MINUTES OF THE TWENTY-THIRD EXPLOSIVES SAFETY SEMINAR

Volume I

HYATT REGENCY HOTEL
ATLANTA, GA
9-11 AUGUST 1988

Sponsored By
Department of Defense Explosives Safety Board
Alexandria, VA

MINUTES OF THE

TWENTY-THIRD EXPLOSIVES SAFETY SEMINAR

Volume I

Hyatt-Regency Hotel

Atlanta, Georgia

9 - 11 August 1988

Sponsored by

Department of Defense Explosives Safety Board

Alexandria, Virginia 22331-0600

Approved for public release; distribution unlimited

REPRODUCTION QUALITY NOTICE

This document is the best quality available. The copy furnished to DTIC contained pages that may have the following quality problems:

- Pages smaller or larger than normal.
- Pages with background color or light colored printing.
- Pages with small type or poor printing; and or
- Pages with continuous tone material or color photographs.

Due to various output media available these conditions may or may not cause poor legibility in the microfiche or hardcopy output you receive.

☐ If this block is checked, the copy furnished to DTIC contained pages with color printing, that when reproduced in Black and White, may change detail of the original copy.

PREFACE

This Seminar is held as a medium by which there may be a free exchange of information regarding explosives safety. With this idea in mind, these minutes are being provided for your information. The presentations made at this Seminar do not imply indorsement of the ideas, accuracy of facts presented, or any product, by either the Department of Defense Explosives Safety Board or the Department of Defense.

THOMAS F. HALL, JR.
Colonel, USA
Chairman

These proceedings are published for the information and benefit of the Seminar participants. The Department of Defense Explosives Safety Board cannot accept responsibility for the accuracy of papers directly reproduced from copies furnished by the authors.

The Twenty-third Explosives Safety Seminar was held August 9-11, 1988 at the Hyatt-Regency Hotel in Atlanta, Georgia. Topics in this issue include:

TABLE OF CONTENTS

VOLUME I

Cont'd

Cont'd

contd

Cont'd

Cont'd

cont'd

Cont'd

Keywords: ORDNANCE, Ammunition, Explosives, Shaped Charge Jets, Magazines (ordnance), Magnesium Powder, Shear Reinforcement, Tunnels, Triboelectric Phenomena, Electric Blasting Caps, Packaging, Buildings. (AW)

OPENING REMARKS

By

Colonel Thomas F. Hall, Jr.
Chairman, Department of Defense
Explosives Safety Board

At

Twenty-Third Department of Defense Explosives Safety Seminar
Atlanta, Georgia
August 9, 1988

9 August 1988

Ladies and Gentlemen:

Welcome to the Twenty-Third Explosives Safety Seminar. The Department of Defense Explosives Safety Board is pleased to cooperate with the Military Services, US industry and the international community in offering this opportunity to you the representatives from the national and international explosives community to become better informed about current matters relating to explosives safety. Our purpose is to exchange and stimulate ideas within that framework. Your active participation is encouraged.

KEYNOTE ADDRESS

DOD EXPLOSIVES SAFETY SEMINAR

By

Honorable Grant S. Green, Jr.

Assistant Secretary of Defense

(Force Management and Personnel)

0900, Tuesday, August 9, 1988

Hyatt Regency Hotel

Atlanta, Georgia

Thank you Tom (Colonel Hall)

Ladies and Gentlemen, I want to thank you for attending this Seminar which gives us all the opportunity to listen, learn, and to share our ideas and latest developments in the safe handling of explosives. It is a rare opportunity indeed when a group such as this can gather. I understand that we not only have representatives from throughout the Department of Defense, but also from other U.S. Government Agencies, representatives from our NATO allies, and friends from all around the world. I want to welcome you all to the 23rd Department of Defense Explosives Safety Seminar.

It can be rather difficult to address such a group in these spectacular surroundings, however, while it appears festive at first glance, this forum is not a celebration. We are here despite increasingly austere defense budgets to handle serious business. Primarily, it's the business of defending this Nation, and meeting our commitments to help our friends and allies to defend freedom around the globe. If this Seminar is to be a success, we must all be dedicated to that end.

It is a great pleasure to be part of this great assemblage which has become a tradition of sorts in the explosives community. I am told the first such Seminar was held at Indian Head, Maryland in 1959 when one hundred explosives experts gathered to pool their knowledge and insights. The Minutes were 180 pages in length. At the last Seminar in Anaheim, California in 1986, 800 participated and it took two hugh volumes to publish the 2200 pages of Minutes.

It is obvious that over the years the information to be shared has increased and the interest in this conference has increased because we all share a need to learn as much as we can about handling the increasingly volatile, explosive, and dangerous materials that are a necessary part of our security structure. In this select forum, we must be focused on protecting our primary mission from an old and renowned enemy...This enemy is not a Fielded Army or a Modern Armored Division, not a Hostile Fleet or Tactical Fighter Wing. The enemy we must seek to learn how to defend against is perhaps more deadly and costly because it attacks without warning, reason, or cost to the real enemy and takes human life and wastes scarce resources. Our enemy is loss by accident, the catastrophic explosion, the disaster.

Let's examine this enemy. What does it cost us? A catastrophic explosion occurs in a Defense Plant, we lose human life, we lose credibility with the local community who sees the plant as an extension of the Defense Department and the Federal Government. Complaints reach Capitol Hill in Washington. Congressmen take up the challenge for their constituents, and the intense public scrutiny, criticisms, and doubts about our ability to manage national security affairs reaches a fever pitch. The media headlines the details in the most graphic and dramatic terms. As free societies that place a premium on the value of the individual, we will not accept loss of life to anything preventable.

But it doesn't end there. An essential weapon system, production facility, and weapons stockpile may be lost. Due to delays strategic assets are idled, tactics are threatened, and the national interest is comprized. We face a deficiency in our ability to execute the Defense Mission with potentially profound effect in time of war, and we lose the availability of important assets which form an essential element of our deterrent posture. We have to find some way to back up the procurement cycle, or risk falling behind Soviet developments. We are then forced to scramble to obtain other, perhaps less reliable sources to replace the loss.

But it doesn't end there either. The courts determine the penalties to be paid to the survivors of the tragedy. We end up paying millions of dollars for lives money cannot replace, and still it doesn't end. The contractor loses time and resources and the workforce loses jobs. Sometimes, the contractor loses interest in such risky work. The results is that the price of the system always escalates.

Which brings us to the heart of this Seminar. How do we counter this threat?

Today over six hundred are assembled here, representing more than 18 Nations. We come from the Defense Department, the Military Staffs of the three Services, Engineering Staffs, plants, and manufacturing firms. We gather to combine our talents and insights into a massive technological counter-assault against our common enemy--the loss of life and mission due to accident.

At no other time and place is such a group assembled for this purpose. Before this Seminar is over you will hear the latest in the design of protective construction. You will see dramatic films of a recent catastrophic accident. You will be brought up

to date on the results of the latest explosives tests. New approaches in Command Safety Programs will be addressed. A myriad of topics will be presented such as lightning protection, airblast phenomena, hazard classification, transportation, and fragmentation hazards. Computer programs will be discussed and exchanged both formally and informally. You choose the session that fits your area of interest.

There is also more than one level to this Seminar. This is the formal level, but there is an informal level also at work here. Private meetings extend into the wee hours when associates from many separate fields become involved in long, meaningful discussions. Safety professionals from operating theaters of all three Services hold encounter sessions over a cup of coffee.

It is this informal level that is most difficult to organize or evaluate, but it is as important as it is spontaneous. If we pursue these informal contacts it will provide this Seminar experience with a completeness that comes from mixing people with different specialties. It is this informal level which establishes the "Explosives Community" and binds it together with common interests and concerns. The products of the informal Seminar are relationships and cross-specialty understanding.

The product of the formal Seminar is information. This information is forged into reports for use by experts in the field. Commanders rely on their experts to gather this harvest of ideas and concepts to direct their safety programs against the common enemy. The Department of Defense has sent its finest into this assembly. Every level of command is represented in one way or another in search of new insights and incentives. In the final analysis, however, it is the Commander who makes the program a functional reality.

When we consider implementing our safety concerns, we must consider the systems approach. The safety that is built into weapons systems--systems safety--is represented in this gathering. The spectre of an unsafe weapon, or a weapon that may react in a way not recognized during its development, is so dangerous that to us it must be unthinkable.

However, weapons are far more complex than before, following every advance in science and technology as it occurs. While the basic principles of safety may be time-honored and well-proven, these dramatic new systems demand the renewed application of old philosophies and new management techniques perhaps not readily apparent. We are here to seek new answers and to hammer out better approaches to explosives safety.

We must learn to manufacture, store, transport, and train with explosives with increased safety. As I glance down the list of presentations, there are papers covering most of the bread and butter safety issues which concern me.

One that particularly concerns me is Training Safety. By Training Safety, I mean, the entire spectrum from Basic Training to Joint Exercises. These include Combined Arms Live Fire Training, Fleet Exercises, Combat Sorties, and the whole host of other exercises which flex the muscle of military might. Training is the combat of peacetime. It sustains our readiness, and it can be as dangerous as it is essential. Training calls for young Soldiers, Sailors, Airmen, and Marines to deal with weapon systems far more lethal than ever before and of a complexity that was beyond belief just twenty years ago. It calls for procedures to make the complexities and dangers manageable. This mission is realistic and attainable.

Safety in such a scenario is the ultimate challenge to Field Commanders. I am aware of the Quickload Program now under development at the Ballistics Research Laboratory. It is a technological response to ammunition storage problems in forward areas. The Air Force is testing the feasibility of new storage concepts to improve explosives safety in the combat environment. The Navy initiated the Insensitive Munitions Program to improve explosives safety aboard warships. We need to apply and expand these new technologies to our needs in the field of training exercises.

While I will not be able to personally visit all of these sessions, I am confident that those who will attend will certainly benefit themselves, their Commanders, and their organizations.

To those visitors from other Nations, some having traveled tens of thousands of miles to attend this Seminar, I extend our most sincere welcome. It is your presence that gives this Seminar the International dimension necessary if we are to learn, grow, and to apply what we learn everywhere there is human life and liberty to protect. Your cooperation vividly demonstrates the seriousness of our efforts in explosives safety. We intend to reciprocate by attending your excellent seminars and gatherings when possible.

Ladies and Gentlemen, I wish you success in your sessions. We in the Department of Defense have a vested interest in everything that happens at this Seminar. We await with interest the successful culmination of events here, and finally, the publication of the Minutes.

Thank You.

NEW DEVELOPMENTS IN THE ARMY SAFETY PROGRAM

By

MR. LEWIS D. WALKER

DEPUTY FOR ENVIRONMENT, SAFETY AND OCCUPATIONAL HEALTH,

OFFICE OF THE ASSISTANT SECRETARY OF THE ARMY

(INSTALLATIONS AND LOGISTICS)

0930, Tuesday, August 9, 1988

Hyatt Regency Hotel

Atlanta, Georgia

Introduction:

I am pleased and honored to address such a distinguished group and want to thank the Department of Defense Explosives Safety Board for inviting me.

This gathering of vast experience and expertise allows for an interchange of information in an area of extreme importance to the mission of the Department of Defense, that being explosives safety.

The exchange of information here at this seminar in both the formal presentations and during the breaks and social gatherings is so important to our continuing efforts to identify a safe environment for our military and civilians, and in protecting the public when dealing with ammunition and explosives.

As you know, explosives safety is one of the most difficult and demanding safety tasks due to our requirement of striking a balance between operational and explosives safety considerations.

It requires we consider the balance between total protection of life and property and maintenance of operational readiness for a combat ready force.

The advances in explosives and weapons technology must be viewed in conjunction with safety engineering and research and development testing. Many in attendance here have a direct impact in this area and understand the ability and necessity to identify hazards and design or engineer them out or at least control them. This is critical to our overall goal of resource conservation and mission accomplishment. The Army is committed to continued progress toward an improved explosives safety posture.

We are all aware of how an explosives accident can have catastrophic consequences, not only in terms of lives lost or property destroyed, but also in terms of international ramifications that could greatly impair our ability to maintain the mission worldwide.

The perfect lesson on lack of explosives safety awareness and the possible catastrophic results was the April explosion of an ammunition storage area in Pakistan. The U.S. Military Forces and its Allies could ill afford the mass destruction, loss of life, and the millions of dollars worth of ammunition destroyed in that particular incident. Storage there did not adhere to the basic explosives safety principles understood as vitally important in the Department of Defense. Explosives safety quantity distance and compatibility application was not evident in Pakistan. The Explosive Ordnance Disposal after action report states "...the result of the storage configuration was that once any explosion or fire started, there was no barrier or distance to impede or stop all of the ammunition stored to either burn, detonate, be blown out of or away from the depot, or in the case of rocket ammunition become propulsive and shoot out of the compound."

The need for strict implementation of specific explosives safety controls is understood in the Army and is the basis for our expanding programs and training efforts.

Vu-graph #1 - U.S. Army Explosives Safety Program

The Army has designed and implemented a comprehensive, active, integrated explosives safety management program. The program provides for development and execution of planned actions to identify and abate explosives safety deficiencies. It addresses our many areas of concern and is designed to improve our explosives safety posture worldwide.

It strengthens our war fighting capability allowing preservation of resources so important to combat readiness.

In March of 1987, the Director of the Army Staff established a General Officer Steering Committee to guide a special study group in their examination of the management and distribution of Army explosives safety functions. The group had representatives from the Office of the Deputy Chief of Staff for Personnel, the Office of the Deputy Chief of Staff for Logistics, and the Office of Deputy Chief of Staff for Operations and Plans. Other Army staff agencies, major Army commands, Army Secretariat, and the Department of Defense Explosives Safety Board participated in aspects of the study.

The concept and recommendations that evolved from the study allowed the Army's explosives safety technical expertise existing with the major Army commands and other agencies to be used Army-wide. Explosives safety management and policy formulation is maintained at Headquarters, Department of the Army. The concept was approved by Lieutenant General Kicklighter, Director of the Army Staff, and implementation began in February of this year.

Vu-graph #2 - Explosives Safety Management Program

Three key program elements were established by the concept. They are shown here.

Vu-graph #3 - Department of the Army Explosives Safety Council

At the Headquarters, Department of the Army level, a Department of the Army Explosives Safety Council was established to provide an Army staff and major Army command coordinated effort in the development and execution of Army explosives safety policy, procedures, funding, and actions. The Department of the Army Explosives Safety Council is currently chaired by Colonel (P) Mitchiner, the Director of Army Safety.

This council provides the major Army commands direct input into explosives safety policy formulation which they will be responsible to implement. The first meeting in May of this year solidly established the Council's capabilities. Goals have been set for future accomplishments.

Vu-graph #4 - Executive Director for Explosives Safety

The second key element of the program is the Executive Director for Explosives Safety position. It was established and is designated by the Chief of Staff, U.S. Army.

The purpose of establishing this position was to centralize the execution of the Army's explosives safety mission. Lieutenant General Fred Hissong currently serves as the Army's focal point on critical explosives safety actions. He is an extension of Headquarters, Department of the Army in exercising executive management and operational control of the new U.S. Army Technical Center for Explosives Safety.

Vu-graph #5 - U.S. Army Technical Center for Explosives Safety

The key operational element of the program is the U.S. Army Technical Center for Explosives Safety. It executes the missions assigned to the Executive Director for Explosives Safety by Headquarters, Department of the Army and the Department of the Army Explosives Safety Council. It provides assistance and technical services to enhance and support the overall program. The U.S. Army Technical Center for Explosives Safety has authority for day-to-day communication with the Headquarters, Department of the Army staff and major Army command commanders Army-wide to serve and assist in the explosives safety missions. It is being staffed with multi-disciplined personnel to assure all technical aspects of explosives safety are considered and supported.

I am very pleased to report the implementation of the new program is going exceptionally well. The first meeting of the Department of the Army Explosives Safety Council went extremely well and further successes are expected for follow-on Army activities. The Executive Director for Explosives Safety and the U.S. Army Technical Center for Explosives Safety are providing assistance on an expanding scale. In the short period of 6 months since Lieutenant General Kicklighter signed the program documents directing implementation, the U.S. Army Technical Center for Explosives Safety, under Lieutenant General Hissong's direction, is approaching full staffing (20 of 35 authorized positions are filled) and accomplishing its technical assistance role Army-wide.

This management approach is allowing for all elements of the explosives safety community to actively participate or have input into the development of Army explosives safety policy, procedures, and priorities.

We in the Army Secretariat are impressed with the accomplishments to-date and will continue to support his expanded effort to meet our goals and address our complex explosives safety issues.

I wish you success in your seminar. An improved explosives safety posture will be realized through the combined talents and interchanges at this seminar.

Thank you.

U.S. ARMY
EXPLOSIVES
SAFETY
PROGRAM

O <u>EXPLOSIVES SAFETY MANAGEMENT PROGRAM</u>

- KEY ELEMENTS
  - -- DA EXPLOSIVES SAFETY COUNCIL
  - -- EXECUTIVE DIRECTOR FOR EXPLOSIVES SAFETY
  - -- U.S. ARMY TECHNICAL CENTER FOR EXPLOSIVES SAFETY

O <u>THE DEPARTMENT OF THE ARMY EXPLOSIVES SAFETY COUNCIL</u>

- PROVIDES FOR ARMY PRIORITIZATION AND DECISION PROCESS
  - -- DEVELOPMENT OF POLICY, PROCEDURES
  - -- DIRECTOR OF THE ARMY SAFETY IS CHAIRMAN
  - -- MACOM MEMBERS, COLONELS OR HIGHER, AND MACOM SAFETY DIRECTOR

O <u>THE EXECUTIVE DIRECTOR FOR EXPLOSIVES SAFETY</u>

- EXECUTIVE AGENT FOR ARMY EXPLOSIVES SAFETY
- CENTRALIZED EXECUTION OF ARMY EXPLOSIVES SAFETY MISSION
- EXECUTES POLICY AND PRIORITIES DEVELOPED BY THE DAESC
- EXECUTIVE DIRECTOR OF THE TECHNICAL CENTER FOR EXPLOSIVES SAFETY

0 <u>U.S. ARMY TECHNICAL CENTER FOR EXPLOSIVES SAFETY</u>

- OPERATES UNDER THE DIRECTION OF THE EXECUTIVE DIRECTOR FOR EXPLOSIVES SAFETY

- TECHNICAL EXTENSION FOR HEADQUARTERS, DEPARTMENT OF THE ARMY

- MULTI-DISCIPLINED STAFF

DIRECTOR
U.S. ARMY TECHNICAL CENTER FOR EXPLOSIVES SAFETY
ATTN: SMCAC-ES
SAVANNA, IL 61074-9639

AUTOVON: 585-8801
COMMERCIAL: (815) 273-8801

OVERVIEW OF THE CHEMICAL DEMILITARIZATION PROGRAM

By

Brigadier General
David A. Nydam

Program Executive Officer - Program Manager

For Chemical Demilitarization

1000, Tuesday, August 9, 1988

Hyatt Regency Hotel

Atlanta, Georgia

OVERVIEW OF THE CHEMICAL DEMILITARIZATION PROGRAM

GOOD MORNING. I APPRECIATE THE OPPORTUNITY TO ADDRESS THIS CONVENTION. BECAUSE OF THE NATURE OF THE CHEMICAL DEMILITARIZATION PROGRAM - THE INHERENT HAZARDS ASSOCIATED WITH DESTRUCTION OF THE CHEMICAL STOCKPILE, THE PUBLIC CONTROVERSY SURROUNDING THE PROGRAM, AND THE HIGH VISIBILITY -- PUBLIC AND WORKER SAFETY IS OUR OVERRIDING CONCERN.

THIS MORNING I WILL PRESENT AN OVERVIEW OF THE CHEMICAL DEMILITARIZATION PROGRAM, WHERE WE HAVE BEEN, WHERE WE ARE NOW, AND WHERE WE EXPECT TO GO IN THE FUTURE. I WILL ALSO DESCRIBE OUR SAFETY PROGRAM, WITH PARTICULAR EMPHASIS ON RISK MANAGEMENT.

THE CHEMICAL DEMILITARIZATION PROGRAM HAS BEEN AN ONGOING EFFORT SINCE 1970 AND BEGAN WITH THE DISPOSAL OF BULK MUSTARD AGENT AT ROCKY MOUNTAIN ARSENAL, NEAR DENVER, COLORADO.

WE CURRENTLY HAVE SIX DISCRETE DEMILITARIZATION PROGRAMS ONGOING.

THE CHEMICAL AGENT MUNITIONS DISPOSAL SYSTEM (CAMDS), LOCATED AT TOOELE ARMY DEPOT, UTAH, HAS BEEN IN OPERATION SINCE 1979. CAMDS SERVES AS THE TEST BED FOR DEVELOPMENT AND PROVE-OUT OF THE DISPOSAL EQUIPMENT AND PROCESSES TO BE USED IN FUTURE PRODUCTION-SCALE DEMILITARIZATION FACILITIES.

THE FIRST PRODUCTION-SCALE FACILITY, THE JOHNSTON ATOLL CHEMICAL AGENT DISPOSAL SYSTEM (JACADS) IS UNDER CONSTRUCTION NOW AT JOHNSTON ISLAND.

THE FACILITY CONSTRUCTION IS COMPLETE AND EQUIPMENT INSTALLATION IS WELL UNDERWAY. THE JACADS IS SCHEDULED TO BECOME OPERATIONAL IN LATE 1989.

COMPLETED AND NOW IN THE OPERATIONAL PHASE IS A DISPOSAL FACILITY AT PINE BLUFF ARSENAL, ARKANSAS, DESIGNED AND CONSTRUCTED TO DISPOSE OF THE ARMY'S INVENTORY OF INCAPACITATING AGENT BZ. AT THE

COMPLETION OF THE BZ DISPOSAL PROGRAM, THIS FACILITY WILL BE MODIFIED TO DISPOSE OF OTHER CHEMICAL STOCKS AT PINE BLUFF ARSENAL.

THE TECHNICAL APPROACH FOR THE DEMILITARIZATION OF THE CHEMICAL STOCKPILE IS THE DISASSEMBLY-THERMAL PROCESS CURRENTLY BEING CONSTRUCTED AT THE JACADS. THIS TECHNOLOGY HAS BEEN UNDER STUDY FOR A NUMBER OF YEARS AND HAS SUCCESSFULLY DESTROYED SOME 16 MILLION POUNDS OF AGENT WITHOUT ANY SIGNIFICANT ENVIRONMENTAL OR SAFETY PROBLEMS THE TECHNOLOGY USES A REVERSE ASSEMBLY PROCEDURE TO ACCESS AND SEPARATE THE AGENT, EXPLOSIVES, DUNNAGE, AND METAL PARTS FOR THERMAL DECONTAMINATION IN THEIR OWN FURNACE. EACH OF THE FOUR FURNACE SYSTEMS HAS ITS OWN ELABORATE POLLUTION ABATEMENT SYSTEM.

THE CRYOFRACTURE-THERMAL DESTRUCTION PROGRAM IS A RESEARCH AND DEVELOPMENT EFFORT INVOLVING THE DEVELOPMENT OF AN ALTERNATE DEMILITARIZATION TECHNOLOGY IN PARALLEL WITH THE CURRENT DISASSEMBLY-THERMAL TECHNOLOGY BEING EMPLOYED AT JACADS. BOTH TECHNOLOGIES REQUIRE INCINERATION . IT IS THE PROCESSES TO ACCESS THE AGENT THAT ARE DIFFERENT.

WITH CRYOFRACTURE THE ENTIRE MUNITION, AGENT, AND EXPLOSIVES ARE BROUGHT TO SUBFREEZING TEMPERATURES, IN A NITROGEN BATH; CRUSHED WITH A PRESS; AND THEN INCINERATED. HOWEVER, IT REQUIRES ADDITIONAL DEVELOPMENT AS THE DATA BASE IS RESTRICTED TO A FEW AGENT MUNITIONS TESTS ON A RELATIVELY LIMITED BASIS.

THE ACTUAL DEMONSTRATION OF THE ABILITY OF THE CRYOFRACTURE PROCESS TO MEET ENVIRONMENTAL REGULATORY REQUIREMENTS AND ACCUMULATE SUFFICIENT DATA TO ALLOW VALID ENGINEERING COMPARISONS TO THE JACADS TECHNOLOGY REMAIN TO BE DEMONSTRATED. INCORPORATION OF THE CRYOFRACTURE TECHNOLOGY INTO THE DISPOSAL PLAN CANNOT BE ACHIEVED WITH THE CURRENT SCHEDULES.

THE DRILL AND TRANSFER SYSTEM (DATS) IS A TRANSPORTABLE SYSTEM USED TO DEMILITARIZE LEAKING OR UNSERVICEABLE CHEMICAL MUNITIONS AND RECOVERED RANGE ITEMS. USING REMOTE CONTROLS, A HOLE IS DRILLED IN THE MUNITION BODY AND THE CHEMICAL AGENT DRAINED TO AN APPROVED STORAGE CONTAINER. THE MUNITION CASING IS THOROUGHLY DECONTAMINATED AND THE AGENT IS RETURNED TO SECURE STORAGE. DATS HAS OPERATED SINCE 1979 AT SIX INSTALLATIONS AND HAS PROCESSED MORE THAN 900 MUNITIONS.

THE FY83 DEFENSE AUTHORIZATION ACT, OR PUBLIC LAW 99-145, DIRECTED THE DISPOSAL OF THE TOTAL U.S. INVENTORY OF UNITARY CHEMICAL AGENTS AND MUNITIONS BY SEPTEMBER 30, 1994, IN A MANNER THAT WOULD PROVIDE MAXIMUM PROTECTION OF THE ENVIRONMENT, THE GENERAL POPULATION, AND THE WORKFORCE. THE LAW FURTHER DIRECTED THAT THE FACILITIES CONSTRUCTED FOR THE DISPOSAL PROGRAM WOULD BE USED EXCLUSIVELY FOR THE DESTRUCTION OF THE CHEMICAL AGENTS AND MUNITIONS, AND WHEN NO LONGER NEEDED FOR THIS PURPOSE, WOULD BE CLEANED AND DESTROYED.

THE CHEMICAL STOCKPILE IS STORED IN A VARIETY OF MUNITION TYPES AND BULK CONTAINERS AT EIGHT SITES WITHIN THE CONTINENTAL UNITED STATES (CONUS), AT JOHNSTON ISLAND IN THE PACIFIC, AND IN WESTERN EUROPE. THE JOHNSTON ISLAND STOCKS WILL BE DEMILITARIZED IN THE JACADS FACILITY UNDER CONSTRUCTION, AND THE DISPOSITION OF THE EUROPEAN STOCKS ARE BEING DISCUSSED AT THE STATE DEPARTMENT LEVEL.

AS DIRECTED BY PUBLIC LAW 99-145, THE ARMY DEVELOPED A CONCEPT PLAN FOR THE DESTRUCTION OF THE LETHAL CHEMICAL STOCKPILE BY SEPTEMBER 30, 1994, AND SUBMITTED THE PLAN TO CONGRESS IN MARCH OF 1986.

THE PLAN PRESENTED THREE PROGRAMMATIC ALTERNATIVES TO ACHIEVE THIS GOAL:

(1) CONSTRUCTION AND OPERATION OF DISPOSAL FACILITIES AT EACH OF THE EIGHT CHEMICAL STORAGE LOCATIONS;

(2) MOVEMENT OF THE CONUS STOCKS TO TWO REGIONAL DESTRUCTION CENTERS TO BE ESTABLISHED AT ANNISTON ARMY DEPOT FOR THE EASTERN SITES AND TOOELE ARMY DEPOT FOR THE WESTERN SITES; AND

(3) COLLOCATION OF ALL CHEMICAL STOCKS TO ONE DISPOSAL CENTER TO BE ESTABLISHED AT TOOELE ARMY DEPOT.

SINCE THE PREPARATION OF THE DEMILITARIZATION CONCEPT PLAN FOR CONGRESS IN MARCH 1986, SEVERAL OTHER SIGNIFICANT EVENTS HAVE TAKEN PLACE.

THE DRAFT PROGRAMMATIC ENVIRONMENTAL IMPACT STATEMENT (DPEIS) WAS PUBLISHED IN JULY 1986. WITH THE COMPLETION OF THE PUBLIC COMMENT PERIOD, IT WAS DETERMINED THAT SOME AREAS OF THE PROGRAMMATIC EIS REQUIRED A MORE IN-DEPTH REVIEW AND, IN SOME INSTANCES, NEW STUDIES WERE REQUIRED TO SATISFY PUBLIC INTEREST AND CONCERN.

ADDITIONAL REFINEMENTS TO THE RISK AND HAZARD ANALYSIS WERE INCORPORATED INTO THE FINAL

PROGRAMMATIC EIS. A SEPARATE RISK MITIGATION ANALYSIS, AIMED AT REDUCING THE PROBABILITY OF OCCURRENCE OF AN ACCIDENT AND REDUCING THE CONSEQUENCES OF AN ACCIDENT SHOULD IT OCCUR, ACCOMPANIED THE RISK ANALYSIS AS PART OF THE OVERALL EIS PACKAGE. A REVIEW OF THE EMERGENCY RESPONSE PROCEDURES AT EACH CURRENT STORAGE SITE FOUND VARIOUS DEGREES OF DETAILED PLANNING AND INVOLVEMENT WITH THE SURROUNDING COMMUNITIES. AS A RESULT, OFF-POST EMERGENCY RESPONSE PLANS ARE BEING UPDATED TO PROVIDE ADDITIONAL MITIGATION IN THE UNLIKELY EVENT THAT AN ACCIDENT INVOLVING CHEMICAL AGENTS OCCURS. AREAS SUCH AS IMPROVED WARNING SYSTEMS, DETAILED TRAINING OF LOCAL MEDICAL AND LAW ENFORCEMENT PERSONNEL, AND EVACUATION PLANNING ARE ALL UNDER STUDY. THESE TOTAL EFFORTS ARE SUMMARIZED IN THE FINAL PROGRAMMATIC EIS.

WE ALSO DID A DETAILED STUDY ON THE VARIOUS TRANSPORTATION CONCEPTS, BOTH ON AND OFF SITE, AS WELL AS AN EVALUATION OF CURRENTLY AVAILABLE PACKAGES THAT COULD BE USED FOR TRANSPORTATION OF

CHEMICAL MUNITIONS. WE CONDUCTED A STUDY THAT EXAMINED ALL THE POTENTIAL MONITORING REQUIREMENTS WE MAY HAVE IN ORDER TO MAINTAIN STRICT CONTROL OF ALL DEMILITARIZATION RELATED ACTIVITIES AND TO PROVIDE HISTORICAL EVIDENCE THAT WE DID IN FACT CONDUCT THE PROGRAM IN A CONTROLLED MANNER WHICH PRESENTED MINIMAL RISK TO THE PUBLIC. WE ALSO EXAMINED THE FEASIBILITY, COSTS, AND BENEFITS OF TRANSPORTING THE CHEMICAL STOCKPILE AT A REDUCED TEMPERATURE IN ORDER TO REDUCE THE AGENT EVAPORATION RATE IN THE EVENT OF AN AGENT RELEASE. WE ALSO RESEARCHED THE HISTORY OF THE MOVEMENT OF U.S. LETHAL CHEMICAL MUNITIONS AND PREPARED A REPORT BASED ON THAT RESEARCH. THE DRAFT PROGRAMMATIC EIS DID NOT ADDRESS THE RELATIVE VULNERABILITY OF THE VARIOUS DISPOSAL ALTERNATIVES TO SABOTAGE OR TERRORISM, AND WE RECEIVED A NUMBER OF COMMENTS REGARDING THAT OMISSION. AS A RESULT, A TERRORIST VULNERABILITY ASSESSMENT WAS PREPARED. THIS REPORT IS CLASSIFIED SECRET.

DURING THE PUBLIC HEARING AT LEXINGTON-BLUE GRASS ARMY DEPOT, CITIZENS EXPRESSED CONCERNS OVER PORTIONS OF THE DRAFT PROGRAMMATIC EIS AND REQUESTED ARMY FUNDING TO BRING IN EXPERTS TO

ASSIST THE COMMUNITY IN EVALUATING THE HIGHLY TECHNICAL PORTIONS OF THE ENVIRONMENTAL DOCUMENTATION. THE ARMY MADE THE DECISION TO INVOLVE COMMUNITY GROUPS IF THE GROUPS COULD DEMONSTRATE THAT THEY WERE REPRESENTATIVE OF THE ENTIRE COMMUNITY, THAT THEY HAD THE REQUIRED EXPERTISE, AND IF THEY SUBMITTED THE REQUEST IN WRITING. ACCORDINGLY FIVE SUCH CONTRACTS WERE AWARDED TO THE COMMUNITIES NEAR ABERDEEN PROVING GROUND, PINE BLUFF ARSENAL, NEWPORT ARMY AMMUNITION PLANT, LEXINGTON-BLUE GRASS ARMY DEPOT, AND UMATILLA DEPOT ACTIVITY.

THE COMPLEXITY AND VISIBILITY OF THE CHEMICAL STOCKPILE DISPOSAL PROGRAM HAVE INCREASED SIGNIFICANTLY SINCE THE ORIGINAL CONCEPT PLAN WAS SUBMITTED TO CONGRESS IN MARCH 1986. WE MAINTAIN CLOSE LIAISON WITH MANY OF THE REGULATORY AGENCIES SUCH AS THE ENVIRONMENTAL PROTECTION AGENCY, STATE AIR AND WATER REGULATORS, THE DEPARTMENT OF HEALTH AND HUMAN SERVICES, DEPARTMENT OF DEFENSE EXPLOSIVES SAFETY BOARD, THE FEDERAL EMERGENCY PLANNING AGENCY, RESIDENTS COUNCIL ON ENVIRONMENTAL QUALITY, AS WELL AS HEADQUARTERS OF THE DEPARTMENTS OF DEFENSE AND ARMY.

THE FINAL PROGRAMMATIC ENVIRONMENTAL IMPACT STATEMENT WAS PUBLISHED IN JANUARY OF 1988 AND THE UNDER SECRETARY OF THE ARMY ANNOUNCED HIS RECORD OF DECISION THE FOLLOWING MONTH AFTER A ROUND OF HEARINGS AT SEVERAL OF THE SITES.

THAT DECISION CALLED FOR ON-SITE INCINERATION OF THE LETHAL CHEMICAL STOCKPILE.

THE DEFENSE AUTHORIZATION ACT OF FY 88 AND FY89 (PUBLIC LAW 100-180) REQUIRED THE DEPARTMENT OF DEFENSE TO LOOK AT ALL OF THE AVAILABLE DEMILITARIZATION TECHNOLOGIES, EVALUATE THESE TECHNOLOGIES, AND SELECT THE ONE MOST SUITABLE FOR THE CHEMICAL DEMILITARIZATION PROGRAM. THE LAW ALSO REQUIRED THAT THE DEPARTMENT OF DEFENSE PROVIDE FOR FULL SCALE OPERATIONAL VERIFICATION (OVT) AND TO CERTIFY THE CAPABILITIES OF THE SELECTED TECHNOLOGY. SAFETY WAS AND IS THE PARAMOUNT CONSIDERATION. FINALLY, DEPARTMENT OF DEFENSE WAS TO PROVIDE AN IMPLEMENTATION PLAN TO CONGRESS BY THE 15TH OF MARCH 1988 WITH THE REVISED SCHEDULES AND UPDATED BUDGET REQUIREMENTS.

THE IMPLEMENTATION PLAN DREW FROM THE FINAL PROGRAMMATIC ENVIRONMENTAL IMPACT STATEMENT, PROGRAMMATIC RECORD OF DECISION, ALL PREVIOUSLY CONDUCTED SAFETY AND SURETY STUDIES AND INVESTIGATIONS, EFFICIENCY OF OPERATIONS, AND COSTS.

THE PLAN SUBMITTED TO CONGRESS HAS SEVERAL SIGNIFICANT CHANGES FROM THE ORIGINAL CONCEPT PLAN. OF THE TECHNIQUES EVALUATED, RESERVE DISASSEMBLY INCINERATION (BASELINE) WAS SELECTED. THE CRYOFRACTURE/INCINERATION WAS TO BE CONTINUED IN RESEARCH AND DEVELOPMENT AS AN AUGMENTATION POSSIBILITY. THE 1994 COMPLETION DATE WAS EXTENDED BY THREE YEARS TO 1997. THE SCHEDULES INCLUDED A 16 MONTH OPERATIONAL VERIFICATION TEST PHASE AT THE JACADS FACILITY ON JOHNSTON ISLAND. THE PLAN CALLS FOR STAGGERED PLANT CONSTRUCTION, EQUIPPING, AND OPERATION AS COMPARED TO THE ORIGINAL CONCEPT OF CLONING MADE NECESSARY BY THE MANDATED 1994 END DATE. INCLUDED IN THE PLAN ARE PROVISIONS FOR FUNDING EMERGENCY PREPAREDNESS BOTH ON THE INSTALLATION AND IN THE LOCAL COMMUNITIES. IT ALSO PROVIDES FOR DEVELOPMENT OF AN ON-SITE TRANSPORTER

TO ENHANCE SAFETY WHILE MOVING THE MUNITIONS FROM THE IGLOOS TO THE DEMILITARIZATION FACILITY. AT THIS TIME CONGRESSIONAL COMMITTEE REPORTS HAVE SUPPORTED THE IMPLEMENTATION PLAN TO INCLUDE SCHEDULES AND PROGRAM COSTS.

THE MOST SIGNIFICANT NEAR-TERM ACTIONS INVOLVE THE CONSTRUCTION OF A FULL-SCALE BASELINE PLANT AT TOOELE IN FY 1989; THE CONSTRUCTION OF THE CENTRAL TRAINING FACILITY AT ABERDEEN PROVING GROUND IN FY 1989; THE INITIATION OF ALL SITE SPECIFIC ENVIRONMENTAL DOCUMENTATION AND SITE SPECIFIC PERMITTING ACTIVITIES; AND SITE SPECIFIC EMERGENCY PREPAREDNESS PLANNING. THERE WILL BE THE ESTABLISHMENT OF INTER-GOVERNMENTAL CONSULTATION AND COORDINATION BOARDS IN A TIERED APPROACH AT BOTH THE NATIONAL AND THE INSTALLATION LEVEL. THE NATIONAL ACADEMY OF SCIENCE, NATIONAL RESEARCH COUNCIL, WILL CONTINUE THEIR OVER SIGHT ROLE.

WE HAVE TAKEN A SYSTEM SAFETY/RISK MANAGEMENT APPROACH IN OUR PROGRAM IN ORDER TO ASSURE MAXIMUM PROTECTION FOR THE ENVIRONMENT, THE GENERAL PUBLIC, AND PLANT WORKERS. THIS APPROACH IS NECESSARY

BECAUSE OF THE MAGNITUDE AND COMPLEXITY OF THE PROGRAM, THE SEVERITY OF THE POTENTIAL HAZARDS ASSOCIATED WITH HANDLING AND PROCESSING A MIX OF LETHAL AGENTS AND EXPLOSIVES, AND THE TYPES OF OPERATIONS INVOLVED.

OUR SYSTEM SAFETY APPROACH IS TAILORED FROM THE SYSTEM SAFETY AND RISK MANAGEMENT GUIDELINES CONTAINED IN MIL-STANDARD 882B AND DOD INSTRUCTION 5000.36. THE CENTRAL THRUST IS A SYSTEMATIC METHOD FOR IDENTIFICATION AND EVALUATION OF EVENT HAZARD PROBABILITIES AND SEVERITIES AND TO ELIMINATE OR REDUCE THE ASSOCIATED RISK TO AN ACCEPTABLE LEVEL.

WE HAVE RECENTLY COMPLETED A COMPREHENSIVE ASSESSMENT OF THE RISK THE CSDP PRESENTS TO THE PUBLIC AND THE ENVIRONMENT. THE DESIGN AND OPERATION OF EACH OF THE EIGHT CSDP FACILITIES WILL BE SUBJECTED TO VIGOROUS HAZARDS ANALYSES TO INSURE MAXIMUM PROTECTION TO THE PUBLIC, AND ENVIRONMENT, AND TO OUR WORKERS. ADDITIONAL ANALYSES OF JACADS OPERATIONS ARE SCHEDULED TO BE COMPLETED THIS YEAR, PRIOR TO STARTUP OF THE FACILITY.

WE HAVE COMPLETED COMPREHENSIVE ANALYSES OF OUR ONGOING OPERATIONS AT THE CHEMICAL AGENT DISPOSAL MUNITIONS SYSTEM (CAMDS) AT TOOELE ARMY DEPOT IN UTAH, AT THE BZ DISPOSAL FACILITY AT PINE BLUFF ARSENAL, ARKANSAS.

THE APPROACH WE USE FOR RISK MANAGEMENT IS DIFFERENT THAN THE APPROACH USED WITHIN DOD FOR FACILITY SITING AND CONSTRUCTING. THE ACCEPTED APPROACH USED WITHIN DOD IS TO FIRST ASSUME A MAXIMUM CREDIBLE EVENT BASED ON A MUNITION CONFIGURATION AND THEN TO PERFORM A DOWNWIND HAZARD CALCULATION USING ACCEPTED DISPERSION MODELLING TECHNIQUES. THE CRITERIA DEFINED AS ACCEPTABLE IS LESS THAN 1 PERCENT OF AN OFF-POST POPULATION EXPOSED TO THE PLUME BEING KILLED BY THAT EXPOSURE.

OUR APPROACH TO RISK MANAGEMENT, WHICH HAS BEEN ENDORSED BY THE DEPARTMENT OF HEALTH AND HUMAN SERVICES, STRESSES THE REDUCTION OF RISK AND NOT JUST CONSEQUENCE REDUCTION. WE ATTEMPT TO IDENTIFY ALL POTENTIAL ACCIDENT SCENARIOS, DEVELOP PROBABILITY AND CONSEQUENCE ESTIMATES FOR THOSE SCENARIOS, AND ESTIMATE HAZARD DISTANCES BASED ON A

NO DEATHS RATHER THAN A 1 PERCENT LETHALITY DOSAGE. WE TAKE THIS APPROACH BECAUSE IT GIVES US A GOOD BASIS FOR COMPARISON OF RISKS AND ALLOWS US TO CONCENTRATE OUR RESOURCES WHERE THEY WILL DO THE MOST GOOD WITH REGARD TO REDUCTION OF PUBLIC RISK. WE ALSO TAKE THIS APPROACH BECAUSE THE DEPARTMENT OF HEALTH AND HUMAN SERVICES HAS TAKEN THE POSITION THAT WE MUST ANALYZE BOTH EVENT PROBABILITIES AND EVENT CONSEQUENCES WHEN CONSIDERING THE IMPACT OF OUR PROGRAM ON PUBLIC HEALTH AND SAFETY. DHHS HAS ALSO STATED THAT THE ACCEPTANCE OF 1 PERCENT LETHALITY IS UNACCEPTABLE TO THEM, AND THAT OUR HAZARD ARCS MUST EXTEND OUT TO THE NO DEATHS DISTANCE.

FOR PURPOSES OF FACILITY SITING, HOWEVER, WE COMPLY WITH THE DOD REQUIREMENTS IN THAT WE ASSUME A MAXIMUM CREDIBLE EVENT, DO THE DOWNWIND HAZARD CALCULATIONS OUT TO THE 1 PERCENT LETHALITY DISTANCE, AND SUBMIT OUR SITE PLANS IN ACCORDANCE WITH DEPARTMENT OF DEFENSE EXPLOSIVES SAFETY REQUIREMENTS.

IN THE SPECIALIZED SUBJECT SESSIONS THAT WILL OCCUR OVER THE NEXT THREE DAYS, THERE WILL BE ELEVEN PAPERS PRESENTED THAT ARE THE RESULT OF SOME OF THE SAFETY RELATED ACTIVITIES ASSOCIATED WITH THE

CHEMICAL DEMILITARIZATION PROGRAM. SEVERAL OF THE PRESENTATIONS ARE DIRECTLY RELATED TO MY COMMENTS ON RISK MANAGEMENT, BUT I THINK YOU WILL FIND ALL OUR PRESENTATIONS INTERESTING AND INFORMATIVE.

COL MURPHY, I THANK YOU FOR THE OPPORTUNITY TO ADDRESS THIS GROUP. I AM SURE THAT THIS SEMINAR WILL RESULT IN A LOT OF USEFUL INTERCHANGE AMONG THE PEOPLE IN THIS ROOM AND THAT THEY WILL RETURN TO THEIR HOME BASES WITH A LITTLE MORE KNOWLEDGE AND INSIGHT INTO SOLVING SAFETY PROBLEMS ASSOCIATED WITH AMMUNITION AND EXPLOSIVES SAFETY.

THANK YOU.

FRAGMENT HAZARD COMPUTER PROGRAM (FRAGHAZ)

by

Frank McCleskey
Kilkeary, Scott and Associates, Inc.
703-775-7210

ABSTRACT

The Fragment Hazard Computer Program was developed for the DOD Explosives Safety Board to provide a means for estimating fragment hazards produced by the inadvertent detonation of munitions stacks. It is written in FORTRAN 77 and consists of almost 1000 lines with over 200 variables. The fragmentation data used are derived from small-scale arena tests. A separate trajectory is calculated for each recovered fragment using Fourth-Order Runge-Kutta numerical procedures. The program incorporates a true three dimensional simulation. Any target may be simulated which can be approximated by a rectangular parallelepiped. Wind, altitude and fragment ricochet are included. Monte Carlo and Full Factorial options are provided. For the Monte Carlo option, a portable Random Number Generator is included. It is portable in the sense that, given the same seed, the same sequence of random numbers can be produced on almost any computer. Output includes fragment hazard range versus number of munition units for both areal number density an probability of hit criteria. An important aspect of the program is the ease with which it can be modified to investigate specific problems like barricade efficiency and fragment hazards to vehicles on Public Traffic Routes.

FOREWORD

The INTRODUCTION and GENERAL PROGRAM DESCRIPTION which follow were taken verbatim from the documentation report for the FRAGHAZ computer program. As such references to other parts of the documentation report have been retained and serve to indicate the scope of the report. For copies of the report make requests to:

Commander, Naval Surface Warfare Center
Dahlgren, Virginia 22448
Attn: Technical Library Code E231

Ask for the following title:
McCleskey, Frank, Quantity - Distance Fragment Hazard Computer Program (FRAGHAZ), NSWC TR 87-59, February 1988, UNCLASSIFIED

INTRODUCTION

Historically, hazards from stacks of explosive ordnance have been stated in terms of hazard distance due to blast overpressures. These hazard distances, presented as quantity versus distance (QD criteria), have not adequately addressed the fragment hazards. The fragment hazards were specified in terms of specific number of weapons and were derived using many simplifying assumptions. As a result, the validity of these QD criteria have always been questionable.

The Department of Defense Explosives Safety Board (DDESB) decided to begin detailed studies and experiments concerning the hazards posed by fragments from stacks of detonating munitions in the early 1970s. The Naval Surface Warfare Center (NSWC) was requested to characterize weapons of interest to the DDESB and to establish analytical techniques that would predict the fragment hazards for stored munitions.

Many fragmentation experiments were conducted and a number of predictive analytical techniques were explored. The analytical techniques were all characterized by integral and differential equations whose solutions would provide estimates of hazard distances for fragmenting munitions. These analytical approaches suffered from the need to restrict the number of variables to a manageable level. As a result, many variables had to be averaged or held constant. Many conditions such as wind, ricochet, and variable drag coefficient had to be ignored to make the equations manageable.

In 1981, recognizing the limitations of the analytical methods, a new approach was established that had the promise of overcoming the restrictions imposed by analytical equations. The new approach relied on numerical procedures where as many equations as needed could be solved sequentially. In the numerical procedure, a complete trajectory for each fragment representing a particular munition is calculated, and hazard calculations made when the trajectory intersected the target. These numerical procedures are often referred to as MONTE CARLO or FULL FACTORIAL procedures. This report contains the description of numerical procedures currently established for predicting the hazards from fragmenting munitions. There is a general description designed to orient the reader as to the many qualitative aspects of the procedure. This is followed by a detailed line-by-line description of the computer code. Supporting this thorough description of the computer code is a number of appendices containing information too detailed to be included in the main body of the report. Such things as glossaries, mathematical proofs, program listings, and example problems are included in the appendices.

Although future changes are inevitable, the computer program has advanced to a stage where documentation is warranted. All significant factors affecting the hazards from fragments have been incorporated. The program is coded in Microsoft FORTRAN 77, which is common to many computers ranging from MICROS to MAIN FRAMES. FORTRAN 77 represents a compromise between BASIC and FORTRAN IV. The program has been structured to minimize running time such that it can be run practically on MICRO computers. A typical run on the IBM PC-AT using compiled FORTRAN 77 takes approximately 6 hr, whereas on a MAIN FRAME the run would be measured in minutes.

GENERAL PROGRAM DESCRIPTION

The QD Fragment Hazard (FRAGHAZ) Computer Program provides a method for predicting the fragment hazard produced by the detonation of munitions. FRAGHAZ requires fragment characteristic data obtained from small-scale tests representative of larger stacks of munitions. In the case of 155mm projectiles, for example, the small-scale test may consist of one or more pallets (eight projectiles per pallet) positioned and detonated to yield a representative sample of fragment data from an entire stack. Full trajectories are calculated for each fragment recovered in the small-scale test. Appropriate calculations are made during the fragment trajectory to establish the hazard to a specified target.

STACK FRAGMENTATION CHARACTERISTICS

Past tests have demonstrated that virtually all the fragments going downrange are produced by the munitions (projectiles, bombs, etc.) on the face of the stack toward the target area. Fragmentation from the ordnance in the interior of the stack is, for the most part, contained within the stack. When a stack with units close together is detonated, fragment jets are produced between adjacent munitions on the face of the stack. The width of the jet depends on the method of stack initiation. When all units are detonated simultaneously, the jet is typically 10 deg wide. If only one or two donor units are initially detonated, the jet width is more typically 20 to 30 deg. Stack detonation by donor units is called natural communication and all current testing (presented here) uses this technique.

The jet produced between adjacent units is called an interaction area. The greatest fragment densities and highest fragment velocities are produced within the interaction areas. For safety purposes, the fragmentation characteristics of the interaction areas are used for input to the computer model. The interaction areas overlap at relatively short distances downrange and their effects can therefore be added to represent the cumulative effects of large ammunition stacks.

HAZARD CRITERIA

The FRAGHAZ program requires that hazard criteria be specified for the target being considered. Most work to date has been concerned with the personnel target. The DDESB has specified the following hazard criteria for personnel:

1. Fragment impact kinetic energy of at least 58 ft-lb
2. Hazardous fragment areal number density of at least one hazardous fragment per 600 ft^2

The hazardous fragment areal number density criterion is approximately equivalent to a hit probability of 0.01 given that the presented area of a man is considered to be 6.2 ft^2. Similar criteria must be specified for other targets being considered.

MONTE CARLO AND FULL FACTORIAL OPTIONS

FRAGHAZ runs under a MONTE CARLO or FULL FACTORIAL option. Both options provide methods for handling the uncertainty associated with random variables. The program includes seven random variables for each option:

1. Initial fragment elevation angle
2. Initial fragment velocity
3. Fragment drag coefficient
4. Height of the fragment trajectory origin above the ground surface
5. Soil constant for ricochet
6. Wind speed
7. Altitude of the ammunition stack site

The first three random variables have to do with the specific characteristics of each fragment. The remaining four variables are more like background conditions.

The following analogous terms are associated with the two options:

MONTE CARLO	FULL FACTORIAL
Variable	Factor
Value	Level
Replication	Treatment

In the MONTE CARLO procedure a variable is any one of the random variables listed above. In the FULL FACTORIAL option, these random variables are called factors. Likewise, value and level pertain to any single value for any single random variable. Replication and treatment are also essentially synonymous, and are explained in the following.

In the MONTE CARLO option, each replication represents a simulation of a full-scale test. For example, suppose there were 250 fragments recovered in a small-scale test representing a particular munition. Each random variable associated with the fragments would have a known or assumed range of uncertainty. Random numbers are then used to designate a particular value for each random variable. Trajectories would be calculated for each of the 250 fragments with an effective number of fragments associated with each trajectory commensurate with the full-scale stack. Hazardous intersections with the target would be recorded and accumulated in the program. This would constitute one replication. Because of the uncertainty in the random variables, this would constitute only one possible outcome for the full-scale ammunition stack under consideration. As a result a second replication would be conducted using a new set of random numbers to define new values for the random variables. A new outcome would be produced and would be recorded and accumulated along with the outcome of the first replication. This procedure would continue until the outcomes of as many as 60 replications were recorded and accumulated. At that time the program calculates the desired hazard statistics from the hazard data in each replication. These final statistics can be in the form of averages, minima, maxima, percentiles, etc. If there were 250 fragments and 60 replications, then the program would have to calculate 250 x 60 = 15000 complete trajectories. Trajectory calculations consume about 90 percent of the program running time. The remaining 10 percent is taken up with bookkeeping (recording and accumulating hazard data) and output calculations.

The FULL FACTORIAL option differs from the MONTE CARLO option only in the way the values of the random variables are selected. In the MONTE CARLO option, if we had 60 replications, then 60 different values for each random variable for a particular fragment would be selected. For example, suppose a single

simulate the downrange hazard volume. A hazardous fragment is only of concern when its trajectory lies within the pie-shaped hazard volume. The height of the sector is equal to the height of the target selected. In Figure 1, this height is shown for a personnel target. The angular width of the sector is typically 10 deg. This value has been selected to match the 10-deg sector width used in the fragment pickup from full-scale tests. In this way, one can compare the program predictions with actual pickup test data to gage the validity of the computer model. The hazard volume is divided into 100-ft segments from zero to the maximum range specified for the program calculations. Without wind, the maximum calculated range is on the order of 4800 ft. All calculations of fragment numbers, fragment density, and probabilities of hit are made with reference to these 100-ft segments. Later in the simulation, the results in each 100-ft segment may be combined to yield results for 200, 300, and 400-ft increments. These larger increments sometimes assist in plotting and interpreting the output data.

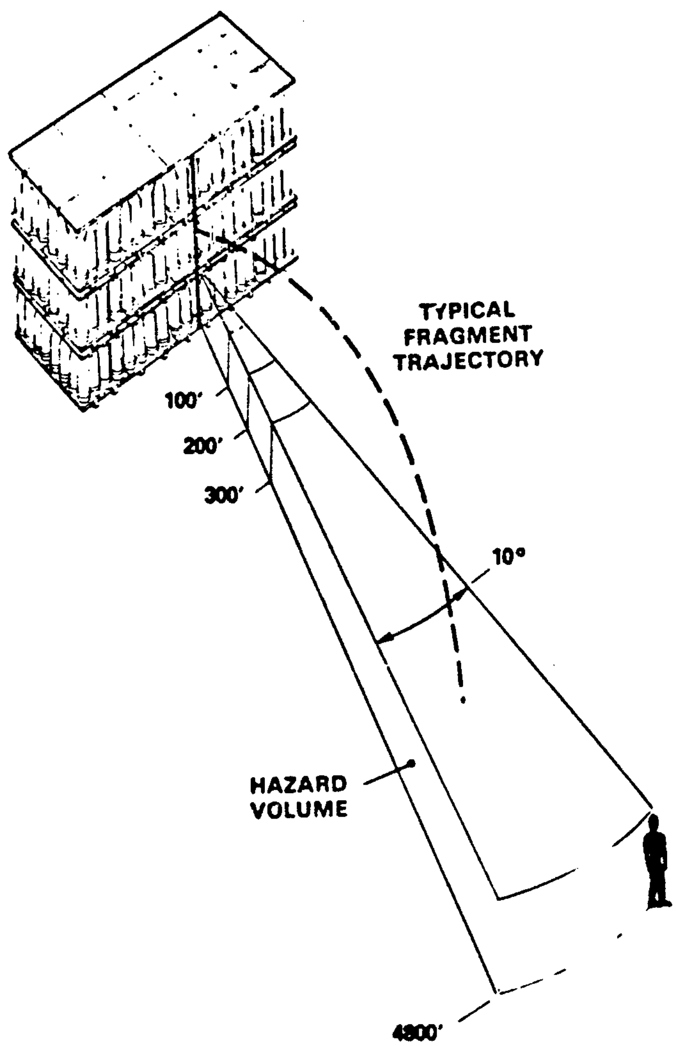

FIGURE 1. STACK FRAGMENTATION SIMULATION

FRAGMENT TRAJECTORY

Figure 2 shows a more detailed picture of the fragment trajectory. Wind is included as a two-dimensional velocity vector, which can have both range and cross-range components. There is no vertical component to the wind vector, since this is seldom reported in practice. The wind, therefore, is always contained in a horizontal plane at the point of calculation. The origin of the trajectory is at a designated height selected by the MONTE CARLO or FULL FACTORIAL option. The trajectory is calculated using a fourth-order Runge-Kutta routine. Calculations can be made in three dimensions with the effects of wind included. The Runge-Kutta routine requires only initial conditions for fragment velocity and elevation angle at the origin. These conditions are obtained from small-scale arena tests of the munition being considered. Each point along the trajectory is calculated from the conditions existing at the previous point. The velocity and trajectory angle are computed at each point. When the trajectory is within the hazard volume, the kinetic energy of the fragment is calculated and compared with the hazard kinetic energy criterion to determine whether the fragment is hazardous or not. The trajectory angle is used in subsequent fragment density and probability of hit calculations. Range, cross-range, and distance are computed and are used for associating the hazard to a particular 100-ft-hazard segment. Currently, the initial fragment velocity vector is constrained to the vertical X-Y plane. However, since the model uses a true three-dimensional routine, there is complete three-dimensional freedom for establishing the initial conditions. Trajectory calculations are made for each fragment recovered in the small-scale arena test.

A tail wind has three adverse effects on hazard conditions. First, a tail wind will increase the range of a fragment. Second, it will increase the striking velocity of a fragment thereby increasing its hazard to the target. Third, a tail wind will decrease the angle of strike thereby increasing the presented area of a target with a large vertical dimension (a man for example). The increased presented area results in larger probabilities of hit. The increased range due to a tail wind is approximately equal to the time of flight multiplied by the wind speed. In the far range where the time of flight can be approximately 10 sec, a tail wind speed of 50 ft/s will result in a range increase of about 500 ft.

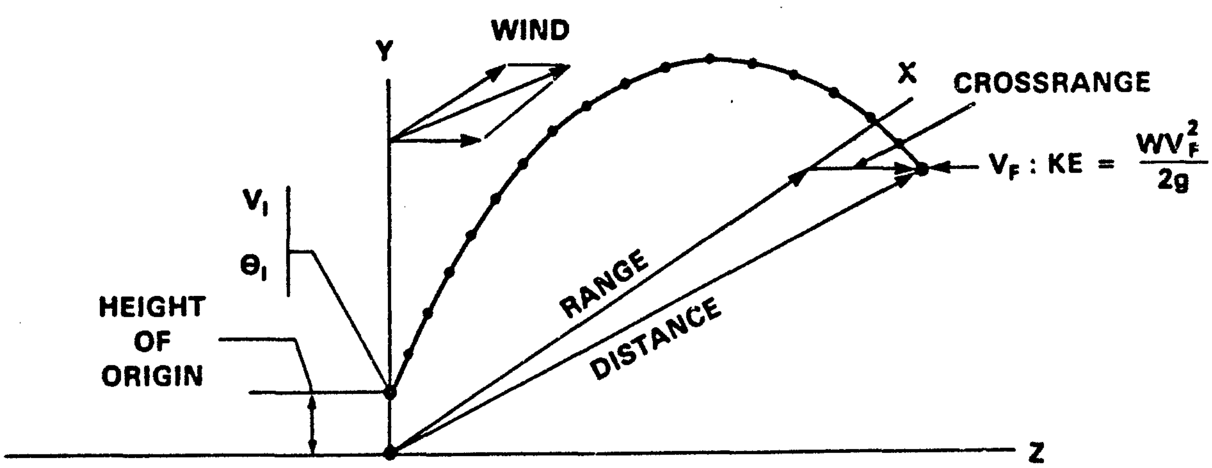

FIGURE 2. FRAGMENT TRAJECTORY

Figure 3 shows the two types of trajectories considered in the FRAGHAZ model. The normal or nonricochet trajectory has been considered previously. The ricochet trajectory is based on experiments conducted by the Ballistic Research Laboratories at Aberdeen, Maryland, in the late 1960s.[1] In both types of trajectories the points at which the fragment strikes the ground and either enters or leaves the hazard volume (large dots in Figure 3) are accurately calculated in the model. This permits the hazard data to be definitely associated with the proper 100-ft hazard segment. When a fragment impacts the ground, its impact angle is compared with a critical ricochet angle to determine whether the fragment will ricochet. The critical ricochet angle is dependent on the type of soil. Once it is determined that the fragment will ricochet, the angle and velocity of ricochet are determined from the incident angle and velocity together with the effect of soil type.

Since all the dynamic characteristics of the fragment are known at each point calculated in the Runge-Kutta routine, all fragment hazard data can be calculated at each point. When more than one point is contained in a 100-ft hazard increment, averages are used to determine the hazard data for the increment.

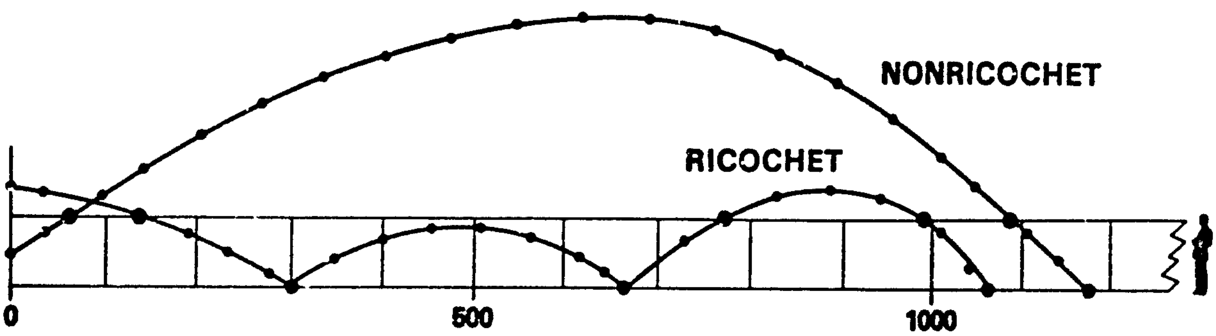

FIGURE 3. TYPES OF TRAJECTORIES

HAZARD CALCULATIONS

Figure 4 shows how hazard density and hazard probability of hit are calculated for a personnel target. The number of hazardous fragments (N_F) is dependent on the number of ordnance units on the face of the stack toward the target area. Since the trajectories are calculated point by point, the 100-ft hazard volume increment through which the trajectory is passing can be determined. The fragment mass and velocity are also known at each point and, therefore, it can be determined whether the fragment possesses sufficient kinetic energy to exceed the hazardous kinetic energy criterion. After the fragment has been determined hazardous, the presented areas of the target (represented as a parallelepiped) and of the total volume of the 100-ft hazard volume segment can be calculated in the plane perpendicular to the fragment trajectory. This can be done because the trajectory angle with respect to the horizontal is calculated at each point along the trajectory. Once the presented areas are known, the density and probability of hit can be calculated using the formulas shown in Figure 4.

[1]Reches, M., *Fragment Ricochet Off Homogeneous Soils and Its Effects on Weapon Lethality (U)*, Army Material Systems Analysis Agency Technical Memorandum No. 79, August 1970 (CONFIDENTIAL).

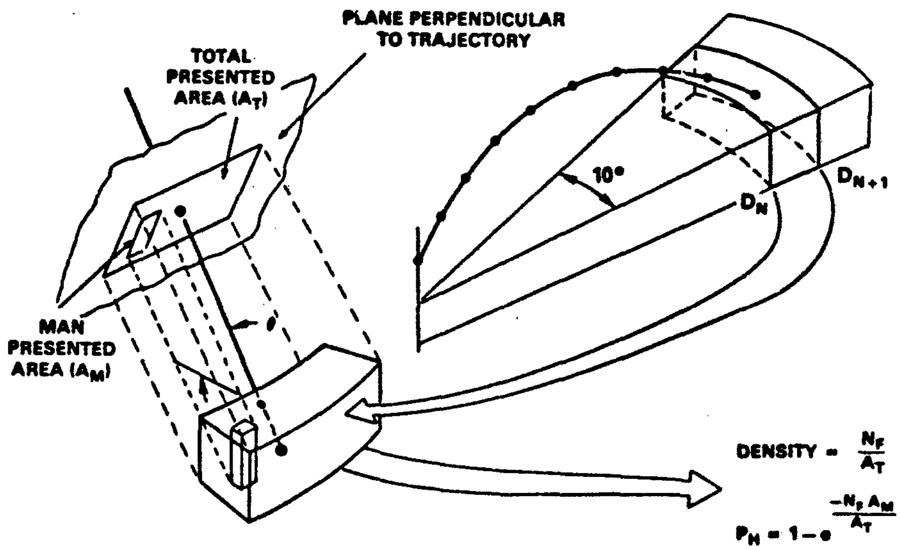

FIGURE 4. HAZARD CALCULATIONS

TYPICAL FRAGMENT DATA INPUT

Table 1 shows typical fragmentation input data. Each fragment recovered in the small-scale arena test has its own set of five elements.

TABLE 1. TYPICAL FRAGMENTATION INPUT DATA

Fragment No.	Polar Angle (deg)	Weight (grains)	Initial Velocity (ft/s)	A/M (in.²/lb)	Presented Area Ratio (max/avg)
1	10	623	3246	10.24	1.73
2	10	815	3246	9.16	1.26
3	20	1522	4112	11.31	1.41
4	30	711	4112	6.43	1.64
.	.	.	.	.	.
.	.	.	.	.	.
.	.	.	.	.	.
.	.	.	.	.	.
89	60	1152	5316	7.37	1.59
90	60	847	5316	8.68	1.42
91	70	1634	6123	11.74	1.65
.	.	.	.	.	.
.	.	.	.	.	.
.	.	.	.	.	.
.	.	.	.	.	.
247	100	1713	5312	8.62	1.59
248	100	652	5312	9.14	1.27
249	110	918	6597	6.23	1.64
250	110	1314	6597	11.89	1.59

Usually all fragments less than 300 grains are eliminated, since they seldom reach and are usually nonhazardous in the far-field. The upper bound of the polar zone is listed under Polar Angle. In this case, the polar zones are 10-deg wide. A polar angle of 70 deg identifies the 60 to 70-deg polar zone. The lower limit of the 10-deg elevation zone used in the program is equal to

$$EA = 90 - PA$$

where

EA = Lower angle of elevation zone
PA = Upper angle of polar zone

A 60 to 70-deg polar zone would therefore be associated with the 20 to 30 deg elevation zone as measured from the horizontal. A 100 to 110-deg polar zone would be associated with the -20 to -10-deg elevation zone. Currently the maximum critical ricochet angle is about 20 deg and, therefore, collection of fragments in polar zones greater than 110 deg is not necessary. In anticipation of possible future changes, tests have been designed to collect fragments to the 130-deg polar angle.

The fragment weight is measured by a scale and used in kinetic energy and A/M ratio calculations. The velocity is the average initial velocity for a particular 10-deg polar zone. As such, all fragments from the same polar zone have the same average initial velocity.

The A/M ratio is used in the drag equation. It is the ratio of the average presented area (in.^{2}) to the weight (lb) of a fragment.

The Presented Area Ratio is the maximum presented area divided by the average presented area of the fragment. This ratio correlates with the low subsonic ($M = 0.1$) drag coefficient. By using this ratio, the uncertainty in the drag coefficient for a fragment can be reduced by about 40 percent as explained under FUTURE IMPROVEMENTS (Drag Coefficients) in the DETAILED PROGRAM DESCRIPTION SECTION.

OUTPUT

There are three basic outputs for the program: Number of Final Ground Impacts versus Distance, Hazard Density and Probability of Hit versus Distance, and Number of Units Required to exceed the density and P-Hit Hazard Criteria versus Distance.

Number of Final Ground Impacts Versus Distance

Suppose we have 250 fragments representing the munition and we use 60 replications or treatments. For the first replication or treatment, the 250 fragments will come to rest in a set of 100-ft hazard segments. On the subsequent replication, the 250 fragments will come to rest with a different distribution because of the different values used for the input variables. We will end up with 60 different distributions of final ground impacts from ricochet and nonricochet fragments. The 60 values for each 100-ft hazard segment are then sorted from the smallest to the largest numbers. The first value in the sorted numbers becomes the minimum number of final ground impacts for the particular 100-ft hazard segment being considered. Likewise the 60th value is the maximum number. Adding all 60 values and dividing the sum by 60 yields the average number of final ground impacts for the associated 100-ft hazard increment. The minimum and maximum number are compared with actual ground pickup from full-scale tests. If the predictive capability of the program is valid, then the actual number of fragments picked up in a full-scale test (analogous to one replication or treatment) should fall within the maximum and minimum limits predicted by the program. Currently two such comparisons are available. Figures 5 and 6 show this comparison for 155mm projectiles and Mk 82 GP Bombs, respectively. The comparisons support the contention that the predictive capabilities of the program are valid.

Hazard Density and Probability of Hit

These quantities are handled similar to the number of Final Impacts. Assuming 60 replications or treatments, there will be density and probability of hit entries in each 100-ft hazard segment for each replication or treatment. By sorting from smallest to largest, we may establish minimum, maximum, and average values. In calculating these quantities, only those fragments exceeding the kinetic energy criterion are used.

An additional hazard measure is used in calculating hazard density and probability of hit. This measure is called a percentile value. The percentile measurement may be thought of as a confidence level. If we were to use a 90th percentile value, one could understand this to mean that we would be 90 percent confident that the hazard densities and probabilities of hit would not exceed the values listed. The 90th percentile value will have 10 percent of the distribution above it. For example, after sorting the 60 values at a particular 100-ft hazard segment, the 54th largest would be the 90th percentile value.

Number of Units to Exceed the Hazard Criterion

These data are used primarily for establishing the hazard ranges versus number of units for stacked munitions of interest to the DDESB. Two tables are output, one based on the hazard density criterion and one based on the hazard probability of hit criterion. Table 2 is an example of the output table based on the hazard density criterion. The number of units required is equal to the hazard density criterion (one hazardous fragment per 600 ft^2) divided by the hazard density for one unit. Note the reciprocal nature of the calculation; the higher the hazard density the less the number of units required and the greater the hazard. Only the 90th percentile column is shown; the other columns would have analogous entries.

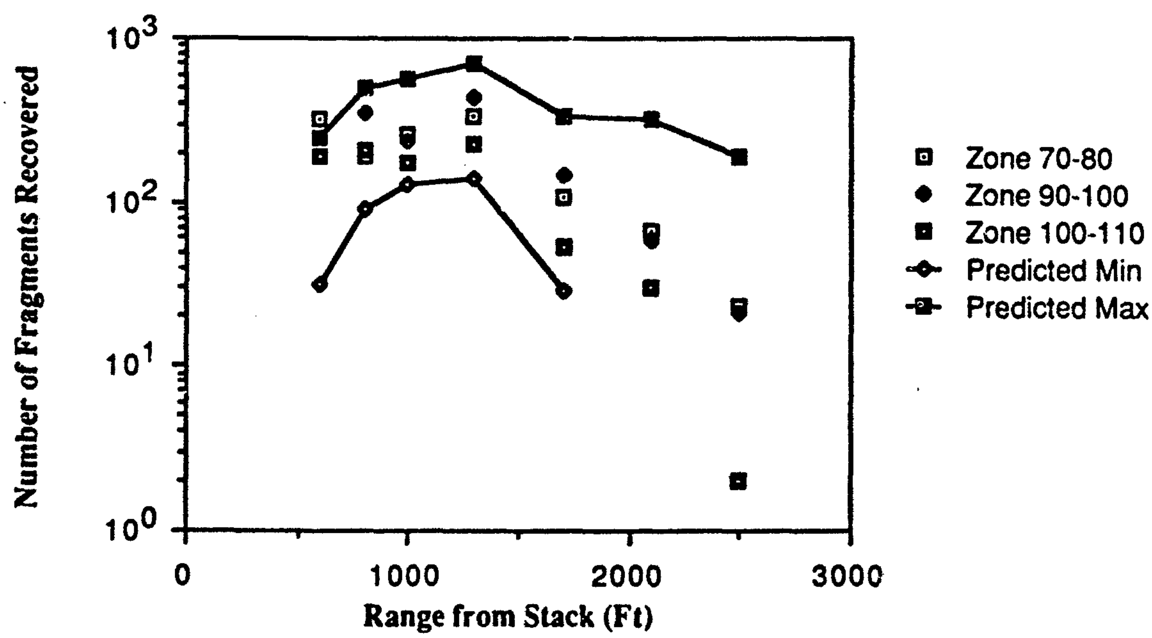

FIGURE 5. ACTUAL VERSUS PREDICTED RECOVERY DATA FOR 36 PALLETS OF 155MM PROJECTILES

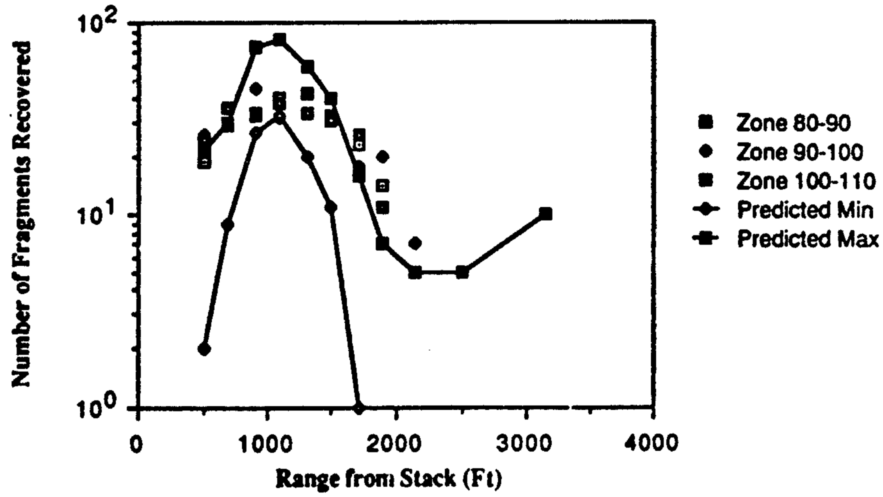

FIGURE 6. ACTUAL VERSUS PREDICTED RECOVERY DATA FOR A SINGLE PALLET OF MK 82 BOMBS

TABLE 2. NUMBER OF UNITS REQUIRED TO JUST EXCEED THE HAZARD DENSITY CRITERION

Range	Minimum	90%	50%	Maximum
50		0.12		
150		0.24		
250		0.43		
350		0.62		
450		2.31		
550		5.16		
650		8.14		
750		12.72		
850		~~27.35~~		
950		20.41		
1050		34.63		
1150		53.12		
1250		~~69.17~~		
1350		~~102.61~~		
1450		~~94.89~~		
1550		67.73		
1650		~~108.12~~		
1750		84.73		
1850		150.71		
1950		~~230.63~~		
2050		214.91		
2150		335.26		
2250		999999.00		
2350		999999.00		

Note that the range (distance) is given as the midpoint of each 100-ft hazard segment and is ready for plotting. Four columns of data are provided, one each for the minimum, selected percentile, 50th percentile, and maximum number of units required to just exceed the hazard density criterion. From a practical standpoint, each column of numbers can present a problem of interpretation. For example, the entry at 850 ft is 27.35 and the entry at 950 ft is 20.41. This leads to a contradiction from a safety standpoint even though the entries are quite plausible. The lesser number of units required at the greater range implies that when we add units to a stack, the hazard range can decrease. Since 20.41 is contained in 27.35, the 20.41 number should predominate and the 27.35 point should be eliminated. A systematic way of going about point elimination is to start at the top of the table and go down point by point. At each point, look back and if any previous points are equal to or greater than the point you are at then eliminate those points. Continue down in this way until you run out of points or all succeeding points are 999999.00. The 999999.00 points indicate no hazard; that is, no hazardous fragments are in those 100-ft hazard segments. When you are finished, you should have a set of points that are constantly getting bigger with range. Figure 7 shows both retained and eliminated points plotted versus hazard distance. If lines are drawn connecting the retained points, we form an upper bound. This upper bound can be somewhat erratic owing to the uncertain input data and the many non-linear relationships associated with trajectory calculations. A regression curve may be calculated using the retained points. A practical equation form for regression is:

$$R = A_1 + A_2 \ln N + A_3 \ln^2 N$$

where

R	=	Range or distance
N	=	Number of units required
ln	=	Natural log
A_1 A_2 A_3	=	Constants determined by regression

A regression program listing is contained in Appendix A. Figure 7 shows the regression curve for the retained points in Table 2.

SUMMARY

The FRAGHAZ computer model provides a flexible tool for predicting the fragment hazards of stacks of ammunition. The program has the inherent capability of considering the multidimensional problem posed by fragmentation hazards. The program has more than 200 variables. Its modular characteristics make it relatively easy to modify for specific problems like barricade effectiveness and public traffic route studies. The essential characteristics of the program are as follows:

- MONTE CARLO and FULL FACTORIAL options
- Individual three-dimensional fragment trajectories
- Two-dimensional wind vectors (horizontal plane)
- Fourth order Runge-Kutta trajectory calculations
- Fragment ricochet included
- Incorporates three-dimensional targets
- Can use different hazard criteria
- Air density and sound speed a function of altitude
- Storage sites may be at different altitudes
- Drag coefficient a function of the fragment presented area ratio and Mach number
- Predicts distribution of final fragment impacts in the ground plane
- Predicts hazard density, and probability of hit as a function of range for different hazard levels (MIN, PCT, 50th PCT, MAX)
- Predicts hazard distance values for different hazard levels (MIN, PCT, 50th PCT, MAX) as a function of number of units required in terms of two hazard criteria, density and probability of hit

fragment had an elevation angle somewhere between 20 and 30 deg as determined in the small-scale test. We would only know that the fragment elevation was between these two limits and not its exact value. For each replication we would use a random number to specify the exact value of the elevation angle for that particular fragment; that is, 60 different angles between 20 and 30 deg. In the FULL FACTORIAL option, only a few levels would be specified. For example, taking three random variables (factors) -- elevation angle, height of origin, and drag coefficient, the levels might be specified as follows:

FACTOR	LEVELS
E	0.1, 0.5, 0.9
H	0.5
C_D	0.1, 0.9

The levels represent the percent up from the minimum. In the previous example, the elevation angle for the fragment was known to be between 20 and 30 deg. The levels being 0.1, 0.5, 0.9 the corresponding angles to be considered in the FULL FACTORIAL option would be 21, 25 and 29 deg. These would be the only angles considered. The treatments would be all the combinations of the three factor levels as presented below:

TREATMENT	FACTOR LEVELS
1	E (0.1), H (0.5), C_D (0.1)
2	E (0.1), H (0.5), C_D (0.9)
3	E (0.5), H (0.5), C_D (0.1)
4	E (0.5), H (0.5), C_D (0.9)
5	E (0.9), H (0.5), C_D (0.1)
6	E (0.9), H (0.5), C_D (0.9)

The number of treatments is equal to the product of the number of factor levels, $3 \times 1 \times 2 = 6$. Since H has only one level, it is constant throughout the procedure. This might be the case if we knew from previous experience that the outcome was insensitive to this variable. Again, trajectories would be calculated for all 250 fragments for each treatment using the factor level combinations given above. The recording, accumulating, and output would be calculated in the same way as for the MONTE CARLO option.

Each of the calculation options has its strengths and weaknesses. The nature of the problem being considered will usually dictate the choice. The program as written in this report uses a personnel target. However, with modification, the FRAGHAZ program has been used to evaluate barricades and compute probability of hit for vehicles moving on a public traffic route.

HAZARD VOLUME

Figure 1 shows the essential elements of the model. Since interaction areas overlap at relatively short distances downrange, all fragments are assumed to emanate from a vertical line at the center of the stack. The height of the vertical line is made consistent with the typical stack height of the ordnance under consideration. The height at which an individual fragment originates is selected randomly for the MONTE CARLO option and at specific levels for the FULL FACTORIAL option. A pie-shaped sector is used to

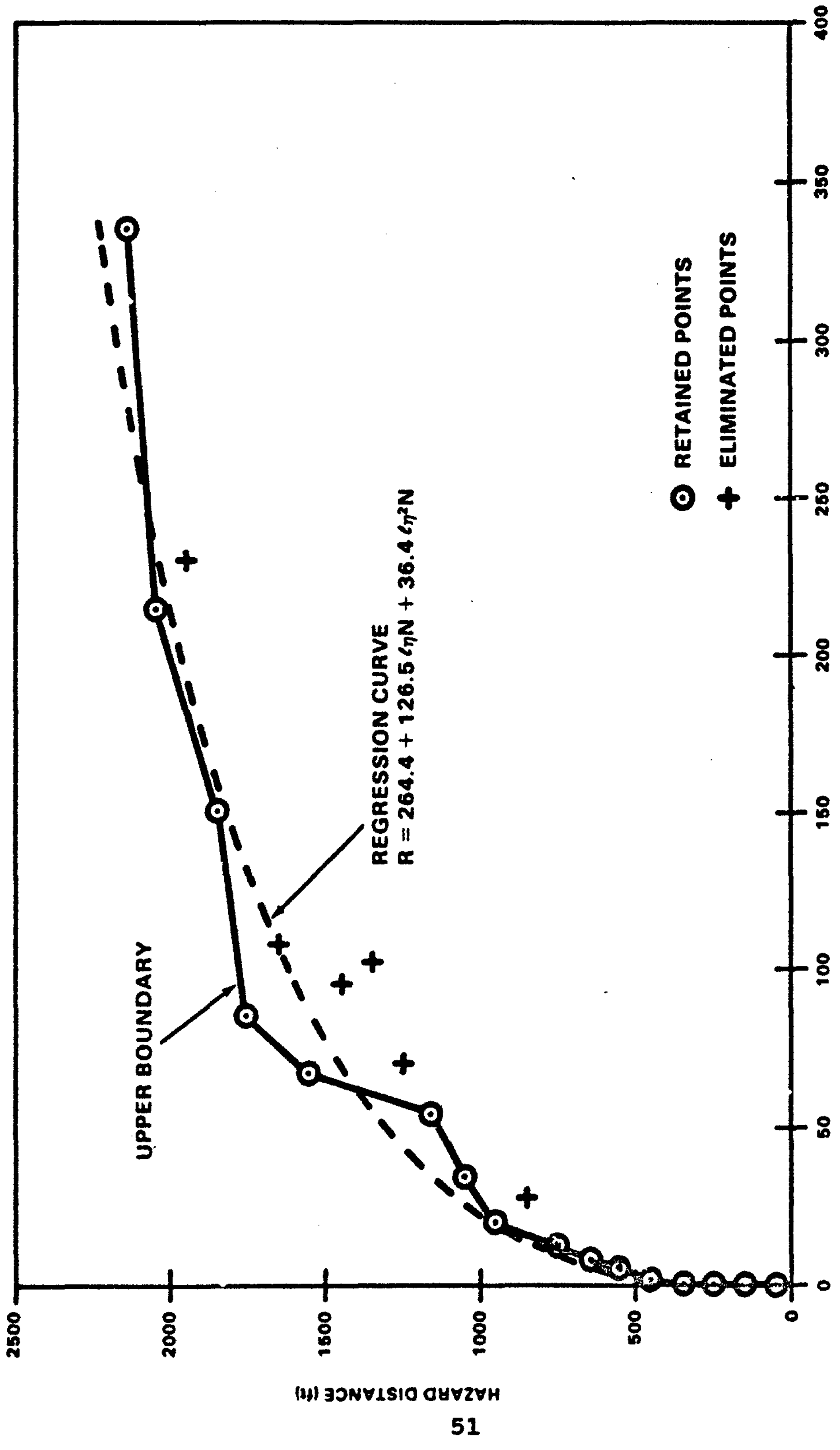

FIGURE 7. NUMBER OF UNITS TO JUST EXCEED HAZARD CRITERION VS. HAZARD DISTANCE FOR PROJECTILE XXX 90TH PERCENTILE

EFFECTIVE UTILIZATION OF THE QUANTITY DISTANCE MODEL FRAGHAZ

by
W. D. Smith
Advanced Technology, Inc.

INTRODUCTION

The Department of Defense Explosives Safety Board (DDESB) has funded a continuing study of the quantity distance (QD) requirements for Class 1, Division 1 ammunition (mass detonating). The focus of this effort has been on M107 155mm projectiles and Mk82 bombs. Small-scale arena tests and large-scale multiple pallet detonation tests demonstrated that the far-field fragment density is directly proportional to the number of units in the side of the stack facing the collection area[1,2]. This combined test and analysis effort lead to the development of a Monte Carlo simulation model (FRAGHAZ)[3] which uses fragmentation characterization data (ejection angle, velocity, mass and presented area) and a three dimensional particle trajectory routine to predict the far-field fragment density. The minimum and maximum fragment density predicted by FRAGHAZ for M107 155mm projectile pallets and Mk82 bomb pallets fragmentation data is compared to actual test data in Figures 1 and 2.[4] It can be seen that the FRAGHAZ model accurately brackets the far-field fragment density recorded on the actual multiple pallet tests. Based upon these results the model was considered "validated".

This paper discusses the utilization of the FRAGHAZ model to:

a. predict QD requirements for mass detonating and non-mass detonating ammunition.

b. evaluate potential changes in current DDESB hazard criteria (fragment kinetic energy and density).

c. evaluate using probability of hit criteria for personnel using the DDESB hazardous fragment criterion.

In addition, other potential applications of the program and future studies will be presented.

QUANTITY DISTANCE REQUIREMENTS

Mass Detonating Ammunition

The FRAGHAZ model calculates QD requirements based upon the predicted far-field fragment density, the terminal ballistics of the

fragments and the DDESB hazard criteria (kinetic energy >=58 ft-lbf and one fragment per 600 sq ft.). The QD requirements are provided as the number of units (N_p) in the face of the stack toward the collection area. Figure 3 presents a comparison of the QD requirements for M107 155mm projectiles, Mk82 bombs and Mk64 5in/54 projectiles. It can be seen that the model predicts that N_p reaches infinity as the range approaches 3000 ft for 155mm projectiles, 3500 ft for Mk82 bombs and ft for Mk64 5in/54 projectiles. This is apparently related to the limits of fragment flight provided by gravity, drag and fragment ricochet. The current DDESB QD requirement for Class 1, Division 1 ammunition is

$$R = 40W^{1/3} \qquad (1)$$

where R = range in ft
W = weight of explosive in the stack in lbs

Substituting the predicted maximum ranges for each ammunition in equation (1) and calculating the allowed W results in the comparison of the existing DDESB QD requirement and the FRAGHAZ predictions in Table 1.

Table 1

Ammunition	FRAGHAZ Range (ft)	W(lbs)	Number of Pallets
M107 155mm	3000	422,000	3516
Mk82 Bomb	3500	670,000	588
Mk64 5in/54	2500	244,000	1196

Non-Mass Detonating Ammunition

The QD requirements for Class 1, Division 2 ammunition are currently being studied using the FRAGHAZ model. The M1 105mm projectile and the 40mm AA cartridge are being used as the test units. These ammunition do not detonate enmasse, but rather progressively when exposed to the thermal environment of a fire. Consequently, the test effort required for these ammunition is based upon the DDESB bon-fire[5] procedure. The present data base contains large-scale multiple pallet detonating tests (up to 36 pallets) with far-field fragment recovery for both the 105mm and 40mm ammunition[6] and a small-scale fragmentation arena of single 105mm projectile[7]. This data is being analyzed to determine if the FRAGHAZ model can accurately bracket the far-field fragment recovery observed on the multiple pallet tests. It is currently uncertain whether the basic, underlying assumption of the FRAGHAZ model that the far-field fragment density is directly proportional to the number of units in

the face of the stack is valid. Additional analysis is required to determine what modifications are required to validate the model for non-mass detonating ammunition.

HAZARD CRITERIA

Fragment Kinetic Energy

Figure 4 presents a comparison of the QD requirements for M107 155mm projectiles using the existing DDESB kinetic energy criteria of 58 ft-lbf and 10 ft-lbf. The density requirement was maintained at one fragment per 600 sq ft. It can be seen that this increases the maximum range by approximately 1150 ft (3000 ft for 58 ft-lbf and 4150 ft for 10 ft-lbf). In addition, a fewer number of projectiles in the face of the stack is required to reach the maximum range. Similar results can be generated for the Mk82 bomb and Mk64 5in/54 projectile.

Fragment Density

Figure 5 presents a comparison the the QD requirements for the M107 155mm projectile using the current DDESB density requirement of one fragment per 600 sq ft and one fragment per 6000 sq ft. The kinetic energy criteria was 58 ft-lbf for both cases. It can be seen that the density criteria does not significantly increase the maximum range (approximately 600 ft. increase). It is also apparent that a fewer number of projectiles in the face of the stack is required to reach the maximum range.

Probability of Hit

Figure 6 presents a comparison of the QD requirements for 155mm projectiles using a 1% probability of hitting a standing man (90th percentile dimensions) and the existing DDESB criteria (KE>=58 ft-lbf, one fragment per 600 sq ft). It is apparent that there is little difference between the QD requirements for these two criteria and that the use of a probability of hit criterion would not increase the maximum range requirement for 155mm projectiles.

Wind Affect

Figure 7 demonstrates the effect of a tail wind on the QD requirements for 155mm projectiles. The data show that a 60mph tail wind will increase the maximum range by approximately 750 ft and significantly increases the requirements for smaller stacks.

CONCLUSIONS

The FRAGHAZ model is an excellent predictor of the far-field fragment density produced by the detonation of stacks of mass detonating ammunition. It can be used to generate QD requirements for Mass Detonating (Class 1, Division 1) ammunition. The model is being evaluated as a predictor of the far-field fragment density produced by the detonation of 105mm projectiles in a bon-fire. Additional analysis and testing will be required to validate the model for non-mass detonating ammunition.

The FRAGHAZ model is a useful tool for evaluating the sensitivity of QD requirements to changes in hazard criteria. The model can easily calculate the effects of fragment kinetic energy, fragment density, probability of hitting a target and tail winds on the QD requirements.

REFERENCES

1. Ramsey, R.T., et al, *Fragment Hazard Investigation Program,* NSWC TR-3664, October 1978

2.Powell, J.G., et al, *Fragment Hazard Investigation Program: Natural Communication Detonation of 155mm Projectiles,* NSWC TR 81-54, July 1981

3. McCleskey, F., *Quantitiy Distance Fragment Hazard Computer Program (FRAGHAZ),* NSWC TR 87-59, April 1988

4.Smith, W.D., *Fragment Hazard Investigation Program: Validation of the Monte Carlo Simulation Model,* NSWC TR 86-187, October 1987

5.*Department of Defense Explosives Hazard Classification Procedures,*Army TB 700-2, Navy NAVSEAINST 8020.8, Air Force TO 11A-1-47, Defense Logistics Agency DLAR 8220.1, September 1982

6.Minutes of the 20th DDESB Seminar, *Fragment Hazard Investigation Progrm: Non-Mass Detonating Ammunition Tests,* August. 1982

7.Smith, W.D., *Fragment Hazard Investigation Program: Quantity Distance Requirements for 105mm Projectiles,* NSWC TR 88-195, UNPUBLISHED

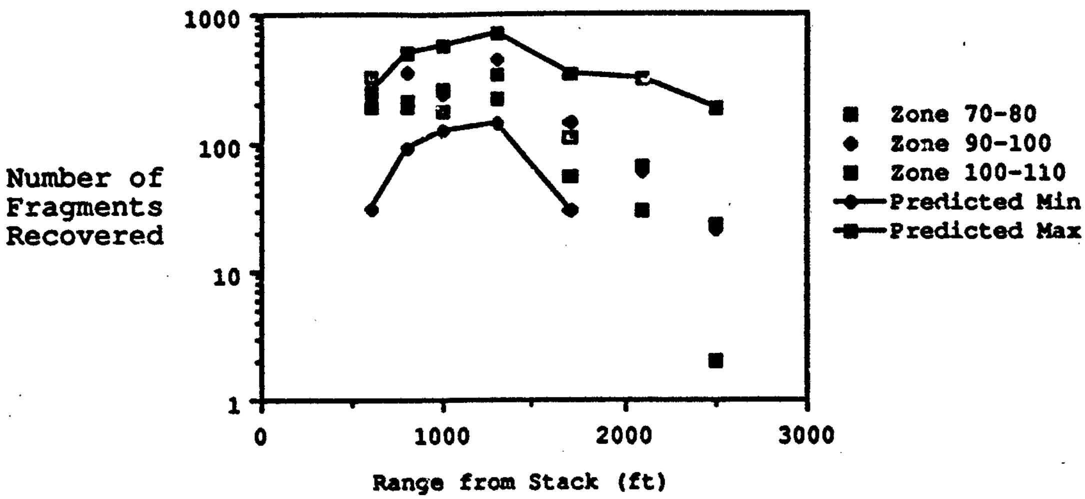

Figure 1
Comparison of Predicted and Actual Fragment
Recovery Data for 36 Pallets of 155mm Projectiles

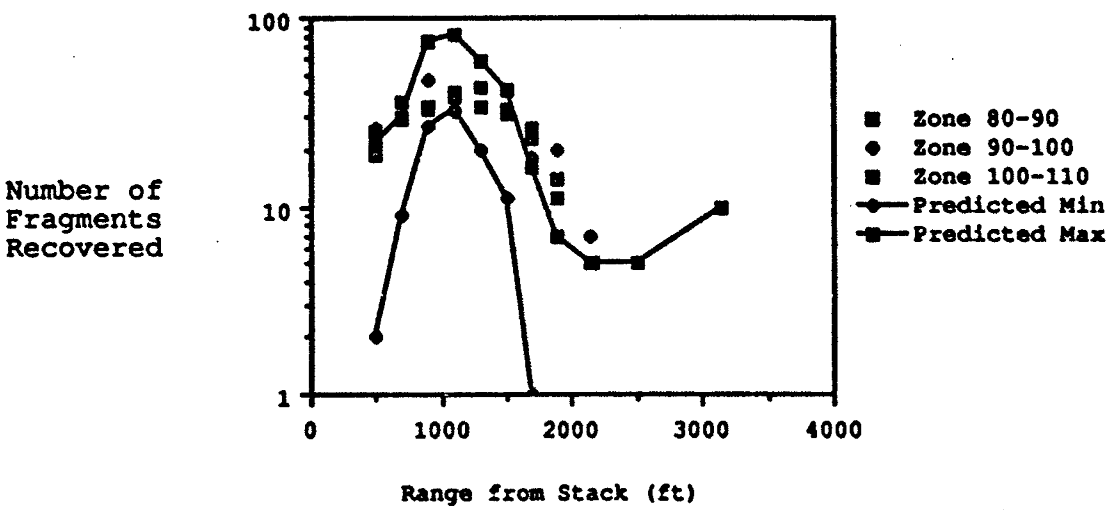

Figure 2
Comparison of Predicted and Actual Fragment
Recovery Data for One Pallet of Mk82 Bombs

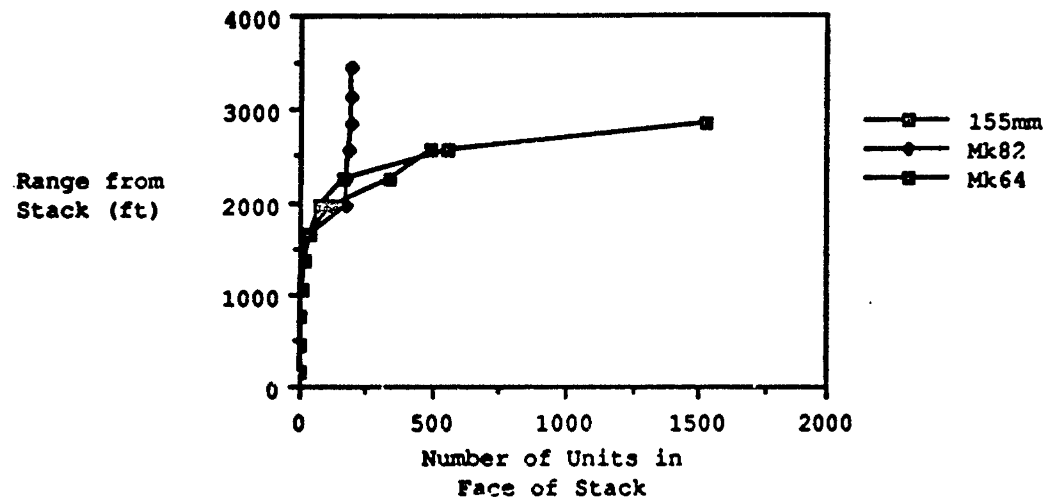

Figure 3
Comparison of QD Requirements for M107 155mm Projectiles, Mk82 Bombs and Mk64 5in/54 Projectiles

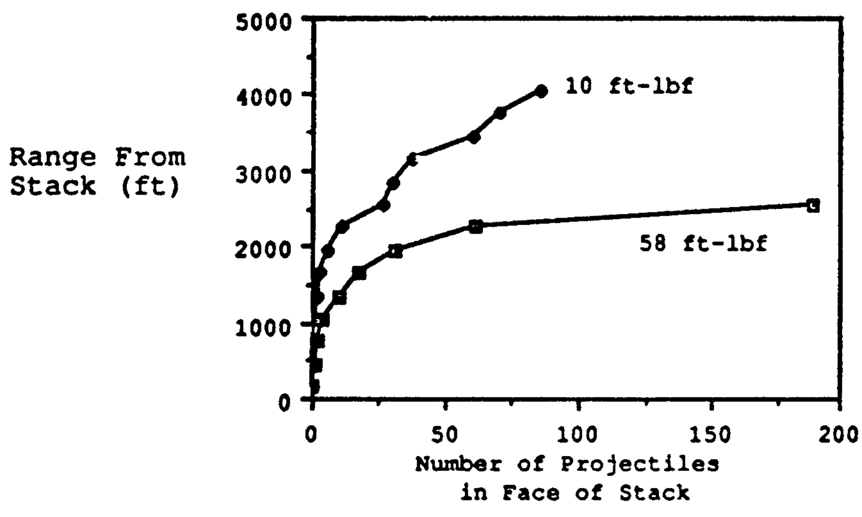

Figure 4
Comparison of the Effect of Kinetic Energy Criteria on the QD Requirments for 155mm Projectiles

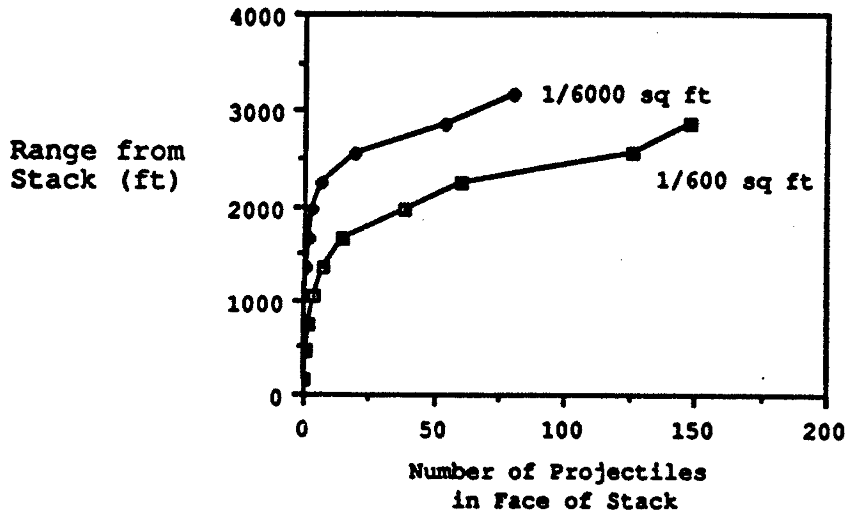

Figure 5
Comparison of the Effect of Density Criterion on the QD Requirements for 155mm Projectiles

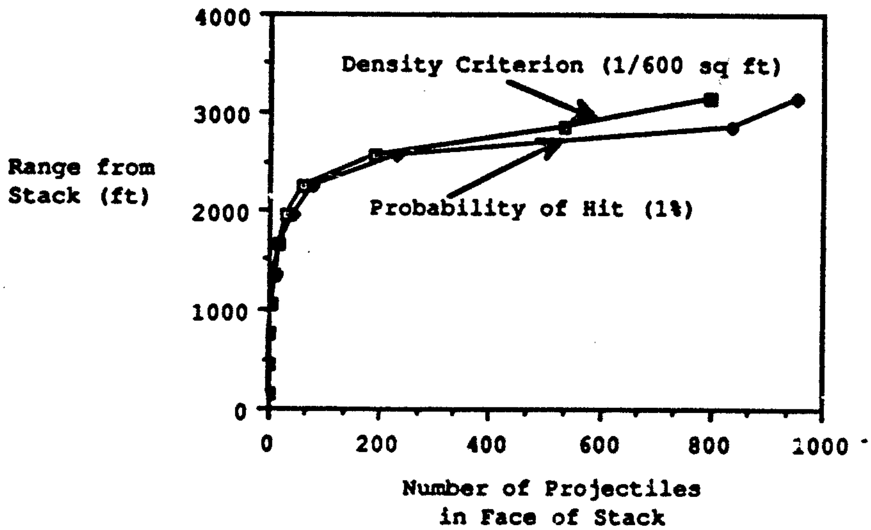

Figure 6
Comparison of Fragment Density and Probability of Hit Criteria on QD Requirements for 155mm Projectiles

STORAGE OF MIXED MUNITIONS IN CONEX CONTAINERS

WILLIAM LAWRENCE

BALLISTIC RESEARCH LABORATORY

ABERDEEN PROVING GROUND, MD. 21005

ABSTRACT

A series of six tests were conducted to identify the debris, fragments, and airblast hazards associated with the detonation of the explosives. First three tests were conducted to determine the external debris and hazard distance, and to check whether the detonation of explosives in one container would detonate the explosives in the adjacent container. Next three tests were conducted by sandbagging the containers on three sides. A lot of fragments were found beyond 300 feet, in Test Nos. 1, 2, 3, and 6. But less fragments were found beyond 300 feet, in Test Nos. 4 and 5. Detonation did not propagate to the adjacent container in any test, even, when the distance between the containers was decreased to eight feet. Ammunition cook off occured in all the tests. Sandbagging the containers decreased the fragment density at large distance but increased the cook off and burning rate of the munitions and other debris, near the location of the test.

INTRODUCTION

A large quantity of different types of munitions are stored in a conex container. Small caliber ammunition, fragmentation grenade, smoke grenade, signal flares, M42 submunition, mines, file destroyer, and rockets are stored in the containers. Table 1 shows a typical basic load of ammunition stored in a container. The study had three objectives. The first objective of this study was to determine the type of debris and fragment hazard distance from point of reaction when the munitions in a single conex container are detonated. The second objective was to prevent propagation of reaction from one container to an adjacent container, and the third objective was to minimize the physical damage to the adjacent conex by the addition of sandbag walls along the three sides of containers.

The project was funded and supported by the Department of Defense Explosive Safety Board and the Project Manager for Ammunition Logistics. The task of designing and conducting the tests and providing the technical data package was undertaken by the Ballistic Research Laboratory, Aberdeen Proving Ground, Maryland.

BACKGROUND

Limited availability of land area for munitions storage at overseas bases, coupled with civilian encroachment, and the need to build additional facilities on available land has placed constraints on munitions storage capabilities. If a fire or explosion should occur, whether it results from accident, enemy attack or sabotage, then the adjacent explosive container and facilities including personnel in the vicinity of the explosion site must be protected, to a predetermined, practical standard. The explosion must not propagate from one container to other. Generally, when ignited, explosives burn and explode, producing fast fragments from metal touching or near the explosive, airblast, cratering, ground shock, flame and radiant heat, and debris and explosive items.

TEST APPROACH AND RESULTS

A series of six tests were performed to identify debris, fragments, and airblast hazards associated with the detonation of the explosives (inside a container) and to check whether the mass detonation of explosives in one container would propagate to the adjacent container. A conex container is made of 1/8 inch thick corrugated steel. The inside dimensions of the conex container are: 92 inches long, 72 inches wide, and 70 inches high.

Fuzed 66mm M72A2 rockets and 40mm M433 cartridge were considered safety hazards (fuzed rockets might go off during the fragment recovery process and M433 contains phosphorous which might cause bodily harm), therefore, in the tests, M433 cartridges were replaced with M42 grenades and unfuzed rockets replaced fuzed rockets.

The center of explosion for each test was established and a search pattern grid was laid. Each area (sector) was marked off with white tape/paint. Fragments were collected in 12 thirty degree wide collection zones 360 degree around the container to a distance of 600 feet. All fragments were identified by collecting them into nearby marked sector in which they were found.

TEST 1

The goal of this test was to identify the external debris, fragments, and to determine the quantity-distance arcs when the explosive (in the conex container) is detonated. Three wooden racks were built and placed inside the container. The munitions were placed on the racks. Twelve mines, M18A1, were placed in the middle of the container. Net explosive (mines, grenades, rockets, M42, etc.) weight, stored in the container, was 160 pounds. Table 2 lists the ammunition placed inside the container. Figure 1 shows the layout configuration of the munitions inside the container.

These mines were remotely detonated. The container and many of the ammunition boxes were broken up into many fragments. Most of the fragments and other debris were located within 100 feet from the point of detonation, but Some of the fragments were found beyond 350 feet from the test location. Three metal fragments (from conex) were located between 320 feet and 375 feet from the point of reaction. Five fragmentation grenades were located at 375 feet.

TEST 2

The goal of this test was to assess the damage to the acceptor container and its contents when the explosive, in the donor conex, is detonated. The acceptor container was placed at a distance of 15 feet (arbitrarily chosen) from the donor container. Same amount and type of munitions were placed in the donor container as was in Test No. 1. The mines were not available at the time of this test, instead, a 20 lbs C-4 charge was placed in the donor container. This increased the net explosive weight from 160 lbs to 162 lbs. The wooden boxes, filled with the sand (instead of munitions), were placed on the wooden racks, inside the acceptor conex.

It was also decided to make pressure measurements. The pressure transducers were placed, in front of donor container, at 30 feet, 60 feet, and 90 feet from the container. The locations for the pressure transducers were arbitrarely selected. Figure 2 shows the set-up configuration of the acceptor and the donor containers.

C-4 charge was detonated. The wooden ammunition boxes and other debris burned for more than one hour, near the acceptor container. The acceptor container was turned over and sustained some physical damage. The sand filled boxes were broken.

The donor was broken up into many fragments. Many of these fragments were thrown at a distance greater than 300 feet. Some fragments and unexploded rounds were found beyond 375 feet from the test location, but most of the fragments were located within a radius of 100 feet.

Peak pressures of 6.7 PSI at 30 feet and 3.40 PSI at 60 feet locations were registered by the transducers. No signal was obtained at 90 feet location.

TEST 3

The goal of this test was to assess the damage to the live munitions, inside the acceptor conex, by decreasing the separation distance (distance between the containers) from 15 feet to 8 feet.

Same amount and type of munitions were placed in the donor container as was in Test No. 1. Live ammunition (rockets, grenades, mines and M42) and sand boxes were placed in the acceptor conex.

No pressure signal was recorded by the pressure transducer at 90 feet location (in Test No. 2), so the location of this transducer was changed from 90 feet to 75 feet. The locations of the other two transducers remained the same (30 feet and 60 feet). Figure 3 shows set-up configuration.

Twelve mines, placed in the middle of the donor container, were detonated. The wooden boxes and other fragments burned, in the space between the two containers, for one to two hours. The fire and heat made some of the munitions (grenades, flares, etc.) to cook off.

The acceptor container was flipped over and caved in. The live munitions, inside the acceptor conex, did not detonate. Some of the munition boxes were broken, but no damage was done to the munitions.

The fragments and other debris were thrown out at a distance greater than 300 feet from the point of reaction. Ten metal fragments were found between 300 feet and 335 feet from the test location. Thirty five M42, two smoke grenade, and one fragmentation grenade were found between 300 feet and 350 feet.

The pressures registered by the transducers were not as high as compared to the pressures obtained in Test No. 2. Peak pressures of 3.33 PSI at 30 feet, 2.4 PSI at 60 feet, and 0.3 PSI at 75 feet were recorded by the transducers in this test.

TEST 4

The aim of this test was to check whether some kind of sandbag wall/shield will prevent the acceptor container from overturning and sustaining the physical damage. Same amount and type of munition was placed in the donor container as was in Test No. 1. The acceptor conex was partially filled with the munition. The sandbag walls, about one foot taller than the height of the container, were built along three sides of the containers. No sandbag walls were built on the front sides of the containers. The pressure transducers were placed at the same locations as were in Test No. 3. Figure 4 shows the set-up configuration. Again twelve mines, inside the donor conex, were detonated.

The wooden boxes and other debris burned for more than two hours. Some munitions (grenades, flares, etc.) were cooked off. The middle sandbag wall was partially collapsed. The acceptor conex did not move or flip over and no damage was done to munitions, inside the acceptor conex. Much of the blast was absorbed by the sandbag wall, thus, preventing the acceptor conex to sustain much damage.

The donor container and other munition boxes were broken into many fragments. Two fragments (3 X 6 feet) from conex door were located at 369 and 561 feet from the test location. One fragment from conex was found at 450 feet. One 66mm rocket (warhead) was found at 305 feet.

The pressures recorded by the transducers were higher than the pressures obtained in Test No. 3. Peak pressures of 6 PSI at 30 feet, 4 PSI at 60 feet, and 3 PSI at 75 feet were registered by the transducers.

TEST 5

The aim of this test was to learn about the extent of the fragments/debris hazards by detonating the same amount of the explosives in the donor conex when sandbags were placed on top of the donor container. Same type of sandbag walls were built along three sides of the containers as in Test No. 4. Same type and amount of explosives were placed in the containers as was in Test No. 4.

Twelve mines were detonated, inside the donor container. It was not a big explosion as compared to the explosions in the last four tests. The door of the donor conex was found between 50 and 60 feet from the container. The roof of the donor container flew up but fell right back in the container.

The debris and fragments did not go very far from the point of detonation. A few parts of the signal flares were located beyond 300 feet from the test location. Most of the munitions and other fragments burned inside the donor container and continued burning for more than three hours.

The sandbag wall, between the acceptor and the donor containers, was partially collapsed. The walls of the acceptor container suffered some damage but container, itself, remained intact. The acceptor container did not flip or turn over.

TEST 6

It was requested by Department of Defense Explosive Safety Board to conduct a test by detonating 160 lbs (100 lbs bare charge and 60 lbs explosives in other munitions) explosives inside the donor container. The sandbag walls, built along three sides of the acceptor and the donor containers in Test Nos. 4 and 5, were very massive and time consuming, so it was decided to modify the sandbag wall configuration.

Double sandbag walls, along the three sides of the containers, were built for Test No. 6. Munition placement, inside the donor conex, was changed without changing the total amount of explosive. This time, a 60 lbs of

explosives (rockets, M42, and fragmentation grenades) were placed close to a 100 lbs of C-4 bare charge. The 160 lbs of explosive was placed against the inside wall of the donor conex (the wall close to the acceptor conex) and on the lower shelf of the wooden rack. Figure 6 shows the actual configuration of the ammunition placement in the donor and acceptor containers.

The 100 lbs explosive was detonated. A big fire ball was seen and a tremendous explosion was heard. A few flares and grenades burned for a few minutes. No other fire was observed in this test.

No explosive (rockets, mines etc.) was recovered. This means that all 160 lbs of explosive was consumed during the explosion process. The detonation did not propagate to the live munitions, inside the acceptor conex.

One side (side towards the donor conex) of the acceptor conex was caved in but it did not flip over. The donor container and some of the munition boxes were broken up into many fragments. These fragments were found at different locations. Twenty six metal fragments (8 inch to 5 feet long) were found in zones A and B (440 feet to 673 feet range).

OVERALL RESULTS

The locations where the debris/fragments were found varied from test to test. In some tests the debris/fragments did not go beyond 300 feet from the point of detonation but in other tests some debris/fragments were found beyond 600 feet. The kick out data, from these tests, are given in Tables III - VIII. The photographs of the recovered munitions/fragments and other debris are given in Appendix.

In some tests the fire started a few minutes after the detonation and lasted for a few minutes, but in other tests the fire started and lasted for some time, and restarted and kept on burning for a long time (many hours). In Test Nos. 2 and 3 the fragments/debris burned for one to two hours, in the space between the containers. In Test No. 4 the fire lasted for more than two hours. In Test No. 5, the fragments and munitions burned for more than three hour. No appreciable fire was observed in Test No. 6.

Several rounds (7.62mm, 5.56mm, 50 cal, flares, grenades, etc.) were cooked-off as a result of fire or heat. Some of the live munitions were recovered in each test. It was estimated that, from the recovered munitions, about 25 to 35 lbs of explosive was consumed, during the detonation process, in each of the first four tests. It is estimated that all 160 lbs of the explosive was expended in Test No. 6, because no explosive was recovered in this test.

The acceptor conex was turned/flipped over and caved in, thus, sustaining some physically damage (tests 2 and 3). No appreciable damage was done to the contents of the acceptor container. The acceptor conex did not move or flip over in Test Nos. 4, 5, and 6. Much of the blast was absorbed by the sandbag wall (between the containers), thus, preventing the acceptor container to

sustain much damage.

When the explosive was detonated, inside the donor conex, a very high pressure was developed instantaneously. The blast inside the donor conex was so high that it created a 2 to 3 feet deep crater underneath the donor conex.

SUMMARY AND CONCLUSIONS

A series of tests were conducted to determine the fragments hazard distance when the explosive, inside the donor conex, is deliberately or accidently detonated. First three tests were conducted to determine the external debris and hazard distance, and to check whether the detonation of explosives in one container would detonate the explosives in the adjacent container. Next three tests were conducted by sandbagging the containers on three sides.

A lot of fragments and debris were found beyond 300 feet, in first three tests. But less fragments and other debris were found beyond 300 feet, in tests 4 and 5. Again a lot of fragments/debris were found beyond 300 feet, in Test No. 6.

Detonation did not propagate to the adjacent container in any test, even, when the distance between the containers was decreased to eight feet. Eight feet separation distance was selected because, at overseas bases, the containers were separated by a distance of greater than six feet.

Ammunition cook off occured in all the tests. Sandbagging the containers decreased the fragment density at larger distances but it increased the cook off and burning rate of the munitions and other debris, near the location of the test. So the probability of cook off or burning of the munitions and other fragments/debris is greater when the containers are sandbagged on three sides.

The following conclusions can be derived from this study.

Detonation of explosives in one container did not propagate to the explosives in an adjacent container when the separation distance (between the containers) was eight feet (no test was conducted by decreasing the distance further).

Sandbagging the acceptor and the donor containers prevented the adjacent container and its contents from extensive physical or mechanical damage when the explosive, in the donor conex, was (accidently or deliberately) detonated.

Sandbagging the containers decreased the fragment density at large distances but increased the cook off and burning rate of the munitions and other debris (close to the ground zero).

TABLE I

A Typical Basic Load of Ammunition Stored in a Conex Container

CTG Cal .45 Ball	1360 Rds
CTG .50 Cal	1800 Rds
CTG 5.5mm Ball M16	23600 Rds
CTG 5.56mm Tracer M16	4930 Rds
CTG 7.62mm Ball & Tracer Lined	9370 Rds
CTG 40mm M433	144 Rds
Grenade Fragmentation M67	195 EA
Grenade Smoke Green	8 EA
Grenade Incendiary	130 EA
Grenade Smoke Red	8 EA
Grenade Smoke HC	8 EA
Grenade Smoke Voilet	10 EA
Grenade Smoke Yellow	8 EA
Fire Starter	8 EA
Grenade Launcher Smoke Screening	8 EA
Signal Illum Grenade	36 EA
RKT 66mm M72A2	15 EA
Mines M18A1	12 EA
File Destroyer M4	1 EA
Signal Illum Ground Red Star	72 EA
Illum Star Ground White	72 EA
Signal Illum Ground Green Star	72 EA

TABLE II

Ammunition in a Conex Container

CTG, Cal .45 Ball and .50 Cal	3160 Rds
CTG, 5.56mm Ball/Tracer M16	28530 Rds
CTG, 7.62mm Ball & Tracer Lined	9370 Rds
Grenade, Fragmentation M67	195 EA
Grenade, Smoke	175 EA
RKT, 66mm M72A2 (unfuzed)	15 EA
Mines, M18A1	12 EA
File Destroyer, M4	1 EA
Signal, Illum Ground	260 EA
Rifle Grenade, M42	216 EA

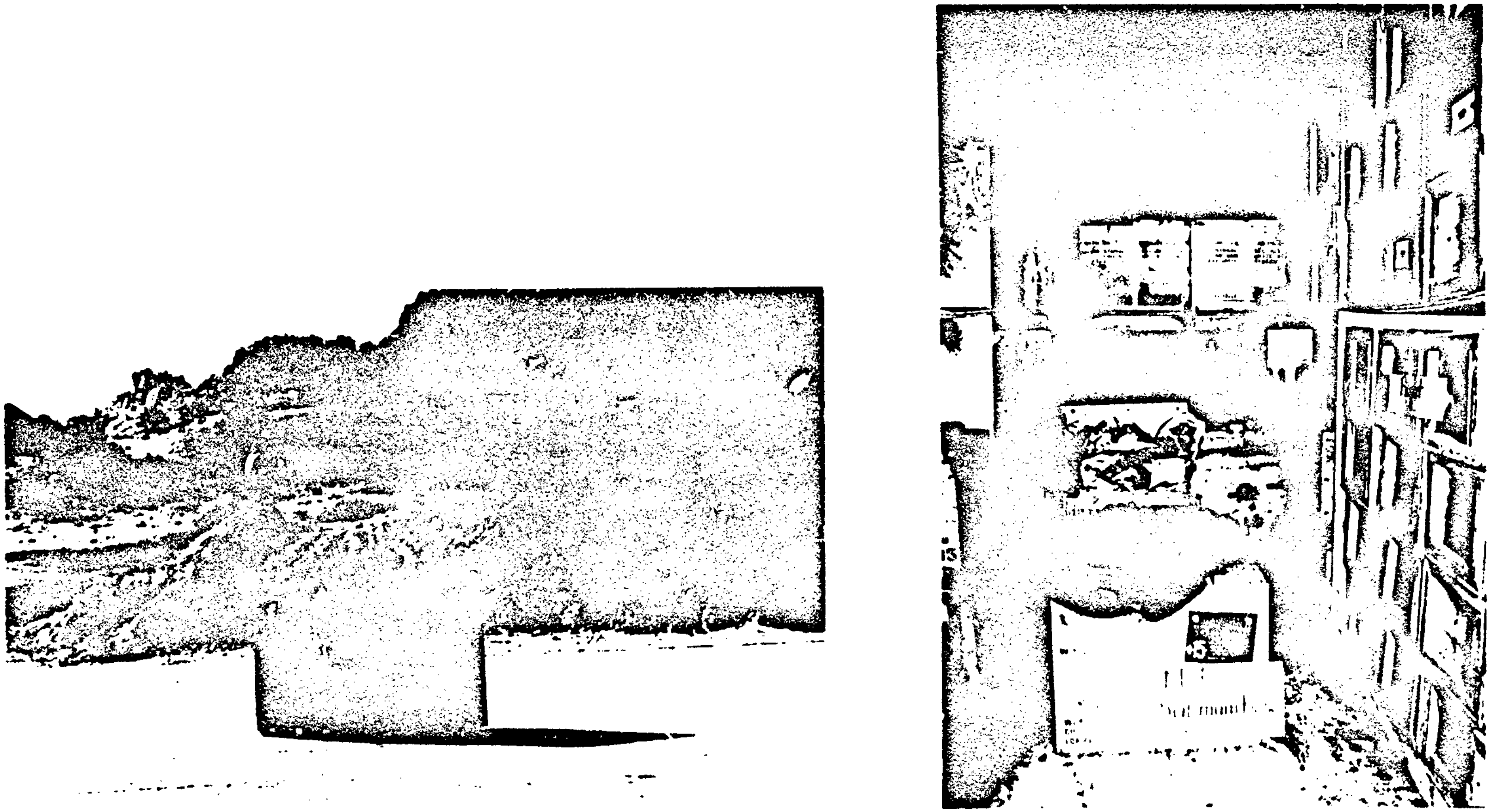

Figure 1. A Conex Container (Left) and Ammunition in the Container (Right), Test No. 1.

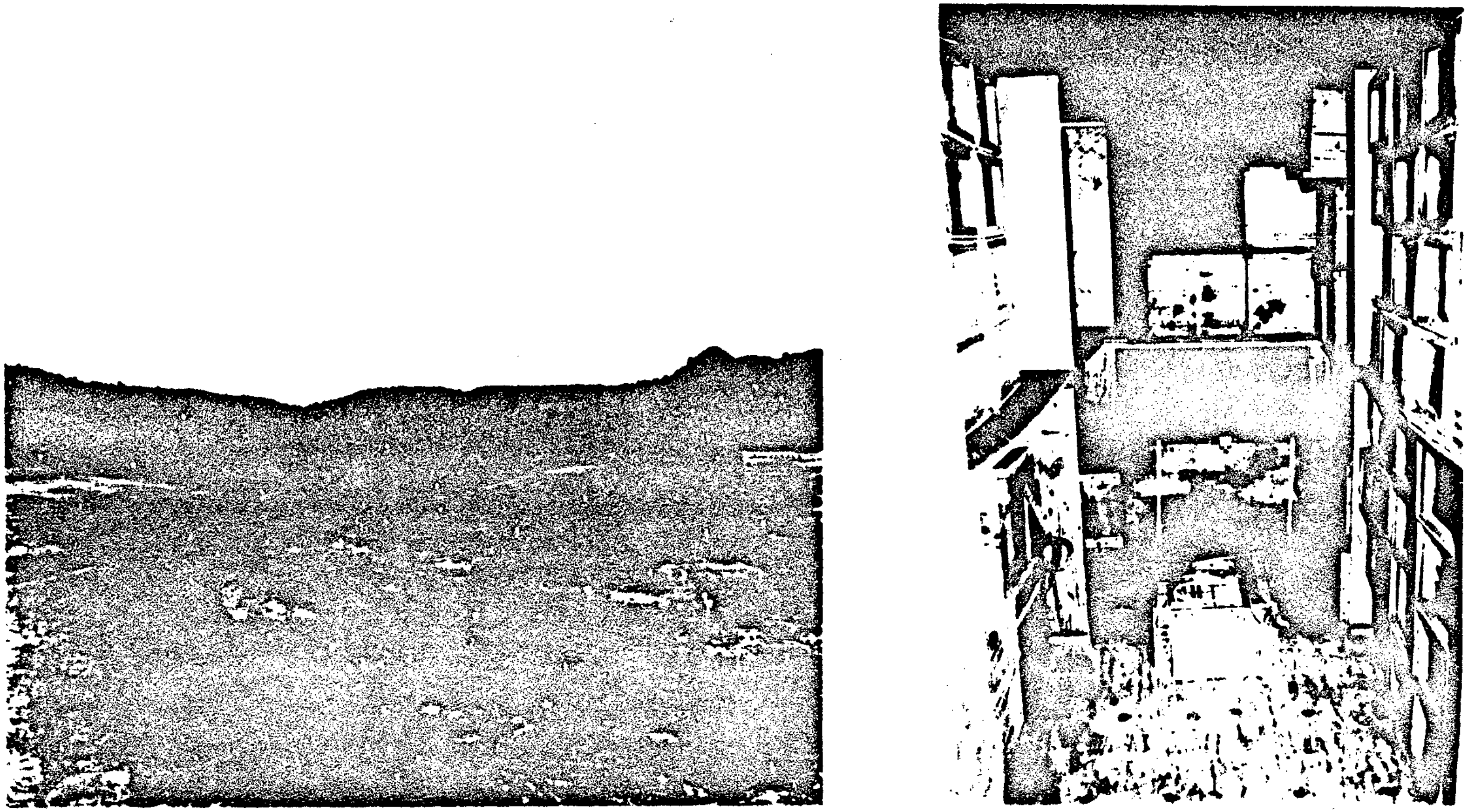

Figure 2. Donor and Acceptor Containers (Left). Ammunition in the Container (Right), Test No. 2.

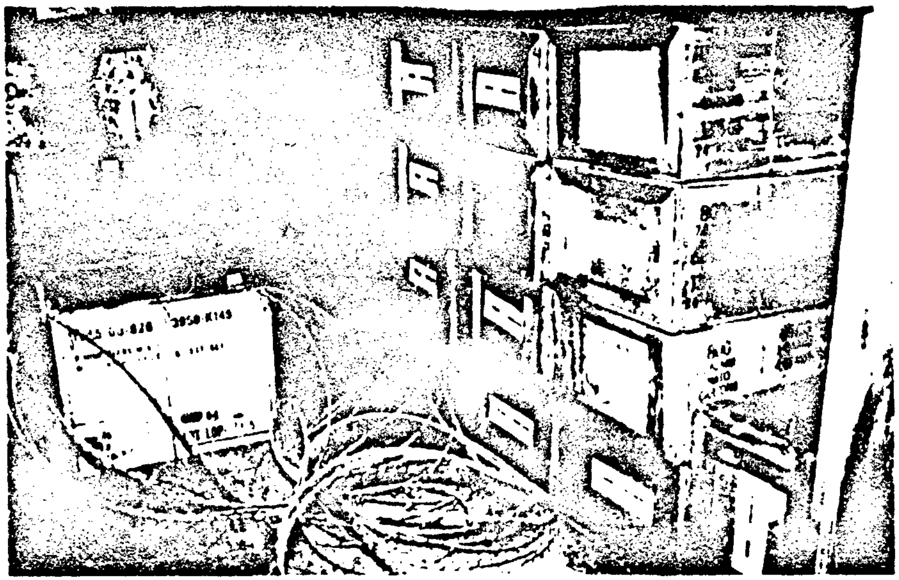

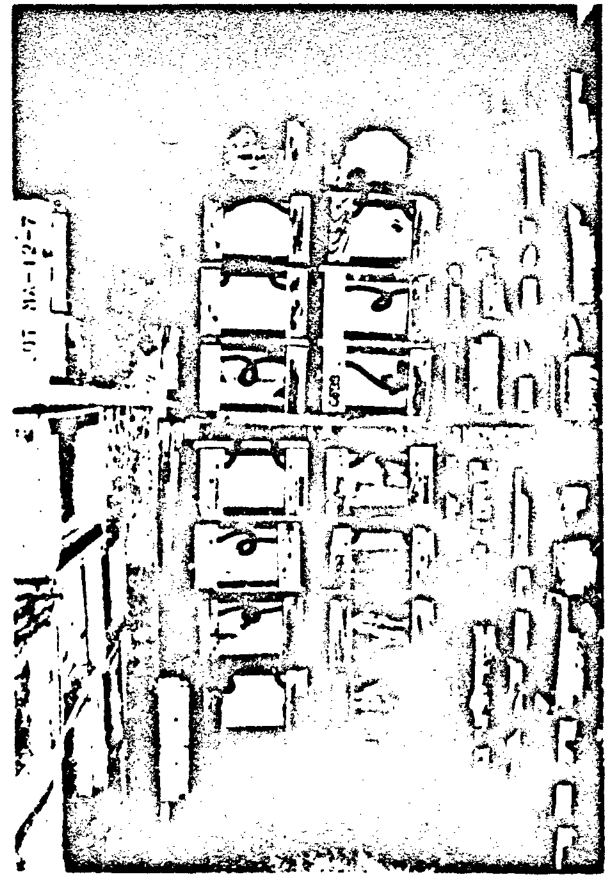

Figure 3. Mines with Prime-A-Cords (Left) and other Ammunition in the Container (Right), Test No. 3.

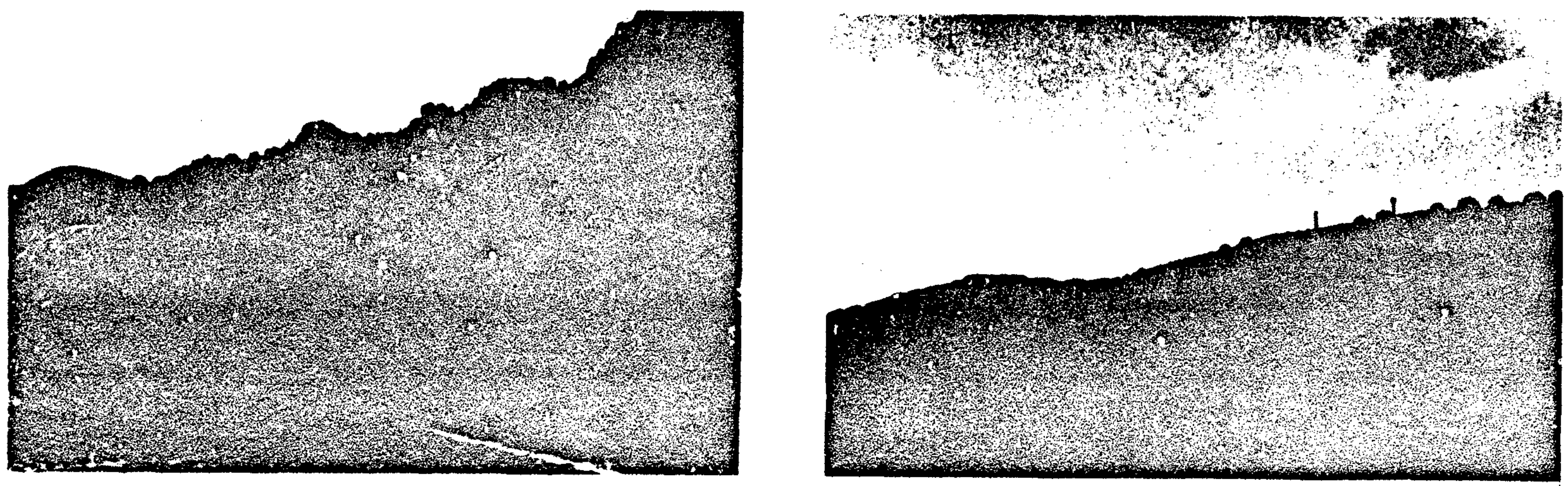

Figure 4. Donor and Acceptor Containers Confined by Sandbag Walls. Front Side (Left) and Back Side (right) of the walls, Test No. 4.

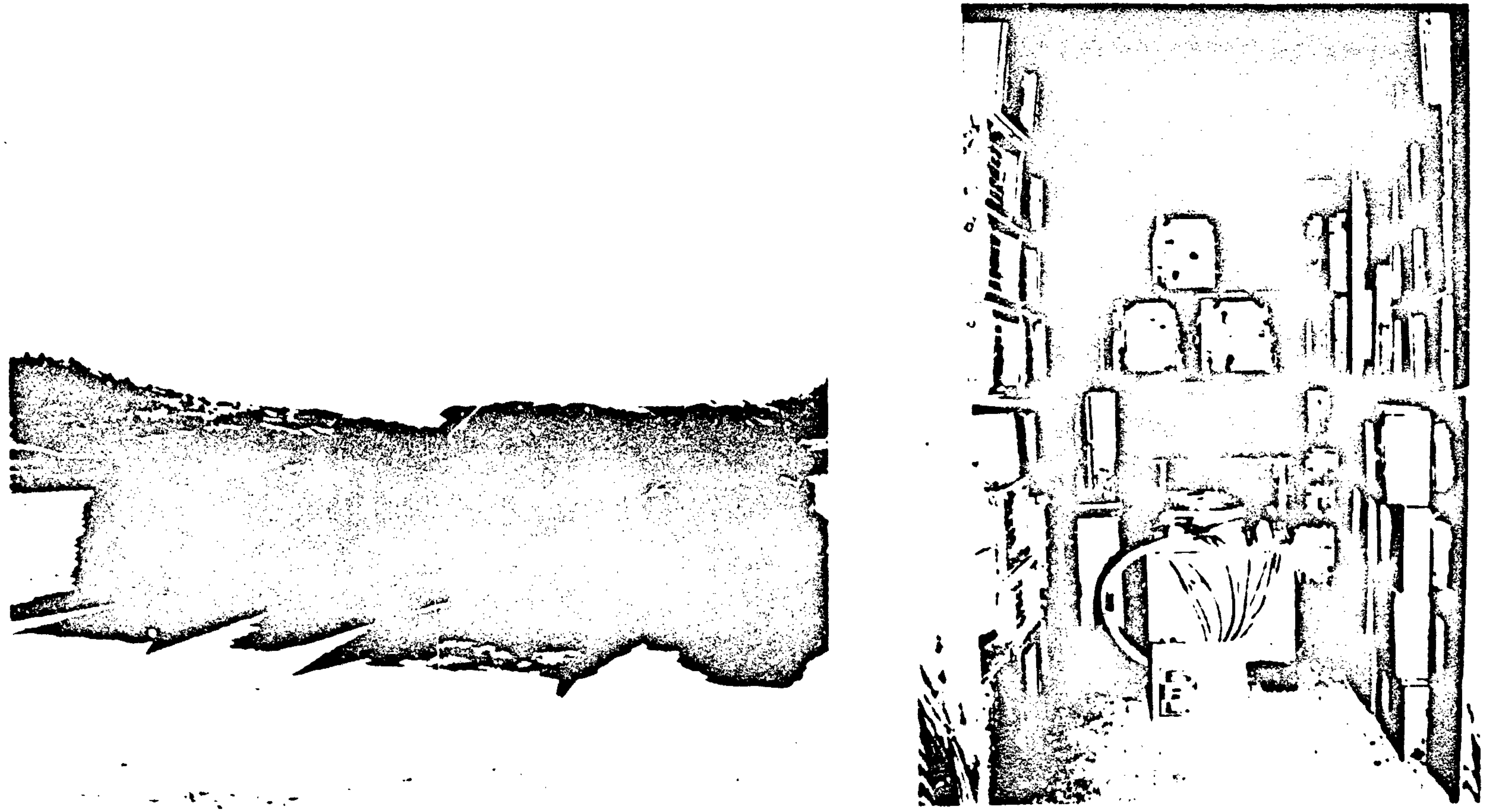

Figure 5. Donor and Acceptor Containers (Left) confined by the Sandbag Walls and Ammunition inside the Donor Container (Right), Test No. 5.

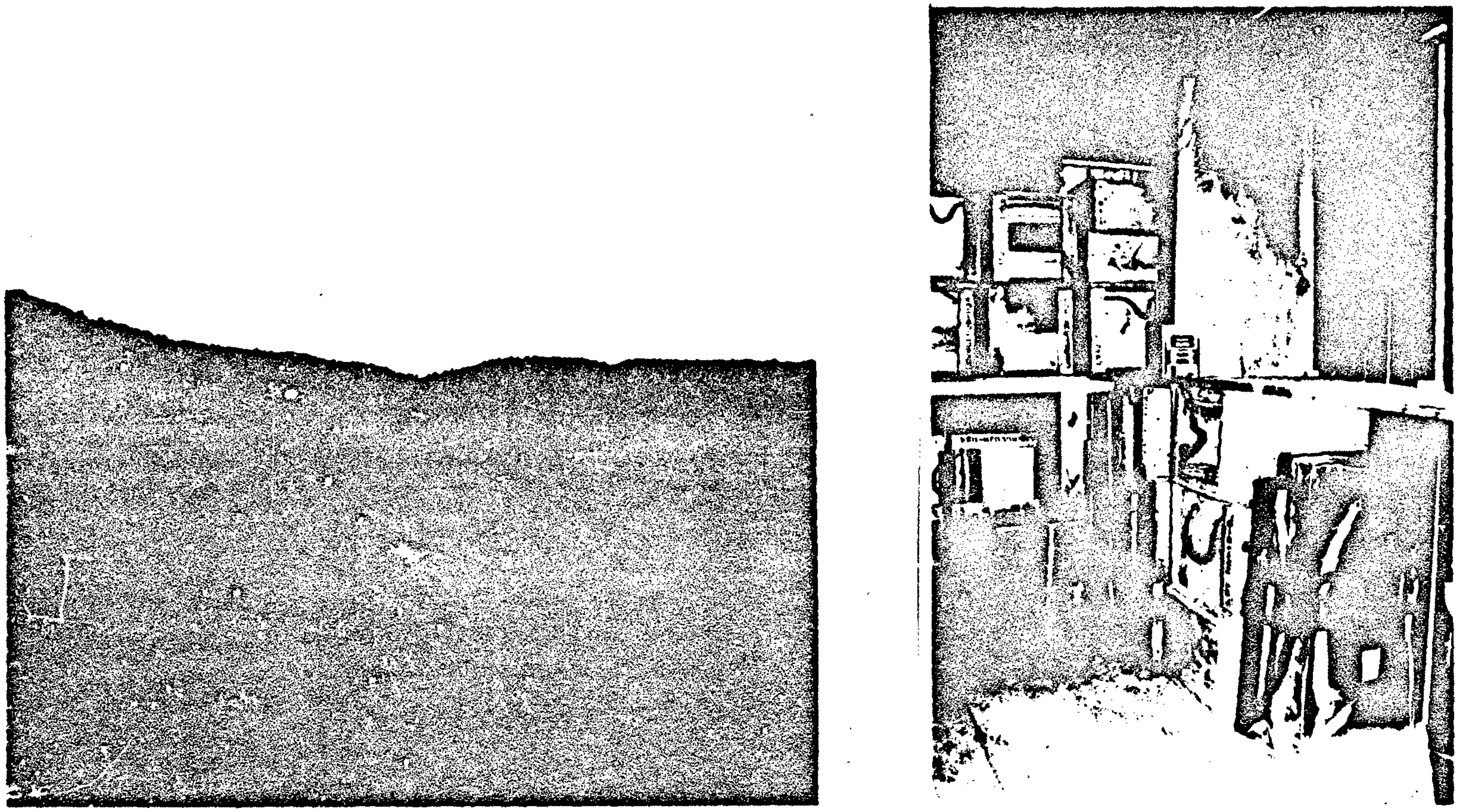

Figure 6. Donor and Acceptor Containers (Left) and Munitions in the Donor Container (Right).

TABLE III

CONEX TEST 1

Zone	A	B	C	D	E	F
9	1-MF					
8	2-MF		10-SG 20-M42 1-MF	25-SG 7-M42 1-MF		
7	1-MF		1-SG 4-M42 1-MF	4-SG 2-M42		
6		1-MF				1-MF
5			27-M42	4-SG		
4		1-MF	9-M42 2-SG	5-SG 2-MF	4-SG	1-MF 1-WF
3			15-M42 8-SG 1-WF	7-SG 1-M42	2-SG 1-M42	1-FDF 1-SG 3-WF
2	3-WF		1-SG	4-SG	5-SG 1-M42 2-WF	2-FDF 7-SG 1-MF
1	1-WF	1-WF	2-SG	5-66 17-S 1-MF 1-M42	6-SG	11-FDF 5-SG 1-MF
0	84-M42 24-SG 3500-50 10-66			1-FG 50-SG 2-M42		

TABLE III (continued)

CONEX TEST NO. 1

ZONE	G	H	I	J	K	L
9				1-MF 5-FG		1-MF
8	4-MF			5-FG		1-MF
7	1-MF 1-WF					1-MF
6	2-MF 1-WF 2-FDF			12-FG	1-MF	2-MF
5				2-MF 7-FG 1-WPF		2-50C
4	1-FDF		9-FG 1-66 13-WPF	1-FG 1-WPF 5-MF		2-50C 3-MF
3	2-FDF		400-752 3-FG	490-762 1-FG		1-MF 1-WF
2	8-FDF 2-SG		10-WPF 15-FG 200-762	2-MF 200-762	1-50C	1-WF
1		4-WP 6-SG 1-FG	1-FG 2-WPF 1-WF	1-WF		
0	1-MF, 24000-762 131-FG , 203-WPF			2-MF 387-762		

TABLE III (continued)

MUNITION, DISTANCE AND ANGLE DESIGNATION FOR CONEX TESTS

Munition	Designation	Munition	Designation
0.50	50	File Dest. M4	FDF
7.62mm	762	RKT 66mm M72A2	66
5.56mm	556	Metal Frag - Conex	MF
M42 Submunition	M42	Wood Frag.	WF
Frag Grenade	FG	Burned Munition	B
Smoke Grenade	SG	Casing	C
White signal Flare	WPF	Projectile	P
White Signal Flare Part	WPFF	Casing / Projectile	C/P

5-M42 = Five rounds of M42

Distance	Designation	Distance	Designation
0 - 60 Feet	0	60 - 90 Feet	1
90 - 120 Feet	2	120 - 150 Feet	3
150 - 180 Feet	4	180 - 210 Feet	5
210 - 240 Feet	6	240 - 270 Feet	7
270 - 300 Feet	8	> 300 Feet	9

Distance	Designation	Distance	Designation
0 - 30 Deg	A	30 - 60 Deg	B
60 - 90 Deg	C	90 - 120 Deg	D
120 - 150 Deg	E	150 - 180 Deg	F
180 - 210 Deg	G	210 - 240 Deg	H
240 - 270 Deg	I	270 - 300 Deg	J
300 - 330 Deg	K	330 - 360 Deg	L

TABLE IV

CONEX TEST NO. 2

ZONE	A	B	C	D	E	F
9		1-MF	28-M42 1-S	6-M42 22-SG 1-MF		
8	3-MF	2-M42	6-M42 4-SG 2-MF	2-MF 2-SG		
7	2-MF		5-M42 1-MF	3-MF	1-SG	
6	2-MF	1-M42	1-MF 4-M42	1-MF 1-M42 2-SG	2-SG	
5	3-MF		7-M42	2-SG	1-SG	1-MF
4	3-MF		9-M42	2-MF		1-MF
			1-SG	3-M42 4-SG		1-66W
3	1-MF 1-WF	1-MF	1-MF 5-M42	1-MF 1-66P 3-SG 1-M42	1-66P 1-FG 1-WF	1-66L 3-556 1-WF
2	1-MF	1-M42 2-W	1-MF 7-M42	5-SG 3-M42 1-SG	1-MF 1-SG	4-SG 1-WF
1	2-M42 1-WF		26-M42 1-WF	10-SG 1-66	4-SG 1-66P	8-SG
0	2800-50, 40-M42,	5-SG, 1-FG		150-50, 11-66, 114-SG 1-FG, 2-M42, 2-66P		

Table IV (continued)

CONEX TEST No. 2

ZONE	G	H	I	J	K	L
9		1-MF	1-MF 12-FG	5-556 2-FG		
8	1-MF		1-FG 1-M42	76-556 4-FG		
7			1-MF 1-66P	820-556 1-FG		
6	1-MF	1-66C	4-FG	1-MF 48-556 1-FG	1-50	1-MF
5			3-FG	200-556	1-66W	
4	2-MF		9-FG	1-MF 1-FG 1-WF 15-556	1-M42	1-MF
3	1-66P 2-FG 3-MF		14-FG	1-MF 24-556 1-WF	5-556	1-MF
2	8-FDF	1-WPF	8-FG	60-556 1-FG	2-50 38-556	1-WF
1	20-FDF 1-SG 1-M42 1-WPF	1-WPF 1-WF	2-FG 2-WF	49-556 1-MF	30-556 4-50 1-FG	4-556 1-50 3-M42 1-MF
0	2460-556, 200-762, 9-50 216-WPF, 110-FG, 9-FDF 2-SG, 1-MF			9400-762, 22140-556, 40-50 13-M42, 3-FG, 8-MF, 5-WF		

Table V

CONEX TEST NO. 3

ZONE	A	B	C	D	E	F
9		12-M42 2-MF 1-SG	23-M42 1-SG	2-M42		
8			8-M42			
7	1-MF		14-M42 3-MF	1-M42B 5-M42 1-WF 6-MF	1-M42B	1-MF 1-FDFP
6	2-MF	1-762C 1-M42 2-MF	9-M42 1-MF	4-SG 5-M42 3-MF		1-MF
5	3-MF 1-762C	1-762C 2-MF	9-M42 1-MF	5-M42 2-SG 1-MF		1-WPF 1-MF
4	6-MF 1-WF 3-762C	1-762C	1-66P 3-M42 1-MF	2-SG 2-M42 1-WF 1-MF		1-WF
3	2-MF	2-M42 1-WF	5-M42 2-MF	2-M42 5-SG	1-SG	2-WF
2	1-MF	3-M42 1-762B 1-MF 3-WF	1-M42B 2-M42 1-MF 4-WF	8-SG 3-M42 1-WF	1-SG	1-MF 1-FDF .
1	2-MF	3-M42 3-WF	17-M42 1-WF 1-MF	13-SG 9-762B 2-WF	1-SG 1-WF	11-FDFP 10-SG 1-WPF 1-WPFB 1-WF
6	1-WPFB, 1-SG, 1-MF, 1-WF 1-M42, 1-66, 3600-50			32-WPF, 24-WPFB, 1-FDFP 1-M42, 159-SG, 3-66B, 10-66		

TABLE V (continued)

CONEX TEST NO. 3

ZONE	G	H	I	J	K	L
9				1-FG 2-WF		8-MF
8			1-MF 1-FG	2-FG 1-762P		3-MF
7				2-FG		
6	1-FDF 2-MF		2-FG 1-66P			3-MF
5	1-FDFP	1-MF	2-FG	1-MF		
4	1-FDFP		1-556B 3-762C 1-762	2-MF 1-FG	1-762P 1-762C	3-762C 2-MF 1-WF
3	1-WPFB 1-FDFP 1-FG	1-WF	1-FG 1-MF	3-762P 3-556C 1-556P	1-556C 1-556 1-WF	1-MF
2	8-FDF 2-MF 1-WF	3-762	1-762 1-556B	1-556B 1-WF	1-FG 1-MF 4-556B 2-762B	2-MF 2-762B
1	15-FDFP 4-WPF 2-MF 1-WF	5-556B 1-FG	14-FG 1-762B 2-556B		5-556B 1-762B 1-WF	
0	1-WPFB, 192-WPF, 58-FGB 215-762, 5-762B, 4-MF 61-FG, 1640-556B			5000-762, 21320-556B, 2460-556, 5059-762B 43FGB, 9-FG, 3-WF		

Table VI

CONEX TEST NO.4

ZONE	A	B	C	D	E	F
9	1-MF 561 ft 1-66WH		1-MF 450 ft			
8					1-M42	
7	2-50C 3-50P	1-MF 2-50P		1-WPF		
6	1-MF 8-50C/P 1-762P 1-556C	10-50C/P 1-556P 1-WPF 1-762P	1-M42 1-WPFC 7-762P			1-50P
5	1-50P 1-WPFC 2-762P	1-WPFP 2-762P/C 2-50P/C	2-50P	3-50P 2-556P/C 1-WPFC		1-50P 1-50C
4	1-WF 3-50P 1-WPFP 1-762P 1-556C	2-50P 2-50C 2-762P	3-50C 3-50P 2-762P	2-50C 1-50P 1-M42C 3-556P	2-50P	
3	2-MF 3-50P 1-M42 4-50C	6-50C 1-50P 1-WPFC	7-50C 3-50P 1-SG 1-WPF 1-762P	1-556P 1-50C	2-50C 1-50P 1-556P	2-50C 1-MF 1-762C
2	1-MF 13-50P/C 1-M42 1-556C 1-762C 1-WF	3-50C 5-50P 1-MF 1-WPFC 1-556P	3-M42 1-SG 8-50C/P 1-556P 2-762P	2-50C 2-50P 1-556C 1-WPF	2-50C	1-50C 1-50P 1-556P 1-SGC
1	9-50C/P 3-762C 1-MF 1-WF	9-50C/P 1-M42 5-762C 1-WPFC	7-50C 1-WPFC 1-50P 6-556C	5-50C 2-50P 2-556P 1-556C	4-50C 1-50P 2-762P 1-556P	1-762P 1-50C 1-50P
0	38-SG, 2-SGB, 1-WPF, 10-FG 4-WPFB, 61-FGB, 86-M42 7-66, 1-66P			57-WPF, 25-50, 3-SG, 3-M42 1-66, 1-FG, 6-762C, 1-WF 5-556C, 1-M42C, 1-MF		

TABLE VI (continued)

CONEX TEST NO. 4

ZONE	G	H	I	J	K	L
9						1-MF 369 ft
6	1-MF			1-MF	13-50C/P 1-762C 1-SG 1-M42	4-50C 1-762P
5				3-50C 1-762C	1-50C	8-50C/P 1-MF
4				3-50C/P 1-556P	1-50C	5-50C
3	2-50C/P 3-762C [illegible]-MF	1-50C 1-M42	3-50C 1-50P	6-50C/P 1-762C 2-MF	7-50C	7-50C 1-50P
2	3-50C 1-5[illegible] 1-762P 1-762C	3-50C 1-50P	8-50C 3-50P 2-WPF 1-SG	2-762C 1-762P 1-50C 1-MF 2-556C	1-50C 1-762C 2-556C 1-SG 1-MF	1-50C 1-WF
1	3-50C 3-50P 1-762C 1-MF	5-50C 3-50P 1-762P	3-50C 2-50P 1-762C 1-WPFC	7-50C 3-50P 1-WPF 3-762C	5-50C 1-M42 1-762P	3-M42 2-50C 1-66 1-SG. 1-WPF
0	91-WPF, 4-FDFP, 2-M42 39-FG, 20-50, 18-SG			78-FG, 33-WPF, 26-WPFB 5-M42, 366, 10-SG, 1-SGB 600-762, 2700-50, 3280-556 19680-556B, 8000-762B		

TABLE VII

CONEX TEST NO. 5

ZONE	A	B	C	D	E	F
9						1-WPF
8	5-50C/P					3-WPF
7	2-WPFP	4-50P			1-WPF	
6	2-50C 2-50P 1-762C	2-50C/P 1-762C 1-WPFP			2-50P 1-M42CP	1-WPF
5	2-50P 2-50CP 1-WPF	2-50P 2-WPF 1-M42P		1-WPF		1-50P
4	5-50C/P 2-WPFP		1-WPF	1-66P		1-50C 1-762P
3	4-50P 2-50C 1-WPFP	1-556P 3-50P 2-WPFP	2-556C/P 2-50C/P 2-WPFP 1-M42P	1-50P 1-WPFP	1-50C 1-762P 2-WPFP	1-556P 1-762P 1-50C 1-WPFP
2	1-MF 5-50P 1-50C 1-WPFP	2-556C 1-50C 6WPFP	1-556P 2-50P 1-WPFP 1-M42CP	1-WPFP	2-762P 1-762C 2WPFP	2-50C/P 1-556C 2-762P 1-WPFP
1	4-556C/P 3-762C/P 16-50C/P 5-WPFP	3-556C 2-50P 3-WPFP 1-M42P	1-556C 1-50P 1-762P 2-WPFP	1-50P 2-WPFP	2-50C 1-762P 1-WPFP 1-M42P	1-50P 1-762C 1-50C 1-762P
0	2-MF, 25-556C, 5-556P, 12-50 114-50C, 52-50P, 6-762C 1-762P, 60-WPFBP, 2-M42B 2-M42p, 1-66BP			2-50, 8-50C, 8-50P, 1-556P 4-556C, 5-762P, 1-SG, 4-M42P, 43-WPFP		

TABLE VII (Continued)

CONEX TEST No. 5

ZONE	G	H	I	J	K	L
9	1-WPFP					2-WPFP
8				3-50C/P 3-WPFP 1-M42P	2-50P 2-WPFP 1-M42P	
7		1-50P		1-50P 1-50C 3-WPFP		4-50C/P 1-762P 2-WPFP
6			1-50P 1-WPFP		1-50P 1-50C	4-50P 2-50C
5	1-50C		3-50C	1-50P 1-M42P	1-50P 2-50C 2-556P	6-50C/P 1-556P 1-762C 2-WPF
4			2-50P 1-762c 1-WPFP	3-50C/P 1-556P 1-762C	4-50C	3-50P 3-50C 1-M42P
3	3-50C	2-50C 1-WPFP		1-50P 3-WPFP 2-M42P	4-50C 1-556C 1-M42CP	9-50C/P 1-M42P 1-WPFP
2	1-50P	1-50P 1-50C 3-WPFP	1-50P 3-50C 2-WPFP	1-556P 2-50P 2-50C 2-WPFP 2-M42P	2-50P 4-50C 2-556P 1-556C 2-WPFP	1-M42P 5-50C/P 1-762C 4-WPFP 1-Door
1	1-556C 1-50P 2-50C 1-WPFP	2-50C 3-WPFP	3-50P 8-50C 3-WPFP 1-M42P	1-556C 5-50C 2-WPFP 1-M42P	5-50P 7-50C 3-556C 4-WPFP	19-50C/P 2-556C/P 1-WPFP 2-M42P
0	6-50P, 21-50C, 1-762P 13-WPFP, 3-M42, 4-M42P 3-66P			1-5[illegible], 106-50C, 123-50C, 4-SG 3-5[illegible], 5-556P, 71-556C, 1-762C, 5-762P, 80-WPFBP 5-M42P, 5-M42, 8-M42B		

TABLE VIII

CONEX TEST NO. 6

ZONE	A	B	C	D	E	F
9	1-ABF 54-50 707-556 13-FM	1-ABF 32-50P 2-SG 1-WPF 13-MF	2-MF 2-SG 25-50P 4-556 2-762	740-556	100-556	
8	1-ABF 673-556 19-50 1-MF	35-50P 6-50CB 4-MF		1423-556 5-50 1-50CB	169-556 2-556CB 1-556P	
7	1-ABF 217-556 1-762P 8-50 1-MF	820-557	2-ABF 7-SG 121-50 10-556 7-762 1-MF	1-ABF 1-WPF 79-556	2-SG 2-50P 3-M42P 2-WPFP 1-MF	
6	208-556 1-SG 3-ABF 51-50 3-MF	1-SG 12-50 3-762CB 553-556 1-ABF 1-MF	7-SG 36-556 13-762 52-50	81-556 1-WPF 1-ABF		
5	2-ABF 13-50P 45-556 57-50CB	10-50P 6-50CB 2-556 2-MF	6-ABF 6-ABF 160-50 167-762 2-556	2-ABF 1-50P 1590-556 1-556P	820-556 1-SG 2-M42P	

TABLE VIII (continued)

CONEX TEST NO. 6

ZONE	A	B	C	D	E	F
4	1-MF 2-ABF 1-SG 30-656 70-50	1-ABF 123-50 2-556 1-MF	3-ABF 93-762 95-50 2-SG	1-ABF 2-WPF 1504-556 16-762 8-50	1-SG 1-50CB	2-SG 1-WPF
3	214-50 46-656 1-762CB 1-SG	2-ABF 47-50 1-762CB	6-ABF 8-SG 488-50 144-762 1-MF	3-ABF 2-SG 2582-656 423-762 11-50	3-WPF 1-SG 1-50P	5-WPF 4-SG
2	315-50 2-556 1-762CB 2-ABF	3-ABF 156-50 2-762CB	5-ABF 295-762 536-50 3-SG	4-ABF 2-50P 823-656 2420-762	820-656 2-50P 2-762P 3-WPF 1-SG	9-SG 2-WPFP 1-50 1-MF
1	97-50 1-762P 4-ABF 4-MF	4-ABF 6-762CB 430-50 1-WPF	2-ABF 4-SG 232-50 25-762	2-MF 13-ABF 2930-762 1-SG 18-50 3-WPF 943-656	1-MF 1-ABF 1-FDF 2-WPF 1-SG 1-762 1-50CB	1-ABF 3-WPF 3-FDF 11-SG 1-MF
0	12-SG, 134-WPF, 262-50 148-50CB, 281-50P, 24-762P 1-556P, 41-762, 56-762CB 3-656CB, 1-656, 17-ABF 47-WF, 6-MF			10661-656, 3-656P, 30-656CB 34-50CB, 67-50P, 412-762P 5-50, 443-762CB, 3026-762 52-WPF, 35-SG, 33-FDF 14-ABF, 13-MF, 63-WF		

REFERENCES

1. DoD 6055.9 STD, DoD Ammunition and Explosive Safety Stanards, July 1984.

2. AR 385-64, Ammunition and Explosive Safety Standards.

ACKNOWLEDGEMENTS

The author is deeply grateful to Mr. Jerry Watson of Ballistic Research Laboratory for his guidance and many useful suggestions during the testing phase of the program. The author would also like to thank Mr. David Collis and his staff, New Mexico Institute of Technology for conducting the tests.

APPENDIX

After Recovery Photographs of the Munition, Debris and other fragments.

Figure A-1 through Figure A-2, Test No. 1

Figure B-1 through Figure B-2, Test No. 2

Figure C-1 through Figure C-2, Test No. 3

Figure D-1 through Figure D-2, Test No. 4

Figure E-1 through Figure E-2, Test No. 5

Figure F-1 through Figure F-2, Test No. 6

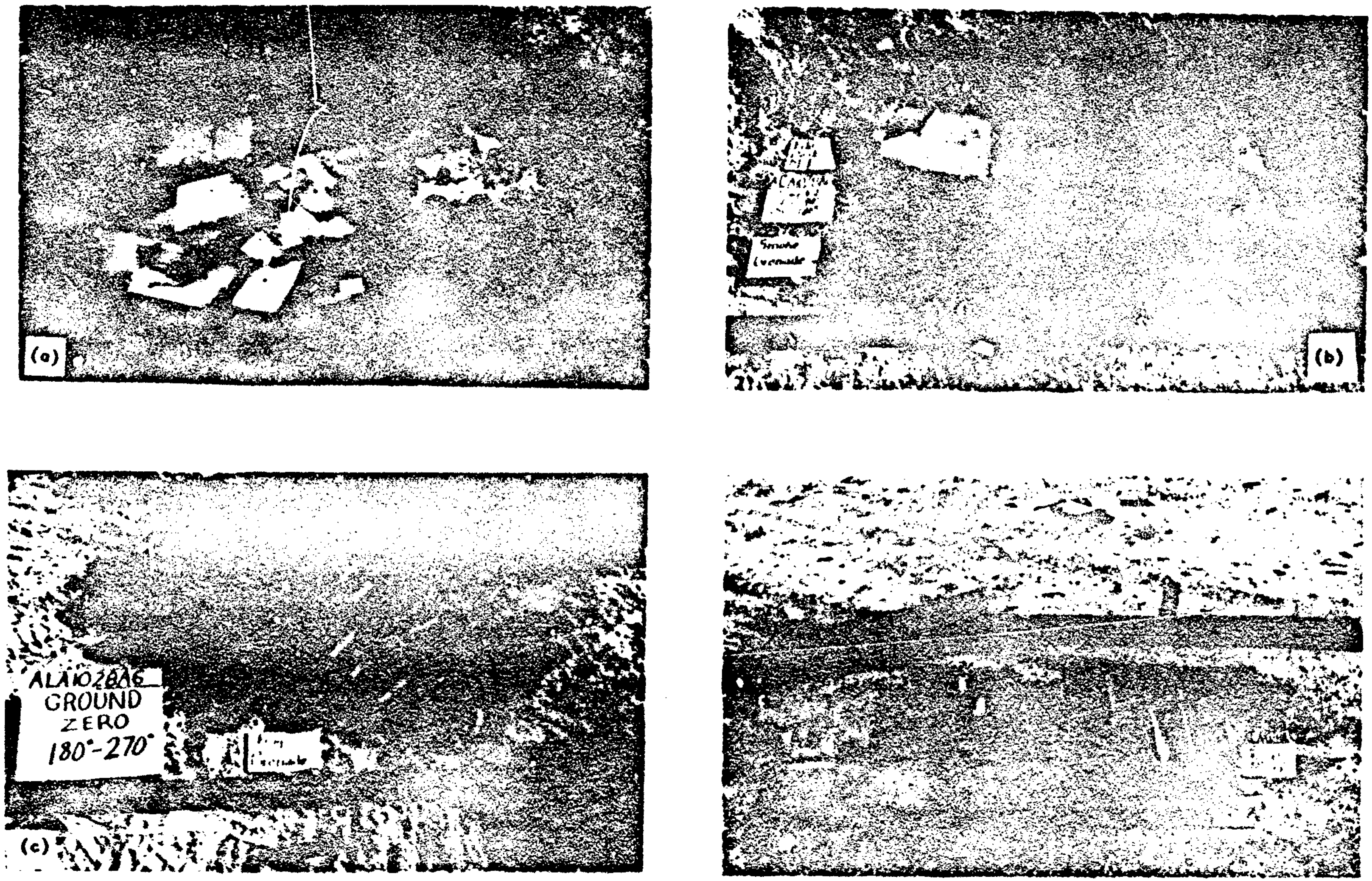

Figure A-1. Test No. 1. (a) File Destroyer, Conex, and Smoke Grenades; (b) Conex and Smoke Grenades; (c) Frag. Grenades; and (d) Smoke Grenades, M42 Submunition, 66mm Rockets.

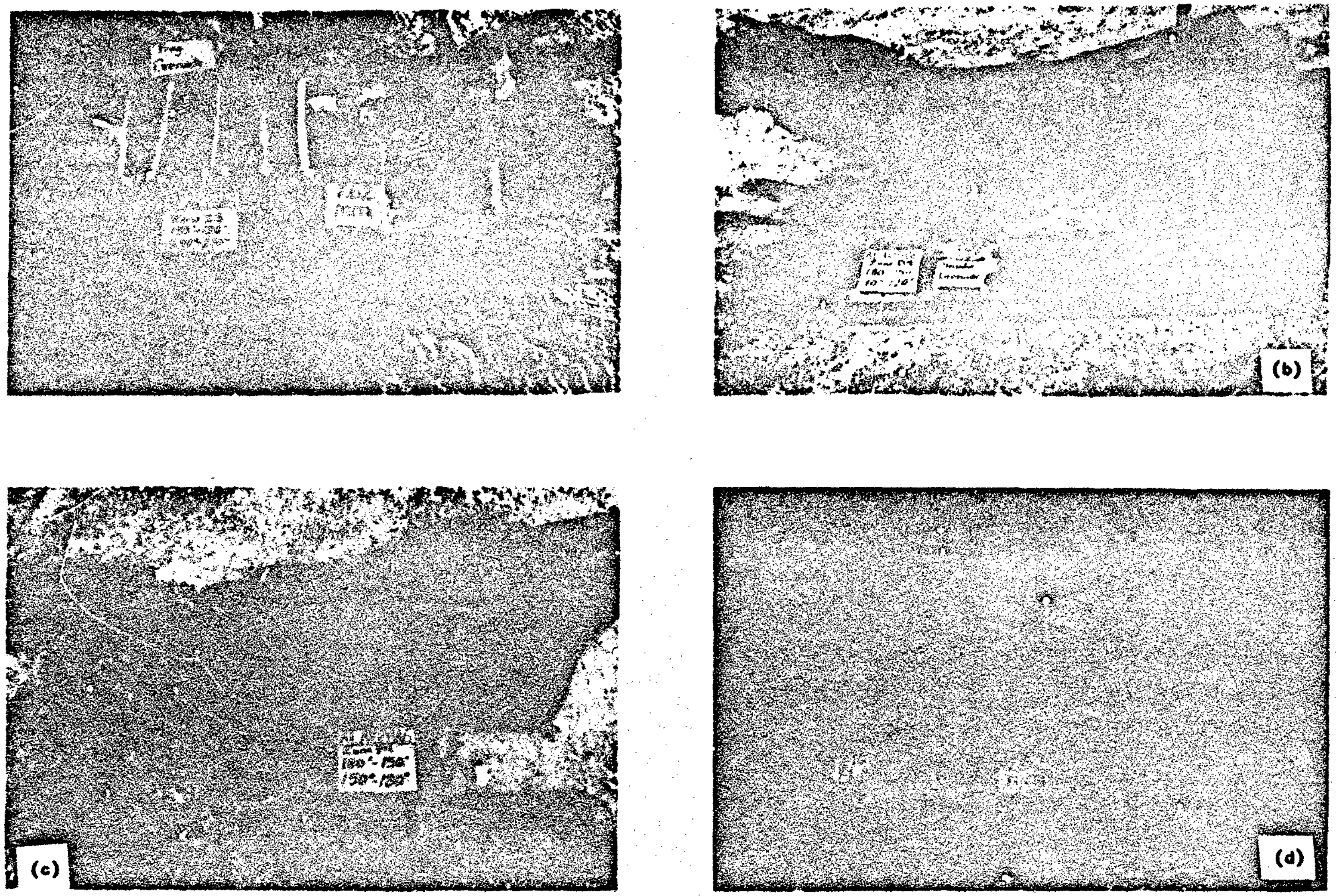

Figure A-2. Test No. 1. (a) Flares, Frag. Grenades, and 7.62mm; (b) Container and Smoke Grenades; (c) Conex Part; and (d) Flares, 7.62mm, Grenades and a part of a Rocket.

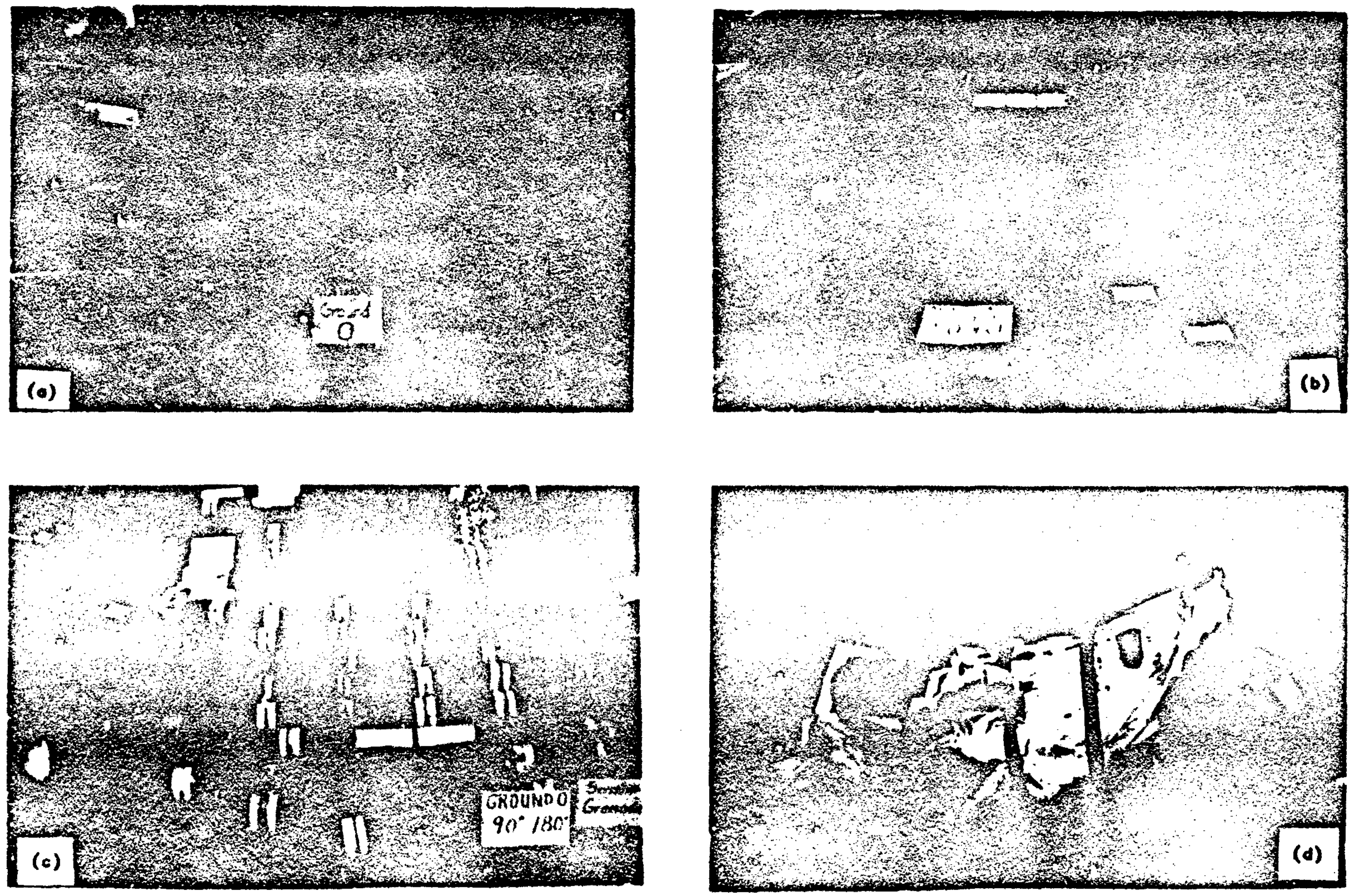

Figure B-1. Test No. 2. (a) Acceptor Conex; (b) 7.62mm, 50 Cal, Frag. Grenades; (c) Smoke Grenades; and (d) 66mm Rocket.

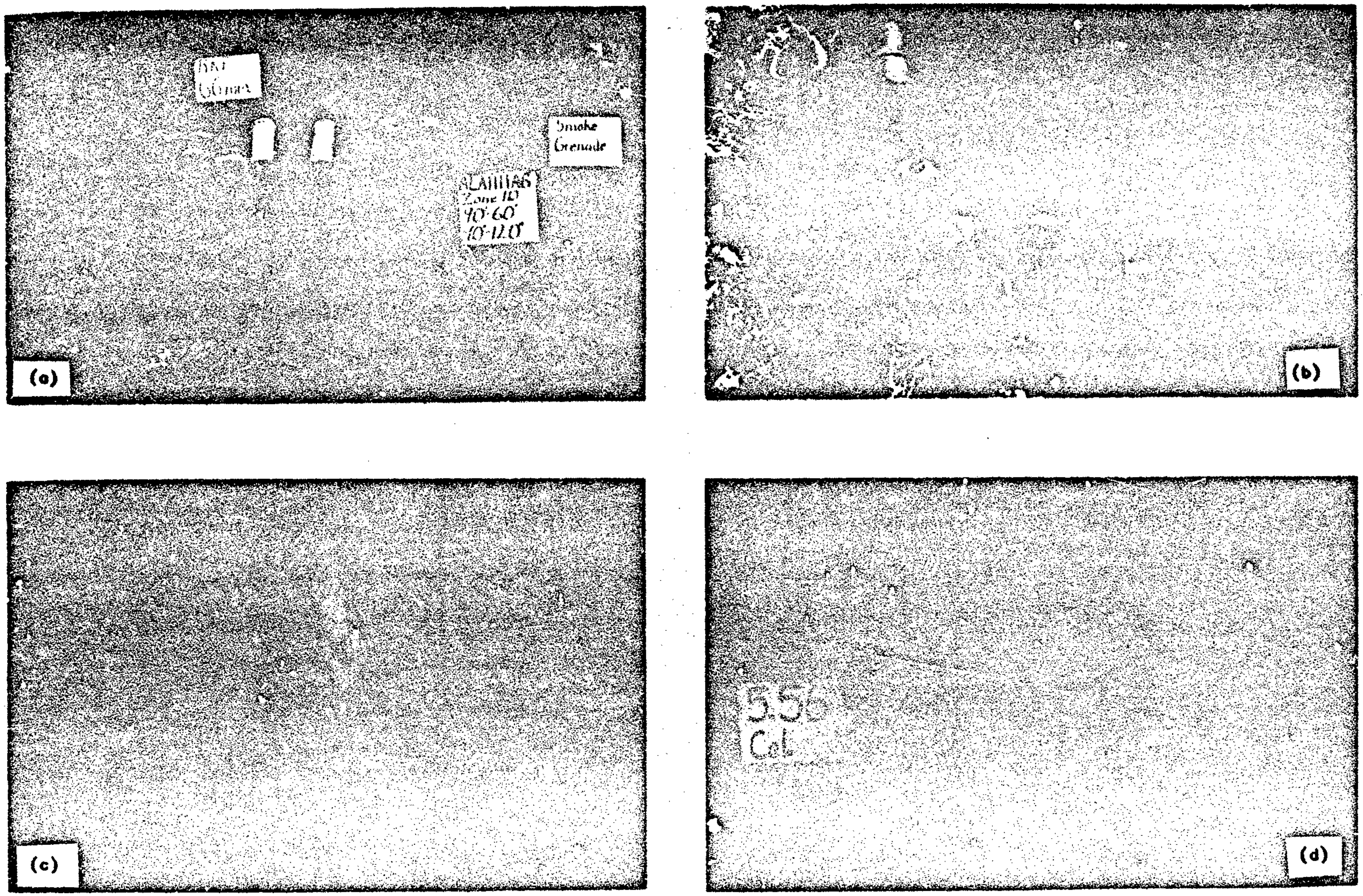

Figure B-2. Test No. 2. (a) 66mm Rockets and Smoke Grenades; (b) Frag. Grenades; (c) Smoke Grenades; and (d) 5.56mm.

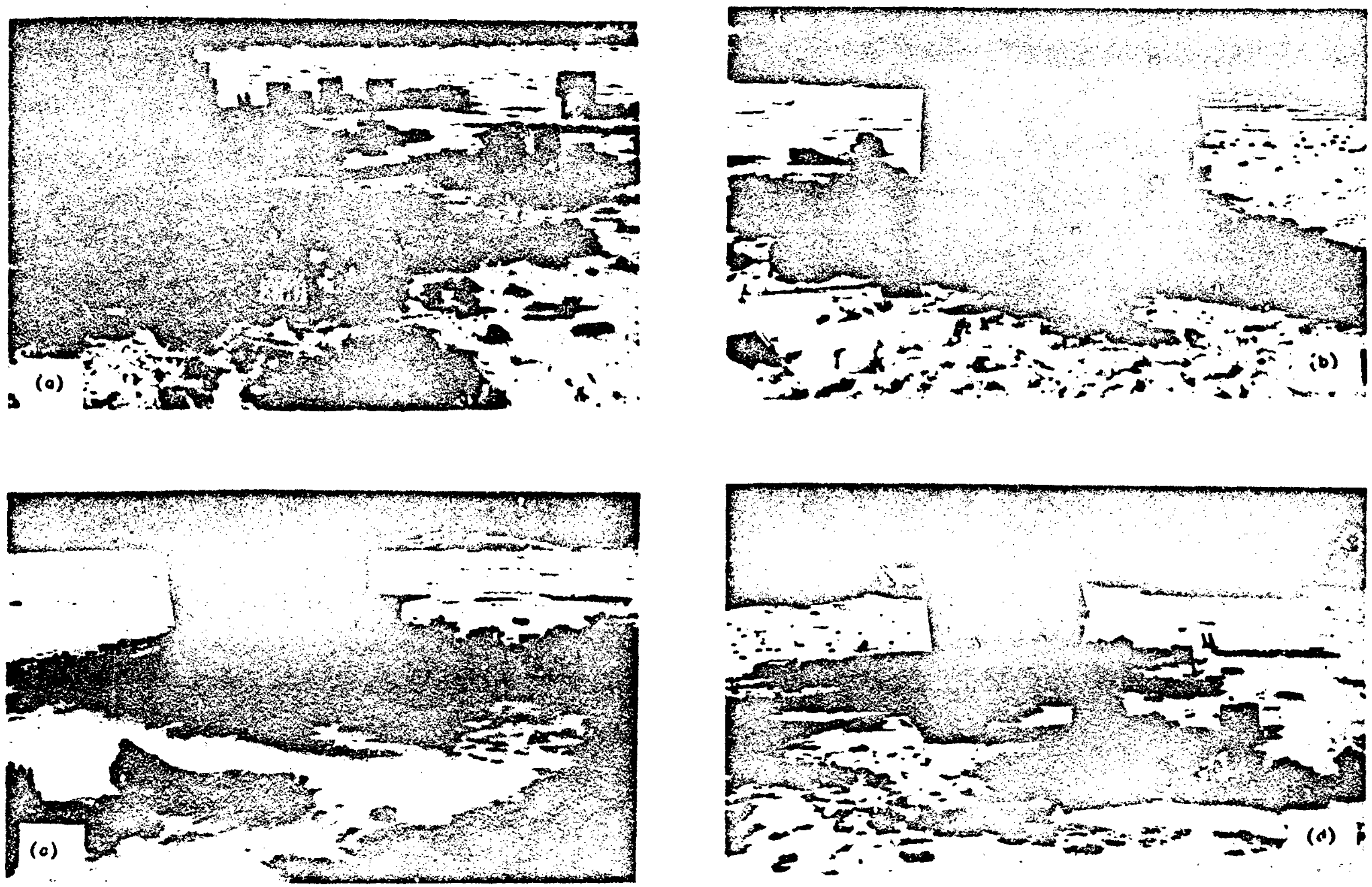

Figure C-1. Test No. 2. (a) Left side, (b) Front side, and (c) Back side of Acceptor Conex; and (d) Acceptor Conex and Munition from Donor Conex.

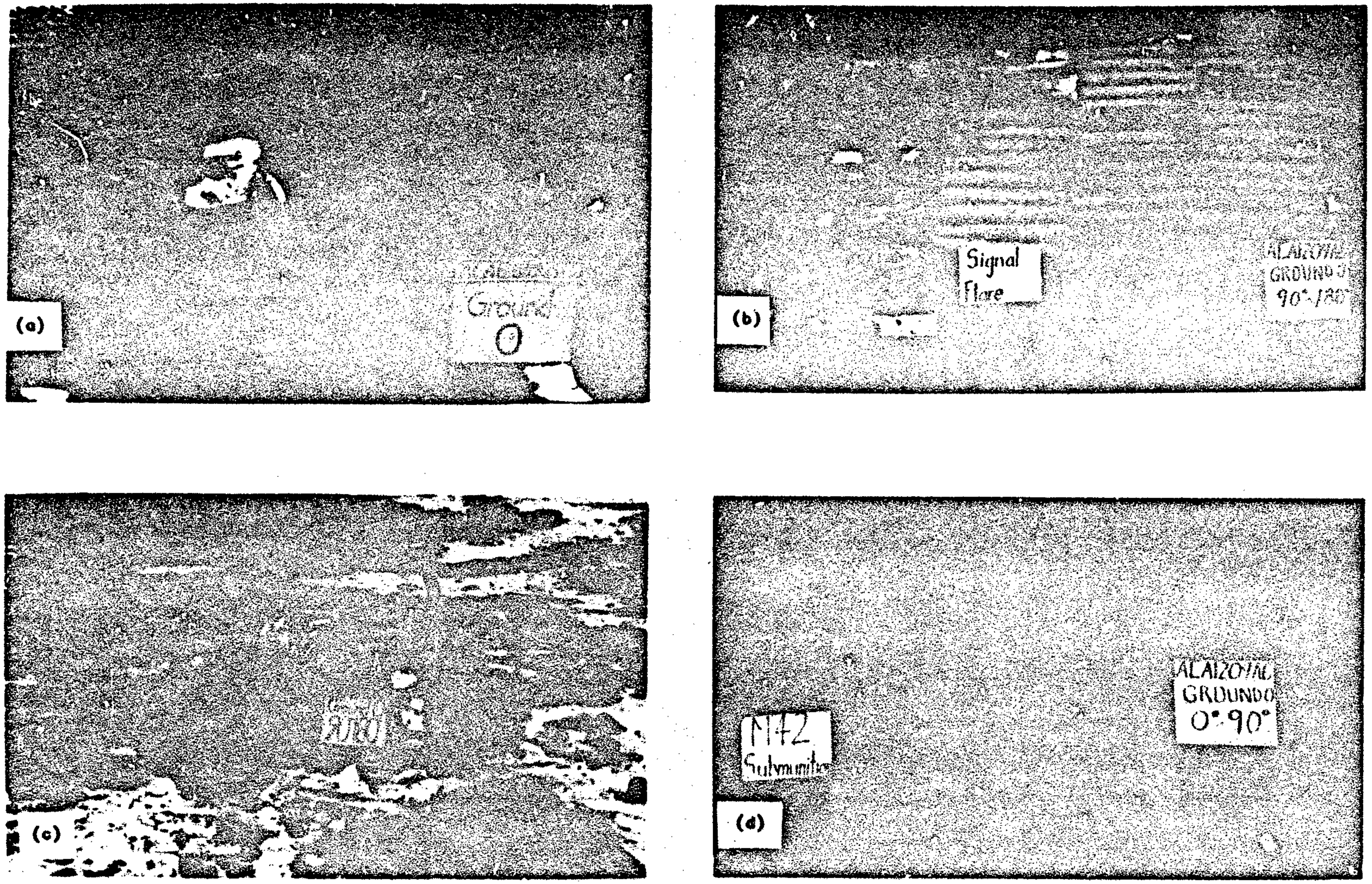

Figure C-2. Test No. 3. (a) Bottom of the Donor Conex; (b) Signal Flares; (c) Mixed munitions from Donor Conex; and (d) M42 Submunition.

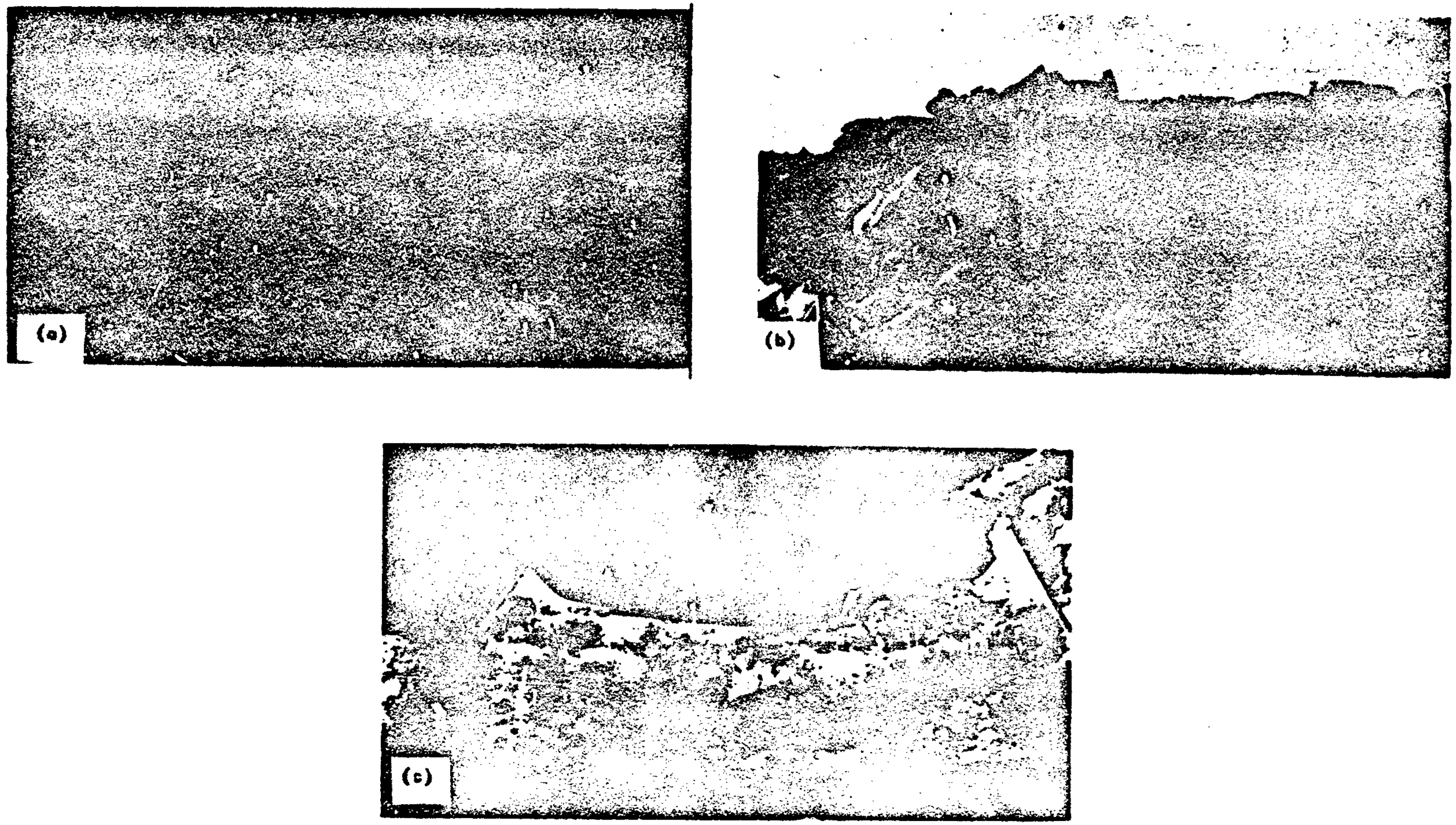

Figure D-1. Test No. 4. (a) Overall View after the Test; (b) Acceptor Conex; and (c) Bottom part of the Donor Conex.

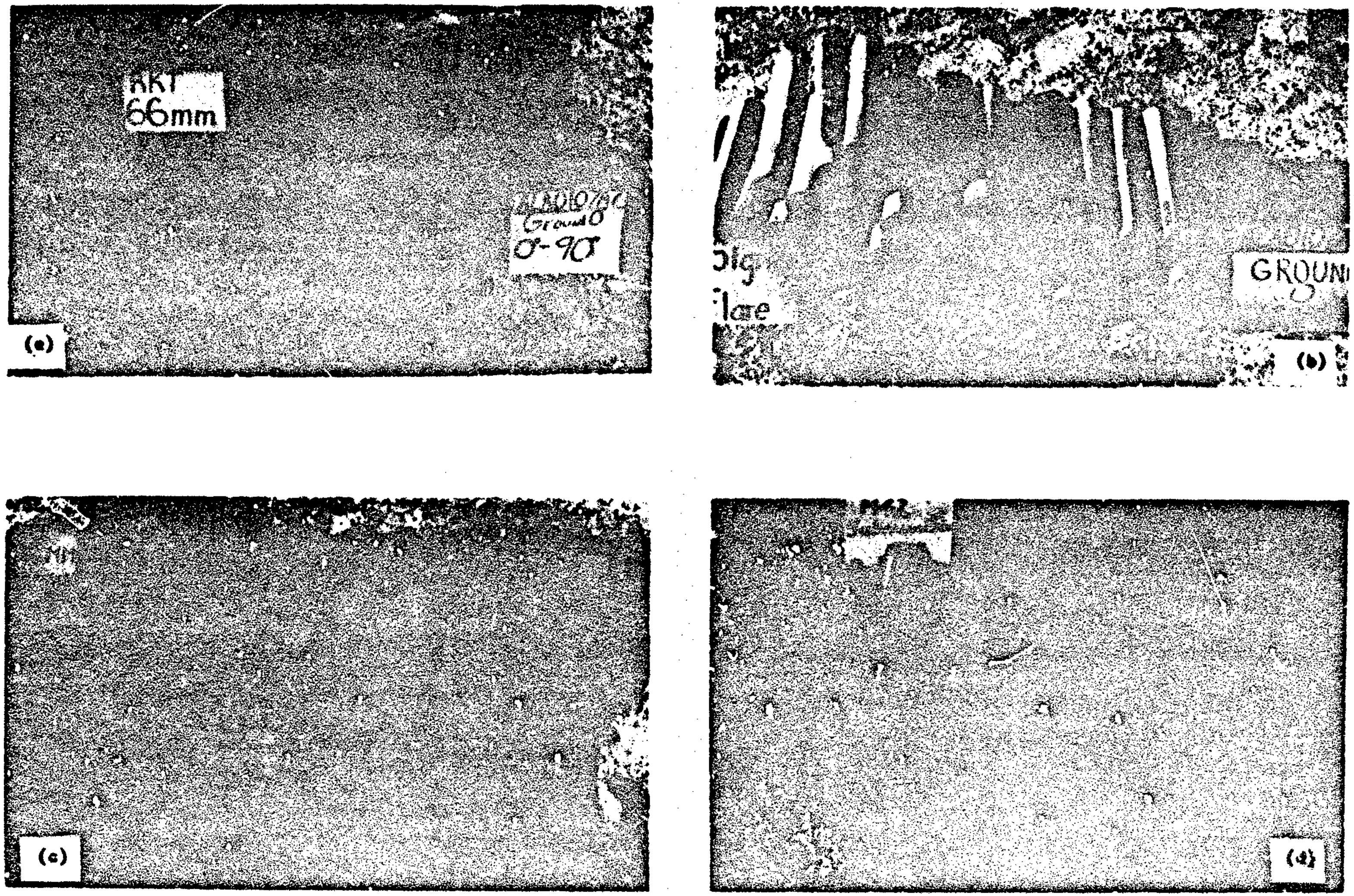

Figure D-2. Test No. 4. (a) 66mm Rockets; (b) Signal Flares; (c) Rocket parts, 50 cal, and 7.62mm; and (d) 50 Cal and M42.

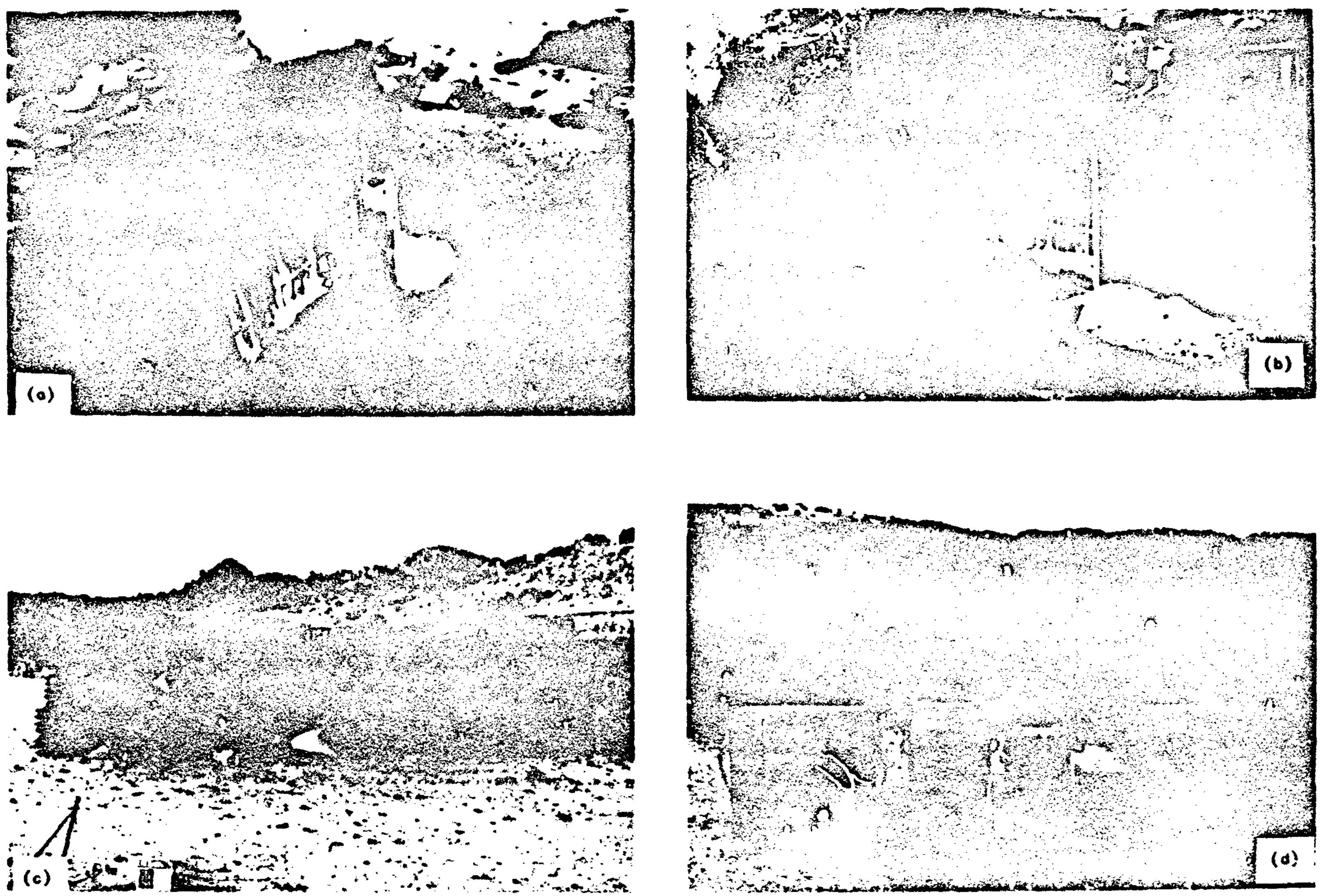

Figure E-1. Test No. 5. (a) Donor Conex; (b,c) Front Side of Donor and Acceptor Conexes; and (d) Munition from Acceptor Conex.

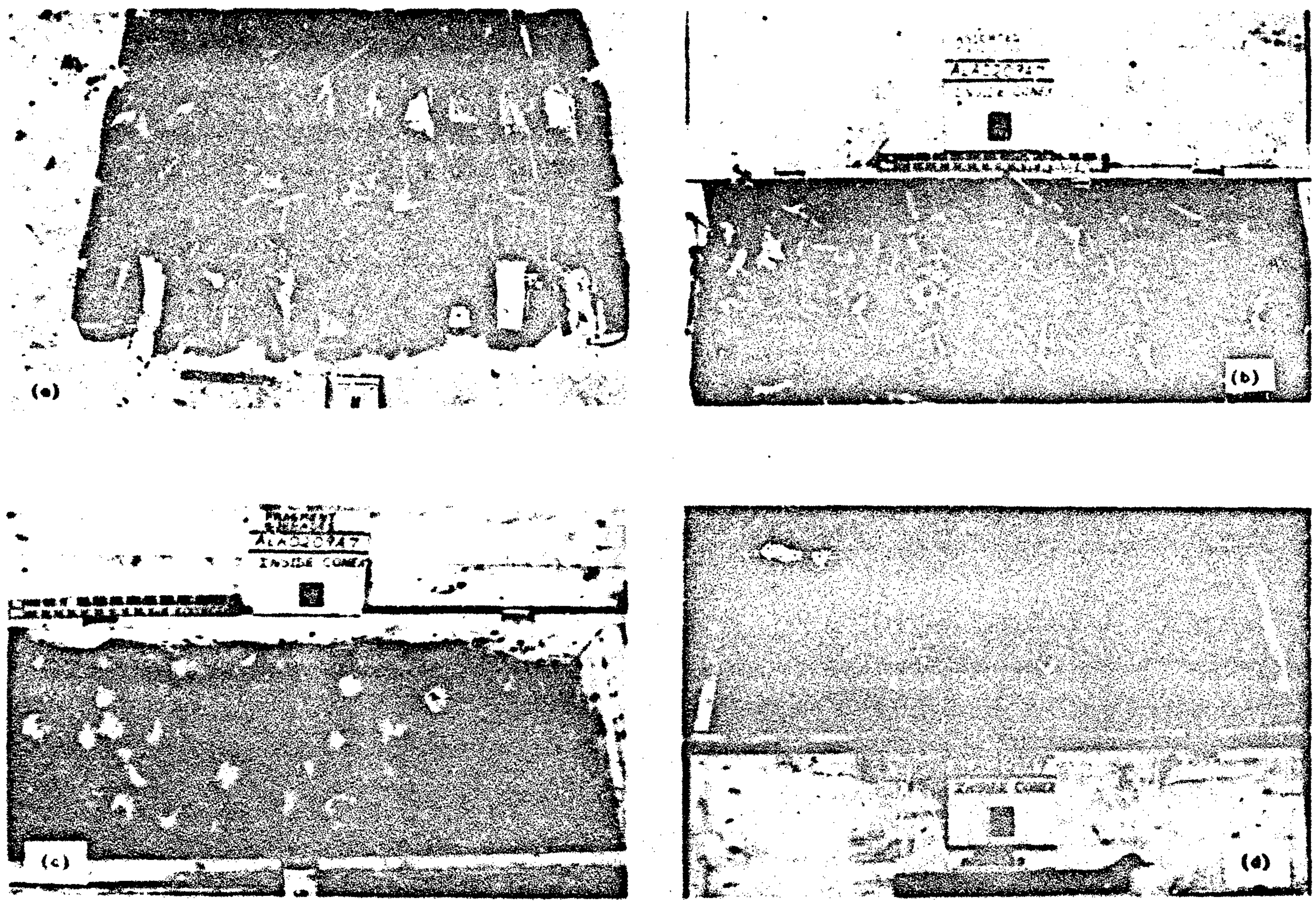

Figure E-2. Test No. 5. (a) 5.56mm Ammunition; (b) Burned Munition; (c) Frag. Grenades; and (d) Smoke Grenades. All burned inside the Donor Conex.

Figure F-1. Test No. 6. (a) 5.56mm, 50 Cal, and 7.62mm; (b) Conex fragment; (c) Ammo Box; and (d) Smoke Grenades, 30 Cal and 5.56mm at 240 - 270 Ft.

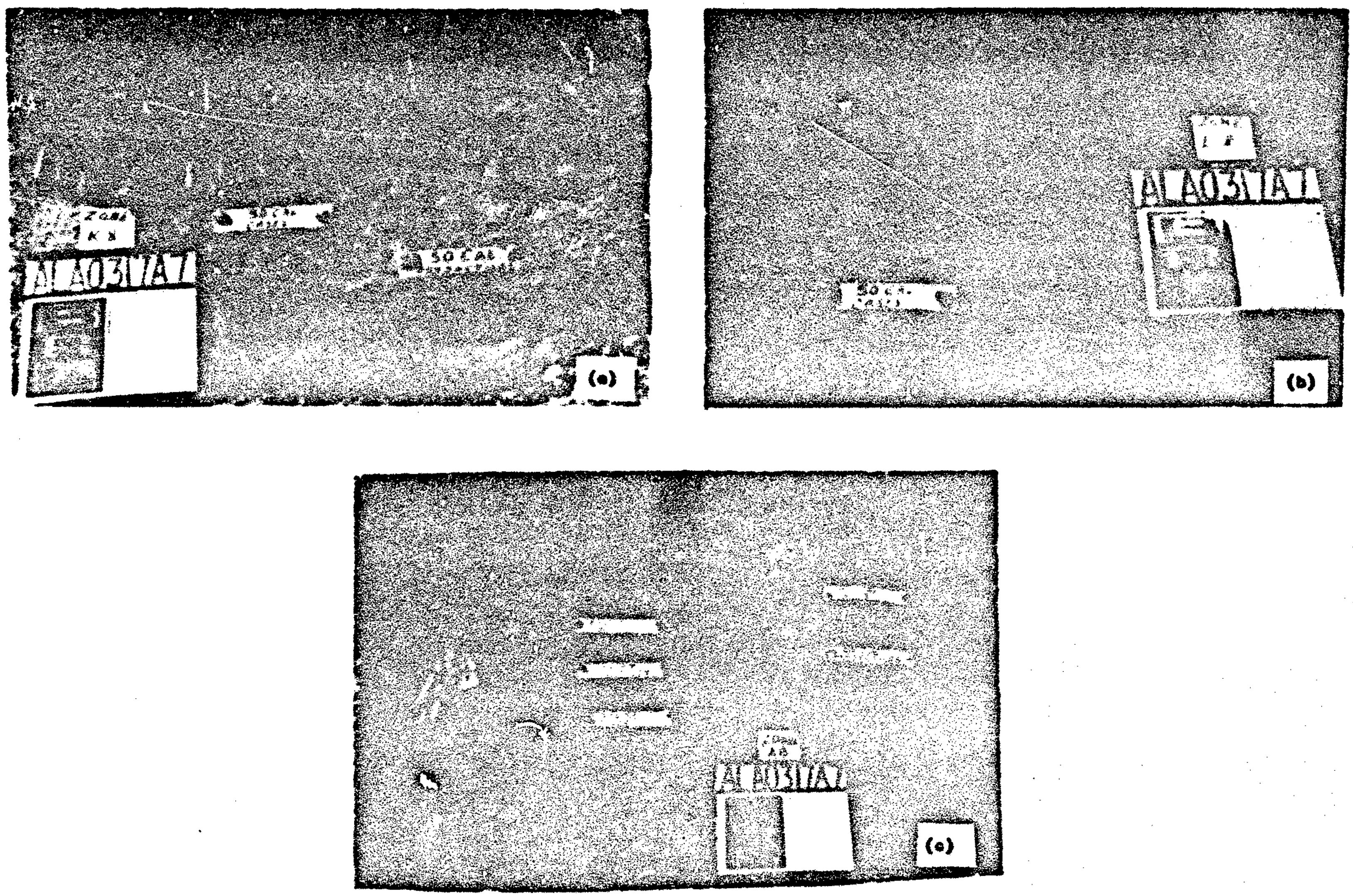

Figure F-2. Test No. 6. (a) 50 Cal; (b) 50 Cal Cases; and (c) 5.56mm and 50 Cal at 270 - 300 Ft.

ESS8/9/88-1

RISK ANALYSIS OF TITAN LAUNCHES OVER SLC 6 AT VANDENBERG AIR FORCE BASE

JON D. COLLINS
ACTA INC.

JOHN J. HARNITCHEK
FEDERAL ELECTRIC CORP.

AUGUST 9, 1988

23RD EXPLOSIVE SAFETY SEMINAR
ATLANTA, GEORGIA

BACKGROUND

- SLC 6 WAS THE LAUNCH FACILITY FOR THE SPACE SHUTTLE AT VAFB (PRIOR TO CANCELLATION).
- TITAN 34D'S ARE LAUNCHED FROM SLC4 AND FLY OVER SLC 6.
- TWO RISK STUDIES WERE MADE REGARDING THE TITAN LAUNCHES:

  (1) RISK TO OCCUPANTS OF THE SPACE SHUTTLE LAUNCH CONTROL CENTER DURING A TITAN OVERFLIGHT.

  (2) RISK (EXPECTED DAMAGE) TO STRUCTURES AT SLC 6 FROM TITAN OVERFLIGHTS.

- THIS PAPER DISCUSSES THE STRUCTURAL RISK ANALYSIS WITH EMPHASIS ON EXPLOSIVE DEBRIS.
  IT INCLUDES A MODEL FOR CATASTROPHE PROBABILITY.

RELATIVE POSITIONS OF SLC 4 AND SLC 6

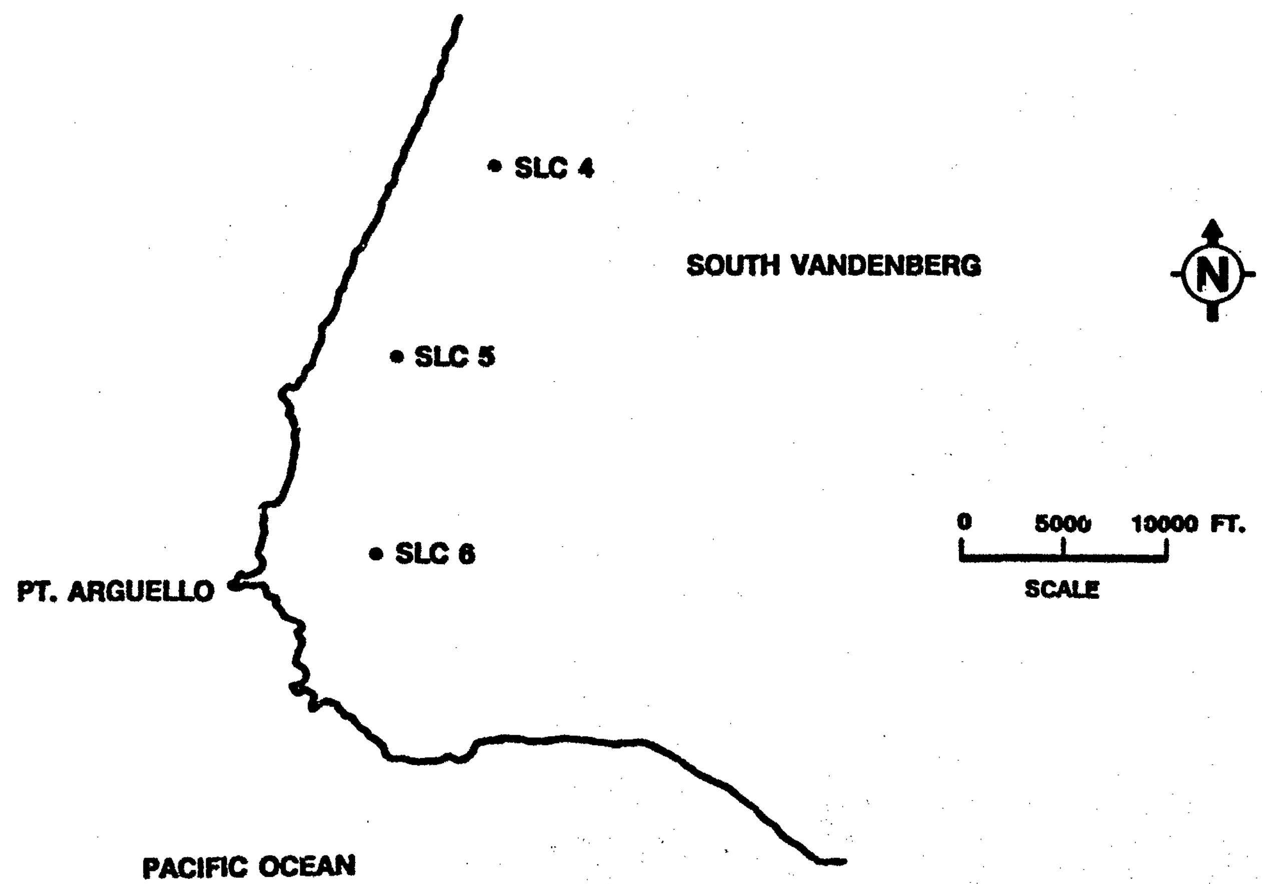

ACTA INC

MAP OF THE SLC 6 COMPLEX

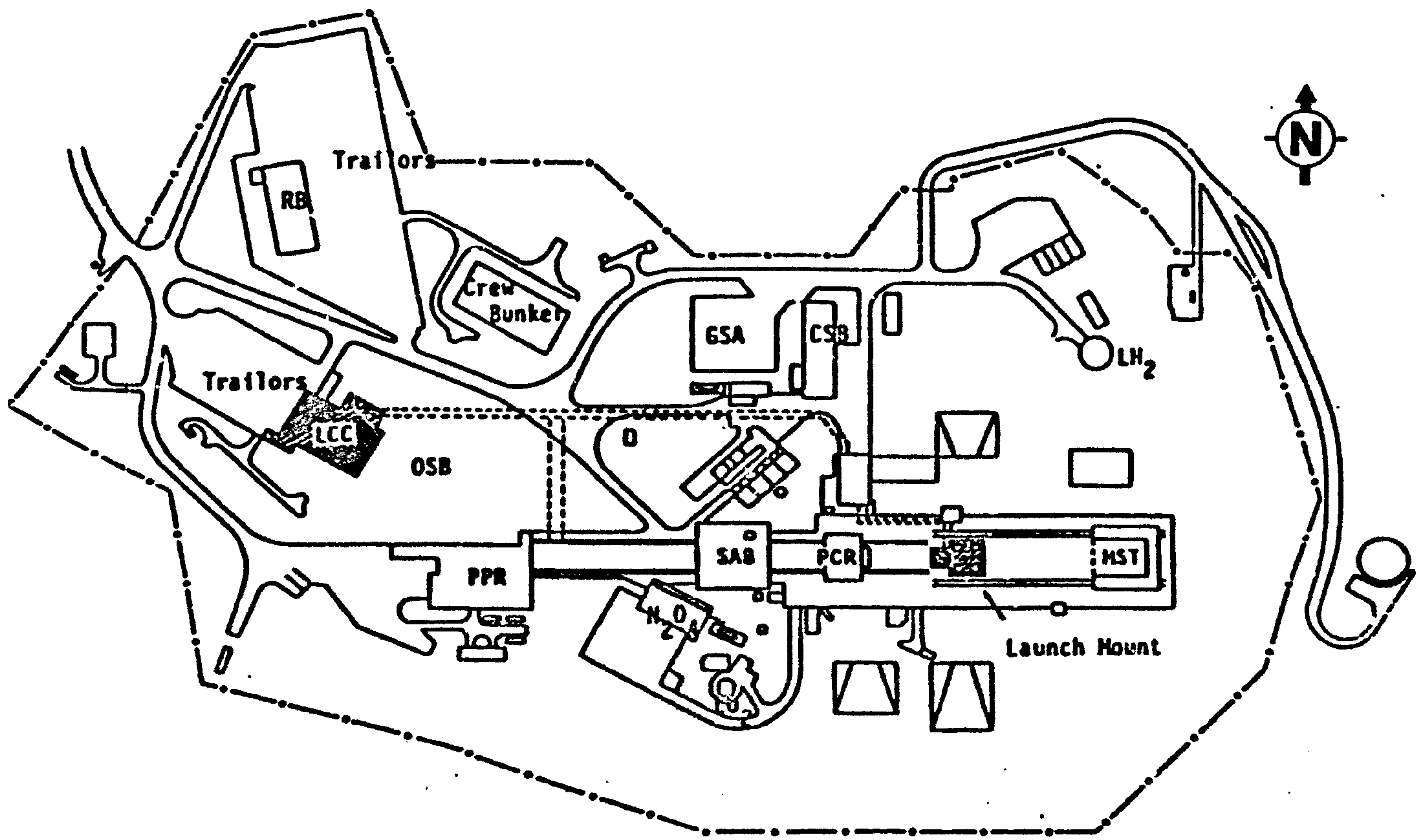

DESCRIPTION OF THE TITAN 34D

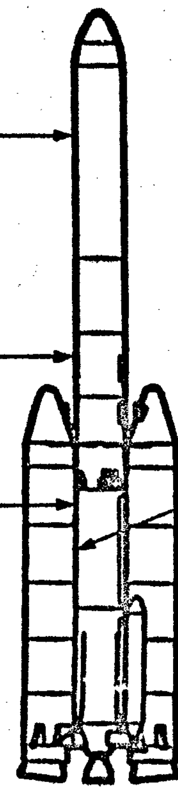

2 STAGES OF HYPERGOLIC PROPELLANTS
N_2O_4 +
AEROZINE 50

APPROX. 850,000 LB. OF SOLID PROPELLANT
(PBAN/PBAA PERCHLORATE COMPOSITE)

ACTA INC

TYPICAL SCENARIO

- VEHICLE FAILS EARLY IN FLIGHT.
- SOLID ROCKET BREAKS FREE INITIATING THE INADVERTENT SEPARATION DESTRUCT SYSTEM.
- THE SOLID ROCKETS BREAK OPEN AND INERT AND BURNING DEBRIS ARE SPREAD OVER THE AREA.
- STRUCTURES ARE THREATENED BY IMPACTS OF DEBRIS AND OVERPRESSURES FROM POTENTIALLY EXPLCSIVE DEBRIS.

ACTA INC

FACTORS THAT INFLUENCE DEBRIS DISPERSIONS AND IMPACT PROBABILITIES

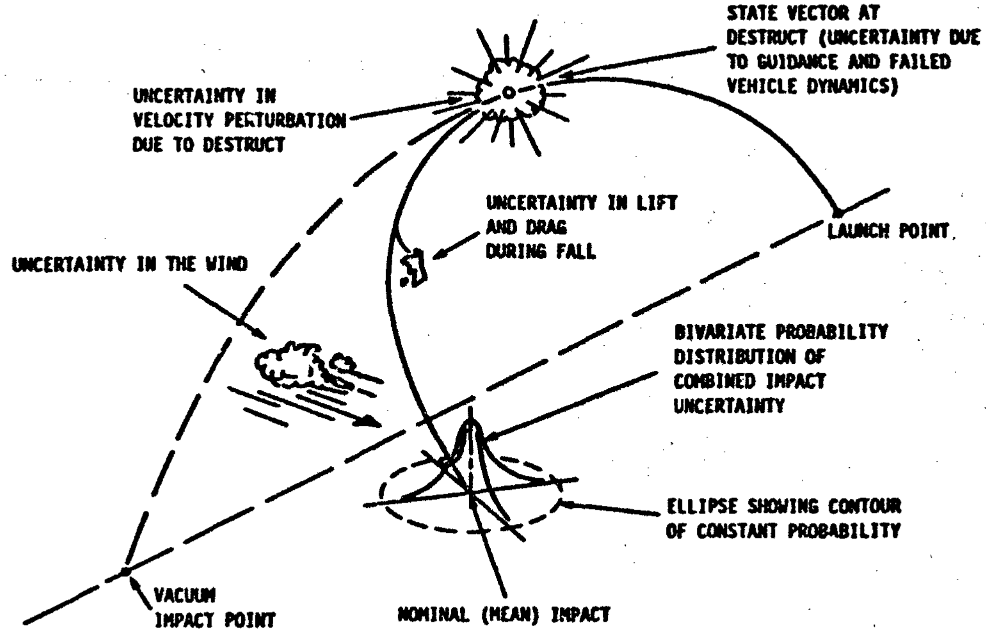

FACTORS

- WIND
- BALLISTIC COEFFICIENT (W/C_DA)
- EXPLOSION VELOCITY
- RATE OF MOVEMENT OF THE INSTANTANEOUS IMPACT POINT

ACTA INC

ESS8/9/88-6

MOTION OF THE DEBRIS PATTERN CENTERLINE TOWARD SLC 6

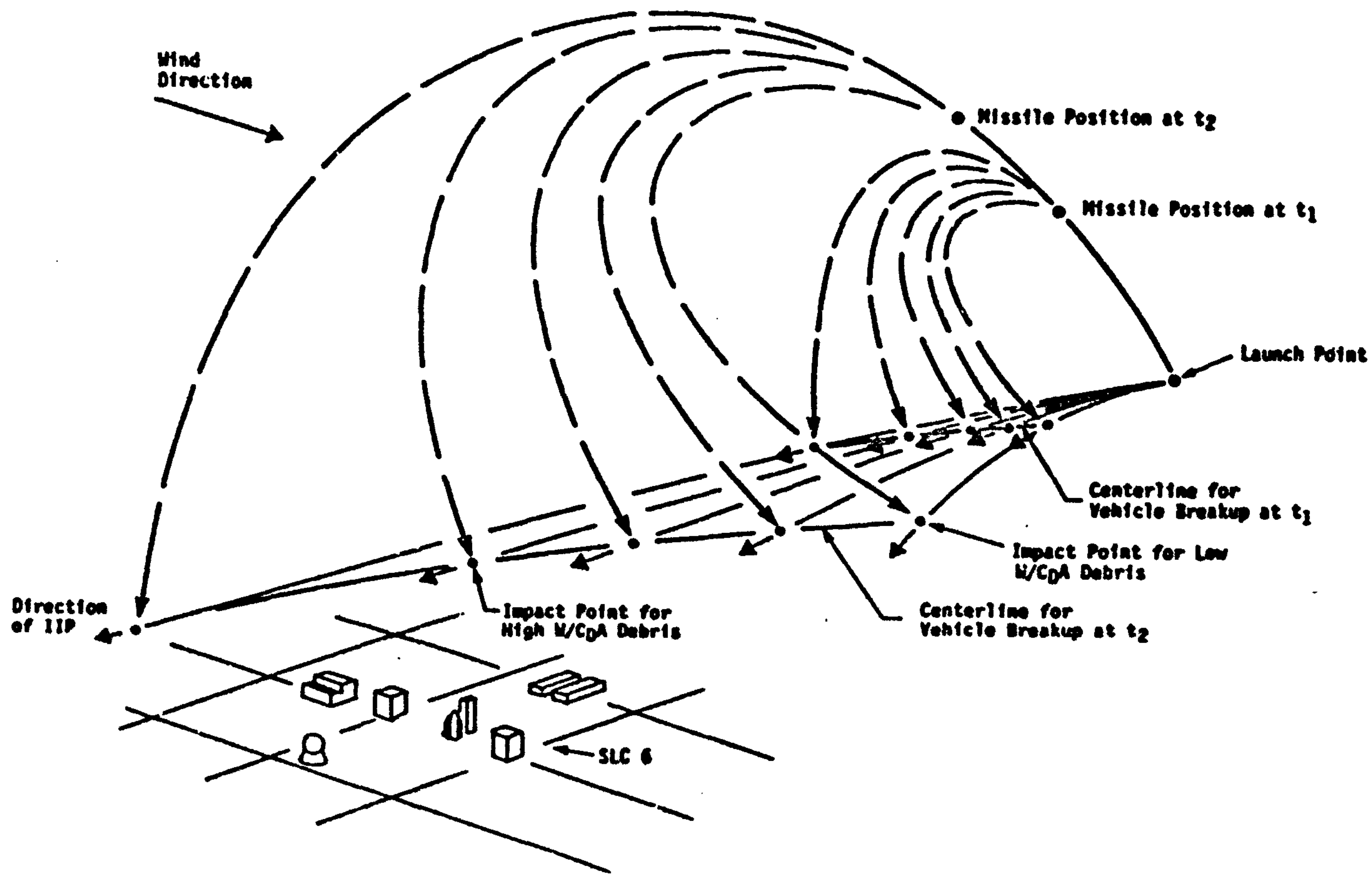

ACTA INC

ESSS/9/C6-8

CONTRIBUTION OF MALFUNCTION TURN TO IMPACT DISPERSIONS

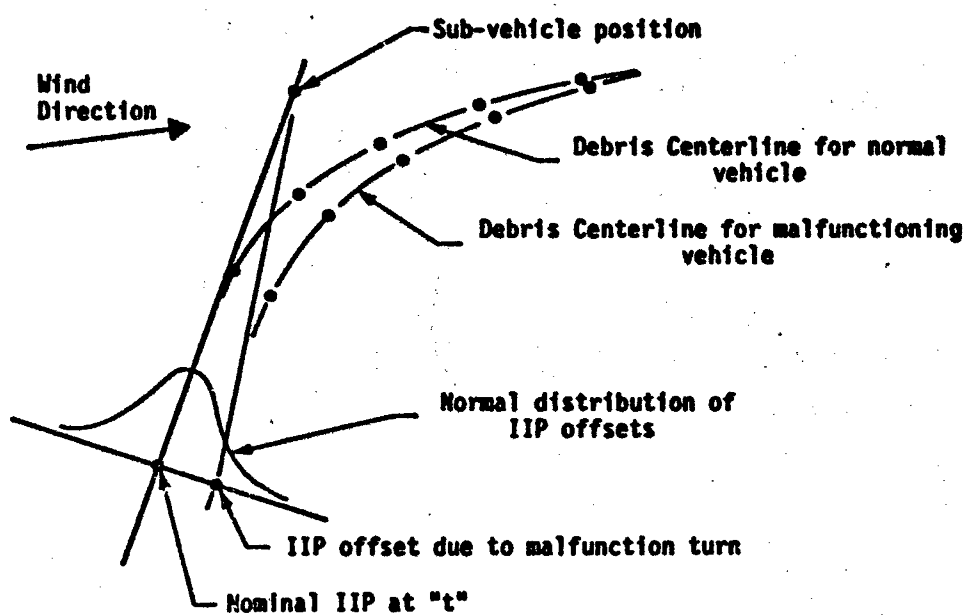

ACTA INC

CONTRIBUTION OF WIND UNCERTAINTY TO IMPACT DISPERSIONS

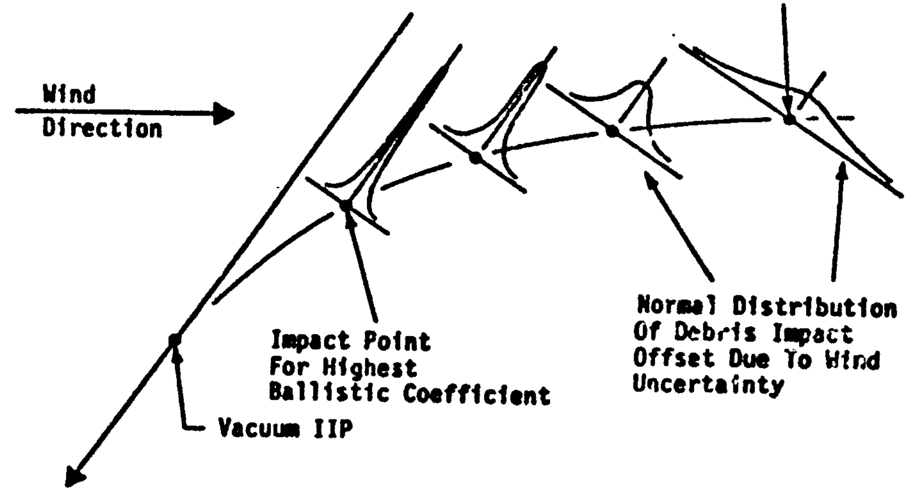

EXPLOSIVE BLAST DAMAGE MODEL

- VERY LIMITED DATA BASE.
- REVIEWED STRUCTURAL DAMAGE DATA FROM ACCIDENTAL EXPLOSIONS.
- USED NCEL STUDY (TANCRETO, 1981) AS A BASIS FOR DAMAGE AS A JOINT FUNCTION OF OVERPRESSURE AND IMPULSE.

$D = a\,P^b\,I^c, \qquad 0 \leq D \leq 100\%$

P - OVERPRESSURE (PSI)
I - IMPULSE (PSI-SEC)
a,b,c - CONSTANTS FIT BY REGRESSION

	a	b	c
WOOD FRAME HOUSE	7.99	2.07	0.30
LT. STEEL FRAME INDSTR. BLDG.	6.04	0.94	0.32
STEEL FRAME E.Q. RESIST. MULTI-STORY OFFICE BUILDING	3.80	0.67	0.38

ACTA INC

ES58/8/88-12

EXPLOSIVE BLAST DAMAGE MODEL (CONCL.)

- ADJUSTMENTS WERE MADE TO LIMIT UNREALISTIC DAMAGE FROM SMALL BUT VERY CLOSE EXPLOSIONS.
- DAMAGE PERCENTAGES ACCUMULATING TO GREATER THAN 60% DAMAGE TO A STRUCTURE FROM A SINGLE EVENT WERE AUTOMATICALLY SET AT 100%.
- FOR DIRECT EXPLOSIVE IMPACTS, PERCENT DAMAGE WAS COMPUTED USING (A SOMEWHAT ARBITRARY MODEL).

$$D = \frac{\pi d^2 W^{2e}}{\text{Bldg. Area } (ft^2)} \qquad 0 \leq D \leq 100\%$$

W - TNT EQUIV. WT. (LB.)
d,e - ESTIMATED CONSTANTS
(d RANGED FROM 10 TO 45, e = 1/3)

STRUCTURAL EVALUATION PROCEDURE

- USED NCEL CATEGORIES PLUS TWO ADDITIONAL AS GENERIC STRUCTURE TYPES.
- COMPUTED THE COEFFICIENTS FOR EACH OF THE GENERIC TYPES.
- SELECTED THE EIGHTEEN MOST SIGNIFICANT STRUCTURES AT SLC 6.
- VISITED EACH OF THE STRUCTURES AND ATTEMPTED TO PUT EACH STRUCTURE INTO ONE OF THE CATEGORIES.
- NO DETAILED ENGINEERING ANALYSIS WAS ATTEMPTED EXCEPT FOR THE LAUNCH CONTROL CENTER. THE RESULTS MUST BE CONSIDERED VERY APPROXIMATE SINCE MANY SPECIALIZED STRUCTURES DO NOT FIT THE GENERIC CATEGORIES VERY SATISFACTORILY.
- OBTAINED STRUCTURE VALUES FROM THE BASE ENGINEER. NO SPACE SHUTTLE COMPONENTS WERE INCLUDED.
- COMPUTED DOLLAR DAMAGE BASED ON PERCENT DAMAGE TO THE STRUCTURE TIMES THE DOLLAR VALUE OF THE STRUCTURE.

ESSB/6/89-14

TYPICAL SETS OF ISO-DAMAGE CURVES CONSTRUCTED USING $D = a\,P^b\,I^c$

OPERATIONS SUPPORT BUILDING (OSB)

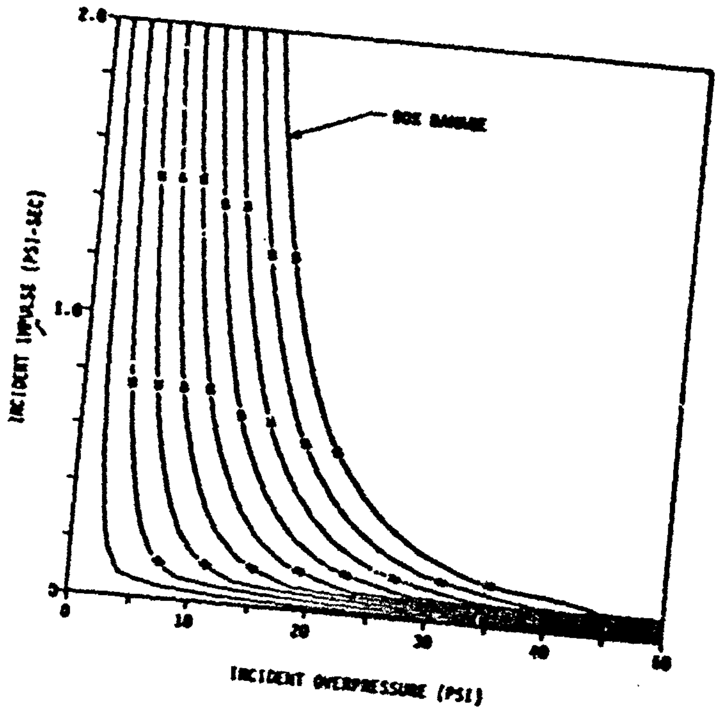

PAYLOAD CHANGEOUT ROOM (PCR)

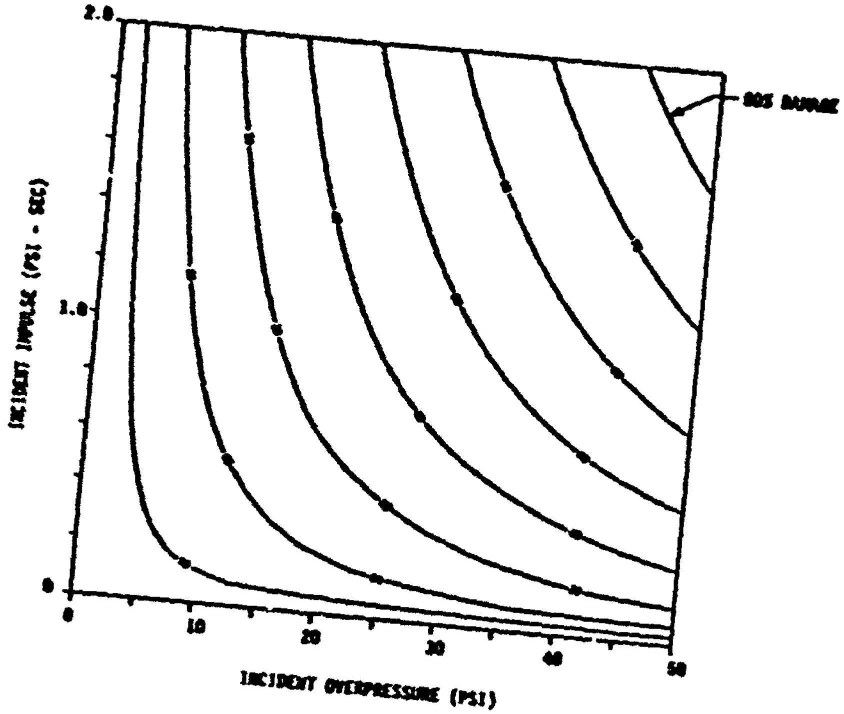

PROPELLANT DEBRIS CATEGORIES

PROPELLANT WEIGHT *	NUMBER OF FRAGMENTS	APPROX. W/C_DA
10	2800	50
35	1400	75
100	840	100
300	420	150
1000	140	220
5000	56	380
20000	11	600

* WEIGHT OF PROPELLANT. THE TNT EQUIVALENT WEIGHT WAS 7% OF THE PROPELLANT WEIGHT.

ESS8/9/88-18

MODELING APPROACH

- SIMULATE A SERIES OF DISCRETE ACCIDENTS (INDIVIDUAL SCENARIOS) WITH VEHICLE DEBRIS IMPACTS MOVING OVER THE FACILITY.
- EACH ACCIDENT HAS A PROBABILITY BASED ON THE PERIOD OF TIME BETWEEN DISCRETE ACCIDENTS AND THE VEHICLE FAILURE RATE.
- RANDOMLY SAMPLE VEHICLE CROSSRANGE DRIFT AND WIND EFFECT.
- COMPUTE THE DAMAGE TO EACH STRUCTURE BY EACH PIECE OF DEBRIS.
- COMPUTE TOTAL LOSSES FOR EACH SCENARIO.
- COMPILE AVERAGE DAMAGE AND PROBABILITY AS A FUNCTION OF DAMAGE LEVEL.

ACTA INC

TOP LEVEL FLOW DIAGRAM OF THE MODEL

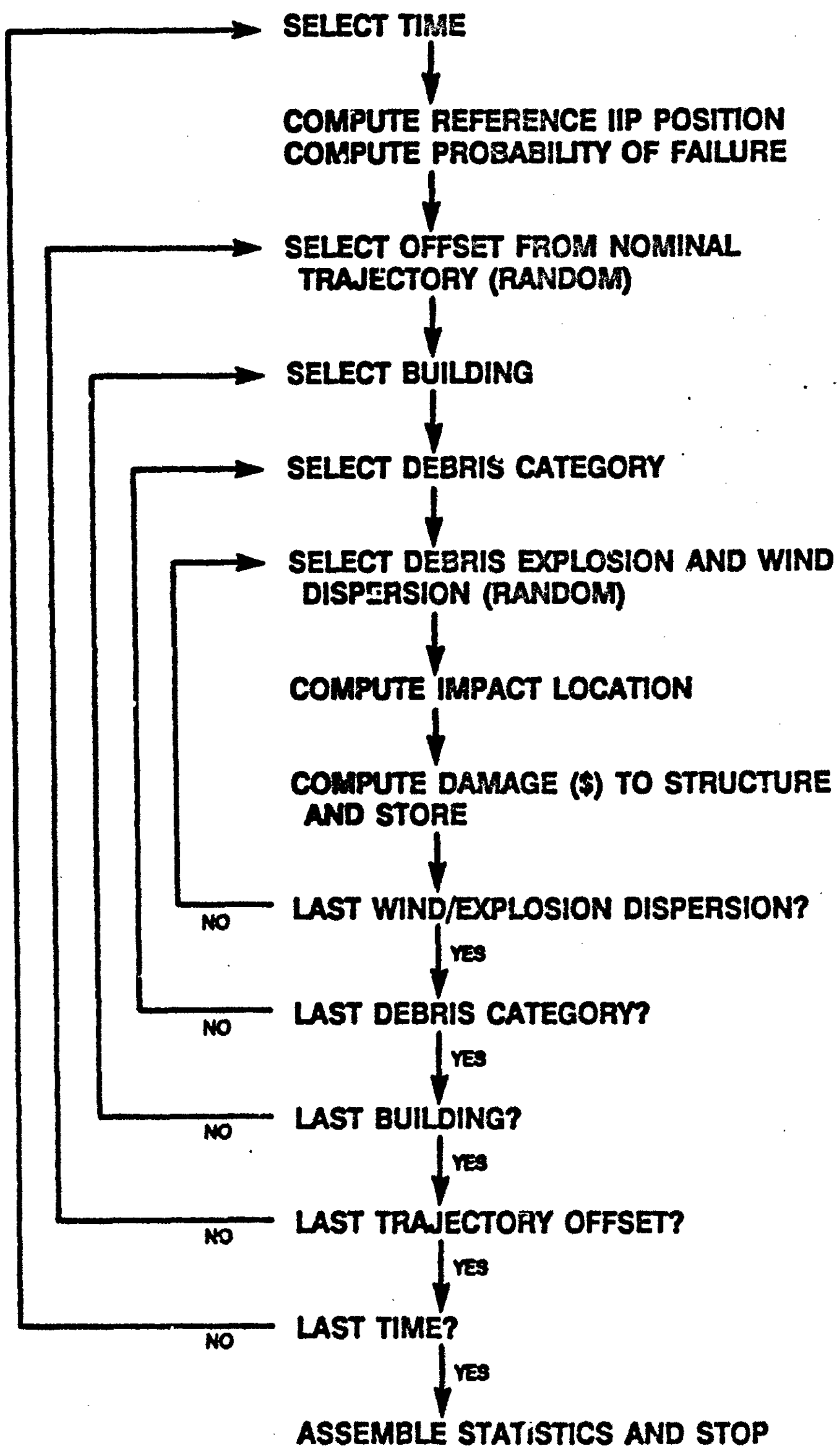

TYPICAL PROBABILITY VERSUS LOSS

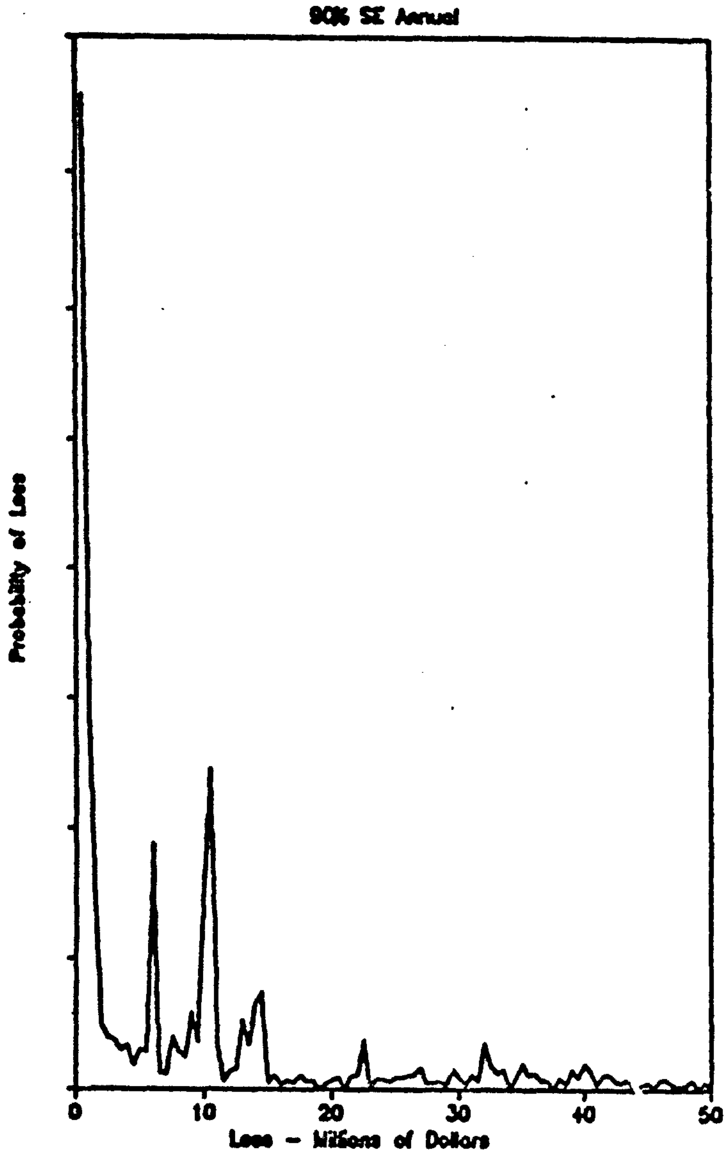

E88/8/88-18

RELATIVE LOSSES FOR VARIOUS WIND PROFILES

WIND PROFILE (IRIG, ANNUAL)	RATIO OF LOSS RELATIVE TO LOSS WITH AVERAGE WIND
AVERAGE WIND	1.0
N.E. 90% WIND	0.28
S.E. 90% WIND	5.27
S.W. 90% WIND	0.15
N.W. 90% WIND	0.12

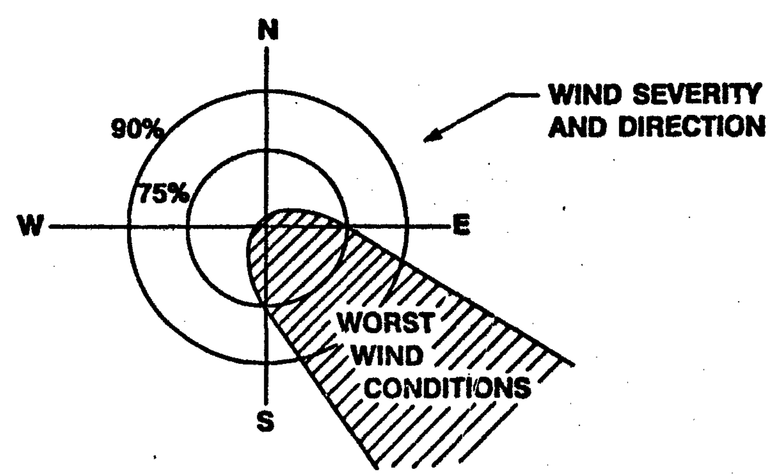

ACTA INC

ESSO/9/88-20

EXPECTED LOSS AS A FUNCTION OF LAUNCH AZIMUTH

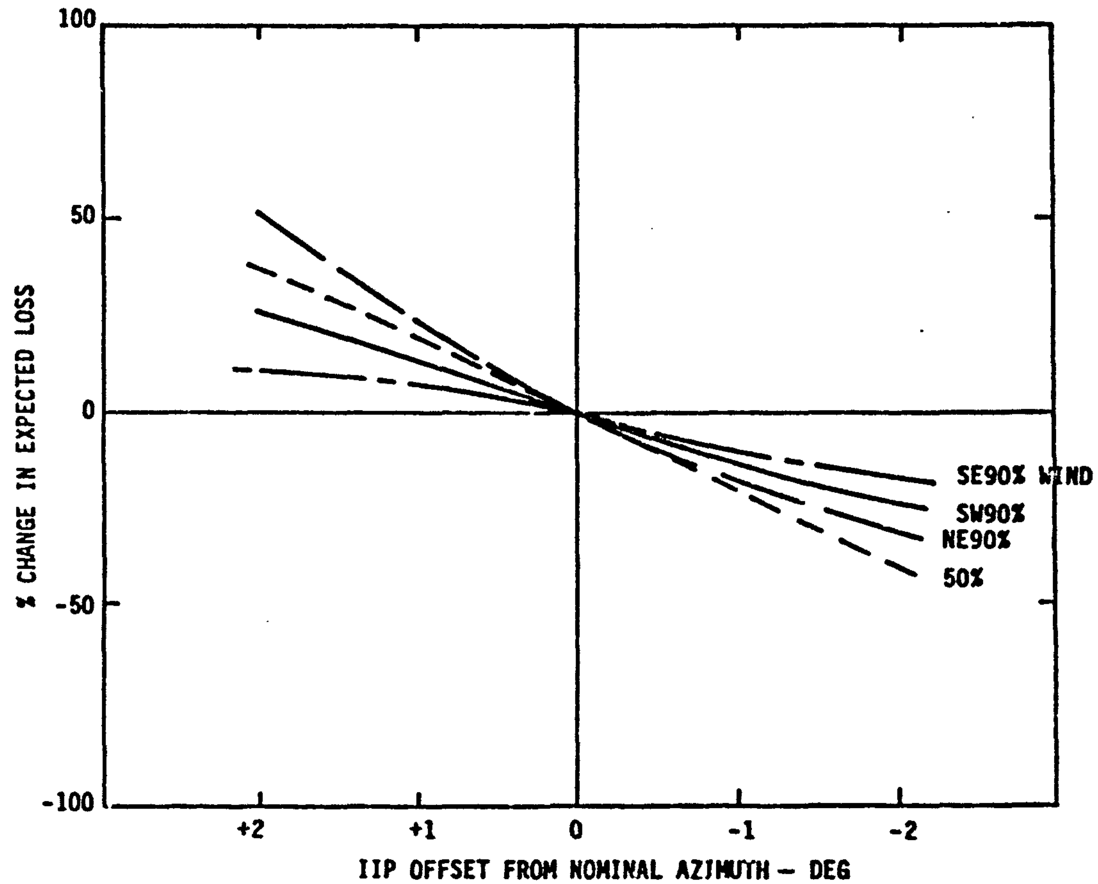

ACTA INC

ESS8/9/88-21

CONCLUSIONS

- NO HIGH PROBABILITY OF LARGE LOSSES.
- WIND CONDITIONS MORE IMPORTANT THAN CHANGING LAUNCH AZIMUTH.
- SUCCESSFULLY MODELED PROBABILITY OF LOSS AS A FUNCTION OF LOSS LEVEL.

ACTA INC

TERRAIN EFFECTS ON SHOCK WAVES AS MEASURED USING A 1:1300 SCALE MODEL OF REITERAPLE PROVING GROUND

G. Bulmash
G. Coulter
C. Kingery
A. Corriggio
R. Abrahams
R. Peterson

Ballistic Research Laboratory
Aberdeen Proving Ground, Maryland

Twenty-Third Department of Defense Explosives Safety Seminar
Atlanta, Georgia
9 - 11 August 1988

ABSTRACT

A 1:1300 scale model of the Reiteralpe Proving Ground large blast simulator and nearby countryside was constructed. The terrain was modeled by stacking 2.54 cm layers of plywood that had been cut to match the natural contours of the mountain; the plywood was smoothed over with plaster to obtain realistic natural contours. A model shock tube was machined from steel pipe having a 0.767 cm inside diameter. Tests were performed and measurements recorded at four geographical locations of interest. For the purpose of comparison, the shock tube was placed on a flat surface and blast parameters were also measured. This paper emphasizes the effects of the terrain on the shock wave and also discusses the problems encountered in modeling at small scale, such as scaling of materials from 1:1300 to full-size, signal to noise ratio, mechanical vibrations, and very small positive phase duration. Valid, consistent, and repeatable blast measurements were made within the shock tube and at four field locations. The shock waves measured at the field stations had the same magnitude as sound waves. At the two near field stations there was blast enhancement, because of reflection which occurred when the shock wave struck the valley floor at an angle and traveled up a slope. At the two far field stations there was blast attenuation, because the shock wave expanded when it entered the lower valley.

1. INTRODUCTION

The large blast simulator is a shock tube that was hollowed out of the Reiteralpe Mountain. It has a closed end inside the mountain and an open end which exits into the surrounding terrain. The facility was constructed to produce blast waves of up to one bar (14.5 psi). Because of the proximity of the shock tube to previously existing inhabited areas, shock wave related damage has occurred which in the past has inhibited the use of the facility. When a shot with a peak overpressure of 0.8 bars was fired, structural damages were incurred[1]. These damages included broken windows and even some minor damage to ceilings and walls in a neighboring village. In order to more fully examine these problems and document the terrain effects, a 1:1300 scale model was constructed of the Reiteralpe shock tube and nearby topography.

2. TEST PROCEDURES

2.1 Terrain Construction. The Federal Republic of Germany (FRG) provided the Ballistic Research Laboratory (BRL) with a contour map of the terrain in the region near the Reiteralpe Facility. The terrain model was confined to the region displayed on this map; see Figure 1 which is a reduced replica. The map provided by FRG describes the contours of the land at a 1:5000 scale. It was concluded that the map should be enlarged to a scale that would allow for a workable shock tube model. The first method of enlargement attempted was by the use of a pantograph which is a device consisting of four jointed bars in parallelogram form that may be used to copy on a predetermined scale. However, a pantograph large enough was not readily available, and it was determined that a great deal of time would be expended to get results by this method. The map was instead photographically reproduced and enlarged in sections roughly following the grid lines already present. By means of this sectioned augmenting process, the map was enlarged 3.8 times to a new scale of 1:1316 (In this paper, the scale is sometimes referred to as 1:1300 and at other times more exactly as 1:1316.) and covered a 2.6 x 3.4 meter (8.5 x 11 ft) area. An increase factor of 3.8 was as much as the available enlarging equipment would allow. To assure that all map sections had the same scale, the photographically enlarged sections were dried at room temperature instead of being heat dried which might have caused distortions.

A large space was cleared in a nearby warehouse to be the work area for this project. An indoor environment was chosen over an outdoor site primarily because of the weather factor. The cover of the warehouse would assure against any weather related side-effects during the actual testing. Additionally, working indoors also assured protection from inclement weather to the workers, maps, and construction tools. The building material chosen for construction of the terrain was plywood because it was readily available in a standard size and thickness of 1.2 m x 2.4 m x 2.54 cm (4 ft x 8 ft x 1 in) and because of its structural stability. A 3.7 x 3.7 meter (12 x 12 ft) platform elevated 15.2 cm (6 in) above the ground was assembled to provide a level base on which to work and plenty of room for cables to run underneath. Fortunately, the 1:1316 scale allowed for a very convenient transference of actual height to scale height. The major map contours ascend in 100 meter increments which converts to 7.62 cm (3 in) at 1:1316 scale with an error of 0.26%. In other words, three thicknesses of plywood equals a scale height of 100.26 meters. So, every 100 meter increase in height on the German mountains would constitute a 7.62 cm height increase on the model. A base altitude of approximately 500 m above sea level was found along the Saalach River near Reiterpoint and deemed the low point on the map. All height delineations were made referencing 500 m as the base, thus placing any altitude from 500-599 m (mostly all of the river basin) flat on the platform. Seven levels or 21 layers of plywood were needed to model the highest mountains on the test site which corresponds to 1200 m above sea level. Figure 2 shows some construction details of the plywood terrain.

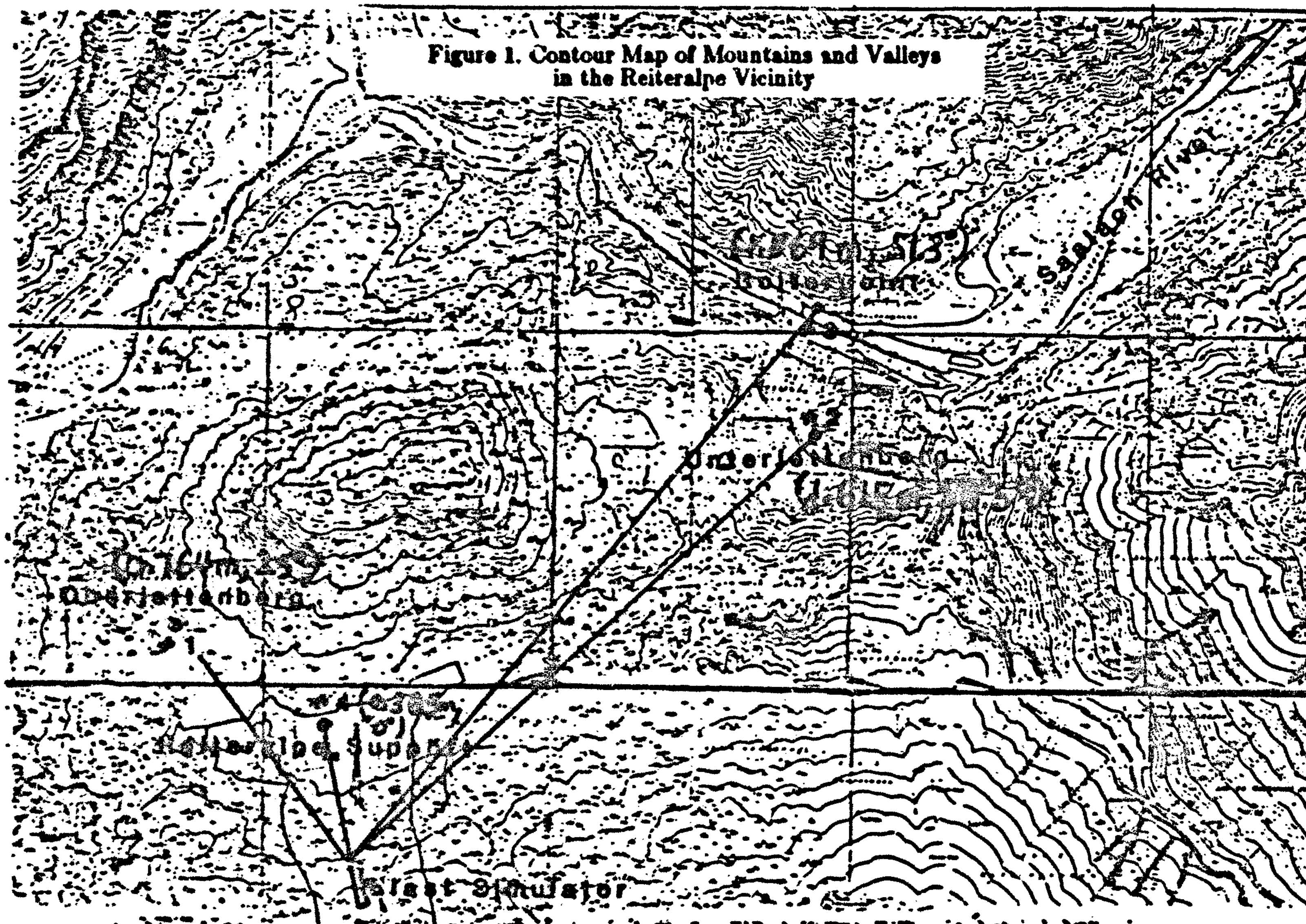

Figure 1. Contour Map of Mountains and Valleys in the Reiteralpe Vicinity

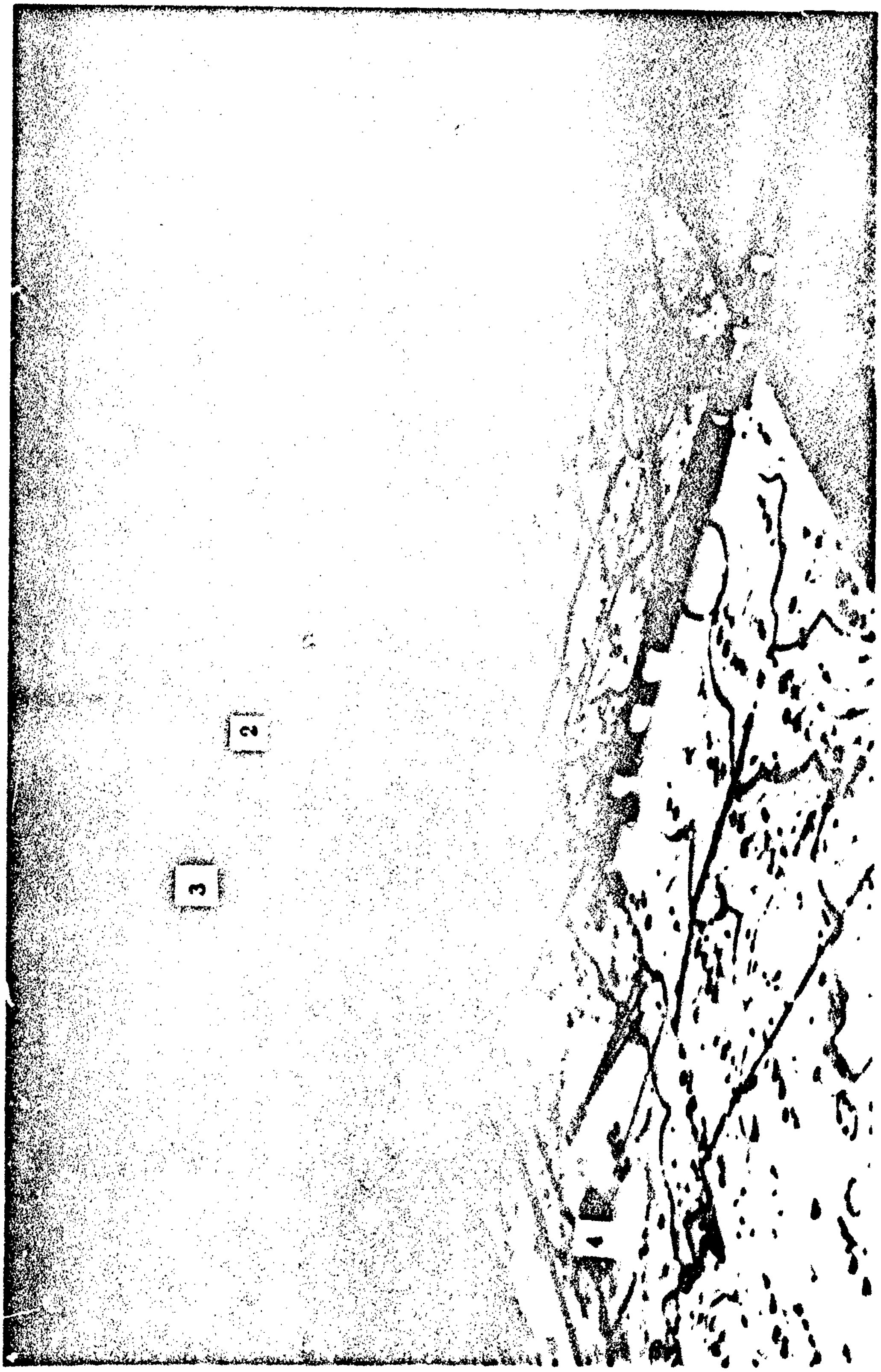

Figure 2. Construction Details of Terrain Model

The wooden contours were covered with plaster in the critical areas to get the finer details of the altitude modeling; a photograph of the test site is shown on Figure 3. In the less critical regions, the plywood was covered with firmly packed soil.

2.2 Shock Tube Model. According to Reference 1, the Reiteralpe large blast simulator has a total length of 106 m, and a cross-section of 76 meter square. The floor is 13 m wide, and the height is 7 m with a 2.5 m vertical part and a semicircle on top. The blast wave generator or driver consists of 144 pressure bottles 6.34 m long clamped horizontally into a frame resting against the shock tube back wall.

From the dimensions reported in Reference 1, the cross-sectional area was calculated to be 75.3 meter square which is 0.7 meter square less than the number reported therein. Using 75.3 m as the cross-sectional area resulted in a hydraulic diameter of 9.79 m. Scaling by 1:1316 gave a hydraulic diameter of 0.744 cm (0.293 in). The scaled shock tube was constructed out of steel pipe having a nominal inside diameter of 0.767 cm (0.302 in). This means that the scaled tube is 3.1% larger than it should be. This small systematic error was considered acceptable for several reasons. It was not possible to locate a drill bit that would allow for machining a pipe to exactly 0.293 in. Also the error was on the conservative side and thus would give higher field pressures than a 0.293 in tube. Lastly, the cross-sectional area reported in Reference 1 was slightly larger than the area used herein.

It was infeasible to scale the 6.34 m high pressure gas bottles by 1:1316 so a simple compressed air driver which was filled from a pair of 6.9 bar (100 psi) bottles was used. The length of the driver, including air in the control valve, was 7.1 cm (2.8 in). The diaphragm material was 0.00635 mm (0.25 mil) mylar for the low pressure range and 0.0127 mm (0.5 mil) mylar for the high pressure range. Mylar was easy to cut, easy to handle, and gave consistent, repeatable results. The mylar diaphragm was ruptured by piercing it with a pin placed in a 1 mm hole in the downstream tube wall. (Other materials that were tried as diaphragms at this scale gave interesting but negative results. Ordinary writing paper was far too strong, aluminum foil was hard to handle without causing wrinkles and therefore did not give repeatable results, and wax paper became porous under pressure.) The downstream or test section of the shock tube was 30.5 cm (12.0 in) long. The driver to test section length ratio was chosen to give a flattop wave at the exit. An Endevco pressure transducer was placed 5.1 cm (2.0 in) from the open end to record the shock pressure within the tube near the exit. The operational shock tube may be seen on both Figures 2 and 3.

The shock tube was very easy to operate and had a turnaround time of only ten minutes. The circular mylar diaphragm was punched out of a sheet of mylar using a custom made hole punch and was placed on an O-ring that was seated at the end of the driver. The downstream section was screwed into the driver forming a pressure tight seal at the O-ring.

2.3 Instrumentation. Pressure-time data were recorded at five locations, one within the model shock tube using an Endevco gage Model 8510 and at 4 field positions using Susquehanna yellow dot gages Model ST-2. Neff Model 122 amplifiers, rated at 100 kz, were used to amplify the gage signals. Pacific Instruments Model 9820 transient data recorders, having 12 bit resolution and a 2 microsecond sampling rate, were used to digitize and store the data which was then transferred to a Hewlett Packard (HP) Model 9807A Integral Personal Computer. The HP electroluminescent monitor produced a graphic display that facilitated analysis of the shots. This very efficient data acquisition scheme made it possible to fire many shots with little turnaround time. In the event of a misfire, erratic diaphragm break, or instrumentation error, a quick look at the shock tube gage record was all that was needed in order to decide to throw out the shot and repeat it. Good shot pressure-time records were then plotted out using an HP Thinkjet printer. The records were

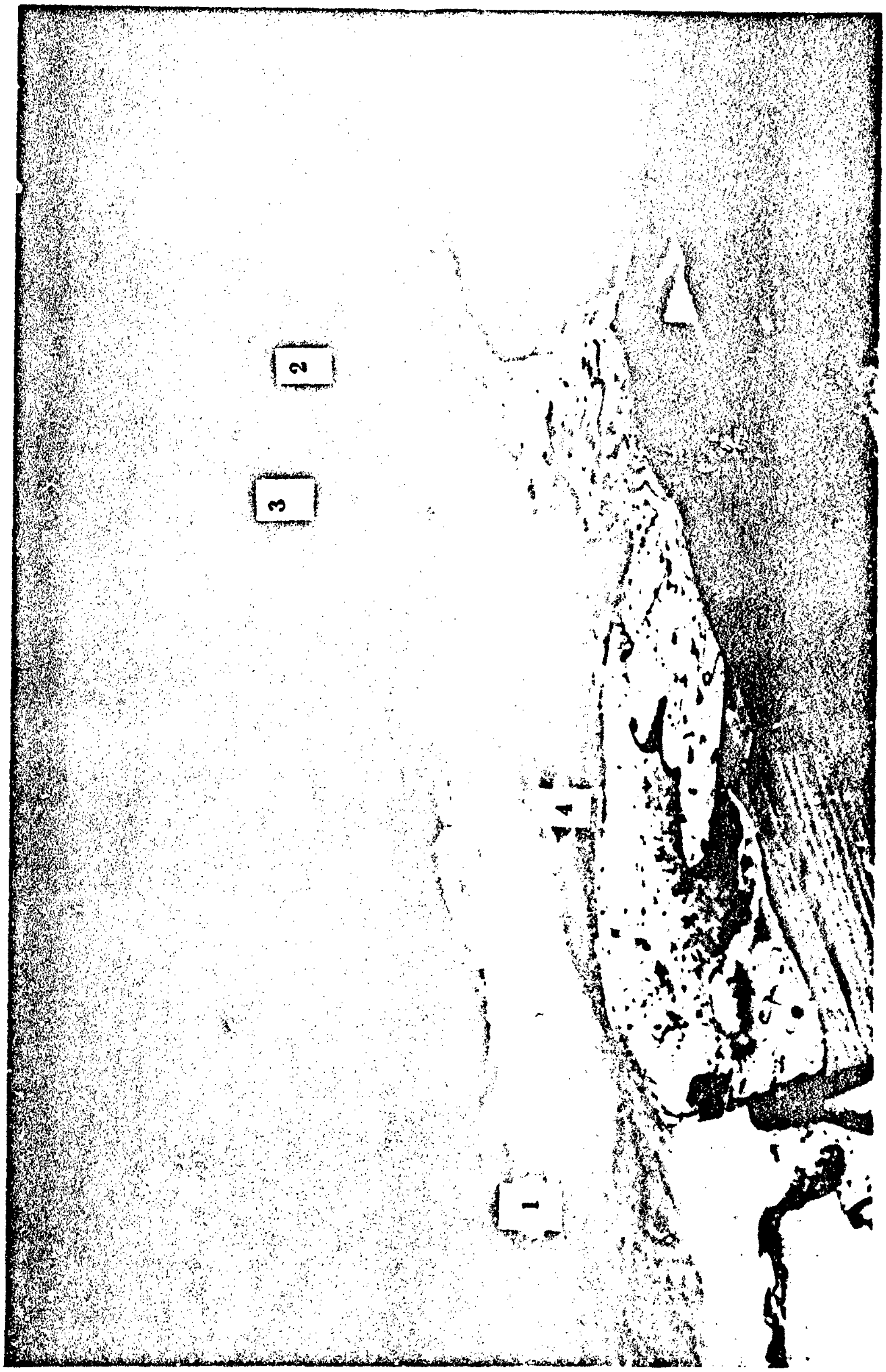

Figure 3. Terrain Model Covered with Plaster and Soil

stored on a 3.25 in, double density, double sided, 1.2 megabyte floppy disks and transferred to cassette tapes for further reduction on a Tektronix 4052A micro-computer, 4631 hardcopier, and 4662 plotter.

The Endevco gage was chosen for the shock tube station because the gage has a 2.34 mm (0.092 in) case diameter with a 1.25 mm (0.05 in) diameter sensing element. A small diameter gage was needed since the shock tube diameter is 7.67 mm (0.302 in), and a larger gage would have obstructed the flow that was being measured. This type gage had one noticeable disadvantage. It has a natural frequency of 100 kz and this periodic ringing was evident on each shock tube station record. The ringing was filtered out by smoothing the records on the Tektronix 4052A computer.

The Susquehanna gage was chosen for the field stations because no other available gages would adequately record these short duration, extremely low pressure records. PCB Inc. piezoelectric gages, having a quartz sensing element, were not sensitive enough to record low pressures. The electronic signal to noise ratio made the records useless when these gages were tried. The Susquehanna gages have 200 kz natural frequency and 100 mv/psi sensitivity, but are unstable to temperature changes. The temperature instability is inherent to gages having a sensing element composed of manmade ceramic crystal material. The temperature problem was solved by calibrating each gage from 60° F to 100° F in 10 degree increments, recording the temperature at the time of each shot, and then making a scalar correction to the gage calibration level. Since only short duration waveforms were being measured, AC coupling was used to cancel most of the baseline drift which was a result of the temperature sensitivity. The Susquehanna gage element diameter is 1.27 cm (0.5 in)

The 1:1300 scale imposed difficulties on the ability of the instrumentation to adequately capture and record the shock. The most significant losses in the field records were a result of the amplifier response time and the yellow dot gage crossing time. As much as 20% of the field record peak pressures may have been lost because of the instrumentation limitations. The largest losses for the shock tube gage were caused by the gage response time and the amplifier response time. The shock tube station losses were insignificant.

2.4 Experiments. Experiments were conducted on the free field plaster board to establish a baseline to compare with results from the topographical model. After this baseline was established, experiments were performed on the topographical model. Shots were fired at two pressure levels, nominally 55 and 96 kPa shock tube exit pressure. Before experiments were conducted on the plaster covered model, preliminary tests were performed on the model which was covered with firmly packed soil. The soil was too rough, granular, and porous to be used on a 1:1300 scale model. Therefore, the pressures recorded on the soil model were low and at the far field stations difficult to interpret. Using a plaster model increased the pressures and made it much easier to interpret the records. Also, the field gages were shock mounted on the plywood board by emplacing the 5.08 cm (2 in) brass gage mounts in oversized mounting holes within the plywood and cushioning the mounts with foam rubber and duct seal (a malleable filler); this was done to reduce the signals transmitted to the gages by mechanical vibration of the solids and was very effective. Even with this measure, however, because the system was recording Pa level pressures, there was still some noise superposed on the records which made it difficult to determine the baseline. To be consistent, the baseline for each record was determined in the same manner; it was set to 0 Pa at the shock discontinuity.

3. RESULTS

The results are summarized in Table 1 and presented graphically in Figures 4 - 8 where the test label 'Plaster FF' refers to the plaster covered flat surface, and the label 'Plaster Model' refers to the plaster covered terrain model.

Table 1. Peak Pressure at the Four Field Gage Positions

Shock Tube Station Pressure (kPa)	Test Configuration	Field Pressure (Pa) Station			
		1	2	3	4
55	Flat Surface	141	54	47	390
	Terrain Model	195	25	18	487
96	Flat Surface	270	86	69	716
	Terrain Model	354	43	32	772

The four gage positions were provided by the FRG and are indicated on Figures 1 - 3. Station 1 is at Oberjettenberg, 0.764 m from the shock tube open end and at an angle of 25° with respect to the shock tube axis; Station 2 at Unterjettenberg, 1.615 m and 58.5°; Station 3 at Reiterpoint, 1.869 m and 51.3°; and Station 4 at the Reiteralpe support facilities, 0.365 m and 0°.

4. DISCUSSION

Figure 4 shows the shock tube exit pressure records at low and high pressure for each plaster shot configuration. These shots were chosen for comparison because the exit pressures are quite similar. Figures 5 - 8 compare the records at Stations 1 - 4 at both low and high pressure. The most important phenomenon observed was the pressure enhancement on the topographical model[2] at Station 1 which was caused by a reflection as the shock wave moved up the slope. Station 4, which is located in the valley directly in front of the shock tube also shows an enhancement because of the reflection that occurs when the shock wave reaches the flat area at the bottom of the valley. Stations 2 & 3 show a clear blast attenuation when compared with the flat surface.

The free field plywood surface results for Stations 1-4 are compared with Equation 1.

$$P_{ss_v} = \frac{B_1 P_{ss} \left(\frac{d}{R}\right)^{B_2}}{1 + \left(\frac{\nu}{B_3}\right)^2} \qquad (1)$$

where,
P_{ss_v} is the expected overpressure in the environment
$B_1 = 1.2 \pm 0.2$
$B_2 = 1.35 \pm 0.08$
$B_3 = 56° \pm 3°$
P_{ss} is the overpressure in the tunnel outlet
d is the tunnel diameter

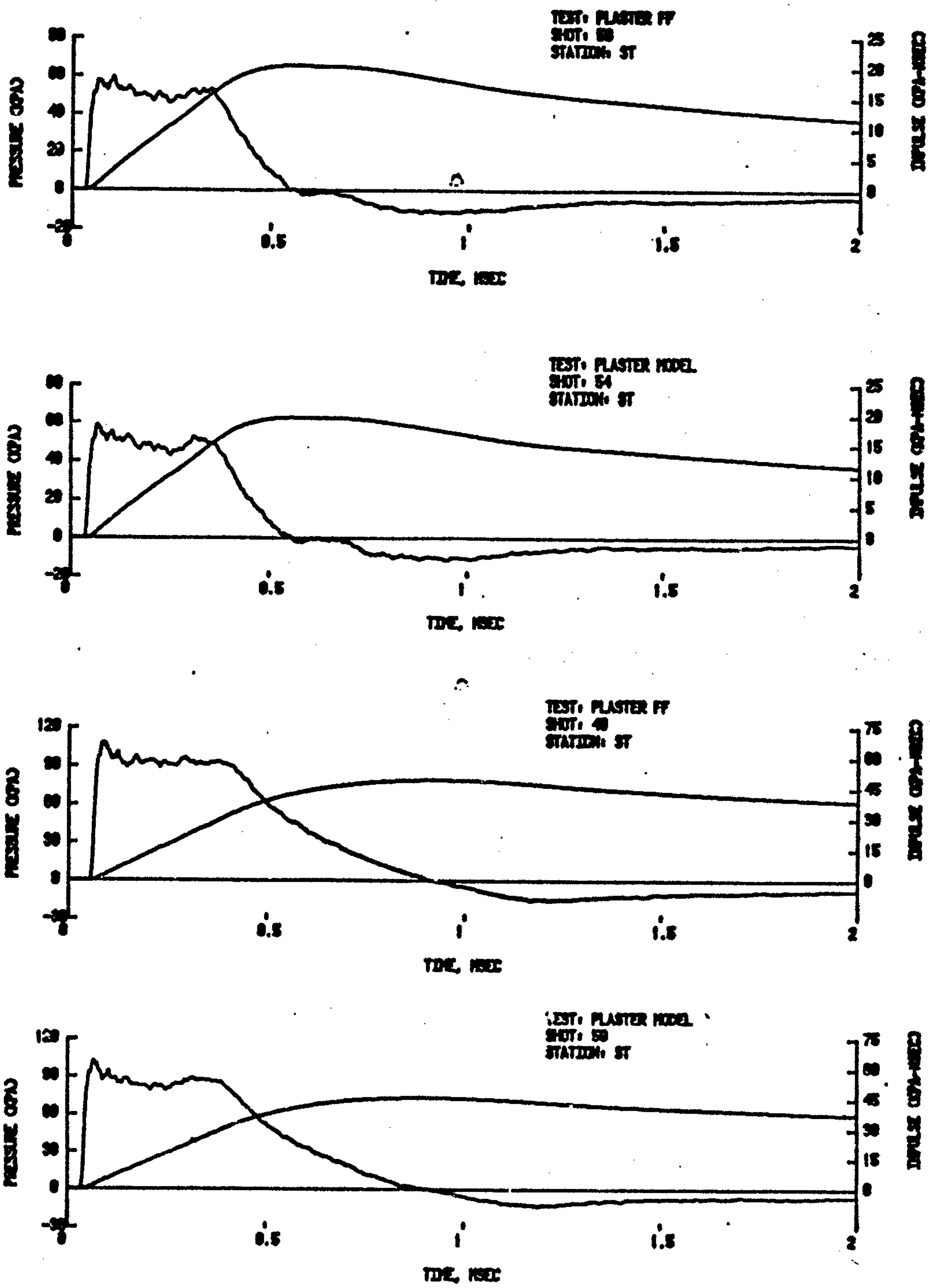

Figure 4. Shock Tube Station Records for Each Test Configuration

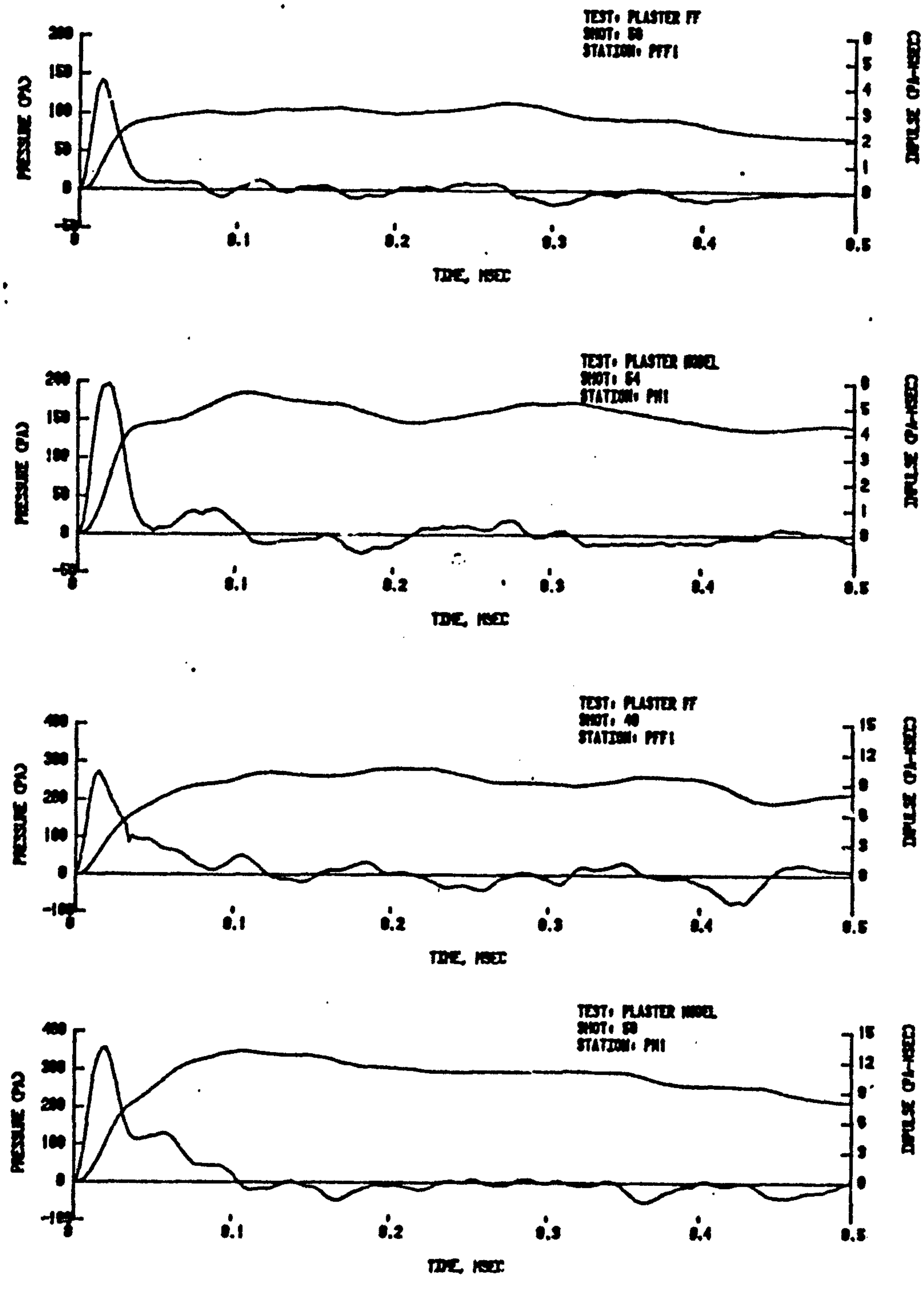

Figure 5. Pressure-time Records at Station 1

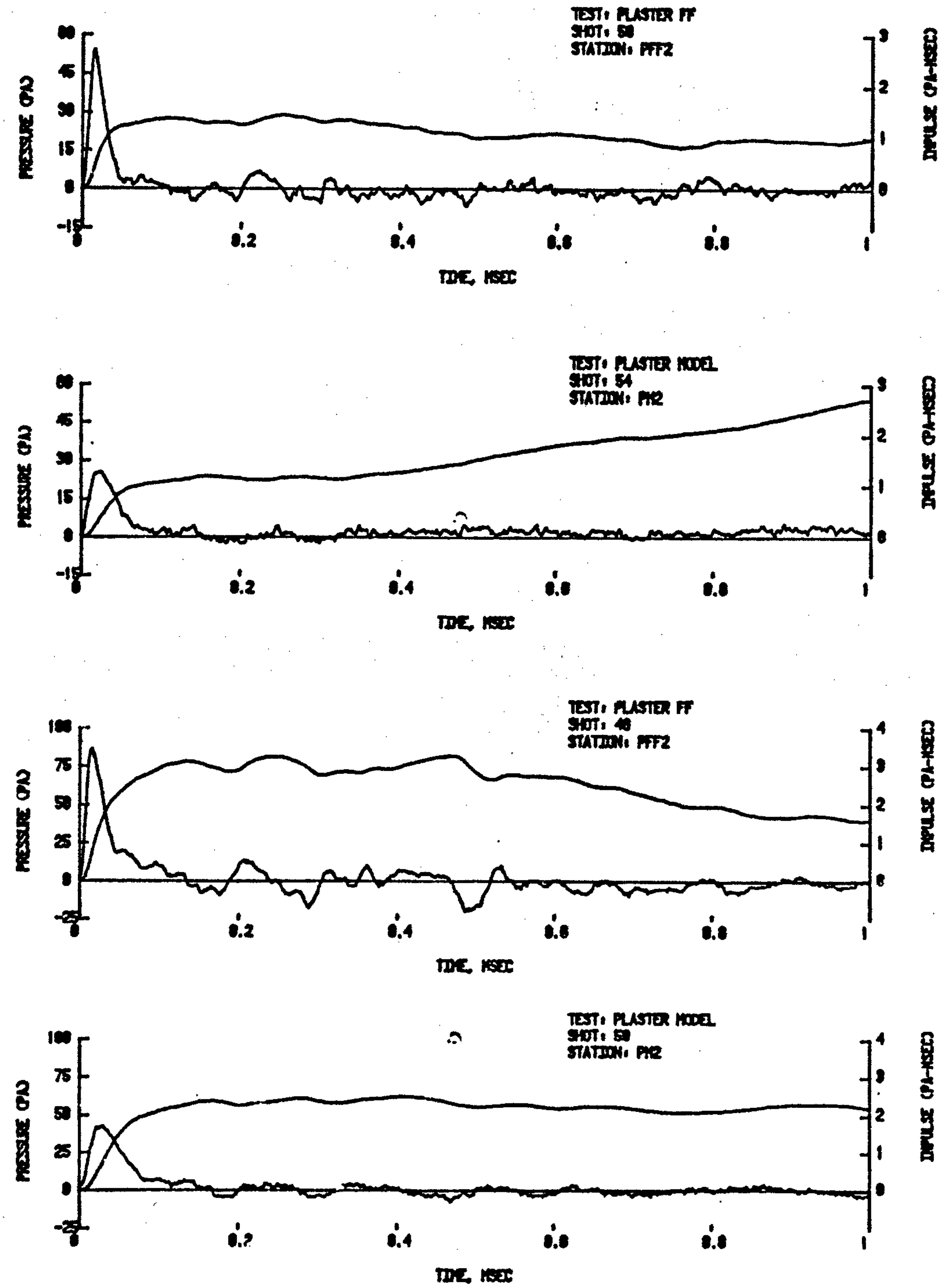

Figure 6. Pressure-time Records at Station 2

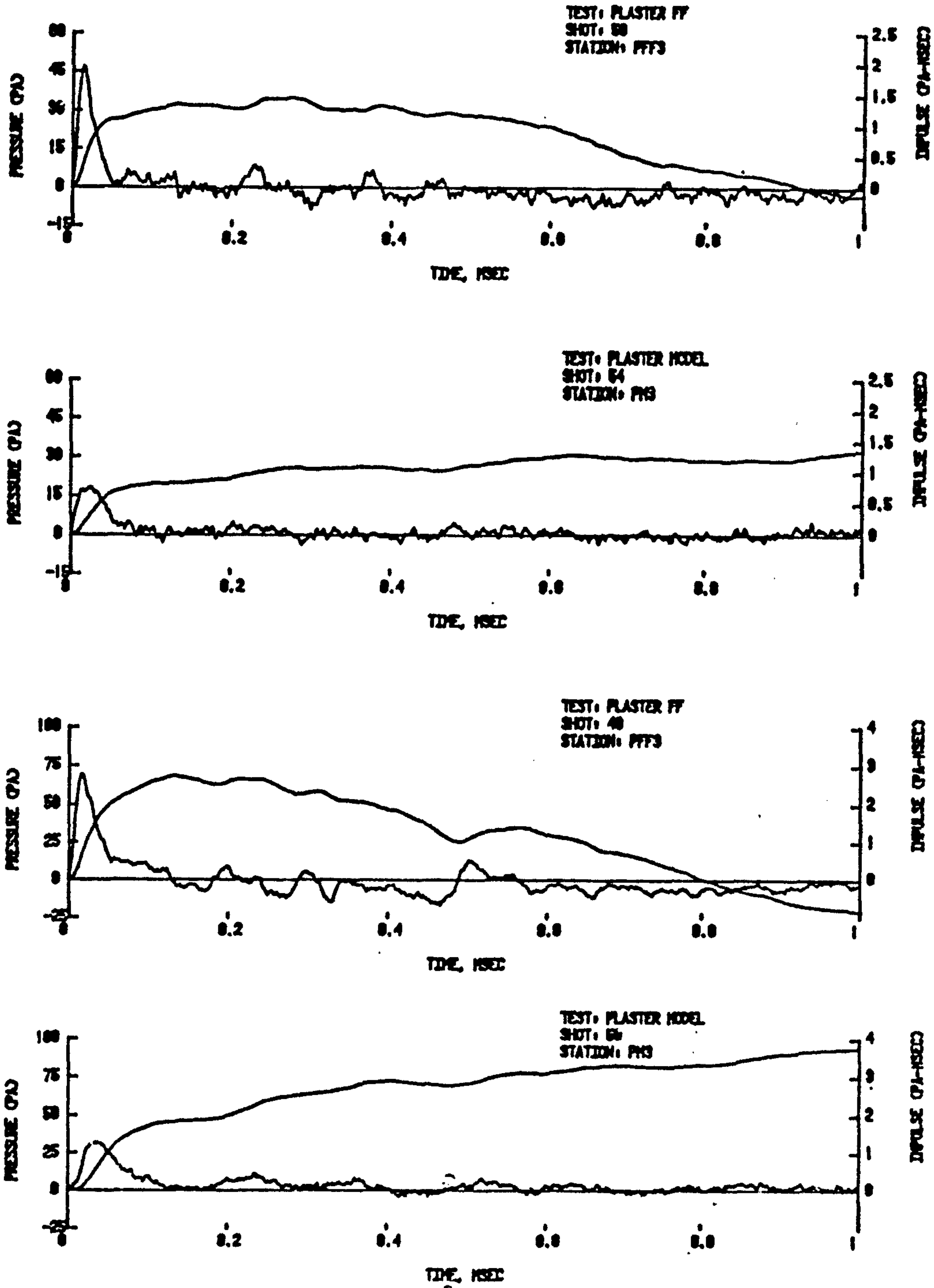

Figure 7. Pressure-time Records at Station 3

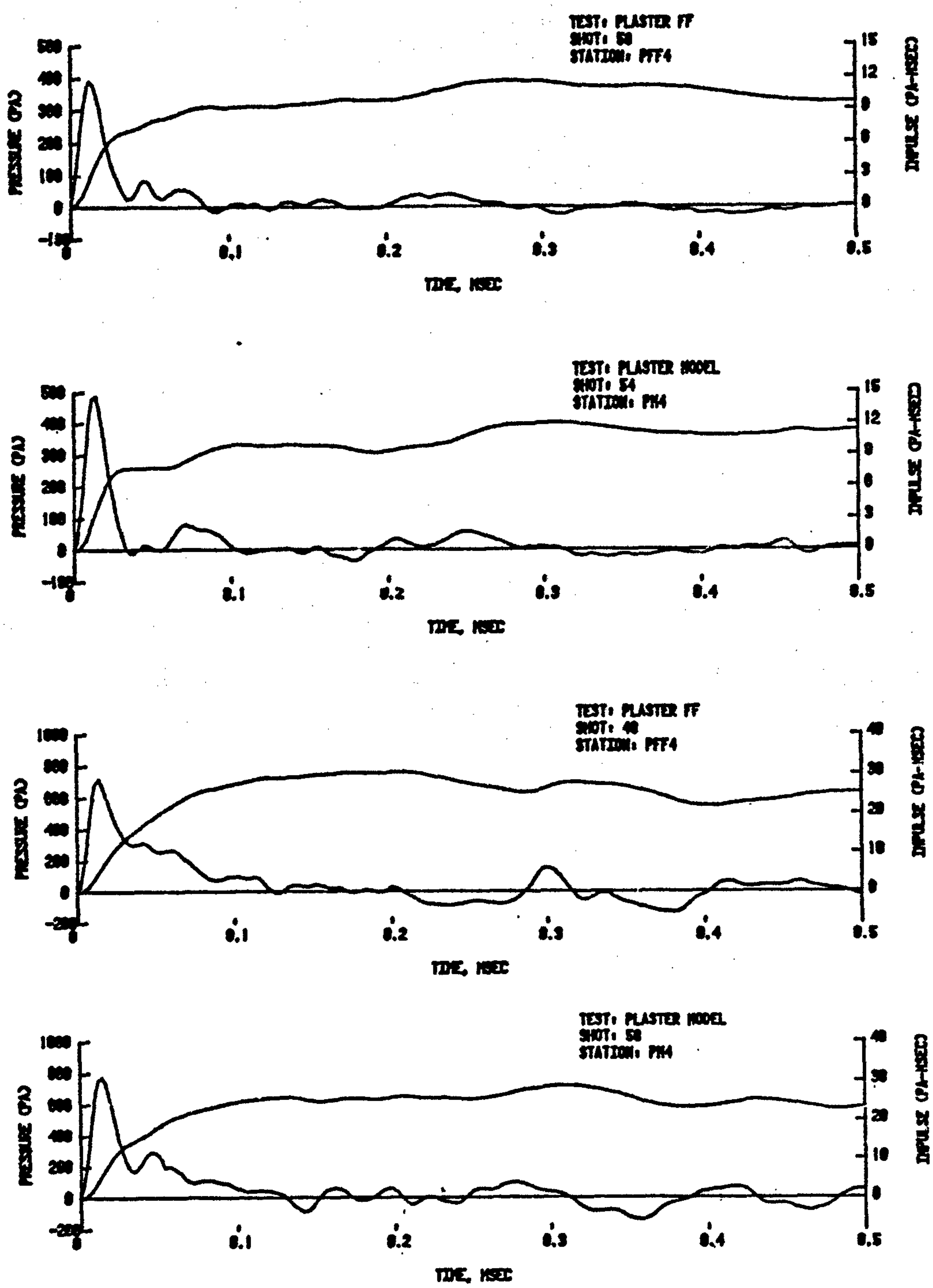

Figure 8. Pressure-time Records at Station 4

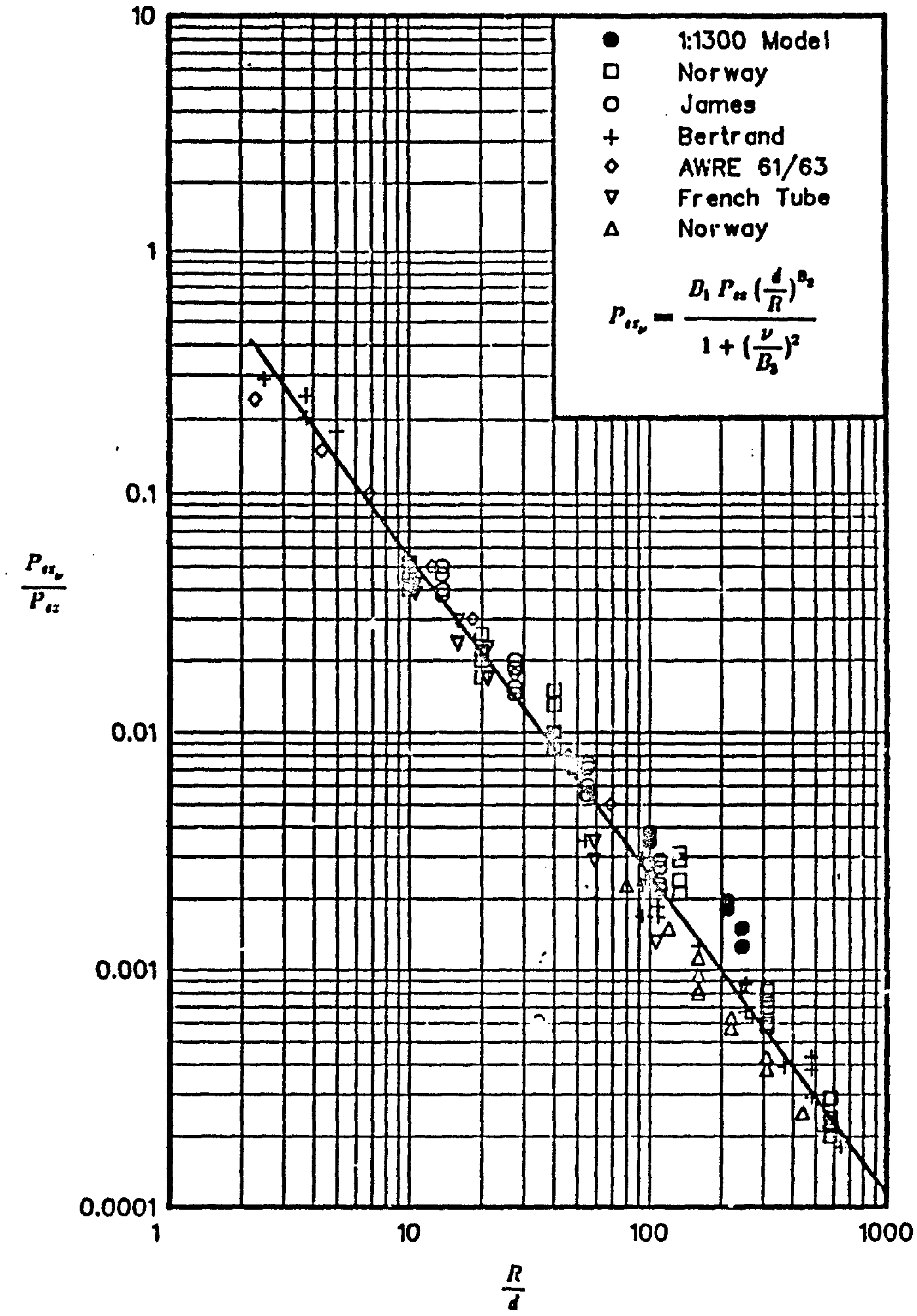

Figure 9. Comparison of Equation 1 with Scale Model Results and Other Data

R is the distance between the tunnel outlet and the object in the environment, and
ν is the angle between the tunnel axis and the radial R.

This formula was reported by Dr. Amann of the Ernst Mach Institute as indicated in Reference 1. (In Reference 1, $B_2 = 1.35 \pm 0.8$) The equation is an empirical fit to data; it was reduced from experiments where TNT charges ranging from 9.5 gm to 151.5 gm were detonated in a non-responding chamber connected by a passageway (tunnel outlet) to the outside environment and was reported at *MABS* 5.[3] According to Reference 3, the data was compared with data from compressed air shock tubes, and the fitted parameters showed qualitative agreement. Kingery[4] has compared this empirically derived equation with other similar equations and found that for a large variety of explosive and shock tube data Equation 1 adequately predicts the environmental overpressure. The predictions generated by Equation 1 are shown as a straight line on Figure 9 and may be compared with the experimental results and other data. A comparison indicates that the results measured on this 1:1300 scale flat surface are similar to what would be measured at full scale.

5. CONCLUSIONS

The enhancement at Station 1 and the attenuation at Stations 2 & 3 are real effects that are present at Reiteralpe. The enhancement at Station 4 may or may not be occurring at Reiteralpe, depending upon just how well the 1:1300 scale model simulates the topography at this near field position.

ACKNOWLEDGEMENTS

There were many people who graciously assisted with this project. Each one would have willingly helped more if required, and the authors are sincerely appreciative. They are John Sullivan, Peter Muller, George Teel, Jim Bernhardt, Ken Holbrook, Brian Bertrand, John Simansky, and Rick Thane all from the Blast Dynamics Branch at BRL. We particularly wish to thank the US Army Ordnance School Photography Laboratory for creating a 2.6 x 3.4 m photograph of the Reiteralpe contour map.

LIST OF REFERENCES

1. J. Ackerman and L. Klubert, "The New Large Blast Simulator of Reiteralpe Proving Ground," Ninth International Symposium on Military Applications of Blast Simulation, Oxford, England, Sept. 1985.

2. K Kaplan, "Effects of Terrain on Blast Prediction Methods and Predictions," Scientific Services, Inc., Redwood City, California, BRL Contract Report ARBRL-CR-00364, Jan. 1978.

3. A. T. Skjeltorp, A. Jenssen, A. Rinnan, "Blast Propagation Outside a Typical Underground Ammunition Storage Site," Fifth International Symposium on Military Applications of Blast Simulation, Stockholm, Sweden, May 1977.

4. C. N. Kingery, "Survey of Airblast Data Related to Underground Munitions Storage Sites," Ballistic Research Laboratory, Aberdeen Proving Ground, Maryland, Technical Report, to be published.

HOB AIRBLAST FROM 1000-LB CANDIDATE
CHARGE DEVELOPMENT EXPLOSIVES

R. E. Reisler, L. A. Dixon, J. H. Keefer

ABERDEEN RESEARCH CENTER
30 DIAMOND STREET, P. O. BOX 548
ABERDEEN, MARYLAND 21001

301 272-4200

HOB AIRBLAST FROM 1000-LB CANDIDATE CHARGE DEVELOPMENT EXPLOSIVES

INTRODUCTION

High explosives have been used rather extensively over the past 25 years as a blast source for research in many weapons effects testing programs. TNT was used in block built configurations for large multi-ton charges and in castable spherical form in the 1000-216 lb weights. Airblast recorded from many of these events exhibited numerous anomalies and in some well documented instances produced a shock which propagated out in front of the main wave. Efforts to resolve these anomalous effects were less than successful.

In the 1970's, TNT for multi-ton charges was replaced by contained ammonia nitrate fuel oil (ANFO). One thousand pound testing programs began using cast Pentolite spherical charges anticipating an improvement over the TNT; however, anomalous conditions continued to occur although on a reduced scale.

In 1982, the Denver Research Institute (DRI) conducted a series of 8-lb tests comparing HMX based explosive PBX 9501 and LX-10 with Pentolite.[1] Sharp, clean shocks were observed from the photography of the fireball from the HMX explosive and clean waveforms were seen in the pressure records. The Pentolite, on the other hand, did not show a clean shock break away from the detonation products and the waveforms were not as good as those from the HMX. These tests prompted an investigation of HMX-based explosives as candidates for a charge development study. When it was discovered that the pressed PBX and LX-10 materials could not be obtained for charge weights greater than 64 lbs, attention was directed toward solid propellants.

---

[1] Wisotski, J. and Plooster, M., "Comparison of Blast Parameters from HMX-Based Explosives to Cast Pentolite," Denver Research Institute, DNA Report TR-81-155, June 1982.

A listing of the characteristics desired of a high explosive charge for high fidelity blast studies was developed and is presented in Table 1. The most important features are the capability to generate a symmetrical and a repeatable blast wave.

Contacts made with a major manufacturer of solid propellants, the Morton Thiokol Inc., resulted in the casting of 8-lb charges using their formulation TPH 3342 which contains 85% HMX. The DRI tested these charges in 1984 and found the results to be very gratifying.[2] The Ballistic Research Laboratory (BRL), under the auspices of the Defense Nuclear Agency (DNA), followed this work with an order for three 500 kg (1100 lb) spherical charges.

Concurrent with the production of the three Morton Thiokol charges, the IRECO company was working with the Air Force Weapons Laboratory to produce a composite castable explosive designated IRESET A-1. The basic material of this composite is ammonium nitrate and since a booster is required for detonation, charges of the 8-lb scale were not produced. Instead, larger charges were cast for the 1000-lb range where 1500 lbs of material was needed to gain the blast equivalency of 1000 lbs of TNT.

Characteristics of the two charge materials are given in Table 2. The TPH 3342 has a high density and a high detonation velocity, is detonable without boosting using an exploding bridge wire but is not oxygen balanced. The IRESET, on the other hand, has a low density and a low detonation velocity, requires a booster to detonate but is oxygen balanced. A spherical container, in this case an aluminum sphere, was placed in the IRESET during the casting process to hold 850 cc of sensitized nitromethane added at the time the charge is armed.

TESTING PROGRAM

Two tests with the TPH 3342 at a height of burst of 19.8 ft were conducted in 1985 over an existing test pad at the Defence Research

---

[2] Wisotski, John, Denver Research Institute, Private Communication.

Table 1. Characteristics Desired of a High Explosive Charge for High Fidelity Blast Studies

High Energy
High Density
High Detonation Velocity
Clean Shock With Early Time Emergence From Fireball
No or Few Anomalies
Minimum Fireball
Castable, No Voids
Self-Supporting
Impervious to Moisture
Long Shelf Life
Repeatable
Symmetrical
Reasonable Cost
Class A (DOT)
High Quality
No Skin Obstruction
Spherical
No Booster (Preferred)
Oxygen Balanced

Table 2. Charge Fact Sheet

	TPH 3342	IRESET A-1
COMPOSITION	HMX (150 -65, 5 -35)-84.80% R45M & IPDI 15.15% THERMAX 0.05%	PROPRIETARY
DENSITY	1.632 g/cc	1.26 g/cc
CASTABILITY	BAYONET & VACUUM CASTING, AIR REMOVED FROM MATERIAL DURING MIXING PROCESS	LAYERED CASTING, SOLIDIFIES ON COOLING
TENSILE PROPERTIES	MAXIMUM STRESS 112 psi STRAIN AT MAX. STRESS 0.26 in/in ELASTIC MODULUS 1010 psi	APPROXIMATELY 38 psi
HOMOGENITY	EXCELLENT	EXCELLENT
SENSITIVITY	LOW, LONG SHELF LIFE, IMPERVIOUS TO WATER	LOW, LONG SHELF LIFE
DOT EXPLOSIVE CLASS	A	BLASTING AGENT
ENERGY (cal/g)	822	880
ENERGY (cal/cc)	-----	1109
GAS VOLUME (moles/kg)	-----	41
MAXIMUM THEORETICAL VELOCITY (km/sec)	9.10	6.4
MAXIMUM THEORETICAL PRESSURE (kbar)	-----	141
PHYSICAL STATE	CAST	CAST
CRITICAL DIAMETER	NONE	4"
CHARGE DIAMETER	1086 lb SPHERE 32.75"	1500 lb SPHERE 39.875"
BOOSTER	NONE	SENSITIZED NITROMETHANE
DETONATOR	REYNOLDS INDUSTRIES RP83	REYNOLDS INDUSTRIES RP83

Establishment, Suffield, Alberta, Canada (DRES), see Table 3. Figure 1 shows a charge in place and ready for detonation. Static and stagnation measurements were made along three radials approximately 120 degrees apart (the north line having the largest number of gages). Symmetry of the blast wave could thus be checked along with repeatability when the second shot was fired.

Two tests with the IRESET at a height of burst of 19.8 ft were conducted in 1986 over a new test pad at DRES. Figure 2 shows the booster material being added to the charge and Figure 3 shows the charge being positioned for the shot. The surface area under the charge consisted of relocatable 2-inch steel plates supported by pea-sized gravel and positioned in the ground zero region. Static and stagnation measurements were made along two lines, 180 degrees apart. As with the TPH 3342, symmetry and repeatability of the IRESET could be examined.

Additional data on the TPH 3342 explosive is included from two shots fired in 1987 at the same site, at heights of burst of 36 ft, see Table 3. These shots used the new test pad discussed above and had one-half the layout dedicated to non-ideal airblast studies and the other half for ideal blast over concrete and soil.

INSTRUMENTATION

The instrumentation for the tests was the analog FM data acquisition system as deployed on past experiments of this size. PCB piezoelectric quartz pressure transducers were connected with line drivers and coupled by coax cabling to 500 kHz wide band II magnetic tape recorders to achieve response times of one to two microseconds. High-speed cameras were used at various locations on the layout to observe the detonation and shock development, while the early time shock structure was observed by the laser photogrammetry technique.[3]

---

[3] Wisotski, John, "Ultra High-Speed Ruby Laser Photographic Light System," Proceedings of the Sixth International Symposium on Military Applications of Blast Simulation, Vol I, Cahors, France, 25-29 June 1979.

Table 3. Shot Information

SHOT	DATE/TIME	EXPLOSIVE/DIA	CHARGE WT (lb)	CHARGE WT (kg)	HOB (ft)	HOB (m)	WIND (mph)	WIND (km/hr)	TEMP °C	ATM PRES (mb)	RELATIVE HUMIDITY %
85-1	30 Sep/12:53	TPH 3342/32.75"	1086	492.6	19.737	6.02	8.9	14.4	8.3	938.9	37
85-2	11 Oct/13:30	TPH 3342/32.75"	1088	493.5	19.779	6.03	17.0	27.35	13.6	919.0	51
86-4	13 Aug/12:56	IRESET A-1/39.875"	1515	688	19.800	6.00	13.6	21.9	24.3	933.8	49
86-5	18 Aug/10:57	IRESET A-1/39.875"	1526	693	19.820	6.00	6.7	10.8	28.3	934.2	26
87-1	14 Oct/13:22	TPH 3342/31.81"	999	453.5	36.127	11.01	2.0	1.24	13.0	930.4	26
87-2	28 Oct/14:11	TPH 3342/31.81"	998	453.1	35.966	10.96	5.5	3.41	17.8	924.2	36

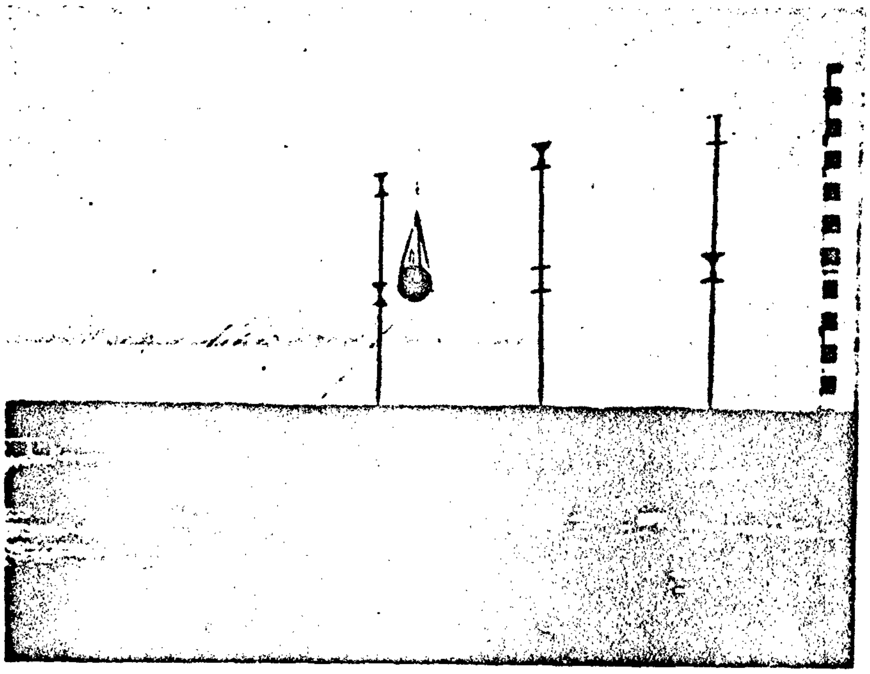

Figure 1. Shot 85-I ready for firing.

Figure 2. Booster material being added to the charge.

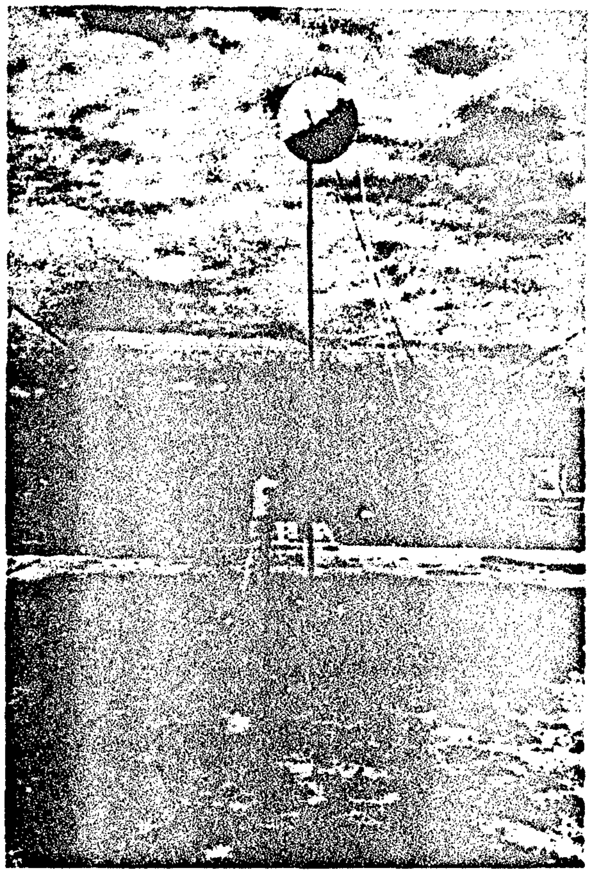

Figure 3. Charge positioning for Shot 86-4.

RESULTS

The shock emerging from the fireball was clear and sharp for each of the explosives as shown by the photographs of the TPH 3342 in Figure 4 and the IRESET in Figure 5. Separation from the detonation products occurred early with no obscuration.

Overpressure-time records obtained at the same station using the same gages and the same data acquisition system on two shots are compared for TPH 3342 in the next three figures. Figure 6.1 shows the static pressure records along the surface for four of the stations instrumented. Excellent repeatability of the double Mach at Stations 19 and 22 is observed. The repeatability of this explosive is again observed in the stagnation records from three stations shown in Figure 6.2. Figure 6.3 shows the East station at 16 ft compared with the mainline station, and the West station compared with the mainline station at 22 ft, 1.5-inch elevation. Good shock symmetry is indicated at these radial distances.

The detonation of the IRESET charges produced a large number of fragments from the breakup of the booster well. These fragments were found throughout the test bed and are presumed to be the cause of perturbations on many of the gage records. Presented in Figure 7.1 are static overpressure records along the surface. The double Mach wave at stations 18 and 19 was not repeated well at all, although stations 16 and 22 show a reasonable measure of repeatability. A good correlation is also seen in Figure 7.2 with static measurements at 40 ft and 60 ft and stagnation measurements at 26 ft and 40 ft. The test pad used for the IRESET allowed measurements to be made at different azimuths along the same radial. Figure 7.3 presents the results from the Stations at the 50 ft radial arc on Shot 4. The A-line gage was approximately six feet from the centerline, the B gage was another two and one-half feet along the arc, and the C gage was six feet farther on. Differences between the two records are considerable. The right side of the figure presents records from the East and West stations at 19 and 30 ft. Considerable differences also occurred at these stations, indicating an asymmetrical shock wave from the IRESET charge.

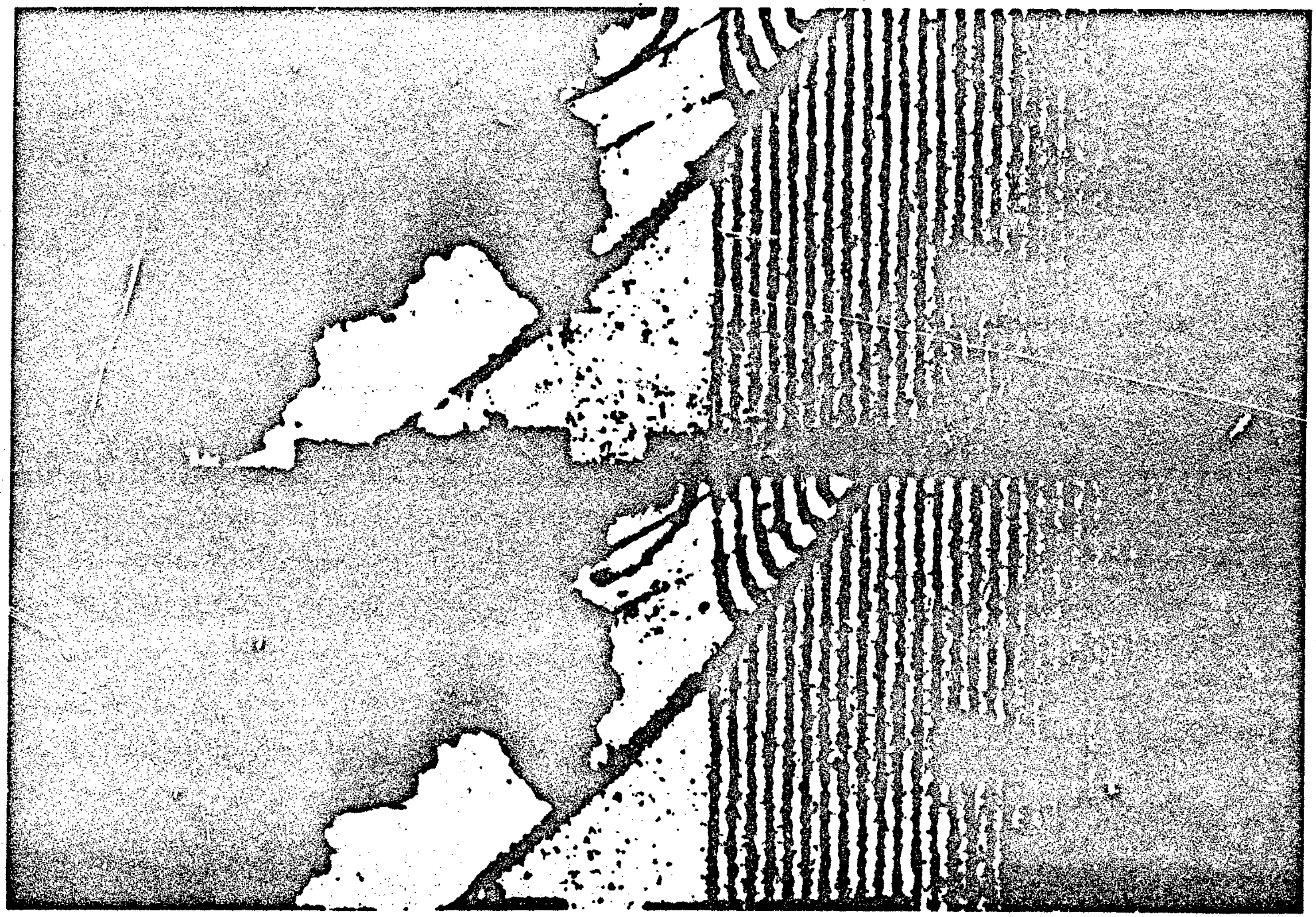

Figure 4. Expanded view of shock front emerging from fireball, 1.825 ms, TPH 3342, Shot 85-1.

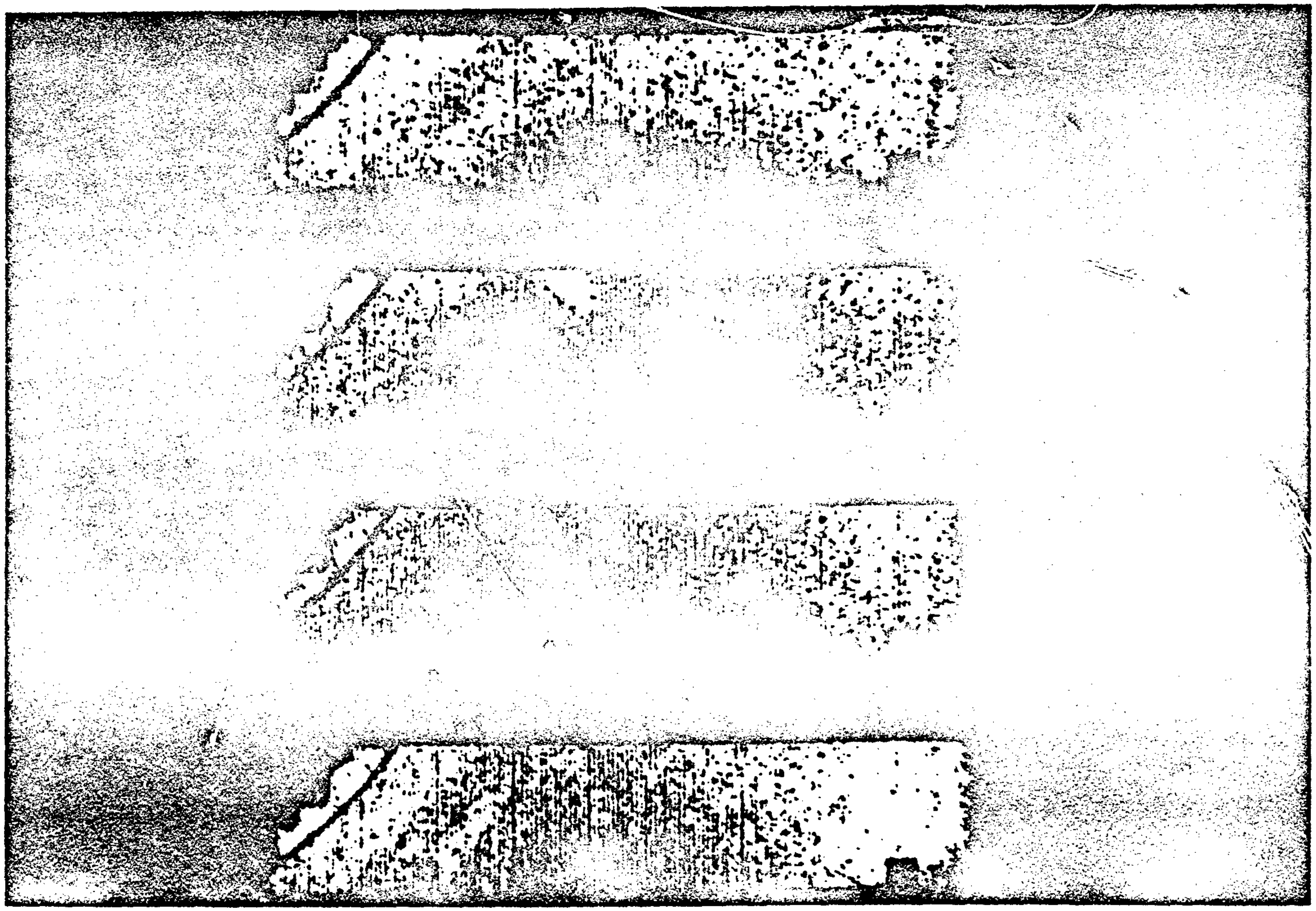

Figure 5. Shock front emerging from fireball, IRESET A-1, Shot 86-4, 1.070 ms.

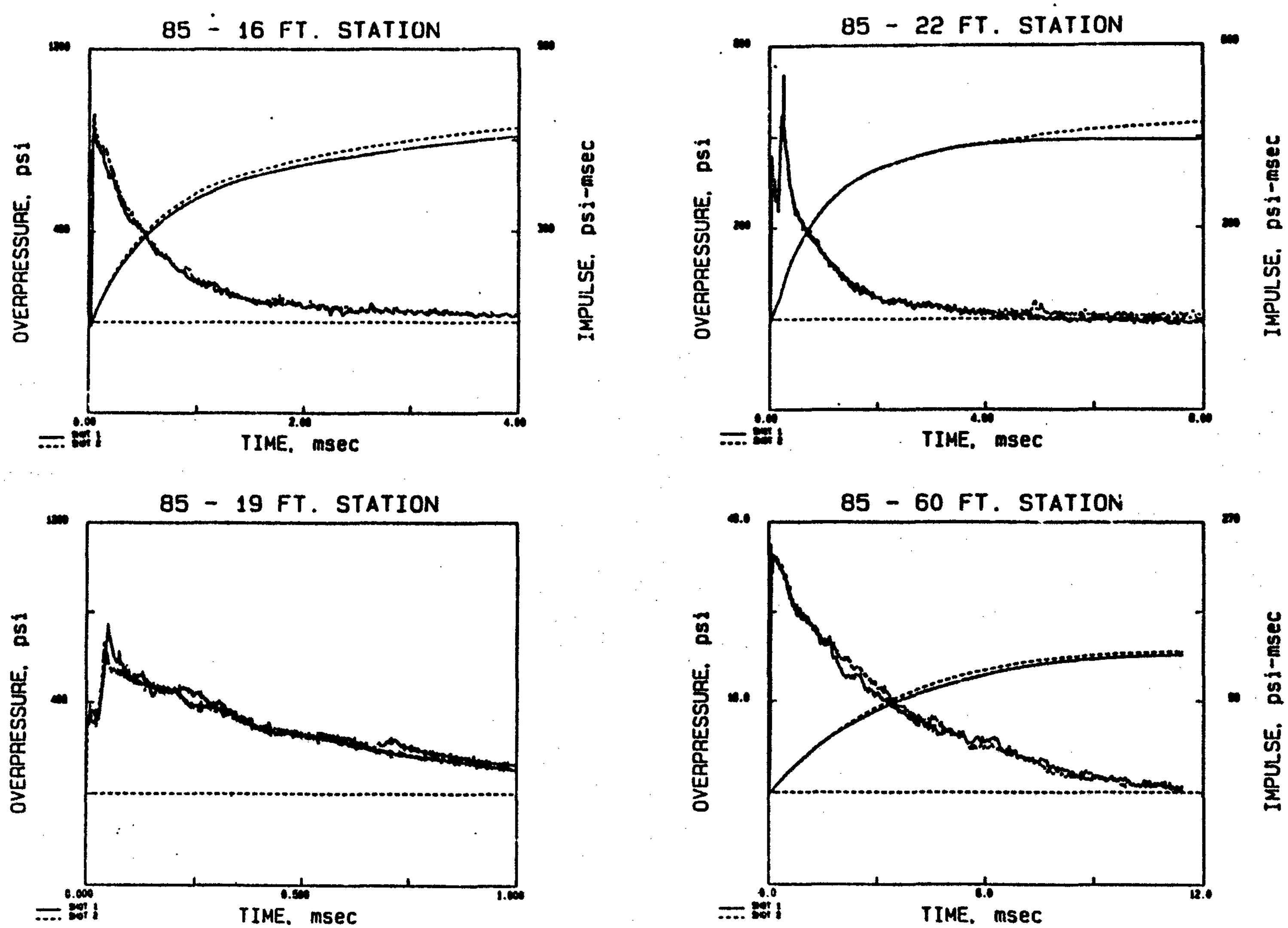

Figure 6.1. Static pressure record comparisons along the surface, TPH 3342, Shots 85-1 and 85-2.

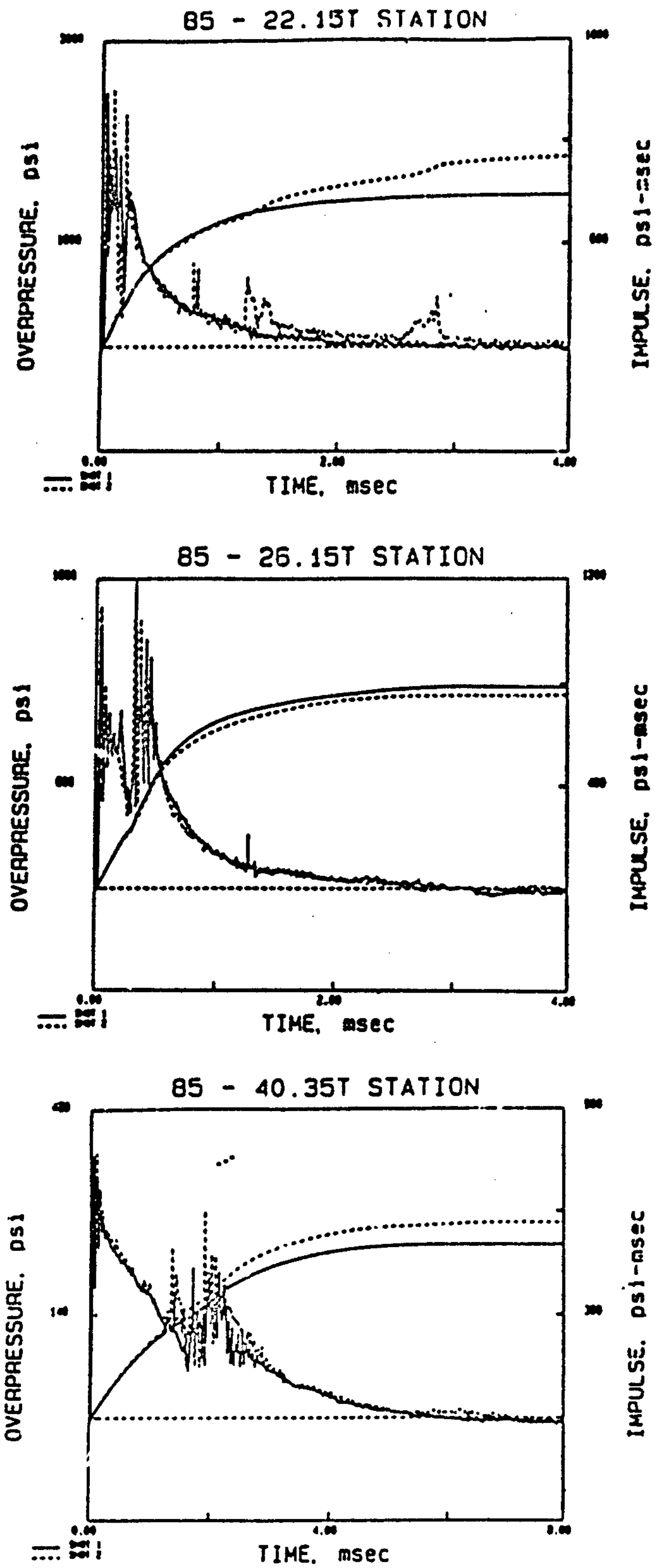

Figure 6.2. Stagnation pressure record comparisons, 1½ and 3½ inch elevation, TPH 3342, Shots 85-1 and 85-2.

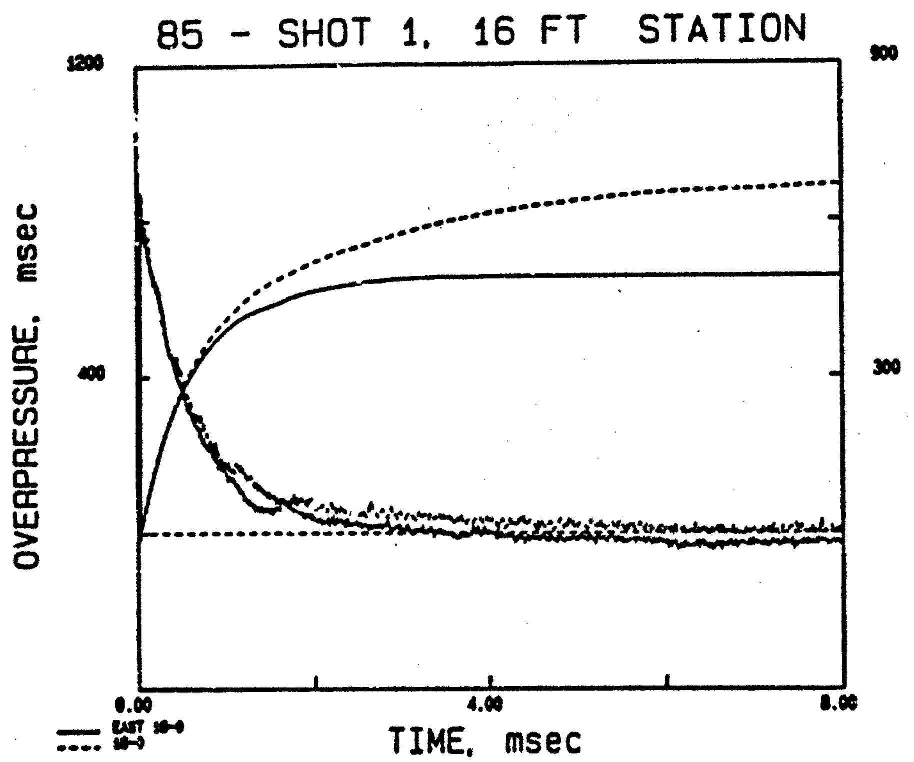

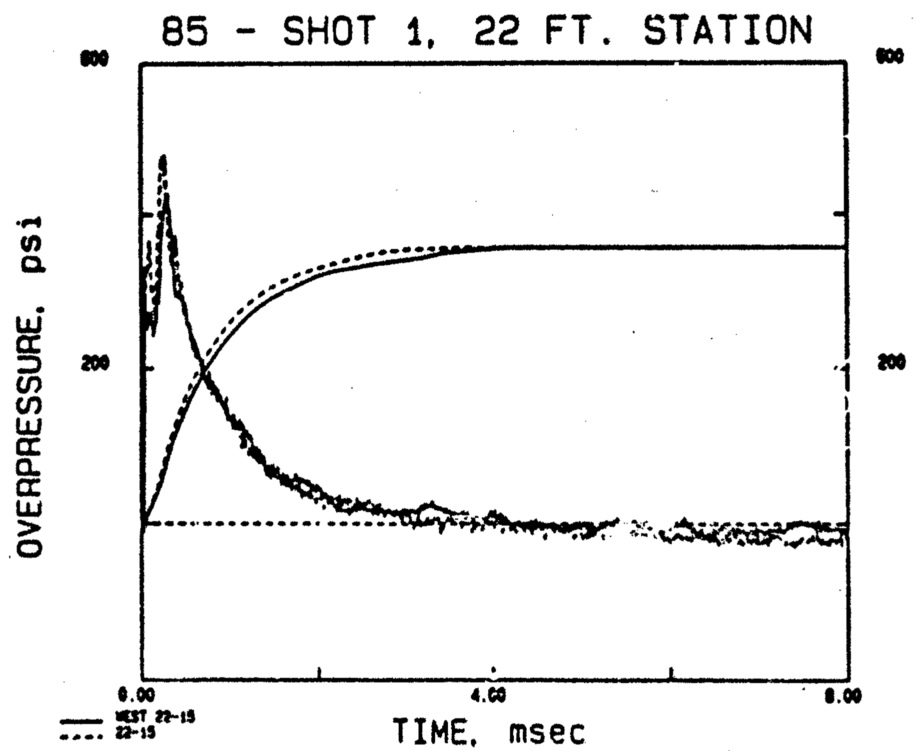

Figure 6.3. Static pressure record comparisons of off-line positions, TPH 3342, Shot 85-1.

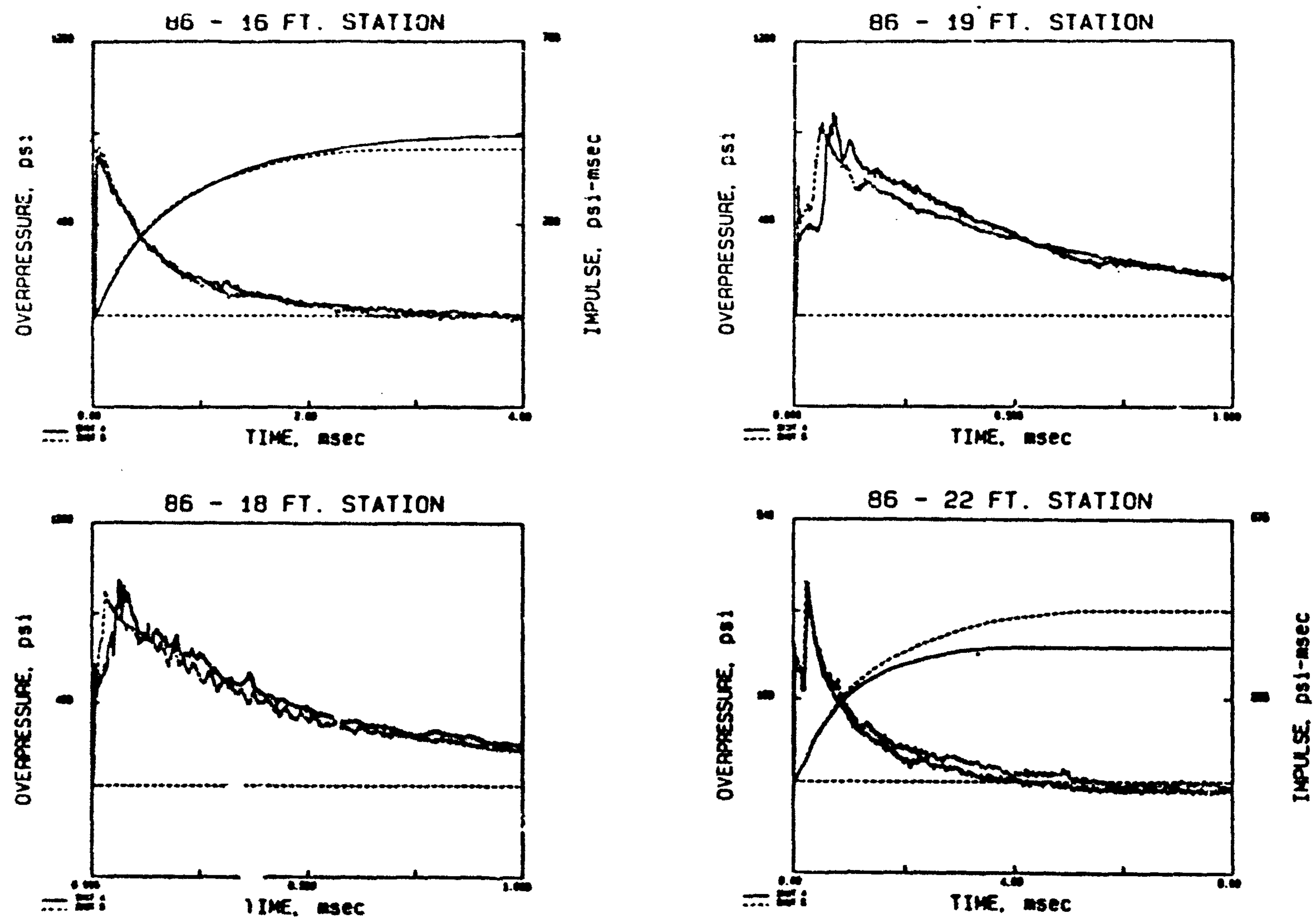

Figure 7.1. Static pressure record comparisons along the surface, IRESET A-1, Shots 86-4 and 86-5.

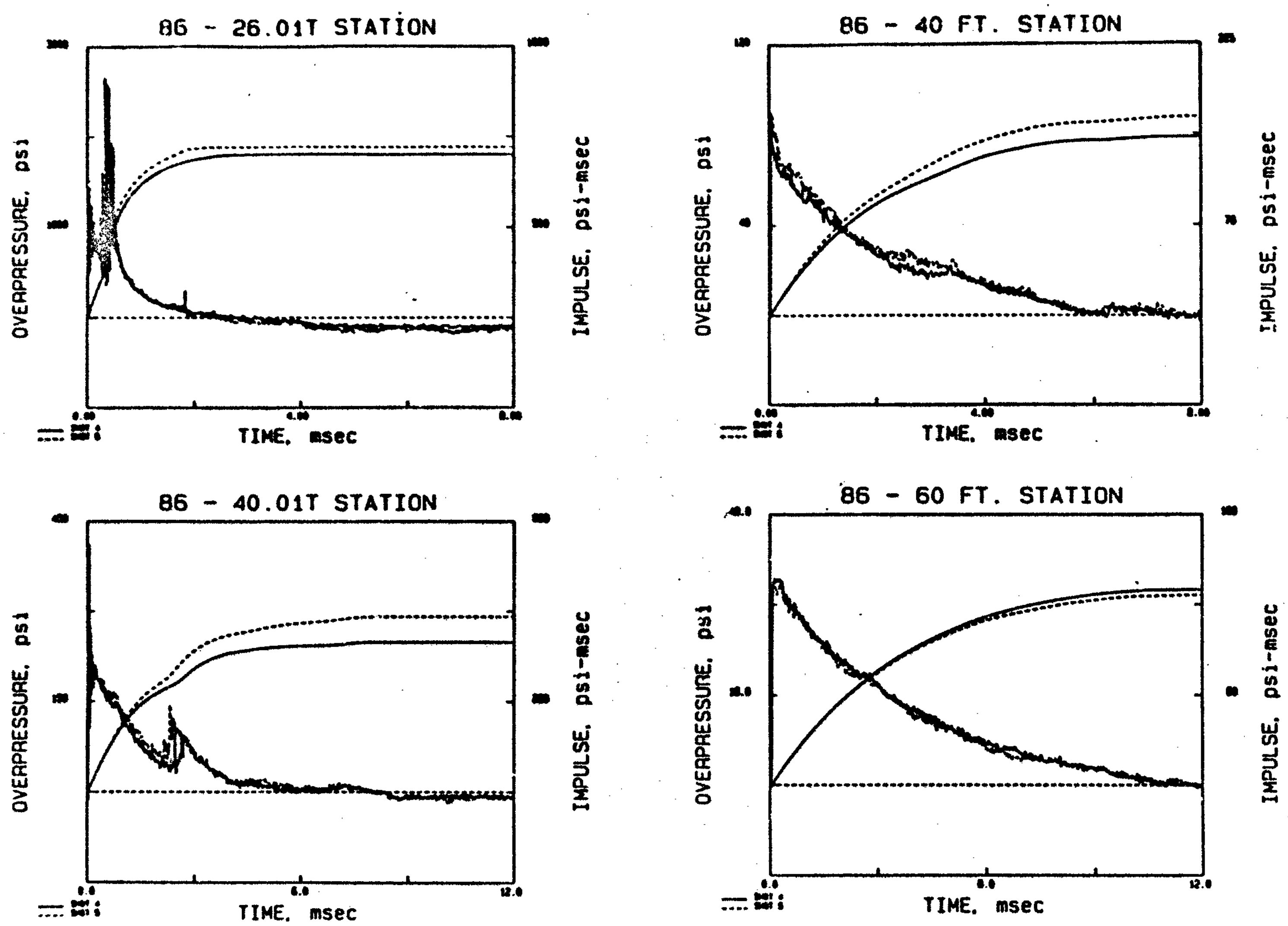

Figure 7.2. Left - Stagnation pressure record comparisons, 1-inch elevation, IRESET A-1, Shots 86-4 and 86-5.
Right - Static pressure record comparisons along the surface, IRESET A-1, Shots 86-4 and 86-5.

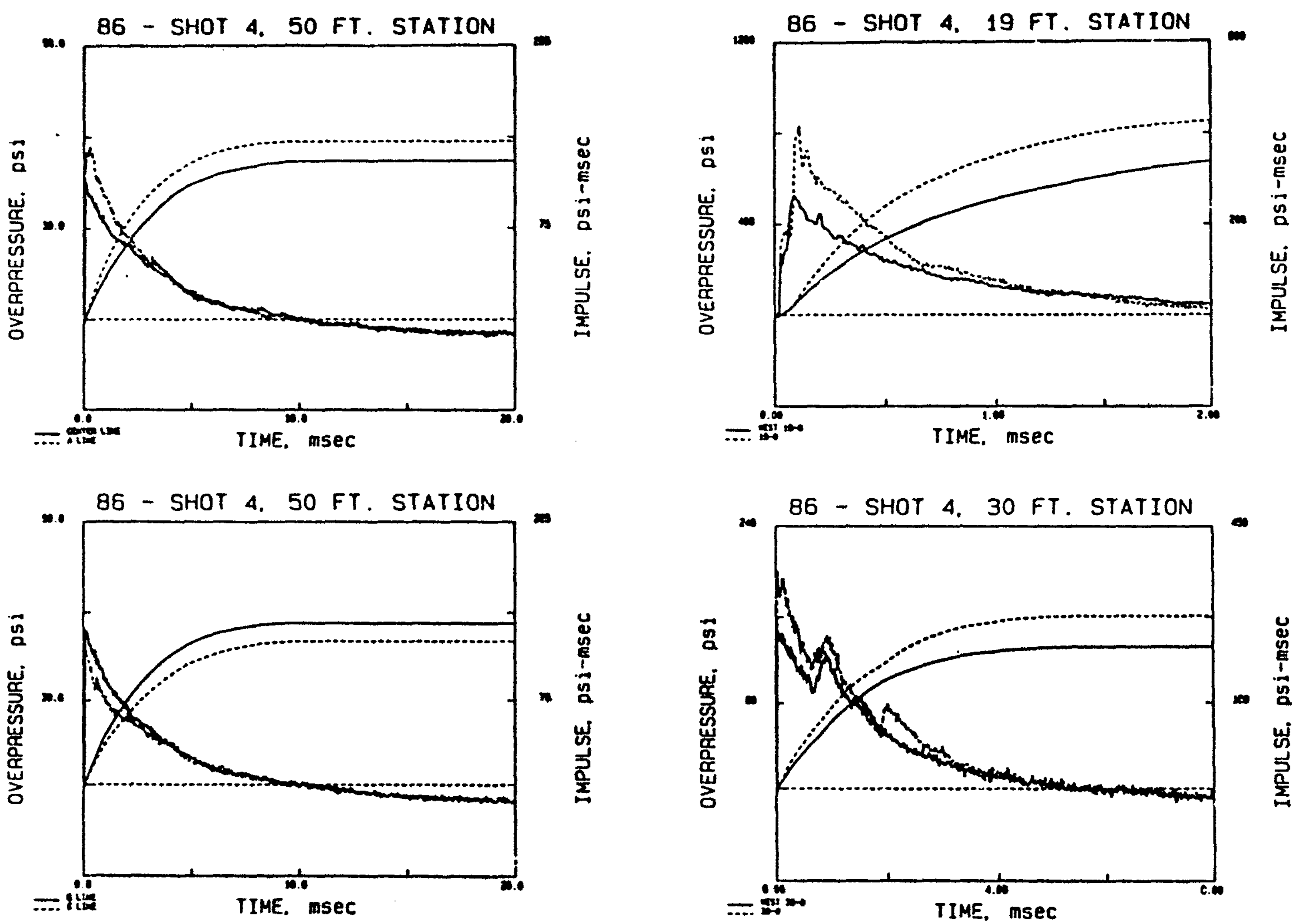

Figure 7.3. Left, static pressure record comparisons at the surface on the 50 ft. arc, IRESET A-1, Shot 86-4. Right, static pressure record comparisons along the surface for west and main line positions, IRESET A-1, Shot 86-4.

The 1987 tests using TPH 3342 provided an opportunity to evaluate repeatability because Shot 87-2 was a repeat of Shot 87-1. Both shots were at a height of burst of 36 feet. Gage stations were selected at random from those placed on the height-of-target study in the ideal section of the layout. The comparisons made are shown in Figures 8.1 and 8.2. Elevated gage stations show both incident and reflected shocks. These were at 10 feet at the 90-foot station, 20 feet at the 120-foot station, 30 feet at the 150-foot station, and 60 feet at the 200-foot station. Excellent repeatability was realized as seen by the figures.

Arrival time versus ground range for the TPH 3342 and IRESET A-1, Shots 85-1 and 86-4 respectively, are compared in Figure 9. The shock velocity of the HMX explosive is much greater than the ammonium nitrate from ground zero out to 40 feet. Since the detonation velocity of TPH 3342 is nearly 50% greater than the IRESET A-1, this difference was expected.

Overpressure versus ground range for the two charges, Shots 85-1 and 86-4, are compared in Figure 10. A larger number of stations were used from the new test pad for the IRESET shots than were available for the HMX shots and this is evident in the plot. Overpressure enhancement was seen in the transition region of Shot 86-4. The charge weights of the shots differ and this is evident in the comparison.

In relating these explosives to Pentolite, it was found that the 1500 lbs of IRESET yielded blast equal to 1000 lbs of Pentolite as indicated by the radius time data related to Goodman's Pentolite data, Figure 11. TPH 3342 weighed 1086 lbs and is related to a 1068-lb Pentolite charge tested in 1980 in the overpressure distance plot of Figure 12. The data indicates the TPH 3342 is slightly more energetic (5-10%) than the Pentolite.

CONCLUSION

The HMX-based TPH 3342 explosive produced excellent waveforms with comparatively few extraneous inflections in the tests conducted. Repeatability and blast symmetry were very good over the entire pressure range. Fireball photography showed a high rate of expansion indicative of a

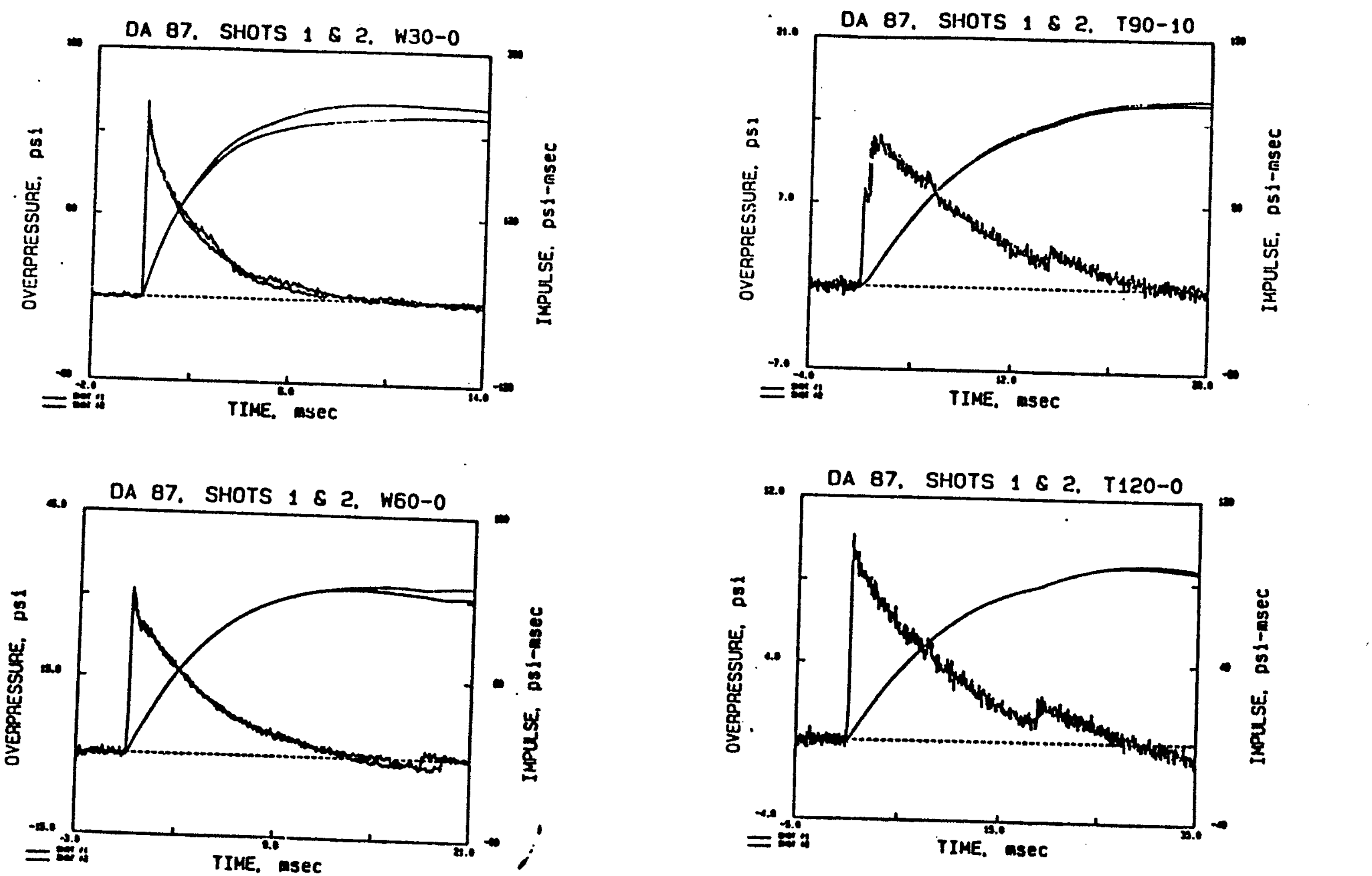

Figure 8.1. Comparison of TPH 3342, Shot 87-1 and 87-2 records, at stations W30.0 and W60.0 (left side), and at stations T90.10 (10-foot elevation, 90 ft.) and T120.0 (right side), ideal sector.

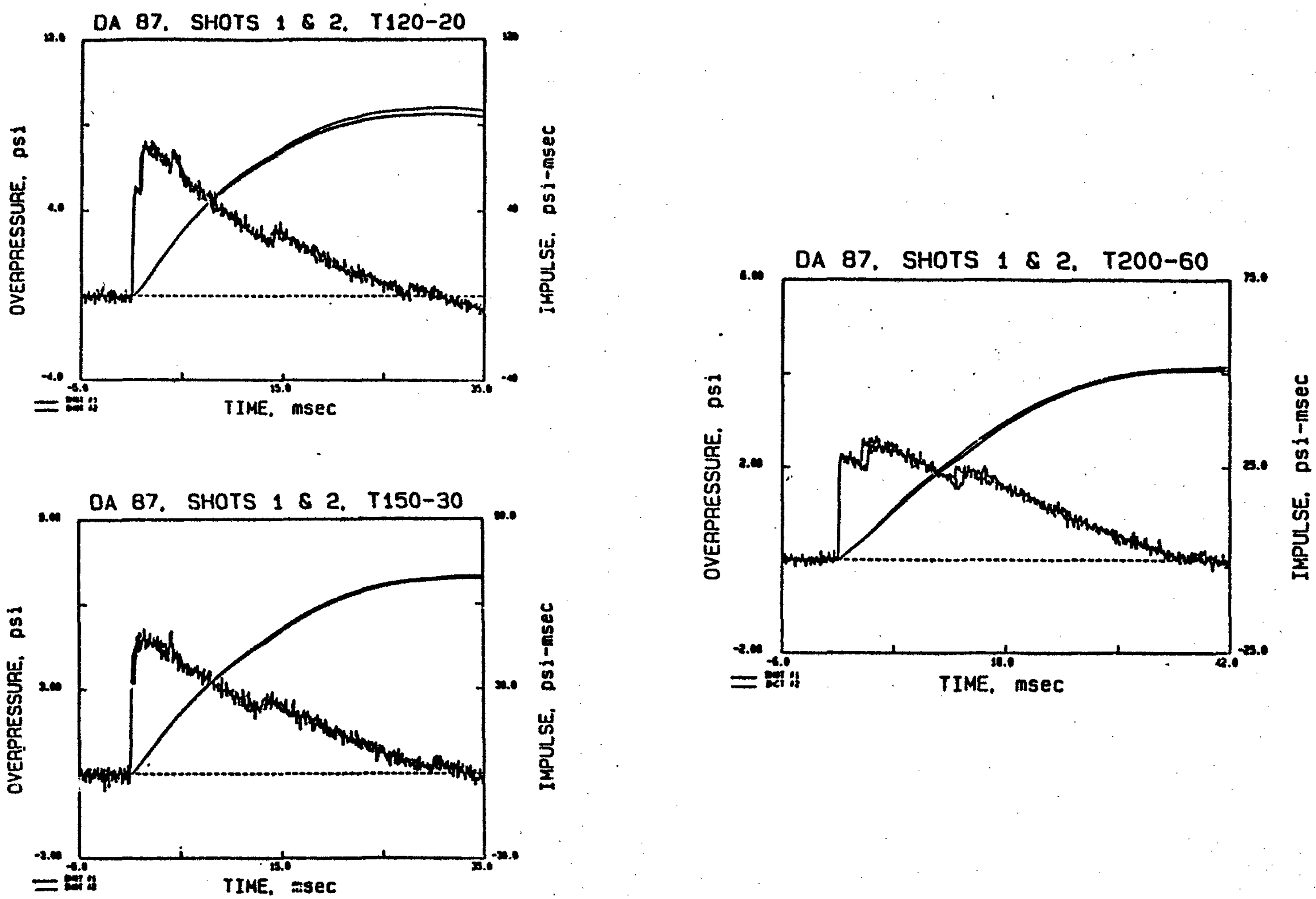

Figure 8.2. Comparison of TPH 3342, Shot 87-1 and 87-2 records at stations T120-20 and T150-30 (20 and 30-foot elevations, left side), and at station T200.60 (60-foot elevation, right side), ideal sector.

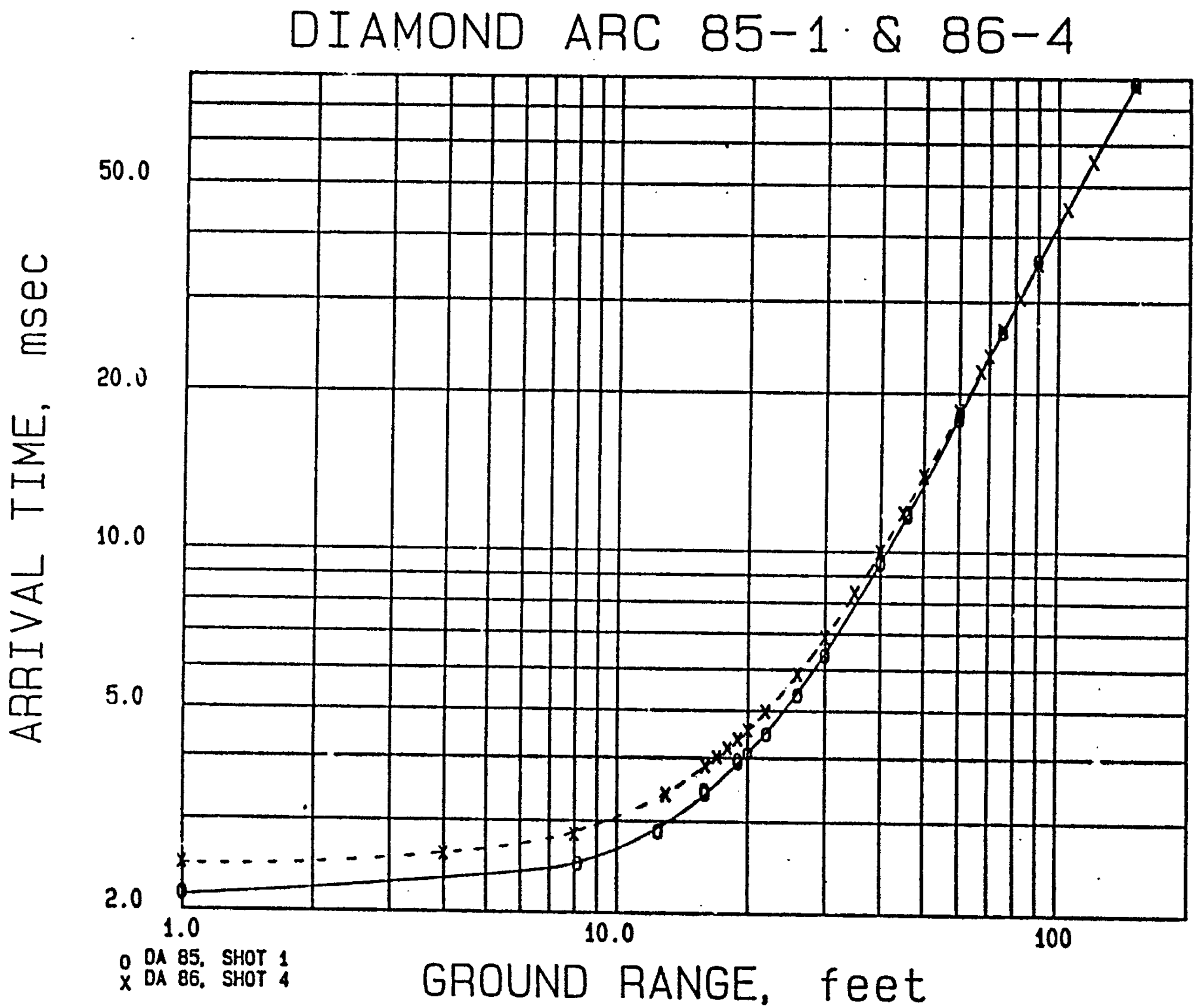

Figure 9. Arrival time versus ground range, Shots 85-1 and 86-4.

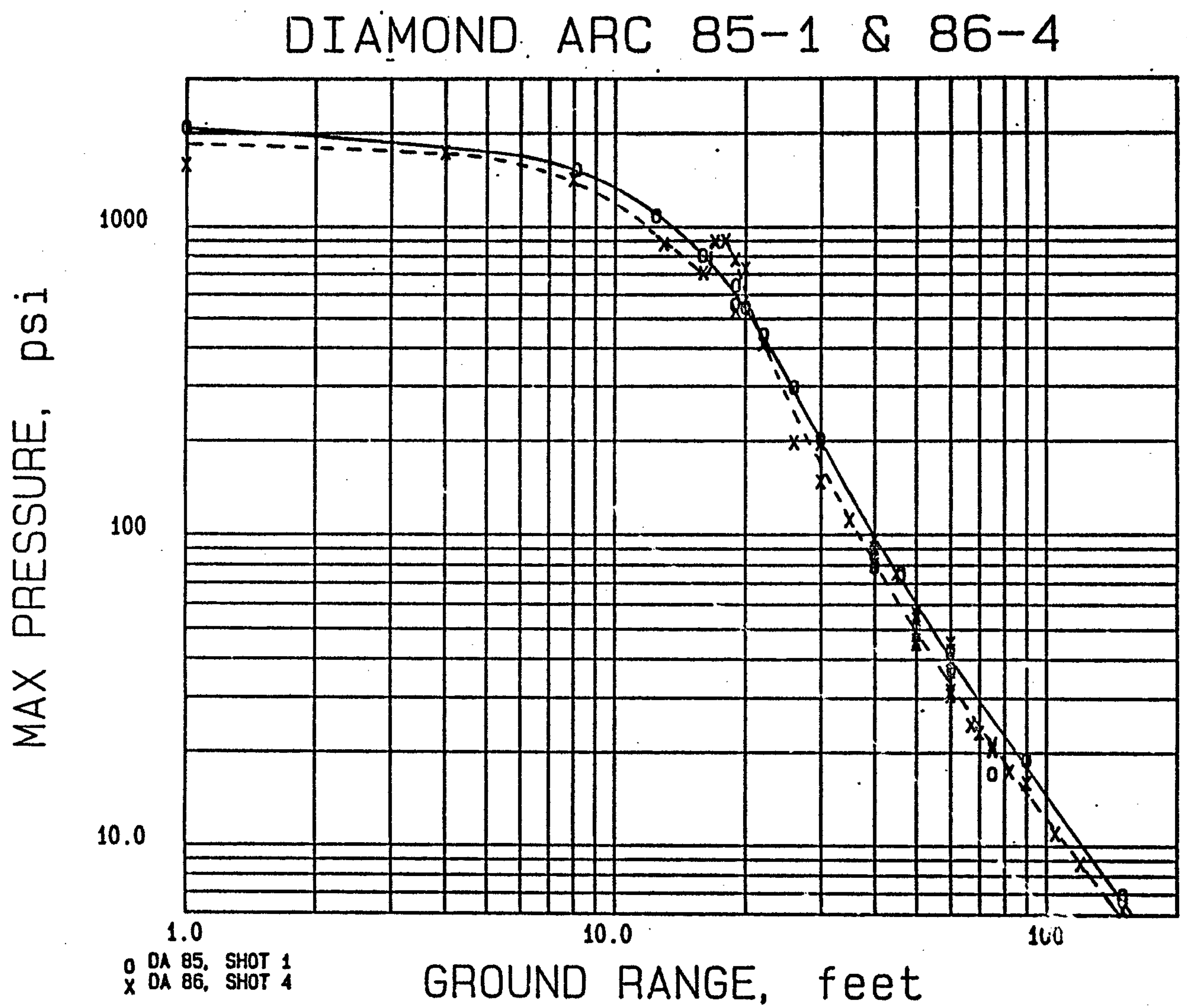

Figure 10. Static overpressure versus ground range, Shots 85-1 and 86-4.

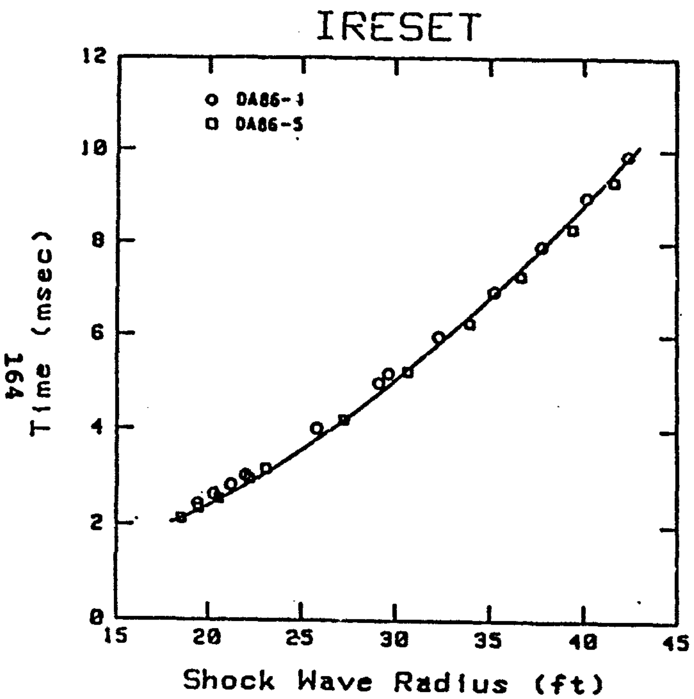

Figure 11. Shockwave Radius-Time from DA86-4 and DA86-5 and Goodman's Pentolite Standard, Scaled.

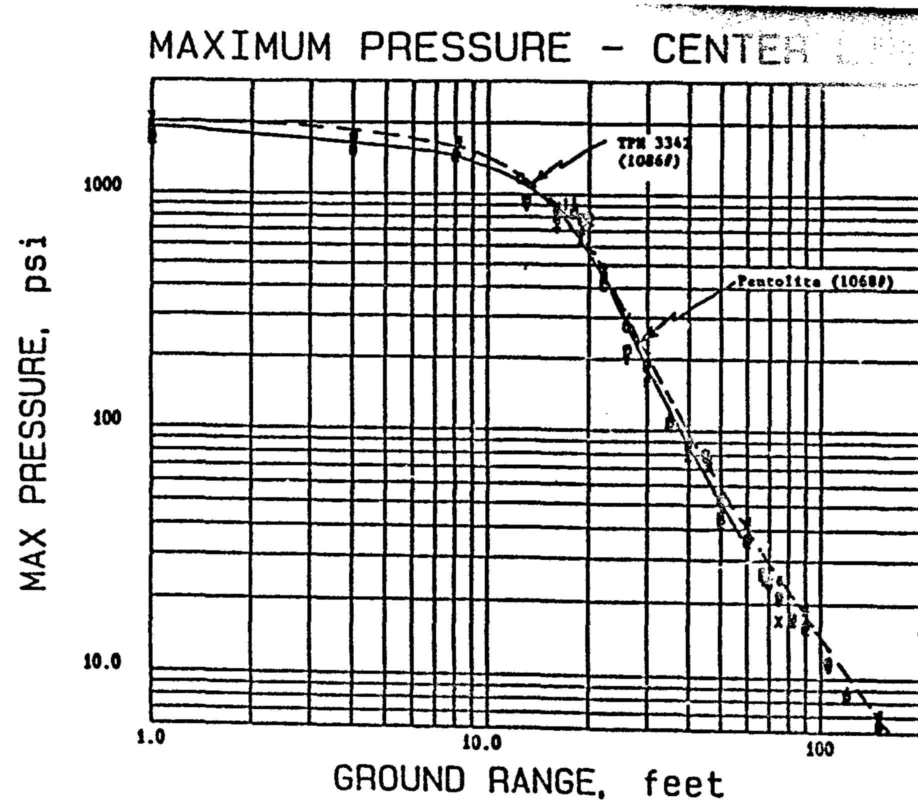

Figure 12. Overpressure versus ground range for Pentolite and TPH 3342.

high detonation velocity explosive. The majority of the criteria established in Table 1 was met.

IRESET A-1, the ammonium nitrate-based explosive produced waveforms of varying quality - many were excellent, however, many showed inflections and some reflections resulting from the breakup of the aluminum charge booster container. Asymmetry and non-repeatability were observed. Fireball photographic data shows a low expansion rate indicative of a low detonation velocity explosive. Although many items in the criteria established in Table 1 were met, the asymmetry and non-repeatability make IRESET A-1 undesirable for high fidelity experimental research.

EXPLOSION AIRBLAST PREDICTIONS ON A PERSONAL COMPUTER AND APPLICATION TO THE HENDERSON, NEVADA, INCIDENT

Jack W. Reed
Ground Motion & Seismic Division
Sandia National Laboratories
Albuquerque, New Mexico

ABSTRACT

An airblast prediction program for explosions, called BLASTO, has been written for use with IBM-PC (or compatible) computers, to produce overpressure-distance curves for a variety of interactive input conditions. Several common units are allowed for each input, but calculation and output are in SI metric units. Explosion yield (chemical or nuclear) and ambient atmospheric pressure are used to generate a referenced 'Standard' overpressure-distance curve. Explosives may be point charges at any height above ground or depth below the earth surface. Buried charges may also be distributed in a sheet, or 'HEST' configuration, but a mining model for a number of point charges with firing delays has not yet been developed.

If upper air weather data or forecasts are available, they can be used to generate directed (wind effects) sound velocity versus height structures which are interpreted to give attenuated or enhanced overpressure-distance curves. These are calculated for incremented directions around the compass or toward specified targets or communities.

Evaluation of the recent accidental explosion at an ammonium perchlorate (A-P) plant in Henderson, Nevada, made use of BLASTO. Damage inspection gave some estimates for incident overpressure at various ranges. These showed considerable scatter, but they generally surrounded an overpressure versus distance curve calculated for 1-kt NE free-air burst. Weather data and directed sound velocity calculations showed that some of the closest residential damages were in directions of minimal weather-dependent blast distortion, allowing the conclusion that the largest explosion could be simulated by a 250-ton HE surface burst. Video-camera recordings, newspaper eye-witness accounts, post-accident aerial photographs, seismic recordings, and a report of the A-P storage pattern have been reviewed to show that this largest blast probably occurred in a 1500-ton A-P collection. This leads to 1:6 TNT airblast equivalence for A-P.

INTRODUCTION

Predicting atmospheric influences on explosion airblast propagation has evolved from a two-hour process of number-punching on an electro-mechanical desk calculator in 1951 [1], through analog computer processing [2] in about 15 minutes - with five 8-ft relay racks of electronic components - for atmospheric nuclear tests from 1955 to 1962, to general assessments of atmospheric structure which can be made on a programmable pocket calculator that allow qualitative safety conclusions. Detailed numerical evaluations for expected damage still require main frame computations for yield-scaled overpressure-distance curves and bookkeeping functions of damage assessment for the distribution of neighbors around a typical explosion test site [3]. The recent proliferation of desk-top personal computers, with large memories and user-friendly operations, now makes feasible a relatively complete airblast prediction program, BLASTO, that is transportable by floppy disk to any PC that is IBM-compatible and uses the MS-DOS operating system.

BLASTO begins with an input explosion definition, considers the burst environment and its effect on airblast source strength, and generates several typical overpressure-distance curves for various weather effects. At this point in planning exercises it is possible to tell whether weather needs to be watched during a countdown. If so, input weather data are used to show directional refractive enhancements or attenuations of airblast propagation with expected overpressure-distance curves for incremental or targeted directions. From these, an off-line estimate of damage may be made for each community of concern.

Diskette copies of BLASTO, along with necessary instructions and input-output examples, are available on request, for field test evaluation.

COMPUTATION MODEL

A flow diagram for BLASTO is shown in Figure 1. An input explosion definition consists of a yield, W, in any of several units for selected explosives, and an environment, a location, elevation, and height-of-burst (HOB). HOB may be zero for a surface burst, positive for an airburst, or negative for an underground burst. Distributed buried charges, such as HEST, CARES, etc., may also be used. The positive HOB function [4] begins with a 2 W apparent yield value for a surface burst, curves up to 5.6 W at optimum HOB, and reduces to a free-air burst 1 W value above about 700 $m/kt^{1/3}$, as shown in Figure 2. Source strength for buried charges depends on the amount of overburden per unit of charge weight [5], as shown in Figure 3. Ambient pressure at the burst is obtained from a weather report, if available, or from the Standard Atmosphere [6] and elevation.

Apparent yield (free-air burst) is then used to scale distances [7] in calculating a Standard [4,8] overpressure-distance function. Typical weather effects on propagation include attenuation by upward acoustic refraction as shown in Figure 4, enhancement by acoustic ducting, and amplification by focusing in complex atmospheric conditions as shown in Figure 5. Empirical

functions were derived [9] for simple sound velocity versus height conditions where the overpressure-distance decay rate depends on the increase or decrease of sound velocity between the surface and about 40 $m/kg^{1/3}$ height as shown in Figure 6. When there is focusing, focal distance cannot be accurately predicted because of its great sensitivity to measurement and turbulent errors in defining sound velocity. For those cases, the envelope of overpressures in Figure 6 contains about 95% of the relatively few data points that have been acquired from tests. The world record focused overpressure magnification of 9.6 X was found during French sonic boom tests [10]. A window damage threshold was established by incidents from atmospheric nuclear tests [2].

Input weather data requirements are for pressure, temperature, and wind vectors to such altitudes as may cause propagation problems [1]. Sound speed depends on air temperature, and directed sound velocity is the sum of sound speed plus the directed wind component. Vertical structure of directed sound velocity then determines the airblast overpressure-distance curve expectation for that direction. This is as far as BLASTO goes at the present time.

Damage prediction requires another empirical approximation, for window damage probability versus incident overpressure [4] derived from accident analyses [11], as shown in Figure 7. Window surveys or estimates based on population census values give the number of exposed window panes, which are multiplied by appropriate probabilities to give the number of broken panes. This may or may not frighten test management into calling a delay for better weather. These manipulations will eventually be included in BLASTO to compute expectations for numbers of broken panes.

FUTURE MODIFICATIONS

Planned expansions for BLASTO include more detailed damage and hazard evaluations, pending final analyses of glass breakage tests at MISTY PICTURE [12]. For countdown decision-making, BLASTO should also provide consideration of localized diurnal variations in surface wind and temperature [13], as well as time-dependent statistical treatments of weather prediction errors and uncertainties [14]. One needs to know, when conditions look good, how close the weather may be to causing a serious incident. Or, when conditions look bad, how much diurnal or statistical change is needed to make a test safe.

Finally, in response to recent requests, a source model for underwater bursts is planned. There has been no attempt to generate graphic outputs, since each PC installation is likely to have its own graphics capability and system. A choice is presented, however, between immediate output to a terminal or creation of an output data file which may be read and rewritten in a local format for graphics preparations. We welcome comments or suggestions about other specific useful modifications to this program.

HENDERSON EXPLOSIONS

A series of large explosions destroyed the Pacific Engineering Company (Pepcon) plant in Henderson, Nevada, which manufactures ammonium perchlorate (A-P) for rocket fuel, beginning about 1151 PDT May 4, 1988. Since a number of Sandians live near the plant, our investigation was made to explain what happened to them. New housing projects, that extend south from Las Vegas into the city limits of Henderson, reached within 2 km of the explosions. A first inspection of damage to these houses left an impression of only slightly less severe blast effects than were encountered in a Civil Defense test [2] that exposed typical houses to 0.5-psi overpressure from Turk, a 1955 atmospheric nuclear test in Yucca Flats. Damage also appeared to be more severe than at the Admin Park for MISTY PICTURE [15], a large chemical explosion test at White Sands Missile Range in 1987, where nearly 0.4-psi overpressure was recorded. As shown in Figure 8, this overpressure range at 2-km distance falls near the Standard curve calculated from BLASTO for a 1-kt NE free-air burst.

A number of other window damage incidents have been analyzed, some as far as 15 km from the plant. The number of broken panes ($\pm$ 0.5) in an area, divided by the number of similar panes exposed, gives a breakage probability range which may be translated to an overpressure range at a map-determined distance. Some results, and many more will be included when analysis is complete, are included in Figure 8 to support the early yield estimate. Since a 1-kt NE free-air burst Standard curve can be duplicated with a 0.5-kt NE (hemispherical) surface burst, and this by a 0.25-kt HE surface burst, considering the 2:1 HE:NE yield equivalence, the largest Pepcon explosion thus appears to have been equivalent to about 250-ton TNT.

Upper air weather conditions were observed at Desert Rock, 100 km northwest of Henderson, about six hours before and after the accident, at internationally scheduled times. Combined with surface weather conditions reported at McCarran Field, Las Vegas airport, an estimated shot-time sounding could be interpolated to give sound-velocity height curves from BLASTO calculations for various directions in Figure 9. The nearest housing damage was nearly crosswind, toward 300°, so it was probably not significantly distorted by atmospheric refractive effects.

There were a number of explosions, according to eye-witnesses, following a first large one which started a mass evacuation from the Pepcon plant as well as from the marshmallow factory next door. A seismic recorder in a Henderson Fire Department station, 3.6 km north of the blasts, showed both fast travelling ground shocks and later ground motion induced by airblast waves. This and other seismic recorders from the Las Vegas area, operated to document ground motion from underground nuclear tests, provide time estimates of 18:53:35.01+ 0.44s UT and 18:57:35.05+ 0.48s UT for the two largest explosions, with a much smaller one at 18:56:15.30 UT.

Video-camera recordings shown on TV, and post-accident aerial photographs taken by EG&G at the request of the Department of Energy, Nevada Operations Office, showed the largest explosion and ground disturbance occurred on the east edge of the Pepcon compound. According to Claude Merrill at Edwards AFB, the eastern A-P storage area contained approximately 3 million pounds, or 1500 tons, of A-P. This accident suggests a 1/6 TNT equivalence for A-P, a value not generally provided for in handling, transport, or manufacture of this material.

REFERENCES

1. Cox, E. F., H. J. Plagge, and J. W. Reed, "Meteorology Directs Where Blast Will Strike," Bull. Amer. Meteorol. Soc., 35, 95-103, 1954.

2. Cox, E. F., and J. W. Reed, "Long-Distance Blast Predictions, Microbarometric Measurements, and Upper-Atmosphere Meteorological Observations for Operations Upshot-Knothole, Castle, and Teapot," WT-9003, AEC-TIS, Oak Ridge, TN, Sep. 20, 1957.

3. Reed, J. W., "Climatology of Airblast Propagations from Nevada Test Nuclear Airbursts," SC-RR-69-572, Sandia Laboratories, Albuquerque, NM, Dec. 1969

4. American National Standards Institute, Estimating Air Blast Characteristics for Single Point Explosions in Air, with a Guide to Evaluation of Atmospheric Propagation and Effects, ANSI S2.20-1983, Acoustical Society of America, New York, NY, 1983.

5. Reed, J. W., "Recent Studies of Airblast from Buried Charges, for Environmental Protection from HEST Events," in Proc. I, MABS-8 Eighth International Symposium on Military Applications of Blast Simulation, Gruppe fur Rustungsdienste, AC-Laboratorium, Spiez, Switzerland, June 1983.

6. NASA, USAF, & USWB, U. S. Standard Atmosphere, 1962, USGPO, Washington, DC, 1962.

7. Glasstone, S., (Editor), The Effects of Nuclear Weapons, Revised Edition, USGPO, Washington, DC, 1977.

8. Needham, C. E., M. L. Havens, and C. S. Knauth, "Nuclear Blast Standard (1 kt)," AFWL-TR-73-55 (Rev., USAF Weapons Lab., Kirtland Air Force Base, NM, 1975.

9. Reed, J. W., "Project Propa-Gator Intermediate Range Explosion Airblast Propagation Measurements," in Minutes, 19th DOD Explosive Safety Seminar, DOD ESB, Washington, DC, Sep. 9-11, 1980.

10. Wanner, J. L., J. Vallee, C. Vivier and C. Thery, "Theoretical and Experimental Studies of Focus of Sonic Booms," J. Acoust. Soc. Amer., 52, 1 (Pt. 1), July 1972.

11. Reed, J. W., B. J. Pape, J. E. Minor, and R. C. DeHart, "Evaluation of Window Pane Damage Intensity in San Antonio Resulting from Medina Facility Explosion on November 13, 1963," Ann. N.Y. Acad. Sciences, 152, Oct. 28, 1968.

12. Dillingham, R. A., ed., "MISTY PICTURE Data: Window Glass Experiment," Final Data Report, GR&TL, Texas Tech Univ., Lubbock, TX, Dec. 1987.

13. Reed, J. W., "Predictions of Nuisance Damage and Hazard from Accidental Explosions During Trident Missile Test Flights," SAND 79-0626, Sandia National Laboratories, Albuquerque, NM, March 1980.

14. Daniels, R. D., and K. Overbeck, "Development of a Blast Damage Assessment Prediction Model," Tech. Rpt. No. 80-1351, J. H. Wiggins Co., Redondo Beach, CA, March 1980.

15. Reed, J. W., H. W. Church, and T. W. Huck, "MISTY PICTURE Weather-Watch & Microbarograph Project," Proc. MISTY PICTURE Symposium, Defense Nuclear Agency, Washington, DC, in preparation.

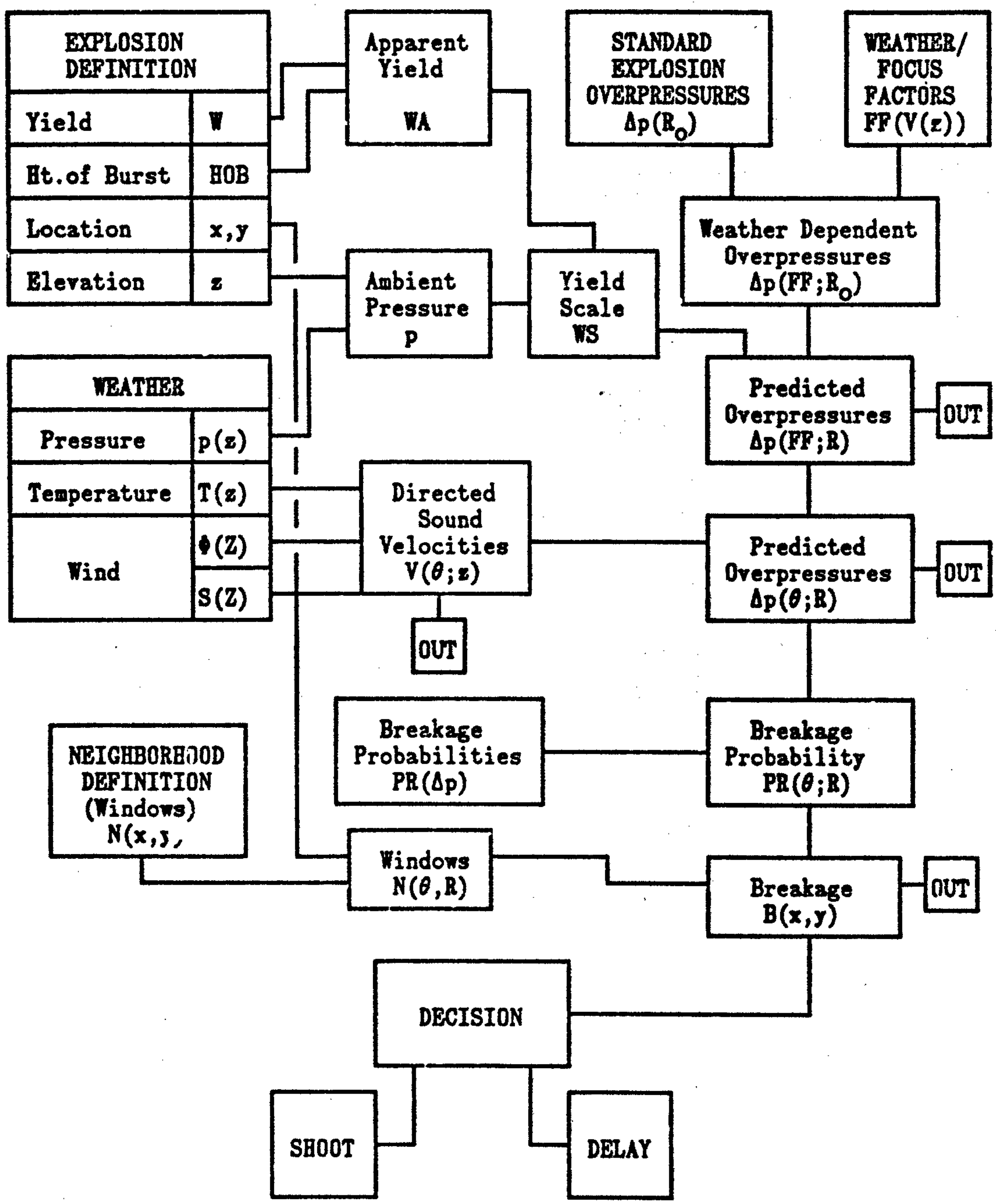

Figure 1. BLASTO Airblast Prediction Flow Chart.

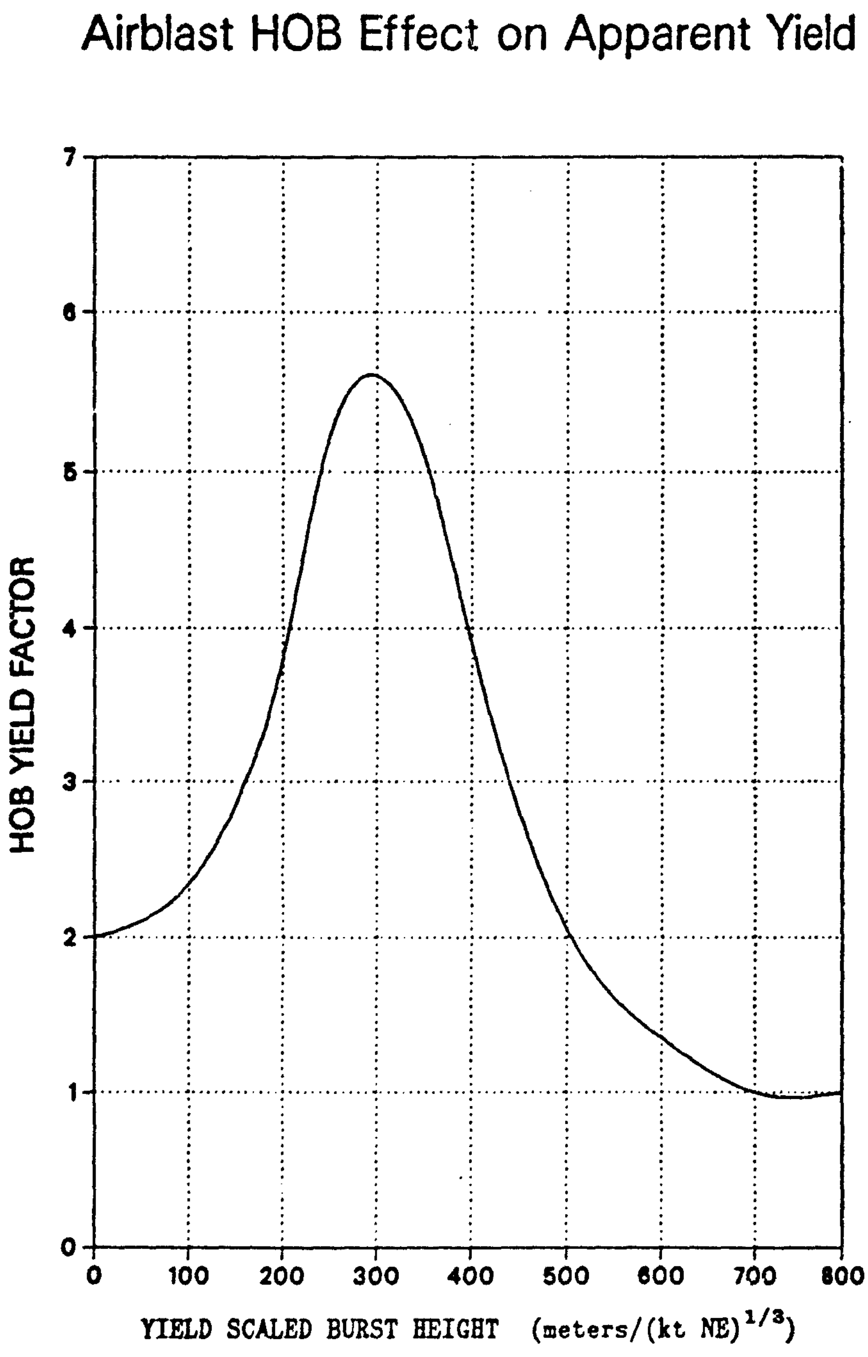

Figure 2. Airblast Height-of-Burst Effect on Apparent Yield.

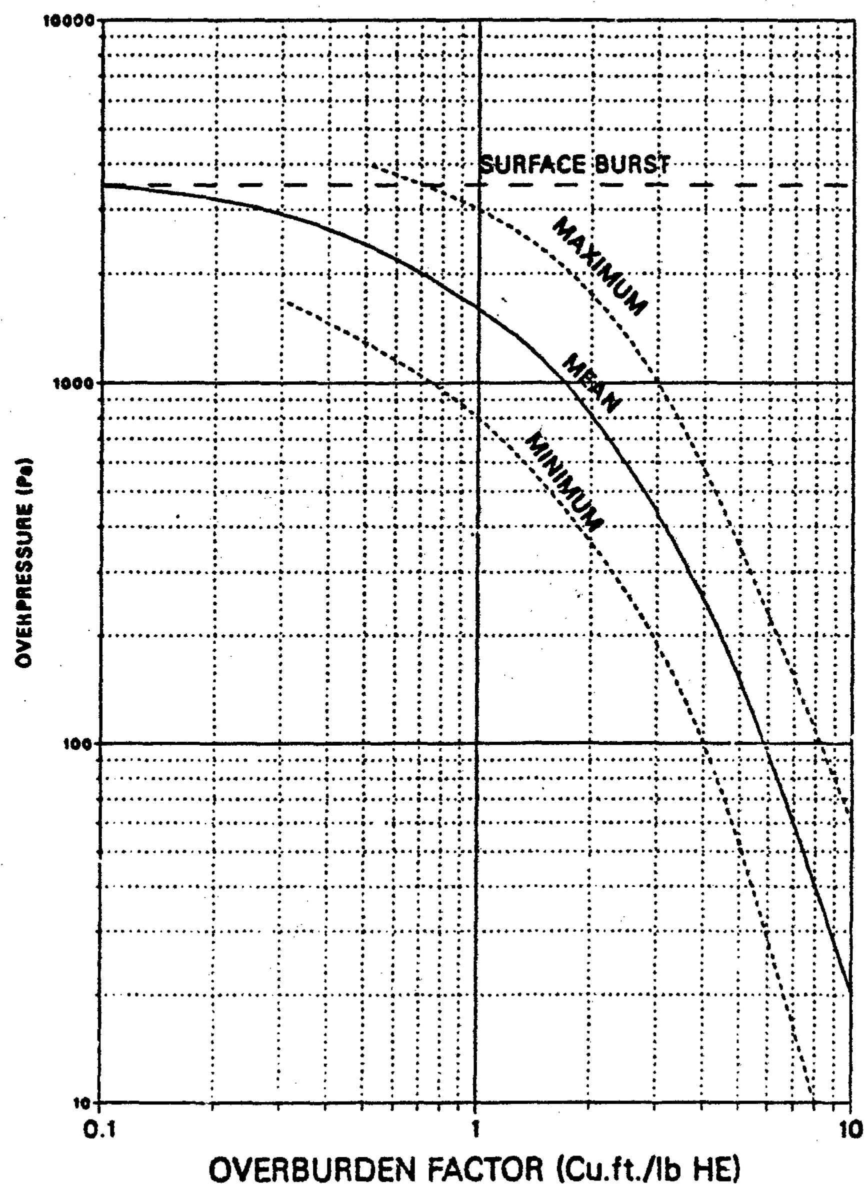

Figure 3. Reference Overpressures (914 m from 18 Mg HE) Versus Overburden Factors for HEST and Cratering Test Explosions.

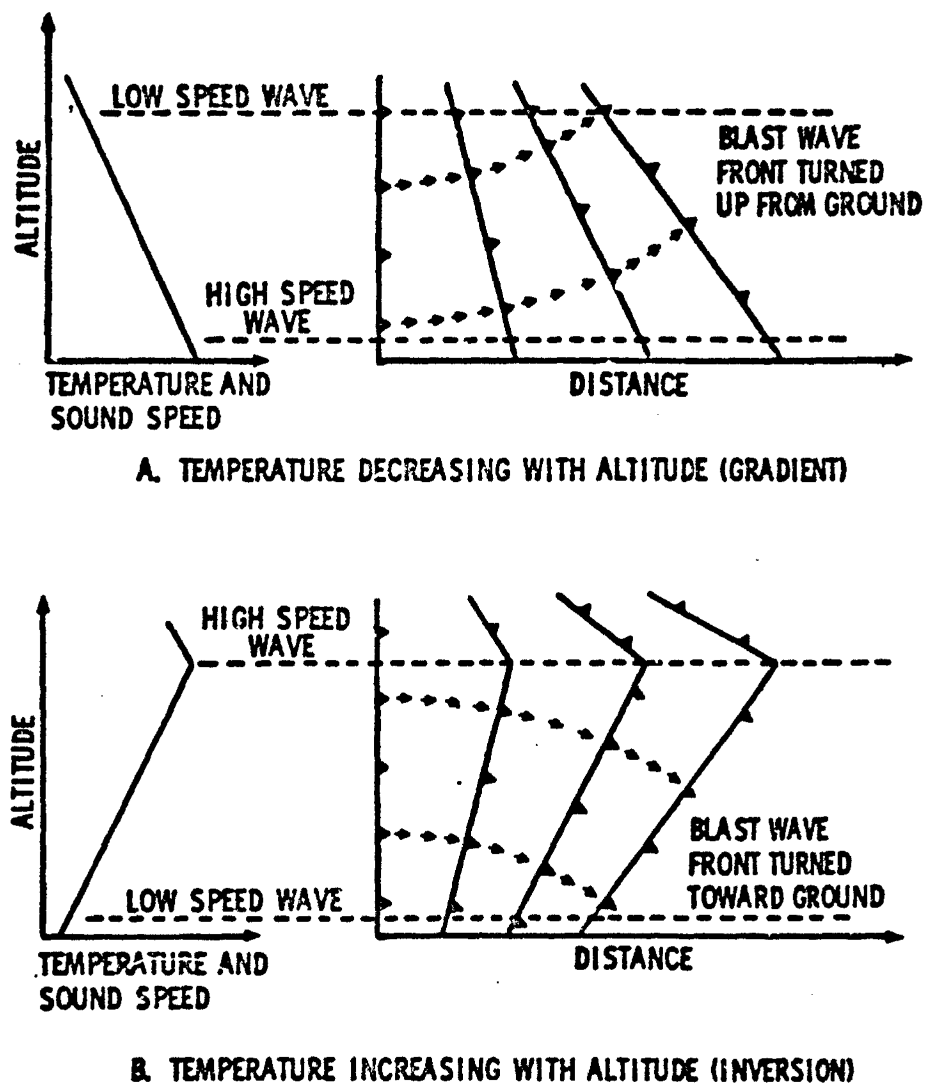

Figure 4. Blast Wave Distortions Caused by Atmospheric Conditions.

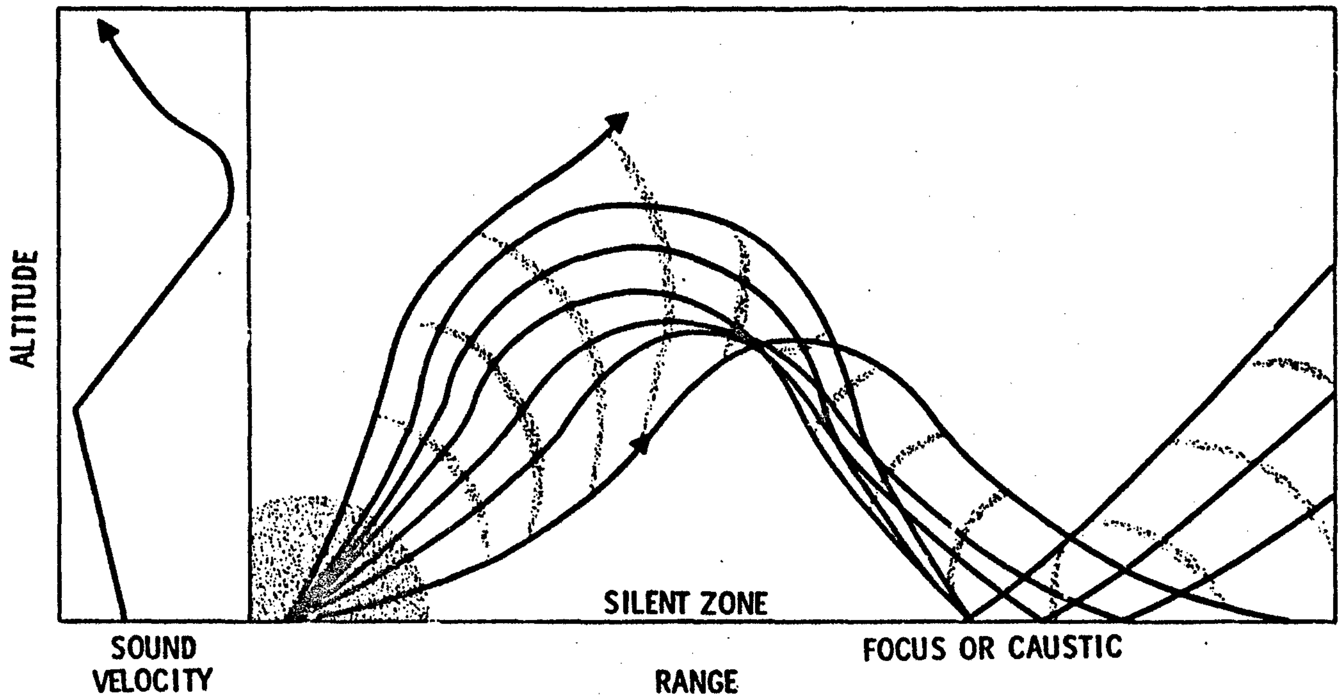

Figure 5. Typical Explosion Ray Paths under Complex Conditions.

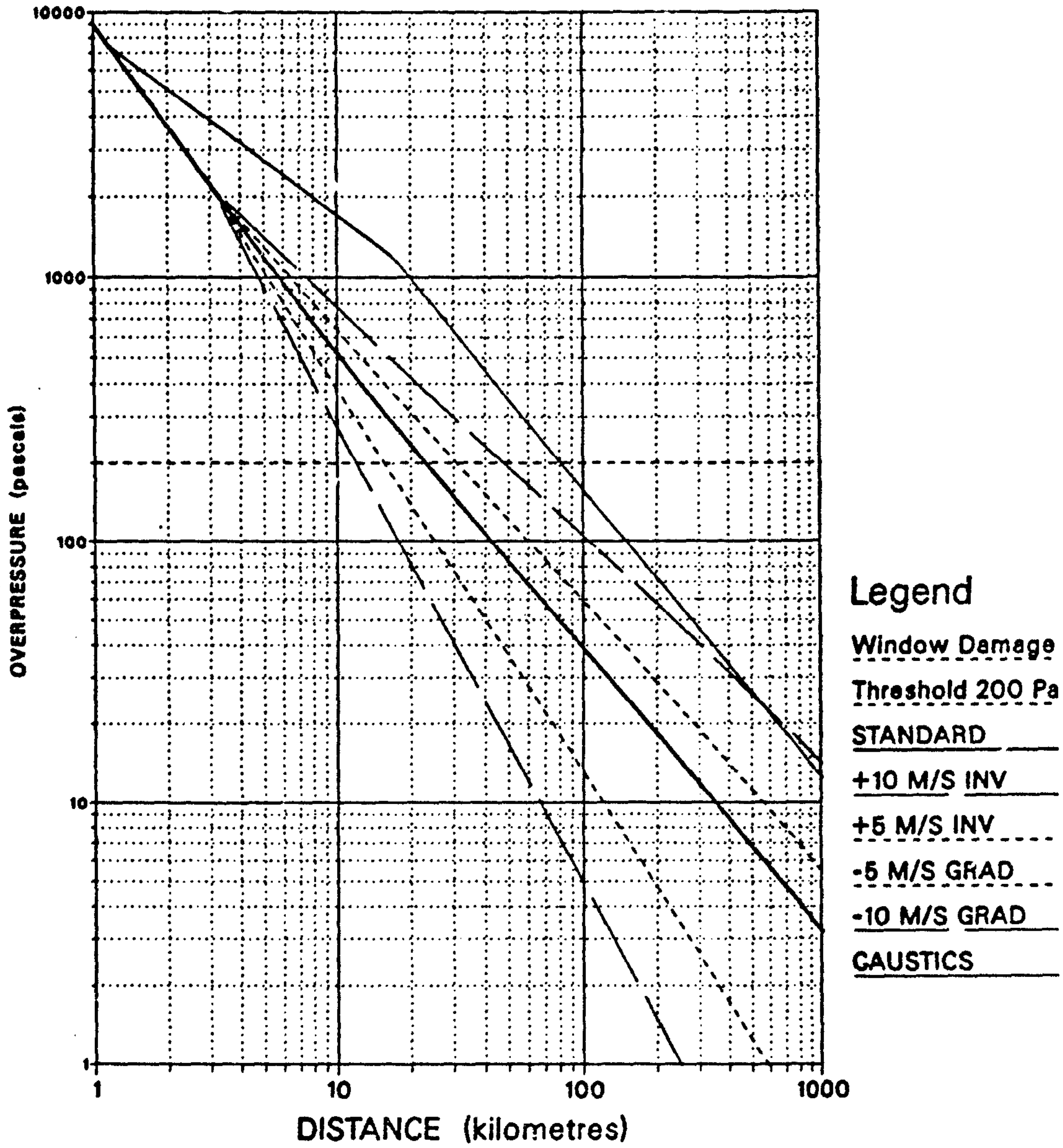

Figure 6. Overpressure Versus Distance Curves for a 1-kt Nuclear Free-Air Burst Standard Explosion in Various Atmospheric Conditions.

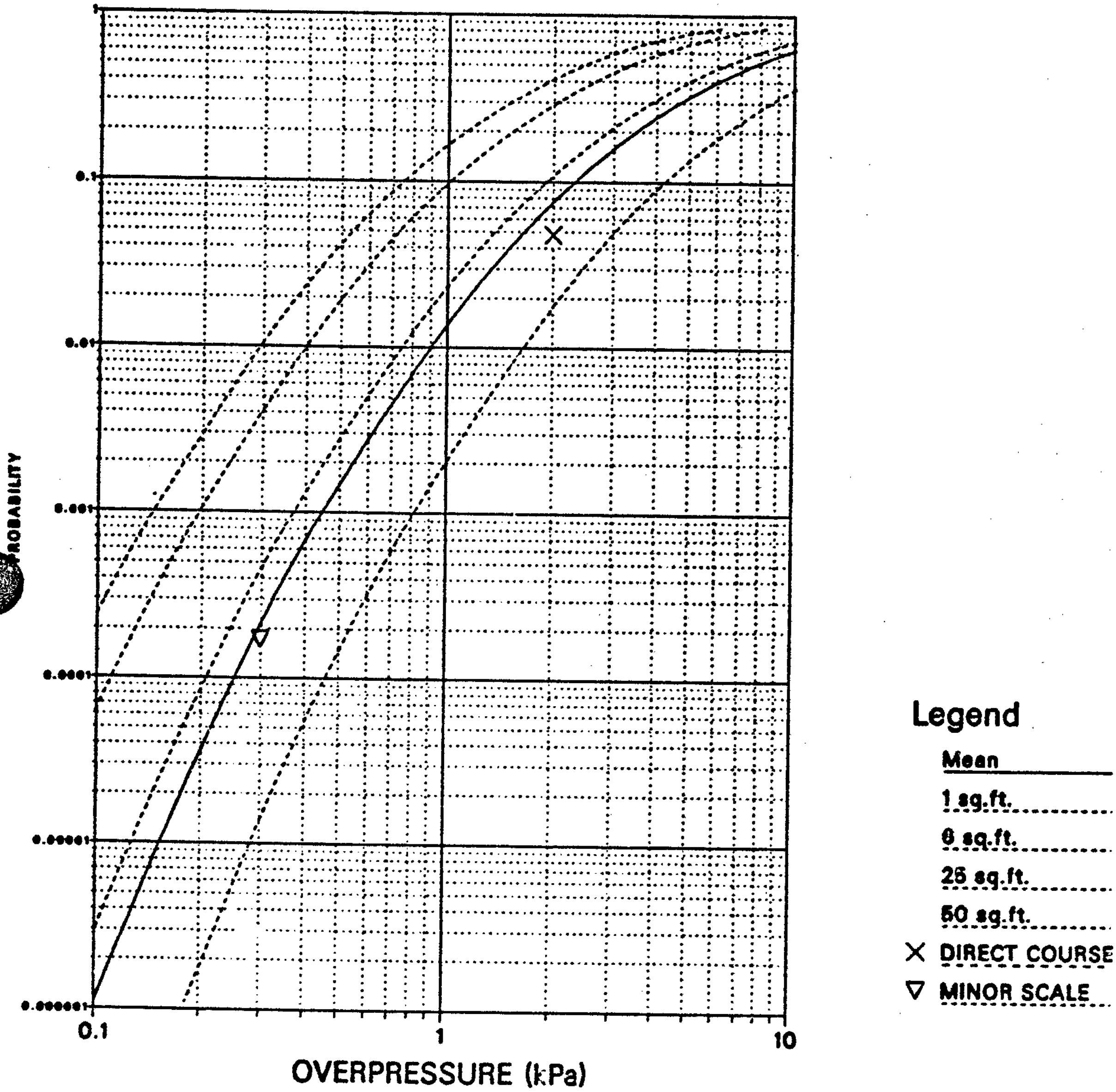

Figure 7. Window Damage Probability Versus Incident Airblast Overpressure.

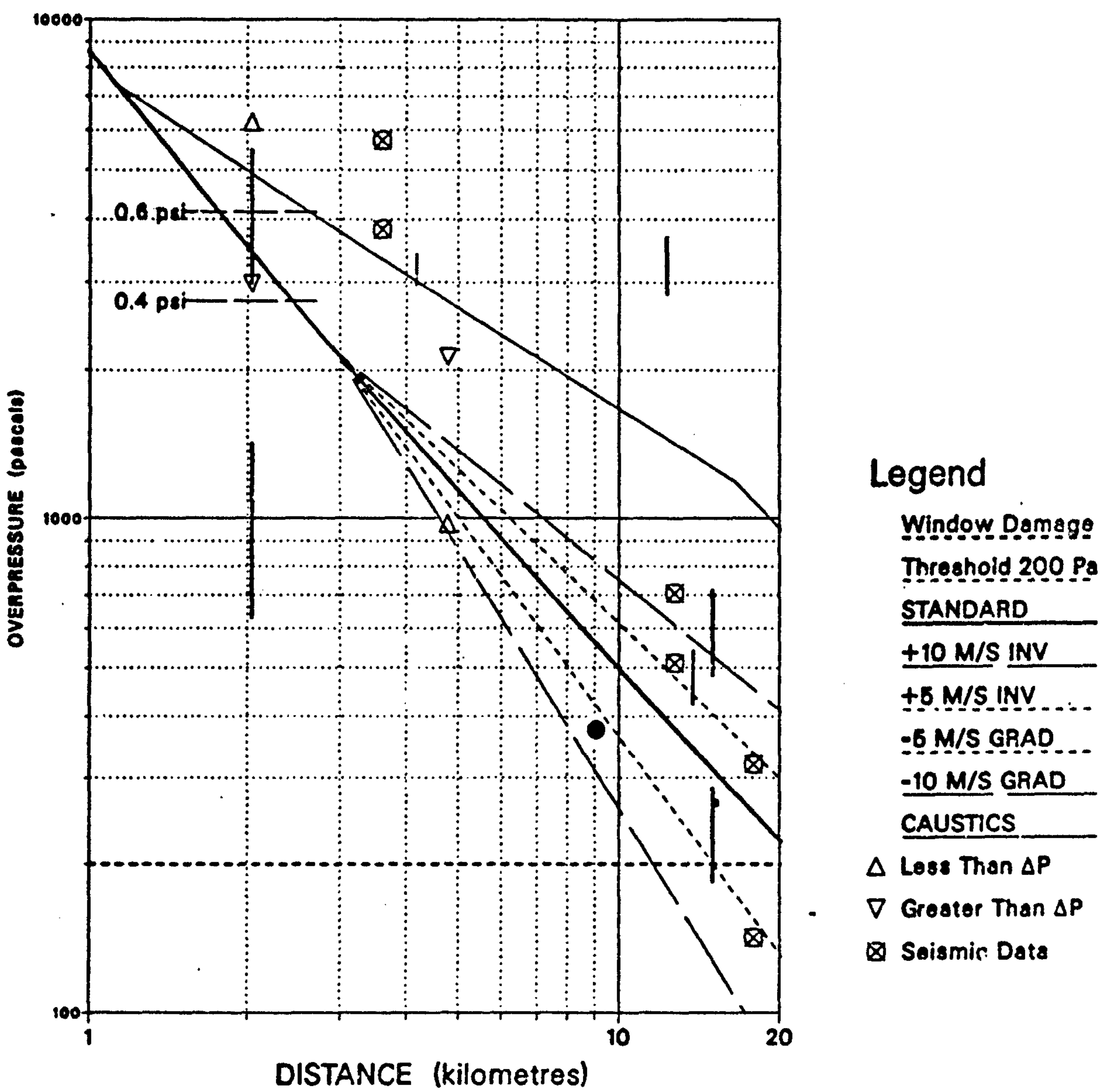

Figure 8. Incident Overpressures Estimated from Blast Damage by Pepcon Explosions.

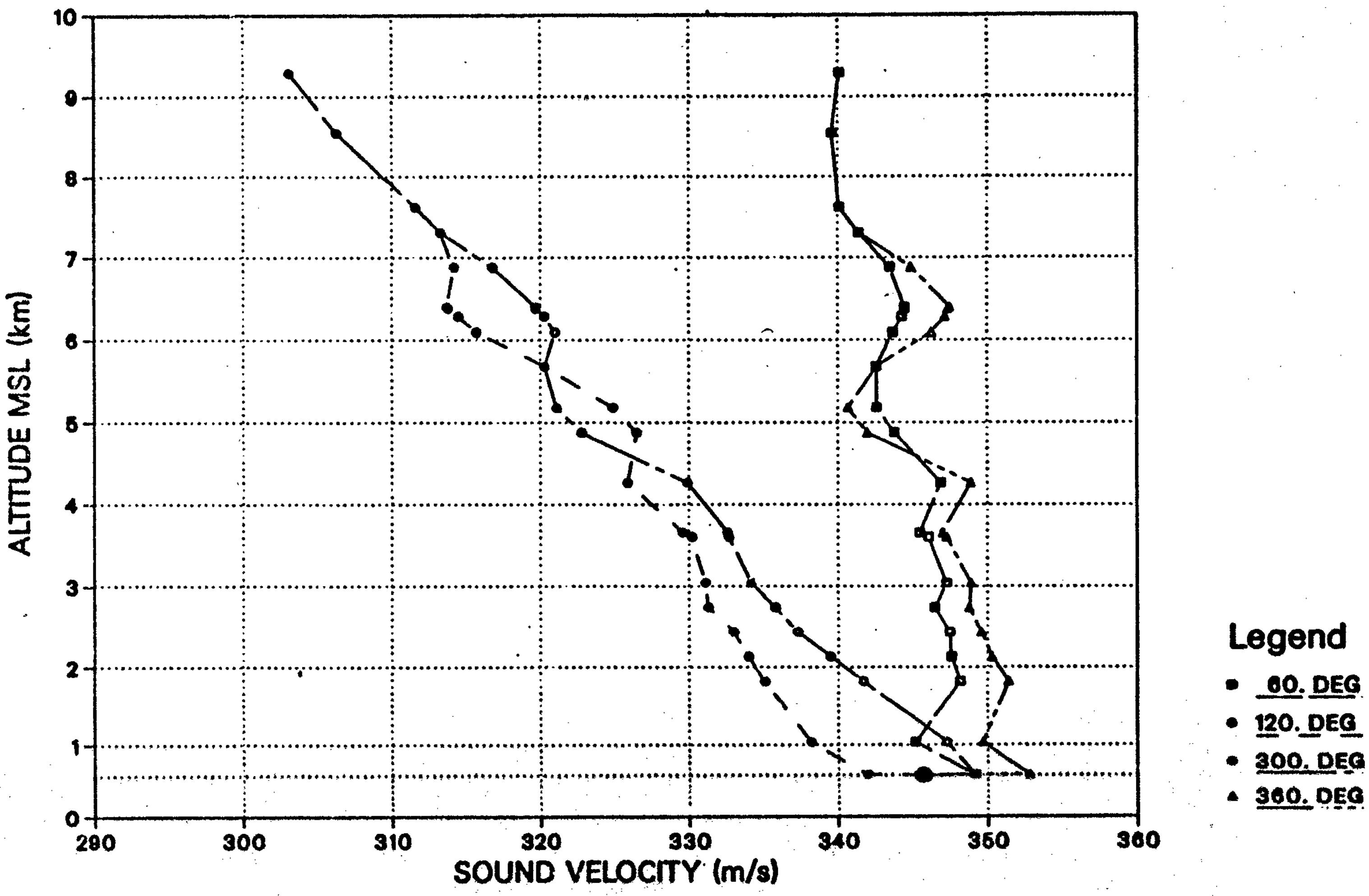

Figure 9. Sound Velocity Versus Height Curves, Composite Sounding for Henderson, Nevada, 1200 PDT, 4 May 1988.

Case Effects on Airblast for Cylindrical Charges

by
Gerhard H. Guerke
Fraunhofer-Institut fuer Kurzzeitdynamik
Ernst-Mach-Institut
Freiburg, Germany

Abstract

The effect of steel case weight to the variation of airblast parameters was studied. A series of tests were made with cylindrical RDX-charges that were either bare or cased by steel cylinders of different thickness. The test results show a more distinct case effect on the blast impulse. Various approximation formulae to determine the equivalent bare charge weight for cased charges have been suggested. All of these formulae do not meet the definition that the equivalent bare charge weight must be zero if there is no charge in the metal case. It is suggested that different formulae should be used to describe the case effect for

peak overpressure $CP = \left[\frac{W}{M + W}\right]^{1/2} = \sqrt{a}$

and for

specific blast impulse $CJ = \left[\frac{W}{2M + W}\right]^{1/2} = \sqrt{\frac{a}{2 - a}}$;

W = charge weight   M = steel case weight

$a = \frac{W}{M + W}$ = charge weight to total weight ratio

The effective bare charge weight will be calculated by using CP and CJ as factors to the actual weight of explosive in the steel cased cylinder. Both formulae meet the condition mentioned above and fit to the test results as well as to data taken from references. Besides, there is a close relationship to the Gurney energy equation.

Introduction

Experimental data indicate that blast parameters of cased HE are significantly different from those determined for bare charges. A number of methods have been proposed to relate cased and bare cylindrical charges. One approach is to assume that the only variable significantly contributing to the blast parameters other than charge weight W and standoff R is casing weight M. An equivalent bare charge weight W' can then be defined. An equivalent scaled distance Z' is calculated and the blast parameters are obtained as for bare charges. One is interested in this approach as standard curves for bare charges are available.

Many different casing formulae have been proposed in the past. There are empirical approximation formulae as proposed e.g. by Baker (SwRI) and Proctor (NOL) (Lit.6; 7) that are shown in Figure 5. Also semi-empirical formulae have been proposed, e.g. by Gurney, Fano, J. Dewey (BRL) and by British authors, that are shown in Figure 6. None of these approaches seemed to be suited to describe well the experimental data. Hence a new approach has been stated to find a better formula.

By definition the equivalent charge weight factor must be 1 for bare charges, a condition that will be met by all the approximation formulae. If there is no charge in the metal case, then the casing factor must be 0. It is a drawback of all the approximation formulae that they do not meet this condition. It will be shown that the equivalent bare charge weight for the peak overpressure can be determined by formulae that meet the conditions mentioned above and also fit to the test results.

Test Arrangement and Test Results

A test program has been planned under the premise that as few parameters as possible should be varied. Cylindrical charges having the length to diameter ratio of 1 were selected. All charges were made of pressed RDX with nominal weight of W = 1 kg. Bare charges have been detonated. In order to check casing effects cylindrical cases made of mild steel with 3 different nominal weights of 1 kg, 2 kg and 4 kg were put on the charges as shown in Figure 1. Heavy steel plates were put on top and base of the charges. Ignition took place at the top center. As a result, one can say that the only variable significantly contributing to the variation of the blast parameters is the casing weight M.

Each of the 4 test arrangements as shown in Figure 1 has been fired 5 times. Side-on pressure-time histories were measured at 8 stations along two blast lines perpendicular to each other. Gage distances were located between 5 m and 30 m from GZ. Absolute distances are identical with scaled distances in $m/kg^{1/3}$ as only 1 kg charges were used. The test results are valid in the medium-to-far field below 100 kPa peak overpressure.

The data was reduced with an evaluation program using an HP 9845 desk computer. About 160 pressure-time records were analyzed to determine shock front arrival time, shock front overpressure, specific overpressure impulse and positive phase duration. Graphical plots of the blast parameters have been generated, as shown in Figure 2 for one example. The straight lines in this figure represent smothed, numerical fits to the experimental data.

Experimental results for equivalent bare charge weight factors were determined by calculating the bare charge that produces the identical side-on peak overpressure PS or side-on specific blast impulse IS at the identical standoff R (in m). The final result of the data reduction process is summarized in Figure 3. These data will be used in order to find an equation to determine the effects on airblast of a steel casing surrounding a cylindrical charge.

Discussion

Four statements are to be made at the beginning of the discussion:

A. The working hypothesis is used that part of the detonation energy is used up to plastically deform and brake up the case, to heat and accelerate the fragments. As long as this hypothesis holds the effective bare charge weight W' for airblast will be smaller than the actual weight of explosive W in the steel cased cylinders. Experimental data indicate that the hypothesis proves well for cylindrical charges made of RDX or Comp B and cases made of mild steel.

B. The assumption is made that the only variable significantly contributing to change the blast parameters is the casing weight M. It is this assumption that limits the range of validity of different casing formulae.

C. The "casing factor" C is used in order to calculate the airblast-effective bare charge weight W' of a steel-cased HE cylinder from the actual weight of explosive W. By definition this nondimensional factor is C = 1 for a bare charge without any case and C = 0 for a steel case without any charge in it.

D. A simple formula for C is desired that meets the conditions mentioned above and also fits to the experimental data. It will be shown that the nondimensional charge to total weight ratio parameter a = W/W + M is suited to describe such a formula. This parameter varies from a = 1 for a bare charge without any case to a = 0 for a steel case without any charge in it. The discussion of casing formulae should be restricted to the range $0.2 < a < 0.8$. Outside this range other parameters than the casing weight M may strongly affect the test results.

In Figure 4 the experimental results are summarized. Each data point represents at least 5 shots. The actual charge was for all shots a 1 kg RDX cylinder at the length-to-diameter ratio of 1. Three different cases made of 1 kg (a = 0.5); 2 kg (a

= 0.33) and 4 kg (a = 0.2) of mild steel were used. It is clearly to be recognized from this diagram that the casing factor C for the specific blast impulse is smaller than for the peak overpressure. Hence two different casing formulae will be needed.

In Figure 5 two empirical approximation formulae are shown. The equation

$$C = 0.2 + 0.8\ a$$

fits the data points for blast impulse rather well. Some data points from Lit. 6 and Lit. 7 have been added to the diagram. For certain purposes the equation

$$C = 0.4 + 0.6\ a$$

could be useful in order to describe the case effect for peak overpressure measurements. A principal drawback of both formulae is that they do not meet the condition that the casing factor must be zero ($C = 0$ or $W' = 0$) for cases without explosive content ($W = 0$ or $a = 0$).

A semi-empirical relationship has been developed many years ago by Gurney (Lit. 4) that allows the evaluation of the initial velocity of fragments for a charge which consists of an evenly distributed explosive in a cylindrical metal case of uniform thickness. The initial velocity V_0 is described in terms of the type of explosive e, the weight of explosive W and the weight of the cylindrical portion of the metal casing M.

$$V_0 = (2\ e)^{1/2} \left(\frac{W/M}{1 + W/2M} \right)^{1/2} = (2\ e)^{1/2} \cdot \left(\frac{W}{M + 0.5W} \right)^{1/2} \qquad (1)$$

Where $(2e)^{1/2}$ is the Gurney Energy Constant which was developed from empirical data for various explosive materials contained in mild steel casings.

To develop equation (1), it was assumed that the yield or total explosive energy $E_0 = e \cdot W$ is transformed to kinetic energy of the metal case and part of the detonation products. The energy equation was used for cased cylindrical charges:

$$e \cdot W = \frac{1}{2} (M + 0.5\ W) \cdot V_0^2 \tag{2}$$

that can be transformed to

$$e \cdot W = 0.5\ M\ V_0^2 + 0.25 \cdot W \cdot V_0^2 \tag{3}$$

In order to estimate the airblast-effective bare charge W', it has been argued that the airblast is produced by the energy of the detonation products only

$$E_0' = e \cdot W = 0.25 \cdot W \cdot V_0^2 = \frac{(e \cdot W) \cdot W}{W + 2M} \tag{4}$$

As a result, the following casing factor was calculated with $E_0 = e\ \ W$

$$\frac{E_0'}{E_0} = \frac{W'}{W} = \frac{W}{W + 2M} = \frac{a}{2 - a} \tag{5}$$

It has been detected long ago, and may be seen from Figure 6 that formula (5) does not meet the experimental results. Fano (Lit. 4) has suggested a modification of formula (5) by arguing that a constant portion 0.2 W of the actual weight of explosive charge contributes to the airblast effective weight independent of the type of metal casing. The rest of the Fano-formula is taken from Gurney's energy equation:

$$C = \frac{W'}{W} = 0.2 + \frac{0.8 \cdot W}{W + 2M} = \frac{1}{2 - a}\ (0.4 + 0.6a) \tag{6}$$

It is shown in Figure 6 that Fano's formula does not meet the experimental data either. Some more modifications of Fano's casing factor have been proposed by different authors (Lit. 4; 10; 13), as was shown in Figure 6. All the formulae of the Fano-type do not meet the definition that the airblast-effective bare charge weight W' must be zero (W' = 0) for a steel case without any charge in it (W = 0). They also show the wrong curvature in order to meet the experimental data.

Another modification of Gurney's casing factor is proposed in Figure 7. Not the term a/2 - a but the square root:

$$CJ = \frac{W'}{W} = \sqrt{\frac{W}{W + 2M}} = \sqrt{\frac{a}{2 - a}} \tag{7}$$

describes well the data points and is recommended here for casing factor CJ accounting for the specific blast impulse.

To get a casing factor accounting for the peak overpressure, a different energy equation will be used. Years ago at the Explosive Safety Seminars there were many presentations on the Navy Explosives Safety Improvement Program (NESIP). The Unified Theory of Explosions (UTE) was part of this program. In UTE it was assumed that the yield or total explosive energy E_0 is partitioned equally among the total mass present, HE plus case, or W + M. It was taken into consideration that, when the shock emerges from the case, a strong rarefaction wave moves inward to the center of explosion which converts all the local energy to kinetic energy. By setting the kinetic energy equal to the yield

$$e \cdot W = \frac{1}{2}(M + W) \cdot V_0^2 \tag{8}$$

the proper average velocity gives

$$V_0 = (2\,e)^{1/2} \left(\frac{W}{W + M}\right)^{1/2} = \sqrt{2e} \cdot \sqrt{a} \tag{9}$$

It was emphasized in the UTE presentation that this approach takes care of the fact that the blast energy is peaked at the front, which was omitted by the Gurney-Fano approach.

The energy equation (8) can be transformed to

$$e \cdot W = 0.5\ M\ V_0^2 + 0.5\ W\ V_0^2 \tag{10}$$

Under the assumption that the blastwave is generated by the energy of the detonation products only results:

$$E_0' = eW' = 0.5 \cdot W \cdot V_0^2 = \frac{(e \cdot W) \cdot W}{W + M} \tag{11}$$

with $E_0 = e\ W$

$$\frac{E_0'}{E_0} = \frac{W'}{W'} = \frac{W}{W + M} = a \qquad (12)$$

In Figure 8 is shown that the term:

$$CP = \sqrt{\frac{W}{W + M}} = \sqrt{a} \qquad (13)$$

the square root of the charge to total weight ratio describes well the casing factor accounting for the peak overpressure. It is also shown that the linear equation CP = a does not meet by far the experimental data.

Finally, in Figure 9 the ratio:

$$\frac{CP}{CJ} = \sqrt{2 - a} \qquad (14)$$

that describes the difference between the casing factors accounting for peak overpressure (13) and for specific blast impulse (7) is compared to results from the literature. Petes (Lit. 8) derived a constant factor 1.19 from the experiments that were made at the Naval Ordnance Laboratory. In England tests were made with different ordnance (Lit. 4). The Fano formula was used for the casing factor accounting for specific blast impulse and a modified Fano formula for peak overpressure as shown in Figure 6. It may be recognized that in any case the impulse casing factor was found to be smaller than the peak overpressure casing factor. In the region where tests were made with different ordnance the three approaches are in satisfactory agreement, indicating that the new approach is in coincidence with former experimental results.

Conclusions

For practical application in the field of explosive safety, approximation formulae of the linear type as shown in Figure 5 are well suited. Semi-empirical formulae of the Fano-type as shown in Figure 6 do not better meet the experimental data, they have the wrong curvature and do not fulfill the boundary conditions. They are not more useful than approximation formulae of the linear type and do not allow more insight in the physics of the casing effect. Formulae as proposed in Figure 7 and Figure 8 meet the experimental data and fulfull the boundary conditions, A further discussion may allow more insight in the physics of the casing effect. The casing factors CI and CP are proportional to the square root of the expressions that were derived from energy equations. Possibly that is a hint that the impulse of the fragments and the detonation products are more important to describe the casing process than the kinetic energy.

List of Symbols

W	actual weight of explosive charge in kg
e	specific energy of explosive in kJ/kg
$E_0 = e\ W$	yield or total working performance of explosive charge in kJ
V_0	initial velocity in ms^{-1} for fragments and detonation products
W'	airblast-effective charge weight of steel cased cylinders in kg
M	case weight in kg of the cylindrical portion of the steel casing
M/W	metal to charge weight ratio
$a = \frac{W}{W+M} = \frac{1}{1+M/W}$	charge to total weight ratio

C = W'/W casing factor

CP = W'/W casing factor accounting for peak overpressure

CI = W'/W casing factor accounting for specific blast impulse

References

1. G. Gürke, G. Scheklinski-Glück, "Blastparameter bei der Oberflächendetonation senkrecht stehender Explosivstoffzylinder mit den Streckungen L = 1D bis L = 6D", Bericht des Ernst-Mach-Instituts, E 16/85, Juni 1985

2. G. Gürke,"TNT-Äquivalentfaktoren für Projektile unter Berücksichtigung von Form- und Casingfaktoren", Bericht des Ernst-Mach-Instituts, V 2/84, September 1984

3. K.-H. Boelke, "Ermittlung der Blastparameter bei stehenden Explosivstoffzylindern", Erprobungsstelle 91 der BW, Bericht Nr. 22/86/91-334, Oktober 1986

4. Handbuch Munitionsbewertung, BWB, WM VI 2, M. Held, "Blastwellen bei Detonationen in Luft", Ausgabe A - 1981, Abschnitt 4.2, 1981

5. Waffenwirkungen und Schutzraumbau, D. Itschner, "Konventionelle Waffen", Forschungsinstitut für Militärische Bautechnik, Zürich FMB 73-11(10), 1976

6. "A Manual for the Prediction of Blast and Fragment Loading on Structures". US Department of Energy, DOE/TIC-11268, November 1980

7. J. F. Proctor, "Internal Blast Damage Mechanisms Computer Program", Naval Ordnance Laboratory, NOLTR 72-231, AD-759002, August 1972

8. J. Petes, "Blast and Fragmentation Characteristics", Annals of the New York Academy of Sciences, Vol. 152, p. 368, 1968

9. M. M. Swisdak, "Explosion Effects and Properties Part I - Explosion Effects in Air", Naval Surface Weapons Center, NSWC/NOL/TR 75-116, October 1975

10. W. S. Filler, "A New Approach to Airblast from Cased Explosives", Naval Ordnance Lab., NOLTR 70-66, October 1970

11. F. B. Porzel, "Technology Base of the Navy Explosives Safety Improvement Program", NSWC MP 79-311, 1979 (Expl. Safety Seminar, 1980)

12. G. F. Kinney, K. J. Graham, "Explosive Shocks in Air", Springer-Verlag, New York, 1985

13. Fragment and Debris Hazards, Department of Defense Explosives Safety Board, Technical Paper No. 12, July 1975

14. Suppressive Shields, Structural Design and Analysis Handbook, U.S. Army Corps of Engineers, HNDM-1110-1-2, November 1977

15. Structures to Resist the Effects of Accidental Explosions, TM5-1300, 1969

16. Meyer, Explosivstoffe, Weinheim, 1979

17. "Computer Program for Predicting Casualties and Damage from Accidental Explosions", Department of Defense Explosives Safety Board, Washington D.C., Technical Paper 11, May 1975

18. E. M. Fisher, "The Effect of the Steel Case on the Air Blast High Explosives", NAVORD Report 2753, 1953

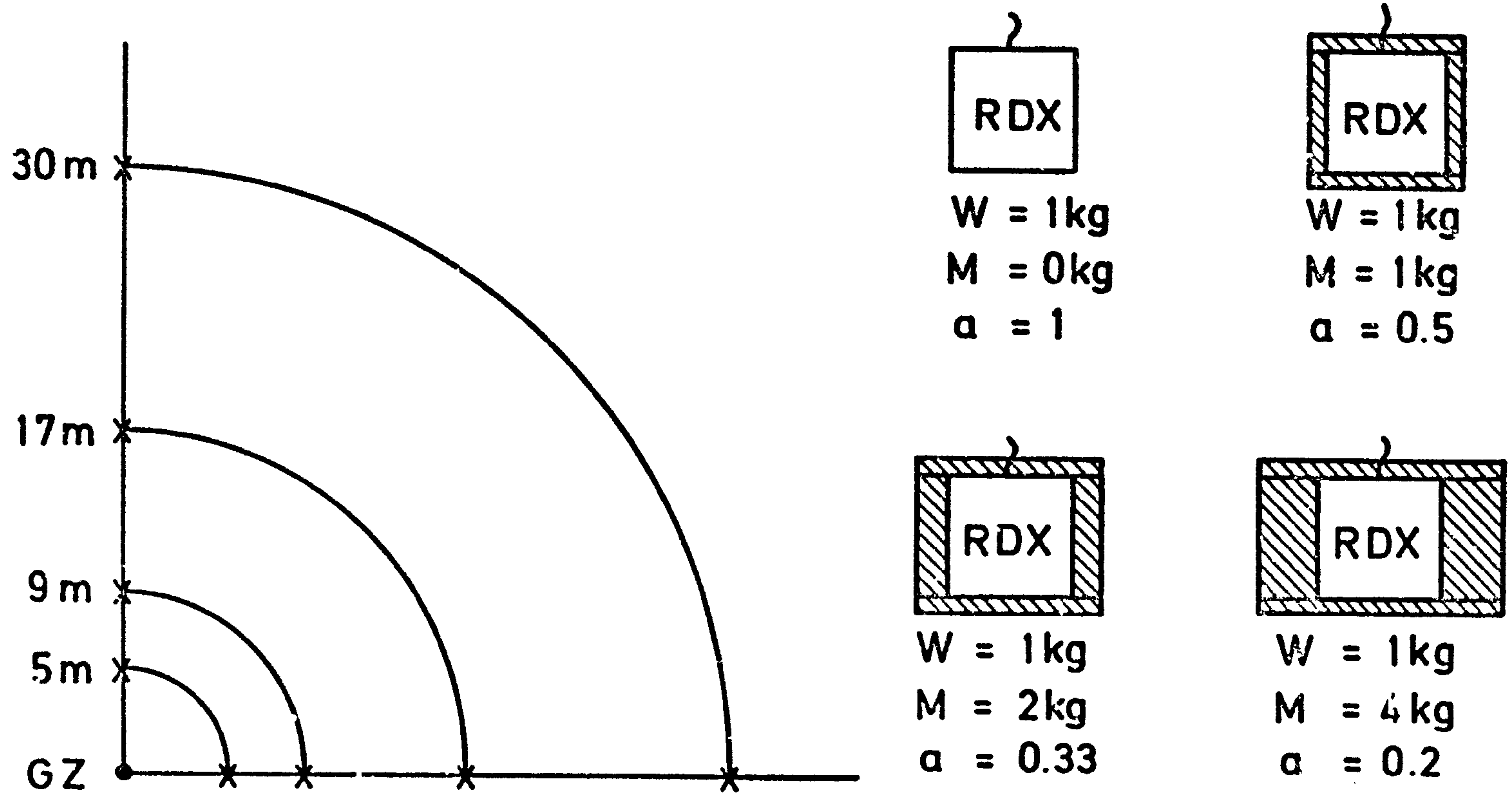

Figure 1 **Test Arrangement**

Cylindrical 1kg - RDX Charges with different mild steel cases. Side-on pressure measurements at 8 point along two axes.

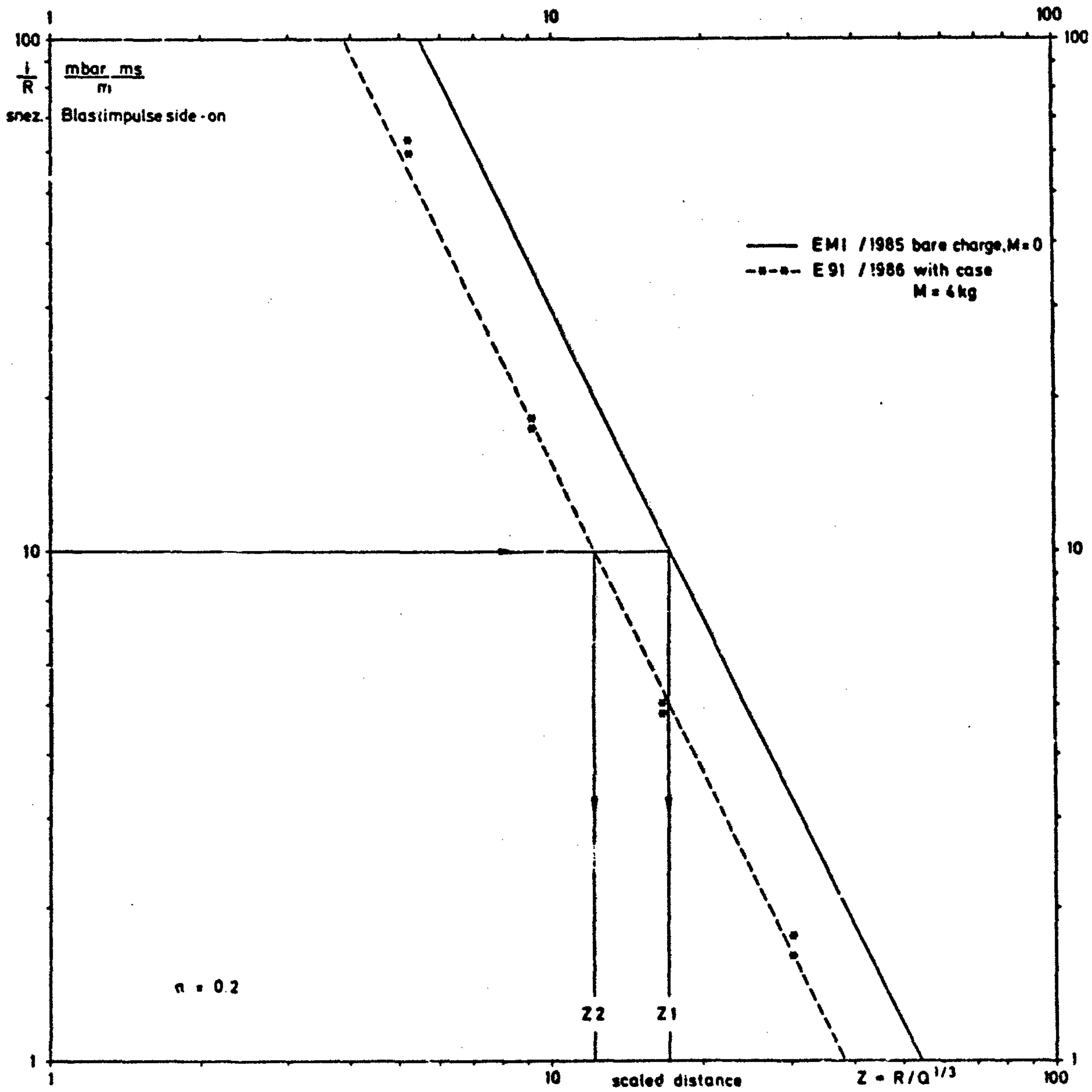

Figure 2

Casing - Diagram to determine the airblast - effective equivalent weight W' for specific blast impulse

$W' = \left(\frac{Z\,2}{Z\,1}\right)^3 \cdot W$

Figure 3 Test Results

W kg	M kg	a	CP	CI
1	0	1	1	1
1	1	0,5	0,685	0,60
1	2	0,33	0,57	0,435
1	4	0,20	0,44	0,35

W actual weight of explosive in kg

M steel case weight in kg

$a = \frac{W}{W+M}$ charge to total weight ratio

CP casing equivalent weight factor for peak overpressure

CI casing equivalent weight factor for specific blast impulse

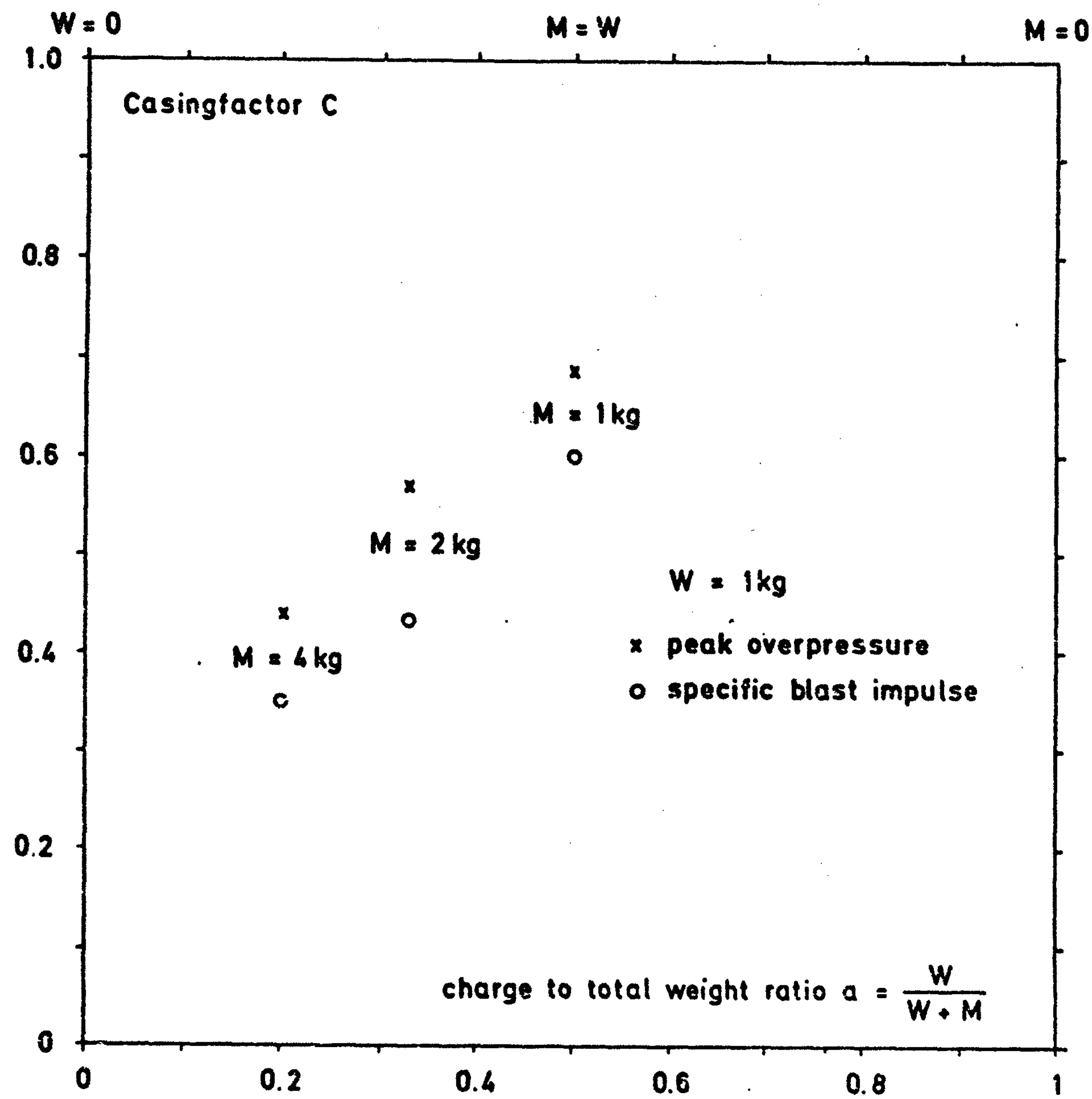

Figure 4

Casing - Collection of Experimental Results for Cylindrical Charges with Cases of Mild Steel

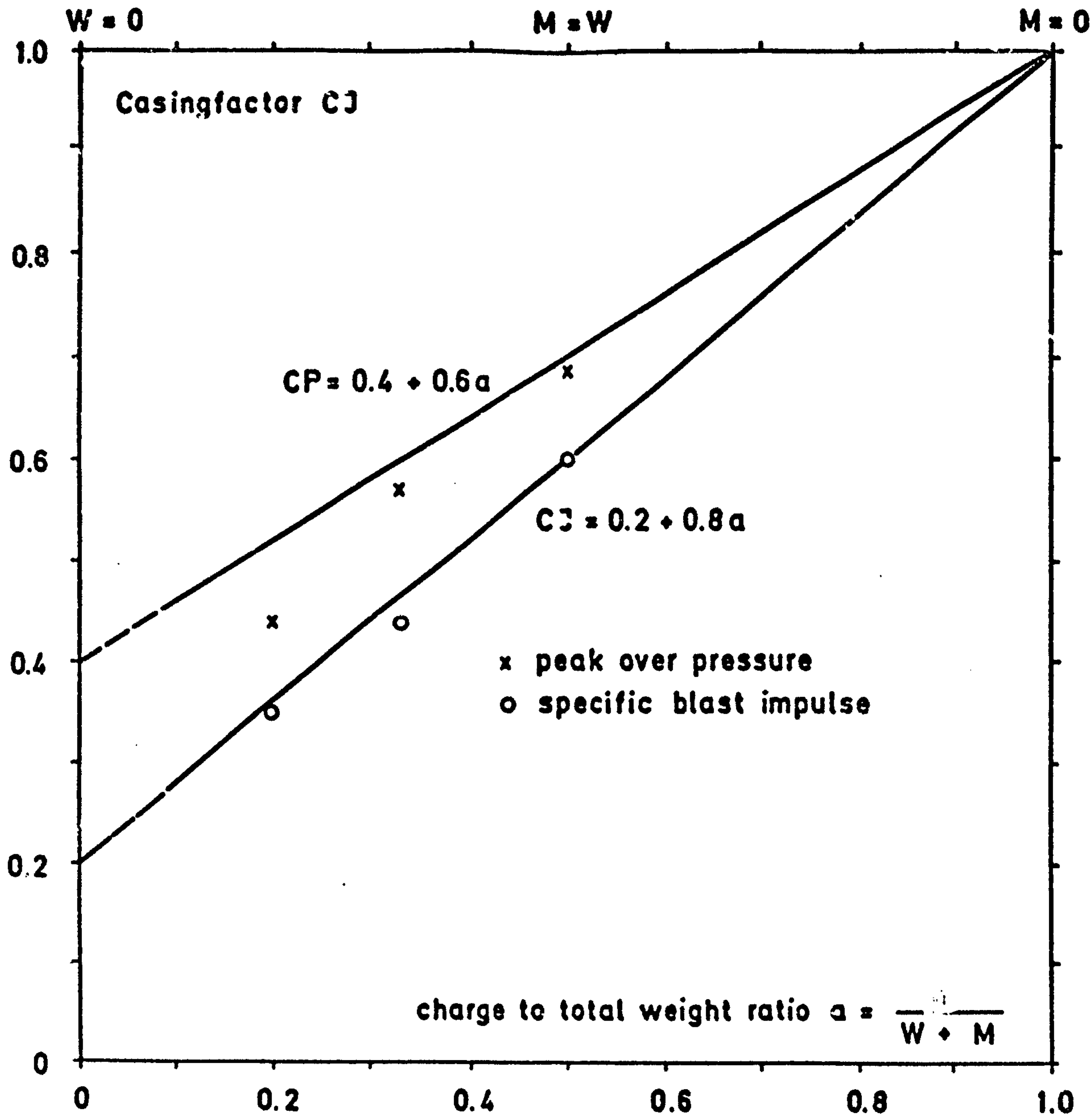

Figure 5

Casing - Empirical Approximation Formulare

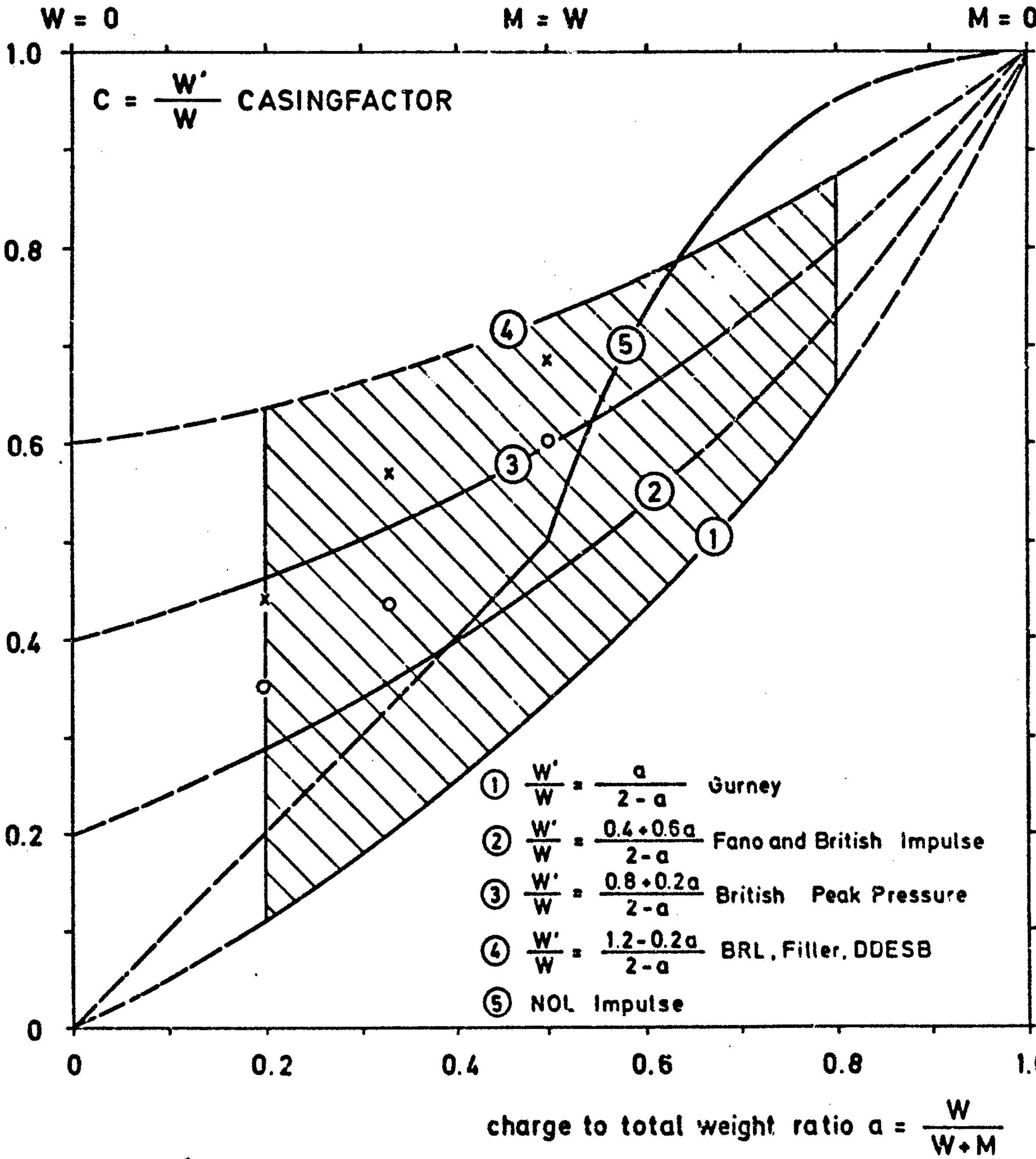

Figure 6

Casing - A Selection of Casing Formulae of the GURNEY - FANO - type

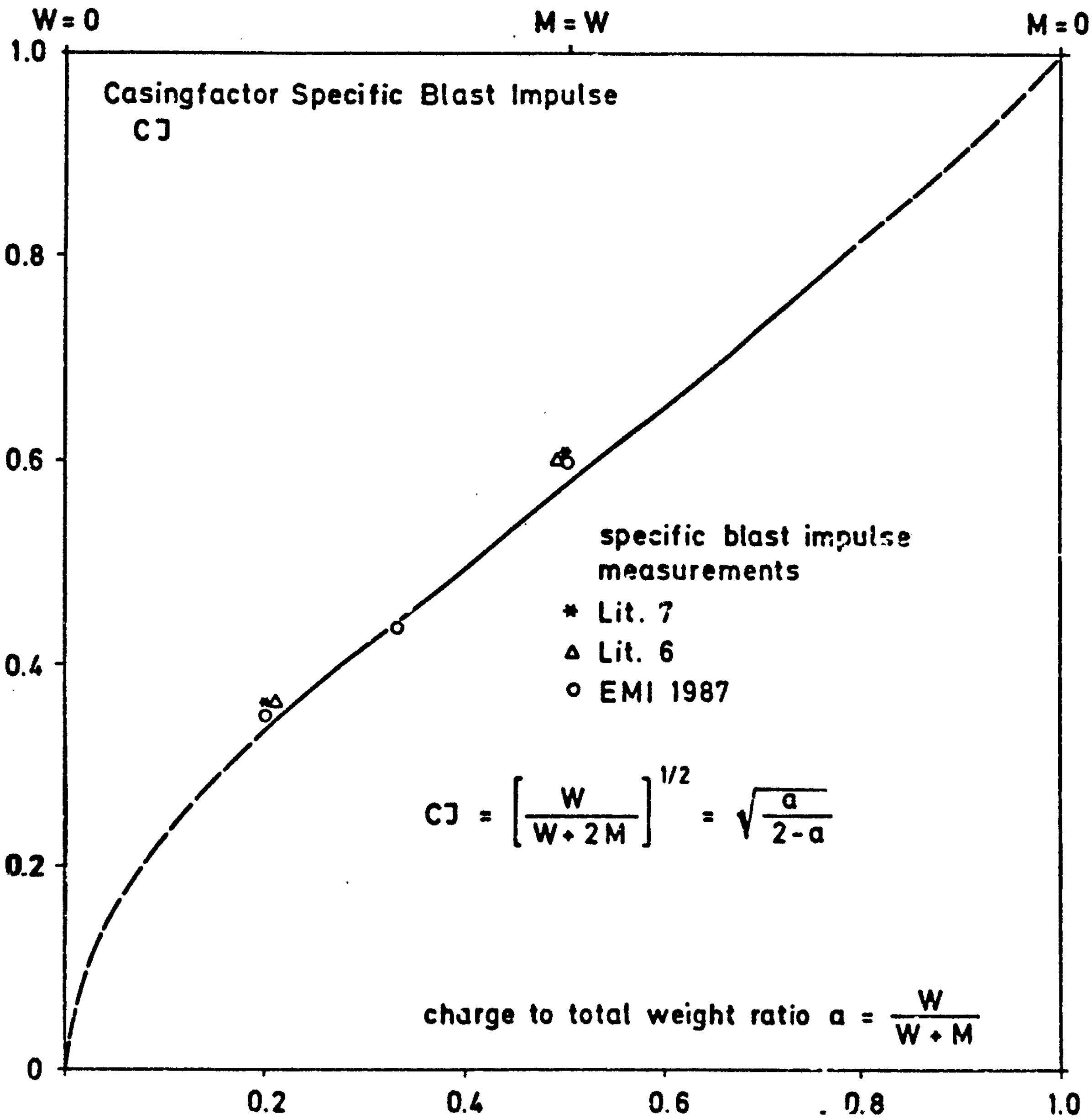

Figure 7

Casing - Formula to Describe the Case Effect on Specific Blast Impulse

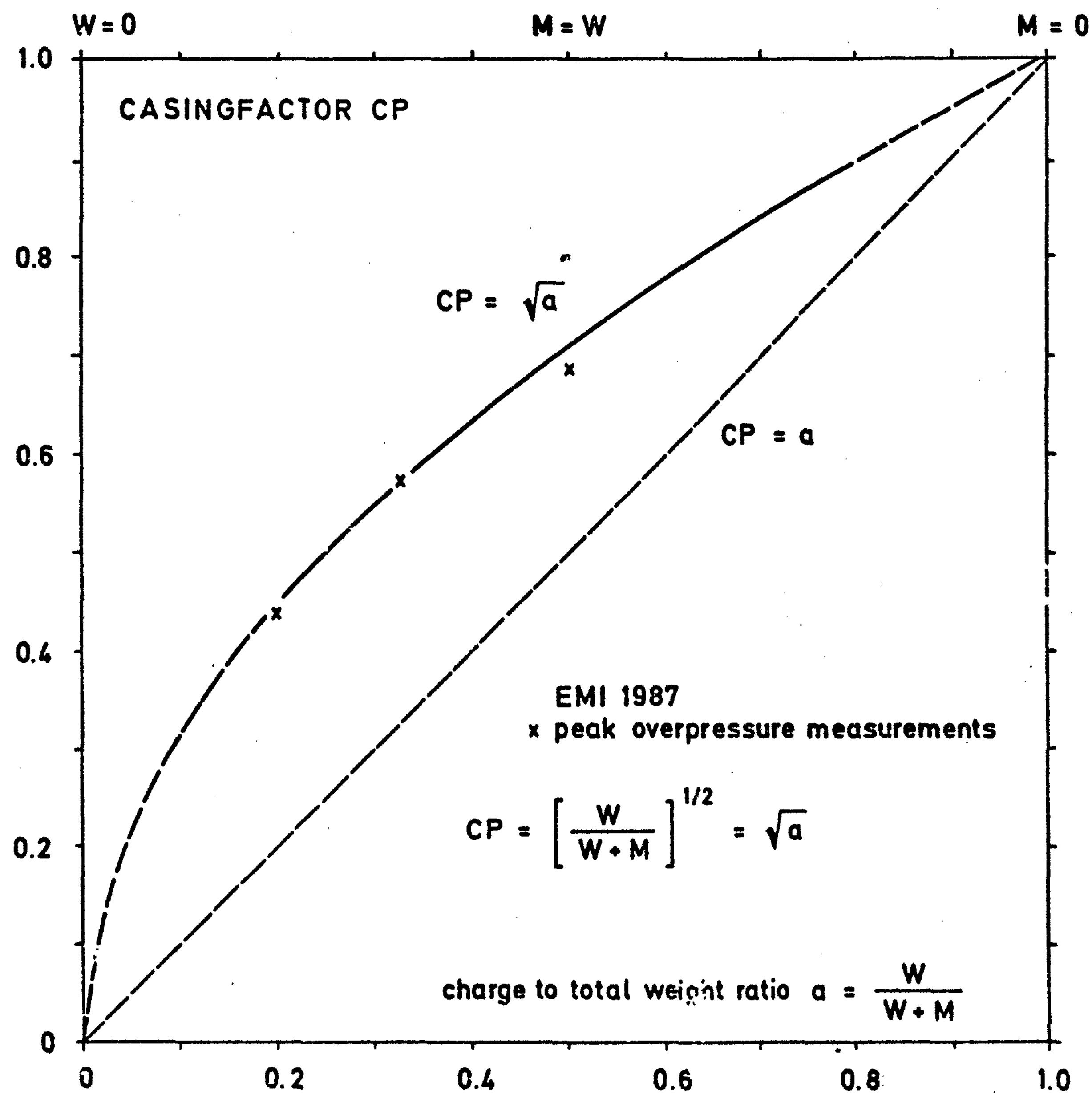

Figure 8

Casing - Formula to Describe the Case Effect on Peak Overpressure

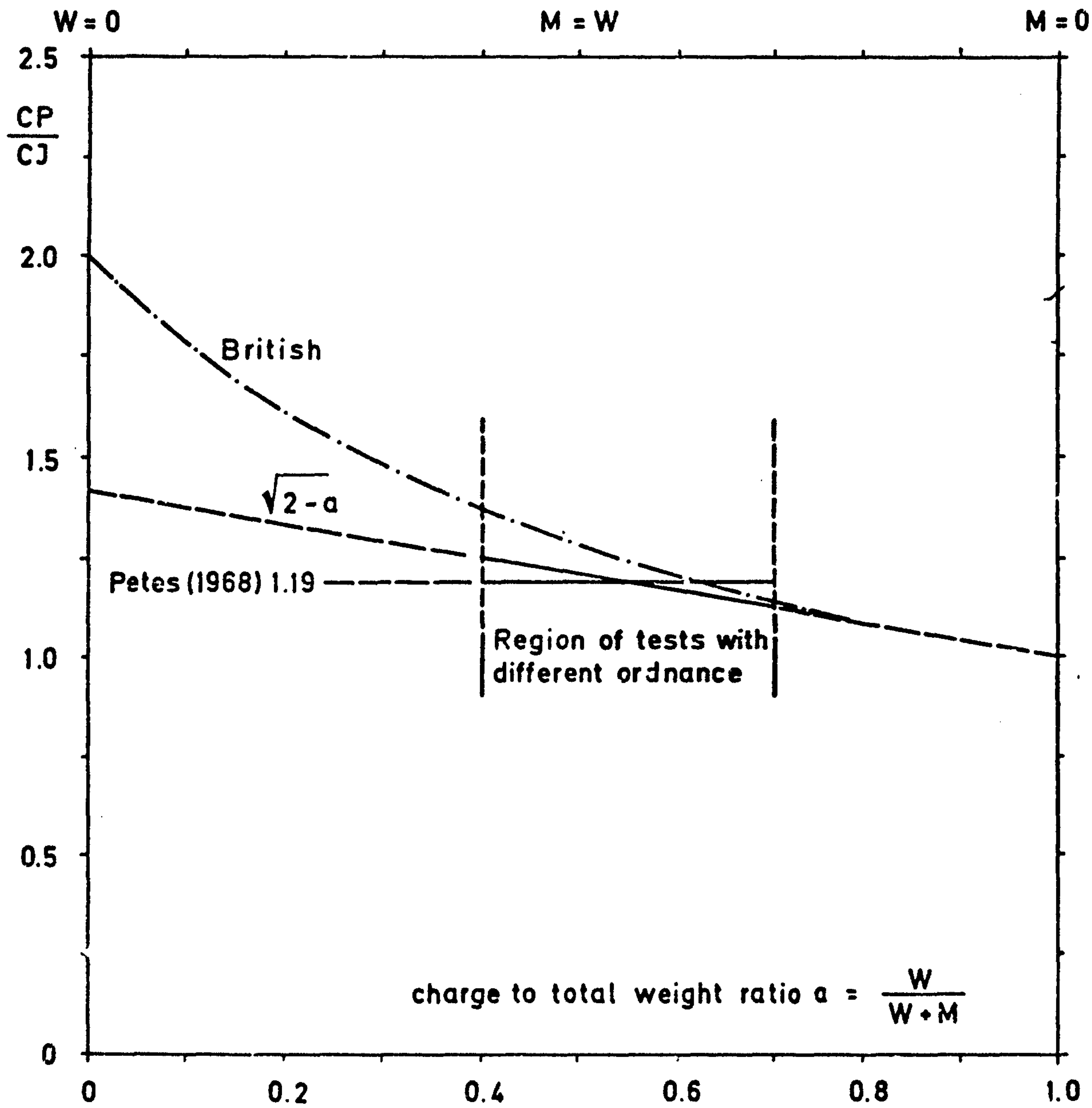

Figure 9

Casingfactors - checking the difference between effective bare charge weight factors for peak overpressure and specific blast impulse from different references

Significant Hazards and Risks of the Chemical Stockpile Disposal Program

Thomas S. Kartachak
Willard E. Fraize
Robert Cutler
William Duff
John Perry
Brian Price

August 1988

U.S. Army, Office of The Program Executive Officer-
Program Manager for Chemical Demilitarization

and

The MITRE Corporation
Civil Systems Division

TABLE OF CONTENTS

1.0 INTRODUCTION

The U.S. Army's stockpile of chemical munitions is stored at eight sites throughout the continental United States. (See Figure 1.) The Army's Program Executive Officer-Program Manager for Chemical Demilitarization (PEO-PM Cml Demil) has the responsibility for disposing of the existing stockpile. PEO-PM Cml Demil has developed the Chemical Stockpile Disposal Program (CSDP) and has prepared a Programmatic Environmental Impact Statement (PEIS) to evaluate the environmental impacts of alternative approaches to disposing of the lethal chemical agent and munition stockpile. A comprehensive assessment of the frequency and magnitude of chemical agent release and associated consequences was performed to assist in selecting the preferred alternative.

1.1 Purpose of the Risk Analysis

The major purpose of this risk analysis was to provide the Army with a consistent and quantitative comparison of the risks associated with each one of the disposal alternatives. The relative risk to public safety of the alternatives was evaluated on the basis of risk to the public (individuals outside the boundaries of the military installation) at proposed disposal sites and along potential transportation corridors.

This document summarizes the results of a comprehensive probabilistic risk analysis for the storage, handling, on-site transportation, off-site transportation, and chemical demilitarization plant operations associated with disposal of the chemical stockpile.

An essential first step in risk analysis is the identification of potential accidents that contribute significantly to risk. This requires that the risk analysis be performed on an accident-specific basis.

Since risk analysis deals with potential future occurrences, uncertainty in the results is unavoidable. In addition, uncertainty in the risk analysis arise from gaps in data in our understanding of the accident phenomena, which require that many assumptions be made in the analysis. Estimates of uncertainty in the probability of accident occurrences were developed, and are displayed with the risk estimates. Another paper in this seminar describes how uncertainty in the results was addressed.

Despite uncertainties in the results, risk analysis remains the best available means for systematically identifying major sources of risk, quantifying safety concerns, and comparing the relative risk of the different alternatives. Subjective factors related to developing a sound safety philosophy (e.g., administrative controls) and to managing risks that are difficult to quantify (e.g., sabotage, procedural errors) are important also, and need to be considered along with the insights offered by quantitative risk analysis.

The data used in this risk analysis are of two broad types: historical data — that is, data derived from records of a large number of actual events which are related to specific types of accidents, or events leading to them; and hypothesized data — data derived from largely subjective modeling of assumed accident sequences with the aid of fault and event trees describing the process. (The use of fault and event trees is a standard procedure to investigate sequences

ORNL DWG [illegible]

Stockpile Distribution Throughout the Country

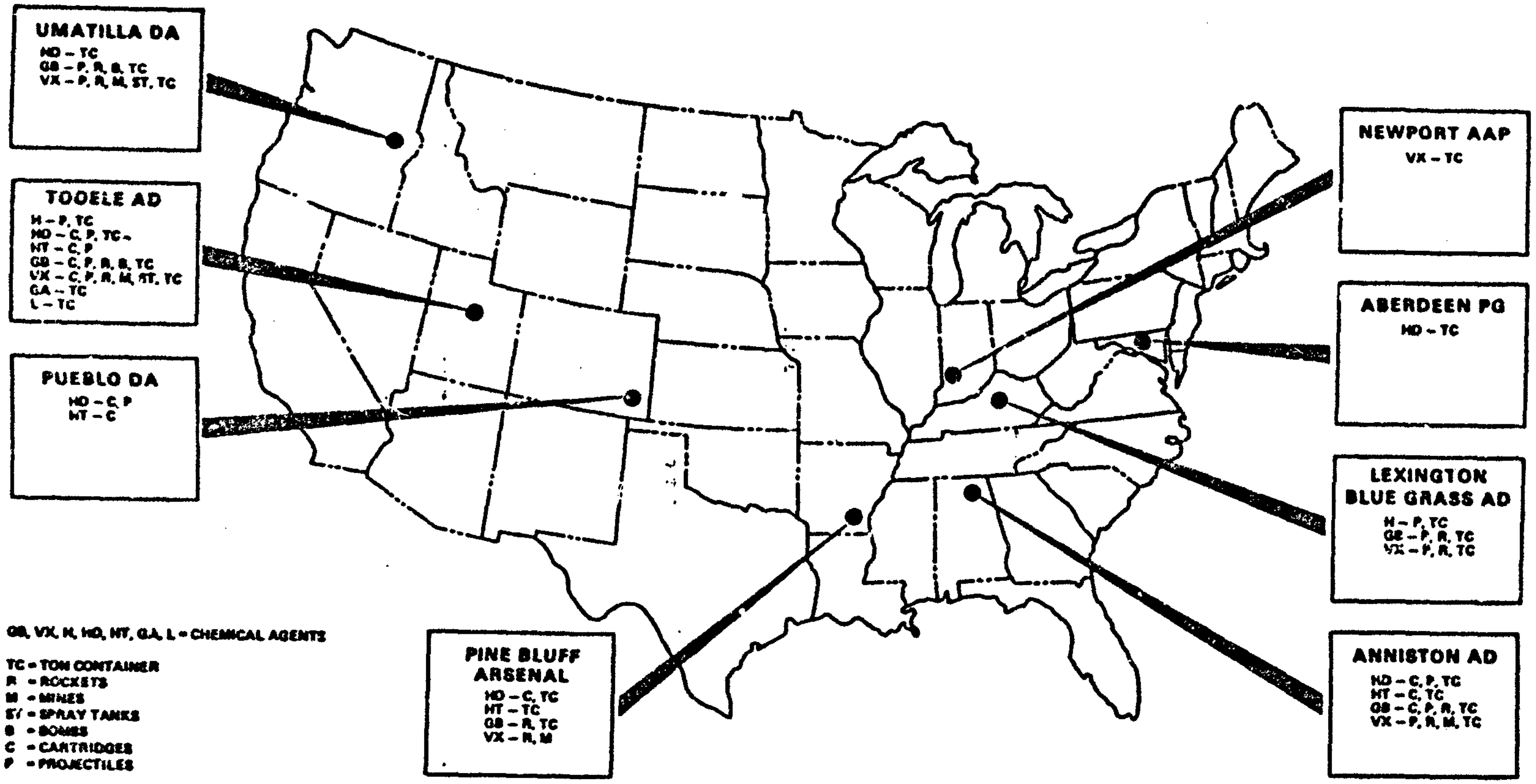

FIGURE 1

of occurrences in a complex system.) Risk data for externally-caused accidents such as those due to aircraft crashes and destructive natural phenomena, as well as data related to off-site transportation (via rail freight, air, barge, etc.) can be drawn from historical data bases. Modeling data, based on analysis of hypothesized sequences involved in the accident scenarios, must be developed for those events which are unique to the handling and processing of chemical munitions, and for which there are very few historical data.

1.2 Risk Elements of the CSDP

To understand the ways in which the CDSP might present risk to the public, one needs first to identify the major features of the CSDP, including:

- o the disposal alternatives, including the "no-action" alternative (continued storage);
- o the disposal activities (e.g., handling, transportation, plant operations) that make up the alternatives;
- o the chemical agents themselves and the munition configurations in which they are stored; and
- o the various accident initiators (e.g., human error, equipment failure, natural event) and accident types that could lead to agent release.

Each of these features is discussed below.

1.2.1 The Disposal Alternatives

For purposes of the risk assessment, the disposal alternatives are defined by where, not how, the destruction of the chemical stockpile takes place. The disposal technology assumed here for all alternatives is the "baseline" technology which consists primarily of mechanical disassembly of the munitions, draining of the chemical agent, destruction of the agent in liquid incinerators, incineration of "energetics" (propellants, bursters, etc.) in deactivation furnaces or kilns, and destruction of residual agent in metal parts and dunnage furnaces. The disposal alternatives are, therefore, distinguished by the logistics of munition movement and the location of the disposal activities. The alternatives can be summarized as follows:

- o on-site disposal: all chemical agents are destroyed at the sites where they are now stored;
- o regional disposal: munitions stored in the eastern region of the country are shipped by rail to ANAD, Alabama, while those in the West are shipped to TEAD, Utah;
- o national disposal: all munitions in the continental U.S. are shipped by rail to TEAD for destruction; and
- o partial relocation: on-site disposal at all sites except for relocation of the stockpile from selected sites:

- the APG, MD stockpile moved by air to TEAD and/or
- the LBAD, KY stockpile moved by air to TEAD

o continual storage: munitions currently in storage remain in storage with routine maintenance and surveillance.

The risk implications of the disposal alternatives are apparent in the potential for the redistribution and, it is expected, the reduction of overall risk. Movement of the stockpile from one site, in what could be a densely populated region, to a second site, in what could be a sparsely populated region, might reduce the risk to the population around the first site, at the expense of added risk to people along the transportation corridor and around the second site. The magnitude of these risk differences is one of the questions answered by the risk analysis.

1.2.2 Disposal Activities

Each of these disposal alternatives comprises many activities. These range from the relatively simple activities associated with continuing to store the munitions, to the more complex activities associated with handling, shipping, or disassembly/destruction of the stockpile elements. Since these activities involve some contact with the chemical stockpile, they all could pose some risk to the public.

Figure 2 illustrates the major activities associated with each disposal alternative. Many of these activities are common to some or all of the disposal alternatives.

The "no-action" alternative, continued storage, involves the risks associated with the storage in fixed sites (igloos, warehouses, or open fields). The major risk elements are relatively rare, external or natural catastrophic events, such as tornadoes and aircraft crashes; maintenances and surveillance activities for the stored stockpile also contribute to risk. Storage-related accidents are typically very low in their probability of occurrence, but very high in potential consequence, because of the large inventory of agent likely to be affected by any one event.

The on-site disposal alternative involves risk posed by the following activities:

o handling activities, required to move the stockpile elements from their storage areas to on-site transportation containers, and from the transportation containers to the on-site disposal facility, and from one operation to another within the facility;

o on-site transport activities, moving the stockpile by truck from storage area to plant over on-site roads; and

o plant operations activities, including all steps required to disassemble, drain, and incinerate the chemical agents and munitions.

The national, regional, and partial relocation disposal alternatives introduce several different classes of activity posing some risk:

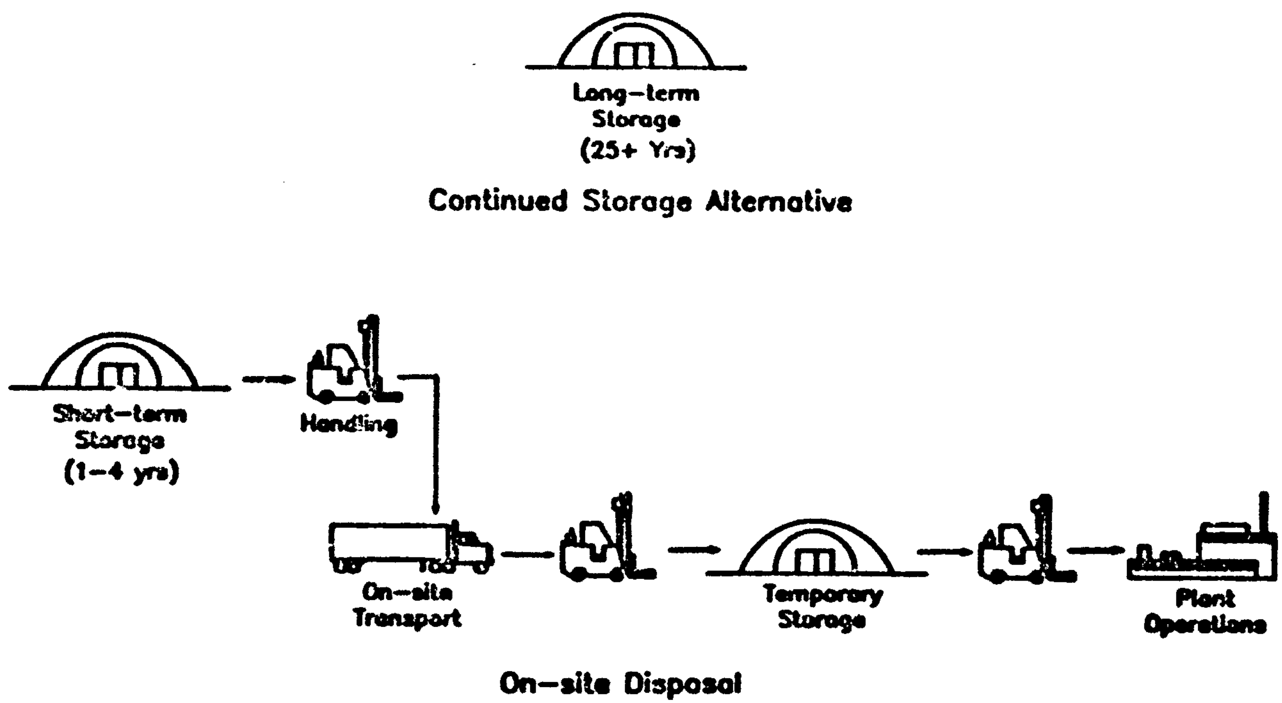

FIGURE 2

DISPOSAL ACTIVITIES INVOLVING SOME RISK

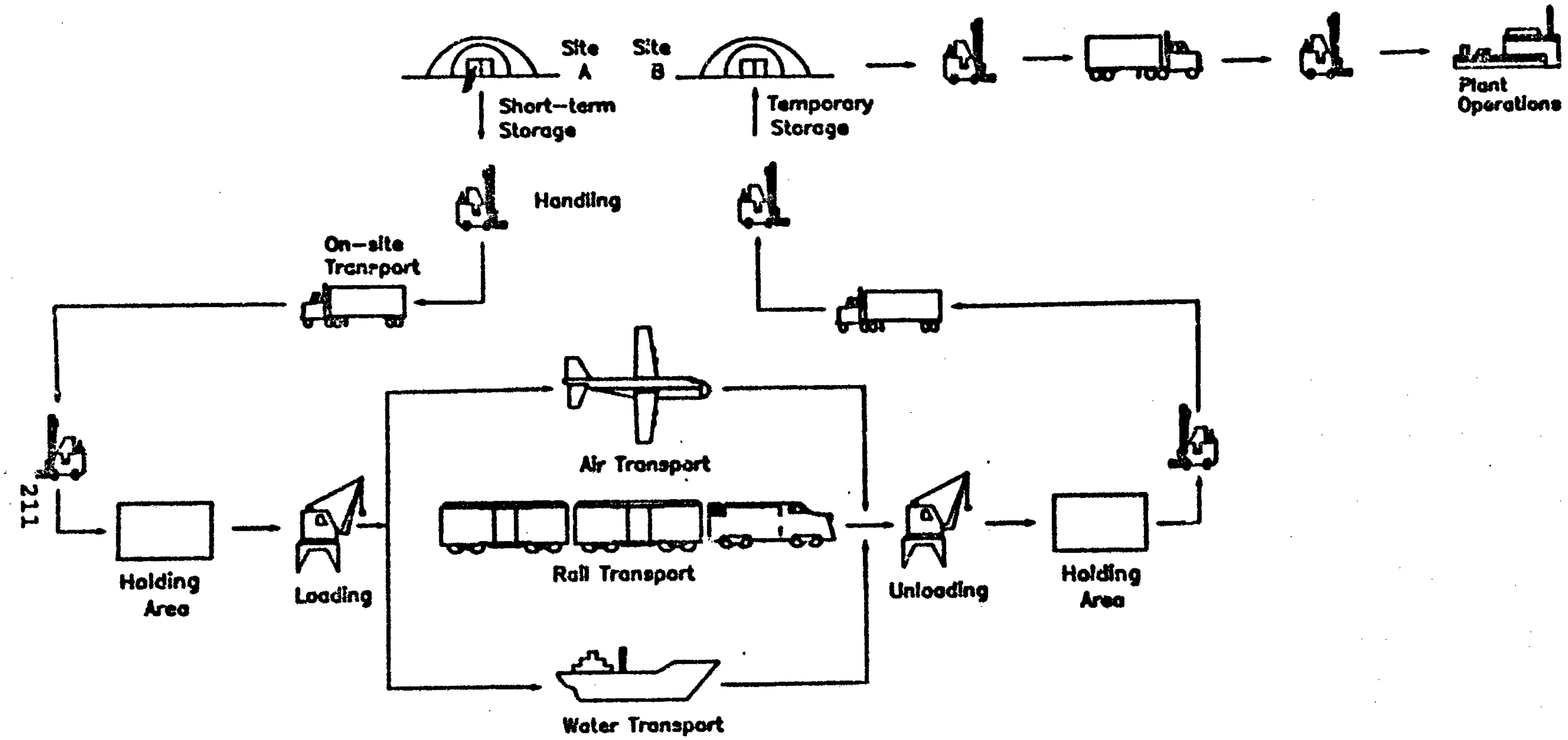

Disposal Alternatives Involving Transportation

FIGURE 2 (Concluded)

DISPOSAL ACTIVITIES INVOLVING SOME RISK

- additional handling activities, involving stockpile movement from storage to the packing/holding/loading areas (essentially the same risk as movement of the stockpile from storage to on-site disposal plant) for subsequent off-site transport, plus handling at the transportation container unloading/holding/unpacking areas and handling at the destination site (essentially a reversal of the activities at the sending site); and

- off-site (inter-site) transport activities, involving long distance transport by one of three modes, depending on which disposal alternative is being considered.

1.2.3 Agents and Munition Types

Each of the disposal alternatives involves the full range of chemical agent and munition types in the chemical stockpile. The characteristics of each are accounted for in the risk analysis. Risk associated with each of the agent types is different, since their physical and toxicological properties differ. Physical properties of greatest importance in estimating risk as a function of agent type include: vapor pressure (determines the rapidity with which spilled agent might evaporate); freezing point; and molecular weight. These and other physical properties, as well as toxicological characteristics, are encoded into the Army's D2PC computer model for chemical hazard prediction (C.G. Whitacre, et al., 1987), which provides estimates of the downwind distance the chemical hazard might extend in a particular accident. Use of the model in this risk analysis is described in another paper at this seminar.

The munition types included in the stockpile are shown in Table 1. Major munition characteristics accounted for in the risk analysis include: munition size and agent inventory, susceptibility to failure by puncture, crash, fire or impact; packing density; and presence of energetic materials (bursters, fuzes, and propellants).

1.2.4 Accident Types

Potential chemical accidents are defined in specific accident scenarios, which are sequences of possible events leading to a release of agent. Accident scenarios have been identified for major classes of accident causes, including natural phenomena (e.g., wind, earthquake), other external events (e.g., aircraft crash), equipment failures (e.g., pipe rupture, control system breakdown), and human error. A multifaceted approach was used to identify potential initiating events, screening those which should not affect overall risk and selecting those events warranting further analysis. The approach consisted of:

- Developing a master logic diagram (MLD), a tool described in the NUREG/CR2300, "PRA Procedures Guide" for systematically examining potential modes of release, pathways for release, barriers against release, and mitigating safety functions together with initiators of release. Figures 3a through 3i shows the Level and and Level 2 MLDs used in this risk analysis.

- Dividing the demilitarization facility into spatial zones and examining potential sources of release in each zone to identify internal initiating events for plant operations.

Table 1 Description of Lethal Chemical Agent Munitions

Munition	Model/Agent	Dimensions: Diameter	Dimensions: Length[c] (in.)	Dimensions: Weight[c] (lb)	Agent: Type	Agent: Weight[c] (lb)	Burster: Model	Burster: Explosive	Burster: Weight[c] (lb)	Propellant: Model	Propellant: Weight[c] (lb)	Fuze Model	Other Energetic Components
105-mm cartridge	M60	105 mm	31.1	42.92	HD[a]	2.97	M5	Tetrytol	0.3	M67	2.83	M57	M28B2 primer
		105 mm	31.1	42.92	HD	2.97	M5	Tetrytol	0.3	M67	2.83	M51A5	M22 booster
	M360	105 mm	31.1	43.86	GB	1.63	M40	Tetrytol	1.12	M67	2.83	M508	M28B2 primer
		105 mm	31.1	43.86	GB	1.63	M40A	Comp B	1.12	M67	2.83	M508	M28B2 primer
		105 mm	31.1	43.86	GB	1.63	NA[b]	NA	1.12	M67	2.83	M557	NA
105-mm projectile	M360	105 mm	16.0	32	GB	1.63						0	
4.2-in. mortar	M2	4.2 in.	21.0	24.67	HD	6.0	M14	Tetryl	0.14	M6	0.4	M8	M2 primer
	M2	4.2 in.	21.0	24.67	HT[a]	5.8	M14	Tetryl	0.14	M6	0.4	M8	M2 primer
	M2A1	4.2 in.	21.0	24.67	HD	6.0	M14	Tetryl	0.14	M6	0.4	M8	M2 primer
155-mm projectile	M104	155 mm	26.8	98.9	HD	11.7	NA	NA	0.41				
		155 mm	26.8	98.9	HD	11.7	M6	Tetrytol	0.41				
		155 mm	26.8	98.9	H	11.7	M6	Tetrytol	0.41				
	M110	155 mm	26.8	98.9	HD	11.7	NA	NA	0.41				
		155 mm	26.8	98.9	H	11.7	M6	Tetrytol	0.41				
		155 mm	26.8	98.9	HD	11.7	M6	Tetrytol	0.41				
		155 mm	26.8	98.9	H	11.7	M6	Tetrytol	0.41				
	M121	155 mm	26.8	96.4	GB	6.5							
	M121A1	155 mm	26.8	98.9	VX	6.3	M71	Comp B	2.45				
	M121A1	155 mm	26.8	98.9	GB	6.5	M71	Comp B	2.45				
	M122	155 mm	26.8	98.9	GB	6.5	M37	Tetrytol	2.45				
8-in. projectile	M426	8 in.	35.1	203	VX	14.5	M83	Comp B	7.0				
		8 in.	35.1	203	GB	14.5	M83	Comp B	7.0				
		8 in.	35.1	203	GB	14.5	NA	NA	7.0				
Land mine	M23	13.5 in.	5	23	VX	10.5	M38	Comp B	0.8			M603	
Rocket	M55	115 mm	78.0	57	GB	10.7	M34	Comp B	3.2	M28	19.3	M417	M62 primer
		115 mm	78.0	57	GB	10.7	M36	Comp B	3.2	M28	19.3	M417	M62 primer
		115 mm	78.0	57	VX	10.0	M34	Comp B	3.2	M67	19.3	M417	M62 primer
		115 mm	78.0	57	VX	10.0	M36	Comp B	3.2	M67	19.3	M417	M62 primer
500-lb bomb	MK94-0	10.8	60.0	441	GB	108							
525-lb weteye	MK116-0	14 in.	86.0	525	GB	347							
750-lb bomb	MC-1	16.0	50.0	725	GB	220							
Spray tank	TMU-28/B	22.5	185.5	1,935	VX	1,356							
Bulk containers	Agent GB	30.1	85.1	2,900	GB	1,300							
	Agent H	30.1	85.1	3,100	H	1,700							
	Agent HD	30.1	85.1	3,100	HD	1,700							
	Agent HT	30.1	85.1	3,100	HT	1,700							
	Agent L	30.1	85.1	3,100	L	1,700							
	Agent VX	30.1	85.1	3,000	VX	1,600							
	Agent GA	30.1	85.1	NA	GA	NA							

[a] HD, HT, H are referred to as Mustard.
[b] NA = information not available.
[c] For conversion of the English units to metric units 1 in. = 2.54 cm and 1 lb = 0.454 kg.

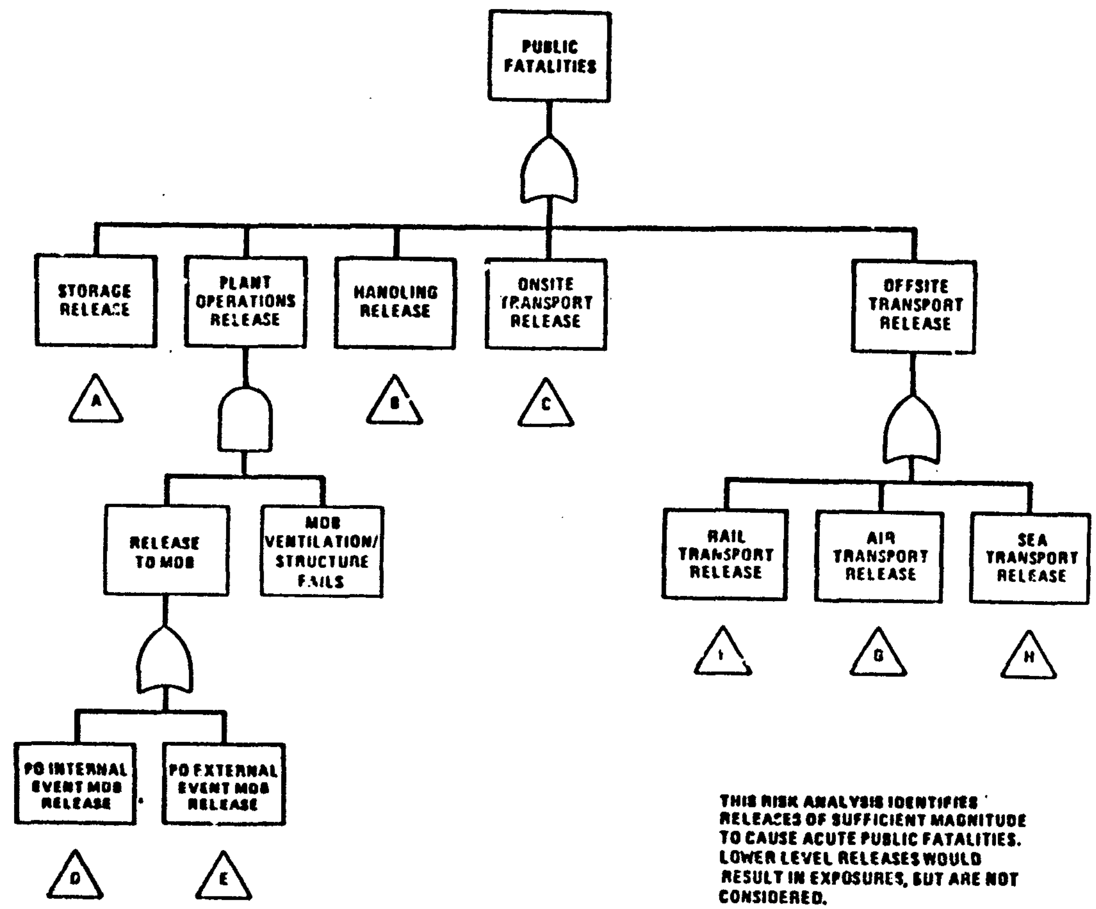

Figure 3a Master Logic Diagram – Level 1

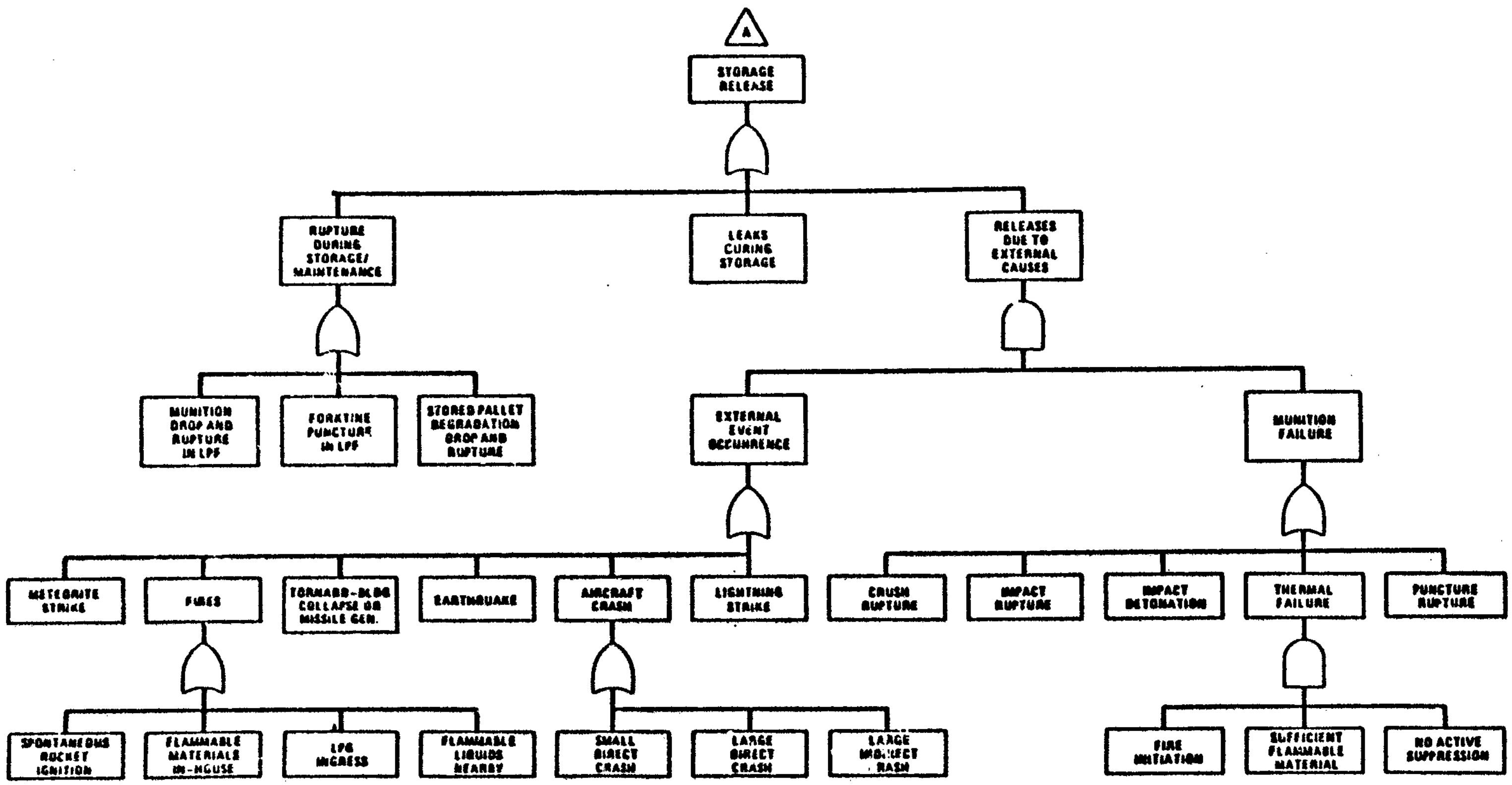

Figure 3b Master Logic Diagram - Level 2. Storage Release

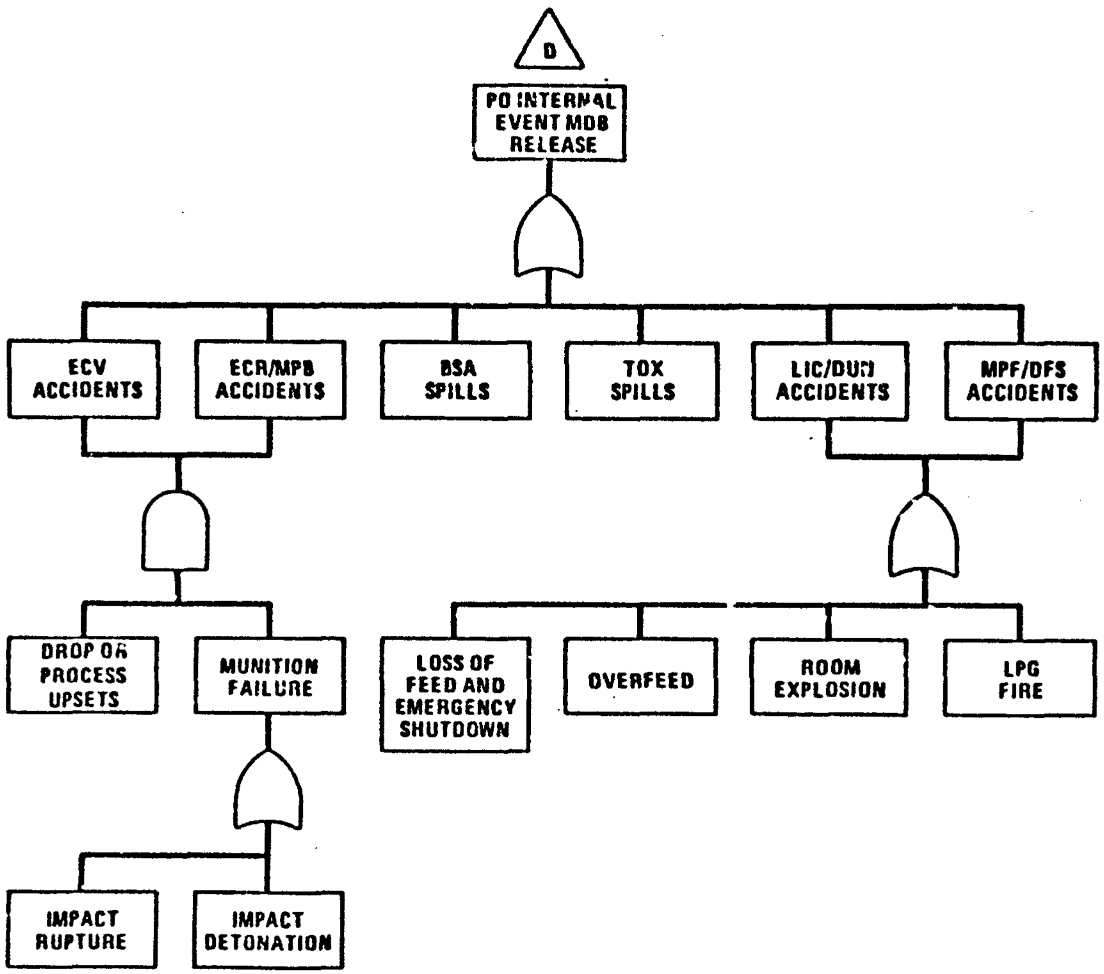

Figure 3c Master Logic Diagram - Level 2 - Plant Operations Internal Events

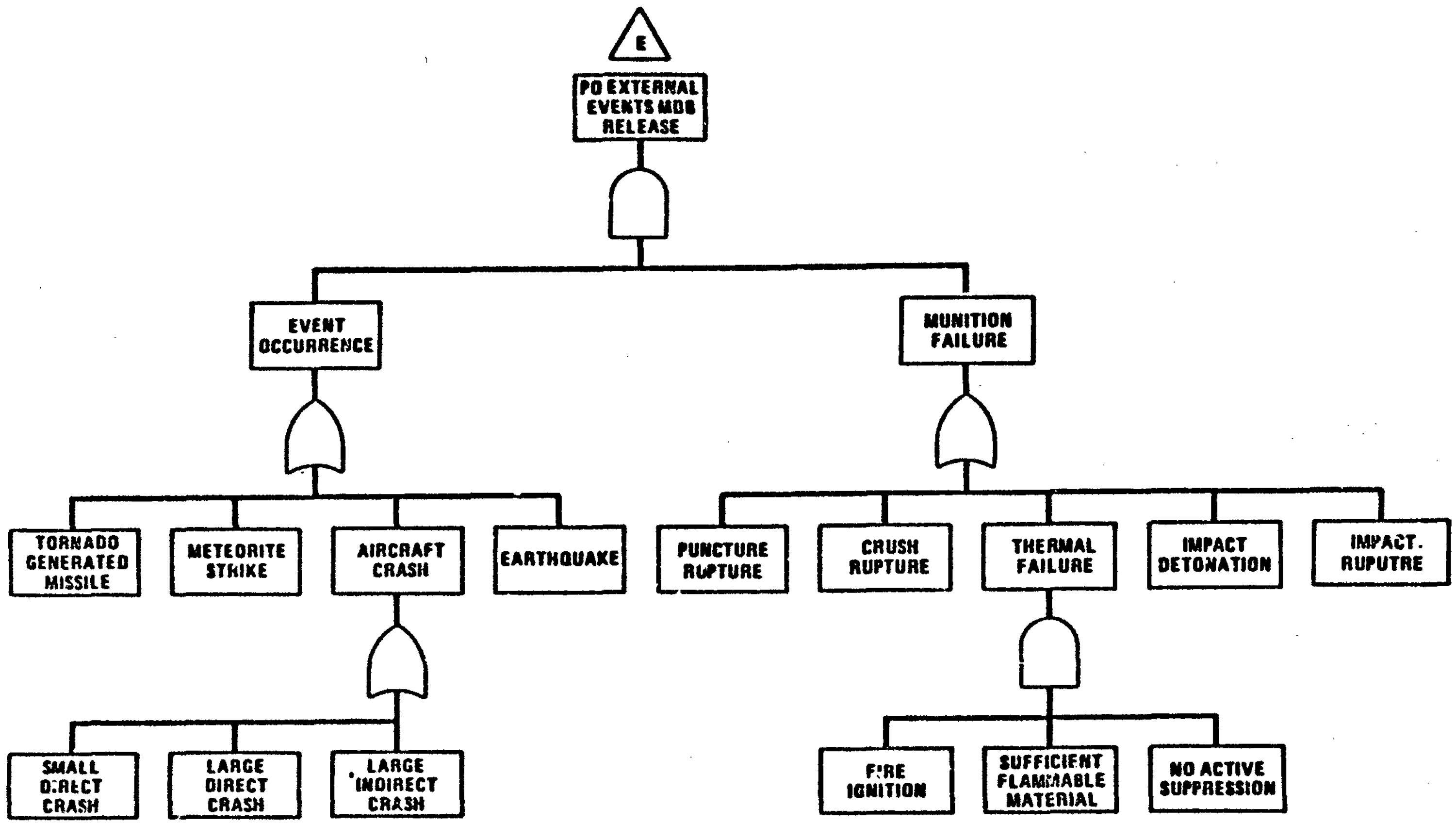

Figure 3d Master Logic Diagram - Level 2. Plant Operations External Events

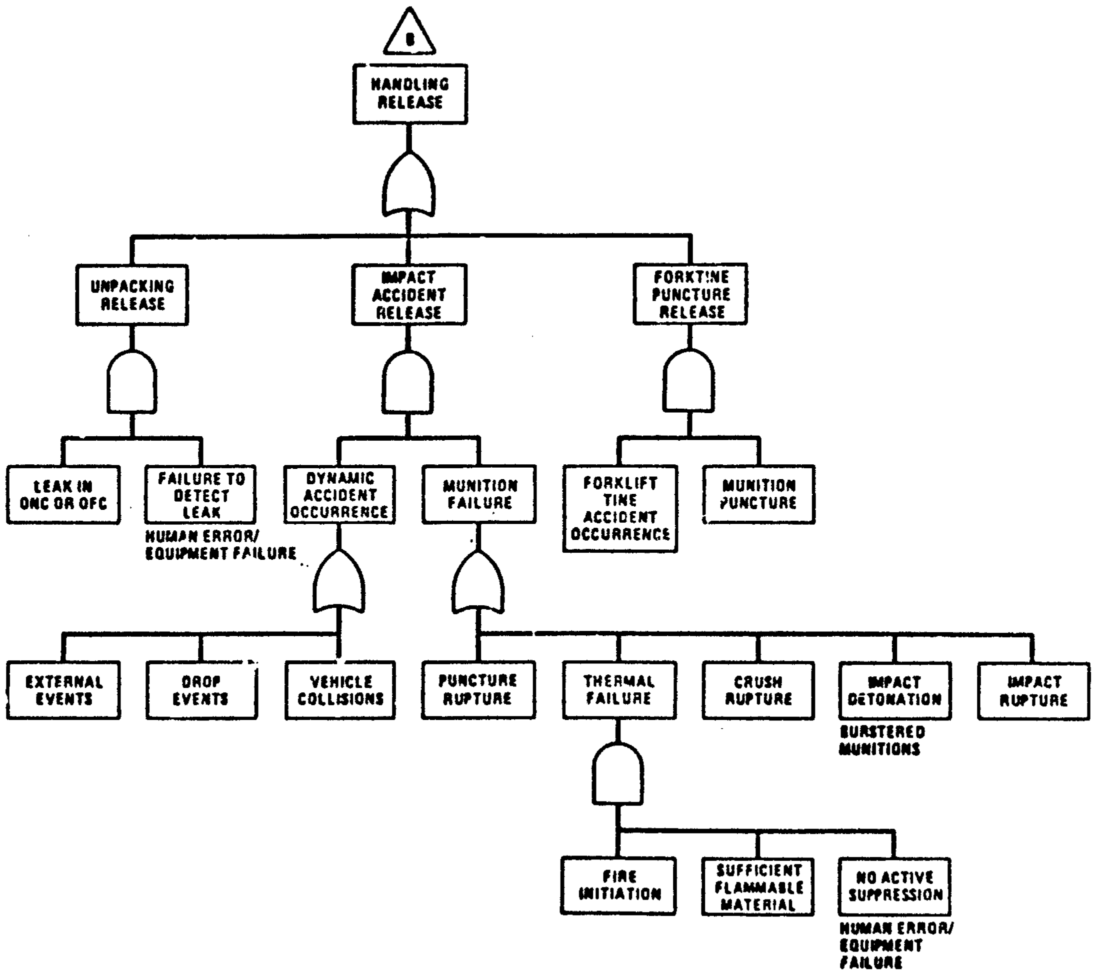

Figure 3e Master Logic Diagram - Level 2. Handling Release

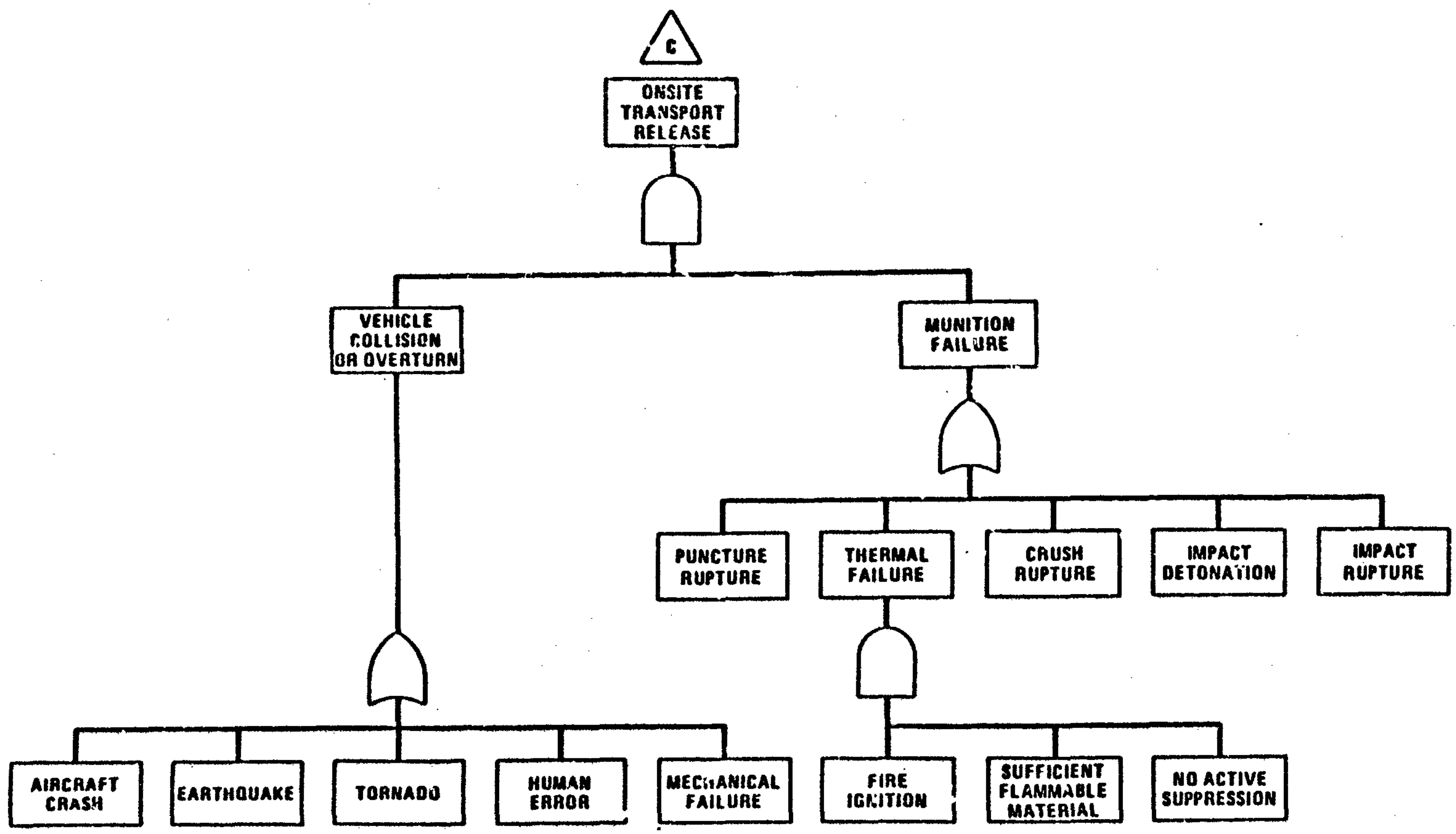

Figure 3f Master Logic Diagram – Level 2. Onsite Transport Release

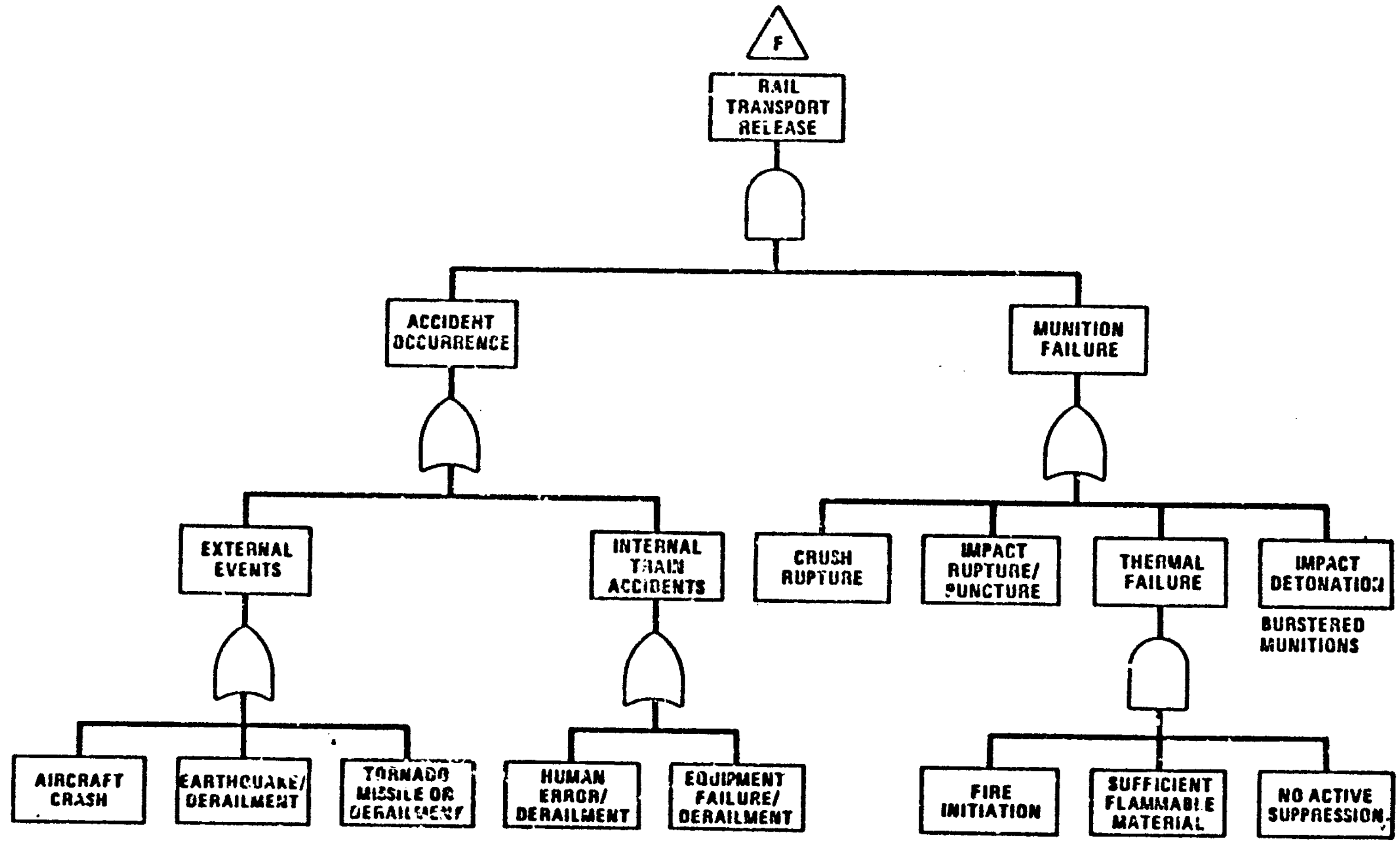

Figure 3g Master Logic Diagram - Level 2. Offsite Rail Transport Release

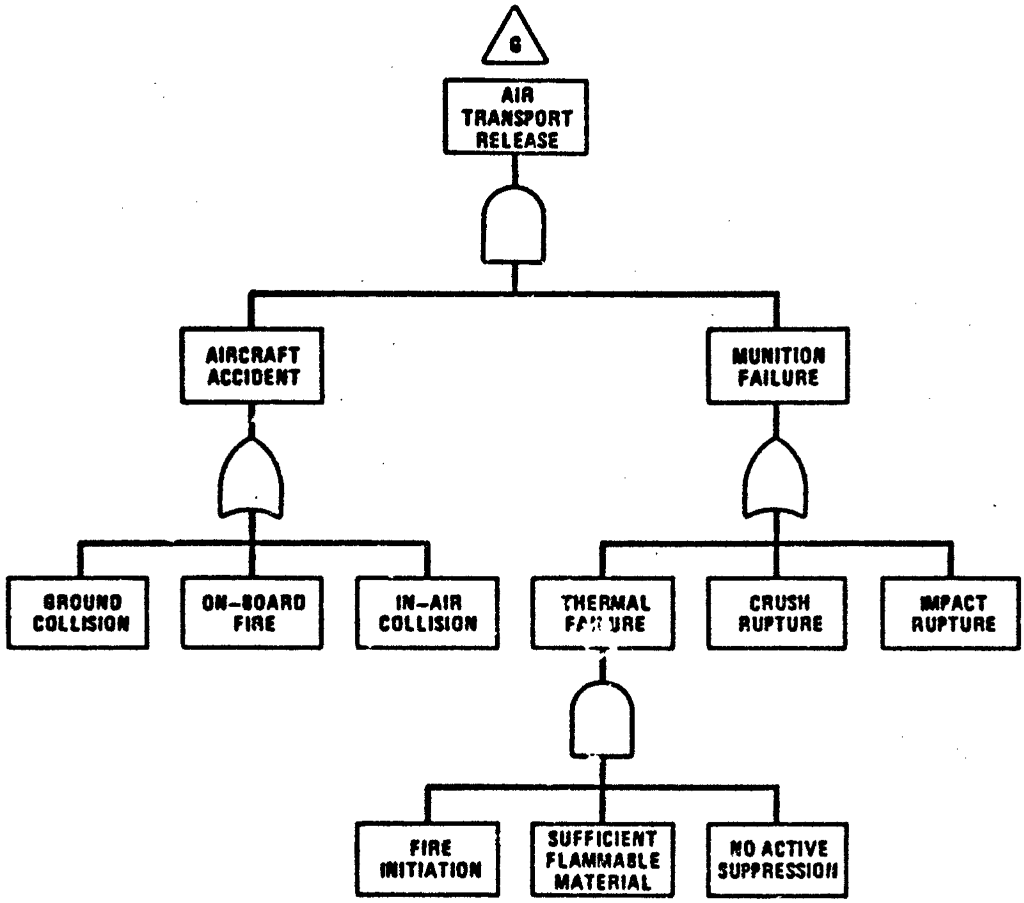

Figure 3h Master Logic Diagram - Level 2. Offsite Air Transport Release

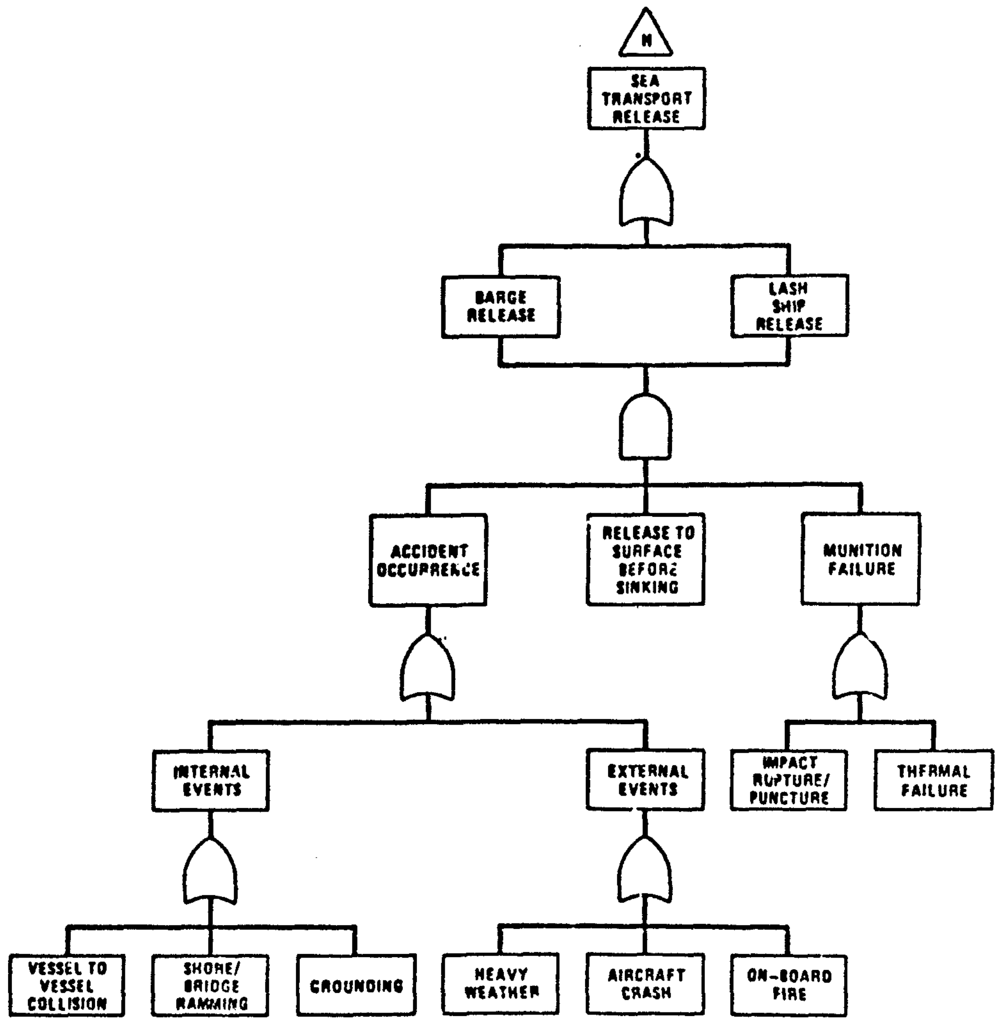

Figure 31 Master Logic Diagram - Level 2. Offsite Sea Transport Release

- Cross-referencing the results from the MLD with a list of accident scenarios from safety related studies on the chemical demilitarization program.

Two criteria were used to screen accident scenarios: (1) accidents with extremely low frequency (below 10^{-10} per year), and (2) accidents with low release amounts that could not cause human fatalities .5km from the incident under worst case meteorological conditions (amount of agent release below 0.3 lb GB, 14 lb H or 0.4 lb VX).

All accident scenarios analyzed are presented in Appendix A of this report.

1.3 Prior Studies

This risk analysis is founded on a number of prior hazard and risk analyses. Quantitative hazard analyses were performed in the proposed disposal of M55 rockets utilizing a technique known as hazard and operability analysis (HAZOP) (Arthur D. Little, 1985[a], 1985[b], 1985[c], 1985[d]). Qualitative analyses of the Johnston Atoll Chemical Agent Disposal System (JACADS), using a failure mode and effects analysis (FMEA) method were carried out by the R. M. Parsons Company (1983, 1985).

Deductive system logic models, such as fault trees, were used to assess the probability of agent release in off-site transportation accidents (Rhyne, 1985[a], 1985[b]). Rhyne's study incorporated the transportation accident data base prepared by Sandia National Laboratories (Clark, et al., 1976). An analysis of disposal of M55 rockets by Science Applications International Corporation (1985) focused on the storage, handling and on-site transportation of chemical munitions, using both the event tree and fault tree methodologies.

For the draft PEIS for the CSDP (U.S. Army Program Manager for Chemical Demilitarization, 1986), The MITRE Corporation outlined an approach for using the risk data prepared in support of the M55 rocket disposal program as the basis of an accident scenario data base applicable to the entire stockpile (Fraize, et al., 1987). MITRE then identified gaps in the accident scenario data base (subsequently addressed by GA Technologies), and proceeded to develop a framework for analyzing the risk associated with this resulting accident scenario data base and identifying representative worst-case accidents for the CSDP/EIS. This framework and the preliminary accident scenario data base, as updated and completed by GA Technologies, was used to prepare the risk analysis supporting the draft PEIS (U.S. Army Program Manager for Chemical Demilitarization, 1986).

1.4 Data Sources for this Analysis

With the studies listed above as the starting point, GA Technologies (GA Technologies, 1987[a], 1987[b], 1987[c]), with technical assistance from H&R Technical Associates, JBF Associates, and Battelle-Columbus Laboratories, conducted a comprehensive assessment of accident probabilities for all munitions types. Event and fault tree analyses, together with information on mechanical and thermal failure threshold conditions for each munition type, were used to estimate the probability of agent release in each of nearly 3000 potential accidents, and the amount of agent that could be released.

Downwind dispersion of lethal plumes was determined by a method incorporated in the D2PC plume dispersion model developed by the Army (Whitacre, et al., 1987). Demographic data and potential fatality estimates for generic accidents (defined by lethal plume length and meteorological conditions) for all sites and transportation corridors were provided by Oak Ridge National Laboratory.

2.0 METHODOLOGY OF THE RISK ANALYSIS

The purpose of this section is to present basic principles involved in estimating risk to the public, and to show how these principles have been applied to the CSDP.

2.1 Introduction to Risk Assessment Concepts

Risk is a measure of the potential for exposure to unwanted events or consequences (e.g., injuries or fatalities). Any danger to the public associated with the proposed CSDP may be described in terms of risk. For purposes of this study, risk is considered to be that due only to accidental release of and potential public exposure of agent to chemical agent. Only accidents that could result in a release of agent sufficient to expose the public to potentially lethal doses are included. For purposes of this study, the term "public" excludes persons within the boundaries of the military installations.

2.1.1 Risk Descriptors: Probability and Consequence

The risk associated with any activity (e.g., living near a geologic fault, driving a car, riding a roller-coaster, or living under an airplane flight path) may be described as the product of two quantities: the probability of the unwanted event occurring and the consequence to an individual or the public, if the event does occur.

The probability of a potential accident is a quantitative statement of the "odds" of that accident occurring, given many repetitions of the activity or condition that can lead to the accident. For instance, analysis of the accident and all of the separate events leading up to it might show that the odds of the accident occurring at some time during the CSDP might be 1 in 200,000: we can express the probability of that event occurring in just that way — 1 in 200,000 — or in the following equivalent ways: 0.000005; 1/200,000; or, in scientific notation, 5×10^{-6}. For this analysis, the probability of an accident is expressed as the likelihood (or "odds") of its occurring once during the stockpile disposal program. The only exception is for long-term storage accidents where probability has been expressed as the likelihood of occurrence during a 25-year period (the assumed duration of the "no-action" alternative).

The consequence of a potential accident can be expressed in several ways, depending on the intended use of the results. For the purposes of the CSDP risk analysis, there are two principal measures of the consequence of any given accident:

- size of the lethal plume produced by the accident. Size of the lethal plume is defined as the distance to the downwind locations where the "exposure" (the product of agent concentration and time) is equal to the estimated minimum lethal value. This distance is also referred to as the "no-deaths" hazard distance. Plume size, or downwind

hazard distance, is dependent on the agent type (physical characteristics), agent quantity released and the meteorological conditions governing the atmospheric dispersion of the agent.

- potential fatalities per event. This measure is the most direct indicator of potential accident consequences to the population. Estimation of potential fatalities requires knowledge of the source term (quantity and mode of agent release), the atmospheric dispersion mechanism (specified by local meteorological conditions), the population distribution (by distance and direction), and the estimated human response to chemical agent exposure.

The present risk analysis is limited to airborne release of agent. Other modes for dispersion of released agent, such as through ground water or surface water, are beyond the scope of this analysis. Only acute and lethal toxicity are considered in the analysis; chronic and sub-lethal effects are not evaluated.

2.1.2 Two Perspectives on Risk

Risk can be viewed from two basic perspectives:

- risk to an individual at a specified location; and
- risk to the affected populations.

In the first case, risk to an individual is the probability that he or she will be harmed while at a fixed location. Risk to the affected population (the expected number of individuals who might be adversely affected by the event) may be more useful to a decision-maker who needs to assess total effects on the public.

An individual tends to view risk in very personal terms, such as the probability that an unwanted event will occur to him or to his family. Many risky activities or situations to which an individual is exposed are voluntary (e.g., a canoe ride) and their risk is accepted in return for the benefit the activity brings. Others (e.g., being struck by lightning) are "acts of God or nature" and the associated risk is generally accepted as a part of living. Still others (e.g., living near a nuclear power plant or along a rail route that carries hazardous chemicals) are viewed as involuntary, the result of man-made intrusions, and often are less willingly accepted. In this risk analysis, we are dealing with a man-made activity that the public may view as an imposed or involuntary risk. Risk comparable in character (not necessarily magnitude) to that potentially imposed by the CSDP might be that associated with living next to a chemical plant processing hazardous chemicals or living along a transportation route carrying such materials.

Community or social risk is, in effect, the aggregate of individual risk to which all members of the local population are exposed. Thus, individual risk is independent of the number of individuals at risk; community or societal risk is not.

2.2 Application of Risk Concepts to the CSDP

2.2.1 Computation of Individual Risk (General Case)

The risk to an individual is calculated by multiplying together probabilities of each of the circumstances necessary to produce a fatality. This combined probability of occurrence is multiplied by the consequence to determine risk; in the individual case, consequence is always equal to 1 (the death of the individual), and so does not affect the risk value we calculate. Figure 4 illustrates the risk to an individual posed by a potential release of chemical agent; these factors are:

- the probability that an accidental release will occur;
- the probability (along transportation corridors only) that a transport vehicle will be in the vicinity of the individual when the accident occurs;
- the probability of being downwind of the release;
- the probability of being within the plume width;
- the probability that an individual within a given lethality zone of the plume will die.

For the case of individual risk along a transportation corridor, the analysis is based on determining the route length over which an accident can occur and still affect an individual at a given location. This is equivalent to basing individual risk exposure time. Basically, the analysis computes average individual risk along the transportation corridor, based on average distances, speeds, and exposure times along the route.

Whether along a transportation route or near a fixed site, the total risk to an individual is the sum of the individual risks posed by each identified accident scenario that could happen at the individual's location (either along a corridor or near a site).

2.2.2 Risk to the Population (Community/Societal Risk)

To estimate the risk to the general population, the factors defining risk to an individual, discussed above (Section 2.2.1), must be applied to the total number of individuals at risk. Risk to the public was calculated for each accident by overlaying the lethal plume (under "most-likely" weather conditions) associated with the accident on a map of the residential population about the site or adjacent to a transportation corridor and estimating the number of potential fatalities from each accident within the plume. Next, expected fatalities from each accident were computed as the product of potential fatalities and the probability of the accident occurring. The total population risk is then determined by summing expected fatalities for all applicable accidents.

This concept is illustrated by Figure 5. The concentric arcs in the figure represent hazard distance zones from the potential accident site. For example, the distance zones used in this analysis are the following:

Concept:

The Probability of a Potential Individual Fatality Depends on Several Factors

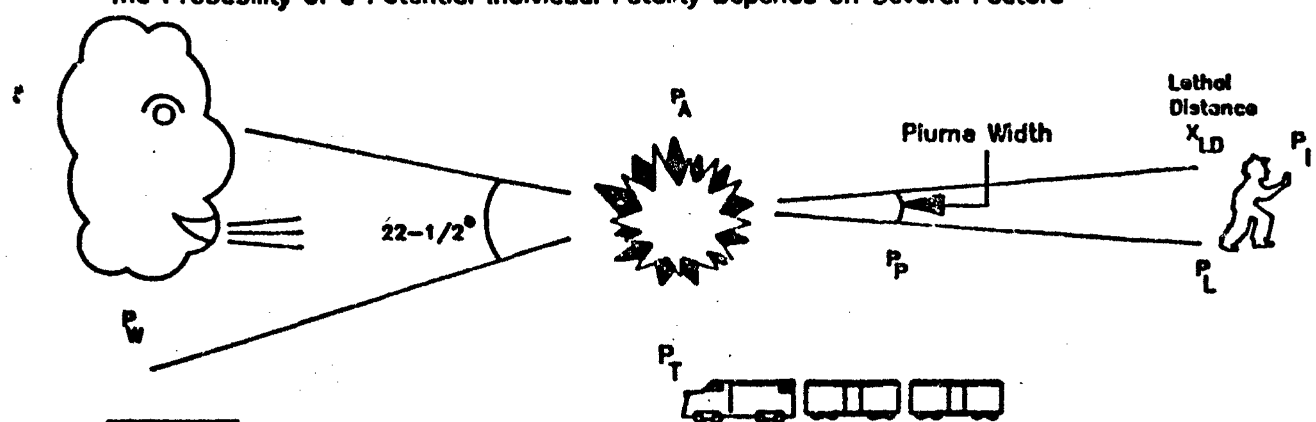

Formula:

$P_I = P_W \times P_A \times P_T \times P_P \times P_L$ Where:

P_I = Probability of an Individual Fatality
P_W = Probability of Wind Directed from an Appropriate Sector
P_A = Probability of an Accidental Release of Agent
P_T = Probability of a Train being Present (as applicable)
P_P = Probability of an Individual Being within the Plume Width
P_L = Probability of a Potential Fatality for an Individual within the Plume

Typical Data are:

$P_I = 0.06 \times P_A \times 1.0 \times 0.3 \times 0.2 = 0.004 \times P_A$

FIGURE 4

ILLUSTRATION OF INDIVIDUAL RISK

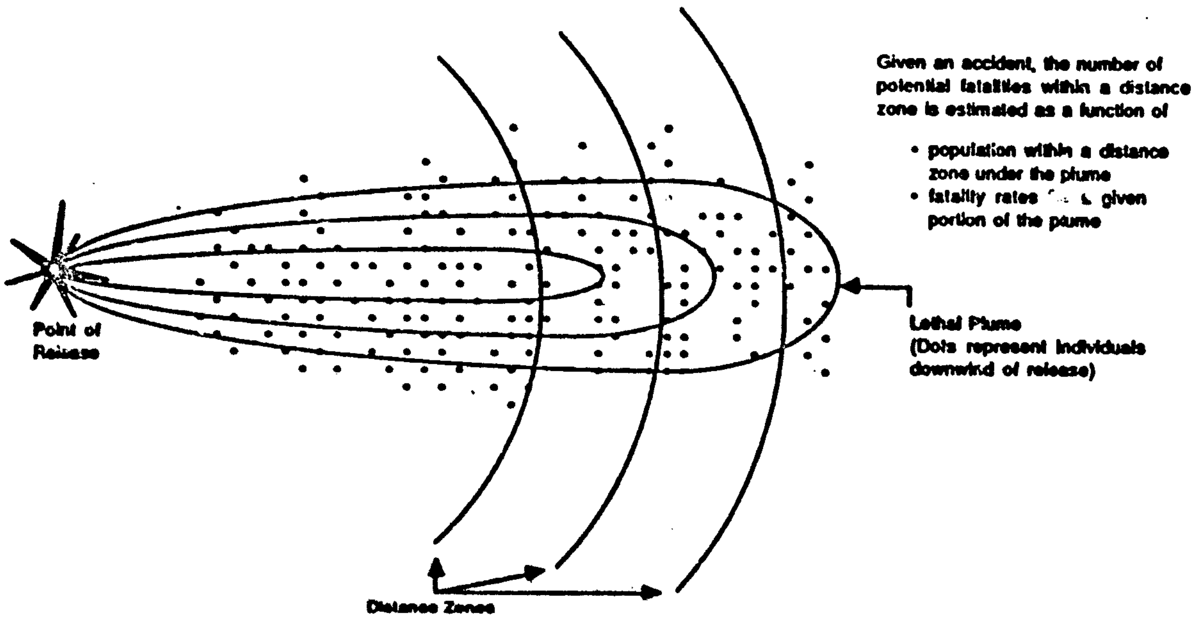

FIGURE 5

ILLUSTRATION OF POPULATION RISK

Greater than 0.0 - 0.1 km	Greater than 2 - 5 km
Greater than 0.1 - 0.2 km	Greater than 5 - 10 km
Greater than 0.2 - 0.5 km	Greater than 10 - 20 km
Greater than 0.5 - 1.0 km	Greater than 20 - 50 km
Greater than 1 - 2 km	Greater than 50 - 100 km

An accident having a "no-deaths" plume length of 12 km is assumed to result in a fatality count for the zone which is 10 - 20 from the accident site. If an accident causes a plume that reaches into the 10 - 20 km population zone, then all those in the inner population rings, closer to the agent source, are at even more risk since the dosages become higher as one approaches the accident site. Similarly, within a given distance zone, individuals will be affected not only by those scenarios for which the plume just reaches their zone, but also those for which the magnitude for which the plume reaches into the outer zones. While plume lengths exceeding 100 km may be estimated in the D2PC model for the worst of the potential accidents, a correction has been made to exclude fatalities that would occur farther than 100 km from the potential accident location.

2.3 Principle Measures of Risk

To compare the public risks of the disposal alternatives, the following measures, each of which provides a different perspective on program risk, were used:

- <u>maximum individual risk</u>, equal to the probability of an individual's death if he/she spent the entire duration of the CSDP at the site boundary (assumed to be 0.5 km from the on-site disposal/storage operations) or as close as 0.1 km to the center line of a transportation corridor. This indicator is dependent only on the mix of potential accidents that could happen at the individual's location; it is independent of population density (the number of individuals who could be so maximally exposed;

- <u>maximum lethal distance</u>, equal to the maximum downwind length ("no-deaths" exposure level) of the plume from the worst of all identified potential accidents under worst-case weather conditions at a specific location. Conversely, it is also the minimum distance an individual could be from a given site or transportation corridor and have no risk of lethal exposure during the CSDP;

- <u>maximum total time at risk</u>, representing the maximum length of time an individual could be at risk at a fixed location near a site or along a transportation corridor. For those living within a radius equal to or less than the maximum lethal hazard distance, the time at risk is the total time during which stockpile disposal activities will take place at that site, regardless of where the individual is located. For those individuals along the transportation corridors, the time depends on the distance from the rail line or air corridor; the maximum time is assumed to occur if the individual is located at a 0.1 km distance from the rail track or centerline of the air corridor. These persons are exposed to a hazard only when a train or aircraft is in the vicinity (defined as the maximum lethal hazard distance in either direction) of them. This time

is summed for each agent-bearing train or aircraft that would pass by in each alternative. Since maximum lethal hazard distance is used in this determination, the worst-case meteorological conditions apply;

- <u>probability of one or more fatalities</u>, a public risk indicator equal to the chance that there will be at least one fatality at a given site or for the nation as a whole during the CSDP. This measure is calculated by summing the probabilities of all accidents that could cause one or more fatalities. Included in this sum are all accidents for which the potential fatality estimate, based on assuming uniform population densities, is less than unity. (This means that an accident is expected to cause a fatality for only a fraction of the time it occurs; for the remaining fraction of occurrences, that event would not cause a fatality. For such accidents, the probability of occurrence is reduced so that only the fraction of events expected to cause a fatality are counted). (To illustrate: On the basis of average population density and lethality rate variations within the chemical agent plume, an accident could have a potential fatality value of say, 0.2 and a probability of occurring estimated at 10^{-4}; the potential fatality value of 0.2 means that 20%, or 1 out of every 5 occurrences of the event in question could cause a fatality. Those 4 occurrences that cause, on average, no fatality are not counted and the accident is, in effect, redefined to be the 1-in-5 event that leads to a fatality -- having a correspondingly reduced probability, equal to the fraction of fatal accidents times the probability of all occurrences, or 0.2×10^{-4});

- <u>maximum number of fatalities</u>, equal to the maximum consequence of all accidents at a site or for the nation. This risk measure is based on worst-case weather conditions, actual population densities (1980 census data, as analyzed by Oak Ridge National Laboratories), and worst possible wind direction (i.e., plume striking the highest number of people without any allowance for preventive/emergency response measures);

- <u>expected fatalities</u>, equal to the sum of the risk contribution of all accidents at a site or for the nation, where risk for each accident is the potential fatality count (if the accident were to occur) multiplied by the probability of the accident occurring. Note that expected fatalities is proportional to the probability of a fatality-causing event occurring, and will nearly always be a small number -- well less than unity. For example, an accident with a <u>potential</u> fatality estimate of 12 and a probability of 10^{-6} (odds of 1 in a million of occurring during the CSDP) would have an expected fatality value of 12×10^{-6}. At the programmatic level, the expected fatalities value is the sum of the expected fatality contribution of several hundreds of potential events and might lie somewhere in the range of 10^{-3}, or 0.001. This typical value can be interpreted in the following way: The program can be expected to cause, on average, one fatality every 1000 times the program is executed; since the program consists of many events which could cause multiple fatalities, a more typical interpretation would be made up of several parts, such as: one fatality every 10,000 programs (expected fatality contribution of 1/10,000 = 0.0001) <u>plus</u> a 10-fatality event every 25,000 programs (contribution of 10/25000 =

0.0004 plus a 100-fatality event every 200,000 programs (contributing 100/200,000 = 0.0005), for a total expected fatality value of 0.001; and

- person-years-at-risk, equal to the population living within all zones (defined in Section 2.2.2) that could experience potentially lethal agent exposure multiplied by the time period over which that worst-case event could take place (typically, the duration of disposal operations at fixed sites or the time during which transport vehicles might be within lethal plume reach of population groups along the corridors). This measure does not account for the fact that individuals within the affected population groups who are farther from the potential accident site are a lower risk of suffering ill effects of exposure: all affected individuals are counted if they have any risk at all. (This measure is discussed in more detail in Section 3.3.3.2).

The first three risk measures are indicators of risk to the individual. The next three apply to community/societal (population-based) risk, with each measure representing one of the three major features of the cumulative risk curve: vertical scale intercept (probability: horizontal scale intercept (maximum fatalities -- worst-case value); and area under the risk curve (expected fatalities) (Note: Equating expected fatalities with the area under the risk curve applies only if the curve were plotted using linear scales - equal increments for equal changes in the value of the plotted parameters -- instead of the logarithmic scales -- equal increments for each 10-fold multiple of the value of the plotted parameters -- necessitated by the very wide range of the risk data.) Person-years-at-risk is also a community/societal risk measure.

2.4 Methods for Portraying Risk

Estimates of risk to the population can be displayed in a variety of ways. They are described in another paper at this seminar.

3.0 PRESENTATION OF RESULTS

This section is a summary of the significant accidents for both programmatic (all locations combined, for each disposal alternative) and location-specific considerations.

Unless stated otherwise, the term risk will refer to expected fatalities, while plume length will mean the "no-deaths" hazard distance under most-likely meteorological conditions.

3.1 Overview of Risk Data

Throughout this section, we will refer to the following three descriptors of the accident scenario set of interest:

- Disposal Alternative (see below)
- Site-Stockpile (see below)
- Location/Locale of Risk as defined by:

OS = Originating Site

DS = Destination Site
TC = Transportation Corridor

For programmatic risk portrayal, all three locales are combined. For site or location-specific risk portrayal, the risk at only one locale is shown.

3.1.1 Disposal Alternatives and Site-Stockpiles Considered

The eight site-stockpiles considered in this analysis are identified in Figure 1. The codes used throughout this analysis to signify particular sites are tabulated below:

G = APG = Aberdeen Proving Ground, MD
L = LBAD = Lexington-Blue Grass Army Depot, KY
B = PBA = Pine Bluff Arsenal, AR
N = NAAP = Newport Army Anniston Plant, IN
P = PUDA = Pueblo Depot Activity, CO
U = UMDA = Umatilla Depot Activity, OR
A = ANAD = Anniston Army Depot, AL
T = TEAD = Trоele Army Depot, UT

Eight disposal alternatives were analyzed; five were selected by the Army for detailed analyses. Their one-line descriptions, and the codes used to represent them in the analysis and in the presentation of the results are given below:

S = STR = Continued Storage (for 25 years)
O = ONS = On-Site Disposal
R = REG = Regional Disposal (via rail)
N = NAT - National Disposal (via rail)
B = PRB = Partial Relocation — On-Site Disposal, except APG & LBAD
Stockpiles to TEAD via air (C141 aircraft)

3.1.2 Treatment of Mitigation

The accident scenario data base was analyzed for the unmitigated case plus two levels of mitigation, the details for which are described in another report at this seminar.

3.1.3 Treatment of Uncertainty

Uncertainties in risk estimation arise due to many causes, including the inadequacy of data, inaccuracies in modeling, and the incomplete identification and understanding of accident phenomena. The analysis of accident scenarios carried out by GA Technologies provides an error factor for each accident probability "point estimate". This error factor was used to characterize the uncertainty inherent in each estimate. The contribution to risk uncertainty of consequence estimation (for example, in estimating potential public fatalities as a result of an agent release) is represented separately (though incompletely) by considering most likely and worst-case meteorological conditions. However, since worst-case conditions occur relatively rarely and have greater consequences, they may have little effect on a risk curve.

In this report, uncertainty is portrayed on the risk curves and on the expected fatality plots where upper and lower uncertainty bounds (at the 95 percent and 5 percent levels) are indicated.

3.1.4 Description of Data

Risk data are summarized in several forms. Risk data for the programmatic level (no location-specific information) are presented for the unmitigated CSDP in three forms:

- o semi-quantitative, graphical/pictorial comparisons of major risk parameters in pictograms;
- o graphical comparisons of expected fatality estimates, with upper and lower uncertainty bounds; and
- o cumulative risk curves, with upper and lower uncertainty bounds.

3.2 Programmatic Risk of Alternatives

3.2.1 General Comparison

Figure 6 displays in pictogram format (using matrix elements shaded according to four numerical equivalence ranges) the four major risk measures plus a fifth measure — the expected value of plume area (provided for the purpose of evaluating ecological risk in the FPEIS) for the five FPEIS disposal alternatives. The shadings are chosen so that higher risk is connoted by darker shading. The numerical ranges were chosen so that the full range of values for all alternatives could be displayed and readily differentiated. The shading assigned to any entry in the pictograms is strictly defined by the mean value of the risk measure relative to the numerical boundaries of the ranges. Differences in shading should not be interpreted as indicating a significant difference in risk. Note that the numerical equivalence scale chosen for this programmatic chart (involving the larger values associated with the summation of risk at individual locations) is higher (by one order of magnitude or distance category) than the numerical equivalence scale for the location-specific pictograms displayed in Section 3.3.

Discussion of comparative risks, as presented in this section, are based on reference to the actual data from the risk analysis; the quantitative comparisons cannot be derived from the pictograms. To support the programmatic risk comparisons in this subsection, actual values for the risk measure for the five FPEIS alternatives are presented in Table 2; data are provided for the unmitigated case.

The continued storage alternative has the greatest probability of causing one or more fatalities of the five alternatives. The remaining four alternatives have approximately a factor of 10 lower probability of causing one or more fatalities.

The maximum number of fatalities of the five FPEIS alternatives ranging between approximately 5,000 and 90,000, with continued storage having the greatest number and on-site disposal having the least. Continued storage has 16 times more maximum fatalities than on-site disposal; the national or regional alternatives

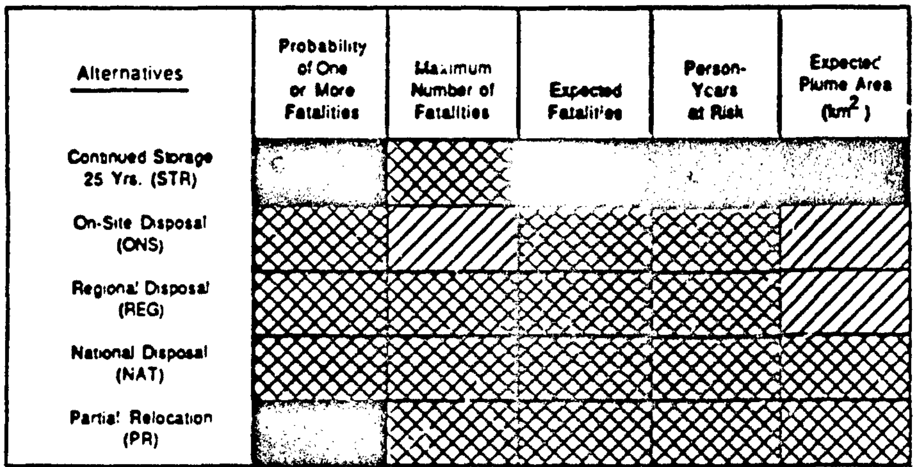

Note: Because this chart combines risk from all locations, the shading scale is a factor of 10 higher than the scale for all site-specific pictograms

Numerical Equivalents

Legend

Relative Risk	Shading	Probability of One or More Fatalities	Maximum Number of Fatalities	Expected Fatalities	Person-Years at Risk	Expected Plume Area (km^2)
Higher		$>10^{-2}$	>100,000	>0.1	$>10^{7}$	>0.1
		10^{-3} - 10^{-2}	10,000-100,000	10^{-2} - 0.1	10^{6} - 10^{7}	10^{-2} - 0.1
		10^{-4} - 10^{-3}	1000 - 10,000	10^{-3} - 10^{-2}	10^{5} - 10^{6}	10^{-3} - 10^{-2}
Lower		$<10^{-4}$	<1000	$<10^{-3}$	$<10^{5}$	$<10^{-3}$

FIGURE 6

RISK COMPARISON FOR PROGRAMMATIC ALTERNATIVES
ALL LOCATIONS COMBINED

TABLE 2

QUANTITATIVE COMPARISON OF RISK MEASURES FOR PROGRAMMATIC ALTERNATIVES
-ALL LOCATIONS COMBINED-

Unmitigated Risk

Alternatives	Probability of One or More Fatalities	Maximum Number of Fatalities	Expected Fatalities	Person-Years at Risk	Expected Plume Area (km^2)
Continued Storage 25 Yrs. (STR)	6.4×10^{-2}	8.9×10^{4}	19.3	1.4×10^{8}	2.1
On-Site Disposal (ONS)	7.3×10^{-3}	5.4×10^{3}	1.0×10^{-2}	2.3×10^{6}	7.2×10^{-3}
Regional Disposal (REG)	4.8×10^{-3}	4.2×10^{4}	1.2×10^{-2}	5.5×10^{6}	9.3×10^{-3}
National Disposal (NAT)	5.1×10^{-3}	4.2×10^{4}	3.1×10^{-2}	5.4×10^{6}	1.2×10^{-2}
Partial Relocation (PR)	1.1×10^{-2}	2.3×10^{4}	3.4×10^{-2}	3.1×10^{6}	1.3×10^{-2}

have 7 times more than on-site disposal alternative and the partial relocation alternative has 4 times more than the on-site disposal alternative.

The continued storage alternative has the greatest expected fatalities, while the on-site disposal and regional disposal alternatives have the least. The value of expected fatalities for the partial relocation and national disposal alternatives is approximately three times that for the on-site disposal alternative, while the value for the continued storage alternative (25 years) is approximately 1,900 times greater than for the on-site disposal alternative. This significant difference is not displayed on the pictogram, since the darkest shading category, in which continued storage falls, is unbounded on the higher end.

The difference between the expected fatalities for the continued storage alternative and the other four alternatives is more precisely shown in a plot of expected fatality estimates. Figure 7 portrays the expected fatality estimates, with upper and lower bounds, for each of the five unmitigated alternatives. The data show the dominance of expected fatalities associated with 25 years of continuing storage over expected fatalities associated with any of the disposal alternatives. Continued storage shows a mean expected fatality value of approximately 20, indicating that the analysis predicts a public fatality rate averaging roughly one per year. The fact that no deaths to the public have occurred after the decades of storage does not mean the analysis is greatly in error or unduly conservative, rather, it is because the continued storage accidents are predicted to be infrequent (occurring far less than 1 per year) but severe (multiple fatalities).

Person-years-at-risk are approximately equal for the on-site disposal and partial relocation alternatives. The national and regional disposal alternatives have approximately five times more person-years-at-risk than the on-site disposal alternative; and the continued storage alternative has approximately 60 times more person-years-at-risk than the on-site disposal alternative.

Expected plume area is greater for the continued storage alternative and least for the on-site disposal alternative.

3.2.2. Major Sources of Risk in Each Alternative

Figures 8 through 12 display the cumulative risk for the five disposal alternatives. Each curve shows the probability that the number of fatalities indicated by the horizontal scale is estimated to occur during the course of the entire disposal program. The intercept of the risk curve with the vertical axis, at a potential fatality of value 1, is the probability of one or more fatalities — one of the chosen major measures of programmatic risk. The area under each risk curve is numerically equal to another of the principle risk measures — the expected fatalities of the alternative. Finally, the horizontal intercepts (at probability = 10^{-10}) indicate the maximum fatalities that potentially could occur, although at very low probability, during the execution of the disposal alternative. The intercept for the lower bound curve indicates maximum fatalities for most-likely meteorology with wind directed at the average population density; the dashed vertical line at the right of each curve indicates the maximum fatalities for worst-case meteorology with wind directed toward the maximum potentially affected population. The latter for maximum fatalities (i.e., worst-case conditions) is the measure represented in the pictograms.

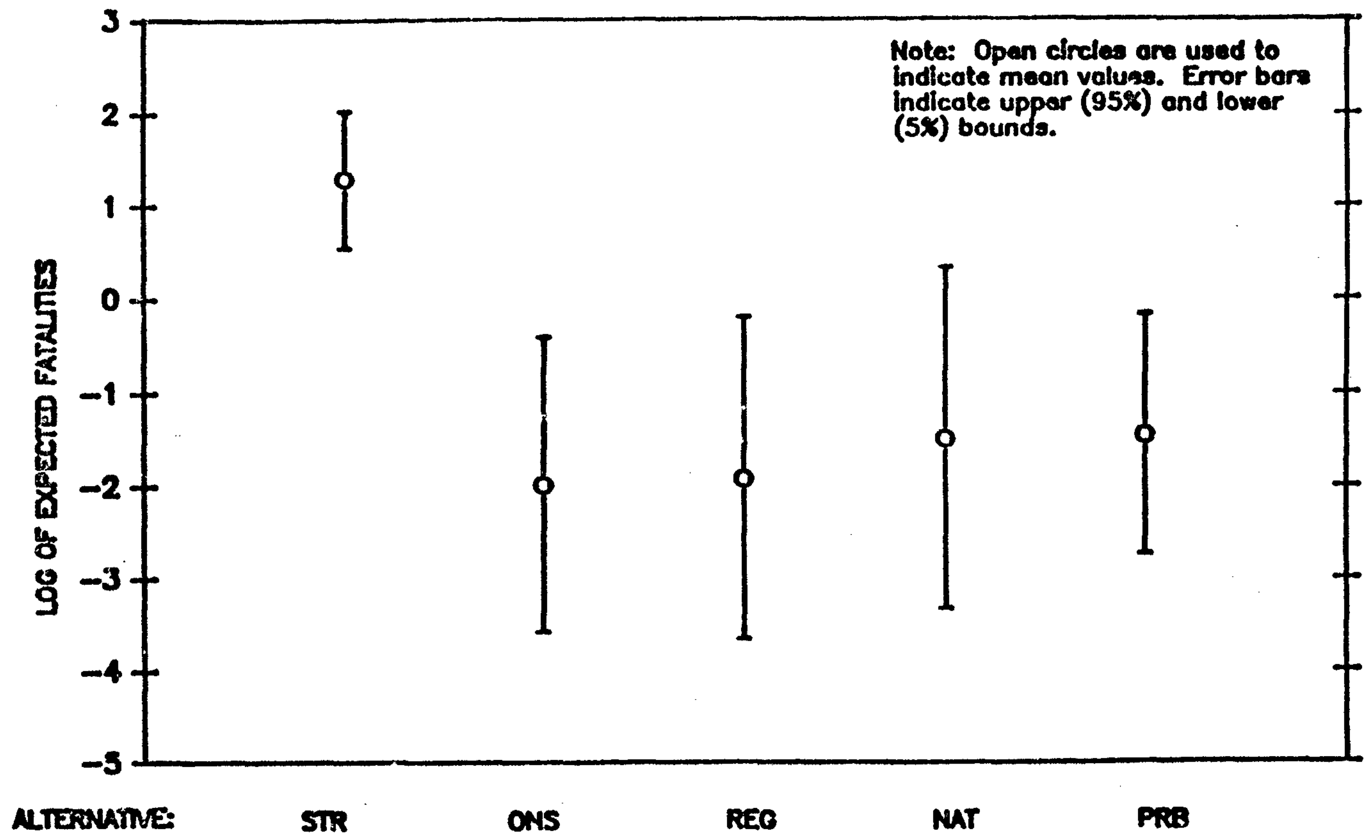

FIGURE 7

SOCIETAL RISK (EXPECTED FATALITIES) FOR PROGRAMMATIC ALTERNATIVES UNMITIGATED

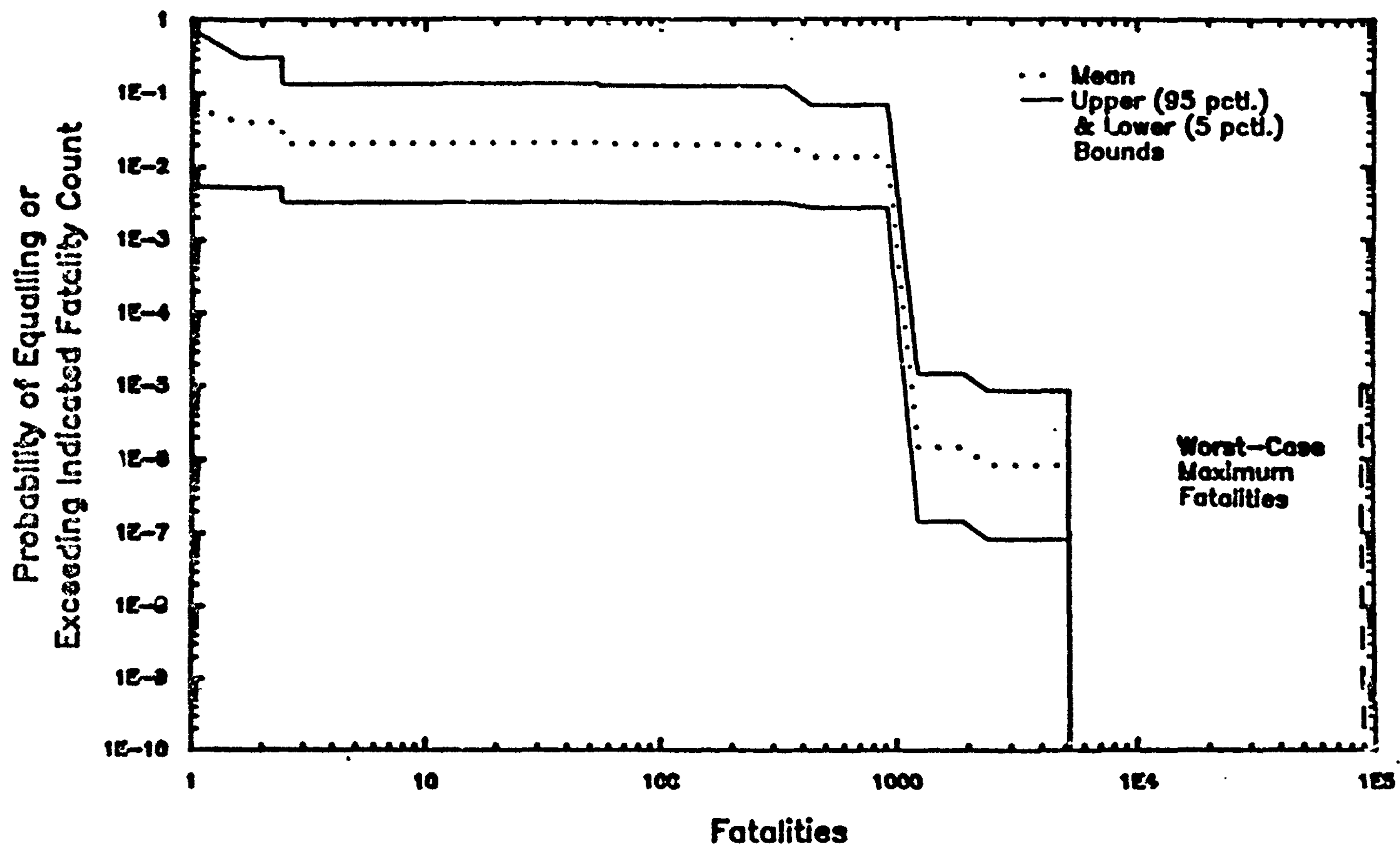

FIGURE 8

SOCIETAL RISK FOR PROGRAMMATIC ALTERNATIVE: STR CONTINUED STORAGE – 25 YEARS

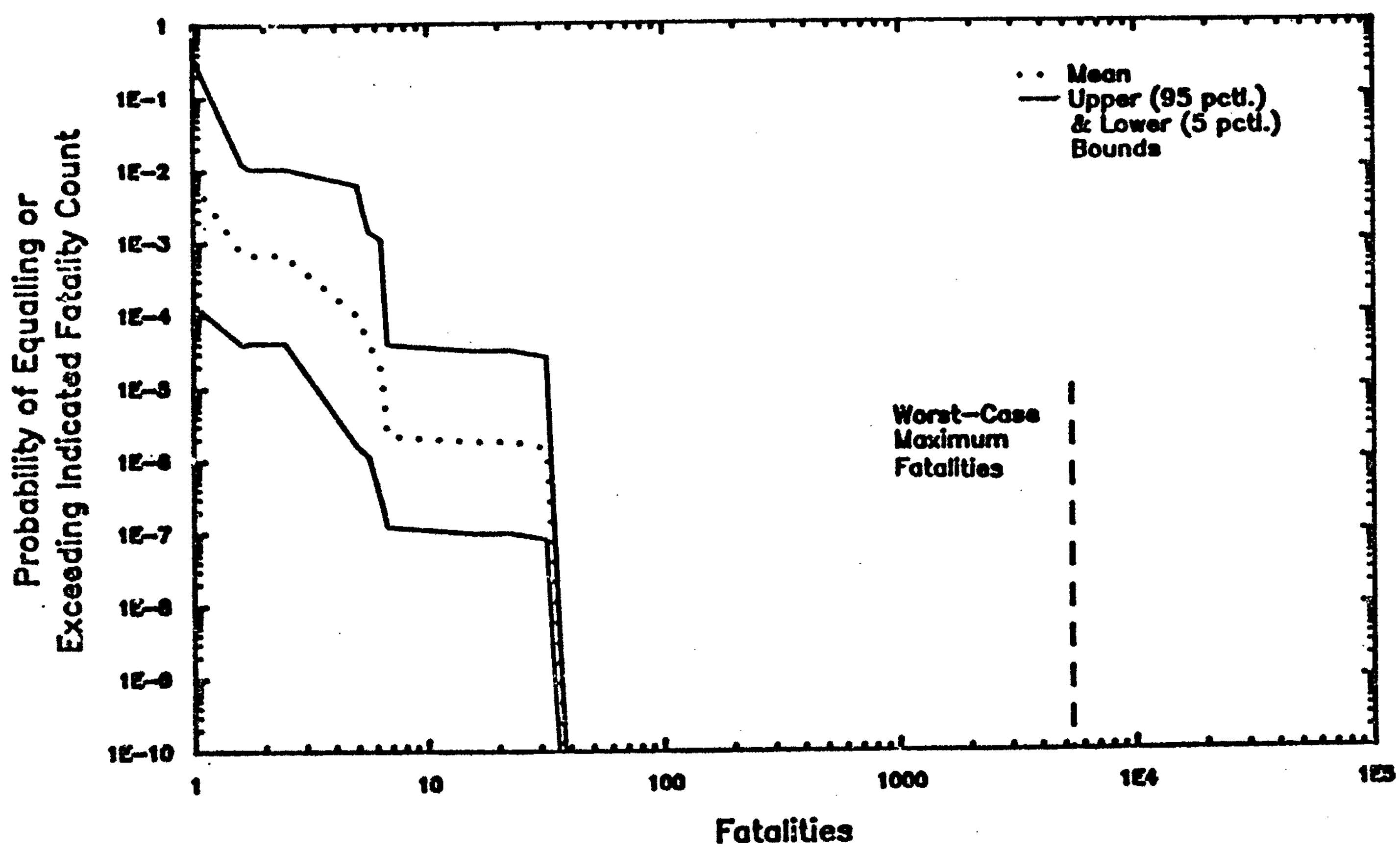

FIGURE 9

SOCIETAL RISK FOR PROGRAMMATIC ALTERNATIVE: ONS ON-SITE DISPOSAL

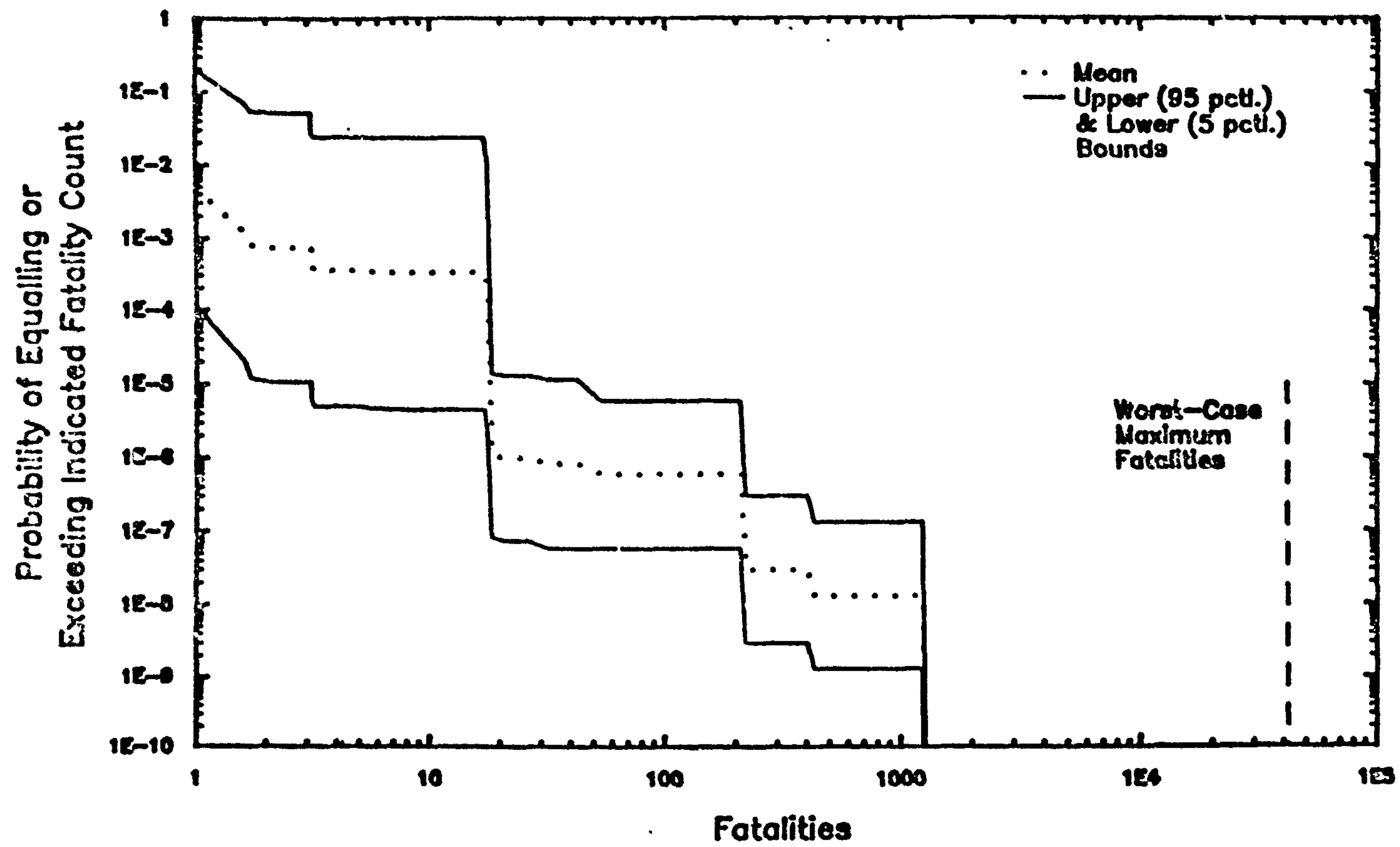

FIGURE 10

SOCIETAL RISK FOR PROGRAMMATIC ALTERNATIVE: REG REGIONAL DISPOSAL (RAIL)

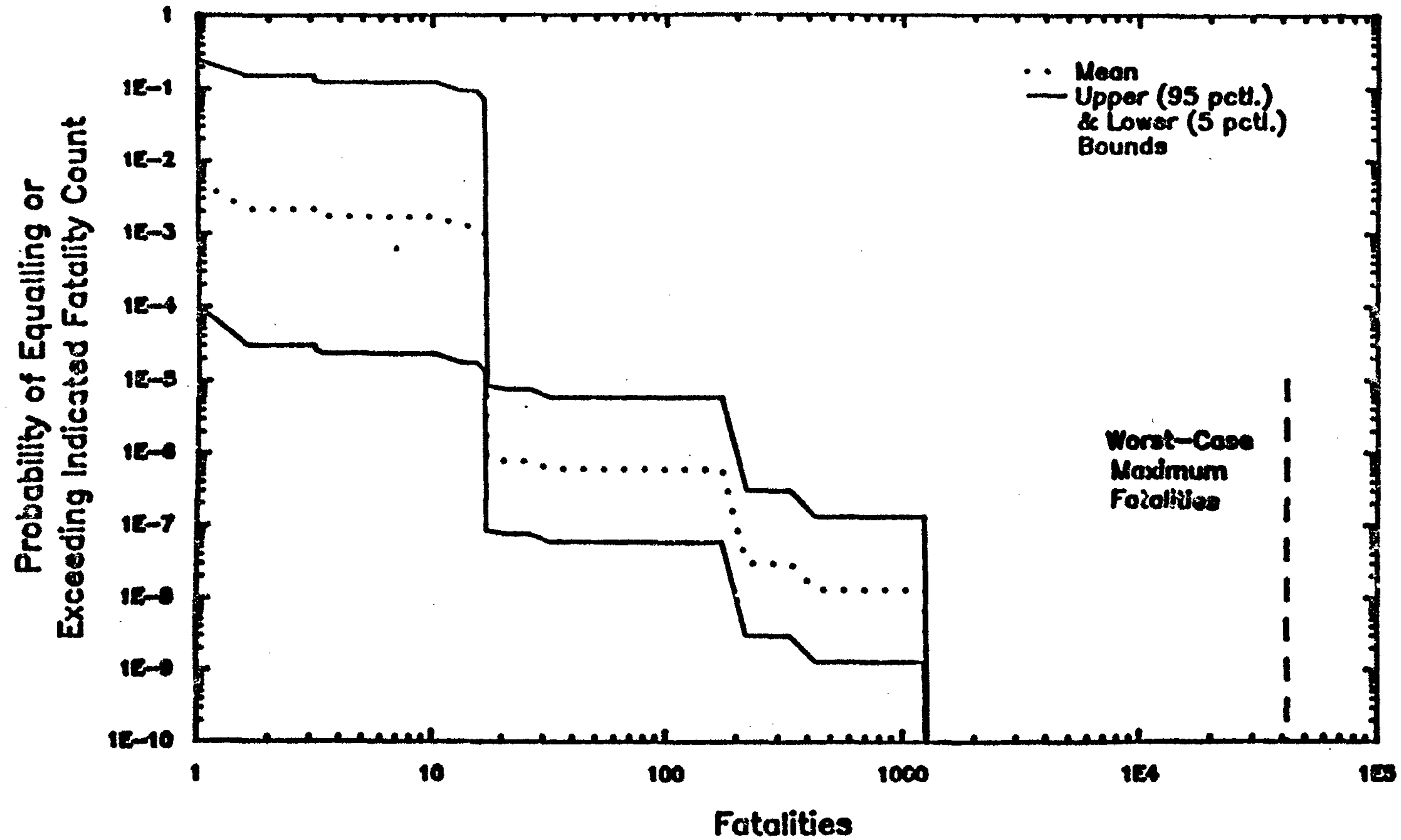

FIGURE 11

SOCIETAL RISK FOR PROGRAMMATIC ALTERNATIVE: NAT NATIONAL DISPOSAL (RAIL)

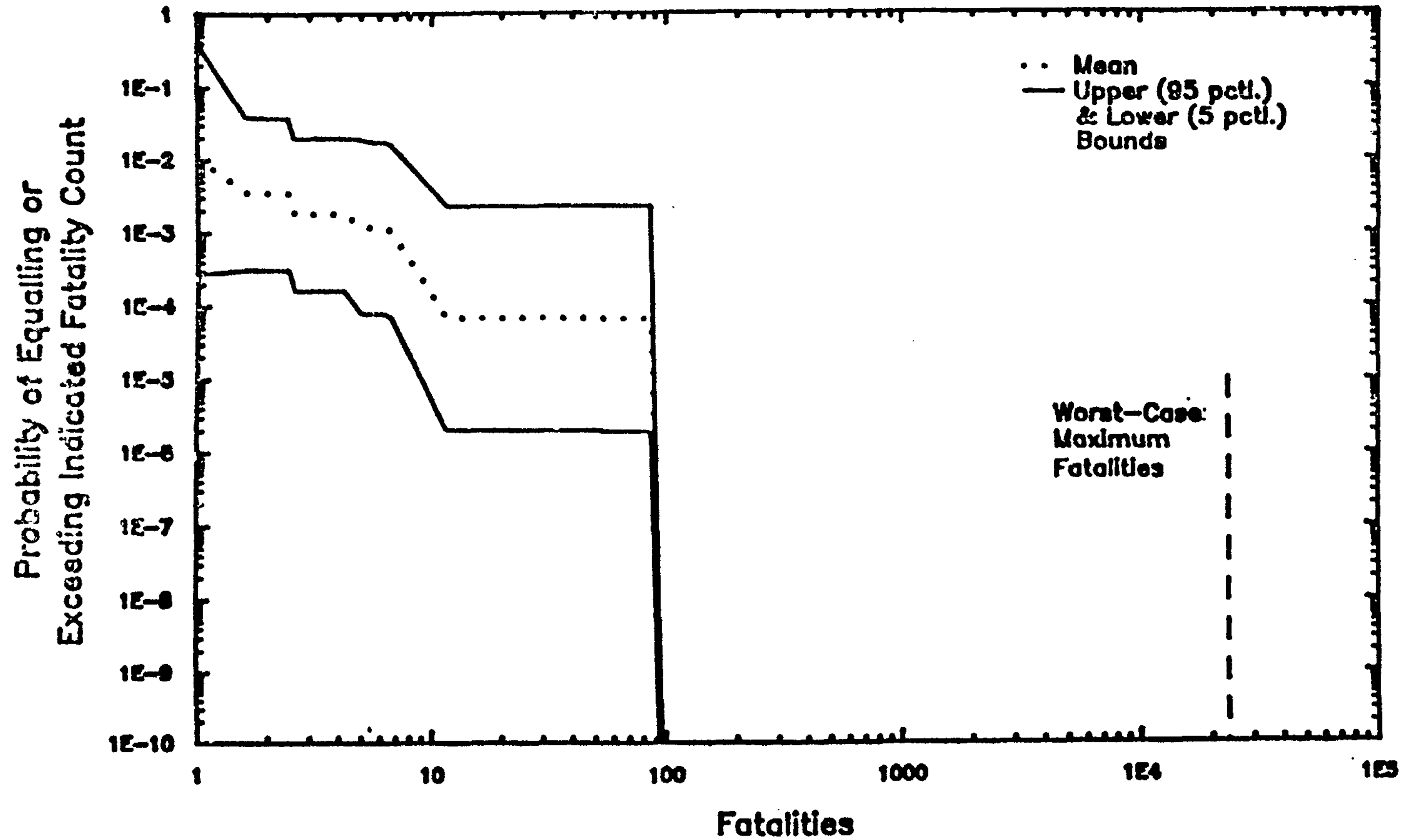

FIGURE 12

SOCIETAL RISK FOR PROGRAMMATIC ALTERNATIVE: PRB PARTIAL RELOCATION: APG & LBAD TO TEAD BY AIR (C141)

The risk curves show mean values as the dotted curve, as well as upper and lower uncertainty bounds (95 percent and 5 percent levels). The uncertainty bounds have been estimated through the use of the range factor data supplied by GA Technologies as a part of the accident scenario data base (GA Technologies, 1987[a], 1987[b], 1987[c]). Note that the uncertainty estimates are based on uncertainty in the estimated probability that an accident will take place, not on uncertainty in the consequence of an accident; nor do the uncertainty estimates include the uncertainty in population density, atmospheric conditions, and dose response. Uncertainty in wind direction is implied by assuming a uniform wind rose (equal probability for any direction) in conjunction with the assumptions of most-likely meteorological conditions and average population densities used for all probabilistic risk computations.

3.2.2.1 Continued Storage. The programmatic risk due to the continued storage alternative is portrayed in Figure 8. The risk is made up of both internally- and externally-initiated potential accidents. Storage of bulk containers account for 99 percent of the risk. Externally-initiated events, and, in particular, relatively mild earthquakes that result in fires affecting warehouse storage of bulk containers of mustard or VX at three sites (NAAP, UMDA, and TEAD), account for nearly all of the risk as measured by expected fatalities (the area under the cumulative risk curve), with earthquakes at the NAAP warehouse dominating. The probability of these earthquake events occurring in any given year is in the range of 10^{-4} to 10^{-5}, and the amount of agent potentially released is in the range of 10,000 to 100,000 pounds or more — an amount which, because it can be released as a vapor cloud fed by burning agent, can cause downwind plume lengths ("no-deaths" hazard distances, most-likely weather) of 20 to 50 km. Such large plumes could result in large numbers of fatalities, even in remote areas.

The next most significant contributor to risk of continued storage is the result of another external event — a small aircraft crash into the open storage yard, containing two containers of mustard, at APG. Like the warehouse accidents, this scenario involves the fire-included release of mustard agent. The frequency expected for this accident is 10^{-5} per year and the quantity of agent released is in the range of 5000 lbs, which can result in a plume length of approximately 3 km.

The analysis has identified a number of highly probable agent-releasing handling accidents associated with movement of the stockpile for maintenance and surveillance. These accidents, although estimated to occur more frequently than earthquakes or aircraft accidents (frequency 10^{-2} per year) release small quantities of agent since the contents of only one munition or pallet is involved, and the accident can be cleaned up more quickly. Because the release quantities are smaller, the downwind hazard distances are less. Therefore, handling accidents during storage do not contribute significantly to the population risks associated with the continued storage alternative.

The risk curve shows that accidents with consequences greater than 5000 fatalities could occur. These accidents involve aircraft crashing into the warehouse at NAAP resulting in fire-induced release of agent VX. However, the probability of these potential accidents is less than 10^{-7}, and the resulting contribution to expected fatalities is relatively low. The risk curve also shows a probability to expected fatalities of one or more fatalities (the Y-axis intercept) to be 0.05 with a range factor of approximately 10. This means that

the chance of a fatal accident (one or more deaths) per year is 0.05/25 = 0.002, with the same range factor. Thus, the risk analysis predicts a fatal event every 500 years (500 = 1/0.002), give or take a factor of 10.

3.2.2.2 On-Site Disposal. The programmatic risk of on-site disposal is displayed in Figure 9. Several activity categories contribute to on-site disposal risk; 93 percent being caused by chemical disposal plant operations; 2 percent caused by handling in the storage area and at the disposal facility; and 4 percent being caused by on-site storage transportation. The major contributors to on-site disposal risk are earthquakes damaging the disposal plant and human-error-induced accidents involving inadvertent feed of a burstered munition to the dunnage incinerator. These accidents are among the most frequent of all those identified for this alternative; they have a probability of occurring during the stockpile program of approximately 10^{-3}. The agent release for the earthquake scenario is large because the munition demilitarization building (MDB) is assumed to be severely damaged and bulk agent quantities and/or multiple munitions are involved; the estimated potential release, via fire, is sufficient to generate a lethal plume approximately 3 km long. The dunnage furnace scenarios involve lesser release quantities, since only single munitions are involved. Aircraft crashes into the disposal plant do not contribute significantly to risk because of the relatively small size of the target and of the local inventory available for release, and because of the relatively short time the plant is in operation (less than 3 years at most sites).

On-site transport of munitions also contributes significantly to on-site risk because large quantities of agent can be involved in vehicle accidents, and because the probability of occurrence, although only 10^{-10} accidents per vehicle-mile, is relatively high because there are many vehicle-miles involved in the CSDP.

Handling accidents which contribute most significantly to on-site risk are the dropping of an on-site container or a pallet of munitions.

The on-site disposal alternative has the lowest maximum consequence accident (most-likely meteorological conditions) of any alternative. The maximum potential fatality event could cause an estimated 54 deaths (under these most-likely conditions) as a result of either an earthquake, leading to a fire in the disposal plant, or a serious on-site transport vehicle accident; all these maximum consequence accidents involve the fire-borne or detonation-caused release of agent VX.

In addition to the dunnage incinerator accidents discussed above, other accidents having probabilities in the range of 10^{-4} to 10^{-3} per stockpile also include handling operations both at the storage yard and at the plant; these handling accidents, with the exception of accidents during handling of ton-containers containing GB, do not result in consequences beyond the boundaries of the military reservation.

3.2.2.3 Regional Disposal (Rail). Figure 10 illustrates the programmatic risk for the regional disposal alternative. Over 60 percent of the total risk (expected fatalities) is due to potential off-site transport accidents; 25 percent of the risk is due to plant operations and less than 10 percent results from on-site transport; short-term storage and handling together contribute to less than 5 percent of the total risk. Of the risk contributed by off-site

transportation, 8 percent is due to the transport of rockets, followed in significance by an 11 percent contribution due to transport of mines. Of total regional disposal risk, over 60 percent is due to rockets.

Among individual accident scenarios, those contributing most to risk are due to off-site rail transport of rockets. Of nearly equal risk are dunnage incinerator accidents involving rockets and mines.

In contrast to the on-site disposal risk curve (Figure 9), the regional alternative includes potential accidents with much higher consequences (most-likely conditions): greater than 1400 maximum fatalities vs. 54 for on-site. The highest consequence involves short-term storage of the transportation containers of rockets in the holding area. However, the probability of this high consequence accident is low: less than 10^{-7}.

The highest probability accidents for this alternative are those due to inadvertent feeding of burstered munitions into the dunnage incinerator and handling accidents involving single munitions or a pallet of munitions. These high probability accidents are not of sufficient consequence, under most-likely conditions, to cause fatalities beyond the boundaries of the military reservation with the exception of dunnage furnace accidents involving mines and rockets.

3.2.2.4 National Disposal (Rail). The programmatic risk due to the national disposal alternative is portrayed by Figure 11. The risk curve appears to be very similar to that for the regional disposal, as one might expect since the mix of activities is the same, with the major differences due to where the accidents might take place. Relative to regional disposal, the national alternative involves the transportation of the ANAD stockpile and the shift of all plant operations to TEAD.

Of the total risk, approximately 90 percent is caused by off-site transportation and less than 5 percent is caused by chemical disposal plant operations. Of the off-site transportation risk, over 95 percent is caused by transportation of energetic munitions, approximately 55 percent of that being caused by transportation of rockets, and 25 percent by transportation of projectiles.

As with regional disposal, the major contributors to risk among individual accident scenarios are the off-site rail transportation accidents. However, for this alternative, the highest risk accidents include those due to projectiles and mines, representing the risk due to transport of the ANAD stockpile to TEAD.

The highest consequence scenario, involving potential fatalities of over 1400, is the same as for the regional alternative: short-term storage of rockets in the holding area.

Highest probability accidents (probability greater than 10^{-4}) for national disposal are due to plant operations (inadvertent feed of burstered munitions to dunnage incinerators), handling, and off-site rail transportation. Of these, the handling accidents do not lead to plume lengths which exceed the boundary of the military reservation with the exception of those involving ton containers of GB, and therefore do not contribute significantly to risk.

3.2.2.5 Partial Relocation. APG & LBAD to TEAD by Air (C141). Programmatic risk for the partial relocation alternative, on-site disposal at all sites except for transport of the APG and LBAD stockpiles to TEAD via C141 aircraft, is shown in Figure 12. Of total risk, 71 percent is due to off-site transportation and 27 percent results from plant operations. Accidents involving rockets contribute 77 percent of total risk. In-flight air accidents (along the transportation corridor) account for 46 percent of total risk for this alternative.

The highest consequence accidents, under most-likely conditions, for this alternative (112 potential fatalities) are due to aircraft take-off accidents involving rockets and projectiles containing GB.

The probability of one or more fatalities for this alternative is approximately 10^{-2}.

3.3 Location-Specific Risk

In this section, the distribution of risk according to location (storage/disposal — i.e., "fixed" — sites and transportation corridors) is presented by means of the pictogram display of the major risk parameters as shown in Figures 13 through 28. The first 5 pictograms, Figures 13 through 17, compare the risk measures for each of the five FPEIS disposal alternatives at each of the eight sites for the unmitigated case. Figures 18 through 20 present the risk to the transportation corridor populations (which is not affected by the proposed mitigation measure) for the three alternatives involving off-site transport of the stockpile. Figures 21 through 28 present the pictogram displays of risk measures for each of the eight sites and for the unmitigated case plus two levels of mitigation. Although the relevant values (shadings) in Figures 13 through 17 are identical to those for Figures 21 through 28, the information is presented on a site-by-site basis for the latter figures to facilitate comparison of risks at a site for the different alternatives. The reader should note that all figures displaying site risk do not incorporate risks along a transportation corridor. (The corresponding pictogram for all locations combined was presented as Figure 6.)

3.3.1 Distribution of Progammatic Risk by Location

In addition to the differences in overall programmatic risk among the disposal alternatives, as presented in section 3.2, there are major differences in how that risk (as measured by expected fatalities) is distributed among the affected population groups. The pictograms supporting this discussion are those presented in Figures 13 through 20. In this regard, we note the following:

- For continued storage, the risk is borne primarily by two sites: NAAP with 85 percent of the total, and UMDA with 14 percent.
- Risk is somewhat more evenly shared for the unmitigated on-site disposal alternative, but even here, large disparities exist: 48 percent of the total risk would be experienced at PBA, with 2 percent or less of the total borne at each of four sites — APG, LBAD, PUDA, and UMDA.
- For the regional alternative, 63 percent of the total programmatic risk is borne by the population groups along the transportation corridors, and only 3 percent is felt by the populations near the

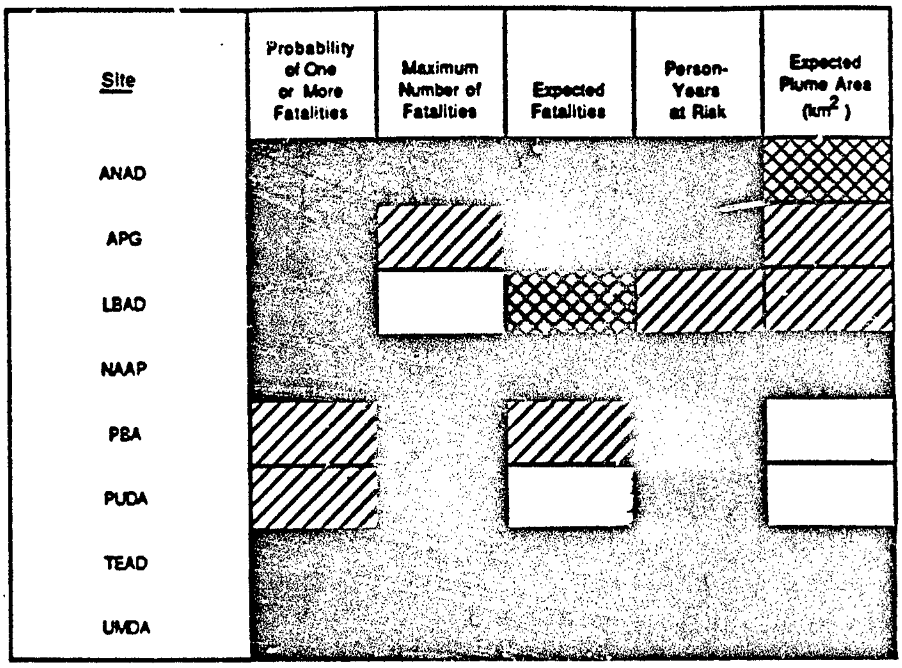

Numerical Equivalents

Legend Relative Risk	Shading	Probability of One or More Fatalities	Maximum Number of Fatalities	Expected Fatalities	Person-Years at Risk	Expected Plume Area (km^2)
Higher		$>10^{-3}$	>10,000	$>10^{-2}$	$>10^{6}$	$>10^{-2}$
		$10^{-4} - 10^{-3}$	5000 - 10,000	$10^{-3} - 10^{-2}$	$10^{5} - 10^{6}$	$10^{-3} - 10^{-2}$
		$10^{-5} - 10^{-4}$	1000 - 5000	$10^{-4} - 10^{-3}$	$10^{4} - 10^{5}$	$10^{-4} - 10^{-3}$
Lower		$<10^{-5}$	<1000	$<10^{-4}$	$<10^{4}$	$<10^{-4}$

FIGURE 13

SITE-SPECIFIC COMPARISON OF RISK FOR CONTINUED STORAGE (STR) 25 YEARS

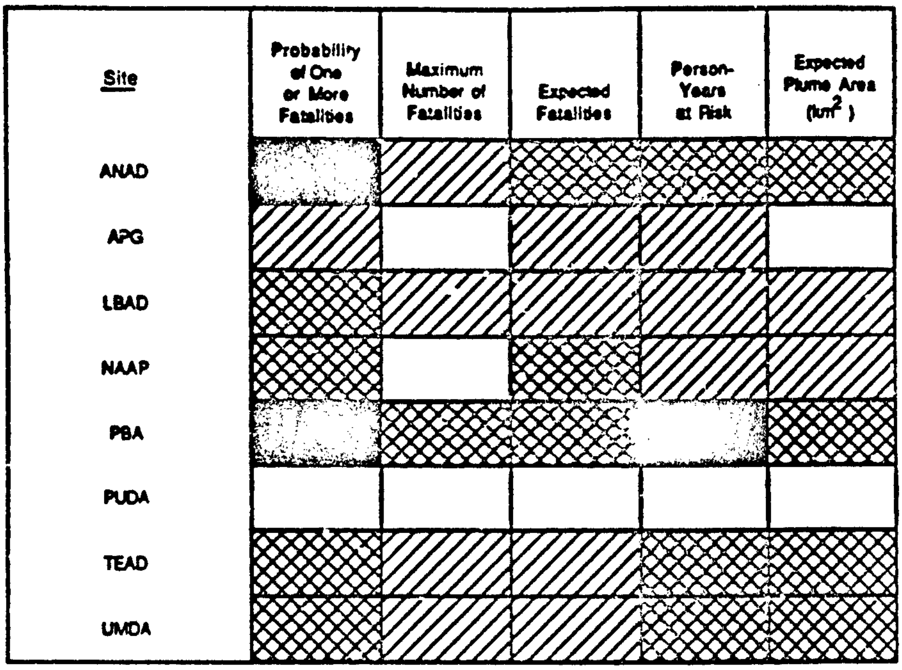

Legend:

Relative Risk	Shading	Probability of One or More Fatalities	Maximum Number of Fatalities	Expected Fatalities	Person-Years at Risk	Expected Plume Area (km^2)
		Numerical Equivalents				
Higher		$>10^{-3}$	>10,000	$>10^{-2}$	$>10^{6}$	$>10^{-2}$
		$10^{-4} - 10^{-3}$	5000 - 10,000	$10^{-3} - 10^{-2}$	$10^{5} - 10^{6}$	$10^{-3} - 10^{-2}$
		$10^{-5} - 10^{-4}$	1000 - 5000	$10^{-4} - 10^{-3}$	$10^{4} - 10^{5}$	$10^{-4} - 10^{-3}$
Lower		$<10^{-5}$	<1000	$<10^{-4}$	$<10^{4}$	$<10^{-4}$

FIGURE 14

SITE-SPECIFIC COMPARISON OF RISK FOR ON-SITE DISPOSAL (ONS)

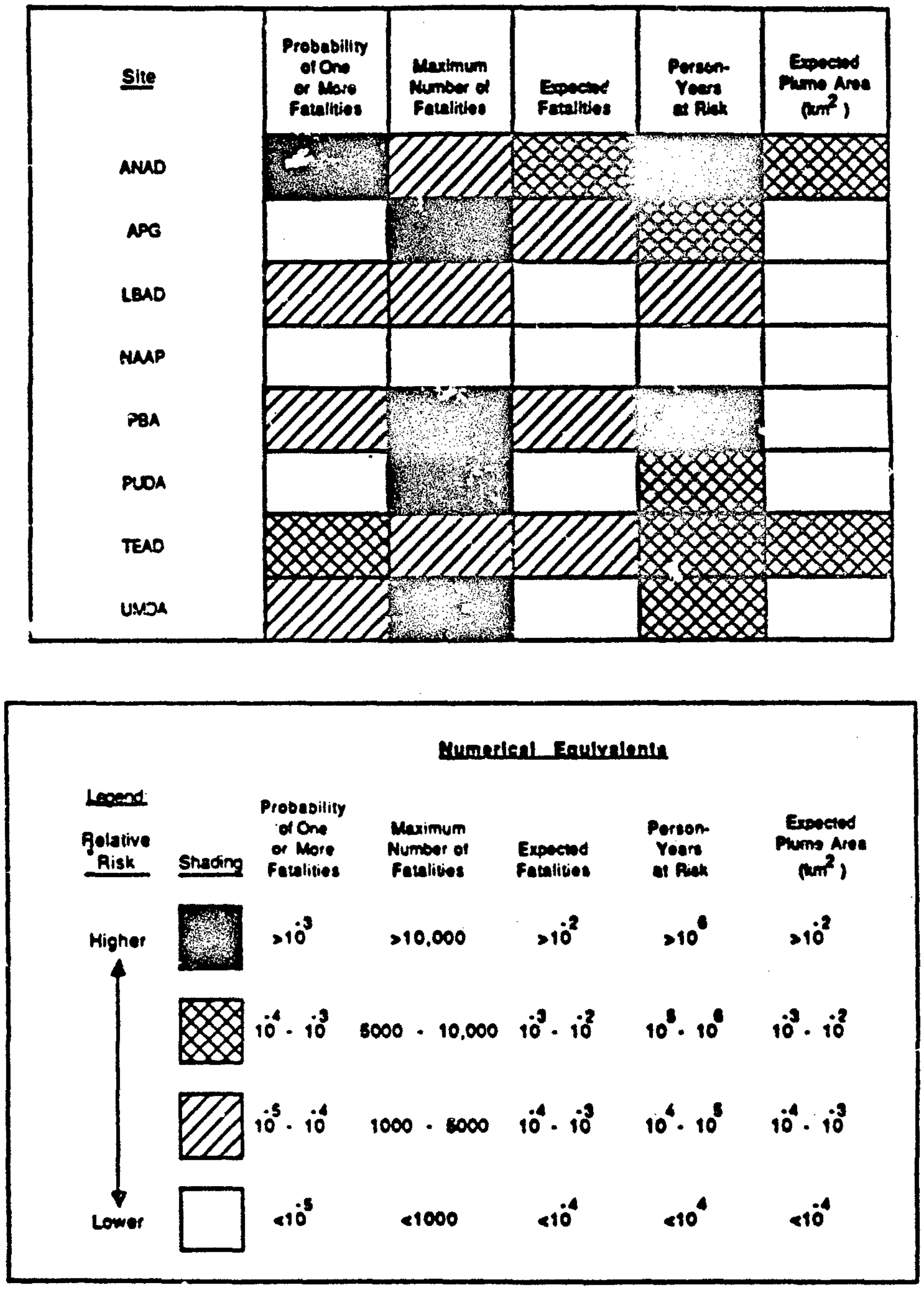

FIGURE 15

SITE-SPECIFIC COMPARISON OF RISK FOR REGIONAL DISPOSAL (REG)

(Risk along transportation corridors not included)

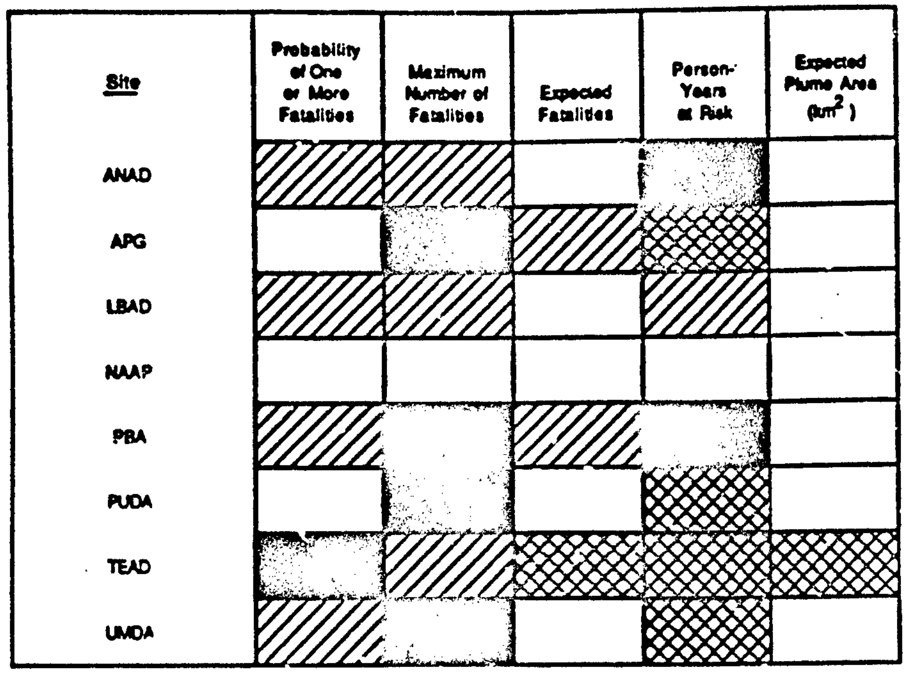

Numerical Equivalents

Legend Relative Risk	Shading	Probability of One or More Fatalities	Maximum Number of Fatalities	Expected Fatalities	Person-Years at Risk	Expected Plume Area (km^2)
Higher		$>10^{-3}$	>10,000	$>10^{-2}$	$>10^{6}$	$>10^{-2}$
		$10^{-4} - 10^{-3}$	5000 - 10,000	$10^{-3} - 10^{-2}$	$10^{5} - 10^{6}$	$10^{-3} - 10^{-2}$
		$10^{-5} - 10^{-4}$	1000 - 5000	$10^{-4} - 10^{-3}$	$10^{4} - 10^{5}$	$10^{-4} - 10^{-3}$
Lower		$<10^{-5}$	<1000	$<10^{-4}$	$<10^{4}$	$<10^{-4}$

FIGURE 16

SITE-SPECIFIC COMPARISON OF RISK FOR NATIONAL DISPOSAL (NAT)

(Risk along transportation corridors not included)

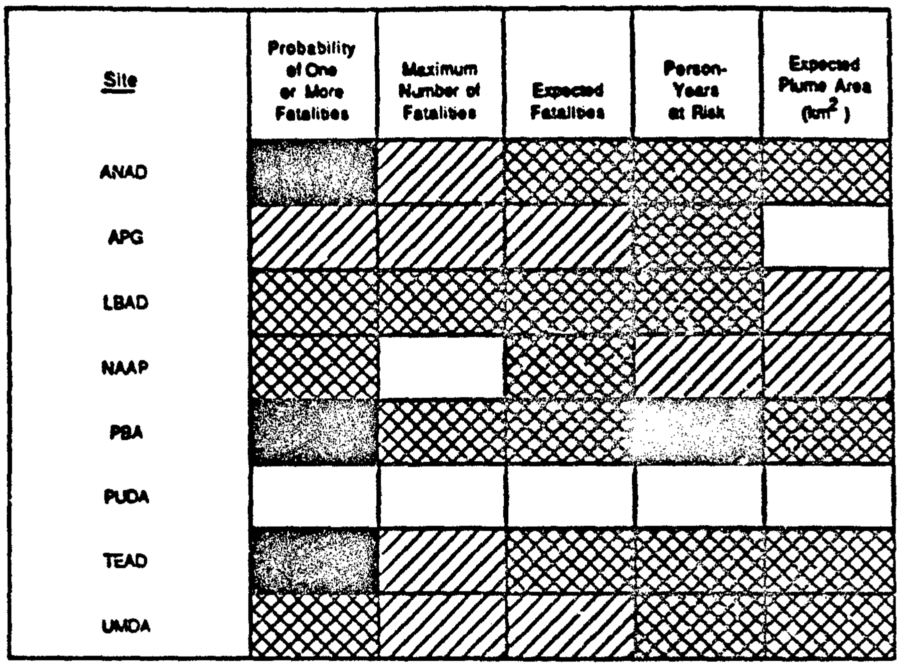

Legend Relative Risk	Shading	Probability of One or More Fatalities	Maximum Number of Fatalities	Expected Fatalities	Person-Years at Risk	Expected Plume Area (km^2)
		Numerical Equivalents				
Higher		$>10^{-3}$	>10,000	$>10^{-2}$	$>10^{6}$	$>10^{-2}$
		10^{-4} - 10^{-3}	5000 - 10,000	10^{-3} - 10^{-2}	10^{5} - 10^{6}	10^{-3} - 10^{-2}
		10^{-5} - 10^{-4}	1000 - 5000	10^{-4} - 10^{-3}	10^{4} - 10^{5}	10^{-4} - 10^{-3}
Lower		$<10^{-5}$	<1000	$<10^{-4}$	$<10^{4}$	$<10^{-4}$

FIGURE 17

SITE-SPECIFIC COMPARISON OF RISK FOR PARTIAL RELOCATION (PR)

(Risk along transportation corridors not included)

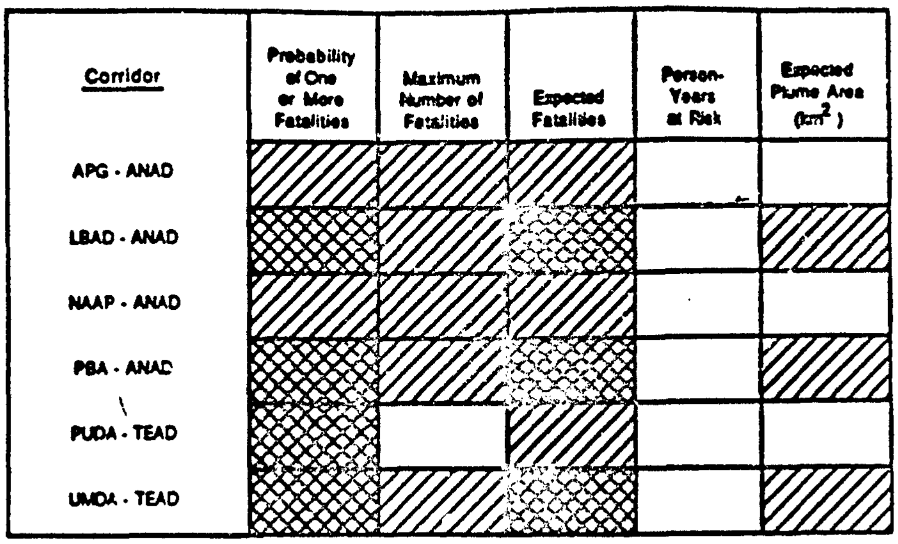

Numerical Equivalents

Legend:

Relative Risk	Shading	Probability of One or More Fatalities	Maximum Number of Fatalities	Expected Fatalities	Person-Years at Risk	Expected Plume Area (km^2)
Higher		$>10^{-3}$	>10,000	$>10^{-2}$	$>10^{6}$	$>10^{-2}$
		$10^{-4} - 10^{-3}$	5000 - 10,000	$10^{-3} - 10^{-2}$	$10^{5} - 10^{6}$	$10^{-3} - 10^{-2}$
		$10^{-5} - 10^{-4}$	1000 - 5000	$10^{-4} - 10^{-3}$	$10^{4} - 10^{5}$	$10^{-4} - 10^{-3}$
Lower		$<10^{-5}$	<1000	$<10^{-4}$	$<10^{4}$	$<10^{-4}$

FIGURE 18

RISK ALONG RAIL TRANSPORTATION CORRIDORS
FOR REGIONAL DISPOSAL
- ALL MITIGATION LEVELS -

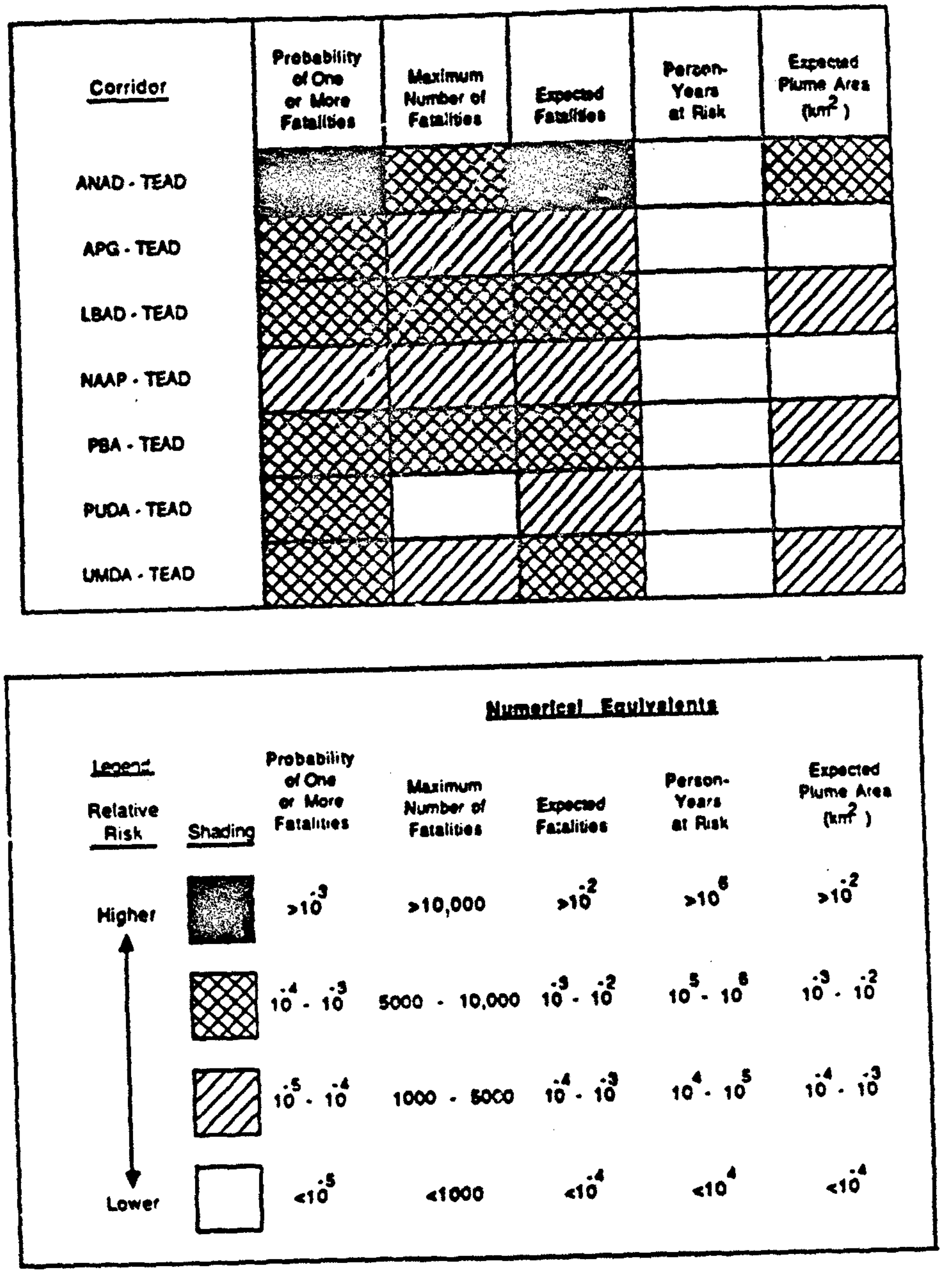

FIGURE 19

RISK ALONG RAIL TRANSPORTATION CORRIDORS
FOR NATIONAL DISPOSAL
- ALL MITIGATION LEVELS -

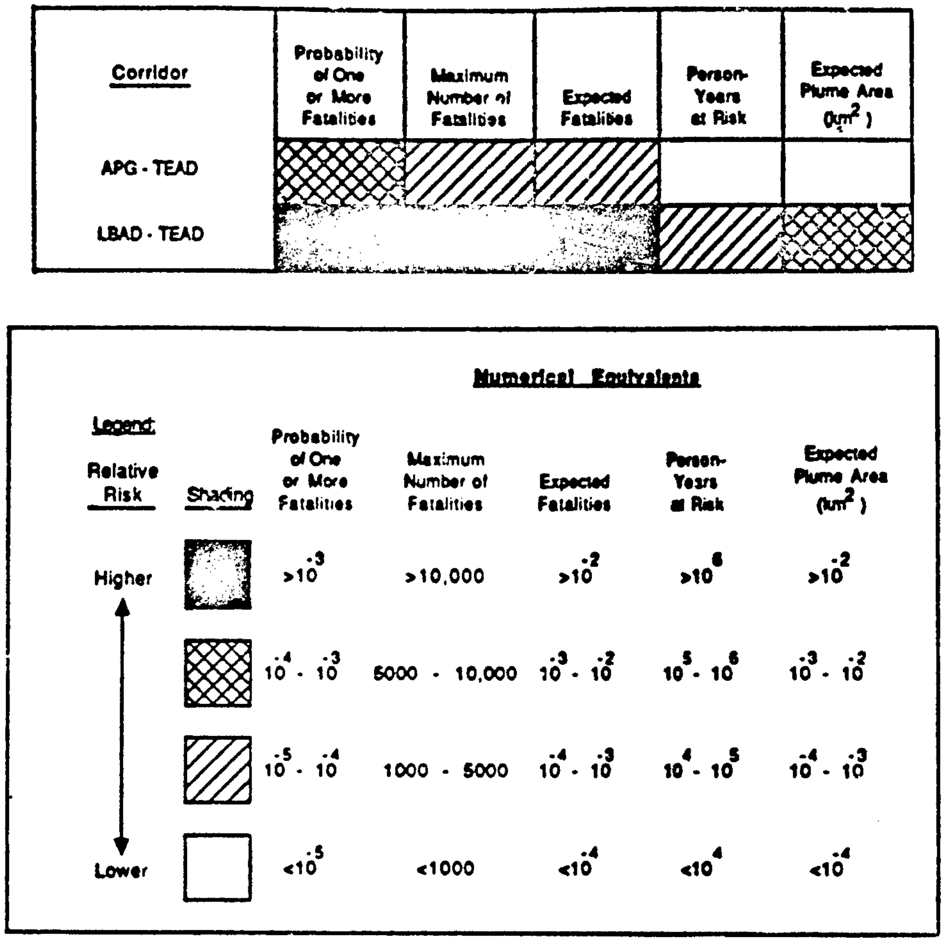

FIGURE 20

RISK ALONG AIR TRANSPORTATION CORRIDOR FOR PARTIAL RELOCATION DISPOSAL - ALL MITIGATION LEVELS -

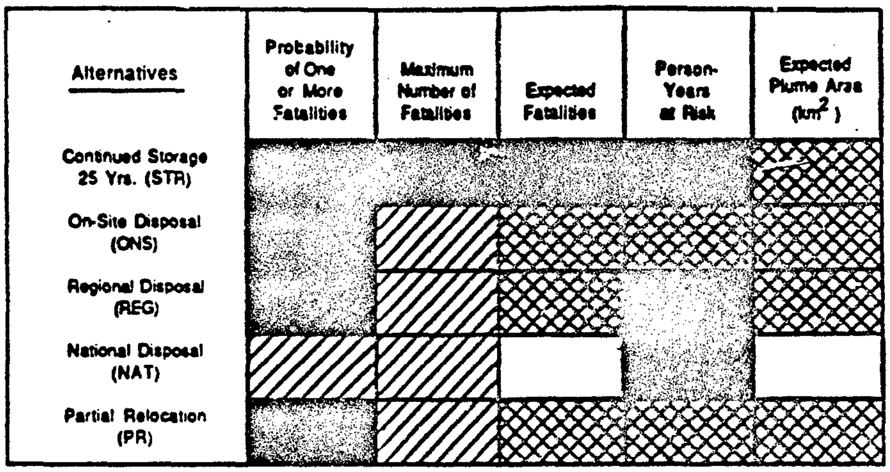

Numerical Equivalents

Legend

Relative Risk	Shading	Probability of One or More Fatalities	Maximum Number of Fatalities	Expected Fatalities	Person-Years at Risk	Expected Plume Area (km²)
Higher		$>10^{-3}$	>10,000	$>10^{-2}$	$>10^{6}$	$>10^{-2}$
		$10^{-4} - 10^{-3}$	5000 - 10,000	$10^{-3} - 10^{-2}$	$10^{5} - 10^{6}$	$10^{-3} - 10^{-2}$
		$10^{-5} - 10^{-4}$	1000 - 5000	$10^{-4} - 10^{-3}$	$10^{4} - 10^{5}$	$10^{-4} - 10^{-3}$
Lower		$<10^{-5}$	<1000	$<10^{-4}$	$<10^{4}$	$<10^{-4}$

FIGURE 21

RISK IN THE VICINITY OF ANNISTON ARMY DEPOT (ANAD) FOR PROGRAMMATIC ALTERNATIVES

(Risk along transportation corridors not Included)

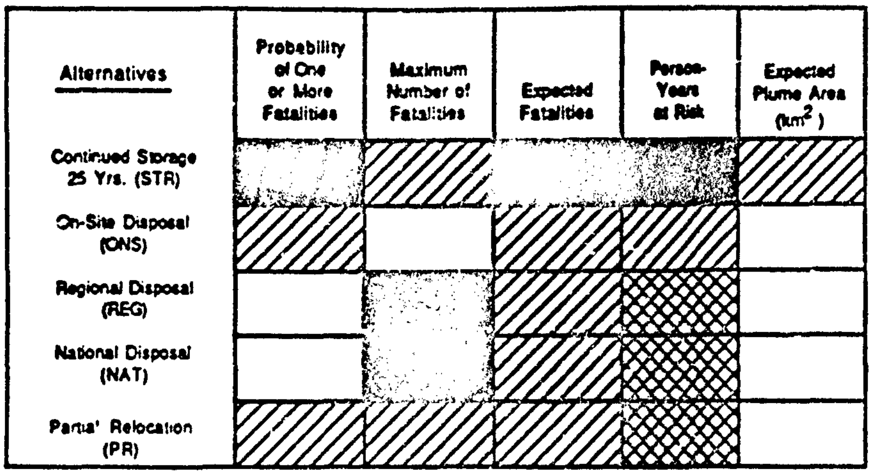

Numerical Equivalents

Legend: Relative Risk	Shading	Probability of One or More Fatalities	Maximum Number of Fatalities	Expected Fatalities	Person-Years at Risk	Expected Plume Area (km²)
Higher		$>10^{-3}$	>10,000	$>10^{-2}$	$>10^{6}$	$>10^{-2}$
		$10^{-4} - 10^{-3}$	5000 - 10,000	$10^{-3} - 10^{-2}$	$10^{5} - 10^{6}$	$10^{-3} - 10^{-2}$
		$10^{-5} - 10^{-4}$	1000 - 5000	$10^{-4} - 10^{-3}$	$10^{4} - 10^{5}$	$10^{-4} - 10^{-3}$
Lower		$<10^{-5}$	<1000	$<10^{-4}$	$<10^{4}$	$<10^{-4}$

FIGURE 22

RISK IN THE VICINITY OF ABERDEEN PROVING GROUND (APG) FOR PROGRAMMATIC ALTERNATIVES

(Risk along transportation corridors or not included)

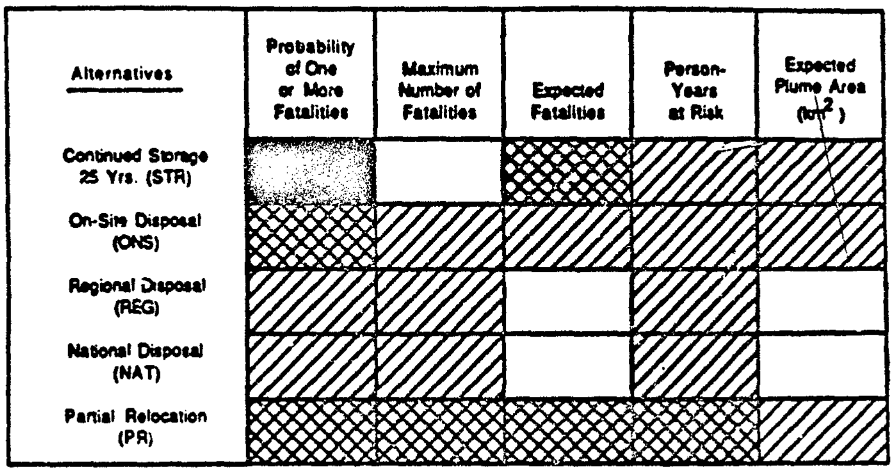

Numerical Equivalents

Legend Relative Risk	Shading	Probability of One or More Fatalities	Maximum Number of Fatalities	Expected Fatalities	Person-Years at Risk	Expected Plume Area (km^2)
Higher		$>10^{-3}$	>10,000	$>10^{-2}$	$>10^{6}$	$>10^{-2}$
		$10^{-4} - 10^{-3}$	5000 - 10,000	$10^{-3} - 10^{-2}$	$10^{5} - 10^{6}$	$10^{-3} - 10^{-2}$
		$10^{-5} - 10^{-4}$	1000 - 5000	$10^{-4} - 10^{-3}$	$10^{4} - 10^{5}$	$10^{-4} - 10^{-3}$
Lower		$<10^{-5}$	<1000	$<10^{-4}$	$<10^{4}$	$<10^{-4}$

FIGURE 23

RISK IN THE VICINITY OF LEXINGTON-BLUE GRASS ARMY DEPOT (LBAD) FOR PROGRAMMATIC ALTERNATIVES

(Risk along transportation corridors not included)

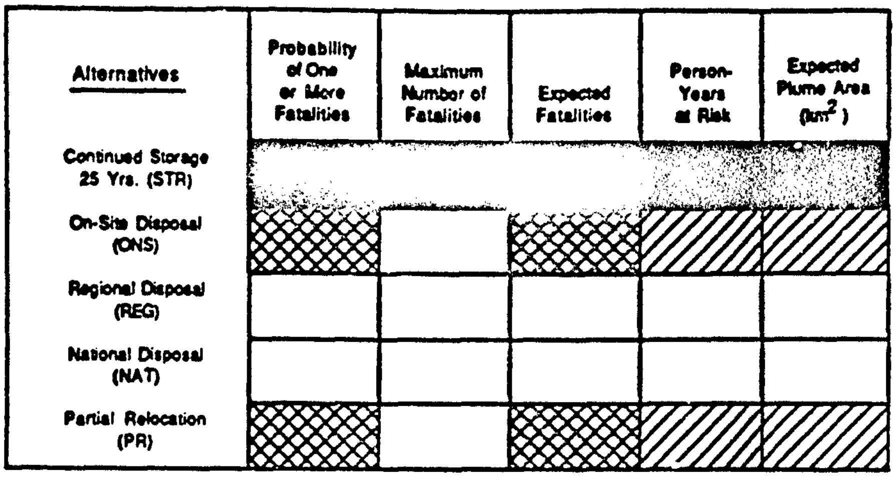

Numerical Equivalents

Legend:

Relative Risk	Shading	Probability of One or More Fatalities	Maximum Number of Fatalities	Expected Fatalities	Person-Years at Risk	Expected Plume Area (km^2)
Higher		$>10^{-3}$	>10,000	$>10^{-2}$	$>10^{6}$	$>10^{-2}$
		10^{-4} - 10^{-3}	5000 - 10,000	10^{-3} - 10^{-2}	10^{5} - 10^{6}	10^{-3} - 10^{-2}
		10^{-5} - 10^{-4}	1000 - 5000	10^{-4} - 10^{-3}	10^{4} - 10^{5}	10^{-4} - 10^{-3}
Lower		$<10^{-5}$	<1000	$<10^{-4}$	$<10^{4}$	$<10^{-4}$

FIGURE 24

RISK IN THE VICINITY OF NEWPORT ARMY AMMUNITION PLANT (NAAP) FOR PROGRAMMATIC ALTERNATIVES

(Risk along transportation corridor not included)

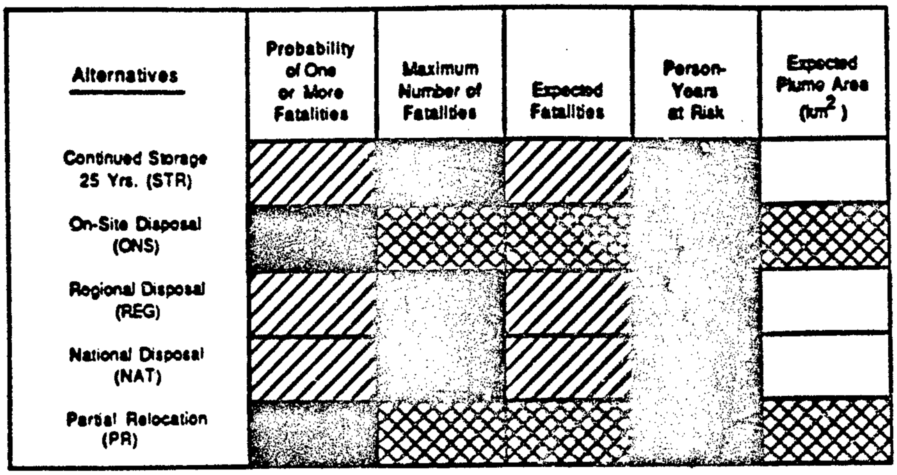

Numerical Equivalents

Legend

Relative Risk	Shading	Probability of One or More Fatalities	Maximum Number of Fatalities	Expected Fatalities	Person-Years at Risk	Expected Plume Area (km^2)
Higher		$>10^{-3}$	>10,000	$>10^{-2}$	$>10^{6}$	$>10^{-2}$
↑		$10^{-4} - 10^{-3}$	5000 - 10,000	$10^{-3} - 10^{-2}$	$10^{5} - 10^{6}$	$10^{-3} - 10^{-2}$
↓		$10^{-5} - 10^{-4}$	1000 - 5000	$10^{-4} - 10^{-3}$	$10^{4} - 10^{5}$	$10^{-4} - 10^{-3}$
Lower		$<10^{-5}$	<1000	$<10^{-4}$	$<10^{4}$	$<10^{-4}$

FIGURE 25

RISK IN THE VICINITY OF PINE BLUFF ARSENAL (PBA) FOR PROGRAMMATIC ALTERNATIVES

(Risk along transportation corridors or not Includea)

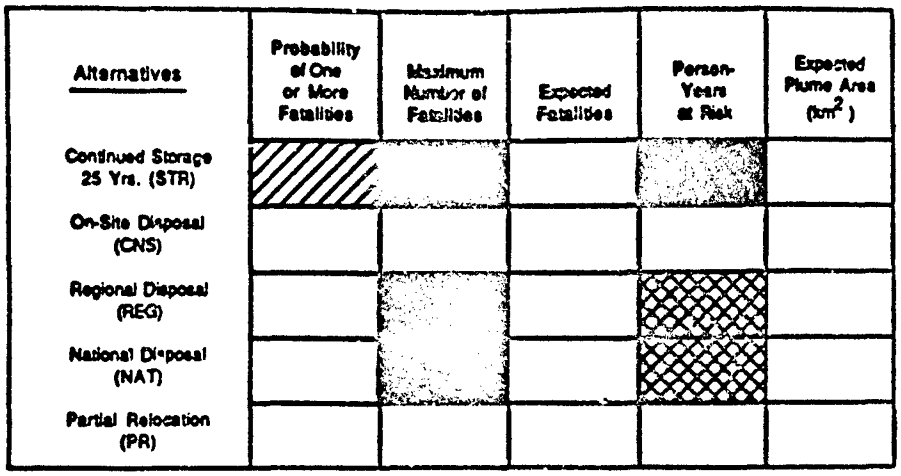

Legend:

Relative Risk	Shading	Probability of One or More Fatalities	Maximum Number of Fatalities	Expected Fatalities	Person-Years at Risk	Expected Plume Area (km^2)
		Numerical Equivalents				
Higher		$>10^{-3}$	>10,000	$>10^{-2}$	$>10^{6}$	$>10^{-2}$
		10^{-4} - 10^{-3}	5000 - 10,000	10^{-3} - 10^{-2}	10^{5} - 10^{6}	10^{-3} - 10^{-2}
		10^{-5} - 10^{-4}	1000 - 5000	10^{-4} - 10^{-3}	10^{4} - 10^{5}	10^{-4} - 10^{-3}
Lower		$<10^{-5}$	<1000	$<10^{-4}$	$<10^{4}$	$<10^{-4}$

FIGURE 26

RISK IN THE VICINITY OF PUEBLO DEPOT ACTIVITY (PUDA) FOR PROGRAMMATIC ALTERNATIVES

(Risk along transportation corridors not included)

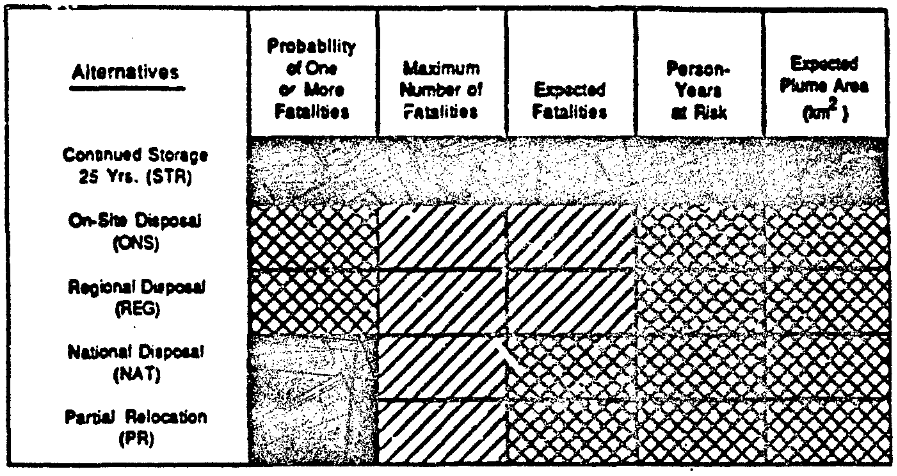

Numerical Equivalents

Legend Relative Risk	Shading	Probability of One or More Fatalities	Maximum Number of Fatalities	Expected Fatalities	Person-Years at Risk	Expected Plume Area (km^2)
Higher		$>10^{-3}$	>10,000	$>10^{-2}$	$>10^{6}$	$>10^{-2}$
		10^{-4} - 10^{-3}	5000 - 10,000	10^{-3} - 10^{-2}	10^{5} - 10^{6}	10^{-3} - 10^{-2}
		10^{-5} - 10^{-4}	1000 - 5000	10^{-4} - 10^{-3}	10^{4} - 10^{5}	10^{-4} - 10^{-3}
Lower		$<10^{-5}$	<1000	$<10^{-4}$	$<10^{4}$	$<10^{-4}$

FIGURE 27

RISK IN THE VICINITY OF TOOELE ARMY DEPOT (TEAD) FOR PROGRAMMATIC ALTERNATIVES

(Risk along transportation corridors not included)

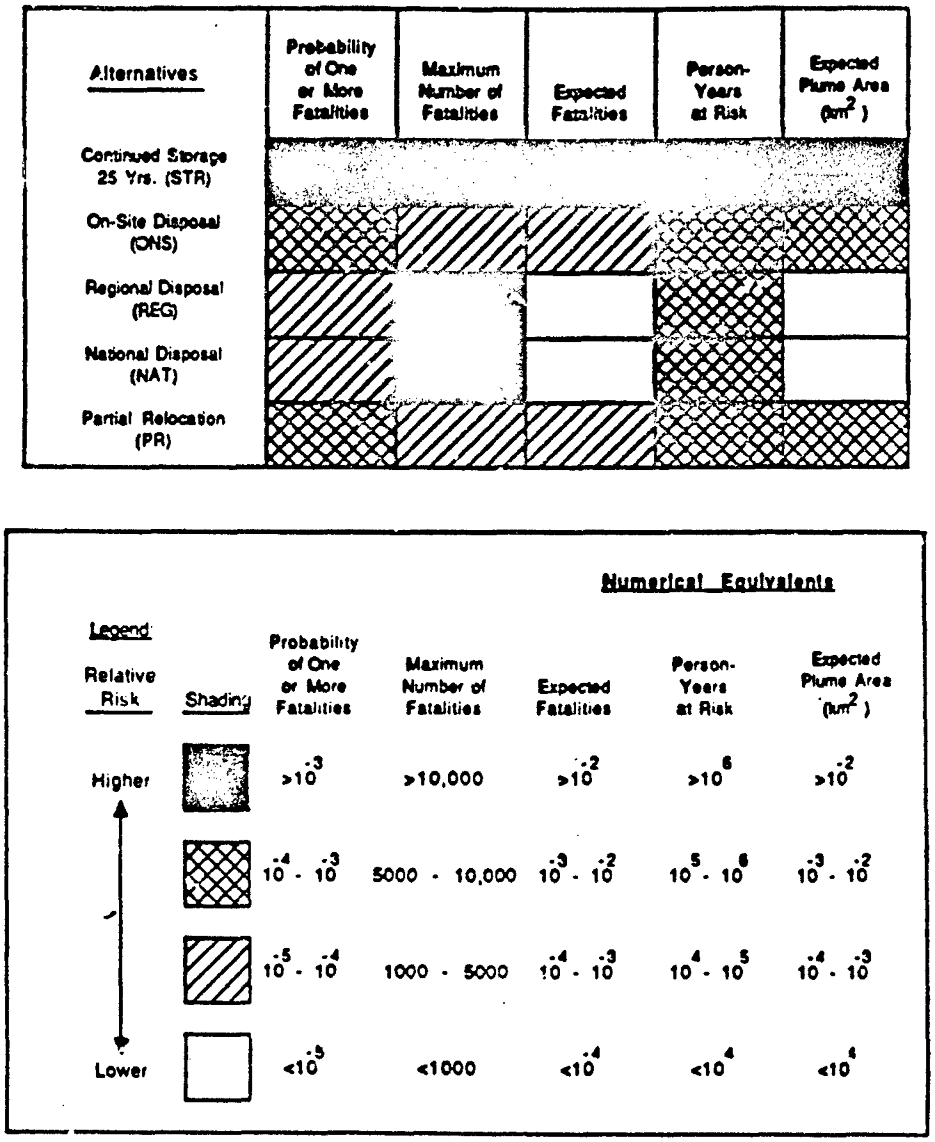

FIGURE 28

RISK IN THE VICINITY OF UMATILLA DEPOT ACTIVITY (UMDA) FOR PROGRAMMATIC ALTERNATIVES

(Risk along transportation corridors not included)

originating sites; the remaining 34 percent is borne by the destination site populations (ANAD and TEAD), with ANAD's share three times TEAD's. Risk along the transportation corridors is due principally to shipment of the PBA and LBAD stockpiles.

- Ninety-two percent of the risk for the national alternative is distributed along the transportation corridors, leaving less than 2 percent of the risk to be borne by the originating sites. The remaining 6 percent of the total is felt by the TEAD population group. Of the transportation corridor risk, over 50 percent is the result of transporting the ANAD stockpile; the LBAD and PBA stockpiles also contribute nearly 20 percent each.

- For the partial relocation alternative, nearly half the risk is borne by the corridor populations, with the air-movement of the LBAD stockpile contributing over 98 percent of the corridor risk (68 percent of the total risk for the alternative). TEAD sees only 3 percent of the risk, while LBAD and APG as the originating sites contribute roughly 25 percent and 5 percent, respectively; risk at the remaining sites is the same as for the on-site alternative.

3.3.2 Factors Contributing to Community/Societal Risk, by Location

Risk at disposal/storage sites includes all activities that take place there. These include both storage and disposal activities, as well as any activities (such as extra handling and temporary storage while awaiting shipment) that could be associated with preparing the stockpile for off-site transport. The sites are identified by the codes listed in section 3.1.1.

3.3.2.1 Anniston Army Depot (ANAD). Figure 21 displays the major risk measure for all applicable disposal alternatives at ANAD. For all major risk measures, continued storage poses the highest risk of any alternative. Among the disposal alternatives, all appear to pose the same risk (within the numerical ranges defining the 'pictogram' shadings) to the public except for national disposal for which risk is one or two categories lower for probability of one or more fatalities and expected fatalities. Person-years-at-risk is high for the national and regional alternatives.

For the case of no mitigation, the major contributors to community/societal risk to the community in the vicinity of ANAD, as measured by expected fatalities, for each of the disposal alternatives is summarized below:

- Continued storage risk at ANAD is mostly (90 percent) due to handling activities; the remainder of the risk results from external events affecting the stockpile. Furthermore, over 90 percent of the risk is due to projectiles.

- For the on-site and partial relocation (which, for ANAD, is the same as on-site) alternatives, 97 percent of the risk is due to plant operations, and of that risk, roughly 70 percent is due to the disposal of mines with most of the remainder due to rockets.

- o The regional disposal risk is due primarily (75 percent) to plant operations; most of the remainder (22 percent) results from on-site transport. Roughly 40 percent of total risk is due to rockets; another 40 percent is due to mines; only 1 percent of the risk results from the disposal of bulk agent. The reason for the relatively high risk of the regional alternative is the need to process the additional inventory of munitions shipped in by rail from other sites.

- o The national alternative, 62 percent of the risk is due to on-site transport accidents and 37 percent results from handling accidents. Among the munition types, nearly 80 percent of the risk results from rockets, with the remainder split evenly between mines and projectiles.

3.3.2.2 APG. The risk from various disposal alternatives to the population about APG is illustrated by the pictogram in Figure 22. Except for the probability of one or more fatalities, all risk measures indicate that the on-site alternative poses the least risk. On the basis of expected fatalities, the risk due to the disposal alternatives is roughly the same (within 25 percent) for all. Risk associated with the continued storage alternative is greater than for any of the disposal alternatives by a factor of 10 - 100.

The major contributors to risk for each unmitigated alternative at APG are summarized below:

- o 100 percent of the continued storage risk is due to external events (aircraft crashes) during storage; there are no handling events of risk significance, a result of the fact that APG's stockpile consists only of mustard agent in bulk containers, and the handling accidents lead only to spill or spills with fire which do not create plume that move beyond the boundary of the military reservation.

- o For the on-site alternative, 100 percent of the risk results from plant operation.

- o The risk due to regional and national alternatives (the same for those living near APG) is due entirely to accidents during short-term storage related to off-site transportation via rail.

- o For the partial relocation — air mode alternative, more than 95 percent of the risk arises from off-site transportation-related activities — mainly crashes of aircraft carrying bulk containers of mustard, during take-off. The remainder of the risk results from short-term storage activities.

- o For the partial relocation — water mode alternative, the risk is about evenly split between off-site transportation-related accidents — and short-term storage accidents — an aircraft crashing into a loaded LASH while still moored in the Aberdeen area.

3.3.2.3 LBAD. Figure 23 contains the pictogram representation of risk at LBAD. The pictogram for the unmitigated case indicates that the regional and national alternatives (identical in terms of originating site activities and risk at LBAD) pose the least risk to the population surrounding LBAD. On the basis of expected fatalities, the risk due to the national/regional alternatives is less

than that due to on-site disposal by a factor of 3 or 4, while the risk due to the partial relocation (air mode) alternatives dominate by one-to-two orders of magnitude.

The contributions to risk for each unmitigated disposal alternative are summarized below:

- For continued storage at LBAD, essentially all of the risk arises from handling accidents associated with the maintenance of projectiles. The highest risk accidents are due to the movement of munitions for maintenance purposes.

- The risk to on-site disposal results primarily (61 percent) from plant operations, with the remainder of the risk coming from on-site transportation accidents. Among munition types, rockets contribute 96 percent of the risk.

- For the regional/national alternatives, 100 percent of the risk results from rockets. Among activity types, 93 percent of the risk is due to on-site transportation, with handling contributing to the remainder.

- For the partial relocation -- air mode alternative, 99 percent of the risk is due to off-site transportation-related accidents -- aircraft crashes on take off. Ninety percent to 95 percent of the total risk results from the transport of rockets.

3.3.2.4 NAAP. The risk at NAAP is illustrated by the pictogram in Figure 24. The comparison of risk among the unmitigated alternatives becomes very obvious for this site: Continued storage poses the highest risk of all measures. Regional and national disposal represent the least (in fact, very low) risk at NAAP, while the risk due to on-site disposal fall between these extremes. At NAAP, the partial relocation disposal alternative is identical to the on-site disposal alternative.

The major contributions to risk for each unmitigated alternative are discussed below:

- The entire risk associated with continued storage at NAAP is due to external events damaging the stored agent (all of which is agent VX in ton containers in a warehouse.) In particular, the potential accident posing the highest risk, by far, is an earthquake-induced failure of the storage warehouse with a resulting fire. Handling during storage poses only a negligible risk.

- For on-site disposal, essentially the entire (all but a fraction of a percent) risk is posed by plant operations, for which the major contributing accident, as with continued storage, is an earthquake-induced failure of the demilitarization building and simultaneous failure of the fire suppression system.

- The very small risk (expected fatalities less than 10^{-4}) of regional and national disposal to the NAAP population is due entirely to a handling accident leading to a short duration fire.

3.3.2.5 PBA. The risk to the PBA population is portrayed by the pictograms in Figure 25. The pictogram for the unmitigated case illustrates a more complex situation than is portrayed for NAAP. On-site disposal appears to pose the highest risk, both in terms of the number of risk measures which are in the higher risk categories, an on the basis of expected fatalities. (As for all sites but APG , LBAD, and TEAD, the programmatic partial relocation alternative calls for on-site disposal at PBA). Continued storage poses the least risk, with the regional/national transportation alternatives responsible for an intermediate level of risk.

Contributions to risk for each unmitigated disposal alternative at PBA are discussed briefly below:

- Over 90 percent of the continued storage risk at PBA results from external events (aircraft crashes or meteorite strikes) causing fire-borne release of mustard agent from the ton containers in open storage. The remainder of the risk is due almost to handling accidents (the dropping of a pallet leading to detonation affecting stored rockets.

- For on-site disposal, nearly 95 percent of the risk results from plant operations; the remainder is due to on-site transportation. Over 90 percent of the plant operations risk is caused by inadvertent feed of rockets and mines to the dunnage incinerator. Rockets and mines, together, are responsible for essentially all of the risk at PBA; bulk containers contribute a negligible fraction (well less than 1 percent).

- For the regional and national disposal alternatives, nearly 60 percent of the risk to the population near PBA results from on-site transportation accidents involving rockets; the remainder of the risk is roughly split between handling and short-term storage, again involving rockets. In fact, all but 2 percent of the risk for all activities is due to rockets. Accidents involving a release of agent GB dominate the risk.

3.3.2.6 PUDA. Figure 26 displays in pictogram form the comparative risk for the applicable disposal alternatives at PUDA. For the unmitigated case, the continued storage alternative appears to pose the highest risk, but only to the basis of the probability of one or more fatalities, relative to the regional and national disposal alternatives. On-site disposal results in the least risk to the population near PUDA if all risk measures are considered. On the basis of expected fatalities alone, all disposal alternatives pose low risk (less than 10^{-4}) at PUDA with on-site disposal posing the least.

The factors contributing to unmitigated risk at PUDA are summarized below:

- The risk at PUDA during continued storage arises entirely from potential aircraft crashes into the storage facility, leading to detonation and/or fire. Projectiles account for nearly 80 percent of the risk. Although the risk, as measured by expected fatalities is very low, that risk is made up of highly improbable but very severe potential accidents for which the "no-deaths" plume length, worst-case weather, could exceed 50 km and lead to over 15,000 potential fatalities. The

fact that probability of one or more fatalities is relatively high is the result of a single highly probable handling accident of negligible consequence.

- For on-site disposal, plant operations account for nearly 95 percent of the risk, with the major event being earthqake-initiated fires in the munition demil building. The most severe accident involves a "no-deaths" plume length of approximately 1 km (most-likely weather). The remainder of the risk is due to an on-site vehicle accident leading to detonation and fire.

- The risk at PUDA due to regional and national disposal is entirely the result of short-term storage associated with off-site real transportation. Most (90 percent) of the risk is due to projectiles. The scenarios contributing the most risk are those involving aircraft crashes into the transportation containers in the holding area. As with continued storage, the risk as measured by expected fatalities is low but it is comprised of a few high-consequence, low-probability events. The most severe accident leads to a worst-case weather, "no-deaths" plume length greater than 50 km with the potential to cause over 15,000 fatalities.

3.3.2.7 TEAD. Figure 27 contains the pictogram comparisons of risk measures for TEAD. Continued storage is seen to be the most risky on the basis of all risk measures. The lowest risk alternatives appear to be on-site and regional disposal.

The major contributions to risk for the unmitigated alternatives at TEAD are summarized for each disposal alternative below:

- Over 90 percent of the risk due to continued storage at TEAD is the result of earthquake-initiated damage and/or fire affecting bulk containers of agent VX in warehouse storage. Essentially all of the remainder of the risk is due to handling accidents involving burstered munitions. The events contributing the most to expected fatalities are also those having the most severe consequences (maximum number of fatalities) as well as a relatively high probability of occurring during the CSDP (10^{-4} to 10^{-3}).

- The risk of on-site disposal at TEAD results from plant operations (57 percent of expected fatalities) and handling (42 percent). Nearly half of the risk involves releases from bulk containers or while processing bulk containers, while mines contribute a third of the risk and rockets approximately 10 percent. Over 60 percent of the risk involves agent GB. The scenarios making major contributions to risk are handling accidents involving ton containers of GB, inadvertent passing of rockets and mines into the dunnage incinerator, and earthquakes damaging or causing fire in the demil building.

- For regional disposal, 59 percent of the risk comes from plant operations, 27 percent results from handling activities, and 14 percent is due to on-site transportation. Rockets, mines, and bulk containers each contribute about 25 percent to the risk at TEAD. As with on-site disposal, over 60 percent of the risk involves agent GB. Over 40

percent of the regional disposal risk at TEAD is due to inadvertent feeding of rockets and mines into the dunnage incinerator.

- For regional disposal, where the entire U.S. stockpile is disposed of at TEAD, the contribution to total risk due to plant operations rises to 70 percent, with approximately 20 percent of the risk resulting from handling activities and 10 percent caused by on-site transport. Mines and rockets each contribute one-third to the total risk with nearly 20 percent resulting from bulk agent disposal. Slightly more than half of the risk arises from potential accidents involving agent GB. The major scenarios contributing to risk are essentially the same ones responsible for risk for the regional disposal alternative at TEAD, although the relative importance of some of the scenarios is slightly different due to the different mix if munitions in the inventory to be disposed. Nearly 60 percent of the total risk is due to inadvertent feeding of rockets and mines to the dunnage incinerator; handling of ton containers of GB are another major risk contributor — responsible for 10 - 15 percent of the total. Vehicular accidents during on-site transportation of burstered munitions is next in risk significance.

- For the partial relocation disposal alternatives involving air shipment into TEAD, the risk picture changes significantly. When the C5 aircraft is used (alternative PRA), approximately 3/4 of the risk is due to off-site transportation — aircraft crashes during landing; most of the remainder of the risk results from plant operations. For the air air-mode alternatives, approximately 1/3 of the risk is due to off-site transportation — aircraft crashes during landing; most of the remainder of the risk results from plant operations. Rockets are responsible for 50 percent to 75 percent of the total risk; accidents involving bulk containers are next in importance to risk. Close to 80 percent of risk involves agent GB. For the C5 aircraft mode, over 60 percent of the risk results from aircraft crashes on landing while transporting rockets. Aircraft crashes play a much reduced role in TEAD's risk for other partial relocation alternatives which use the C141 aircraft; for these alternatives, the highest risk event is a handling accident involving ton containers of GB.

3.3.2.8 UMDA. The pictogram comparing risk measures among the applicable disposal alternatives at UMDA are presented in Figure 28. The only obvious conclusion to be drawn from Figure 28, is that the risk due to continued storage exceeds that of any of the disposal alternatives, both in terms of the number of risk measures (all) for which is in the maximum category and in terms of expected fatalities. In fact, the risk of continued storage for 25 years, as measured by expected fatalities, dominates disposal risk by several orders of magnitude.

The major contributions to unmitigated risk for each disposal alternative are summarized below:

- The risk associated with continued storage is due almost entirely (greater than 99 percent) to earthquake-induced damage with the fire in warehouses storing mustard ton containers. This scenario represents a set of potential accidents with probabilities in the range of 10^{-6} to 10^{-4} per year and 'no-deaths' plume lengths of 20 - 30 km, for most likely weather, and 200 - 300 km, for worst-case weather; potential

fatalities exceed 400 for average conditions and approach 50,000 for extreme conditions (worst-case weather and wind direction over peak population density).

- For on-site disposal, plant operations accidents contribute over 90 percent of the total risk; on-site transportation accidents are responsible for most of the remainder. Two-thirds of all risk is due to rockets, with the remainder resulting from the disposal of mines. The inadvertent feeding of rockets and mines to the dunnage incinerator accounts for over 80 percent of the total risk for this alternative; on-site vehicle accidents and earthquake-initiated fire in the demil building during the processing of rockets and mines account for nearly all the remainder of the identified risk. Agent GB is involved in most of the risk; mustard-related accidents are negligible for plant operations (whereas mustard dominates for storage-related accidents because a much larger source of agent is available for release).

- The risk due to national and regional disposal, as measured by expected fatalities, is quite low (less than 10^{-4}) and arises mostly from on-site transportation accidents; short-term storage and handling accidents also make a significant and equivalent contribution to risk Again, approximately 90 percent of the risk is GB-related, with rockets making the dominant contribution; bombs are responsible for most of the remainder of the identified risk. The scenarios contributing most risk are a severe on-site vehicle transporter accident, an aircraft crash into the holding area during short-term storage, and handling accident leading the drop and detonation of a palletized rocket.

3.3.2.9 Transportation Corridors - Regional (Rail) Alternatives. Figure 29 summarizes, in pictogram form the risk measures along the regional (rail) transportation corridors. The rail corridors from LBAD, PBA, and UMDA pose the highest risk in terms of expected fatalities. For these three corridors, rockets are responsible for well over half of the risk. For the other corridors, rockets are responsible for well over half of the risk. For the other corridors (originating from APG, NAAP, and PUDA), the risk is lower primarily because rockets are not a part of the transported stockpile. The risk-dominating accident scenarios are severe train accidents with fire of long enough duration to cause failure of the overpack and the munitions (either by burster detonation or by thermal rupture of bulk containers). The applicable scenario (depends on whether the transported inventory is burstered or not) accounts for at least 95 percent of the risk (greater than 99 percent for three sites) in all corridors.

The most severe potential accidents are those in the LBAD,PBA, and UMDA corridors. They yield worst-case 'no-death' plume lengths in the range of 15 to 20 km and could cause, under extreme conditions, 1000 to 2000 potential fatalities.

3.3.2.10 Transportation Corridors - National (Rail) Alternative. The risk picture is much the same for national disposal as it is for regional, as seen in Figure 30. The major difference is due to the fact that the ANAD stockpile is now transported to TEAD and, because of the size and composition of the ANAD stockpile, the risk in the ANAD - TEAD corridor dominates. In addition, selected risk parameters for APG, LBAD, and PBA are higher for national than for regional, primarily because of the greater travel distance for these stockpiles. For the ANAD - TEAD corridor, virtually all of the risk is associated with the movement of

energetic munitions; the largest contribution to risk results from the transporting of projectiles, with the risk due to rockets not far behind.

The scenarios contributing the most risk are the same severe rail accidents, with long-duration fires, that control risk for the regional corridors. The highest-consequence accident for the ANAD - TEAD corridor is expected to cause a worst-case "no-deaths" plume length of 19 km with the potential for over 6000 fatalities.

3.3.2.11 Transportation Corridors - Partial Relocation Alternatives. The risk along the transportation corridors that might be employed during the partial relocation disposal alternative is depicted in Figure 17. The route emanating from LBAD represents significantly higher risk than those originating from APG. The water mode from APG to JI (Johnston Island) appears to pose very low risk to the public. However, it should be noted that the transportation corridor accidents for this mode do not include the accident scenarios which have been identified for the barge (or "lighter") portion of the trip (from a dock at APG to the moored LASH vessel in the bay) nor do they include those events that could happen while the LASH is still at anchor. Lastly, between the two aircraft options (C5 vs C141), the C141 contributions the lesser risk to the public.

The major contributions to risk along the two corridors are discussed briefly below:

- For the LBAD - TEAD Corridor, via air mode, the risk (when measured, as before, by expected fatalities) associated with the use of the C5 aircraft is nearly a factor of 10 greater than for the C141 aircraft. For both aircraft options, 90 percent of the risk results from the transport of rockets; the rest is due to projectiles. Accidents involving GB constitute over 80 percent of the total corridor risk in both cases. Better than 75 percent of the risk results from a severe potential crash on an aircraft carrying GB-filled rockets; the accident would be of sufficient severity as to rupture both the shipping containers and the munitions, with a possible fire. These high risk accident scenarios also represent the most severe consequences as well: worst-case 'no-deaths' plume lengths of 64 and 31 km for the C5 and C141 options, respectively, with maximum potential fatalities of 73,000 and 23,000 also respectively.

- The risk along the APG - TEAD Corridor, via air mode, is also nearly a factor of 10 higher for the C5 aircraft option. The three scenarios contributing to risk in this corridor all involve severe air crashes with breach of the shipping container and the agent containers. Worst-case plume lengths are considerably a smaller than for the LBAD stockpile —5.2 and 2.3 km for the C5 and C141, respectively; maximum potential fatalities for these worst cases are 7500 and 3500, respectively.

- Along the APG - JI Corridor, via water mode, all identified accidents have both low probabilities and moderately low consequences. Probabilities are all in the range of 10^{-7} to 10^{-5}, and worst case plume lengths are less than 7.5 km — too small to reach major population groups.

4.0 DISCUSSION OF RESULTS

4.1 Statistical Significance of Differences in Risk

The probability that the risk (in terms of expected fatalities) of any programmatic alternative exceeds the risk of any other alternative is shown in Table 7. It should be noted, however, that a number of uncertainties were not explicitly considered in the development of the accident scenario data base used to compute these results. Therefore, it should be understood that the probabilities shown in Table 7 overstate the certainty of risk differences; that is, all of the probabilities should be somewhat closer to 50 percent. More specifically, probabilities in the range of roughly 30 percent to 70 percent do not substantiate true differences in risk, while probabilities below 30 percent or above 70 percent do indicate the likelihood of actual differences in risk.

The main conclusions that may be drawn from Table 7, for the case of unmitigated risk, are the following:

- o Storage for 25 years is the riskiest alternative;
- o Partial relocation alternatives involving air transport are next riskiest; and
- o National (NAT) and regional (REG) relocation by rail, and on-site disposal (ONS) are the least risky alternatives. Within this group, overall risks are indistinguishable.

4.2 Caveats and Limitations

4.2.1 Frequency and Consequence Screening

The accident scenario data base for this risk analysis was screened so that only those accidents with a potential (under worst-case meteorology for causing fatalities beyond the installation boundaries (assumed to be 0.5 km for all sites) and having a probability of occurring during the course of the CSDP (or during a one-year period, in the case of continued storage activities) of at least 10^{-8} are included.

4.2.2 Potential Fatality Estimates and Site Boundaries

The fatality estimates used in the risk analysis were computed by Oak Ridge National Laboratories (ORNL) using population data from census tracts. [It is not possible from such data to determine the precise potential health effects to the general population located outside the military reservations, personnel within the boundaries of the reservations should not be considered.] In an effort to exclude these personnel from consideration, ORNL set all fatality rates to zero for distances of up to 0.5 km from the disposal or storage site where accidents may occur. Thus, no fatalities are computed for low-consequence accidents for which the zero-fatalities distance does not exceed 0.5 km, if the accidents occur within a military reservation.

Using 0.5 km as a cut-off distance for fatality computations is a conservative approach; i.e., the number of fatalities may be overstated. This is because the actual distances from disposal and storage sites to military

reservation boundaries range from 0.9 to 3.5 km. Thus, if the actual boundaries had been used to compute the number of fatalities, the value of "expected fatalities" would have been substantially lower in a number of cases. The most significant reduction (about an order of magnitude) in "expected fatalities would be for the on-site disposal alternative at Anniston, Aberdeen, Pine Bluff, Tooele, and Umatilla. The total of expected fatalities at all sites for the on-site alternative would be approximately 75 percent lower.

REFERENCES

References Cited

Arthur D. Little, Inc. (1988[a]), Analysis of Risk Associated with M55 Rocket Demilitarization Plants, M55-OD-3. Prepared for the U.S. Army Toxic and Hazardous Materials Agency.

Arthur D. Little, Inc. (1985[b]), Analysis of Risks Associated with Operation of the JACADS M55 Rocket Demilitarization Plant, M55-OD-9. Prepared for the U.S. Army Toxic and Hazardous Materials Agency.

Arthur D. Little, Inc. (1985[c]), Analysis of the Converted M55 Rocket Demilitarization Plant at Pine Bluff Arsenal, M55-OD-10. Prepared for the U.S. Army Toxic and Hazardous Materials Agency.

Arthur D. Little, Inc. (1985[d]), Analysis of Risks Associated with Operation of the CAMDS M55 Rocket Demilitarization Plant, M55-OD-11. Prepared for the U.S. Army Toxic and Hazardous Materials Agency.

Chu, S.C. et al. (1987), Transportation of Chemical Agents and Munitions: A Concept Plan, WP-87W00205, McLean, VA: The MITRE Corporation. Prepared for the U.S. Army, Office of the Program Executive Officer-Program Manager for Chemical Demilitarization. SAPEO-CDE-IS-87003.

Clarke, R.D., et al. (1987), Severities of Transporation Accidents, SLA-7400001, Sandia National Laboratories.

Fraize, W.E. et al. Preliminary Risk Analysis Supporting the Chemical Stockpile Disposal Program (CSDP), MTR-86W00004, McLean, VA: The MITRE Corporation, prepared for the U.S. Army Toxic and Hazardous Materials Agency.

GA Technologies Inc. (1987[a]), Risk Analysis of the Onsite Disposal of Chemical Munitions, GA-C18562, (Aug 87). Prepared for the U.S. Army, Office of the Program Executive Officer-Program Manager for Chemical Demilitarization. SAPEO-CDE-IS-87010.

GA Technologies Inc. (1987[b]), Risk Analysis of the Disposal of Chemical Munitions at National or Regional Sites, GA-C18563, (Aug 87), prepared for the U.S. Army, Office of the Program Executive Officer-Program Manager for Chemical Demilitarization. SAPEO-CDE-IS-87008.

GA Technologies Inc. (1987[c]), Risk Analysis of the Continued Storage of Chemical Munitions, GA-C18564, (Aug 87), prepared for the U.S. Army, Office of the Program Executive Officer-Program Manager for Chemical Demilitarization. SAPEO-CDE-IS-87009.

MITRE Corporation (1987), Risk Analysis Supporting The Chemical Stockpile Disposal Program (CSDP), MTR-87W00230. Prepared for the U.S. Army, Office of the Program Executive Officer-Program Manager for Chemical Demilitarization. SAPEO-CDE-IS-87014.

Rasmussen, N. et al. (1975), Reactor Safety Study, WASH-1400, prepared for the Nuclear Regulatory Commission.

Rhyne, W.R., et al. (1985[a]), Probabilistic Analysis of Chemical Agent Release During Transport of M55 Rockets, M55-CD-4, H&R Technical Associates, Inc., Report No. 255-1. Prepared for the U.S. Army Toxic and Hazardous Materials Agency.

Rhyne, W.R., et al. (1985[b]), Probabilistic Analysis of Chemcial Agent Release During Transport of Obsolete Munitions With and Without Additional Protective Packaging,244-3/244-4, H&R Tecnnical Associates, Inc.

Science Applications International Corporation (1985), Probabilities of Selected Hazards in Disposition of M55 Rockets, M55-CS-2. Prepared for U.S. Army Toxic and Hazardous Materials Agency.

The R M. Parsons Company, (1983), JACADS - Preliminary Hazards Analysis of Final Concept Design, Task G-5C Interim Report. Prepared for the U.S. Army Engineers Division.

The R.M. Parsons Company (1985), Fault Tree Analysis, Johnston Atoll Chemical Agent Disposal System, Task G-5C Interim Report. Prepared for the U.S. Army Engineers Division.

U.S. Army Toxic and Hazardous Materials Agency (1986), Chemical Stockpile Disposal Concept Plan (Final Draft), Aberdeen Proving Ground, MD.

U.S. Army, Program Manager for Chemical Demilitarization (1986), Chemical Stockpile Disposal Program - Draft Environmental Impact Statement, Aberdeen Proving Ground, MD.

U.S. Army, Program Executive Officer-Program Manager for Chemical Demilitarization (1987[a]), Mitigation of Public Safety Risks of the Chemical Stockpile Disposal Program, SAPEO-CDE-IS-87014, Aberdeen Proving Ground, MD.

Whitacre, C.G. et al. (1987), Personal Computer Program for Chemical Hazard Prediction, CRDEC-TR-87021, Aberdeen Proving Ground, MD: Chemical Research, Development & Engineering Center.

APPENDIX A

GENERAL APPROACH TO THE RISK ANALYSIS

APPENDIX A: REFERENCE DATA

A.1 Introduction

This appendix contains data that is representative of the details that underlie the risk analysis. Much of the input data, including the accident scenario data base and the D2PC plume dispersion data, have been presented elsewhere in this report or in external documents and will not be repeated here. In this appendix, we will present those additional data items that should assist the reader who wish a detailed understanding of what was done in the risk analysis. In particular, the following data are presented:

- Definition of disposal alternatives in terms of applicable activities;
- Summary descriptions of the accident scenarios;

A.2 Activity-Based Definition of Disposal Alternatives

Table A-1 illustrates how the disposal alternatives are defined, for the purpose of the risk analysis, in terms of the applicable activity codes. The single-letter codes used in Table A-1 for the designation of disposal alternatives and sites are defined in section 3.1.1.

The entries in Table A-1 indicate which activities (that is, which data files from the accident scenario data base) comprise the set of potential accidents for the alternative.

A.3 Summary Descriptions of Accident Scenarios

The accident scenario data includes a textual description of each of the accident scenarios. The scenarios are identified by the activity code (first 2 characters of the scenario ID code — see Table A-2) and the scenario number. For convenience, the scenario descriptions are summarized into a data base format. The results are presented in Table A-3. To facilitate finding a particular scenario description, the list is ordered alphabetically according to the ID. With only two exceptions, the scenario descriptions are independent of munition and agent type. Thus, any given scenario could be the basis for as many as fourteen separate accidents, each one representing the probability and release characteristics of one of the applicable munition-agent combinations.

TABLE A-1

SITE/ALTERNATIVE/LOCAL (SAXX) Activity Selection File
- Originating Site Accidents -

ACTIVITY:

	SITE:	AT	BT	HA	HB	HF	HO	HR	HS	HW	PO	SA	SB	SL	SR	SW	VA	VB	VO	VR	VW	WB
** ALTERNATIVE: A	A					*	*				*								*			
	B					*	*				*								*			
	G	*		*								*					*					
	L	*		*								*					*					
	N					*	*				*								*			
	P					*	*				*								*			
	U					*	*				*								*			
** ALTERNATIVE: B	A					*	*				*								*			
	B					*	*				*								*			
	G		*		*								*					*				
	L		*		*								*					*				
	N					*	*				*								*			
	P					*	*				*								*			
	U					*	*				*								*			
** ALTERNATIVE: C	A					*	*				*								*			
	B					*	*				*								*			
	N					*	*				*								*			
	P					*	*				*								*			
	U					*	*				*								*			
** ALTERNATIVE: N	A							*							*					*		
	B							*							*					*		
	G							*							*					*		
	L							*							*					*		
	N							*							*					*		
	P							*							*					*		
	U							*							*					*		
** ALTERNATIVE: O	A					*	*				*								*			
	B					*	*				*								*			
	G					*	*				*								*			
	L					*	*				*								*			
	N					*	*				*								*			
	P					*	*				*								*			
	T					*	*				*								*			
	U					*	*				*								*			

SITE/ALTERNATIVE/LOCAL (SAXX) Activity Selection File
- Originating Site Accidents -

ACTIVITY:

ALTERNATIVE	SITE:	AT	BT	HA	HB	HF	HO	HR	HS	HW	PO	SA	SB	SL	SR	SW	VA	VB	VO	VR	VW	WB
** ALTERNATIVE: R	B							*							*					*		
	G							*							*					*		
	L							*							*					*		
	N							*							*					*		
	P							*							*					*		
	U							*							*					*		
** ALTERNATIVE: S	A								*					*								
	B								*					*								
	G								*					*								
	L								*					*								
	N								*					*								
	P								*					*								
	T								*					*								
	U								*					*								
** ALTERNATIVE: W	A					*	*				*								*			
	B					*	*				*								*			
	G									*						*					*	*
	L					*	*				*								*			
	N					*	*				*								*			
	P					*	*				*								*			
	T					*	*				*								*			
	U					*	*				*								*			

SITE/ALTERNATIVE/LOCAL (SAXX) Activity Selection File
- Transportation Corridor Accidents -

ACTIVITY:

Alternative	SITE:	AF	BF	RN	RR	WC	WI	WS
** ALTERNATIVE: A	G	*						
	L	*						
** ALTERNATIVE: B	G		*					
	L		*					
** ALTERNATIVE: C	G					*	*	*
	L		*					
** ALTERNATIVE: N	A			*				
	B			*				
	G			*				
	L			*				
	N			*				
	P			*				
	U			*				
** ALTERNATIVE: R	B				*			
	G				*			
	L				*			
	N				*			
	P			*				
	U			*				
** ALTERNATIVE: W	G					*	*	*

SITE/ALTERNATIVE/LOCAL (SAXX) Activity Selection File
- Destination Site Accidents -

ACTIVITY:

ALTERNATIVE	SITE:	AL	BL	HA	HB	HF	HR	PO	SA	SB	SR	VA	VB	VO	VR
** ALTERNATIVE: A	T	*		*		*		*	*			*		*	
** ALTERNATIVE: B	T		*		*	*		*		*			*	*	
** ALTERNATIVE: C	T		*		*	*		*		*			*	*	
** ALTERNATIVE: N	T					*	*	*			*				*
** ALTERNATIVE: R	A					*	*	*			*				*
	T					*	*	*			*				*

TABLE A-2
ACCIDENT SCENARIO IDENTIFICATION CODE

Scenario ID is of the form: XXYZWQnnn

where: XX = Activity Code W = Release Mode Code
Y = Munition Code Q = Special Code
Z = Agent Code nnn = Scenario Number (See App. C)

ACTIVITY CODE (XX) DEFINITION

AF/AL/AT: Air transportation (C5A)* -- in-Flight/Landing/Take-off
BF/BL/BT: Air transportation (C141)*
HA/HB: Handling associated with air modes (A & B)
HF: Handling at the disposal facility
HO: On-site handling away from the disposal facility
HR: Handling associated with rail mode
HS: Handling during long-term storage*
HW: Handling associated with water mode
WB: Water transportation, barge in inland waterways*
WC: Water transportation, LASH ship in coastal waterways*
WI: Water transportation, LASH ship in inland waterways*
WS: Water transportation, LASH ship on the open seas*
PO: Plant operations
RN: Rail transportation, National
RR: Rail transportation, Regional
SL: Long-term storage
SR/SA/SB/SW: Temporary storage associated with transportation by rail, air(mode A), air(mode B), water, respectively
VO/VR/VA/VB/VW: On-site transportation associated with on-site, rail, air(A/B), and water disposal alternatives

MUNITION CODE (Y) DEFINITION

B: Bombs
C: Cartridges (105mm)
D: Mortar Shells (4.2in)*
K: Bulk ("ton") containers
M Mines
P: Projectiles (155mm)
Q: Projectiles (8in)*
R: Rockets
S: Spray tanks
W: Wet-eye bombs*
A: All munitions

AGENT CODE (Z) DEFINITION

G: Agent GB ("Sarin")
H: Agents H, HT, HD ("Mustard")
V: Agent VX
A: All agents

RELEASE MODE CODE (W) DEFINITION

A: Detonation
C: Complex mode (incl. indoor releases affected by building systems) or a combination of simple modes
F: Fire (incomplete combustion)
S: Spill (leading to partial evaporation

SPECIAL CODE (Q) DEFINITION

W: Warehouse Storage
O: Open Storage
6/8/9: 60/80/89 ft. Igloo

* Defined for the June '87 accident scenario data base.

TABLE A-3 CSDP/FEIS RISK ANALYSIS
- Accident Scenario Descriptions -
(Data File: MASTER4.DBF)
as of 15 October 1987

RECORD NUMBER	ID		SCENARIO
** AF			
384	AF	001	A severe ground collision involving an aircraft with munitions occurs and impact forces fail the agent package and munitions.
385	AF	002	A severe ground collision involving an aircraft with munitions occurs and impact forces fail the agent package and munitions. A subsequent fire occurs with a duration less than 2 h.
386	AF	003	A fire occurs aboard an aircraft with munitions and causes rupture of the compartment due to thermal expansion of the agent.
387	AF	004	A severe ground collision involving an aircraft with munitions occurs and impact forces fail the agent package and munitions. A subsequent fire occurs with a duration greater than 2 h.
388	AF	005	A moderate ground collision involving an aircraft with munitions occurs causing a breach of the package. A subsequent fire occurs causing a breach (by detonation or thermal expansion) of the agent compartment and agent is released.
** AL			
389	AL	001	A severe ground collision involving an aircraft with munitions occurs and impact forces fail the agent package and munitions.
390	AL	002	A severe ground collision involving an aircraft with munitions occurs and impact forces fail the agent package and munitions. A subsequent fire occurs with a duration less than 2 h.
391	AL	003	A fire occurs aboard an aircraft with munitions and causes rupture of the compartment due to thermal expansion of the agent.
392	AL	004	A severe ground collision involving an aircraft with munitions occurs and impact forces fail the agent package and munitions. A subsequent fire occurs with a duration greater than 2 h.
393	AL	005	A moderate ground collision involving an aircraft with munitions occurs causing a breach of the package. A subsequent fire occurs causing a breach (by detonation or thermal expansion) of the agent compartment and agent is released.
** AT			
394	AT	001	A severe ground collision involving an aircraft with munitions occurs and impact forces fail the agent package and munitions.
395	AT	002	A severe ground collision involving an aircraft with munitions occurs and impact forces fail the agent package and munitions. A subsequent fire occurs with a duration less than 2 h.
396	AT	003	A fire occurs aboard an aircraft with munitions and causes rupture of the compartment due to thermal expansion of the agent.
397	AT	004	A severe ground collision involving an aircraft with munitions occurs and impact forces fail the agent package and munitions. A subsequent fire occurs with a duration greater than 2 h.
398	AT	005	A moderate ground collision involving an aircraft with munitions occurs causing a breach of the package. A subsequent fire occurs causing a breach (by detonation or thermal expansion) of the agent compartment and agent is released.
** BF			
399	BF	001	A severe ground collision involving an aircraft with munitions occurs and impact forces fail the agent package and munitions.
400	BF	002	A severe ground collision involving an aircraft with munitions occurs and impact forces fail the agent package and munitions. A subsequent fire occurs with a duration less than 2 h.
401	BF	003	A fire occurs aboard an aircraft with munitions and causes rupture of the compartment due to thermal expansion of the agent.
402	BF	004	A severe ground collision involving an aircraft with munitions occurs and impact forces fail the agent package and munitions. A subsequent fire occurs with a duration greater than 2 h.

CSDP/FEIS RISK ANALYSIS
Accident Scenario Descriptions
(Data File: MASTER4.DBF)
as of 15 October 1987

	RECORD NUMBER	ID		SCENARIO
	403	BF	005	A moderate ground collision involving an aircraft with munitions occurs causing a breach of the package. A subsequent fire occurs causing a breach (by detonation or thermal expansion) of the agent compartment and agent is released.
** BL				
	404	BL	001	A severe ground collision involving an aircraft with munitions occurs and impact forces fail the agent package and munitions.
	405	BL	002	A severe ground collision involving an aircraft with munitions occurs and impact forces fail the agent package and munitions. A subsequent fire occurs with a duration less than 2 h.
	406	BL	003	A fire occurs aboard an aircraft with munitions and causes rupture of the compartment due to thermal expansion of the agent.
	407	BL	004	A severe ground collision involving an aircraft with munitions occurs and impact forces fail the agent package and munitions. A subsequent fire occurs with a duration greater than 2 h.
	408	BL	005	A moderate ground collision involving an aircraft with munitions occurs causing a breach of the package. A subsequent fire occurs causing a breach (by detonation or thermal expansion) of the agent compartment and agent is released.
** BT				
	409	BT	001	A severe ground collision involving an aircraft with munitions occurs and impact forces fail the agent package and munitions.
	410	BT	002	A severe ground collision involving an aircraft with munitions occurs and impact forces fail the agent package and munitions. A subsequent fire occurs with a duration less than 2 h.
	411	BT	003	A fire occurs aboard an aircraft with munitions and causes rupture of the compartment due to thermal expansion of the agent.
	412	BT	004	A severe ground collision involving an aircraft with munitions occurs and impact forces fail the agent package and munitions. A subsequent fire occurs with a duration greater than 2 h.
	413	BT	005	A moderate ground collision involving an aircraft with munitions occurs causing a breach of the package. A subsequent fire occurs causing a breach (by detonation or thermal expansion) of the agent compartment and agent is released.
** HA				
	171	HA	001	Drop of bare pallet or single item at storage area.
	221	HA	002	Forklift collision with short duration fire at storage area involving bare munitions.
	173	HA	003	Forklift tine accident at storage area involving bare munitions.
	175	HA	004	Forklift collision accident at storage area involving bare munitions.
	177	HA	005	Drop of onsite container.
	179	HA	006	Forklift collision accident with short duration fire during handling of onsite container.
	181	HA	007	Forklift collision without fire during handling of onsite container.
	183	HA	008	Drop of offsite container.
	185	HA	009	Collision accident with short duration fire during handling of offsite container.
	187	HA	010	Collision accident without fire during handling of offsite container.
	189	HA	011	Drop of bare palletized munition leads to detonation.
	191	HA	012	Forklift collision accident at storage area leads to detonation.
	193	HA	017	Drop of pallet containing a leaking munition during leaker isolation operations.
	195	HA	018	Drop of single leaking in leakers processing facility.
	197	HA	019	Forklift tine puncture during leaker isolation.
	199	HA	021	Collision accident without fire during handling of leaking munition.
	201	HA	022	Drop of munition in onsite container leads to detonation.

CSDP/FEIS RISK ANALYSIS
- Accident Scenario Descriptions -
(Data File: MASTER4.DBF)
as of 15 October 1987

RECORD NUMBER	ID		SCENARIO
203	HA	023	Drop of munition in offsite container leads to detonation.
205	HA	024	Collision accident during munition handling in onsite container leads to detonation.
207	HA	025	Collision accident during munition handling in offsite container leads to detonation.
209	HA	026	Collision accident in onsite container with prolonged fire lead to thermal detonation.
211	HA	027	Collision accident in offsite container with prolonged fire lead to thermal detonation.
213	HA	029	Drop of pallet containing leaker leads to detonation.
215	HA	030	Drop of single leaking munitions leads to detonation.
217	HA	031	Collision accident involving a leaking munitions leads to detonation.
219	HA	032	Failure to detect a leak in the offsite container.
** HB			
414	HB	001	Drop of bare pallet or single item at storage area.
415	HB	002	Forklift collision with short duration fire at storage area involving bare munitions.
416	HB	003	Forklift tine accident at storage area involving bare munitions.
417	HB	004	Forklift collision accident at storage area involving bare munitions.
418	HB	005	Drop of onsite container.
419	HB	006	Forklift collision accident with short duration fire during handling of onsite container.
420	HB	007	Forklift collision without fire during handling of onsite container.
421	HB	008	Drop of offsite container.
422	HB	009	Collision accident with short duration fire during handling of offsite container.
423	HB	010	Collision accident without fire during handling of offsite container.
424	HB	011	Drop of bare palletized munition leads to detonation.
425	HB	012	Forklift collision accident at storage area leads to detonation.
426	HB	017	Drop of pallet containing a leaking munition during leaker isolation operations.
427	HB	018	Drop of single leaking in leakers processing facility.
428	HB	019	Forklift tine puncture during leaker isolation.
429	HB	021	Collision accident without fire during handling of leaking munition.
430	HB	022	Drop of munition in onsite container leads to detonation.
431	HB	023	Drop of munition in offsite container leads to detonation.
432	HB	024	Collision accident during munition handling in onsite container leads to detonation.
433	HB	025	Collision accident during munition handling in offsite container leads to detonation.
434	HB	026	Collision accident in onsite container with prolonged fire lead to thermal detonation.
435	HB	027	Collision accident in offsite container with prolonged fire lead to thermal detonation.
436	HB	029	Drop of pallet containing leaker leads to detonation.
437	HB	030	Drop of single leaking munitions leads to detonation.
438	HB	031	Collision accident involving a leaking munitions leads to detonation.
439	HB	032	Failure to detect a leak in the offsite container.
** HF			
223	HF	001	Munition pallet or container dropped during movement from MHI to MDB.
12	HF	002	Bare single munition dropped during handling inside the MDB.
224	HF	003	Forklift collision accident with short duration fire during handling from MHI to MDB.
225	HF	004	Forklift tine accident handling from the MHI to MDB.
226	HF	005	Collision accident with prolonged fire during handling from MHI to MDB leads to detonation or hydraulic rupture.
227	HF	007	Collision accident without fire.

CSDP/FEIS RISK ANALYSIS
Accident Scenario Descriptions -
(Data File: MASTER4.DBF)
as of 15 October 1987

RECORD NUMBER	ID		SCENARIO
228	NF	008	Munition dropped inside the MDB.
229	NF	009	Forklift tine accident inside the MDB.
13	NF	010	Collision without fire inside the MDB.
230	NF	011	Drop of munition pallet from the MHI to MDB leads to detonation.
231	NF	012	Drop of bare single munition inside the MDB leads to detonation.
232	NF	013	Drop of palletized munition (in container) inside the MDB leads to detonation.
233	NF	014	Collision accident from the MHI to the MDB leads to detonation.
** NO			
1	NO	001	Drop of bare pallet or single item at storage area.
2	NO	002	Forklift collision with short duration fire at storage area involving bare munitions.
3	NO	003	Forklift tine accident involving bare munitions at storage area.
4	NO	004	Forklift collision accident without fire at storage area involving bare munitions.
5	NO	005	Drop of onsite container.
6	NO	006	Forklift collision with short duration fire during handling of onsite container.
7	NO	007	Forklift collision without fire during handling of onsite container.
8	NO	011	Drop of bare palletized munition leads to detonation.
9	NO	012	Forklift collision accident at storage area leads to detonation of burstered munition.
10	NO	024	Collision accident during munition handling in onsite container leads to detonation due to impact.
11	NO	026	Collision accident in onsite container with prolonged fire leads to thermal detonation.
490	NO	027	Collision accident in offsite container with prolonged fire leads to thermal detonation.
491	NO	028	Drop of single munitions at maintenance facility leads to detonation.
492	NO	029	Drop of pallet containing leaker leads to detonation.
493	NO	030	Drop of single leaking munition leads to detonation.
494	NO	031	Collision accident involving a leaker leads to detonation due to impact.
495	NO	032	Failure to detect a leak in the offsite container.
** HR			
440	HR	001	Drop of bare pallet or single item at storage area.
441	HR	002	Forklift collision with short duration fire at storage area involving bare munitions.
442	HR	003	Forklift tine accident at storage area involving bare munitions.
443	HR	004	Forklift collision accident at storage area involving bare munitions.
444	HR	005	Drop of onsite container.
445	HR	006	Forklift collision accident with short duration fire during handling of onsite container.
446	HR	007	Forklift collision without fire during handling of onsite container.
447	HR	008	Drop of offsite container.
448	HR	009	Collision accident with short duration fire during handling of offsite container.
449	HR	010	Collision accident without fire during handling of offsite container.
450	HR	011	Drop of bare palletized munition leads to detonation.
451	HR	012	Forklift collision accident at storage area leads to detonation.
452	HR	017	Drop of pallet containing a leaking munition during leaker isolation operations.
453	HR	018	Drop of single leaking in leakers processing facility.
454	HR	019	Forklift tine puncture during leaker isolation.
455	HR	021	Collision accident without fire during handling of leaking munition.
456	HR	022	Drop of munition in onsite container leads to detonation.

CSDP/FEIS RISK ANALYSIS
- Accident Scenario Descriptions -
(Data File: MASTER4.DBF)
as of 15 October 1987

RECORD NUMBER	ID		SCENARIO
457	HR	023	Drop of munition in offsite container leads to detonation.
458	HR	024	Collision accident during munition handling in onsite container leads to detonation.
459	HR	025	Collision accident during munition handling in offsite container leads to detonation.
460	HR	026	Collision accident in onsite container with prolonged fire lead to thermal detonation.
461	HR	027	Collision accident in offsite container with prolonged fire lead to thermal detonation.
462	HR	029	Drop of pallet containing leaker leads to detonation.
463	HR	030	Drop of single leaking munitions leads to detonation.
464	HR	031	Collision accident involving a leaking munitions leads to detonation.
465	HR	032	Failure to detect a leak in the offsite container.
** HS			
478	HS	001	Drop of pallet or container in storage area or maintenance facility; munition punctured.
479	HS	002	Forklift collision with short duration fire.
480	HS	003	Forklift tine puncture.
481	HS	004	Forklift collision without fire.
482	HS	005	Drop of munition leads to detonation.
483	HS	006	Collision accident leads to detonation.
484	HS	007	Collision accident with prolonged fire.
485	HS	008	Munition pallet dropped during pallet inspection.
486	HS	009	Forklift tine puncture during pallet inspection.
487	HS	010	Forklift collision during pallet inspection.
488	HS	011	Munition pallet dropped during pallet inspection; detonation occurs.
489	HS	012	Forklift collision; detonation occurs.
** HW			
172	HW	001	Drop of bare pallet or single item at storage area.
222	HW	002	Forklift collision with short duration fire at storage area involving bare munitions.
174	HW	003	Forklift tine accident at storage area involving bare munitions.
176	HW	004	Forklift collision accident at storage area involving bare munitions.
178	HW	005	Drop of onsite container.
180	HW	006	Forklift collision accident with short duration fire during handling of onsite container.
182	HW	007	Forklift collision without fire during handling of onsite container.
184	HW	008	Drop of offsite container.
186	HW	009	Collision accident with short duration fire during handling of offsite container.
188	HW	010	Collision accident without fire during handling of offsite container.
190	HW	011	Drop of bare palletized munition leads to detonation.
192	HW	012	Forklift collision accident at storage area leads to detonation.
194	HW	017	Drop of pallet containing a leaking munition during leaker isolation operations.
196	HW	018	Drop of single leaking in leakers processing facility.
198	HW	019	Forklift tine puncture during leaker isolation.
200	HW	021	Collision accident without fire during handling of leaking munition.
202	HW	022	Drop of munition in onsite container leads to detonation.
204	HW	023	Drop of munition in offsite container leads to detonation.
206	HW	024	Collision accident during munition handling in onsite container leads to detonation.
208	HW	025	Collision accident during munition handling in offsite container leads to detonation.

CSDP/FEIS RISK ANALYSIS
- Accident Scenario Descriptions -
(Data File: MASTER4.DBF)
as of 15 October 1987

RECORD NUMBER	ID		SCENARIO
210	HW	026	Collision accident in onsite container with prolonged fire lead to thermal detonation.
212	HW	027	Collision accident in offsite container with prolonged fire lead to thermal detonation.
214	HW	029	Drop of pallet containing leaker leads to detonation.
216	HW	030	Drop of single leaking munitions leads to detonation.
218	HW	031	Collision accident involving a leaking munitions leads to detonation.
220	HW	032	Failure to detect a leak in the offsite container.
512	HW	034	Drop of lighter while loading with shipboard crane crushes vault.

** PO

RECORD NUMBER	ID		SCENARIO
342	PO	001	Tornado-generated missile puncture/crush munitions in the MHI.
343	PO	002	Tornado-generated missile detonate munitions in the MHI.
344	PO	003	Tornado-generated missile puncture/crush munitions in the UPA.
345	PO	004	Tornado-generated missile detonate munitions in the UPA.
346	PO	005	Tornado-generated missile damages the agent piping system between the BDS and TOX at TEAD (bulk-only facility).
347	PO	006	Meteorite strikes the MHI.
348	PO	007	Meteorite strikes the UPA.
350	PO	008	Meteorite strikes the agent piping system between the BDS and TOX at TEAD (bulk-only facility).
351	PO	009	Direct large aircraft crash onto the MHI, no fire.
280	PO	010	Direct large aircraft crash onto the MHI; fire not contained in 0.5 hours
281	PO	011	Direct large aircraft crash onto the MHI; fire contained in 0.5 hours
282	PO	012	Direct large aircraft crash damages the MDB; no fire
283	PO	013	Direct large aircraft crash damages the MDB; fire not contained in 0.5 hours
284	PO	014	Direct large aircraft crash damages the MDB; fire contained in 0.5 hours
285	PO	015	Indirect large aircraft crash damages the MHI; no fire
286	PO	016	Indirect large aircraft crash damages the MHI; fire not contained in 0.5 hours
287	PO	017	Indirect large aircraft crash damages the MHI; fire contained in 0.5 hours
288	PO	018	Indirect large aircraft crash damages the MDB; no fire
289	PO	019	Indirect large aircraft crash damages the MDB; fire not contained in 0.5 hours
290	PO	020	Indirect large aircraft crash damages the MDB; fire contained in 0.5 hours
352	PO	021	Direct crash of a large or small aircraft damages the outdoor agent piping system at TEAD, no fire.
353	PO	022	Direct crash of a large or small aircraft damages the outdoor agent piping system at TEAD, fire occurs and not contained.
354	PO	023	Earthquake causes the munitions in the MHI to fall and be punctured.
355	PO	024	Earthquake causes munitions in the MHI to fall and detonate.
356	PO	025	Earthquake damages the MDB structure, munitions fall and are punctured, fire suppressed.
357	PO	026	Earthquake damages the MDB structure, munitions fall and are punctured, earthquake also initiates fire, fire suppression system fails.
359	PO	028	Earthquake damages the MDB structure, munitions fall and are punctured, TOX damaged, fire occurs, fire suppression system fails.
291	PO	029	Earthquake damages the MDB; munitions are intact; fire occurs; fire suppression system fails
360	PO	030	Earthquake damages the MDB, munitions are intact, TOX damaged, no fire occurs.
362	PO	031	Earthquake damages the MDB, munitions are intact, TOX damaged, fire occurs, fire not suppressed.
363	PO	032	Earthquake causes munitions to fall and detonate, MDB breached by detonation, the TOX is intact, no fire.
364	PO	033	Earthquake causes munitions to fall but no detonation occurs, the MDB is intact, the TOX is intact, earthquake also initiates fire, fire suppression system fails.

CSDP/FEIS RISK ANALYSIS
- Accident Scenario Descriptions -
(Data File: NASTER4.DBF)
as of 15 October 1987

RECORD NUMBER	ID		SCENARIO
365	PO	034	Earthquake causes munitions to fall but no detonation occurs, the MDB is intact, the TOX is damaged, fire occurs, fire suppression system fails.
234	PO	041	Failure to stop agent feed to the LIC, overloads the ventilation system.
235	PO	042	MPF explosion due to failure to stop fuel flow after a shutdown.
236	PO	043	MPF explosion due to hydraulic rupture of an unpunched bulk item. MPF room and ventilation integrity maintained.
237	PO	044	MPF explosion due to hydraulic rupture of an unpunched bulk item. MPF room or ventilation integrity lost.
238	PO	045	Ton container is spilled in the ECV, MDB structure fails due to subsequent agent fire.
239	PO	046	Munition detonation in the ECV, no fire.
240	PO	047	Munition detonation in the ECV, fire results but does not propagate.
241	PO	048	Munition detonation in the ECV, fire results and propagates.
242	PO	049	Munition detonation in ECR causes structural and ventilation system failure.
243	PO	050	Munition detonation in ECR causes structural failure, a fire, and ventilation failure.
244	PO	051	Ton container spill in the MPB results in fire and structural failure.
249	PO	052	A burstered munition is fed to the DUN.
266	PO	053	A burstered munition is fed to the DUN.
349	PO	A07	Meteorite strikes the TOX.
358	PO	A28	Earthquake damages the MDB structure, munitions fall and are punctured, TOX damaged, fire occurs, fire suppressed.
361	PO	A31	Earthquake damages the MDB, munitions are intact, TOX damaged, fire occurs, fire suppressed.
** RN			
496	RN	001	A train accident involving a munitions railcar occurs and crush forces fail the agent containment.
497	RN	002	A train accident involving a munitions railcar occurs and impact forces fail the agent containment.
120	RN	003	A train accident involving a munitions railcar occurs and puncture forces fail the agent containment.
121	RN	004	A train accident with fire occurs. Either the package insulation is torn away due to mechnical forces and the fire is able to heat the munitions inside the package, or the fire last long enough to cause burstered munitions in the package to detonate. Undue force created by the accident may also cause burster detonation.
122	RN	005	A train accident with fire occurs. Either the package insulation is torn away due to mechanical forces and the fire is able to heat the munitions inside the package, or the fire lasts long enough to cause thermal ruture of the munitions inside the package.
123	RN	006	An aircraft crashes on a munitions railcar. No fire occurs, but impact forces lead to detonations and/or failure of agent containment.
124	RN	007	An aircraft crashes on a munitions railcar. Fire occurs, but impact forces lead to detonations and/or failure of agent containment.
498	RN	008	Combined with scenario RN007.
499	RN	009	A severe earthquake occurs involving a munitions railcar and crush forces fail the agent containment.
500	RN	010	A severe earthquake occurs involving a munitions railcar and impact forces fail the agent containment.
125	RN	011	A severe earthquake occurs involving a munitions railcar and puncture forces fail the agent containment.
126	RN	012	A severe earthquake occurs involving a munitions railcar and subsequent fire detonates burstered.
127	RN	013	A severe earthquake occurs involving a munitions railcar and subsequent fire fails nonburstered munitions.
128	RN	014	A tornado-generate missile leads to failure of the agent containment, or a tornado occurs, causing overturn or derailment of a munitions railcar.
129	RN	015	A earthquake or a tornado occurs, generating undue mechanical forces which cause detonation of burstered munitions.
** RR			
501	RR	001	A train accident involving a munitions railcar occurs and crush forces fail the agent containment.

CSDP/FEIS RISK ANALYSIS
- Accident Scenario Descriptions -
(Data File: MASTER4.DBF)
as of 15 October 1987

RECORD NUMBER	ID		SCENARIO
502	RR	002	A train accident involving a munitions railcar occurs and impact forces fail the agent containment.
267	RR	003	A train accident involving a munitions railcar occurs and puncture forces fail the agent containment.
268	RR	004	A train accident with fire occurs. Either the package insulation is torn away due to mechnical forces and the fire is able to heat the munitions inside the package, or the fire last long enough to cause burstered munitions in the package to detonate. Undue force created by the accident may also cause burster detonation.
269	RR	005	A train accident with fire occurs. Either the package insulation is torn away due to mechanical forces and the fire is able to heat the munitions inside the package, or the fire lasts long enough to cause thermal ruture of the munitions inside the package.
270	RR	006	An aircraft crashes on a munitions railcar. No fire occurs, but impact forces lead to detonations and/or failure of agent containment.
271	RR	007	An aircraft crashes on a munitions railcar. Fire occurs, but impact forces lead to detonations and/or failure of agent containment.
503	RR	008	Combined with scenario RN007.
504	RR	009	A severe earthquake occurs involving a munitions railcar and crush forces fail the agent containment.
505	RR	010	A severe earthquake occurs involving a munitions railcar and impact forces fail the agent containment.
272	RR	011	A severe earthquake occurs involving a munitions railcar and puncture forces fail the agent containment.
273	RR	012	A severe earthquake occurs involving a munitions railcar and subsequent fire detonates burstered.
274	RR	013	A severe earthquake occurs involving a munitions railcar and subsequent fire fails nonburstered munitions.
275	RR	014	A tornado-generate missile leads to failure of the agent containment, or a tornado occurs, causing overturn or derailment of a munitions railcar.
276	RR	015	A earthquake or a tornado occurs, generating undue mechanical forces which cause detonation of burstered munitions.
** SA			
366	SA	001	Large aircraft direct crash onto transportation containers in holding area; no fire.
367	SA	002	Large aircraft direct crash onto transportation containers in holding area, fire not contained.
368	SA	003	Large aircraft direct crash onto transportation containers in holding area; fire contained.
369	SA	004	Small aircraft direct crash onto transportation containers in holding area; no fire.
370	SA	005	Small aircraft direct crash onto transportation containers in holding area; fire not contained.
371	SA	006	Small aircraft direct crash onto transportation containers in holding area; fire contained.
372	SA	007	Tornado-generated missiles strike munitions in transportation containers in holding area; no detonation.
373	SA	008	Tornado-generated missiles strike munitions in holding area; detonation occurs.
374	SA	009	Meteorite strikes munitions in transportation containers in holding area; fire occurs; detonation (if burstered).
** SB			
375	SB	001	Large aircraft direct crash onto transportation containers in holding area; no fire.
376	SB	002	Large aircraft direct crash onto transportation containers in holding area, fire not contained.
377	SB	003	Large aircraft direct crash onto transportation containers in holding area; fire contained.
378	SB	004	Small aircraft direct crash onto transportation containers in holding area; no fire.
379	SB	005	Small aircraft direct crash onto transportation containers in holding area; fire not contained.
380	SB	006	Small aircraft direct crash onto transportation containers in holding area; fire contained.
381	SB	007	Tornado-generated missiles strike munitions in transportation containers in holding area; no detonation.
382	SB	008	Tornado-generated missiles strike munitions in holding area; detonation occurs.
383	SB	009	Meteorite strikes munitions in transportation containers in holding area; fire occurs; detonation (if burstered).

CSDP/FEIS RISK ANALYSIS
- Accident Scenario Descriptions -
(Data File: MASTER4.DBF)
as of 15 October 1987

** SL

RECORD NUMBER	ID		SCENARIO
292	SL	001	Munitions develops a leak during the in between inspection period.
293	SL	002	Munition punctured by forklift tine during leaker-handling activities.
294	SL	003	Spontaneous ignition of rocket during storage (not analyzed for lack of quantitative data).
295	SL	004	Large aircraft direct crash onto storage area; fire not contained in 30 min. (Note: Assume detonation occurs if burstered munitions hit, fire involving burstered munitions not contained at all.
296	SL	005	Large aircraft indirect crash onto storage area; fire not contained in 30 min. (See note in SL4.)
297	SL	006	Tornado-generated missiles strike the storage magazine, warehouse, or open storage area; munitions breached (no detonation).
298	SL	007	Severe earthquake breaches the munitions in storage igloos, no detonations.
299	SL	008	Meteorite strikes the storage area; fire occurs; munitions breached (if burstered, detonation also occurs).
300	SL	009	Munition dropped during leaker isolation operation, munition punctured.
301	SL	010	Storage igloo or warehouse fire from internal sources.
302	SL	011	Munitions are dropped due to pallet degradation.
303	SL	012	Liquid petroleum gas (LPG) infiltrates igloo/building.
304	SL	013	Flammable liquids stored in nearby facilities explode, fire propagates to munition warehouse (applies to NAAP).
305	SL	014	Tornado-induced building collapse leads to breeching/detonation of munitions.
306	SL	015	Small aircraft direct crash onto warehouse or open storage yard, fire occurs, not contained in 30 min.
307	SL	016	Large aircraft direct crash, no fire, detonation (if burstered).
308	SL	017	Large aircraft direct crash, fire contained within 30 min (applies to nonburstered munitions only).
309	SL	018	Small aircraft direct crash onto warehouse or open storage yard, no fire.
310	SL	019	Small aircraft direct crash onto warehouse or open storage yard, fire contained in 30 min.
311	SL	020	Large aircraft indirect crash onto storage area, no fire.
312	SL	021	Large aircraft indirect crash onto storage area, fire contained in 30 min.
313	SL	022	Severe earthquake leads to munition detonation.
314	SL	023	Tornado-generated missiles strike the storage igloo and leads to munition detonation.
315	SL	024	Lightning strikes ton containers stored outdoors.
316	SL	025	Munition dropped during leaker isolation, munition detonates.
317	SL	A26	Earthquake occurs, NAAP warehouse is intact, no ton containers damaged, fire occurs.
322	SL	A27	Earthquake occurs, TEAD warehouses intact, munitions intact, fire occurs at one warehouse.
327	SL	A28	Earthquake occurs, UMDA warehouses intact, munitions intact, fire occurs at one warehouse.
318	SL	B26	Earthquake occurs, NAAP warehouse is intact, ton container damaged, no fire.
323	SL	B27	Earthquake occurs, TEAD warehouses intact, munitions intact, fire occurs at two warehouses.
328	SL	B28	Earthquake occurs, UMDA warehouses intact, munitions intact, fire occurs at two warehouses.
319	SL	C26	Earthquake occurs, NAAP warehouse is intact, ton container damaged, fire occurs.
324	SL	C27	Earthquake occurs, one TEAD warehouse is damaged, munitions intact, fire occurs at one warehouse.
329	SL	C28	Earthquake occurs, UMDA warehouses intact, munitions in one warehouse damaged, no fire occurs.
320	SL	D26	Earthquake occurs, NAAP warehouse is damaged, ton containers damaged, fire occurs.
325	SL	D27	Earthquake occurs, one TEAD warehouse is damaged, munitions intact, fire occurs at two warehouse.
330	SL	D28	Earthquake occurs, UMDA warehouses intact, munitions in one warehouse damaged, fire occurs at warehouse with damaged munitions.
321	SL	E26	Earthquake occurs, NAAP warehouse is damaged, ton containers damaged, no fire occurs.
326	SL	E27	Earthquake occurs, two TEAD warehouses damaged, munitions intact, fire occurs at one warehouse.

CSDP/FEIS RISK ANALYSIS

- Accident Scenario Descriptions -

(Data File: MASTER4.WRF)

as of 15 October 1987

RECORD NUMBER		ID	SCENARIO
331	SL	E28	Earthquake occurs, UNDA warehouses intact, munitions in one warehouse damaged, fire occurs at warehouse with undamaged munitions.
313	SL	F27	Earthquake occurs, 2 TEAD warehouse damaged; munitions intact; fire occurs at 2 warehouses.
332	SL	F28	Earthquake occurs, UNDA warehouses intact, munitions in one warehouse damaged, fire occurs at two warehouses.
333	SL	G28	Earthquake occurs, UNDA warehouses intact, munitions in two warehouses damaged, no fire occurs.
334	SL	H28	Earthquake occurs, UNDA warehouses intact, munitions in two warehouses damaged, fire occurs at warehouse with damaged munitions.
335	SL	K28	Earthquake occurs, one UNDA warehouse damaged, munitions in one warehouse damaged, fire occurs at warehouse with damaged munitions.
336	SL	L28	Earthquake occurs, one UNDA warehouse damaged, munitions in one warehouse damaged, fire occurs at two warehouses.
337	SL	M28	Earthquake occurs, one UNDA warehouse damaged, munitions in two warehouses damaged, no fire occurs.
338	SL	N27	Earthquake occurs, one UNDA warehouse damaged, munitions in two warehouses damaged, fire occurs in warehouse with damaged munitions.
339	SL	O28	Earthquake occurs, one UNDA warehouse damaged, munitions in two warehouses damaged, fire occurs at two warehouses.
340	SL	P28	Earthquake occurs, two UNDA warehouses damaged, munitions in two warehouses damaged, no fire occurs.
341	SL	Q28	Earthquake occurs, two UNDA warehouses damaged, munitions in two warehouses damaged, fire occurs at both warehouses.

** SR

RECORD NUMBER		ID	SCENARIO
14	SR	001	Large aircraft direct crash onto transportation containers in holding area; no fire.
15	SR	002	Large aircraft direct crash onto transportation containers in holding area; fire not contained.
16	SR	003	Large aircraft direct crash onto transportation containers in holding area; fire contained.
17	SR	004	Small aircraft direct crash onto transportation containers in holding area; no fire.
18	SR	005	Small aircraft direct crash onto transportation containers in holding area; fire not contained.
19	SR	006	Small aircraft direct crash onto transportation containers in holding area; fire contained.
20	SR	007	Tornado-generated missiles strike munitions in transportation containers in holding area; no detonation.
21	SR	008	Tornado-generated missiles strike munitions in transportation containers in holding area; detonation occurs.
279	SR	008	Tornado-generated missile penetrates containers; detonation occur.
22	SR	009	Meteorite strikes munitions in transportation containers in holding area: fire occurs; detonation (if burstered).

** SW

RECORD NUMBER		ID	SCENARIO
23	SW	001	Large aircraft direct crash onto transportation containers in holding area; no fire.
24	SW	002	Large aircraft direct crash onto transportation containers in holding area; fire not contained.
25	SW	003	Large aircraft direct crash onto transportation containers in holding area; fire contained.
26	SW	004	Small aircraft direct crash onto transportation containers in holding area; no fire.
27	SW	005	Small aircraft direct crash onto transportation containers in holding area; fire not contained.
28	SW	006	Small aircraft direct crash onto transportation containers in holding area; fire contained.
277	SW	007	Tornado-generated missile penetrates vault
29	SW	008	Meteorite strikes munitions in transportation containers in holding area; fire occurs.
278	SW	009	Meteorite strikes vault
30	SW	010	Large aircraft direct crash onto a flotilla of lighers; no fire.
31	SW	011	Large aircraft direct crash onto a flotilla of lighers; fire not contained.
32	SW	012	Large aircraft direct crash onto a flotilla of lighers; fire contained.
33	SW	013	Small aircraft direct crash onto a flotilla of lighers; no fire.
34	SW	014	Small aircraft direct crash onto a flotilla of lighers; fire not contained.
35	SW	015	Small aircraft direct crash onto a flotilla of lighers; fire contained.

CSDP/FEIS RISK ANALYSIS
- Accident Scenario Descriptions -
(Data File: MASTER4.DBF)
as of 15 October 1987

	RECORD NUMBER	ID		SCENARIO
	36	SW	016	Large aircraft direct crash onto LASH vessel (at rest); no fire.
	37	SW	017	Large aircraft direct crash onto LASH vessel (at rest); fire not contained.
	38	SW	018	Large aircraft direct crash onto LASH vessel (at rest); fire contained.
	39	SW	019	Small aircraft direct crash onto LASH vessel (at rest); no fire.
	40	SW	020	Small aircraft direct crash onto LASH vessel (at rest); fire not contained.
	41	SW	021	Small aircraft direct crash onto LASH vessel (at rest); fire contained.
** VA				
	150	VA	001	A munitions vehicle collision/overturn occurs and crush forces fail the agent containment.
	151	VA	002	A munitions vehicle collision/overturn occurs and impact forces fail the agent containment.
	152	VA	003	A munitions vehicle collision/overturn occurs and puncture forces fail the agent containment.
	153	VA	004	Detonation of burstered munitions occurs by either 1) fire-only accident, 2) mechanical force and fire, 3) truck collision/overturn impact - induced rocket propellant ignition, or 4) truck collision/overturn - induced undue force detonation.
	251	VA	005	A munitions vehicle accident with fire occurs, causing non-burstered munitions to fail.
	154	VA	006	An aircraft crashes on a munitions vehicle. No fire occurs; impact forces fail the agent containment.
	155	VA	007	An aircraft crashes on a munitions vehicle. Fire occurs but impact forces fail the agent containment.
	156	VA	009	A severe earthquake occurs, causing a munitions vehicle accident and crush forces fail the agent containment.
	157	VA	010	A severe earthquake occurs, causing a munitions vehicle accident and impact forces forces fail the agent containment.
	158	VA	011	A severe earthquake occurs, causing a munitions vehicle accident and puncture forces forces fail the agent containment.
	159	VA	012	A severe earthquake occurs, causing a munitions vehicle accident and fire detonates burstered munitions.
	250	VA	013	A severe earthquake occurs, causing a munitions vehicle accident and fire fails nonburstered munitions.
	160	VA	014	A tornado occurs, generating under mechanical forces which cause detonation of burstered munitions.
	161	VA	015	A earthquake or tornado occurs, generating under mechanical forces which cause detonation of burstered munitions.
** VB				
	466	VB	001	A munitions vehicle collision/overturn occurs and crush forces fail the agent containment.
	467	VB	002	A munitions vehicle collision/overturn occurs and impact forces fail the agent containment.
	468	VB	003	A munitions vehicle collision/overturn occurs and puncture forces fail the agent containment.
	469	VB	004	Detonation of burstered munitions occurs by either 1) fire-only accident, 2) mechanical force and fire, 3) truck collision/overturn impact - induced rocket propellant ignition, or 4) truck collision/overturn - induced undue force detonation.
	470	VB	006	An aircraft crashes on a munitions vehicle. No fire occurs; impact forces fail the agent containment.
	471	VB	007	An aircraft crashes on a munitions vehicle. Fire occurs but impact forces fail the agent containment.
	472	VB	009	A severe earthquake occurs, causing a munitions vehicle accident and crush forces fail the agent containment.
	473	VB	010	A severe earthquake occurs, causing a munitions vehicle accident and impact forces forces fail the agent containment.
	474	VB	011	A severe earthquake occurs, causing a munitions vehicle accident and puncture forces forces fail the agent containment.
	475	VB	012	A severe earthquake occurs, causing a munitions vehicle accident and fire detonates burstered munitions.
	476	VB	014	A tornado occurs, generating under mechanical forces which cause detonation of burstered munitions.
	477	VB	015	A earthquake or tornado occurs, generating under mechanical forces which cause detonation of burstered munitions.
** VO				
	130	VO	001	A munitions vehicle collision/overturn occurs and crush forces fail the agent containment.
	131	VO	003	A munitions vehicle collision/overturn occurs and puncture forces fail the agent containment.
	132	VO	004	A munitions vehicle accident with fire occurs, causing detonation of burstered munitions. Ignition of the propellant by

CSDP/FEIS RISK ANALYSIS
- Accident Scenario Descriptions -
(Data File: MASTER4.DBF)
as of 15 October 1987

RECORD NUMBER	ID		SCENARIO
			a probe could also detonate the burster of a cartridge and the burster of a rocket could be detonated by impact-induced ignition of the rocket propellant.
133	VO	005	A munitions vehicle accident with fire occurs, causing non-burstered munitions to fail.
134	VO	006	An aircraft crashes on a munitions vehicle. No fire occurs; impact forces fail the agent containment.
135	VO	007	An aircraft crashes on a munitions vehicle. Fire occurs; but impact forces fail the agent containment.
136	VO	009	A severe earthquake occurs, causing a munitions vehicle accident and crush forces fail the agent containment.
212	VO	010	A severe earthquake occurs, causing a munitions vehicle accident and impact forces fail the agent containment.
137	VO	011	A severe earthquake occurs, causing a munitions vehicle accident and puncture forces fail the agent containment.
138	VO	012	A severe earthquake occurs, causing a munitions vehicle accident and fire fails detonates burstered munitions.
139	VO	013	A severe earthquake occurs, causing a munitions vehicle accident and fire fails nonburstered munitions.
140	VO	014	A tornado occurs, generating a missile or causing a truck overturn and mechanical forces fail agent containment.
141	VO	015	A truck collision/overturn occurs generating undue mechanical forces which cause detonation of burstered munitions.
** VR			
253	VR	001	A munitions vehicle collision/overturn occurs and crush forces fail the agent containment.
254	VR	002	A munitions vehicle collision/overturn occurs and impact forces fail the agent containment.
162	VR	003	A munitions vehicle collision/overturn occurs and puncture forces fail the agent containment.
163	VR	004	Detonation of burstered munitions occurs by either 1) fire-only accident, 2) mechanical force and fire, 3) truck collision/overturn impact-induced rocket propellant ignition, or 4) truck collision/overturn-induced undue force detonation.
255	VR	005	A munitions vehicle accident with fire occurs, causing nonburstered munitions to fail.
164	VR	006	An aircraft crashes on a munitions vehicle. No fire occurs; impact forces fail the agent containment.
165	VR	007	An aircraft crashes on a munitions vehicle. Fire occurs; but impact forces fail the agent containment.
256	VR	009	A severe earthquake occurs, causing a munitions vehicle accident and crush forces fail the agent containment.
257	VR	010	A severe earthquake occurs, causing a munitions vehicle accident and impact forces fail the agent containment.
166	VR	011	A severe earthquake occurs, causing a munitions vehicle accident and puncture forces fail the agent agent containment.
167	VR	012	A severe earthquake occurs, causing a munitions vehicle accident and fire detonates burstered munitions.
168	VR	013	A severe earthquake occurs, causing a munitions vehicle accident and fire fails nonburstered munitions.
169	VR	014	A tornado occurs, generating a missile or causing a truck overturn, and mechanical forces fail agent containment.
170	VR	015	An earthquake or tornado occurs, generating undue mechanical forces which cause detonation of burstered munitions.
** VW			
506	VW	001	A munitions vehicle collision/overturn occurs and crush forces fail the agent containment.
507	VW	002	A munitions vehicle collision/overturn occurs and impact forces fail the agent containment.
142	VW	003	A munitions vehicle collision/overturn occurs and puncture forces fail the agent containment.
143	VW	005	A munitions vehicle accident with fire occurs, causing nonburstered munitions to fail.
144	VW	006	An aircraft crashes on a munitions vehicle. No fire occurs; impact forces fail the agent containment.
145	VW	007	An aircraft crashes on a munitions vehicle. Fire occurs; but impact forces fail the agent containment.
146	VW	009	A severe earthquake occurs, causing a munitions vehicle accident and crush forces fail the agent containment.
508	VW	009	A severe earthquake occurs, causing a munitions vehicle accident and crush forces fail the agent containment.
147	VW	010	A severe earthquake occurs, causing a munitions vehicle accident and impact forces fail the agent containment.
509	VW	010	A severe earthquake occurs, causing a munitions vehicle accident and impact forces fail the agent containment.
148	VW	011	A severe earthquake occurs, causing a munitions vehicle accident and puncture forces fail the agent containment.
510	VW	013	A severe earthquake occurs, causing a munitions vehicle accident and fire fails nonburstered munitions.
149	VW	014	A tornado occurs, generating a missile or causing a truck overturn, and mechanical forces fail agent containment.

CSDP/EIS RISK ANALYSIS
- Accident Scenario Descriptions -
(Data File: MASTER4.DOF)
as of 15 October 1987

RECORD NUMBER	ID		SCENARIO
** WB			
311	WB	001	A collision occurs and crush forces fail agent containment.
44	WB	002	A collision occurs and crush forces fail agent containment. Sinking also occurs.
43	WB	003	A collision occurs and crush forces fail agent containment. A fire breaks out.
52	WB	004	A collision occurs and crush forces fail agent containment. A fire breaks out and sinking occurs.
56	WB	005	A ramming occurs and crush forces fail agent containment.
50	WB	006	A ramming occurs and crush forces fail agent containment. Sinking also occurs.
259	WB	007	A ramming accident occurs and crush forces fail agent containment. A fire breaks out.
57	WB	008	A ramming occurs and crush forces fail agent containment. A fire breaks out and sinking occurs.
260	WB	009	A grounding accident occurs and crush forces fail agent containment.
74	WB	010	A grounding accident occurs and crush forces fail agent containment. Sinking also occurs.
261	WB	011	A grounding accident occurs and crush forces fail agent containment. A fire breaks out.
61	WB	012	A grounding accident occurs and crush forces fail agent containment. A fire breaks out and sinking occurs.
252	WB	013	Structural damage due to heavy weather occurs. Crush forces fail agent containment.
80	WB	014	Structural damage due to heavy weather occurs. Crush forces fail agent containment. Sinking also occurs.
253	WB	015	Structural damage due to heavy weather occurs. Crush forces fail agent containment. A fire breaks out.
95	WB	016	Structural damage due to heavy weather occurs. Crush forces fail agent containment. A fire breaks out and sinking occurs.
254	WB	017	Spontaneous fire occurs.
255	WB	018	Spontaneous fire occurs. Sinking also occurs.
105	WB	019	Collision accident occurs with no immediate release. Sinking also occurs.
109	WB	020	Ramming accident occurs with no immediate release. Sinking also occurs.
112	WB	021	Grounding accident occurs with no immediate release. Sinking also occurs.
115	WB	022	Structural damage due to heavy weather occurs with no immediate release. Sinking also occurs.
[illegible]	WB	023	Aircraft crashes into marine vessel.
** WC			
258	WC	001	A collision occurs and crush forces fail agent containment.
46	WC	002	A collision occurs and crush forces fail agent containment. Sinking also occurs.
53	WC	003	A collision occurs and crush forces fail agent containment. A fire breaks out.
56	WC	004	A collision occurs and crush forces fail agent containment. A fire breaks out and sinking occurs.
58	WC	005	A ramming occurs and crush forces fail agent containment.
62	WC	006	A ramming occurs and crush forces fail agent containment. Sinking also occurs.
65	WC	007	A ramming occurs and crush forces fail agent containment. A fire breaks out.
69	WC	008	A ramming occurs and crush forces fail agent containment. A fire breaks out and sinking occurs.
72	WC	009	A grounding accident occurs and crush forces fail agent containment.
76	WC	010	A grounding accident occurs and crush forces fail agent containment. Sinking also occurs.
79	WC	011	A grounding accident occurs and crush forces fail agent containment. A fire breaks out.
83	WC	012	A grounding accident occurs and crush forces fail agent containment. A fire breaks out and sinking occurs.
[illegible]	WC	013	Structural damage due to heavy weather occurs. Crush forces fail agent containment.
92	WC	014	Structural damage due to heavy weather occurs. Crush forces fail agent containment. Sinking also occurs.
93	WC	015	Structural damage due to heavy weather occurs. Crush forces fail agent containment. A fire breaks out.
97	WC	016	Structural damage due to heavy weather occurs. Crush forces fail agent containment. A fire breaks out and sinking occurs.
100	WC	017	Spontaneous fire occurs.

CSDP/FEIS RISK ANALYSIS
- Accident Scenario Descriptions -
(Data File: MASTER6.DBF)
as of 15 October 1987

	RECORD NUMBER	ID		SCENARIO
	103	WC	018	Spontaneous fire occurs. Sinking also occurs.
	107	WC	019	Collision accident occurs with no immediate release. Sinking also occurs.
	111	WC	020	Ramming accident occurs with no immediate release. Sinking also occurs.
	114	WC	021	Grounding accident occurs with no immediate release. Sinking also occurs.
	118	WC	022	Structural damage due to heavy weather occurs with no immediate release. Sinking also occurs.
	247	WC	023	Aircraft crashes into marine vessel.
** WI				
	42	WI	001	A collision occurs and crush forces fail agent containment.
	45	WI	002	A collision occurs and crush forces fail agent containment. Sinking also occurs.
	49	WI	003	A collision occurs and crush forces fail agent containment. A fire breaks out.
	53	WI	004	A collision occurs and crush forces fail agent containment. A fire breaks out and sinking occurs.
	57	WI	005	A ramming occurs and crush forces fail agent containment.
	61	WI	006	A ramming occurs and crush forces fail agent containment. Sinking also occurs.
	64	WI	007	A ramming occurs and crush forces fail agent containment. A fire breaks out.
	68	WI	008	A ramming occurs and crush forces fail agent containment. A fire breaks out and sinking occurs.
	71	WI	009	A grounding accident occurs and crush forces fail agent containment.
	75	WI	010	A grounding accident occurs and crush forces fail agent containment. Sinking also occurs.
	78	WI	011	A grounding accident occurs and crush forces fail agent containment. A fire breaks out.
	82	WI	012	A grounding accident occurs and crush forces fail agent containment. A fire breaks out and sinking occurs.
	85	WI	013	Structural damage due to heavy weather occurs. Crush forces fail agent containment.
	89	WI	014	Structural damage due to heavy weather occurs. Crush forces fail agent containment. Sinking also occurs.
	92	WI	015	Structural damage due to heavy weather occurs. Crush forces fail agent containment. A fire breaks out.
	96	WI	016	Structural damage due to heavy weather occurs. Crush forces fail agent containment. A fire breaks out and sinking occurs.
	99	WI	017	Spontaneous fire occurs.
	102	WI	018	Spontaneous fire occurs. Sinking also occurs.
	106	WI	019	Collision accident occurs with no immediate release. Sinking also occurs.
	110	WI	020	Ramming accident occurs with no immediate release. Sinking also occurs.
	113	WI	021	Grounding accident occurs with no immediate release. Sinking also occurs.
	117	WI	022	Structural damage due to heavy weather occurs with no immediate release. Sinking also occurs.
	246	WI	023	Aircraft crashes into marine vessel.
** WS				
	43	WS	001	A collision occurs and crush forces fail agent containment.
	47	WS	002	A collision occurs and crush forces fail agent containment. Sinking also occurs.
	51	WS	003	A collision occurs and crush forces fail agent containment. A fire breaks out.
	55	WS	004	A collision occurs and crush forces fail agent containment. A fire breaks out and sinking occurs.
	59	WS	005	A ramming occurs and crush forces fail agent containment.
	63	WS	006	A ramming occurs and crush forces fail agent containment. Sinking also occurs.
	66	WS	007	A ramming occurs and crush forces fail agent containment. A fire breaks out.
	70	WS	008	A ramming occurs and crush forces fail agent containment. A fire breaks out and sinking occurs.
	73	WS	009	A grounding accident occurs and crush forces fail agent containment.
	77	WS	010	A grounding accident occurs and crush forces fail agent containment. Sinking also occurs.
	80	WS	011	A grounding accident occurs and crush forces fail agent containment. A fire breaks out.

CSDP/FEIS RISK ANALYSIS

- Accident Scenario Descriptions -

(Data File: MACTER4.DBF)

as of 15 October 1987

RECORD NUMBER	ID		SCENARIO
84	WS	012	A grounding accident occurs and crush forces fail agent containment. A fire breaks out and sinking occurs.
87	WS	013	Structural damage due to heavy weather occurs. Crush forces fail agent containment.
91	WS	014	Structural damage due to heavy weather occurs. Crush forces fail agent containment. Sinking also occurs.
94	WS	015	Structural damage due to heavy weather occurs. Crush forces fail agent containment. A fire breaks out.
98	WS	016	Structural damage due to heavy weather occurs. Crush forces fail agent containment. A fire breaks out and sinking occurs.
101	WS	017	Spontaneous fire occurs.
104	WS	018	Spontaneous fire occurs. Sinking also occurs.
108	WS	019	Collision accident occurs with no immediate release. Sinking also occurs.
115	WS	[illegible]	Grounding accident occurs with no immediate release. Sinking also occurs.
119	WS	022	Structural damage due to heavy weather occurs with no immediate release. Sinking also occurs.
248	WS	023	Aircraft crashes into marine vessel.

RISK MITIGATION FOR THE CHEMICAL STOCKPILE DISPOSAL PROGRAM: IDENTIFICATION OF OPPORTUNITIES AND ESTIMATION OF POTENTIAL BENEFITS

Robert B. Perry
Office of the Program Executive Officer
Program Manager for Chemical Demilitarization
Aberdeen Proving Ground, Maryland

William W. Duff
The MITRE Corporation
McLean, Virginia

TWENTY-THIRD DOD EXPLOSIVES SAFETY SEMINAR
HYATT REGENCY HOTEL
ATLANTA, GEORGIA

9-11 AUGUST 1988

TABLE OF CONTENTS

TABLE OF CONTENTS (Continued)

Page

TABLE OF CONTENTS (Concluded)

LIST OF FIGURES

LIST OF TABLES

1.0 INTRODUCTION

The Department of Defense was directed by Congress (Public Law 99-145, Title 14, Part B, Section 1412) to destroy the stockpile of lethal unitary chemical agents and munitions in such a manner as to provide, among other precautions, maximum protection to the general public. One part of the Army's effort to comply with this directive is the subject of this paper.

1.1 Background

In response to the requirements of Public Law 99-145, in March 1986 the Army produced a concept plan for destruction of the lethal chemical stockpile by 1994 (USATHAMA, 1986). The plan for the Chemical Stockpile Disposal Program (CSDP) presented three programmatic alternatives:

1. On-site destruction of the chemical stocks at their present storage locations.

2. Movement of the Continental United States (CONUS) stocks to two regional destruction centers.

3. Collocation of all CONUS stocks to a national destruction center.

In July 1986 a Draft Programmatic Environmental Impact Statement (DPEIS) was issued, followed in January 1988 by a Final Programmatic Environmental Impact Statement (FPEIS); the FPEIS considered the disposal alternatives listed above and two additional alternatives:

4. Relocation of the stocks from two sites by air to alternative sites, with the remainder destroyed at their present storage locations.

5. Continued storage of the stocks at their present locations (the no-action alternative required by the National Environmental Policy Act).

In an effort to comply with the safety directive from Congress, the FPEIS contains estimates of risk to the public for each of the five alternatives. A risk analysis was performed, in support of the FPEIS, to quantify the public risk for each alternative. While performing the risk analysis and during the development of the transportation concept plan some measures to reduce risk were identified and incorporated into the disposal plan. The safety measures included in the plan since the DPEIS are listed in Table 1-1. The risk analysis in support of the FPEIS also includes these measures.

After the completion of this risk analysis a further study was undertaken to identify and evaluate additional measures for reducing the

TABLE 1-1
SAFETY IMPROVEMENTS ADDED SINCE THE DPEIS[a]

Handling and Preparation for Shipment

- Propellant and fuzes removed from 105-mm cartridges and 4.2-in mortar projectiles.
- Valves and plugs replaced on ton containers before shipping.
- Use of on-site shipping container (or protective overpack) for all munition handling activities in the disposal plant yard and Munitions Holding Igloo (eliminates handling bare munitions in the disposal plant yard).
- On-site shipping container designed to be handled with lifting beam; reduces probability of a drop by a factor of 10 compared with conventional forklift with tines.

On-Site Transport

- Use of on-site shipping container.
- Amount of fuel in trucks limited so as not to exceed a 10-min fire. (The on-site container is designed to provide fire resistance for a 15-minute all-engulfing fire).

Off-Site Transport

- Use of off-site shipping container for all munitions (rather than just thin-walled munitions).
- Loading munitions into the off-site package at the igloo/storage area apron rather than the shipping dock; eliminates the transport of bare munitions from the storage area to the shipping area and handling bare munitions at the shipping area.
- For air transport special selection of aircraft to meet highest standards of reliability; procedures would be developed for chemical munition transport similar to those used for selecting and maintaining aircraft for transportation of nuclear weapons.
- Air transport limited to good weather conditions.

TABLE 1-1
SAFETY IMPROVEMENTS ADDED SINCE THE DPEIS[a]
(Concluded)

Plant Operations

- Upgraded the earthquake survivability of the toxic cubicle; specifically the toxic room, agent tanks, and piping are being redesigned to meet the more stringent Nuclear Regulatory Commission (NRC) seismic standards [instead of the Uniform Building Code (UBC)].
- Reduced the size of the agent storage tanks in the toxic cubicle; this reduced the inventory of agent in the plant.
- Increased the size of the sump in the toxic cubicle to contain the entire contents of an agent storage tank; this reduced the area of the puddle and hence reduced the agent evaporation in the event the contents of the tank are spilled.
- Added a dry chemical fire protection system in the toxic cubicle.
- Added pressure and vacuum relief valves to agent storage tanks.
- Extend the time that the uninterruptible power supply can operate critical plant safety systems in the event of total loss of commercial and emergency power.
- Added redundant induced draft fans to all furnace systems.
- Redesigned damper systems on agent containing furnaces to fail in "fail safe" position (instead of manual positioning).
- Enclosed the deactivation furnace system cyclone discharge and added agent monitors to the enclosure.

[a]Measures are incorporated in the risk analysis by GA Technologies Inc. (U.S. Army 1987a, 1987b, 1987c).

public safety risk during the course of the CSDP. It is this additional study which is described in the present paper.

The term "mitigation" as used in this paper is different from the definition normally applied to it in nuclear risk assessments. We refer to "mitigation" as the reduction or elimination of risk contributors (frequencies and/or agent source terms), whereas in the nuclear industry "mitigation" normally refers to the reduction of the effects from radionuclide releases once the event occurs. Therefore, mitigation measures proposed in the study were evaluated for their effectiveness in (1) reducing the frequency of an accident and (2) reducing the size of the accident.

1.2 Overview of the Chemical Stockpile Disposal Program

1.2.1 Description of the Stockpile

The chemical agents are stored in three types of configurations: (1) projectiles, cartridges, and rockets containing propellant and/or explosive components, (2) munitions for aircraft delivery that do not contain explosives, and (3) bulk agent stored in ton containers. The chemical agents covered by this program are the persistent nerve agent VX, the nonpersistent nerve agent GB, and the persistent blister agents known as mustards. The CONUS stockpile is currently stored at eight Army installations throughout the nation, as shown in Figure 1-1.

1.2.2 Activities Associated with the Disposal Program

The activities associated with the disposal program alternatives include storage, handling, on-site transport, off-site transport, and plant operations.

Storage

All chemical munition/agent storage is currently maintained within a chemical exclusion area at each installation. Extensive security precautions are used to deter entry to these storage areas. Current storage operations will continue until the stockpile is completely destroyed. For purposes of the risk analysis in support of the FPEIS the Continued Storage (no-action) alternative was assumed to continue for 25 years.

Munitions containing explosives are stored in igloo magazines specifically designed for the storage of ammunition and explosives. The igloos are constructed of reinforced concrete, have steel doors, are covered with earth, and have lightning protection. All GB-filled and most VX-filled munitions without explosives and bulk containers are also stored in igloos. The exceptions are VX ton containers at Newport Army Ammunition Depot (NAAP) and VX spray tanks at Tooele Army Depot (TEAD) which are stored in warehouses. Ton containers of mustard are stored in warehouses at Umatilla

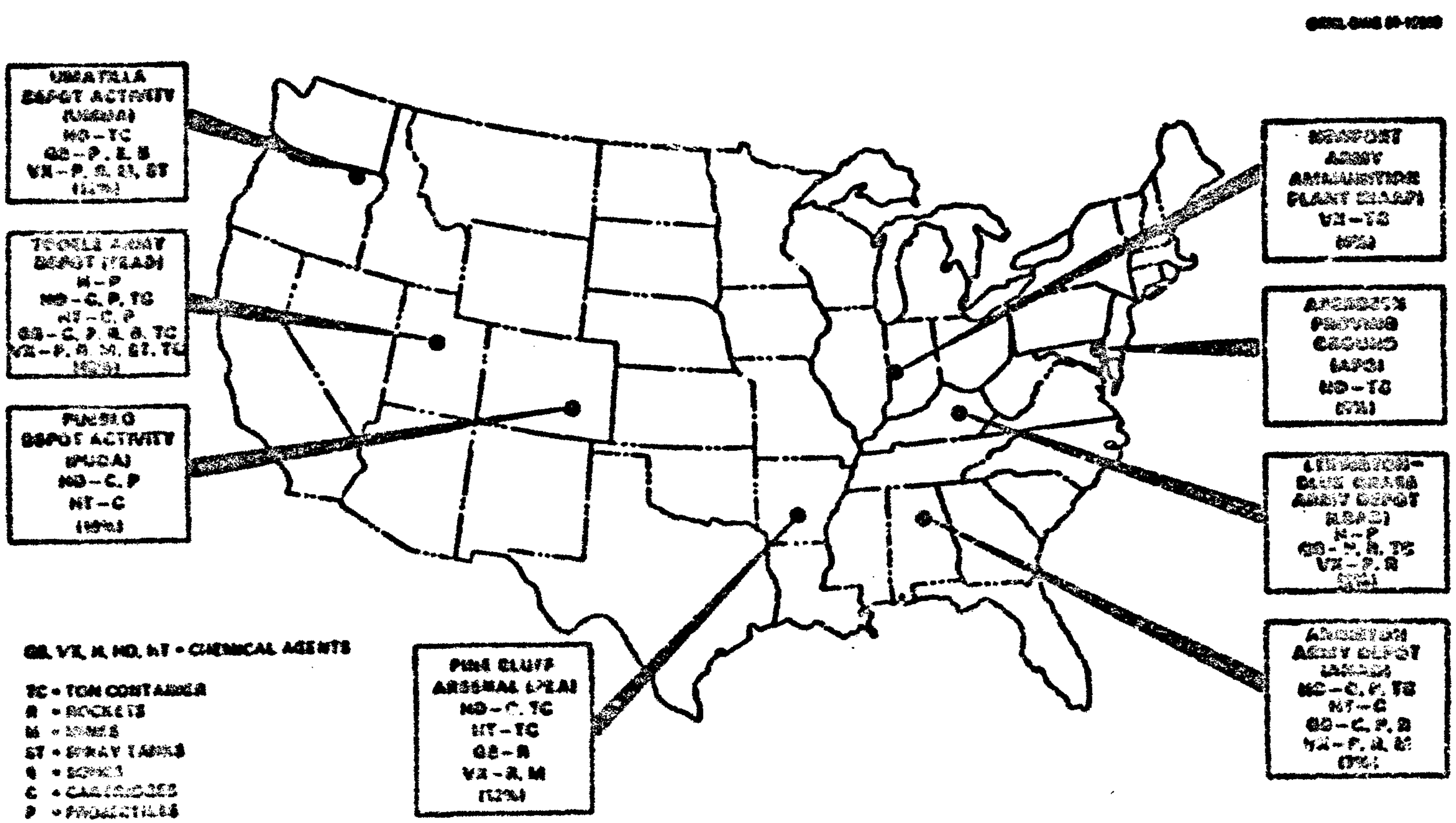

FIGURE 1-1
LOCATION OF CHEMICAL AGENTS AND MUNITIONS
IN THE UNITED STATES

Depot Activity (UMDA); in outdoor storage yards at Aberdeen Proving Ground (APG), Pine Bluff Arsenal (PBA), and TEAD; and in igloos at Anniston Army Depot (ANAD).

The munitions are monitored routinely and are periodically maintained. Moving and/or restacking of munitions is involved in routine inspection and maintenance activities. The total inventory at an installation is handled on the average over approximately a five-year period.

All chemical agents in the stockpile are at least 19 years old, and some are more that 40 years old. Some of the munitions have started to leak. The M55 rockets in a few lots (about two percent of the GB-filled rockets) have exhibited the greatest incidence of leakage, while the remaining munitions and containers have relatively few leakers. As leakers are discovered, they are placed in protective overpacks to prevent agent leakage to the environment. Further protective measures are taken as appropriate. A drill and transfer system has been used to drain agent from some leaking munitions to a bulk container, followed by decontamination of the munition body.

Handling and Transport

Disposal of the chemical stockpile will require the movement of munitions and containers from the storage area to the headend of the disposal process and involve a number of handling steps, as illustrated in Figure 1-2. The descriptions given below represent the movements and procedures used in the risk analysis and are in the process of being revised.

For on-site disposal a pallet of munitions or bulk container is removed from storage and placed into an on-site transportation package using a forklift. Packing operations occur on or adjacent to the igloo apron or storage area. The shipping package is designed to provide the munitions with protection from collision and fire. The package is loaded on a flat-bed truck and transported to a Munitions Handling Igloo (MHI) at the disposal facility. Two exceptions are the TMU-28/B spray tanks and the MK-116 Weteye bombs which are transported directly in the protective steel overpacks in which they are stored. The munition truck is accompanied by two security trucks, an emergency vehicle, and decontamination vehicle. The convoy speed is limited to 20 mph maximum and the amount of fuel in trucks is limited so as not to exceed a ten- minute fire. Upon arrival at the disposal facility the packages are unloaded from the truck and moved into the MHI for temporary storage. Later the package is carried to the Munitions Demilitarization Building (MDB) with a forklift, placed on an elevator, removed from the elevator, and moved to the unpacking area, where the palletized munitions are removed from from the transport package.

For regional and national disposal or partial relocation alternatives the off-site transportation package is used. This package is larger than

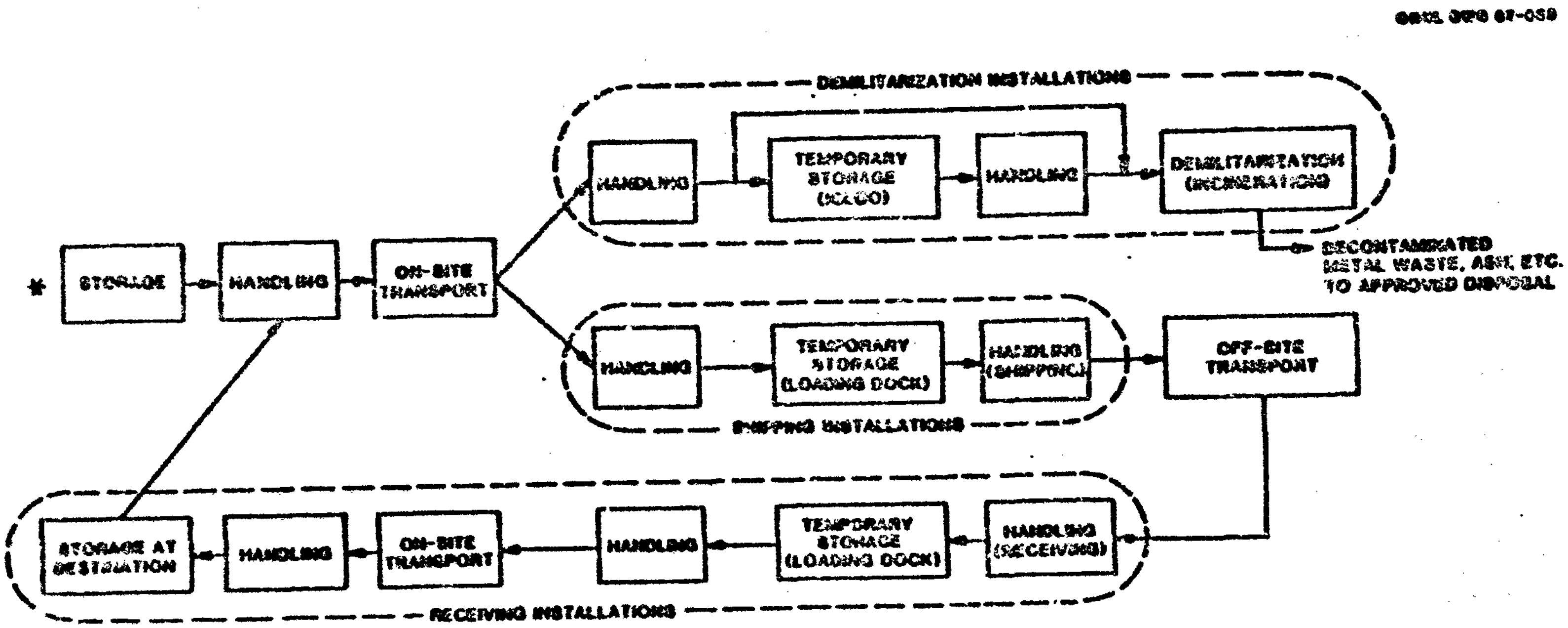

FIGURE 1-2
SIMPLIFIED FLOW CHART FOR DISPOSAL ACTIVITIES

the on-site package. Palletized munitions or bulk items are loaded into the package at the igloo or storage area. The package is moved by truck to an open holding area and unloaded using standard cargo handling equipment. From there the packages are loaded on the off-site transporter (rail car or plane) and transported to the destination site. At the receiving site the package is unloaded, placed in an open holding area temporarily and then transported by truck to the storage area. The munitions are removed from the off-site package and placed in a storage facility (e.g., igloo). When the disposal plant is ready the munitions are removed from storage and placed in an on-site transportation package for movement to the disposal facility. Handling and movement to the MHI and MDB are performed as described above for on-site disposal.

Disposal

The risk analysis is based on the "Baseline" demilitarization process, which involves mechanical separation of explosive components and draining agent followed by incineration and/or decontamination of the components. The MDB, in which the process is performed, is designed for the confinement of agent. The building is under negative pressure and zoned with air flow from areas of no or low contamination to higher contamination. The building ventilation exhaust is treated with charcoal filters to remove agent before release. The stack and building ventilation exhaust are monitored for agent as well as the building work areas. The steps involved in the destruction process are described below.

Explosively configured munitions are separated and drained in special explosion containment rooms. Rockets are sheared to separate propellant and explosive components, drained, and fed to a deactivation furnace. M23 mines are punched and drained; the explosive components are punched out and fed with the empty mines to the deactivation furnace. The explosives are removed from the other burstered munitions by a machine, sheared, and fed to the deactivation furnace; the munitions are drained and fed to the metal parts furnace. In all cases, the drained agent is fed to a storage tank prior to incineration.

Bulk items, which have no explosives, are punched and drained. The agent is fed to a storage tank and the empty bulk container is then conveyed to the metal parts furnace.

The Army has selected incineration as the best technology for destroying chemical agents. Incineration has been endorsed by the National Academy of Science as the method of choice for destroying chemical agents (National Research Council, 1984). Four types of furnace systems are used in the process. The agent drained from the munitions is destroyed in the liquid incinerator. The deactivation furnace is used to destroy explosives and propellants and to decontaminate certain munition hardware. The metal parts furnace burns out agent residues and detoxifies projectile and mortar

shells and bulk item containers. The dunnage incinerator treats other combustibles (wooden dunnage, packing material, spent charcoal filters, etc.). The furnace systems and associated feed systems for toxic materials are located in special confinement cubicles and operated remotely. The deactivation furnace is housed in a blast containment room and is equipped with blast gate valves and blast attenuating duct on the exhaust.

Each furnace has its own pollution abatement system to remove acid gases and particulates. Liquid wastes are processed to dry solids and packaged for appropriate disposal. Spent decontamination and suspect liquid wastes are incinerated. There is no liquid effluent from the process. Combustible wastes are incinerated.

2.0 SELECTION OF ACCIDENTS FOR MITIGATION STUDY

Public safety risks are defined in terms of two factors: (1) the probability or likelihood that public safety will be threatened; and (2) the impact or consequences that could result from that threat. The public safety risks of the CSDP alternatives were evaluated in the risk analysis by: (1) identifying potential accidents that could result in release of chemical agents to the environment; (2) estimating the likelihood of such accidents; and (3) estimating the severity of the potential accidents in terms of the quantity of agent released and the distance a cloud or plume of agent could travel with lethal consequences. The accident scenarios identified in the risk analysis were screened to remove from consideration events with a very low probability of occurrence or whose consequences would have a minor effect on public health. Accidents scenarios which exceeded the screening factors were analyzed for possible mitigation measures.

2.1 Risk Descriptors

2.1.1 Probabilities

The risk analysis in support of the FPEIS was based on a quantitative hazard analysis of events that would lead to agent release to the environment (GA Technologies, 1987). In this study, numeric estimates of the probabilities of such accidents occurring were made by combining the probabilities of the events that comprise each accident scenario. The probabilities were given in terms of events per unit time, per storage unit-year, or per mile.

The GA Technologies' data was converted to a munition-per-stockpile basis by utilizing information on the classified inventory for each site. Finally, the total (programmatic) probability of an accident scenario was determined by combining the probabilities for each of the munitions at each of the sites.

The probability estimates, while made on the basis of sound engineering data and principles, are not precise values. The data bases for calculating probabilities are limited.

2.1.2 Consequences

The consequences of an accident are partly a function of the size of the impacted area. The risk analysis utilized a Gaussian-plume dispersion model, D2PC, developed by the Army to predict the areas affected by releases of agent (Whitacre *et al.*, 1986). For screening purposes in the present study the severity of each potential accident was estimated, using the D2PC model, of the maximum downwind distance a cloud or plume of agent

could travel with lethal consequences. This is called the "no deaths" distance in the model, defined as the maximum distance downwind to the location where the "dosage" no longer causes deaths to the affected population. It indicates how far from a potential accident site an individual or population group should be to avoid any potentially lethal exposure to agent. This measure takes account of the quantity of agent released to the environment, the mechanism for dispersing the released agent, and the toxicities of the different agents. In this study we use the term "maximum hazard distance" for the no-deaths distance under "worst-case" weather conditions: Pasquill stability E and 1 m/sec wind velocity.

The transport and diffusion portion of the D2PC model has certain shortcomings which affect the results at large distances. At large distances the Gaussian-plume model overestimates the concentrations or, in the case of the D2PC model, overestimates the hazard distances. All meteorological conditions, including wind direction, are constant within any D2PC run. In actuality, such conditions change with both time and distance. A change in wind direction can greatly reduce the maximum downwind agent concentration at a specified distance. Thus, for accidents where a large hazard distance is predicted, the results should be regarded as only a relative indicator.

2.2 Screening to Identify Accidents for Mitigation Analysis

The risk analysis data base was screened using the factors presented in Table 2-1. The action levels for mitigation study are a probability of 10^{-8} or greater events per stockpile for on-site accidents which release enough agent that members of the general public might be exposed to lethal concentrations under "worst case" weather conditions. The requirement that the general public be exposed implies that the downwind distance to the "no deaths" dosage exceeds the site boundary distance. For purposes of screening a distance of 0.5 km was used from the source for on-site accidents (at no site is the distance from the disposal site to the boundary of the military reservation less than 0.5; at most installations it is 1 to 2 km). For transportation accident scenarios which occur off-site the screening factor is a frequency greater than 10^{-8} events per stockpile and any release of agent, since the accident could occur at any public area along the transportation route.

The probabilities used for screening are the sum of the probabilities over all agent/munition types and all sites to which the accident scenario applies which have a maximum hazard distance exceeding 0.5 km. For any given accident scenario the consequences will vary according to the type of munition or agent involved. The probability used for screening is the likelihood that the accident might occur, not the probability that worst-case consequences would occur. For storage the probabilities are per stockpile year and the risks recur year after year until the stockpile is

TABLE 2-1
FACTORS FOR SCREENING TO IDENTIFY ACCIDENTS
FOR MITIGATION ANALYSIS

Activity	Screening Factors
Storage[a]	Probability $>10^{-8}$ events per storage year and a 'no-deaths, worst case' hazard distance >0.5 km[b]
Handling, on-site transport, demilitarization	Probability $>10^{-8}$ events per stockpile and a 'no-deaths, worst case' hazard distance >0.5 km
Off-site transport	Probability $>10^{-8}$ events per stockpile and any release of agent if accident occurs off-site

[a]Includes handling related to leakers during storage.

[b]Hazard distance calculated with the D2PC model; "worst-case" meteorology (E stability, 1 m/sec).

destroyed. For disposal activities the probabilities are for the one-time disposal of the entire stockpile based on the three year disposal schedule in the Chemical Stockpile Disposal Concept Plan (USATHAMA, 1986).

The accident scenarios selected for risk mitigation study by application of the screening factors are presented in Table 2-2.

TABLE 2-2
ACCIDENT SCENARIOS SELECTED FOR RISK MITIGATION

<u>Storage Accident Scenarios</u>

1. A small or large aircraft crash on, or adjacent to, munition storage or holding area leads to a fire.
2. A small or large aircraft crash on, or adjacent to, munition storage or holding area without fire (detonation may occur).
3. Earthquake leads to a spill.
4. Earthquake leads to a detonation.
5. Earthquake leads to a warehouse fire.
6. Meteorite strikes with a fire/detonation.
7. Munition dropped during leaker isolation leads to a spill or a detonation.

<u>Handling Accident Scenarios</u>

1. Dropped munition or container results in a spill.
2. Forklift collision results in a spill.
3. Forklift collision results in a spill with a fire.
4. Forklift tines puncture munition.
5. Dropped munition or container results in detonation.
6. Collision results in a detonation.

<u>On-Site Transport Accident Scenarios</u>

1. Vehicle accident or earthquake crushes or punctures munition, resulting in a spill.
2. Vehicle accident with fire and/or detonation.

TABLE 3-2
ACCIDENT SCENARIOS SELECTED FOR RISK MITIGATION
(Concluded)

Off-Site Transport Accident Scenarios

1. Rail accident crushes or punctures munition, resulting in a spill.

2. Rail accident results in a fire and /or detonation.

3. Aircraft carrying munitions crashes without a fire; spill occurs.

4. Aircraft carrying munitions crashes with fire; detonation may occur.

Plant Operations Accident Scenarios

1. Direct or indirect aircraft crash with or without fire.

2a. Earthquake damages MDB; munitions fall, fire starts; munitions punctured and fire suppressed.

2b. Earthquake damages MDB; munitions fall, fire starts; munitions punctured and fire suppression fails.

2c. Earthquake damages MDB; munitions fall, fire starts; munitions intact and fire suppression fails.

2d. Earthquake does not damage MDB; munitions fall, fire starts, and fire suppression fails.

3. Metal parts furnace explosion due to fuel shutoff failure.

4a. Munition falls from ECV conveyor and detonates; no fire occurs.

4b. Munition falls from ECV conveyor and detonates; fire starts.

5a. Munition detonation fails ECR and ventilation system.

5b. Munition detonation fails ECR and ventilation system; fire starts.

6. Burstered munition fed to dunnage incinerator.

3.0 MITIGATION MEASURES CONSIDERED

The mitigation measures that were considered feasible for accidents involved in storage, handling, on-site and off-site transportation, and plant operations are discussed below. A brief description of each is given, together with comments about its practicability and expected benefits. The action the Army proposes to take with regard to the mitigation measures is given at the end of each section.

3.1 Mitigation of Storage Risks

Seven types of storage accident scenarios were identified as accidents which should be studied to determine if mitigation measures could be applied. Of these, six are externally-caused accidents and one is caused by worker error. The accidents with the most serious consequences are those involving a fire, which causes the evaporation of large amounts of agent. Potentially, the most serious consequences could result at NAAP and UMDA where ton containers of VX and mustard, respectively, are stored in warehouses.

Four measures were considered for mitigation of most of the externally-caused accidents: (1) restricting air space, (2) installing a warehouse fire suppression system, (3) moving agent not in igloos into igloos, and (4) deenergizing the warehouse electrical system. One measure was considered for mitigation of the accident caused by worker error: securing the lift truck load. No mitigation measures were identified for earthquake-caused accidents resulting in a spill or a detonation. Table 3-1 provides a summary of storage accident scenarios and mitigation measures.

3.1.1 Mitigation Measure: Restrict Air Space

Establishing air space restrictions for civilian and military aircraft could substantially reduce the expected frequency of an aircraft crash on storage areas. Studies would have to be conducted to determine the extent of the exclusion area required and the disruption of air traffic that would result at each site. These would require considerable time and effort but a good case might be made for such restrictions at some sites. The Department of Defense could restrict military aircraft if it were determined that military operations would not be seriously affected. To obtain restrictions on civilian aircraft, the Army would have to file a proposal with the local FAA regional office. After the Army and the regional office agreed on the conditions to be applied, the proposal would follow the public notice procedure process, including publication in the Federal Register and a waiting period for public comments. If no problems were raised the process could take from 6 months to a year. The cost of the study would probably not exceed $200,000 per site. The cost of disrupting commercial and general aviation is not known at this time.

TABLE 3-1
SUMMARY OF STORAGE ACCIDENT SCENARIOS AND MITIGATION MEASURES

Accident Scenario	Max. Hazard Distance (km)	Probability	Mitigation Measure	Cost	Expected Benefit: Maximum Hazard Distance (km)	Expected Benefit: Probability
A small or large aircraft crash on, or adjacent to, munition storage or holding area leads to a fire	297	$2x10^{-5}$	Restricted airspace	\$ 200,000/site[a]	--	$2x10^{-6}$
			Warehouse fire suppression system	500,000/whse	40[b]	--
			Move munitions from warehouse and storage to igloos	\$80,000,000	--	$2x10^{-6}$
A small or large aircraft crash on, or adjacent to, munition storage or holding area without fire (detonation may occur)	178	$3x10^{-6}$	Restricted airspace	\$ 200,000/site[a]	--	$2x10^{-7}$
Earthquake leads to a spill	2.3	$1x10^{-5}$	None	--	--	--
Earthquake leads to a detonation	5.4	$2x10^{-6}$	None	--	--	--
Earthquake leads to warehouse fire	314	$7x10^{-4}$	Warehouse fire suppression system	\$ 500,000/whse	41	--
			Deenergize electrical system	100,000	--	$1x10^{-5}$
Meteorite strikes with fire/detonation	293	$2x10^{-8}$	Warehouse fire suppression system	\$ 500,000/whse	54[c]	--
Munition dropped during leaker isolation leads to a spill or a detonation	5.4	$1x10^{-5}$	Lift truck load secured	\$ 900,000	--	$2x10^{-7}$

[a]Does not include cost of disruption to air traffic.
[b]Reduction in hazard distance applicable only to warehouse fires caused by indirect aircraft crashes.
[c]Maximum hazard distance for warehouse fires reduced from 203 km to about 54 km. The maximum hazard distance for igloo fires remains unmitigated at 180 km.

Using the flight data for the Newport site as the basis of the estimate, the expected frequency of the aircraft crashes at NAAP would be reduced by 92 percent if the restriction were applied to a 50-mile distance from the site. The reduction in the probabilities of the aircraft crash accidents shown in Table 3-1 would result if a reduction similar to the NAAP reduction were possible at all eight CONUS sites. The greatest reduction in the probability of such an accident would result if military aircraft were restricted at APG.

3.1.2 Mitigation Measure: Install Warehouse Fire Suppression System

Although fire-fighting equipment and crews are available at each site, a warehouse fire caused by an aircraft crash, earthquake, or meteorite could get out of control before the fire crew arrived on the scene. Therefore, the installation of a fire suppression system for containing the fire until the fire protection unit arrived was considered.

A system automatically actuated by detection devices could be installed in the chemical agent storage warehouses at NAAP, UMDA, and TEAD. The system would be designed to drench the agent containers with water. The water delivery system should be located far enough from the warehouse to preclude its destruction if an aircraft hit the warehouse. Several parallel distribution systems would assure the operation of the remaining sections if one of them were damaged. Excess-flow valves in distribution lines would shut off flow to a ruptured section, preventing loss of pressure throughout the system. Such a system could probably be installed in a warehouse for about $500,000.

A fire suppression system might not control fires in all cases of aircraft crashes, but could mitigate the consequences of some fires, especially those caused by small aircraft. The redundancy in the distribution lines should permit the system to operate successfully in the event of an earthquake or meteorite strike. It was estimated that, in the event of a direct crash by a small plane, an indirect crash by a large plane, an earthquake, or meteorite strike, the fire suppression system would reduce the amount of agent release by about 99 percent. This would result in a substantial reduction in the maximum hazard distance, as indicated in Table 3-1. No credit was taken for the benefit in mitigating the accident scenarios involving the direct crash of a large aircraft on a warehouse.

3.1.3 Mitigation Measure: Move Agent Not in Igloos to Igloos

Hardened storage magazines (i.e., igloos) are not designed to withstand all external events but against small aircraft crashes they are expected to be effective. Since agent stored in warehouses or outdoors is vulnerable to small aircraft, accidents resulting from small aircraft could be mitigated by moving the agent to igloos. Over 200 igloos would be

required to store all the inventory now in warehouses (at NAAP, UMDA, and TEAD) and outdoors (APG, PBA, and TEAD) at a cost of over $60 million. The cost of constructing igloos only for the stocks now in warehouses would probably exceed $20 million; this option could be considered because agent concentrated in a warehouse is more vulnerable than in open storage. Moving the agent into the new igloos is not without risk because of the extensive handling required.

Moving agent into igloos effectively reduces the probability of agent release from a small aircraft crash to a non-credible event. Assuming the threat of large aircraft crashes would remain, the overall probability of the accident scenario in which an aircraft crash causes a fire is reduced by about one order of magnitude, as shown in Table 3-1. The added risks incurred with handling and transportation while transferring these stocks to the igloos have not been quantified.

3.1.4 Mitigation Measure: Deenergize Warehouse Electrical System

The agent warehouses at NAAP, UMDA, and TEAD contain electrical systems inside and security lighting mounted on the exterior. In the event of an earthquake, damaged power lines could provide an ignition source for a fire. Deenergizing the electrical system would remove a major ignition source, thus decreasing the probability of a fire. This could be done by disconnecting the electrical leads at all times except when personnel are working in the building. A new security lighting system located away from the building would have to be provided. Another method would be to install a seismic sensor which would open a circuit breaker in the power line in the event of an earthquake. The sensor could be set to actuate the circuit breaker if ground acceleration exceeded the design criteria for the warehouse (in the range of 0.07 to 0.14 g).

While the existence of some unidentified ignition source cannot be ruled out, it is reasonable to to expect that elimination of power during an earthquake would reduce the probability of a fire by 98 percent.

3.1.5 Mitigation Measure: Secure the Lift Truck Load

Munitions in storage are moved by lift truck when checking for leakers or performing maintenance. If a munition or container is dropped it may rupture or, in the case of a burstered munition, a detonation could occur. The probability of dropping a munition could be reduced if the lift trucks were equipped with mechanical devices to prevent munitions or pallets of munitions from being dropped.

Lift trucks used for palleted munitions could be provided with a heavy rail which would surround the pallet on three sides and prevent it from dropping off the lift during movement or collision. A U-shaped rail pivoted at each end would be lifted out of the way when the tines were

being placed under the pallet prior to lifting. The lifting device used to move ton containers is equipped with a horizontal lifting beam with clamps at each end which grip the chimes at each end of the container. The device could be equipped with cables, attached at one end to the top of the boom and clamped at the other end to the chimes of the ton container. Such a device would provide a measure of redundancy, thus reducing the likelihood of a ton container falling to the ground. The total cost of these devices is expected not to exceed $900,000.

This mitigation measure was estimated to reduce the probability of a spill or detonation due to a drop by 98 percent. However, the operators are likely to find them a nuisance and enforcing their use is likely to be difficult. Malfunction or careless use of the devices could increase injuries to workers.

3.1.6 Proposed Action

The most promising and cost-effective measure for mitigating air crash accidents appears to be restricting air space in the vicinity of the storage areas. Although the Army cannot commit to air space restrictions at this time, a study could be undertaken to determine whether such restrictions can and should be implemented. The most promising sites for such restrictions are NAAP, UMDA, TEAD (because these sites have warehouses), and APG (because this site has the highest potential for an air crash).

The most effective measure for mitigating an earthquake-caused warehouse fire, which is the storage accident with the greatest risk, is to deenergize the electrical system. The Army plans to implement this mitigation measure.

The Army does not plan to design devices for providing redundant protection against dropping during handling. It is uncertain whether a workable device for securing munitions could be devised, tested, and manufactured before the destruction of stored munitions commences. There are also uncertainties about worker acceptance of such a device.

3.2 Mitigation of Handling Risks

Six handling accident scenarios were identified as accidents which should be studied to determine if mitigation measures could be applied. Four are accidents in which munition agent compartments are breached and agent is spilled. In addition to the spilled agent, one of the accidents involves a fire. Two accidents involve detonations of burstered munitions.

Five measures were considered for mitigation of accidents involving agent spills: (1) securing the lift truck load, (2) installing grating over the surface, (3) sloping the surface, (4) reducing the response time for containment or destruction, and (5) installing blunt bumpers on tines.

Securing the lift truck load was also considered for mitigating the accident involving a drop which resulted in a detonation. Using battery-powered lift trucks was considered for mitigating the accident resulting in a fire. No mitigation measure was identified for the forklift collision resulting in a detonation. Table 3-2 provides a summary of handling accident scenarios and mitigation measures.

3.2.1 Mitigation Measure: Secure the Lift Truck Load

This mitigation measure is described above in Section 3.1.5.

3.2.2 Mitigation Measure: Install Grating Over the Surface

If a spill occurs on a concrete surface, the liquid agent spreads out as a shallow pool, providing a large area from which agent can evaporate. For example, it is estimated that agent from a ruptured GB ton container could cover an 8400 square foot area. The maximum hazard distance for such an accident is 8.4 km. The size of the pool could be substantially reduced by altering the surfaces over which lift truck operations are performed. This may be done by installing a grating over the surface on which handling operations are performed. The agent would be contained in its interstices and would be somewhat protected from the effect of air movement. The cost of providing movable grating for all eight sites is expected to be about $800,000.

The lower rate of evaporation provided by the grating is expected to reduce the maximum hazard distance from 8.4 km to about 0.8 km. However, decontamination and clean-up would be more difficult and potentially hazardous to the decontamination crew.

3.2.3 Mitigation Measure: Slope the Surface

Another way to reduce the agent surface area available for evaporation would be to slope the surface to drains at the edge of the lift truck operating area. The drain would direct the flow into a sump where the agent could be contained and destroyed by the decontamination crew. The sumps would have to be equipped with overflow valves for discharging rain water, which would have to be drained from the sumps. The cost of installing such a system at all sites is expected to be about $400,000.

The area associated with the slope, drain, and sump system was estimated to be about 375 square feet, thus reducing the effective area for evaporation (in the case of a ruptured ton container, for example) by 95 percent. The maximum hazard distance would be reduced from 8.4 km to about 1.8 km. The benefit for smaller smaller spills would be proportionately less.

TABLE 3-2
SUMMARY OF HANDLING ACCIDENT SCENARIOS AND MITIGATION MEASURES

Accident Scenario	Max. Hazard Distance (km)	Probability	Mitigation Measure	Cost	Expected Benefit: Maximum Hazard Distance (km)	Expected Benefit: Probability
Dropped munition or container results in spill	8.4	$2x10^{-3}$	Lift truck load secured	$ 900,000	--	$4x10^{-5}$
			Install grating	800,000	0.8	--
			Slope surface	400,000	1.8	--
			Cover spill within 15 min.	900,000	4.8	--
Collision results in spill	8.4	$7x10^{-4}$	Install grating	$ 800,000	0.8	--
			Slope surface	400,000	1.8	--
			Cover spill within 15 min.	900,000	4.8	--
Collision results in spill with fire	7.8	$8x10^{-5}$	Battery powered lift trucks	$1,300,000	--	$8x10^{-5}$
Forklift tines puncture munition	0.8	$8x10^{-4}$	Blunt bumpers on tines	$ 80,000	--	$3x10^{-4}$
			Install grating	800,000	0.1	--
			Slope surface	400,000	0.2	--
			Cover spill within 15 min.	900,000	0.5	--
Dropped munition or container results in detonation	6.0	$8x10^{-4}$	Lift truck load secured	$ 900,000	--	$2x10^{-5}$
Collision results in detonation	6.0	$2x10^{-5}$	None	--	--	--

3.2.4 Mitigation Measure: Reduce the Response Time by Covering the Spill

The consequences of an accident resulting in a spill could be mitigated by reducing the time required to respond to the spill and contain or destroy it. The risk analysis assumes that a spill resulting from a handling accident has a duration of up to one hour, during which time agent continues to evaporate. The time of evaporation could be reduced by immediately covering any spill with foam or other material to blanket the spill. The blanketing material would be applied by a standby vehicle carrying foam dispersion equipment. Its function would be to prevent evaporation until decontamination solution could be applied to the spill. There would be an added advantage if the components of the foam included substances that destroy agent.

Foam equipment of this type is commercially available. Some laboratory work would be needed to select a suitable blanketing material. The cost of providing suitable foam-delivery systems is expected to be under $900,000. This does not include the added labor cost that might be required for standby crews.

A standby blanketing system is expected to stop the evaporation from a spill in less than 15 minutes. Since the original response time was up to one hour, the amount of agent released would be reduced by about 75 percent, reducing the maximum hazard distance from 8.4 km to about 4.8 km.

3.2.5 Mitigation Measure: Install Blunt Bumpers on Tines

When a forklift operator is attempting to place the forklift tines under a pallet, an error could result in a tine puncturing an agent compartment, spilling the agent. The probability that a puncture will occur would be reduced by increasing the area which strikes the munition and by making the tip of softer material such as rubber. A bumper about eight inches across and one inch wide would accomplish this and would also fit under the pallets. The total cost of implementing this measure is expected to be about $80,000.

It was estimated that increasing he cross-sectional area of the tines would reduce the probability of a puncture by about 65 percent. No credit was taken in this estimate for the cushioning effect of the rubber because the energy absorption capabilities of the material are not known. Forklift operators might experience some difficulty in using the modified lift truck.

3.2.6 Mitigation Measure: Use Battery-Powered Lift Trucks

If a handling accident results in an agent spill a fire could occur at the same time. In the risk analysis the fire is presumed to be externally

initiated -- that is, fuel (e.g., diesel fuel from the lift truck) is ignited and the fire spreads to the agent, which provides additional fuel for the fire. Since the duration of the fire is not expected to exceed ten minutes the available fire-fighting capability has little mitigative effect on this accident.

The probability of the accident occurring can be reduced by removing fuel from the immediate vicinity of the handling operation by using only battery-powered lift trucks for all movements. Battery-powered trucks are now in use for all movements requiring igloo entry. Although battery-powered trucks capable of lifting off-site containers are not commercially available, batery-powered lifting devices could be built to meet this requirement. As an additional precaution, battery-charging stations should be located remotely from the storage area to prevent fires from being initiated by electrical discharges or flammable gas generation. The total cost of using battery-powered equipment is expected to be about $1.3 million over the cost of diesel-powered equipment for the on-site alternative. The cost increase for the collocation alternative would be greater.

3.2.7 Proposed Action

Reducing the evaporation time to 15 minutes or less by covering a spill with a blanket of foam or other material appears to be the most likely mitigation measure to succeed in providing substantial benefits. Therefore, the Army plans to take steps to implement this measure. Since installing blunt bumpers on forklift tines does not appear to be difficult to do and will provide some benefits, the Army also plans to implement this measure.

The Army also plans to reduce the likelihood of a fire by using only battery-powered forklifts.

3.3 Mitigation of On-Site Transport Risks

Two types of on-site transport accident scenarios were identified as accidents which should be studied to determine if mitigation measures could be applied. One is an accident which results in an agent spill; the other results in a detonation, with or without a fire. The latter accident does not involve bulk agent containers because a vehicle fire is expected not to last long enough to rupture a container. According to the risk analysis an impact-caused detonation is more than 100 times more likely than a fire-caused detonation.

Two measures were considered for mitigation of accidents resulting in spills: (1) reducing the response time for containment or destruction and (2) reducing the agent temperature. No measures were considered adequate

to prevent a detonation but a protected fire-fighting vehicle was considered for the mitigation of accidents involving fires. Table 3-3 provides a summary of on-site transport accident scenarios and mitigation measures.

3.3.1 Mitigation Measure: Reduce Response Time by Covering the Spill

Vehicle accidents involving agent spills may be mitigated by reducing the time required to respond to the spill and contain or destroy the agent. The risk analysis assumes that a spill resulting from an on-site transportation accident has a duration of up to two hours, during which agent continues to evaporate. The time of evaporation could be reduced by immediately covering the spill with a blanket of foam or other material. The concept is discussed above in Section 3.2.4.

The blanketing system is expected to stop evaporation within 15 minutes. Since the original response time was up to two hours, the amount of agent released would be reduced by 87 percent, reducing the maximum hazard distance from 4.2 to 1.5 km.

3.3.2 Mitigation Measure: Reduce Agent Temperature

Reducing the temperature of agent can reduce the amount evaporated because the evaporation rate is lower at the reduced vapor pressure. Munitions could be chilled to about 0°F by circulating chilled air through the igloos where the munitions are stored. The chilled munitions would then be placed in insulated containers for transport. The use of movable refrigeration units would allow the units to be moved from one igloo to another. Refrigeration of all GB stocks could be accomplished by about 60 mobile igloo refrigeration units. Installation and operating costs are expected to be about $14 million.

Only GB stocks were considered for this mitigation measure because VX and mustard spills during on-site transportation do not pose a significant public risk. GB spills, especially from ton containers at TEAD, are a risk to the public.

Refrigerating agent is not without risk. Handling chilled munitions might be hazardous because of the possibility of ice and fog forming at the entrance of the chilled igloo. The fuel used to power the refrigeration systems would be a minimal hazard because the generator could be located some distance from handling operations.

Transporting GB stocks that have been chilled would reduce the amount of agent released to the atmosphere during the first hour after an accidental spill. After the first hour, the spilled agent reaches the ambient temperature and the amount released is the same as it would have been without refrigeration. Thus, the magnitude of the benefit depends on the length of time required to contain or destroy the agent. For example, if

TABLE 3-3

SUMMARY OF ON-SITE TRANSPORT ACCIDENT SCENARIOS AND MITIGATION MEASURES

Accident Scenario	Max. Hazard Distance (km)	Probability	Mitigation Measure	Cost	Expected Benefit Maximum Hazard Distance (km)	Expected Benefit Probability
Vehicle accident or earthquake crushes or punctures munition, resulting in a spill	4.2	$4x10^{-5}$	Cover spill within 15 min.	$ 800,000	1.5	--
			Reduce agent temperature	14,000,000	3.6	--
Vehicle accident with fire and/or detonation	33	$6x10^{-5}$	Protected fire-fighting vehicle	$ 2,400,000	--	--

[a]Cost of chilling munitions for on-site transport is $3,000,000 incremental over cost chilling for off-site transport if off-site transport of chilled munitions is adopted.

the clean-up time is two hours, the maximum hazard distance is reduced from 4.2 km to about 3.6 km by chilling.

3.3.3 Mitigation Measure: Protected Fire-Fighting Equipment

Ordinary fire-righting equipment is not effective against fires where explosives are present because of the danger to personnel attempting to bring the fire under control. If the fire-fighting crew could be protected, such fires could be brought under control, in all or most cases, before the fire caused the explosives to detonate. This could be accomplished by placing the crew in a vapor-sealed armored personmer carrier with remotely-operated, trailer-mounted fire-fighting equipment in tow. The equipment would include a tank of water, a tank of foam concentrate, a high-head diesel-powered pump and nozzle capable of delivering foam to a distance of 200 feet. The turret would be remotely operated by the crew in the personnel carrier. With this equipment, a properly trained crew could safely approach within 200 feet of a burning vehicle and bring the fire under control in a few minutes.

Alternatively, an airport crash truck equipped with a foam delivery device could be modified to provide protection for the crew inside the truck. It is estimated that 12 such vehicles (two for each of the six sites where on-site transport is required) would cost about $2.4 million.

Using a protected, mobile fire-fighting system is expected to bring a vehicle fire under control in time to prevent fire-caused detonations about 99 percent of the time. However, the probability of a fire-caused detonation is less than one percent of the probability of an impact-caused detonation. Therefore this mitigation measure will not appreciably reduce the probability of a detonation in the event of a vehicle accident.

3.3.4 Proposed Action

The most promising and cost-effective measure for mitigating an accident which results in a spill is to reduce the evaporation time by covering the spill with a foam blanket. The Army plans to provide the equipment necessary to do this.

The Army plans to consider methods of protecting fire-fighting crews to enable them to effectively control vehicle fires during on-site transportation of burstered munitions.

3.4 Mitigation of Off-Site Transport Risks

Two modes of of-site transportation were included in the risk analysis: (1) rail and (2) air from Lexington and Aberdeen to Tooele.

Two rail accident scenarios described in the risk analysis were identified as accidents which should be studied to determine if mitigation measures could be applied. Two air accident scenarios were similarly identified. One rail scenario and one air scenario represent accidents that result in an agent spill. The other scenarios represent accidents resulting in fire and/or detonation.

The only practicable measure for mitigating a spill accident that was identified was to transport stocks at a low temperature. No mitigation measures were identified for transportation accidents resulting in fire or detonation. Table 3-4 provides a summary of off-site transport accident scenarios and mitigation measures.

3.4.1 Mitigation Measure: Transport at Low Temperature

Reducing the the temperature of agent can reduce the amount evaporated in two ways:

1. Reducing the temperature lowers the vapor pressure, thus decreasing the evaporation rate.

2. In the case of mustard, which is readily frozen, solidified agent will not spread out and provide a large area for evaporation. Thus, the evaporation rate is reduced.

Transporting at a reduced temperature would mitigate the consequences of accidents involving mustard or GB. It would not appreciably mitigate accidents involving VX because it has a very low vapor pressure at ambient temperature.

As described in Section 3.3.2, munitions stored in an igloo could be chilled by circulating refrigerated air through the igloo. The use of movable refrigeration units would allow the units to be moved from one igloo to another. Munitions not stored in igloos could be moved to empty igloos for chilling; at sites where there are no igloos, agent could be chilled in a refrigerated building. Chilled munitions and agent would then be placed in insulated or refrigerated containers for transport by rail or air.

Refrigeration of all GB and mustard stocks that would be moved off-site could be accomplished by about 64 mobile refrigeration units and one refrigerated building. Installation and operating costs for the national disposal alternative are expected to be about $17 million. For the regional alternative, 52 mobile units and one refrigerated building would be required and the total cost would be about $14 million. The cost of refrigerating the stocks at LBAD and APG for air transport would be about $4.7 million.

TABLE 3-4
SUMMARY OF OFF-SITE TRANSPORT ACCIDENT SCENARIOS AND MITIGATION MEASURES

Accident Scenario	Max. Hazard Distance (km)	Probability	Mitigation Measure	Cost	Expected Benefit: Maximum Hazard Distance (km)	Expected Benefit: Probability
Rail accident crushes or punctures munition, resulting in a spill	2.2	9×10^{-4}	Transport at low temperature	$17,000,000	2.0	--
Rail accident results in fire and/or detonation	19.1	2×10^{-4}	None	--	--	--
Aircraft carrying munitions crashes without fire; spill occurs	31[a]	1×10^{-3}[a]	Transport at low temperature	$ 4,700,000	31[b]	--
Aircraft accident with fire; detonation may occur	25[c]	7×10^{-4}[c]	None	--	--	--

[a]Values given in the table are for C-141 aircraft; for C5A aircraft the maximum hazard distance = 64 km and the probability = 2×10^{-3}.
[b]There is negligible benefit if it takes 24 hours to destroy or contain a GB spill; an 8 percent reduction in hazard distance is expected if the duration is 6 hours.
[c]Values given in the table are for C-141 aircraft; for C5A aircraft the maximum hazard distance = 39 km and the probability = 1×10^{-3}.

Transporting GB stocks that have been chilled would reduce the amount of agent released to the atmosphere only during the first hour after an accidental spill. Thus, the magnitude of the benefit depends on the length of time required to contain or destroy the spilled agent. For example, if six hours (the maximum time assumed in the risk analysis for a rail accident) is used, the maximum hazard distance is reduced from 2.2 km to about 2.0 km by chilling GB. Similarly, the maximum hazard distance for an air accident would be reduced from 31 km to 28.5 km if the spill is cleaned up in 6 hours. However, if the spill is not contained for 24 hours (the maximum time assumed in the risk analysis for air accidents) the benefit is negligible.

The benefit for chilling mustard stocks is greater because mustard is readily frozen and in the solid state does not evaporate as easily as in the liquid state. For example, if the cleanup time is six hours, the maximum hazard distance for a rail accident is reduced from 0.4 to 0.1 km by chilling. For an aircraft accident the maximum hazard distance is reduced from 3.0 to 1.2 km.

3.4.2 Proposed Action

Chilling munitions does not appear to provide a significant reduction in the consequences of a GB agent spill during transport. Therefore, the Army does not plan to implement this mitigation measure for munitions or bulk items containing GB. However, since there are more substantial benefits for freezing bulk mustard, the Army plans to ship ton containers of mustard in a frozen state, if off-site transportation is required.

3.5 Mitigation of Plant Operations Risks

Eleven plant operations accident scenarios were selected for review. Five of the scenarios are accidents caused by external events (earthquakes and aircraft crashes). The remaining scenarios involve detonations caused by equipment failure or operator error. The high-consequence accidents (maximum hazard distance >27 km) are all externally-caused. The maximum hazard distances for the internally-caused accidents range from 1.5 to 6.1 km.

For the aircraft crash accident the mitigation measure considered was restricting air space. Four mitigation measures were considered for earthquake-caused accidents: (1) installing seismic-actuated gas cutoff valves and lighting circuit breakers; (2) reducing the presence of probes in the Unpack Area (UPA); (3) reinforcing the UPA; and (4) modifying the conveyor.

The mitigation measures considered for internally-caused accidents concentrate on eliminating equipment failure and reducing the potential for human error. Four measures were considered for mitigating an explosion

TABLE 4-1
MITIGATION MEASURES WHOSE EFFECT IS EVALUATED

A. Mitigation Revision 1

The following mitigation measures are those that the Army plans to implement:

1. Reduce the response time for containing or destroying a spill by covering the spill.

2. Use battery-powered lifing devices for handling.

3. Install blunt bumpers on lift truck tines.

4. Use improved mobile device to control vehicle fire during on-site transportation.

5. Install seismic-actuated gas cutoff valves and category 3 circuit lighting circuit breakers in the MDB.

6. Install a metal shield over the conveyor between the UPA and the ECR.

7. Implement changes in the UPA to prevent mines and rockets from being accidentally conveyed to the DUN. All measures necessary to reduce by two orders of magnitude the probability of a munition reaching the DUN will be implemented.

8. Transport mustard ton containers in a frozen state if off-site transportation is required.

9. De-energize warehouse electrical systems using seismically-actuated circuit breakers or disconnected electrical leads.

B. Mitigation Revision 2

Mitigation revision 2 includes all of the above mitigation measures with the additional step of restricting air space and eliminating military flights at all of the sites.

in the Metal Parts Furnace (MPF): (1) installing a redundant fuel cutoff valve; (2) using steam to purge the furnace; (3) using nitrogen to purge the furnace; and (4) using gas from an inert gas generator to purge the furnace. Two measures were considered for preventing munitions from falling from the conveyor and detonating: (1) reducing conveyor speed and (2) installing a metal cage over the conveyor. Finally, four measures were considered for reducing the likelihood of a munition being fed to the Dunnage Incinerator (DUN) and detonating: (1) using x-rays to screen dunnage; (2) interlocking a metal detector with the conveyor; (3) interlocking a mine counter with the conveyor; and (4) using a mechanical hoist to move rockets. No practicable measure was identified for mitigation of detonations in the Explosive Containment Room (ECR).

Table 3-5 provides a summary of plant operations accident scenarios and mitigation measures.

3.5.1 Mitigation Measure: Restrict Air Space

Establishing air space restrictions could substantially reduce the expected frequency of an aircraft crash on the disposal plant. According to the risk analysis, the building will be designed to withstand small aircraft crashes; therefore, this mitigation measure is directed against crashes of large aircraft only. This mitigation measure is discussed in Section 3.1.1.

3.5.2 Mitigation Measure: Install Seismic-Actuated Gas Cutoff Valves and Lighting Circuit Breakers

The most serious consequences of an earthquake-initiated accident occur when the fuel lines are damaged and a fire occurs. This accident may be mitigated by shutting off the fuel supply and eliminating the most likely source of ignition (broken power lines).

A valve designed to actuate under earthquake forces to shut off gas flow could be placed on the main gas supply line to the Munitions Demilitarization Building (MDB). The purpose of the valve would be to limit fuel to any fire that could occur within the building. It would also prevent further damage to the building by precluding a gas explosion.

A special test circuit circuit breaker could be placed on the lighting circuits in the UPA to prevent initiation of a fire by short circuiting lighting fixtures. Normal circuit breakers might "chatter" during an earthquake and not cut current even though a short had occurred. The special breaker is considered necessary only for lighting circuits because other circuits are more substantial and less prone to damage.

This mitigation measure is expected to cost about $30,000 at each site. The estimated risk reduction depends on the scenario. For those

TABLE 3-5
SUMMARY OF PLANT OPERATION ACCIDENT SCENARIOS AND MITIGATIVE MEASURES

Accident Scenario	Max. Hazard Distance (km)	Probability	Mitigation Measure	Cost	Expected Benefit: Maximum Hazard Distance (km)	Expected Benefit: Probability
Aircraft crash direct/indirect with/without fire (PO 12, 13, 18 and 19)	46.5	3.1×10^{-7}	Restrict airspace	--	46.5	3.1×10^{-8}
Earthquake scenario measures identified below are common to several scenarios. Effectiveness changes with scenario.						
Earthquake damages MDB, munitions fall, fire starts, munition is punctured, and fire is suppressed (PO 25)	5.5	1.2×10^{-5}	Seismic-actuated gas cutoff and special UPA lighting breakers	$ 30,000	5.5	1.2×10^{-5}
			Probe reduction	Minimal	5.5	1.2×10^{-6}
			Reinforce UPA	$900,000	5.5	6.0×10^{-6}
			Modify conveyor	Minimal	5.5	6.0×10^{-6}
Earthquake damages MDB, munitions fall, fire starts, munition is punctured, and fire suppression fails (PO 28)	27.8	6.3×10^{-7}	Seismic-actuated gas cutoff and special UPA lighting breakers	$ 30,000	27.9	1.1×10^{-7}
			Probe reduction	Minimal	27.9	6.3×10^{-8}
			Reinforce UPA	$900,000	27.9	4.2×10^{-7}
			Modify conveyor	Minimal	27.9	3.2×10^{-7}
Earthquake damages MDB, munitions fall, fire starts, munition remains intact, and fire suppression fails (PO 29)	27.8	3.8×10^{-4}	Seismic-actuated gas cutoff and special UPA lighting breakers	$ 30,000	27.9	5.2×10^{-5}
			Probe reduction	Minimal	27.9	3.8×10^{-4}
			Reinforce UPA	$900,000	27.9	2.5×10^{-4}
			Modify conveyor	Minimal	27.9	3.8×10^{-4}

TABLE 3-5
SUMMARY OF PLANT OPERATION ACCIDENT SCENARIOS AND MITIGATIVE MEASURES
(Continued)

Accident Scenario	Max. Hazard Distance (km)	Probability	Mitigation Measure	Cost	Expected Benefit: Maximum Hazard Distance (km)	Expected Benefit: Probability
Earthquake does not damage MDB, munitions fall, fire starts, and fire suppression fails (PO 33)	27.9	6.8×10^{-5}	Seismic-actuated gas cutoff and special UPA lighting breakers	$ 30,000	27.9	3.1×10^{-6}
			Probe reduction	Minimal	27.9	6.8×10^{-5}
			Reinforce UPA	$900,000	27.9	6.8×10^{-5}
			Modify conveyor	Minimal	27.9	6.8×10^{-5}
MPF explosion due to fuel shutoff failure (PO 42)	6.1	1.1×10^{-7}	Redundant fuel-cutoff valve on MPF main gas supply line	$ 25,000	6.1	1.0×10^{-7}
			Insert gas purge using steam	$250,000	6.1	1.1×10^{-7}
			Insert gas purge using nitrogen	$150,000	6.1	1.1×10^{-7}
			Insert gas purge using an inert gas generator	$500,000	6.1	1.1×10^{-9}
Munition falls from ECV conveyor and detonates				--		
Munition falls from ECV conveyor and detonates. No fire (PO 45)	1.9	4.7×10^{-7}	Lower conveyor speed for 8-in. projectiles	Minimal	1.9	4.7×10^{-7}
			Install metal cage (shield) over conveyor	Minimal	1.9	4.7×10^{-7}

TABLE 3-5
SUMMARY OF PLANT OPERATION ACCIDENT SCENARIOS AND MITIGATIVE MEASURES
(Concluded)

Accident Scenario	Max. Hazard Distance (km)	Probability	Mitigation Measure	Cost	Expected Benefit: Maximum Hazard Distance (km)	Expected Benefit: Probability
Munition falls from ECV conveyor and detonates. Fire starts (PO 47)	1.5	6.3×10^{-8}				
			Lower conveyor speed for 8-in. projectiles	Minimal	1.5	6.3×10^{-8}
			Install metal cage (shield) over conveyor	Minimal	1.5	6.3×10^{-10}
Munition detonates in ECR						
Munition detonation fails ECR and ventilation system (PO 49)	3.5	5.1×10^{-6}	No mitigative measure proposed. Further study required	--	--	--
Munition detonation fails ECR and ventilation. Fire starts (PO 50)	3.5	8.8×10^{-7}	No mitigative measure proposed. Further study required	--	--	--
Burstered munition fed to DUN (PO 52)	2.9	1.1×10^{-2}	Further study required before measures are incorporated			
			Use X-rays to screen dunnage	$250,000	2.9	3.7×10^{-3}
			Interlock metal detector to stop conveyor	$ 50,000	2.9	3.7×10^{-3}
			Interlock mine counter to stop dunnage	Minimal	2.9	3.6×10^{-3}
			Use mechanical effector to move rockets	$ 30,000	2.9	8.3×10^{-3}

earthquake-caused accidents resulting in fire the probability of the event would be reduced by 82 to 95 percent.

3.5.3 Mitigation Measure: Reduce the Presence of Probes in the UPA

In the event of an earthquake, munitions may fall on sharp objects (probes). A punctured munition may either contribute fuel to a fire in the UPA or directly release agent into the atmosphere. Although the UPA is generally devoid of objects on the floor that would puncture falling munitions, this mitigation measure calls for reviewing equipment design and redesigning where necessary to eliminate potential probes. An analysis would also be done of the path of travel of munitions and bulk containers to identify potential primary probes in the path and to identify secondary probe-producing objects (e. g., sprinkler piping). Although the estimated cost of this measure is expected to be minimal, the impact of of redesign or removal of equipment is difficult to predict.

The estimated risk reduction for this measure depends on the scenario. Accidents involving puncture are reduced in probability one order of magnitude. Other earthquake-caused accidents are not affected.

3.5.4 Mitigation Measure: Reinforce the UPA

The probability of a breach of the UPA in an earthquake could be reduced by designing the building for structural unity at higher ground acceleration. Designing for higher ground acceleration does not, on its own, reduce the probability of this breach. Instead, the area of the UPA must be considered as a unit and designed to maintain ductility throughout the combined acceleration/velocity/displacement-versus-time history. Building material and stiffening methodology would have to be developed. There would be a substantial program delay to accomplish this significant design change. The estimated cost would be about $900,000 at each site.

The benefits for this mitigation measure depend on the scenario. The probability would be reduced by about 1/3 for those accident which result in building damage. There is no benefit in the case of an earthquake which causes munitions to fall but does not damage the building.

3.5.5 Mitigation Measure: Modify the Conveyor

In an earthquake, munitions being moved by conveyor may fall off and be ruptured. The conveyor could be modified to reduce the potential for the munitions to fall. This would involve placing stops at the conveyor ends and deepening the channels on the conveyor sides. The cost would be minimal.

A reduction of about 50 percent is expected for those accidents in which a munition falls and is ruptured. There are potential human factors

and operational difficulties associated with this measure because of the reduced clearances and a corresponding increase in pinch points on the conveyor.

3.5.6 Mitigation Measure: Install a Redundant Fuel Cutoff Valve

When the MPF is shut down there is a possibility that the logic controllers will fail or that the fuel cutoff valves will fail to shut off fuel. Thus, an explosive mixture could occur which could result in an explosion in the MPF.

One way to mitigate this accident is to provide redundancy by installing an additional automatically actuated cutoff valve to the main gas supply line to the furnace. It is expected that this measure would cost about $25,000 at each site.

This measure is expected to reduce the probability of failure by only ten percent. The reason for the limited benefit is the potential for common cause failures to affect all the valves within the train. Precautions should be taken when adding the valve to the system that common cause failures are avoided so that the valve will provide true redundancy. The following administrative and design measures are suggested: (1) Use different valve suppliers; (2) use different valve actuation mechanisms; (3) require routine, periodic tests of valve function and demonstration tests following valve maintenance; and (4) incorporate position-proving fuel valve shutoff switches, fuel line flow sensors, or combustion gas analyzers to alarm on potential fuel flow or explosive atmosphere. Although the effect of these precautions was not evaluated, it is expected that a close approach to full redundancy can be achieved.

3.5.7 Mitigation Measure: Use Steam to Purge the Furnace

An explosion in the MPF could be precluded if the formation of an explosive atmosphere within the furnace were prevented. One way to do this would be to inject steam into the furnace. The estimated cost of this measure is $20,000 at each site.

Although steam injection is technically feasible, there are some drawbacks to this measure. The chief difficulty would be in determining when to initiate the purge, in establishing how long a purge is required, and in maintaining a sufficiently long purge. Moreover, the fuel would continue to flow into the furnace until some other measure were taken to shut it off. Steam injection could complicate destruction of agent within the furnace and subsequent furnace decontamination. Steam could also degrade the furnace lining to the point where it would need replacement. Consideration of these difficulties led to the conclusion that this measure would not reduce the risk of an explosion in the MPF.

3.5.8 Mitigation Measure: Use Nitrogen to Purge the Furnace

Another way of preventing the formation of an explosive atmosphere in the MPF would be to inject nitrogen into the furnace. The estimated cost is $150,000.

As in the case of steam injection, it would be difficult to determine when to initiate the purge and how long a purge is required, and to maintain a sufficiently long purge. It would also be necessary to take some other action to shut off the fuel. There could be some adverse impact on agent destruction in the furnace. Because of these difficulties, nitrogen injection is not expected to reduce the risk of an explosion in the MPF.

3.5.9 Mitigation Measure: Use Gas from an Inert Gas Generator to Purge the Furnace

A third way of preventing the formation of an explosive atmosphere in the MPF was also considered. This involves the use of an inert gas generator to provide an inert atmosphere and to combust the fuel released during the accident. If used with a feedback loop, the generator could positively result in neutralization of any explosive atmosphere that could be formed within the furnace. Thus, unlike the injection of steam or nitrogen, an inert atmosphere could be maintained within the furnace. Since the generator would maintain temperature in the furnace, there should be no problem with agent destruction. There might be a design delay due to the requirement to integrate the generator system with the furnace and its control system. The estimated cost of this measure is $500,000.

The probability of an explosion in the MPF is expected to be reduced by two orders of magnitude. Although this measure does not appear to have the most serious drawbacks of steam or nitrogen injection, there is still the difficulty of determining when a purge is required. Moreover, the reliability of the generator system is uncertain because of its complexity.

3.5.10 Mitigation Measure: Reduce Conveyor Speed

Munitions are moved from the UPA to the ECR by a conveyor with devices to center the munitions as they are conveyed. For projectiles, the conveyors will have rollers that are slightly dished and for rockets guide rails that come slightly above the centerline will be provided. Despite these design features, the possibility exists that a munition could fall from the conveyor and detonate. 8-inch projectiles have been observed to oscillate in a vertical plane as they are conveyed at the design speed of 120 linear feet per minute.

A mitigative measure applicable to 8-inch projectiles is to reduce the speed of the conveyor during movement of these munitions. The other munitions would be conveyed at the higher speed in order to maintain production rates. This would require incorporation of a two-speed drive into the conveyor. This measure could be implemented at a minimal cost.

Although a slower conveyor speed would appear to reduce the chance of a fall, no appreciable reduction in the probability of this accident could be determined.

3.5.11 Mitigation Measure: Install a Metal Cage over the Conveyor

Munitions could be prevented from falling off the conveyor by installing metal cage over the conveyor. The cage would be permanently installed but would have bars spaced in such a manner as to allow access to conveyor components. Alternatively, a removable metal shield more thoroughly covering the conveyor could be used. The exact design would be determined following an analysis of maintenance and changeover requirements. The cage could be installed at a minimal cost.

3.5.12 Mitigation Measure: Use X-Rays to Screen Dunnage

An operator error during dunnage transfer in the UPA could result in a munition being accidentally placed in a dunnage box and conveyed to the DUN, where the munition detonates. The DUN is not designed for explosive containment. The operator error is considered possible only with small munitions (105-mm cartridges, mines, and rockets) that can be easily handled by one person. There will be a number of personnel (operators, a supervisor, a quality assurance specialist) who would be likely to notice an operator error of this magnitude, especially in the case of cartridges and rockets. Mines are removed from drums in a glovebox which will restrict visibility of dunnage transfer to operators.

One method of providing additional scanning would be to use an x-ray scanner to monitor the dunnage box. The scanner would be located at the airlock into the DUN, which would not open without a positive signal from the scanner operator. The cost of this measure is expected to be $250,000 at each site where this accident could occur.

The x-ray scanner is expected to reduce the probability of a detonation in the DUN by about 66 percent. The major problems with this measure would be maintenance and the human error rate associated with repetitive scans. Maintenance would probably have to be done by outside technicians and could entail extensive interruptions to the operation of the UPA.

3.5.13 Mitigation Measure: Interlock a Metal Detector with the Dunnage Conveyor

A metal detector could be used to detect the presence of munitions in the dunnage box. The detector could be interlocked with the DUN airlock, which would not open unless it received a signal from the detector. The system could be used for cartridges and rockets. It could be used for mines only if the drums in which mines are transported were not sent to the DUN. The cost is expected to be $50,000 at each site where this accident could occur.

The metal detector is expected to reduce the probability of a detonation in the DUN by about 66 percent. The chief drawback of this measure is the potential for false alarms triggered by other metal (e.g., metal banding). The unit could be calibrated to respond to a given mass of metal and could be adjusted to minimize the false alarms. Actual tests of the detectors would be required to determine the false positive alarm rates for different munitions.

3.5.14 Mitigation Measure: Interlock a Mine Counter with the Dunnage Conveyor

The probability of a mine entering the DUN and being detonated there would be reduced if counters for explosive components and mines at the mine glovebox were interlocked to the feed to the dunnage conveyor. Interlocking the counters also to the drum crushing station would have the added benefit of preventing a mine detonation there. Multiple sensors would be used to detect mines and explosive components inserted through silhouette holes, thus ensuring that dunnage cannot trip counters if inserted through mine and explosive out ports. A secondary check could be provided by weighing items fed to the drum-crushing station. The feed to the dunnage conveyor will not function if the counters do not account for all the mines or if the expected weights are exceeded. The programmable logic controller will automatically screen sensors to determine potential sensor malfunction.

The direct cost of this measure is minimal because it can be done in conjunction with the redesign of the mine glovebox, which is being done to incorporate a drum crushing unit. The indirect cost associated with operational changes cannot be estimated at this time. There could be an impact on furnace operations and buffering both on the bypass conveyor and in the UPA.

Since this measure is applicable only to mines, no credit was taken for mitigation of accidents involving other munitions. The overall probability of a detonation in the DUN would be reduced by about 67 percent.

3.5.15 Mitigation Measure: Use a Mechanical Hoist to Move Rockets

Using a mechanical hoist (effector system) to lift rockets from the pallet would reduce manual handling and the potential for mistaking a rocket as dunnage. The effector unit would lift five rockets at a time from the pallet, placing them on the conveyor feed table. Two persons would position and guide the unit. Vertical rails would extend upward from the frame to aid operators to position the unit. Rails extending down around the edges of the frame would protect rockets from being bumped. The estimated cost is $30,000 for each device.

Since this measure applies only to rockets, no credit was taken for mitigation of accidents involving other munitions. The overall reduction in the probability of this accident occurring is about 25 percent. Disadvantages of the effector system include the difficulty in positioning the unit over the rockets and the potential awkwardness in handling five rockets at a time. There could be potential hazards if rockets were not gripped securely or if the effector unit hit the shipping and firing tubes with force while being lowered.

3.5.16 Proposed Action

Restricting air space is potentially a cost-effective way to mitigate accidents resulting from aircraft crashes (see Sections 3.1.1 and 3.5.1). However, it is not certain that this can be done. Although the Army cannot commit to air space restrictions at this time, a study could be undertaken to determine whether such restrictions can and should be implemented.

Accidents resulting from earthquakes can best be mitigated by installing seismic-actuated cutoff valves and special test lighting circuit breakers (see Section 3.5.2). This measure is relatively cost-effective, can be implemented without program delay, and can reduce the probability of the highest severity/most probable accidents by approximately one order of magnitude.

An explosion in the MPF can best be mitigated by installing a redundant fuel cutoff valve (see Section 3.5.6). Although common cause failures may lessen the expected risk reduction, the recommended administrative and design measures should lessen their effect. The use of either steam or nitrogen to inert the furnace does not appear to be effective and the reliability of the inert gas generator system is questionable. Moreover, the various purge options require significant redesign of the furnace and pollution abatement system.

The Army plans to implement both of the measures considered for preventing munition from falling off the conveyor and detonating. Reducing the conveyor speed (Section 3.5.10) is being considered anyway to reduce

impact stresses on conveyor stops. Installing a metal cage over the conveyor will provide more positive assurance that no munitions fall off the conveyor.

The Army plans to reduce the probability of mines entering and detonating in the DUN by interlocking mine and explosive component counters with the dunnage conveyor feed (see Section 3.5.14). The other mitigation measures considered require additional human factors analysis. The Army plans to continue to pursue mitigative measures until at least a two-order-of-magnitude reduction in probability is achieved.

4.0 POTENTIAL EFFECT OF MITIGATION MEASURES ON RISK

Since the purpose of the effort to identify mitigation measures was to reduce the public risk of the CSDP, we have attempted to quantify the risk reduction that would result if the mitigation measures were implemented. According to the analysis described in Section 3.0, some of the measures were found to be more effective or practicable than others. Therefore, when evaluating the potential effect of mitigation we selected those items that the Army has decided to carry out as part of the disposal program. The mitigation measures listed in Table 4-1 represent two revisions to the disposal plan. Those listed under Revision 1 are the measures the Army has included in its plan. The Army is uncertain at this time about whether air space can or should be done; therefore Revision 2, which includes this mitigation measure, represents mitigation that might be undertaken at a later time.

For the purpose of showing the potential risk reduction due to mitigation, we have chosen to use "expected fatalities" as the measure of risk. Expected fatalities is a value that is calculated as follows:

1. The probability of each potential accident is multiplied by the number of fatalities that could occur if that accident happened.

2. The values obtained in this calculation are summed for all of those accidents involved in a given alternative at a given site.

The values for expected fatalities at each of the eight CONUS sites were calculated in this way to determine the site-specific risk for three cases: (1) unmitigated risk, (2) risk with Mitigation Revision 1 implemented, and (3) risk with Mitigation Revision 2 implemented. The programmatic (overall) risk for each of these cases was determined by adding the site-specific values of expected fatalities.

4.1 Reduction in Programmatic Risk

The effect of mitigation on the programmatic risk is illustrated in Figure 4-1. The bars show the potential effect of mitigation on expected fatalities for each of the CSDP alternatives.

The mitigation measures selected for implementation are expected to substantially reduce the risk of continued storage and on-site disposal. Mitigation Revision 1 has the potential for reducing expected fatalities by at least an order of magnitude for continued storage. This is attributable primarily to reducing the likelihood of a warehouse fire in the event of an earthquake. Restricting air space (Revision 2) could further reduce the risk by 15 percent.

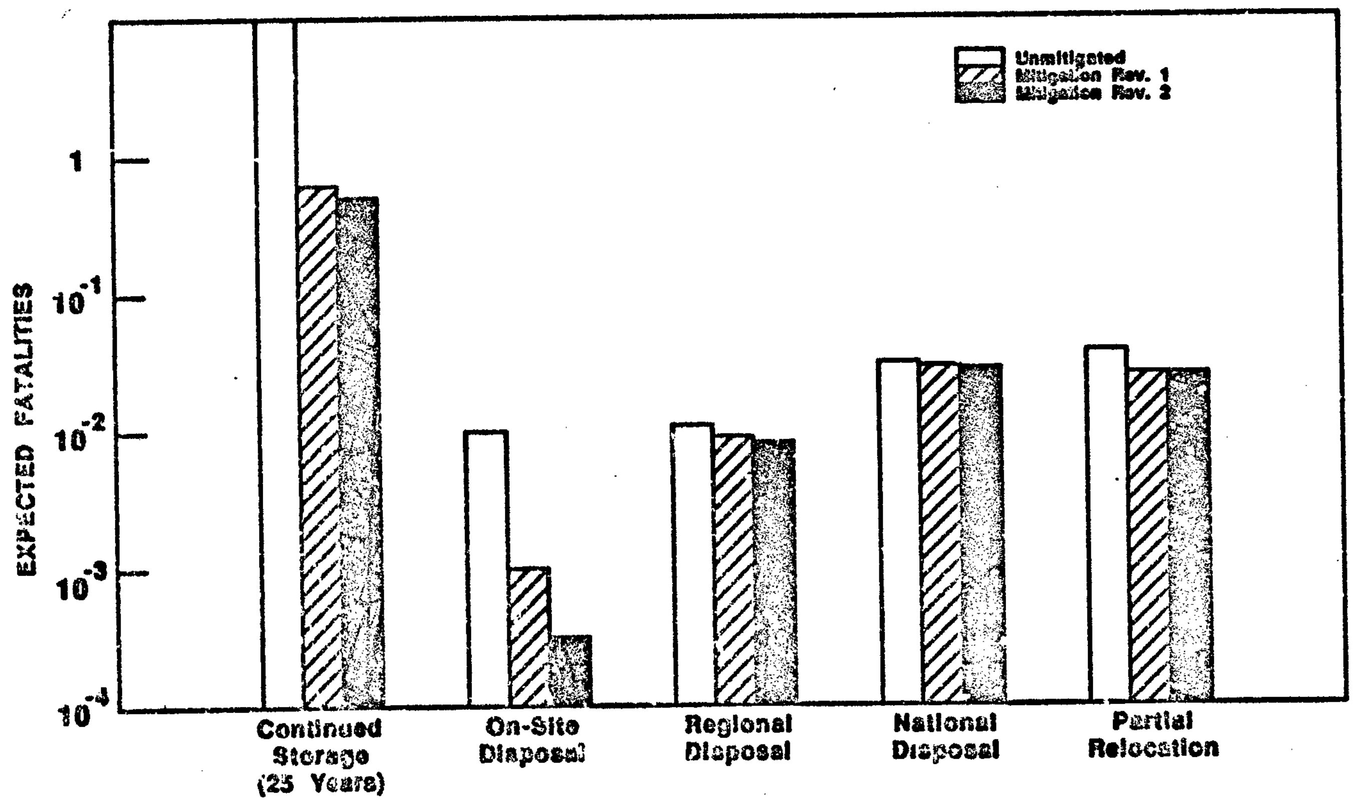

FIGURE 4-1
RISK COMPARISON FOR PROGRAMMATIC ALTERNATIVES
ALL LOCATIONS COMBINED

For the on-site disposal alternative, Mitigation Revision 1 also has the potential for reducing risk by an order of magnitude. This reduction is attributable primarily to mitigation of plant operations accidents. An additional 30 percent reduction could be achieved by restricting air space.

The modest reductions achieved in the alternatives involving movement of munitions is a reflection of the difficulty of mitigating accidents that occur during transportation, as can be seen in Section 3.4. The 25 percent reduction in risk for the partial relocation alternative is entirely attributable to the effect of mitigation at the sites where disposal is carried out; mitigation has little effect at Lexington-Blue Grass and Aberdeen, the sites from which stocks are moved.

4.2 Reduction in Risk at Each Site

The effect of mitigation on a site-specific basis is illustrated in Figures 4-2 through 4-6 for each of the alternatives. Exact values of expected fatalities are not represented on these bar graphs because such information could reveal classified information. Instead, values are given to the nearest order of magnitude. Thus, the mean value for expected fatalities is shown on the graph in the center of the order-of-magnitude range in which it falls. For example, if the value of expected fatalities is 8×10^{-4}, the top of the bar is placed between 10^{-3} and 10^{-4}. The reader should note that the figures for regional disposal, national disposal, and partial relocation do not incorporate the risk along the transportation corridors. There is no measurable effect of mitigation on the risk during transportation.

Mitigation should substantially reduce the risk for continued storage at all sites except Pine Bluff and Pueblo, as shown in Figure 4-2. The reduction in risk due to Mitigation Revision 1 at Newport, Tooele and Umatilla is largely attributable to mitigation of the accident scenario involving an earthquake-caused warehouse fire. At Anniston and Lexington-Blue Grass the mitigation of handling accidents is the major contributor to the reduction in risk. Mitigation Revision 2 reduces the risk at Aberdeen by two orders of magnitude by reducing the probability of an an aircraft crash on ton containers in open storage. Air space restrictions reduce the storage risk at Anniston by about 90 percent by reducing the probability of an aircraft crash on an igloo.

All sites are benefitted by Mitigation Revision 1 for the on-site disposal alternative, as illustrated in Figure 4-3. At Pueblo the value of expected fatalities is too low to show the benefit for mitigation. At all of the sites the major contributor to the reduction in risk is the mitigation of plant operations accidents. At Aberdeen, Newport, and Pueblo the mitigation of the effects of an earthquake provides the greatest benefit; at the other sites, reducing the probability of a detonation in the DUN is

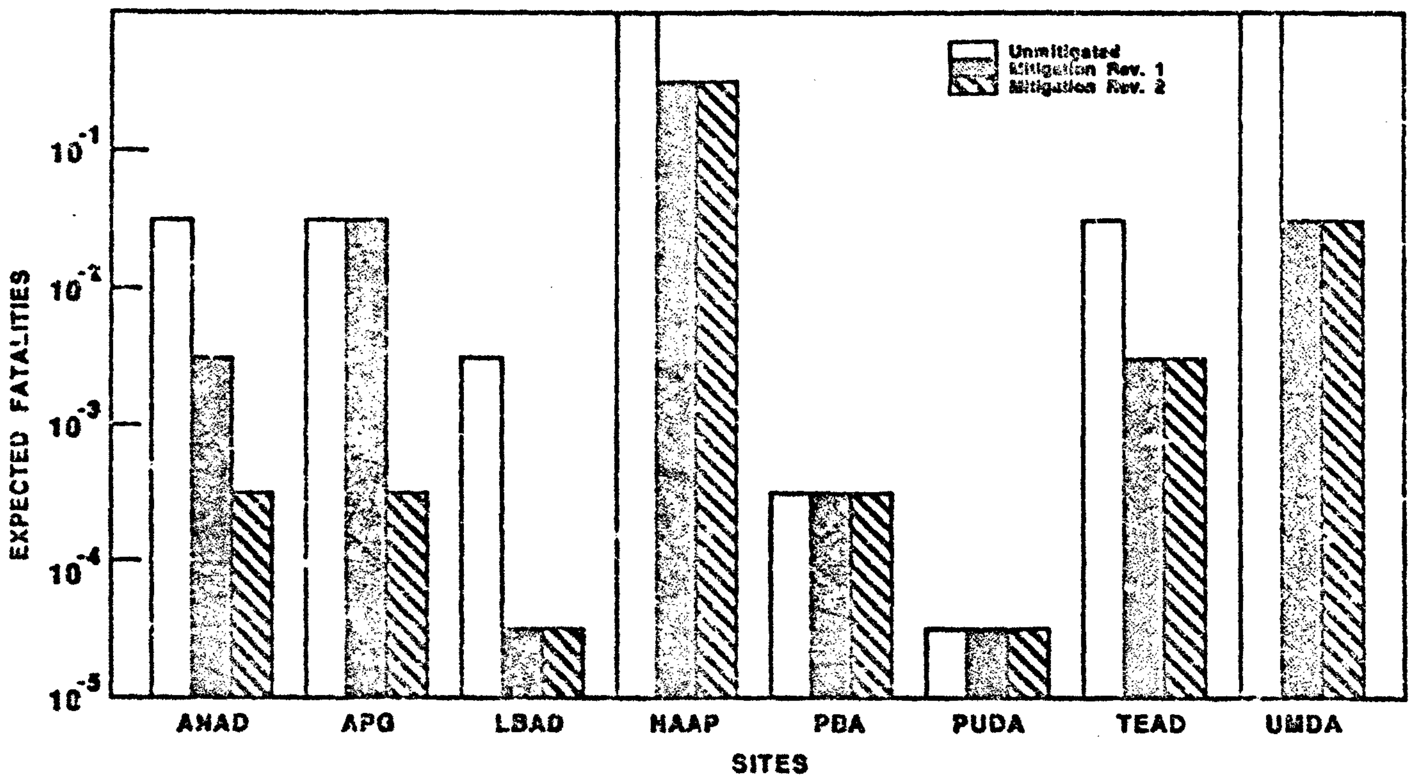

FIGURE 4-2
RISK COMPARISON FOR CONTINUED STORAGE ALTERNATIVE

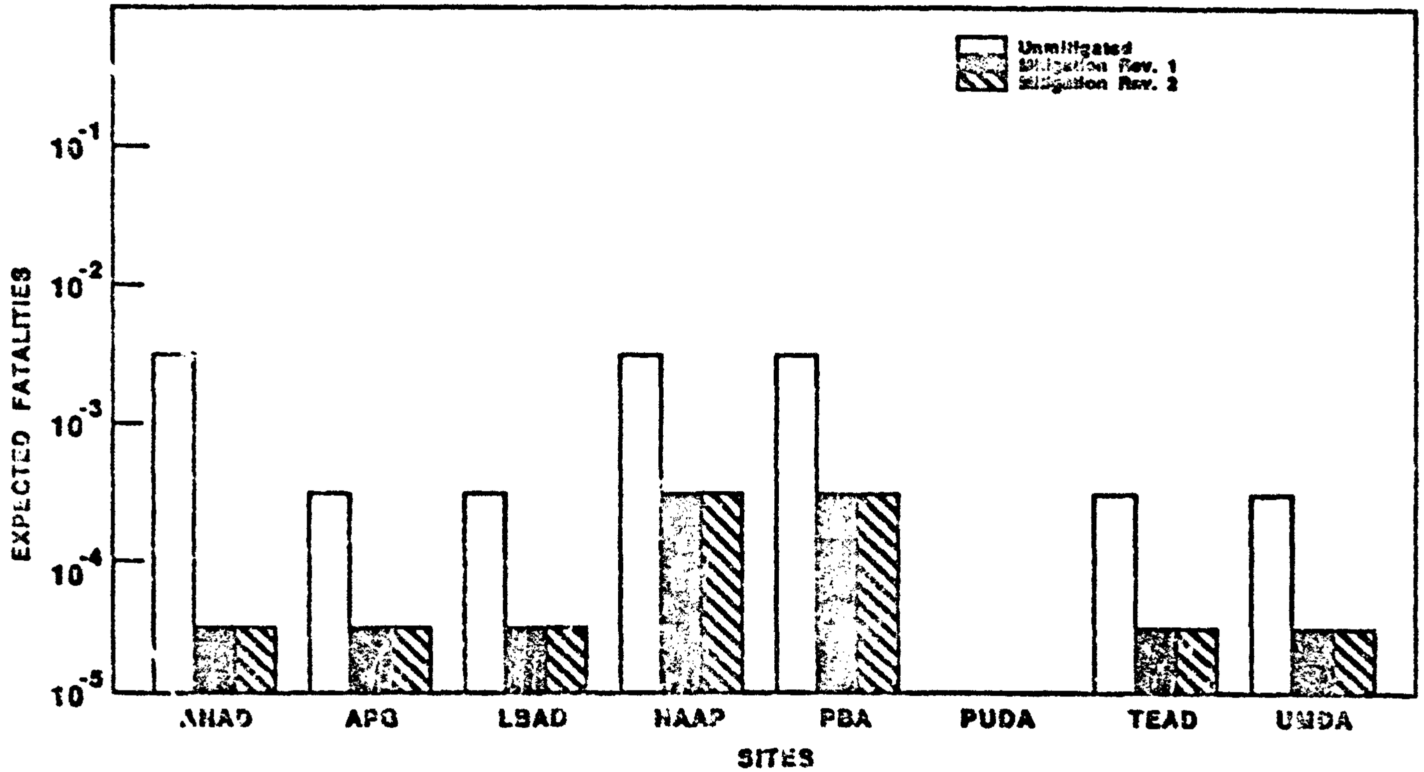

FIGURE 4-5
RISK COMPARISON FOR ON-SITE DISPOSAL ALTERNATIVE

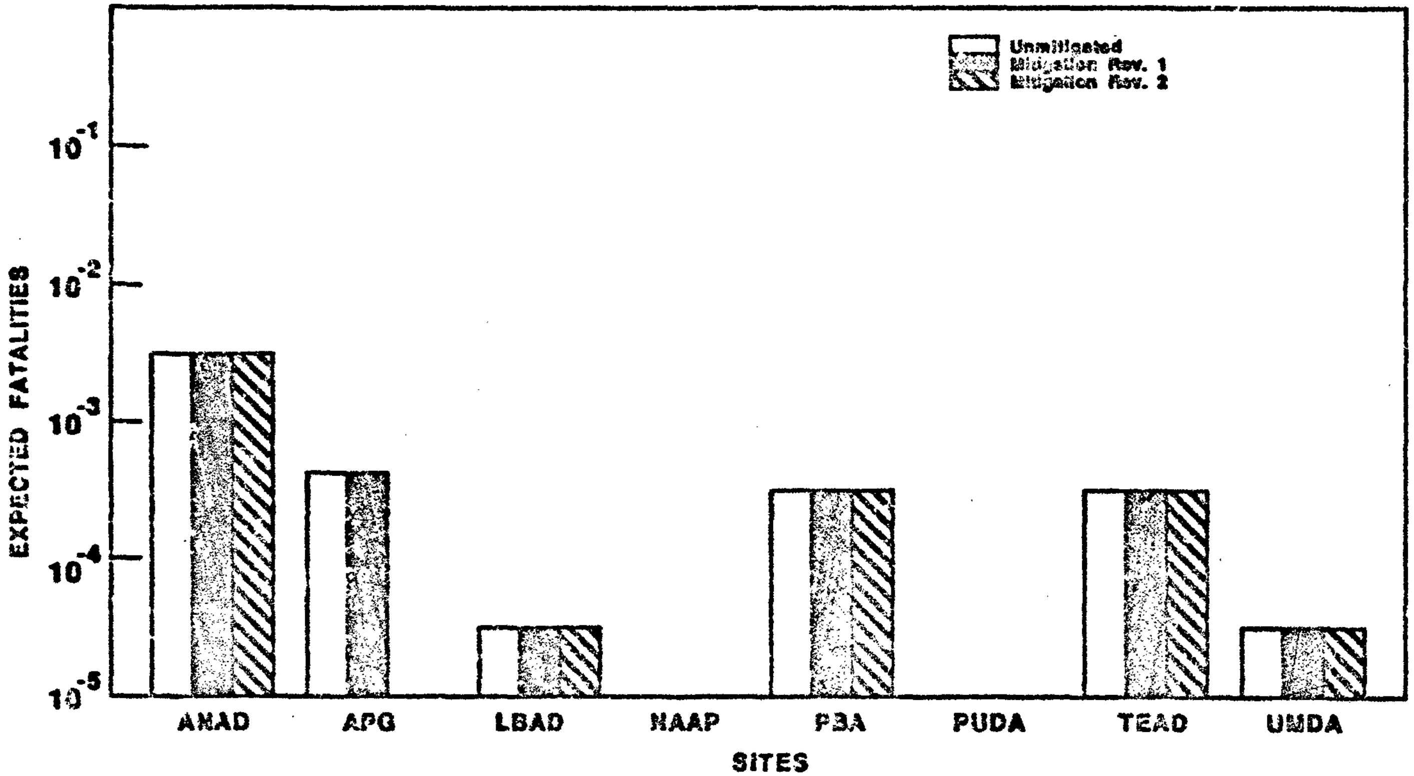

(Risk Along Transportation Corridor Not Included)

FIGURE 4-4

RISK COMPARISON FOR REGIONAL DISPOSAL ALTERNATIVE

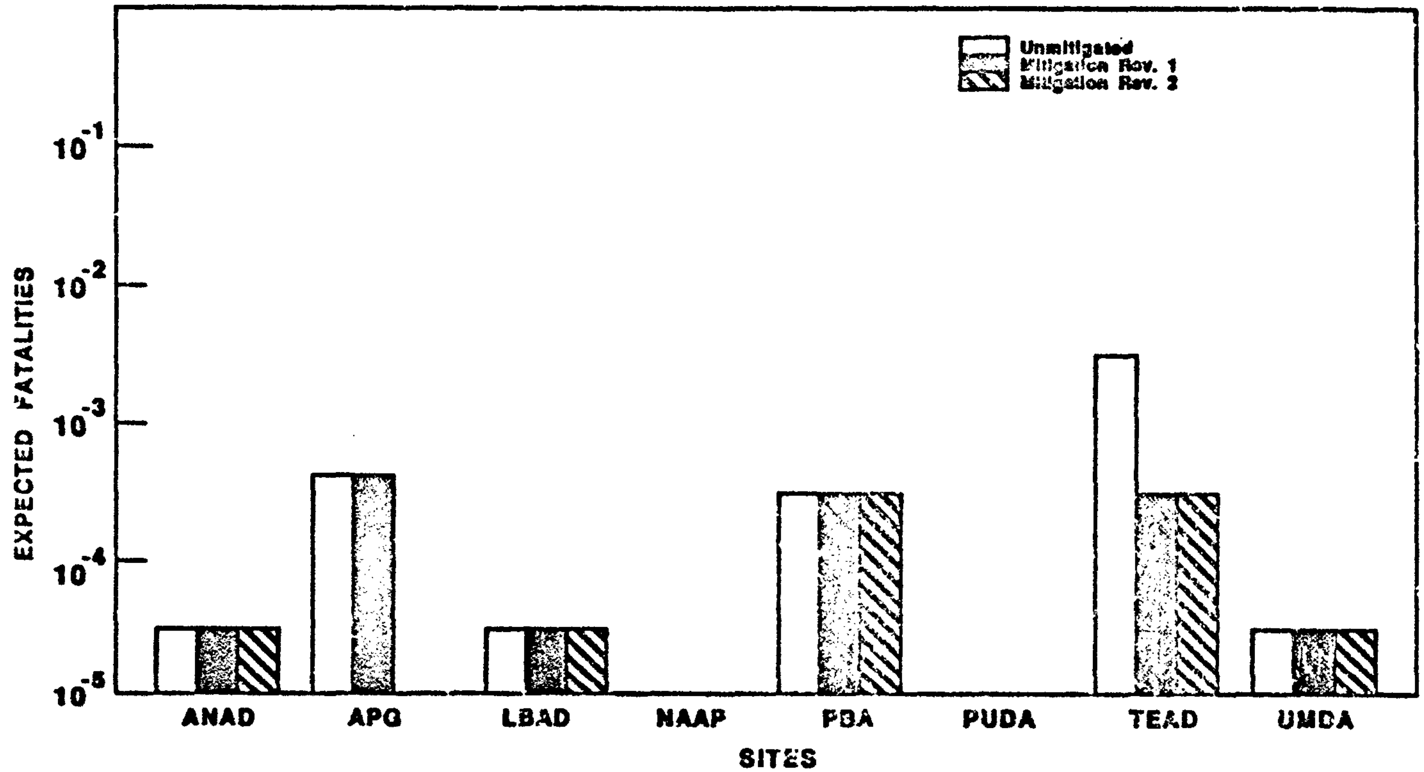

(Risk Along Transportation Corridor Not Included)

FIGURE 4-5

RISK COMPARISON FOR NATIONAL DISPOSAL ALTERNATIVE

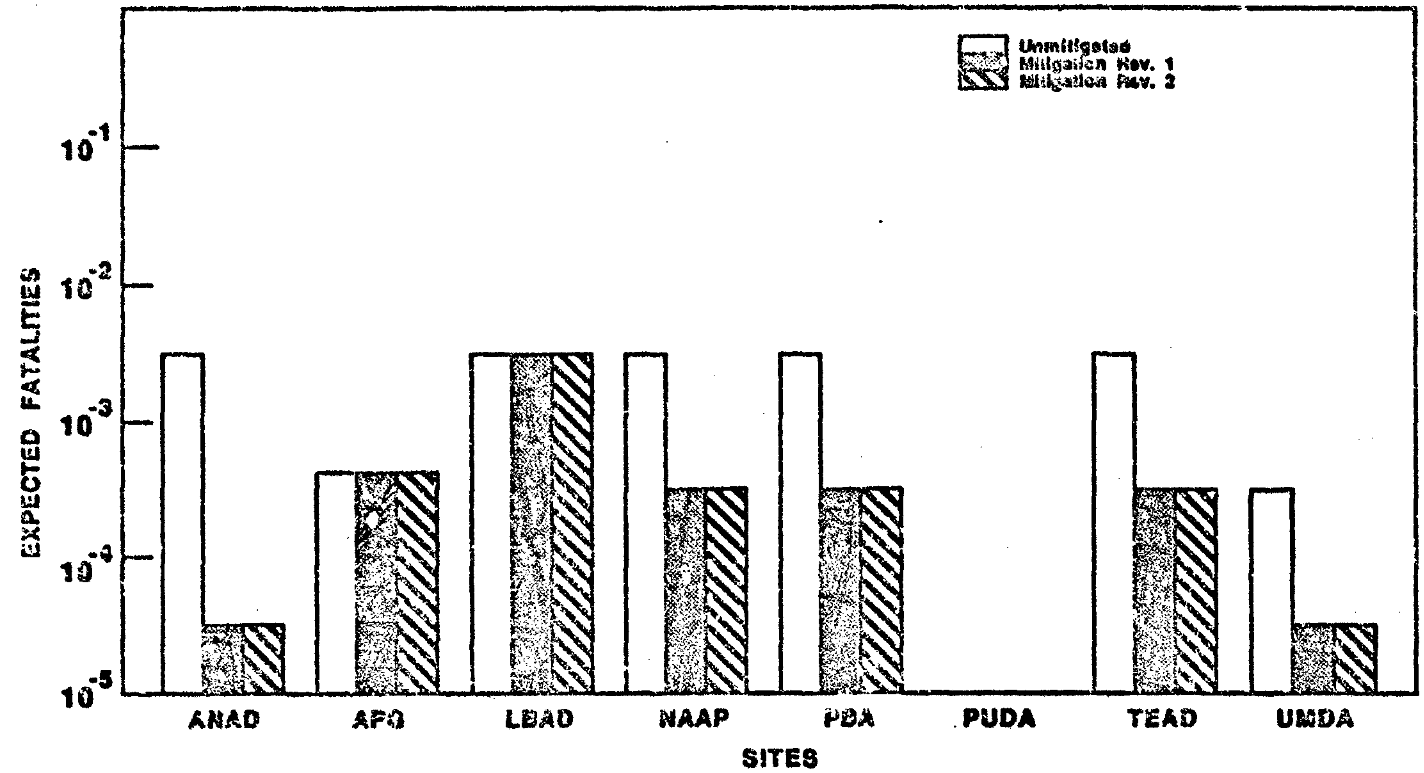

(Risk Along Transportation Corridor Not Included)

FIGURE 4-6

RISK COMPARISON FOR PARTIAL RELOCATION ALTERNATIVE

the most important mitigation measure. At Tooele the mitigation of handling accidents also has an appreciable effect on risk. Restricting air space does not appreciably reduce risk for on-site disposal.

Figures 4-4 and 4-5 illustrate the fact that mitigation has little potential for reducing the risk for the regional or national disposal alternatives. At no site is the effect sufficient to reduce the expected fatalities from one range of values to another, except at Tooele (national disposal). In this case, the reduction is less than one order of magnitude but is shown on the graph as a reduction because the value moves from one range to another.

As shown in Figure 4-6, there is no appreciable reduction in risk at the two sites (Aberdeen and Lexington-Blue Grass) from which stocks are moved by air. The effect of mitigation at the other sites is attributable primarily to mitigation of plant operations accidents.

REFERENCES

National Research Council (1984). Disposal of Chemical Munitions and Agents. National Academy Press, Washington, D.C.

U.S. Army Toxic and Hazardous Materials Agency (15 March 1986). Chemical Stockpile Disposal Concept Plan. Report AMXTH-CD-FR-85047. Aberdeen Proving Ground, Maryland.

U.S. Department of the Army (1987a). Risk Analysis of the Continued Storage of Chemical Munitions, SAPEO-CDE-15-87009. Prepared by GA Technologies Inc. for Program Executive Officer-Program Manager for Chemical Demilitarization, Aberdeen Proving Ground, Maryland.

U.S. Department of the Army (1987b). Risk Analysis of the On Site Disposal of Chemical Munitions, SAPEO-CDE-15-87010. Prepared by GA Technologies Inc. for Program Executive Officer-Program Manager for Chemical Demilitarization, Aberdeen Proving Ground, Maryland.

U.S. Department of the Army (1987c). Risk Analysis of the Disposal of Chemical Munitions at Regional or National Sites, SAPEO-CDE-15-87008. Prepared by GA Technologies Inc. for Program Executive Officer-Program Manager for Chemical Demilitarization, Aberdeen Proving Ground, Maryland.

U.S. Department of the Army (1986) Draft Programmatic Environmental Impact Statement, Chemical Stockpile Disposal Program. Office of the Program Manager for Chemical Demilitarization, Aberdeen Proving Ground, Maryland.

U.S. Department of the Army (1988) Final Programmatic Environmental Impact Statement, Chemical Stockpile Disposal Program. Office of the Program Manager for Chemical Demilitarization, Aberdeen Proving Ground, Maryland.

Whitacre, G.C. *et al.* (1988). Personal Computer Program for Chemical Hazard Prediction (D2PC). U.S. Army Chemical Research and Development Center, Aberdeen Proving Ground, Maryland.

FACILITY SYSTEM SAFETY FOR THE CHEMICAL STOCKPILE DISPOSAL PROGRAM

Presented at the 23rd Annual
Department of Defense (DOD) Explosive Safety Seminar

By

C. DAVID DOUTHAT, P.E., CSP
U.S. Army Corps of Engineers
Huntsville Division
Huntsville, AL

And

BERNIE BINDEL
Program Executive Officer - Program Manager
for Chemical Demilitarization
Aberdeen Proving Ground, MD

INTRODUCTION

The purpose of this paper is to provide an overview of the comprehensive Facility System Safety (FASS) effort that has been implemented for the Chemical Stockpile Disposal Program (CSDP) facility and process design. This system safety effort will ensure that the destruction of the chemical agent stockpile is accomplished in a manner that protects the environment, the general public, and the personnel involved in the destruction process.

BACKGROUND

The enactment of Public Law 99-145 directed the Department of Defense (DOD) to destroy this nation's stockpile of lethal unitary chemical (nerve and blister) agents stored in various munition items and bulk containers at eight Army installations throughout the continental United States. These locations include:

- Aberdeen Proving Grounds (APG), Maryland
- Anniston Army Depot (ANAD), Alabama
- Lexington-Blue Grass Army Depot (LBAD), Kentucky
- Newport Army Ammunition Plant (NAAP), Indiana
- Pine Bluff Arsenal (PBA), Arkansas
- Pueblo Depot Activity (PUDA), Colorado
- Tooele Army Depot (TEAD), Utah
- Umatilla Depot Activity (UMDA), Oregon

The lethal agent stockpile consist of two types--nerve and blister--and are configured in explosive and nonexplosive munition items and bulk type containers. A listing of these chemical munitions and their locations are summarized in Table 1.

DESTRUCTION PROCESS

Presently, there are two technologies available for destruction of the chemical agent stockpile. These include the baseline technology, which has had extensive testing at the Army's Chemical Agent Munition Disposal System (CAMDS) at Tooele, Utah, and the cryofracture technology, which has been under research and development for the past six years. The major difference between the two technologies is the method by which access is made to the explosive component and chemical agent. The baseline technology consists of mechanical disassembly or penetration of the munitions, separation of the agent and any energetic materials (explosives and propellants). The cryofracture utilizes liquid nitrogen to embrittle the munition items and a mechanical process to fracture and expose all the contents. Both technologies ultimately provide thermal destruction of the agents and explosive components in specially designed incinerators. The technology that has been selected and will be utilized for the CSDP is the baseline technology. Research and development is continuing for the cryofracture technology with a pilot plant eventually to be located at Tooele Army Depot.

FACILITY SYSTEM SAFETY

The overall objective of the CSDP is to provide for safe destruction of the chemical agent stockpile. This is an objective that is shared by

TABLE 1. Chemical munitions stored in the continental United States

Chemical munitions/agent	APG	ANAD	LBAD	NAAP	PBA	PUDA	TEAD[a]	UMDA
Mustard agent (H, HD, or HT)								
105-mm projectile (HD)		X				X		
155-mm projectile (H, HD)		X	X			X	X	
4.2-in. mortar (HD, HT)		X				X	X	
Ton container (HD)	X	X			X	X[b]	X	X
Ton container (HT)					X			
Agent GB								
105-mm projectile		X					X	
155-mm projectile		X					X	X
8-in. projectile		X	X				X	X
M-55 rocket		X	X		X		X	X
500-lb bomb								X
750-lb bomb							X	X
Weteye bomb							X	
Ton container		X[b]	X[b]		X[b]		X	X[b]
Agent VX								
155-mm projectile		X	X				X	X
8-in. projectile							X	X
M55 rocket		X	X		X		X	X
M23 land mine		X			X		X	X
Spray tank							X	X
Ton container				X				X[b]

[a]Small quantities of Lewisite(L) and tabun (GA) are stored in ton containers at TEAD.
[b]Small quantities of agent drained as part of the DATS/M55 assessment.

management, designers, and safety personnel alike. This understanding by the design team of the risks involved in agent and explosive component destruction has enabled this design to proceed achieving a balance of safety, cost and operational effectiveness.

SYSTEM SAFETY PROGRAM PLAN (SSPP)

The SSPP for the CSDP was prepared to implement and manage the system safety effort in accordance with MIL STD 882B, AMC-R 385-3, AR 385-16, DODI 5000.36, and HNDP 385-3-1. The SSPP documents how the contractual safety tasks will be performed to assure the highest attainable level of safety. The SSPP describes interfaces between various program elements and their schedule and the system safety program elements. (Figure 1).

The SSPP detail methods and procedures that will be used in evaluating and accessing the risks associated with operations of the CSDP. The risk assessment methods that were developed are used to access the impact of an incident on workers, the general population and the system. This required establishing and defining levels of hazard severity and frequency unlike most risk matrix assessment approaches in that it required the evaluation of hazards of toxic agent release to both on post and off post. This was done from downwind hazard calculations from postulated agent release scenarios. Table 2 is used to assign hazard severity classifications to various populations and to the facility, based on incidents that could occur. Hazard probability levels (Table 3) incorporate quantitative probabilities to an otherwise qualitative assessment. The advantage of this approach is that the safety review group, which all have extensive safety and hazard analysis experience, can easily apply quantitative probability levels rather than generic qualitative description of hazard probabilities. A risk matrix Table 4 provides for evaluation and defines acceptability criteria for the identified hazards.

SAFETY DESIGN REQUIREMENTS MANUAL

The Safety Design Requirements Manual for the CSDP was developed to provide special safety requirements for incorporation in the design of facility and process equipment. This manual is utilized by the design team as a design tool to ensure that existing safety design criteria, requirements developed for the CAMDS, the Johnston Atoll Chemical Agent Disposal System (JACADS), as well as other Army and industrial standards are fully incorporated into the design. In addition, many special safety design criteria have been developed and incorporated in the manual, addressing specific potential toxic and explosive hazards associated with the demilitarization process.

An example of these design requirements was the unique requirements for agent vapor control. Due to the toxicicity of the agents, specific ventilation design criteria was established by this design manual to collect and prevent agent contamination of work areas as well as release to the outside. The general approach was to:

- Collect and exhaust agent vapors from the work areas.
- Provide mixing of air that was essential for monitoring work areas with agent detection devices.
- Provide negative pressure within work area to eliminate the escape of agent vapors.

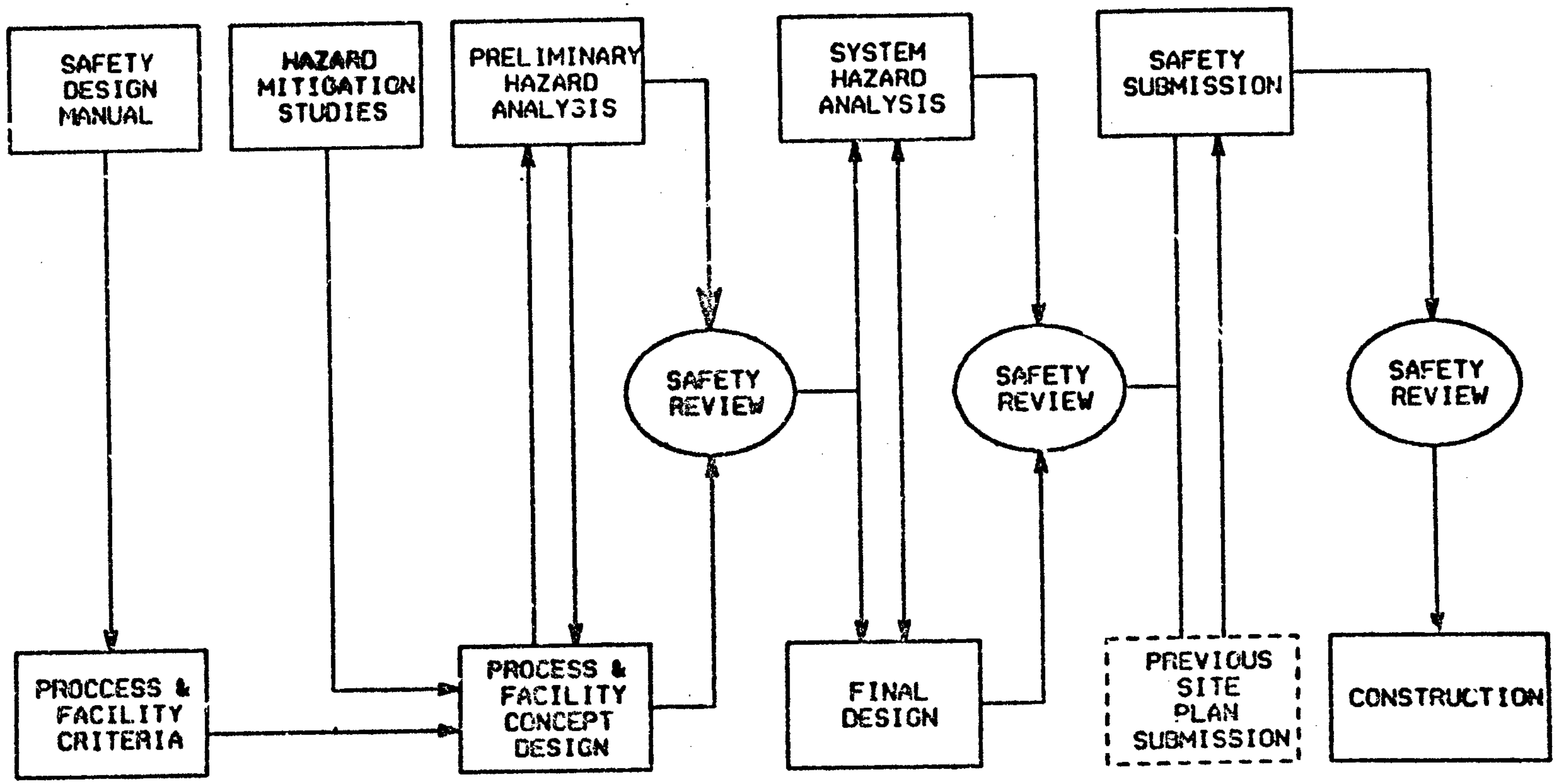

FIGURE 1
SYSTEM SAFETY PROGRAM ELEMENTS

TABLE 3 - CSDP Hazard Severity Levels*

Severity Level	Toxic Chemical Agent Release Off Post	Toxic Chemical Agent Release On Post	Personnel	System Loss
I Catastrophic	Dosages equal to or exceeding the no-deaths level	Agent concentration exceeding IDLH levels for unprotected workers inside chemical limited areas	Injury, illness, death or personal injury (permanent total disability)	>25% and >1 month to repair
II Critical	Dosages exceeding the no-effects level	Agent concentrations exceeding PELs for nonagent workers inside chemical limited area	Injury involving permanent partial disability	10% to 25% 1 week to 1 month to repair
III Marginal	Dosages of less than the no-effects level	Agent concentrations exceeding PELs for unmasked workers inside chemical limited areas	Injury involving temporary total disability	<10% <1 week to repair
IV Negligible	Dosages that could not be detected by monitors at installation boundaries	Agent concentrations less than PEL inside chemical limited area	Injury involving only first aid or minor supportive treatment	No system loss or downtime

*Above agent release levels are based on agent concentration action levels contained in DoD 6055.9 and in DARCOM R 385-102 and DARCOM R 385-31. Levels for personnel effects were based on AR 385-40 accident definitions. Levels for system loss were based on information contained in AMCCOM Supplement 1 to DARCOM R 385-3 and on information provided by USAEDH.

TABLE 3 - Assigned CSDP Probability Levels

Qualitative Probability	Agent Release Off Post	Agent Release On Post	Personnel Injury/Illnesses	System Loss
A - Frequent	$\geq 1 \times 10^{-2}$	$\geq 1 \times 10^{-1}$	$>1.2 \times 10^{1}$/yr	$>1 \times 10^{0}$
B - Probable	$\geq 1 \times 10^{-3}$	$\geq 1 \times 10^{-2}$	$>1 \times 10^{0}$/yr	$>1 \times 10^{-1}$
C - Occasional	$\geq 1 \times 10^{-4}$	$\geq 1 \times 10^{-3}$	$>1 \times 10^{-3}$/yr	$>1 \times 10^{-2}$
D - Remote	$\geq 1 \times 10^{-5}$	$\geq 1 \times 10^{-4}$	1×10^{-4}/yr	$>1 \times 10^{-3}$
E - Improbable	$<1 \times 10^{-5}$	$<1 \times 10^{-4}$	$>1 \times 10^{-4}$/yr	$<1 \times 10^{-4}$

TABLE 4 - Risk Assessment Code (RAC) Matrix

Qualitative Probability	Severity Level I	II	III	IV
A	1	1	1	3
B	1	1	2	3
C	1	2	3	4
D	2	2	3	4
E	3	3	3	4

Acceptability criteria:

RAC	Description
1	Unacceptable
2	Undesirable
3	Acceptable with controls
4	Acceptable

The ventilation criteria (Table 5) established minimum capture velocities, minimum room air change requirements, and minimum pressure differential requirements for the facility.

This manual has been extremely important for the designer and will ensure consistent application of safety design criteria to the CSDP throughout the design effort.

SAFETY REVIEW

The purpose of the safety review is to verify that the criteria established in the Safety Design Requirements Manual is incorporated in the design and to verify that the hazards identified in the various hazard analyses are adequately mitigated. In addition, verification and resolution of various safety problems are monitored as a portion of this effort.

Application of the safety review task is being conducted throughout the design effort. This safety review process is being utilized to track hazards or design deficiencies to ensure compliance with design goals or criteria and to identify the risk before and after mitigation. The safety review task has been an effective safety engineering tool to ensure that hazards are identified and monitored until corrective action has been completed.

PRELIMINARY HAZARD ANALYSIS (PHA)

The PHA is being developed to ensure that potentially hazardous system failures are identified early in the design process and that corrective design changes are implemented. The output of the PHA has identified numerous design deficiencies that have been corrected in the early design phase with minimal impact on cost or schedule.

The PHA utilizes failure modes and effects analysis (FMEA) methodology for the analysis (Figure 2). Thus far, over 700 events have been analyzed for their effect on system performance. The PHA has been effective in identifying, evaluating, and assessing the risk on this complex project The PHA has focused primarily on explosive and/or toxic chemical hazards but has been useful in identifying general industrial hazards.

SYSTEM HAZARD ANALYSIS (SHA)

The SHA is presently under development for the CSDP. The current SHA is essentially a continuation of the PHA, utilizing more advanced techniques and procedures in an attempt to analyze the complicated process that has developed. The approach for the SHA has been to use available software programs to analyze a number of accident initiating events.

One of the major efforts for this task has been the development and identification of accident sequences and their potential consequences. This effort utilizes the event tree methodology and has developed a list of major potential accident sequences that will be quantified using the fault tree methodology.

TABLE 5 - CSDP Ventilation Criteria

Ventilation Category	Minimum Capture Velocity[a] (ft/min)	Minimum delta P[b] (in. water)	Minimum Airflow[c] (changes/ hr.)	Contamination	Treatment
A	150	-0.75 to -1.25	20	Probable liquid and vapor	Incinerate or filter
B	150	-0.40 to 0.60	10	Possible vapor only	To higher concentration, incinerate, or filter
C	150	-0.25	6	Not expected but possible (vapor)	To higher concentration, incinerate, or filter
D	NA	Atmospheric	Normal industrial practice	No agent	None
E	NA	+0.1 to +0.2	Positive pressure	No agent	Filter on inlet and return air

[a] Referenced to next lower vent category.
[b] Referenced to atmospheric pressure; values are derived and may change for different building designs.
[c] Air changes/hr. are only approximate; the need is for adequate air circulation (no dead-air spaces) and local ventilation at probable sources of release (e.g., punch and drain station).

NOTES:

(1) Makeup air for Category A areas will not, as a general rule, be taken from Category C or D work areas unless special provisions are incorporated to preclude (a) release of vapor in the event of ventilation failure, and (b) escape of liquid agent in the event such material is accidently released inside the operating area.
(2) Priority of ventilation criteria will be as follows: capture velocity, pressure differentials, air changes.
(3) Ventilation inlet ducts to Category A areas will be designed to avoid line of sight to supply area so that washdown water/decon will not pass to or drain through ducts to supply side.

PARSONS FAILURE MODE AND EFFECTS ANALYSIS DATA (FMEA) CHEMICAL STOCKPILE DISPOSAL PROGRAM JOB NO. [illegible]	FMEA APPLIED TO DRAWING NO: ____ REVISION ____ DATE ____ OTHER REFERENCES ____	PROTECTION DEVICE TYPES P - PASSIVE A - ACTIVE W - WARNING MEASURES D - DESIGN (OTHER CHANGES) O - OTHER (PROCEDURAL)	RISK LEVEL INDICATORS SEVERITY (S) 1 CATASTROPHIC 2 CRITICAL 3 MARGINAL 4 NEGLIGIBLE	PROBABILITY (P) A FREQUENT B PROBABLE C OCCASIONAL D REMOTE E IMPROBABLE	PREPARED BY ____ DATE ____ SHEET ____ OF ____ NOTES ____

REF. NO.	LOCATION	ITEM TAG NO./DESCRIPTION	FAILURE MODE	EFFECT(S)	EXISTING PROTECTIVE DEVICE(S)	TYPE	RECOMMENDED DEVICE(S)/MEASURE(S) *	TYPE	RISK LEVEL [illegible]: RELEASE [illegible] S	P	[illegible] S	P	PERS. S	P	SYS. S	P	REMARKS

FIGURE 2
FAILURE MODE AND EFFECTS ANALYSIS WORK SHEET

RISK MITIGATION

In support of the Environmental Impact Statement (EIS) for the CSDP, risk analyses were performed to identify and evaluate measures for reducing the public safety risk from implementing the various alternatives under consideration for disposal of the chemical agent stockpile. These analyses evaluated major activities for storage, handling, on-site transport, plant operations, and off-site transport for the relocation alternatives. These analyses were performed by Oak Ridge National Laboratory, The MITRE Corporation, and GA Technologies, Incorporated. The role played by the FASS Program was the evaluation of the alternatives required to mitigate the unacceptable risk during plant operations.

For those identified risks, alternatives were evaluated to (1) reduce the frequency of occurrence of an accident, (2) reduce the quantity of an agent source present, and/or (3) reduce the dispersion in the environment following the occurrence. Those risks associated with plant operations were evaluated as a part of the FASS effort. This provided an established procedure for evaluating risk and recommending mitigation measures that were consistent with the overall design effort.

QUALITY ASSURANCE, SIGNIFICANT ITEM LIST

As a part of the Quality Assurance (QA) effort for the CSDP, significant items for the process are being identified. A significant items list (SIL) for facility and process equipment is being developed to ensure that the appropriate quality control measures are applied to equipment.

The QA classifications established in the General Design Criteria (GDC) for the CSDP facilities are as follows:

(1) QA Class I: Applies to those structures, systems, or components whose failure or malfunction would detrimentally affect the following safety functions:

(a) Containment (liquid/vapor agent or explosion).

(b) Plant safe shutdown and safety of plant personnel.

(c) Off-site release of toxic material affecting the health and safety of the public.

In addition, QA Class I includes those items and activities that, as a result of being defective, cause extensive damage to equipment or long-term stoppage of the process. Thus, the most proficient degree of controls for the applicable QA/QC elements identified within military specification MIL-Q-9858A shall be implemented, including audits of documentation and records.

(2) QA Class II: Includes those items and activities that, as a result of being defective, could adversely affect the reliability, operability, and/or safety of the facility/equipment and personnel, causing limited damage or temporary shutdown of the process. Accordingly, sufficient controls shall be applied to QA/QC elements

for inspection, test, nonconformance, corrective action, documentation, and records in accordance with MIL-I-45208A during design, procurement, and construction. When design changes under configuration controls are also required, the QA/QC element required for design activities shall also adhere to MIL-Q-9858A.

(3) QA Class III: Includes those items and activities that do not adversely affect the reliability, capability, and/or safety of the facility or equipment if failure were to occur. Appropriate referencing of industrial codes or standards (in combination with testing, inspections, and good workmanship), both specified within the specification and procurement documents, are sufficient. Documents specifically required shall be delineated in technical data packages. Off-the-shelf items may be included in this classification.

As the required quality of a particular piece of equipment is based upon its ability to provide containment of vapor and/or liquid agent, contain explosive forces, provide safe shut down of the plant, etc., it was logical to apply system safety procedures to evaluating the SIL. Many items of the SIL had already been evaluated during development of the PHA and application of the same procedures in evaluating the remaining items is ensuring a consistent method for assigning QA Classifications. The logic for determining the QA classification is shown in Figure 3. Application of the established Risk Assessment Criteria has ensured consistency in evaluation of the risks associated with the use and failure of equipment.

SAFE RESPONSE OF PLANT SYSTEMS TO POSTULATED FAILURES

This study was performed to evaluate safe response of the CSDP plant systems and the required operator actions in the event of a postulated failure. The report reviewed 24 selected postulated failures describing both plant and operator responses to the failure. The criteria that was used to evaluate potential safety concerns were:

(1) Migration of detectable quantity of agent from toxic to nontoxic areas.

(2) Agent release to the outside environment.

(3) Increased risks to the health or safety of plant workers, installation personnel, or general public.

(4) Major equipment or facility damage.

In general, the study revealed that the plant responded appropriately to the postulated failures and identified areas for design changes or additional study.

POWER SYSTEM AVAILABILITY

This study was to determine the maximum time that a total power outage could exist without compromising the integrity of the Munition Demilitarization Building (MDB). The integrity of the MDB was considered

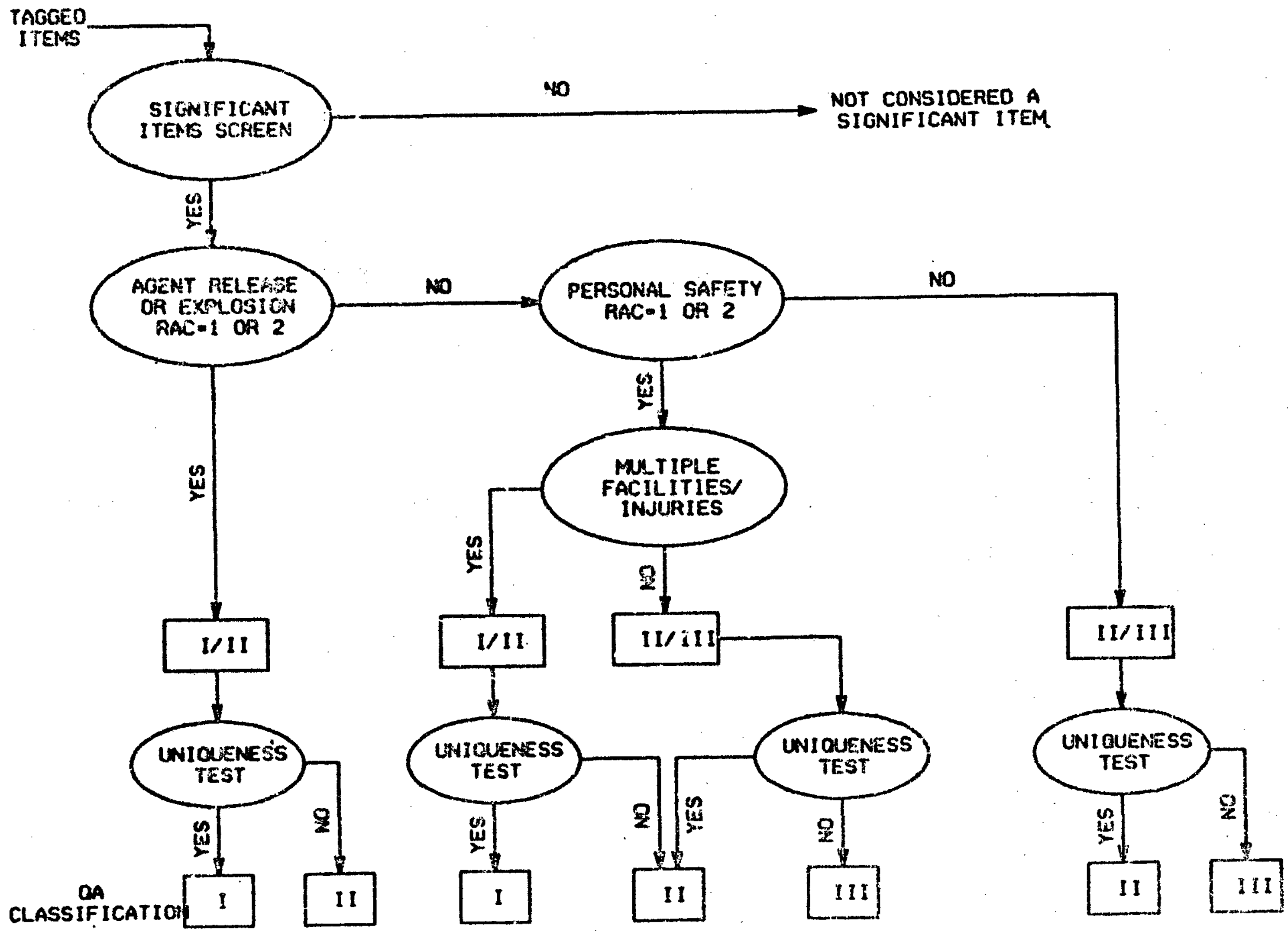

NOTE: Any items screened as being significant will be a minium of QA Class III.

FIGURE 3
SIGNIFICANT ITEM LIST EVALUATION TREE

to be compromised when toxic agent is above the acceptable level in one or more nontoxic areas or when agent is released to the outside environment. The results of this study established additional safety criteria for safe operation and shut down during plant upset conditions.

HUMAN FACTOR ENGINEERING (HFE) DESIGN CRITERIA

Similar to the requirements for the Safety Design Criteria Manual and safety review effort, an HFE design criteria manual was developed to ensure that the unique man-machine interface requirements are maintained.

The criteria is intended to ensure that:

(1) Personnel can safely and adequately perform required operator and technician functions when wearing protective clothing.

(2) Operators can effectively monitor and remotely control equipment operations normally controlled automatically by the control system.

(3) Personnel can safely handle highly toxic and explosive materials using gloveboxes, if required.

(4) Workspace, environment, maintainability, communications, control/display panel, and hazard protection and safety designs conform to well-established human factors engineering criteria.

The design is continually reviewed to ensure adherence to the HFE design criteria.

CONCLUSION

The FASS effort for the CSDP process and facility design is ensuring that risks associated with this demilitarization program are maintained at a level consistent with mission requirements. This FASS effort is perhaps the most intensive safety effort ever applied to a DOD facility/process design. Its success is a result of managers and designers commitment to providing a design that will safely dispose of this nations unitary chemical agent stockpile.

The FASS techniques and studies that have been discussed represent a portion of the overall safety effort thus far performed on the CSDP design. Additional safety studies will be required as the design progresses, and they too will be managed in accordance with the SSPP to ensure consistent application of the established safety criteria.

The CSDP Program has had and will continue to have oversight by environmental and public concerns. This FASS effort will serve to demonstrate that extraordinary efforts are being made to ensure the safe design and operation of the demilitarization facility.

DESIGN AND ACQUISITION OF STANDARD FACILITIES FOR THE DISPOSAL OF OBSOLETE LETHAL CHEMICAL MUNITIONS

Paul M. LaHoud, U.S. Army Engineer Division, Huntsville
Huntsville Alabama, 35807-4301

ABSTRACT

Public Law 99-145 (1986) requires that the Department of Defense design, procure and operate process disposal facilities for the sole purpose of destroying the U.S. stockpile of obsolete unitary lethal chemical munitions. Almost 94% of these stockpiles is stored at eight locations in the U.S. and constitute a serious long term hazard to the public safety and the environment, as well as a significant security risk. The direct implementation of this disposal mission lies with the Department of the Army. The extremely hazardous nature of these disposal operations require that all facilities will be adaptations of a standard design developed from a prototype plant. This paper discusses the development of these facility designs and the multiple safeguards provided to assure safe operations.

BACKGROUND

The Department of Defense (DOD) currently maintains a large stockpile of munitions and bulk storage items containing unitary lethal chemical agents. These stockpiles are maintained as a deterrent to the use of similar weapons by other nations. Figure 1 gives the types of agent and storage configuration maintained in the stockpile. Almost 94% of the total stockpile is stored within the Continental United States (CONUS). Approximately 61% of this stockpile is stored in bulk form (ton containers or spray tanks). Figure 2 shows the storage sites.

The munitions and storage containers in the stockpile were manufactured and assembled from twenty to forty years ago. Many of these munitions and bulk containers, as well as the explosives, propellant and agent contained in them, are deteriorating and are beginning to represent a serious long term storage problem. Significant maintenance efforts are required to assure continued environmental and personnel safety at the storage sites. In addition, weapons systems capable of delivering many of these munitions are no longer in use within the U.S. military services. Adding to these concerns in recent years is the perceived risk of terrorism. As a result, physical security has become a major issue.

Prior to 1970 ocean dumping was the principal means of elimination. However rising worldwide environmental concerns resulted in a moratorium on this disposal procedure. The Department of the Army (DA) commissioned a study by the National Academy of Sciences (NAS) to address this issue (Ref 1). The NAS recommended that DA avoid ocean dumping in the future and initiate systematic studies to accomplish environmentally safe disposal at the storage sites. DA subsequently initiated research to evaluate and develop technologies suitable for this purpose. In 1979 the first prototype disposal facility became operational (Ref 2). This plant served as the test bed for evaluation of alternative disposal technologies to be used for subsequent full scale production facilities.

CHEMICAL STOCKPILE DISPOSAL PROGRAM

Concern at the national level with the deteriorating condition of the stockpile resulted in congressional action through Public Law 99-145 (Defense Appropriations Act of 1986). This law required that DA develop a plan to implement the complete destruction of all unitary lethal chemical munitions by September 1994 (Ref 3). The mission was identified as the Chemical Stockpile Disposal Program (CSDP).

Alternatives considered for the CSDP included a single national disposal facility, two regional facilities and on-site destruction. The Programmatic Environmental Impact Statement (PEIS) recommended on-site destruction as the safest and therefore preferred method of disposal. Extended environmental reviews, as well as a delay in the necessary appropriations, have resulted in the estimated completion of the CSDP being revised to late 1997. Figure 3 summarizes the Army's subsequent actions to implement the CSDP (Ref 5). The 1989 Defense Appropriations Act accepted the recommendations of the Army and provided initial funding to achieve that objective.

PROGRAM MANAGEMENT

Under the acquisition strategies now employed within DA, program management responsibility for the CSDP lies with the Program Executive Officer for Chemical Demilitarization (PEO-PM-CML-DML) located at Edgewood Arsenal. Contracting for engineering services for both the process and facility designs is being provided by the Huntsville Division, Corps of Engineers (CEHND) located in Huntsville Alabama. Corps of Engineer Districts will provide engineering services within their geographic regions during construction. Design services for both process and facilities have been contracted by CEHND to The Ralph M. Parsons Company, Pasadena California.

DISPOSAL PROCESS

The Army has systematically pursued development of the necessary technology for production scale chemical agent demil plants since 1979. The guidelines for this work in agreement with NAS recommendations are:

- ABSOLUTE SAFETY AND SECURITY RATHER THAN COST OR TIME
- MAXIMUM PROTECTION FOR OPERATING PERSONNEL
- ABSOLUTE ASSURANCE OF TOTAL AGENT CONTAINMENT
- ABSOLUTELY NO ENVIRONMENTAL POLLUTION

The result of this effort has been the development of the so-called reverse assembly process. Using specially designed remotely controlled equipment, munitions or agent containers are disassembled, punched, and drained. All agent, explosive and propellant are then incinerated, along with any other combustible components or packing materials. Metal munitions bodies, drained bulk containers, and other noncombustible residue of the process are thermally decontaminated and scrapped. Figure 4 summarizes the mechanical technologies required for all demil operations. Figure 5 is a functional block diagram of

processing activities. Munitions with explosives or propellants are separated from the energetic components in an Explosive Containment Room (ECR). All other munitions or bulk containers are handled separately and drained. Ammunition Peculiar Equipment (APE) developed for the demil process is given for each site in Table 1. All incineration and thermal decontamination is accomplished in four special incinerators, each with its own Pollution Abatement System (PAS). Table 2 lists these incineration systems and their function.

R&D TECHNOLOGY DEVELOPMENT

The reverse assembly technology was developed and verified in more than 10 years of research and development using the Chemical Agent Munition Disposal System (CAMDS) located at Tooele Depot. Operations at this facility led to development and prove out of the APE, process control systems, incineration /pollution abatement systems, and monitoring equipment. In addition, extensive operational experience was accumulated in the processing of lethal agent. Figure 6 shows the CAMDS R & D disposal facility. Based on the results obtained from CAMDS and other research, design of a prototype production disposal plant was initiated.

PROTOTYPE DISPOSAL FACILITIES

The prototype lethal agent production disposal facility was the Johnston Atoll Chemical Agent Disposal System (JACADS). This facility was designed based on the technology created at CAMDS and further developed for use in a sustained production environment. It is located on Johnston Atoll, approximately 700 nautical miles southwest of Hawaii, where a significant agent stockpile has been stored for a number of years. Figure 7 provides the current status of the JACADS program. Initial operations at JACADS will serve as the verification test bed for the CSDP on-site disposal facilities. Details of the JACADS plant are discussed in detail in References 6-7.

A non-lethal disposal plant has also designed and constructed at Pine Bluff Arsenal. This facilitiy is required for the destruction of the incapacitating agent BZ which is stored only at this site. This plant is also based on the reverse assembly incineration process and its background is summarized in Figure 8. The BZ facility is currently in operation and is providing operational data which will support the future lethal plant operations.

BASIS OF STANDARD DESIGNS

The hazardous nature of the chemical agents being destroyed dictated that the design of the CONUS on-site disposal plants be intensely scrutinized and managed. Normal design development and coordination activities are not considered adequate. Similarly, standard procedures for the oversight of facility construction, equipment acquisition and installation, acceptance testing and operations are also not acceptable. The intent of the CSDP was therefore to develop closely integrated acquisition procedures based on "standard" disposal plant designs. These designs would be as nearly identical as possible, given the variations in environmental conditions, siting and inventory at each disposal site. The entire life cycle of the design,

acquisition and operations would be subject to comprehensive systems engineering controls, including in-depth safety analysis, quality assurance programs and rigid configuration management. The safety engineering tasks being performed for the CSDP are shown in Figure 9. These safety tasks were initially performed on the JACADS plant and then modified to reflect the site specific requirements of the CSDP facilities. Hazard analyses performed in support of the PEIS identified necessary changes to the JACADS design resulting from hazards specific to CONUS operations. Risk Assessment Codes (RAC) were the basis for identifying safety critical process and facility equipment and developing quality assurance requirements. Standardization of designs at all sites would assure the highest degree of conformance with critical safety and environmental requirements.

DESIGN CRITERIA

Comprehensive design criteria were developed to ensure standardization. These include a program level General Design Criteria Document, and subsequent lower level implementation guidance. Figure 10 shows a document tree for program guidance. Detailed design criteria were established for both facilities and process operations. Once these criteria were established configuration management was implemented and development of the CSDP "standard" designs initiated. Evolution in the process systems resulting from ongoing testing at CAMDS and JACADS as well as operations at the BZ plant are incorporated on a continuing basis through the Engineering Change Proposal (ECP) procedures of the configuration management system. These formally controlled design criteria maximize the standardization of the design efforts. Use of proven JACADS technology is a major programmatic objective. Identical process equipment and systems are to be used for all on-site disposal plants unless specific variation is approved by ECP.

INTEGRATED DESIGN

Conventional engineering practice within the Army would normally result in separate designs of the demil process systems and the facilities. Usually the process design would be accomplished prior to, and generally independent of, the design of the facilities and be performed by a different design firm. The design of the JACADS plant was accomplished in this fashion. Lessons learned during the design, construction and equipment installation for JACADS clearly indicated that a higher degree of coordination and design integration would be needed to implement the design of standard disposal facilities at multiple sites in the CSDP. This integration was achieved through the use of a single design contract to accomplish both process and facility designs. Thus a single design team would become intimately familiar with all the design criteria and develop a programmatic learning curve. This design team would develop the "standard" disposal plant and then adapt it to each on-site location. This process was nicknamed "cloning" for obvious reasons. All design drawings were developed on a Computer Aided Drafting (CAD) system. Once the initial standard design was completed all subsequent on-site designs would use all existing available system and facility design drawings and specifications, requiring only site adaptation design efforts. This procedure greatly reduces the design effort as well as improving configuration control and quality assurance.

STANDARD DESIGNS

Criteria requirements, site specific munitions inventories, local environmental conditions and life cycle costs studies resulted in development of two standard disposal plant designs. One design will be a mixed munition plant which will be capable of processing all agent configurations. There will be a requirement for five such facilities; Tooele (TEAD), Anniston (ANAD), Umatilla (UMAD) Pueblo (PUAD) and Lexington (LBAD). The second standard will be a bulk item plant. This design will be used at locations which do not have any explosively configured munitions. This plant will be required at two locations; Newport (NAAP) and Aberdeen (APG). Only minor changes will be made to adapt either of these standard plants to local environmental conditions at each site. All support facilities will also be site adaptable standard designs.

In addition to the two standard designs, two other designs will also be required to complete the CSDP. One of these is a modification of the existing non-lethal BZ plant now in operation at Pine Bluff Arsenal (PBA). A unique design will be required to adapt this plant for lethal agent after it completes its current mission. This retrofit design will still be standardized to the maximum extent practicable, and will be required to conform to all critical programmatic criteria. The other unique design is that of a Central Training Facility (CTF), to be located at Edgewood Arsenal near the Program Manager's office. This facility will be used to provide highly standardized central training for initial and recurrent certification for all plant operating personnel. The programmatic schedule has resulted in the first designs being the mixed munition plant at Tooele, Utah, and the Central Training facility at Edgewood Arsenal.

ENGINEERING MODELS

In addition to the use of CAD for the design process, the CSDP will make maximum use of engineering scale models. These models will be constructed during the design and will be used for coordination and checking of the process and facility drawings. Subsequently a model will be located at each site during construction, equipment installation and operations. Such models are indispensible for facilities of the complexity of Demil plants. A model will also be located at the CTF during training operations.

CRITICAL SAFETY FEATURES OF PLANTS

Total containment of chemical agent is the predominant safety goal of the CSDP disposal facilities. Agent in any form must not be allowed to escape during processing. To achieve this the facilities are designed as tightly sealed cascaded negative pressure ventilation structures. Air handling units provide supply air which is then distributed through functional areas of the building with progressively greater negative pressures. The required negative pressure in any area is a function of the probability of agent contamination in that area during processing. In addition to negative pressures, minimum air changes are also required for each ventilation category. Table 3 defines the criteria used to establish ventilation requirements in the facility.

Since the mixed munitions plants must process weapons with explosives, propellants and other energetic materials, operations for removal of these

hazardous components are performed remotely in Explosive Containment Rooms (ECRs). Figure 12 shows the general configuration of the ECRs within the facility. These rooms are designed in accordance with procedures given in TM5-1300 as described in detail in Reference 7.

The continuous maintenance of negative pressures within the Munitions Demil Building is critical to the containment criteria and requires a high degree of reliability in the electrical power system. Extensive analysis for each site is required to define the degree and type of redundancy provided. Typically each plant will be provided with a single commercial power source, backed up by two emergency generators. Each emergency generator can support 100% of all electrical loads defined as "essential" to safe shutdown of the plant, including the ventilation system. In addition a 100% redundant 45-minute uninterruptible power supply (UPS) is also provided for life safety critical systems. Table 4 shows the allocation of electrical loads to each type of back-up system.

Extensive agent monitoring systems are provided within the Munitions Demil Building, the associated support facilities and on the installation areas adjacent to the site. Rapid monitoring response is critical to life safety. The primary monitoring system for this purpose will be the Automatic Continuous Air Monitoring System (ACAMS).

An in-depth Quality Assurance (QA) program has been developed for the entire CSDP. Risk Assessment Codes (RAC) are developed in accordance with procedures defined by the System Safety Program Plan, based on methodologies given in Mil-Std-882B. These RAC levels are used as the the basis for development of a Significant Items List (SIL). QA classes for the SIL are assigned in accordance with criteria given in the programmatic General Design Criteria and repeated in Table 5.

PROGRAMMATIC SUMMARY

The detailed implementation plan for the CSDP is described in Reference 5. The schedule presented in the plan is shown in Figure 13. Current estimated programmatic costs are given in Table 6.

Acquisition strategies for the CSDP are based on the use of three special contracts. Major safety critical process equipment will be provided by the same contractor and vendors that supplied the JACADS plant. This will assure the standardization of these systems program wide. Other process equipment will be provided by a program level Equipment Acquisition Contractor (EAC) who will be selected to supply all other standardized equipment. Finally, A System Contractor (SC) will be selected to operate each site. This contractor will be responsible for construction, equipment installation, acceptance testing, operations and plant closure. One Request For Proposal (RFP) for will be issued in 1989, 1991 and 1992. It is possible that a single SC may operate multiple sites. All SC plant operating personnel will be trained and certified at the CTF. Both the designer RMP, and the Program manager will maintain field offices at each site from the start of construction through acceptance testing. PEO-PM-CML-DML will continue to provide program management throughout the life of the Program. This programmatic standardization of equipment, facilities, training and management is intended to minimize risk and provide the maximum probability of a safe successful program.

CONCLUSIONS

The DA has entered into one of the most nationally significant and environmentally sensitive programs in history. The Program is subject to widespread and intense management as well as independent oversight (See Figure 14). Every effort has been made to develop a comprehensive, coordinated engineering strategy to implement this program. Standardization of design activities, facilities, equipment, operations and training are key elements in in this strategy. Many of the techniques, both in engineering and procurement may serve as forerunners for future DA programs.

ACKNOWLEDGEMENTS

I would like to express my appreciation to Robert Ager, Civil Structures Branch, Huntsville Division, for his dedication and effort in preparing graphics and final text for this paper.

REFERENCES

1. "Report of the Disposal Hazards of Certain Chemical Agents and Munitions," Prepared by An Ad-Hoc Advisory Committee of The National Academy of Sciences, Washington D.C., June 1969.

2. "Final Demilitarization Plan for The Chemical Agent Disposal System (CAMDS) at Tooele Army Depot," Department of the Army Office of the Program Manager for Chemical Demilitarization and Installation Restoration, Aberdeen Proving Ground, Md, September 1978.

3. "Chemical Stockpile Disposal Plan," Report AMXTH-CD-FR-85047, U.S. Army Toxic And Hazardous Materials Agency. Aberdeen Proving Ground, Md., March 15, 1986.

4. "Chemical Stockpile Disposal Program Final Programmatic Environmental Impact Statement," Program Executive Officer-Program Manager for Chemical Demilitarization, Aberdeen Proving Ground Md.,January 1988.

5. "Chemical Stockpile Disposal Program, Implementation Plan," Program Executive Officer-Program Manager For Chemical Demilitarization, Aberdeen Proving Ground, Md., March 15, 1988.

6. "Chemical Demilitarization: Disposal Of The Most Hazardous Waste," Scott, J.A., Rife, R., Minutes Of The Twenty-First Explosive Safety Seminar, Volume II, Houston Texas, August 1984.

7. "The Design Of Explosive Containment Rooms For Demilitarization of Chemical Munitions," LaHoud, P.M., Minutes Of The Twenty-First Explosive Safety Seminar, Volume I, Houston, Texas, August 1984.

MUNITION TYPES

- ROCKETS
- MINES
- PROJECTILES
  - 4.2" MORTARS
  - 105 MM PROJECTILE
  - 105 MM CARTRIDGE
  - 155 MM
  - 8"
- BULK
  - SPRAY TANKS
  - 750# BOMBS
  - 500# BOMBS
  - WETEYE BOMBS
  - TON CONTAINERS

FIGURE 1 - CHEMICAL AGENT MUNITIONS TYPES

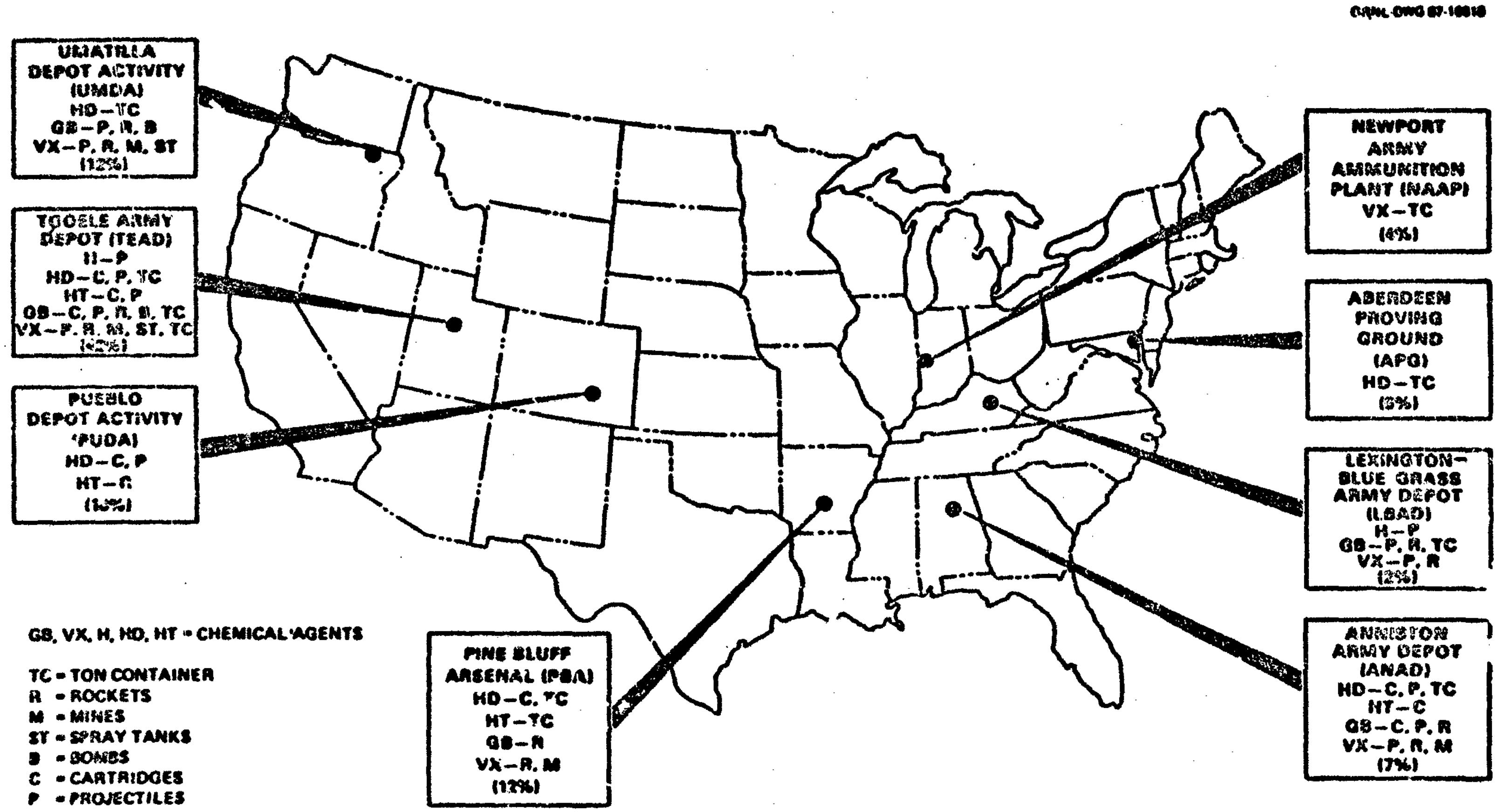

FIGURE 2 - CONUS STORAGE LOCATIONS

CHEMICAL STOCKPILE DISPOSAL
RECENT PROGRAM EVENTS

3 DEC 87 - DRAFT PROGRAMMATIC EIS ISSUED

23 FEB 88 - RECORD OF DECISION: (ON-SITE)

15 MAR 88 - IMPLEMENTATION PLAN TO CONGRESS

22 MAR 88 - CONGRESSIONAL HEARING (HAC)

FIGURE 3 - SUMMARY OF RECENT ARMY ACTIONS

MECHANICAL TECHNOLOGIES

DISPOSAL OPERATION	MUNITION TYPE: ROCKETS	MINES	PROJECTILE	BULK
REMOVE EXPLOSIVES	NONE	PUNCH BOOSTER	REVERSE ASSEMBLY	N/A
DRAIN AGENT	PUNCH AND DRAIN	PUNCH AND DRAIN	PULL BURSTER WELL AND DRAIN	PUNCH AND DRAIN
METAL PARTS	SHEAR	NO SIZE RETUCTION	NO SIZE REDUCTION	NO SIZE REDUCTION
DUNNAGE	NO SIZE REDUCTION	NO SIZE REDUCTION	NO SIZE REDUCTION	N/A

FIGURE 4 - MECHANICAL TECHNOLOGIES

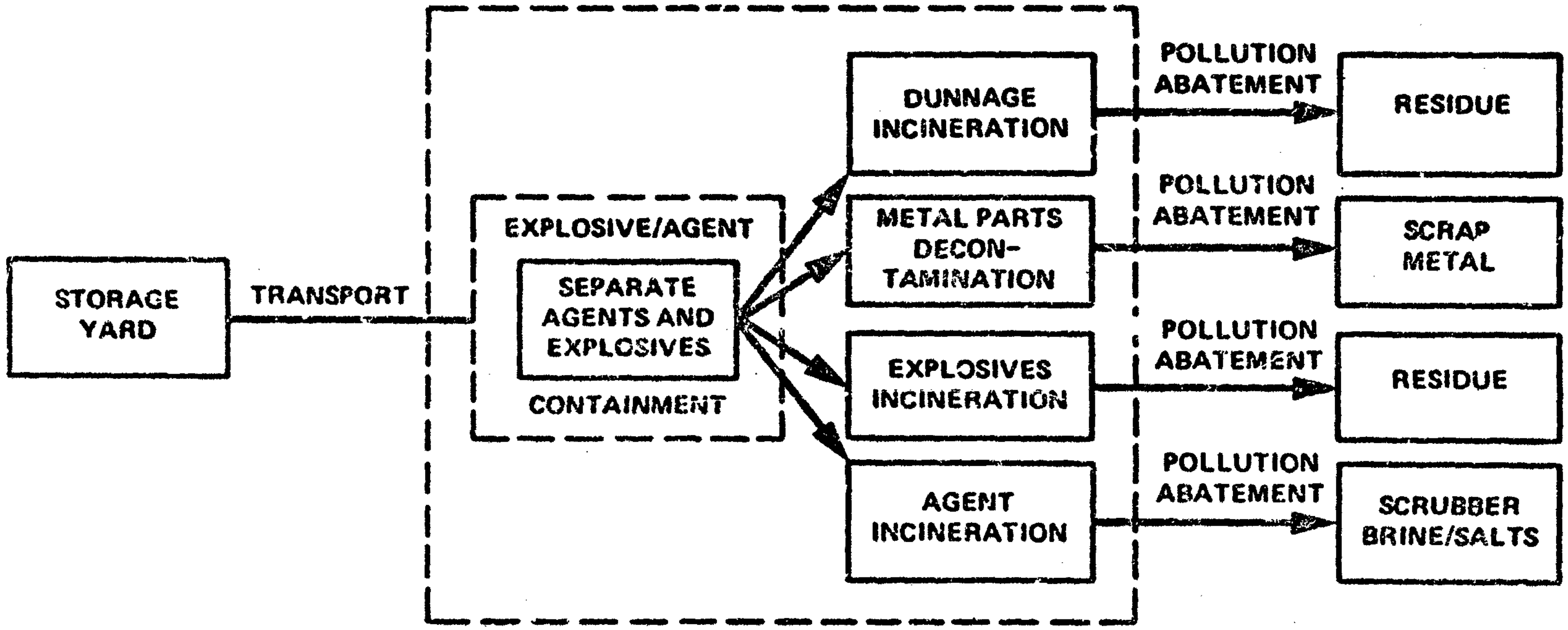

FIGURE 5 - DISPOSAL PROCESS BLOCK DIAGRAM

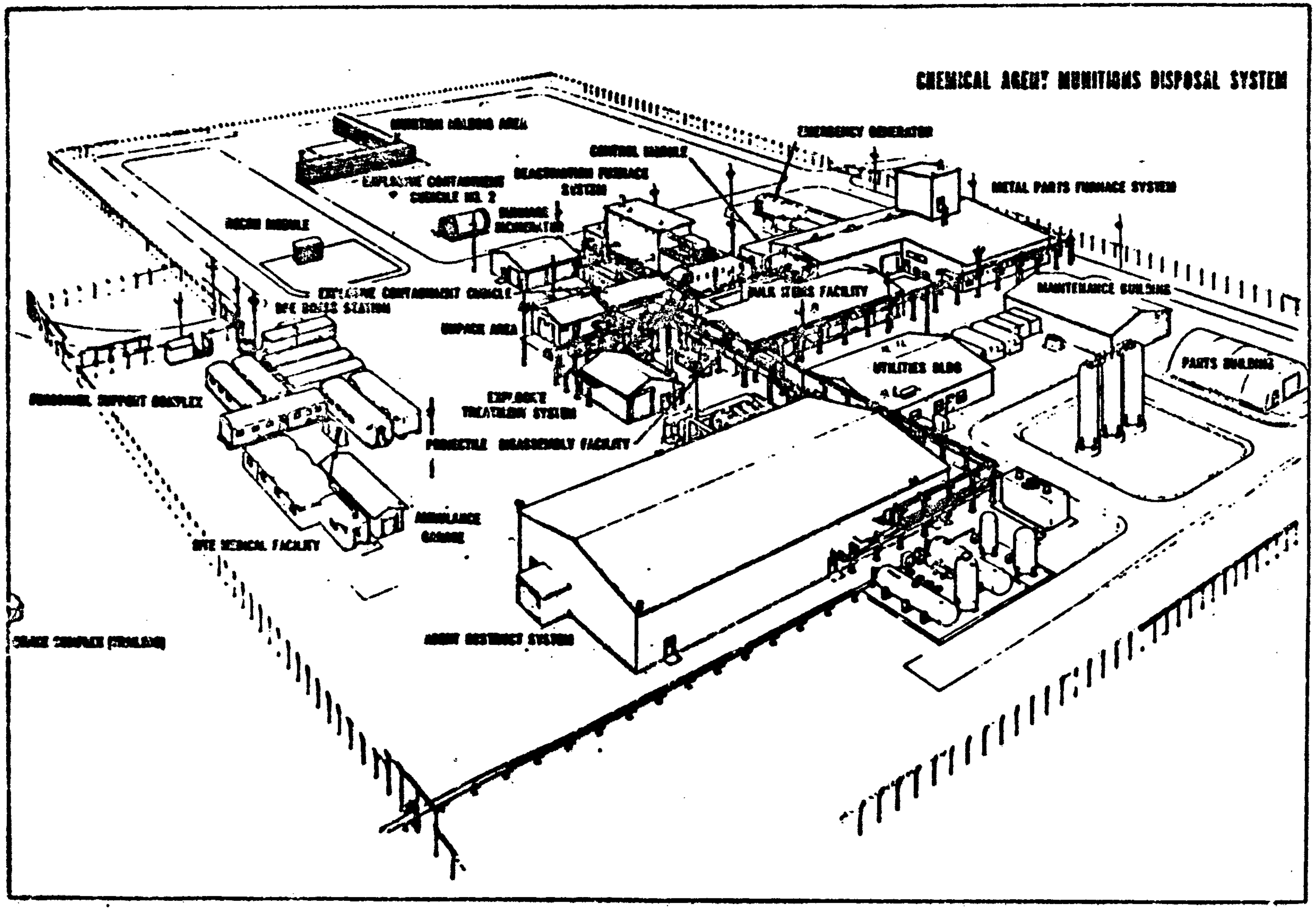

FIGURE 6-CAMDS FACILITY

JACADS PROGRAM MILESTONES

o START FACILITY CONSTRUCTION	JAN 86
o AWARD O&M CONTRACT	AUG 86
o OCEAN SHIPMENT I (EQUIPMENT)	MAR 87
o COMPLETE FACILITY CONSTRUCTION	AUG 87
o OCEAN SHIPMENT II (EQUIPMENT)	MAR 88
o RECORD OF DECISION JACADS SEIS	MAY 88
o COMPLETE EQUIPMENT INSTALLATION	OCT 88
o SYSTEM INTEGRATION/SHAKEDOWN	OCT 88 - SEP 89
o START OPERATIONAL VERIFICATION TESTING	SEP 89
o START ROCKET OPERATIONS	JAN 91

FIGURE 7 - JACADS PROGRAM SUMMARY

BZ PROGRAM MILESTONES

o COMPLETE MCA FACILITY CONSTRUCTION	JAN 86
o COMPLETE PROCESS EQUIPMENT INSTALLATION	JAN 87
o BEGIN PLANT TESTING/OPERATOR TRAINING	JAN 87
o COMPLETE PLANT PROVEOUT	APR 88
o BEGIN BZ DISPOSAL OPERATIONS	APR 88
o COMPLETE BZ OPERATIONS/ CLEANUP	MAR 90

FIGURE 8 - BZ PROGRAM SUMMARY

SYSTEM SAFETY PROGRAM PLAN

SAFETY DESIGN REQUIREMENTS MANUAL

SAFETY DESIGN REVIEWS

PRELIMINARY HAZARD ANALYSIS

RISK MITIGATION STUDIES

HUMAN FACTORS ENGINEERING CRITERIA

HUMAN FACTORS DESIGN REVIEWS

FIGURE 9 - PROGRAM SAFETY ACTIVITIES

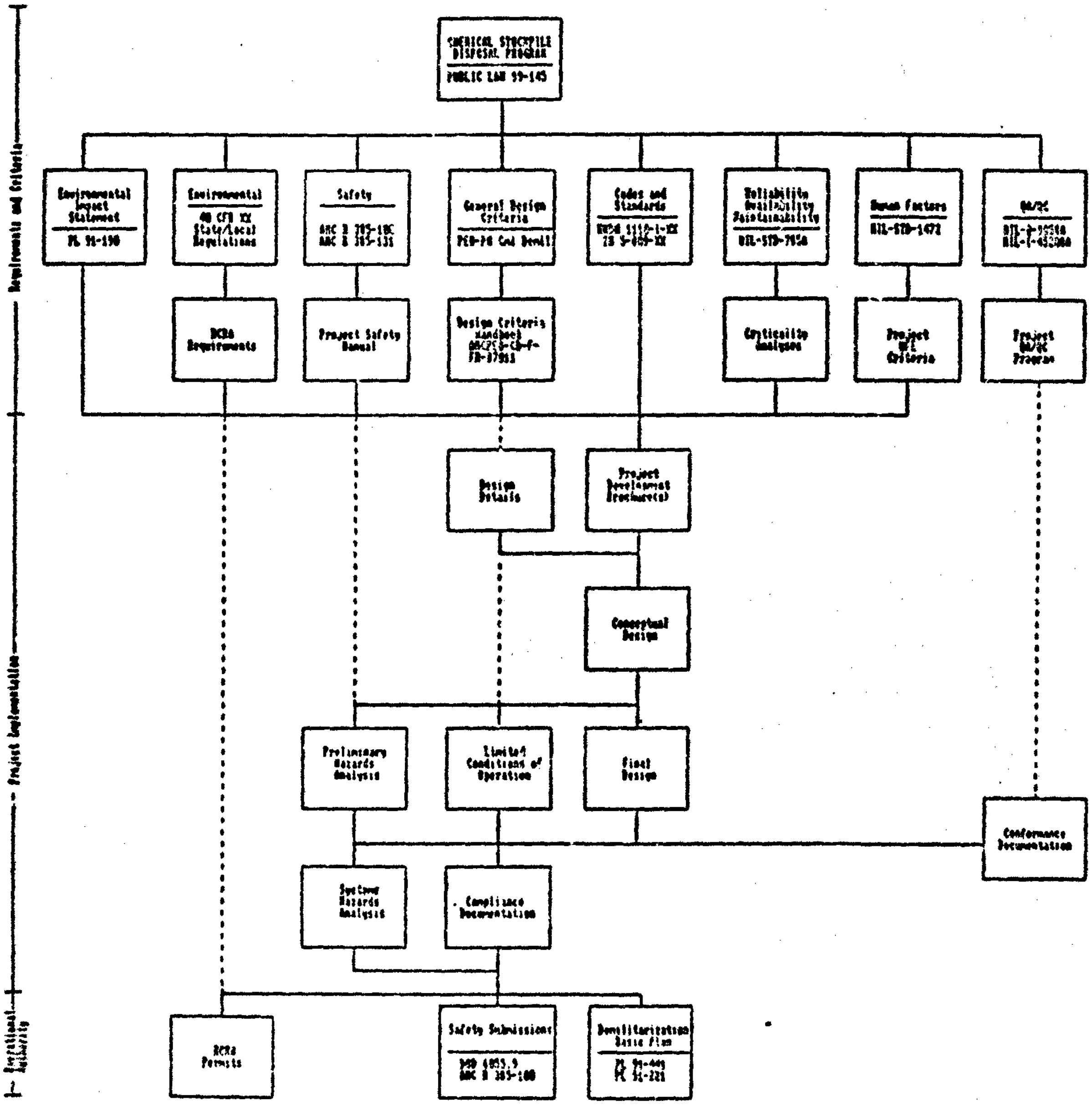

FIGURE 10-PROGRAM SAFETY ACTIVITIES

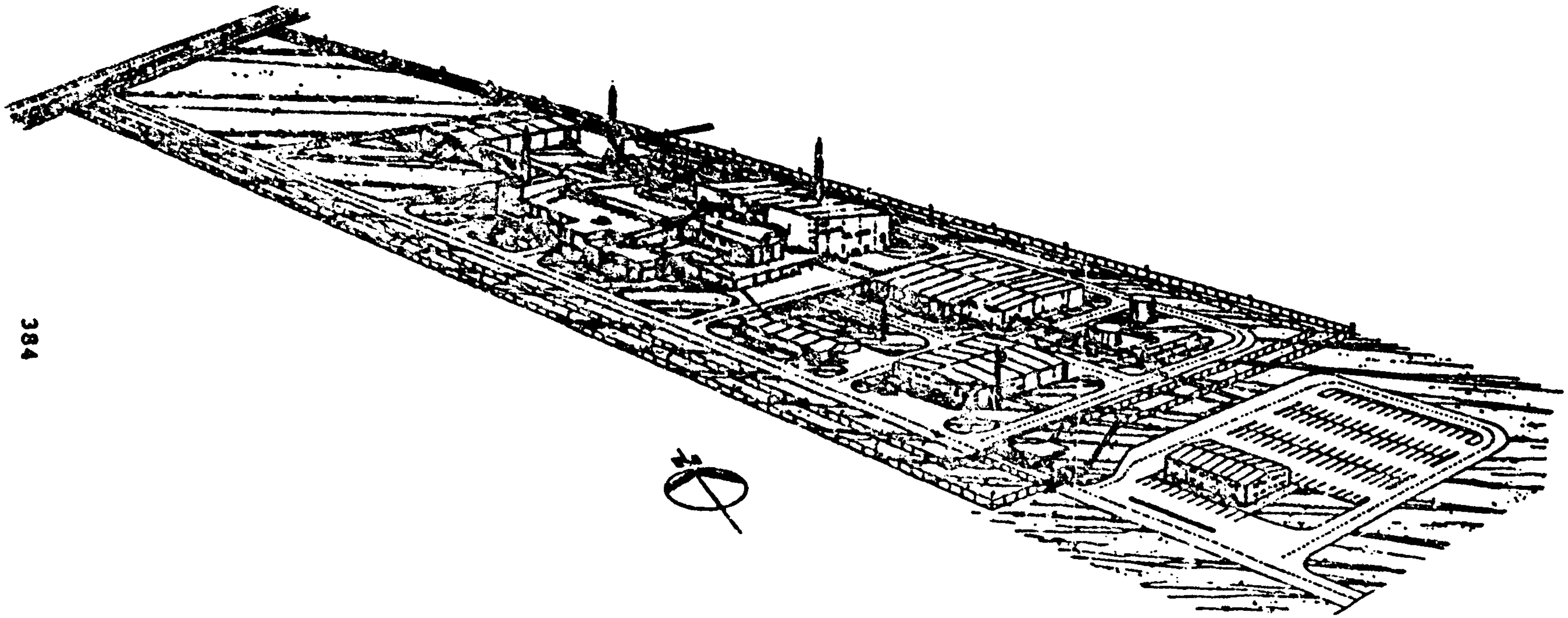

OVERALL PERSPECTIVE

FIGURE 11 - MIXED MUNITIONS PLANT

SECTION THROUGH ECR/DFS

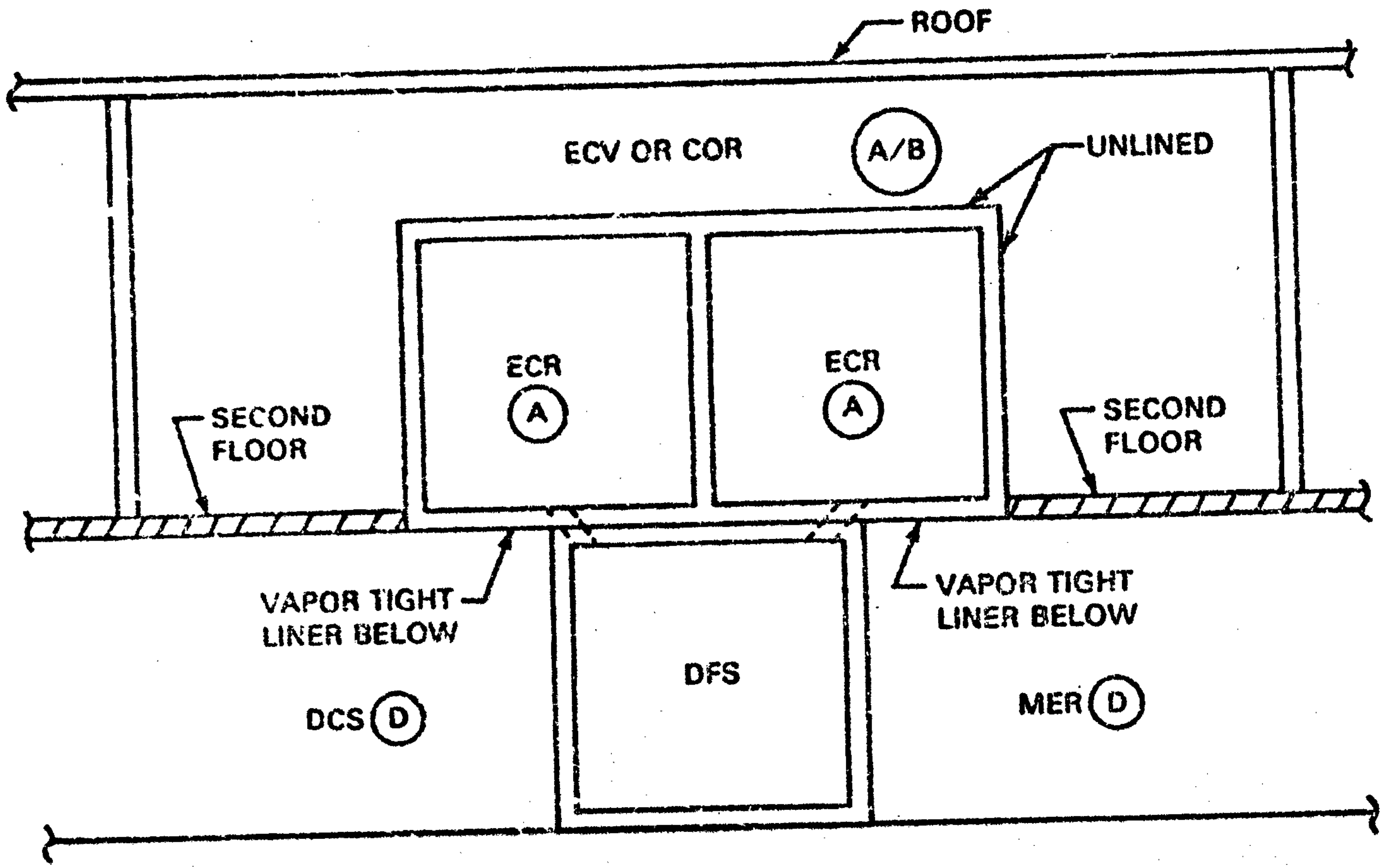

FIGURE 12 - TYPICAL ECR STRUCTURES

BASELINE SCHEDULE

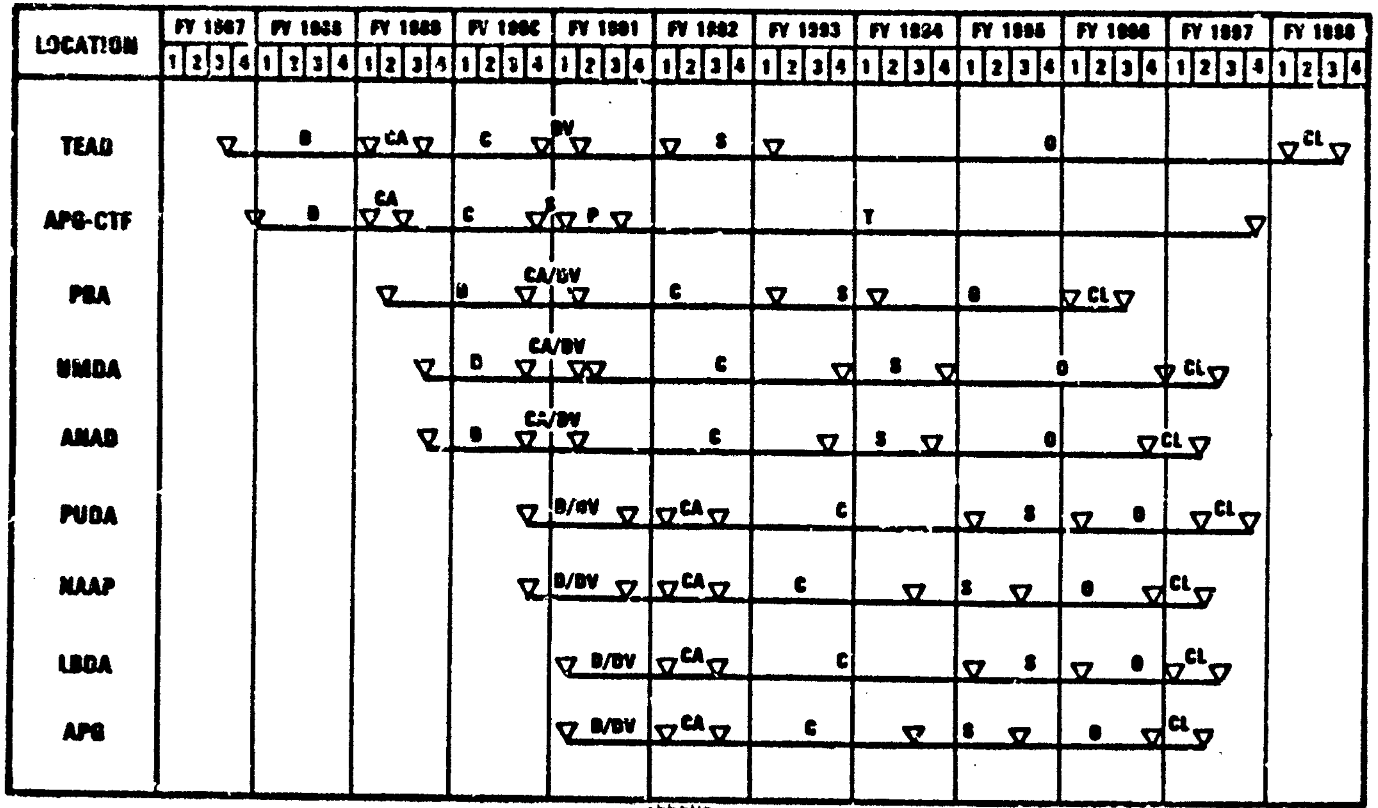

LEGEND

D - DESIGN
DV - DESIGN VERIFICATION
CA - CONSTRUCTION AWARD
C - CONSTRUCTION
S - SYSTEMIZATION
O - OPERATIONS
CL - CLOSURE
P - PREPARATION
T - TRAINING

FIGURE 13 - CSDP SCHEDULE

OVERSIGHT/INTERFACE MECHANISMS
CHEMICAL DEMILITARIZATION PROGRAM

- CONGRESS (LEGISLATION AND HEARINGS)
- COUNCIL ON ENVIRONMENTAL QUALITY
- DEPARTMENT OF HEALTH AND HUMAN SERVICE
- ENVIRONMENTAL PROTECTION AGENCY
- NATIONAL RESEARCH COUNCIL (OVERSIGHT PANEL)
- GENERAL ACCOUNTING OFFICE
- LOCAL AND STATE ELECTED OFFICIALS
- STATE REGULATORS
- DEPARTMENT OF DEFENSE EXPLOSIVES SAFETY BOARD
- US ARMY SURETY FIELD ACTIVITY
- US ARMY FIELD SAFETY ACTIVITY
- MEDIA
- PUBLIC COMMENT (WRITTEN, HEARINGS, MEETINGS)
- HEADQUARTERS DEPARTMENT OF ARMY
- MAJOR ARMY COMMANDS (AMC, HSC, WESTCOM)
- MAJOR SUBORDINATE COMMANDS (AMCCOM, DESCOM, TECOM)
- CORPS OF ENGINEERS
- INSTALLATIONS
- CONTRACTORS

FIGURE 14 - PROGRAM OVERSIGHT

Installation	Facility	Processing features[a]			
		RDS/RSM[b]	PMD/BSR[c]	MDS/MIN[d]	BDS[e]
APG	JACADS-adapted bulk design				X
ANAD	JACADS-type facility	X	X	X	X
LBAD	JACADS-type facility with one projectile line and rocket processing only	X	X		
NAAP	JACADS-adapted bulk design				X
PBA	Modified BZ facility[f]	X		X	X
PUDA	JACADS-type facility with projectile and mortar equipment only		X		
TEAD	JACADS-type facility and JACADS-adapted CAMDS bulk facility	X	X	X	X
UMDA	JACADS-type facility	X	X	X	X

[a]All on-site disposal facilities will have the following processing features, except as noted: (a) unpacked area (UPA); (b) explosive containment vestibule (ECV) and explosive containment room (ECR), except at APG and NAAP; (c) munition processing bay (MPB); (d) toxic cubicle tankage (TOX); (e) liquid incinerator (LIC); (f) deactivation furnace system (DFS), except at APG and NAAP; (g) metal parts furnace (MPF); and (h) dunnage incinerator (DUN).

[b]RDS/RSM—rocket punch and drain system and rocket shearing machine; located in explosive containment room (ECR).

[c]PMD/BSR—projectile/mortar disassembly machine and burster size reduction machine; located in explosive containment room (ECR).

[d]MDS/MIN—mine punch and drain system and mine machine for burster removal; located in explosive containment room (ECR).

[e]BDS—bulk drain system for bombs, spray tanks, and ton containers; located in munitions processing bay (MPB).

[f]The modified BZ facility at PBA is expected to have incineration and pollution abatement systems similar to a JACADS-type facility.

TABLE 1 - DEMIL PROCESS EQUIPMENT

DEACTIVATION FURNACE SYSTEM

A rotary kiln type furnace used to process all components of rockets and mines as well as bursters and fuses from other munitions. Will incinerate small amounts of agent residual to rocket and mine bodies after draining. Also incinerates all explosive, propellant fuses and decontaminates remaining metal parts. Followed by a dedicated Pollution Abatement system.

LIQUID INCINERATOR

A two stage liquid incinerator intended to destroy all agent drained from the munitions and bulk containers. Also used to incinerate spent decon solutions. Supported by its own Pollution Abatement system.

METAL PARTS FURNACE

Two stage furnace to thermally decontaminate large metal parts including drained projectile bodies, bulk containers and spray tanks. Designed to accomodate approximately 5% residual agent in containers. dedicated Pollution Abatement system.

DUNNAGE INCINERATOR

Two stage furnace to incinerate all dunnage from packing containers as well as contaminated clothing. Will also thermally decontaminate empty mine drums, metal banding as well as spent carbon filter materials. dedicated wet Pollution Abatement system.

TABLE 2 - CSDP INCINERATION SYSTEM

The ventilation system is a parallel/cascade system in which air flows progressively from areas with lower probability of contamination toward areas of greater probability and then to the filtration system and the exhaust stack. The supply air flows first to the Category C areas and then, in sequence, to Category B and Category A areas before being filtered and exhausted to the atmosphere.

The airflow to each category was determined by the following minimum air change rates:

Category	Air Changes/hr
A	20
B	10
C	6
D	Industry standards

The differential pressure between categories is:

Category	Inches of Water
A	-0.75 to -1.25
B	-0.40 to -0.60
C	-0.25
D	Atmospheric (0.0)
E	+0.1 to +0.25

A. Area Classifications

The TEAD facility, and the MDB in particular, has been subdivided into a series of five categories that designate the potential agent contamination in various work areas. These categories are defined as follows:

Category	Definition
A	Areas that have routine contamination, either agent liquid or vapor
B	Areas with a high probability of agent vapor contamination resulting from routine operations
C	Areas with a low probability of agent vapor contamination
D	Areas that are unlikely to ever have agent contamination
E	Areas maintained to be free from any chance of agent contamination.

These classifications will determine the type and magnitude of contamination control measures required in a particular area.

TABLE 3-VENTILATION CRITERIA

Power Load	Property Damage	Life Safety	How Soon Needed	Current (JACADS)	Recommended (for CSDP)	Load Classification
Agent annunciation system	-	x	Immediately	BP	BP	Critical
Fire alarm	x	x	Immediately	BP	BP	Critical
UPS radio base station	-	x	Immediately	UPS	BP[f]	Critical
ACAMS agent monitors	-	x	Immediately	BP	BP	Critical
Emergency lighting in nontoxic areas	-	x	Immediately	BP/UPS	BP	Critical
Emergency lighting in toxic areas	-	x	Immediately	BP	BP[a]	Critical
Load center and electrical switchgear controls	-	-	-[e]	BP	BP	Critical
Bubblers	-	-	-[e]	EP	-[d]	Critical
Rotary retort DFS drive	x	-	Immediately	EP	UPS	Critical
DFS retort lube oil pump	x	-	Immediately	EP	UPS	Critical
Cooling water circulating pump	x	-	Immediately	EP	UPS	Critical
CCTV	-	x	Immediately	EP	UPS	Critical
Public address system	-	x	Immediately	UPS	UPS	Critical
Potable water pump	-	x	Immediately	N/A	UPS	Critical
Instrumentation (CON, PLCs, microprocessors)	-	-	-[e]	UPS	UPS	Critical
Control room ventilation (air handling)	-	x	11 hr	EP	EP	Essential
UPS (power to)	-	-	-[b]	EP	EP	Essential
LAB building	-	x	-[e]	EP[c]	EP[c]	Essential
Life support system air compressor	-	x	11 min[e]	EP	EP[b]	Essential
Air filtration system	x	x	11 hr	EP	EP	Essential
Instrument air compressor	-	x	11 hr	EP	EP	Essential
ACAMS agent monitor receptacles	-	x	5 hr	EP	EP	Essential
Battery room exhaust	x	x	N/A	EP	EP	Essential
Fuel oil transfer pump and spare	x	x	2 hr	EP	EP	Essential
Plant air	x	x	-[e]	N/A	EP	Essential
Facility heating	x	-	-[e]	N/A	EP	Essential
Decon supply pump and spare	-	x	-[e]	EP	EP	Essential
Process water supply pumps and spare	-	x	-[e]	EP	EP	Essential
Stack lighting	x	x	-[e]	EP	EP	Essential
MPF/DUN/DFS/ECR feed and exit	x	x	Immediately	EP	UPS	Critical
ID fans (DFS)	-	-	-	EP	None	Utility
ID fan lube oil pumps	-	-	-	EP	None	Utility
Quench brine pumps	-	-	-	EP	None	Utility
Control room air conditioning	-	-	-	EP	EP	Essential
Elevators/doors	-	-	-	EP	None	Utility

BP = self contained battery pack; UPS = solid-state uninterruptible power supply; EP = emergency power; None = normal power only.
[a]Battery packs are located in nontoxic areas.
[b]UPS and emergency support should be sized to support evacuation of building.
[c]Portions of the LAB building should be on MDB, separate UPS, or self-contained battery packs.
[d]Bubblers need power immediately and should have their own batteries or be tied to the UPS. Chiller should be on emergency power.
[e]See discussion.
[f]8-hr telephone battery.

TABLE 4 - ELECTRICAL LOADS

(1) QA Class I applies to those structures, systems, or components whose failure or malfunction would detrimentally affect the safety function of the following:

(a) Containment (liquid or vapor agent or explosion)

(b) Plant safe shutdown and safety of plant personnel

(c) Offsite release of toxic material affecting the health and safety of the public

In addition, QA Class I includes those items and activities that, as a result of being defective cause extensive damage to equipment or long-term stoppage of the process. Thus, the most proficient degree of controls for the applicable QA/QC elements identified within military specification MIL-Q-9858A, including audits of documentation and records, shall be implemented.

(2) QA Class II includes those items and activities that, as a result of being defective, could adversely affect the reliability, operability, and/or safety of the facility/equipment and personnel, causing limited damage or temporary shutdown of the process. Accordingly, sufficient controls shall be applied to QA/QC elements for inspection, test, nonconformance, corrective action, documentation, and records in accordance with MIL-I-45208A during design, procurement, and construction. When design changes under configuration control are also required, the QA/QC element required for design activities shall adhere to MIL-Q-9858A, additionally.

(3) QA Class III includes those items and activities that do not adversely affect the reliability, capability, and/or safety of the facility or equipment if failure were to occur. Appropriate referencing of industrial codes or standards in combination with testing and inspections and good workmanship, both specified within the specification and procurement documents, are sufficient. Documents specifically required shall be delineated in technical data packages. Off-the-shelf items may be included in this classification.

TABLE 5 - CRITERIA FOR SIL CLASSIFICATION

CHEMICAL STOCKPILE DISPOSAL PROGRAM

LIFE CYCLE COSTS

(MILLIONS OF CONSTANT FY 1988 DOLLARS)

COST ELEMENT	
DESIGN AND ENGINEERING	76.2
EQUIPMENT	709.9
CONSTRUCTION	273.2
TRAINING	81.2
SYSTEMIZATION AND PREOPERATIONS	165.4
OPERATIONS	630.1
CLOSURE	44.3
ON-SITE SUPPORT	327.1
PROGRAM SUPPORT	390.8
EUROPEAN STOCKPILE	28.4
TOTAL	2,726.6

TABLE 6 - PROGRAMMABLE COST ESTIMATES

A PROCEDURE TO ASSESS EXPLOSION DAMAGE TO BUILDINGS OF COMMON CONSTRUCTION

by
Mark G. Whitney
Donald E. Ketchum
Charles J. Oswald

Abstract

Manuals are available for the design and analysis of hardened structures exposed to explosion loads. These documents are typically concerned with substantial reinforced concrete or steel structures and include factors of safety and design conservatism. Buildings designed for conventional loads (wind, snow, seismic, etc.) are not fully addressed by such manuals, particularly if the goal is to obtain a realistic prediction of explosion damage to buildings. A procedure has been developed which utilizes prediction tools based upon correlations with test data. This procedure has been documented in a Guide which provides facility planners the means to make credible estimates of damage to buildings of common construction. This paper previews the Guide, overviews the development of damage assessment tools, and provides examples of building damage, repair, and reuse curves from the Guide.

I. INTRODUCTION

Design documents are available, such as the recently revised NAVFAC P-397 triservice document (also known as TM5-1300 and AFM 88-22, Reference 1), which provide conservative procedures for designing structures to be resistant to explosion loads. Many explosion handling facilities have structures which were designed for conventional loadings and hence are not blast hardened. While personnel safety must be provided by compliance with inhabited building distances or through the use of barriers or blast containment design based upon NAVFAC P-397, it

is desirable to have a method of predicting non-hardened structure damage which does not include safety factors or design conservatism that is inherent in manuals and design guides. Such a procedure provides realistic predictions of explosion damage to buildings, particularly those of common construction. The procedure is documented in Reference 2, "Blast Vulnerability Guide," which will be referred to as the "Guide" throughout this paper. The Guide allows prediction of damage based upon a correlation of past explosion test data to observed structural damage instead of utilizing standard design procedures which provide conservative estimates of structural component response. A similar effort was completed by Tancreto [3] which established direction and guidelines for preparation of the Guide. The engineering basis for development of the Guide is documented in a separate report by Oswald, et al.[4], in a report entitled "Blast Damage Assessment Procedures for Common Construction Categories."

Many different construction practices are addressed by the Guide. These include the following:

- Reinforced concrete
- Tilt-up concrete panels
- Masonry (reinforced and unreinforced)
- Structural steel-framed buildings
- Butler buildings
- Wood frame buildings
- Heavy timber

The Guide considers explosions external to structures utilizing one or more of these types of construction. The Guide addresses explosive quantities up to 4000 pounds at distances ranging from nearby to 1000 feet away. This covers a range of side-on overpressures from less than 1 psi to several thousand psi. Loadings due to impact of primary fragments from cased munitions and debris from packaging or vehicles transporting the explosives were also addressed in the Guide. The explosion scenarios addressed are limited to those occurring in the open

or during transport, and not inside another structure. Hence, building debris, which can be an important explosion hazard, is not addressed.

II. BLAST DAMAGE PREDICTION PROCEDURE

The general procedure for estimating building damage is outlined in the following paragraphs. The approach taken is to consider the building as an assembly of structural components or elements. Blast and fragment loads are determined for each component based upon the HE amount, the building orientation, and distance to the explosion. Damage to each structural element is predicted. Total building damage is calculated by a sum of the damage to components allowing for the importance each element contributes to the integrity of the building. The procedure outlined in the Guide includes the following steps:

1. Select a specific threat. This includes defining:

   - charge quantity
   - casing description
   - distance from explosion to building
   - orientation of explosion to building

2. Identify the various structural components of the building. The type and number of structural components depend upon the building under analysis. Components typically include wall panels, columns, beams, roof panels, joists, etc. Identify the following parameters for each component where applicable:

   - spans
   - thickness or dimensions
   - mass
   - boundary conditions
   - construction details (if available)

Construction details include information such as reinforcement, size and location of stiffeners, and material properties (compressive, tensile,

and shear strengths). This type of information may not be available, forcing estimates to be made. Direction is provided in the Guide for making such estimates.

3. Blast pressure and impulse and missile loading on the structure are defined utilizing the curves provided in the Guide. Blast curves are for both reflected and side-on parameters. Two types of missiles are discussed: fragments from cased munitions or bombs and debris from vehicles. Small fragments will perforate a structural element upon impact and will reduce its load carrying capacity. Large debris impact increases the gross structural motion of the element in addition to that resulting from the blast wave.

4. Pressure-Impulse (P-I) diagrams are used to predict the blast damage expected for each structural component. A brief description of the P-I diagram development is provided in Section III of this paper. For each component of the structure under consideration, use of the P-I diagram results in a damage level (0.0, 0.3, 0.6, or 1.0) for that component.

5. The damage to individual components of a building is then related to damage to the building as a whole. A "weight" is assigned to each component based on its worth as a structural member. "Weighting" factors are suggested in the Guide for various structural components; however, the procedures are general enough for the user to choose and use his or her own values. A summation of the weighted damage to all components is made to determine total building damage which always will be a value between 0.0 and 1.0; where 1.0 represents complete building collapse, and 0.0 is an undamaged structure. The Guide goes further to relate building damage to a criterion of whether the structure can be repaired or if demolition and replacement is required. Reusability of the building space after minor repairs is also addressed. In Section IV an example is provided of damage, repair, and reuse curves developed for a typical building using this procedure.

III. DAMAGE ASSESSMENT CURVES

It was desired to develop a set of damage prediction curves for a variety of common structural components based upon test data and not analysis predictions. Oswald, et al., [4] performed an extensive literature survey to collect an empirical data base concerning blast damage to structural elements with an emphasis on conventional structures. A total of 36 documents were reviewed, and data was identified for the following:

- Reinforced concrete slabs, beams, and columns
- Unreinforced concrete masonry units
- Unreinforced brick walls
- Steel beams and columns
- Heavy timber beams
- Wood frame walls or roofs
- Wood decking over joists
- Corrugated metal or cement-asbestos wall and roof panels
- Lightweight concrete over decking (roof)
- Metal stud walls
- Shear walls
- Movement resisting steel frames
- Movement resisting concrete frames
- Windows
- Doors

Reference 4 summarizes the literature search effort and the data collected.

A review of the documents indicated that insufficient data existed to define completely damage curves for the building components. This required a combined theoretical-experimental approach to the problem, in which a general theoretical solution was developed and then verified or modified by the comparisons with the experimental data. Following this approach, P-I diagrams that had been previously developed by Baker, Cox, and Westine [5] for various structural components were used. P-I

diagrams existed for beams, plates, membranes, and columns. For cases in which no previous solutions existed, for example, for unreinforced masonry, new theoretical solutions were developed. The P-I diagram with non-dimensional terms was chosen for use in the analysis as this format provides great flexibility in representing structural element and blast load parameters. This format does not refer to specific structural spans or thickness and can represent a variety of support conditions. Also, the curves generally apply to any blast load which can be represented by a single triangular pulse of peak pressure, p, and impulse, i. This type of generality is an essential aspect of the technical solution developed.

The procedure for developing P-I diagrams was to find the asymptotes to the general solutions and estimate the transition region between the asymptotes. The asymptotes were found by equating the strain energy in the structure to the work done by the pressure (pressure asymptote) or to the kinetic energy imparted to the structure by the impulse (impulsive asymptote). For either existing or new solutions, the resulting curves are then adjusted to match the experimental data. The development of a typical set of damage curves is illustrated below with the example of a P-I diagram for steel beams.

Figure 1, taken from Reference 5, was used as the basis for the steel beam solution. The terms in Figure 1 are defined in Table 1. This figure gives an elastic-plastic solution for beams with four different boundary conditions when subjected to arbitrary blast loading. Although the solution is theoretical, the impulsive asymptote was previously verified by comparison with experimental data [5] for idealized beams of rectangular cross section. Comparisons were made in [4] with more representative structural elements to avoid conservatism. Data for comparison with the solution in Figure 1 included blast-loaded steel beams and prefabricated steel panels which responded as beams in the tests.

Comparisons between the theoretical solution and the experimental data are shown on Figure 2. The curves in Figure 2 are the same as

those in Figure 1. The number given for each data point indicates the calculated value of the nondimensional group $\bar{\mu}$.

The components exhibit less damage than is predicted by the theoretical solution. To compensate for the apparent conservatism in the theoretical solution, the curves were shifted to better match the data (see Figure 3).

The terms $\bar{i}$ and $\bar{p}$ are calculated based upon the applied load, beam properties, and boundary conditions. When a point is plotted, a value of $\bar{\mu}$ is obtained. Using the equation which defines $\bar{\mu}$, one can obtain a value of ductility, μ, and an equation is provided in the Guide for calculating deflection, Δ. Damage to the element was defined based upon a modification to criteria for ductility and hinge rotations in Healey, et al. [6], and the revision to NAVFAC P-397 [1]. The final P-I diagram presented in the Guide is illustrated in Figure 4, where damage to the component is calculated at discrete values of either 0, 30%, 60%, or 100% damage depending upon Δ (which is related to θ) and μ.

Similar P-I diagrams were developed for each of the components listed in Table 2 and are available in the Guide. Structures that are not steel (concrete, masonry, or wood) have established damage criteria taken directly from observations in the data as the data base was more complete than that for steel structures. Prediction of μ or Δ is not necessary, as damage levels are plotted directly on the P-I diagram as indicated on Figure 5 for one-way reinforced concrete slabs.

IV. BUILDING DAMAGE CURVES

Twelve example buildings were evaluated using the procedures in the Guide for a variety of explosive quantities and standoffs for determination of damage, reusability, and repairability. The twelve buildings cover a wide range of construction types including reinforced concrete, tilt-up panels, masonry, steel, prefabricated buildings, and wood frame buildings. An example of one building and associated damage

curves is provided in Table 3 and Figures 6-9. These and other curves were developed by applying the methods outlined in the Guide.

V. SUMMARY

Procedures and damage assessment curves have been developed to allow facility planners to make realistic predictions of damage to buildings of common construction subjected to explosion loads. These are presented in a Guide [2] which is previewed in this paper. The damage assessment procedures were applied to twelve common buildings and a set of damage curves for each is presented in the Guide, an example of which is given in this paper.

VI. ACKNOWLEDGEMENTS

The Blast Vulnerability Guide was prepared for the Naval Civil Engineering Laboratory (NCEL) under Prime Contract No. N00123-86-D-0299. The authors wish to acknowledge Ms. Mary Gunther, Mr. Jim Tancreto, and Mr. John Ferritto of NCEL for their review and technical guidance during development of the Guide.

VII. REFERENCES

1. Special Publication ARLCD-SP-84001, "Structures to Resist the Effects of Accidental Explosions," Volumes I - VI, U.S. Army Armament Reserch Development and Engineering Center, Contract No. DAAK10-82-C-0112, 1987.

2. Whitney, M. G., Ketchum, D.E., and Polcyn, M.A., "Blast Vulnerability Guide," Final Report, Southwest Research Institute Project No. 06-1473-040, prepared for the Naval Civil Engineering Laboratory, Prime Contract No. N00123-86-D-0299 under Subcontract to Tecolote Research, Inc., Subcontract No. TRI87107, Job No. 145.09, Oct. 1987.

3. Tancreto, J., "Building Damage Functions for Explosive Threats," Draft Naval Civil Engineering Laboratory TM 88-06, Feb. 1987.

4. Oswald, C.J., Polcyn, M.A., Ketchum, D.E., Marchand, K.A., Cox, P.A., and Whitney, M.G., "Blast Damage Assessment Procedures for Common Construction Categories," Final Report, Southwest Research Institute Project No. 06-1473-030, prepared for the Naval Civil Engineering Laboratory, Prime Contract No. N00123-86-D-0299 under Subcontract to Tecolote Research, Inc., Subcontract No. TRI87107, Job No. 145.08, Oct. 1987.

5. Baker, W.E., Cox, P.A., Westine, P.S., Kulesz, J.J., and Strehlow, R.A., Explosion Hazards and Evaluation, Elsevier Scientific Publishing Company, New York, New York, 1983.

6. Healy, J., Ammar, A., Vellozzi, J., Pecone, G., Weissman, S., Dobbs, N., and Price, P., "Design of Steel Structures to Resist the Effects of HE Explosives," Technical Report 4837, Picatinny Arsenal, Dover, New Jersey, 1975.

BOUNDARY CONDITIONS	ψ_p	ψ_i	ψ_ϵ	ψ_{w_o}
SIMPLE SUPPORT	10.00	0.913	1.250	0.2063
CLAMPED - CLAMPED	23.10	0.861	1.925	0.0625
CLAMPED - PINNED	15.83	0.885	1.979	0.0867
CANTILEVER	3.333	0.577	1.000	0.5000

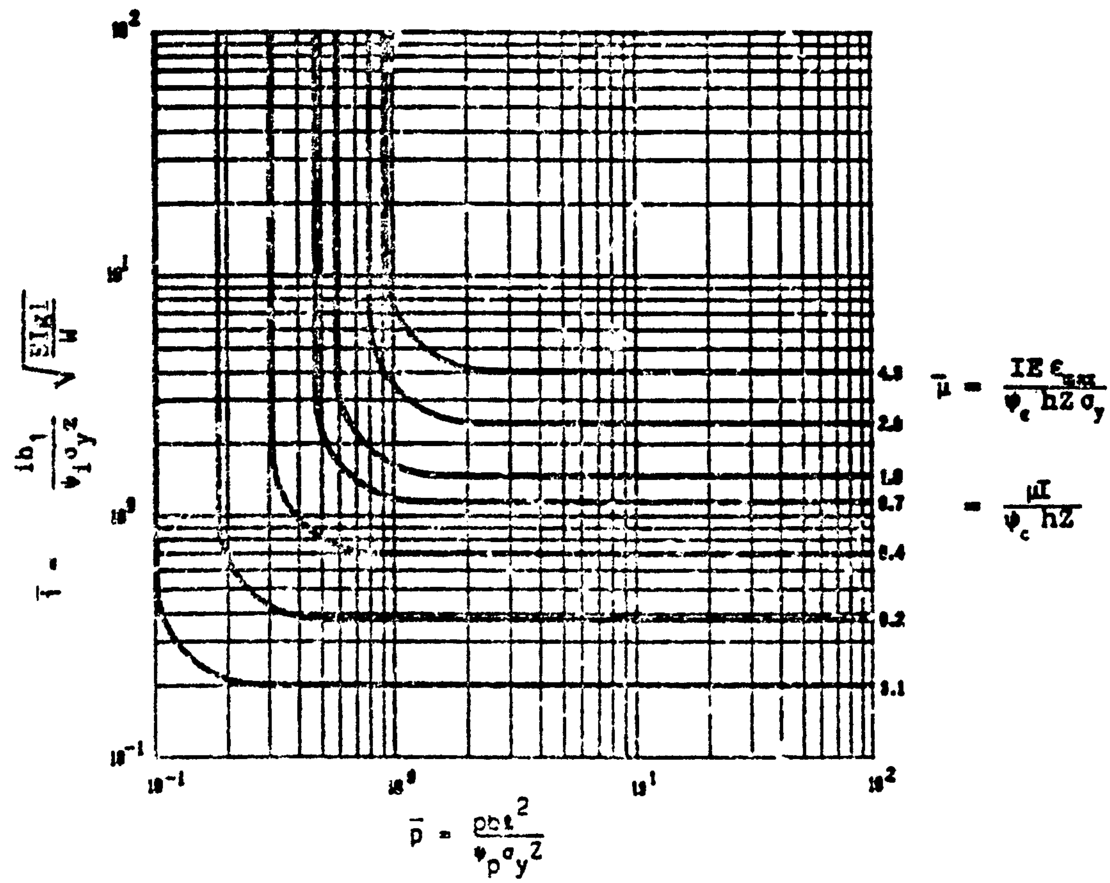

Figure 1
Elastic-Plastic Solution for Bending of Blast-Loaded Steel Beams
(Figure 4-26 of Reference 5)

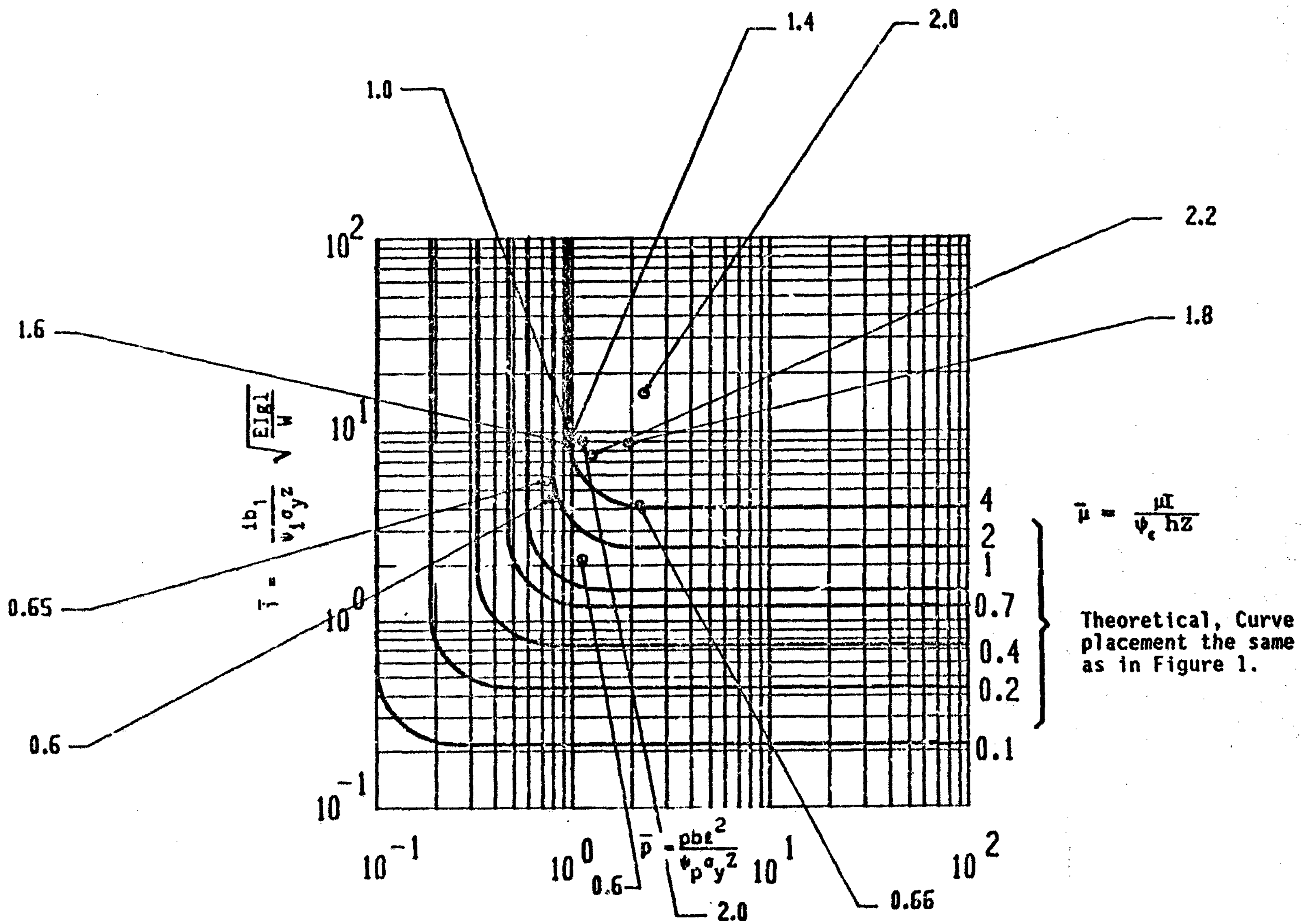

Figure 2
Comparison of the Tehoretical Solution and Experimental Data for Blast-Loaded Beams

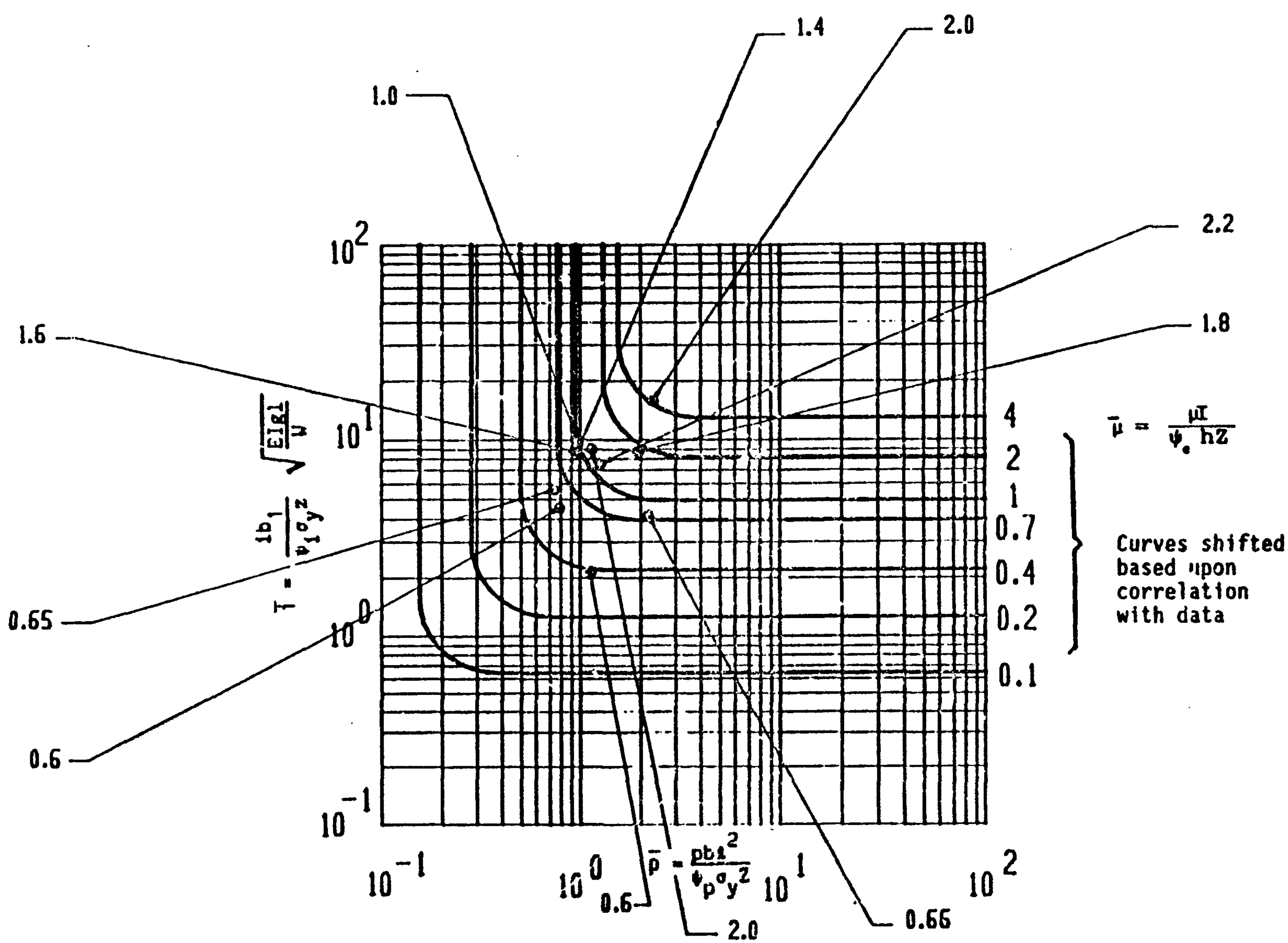

Figure 3
Shifted Theoretical Curves for Better Agreement with Data

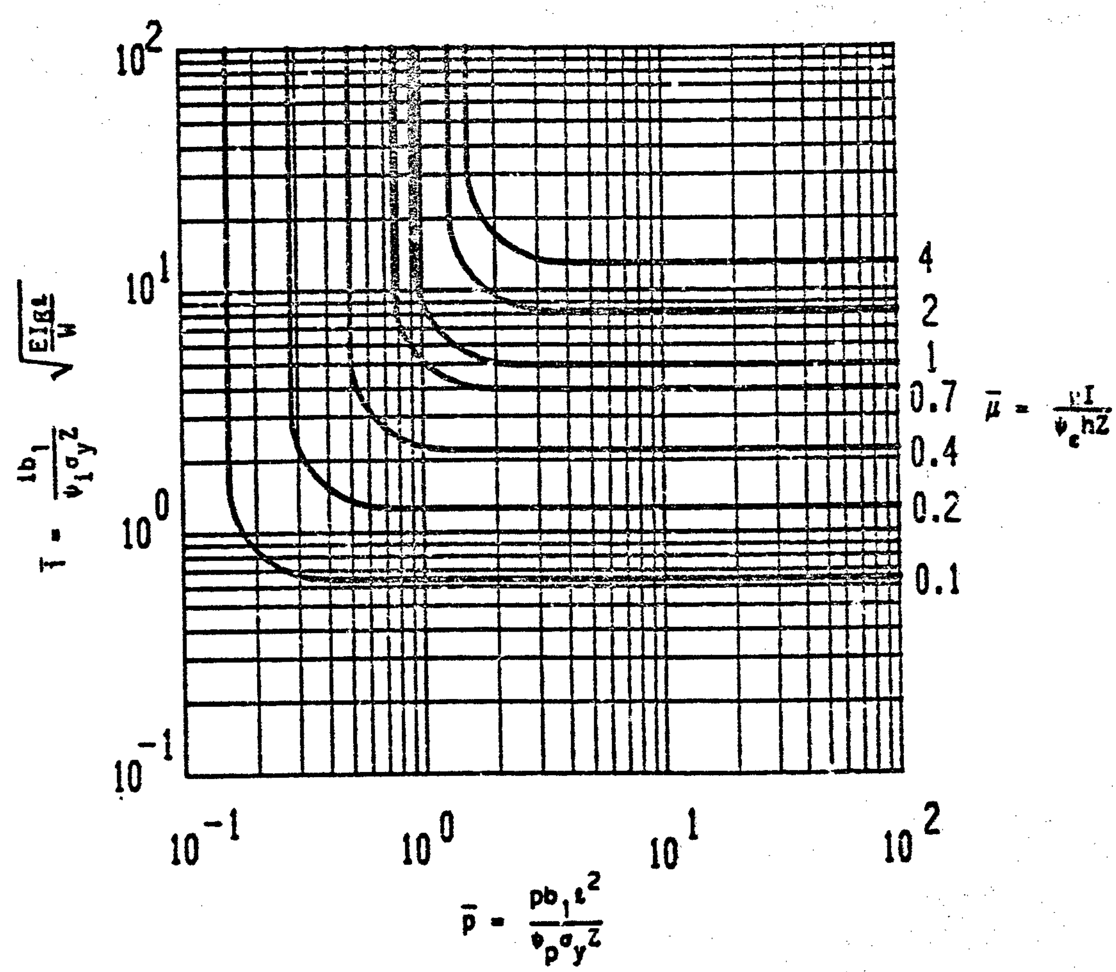

Boundary Conditions	ψ_p	ψ_i	ψ_ϵ	ψ_Δ
Simple-Simple	10.00	0.913	1.250	0.2083
Fixed-Fixed	23.10	0.861	1.925	0.0625

Damage Level	Ductility Ratio Limits	Deflection Limits
0.0	$\mu < 2$	$\Delta/\ell < 1/115$
0.3	$2 < \mu < 7$	$1/115 < \Delta/\ell < 1/30$
0.6	$7 < \mu < 15$	$1/30 < \Delta/\ell < 1/15$
1.0	$\mu > 15$	$\Delta/\ell > 1/15$

Figure 4
Pressure-Impulse Relation for Steel Beams

p	peak applied pressure (F/L^2)
i	applied specific impulse (FT/L^2)
ℓ	beam length (L)
I	moment of inertia (L^4)
Z	plastic section modulus (L^3)
b_1	loaded width (typically beam spacing) (L)
g	acceleration due to gravity (L/T^2)
h	beam depth (L)
E	Young's Modulus (F/L^2)
W	total weight of section plus weight of supported components (F)
ϕ	boundary coefficients (-)
μ	ductility ratio (-)
σ_y	yield stress for steel (F/L^2)
Δ	midspan deflection (L)

$$\Delta/L = \frac{\mu \sigma_y \ell \phi_\Delta}{hE}$$

Notes: Check units of ordinate and abscissa terms to confirm that all units cancel and result in non-dimensional terms.

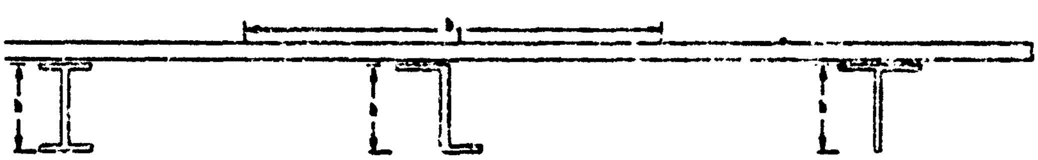

SECTION

Figure 4
Pressure-Impulse Relation for Steel Beams as Presented in the Guide [2]

p	peak applied pressure (F/L^2)
i	applied specific impulse (FT/L^2)
ℓ	slab span (L)
I_{eff}	effective moment of inertia (L^4)
M_p	moment capacity of the section (L-F)
A	cross-sectional area (L^2)
A_s	tensile steel area (L^2)
b	section width (typically rebar spacing) (L)
d	depth of tensile reinforcement (L)
g	acceleration due to gravity (L/T^2)
E	Young's Modulus (F/L^2)
f_y	yield strength of reinforcement (F/L^2)
f_c'	compressive strength of concrete (F/L^2)
γ	weight density of section (F/L^3)
ρ	tensile steel reinforcement area per gross area of section (-)
ϕ	boundary coefficients (-)

$$E = 57000 \sqrt{f_c'} \qquad \rho = A_s/(bd)$$

$$I_{eff} = \frac{bd^3(5.5\rho + 0.083)}{2} \qquad M_p = 0.9\, bd^2 f_y \rho (1 - 0.59 \rho f_y / f_c')$$

Note: 1) Check units of ordinate and abscissa terms to confirm that all units cancel and result in non-dimensional terms.
2) For simple-simple elements calculate tensile steel area, A_s, using the midspan reinforcement at the inside face.
3) For fixed-fixed elements the tensile steel area, A_s, is calculated by averaging the midspan reinforcement at the inside face and the support reinforcement at the outside face.
4) The equation for E above uses f_c' in units of psi and results in E in psi units. If the nondimensional terms on the graph are calculated in other self consistent units, then the value of E must be converted accordingly.

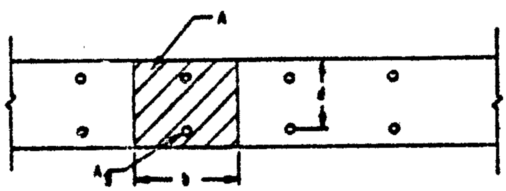

Figure 5
Pressure-Impulse Relation for One-Way Reinforced Concrete Slabs as Presented in the Guide [2]

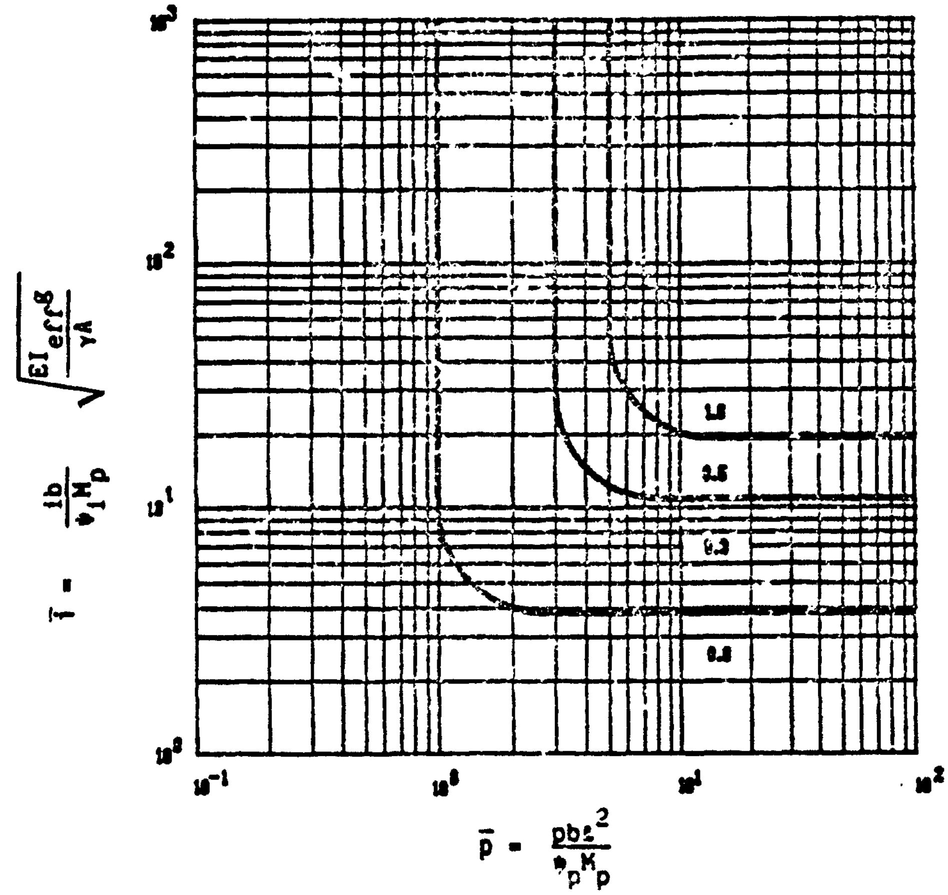

Boundary Conditions	ψ_p	ψ_i
Simple-Simple	10.00	0.913
Fixed-Fixed	23.10	0.851

Figure 5
Pressure-Impulse Relation for One-Way Reinforced Concrete Slabs as Presented in the Guide [2] (Continued)

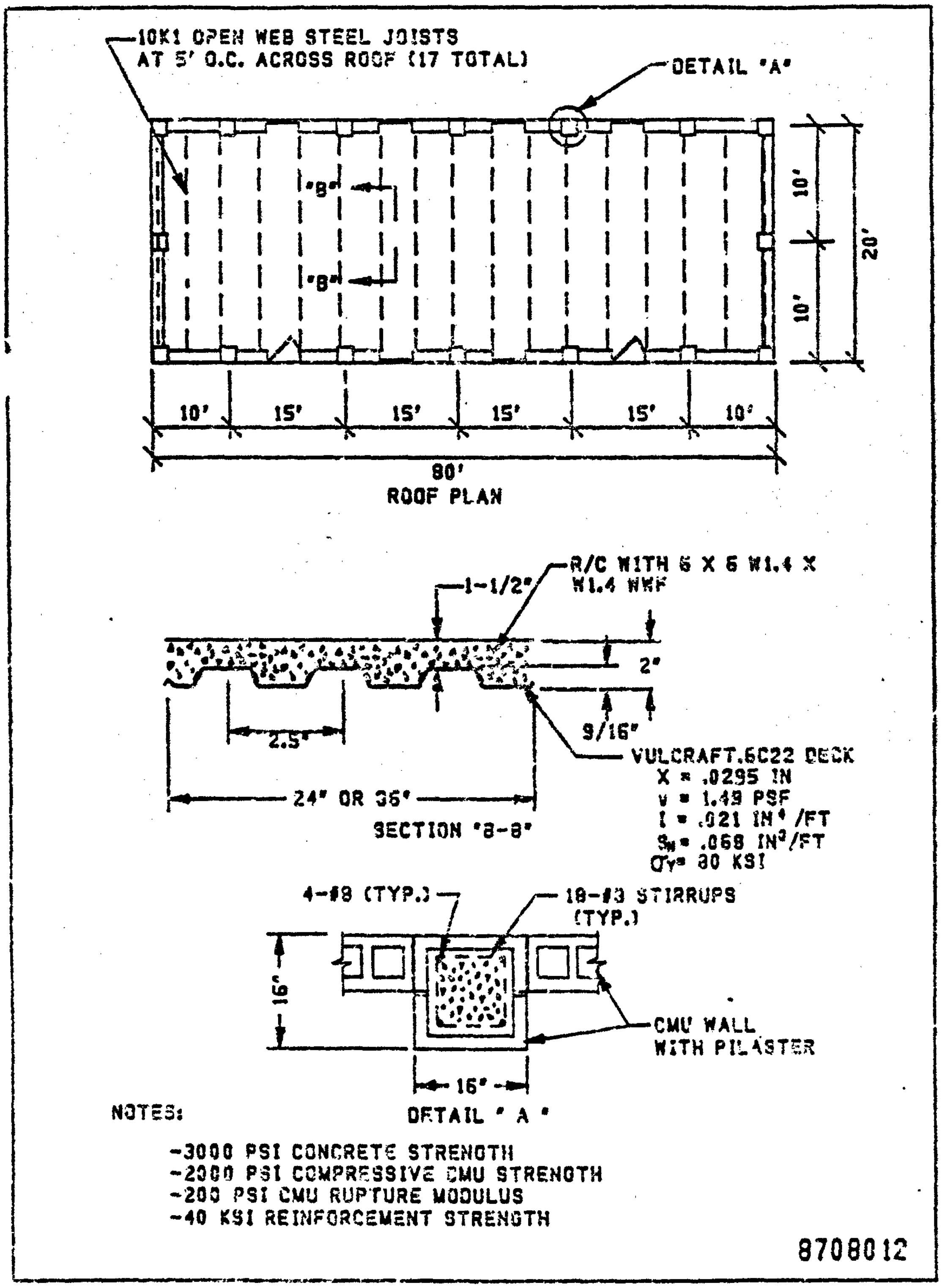

Figure 6
Example Building

TABLE 1.
Nomenclature of Pressure-Impulse Relation for Steel Beams Depicted in Figure 1

p	peak applied pressure (F/L^2)
i	applied specific impulse (FT/L^2)
ℓ	beam length (L)
I	moment of inertia (L^4)
Z	plastic section modulus (L^3)
b_1	loaded width (typically beam spacing) (L)
g	acceleration due to gravity (L/T^2)
h	beam depth (L)
E	Young's Modulus (F/L^2)
W	total weight of section plus weight of supported components (F)
ψ	boundary coefficients (-)
μ	ductility ratio (-)
σ_y	yield stress for steel (F/L^2)
Δ	midspan deflection (L)

$$\Delta/L = \frac{\mu \sigma_y \ell \psi_\Delta}{hE}$$

$$\bar{i} = \frac{i b_1}{\psi_i \sigma_y Z} \sqrt{\frac{EIg\ell}{W}}$$

$$\bar{p} = \frac{p b \ell^2}{\psi_p \sigma_y Z}$$

$$\bar{\mu} = \frac{\mu I}{\psi_\varepsilon h Z}$$

Table 2. List of Components

<u>Reinforced Concrete Components</u>

Beams
One-way slabs
Two-way slabs
Exterior columns (Bending)
Interior columns (Buckling)
Moment-resisting frames

<u>Steel Components</u>

Beams
Metal stud walls
Open-web steel joists (Cord failure)
Open-web steel joists (Web buckling)
Corrugated metal decking
Exterior columns (Bending)
Interior columns (Buckling)
Moment-resisting frames

<u>Masonry Components</u>

One-way unreinforced walls
Two-way unreinforced walls
One-way reinforced walls
Two-way reinforced walls
Pilasters

<u>Wood or Timber Components</u>

Stud walls
Roofs
Beams
Exterior columns (Bending)
Interior columns (Buckling)

TABLE 3. EXAMPLE BUILDING DESCRIPTION

This structure has unreinforced CMU bearing walls with reinforced CMU pilasters. All cells are grouted. The roof supports are open-web steel joists. The roof is constructed of lightweight concrete over corrugated metal decking. This one-story building has 1600 square feet and is 12 feet in height. This structure is comprised of the following components, the quantity of each, and their assigned weights.

No.	Component	Weight
16	13.7′ x 12′ x 7.625" CMU panels, unreinforced, single wythe, considered simply supported, two-way 13.7′ x 12′ loaded area.	4.0
16	12′ x 15.625" x 15.625" CMU pilasters, considered simply supported beams, loaded area is 38% of 15′ x 12′ area, reinforced with 4-#8's at d=12.625."	5.0
17	Open-web steel joists, 20′ span at 5′ on center 20′ x 5′ loaded area, 10 K1 joists (SJI designation).	2.0
16	Corrugated steel/concrete decking, 5′ span, fixed supports, .6C22 panels with 1-1/2" lightweight concrete cover.	1.0
4	Doors and windows, fail at 2.0 psi, located in CMU panels.	0.25

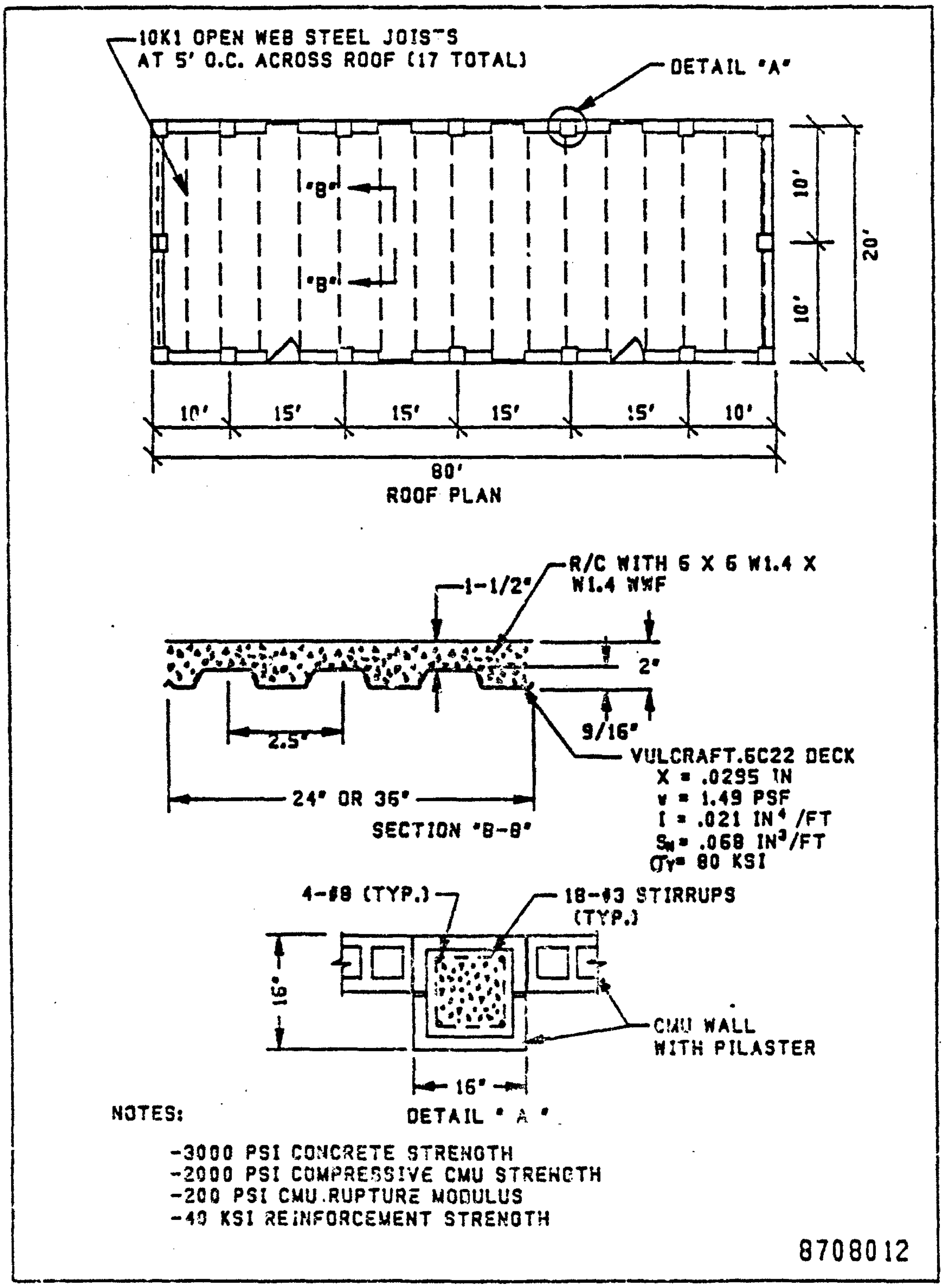

Figure 6
Example Building

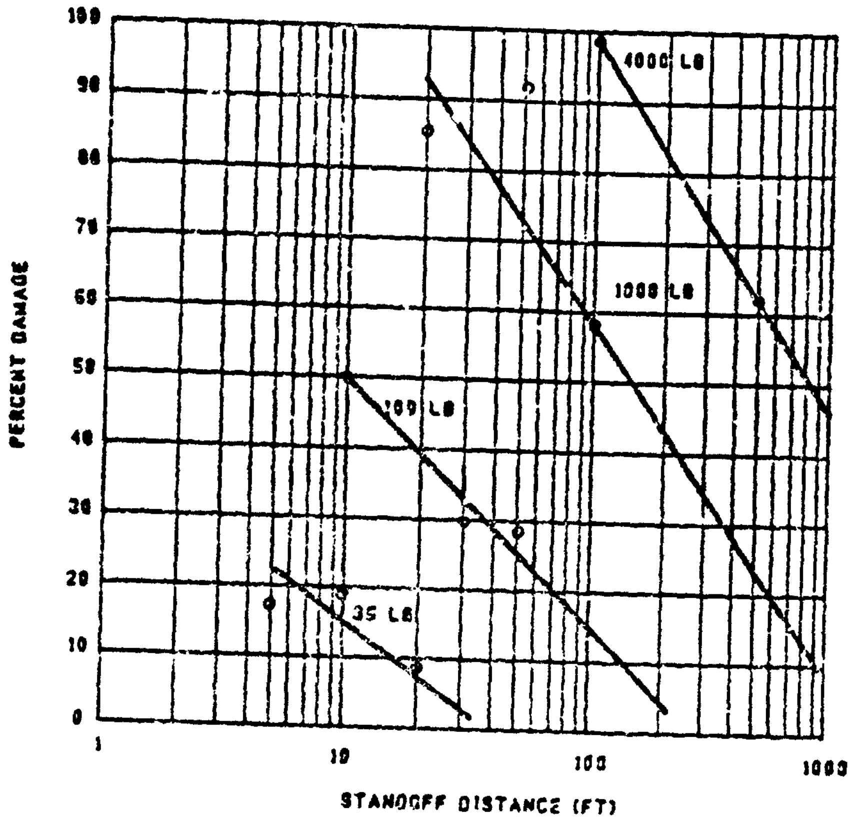

Figure 7
Example Building Damage Curve

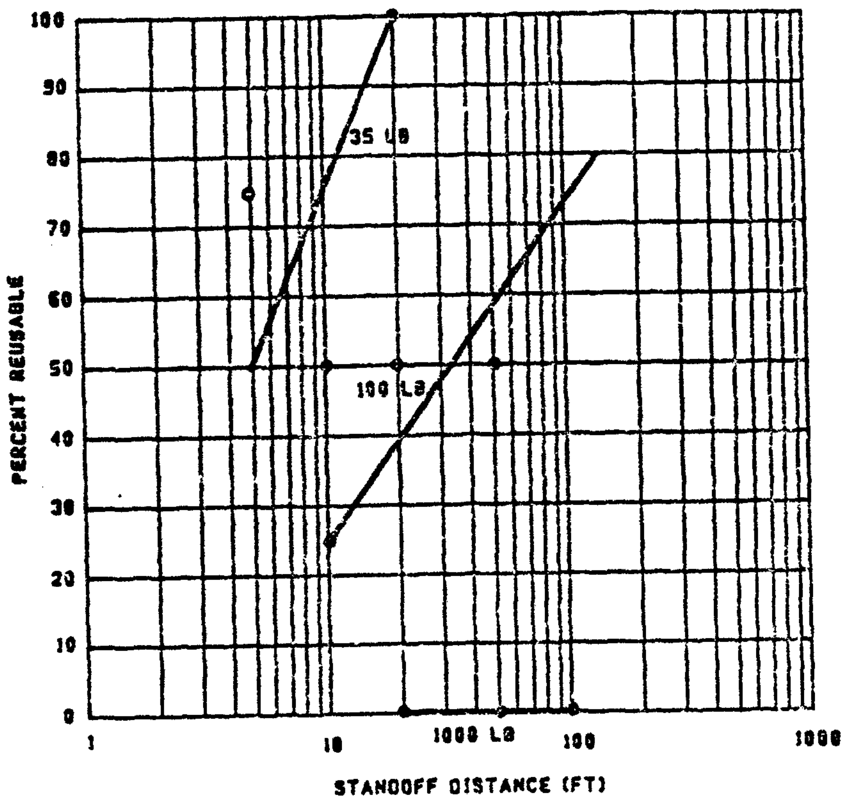

Figure 8
Example Building Reuse Curve

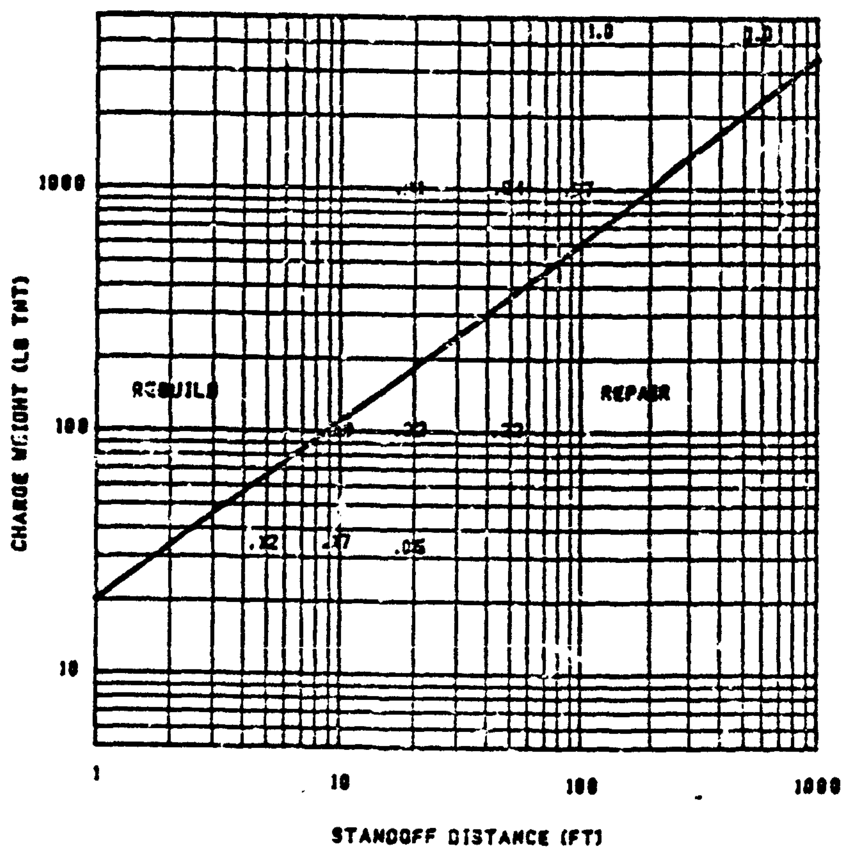

Figure 9
Example Building Repair Curve

RESPONSE OF STRUCTURAL COMPONENTS TO BLAST: ANALYTICAL VERSUS EXPERIMENTAL RESULTS

by
Michael A. Polcyn
and
Kirk A. Marchand

Safety of personnel from accidental explosions at explosive handling facilities is achieved by providing adequate separation distance from potential explosion sources, by providing barriers or protective construction between the explosion source and personnel to reduce shocks and fragments, or by providing some combination of separation distance and protective construction. When space limitations or operational constraints are present, protective construction is required. Manuals such as TM5-1300 and the recent revision to this manual provide analytical procedures to conservatively design most structures. Information concerning loads prediction, dynamic response calculations, dynamic material strengths, and failure criteria is provided in these manuals.

Protection of personnel is always the primary objective and usually overrides any conflicting design considerations such as cost. However, minimizing construction cost is always an important requirement. Therefore, it is of interest to determine the level of conservatism in common design procedures by comparing predicted dynamic response of structural components to the response observed in explosive tests.

Southwest Research Institute (SwRI) was funded by the Naval Civil Engineering Laboratory (NCEL) to develop procedures for predicting blast damage to commonly constructed buildings at Naval Facilities. A wartime or terrorist threat, rather than an accidental explosion threat was of interest. Therefore, damage to structures was correlated to past explosive test data, instead of directly using standard analysis procedures which provide conservative estimates of the response of structural components. This data was used to calibrate an analysis procedure, giving the user a realistic assessment of the potential damage. In doing so, experimental results were compared to analytical results.

Background

The objective when preparing References 1 and 2 was to develop procedures to assess damage to structures resulting from external explosions. Because this type of loading consists only of a shock load, Pressure-Impulse (P-I) diagrams were used to perform the analysis. This provides a simple graphical means of determining the damage to any element type. A typical curve is shown in Figure 1. Each of the lines defines the boundary between increasing component percent damage. These boundaries were initially determined analytically, and plotted along with experimental data points. Boundaries were shifted so that data fell in the appropriate damage level.

The goal for Reference 3 was similar, except that the threat was for internal explosions. This loading condition combines a quasi-static load with the shock load, making the use of P-I diagrams tedious. Therefore it was decided to calculate component damage by solving a modified energy equation. In its basic form, the equation is expressed as

$$KE + Work = \phi_s \times SE \tag{1}$$

where

KE = kinetic energy from the applied shock impulse

Work = work from the applied quasi-static load

ϕ_s = correction factor to relate calculated strain energy to that expected or observed experimentally

SE = component strain energy calculated using standard analysis procedures.

Both the work term and the strain energy term are functions of the maximum deflection of the component. Therefore, by inputting the loads and the appropriate structural parameters, the component response can be calculated. If ϕ_s is chosen properly, the calculated deflection will approximate that which would actually be observed. The remainder of this paper will describe the approach used to calculate the correction factor and present results for several element types.

Procedure for Calculating Correction Factor

The procedure for calculating ϕ_s was set by considering test data for reinforced concrete elements. One-way slabs were analyzed first using test data from Reference 4. The blast loads from these tests were from external explosions and could be represented accurately as a shock impulse. The tests used slab thicknesses of 6 and 8 inches. Both were simply supported with spans of about 98 inches and widths of 47 inches. Concrete compressive strength was 3000 psi, and reinforcement yield strength was 40,000 psi. The reinforcement ratio was 0.0013. Shock loads and observed deflections were provided in the test report.

Using this information, structural parameters including ultimate resistance, stiffness, elastic deflection, and mass were calculated. The slabs were analyzed using an energy equation similar to Equation 1. Because there was no quasi-static load, the work term was neglected. The energy equation used, in detailed form, is as follows:

$$\frac{I^2}{2M_{eff}} = \phi_s \left(\frac{1}{2} R_u \; X_e + R_u \; (X_{max} - X_e) \right) \tag{2}$$

where

I = total applied shock impulse over the slab

M_{eff} = equivalent single degree-of-freedom mass of slab

= (load-mass factor) x (mass)

R_u = total ultimate resistance of slab

X_e = elastic deflection of slab

X_{max} = observed maximum deflection of slab

ϕ_s = strain energy correction factor

For each test, the appropriate structural parameters, the applied load, and the observed deflection were input into the equation, and the correction factor was calculated. These values were averaged and used in Equation 1 for the analysis of any one-way reinforced concrete element.

The similar analysis approach was planned for two-way slabs. However, the durations of the shock loads were approximately the same as the natural periods of the slabs, and treating the load as an impulse resulted in extremely large calculated deflections. Better analytical results were achieved by using a single degree-of-freedom (SDOF) program which allowed the input of the actual shock load history. Test data was taken from References 5-7. Slabs were 12 feet square and about 5 inches thick. About 0.9% reinforcement was provided. The concrete compressive strength was about 4000 psi, and the yield strength of the reinforcement was just under 60 ksi.

The structural parameters used for Equation 2 along with the load history were used as input for the SDOF program. Runs were repeated, increasing the ultimate resistance by a factor of ϕ_r, until the calculated deflections matched the deflections observed in the tests. This corresponding value of ϕ_r was set equal to the strain energy correction factor for that test. The correction factors for all of the tests were averaged for use in Equation 1 when calculating the damage of two-way reinforced concrete elements. It is understood that the corrected strain energy is related to the corrected ultimate resistance only if the elastic portion of the response is negligible; however, the differences actually encountered will be small.

Steel, masonry, and wood elements were also considered in References 1, 2, and 3. Steel components were analyzed using the SDOF program, while the analysis of masonry followed an energy approach using P-I diagrams such as those developed in Reference 1. Wood components were handled in a different fashion, and are not discussed here.

Results

As stated above, both one- and two-way reinforced concrete elements were analyzed. The calculated strain energy correction factors were plotted against support rotations as shown in Figures 2 and 3. Both figures show that the correction factor increases with support rotations. This is expected due to the effects of strain hardening of the reinforcement and additional strength caused by arching in the slab.

The dashed vertical lines in the figures define the boundaries between various component damage levels. Four levels were chosen: 0%, 30%, 60%, and 100% damage. These discrete levels are adequate to define individual component damage, so that when a weighted average of component damage throughout a building is calculated, a number defining percent building damage results. A more detailed discussion of building damage is provided in Reference 2.

Test data for steel elements were taken from References 8, 9, and 10. All of this information was for cold-formed steel panels, girts, and purlins used in the construction of pre-engineered metal buildings. The test loads described in Reference 8 were the result of a nuclear explosion, and were long in duration. The duration of the loads for the tests described in References 9 and 10 are approximately the same as the component natural periods. Therefore, all of the components were analyzed using the SDOF program. The values of ϕ_s for these components also tended to increase with increasing response; however, the range of values was not as great as that calculated for reinforced concrete. The mean value was found to be 1.4, and was recommended for use in Equation 1 for steel components.

Masonry panel test results were taken from References 4, 5, and 11. The test data extracted from these references is shown in Figures 4 and 5 for one-way and two-way masonry panels, respectively. Reference 2 documents the pressure and impulse parameters used to reduce the data to the presented format. All the masonry data includes arching effects, which significantly strengthens the wall flexural capacity. The tests of Reference 4 were performed in a rigid frame. Lightweight concrete masonry units, hollow brick, and solid brick were tested with 8-100 kg spherical charges. The tests of Reference 11 were also performed in a rigid frame. Tailored airblast pulses were produced in a shock tube surrounding the structure. Reference 5 describes tests performed in a nuclear environment. The tests of References 5 and 11 were accomplished using both solid brick and hollow brick units. The damage categories described on the plots are based on a somewhat qualitative assessment of panel response. Slight damage consists of minor flexural cracking. Moderate damage includes flexural damage without mechanism or hinge formation. Severe damage indicates the presence of hinges or a failure mechanism, while failure indicates structural collapse.

This data, like that for reinforced concrete described previously, was also grouped in the 0-100% categories for presentation in Reference 2 in a format similar to that shown in Figure 1. The correction factors varied from 0.8 to 1.8 for the one-way data and from 5.0 to 14.0 for the two-way data using the energy method presented in Reference 12. The dramatic correction factor increase observed in the two-way tests is accounted for almost exclusively by the increase in flexural capacity due to arching.

Closure

Analysis of test data from several sources and concerning several loading environments and response regimes has been completed and compared with energy solutions and single degree of freedom analyses. Correction factors have been determined to equate the analytic results with the

experimental results. These factors were determined for use in vulnerability analyses of structures. However, they illustrate the conservatism that is present in design procedures used for component design in blast resistant construction.

References

1. Oswald, C. J., Polcyn, M. A., Ketchum, D. E., Marchand, K. A., Cox, P. A., and Whitney, M. G., "Blast Damage Assessment Procedures for Common Construction Categories," Final Report for Naval Civil Engineering Laboratory, October 1987.

2. Whitney, M. G., Ketchum, D. E., and Polcyn, M. A., "Blast Vulnerability Guide," Final Report prepared for Naval Civil Engineering Laboratory, October 1987.

3. Polcyn, M. A., Ketchum, D. E., and Whitney, M. G., "Procedures to Assess Internal Blast Damage to Common Construction Categories," Final Report prepared for Naval Civil Engineering Laboratory, May 1988.

4. Forsen, Richard, "Airblast Loading of Wall Panels," FOA Rapport C 20586-D6, Forsvarets Forskningsarstalt, Stockholm, October 1985.

5. Seven, Eugene, "Tests on the Response of Wall and Roof Panels and the Transmission of Load to Supporting Structures," Project 3.5 - Operation Upshot Knothole, May 1955.

6. Black, Michael,"Ultimate Strength Study of Two-Way Concrete Slabs," Journal of the Structural Division - ASCE, January 1975.

7. Keenan, W.A., "Strength and Behavior of Restrained Reinforced Concrete Slabs Under Static and Dynamic Loadings," Technical Report R-621, Naval Civil Engineering Laboratory, April 1969.

8. Johnston, B.G., "Damage to Commercial and Industrial Buildings Exposed to Nuclear Effects," Operation Teapot, Nevada Test Site, Project 31.2, February to May, 1955.

9. Stea, W., Sock, F.E., and Caltagirone, J.P., "Blast-Resistant Capabilities of Cold-Formed Steel Panels," Final Report prepared for U.S. Army Armament Research and Development Command, May 1981.

10. Stea, W., Dobbs, N., Weissman, S., Price, P., and Caltagirone, J., "Blast Capacity Evaluation of Pre-Engineered Building," Final Report prepared for U.S. Army Armament Research and Development Command, March 1979.

11. Wilton, C., et.al, "Shock Tunnel History and results," Scientific Service Inc., March 1978.

12. Baker, W.E., Cox, P.A., Westine, P.S., Kulesz, J.J., and Strehlow, R.A. Explosive hazards and Evaluation, Elsevier, New York, 1983, Page 341.

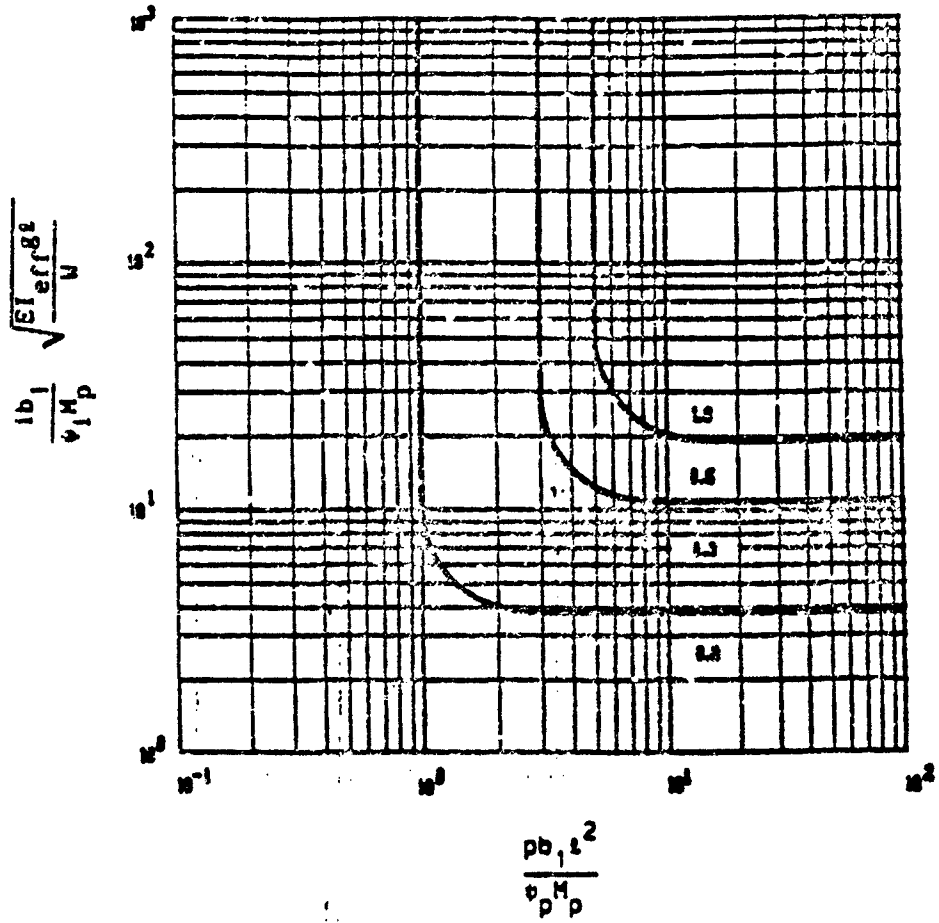

Figure 1. Example P-I Diagram

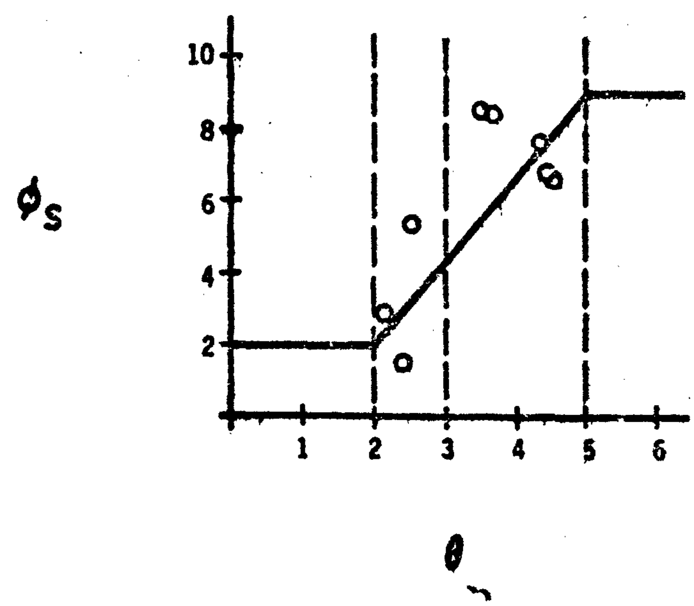

Figure 2. ϕ_s Versus θ for One-Way Reinforced Concrete Slabs

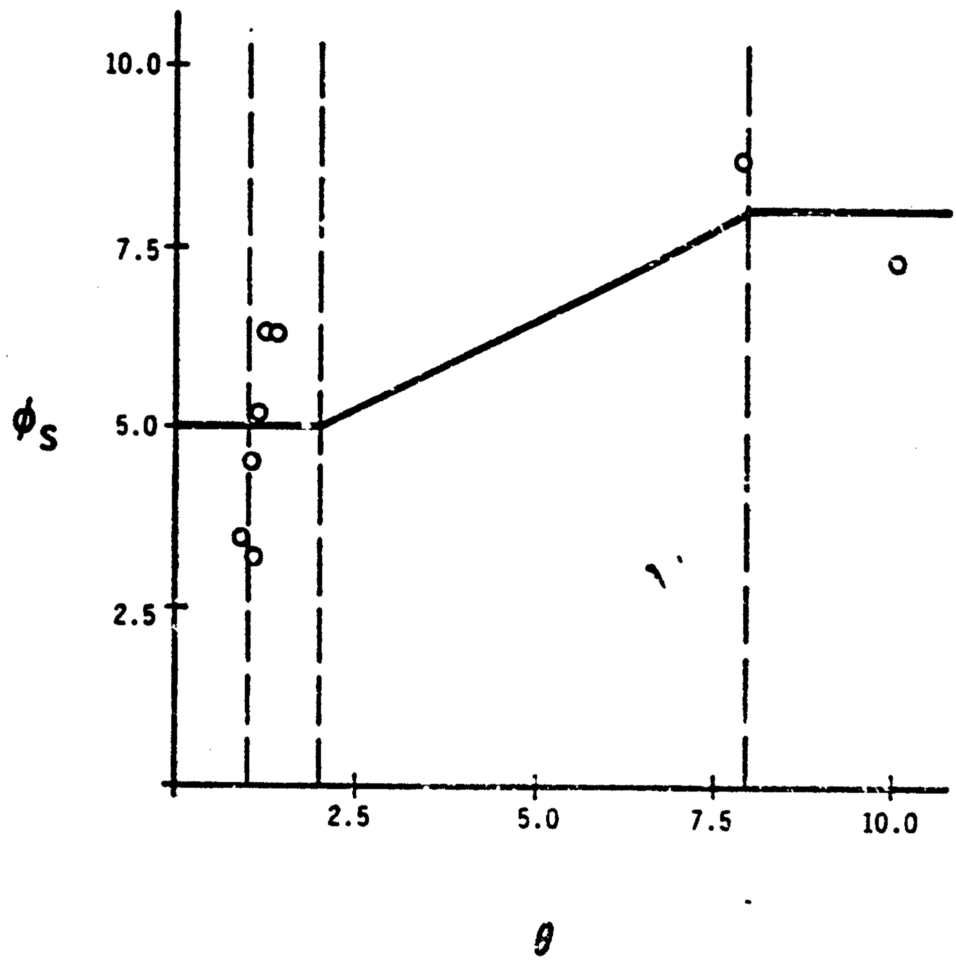

Figure 3. ϕ_s Versus θ for Two-Way Reinforced Concrete Slabs

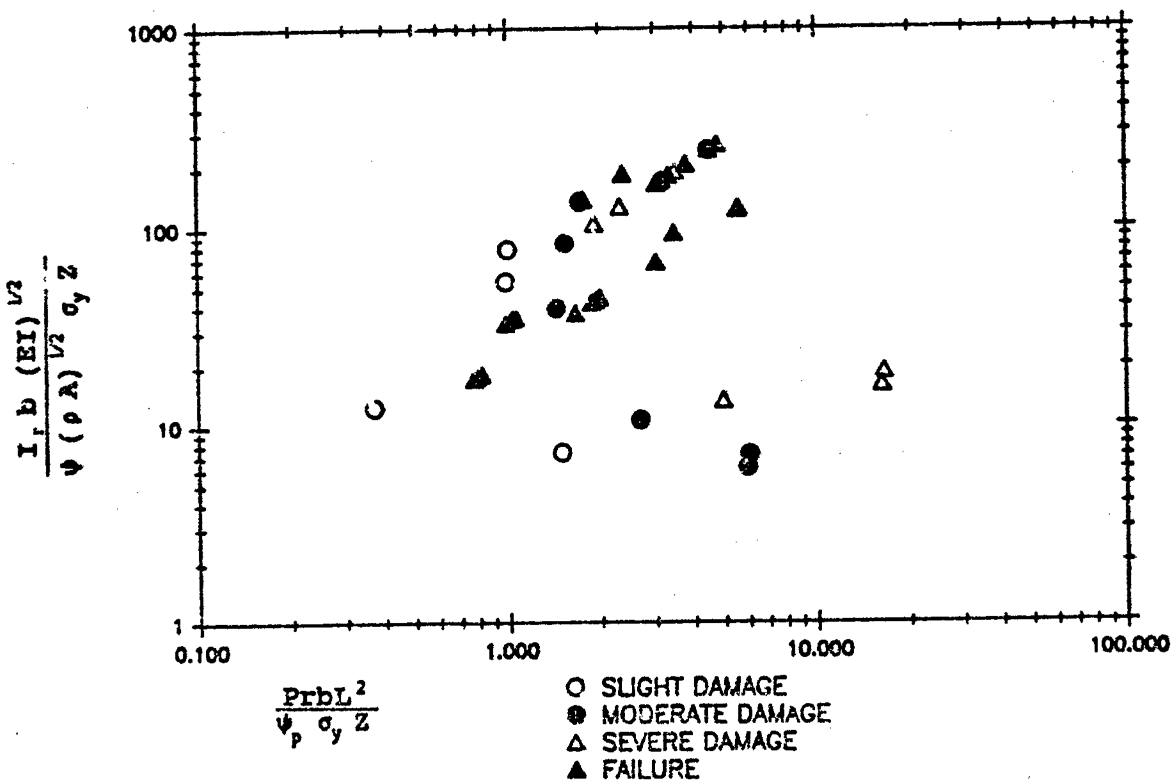

Figure 4. One-Way Unreinforced Masonry

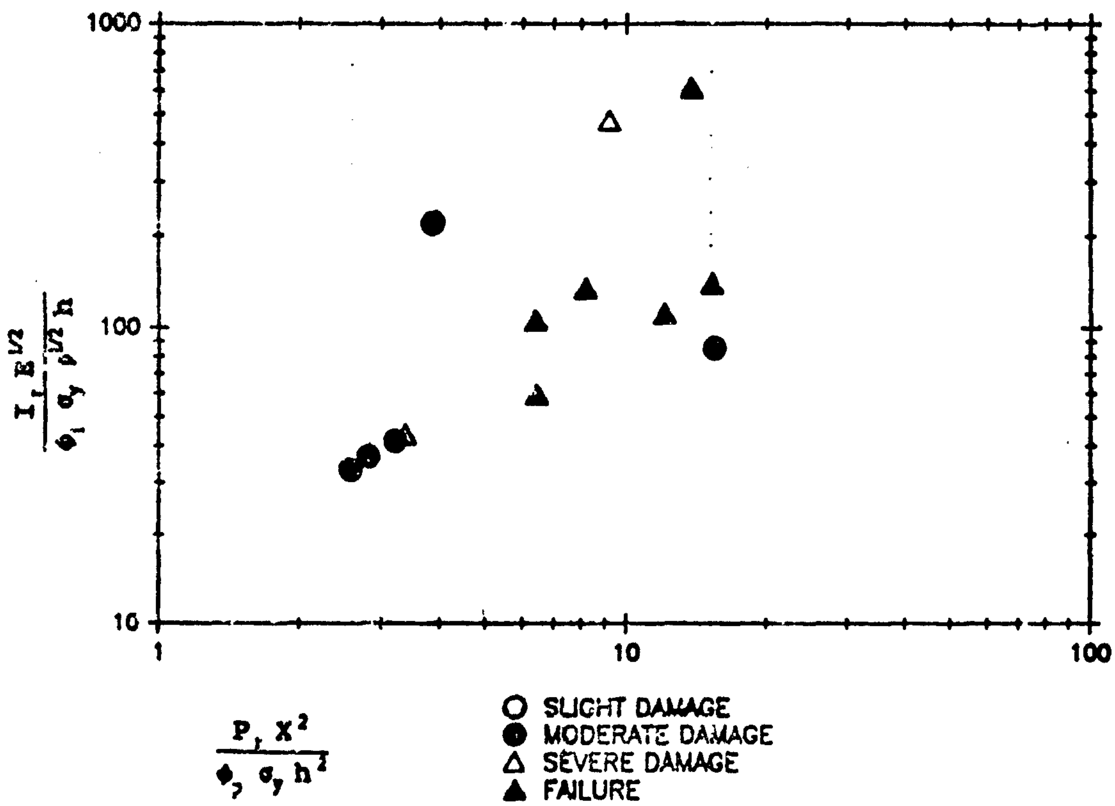

Figure 5. Two-Way Unreinforced Masonry

TWENTY-THIRD DOD EXPLOSIVES SAFETY SEMINAR

9 - 11 AUGUST 1988 - ATLANTA - USA

MODEL TEST OF A PARTICULAR EARTH COVERED WORKSHOP BUILDING

by F.X. BOISSEAU*

ABSTRACT :

This paper presents the main results from a serial of tests conducted by SNPE in 1985 and 1986 with 1/10 th and 1/5 th scale models of a particular earth covered workshop building called "mitigated casemate". This type of structure is designed to partially contain blast and projections effects induced by the accidental explosion of amount of 1.1 product up to 1,000 kg of equivalent TNT.

Different loading densities were tested, blast and roof velocities measurements were made. These results and a comparison with a full scale trial involving 1,000 kg of high explosive are described.

This type of building is designed and used for production or maintenance workshops in establishments where area is very limited.

* SNPE-GTS - P.O BOX n ° 2 - 91710 VERT LE PETIT - FRANCE
TELEX 604479 POUDRES F
TELECOPY (33) (1) 64.93.51.45

1 - INTRODUCTION

In order to build a new type of workshops called mitigated casemate, specially designed to limit effects generated by an internal accidental explosion, SNPE decided to conduct a serial of tests to determine the different hazardous areas.

A few experimental data were already available on a similar structure, issued from a full scale trial, conducted by a French D.O.D. Civil engineering team in 1978, but they did not allow to evaluate blast hazards around the structure in case of explosion, in a precise way. So, an experimental program involving 1/5th and 1/10th scale models was defined and conducted by SNPE in 1985 and 1986.

2 - MITIGATED CASEMATE

This type of building is constitued of 4 reinforced concrete walls, a reinforced concrete roof slab and an access corridor. The whole structure is covered with earth. An internal resistant door, designed to resist the internal explosion, closed the corridor. A description of a mitigated casemate is shown in Figure 1.

There is two types of mitigated casemate, one with a straight corridor, the other with a bent corridor. The roof slab is a flooting slab, i.e a slab not linked to the wall and which in case of explosion will be projected. Walls are lightly linked to each other. For loading densities of interest, i.e 1 kg/m3 to 12 kg/m3 and in case of an internal explosion, the major part of the energy is absorbed by roof and walls which push the earth, the mass of which is very important (the earth cover of the roof is several meters high). Roof slab and walls are designed not to be too severely damaged after being pushed.

3 - SCALING LAWS

We use the classical HOPKINSON laws to scale the phenomenon. That is, if λ is the scale factor between the prototype (full scale) and the model (scale λ related to the prototype).

Distance R : $R_m = \lambda \cdot R_p$		
Mass M : $M_m = \lambda^3 \cdot M_p$		
Time t : $t_m = \lambda \cdot t_p$		
Pressure P : $P_m = 1 \cdot P_p$		m : model index
Impulse I : $I_m = \lambda \cdot I_p$		p : prototype index
Velocity U : $U_m = 1 \cdot U_p$		

4 - TEST PROGRAM

The structure tested in the full scale trial had a bent corridor. The charge was constitued of 1,000 kg of PLANP (1,200 kg of equivalent TNT) which represents a loading density of 12 kg/m3. The interior blast resistant door was closed.

In order to complete our experimental data base, it was decided to test mitigated casemates using 1/10th and 1/5th scale models. We have studied the influence of three parameters on blast propagation outside the structure :

- Shape of the corridor (straight or bent)
- Loading density
- Mass of earth cover/unit area (or heigth)

Table 1 sums up the different configurations tested in 1985 and 1986 by SNPE.

5 - TEST SEP UP

Scale models

Dimensions of a 1/10th scale model are shown in Figure 2 for a straight corridor configuration and in Figure 3 for a bent corridor configuration. Earth is replaced by sand. The models are in steel. The blast resistant door is scaled by a thick steel plate with a system to prevent the rebounding of the door.

Charges

- Charges used in these tests were composed of cylinder of Hexolite 60/40 (60 % RDX - 40 % TNT) initiated by a booster of RDX/WAX (95 % RDX - 5 % Wax) and a High Intensity detonator.

- Mass of charges shot were between 0.084 kg and 8 kg depending on the scale and the loading density tested.

Instrumentation

Blast measurements :

Free field pressure gages were placed in 4 directions for tests involving mitigated casemate with a bent corridor with an angle of 90° between them, and in 3 directions for tests with a straight corridor.

Of course, each time, a line of pressure gages was located in the direction of the corridor entrance.

Locations of pressure gages are shown in Figures 4 and 5 for models with a bent or a straight corridor to illustrate the experimental set up.

Video measurements :

Two high speed camera were used during all tests conducted by SNPE. A 500 frames per second was facing the corridor entrance and a 1500 frames per second was placed perpendicularly to the axe is of the corridor.

In order to have video measurements of the roof slab velocity, a steel bar, 1 m high, with a red flag at the end, was fixed on the center of the roof.

6 - RESULTS

The whole results of all shots can't be described in detail in the present paper, so we will only depict the main results obtained in :

- Comparing blast measurements of the full-scale and 1/10th scale tests on a mitigated casemate with a bent corridor (shots 1 and 2)

- Comparing blast measurements of 1/5th and 1/10th scale tests on mitigated casemate with a straight corridor (shots 3 and 8)

- Comparing roof velocities measured in 1/5 th and 1/10th trials for two loading densities (1 and 12 kg/m3).

Mitigated casemate with a bent corridor

In the full scale test, blast measurements were made only in two directions : 90° and 180° gages lines. Figure 6 and 7 compare side-on overpressures measured in these two directions during the full scale test and 1/10th trials (shots 1 and 2).

90° gages line (corridor entrance) :

Difference observed in values of overpressure measured are probably due to the scaling of the resistant door. In fact, the full scale resistant door had not a system to prevent the rebounding. The door of the model used in shot 1 was also lightly fixed to simulate the full scale door, but models used in shot 2, 3, 4 ... and 9 had all resistant door designed with an anti-rebounding system, because SNPE intend to build in its plants, mitigated casemate with such a system.
So if we examine closely Figure 6, we can see that values recorded in full scale test and shot 1 (1/10 th) at the entrance are quite similar.

180° gages line :

In that direction (see figure 7) we can notice that measures obtained in 1/10th tests and in the full scale trial are in good accordance. The scaling of the resistant door seems to have no influence on blast propagation in the 180° direction.

Mitigated casemate with a straight corridor

Figures 8,9 and 10 compare for the 0°, 180° and 270° gages lines, side-on overpressures measured in the 1/5th (shot 8) and 1/10th (shot 3) scale tests.

0° gages line (corridor entrance) :

Contrary to the bent corridor configuration, we see on figure 8 that measures recorded in 1/5th and 1/10th scale tests are in good accordance. The relatively strong blast measured in that direction is quite surprising because, before doing the test, we thought that the interior resistant door, with its anti-rebounding system, would strongly attenuate the overpressure. We can notice on the film taken with an high speed camera, a flame coming out of the corridor. That is another indication that, despite the presence of the resistant door, a part of the blast manages to go out of the corridor, probably because the gaz pressure inside the structure distends it and let between the floor and the door, or the wall and the door, partial vent area

180° gages line :

Significant difference, about 50 %, can be observed between overpressures measured in the 1/5th test and those recorded in the 1/10th test (see figure 9). But it must be considered that the overpressure levels recorded are very low, 10 mbar or less, so the difference can come as much from scaling problems as from pressure gage precision.

270° gages line :

Comparison between 1/5th and 1/10th tests, describes in Figure 10, shows the good accordance between side-on overpressures measured during both tests, in that direction.

Roof velocities

Roof initial velocities measured with an high speed camera, for shots 3,7, 8 and 9, which concerned 1/5th and 1/10th tests with two loading densities 1 kg/m3 and 12 kg/m3, are described in table 2. Two facts can be noticed :

- Multiplying the loading density by 12, double the initial roof velocity (13 m/s and 30 m/s).

- Comparison between roof velocity measured in the 1/5th test and in the 1/10th test, with a constant loading density shows that using the Hopkinson scaling laws in our case is valuable. We have measured the same initial velocity in the 1/5th test than in the 1/10th test. Of course only the initial velocity is independant of the scale factor, distance of projection cannot be scaled because of the impossibility of scaling the earth gravity.

CONCLUSIONS

Validity of applying the Hopkinson scaling laws in our model test has been verified even for initial velocities of the roof slab.

Different loading densities and design parameters such as shape of the corridor, height of roof earth cover, were studied.

Through the 9 model tests conducted by the Safety Technical Group, SNPE has now a good knowledge of blast and projections hazards, generated by the internal explosion of a charge placed in a mitigated casemate and of modelisation process of buildings.

TABLE 1 : TEST SCHEDULE

SHOT No	SCALE	ROOF EARTH** COVER (m)	LOADING DENSITY (kg/m3)	CORRIDOR SHAPE
1978* TRIAL	1	4	12	Bent
1	1/10	4	12	Bent
2	1/10	4	12	Bent
3	1/10	4	12	Straight
4	1/10	3	7,5	Straight
5	1/10	3	1	Straight
6	1/10	2	7,5	Straight
7	1/10	2	1	Straight
8	1/5	4	12	Straight
9	1/5	2	1	Straight

* NOT CONDUCTED BY SNPE
** Values indicated are for full scale

TABLE 2 : ROOF VELOCITIES MEASURED IN SHOTS 3, 7, 8 AND 9

SCALE	Uo (m/s)	
	d = 1 kg/m3	d = 12 kg/m3
1/10th	13	30
1/5th	13	32

Uo = initial velocity
d = loading density

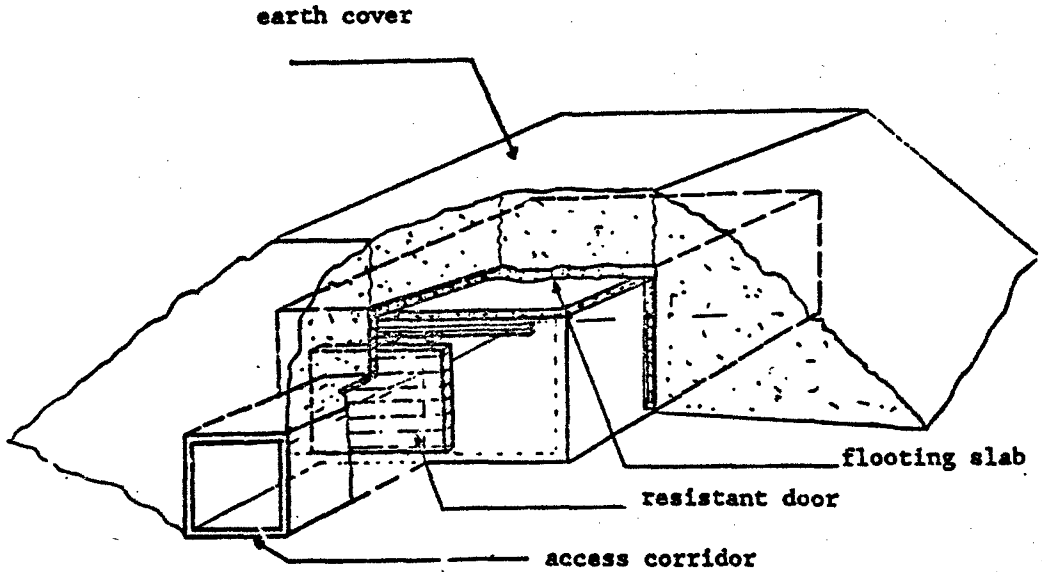

FIGURE 1 : VIEW OF A MITIGATED CASEMATE WITH A STRAIGHT CORRIDOR

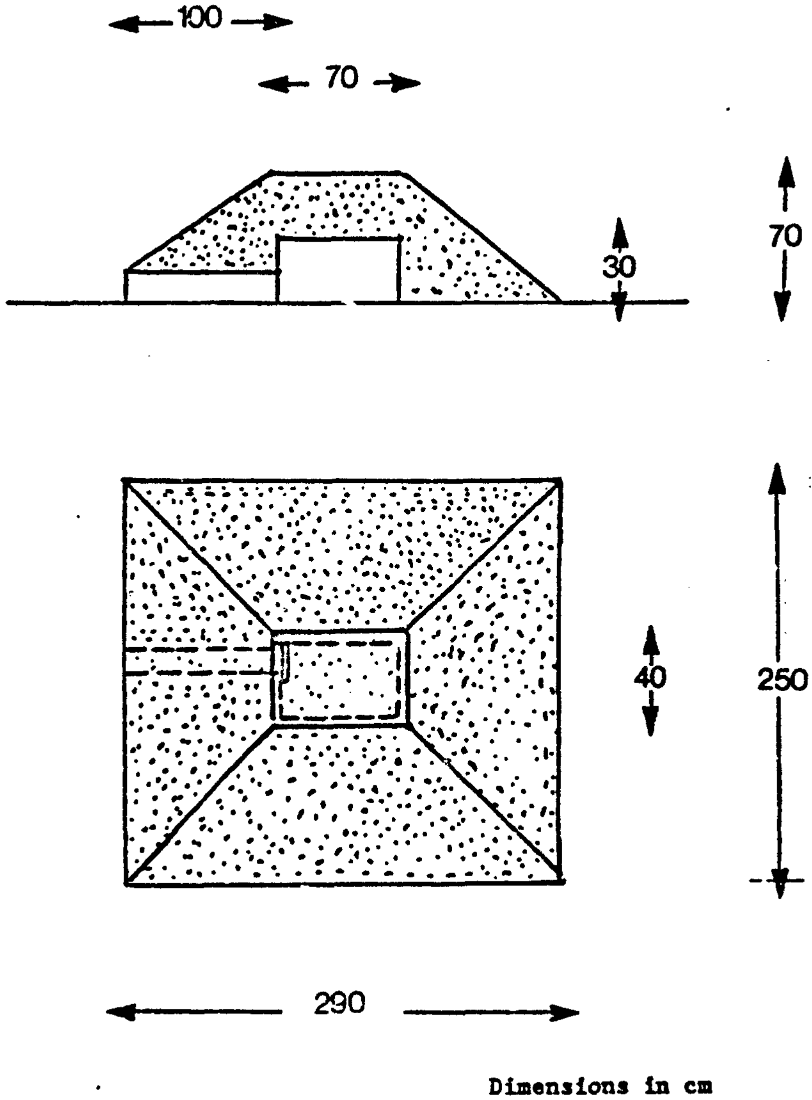

FIGURE 2 : 1/10th MODEL WITH A STRAIGHT CORRIDOR

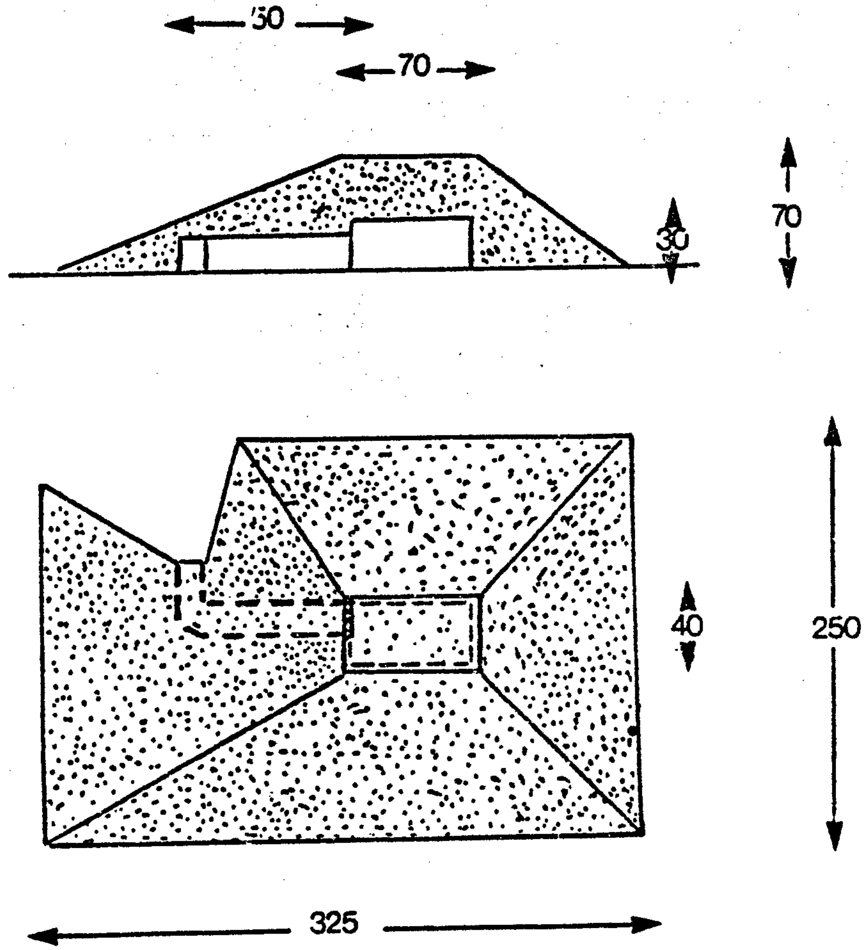

Dimensions in cm

FIGURE 3 : 1/10th MODEL WITH A BENT CORRIDOR

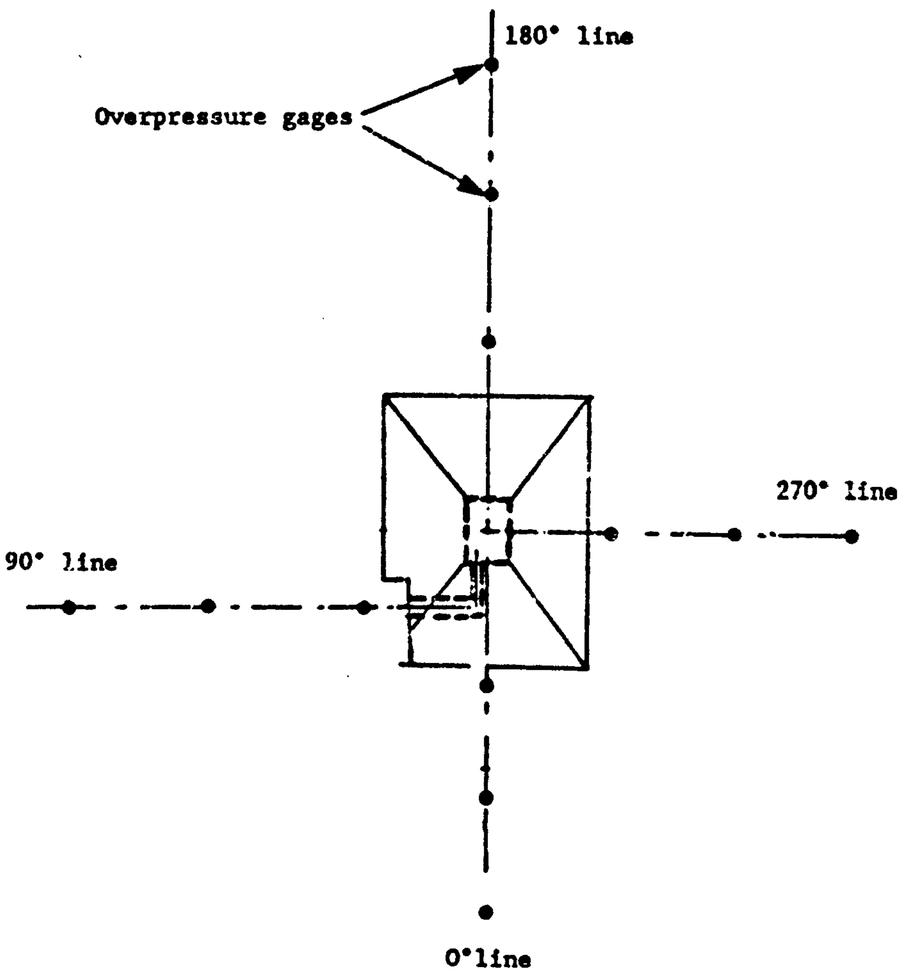

FIGURE N° 4 : PRESSURE GAGES LOCATION FOR MODEL WITH A BENT CORRIDOR

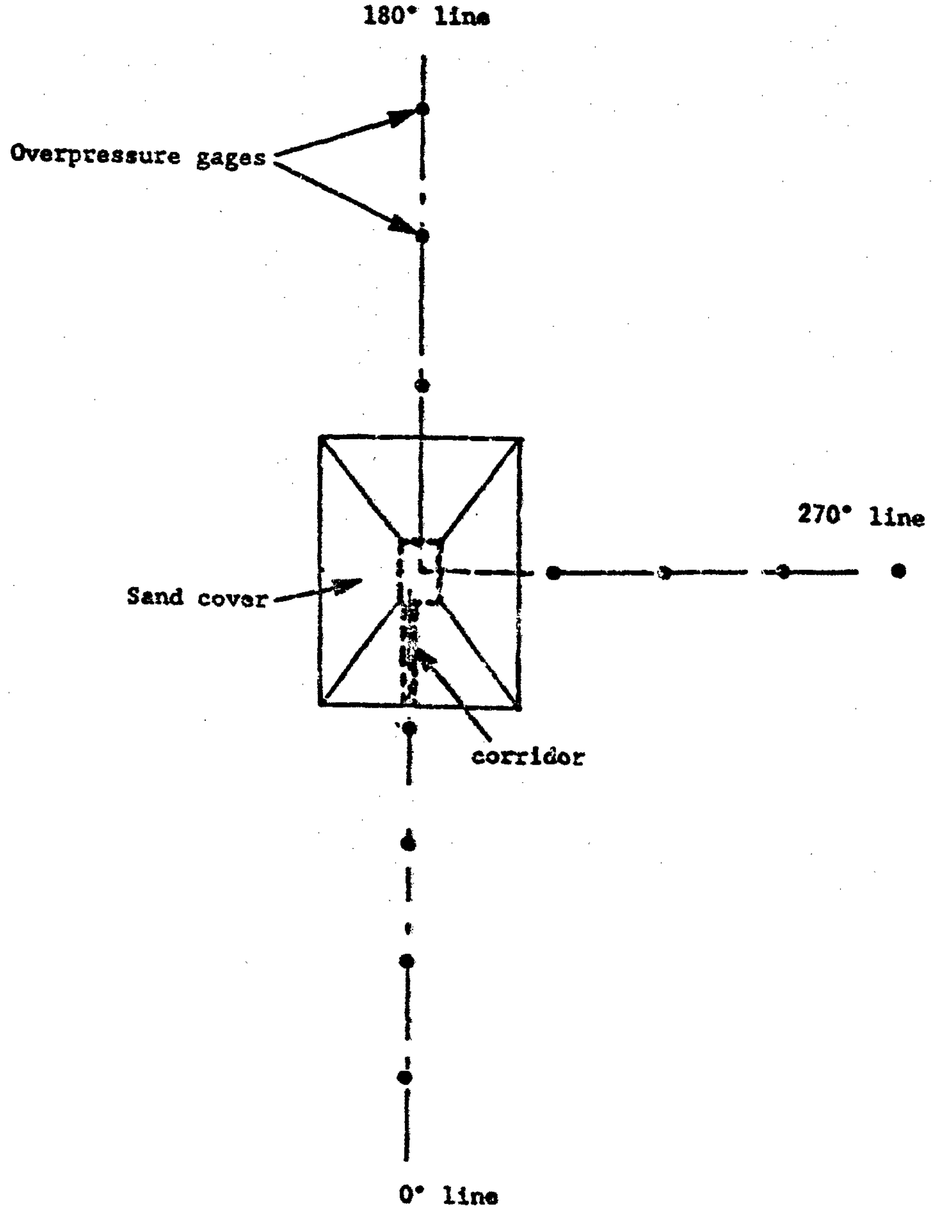

FIGURE 5 : PRESSURE GAGES LOCATION FOR MODEL WITH A STRAIGHT CORRIDOR

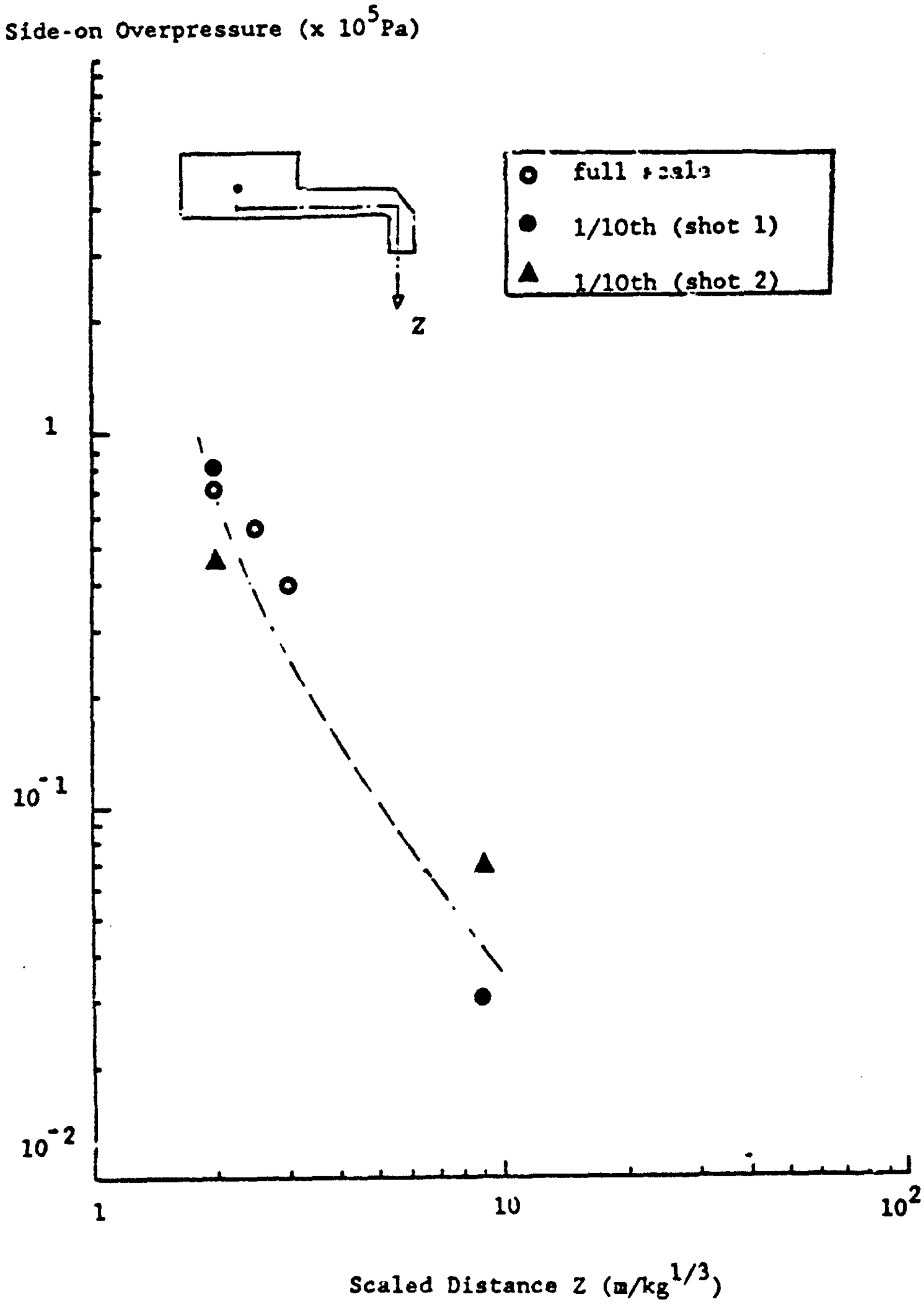

FIGURE 6 : OVERPRESSURES MEASURED ON THE 90° LINE-BENT CORRIDOR CONFIGURATION

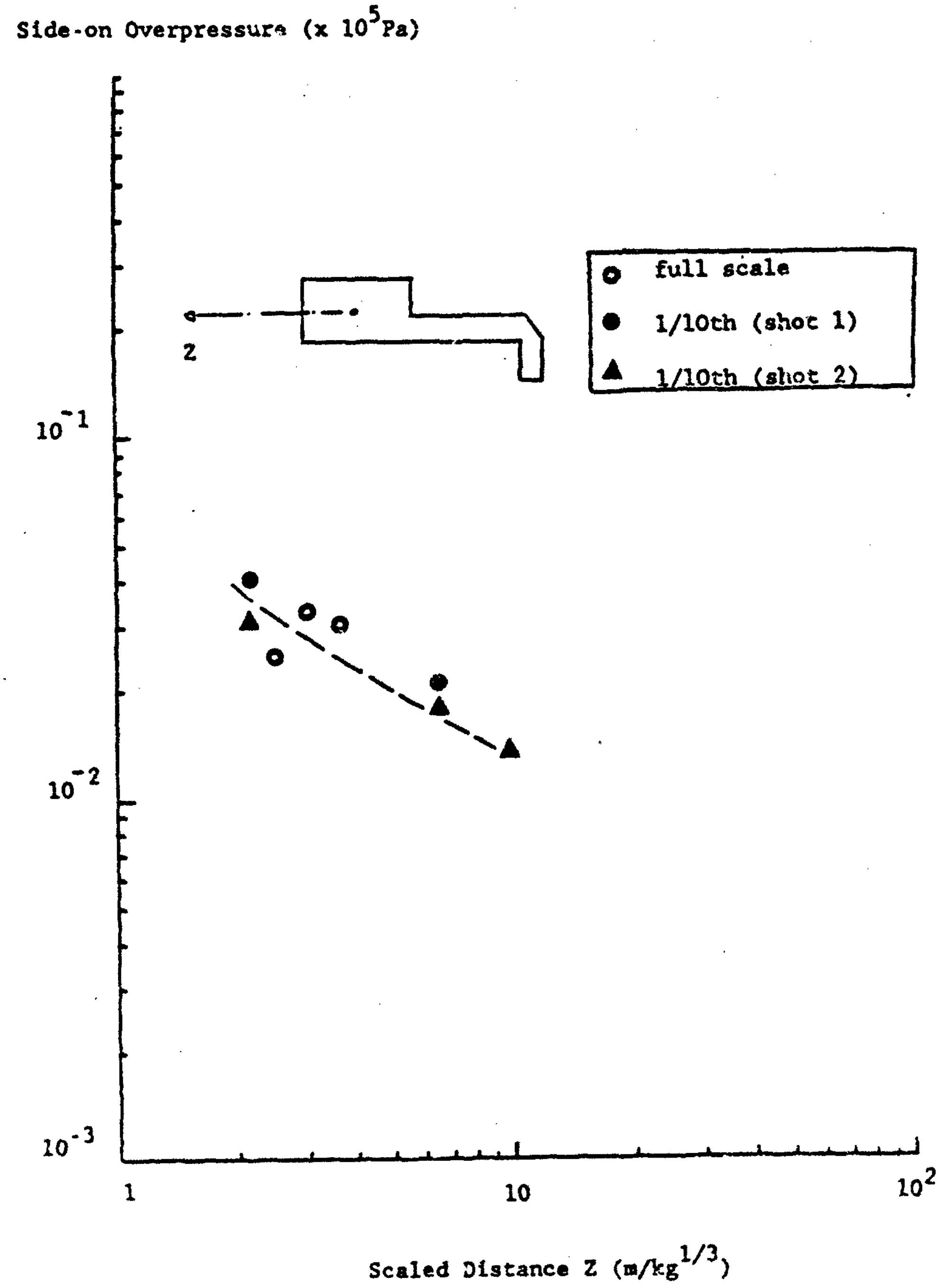

FIGURE N° 7 : OVERPRESSURES MEASURED ON THE 180° LINE-BENT CORRIDOR CONFIGURATION

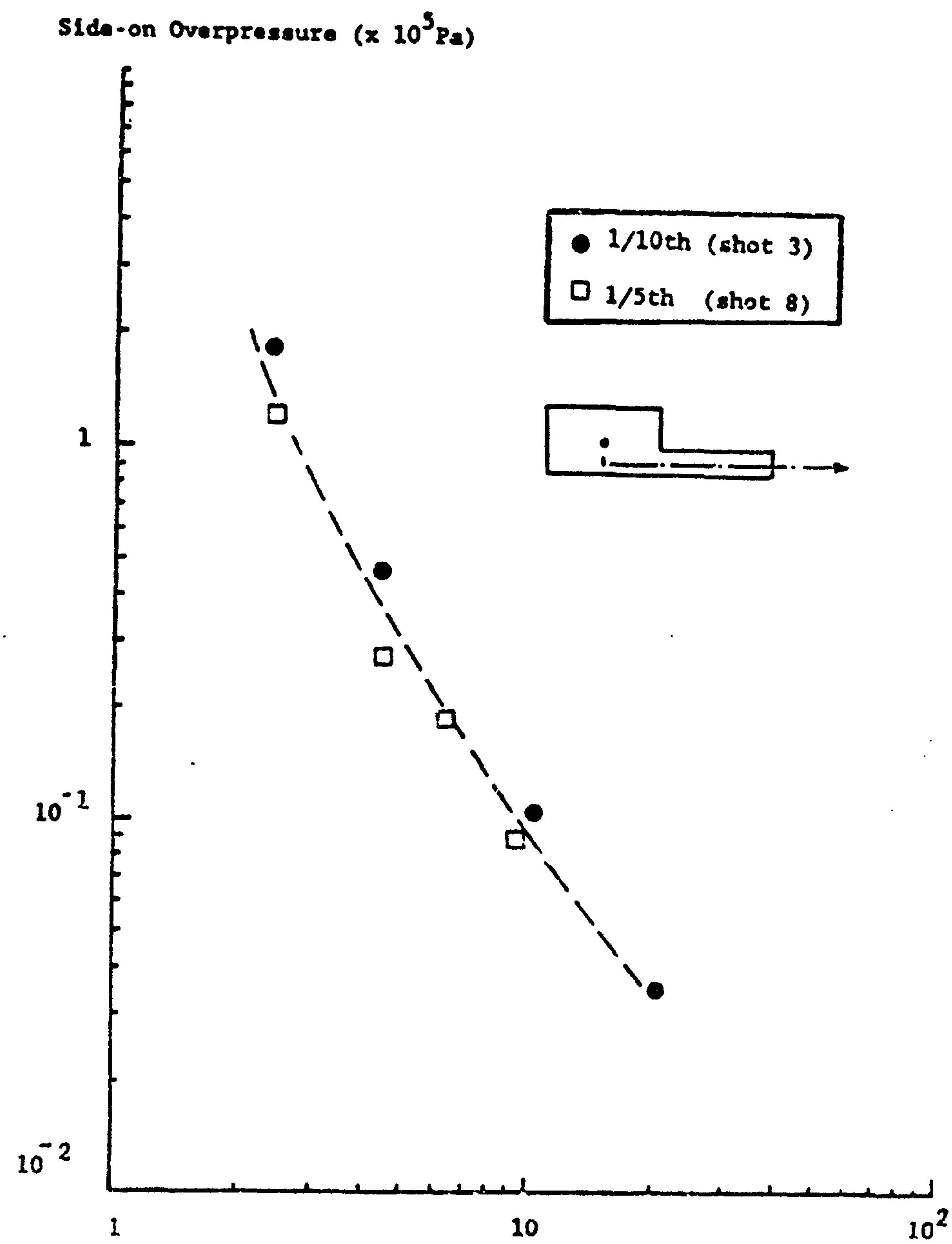

FIGURE 8 : OVERPRESSURES MEASURED ON THE 0° LINE-STRAIGHT CORRIDOR CONFIGURATION

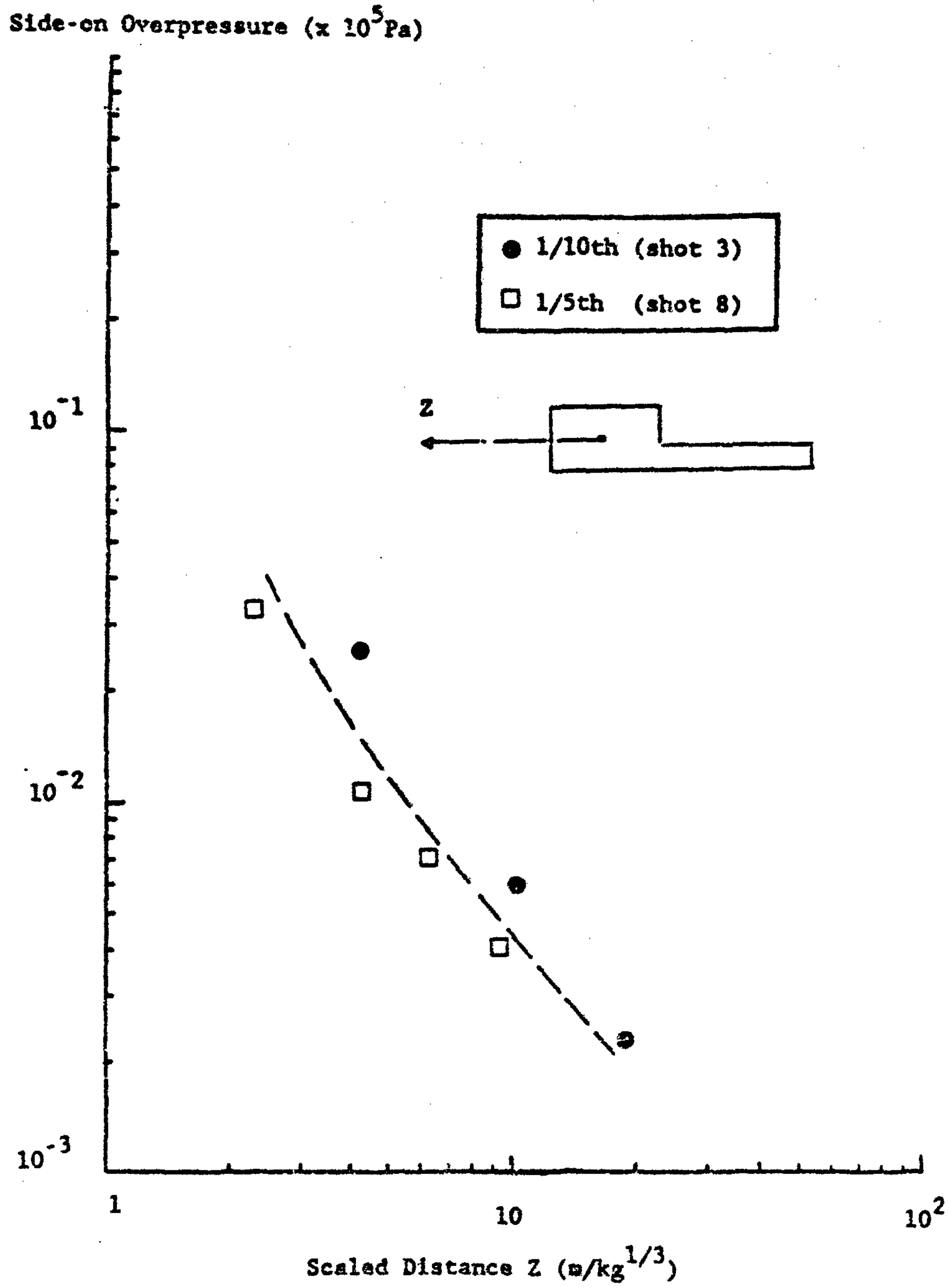

FIGURE [illegible] : OVERPRESSURES MEASURED ON THE 180° LINE-STRAIGHT CORRIDOR CONFIGURATION

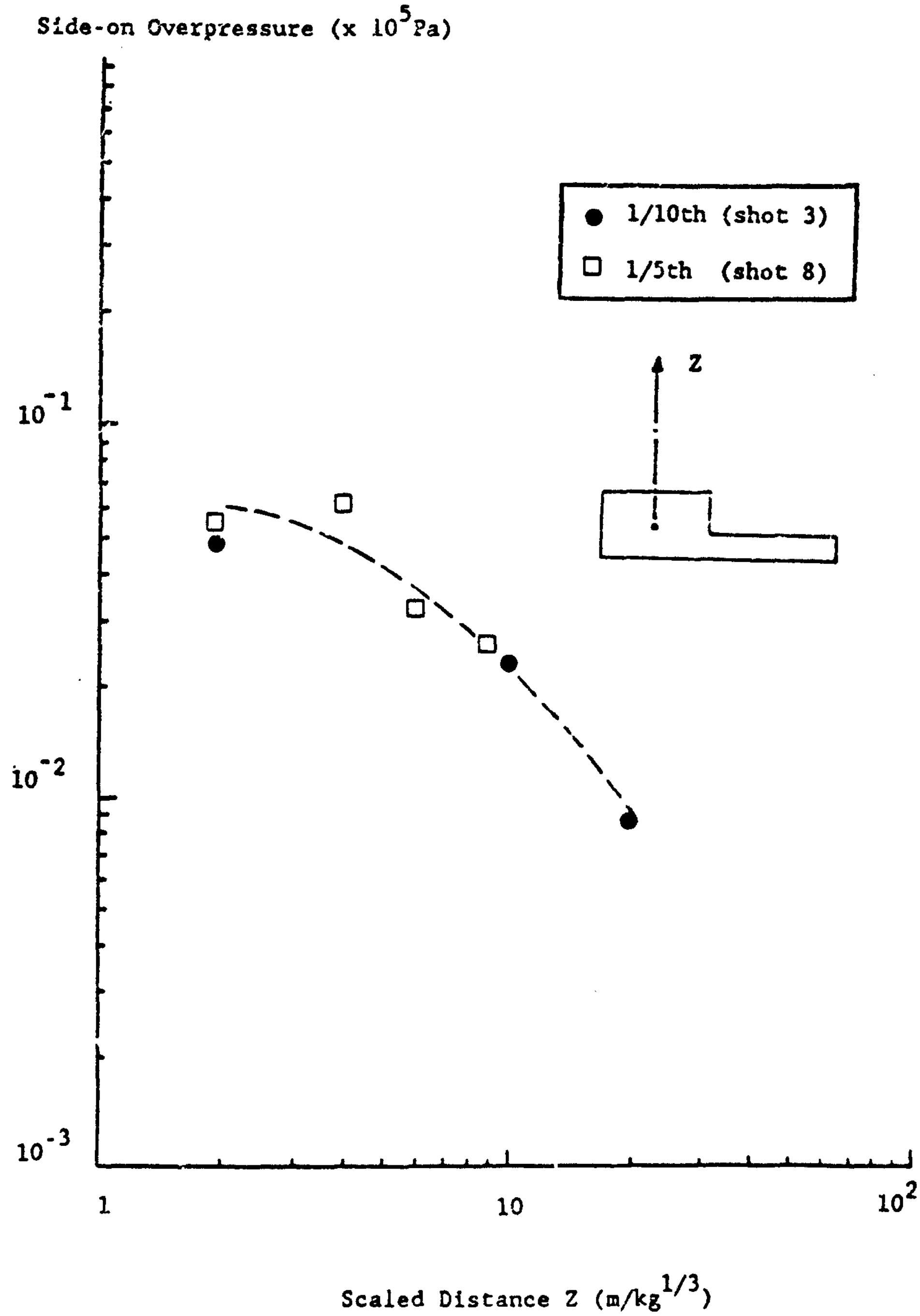

FIGURE 10 : OVERPRESSURES MEASURED ON THE 270° LINE-STRAIGHT CORRIDOR CONFIGURATION

Calculation of Subsequent Structural Effects after an Accidental Explosion in a Test Facility

L. Erik Fugelso[1]
Major Michel Deeter[2]

Advanced Engineering Technology Group
Los Alamos National Laboratory
University of California
Los Alamos, NM 87544

INTRODUCTION

This paper presents an analysis of the deformation and potential damage caused by a small accidental explosion to a critical component of an experiment at the flame source in a high intensity burner. First, the accident is briefly summarized. Then, upper and lower bounds for the explosive load are estimated. Next, a finite element model of one of the tkey structural components is generated and the simplifying assumptions are critically evaluated. Then the results of the appropriate finite element calculation are evaluated and the effect of the accident on the structure is presented.

DESCRIPTION OF THE PROBLEM

The experimental test fixture that serves as the source of a high-intensity flame consists of four burners, two liquid oxygen (LOX) tanks, four gaseous nitrogen tanks, four tanks filled with powdered aluminum, the requisite connecting tubes, control hydraulics, and electronic controls. Figure 1 shows a highly idealized and simplified schematic drawing of a typical section of the test fixture. Powdered aluminum is added by gravity feed to a gaseous nitrogen flow and transported through a pipeline into the center of a mixing nozzle. Liquid oxygen flows through another pipeline into the exterior annulus of this mixing nozzle of the burner, where the oxygen is vaporized. The coaxial streams of gas and aluminum powder mix and form a highly combustible mixture that is ignited by a pilot light. This system creates a vertical plume of a burning mixture with thermal flux properties that can be readily controlled with respect to heat flux intensity, duration, and surface area. Upon completion of each test, the mixing chambers are flushed with their respective inlet gases. When the system is restarted, there is a period of initial gas flow to flush the system of any residual fuel.

One test run was made with a much finer aluminum powder (6μ nominal particle size) to investigate the effect of increased surface area of the dispersed fuel on the thermal flux. The next test was to be done with the normal size (18μ nominal particle size) aluminum powder. During the initial O_2 flush of the mixing chambers, a small explosion took place. No aluminum powder had yet been added to the flow. The exterior annular walls of the mixers were blown off and visual flashes were noted at the two inner burners. Visual examination of the damaged exterior showed scorch marks on the support stands. The nearby liquid oxygen tank is mounted within a large volume of thermal insulation and could not be conveniently examined. This tank is connected to the mixing chamber through a flexible pipe. The explosion was caused by a small amount of unburned very fine aluminum powder that had fallen back into the exterior annulus of the mixing chamber at the termination of that run and that had not been removed by the previous gas flush or by the mechanical cleaning of the apparatus.

The mixer and the external piping systems can be visually examined and quickly repaired or replaced as necessary. Since the liquid oxygen tank and the piping system internal to the thermal insulation cannot be conveniently examined, a finite element calculation was performed to determine whether further inspection of this component was necessary.

METHOD OF APPROACH

We examine in detail the potential structural deformation in the liquid oxygen tank from this event. Upper and lower bounds on the explosive energy release in the mixing chamber are obtained. The transmission of this energy along the connecting tubes is examined. Finally a structural analysis of the stresses and displacements in the liquid O_2 tank was carried out using a finite element analysis, which incorporated a constitutive material model describing work-hardening plasticity to match the behavior of stainless steel at the cryogenic operating temperatures.

BOUNDS ON THE ENERGY RELEASE

We wish to establish a good estimate of the transient load that was incident on the liquid oxygen tank. The blast load will originate at the mixer and then be propagated through the connecting tubes. Thus we will first present the upper and lower bound of the energy released at the mixer. The upper bound on the energy release is obtained by assuming that the mixing chamber was completely filled with pure oxygen at STP and that sufficient aluminum powder was present on the interior surfaces of the mixing chamber to generate a stoichiometric reaction. The volume of the annulus is 280 cm^3 (17 in^3), which would contain 0.40 gm or 0.0125 moles of O_2 at STP. The surface area of the annulus is 265 cm^2 (41 in^2). The volume of Al powder to stoichiometrically react with the oxygen will form a layer 6.3 μ thick. The heat of formation for this reaction is 400 kcal/mol of O_2. This heat release was equated to the detonation energy of an equivalent weight of TNT. The amount of TNT equivalent is 23 gm (0.047 lb). Distributing the blast effects in an equivalent sphere and evaluating the resulting blast pressure of 12.4 MPa (1750 psi) (Baker et. al., 1980) at its radius yielded a peak side-on pressure at the location where the oxygen inlet tube is attached. This estimate required the unlikely combination of 100% efficiency of the reaction and uniform coverage of all interior surfaces by the aluminum powder. We reduced our estimate of the energy release slightly to account for this reduction in the total reaction efficiency. Thus the upper bound estimate used here is 10.3 MPa (1500 psi).

The lower limit on the explosion pressure was obtained by calculating the minimum internal pressure required to effect the observed failure pattern in the annular wall of the mixing chamber. The annular wall of radius 6.35 cm (2.5") is 0.64 cm (0.25") thick. The inlet hole from the liquid oxygen line is 3.81 cm (1.5") in diameter. The failure pattern was a tensile in response to the circumferential tension in the narrow strip between the cutout and the top and bottom edges of the annulus (Figure 2). Using the stress concentration factor from Savin (1961) and a typical ultimate stress for aluminum, we obtain a lower bound of 3.1 MPa (450 psi) for the internal pressure.

ANALYSIS OF THE STRESSES IN THE LOX TANK

The loaded components of the system consist of the liquid oxygen tank and the pipe sections (Figure 3). The tank is held in an aluminum container that provides for handling as well as the insulation of the tank. The tank walls and the piping from the tank to the support structure are type 304 stainless steel. The tank is a cylinder with torospherical head. The main body of the tank is Schedule 5 pipe with a radius of 30.48 cm (12 in) and a thickness of 0.554 cm (0.218 in). The spherical portion of the head has a radius of 60.96 cm (24 in), while toroidal segment has a radius of 3.81 cm (1.5 in). The head has the same thickness as the cylindrical wall. The two stainless steel pipe segments from the tank are symmetrically offset from the center of the torospherical cap and separated by 10.08 cm (4 in). The pipe OD is 4.826 cm (1.9 in) and the wall thickness is 0.368 cm (0.145 in). Each pipe segment has a 90° elbow between the cap and the exterior support structure. The piping exterior to the structure is flexible copper tubing. The temperatures of the tank and of the piping interior to the support structure are maintained at the boiling temperature of liquid oxygen , -183 C (-297 F). The initial internal pressure of the tank is 1.03 MPa (150 psi).

The pressure pulse that is felt at the oxygen tank is transmitted through the fluid contained in about 2 m of flexible copper tubing and the inner stainless steel tubing. The liquid oxygen was flowing at the time of the incident at a velocity of about 0.4 m/s. The blast load is assumed to be a rectangular pulse, the duration of which is determined by the largest interior dimension of the mixing chamber. This upper bound blast pressure in the mixing chamber generates an acoustic pulse propagating backwards in the pipe that, by Joukowsky's formula (Nekrosov 1969) is just sufficient to stop the flow. The pressure in the pipe is transferred to the pipe structure itself at the elbow. The magnitude of the static applied load is equal to the upper bound pressure times the cross section area of the pipe. This load is applied normal to the plane containing the tank axis and the centerlines of the two attached pipes. The "water hammer" model presented here describes a pulse that will traverse the length of the tube essentially unaltered. Estimates of pressure losses due to wall friction, viscosity, pipe curvature, wave reflection at any bends, N-wave dispersion, and acoustic radiation into the surround air or thermal insulation were made and, collectively, the decrement in the shock pressure jump is less than 10% of the initial value. We ignore these losses to remain conservative.

There is one load reduction factor that should not be ignored. The pressure pulse in the pipe has a very short duration that is small compared to the lowest period of vibration of the tank. Thus only a small fraction of the applied force will be activated. For structural motion calculations on a single-degree-of-freedom system a dynamic load factor (DLF) is defined for a rectangular pulse of duration, t, by (Norris et. al., 1959)

$$DLF = 2 \sin (\pi t / T), \; t < T$$

where T is the period of the single-degree-of-freedom structure. The dynamic load factor is the number by which the deflection, which is produced by a static load, is multiplied to obtain the dynamic deflection. For this problem, the pulse duration is about 3×10^{-5}, the fundamental period of the tank is about 3×10^{-3} and, thus, the dynamic load reduction factor is 0.06.

The stresses that might be expected in the liquid oxygen tank were calculated using the commercial finite element code, ABAQUS [Hibbett, Karlsson and Sorenson (1978)]. The assumptions for this calculation are made in a conservative manner and thusthe reported results are a "worst case" scenario. The first assumption is that the pressure wave reaches the external pipe - LOX tank connection unchanged in both magnitude and shape. Pressure pulse losses will probably occur due to shock transmission to the air and to the flexible hosing and due to friction at the liquid-pipe interface. Estimates of the pressure drop in an acoustic mode (e. g. Nekrasov 1969) and in an incompressible waterhammer mode (Parkmakian 1963) suggested that these loss mechanisms would be of the order of 10% to 20% for the transmitted impulse. The second assumption is that the welded connections between the tank head and the exit pipes have no fillets or thickened regions. Further, the angles of the joints are not rounded by the welding material. This is a conservative assumption because most welded joints will exhibit some material thickening at the joint and the rounding off of the sharp angles there. An additional assumption is that the loads are borne solely by the tank itself. In reality, some of the load will be absorbed by the external supporting structure, for example, through deformation of the aluminum wall at the pipe exit supports or by permanent deformation or compaction of the thermal insulation. Aportion of the blast energy is contained in the kinetic energy of a back flow in the liquid oxygen stream. Some portion of this load will not be picked up by the elbow but will initiate a sound pulse into the liquid contents in the tank and, thus dispersed, will be involved with the short-time tank deformation considered here. We ignore this contribution.

The finite element mesh for one quarter of the structure is shown in Figure 4. The LOX tank has two off-center exit tubes (one of which is shown on this drawing). The tank itself is modeled as a thin cylindrical shell with a torospherical head. The tank is subjected to the initial internal pressure of 1.03 Mpa (150 psi) followed by the blast pressure. The blast load in the flowing oxygen stream is a rectangular pulse with a constant pressure equal to the upper bound limit. The total force is the product of the pressure times the cross-section area. This load is

transferred to the inlet pipe at the 90° elbow (only one side of the elbow is shown) and is represented by a tangential force of 750 N (3350 lbs) applied at the top of the pipe stem. The static equivalent tangential load that is applied to the tank and pipe connector system is the above load multiplied by the dynamic load reduction factor appropriate to this problem and is 45 N (200 lbs).

An elastic analysis showed that the elastic limit condition was exceeded in a very small region near the pipe-tank head juncture. An elastic-plastic analysis using a von Mises yield condition and including work hardening to fit the experimental stress-strain curve for type 304 stainless steel at -183 C was used. Figure 5 shows the contours of the maximum octahedral stress for the entire structure. A detail of this stress component near the pipe-tank juncture is shown in Figure 6. The stress concentration is just at yield at the juncture. Consideration of the maximum strain component at that point (Figure 7) shows that the material is still well below ultimate as only 16% of the available plastic work was used. This excursion beyond yield was confined to a very small region.

CONCLUSIONS

The oxygen tank was loaded by a pressure pulse that was transmitted along the fluid in the piping system between the mixing chamber and the tank. The pressure signal that reached the tank should be low enough not to cause any damage. The worst case combination of loads, pipe losses, etc., in the system could generate a load at the tank that would result in a very localized region wherein the stresses were above yield but were well below the ultimate capacity. At the more probable lower limit, the response of the tank would be well below the proportional limit.

[1]Staff Member.

[2]Visiting Staff Member, Formerly, Asst. Prof., U.S. Army Military Academy, West Point, NY. Currently, HHB, 8th Btn, 8th FA, APO, San Francisco, CA.

REFERENCES

Baker, W. E., J. J. Kulasz, R. S. Westine, P. A. Cox and J. S. Wilbeck, "A Manual for the Prediction of Blast and Fragment Loadings on Structures," Technical Report, DOE/TIC-11268, Southwest Research Institute, (1980).

Hibbitt, Karlsson and Sorenson, Inc., "ABAQUS, User's Manual", paged in sections, Providence, RI, (1978).

Nekrosov, B., Hydraulics for Aeronautical Engineers, Trans. V. Talmy, MIR Publishers, Moscow, 295 pp., (1969).

Norris, C. H., R. J. Hansen, M. J. Holley, Jr., J. M. Biggs, S. Namyet, and J. K. Minami, Structural Design for Dynamic Loads, McGraw-Hill NY,453 pp., (1959).

Parmakian, J., Waterhammer Analysis, Dover, NY, 161 pp., (1963).

Savin, G. N., Stress Concentrations Around Holes, Trans. E. Gros, Pergamon Press, NY, 480 pp., (1961).

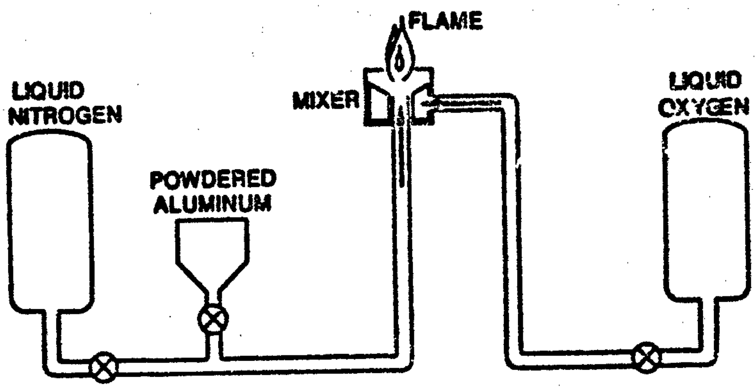

Figure 1. Schematic diagram of the test apparatus.

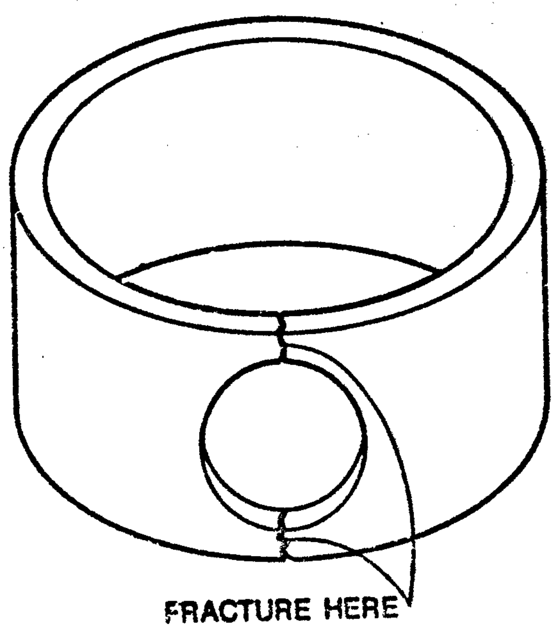

Figure 2. Fracture pattern in the deformed annular shell.

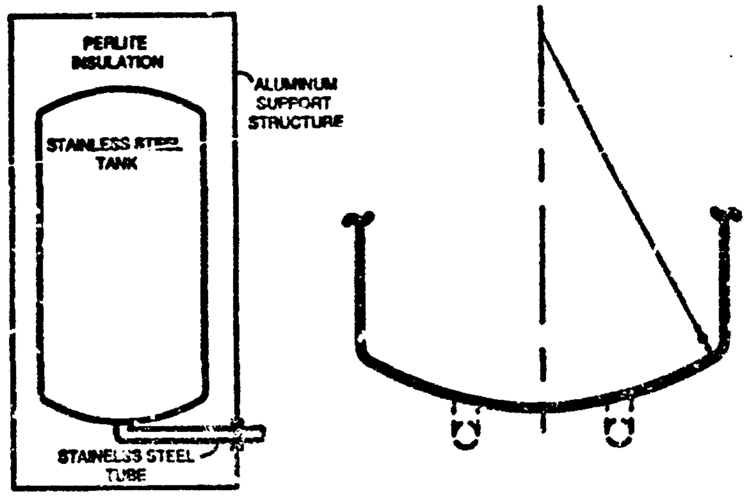

Figure 3. Schematic diagram of the liquid oxygen tank, internal piping, and support structure.

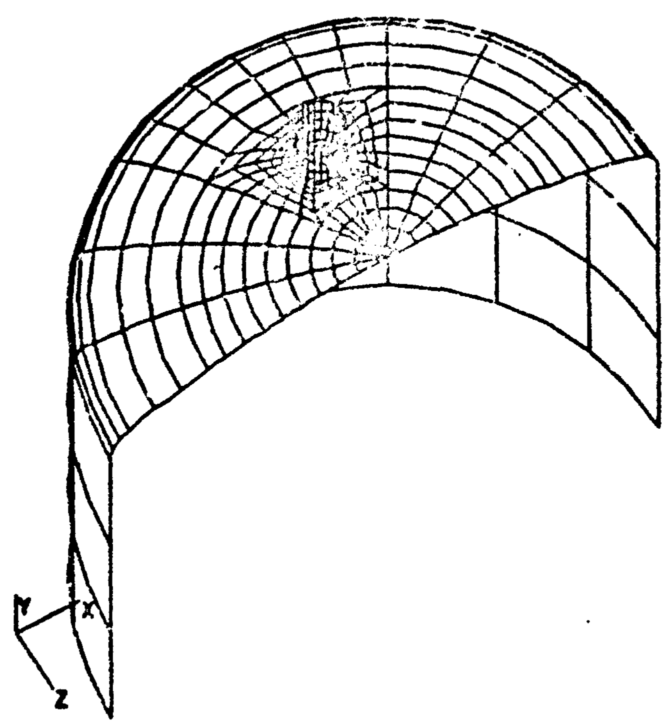

Figure 4. Finite element mesh of the liquid oxygen tank.

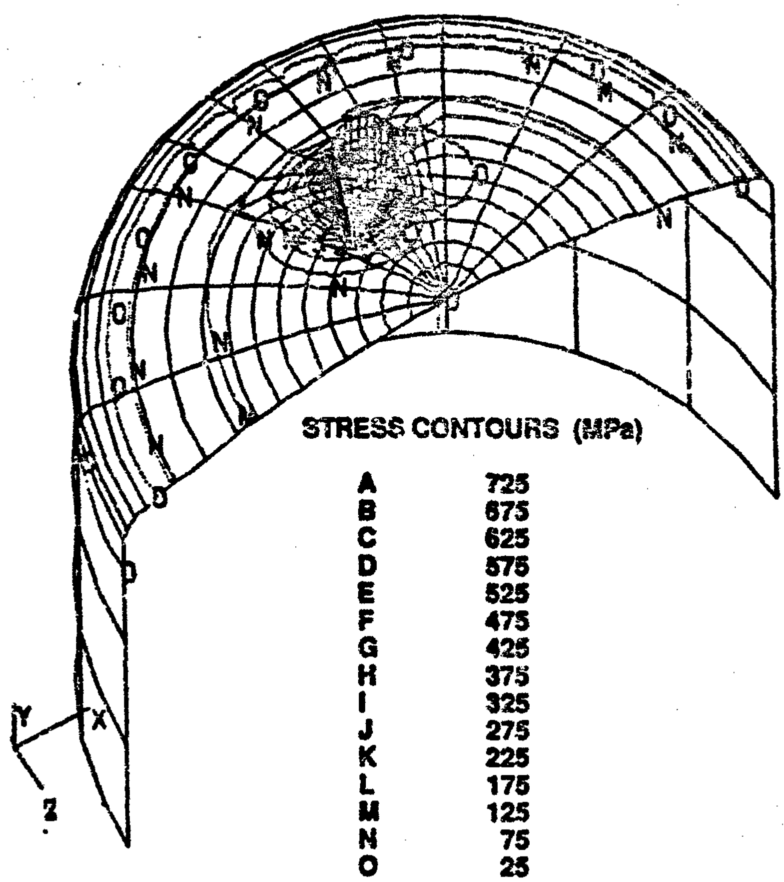

Figure 5. Contours of the octahedral stress, von Mises elastic-plastic model with work-hardening, Type 304 stainless steel at -183 C. 48 N applied tangentially to the pipe stub and normal to the symmetry plane that includes both pipe stubs.

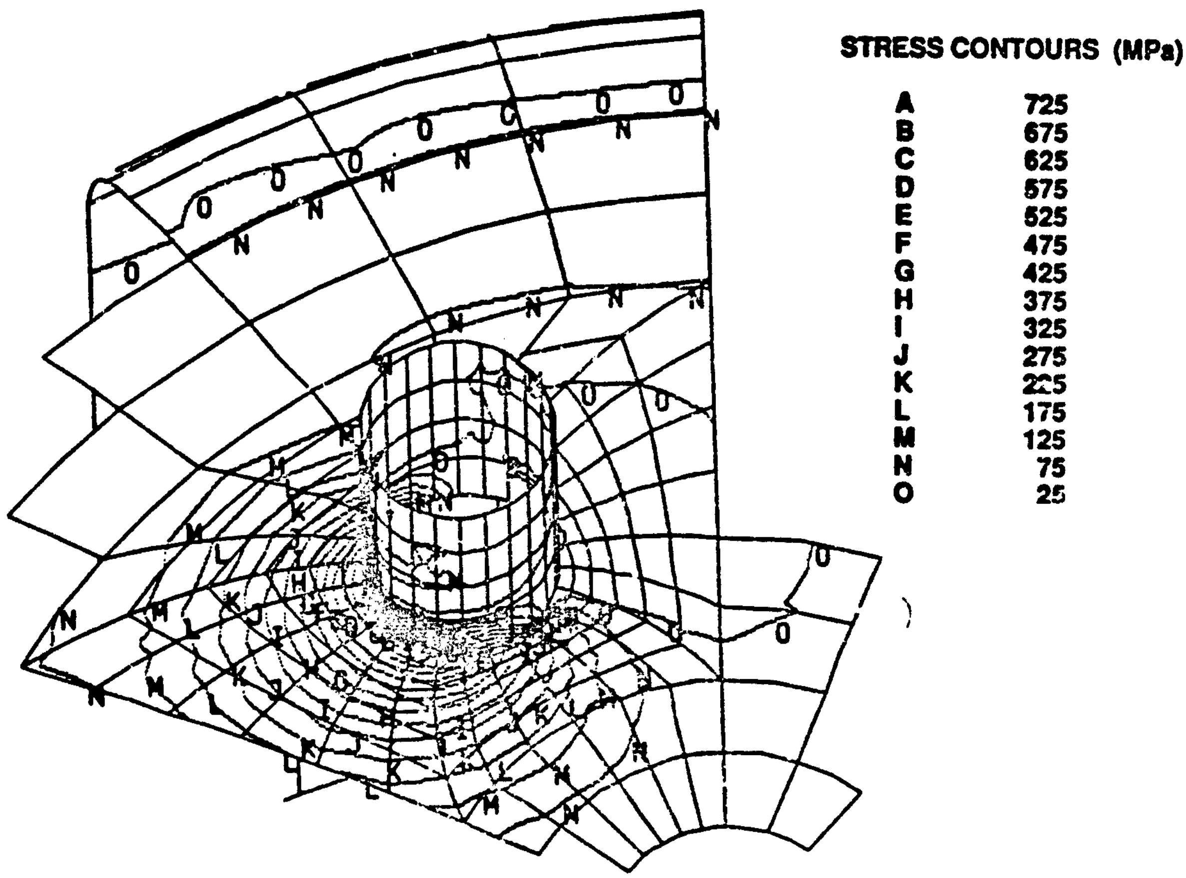

Figure 6. Detail of Figure 5 near the pipe-shell cap junction.

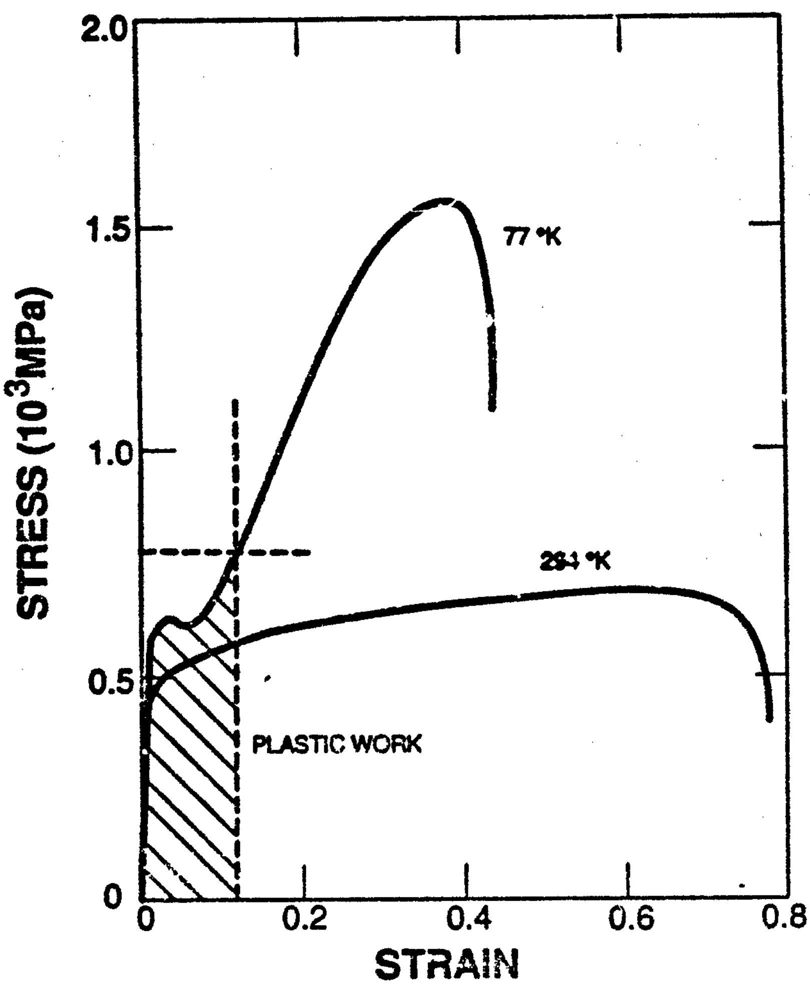

Figure 7. Stress-strain curve for Type 304 stainless steel showing the plastic work done at the location of maximum deformation.

FIVE-PART TEST PROTOCOL FOR EVALUATING REACTIVITY OF EXPLOSIVE CONTAMINATED WASTE SUBSTANCES

By T. S. Bajpayee[1] and Richard J. Mainiero[1]

ABSTRACT

The Bureau of Mines, U.S. Department of the Interior, has conducted research to evaluate the explosive reactivity of explosive-contaminated waste substances generated by U.S. Army ammunition plants. These substances are produced as explosive-contaminated sludge from waste-water treatment plants, residues from burning of munitions and explosives on open ground, and residues from deactivation furnaces. The characterization of explosive reactivity is a prerequisite for disposal of such waste materials, which may be contaminated with primary explosives, pyrotechnic materials, smoke mixtures, signal flares, and missile propellants among others. The Bureau originally suggested a two-part test protocol consisting of gap and internal ignition tests. These tests were proposed to evaluate the sensitivity to shock and thermal stimulus of the test sample. More than 400 samples were tested and reported. However, recently the Bureau revised the test protocol and included three more tests to address the requirements of Title 49 Code of Federal Regulations, Parts 173.51, 173.53, and 173.114a. These tests are thermal stability, impact sensitivity, and electrostatic sensitivity. The purpose of this five-part test protocol is to evaluate the explosive reactivity as defined in Title 40, Code of Federal Regulations, Part 261.23(a)(6) and (7). This paper presents the method of testing and the evaluation criteria of the five-part test protocol.

INTRODUCTION

The Bureau of Mines has conducted research to establish methods and criteria to evaluate the explosive reactivity of explosive-contaminated solid waste substances generated by U.S. Army ammunition plants. These substances are contaminated with various primary explosives, propellants, and pyrotechnic mixtures. The degree of explosive contamination may range from a few parts per million to 10 percent. Such samples are generated as sludge from waste water treatment plants, residue from burning of munitions and explosives on open ground, and residues from deactivation furnaces. Uniform testing methods and assessment criteria were developed to evaluate the explosive reactivity of substances generated from all three sources. The purpose of this research initiative was to develop tests suitable for determining the properties described in 40 CFR 261 Subpart C, "Characteristics of Hazardous Waste," and

---

[1]Supervisory physical scientist, Pittsburgh Research Center, U.S. Department of the Interior, Bureau of Mines, Pittsburgh, PA

in particular, paragraph 261.23(a)(6) and (7), "Characteristic of Reactivity," which defines a solid waste as having the characteristic of reactivity if it has, among others, any of the following properties:

(a)(6) Capable of detonation or explosive reaction if subjected to a strong initiation source, or if heated under confinement.

(a)(7) Readily capable of detonation or explosive decomposition or reaction at standard temperature and pressure.

The Bureau is a recognized expert in the field of explosives and is represented in many national and international organizations. At the request of the U.S. Environmental Protection Agency and the U.S. Department of Defense, the Bureau initiated research to establish testing methods and criteria for characterizing the reactivity of explosive-contaminated solid waste substances. The characterization of explosive reactivity of such substances is a prerequisite for their disposal. This research was aimed at evaluating detonability or explosive reactivity when subjected to a strong initiating source or heated under confinement. Originally two tests were proposed: The Bureau of Mines gap test and the Bureau of Mines internal ignition test.

The gap test is an arrangement for determining the response of a substance to a shock stimulus under confinement. The sample is contained in a length of steel tubing and subjected to the shock stimulus from the detonation of a pentolite booster in contact with the sample. The occurrence of detonation is determined by fragmentation of the tubing, the rate of propagation of the pressure wave in the sample (using an electronic velocity probe), and the perforation of a steel plate at the end of the pipe opposite the booster.

The internal ignition test is an arrangement for determining the response of a sample to heating by internal ignition under confinement. The sample is placed in a steel pipe capped at both ends. An igniter capsule containing 20 g of FFFg black powder inserted in the center of the sample is ignited. The response of the sample is observed according to various degrees of reaction (failure to ignite; partial burning; cap blown off; pipe bulged, split, or laid open; pipe fragmented; and pipe and caps fragmented). The fragmentation of the pipe and/or caps into more than two distinct pieces indicates explosive reactivity. It is considered necessary to perform both tests since there are materials that are sensitive to ignition under confinement but not to shock; there are others that are sensitive to shock but not to ignition under confinement.

The Bureau suggested three more tests to address the requirements of Title 49 Code of Federal Regulations, Parts 173.51, 173.53, and 173.114a. These are the thermal stability test, impact sensitivity test, and electrostatic sensitivity test.

The thermal stability test mandated by 49 CFR 173.51(a) is designed to measure the stability of a substance when subjected to elevated thermal conditions. This test determines if the substance is too hazardous to transport under elevated temperature conditions.

The impact sensitivity test is used to measure the sensitiveness of a substance to mechanical stimuli involving normal impact to determine if the substance is too hazardous to transport.

The electrostatic sensitivity test evaluates the hazard of initiation of explosive substance by electrostatic spark. According to 49 CFR 173.114a, blasting agents should not ignite when exposed to 6 mJ delivered from a 0.002- to 0.004- μF capacitor. This paper provides a description of the five-part test protocol.

EXPERIMENTAL SETUP AND TEST PROCEDURE

Bureau of Mines Gap Test

The apparatus for the Bureau of Mines gap test is shown in figure 1. The test sample is contained in a cylinder of 16-in- (40.6 cm) long, 1-1/2-in-diameter schedule 80 black seamless steel mechanical tubing. The mechanical tubing holds a sample of 425 mL. A mild steel witness plate 6 in (15.24 cm) square and 0.125 in (0.32 cm) thick is mounted at the upper end of the sample tubing and separated from it by spacers of 0.062-in (0.16-cm) thickness. The bottom of the cylinder is closed with two layers of 0.003-in (0.008-cm) thick polyethylene sheet held in place with gum rubber bands and polyvinyl chloride electrical insulating tape. There is no other gap between the pentolite booster and the test sample as used in this test. A continuous velocity of detonation[2] probe made of thin aluminum tube with an axial resistance wire having a resistance of 7.62 ohms/in (3.0 Ω/cm) is mounted on the wall of the sample tubing. The outer tubing of the probe is crimped against the inner wire at the lower end, forming a resistor. When this assembly is inserted in a medium that transmits a shock wave, the outer wall crushes against the inner wire as the wave moves up the tubing, shortening the effective length and changing the resistance. If a constant current (usually 0.06 A) is made to flow between the outer and inner conductors, the voltage between them is proportional to the effective length and can be recorded as a function of time using an oscilloscope. The slope of the oscilloscope trace is thus proportional to the velocity of the shock wave.

The apparatus for the gap test for liquids is the same as that for solids except that a method of injecting bubbles into the liquid sample is provided. The experimental setup is shown in figure 2. The bubbles are injected by means of a 0.925-in (2.35-cm) diameter loop of vinyl plastic tubing located at the bottom of the sample. The tubing is the type used for medical catheterization with an outside diameter of 0.07 in (0.18 cm) and a wall thickness of 0.016 in (0.04 cm). The loop is perforated with two rows of holes diametrically opposite each other with the holes in each row spaced 0.125 in (0.32 cm) apart. The holes are made by inserting a 0.05-in (0.13-cm) diameter needle through the wall of the tubing. Owing to the elastic nature of the tubing, the holes contract almost completely when the needle is withdrawn, so the actual hole diameter is much smaller than 0.04 in (0.1 cm). The tubing is sealed at one end of the loop with epoxy cement, and a length of the tubing from the other end of the loop is led outside to the air supply

---

[2]Ribovich, J., R. W. Watson, and F. C. Gibson. Instrumented Card-Gap Test. AIAA J., v. 6, No. 7, 1968, pp. 1260-1263.

through a hole in the steel tubing, which is also sealed with epoxy cement. Air is supplied at a pressure of 0.3 to 1.0 atm (30 to 100 kPa) to obtain a flow rate of 2.5 ft^3/h (1.2 L/min). Where it is suspected that the sample may react with the steel tube, the inside of the tube is sprayed with a fluorocarbon resin coating.

The sample is loaded to the top of the steel tube. For liquid samples, adequate ullage should be allowed. Solid samples are loaded to the density attained by tapping the cylinder until further settling becomes imperceptible. The sample at 25 ± 3° C is subjected to the shock wave generated by the detonation of a pentolite (50-50 PETN-TNT) pellet, 2 in (5.08 cm) in diameter and 2 in (5.08 cm) thick, having a density of 1.6 ± 0.05 g/cm^3. The pentolite pellet is butted against the bottom of the test sample and initiated with a No. 8 strength electric detonator. The detonator is held in place by a cork detonator holder. Three tests are performed on each sample.

The criteria for detonation propagation are--

(a) The sample tube is fragmented along its entire length, and

(b) A hole is punched in the witness plate, and

(c) A stable propagation velocity greater than 4,900 ft/s (1.5 km/s) is observed.

Bureau of Mines Internal Ignition Test

The experimental arrangement is shown in figure 3. The sample to be tested is contained in an 18-in (45.7-cm) long by 3-in-diameter schedule 80 carbon steel pipe with an inside diameter of 2.9 in (7.37 cm), a wall thickness of 0.30 in (0.76 cm), and capped at both ends with forged steel pipe caps. The pipe holds a sample of 1,950 mL.

The sample is subjected to the thermal and pressure stimuli generated by an igniter consisting of 0.7 oz (20 g) of FFFg black powder located at the center of the sample vessel. The igniter assembly consists of a cylindrical container 0.81 in (2.06 cm) in diameter and 2.5 in (6.4 cm) long, which is made of 0.01-in (0.0254-cm) thick cellulose acetate, held together by two layers of nylon-filament-reinforced cellulose acetate tape. The igniter capsule contains an ignition source that is a resistance heater. The resistance heater consists of a small loop formed from a 1-in (2.54-cm) long nickel-chromium alloy resistance wire 0.012 in (0.030 cm) in diameter having a resistance of 0.343 ohm. This loop is attached to two insulated tinned copper lead wires 0.026 in (0.066 cm) in diameter. The overall wire diameter including insulation is 0.05 in (0.127 cm). The lead wires for the igniter are fed out through a 1/8-in schedule 40 seamless steel pipe attached to one of the pipe caps.

For gelatinous samples, the substance is packed as nearly as possible to its normal shipping density. For granular samples, the substance is loaded to the density obtained by repeated tapping of the pipe against a hard surface. The igniter is fired by a 15-A current obtained from a 20-V transformer. Three tests are performed on each sample. The sample is tested at a temperature of 25 ± 3° C.

The criterion used for interpretation of a positive result is that either the pipe or at least one of the end caps must be fragmented into at least two distinct pieces. Results in which the pipe is merely split or laid open or in which the pipe or caps are distorted to the point at which the caps are blown off are considered to be negative results.

Thermal Stability Test

The test is conducted in two phases. The first phase is used to determine if a sample shows thermal instability by observing whether ignition, explosion color change, weight loss, etc., occurred. The second phase is used to determine the severity of the thermal instability by measuring the extent of temperature rise with thermocouples. The second phase is run only if the first phase does not provide a definite conclusion regarding the stability of the substance.

During the first phase of the test a sample of up to 50 g is transferred to a beaker, covered, and weighed. The beaker, with cover, is placed in an oven and heated at 75° C for 48 h; unless an ignition or explosion occurs in the sample, the beaker is then removed, cooled in a desiccator, and weighed. The volatility (weight loss as a percentage of the sample weight) is calculated. In dealing with an unknown substance, several screening tests with a sample size much less than 50 g are performed to get a feel for the behavior of the substance.

Figure 4 shows the experimental setup for conducting the second phase of the test. Approximately 100 g or 100 mL of the sample is placed in a test tube, and the same quantity of inert reference substance (generally quartz sand) is placed in the other tube. Thermocouples are inserted into the tubes at half-height of the materials. Another thermocouple is used to record the temperature of the oven. The temperature difference (if any) between test sample and reference is measured for 48 h after the sample and reference substance reach 75° C. Unless an ignition or explosion occurs, the sample tube is removed, cooled in the desiccator, and weighed. Evidence of decomposition of the sample is also noted.

The criteria for assessing results follow:

(a) For the first phase of the test, an ignition or explosion indicates a positive result and the sample is considered thermally unstable.

(b) For the second phase of the test, the sample is considered thermally unstable if an ignition or explosion occurs or if a temperature difference of 3° C or more is recorded between the test substance and the reference material.

Impact Sensitivity Test

The impact sensitivity apparatus is designed to study the effect of mechanical impact of a free-falling 3.63-kg (8-lb) weight on the test sample. Figure 5 shows an overview of the impact testing apparatus, and figure 6 shows the sample holder assembly. This test is performed pursuant to 49 CFR 173.53 Note 4. The free-falling weight is guided through two vertical steel guide posts and hits a plunge and plug assembly. The impact is transmitted to the

sample under test, which is placed on a die-and-anvil assembly and confined in a cylindrical casing. The inside diameter of the casing is just sufficient to permit free vertical movement of the plunger and plug. To conduct a test, the free-falling weight is raised to a height of 25 cm (10 in), and approximately 10 mg of the sample is loaded on the die. The anvil and die are placed in the sample housing, and the casing is screwed in. The plug and the plunger are then inserted on the top. The sample assembly is placed in position, and the drop weight is released from a height of 25 cm (10 in). At least 10 tests are performed on each sample.

The criteria for assessing the results are that an audible report, flame and/or smoke, and/or obvious decomposition of the sample indicate a positive result. When testing solid or paste materials, the sample may appear to partially decompose, discolor, or liquify. Unless considerable smoke, noise, and/or other evidence of extensive decomposition is present, the test should be recorded as negative.

Electrostatic Sensitivity Test

This test is designed to determine the ease with which a substance is ignited by electrostatic spark. Figure 7 shows an overview of the spark sensi-tivity test chamber, figure 8 shows the electrode assembly, and figure 9 shows the schematic circuit diagram. Approximately 60 mg of sample is placed on a 0.95-cm-diameter hole in a plastic plate measuring 5 cm by 5 cm by 0.16 cm thick, which is in turn placed atop a copper base plate. A steel needle positioned above the sample acts as an electrode for the discharge of a capaci-tor, thereby producing a spark which passes through the sample to the copper base plate. Prior to testing, the needle is positioned well above the sample and is disconnected from the charged capacitor. For conducting a test, the needle is connected to the charged capacitor through a vacuum relay switch, and a solenoid simultaneously lowers the needle to within 0.32 cm of the base plate. When the needle gets sufficiently close to the sample (a few milli- meters), the intervening air breaks down and the resulting spark passes through the sample. This is called the "approach-gap" mode of operation and is more convenient to use than a fixed gap distance. The spark passing through the sample may or may not cause an ignition, depending on the spark sensitivity of the material and the energy of the spark. The energy is varied by adjusting the voltage and the capacitance. According to 49 CFR 173.114a the sample should not ignite at any trial when exposed to a spark energy level of 0.006 mJ. However, the Bureau recommends additional testing to identify the maximum energy level at which no initiation occurs in 10 successive trials.

The criterion established by the Bureau for a positive reaction is the appearance of flame, smouldering, or glow in the test sample. A visible flash, shooting sparks from the sample, or visibly burned areas in the residual sample indicate positive reaction. Since the spark sometimes scatters the sample (usually finely powdered), even when there is no reaction, sample consumption is not a reliable indicator. The test result is reported as the threshold initiation level, the maximum spark energy level at which no initiation occurs in 10 successive trials.

VALIDATION TESTS

Validation of the gap and internal ignition tests was done as part of the original effort in developing these tests. The rationale of the validation was to set the test stimulus relative to a suite of substances, all of which possess, at least theoretically, some capacity for energy-releasing chemical reaction. In addition to materials with known explosive properties, such as explosives, blasting agents, and propellants, the tests included (1) substances that are of minimal explosive hazard but that still have exhibited some potential to detonate or violently burn with sufficiently strong stimulus and confinement, and (2) substances that, while theoretically capable of releasing energy when decomposed, have not been known to burn or detonate as a result of involvement in transport or storage (such as dense-prilled ammonium nitrate and dinitrotoluene). The stimuli of the two tests were set at values that would give positive results for as many as possible of the first type of substance, while giving negative results for as many as possible of the second type of substance. Table 1 lists reference substances and the test results.

DISCUSSION

The Bureau has evaluated over 400 samples of contaminated soil, sludge, and burning residue using the gap and internal ignition tests. Only two samples showed evidence of explosive reactivity. One sample showed a positive result in the internal ignition test. The sample reacted violently to the thermal stimulus. The end caps were blown off, and the pipe was fragmented into more than three pieces. The other sample reacted violently in the gap and internal ignition tests. In the gap test, the pipe was fragmented into small pieces, a hole of approximately 3-in diameter was punched in the witness plate, and the detonation velocity probe showed a rate in excess of 2 km/s. In the internal ignition test, the end caps were blown off and the pipe fragmented in more than three pieces. However, the majority of the contaminated samples were nonreactive relative to 40 CFR 261.23(a)(6) and (7). Over 20 samples were tested using this 5-part test protocol; none showed any evidence of reactivity.

Table 1. - Examples of validation tests for various reference substances

Type of Reference Substance	Sample Designation	Gap Test	Internal Ignition Test
Blasting Agents	Water gel (TNT sensitized)	P	P
	Ammonium nitrate-fuel oil	P	P
High Explosive	Nitroguanidine	P	P
	Water gel (amine nitrate sensitized)	P	P
	Granular TNT	P	P
	Flake TNT	P	P
Propellants	Propellant (cannon)--sample A	P	P
	Propellant (cannon)--sample B	P	P
	Propellant (cannon)--sample C	P	P
	Propellant (cannon)--sample D	P	P
	Propellant (cannon)--sample E	P	P
	Propellant (cannon)--sample F	P	P
	Propellant (cannon)--sample G	P	P
Marginally Reactive	Benzoyl peroxide, powder	N	N
	Sodium picramate	N	P
	Ammonium perchlorate, coarse crystals	N	P
	Ammonium perchlorate, fine crystals	P	P
	Nitrocellulose, 13.3% N, 20% water	P	P
	Nitrocellulose, 11.5% N, 20% water	P	P
	2,4-Dinitrophenol, granular	P	N
	Guanidine nitrate, granular	P	N
	Nitrocellulose, 13.2% N, 30% ethanol	P	P
	Nitrocellulose, 11.5% N, 30% isopropanol	P	P
	Ammonium perchlorate, fine crystals, low density	P	P
	2,4-Dinitrotoluene, granular	P	N
	m-Dinitrobenzene, dry, fine crystals	P	P
	Smokeless powder (small-arms)	P	P
	Potassium chlorate lactose (50/50)	P	P
	Nitrocellulose 13.3% N, dry	P	P
	Ammonium nitrate prills, low density	N	N
	Ammonium nitrate prills, medium density	N	N
	Ammonium nitrate prills, high density	N	N

P = Positive result; N = Negative result.

UNIT OF MEASURE ABBREVIATIONS USED IN THIS REPORT

A	ampere
atm	atmosphere, standard
°C	degree Celsius
cm	centimeter
ft^3/h	cubic foot per hour
ft/s	foot per second
g	gram
g/cm^3	gram per cubic centimeter
h	hour
in	inch
km/s	kilometer per second
kPa	kilopascal
L/min	liter per minute
mg	milligram
mJ	millijoule
mL	milliliter
μF	microfarad
Ω	ohm
oz	ounce
V	volt

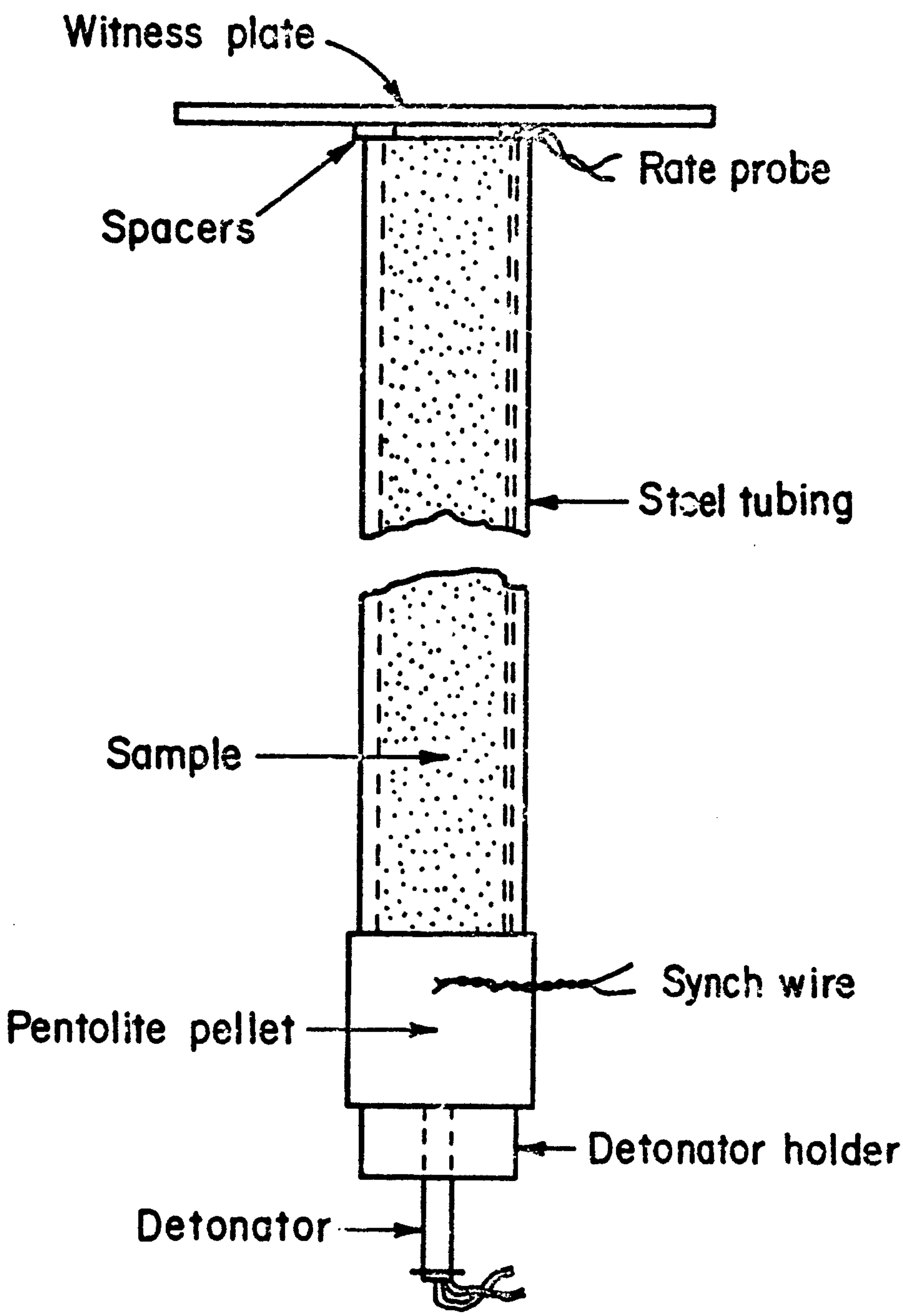

Figure 1 Bureau of Mines Gap Test for Solids

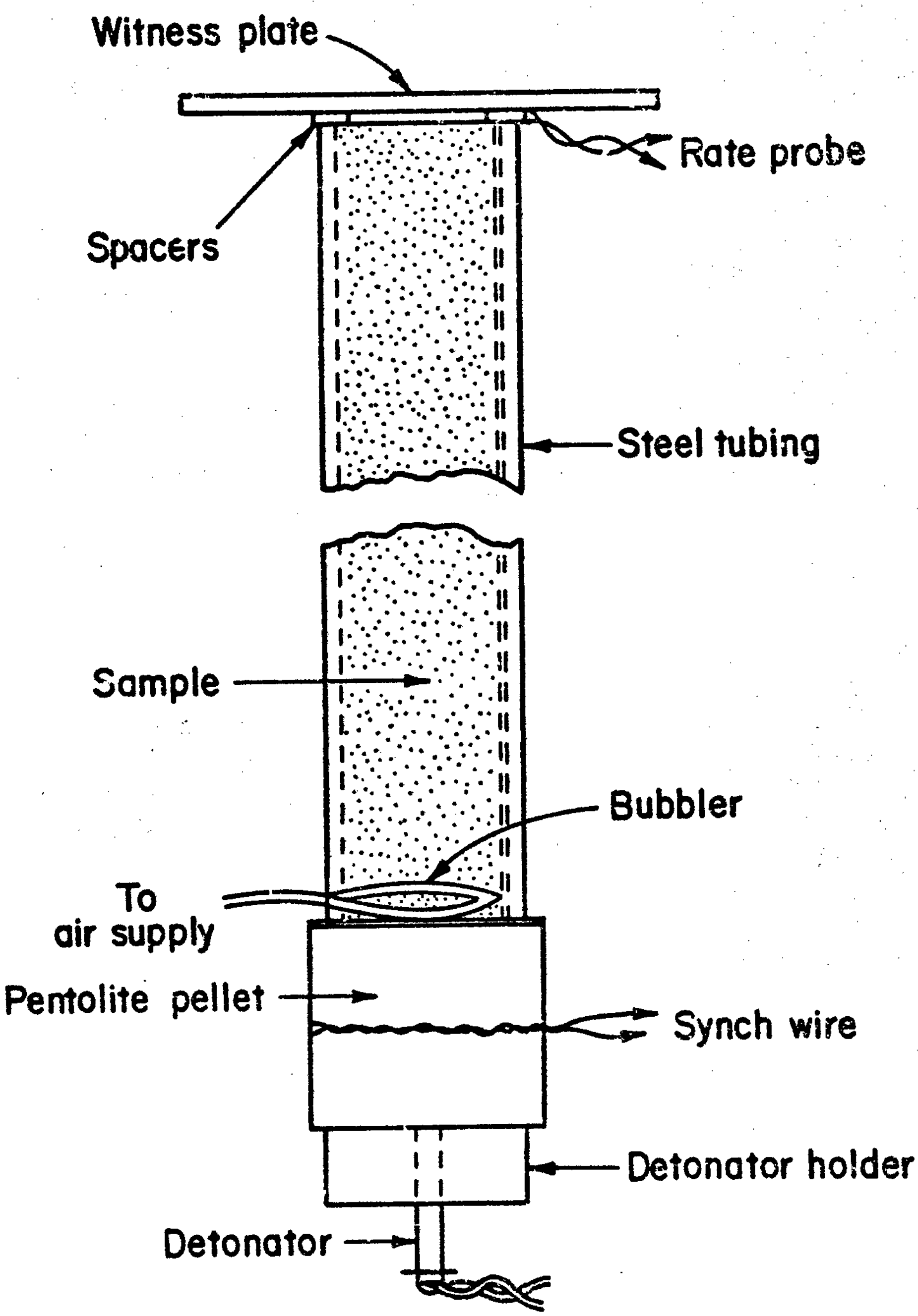

Figure 2. Bureau of Mines Gap Test for Liquids

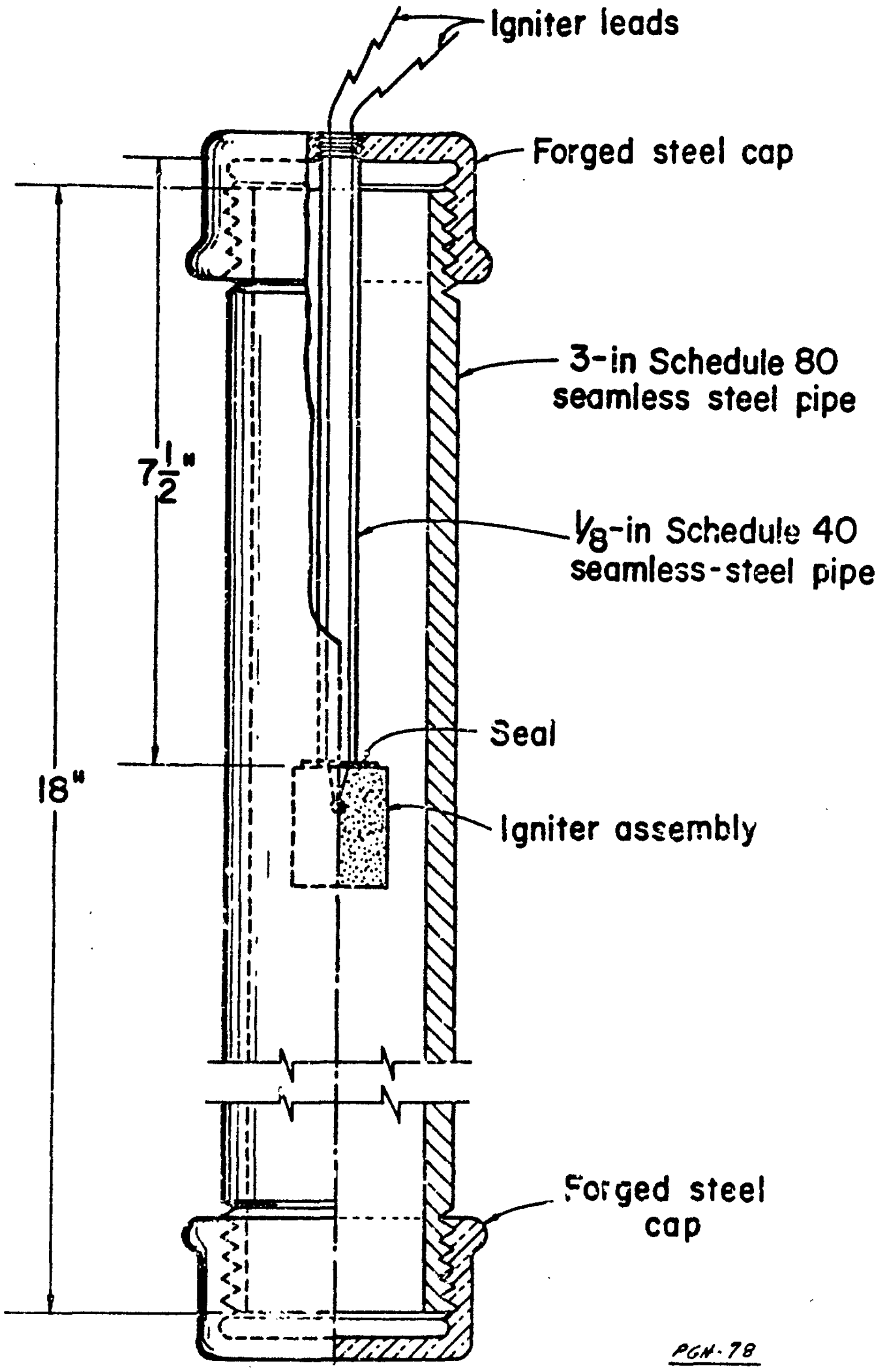

Figure 3. Bureau of Mines Internal Ignition Test

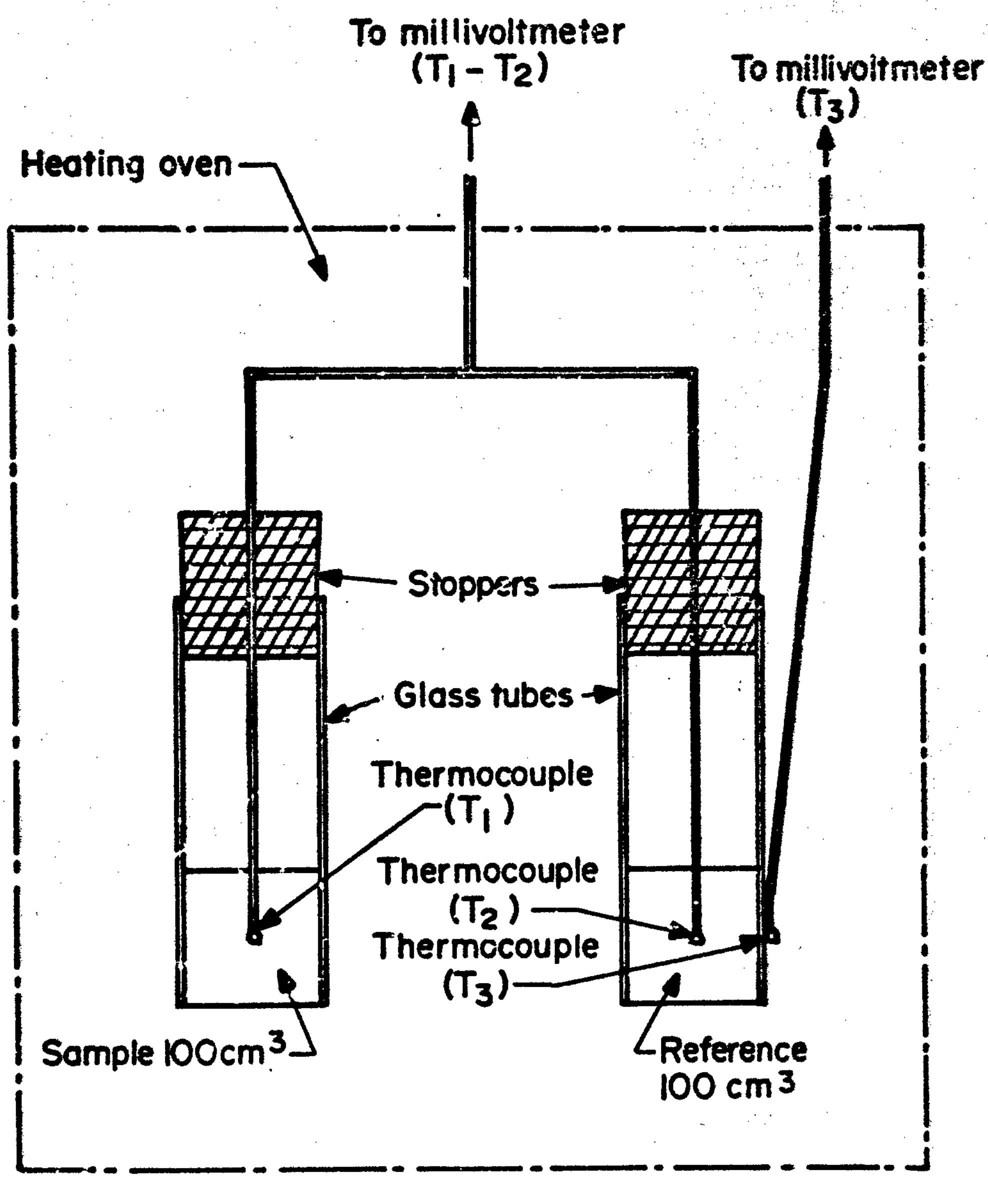

Figure 4. Thermal Stability Test Setup

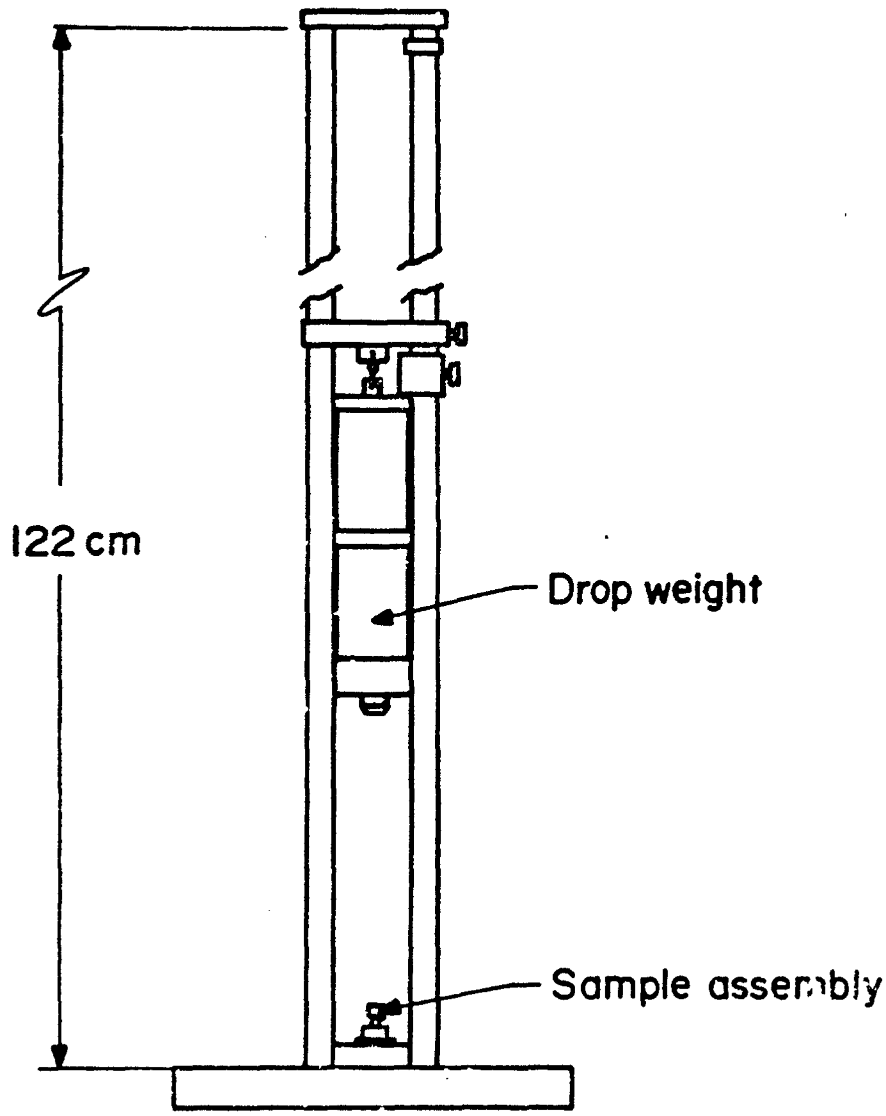

Figure 5. Overview of the Impact Testing Apparatus

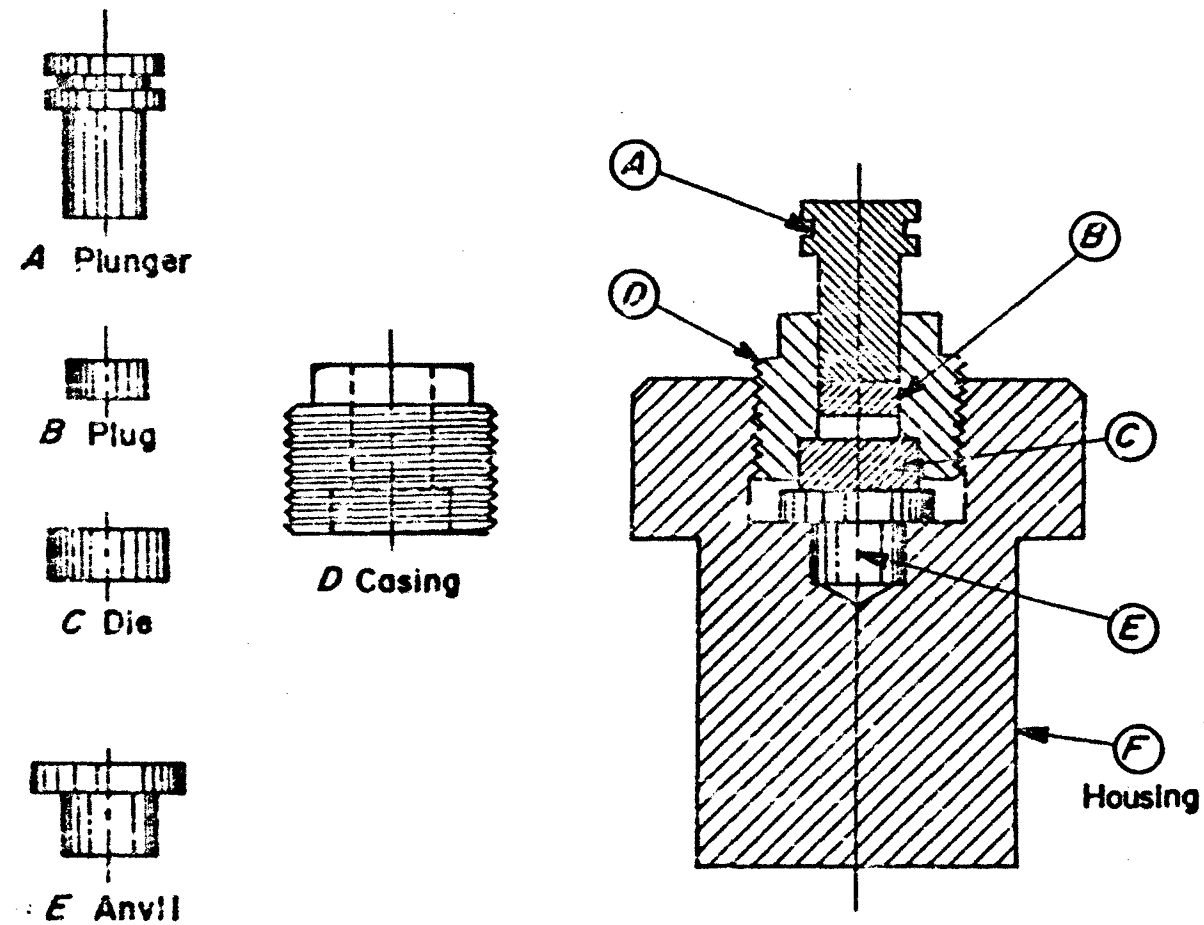

Figure 6. Sample Holder Assembly

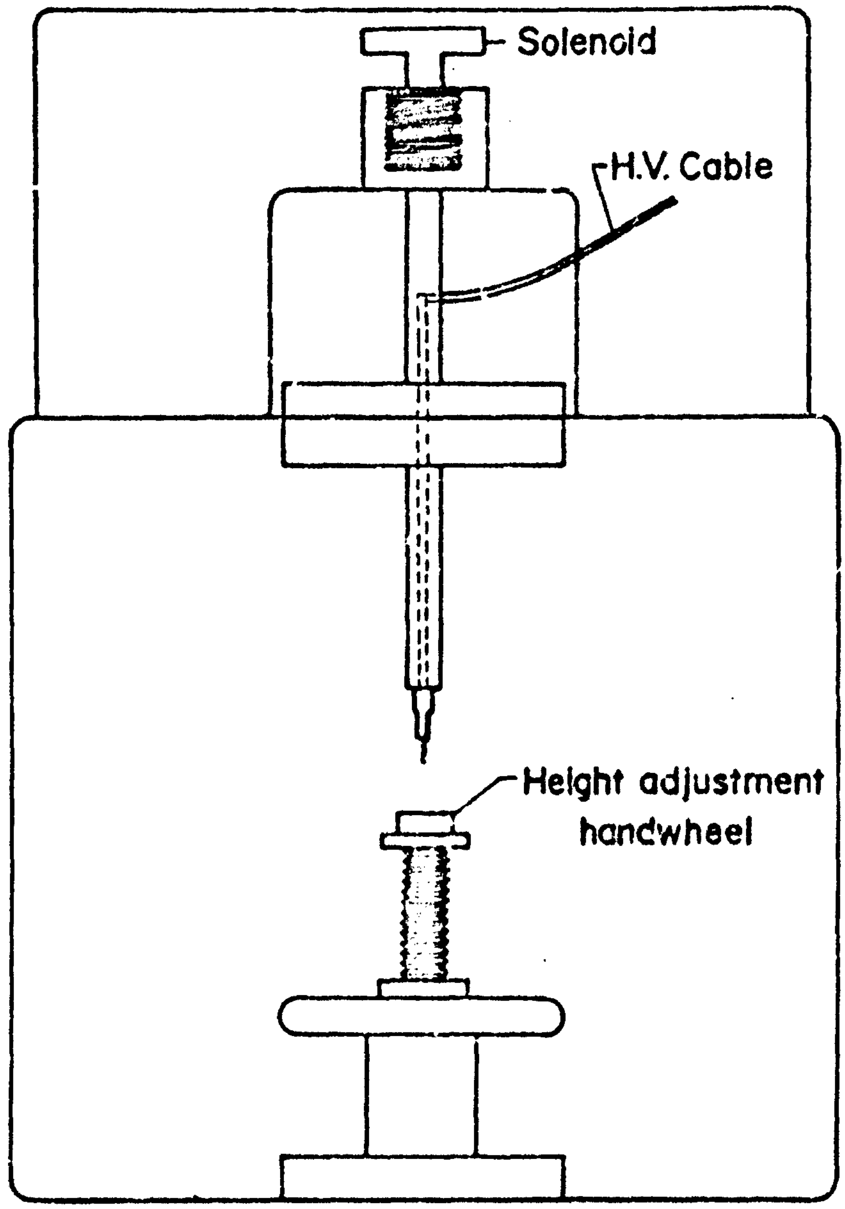

Figure 7. Overview of Spark Sensitivity Test Chamber

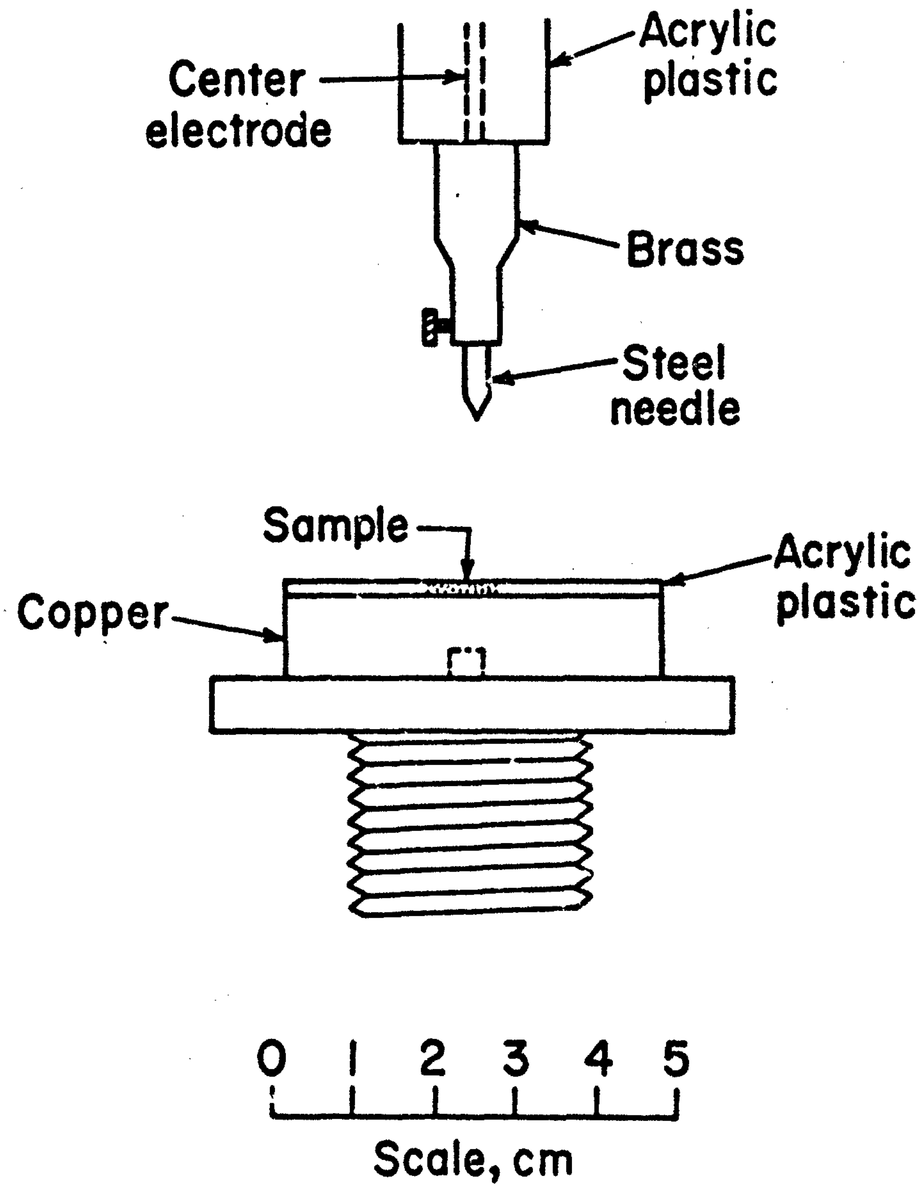

Figure 8. Electrode Assembly

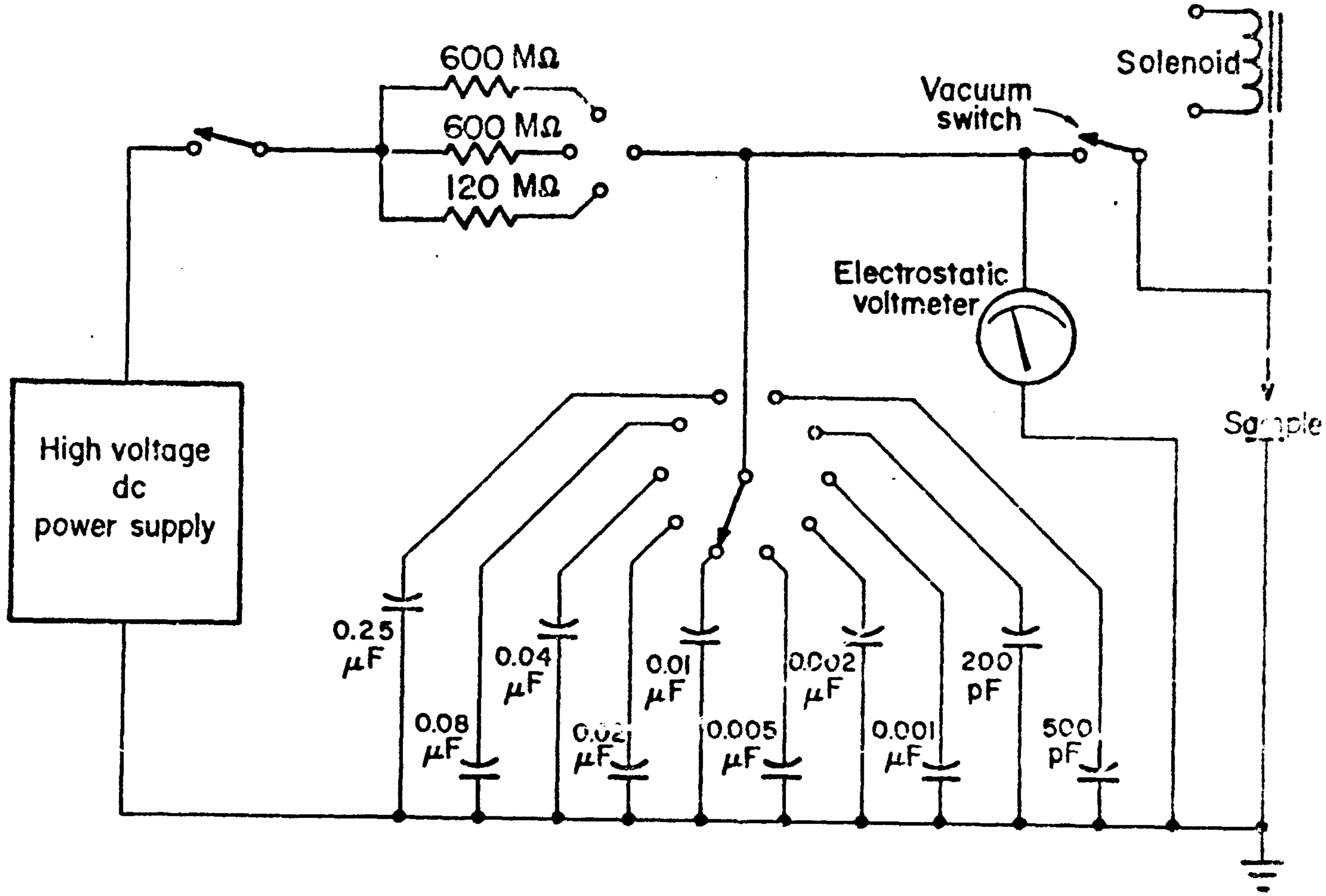

Figure 9. Schematic Circuit Diagram

THE DECONTAMINATION OF PRIDDYS HARD

By L H Armstrong, B Sc, C Eng, M I Chem E, M I Exp E
Ministry of Defence (Navy), DST/AS, Bath, England

Priddy's Hard is a Naval ammunition depot on the South coast of England which was established in 1766, safely to store and supply gunpowder to the Fleet. It was originally a boatyard and wharf owned by Jane Priddy - hence the name - which was bought because there was great anxiety about the storage of so much explosive so near to the Dockyard at Portsmouth.

A magazine was built there to store 14,000 barrels of powder. This building still exists; it is now used as the Naval Armament Museum.

Dr Samuel Johnson once said "If we act only for ourselves, to neglect the study of history is not provident: if we are entrusted with the care of others it is not just". My main problem was to enquire into the history of the site. What had been done where? Some records existed, but they were incomplete. The main source of information was talking to long-service employees, and in particular I am grateful to Mr Jimmy Millar, who worked at Priddy's Hard as a boy, and retired as Head of the Explosive maintenance Division, after a lifetime's work.

All production on the site had ceased, and explosives and ammunition had been removed from the buildings and the site. I will now describe some of the problems found.

The Museum

There was no record of this magazine ever having been declared free from explosives. It was almost certain that this had been done when the museum was founded, but detailed examination was required. Some gaps were seen between floorboards, and because there was no way into the space under the floor, several boards were lifted, so that I could crawl underneath to examine this space. I found nothing, except for a lot of bronze nails and a 19th century gunpowder sampling bottle. The floor had been constructed dustproof; each joint was covered with a wooden lath, and the gap filled with oakum, fibres of old rope. The gaps had been caused when electric cables had been installed under the floor, and the joints had not been made good.

It is likely that all the exhibits are free from explosives, but this must be checked by visual examination. There are problems with the heavier items, and with the sheer quantity of exhibits.

Process Buildings

A careful search of all process buildings was done. Every hidden cavity has to be opened, to ensure that nothing has been hidden there. Many of the buildings were wooden, lined with asbestos cement sheets. It is easier to work from the outside, to strip off the external wood to open the cavities, rather than to remove the lining, and have to take special precautions against the risk of inhaling asbestos dust. Floor coverings are removed, and every sealed ceiling-space opened. Many small components were found.

Five of the buildings were partially surrounded by "moats", ditches made when earth was dug out to make the traverses or berms. I had been warned that small explosive articles had been disposed of in these ditches, so some examination was needed. The moats were pumped out by the local fire brigade; sieves on the end of the suction hoses prevented any article larger than a few millimetres entering the pump.

The initial search was done by the Royal Marines bomb-disposal team. Their excellent work produced several interesting items, including live explosive items from this century and the last, and they said that their technique of using long rods to feel in the mud would find about 60% of what might be there. A second search with similar methods would find about half of the residue. So a better method was needed.

A mechanical digger was used, to remove all the soft mud to a depth of two feet. This mud was then washed through a sieve of 1 inch mesh, to recover anything which might be present. The main difficulty was caused by plant and tree roots, which blocked the sieve and caused much delay. But more live explosive items were found. Some of them were harmless from long immersion in water; the black powder was dissolved out of the primers, for example. But the caps in some of these had survived, and exploded loudly when the primers were put on a fire, ejecting the cap for some yards. The tetryl pellets, the HE filled shell and the base fuzes from large shell were still unharmed, and detonated effectively when they were countermined by the Naval Explosive Ordnance Disposal team, who removed and disposed of all the items found. No incident was caused by the digging or the sieving, because the items found were never trapped between two hard surfaces.

Metal Detectors

The use of metal detectors was proposed and tried. The "Ferex" model 4.021 detector was used by the Royal Marine team, and proved to be sensitive and well able to stand up to the conditions. It can find a 2 pounder shell six or seven feet down without difficulty, and is not harmed by the wet and dirty conditions. Many small detonators were found behind the site of the old proof house; fortunately, they were not sealed, and had been made inert by the water. But the great problem was that of false alarms; every piece of scrap iron produces a response, and it is difficult to motivate a search team for long periods of work in these conditions when no significant explosive article is found.

Shell Filling Buildings

Filling had been done before and during World War I. Filling with Shellite (the eutectic mixture of dinitrophenol and trinitrophenol) and TNT had been recorded in certain buildings, and traces of explosive which had sublimed into the walls and ceiling were clearly detectable with the caustic soda/acetone test. Persistent efforts to cleanse these walls failed, so we had to resort to destruction of the buildings by fire.

Wood was piled to a depth of about four feet in the building. A hole was made in the roof to assure a through draught. Pieces of lead were distributed throughout the building, in intimate thermal contact with the larger girders and walls. If these were melted, we were sure that a temperature of 327 degrees C had been reached, a temperature sufficient to destroy all traces of explosive. It was necessary to wet

all surrounding areas, so that the fire did not spread. The operation was successful, and the burnt buildings were levelled to the ground.

Drains

Some process drains remain to be cleared. A technique developed by Mr Alan Dyer of RARDE, Waltham Abbey is to be used. Each drain is rodded through, and a wire is pulled in. This wire can then pull in a flexible flammable cartridge, made of tubular bandage filled with charcoal briquettes (like those used on a barbeque) soaked in kerosine. A blower supplies the air needed for combustion, and the resulting fire destroys any explosive present, both in the pipe and in and around the joints.

Buried Fuzes

The final problem on the site is that one officer has told me of his memory that boxes of fuzes were buried beneath the foundations of a building. He cannot positively identify which of a set of eight was concerned, so it is planned to remove all eight buildings by an approved asbestos disposal contractor, explosively to disrupt the concrete floor slabs of all eight buildings, and to search with the metal detector. A preliminary search with the detector was inconclusive; false alarms from buried metal were everywhere.

Certification

It will be understood that I cannot honestly certify this site to be completely free from explosives; all that can be done is to complete the detail on the form attached, to declare that the "Best practicable means" have been employed.

CERTIFICATE OF CLEARANCE OF EXPLOSIVE MATERIALS AND OTHER DANGEROUS SUBSTANCES

Location and Map Ref:

Date(s) of search:

1. This site in respect of which this certificate is given is shown coloured/verged .... on the attached plan.

Explosives

2. There being no record or knowledge of explosives having been used or stored, either by MOD or other users, on the site/areas marked .... it is certified that the site/areas has/have been subject to a thorough visual search.

3. Records show/It is known that explosives have been used and/or stored on the site/areas marked ....

   a. An instrument search has been carried out.

   b. An instrument search is unnecessary and a visual search only has been carried out.

   c. Search requirements are beyond the capability of the unit. The site/areas has/have not been searched.

      (Indicate areas not searched)

   The matter has been referred to .... with a request that a search be carried out and a further certificate completed.

4. The site/area indicated .... has been used exclusively for living quarters and has not been searched.

5. No/The following explosives or other dangerous substances have been recovered. They have been removed and/or destroyed in accordance with current regulations.

Other potential dangers

6. In addition, as far as practical, it has been ascertained that:

   a. No oil, gas, chemicals or other dangerous substances are buried or stored within the curtilage of the site and the ground has not been contaminated by such substances.

b. (1) There is no record or knowledge of hazardous radioactive materials being used or stored on the site either by MOD or other users

or

(2) All buildings/areas in which radioactive materials have been used or stored have been monitored and have been certified as free from radioactive contamination.

c. There appear to be no defects in any building which could/would constitute a danger to life or limb.

d. There is no known hazard within the curtilage of the site, which could constitute a danger to life or limb.

7. A potential danger was ....

situated at the positions marked ....

The advice of .... was sought and the following

action taken .... to their satisfaction. (Summarize details in attachment if necessary.) All reasonable steps have been taken to minimize physical hazards, level floors, fill voids, remove or make safe machinery and cut off access to potentially dangerous places and to prevent unauthorized entry.

8. The potential danger is .... situated at the

positions marked .... Clearance is not practical on

grounds of ....

The following action has been taken to minimize the risk ....

The following limitations on future use are recommended ....

9. Any other comments.

Signature ....

Rank ....

Officer i/c Search and Clearance

10. Comments of MOD Sponsor Directorate.

Note: Delete inapplicable clauses of paras 2 to 9 as appropriate.

OPEN BURNING/OPEN DETONATION EMISSIONS STUDY - PHASE I

Summary of Video Presentation
As Presented At The
23rd DOD EXPLOSIVE SAFETY SEMINAR
August, 1988

Mark M. Zaugg and M. Kim Russell
Ammunition Equipment Directorate
Tooele Army Depot, Tooele, Utah

Since the beginning of modern warfare, defective or obsolete munitions have been disposed of by one of two methods. The first is OPEN BURNING, the primary method for disposing of propellant. The second method, used for disposal of munitions containing high explosive, is OPEN DETONATION.

In order to get answers to questions raised on the inpact to the environment by these disposal operations, under the guidence and direction of the US Army Armament Munitions and Chemical Command (AMCCOM), the Ammuniton Equipment Directorate (AED) at Tooele Army Depot in Utah developed and conducted a test program to determine the environmental effects on the air and soil from open burning and open detonation operations.

During a propellant burn operation at the Tooele demil grounds, an opportunity arose to experiment with cloud sampling procedures. A helicopter was provided by Dugway Proving Ground, instrumented with a few simple monitoring devices, and the feasibility of helicopter sampling was tested. One of the concerns was that the intense heat generated by the burning propellant, which was felt by those inside the helicopter, might have an effect on the operation of the helicopter. However, after a cautious beginning, no adverse effect on the operation of the aircraft was noted. After completing this test and after reviewing other possible methods for sampling, it was decided that the helicopter was the best choice.

A go-ahead was provided by AMCCOM to initiate an extensive emissions study of the effects on the environment of open burning and open detonation. The first phase of this study was to identify and confirm the best stacking configurations for the propellants and explosives to be used, and to test sampling equipment and procedures.

Preliminary tests included detonations of TNT-filled hand grenades in increments of 500 pounds, 1000 pounds, and 2000 pounds of explosive. One observation noted was that clouds to be sampled by the instrumented helicopter would be in many varying configurations.

While reviewing the videos tapes of the detonation of bulk TNT, the images were slowed down in order to allow a close look at the development of the fireball during the first second or two of the detonation. It is during the first few milliseconds of 3000-6000 degrees Centigrade temperature that nearly all of the chemical reactions and degradation take place. The high temperatures of the fireball promote good efficient degradation of the explosive. The main constituent of the cloud after the first few seconds is water vapor.

The effectiveness of the fireball in disposing of the explosive varies with its temperature and duration, which themselves are funtions of the type and quantity of the explosive, as well as the configuration of the munition. The size and duration of the fireballs generated during these tests varied widely since munitions of various sizes and containing various explosive fillers were used. Included were projectiles, depth charges, bombs, hand grenades, rockets, torpedo warheads and bulk explosives such as TNT, Composition B, Explosive D and propellants. High Explosive munitions were stacked in 5 stacks per test, in 100, 500, 1,000, 2,000 and 5,000-lb quantities of net explosive weight.

After the configuration of the sampling helicopter was determined, the US Army Aviation Development Test Activity at Fort Rucker, Alabama, supplied a UH-1H helicopter for the duration of the study. Modifications were made to the helicopter including the installation of a 4-inch diameter Teflon-lined PVC sampling probe protruding in front of the helicopter, which entered the helicopter from an opening underneath the fuselage. Sample air was drawn through the probe into a manifold inside the cabin. From the manifold, samples were drawn through teflon tubing into the numerous monitoring devices, each selected with combined consideration for their portability, sensitivity, and response speed.

Included among the monitoring instruments was a hydrogen and carbon monoxide monitor, a particle analyzer which collected, counted and qualified the size of particles at all times while passing through the plumes, a temperature and humidity monitor connected to a probe located inside the manifold, and a carbon dioxide monitor. The date collected by the instruments were passed to an on-board computer where the measurement voltages were collected and stored on magnetic floppy disks. All monitoring instruments were either powered by a DC to AC inverter or by their own internal batteries, the latter being the preferred method.

To an observer looking at the helicopter, the aircraft appeared to be filled to capacity with sample monitoring and collection equipment. A high volume particulate sampler was installed to capture particles on a filter for later analysis. A Volatile Organic Sampling Train filter collected samples from the probe which were later analyzed in the laboratory for organic components.

Installed in an air-tight cabinet were three Teflon-lined sample bags used to collect grab samples of air for later analysis. A vacuum pump was connected to the cabinet to create a negative pressure while sampling. While inside the plume, the valves to the bags were opened allowing the vacuum to expand the bags and the sample air to rush in. After each test was completed the helicopter landed near the test site and the sample bags were removed and immediately taken to the laboratory for extraction and analysis of samples.

Since most demil activities involve obsolete or unserviceable munitions, items from unserviceable stockpiles from around the country were shipped in for this study. Tests were performed on several types of munitions.

An objective of the OBOD study was to burn and detonate bulk explosive (vs. explosive filled munitions) thus eliminating contamination of the samples from metal parts, paints, etc. Therefore, included in this study was bulk Composition B, Explosive D (Ammonium Picrate) and TNT. These bulk explosives were stacked in normal demil configurations and detonated using normal demil procedures, as were all the tests in this study.

In addition to the bulk explosives, munitions with many different filler materials were included in the tests. For example, 500-lb bombs containing explosive H-6, depth charges containing the explosive HBX, and five-inch Navy projectiles filled with a common Navy explosive, Composition A3 were used, among others.

Four camera positions were established to record all of the burns and detonations as well as the location of the helicopter during sampling, each of which included video cameras for both visable and infra-red light and a 35mm slow-speed tracking camera operating a one frame per second. In addition, still photos were taken of the munitions stacking configurations.

When the Test Officer had determined that the EOD personnel had cleared the site, that the camera positions had all called in and declared their readiness, and that the instrumentation personnel aboard the helicopter were ready, the helicopter lifted off and headed for its standby position. The ignition of the munitions was performed by EOD personnel using a manually activated blasting machine located 2,500 meters from the detonation site. Once the munitions were detonated, and as soon as safely possible, the helicopter began its approach and passes through the clouds, usually entering the plumes within one or two minutes of the detonation.

In reviewing the films and videos of the burns and detonations, the quick rising of some plumes to several thousand feet above the test site is in contrast to some instances where the plume hung close to the ground. This created a differing sampling situation so far as the helicopter was concerned and demonstrated the effect of different atmospheric conditions on plume development. Another variable in the testing procedure was the different sizes of the plumes. Also apparent were the convolutions within the plume of which the pilots had to be aware as they entered for sampling. Of course, the earlier the cloud was entered the more effect the motion within the plume had on the helicopter. In some of the first passes, the aircraft was often lifted up and tossed from side to side by the internal turbulance of the plume.

Propellant burns presented their own special problems. Most of the propellant manufactured today is of the smokeless and flashless powder type. Without a normal smoke plume being generated, as is the case with most detonations, the helicopter pilots often had a hard time locating the cloud. This was partially solved by igniting a smoke bomb nearby prior to igniting the propellant to indicate the wind direction to the pilots.

More than 360,000 lbs of explosives were detonated or burned during this series of tests in twenty-four different munition configurations and including 17 different explosive compounds.

Before any of the test results were in, certain threoretical expectations had already been calculated. Indications were that predicted concentrations of gaseous criteria pollutants would be well under OSHA Threshold Limit Values and the EPA Ambient Air Quality Standards within minutes after detonation, and in the case of carbon monoxide, less than 3% of Ambient Air Quality Standards levels. Results of the test indicated that indeed in all cases within minutes of the detonations the levels of pollutants were lower than the standards, by orders of magnitude in most cases.

In addition, the net soil contamination, determined by soil samples taken before, during, and after the tests, was shown to be statistically insignificant. The indications of these and many other results of this study are that open burning and open detonation is not only an efficient and safe method of disposal but also does not present a significant insult to the environment.

END

For more detailed information on the OB/OD Emissions Study please see:

1) Emission Factors From Deactivation of Munitions - Part II, Detection of Pollutants From Open Burning and Open Detonation of PEP & Munitions, CPIA Publication dated 16 December, 1987, minutes of the Joint Army-Navy-NASA-Air Force (JANNAF) Propulsion Meeting at San Diego, California

2) Consolidated Report on the Test Program for the Identification and Characterization of Products and Residues from the Open Burning/Open Detonation of Munitons, Headquarters, U.S. Army Armament, Munitons and Chemical Command, attn: AMSMC-DSM-D, Rock Island, Illinois 61299-6000, June 22, 1987

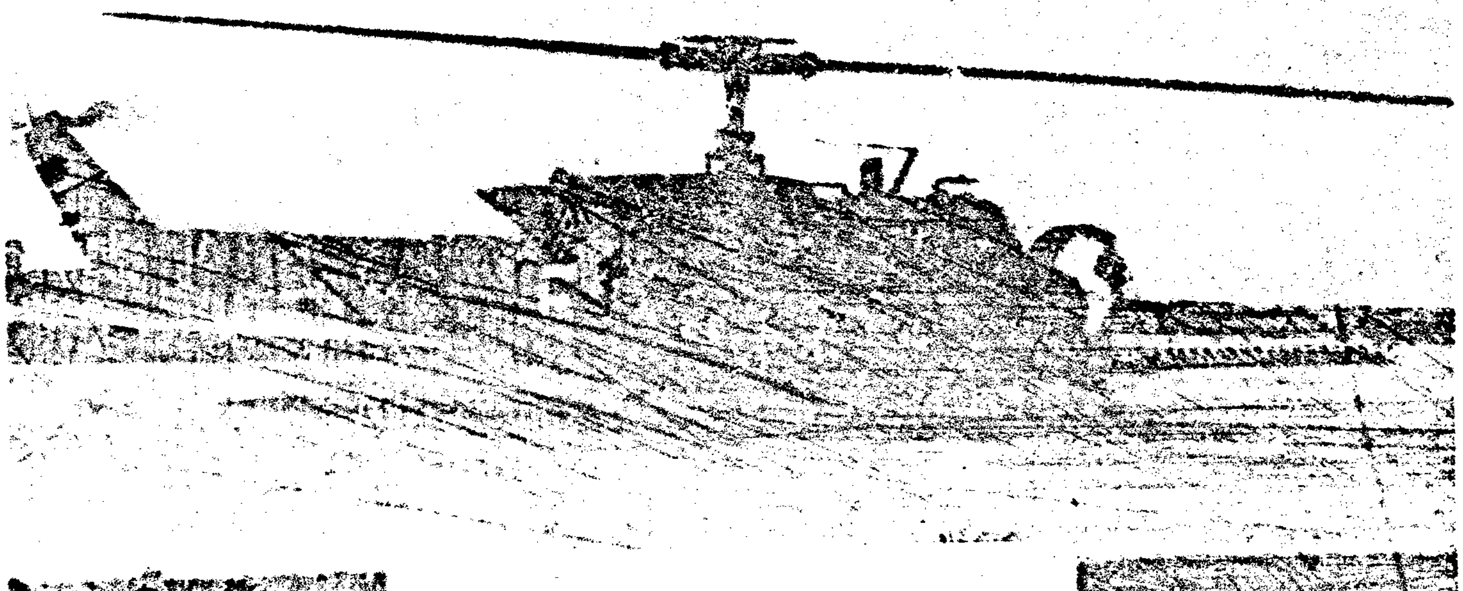

Instrumented UH-1 Helicopter
With Sample Probe

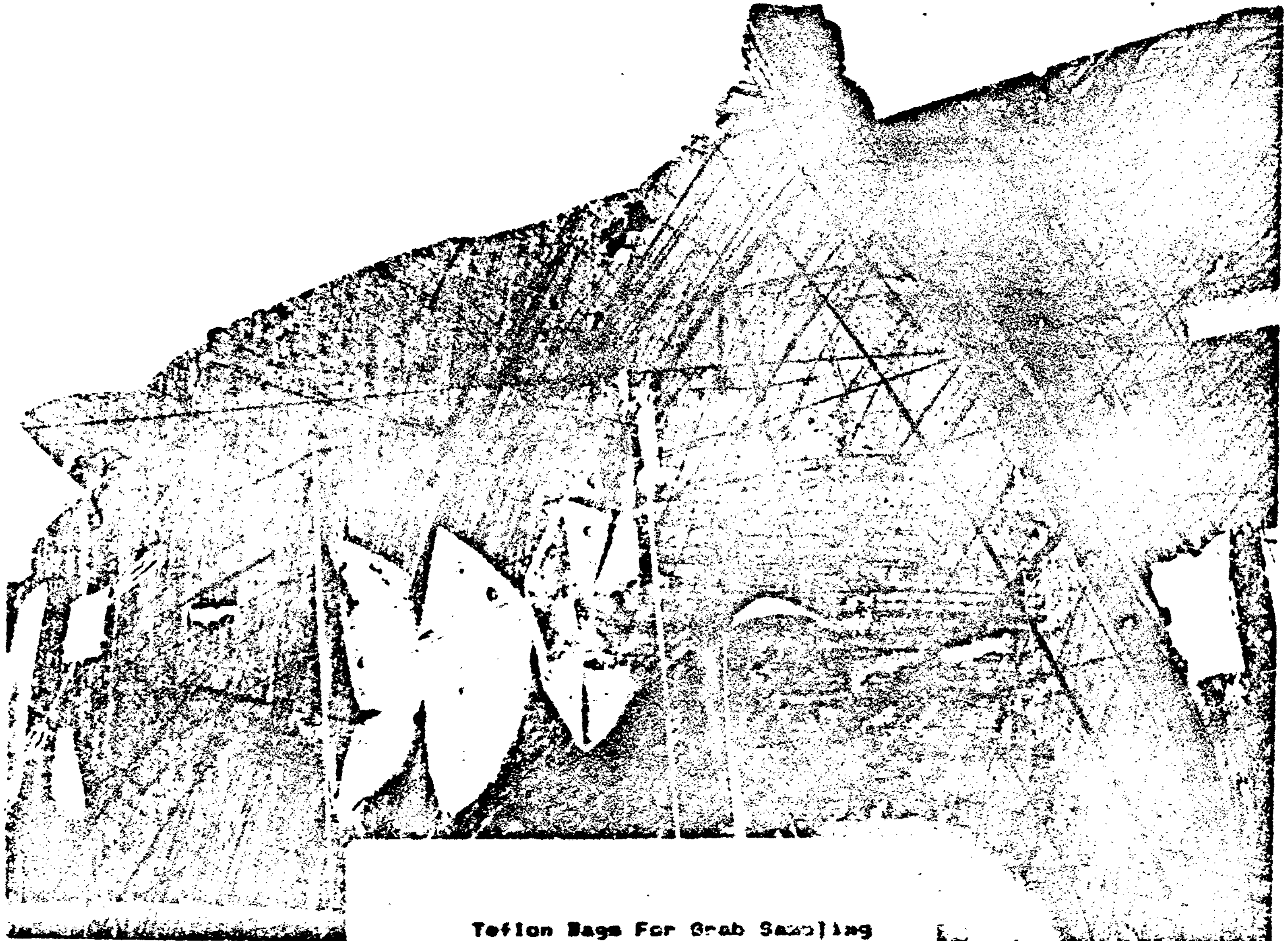

Teflon Bags For Grab Sampling
From Plume

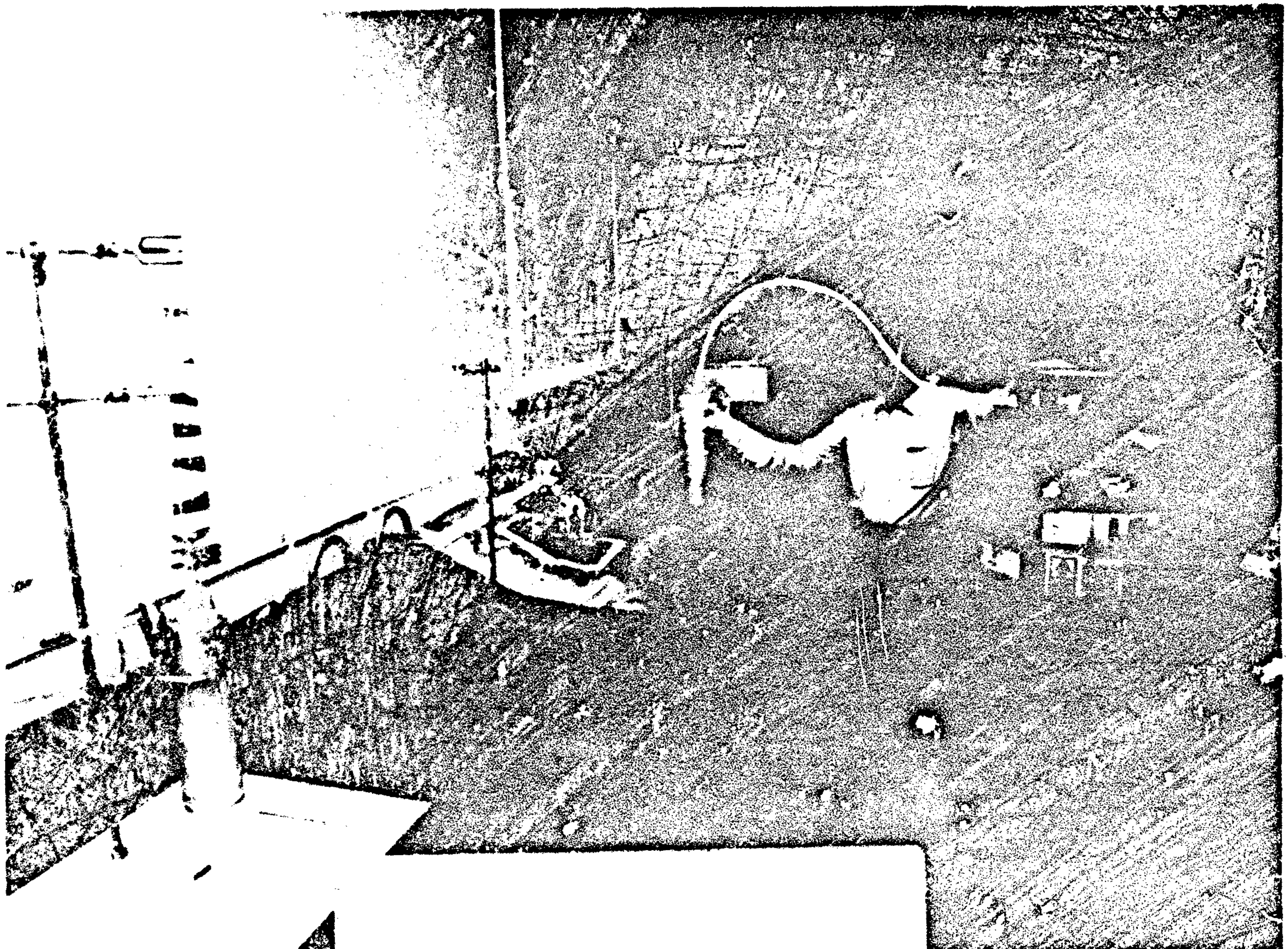

Extraction Of Grab Samples
From Teflon Bags

Typical Set-up For Buried
Detonation Of Projectiles

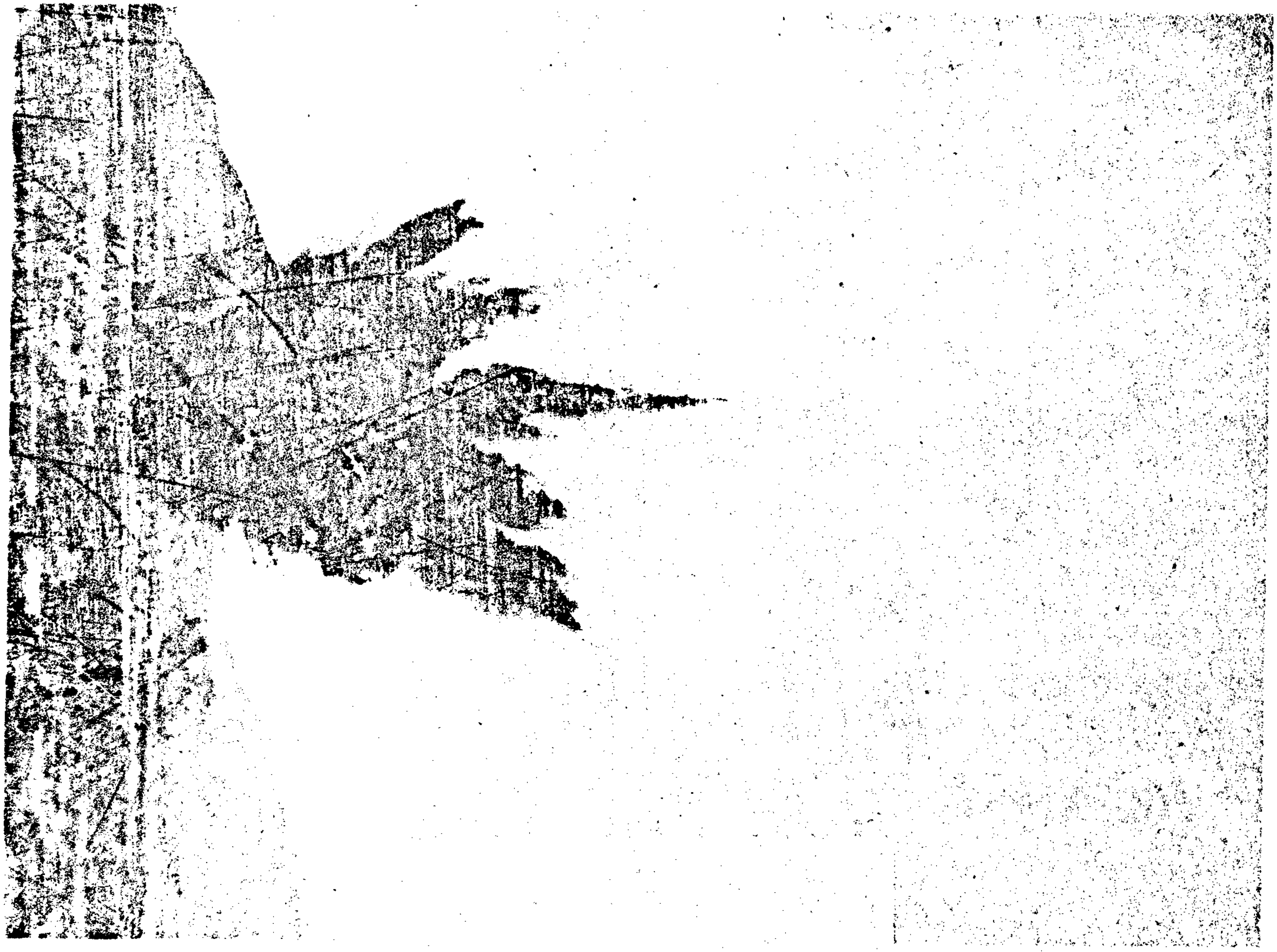

Detonation From Buried Explosives

Typical Set-up For Bulk TNT
Detonation - 5000 lbs.

Fireball Seen At Initial Stages Of Detonation

Example Of Detonation Plume
To Be Sampled

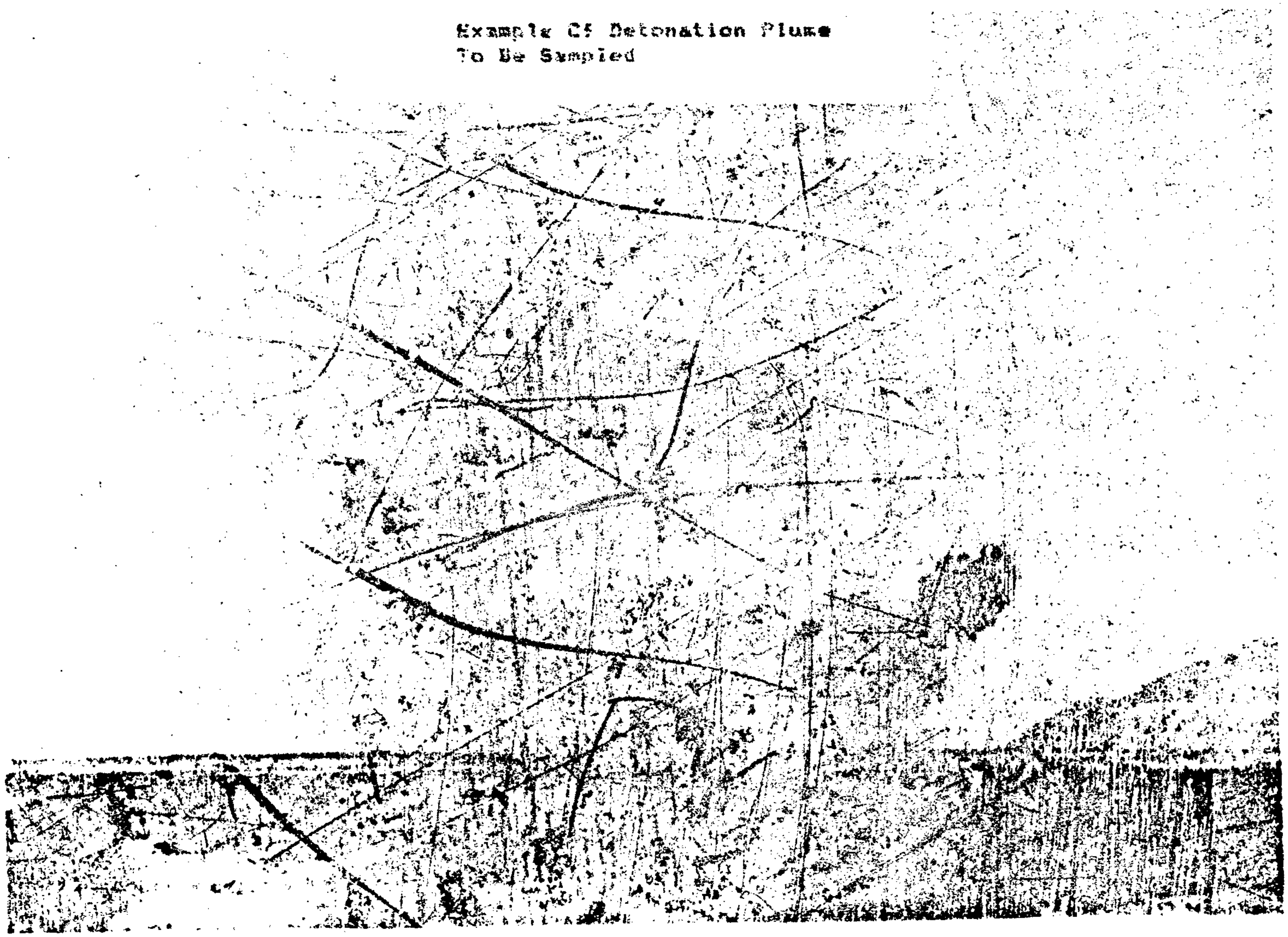

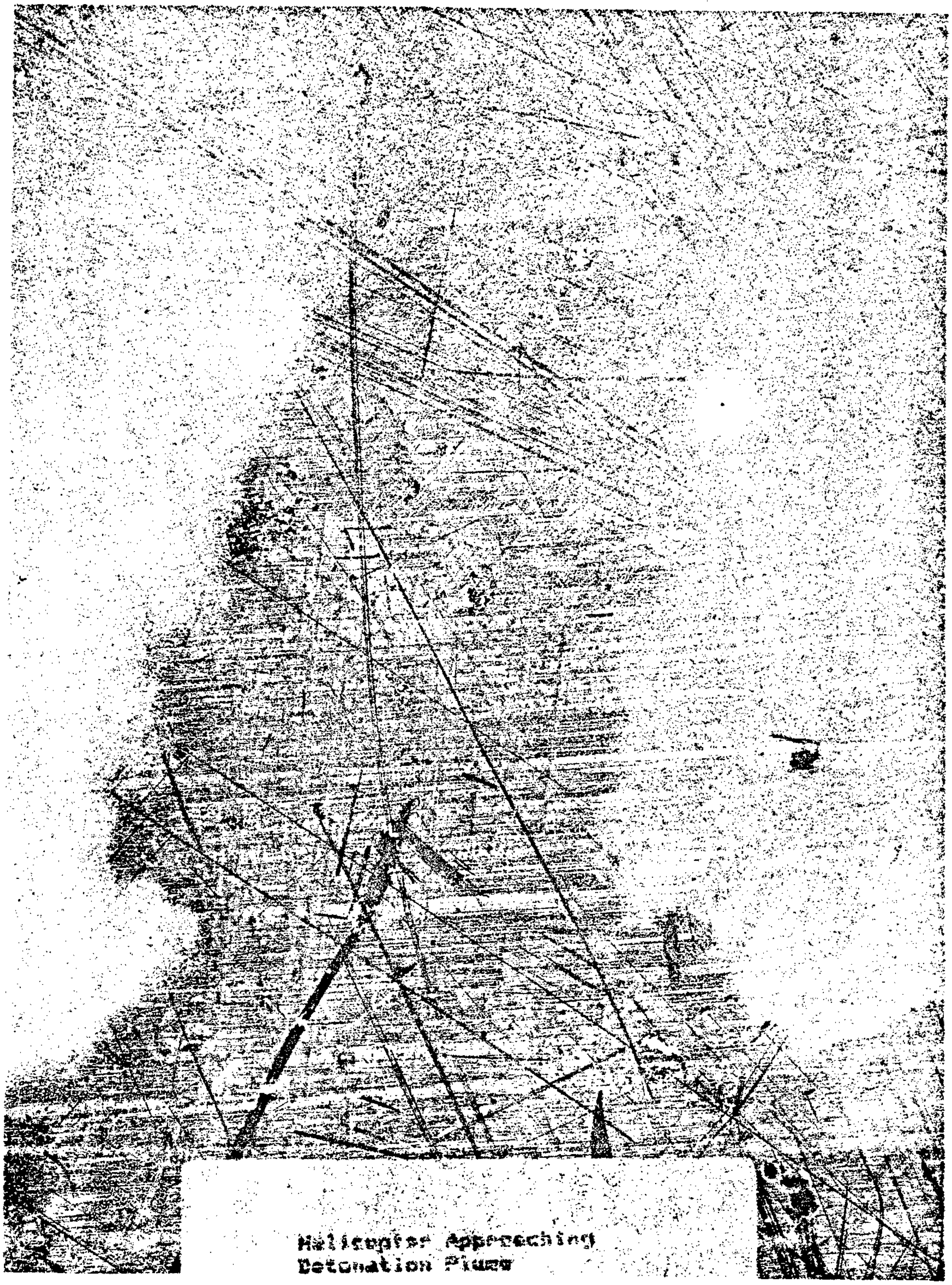

Helicopter Approaching
Detonation Plume

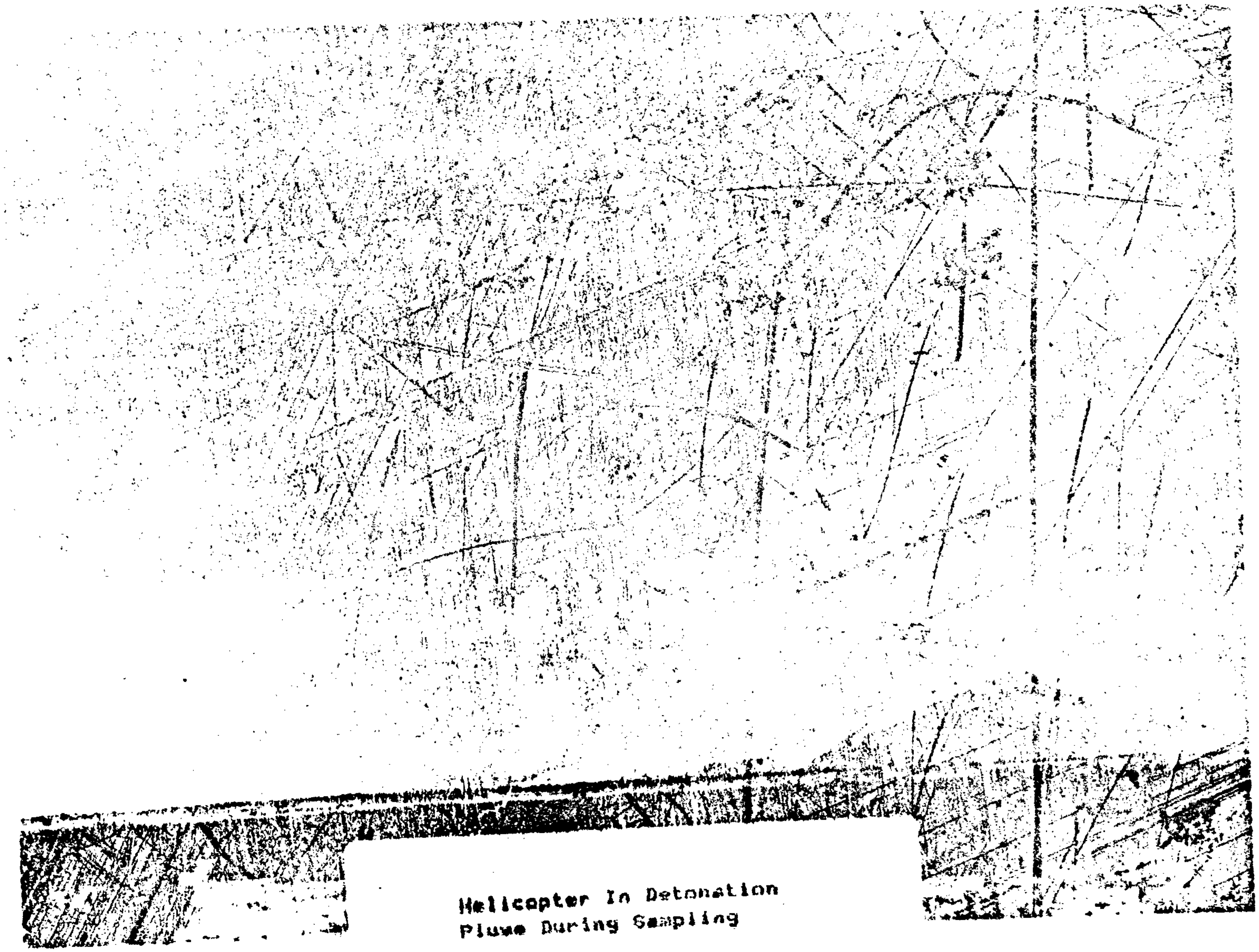

Helicopter In Detonation
Plume During Sampling

Helicopter Exiting Detonation Plume After Collecting Samples

COMPLYING WITH THE NEW EPA HAZARDOUS WASTE PERMITTING REQUIREMENTS FOR OPEN BURNING/OPEN DETONATION (OB/OD) FACILITIES

Beth A. Martin
David C. Guzewich
John W. Bauer
William J.B. Pringle
George Luz, Ph.D.

US Army Environmental Hygiene Agency
Aberdeen Proving Ground, MD 21010

Introduction

Open burning/open detonation (OB/OD) operations have been conducted at DOD installations for many years. It is considered the safest, most cost effective means of treatment of reactive wastes associated with the production, use, maintenance, and demilitarization of munitions and ordnance. Historically, environmental considerations have been secondary to the overriding safety concerns. As a result, OB/OD operations have caused contamination of soil and ground water at numerous locations.

Regulatory Background

Currently, OB/OD units are regulated under 40 CFR Part 265 Subpart P as thermal treatment units. These units must comply with the quantity-distance standards developed by the Defense Explosives Safety Board, in addition to the general facility standards for any permitted unit.

Final Rules for 40 CFR 264, Subpart X were promulgated on 10 December 1987 (reference a). The Subpart X regulations pertain to miscellaneous units. Miscellaneous units include all hazardous waste treatment, storage and disposal (TSD) facilities that were not otherwise specifically regulated under other subparts of 40 CFR 264. The Subpart X regulations apply to OB/OD units as thermal treatment units. OB/OD operations are not considered land disposal. Permit applications for OB/OD units must be submitted to the appropriate EPA Regional Office by 8 November 1988. Failure to submit a permit application by this deadline will result in the loss of interim status if EPA has not issued the final permit by 8 November 1992.

The 40 CFR 264 Subpart X regulations are based on environmental performance standards rather than engineering design and operation standards. Owner/operators are required to design and operate OB/OD units in a manner which protects human health and the environment. The potential contaminant migration pathways which must be addressed include: ground water, air, surface water, and soil.

The specific factors which must be considered when assessing the impact of a unit on ground-water quality are as follows: the volume and physical and chemical characteristics of the waste; the hydrogeologic setting; existing ground-water quality; ground-water flow rate and direction; current and potential ground-water usage; regional land uses; subsurface migration potential of the waste constituents; and, potential impacts on human health, animals, plants, and structures.

The specific factors which must be considered when assessing the impact of a unit on surface water and surface soils are as follows: the volume and physical and chemical characteristics of the waste; effectiveness of containment structures; area topography; rainfall patterns; characteristics of ground-water flow; proximity to surface waters; surface water usage; existing surface water, wetlands, and surface soil quality; water quality standards; and, potential impacts on human health, animals, plants, and structures.

The specific factors which must be considered when assessing the impact of a unit on air quality are as follows: the volume and physical and chemical characteristics of the waste; the effectiveness of systems and structures to prevent gaseous, aerosol, or particulate emissions; the operating characteristics that make air emissions likely; meteorological conditions; existing air quality; and, potential impacts on human health, animals, plants, and structures.

The permit application must include information on each of the factors discussed above to be considered a complete application. The assessments of the potential for adverse effects on each medium must be in sufficient detail to demonstrate minimal impact on those media. The adequacy and findings of the assessments will be evaluated as part of the permit review process.

The U.S. Army has approximately 70 installations that are currently operating OB/OD units under interim status. It is likely that most of these units will require a Part B permit under Subpart X regulations. There may also be many other facilities which will require permits.

The RCRA Part B Permit Writers' Guidance Manual for Department of Defense Open Burning/Open Detonation Units (Permit Writers' Guide)

The Permit Writers' Guidance Manual (reference b) was developed to provide guidance for EPA and state regulatory personnel in preparing RCRA Part B permits for OB/OD units at Department of Defense (DOD) installations. Likewise, the Manual was intended for use by DOD personnel in preparing applications for these permits. The Manual was developed to fulfill a DOD commitment to the EPA to provide a suggested OB/OD Permit Writers' Guide based on DOD's extensive experience with OB/CD operations. It is intended that the use of this manual will ensure a consistent and technically adequate approach in both the preparation and evaluation of permit applications. In addition, it will improve consistency among the various EPA Regions and states in setting final permit requirements. The manual applies to both new OB/OD units and existing units operating under interim status standards. Although this Manual was prepared by the U.S. Army, and is directly applicable for DOD installations, the information and guidance presented will also have application for permitting OB/OD thermal treatment units at non-DOD activities.

Initially, many of the permit writers will have very limited experience with OB/OD units and their operation. Therefore, numerous examples and explanatory sections were included in the Permit Writers' Guide to provide the necessary background needed to assess the applicability of the regulatory requirements to OB/OD units. Note, that EPA commentors felt that more examples and explanations were needed. In addition to addressing the General Facility requirements under 40 CFR 264 and 270, the Manual provides specific permitting guidance for the three general types of OB/OD operations: OB in containment devices (pans), OB on the ground surface, and OD. Appendix A of the Manual is a compilation of reports prepared by the Army that provide the technical basis for the guidance presented. A summary of the results of those studies is provided in the next section.

As discussed in the above section, the Subpart X regulations require the evaluation of several factors relative to each medium. In addition to the evaluation of the three environmental pathways discussed above, the Manual suggests that environmental noise impacts also be evaluated for OD operations. Specific guidance on making these evaluations is provided in the Permit Writers' Guide.

Under the guidance in the Manual, ground-water monitoring would not be required where the design and operation of a unit preclude all contact of waste with the ground surface. Based on the findings of an Army study (reference c), when non-liquid wastes are burned in an area where evaporation exceeds precipitation by more than 2 feet per year, no ground-water monitoring is needed. In areas not meeting this criterion, if the unit is equipped with a leak containment and detection system, no ground-water monitoring is needed. In addition, for any type of unit, if the permit applicant can demonstrate no potential for ground-water contamination, ground-water monitoring may not be required. For OD units where proper operational procedures are followed (particularly management of residues), no ground-water monitoring is needed.

The air quality pathway evaluation requires the permit applicant/writer to evaluate both criteria (those for which National Ambient Air Quality Standards exist) and noncriteria air pollutants. In particular, state and local air toxics requirements must be addressed in the permit. The air quality impact evaluation utilizes a two tiered screening approach. First, a screening technique is required to provide a rapid and inexpensive approach to determine if the unit has the potential to cause adverse health impacts due to air emissions. This involves the use of computer models to estimate air emissions and the resultant ambient downwind concentrations of pollutants of concern with particular attention to sensitive receptors. If this initial screening technique indicates any potential for health impact, or exceedance of any applicable ambient air quality guideline or standard, then a formal health risk assessment must be performed. Since the vast majority of the OB/OD operations occur in remote areas, it is anticipated that the formal risk assessment would not often be required.

Potential adverse effects to surface water quality include consideration of 11 factors. Most of these factors

are the same as those considered for the ground-water and air quality pathways. This aspect requires that the permit applicant consider the existing surface water quality in the vicinity of the OB/OD unit and surface water drainage patterns. The Permit Writers' Guide suggests that, with proper containment of surface water run-on and run-off from OB/OD units, the impact on surface water will not be significant.

The fourth pathway that must be considered is the environmental noise impact. The Permit Writers' Guide suggests that the environmental noise impact be addressed only for OD operations since the environmental noise associated with OB is insignificant. Applicable state noise regulations governing OD or blasting operations should be considered first. In the absence of state or local noise limits, the environmental noise impacts would be quantified using the American National Standard (ANSI) S12-4-1986 for high energy impulse sounds with respect to residential communities. The number of detonations per day, the weight of the explosives and the depth of burial would have to be adjusted so that the predicted noise levels would not exceed "acceptable" levels.

Results of Environmental Studies

The U.S. Army conducted a Ground-water Monitoring Study during the period February 1984 to March 1985 (reference c). The purpose of the study was to evaluate the impact of selected OB and OD facilities on ground-water quality under varying site-specific conditions. Ground-water quality data were collected from 109 monitoring wells around 19 OB/OD units. Nine of the nineteen sites showed some type of ground-water pollution attributable to unit operations. Metals and volatile organics were considered a problem at only two facilities each; however, explosive constituents exceeded criteria at eight locations. In the arid regions of the western U.S., the high ratio of evaporation to precipitation precludes migration of contaminants to the ground water. In the humid east, the predominant condition preventing significant contamination is low soil permeability. Concentrations of explosives in surficial soils was also related to concentrations of explosives found in the ground water.

The U.S. Army conducted a soil contamination study at numerous OB/OD units during the period March 1981 to March 1985 (reference d). Results of the study indicate that OB units

contaminate surficial soils when burning is conducted on the ground. The compounds most commonly detected were lead, barium, and explosives compounds. Run-off is a problem where soil contamination is present. The major recommendations were to control surface water run-on and run-off, to not locate OB units in 100 year floodplains, and to conduct OB in pans.

EPA Comments on the Permit Writers' Guidance Manual

EPA recently completed their review of the Permit Writers' Guide. In general, EPA feels that the Manual needs examples of best management practices and more design information and sketches. They suggest that the Manual provide references for where to find additional information on facility designs and operation. Even though the Subpart X regulations are based on environmental performance standards, EPA intends to apply design standards for other similar TSD facilties wherever possible. For example, OB units equipped with pans may have to meet the double containment requirements for tanks, and units where OB is conducted or the ground may have to meet landfill design specifications. Some of the major specific comments are as follows. EPA suggests that the Manual specify types of wastes that can and cannot be accepted at an OB unit. The manual should distinguish between the types of wastes that can only be treated by OB/OD versus those that can be treated using other technologies. The manual should provide examples of past and present practices; EPA is looking for evidence of technological advances. The waste analysis and closure/post-closure sections need more details. EPA will evaluate requests for exemptions from ground-water monitoring on a case-by-case basis. Fingerprinting of routine wastes and full analysis of off-spec or unknown wastes should conducted in all instances.

Future Actions

One Army Command has contracted for the development of permit applications by 8 November 1988. A great deal of time and money will be spent on this effort. Unfortunately, EPA will almost certainly take 2-4 years to review the applications. This delay in the review process will be due to higher priority permit reviews (i.e., incinerators and land disposal units). We expect that many of the applications will require significant revisions subsequent to EPA review. This will involve another significant expenditure of time and money. In order to ensure that revised

permit applications are adequate, a permit assistance team will be formed to develop a model permit from one of the first applications evaluated. Then, using the model permit as an example, the Army can proceed with permit application revisions while waiting for EPA to complete all of the permit reviews. This should accelerate the permitting process.

Initially, EPA plans to use the Permit Writer's Guidance Manual, supplemented by the EPA comments, in conjunction with the Section 8 - "Health and Environmental Assessment" of the EPA RFI Guidance Document as tools in evaluating permit applications. There is contradictory guidance in the two documents. EPA has not established their position on these controversial issues. Hopefully, many of the controversies will be resolved in the development of the model permit.

Summary

The U.S. Army considers OB/OD to be the safest, most cost effective means of treatment of reactive wastes. In order to continue OB/OD operations, recently promulgated regulations require that owner/operators apply for a RCRA permit by 8 November 1988. The applications must address the impact of the unit on soil, ground water, surface water, and air. The Army developed a Permit Writers' Guidance Manual to assist applicants and permit writers in the permitting process. EPA plans to use this Manual, supplemented by their comments, in conjunction with the EPA RFI Guidance Manual in the permit application review process. Therefore, the Army will also use these documents in developing permit applications. The Army fully intends to submit complete permit applications by 8 November 1988. However, it is anticipated that many of the applications will require significant revision after EPA review.

References

a. Title 40, Code of Federal Regulations (CFR), Parts 144, 260, 264, and 270, Hazardous Waste Miscellaneous Units; Standard; Applicable to Owners and Operators; Final Rule; 10 December 1987.

b. Memorandum, USAEHA, HSHB-ME-SH, 29 May 1987, subject: Hazardous Waste Consultation No. 37-26-1330-87, Resource Conservation and Recovery Act Part B Permit Writers' Guidance Manual for Department of Defense Open Burning/Open Detonation Units, July 1986 - May 1987.

c. Letter, USAEHA, HSHB-ES-G, 28 October 1985, subject: Ground-water Monitoring Study No. 38-26-0457-86, AMC Open Burning/Open Detonation Facilities, February 1984 - March 1985.

d. Letter, USAEHA, HSHB-ES-H, 4 February 1986, subject: Phase 5, Hazardous Waste Study No. 37-26-0593-86, Summary of AMC Open Burning/Open Detonation Grounds Evaluations, March 1981 - March 1985.

UPGRADE OF ARMY APE 1236 DEACTIVATION FURNACES AND
EXPLOSIVE WASTE INCINERATORS TO MEET RCRA

JERRY R. MILLER, P.E.
AMMUNITION EQUIPMENT DIRECTORATE
TOOELE ARMY DEPOT

The Army's attempt to get the Ammunition Peculiar Equipment (APE) 1236 and 2210 Deactivation Furnaces classified by EPA as thermal treatment units instead of hazardous waste incinerators failed. Therefore these furnaces along with the Explosive Waste Incinerators (EWIs), which are essentially deactivation furnaces, are now classified as hazardous waste incinerators and are subject to operating requirements and performance standards promulgated under the Resource Conservation and Recovery Act (RCRA). Under the current configuration the APE furnaces and EWIs do not meet RCRA Standards. These furnaces are presently operating under an interim permit (Part A) until 8 November 1989. If, at that time RCRA Standards are not met, the furnaces will either be closed or only allowed to process Class C munitions. Current EPA guidance does not include all DOT classified Class C munitions as exempt from RCRA, only small arms up through 50 cal. ball ammunition. This is of major concern to the Army.

Special funding has been provided by the Program Executive Office for Ammunition to upgrade eleven APE 1236 furnaces. Funding for the upgrading of the Explosive Waste Incinerators is being provided through other sources. The estimated cost to upgrade each furnace is $800,000 and is broken down into the following general categories:

1.	Gas Monitoring Equipment	$ 50,000
2.	Programmable Control System	70,000
3.	Furnace Burner Control System	15,000
4.	Automated Monitoring of Waste Feed	25,000
5.	Afterburner and Gas Coolers	300,000
6.	Draft Fan and Motor	5,000
7.	In-place Equipment including:	
	Fugitive Emission Furnace Enclosure	305,000
	Start-up and Run-in Costs	30,000
	TOTAL	$ 800,000

Areas for consideration under RCRA or to improve furnace operations which have been discussed during numerous meetings with AMC, AMCCOM and EPA are as follows:

1. Fugitive emission control
2. Automatic waste feed cutoff system
3. Emergency dump stack
4. Monitoring systems - CO, feed rate, combustion gas velocity, temperature
5. Data acquisition and reporting
6. Closed loop control on furnaces
7. Afterburners

As a result of discussions with EPA, the emergency stack dump will be eliminated. An afterburner is necessary to achieve a destruction and removal efficiency (DRE) of 99.99% for principal organic hazardous constituents (POHCs). A high temperature gas cooler and a secondary or low temperature gas cooler will be needed to lower the exhaust gas temperature and protect the baghouse. A larger draft fan will be added to compensate for the losses caused by adding the afterburner and gas coolers. The stack exhaust gases will be monitored for CO levels as an

indicator of destruction efficiency. Stack gas velocity and the operating temperature of the afterburner will be monitored. All of this monitoring is required under RCRA. The monitoring systems, data acquisition, reporting and closed loop control for the furnaces are being developed.

Per guidance received from EPA, a two-piece input conveyor will be incorporated into the redesign. The first section will be stopped in the event of a shutdown of the system while the second section which empties into the furnace input housing hopper will continue to operate for safety reasons.

Two areas where concurrence from EPA has not been totally received are fugitive emissions and automatic waste feed rate monitoring. Correspondence between EPA and AED have been ongoing to try and resolve these issues. Currently, AED is pursuing the design concepts of shrouding the furnace and increasing the furnace draft slightly for fugitive emission control and providing a weighing system with automatic shutoff to meet the automatic waste feed rate monitoring requirement of EPA.

The functional process control diagram depicts how the system functionally fits together.

From an operator's standpoint the general sequence of operation is as follows:

1. Load munition ID into computer as requested.

2. Verify correct item.

3. Operating parameters are sent to equipment via controller.

4. Set munitions in receiving container.

5. Close door and activate system operation.

6. Munition or munitions are weighed.

a. If weight doesn't exceed weight limit as set in the computer, the system cycles and loads the munition(s) onto the conveyor. The cycle is timed to the flights on the conveyor to get the correct spacing and loading.

b. If the weight exceeds the upper limit, the system won't cycle until the operator removes the excess weight and manually toggles the weighing system. This will continue until the correct weight is obtained and the system cycles, allowing the operator to load the container again.

7. If the monitored emission level of CO begins to approach the 100 ppm rolling average, the weighing system will proportionally begin to delay feeding of the munitions onto the conveyor. Under all operating conditions the feed conveyor will operate at the same speed.

8. If the system has an upset condition, the conveyor stops and the monitoring system won't cycle, preventing loading of any additional items onto the conveyor.

9. The conveyor will be shrouded to prevent loading items both before and after the monitor.

10. The above operating sequence may have a tendency to slow down the feed rate to the furnace. Consequently, consideration is being given to a possible method of bulk loading into a holding area from which the furnace control system directs the speed of the weighing system independent of the operator, but in proportion to the set operating parameters.

Specifications have been prepared to procure and install the needed equipment to accomplish the furnace upgrading. The specification packages are divided into the following areas so that we can take advantage of requirement type contracts along with service contracts:

1. Afterburners
2. High and Low Temperature Gas Coolers
3. Furnace Control and Gas Monitoring
4. Miscellaneous — Fuel tanks, conveyors, draft fan and motor, etc.
5. Installation — Install all GFE and interconnect

Tooele Army Depot is scheduled for the pilot model system where it will be tested and evaluated during an operational check and a trial burn. Ideally all of the "bugs" would be worked out of the pilot system before the other furnaces would be upgraded. However, due to dictated scheduling constraints this will not be the case. The following Gantt Chart reflects the most optimum schedule possible. With no major delays this schedule could be met. Some slippages have already occurred in the area of contract awarding. However, we are still optimistic that there will be no delays in the installation of the equipment on the pilot model at TEAD and the schedule of upgrading at each of the other sites.

Usage data records and demil stockpile information was provided to AMCPEO-AMMO for use in determining the locations and sequence of furnace upgrading if limited funding was obtained. The following chart reflects the furnaces presently slated for upgrade including the EWIs:

1. Tooele AD (Pilot)
2. Hawthorne AAP
3. Sierra AD
4. Pueblo ADA
5. Anniston AD
6. Red River AD
7. Seneca AD
8. Umatilla ADA
9. Crane AAA
10. McAlester AAP
11. Lexington - Blue Grass AD
12. Iowa AAP
13. Lake City AAP
14. Kansas AAP

As directed by AMCCOM, all of the designated sites will be done concurrently as was shown on the Gantt chart.

PROPOSED APE 1236 FURNACE LAYOUT

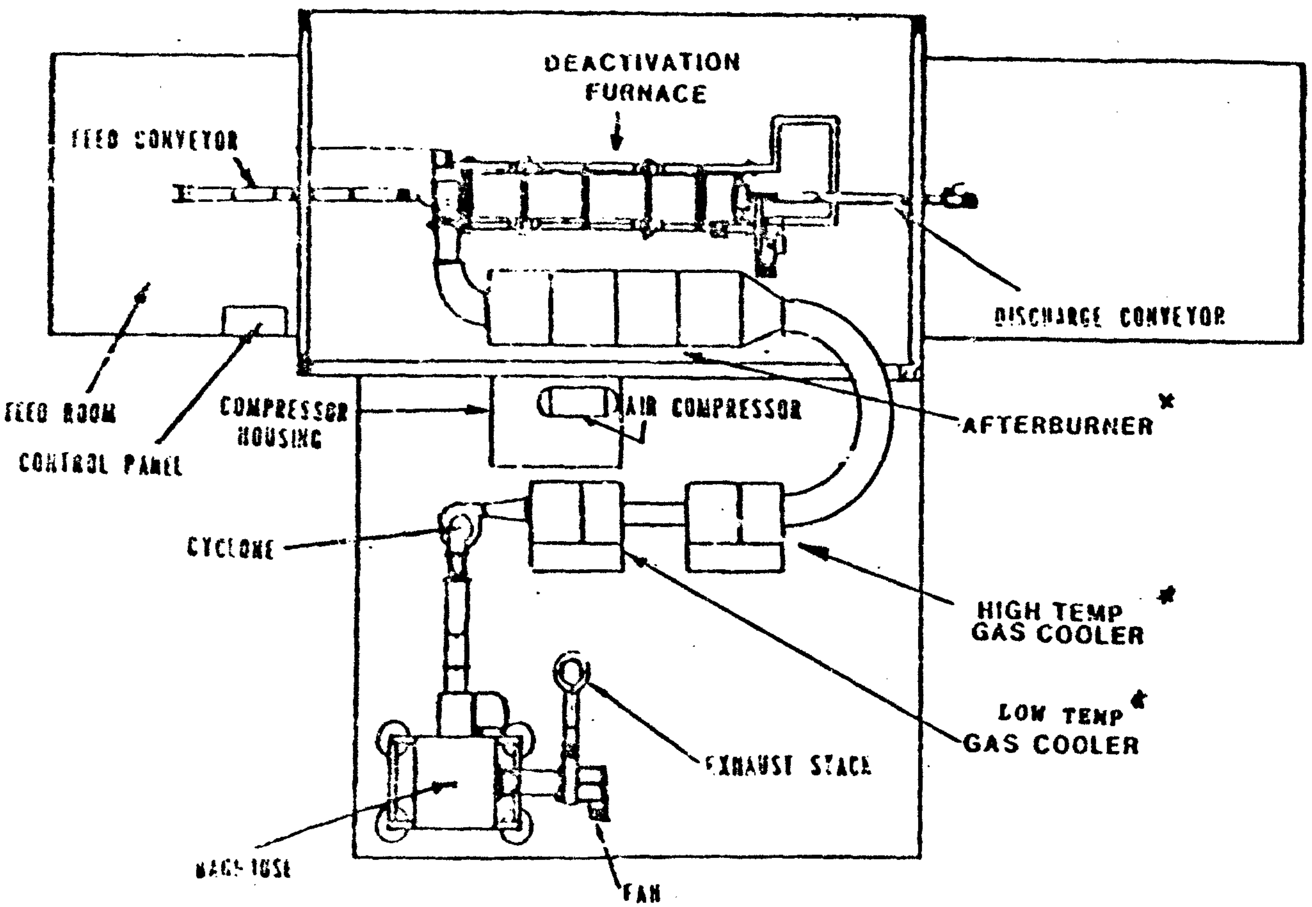

*PROPOSED EQUIPMENT ADDITIONS TO MEET RCRA REQUIREMENTS

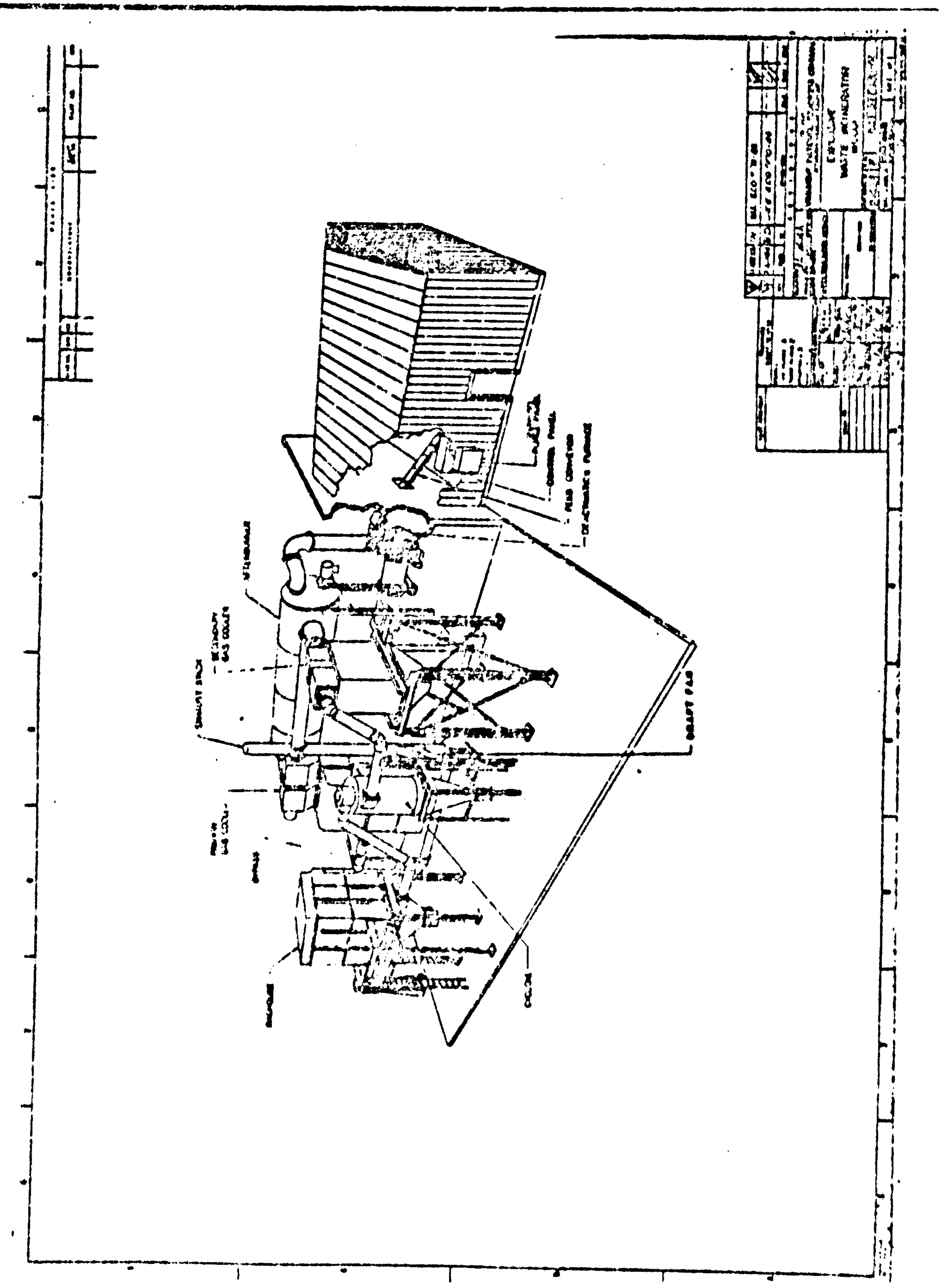

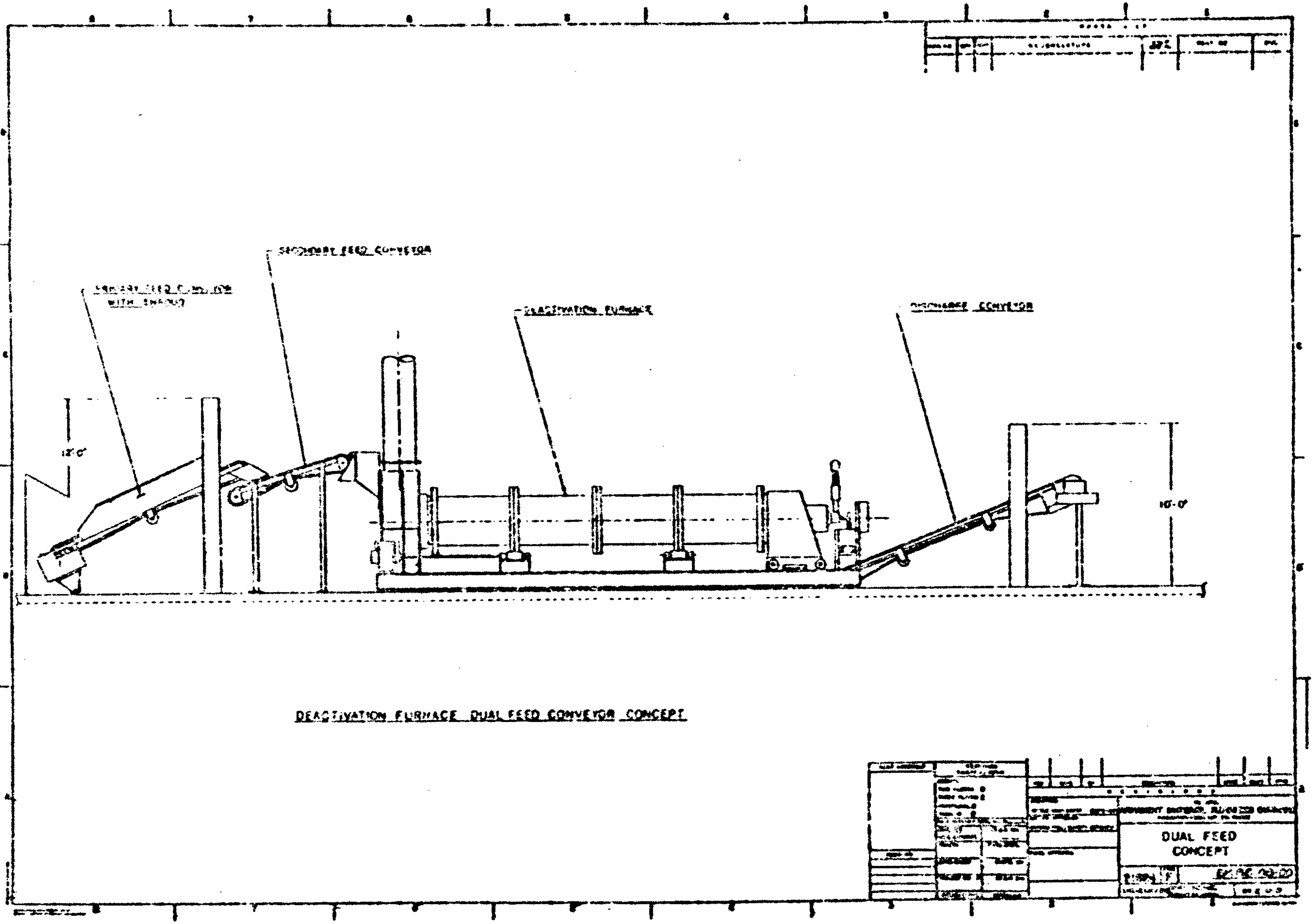
PRIMARY FEED CONVEYOR
WITH SHROUD
SECONDARY FEED CONVEYOR
DEACTIVATION FURNACE
DISCHARGE CONVEYOR
12'-0"
10'-0"
DEACTIVATION FURNACE DUAL FEED CONVEYOR CONCEPT
DUAL FEED
CONCEPT

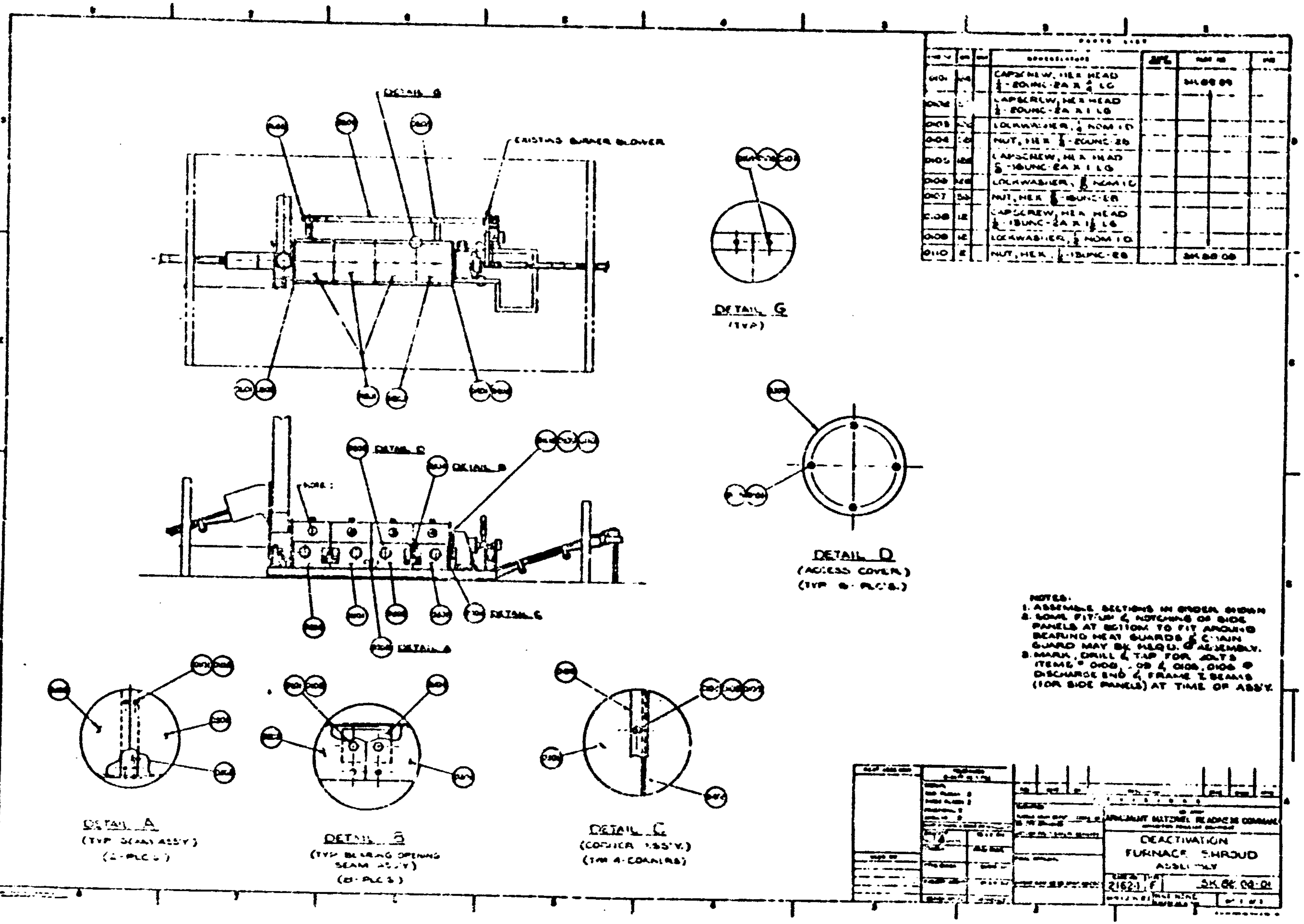

DETAIL G
EXISTING BURNER BLOWER
DETAIL D
DETAIL B
DETAIL C
DETAIL A
NOTE 2
DETAIL G
(TYP)
DETAIL D
(ACCESS COVER)
(TYP 6 PLC'S.)
DETAIL A
(TYP SEAM ASS'Y)
DETAIL B
(TYP BEARING OPENING SEAM ASS'Y)
DETAIL C
(COPIER ASS'Y.)
(TYP 4 CORNERS)
NOTES:
1. ASSEMBLE SECTIONS IN ORDER SHOWN
2. SOME FIT-UP & NOTCHING OF SIDE PANELS AT BOTTOM TO FIT AROUND BEARING HEAT GUARDS & CHAIN GUARD MAY BE REQU. @ ASSEMBLY.
3. MARK, DRILL & TAP FOR BOLTS ITEMS 0106, 08 & 0108, 0109 @ DISCHARGE END & FRAME I BEAMS (FOR SIDE PANELS) AT TIME OF ASS'Y.
PARTS LIST
CAPSCREW, HEX HEAD
CAPSCREW, HEX HEAD
LOCKWASHER
NUT, HEX
CAPSCREW, HEX HEAD
LOCKWASHER
NUT, HEX
CAPSCREW, HEX HEAD
LOCKWASHER
NUT, HEX
DEACTIVATION
FURNACE SHROUD
ASSEMBLY

DODESB IGLOO CONFINEMENT TEST PROGRAM

William R. Herrera and Luis M. Vargas
Southwest Research Institute

INTRODUCTION

This program is the third phase of a study to determine the effects of confinement on the burning rates of propellants and other combustible ammunition. The first phase of this program dealt with the hazards involved with combustion of class 1.3/1.4 materials in the open and with preliminary tests in a confinement. The second phase of this program concerned itself primarily with the effects of confinement on the hazards generated from combustion of these class 1.3/1.4 finished munitions and bulk propellants. Tests were conducted in an instrumented moderate confinement (an 8 foot cubicle fabricated out of Marinite which is a heat resistant material) and also in an instrumented substantial confinement (a 1/10th scale model igloo fabricated out of thin steel). One of the more vital observations resulting from the igloo tests was that at certain propellant loading densities, unburned propellant was being carried outside in the plume and burning outside of the igloo.

This program, Phase 3, is the continuation of the previous efforts and its primary goal is to determine whether typical storage construction configurations are such that if an ignition occurs, the burning material will be substantially confined and whether this confinement will allow the burning rate to escalate to catastrophic failure. If this failure does occur, then storage quantities and subsequent Quantity-Distance requirements may have to be revised. The following is a brief summary of the objectives and results of this ongoing program.

PROGRAM OBJECTIVES AND RESULTS

The Phase 3 program was divided into the following major tasks:

Task I   Review of Phases 1 and 2 of the Program

Task II   Survey of GOCO and GOGO Facilities In Order To Establish a Typical Storage Facility

Task III   Review of the Technical Literature

Task IV   Obtain Thermal Resistance Data for Materials of Construction and Conduct Preliminary Test Program Consisting of Confinement Tests

Task V   Review Quantity-Distance Tables for Class 1.3/1.4 Materials

Task VI   Develop A Full Scale Test Plan

Currently, SwRI has concluded the first four tasks of the program. The major goals achieved as part of this work include the following: the development of a comprehensive listing of typical class 1.3/1.4 munition storage facility construction types and the identification of typical construction materials

(Table 1); the identification of typical vent area ratios (Table 2); the identification of storage configurations with regards to material quantities and loading densities; the development of a table of thermal resistances for the various materials of construction (Table 3); and the conduct of the confinement tests which are described in more detail in the following paragraphs.

CONFINEMENT TESTS

Test Protocol

The confinement tests were performed using an instrumented 1/10th scale model igloo as shown in Figure 1. Temperatures were measured with eight Type K Thermocouples located on the igloo as shown in Figure 2. The thermocouples were of the exposed junction type to increase response time and were situated such that the exposed junction was flush with the inside skin. Three Kiel Probes were located outside of the igloo door and were used to measure plume velocity. Thermocouples were also located adjacent to the Kiel probes for the measurement of the plume temperature. The Kiel probes and thermocouples were mounted on stands as shown in Figure 1 and were placed at various distances from the igloo door in order to profile the plume. A radiometer was placed in the path of the fireball 3 feet from the door opening and it was used to measure the heat flux in the plume. Video cameras were strategically positioned to record the plume sizes and the generation of firebrands.

The actual tests were conducted using two propellants, i.e., IMR 8208 and M1 propellants and the ALA 17 incendiary flares. The quantities of the propellants and the number of flares were varied as was the igloo door opening. A test matrix was developed and is presented here as Table 4. As can be seen in Table 4, propellant quantities of 1, 5, and 10 pounds were tested for each of three scaled vent areas (a series of tests were conducted using 2-, 4-, and 6-pound quantities of the IMR 8208 propellant in combination with a vent area of 144 sq in.). The three scaled vent areas tested were selected to correspond with door and vent areas found in actual plant storage facilities. The three vent sizes were: a large vent size of 12 inches by 12 inches which corresponded to a storage facility with double doors and numerous windows (vent area ratio of 0.1234); a medium vent size of 9 inches by 9 inches which corresponded to an earth-covered igloo with a double door (vent area ratio of 0.07); and a smaller vent size of 6 inches by 6 inches which corresponded to an earth-covered igloo with a single door (vent area ratio of 0.03).

The propellant tests were performed using scaled model cardboard canisters to simulate the actual storage drums used to ship propellants. Two sizes of canisters were used in the tests, a cardboard canister 3.5 inches in diameter which corresponded to a 1/50th scale model of the drum used to store the IMR 8208, and a 4-inch diameter canister which was a 1/65th scale model of the drum used to store the M1 propellant. Molecular sieves (synthetic alkali metal alumino-silicate) having the same size and density of the M1 propellant were used as an inert simulant and several gram quantities were placed in the M1 canisters prior to the tests. Posttest inspections were conducted to determine the length of travel of the inert materials. In all of the propellant tests, the canisters were ignited using an electric match placed just below the top surface of the propellant and multiple canisters were ignited simultaneously. The propellant canisters and the flares were centered inside the igloo under thermocouple

location 3. The ALA 17 flare tests were conducted with the flare bodies out of the metal canister.

Test Program

Propellant Tests

Seven preliminary tests were used to verify instrumentation. Twenty five actual tests were performed with the IMR 8208 and the M1 propellant in the 1/10th scale igloo. Eleven of these tests were performed using a 12-inch square vent (a vent area ratio of 0.1234), seven tests were performed using a 9-inch square vent (a vent area ratio of 0.0597), and seven tests were performed using a 6-inch square vent (a vent area ratio of 0.031). Table 5 presents a summary of these 25 tests and presents data on the plume lengths. As can be seen in Table 5, there are two plume lengths, the maximum length that the fire reached and the length of the plume which exhibited the highest intensity. On all of the propellant tests performed, a region of very high, intense heat was found and its length was always less than the maximum that the flame would reach out to. Thermocouple and radiometer data were recorded for each of the tests.

ALA 17 Flare Tests

A total of seven tests were performed using the ALA 17 flares. Summaries of these tests including plume lengths are also presented in Table 5. Thermocouple and radiometer data were recorded for each of the tests.

Data Analysis

Preliminary analyses of the thermal data, Keil probe data and radiometer data recorded for each of the tests has been conducted. The following paragraphs present details on the analyses performed to date.

Plume Data

A table of plume lengths was developed and is presented in this paper as Table 5. As can be seen in Table 5, there are two plume lengths, the maximum length that the fire extended, and the length of the plume which exhibited the highest intensity. On all of the propellant tests performed, a region of very high, intense heat was found and its length was always less than the maximum length that the flame would extend to. As shown in Table 5, there are several tests where the plume length exceeded 25 feet in the 1/10 scale model tests. The actual plume velocities were calculated for each test using the Keil probe data, which gave a pressure in inches of water and using the plume temperature data recorded by the thermocouples mounted adjacent to the Keil probes in combination with the following equation:

$$V = (P/\text{Gas Density})^{0.5}$$

Where V is the plume velocity, p is the over pressure, and the density of air was used as the density of the plume gas. This density term was corrected for the temperature using the thermocouple data recorded at the Keil probe. A table of velocities for each test is presented here as Table 6. Figure 5 presents the plume velocity data as a function of distance from the igloo door for the 5 pound M1 propellant tests conducted varying the igloo door size (vent area). Figures

4 and 5 present similar data for the 10 pound tests for the M1 and the IMR 8208 propellants respectively. As can be seen in Figure 3, for the 5 pound tests, the velocities increase as the igloo door size or vent area is reduced. Figure 4 presents similar data for the 10 pound M1 propellant test and as can be seen in Figure 4, as the igloo door size is reduced from 12 inches to 9 inches, the plume velocity increased as was expected. However, when the door size was reduced from 9 inches to 6 inches, the plume velocity decreased. Figure 5 presents the data for the 10 pound IMR 8208 tests and similarily to the M1 tests, as the igloo door size was reduced from 9 inches to 6 inches, the plume velocity decreased instaed of increasing. This drop in velocity is indicative of the plume flow becoming choked at the door as was evidenced by the video coverage of the 10 pound IMR 8208 test performed with the 6 inch door. A review of the video recording showed that the hottest portion of the plume separated from the igloo and was pulsing back and forth outside of the igloo doorway indicative of choked or near-choked flow. In reference to the igloo internal pressures, the maximum pressures measured for each test are included in Table 6. Unfortunately, for the majority of the larger tests, the limits for the pressure gauges (0.36 psi) were exceeded during the test and the actual peak pressures were unavailable.

Temperature Profiles

A considerable amount of temperature data was obtained for each test. As previously described in this report, a total of eight type K thermocouples were mounted on the igloo and three thermocouples were located outside of the igloo at varying distances. A sample set of temperature profiles of the maximum recorded temperature for each of the thermocouples for a test has been included as Attachment 1 to this paper. A series of curves have been developed showing maximum thermocouple temperature versus distance from the back wall of the igloo, i.e., a distance of 2 feet corresponds to thermocouple 7 and a distance of 8.2 feet corresponds to the thermocouple located outside of the igloo, thermocouple 9. Figures 6 through 9 present temperature profiles for the 5- and 10-pound tests involving the M1 and IMR 8208 propellants. In each figure, data is presented for the 12-, 9- and 6-inch door vents enabling for direct comparisons to be made.

As can be seen in Figure 6, the higher temperatures for the 5 pound M1 tests are occurring outside of the igloo (the distance of 7.8 feet corresponds to the thermocouple just inside of the igloo door and the distance of 8.2 feet corresponds to the first thermocouple outside of the door) as would be expected and strongly indicates that unburned propellant is being carried out in the plume and combustion of the propellant is occurring outside of the igloo. A similar situation is occurring with the IMR 8208 propellant (see Figure 7) at least for the larger vent (12-inch door); however, for the smaller doors especially the 9-inch door, the temperatures are relatively higher inside of the igloo than they are outside, indicating that more of the combustion is occurring inside of the igloo. The 10-pound M1 tests yielded similar results as shown in Figure 8, with the higher temperatures occurring outside of the igloo rather than inside, and again implying that unburned propellant is being carried out in the plume and burning outside. This phenomena is further verified by the fact that inert particles inserted in the M1 propellant canisters were recovered at varying distances (15 to 25 feet) from the igloo and by the fact that on several of the tests, the propellant grains can be seen burning outside of the igloo as recorded by the video cameras. The 10-pound IMR 8208 test as shown in Figure 9 indicated that as the size of the vent was reduced, the quantity of material burning inside

of the igloo increased. This is indicated by the rise in the inside temperature as compared to the outside temperature. Figure 9 further shows that when the vent has been reduced to 6 inches, the inside temperatures are much higher than the outside temperatures. This would indicate that the majority of the burning is occurring inside of the igloo.

Affects of Plume Lengths On Quantity Distances

The plume lengths measured during these tests showed that on the majority of the larger tests, those involving 10-pound quantities (10,000 pounds full scale) the plumes were reaching lengths of approximately 25 feet, with velocities in excess of 150 feet per second. The plume data can be scaled to the full scale conditions since plume velocity and distance traveled will scale directly. The scaling relationships generated in the Phase 2 program [1] were presented in terms of the geometrical length scale factor, λ, which is the ratio of a length in the model to a corresponding length in full scale. The quantity of propellants must scale as the enclosure volume of reproduce results:

$$(M_1 \sim V0 \sim \lambda^3)$$

where M_1 is the propellant mass and V_0 is the enclosure volume. The vent area will scale as

$$A_e \sim \lambda^2$$

The plume velocity will scale as

$$U_e \sim (M_1/A_e) \sim \lambda$$

This would imply that for the full scale condition of 10,000 pounds of propellant in a full scale underground igloo, the plume would be expected to travel approximately 250 feet and have a velocity in excess of 1500 fps. However, for the larger quantities, it appears from the test data that as the quantity of material is increased, the flow out of the igloo will become choked and the plume will travel less distance out of the igloo. Now, however the failure mechanism is not the plume igniting the adjacent surroundings but is instead, the danger of the propellant burning rate escalating to detonation velocities and the subsequent pressure failure of the igloo.

CONCLUSIONS AND RECOMMENDATIONS

Based on the results of the confinement tests, a number of conclusions can be drawn regarding the combustion behavior of propellants. The velocity data has shown that as either the quantity of propellant burning is increased or the vent area is reduced, the quantity of gases being generated will exceed the capability of the vent and the gas flow will eventually go to a choked condition. The igloo will then respond as a totally closed system and catastrophic failure of the igloo is almost certain. This condition is further verified by the temperature data which indicates that as the plume becomes choked, the primary

---

1 W.R. Herrera, L.M. Vargas, et al. A Study of Fire Hazards from Combustible Ammunition-Effects of Scale and Confinement (Phase II), Prepared for DODESB, December 1984.

combustion of the propellant will occur inside of the igloo and very little material will be carried out in the plume.

The test results to date indicate that the plume length and thermal flux and the distance that firebrands will travel will have an impact on the siting requirements for storage facilities. The potential for the burning rate escalating to a detonation as a result of confinement will have an impact on the quantity of Class 1.3 and 1.4 materials that can be stored in substantially strong and ventilation-limited storage facilities.

Based on the results of the scaled-confinement tests, it is recommended that a number of additional tests be performed. The first type of tests to be performed should involve larger quantities of propellants using the same 1/10th scale igloo. The larger quantities of propellants will demonstrate whether the plume will indeed become choked as was implied by the smaller tests and if choked conditions do occur whether the burning rate inside the igloo will escalate to a detonation. The second series of tests should be performed using a larger scale model to determine whether direct scaling laws apply to the plume velocities and to the plume lengths.

TABLE 1. MATERIALS OF CONSTRUCTION

	Longhorn AAP	Lone Star AAP	Pine Bluff Arsenal	Radford AAP	Indian Head	Lake City AAP
Metal siding	W,R					
Corrugated metal		R	R	R		R
Corrugated AC	W,R			W,R	R	W,R
Hollow tile		W	W		W	
Masonry block			W		W	
Reinforced concrete	W,F	W,F,R	W,F,R,D	W,F,R	W,F,R	F
Wood/sheetrock/ singles	R					
Wood/metal		D	D	D		D
Wood/AC	D			W,R	R	
Glass		V,D				W,D
Wood	P	P,D	P	P		
Steel	D,V	D,V	V	V	D,V	V

W - walls
R - roof
F - floor
D - doors
V - vents and windows
P - pallets

TABLE 2. STORAGE FACILITY VENT AREAS

Facility	Building Type	Dimensions (ft) Dpth x Wdth x Ht	Volume Ft^3	Vent Area Ft^2	Vent Area Ratio $A/V^{2/3}$
SwRI	1/10th Igloo	8'x2.7'x1.35'	23.04	1.0	0.1234
Indian Head	Igloo	39'4"x19'x11'	12915	74.5	0.1353
	Igloo	82'x25'x11'	35421	74.5	0.0691
	Rectangular	51'2"x101'x14'9"	75977	208	0.1160
	Portable	8'x8'x8'	512	0.698	0.0109
	Primer mag.	14'x12'x7'5"	1260	27.5	0.2357
	Rectangular	35'x30'x9'	9450	44.4	0.0992
Lone Star	Rectangular	217'x51'x14'8"	162353	692.0	0.2325
	Rectangular	217'x51'x14'8"	162353	400.0	0.1344
	Igloo	40'x26'6"x12'9"	21146	30.0	0.0392
	Igloo	60'x26'6"x12'9"	31719	30.0	0.0299
Longhorn	Rectangular	150'x80'x12'	144000	831.0	0.3024
	Richmond	61'5"x25'5"x10'	16298	118.0	0.1835
	Richmond	61'5"x26'5"x10'	16298	48.0	0.0747
	Rectangular	220'x52'x12'	137280	673.0	0.1777
Pine Bluff	Igloo	60'x26'6"x12'9"	32204	30.0	0.0297
Radford	Igloo	82'2"x25'x13'	41861	36.0	0.0299
Lake City	Rectangular	25'x45'x10'7"	11906	129.4	0.2482

TABLE 3. THERMAL RESISTANCE OF MATERIALS OF CONSTRUCTION

Material	Time	Reference
Walls		
5" Standard Reinforced Concrete	2.5 hr	1 p7-101
	2.0 hr	2
6" Standard Reinforced Concrete	3.5 hr	1 p7-101
	2.5 hr	2
7" Standard Reinforced Concrete	4.7 hr	1 p7-101
	4.0 hr	2
12" Standard Reinforced Concrete	12.7 hr	1 p7-101
14" Standard Reinforced Concrete	16.9 hr	1 p7-101
7" Hollow Tile Block	3/4 hr	1 p7-92
8" Hollow Tile Block	3/4 to 1 hr	1 p7-92
12" Hollow Cinder Block Filled With Sand	2 1/2 hr	1 p7-92
Standard Cinder Block	1-1/4 hr	1 p7-94
Brick (12" brick (outer wall)/2" air gap/ 4" brick (inner wall)	8 hrs	1 p7-92
Metal Siding (Butler Building Type)	5 min	1
Corrugated AC Siding on 2x6 Studs/ 3" Batt Insulation/1x4 Furring Strips Solid Up To 6ft then every 16" CC/ 1/4" Hardboard Cover	10 min	1 p7-96
Corrugated AC Siding on 2x6 Studs/ 3.5" Batt Insulation/1x4 Furring Strips Solid Up To 6ft then every 16" CC/1/4" Hardboard Cover	10 min	1 p7-96
Roof		
5" Reinforced Concrete	2.5 hr	1 p7-101
	2.0 hr	2
6" Reinforced Concrete	3.5 hr	1 p7-101
	2.5 hr	2
12" Reinforced Concrete	12.7 hr	1 p7-101
14" Reinforced Concrete	16.9 hr	1 p7-101
Corrugated Asbestos Roofing on 2x6 Studs	30 min	1 p7-95
Corrugated Metal	5 min	1
Metal Siding	5 min	1
2x6 Studs with 3/4 in. Sheathing	20 min	1 p7-95
22 ga. G.I. Roof/3/4" Insulation/3/16 in. Asbestos	20 min	1
Tar and Gravel on 1" Solid Sheathing/2x4" Joists on 16" CC/4" Batt Insulation/1/2" Fiberboard	25 min	1 p7-94,96
Built up Tar and Gravel Roofing/7/8" Roof Boards/2" Cross Strip 2x14 at 16"CC Joists/ 3.5" Fiberglass Batt/1/8" Hardboard over 1/2" Fiberboard	30 min	1 p7-95,96
235 Composition Shingles/Sheetrock/2x6 Wood Joists	30 min	1 p7-95

TABLE 3 (CONT'D)

Material	Time	Reference
Roof (Cont'd)		
235 Composition Shingles/1/2" Plywood/Sheetrock/ 2x6 Wood Joists	30 min	1 p7-95
Corrugated Aluminum Roofing/Asbestos Shingles/ 2x6 Joists	10 min	1 p7-95
Doors		
1-3/4" Wood Door with Galvanized Metal Cover Front and Rear with Wire/Glass Window	3/4-1-1/2 hr 3/4 hr	3
1-1/3" Wood Door with Galvanized Metal Cover Front and Rear Metal Clad Door	3/4-1-1/2 hr 3/4 hr	3
1-5/8" Wood Door with Metal Skin--Metal Clad	3/4-1-1/2 hr 20 min*	3
Corrugated Metal on 2x4 Frame--Hollow Metal	3/4-1-1/2 hr 20 min*	3
Galvanized Metal Cover/2x6 Frame--Hollow Metal	3/4-1-1/2 hr 20 min*	3
1/4" Steel/4" Wood/1/4" Steel--Metal Clad	1-1/2 hr 3/4-1 hr	3
1/4" AC/1/2" Plywood/2x6 Frame--Wood Door	20 min; 20 min	3
1/4" AC on Solid 2x6s--Wood Door	20 min 20-30 min	3
3/8" Stl Sheet on Steel Frame--Hollow Metal	3/4-1-1/2 hr 3/4 hr*	3
3/16" Stl Sheet on Steel Frame--Hollow Metal	3/4-1-1/2 hr 3/4 hr*	3
1-5/8" Steel Plate--Metal Door	1-1/2 hr 3/4 hr	3
Thin Metal Rollup--Metal Door	3/4-1-1/2 hr 10 min	3
4" Reinforced Concrete	1-1-1/2 hr	
Windows		
Wood Sash and Frame With Steel Shutters	20 min	2
Standard Glass With Steel Grate	5 min	2
1/4" Steel Plates	1-1/2 hr	2
Mounting Attachments	30 min	3

* if metal only on outside of door

References:

1. Fire Protection Handbook
2. Uniform Building Code Standard 43-9
3. NFPA Codes - (No.80 - p.80-31)

TABLE 4. IGLOO CONFINEMENT TEST MATRIX

Test	Material	Quantity (lb)	Vent Size (in.)
8	IMR 8208	2	12
9	IMR 8208	4	12
10	IMR 8208	6	12
11	M1	1	12
12	M1	5	12
13	IMR 8208	1	12
14	IMR 8208	5	12
15	IMR 8208	10	12
16	M1	10	12
17 (Repeat 12)	M1	5	12
24 (Repeat 16)	M1	10	12
18	IMR 8208	5	9
19	M1	5	9
20 (Repeat 18)	IMR 8208	5	9
21	IMR 8208	1	9
22	M1	1	9
23	M1	10	9
31	IMR 8208	10	9
25	M1	1	6
26	IMR 8208	1	6
27	M1	5	6
28	IMR 8208	5	6
32	M1	10	6
33	IMR 8208	10	6
39	M1	10	6
29	ALA 17	1/2	12
30	ALA 17	1	12
34	ALA 17	1	9
35	ALA 17	1	6
36	ALA 17	2	12
37	ALA 17	2	9
38	ALA 17	2	6

Notes:

Test 12: This test was performed using black powder boosters to initiate the propellant in the canisters.

Test 16: This test had instrumentation problems on Channels 1, 3, 5, and 7.

Test 17: Channel 6 was lost during this test.

Test 27: This test was conducted during gusty wind conditions.

TABLE 5. IGLOO CONFINEMENT TEST MATRIX

Test	Material	Quantity (lb)	Vent Size (in.)	Plume Length (ft) Max	Hot
8	IMR 8208	2	12	10	4
9	IMR 8208	4	12	15	9
10	IMR 8208	6	12	15	12
11	M1	1	12	9	5
12	M1	5	12	17	13
13	IMR 8208	1	12	5	5
14	IMR 8208	5	12	16	14
15	IMR 8208	10	12	25	18
16	M1	10	12	25	15
17 (Repeat 12)	M1	5	12	12	9
24 (Repeat 16)	M1	10	12	25	14
18	IMR 8208	5	9	20	17
19	M1	5	9	15	10
20 (Repeat 18)	IMR 8208	5	9	10	8
21	IMR 8208	1	9	6	5
22	M1	1	9	8	7
23	M1	10	9	25	14
31	IMR 8208	10	9	20	12
25	M1	1	6	8	6
26	IMR 8208	1	6	4	-
27	M1	5	6	20	15
28	IMR 8208	5	6	20	17
32	M1	10	6	13	9
33	IMR 8208	10	6	18	15
39	M1	10	6	18	14
29	ALA 17	1/2	12	10	5
30	ALA 17	1	12	10	5
34	ALA 17	1	9	10	8
35	ALA 17	1	6	10	8
36	ALA 17	2	12	15	12
37	ALA 17	2	9	15	10
38	ALA 17	2	6	25	15

Notes.

Test 12: This test was performed using black powder boosters to initiate the propellant in the canisters.

Test 16: This test had instrumentation problems on Channels 1, 3, 5, and 7.

Test 17: Channel 6 was lost during this test.

Test 27: This test was conducted during gusty wind conditions.

TABLE 6. IGLOO PRESSURES AND VELOCITIES SUMMARY

Test	Material Type	Quantity (lb)	Pressure (psi)	V1 (fps)	V2 (fps)	V3 (fps)
12-Inch Door						
8	IMR 8208	2				
9	IMR 8208	4				
10	IMR 8208	6	0.1	136	124	90
11	M1	1	0.01	47	39	22
12	M1	5	0.18	125	88	88
13	IMR 8208	1	0.01	43	23	0
14	IMR 8208	5	0.18	168	105	112
15	IMR 8208	10	0.18	155	109	113
16	M1	10	0.18	111	68	39
17	M1	5	0.04	116	51	15
24	M1	10	0.14	135	80	67
9-Inch Door						
18	IMR 8208	5	0.18	70	48	42
19	M1	5	0.11	130	59	43
20	IMR 8208	5	0.14	74	39	16
21	IMR 8208	1	0.06	106	67	17
22	M1	1	0.01	38	23	15
23	M1	10	0.34	154	101	68
31	IMR 8208	10	0.18	202	114	48
6-Inch Door						
25	M1	1	0.09	133	51	37
26	IMR 8208	1	0.06	101	34	21
27	M1	5	0.18	165	119	89
28	IMR 8208	5	0.18	165	101	66
32	M1	10	0.18	84	54	15
33	IMR 8208	10	0.36	182	106	88
39	M1	10	0.36	135	85	58
Flares						
29	ALA 17	0.5	0.03	153	104	74
30	ALA 17	1	0.09	205	172	49
34	ALA 17	1	0.08	99	53	15
35	ALA 17	1	0.25	89	63	31
36	ALA 17	2	NA	205	147	26
37	ALA 17	2	NA	294	162	23
38	ALA 17	2	0.36	251	145	41

Notes:
Tests 8-14: Had thermocouples at 3", 3' and 6'
Tests 15: Had thermocouples 3', 6' and 9'
Tests 16-17 and 24: Had thermocouples at 6', 9' and 17'
Tests 21 and 22: Had thermocouples at 3", 3' and 6'
Tests 18-20 and 23 and 31: Had thermocouples at 6', 9' and 17'
Tests 25-28: Had thermocouples at 3", 3' and 6'
Tests 32, 33 and 39: Had thermocouples at 6', 9' and 17'
Tests 29 and 30: Had thermocouples at 3", 3' and 6'
Tests 34-38: Had thermocouples at 6', 9' and 17'

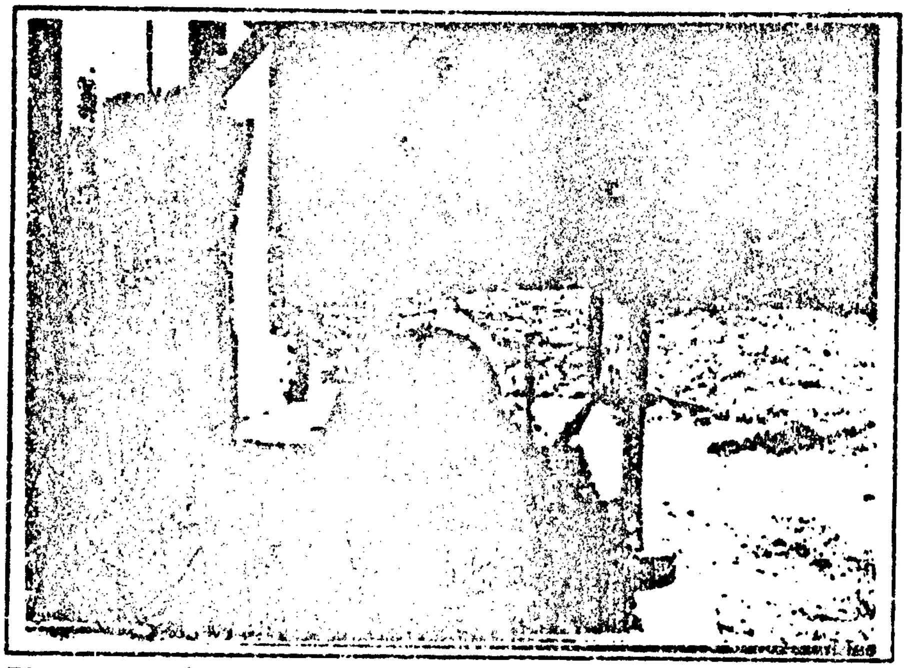

Figure 1. 1/10th Scale Model Igloo

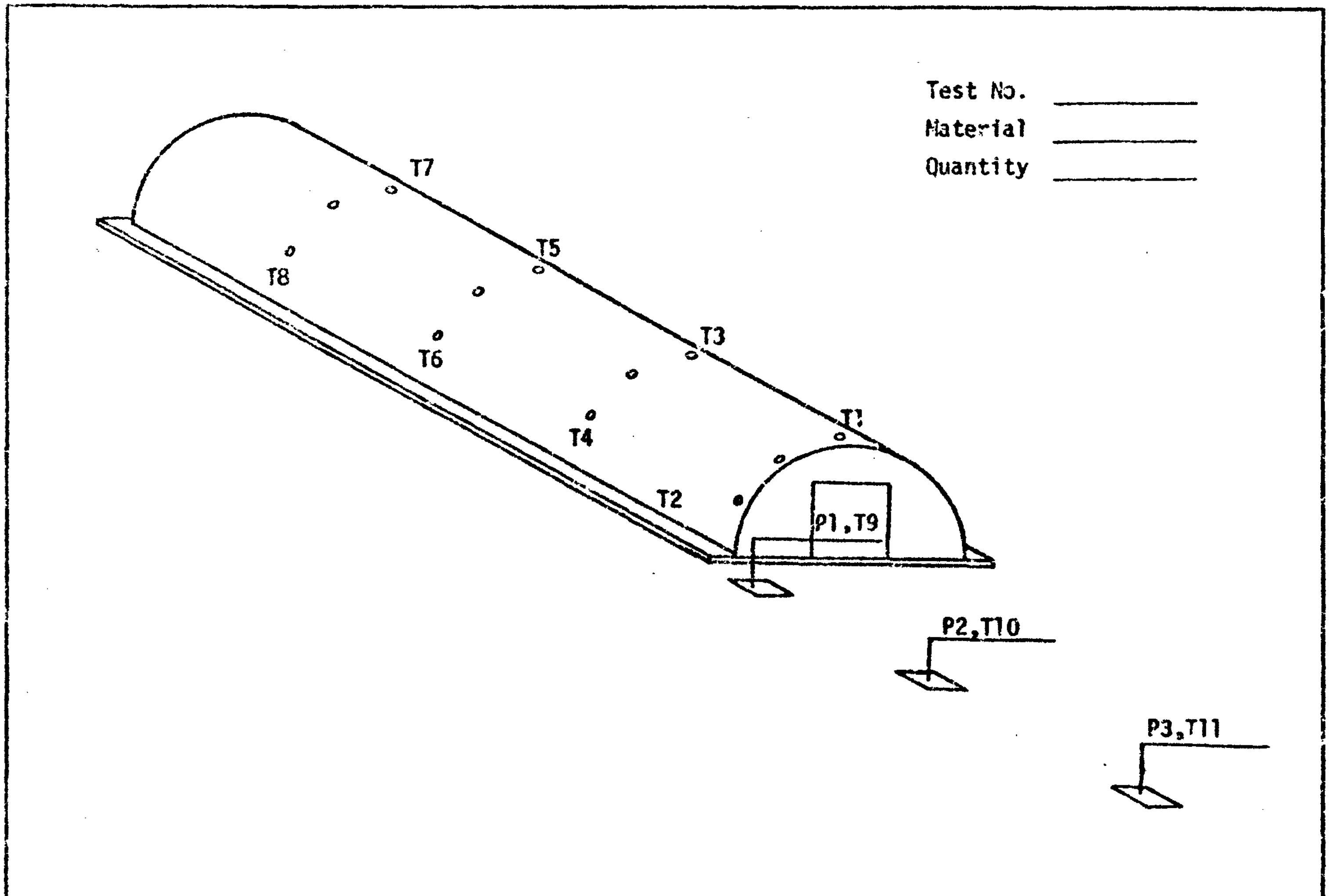

Figure 2. Igloo Confinement Tests

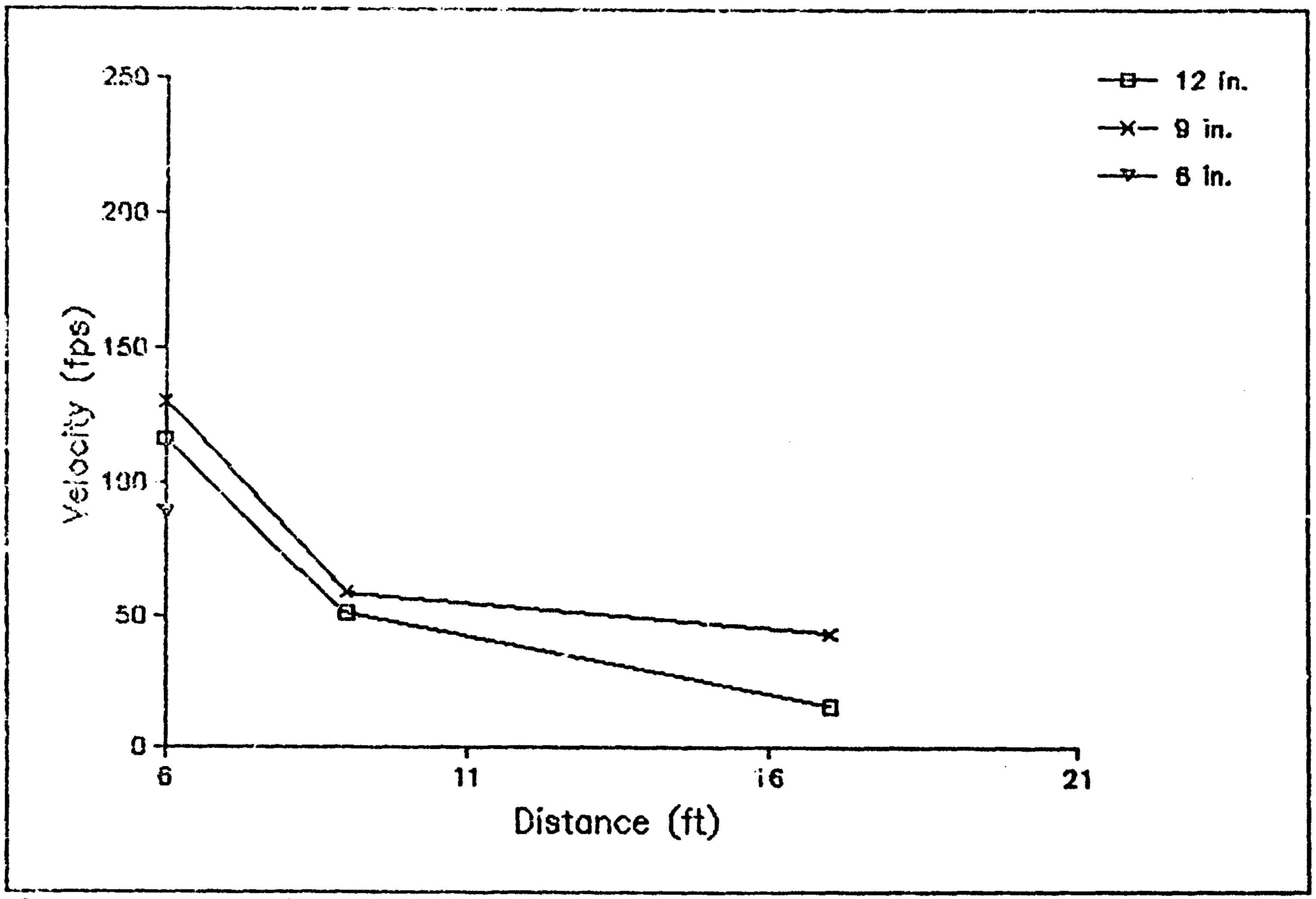

Figure 3. Plume Velocity Comparison of M1 - 5-lb Test

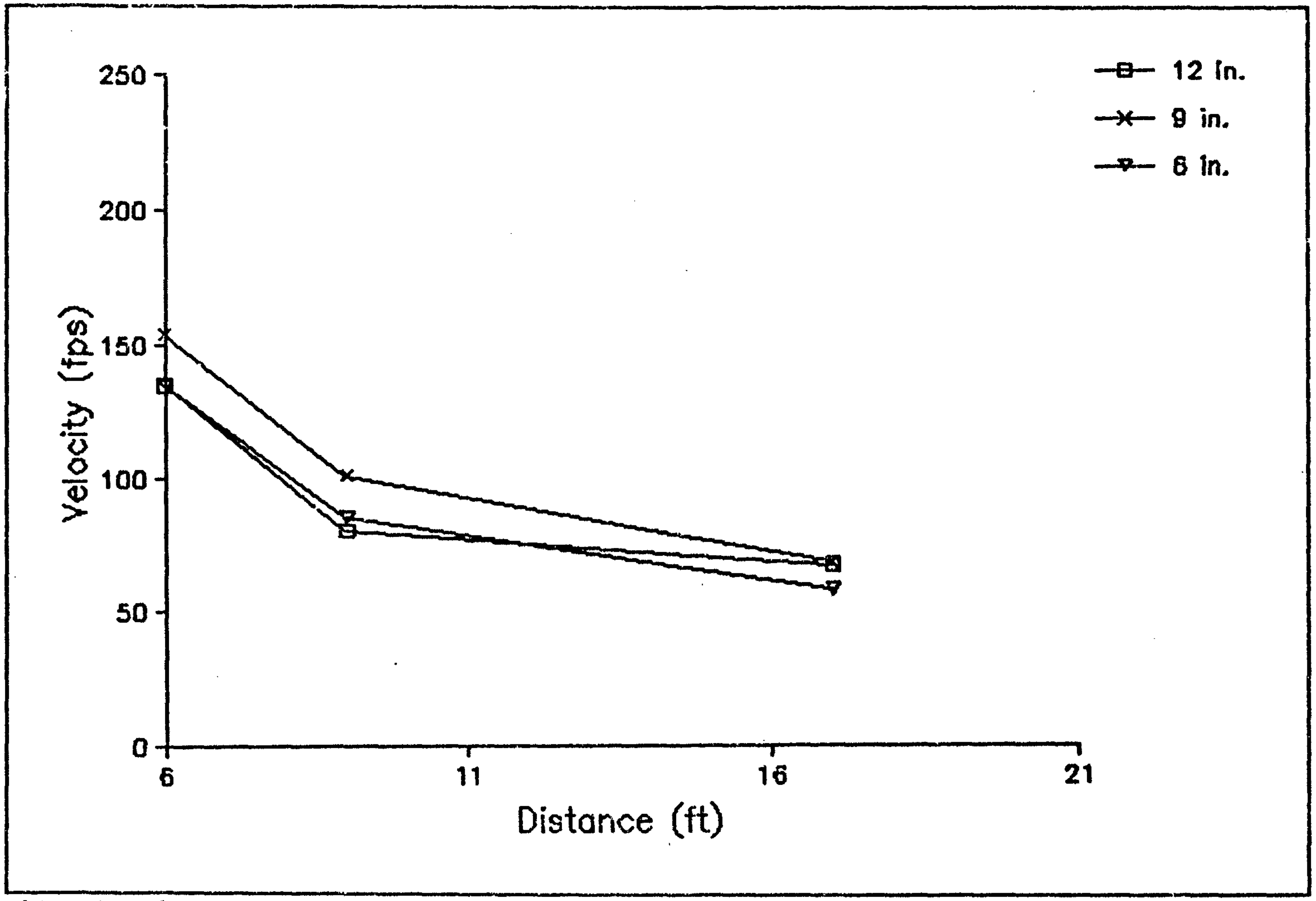

Figure 4. Plume Velocity Comparison of M1 - 10-lb Test

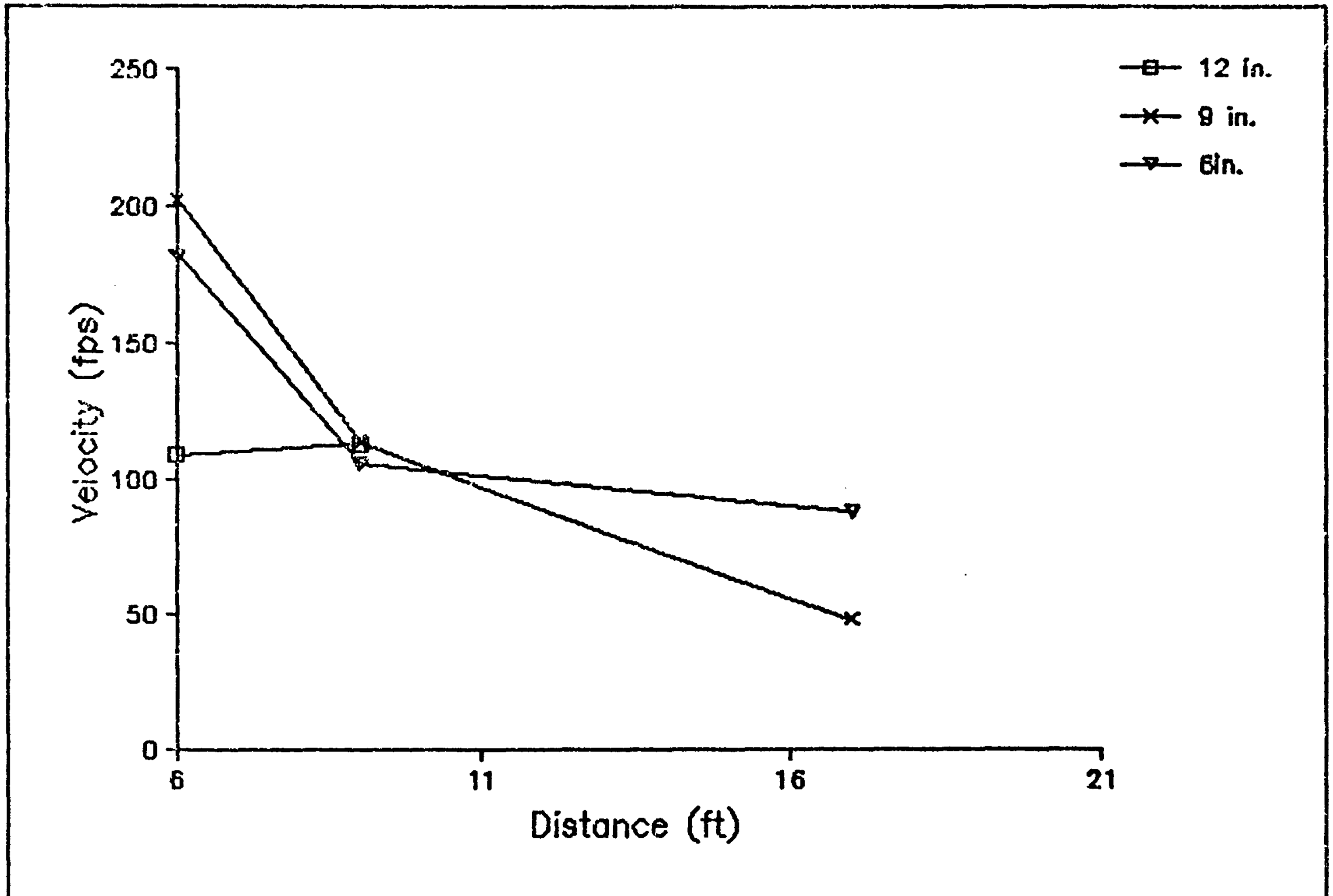

Figure 5. Plume Velocity Comparison of IMR 8208 - 10-lb Test

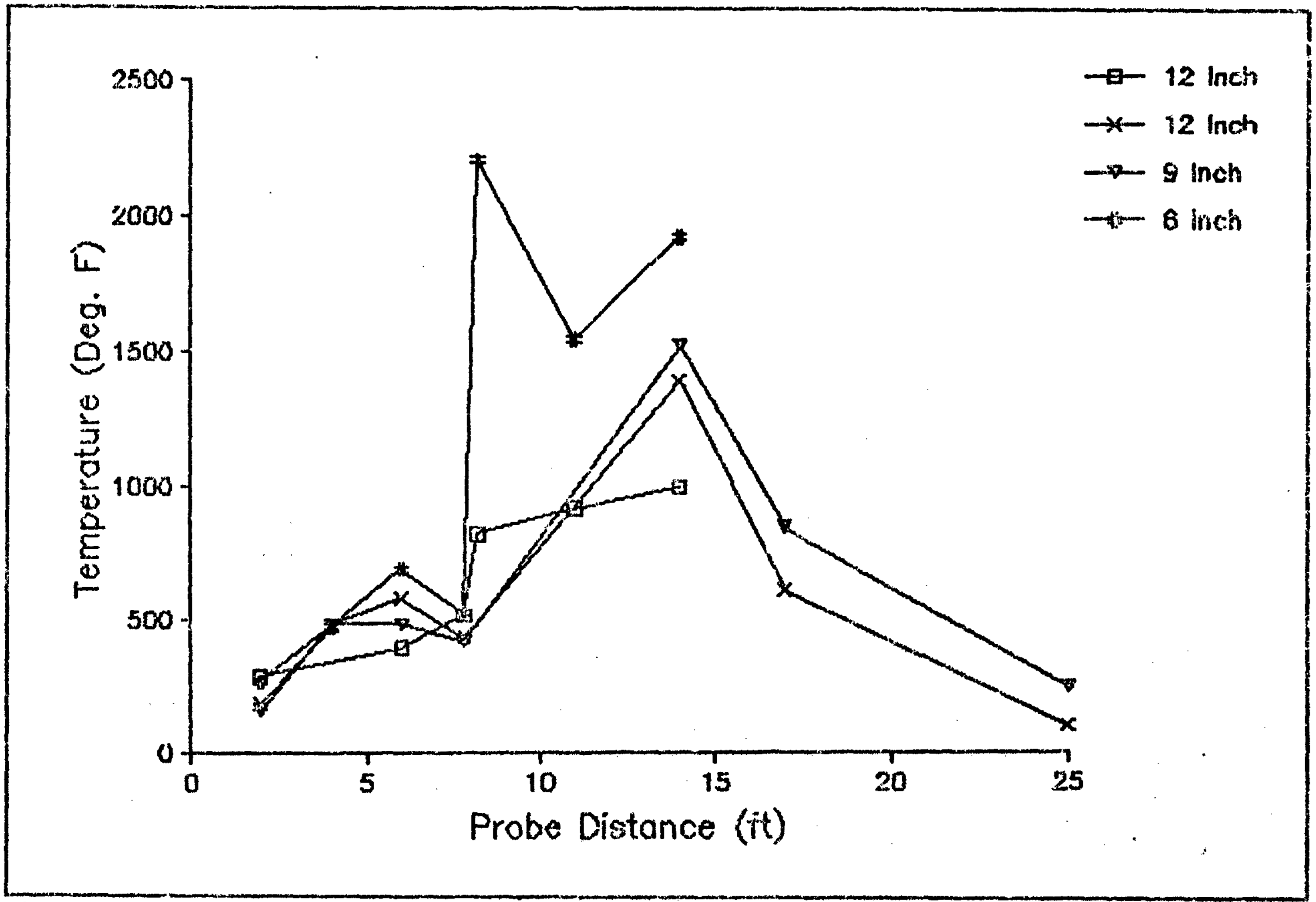

Figure 6. DDESB Door Vent Comparison of M1 - 5-lb Test

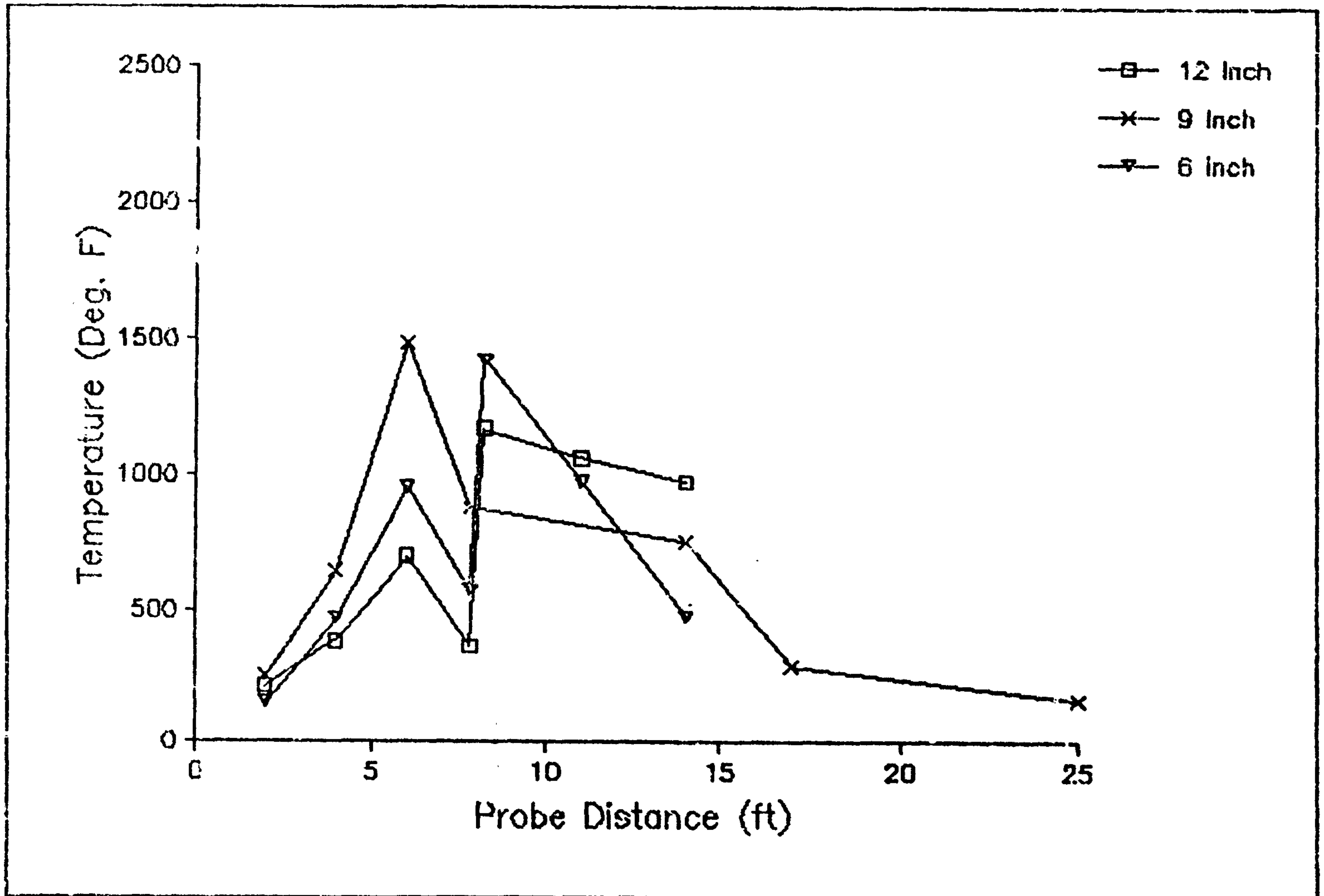

Figure 7. DDESB Door Vent Comparison of IHR 8208 - 5-lb Test

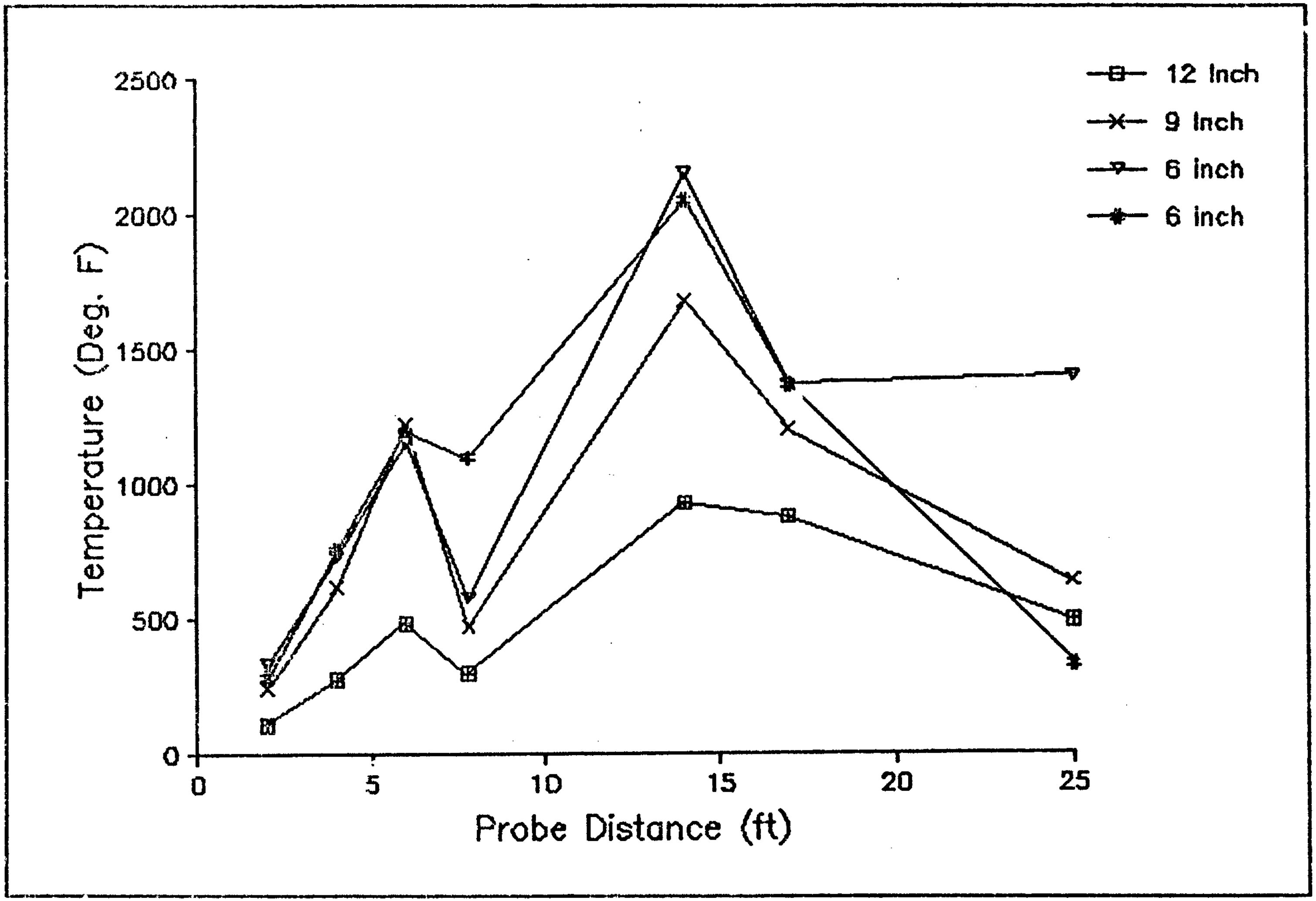

Figure 3. DDESB Door Vent Comparison of M1 - 10-lb Test

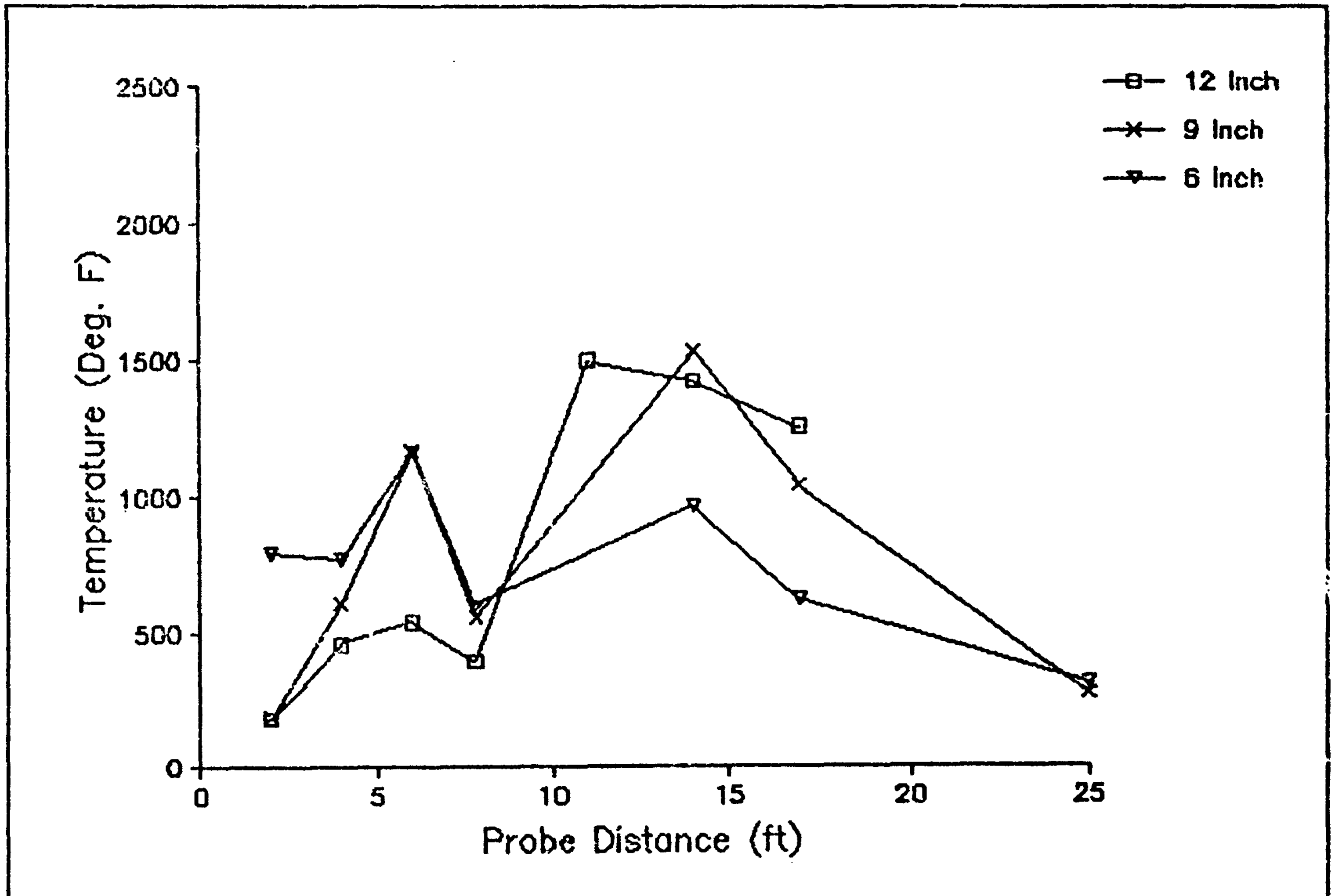

Figure 9. DDESB Door Vent Comparison of IHR 8208 - 10-lb Test

ATTACHMENT 1

18-MAR-88 10:29

COMBUSTIBLE AMMUNITION TEST
TEST NUMBER 032

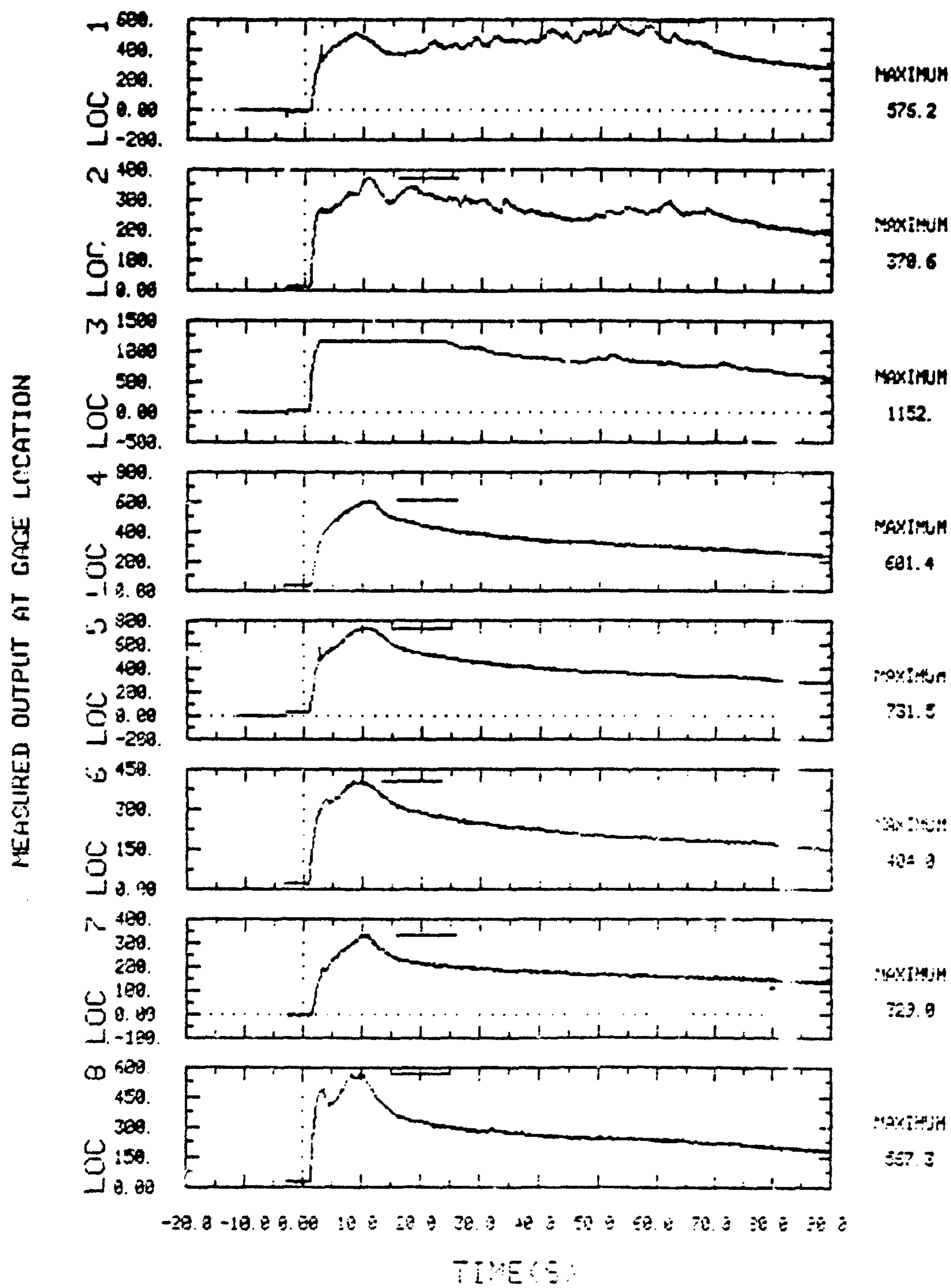

18-MAR-88 10:29

COMBUSTIBLE AMMUNITION TEST
TEST NUMBER 032

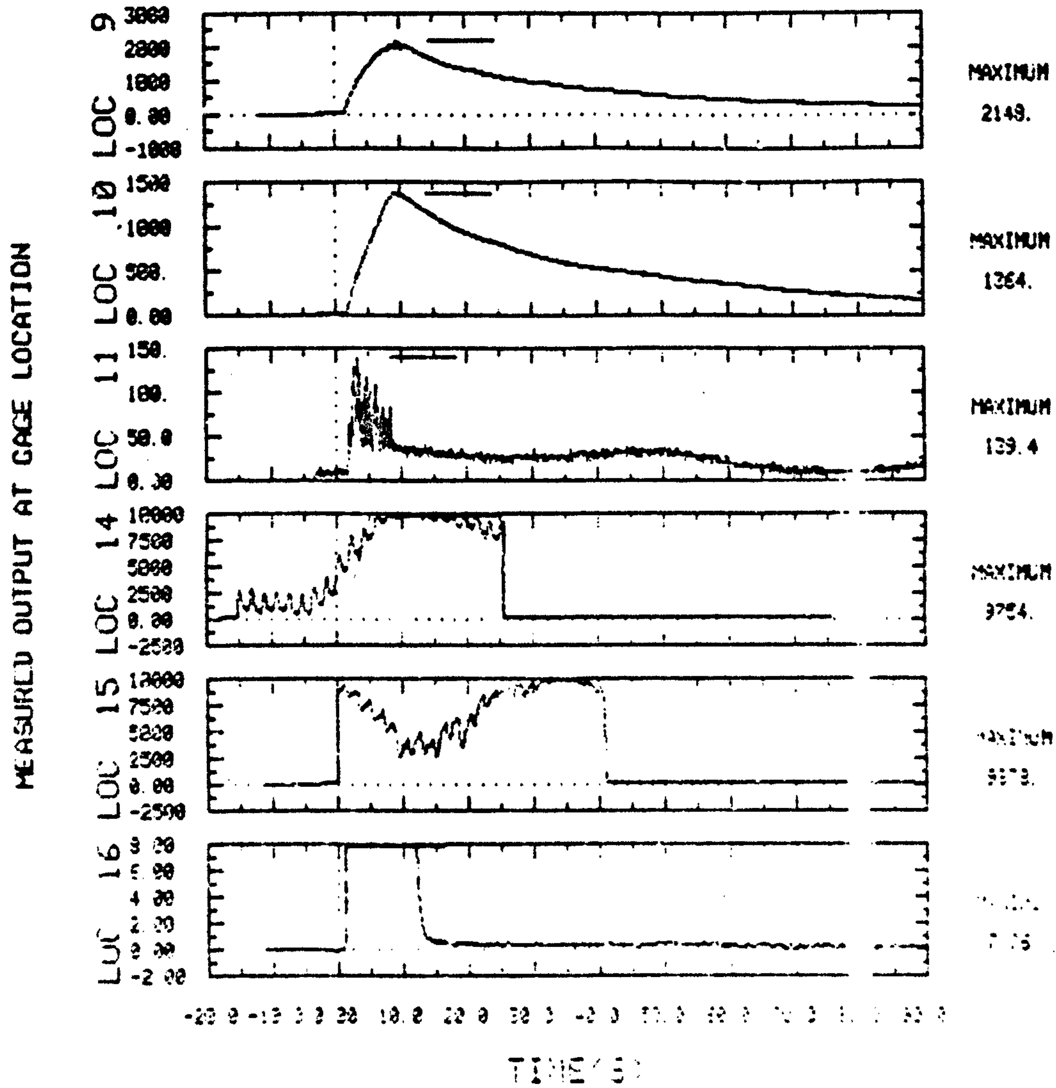

MULTIPLE QUANTITY DISTANCES

U.S. AIR FORCES IN EUROPE

BRIEFER: MR. HAMMEL-MUELLER
HQ USAFE/DEPV

DEPVV/0841b/8 Jul 88

MULTIPLE QUANTITY DISTANCES

PURPOSE:

- EXPLAIN HOW THE DEVELOPMENT AND IMPLEMENTATION OF A SYSTEM OF THREE EXPLOSIVES QUANTITY DISTANCE (QD) ZONES HAS PROVEN TO BE AN EXTREMELY USEFUL RISK MANAGEMENT TOOL
- HOW TO SITE NEW FACILITIES ON LAND PREVIOUSLY UNUSABLE DUE TO QD ZONES NORMALLY REQUIRED BY TRADITIONAL EXPLOSIVES SAFETY STANDARDS
- 200-300 MILLION DOLLARS WORTH OF VIABLE CONSTRUCTION PROJECTS HAVE BEEN SITE APPROVED IN UNITED STATES AIR FORCE IN EUROPE BY USING THIS NEW MANAGEMENT TOOL

MULTIPLE QUANTITY DISTANCES

OVERVIEW:

SITING/QD PROBLEMS AT US AIR FORCE BASES IN EUROPE

- SITING OF HARDENED AIRCRAFT SHELTERS (HAS)
- TYPES OF SEPARATIONS OF HAS

COB/FOL EXEMPTION (COLOCATED OPERATING BASES/FORWARD OPERATING LOCATIONS)

- BENEFITS
- THREE PHASED SITING FOR HAS
- EXPLOSIVES SITE PLAN

THREE-PHASED SITING AT MOBS (MAIN OPERATING BASES)

- BENEFITS
- CURRENT SITING PRACTICE AT MOBS
- THREE-PHASED SITING FOR HAS
- EXPLOSIVES SITE PLAN

RECOMMENDATION ABOUT FUTURE IMPLEMENTATION

SUMMARY

MULTIPLE QUANTITY DISTANCES

<u>SITING/QD PROBLEMS AT US AIR FORCES BASES IN EUROPE</u>

- USAFE FACES A CONSTANT STRUGGLE TO BALANCE WARFIGHTING CAPABILITY WITH EXISTING EXPLOSIVES SAFETY STANDARDS
- INSTALLATIONS IN EUROPE ARE <u>TOO SMALL</u> FOR CONDUCTING PEACETIME, EXERCISE AND WARTIME OPERATIONS WITHOUT <u>SIGNIFICANT EXEMPTION OF EXPLOSIVES SAFETY QUANTITY-DISTANCE CRITERIA</u>
- EXPLOSIVES CLEAR ZONES ENCOMPASS A LARGE AMOUNT OF REAL ESTATE ON THE BASES

MULTIPLE QUANTITY DISTANCES

SITING/QD PROBLEMS AT US AIR FORCE BASES IN EUROPE:

- FACILITIES MAY PHYSICALLY FIT ON THE LAND, BUT EXPLOSIVE SAFETY DISTANCES FOR ADEQUATE AMOUNTS OF MUNITIONS CANNOT BE MET
- ACQUIRING ADDITIONAL REAL ESTATE IS COSTLY AND NOT TIMELY
- INFLEXIBILITY OF ALIGNING AIR FORCE FACILITY SITING POLICY WITH OUR HOST NATIONS POLICY

MULTIPLE QUANTITY DISTANCES

EXAMPLE - Siting of Hardened Aircraft Shelters (HAS)

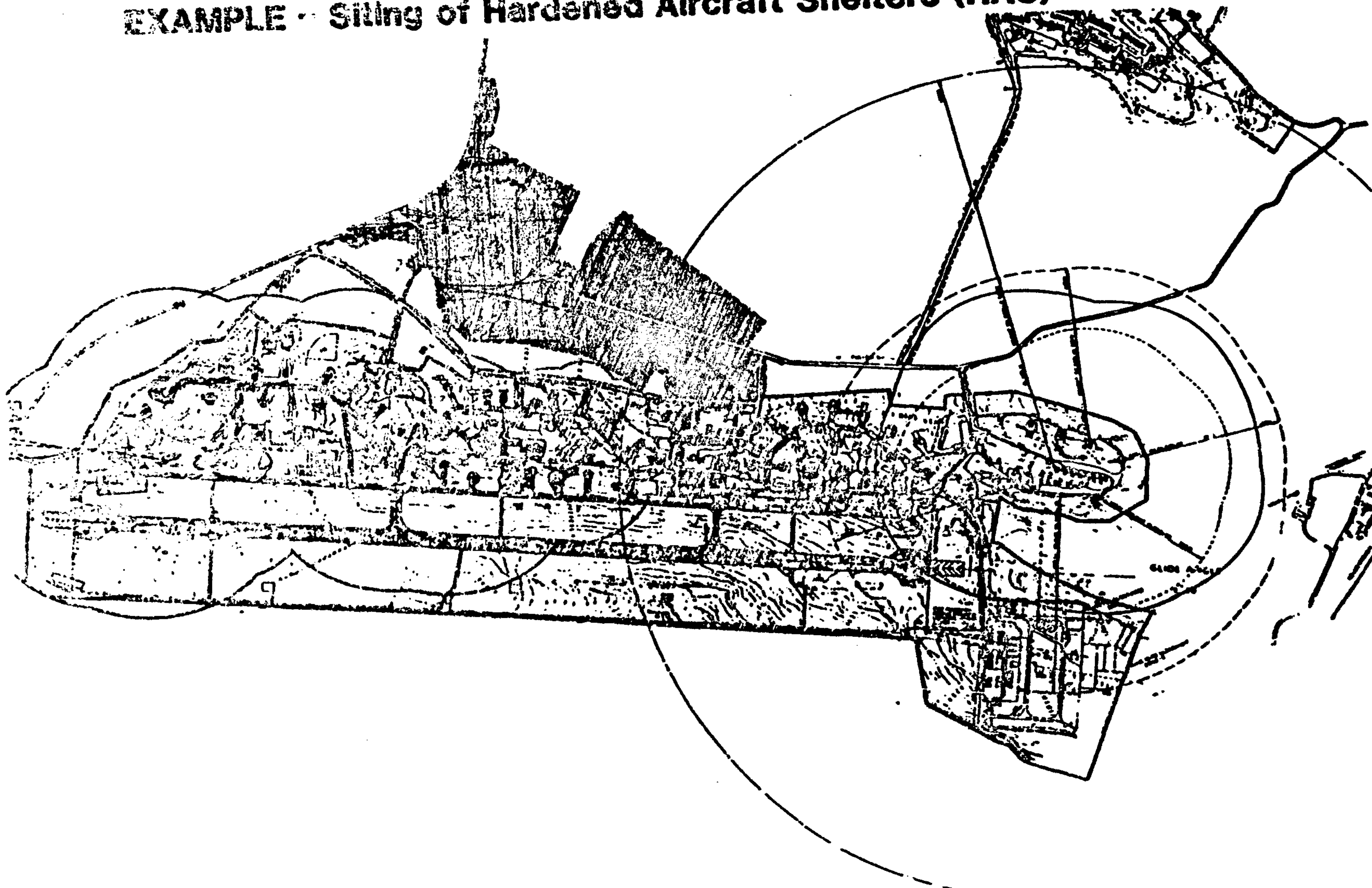

MULTIPLE QUANTITY DISTANCES

EXAMPLE: SITING OF HARDENED AIRCRAFT SHELTER (HAS)

APPROXIMATELY TWO-THIRDS OF THE HAS' AT USAFE BASES CAN'T HOUSE FULLY LOADED COMBAT AIRCRAFT DURING WARTIME DUE TO EXPLOSIVES SAFETY DISTANCE LIMITATIONS

MULTIPLE QUANTITY DISTANCES

<u>EXAMPLE: SITING OF HARDENED AIRCRAFT SHELTERS:</u>

TWO MAJOR FACTORS CONTRIBUTE TO THIS PROBLEM:

- THE CONCEPT OF OPERATIONS FOR HAS
  - -- CHANGED FROM PARKING GARAGES FOR AIRCRAFT TO INTEGRATED COMBAT TURNAROUND FACILITIES
- AIRCRAFT SHELTER DESIGN
  - -- NOT DESIGNED TO CONTAIN INTERNAL EXPLOSION

COMBINED WITH EXISTING LAND CONSTRAINTS, IT IS ALMOST IMPOSSIBLE TO SITE HAS AT USAFE BASES FOR AN ADEQUATE AMOUNT OF MUNITIONS

MULTIPLE QUANTITY DISTANCES

EXAMPLE - Types of Separation for HAS (2500 lbs NEW)

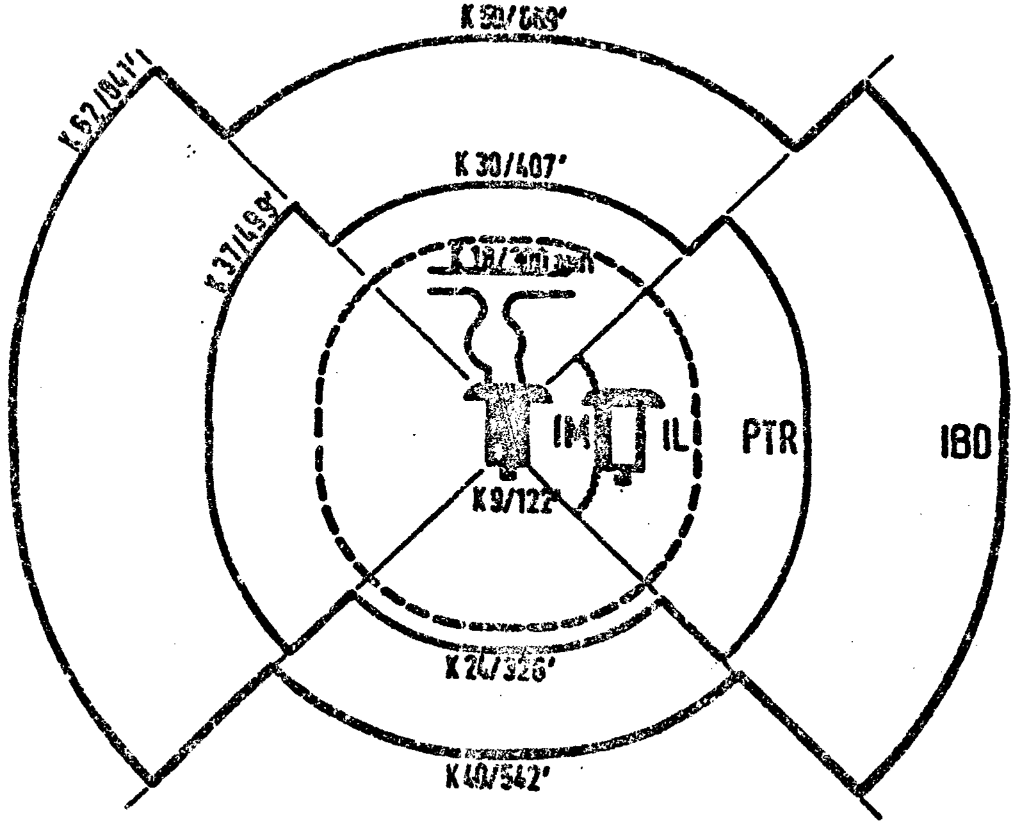

MULTIPLE QUANTITY DISTANCES

COB/FOL EXEMPTION:

- IN AUG 86, COMBINED SAF/HQ AFISC AND A HQ USAFE TEAM CONDUCTED AN IN-DEPTH REVIEW OF THE EXPLOSIVE SAFETY PROBLEMS ASSOCIATED WITH THE USAFE COB AND FOL PROGRAMS IN EUROPE

- THE SECRETARY OF THE AIR FORCE APPROVED AN EXEMPTION TO EXPLOSIVE SAFETY DISTANCED FOR COLLOCATED OPERATING BASES IN SEPTEMBER 1986

MULTIPLE QUANTITY DISTANCES

COB/FOL EXEMPTION-BENEFITS:

- ENSURES TIMELY CONSTRUCTION OF VITAL FACILITIES AT VARIOUS BASES WHERE THE US FORCES ARE TENANTS
- PROVIDES A NEW CONCEPT IN EXPLOSIVE SAFETY SITE PLANNING BY ESTABLISHING PEACETIME. EXERCISE AND WARTIME SAFETY CRITERIA
- ALLOWS USAFE THE FLEXIBILITY TO USE HOST NATION CRITERIA WHEN OUR POTENTIAL EXPLOSIVE SOURCES (PES) PLACE HOST FACILITIES AT RISK. (THE AIR FORCE WILL CONTINUE TO OBSERVE US EXPLOSIVE SAFETY STANDARDS OF EXPOSURES AT THESE FACILITIES)

MULTIPLE QUANTITY DISTANCES

COB/FOL EXEMPTION-BENEFITS:

- BECAUSE OF SEVERE SITING CONSTRAINTS, WARTIME QD CLEAR ZONES MAY ALSO EXPOSE NON-ESSENTIAL, UNINHABITED US RESOURCES

EXAMPLE:

- PPP (PREPOSITIONED PROCUREMENT PACKAGE) STORAGE FACILITIES MUST BE SITED OUTSIDE EXERCISE QD CLEAR ZONES SINCE THESE RESOURCES CANNOT BE RISKED (AS AN ESSENTIAL FACILITY).
- SINCE PPP RESOURCES WILL BE DISPERSED IN WARTIME, THESE FACILITIES MAY BE SITED WITHIN THE WARTIME QD ZONE (AS A NON-ESSENTIAL FACILITY NOW).

MULTIPLE QUANTITY DISTANCES

EXAMPLE - Three Phased Siting for a HAS

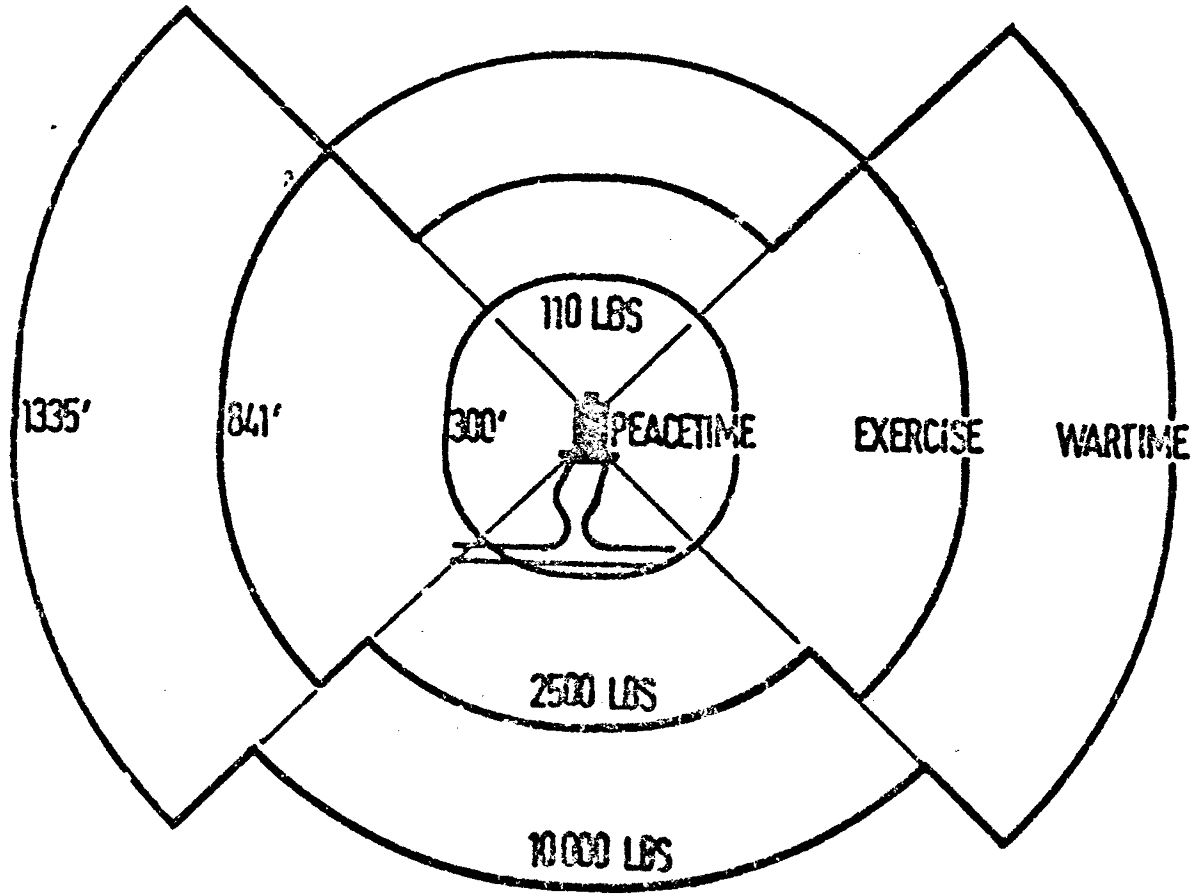

MULTIPLE QUANTITY DISTANCES

<u>COB/FOL EXEMPTION-THREE PHASED SITING FOR HARDENED AIRCRAFT SHELTERS (HAS)</u>

PEACETIME (DAY TO DAY) OPERATION:

- GENERALLY, NO EXPLOSIVES INSIDE THE HAS (110 LBS MAX)
- MINIMUM SEPARATION OF 300 FT REQUIRED FOR ALL OTHER FACILITIES (USAFE REQUIREMENT)

MULTIPLE QUANTITY DISTANCES

<u>COB/FOL EXEMPTION-THREE PHASED SITING FOR HAS</u>

EXERCISE OPERATIONS:

- BASED ON REQUIRED LIVE MUNITIONS
- USE OF INERT MUNITIONS CAN BE CONSIDERED WHERE APPROPRIATE
- EXERCISES WILL OCCUR INFREQUENTLY (ABOUT 3 WEEKS, EVERY 2 OR 3 YEARS)

MULTIPLE QUANTITY DISTANCES

COB/FOL EXEMPTION THREE-PHASED SITING FOR HAS

WARTIME OPERATIONS:

- WARTIME WEIGHTS WILL NOT BE REDUCED BELOW THAT WHICH PROVIDES A REALISTIC WARTIME OPERATIONAL CAPABILITY
- ALL FACILITIES WILL BE SITED FOR A MAXIMUM WARTIME CAPABILITY

MULTIPLE QUANTITY DISTANCES

<u>THREE-PHASED SITING AT MOBS-BENEFITS:</u>

A RECENT STUDY CONDUCTED BY USAFEISC/SEW AND HQ USAFE/DEPV AT A MOB IN GERMANY PROVED THE BENEFITS OF THE MULTIPLE EXPLOSIVES CLEAR ZONE CONCEPT FOR MOBS.

- WILL GENUINELY ENHANCE OUR PEACETIME, EXERCISE AND ULTIMATE WARFIGHTING CAPABILITY
- IMPROVE OPERATIONAL CAPABILITY WITHOUT INCREASING RISK TO PEOPLE, FACILITIES AND EQUIPMENT
- HELP TO SOLVE CRITICAL LAND SHORTAGE PROBLEMS

MULTIPLE QUANTITY DISTANCES

<u>THREE PHASED SITING AT MOBS-BENEFITS</u>

CURRENTLY, PEACETIME EXERCISE AND WARTIME Q-D'S ARE CONSIDERED TO BE ALL THE SAME. PEACETIME ASSETS MAY CONSTRAIN THE WARTIME USE OF CRITICAL ASSETS, SUCH AS HARDENED AIRCRAFT SHELTERS.

<u>EXAMPLE:</u>

- A NONESSENTIAL FACILITY SUCH AS A BASE EXCHANGE (BX) MAY CONSTRAIN THE WARTIME USE OF A HAS, BY LIMITING THE AMOUNT OF EXPLOSIVES ALLOWED IN THE SHELTER SUCH THAT THE BX IS NOT EXPOSED TO AN UNACCEPTABLE LEVEL OF RISK
- SINCE SUBJECT FACILITY WON'T BE INHABITED IN WARTIME, THE WARTIME ZONE CAN BE EXPANDED TO IMPROVE OPERATIONAL CAPABILITY OF THE NEARBY HAS.

MULTIPLE QUANTITY DISTANCES

EXAMPLE - Three Phased Siting at MOBs

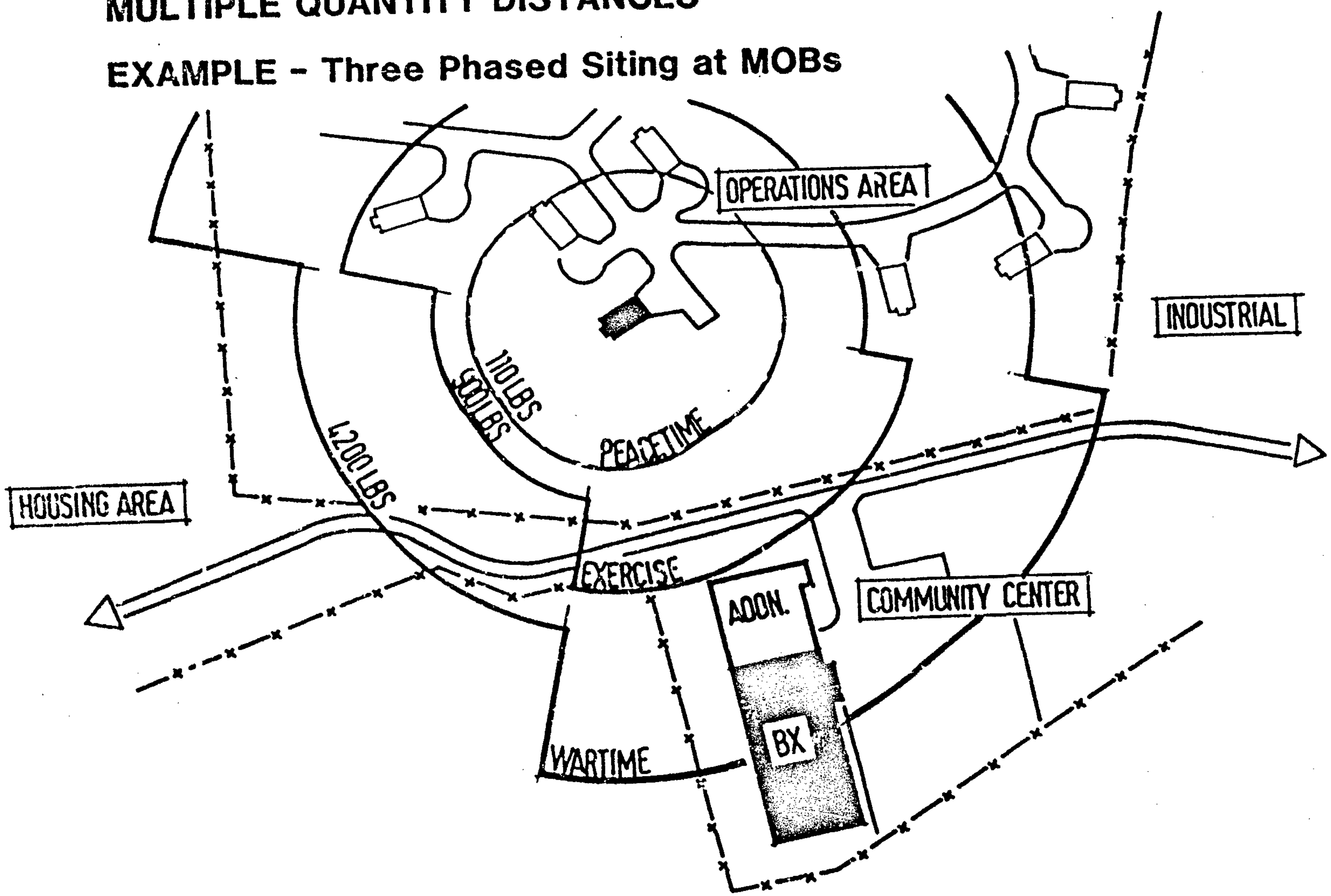

EXAMPLE - Three Phased Siting at MOBs

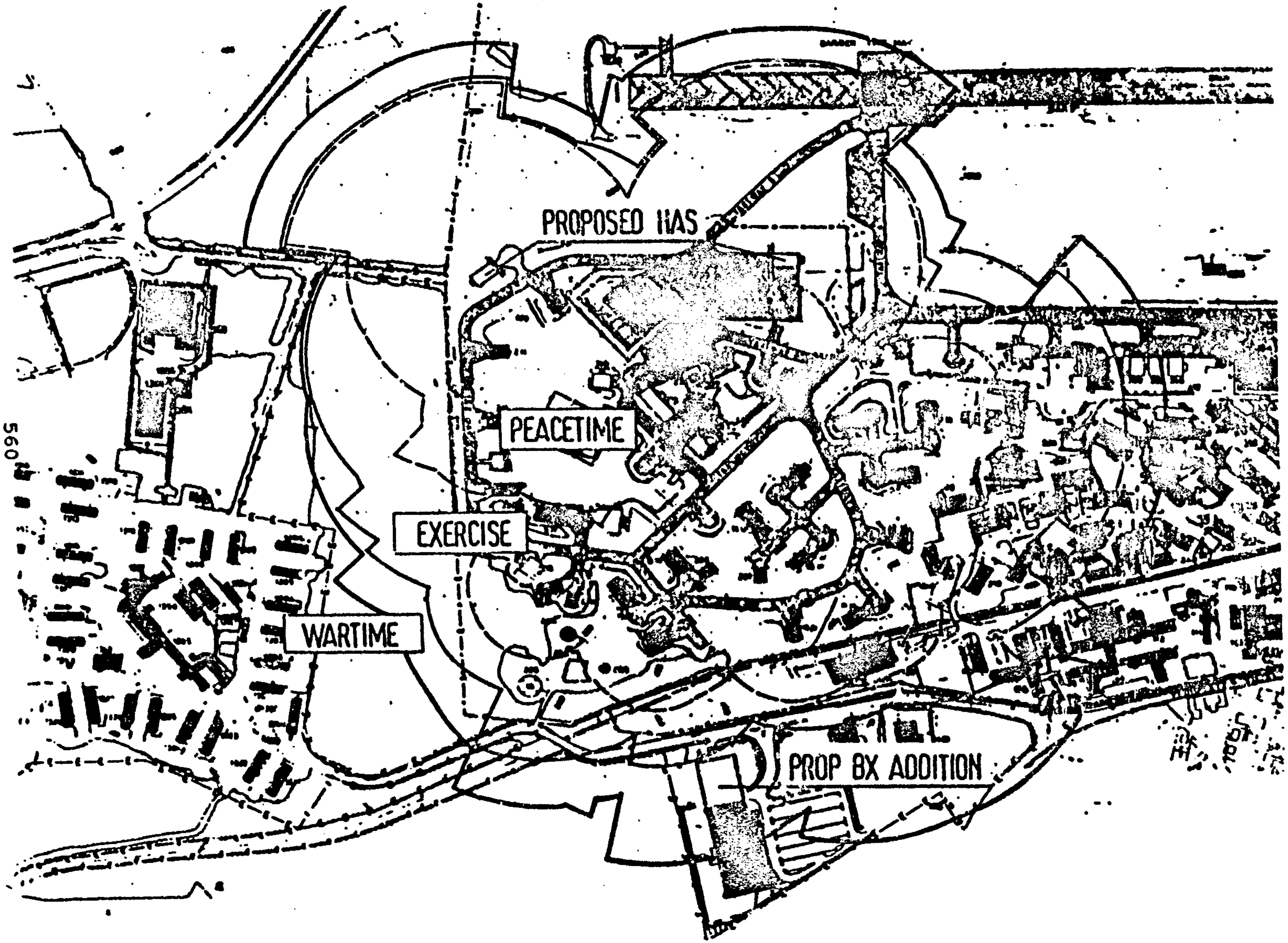

MULTIPLE QUANTITY DISTANCES

<u>THREE PHASES SITING AT MOBS-APPLICABILITY</u>

- EACH FACILITY INSIDE WARTIME EXPLOSIVES CLEAR ZONES HAS TO BE CLASSIFIED AS EITHER ESSENTIAL OR NON-ESSENTIAL IN WARTIME
- ESSENTIAL FACILITIES MUST BE PROTECTED. NON-ESSENTIAL FACILITIES MUST BE CONSIDERED EXPENDABLE
- BUILDINGS INHABITED IN PEACETIME BUT UNINHABITED IN WARTIME ARE CONSIDERED UNINHABITED WARTIME QUANTITY-DISTANCE CALCULATIONS (THE VALUE OF THESE FACILITIES IS CONSIDERED NEGLIGIBLE WITH RESPECT TO INCREASED MISSION CAPABILITY)

MULTIPLE QUANTITY DISTANCES

<u>THREE PHASED SITING AT MOBS-EXPLOSIVES SITE PLAN</u>

THE SITE PLAN WILL CONTAIN AS A MINIMUM:

- EXPLOSIVES SAFETY QD CLEAR ZONES FOR PEACETIME DAY TO DAY, EXERCISE AND WARTIME WEIGHTS, AS APPLICABLE
- CLEARLY IDENTIFY OFF-INSTALLATION AND HOST NATION ON-INSTALLATION EXPLOSIVES SAFETY EXPOSURES WITHIN THE SAFETY QUANTITY-DISTANCE ZONES
- AN EXPLOSIVES SAFETY ANALYSIS OF FACILITIES AND FACILITY USE IN THE AREA BETWEEN THE WARTIME AND EXERCISE QD CLEAR ZONES
- AN ANALYSIS OF FACILITIES AND FACILITY USE IN THE AREA WITHIN THE EXERCISE QD CLEAR ZONE

MULTIPLE QUANTITY DISTANCES

RECOMMENDATIONS:

- IN ORDER TO FURTHER MAXIMIZE WARFIGHTING CAPABILITY OF OUR INSTALLATIONS IN EUROPE, A REALISTIC ENFORCEMENT MECHANISM FOR THREE-PHASED SITING SHOULD BE INSTITUTED (IMPLEMENT INTO AFR 127-100)
- ESTABLISH AND FUND AN AGGRESSIVE, COMPREHENSIVE RESEARCH, DEVELOPMENT AND TESTING PROGRAM TO DETERMINE METHODS BY WHICH MUNITIONS STORAGE CAN BE INCREASED WITHOUT ADDITIONAL RISK
- DEVELOP COMPREHENSIVE FACILITY DESIGN AND USE CRITERIA TO REDUCE THE ADVERSE IMPACTS OF EXPLOSIVES
- KEEP A CONTINUED EMPHASIS ON RISK MANAGEMENT AT ALL EXPLOSIVE LOCATIONS

MULTIPLE QUANTITY DISTANCES

SUMMARY:

- THE MULTIPLE EXPLOSIVE CLEAR ZONE CONCEPTS/THREE-PHASES SITING HAS PROVED TO BE A VALUABLE PLANNING TOOL FOR COBS AND FOLS
- THE CONCEPT FACILITATES THE TIMELY SITING, CONSTRUCTION AND USE OF USAF FACILITIES ($200-300M CONSTRUCTION WORTH) AND ALSO MAXIMIZES WARFIGHTING CAPABILITY AT USAFE INSTALLATIONS IN EUROPE
- HQ USAFE IS NOW IN THE PROCESS OF EXPANDING THREE-PHASED SITING PROVISIONS TO ALL INSTALLATIONS INCLUDING MOBS
- FURTHER PROCESSING OF THREE-PHASED SITING IS PENDING ON ESTABLISHMENT OF A REALISTIC ENFORCEMENT MECHANISM (IMPLEMENTATION IN AFR 127-100)

ASSESSMENT OF THE PROBABILITY OF EXPLOSION EVENTS IN MANUFACTURING AND STORING OF AMMUNITION AND EXPLOSIVES

Authors: Peter Kummer and Andreas F. Bienz
Ernst Basler & Partners Ltd., 8702 Zollikon, Switzerland

Abstract

According to the explosive safety regulations for the Swiss Federal Armament Industry a quantitative risk analysis has to be made for the safety evaluation of each new operation, manufacturing plant, building or storage facility.

To estimate and quantify the actual hazards, the risk analysis has to consider the effects of explosions or fires as well as their respective event probability. Today, explosion effects are generally well documented, or they can easily be established, e.g. by means of model or full-scale tests. However, only little basic data is made ready for the estimation of the event probabilities, so that in practice its determination may be difficult. Basically, there are three approaches to estimate the probability of an event: Statistically, analytically and intuitively.

This paper explains as to how these three approaches are useful for estimating the event probability, either individually or combined. It describes the advantages and disadvantages of each approach as well as the way of putting it into practice. Moreover, a general "Basic Frequency Rate System" will be shown, which represents the combination of all the approaches and allows to consistently assess the probability of explosion events. Several examples demonstrate the practical usefulness of this concept.

Paper presented at the 23rd Department of Defence Explosives Safety Seminar in Atlanta/USA, 9-11 August, 1988

1. THE PROBLEM

Most safety regulations for the manufacturing and storing of explosives and ammunition are still based on the safety distance concept. A typical example are the widely used "NATO Safety Principles for the Storage of Ammunition and Explosives". These safety distance regulations have their roots in those times, when explosions actually happened frequently. They are generally designed so that in case of an explosion the damage in the surroundings would only be very small. Usually, they do not explicitly account for the probability of explosions, for instance in the storage of explosives where, today, we have every reason to believe in the low probability of accidents. On the other hand, those in charge often do not hesitate to believe that the probability of events is very low and "nothing can happen" when the circumstances do not allow to follow the regulations and waivers have to be approved, or in manufacturing plants where the personnel actually has to work with explosives. Likewise, aircraft, buildings etc., and even nuclear power plants have always been said to be safe only because of the very low probability of a major accident.

Regulations in explosives and ammunition handling and storing which are based on the limitation of consequences, usually result in safe, i.e. low-risk installations. But this attitude often leads to an extensive land use and high cost. Moreover, installations requiring large safety distances can no longer be built in densely populated areas.

In Switzerland, with its limited land resources and where the financial means are limited as well as in all other countries, we were forced to apply a more flexible instrument for the evaluation of the safety of installations for the manufacturing and storage of ammunition and explosives. According to the explosive safety regulations for the Swiss Federal Armament Industry, a quantitative risk analysis has to be performed for the safety evaluation of each new operation, manufacturing plant, building or storage facility. Similar regulations, also based on the risk concept, have been used for more than 15 years in the ammunition storage of the Swiss army. Today, quantitative risk analyses have become successfully applied routine work.

I do not intend to explain the methodology of risk analysis in detail (for the methodology of safety analyses see Ref. 1-6). However, I would like to point out again the advantages of this method (Figure 1):

1. thinking quantitively

2. risk thinking, i.e. measuring the danger to persons or material values in terms of actual risks and

3. cost/effectiveness thinking

It is generally accepted today that "risk" has to be a function of the possible consequences C as well as the probability P of an accident, here presented simplified as their product (Figure 2). The two factors are of the same significance. This means that when risk analyses are performed for a certain situation, we must not only quantify possible consequences, but also their probability. But if we actually try to quantify the terms C and P, we realize soon that we are confronted with two entirely different problems.

Today, we find quite a lot of information for quantifying the consequences of an explosion, based on theoretical studies and a large number of experiments which have been performed in the last twenty years. As an example our firm developed a computer program - called EXPLORISK - which allows to calculate the consequences of an explosion in any type of ammunition magazine in detail, according to the above mentioned Swiss regulations (Ref. 7). If more information on a specific problem is needed, there are tools and experience to perform appropriate additional tests.

In contrast to the quantification of the consequences, we can run into big problems when we try to quantify probabilities. How, for instance, can we find out the probability of an explosion in a dynamite storage facility? Or the probability of a melt-loading facility to be involved in a major accident? We cannot even think of a test to find this out!

2. HOW TO QUANTIFY PROBABILITIES

When we talk about probabilities of explosions in the field of explosives and ammunition, we should keep two issues in mind:

1. Probabilities of explosions vary within a wide range (Figure 3). While explosions occur relatively often during, e.g., the pressing process of lead azide, explosions in a TNT storage magazine surely belong to the very improbable events. Between these two extremes, there are many orders of magnitude.

2. From this fact we can deduct that it is obviously not suitable to distinguish just between dangerous and less dangerous activities, but to calibrate the dangerous activities as accurately as possible.

Now, how can probabilities of explosions be determined? I think that there are basically three possible approaches (Figure 4):

1. empirical /statistical approach
2. analytical/theoretical approach
3. subjective/intuitive approach

Today, the **empirical determination** of event probabilities by means of evaluating statistical data is widely used in the field of safety. In the case of high probabilities this normally presents no problems, as there are often sufficient data available. For example, it is usually easy to determine the probability of explosions during the pressing of primary explosives with the data which is available at the respective manufacturing plant. However, it is far more difficult to determine the probability of rare accidents. Here, there often exists no or little reliable information from within the actual field of experience. In such cases the field of experience has to be enlarged, for example from the level of one facility to the system of all national manufacturing plants, maybe even to worldwide installations. In the evaluation of the overall probabilities of explosions in ammunition magazines of the Swiss Army, e.g., we have not only considered our own national data, but also those which were

available from other western countries. Of course, questions arise such as: have we considered all relevant accidents, have we correctly assessed the number of installations to which the data sample refers, can these installations be compared with respect to the frequency of accidents, and so on.

There is no generally acceptable recipe, but our experience shows that such estimates often give plausible results which can be verified. The main pre-requisite for an empirical evaluation of event probabilities is to dispose of suitable accident statistics. In the next chapter, I shall come back to this point.

In the analytical approach event probabilities are deduced by means of physical or mathematical models. Fault-tree analysis is the most widely used method. It splits a hypothetical event up into basic events, until their probability can be determined. Of course, the input of a fault tree analysis is based on empirical data such as failure rates or even subjective estimates. One of the disadvantages is that errors in the partial probabilities can easily sum up so that, as a rule, the calibrating of the results against a more comprehensive system becomes necessary. On the other hand, the analytical investigation of a problem is often the best way to plan adequate measures as it clearly shows the possibly critical elements in a system. Let me give you two examples:

- More than 15 years ago, when we started to perform risk analyses for ammunition magazines, we asked ourselves about the basic causes for major explosions in underground ammunition magazines. Detailed analytical examinations led to the conclusion that approx. 80 % of all major accidents start with a fire, e.g. of packing material or powder. This is the reason why we still equip all our underground ammunition magazines with fire detection and an automatic fire extinguishing system.

- Explosives and ammunition transports between an important manufacturing plant in Switzerland and its storage area cross a main road which was one of the most important transit routes from southern to northern

Europe (Figure 5). The government found this situation intolerable and decided to invest about 7 million Swiss Francs (5 million US dollars) for the construction of an underground passage. Money being scarce in Switzerland as anywhere else, we have been contracted to study cheaper alternatives. Analytical in-depth investigations of the probable sequence of events and their causes showed that it was possible to reduce the original risks by a factor of almost 10 at a cost of only a few hundred thousand Francs. It could be proven unmistakenly that a considerably smaller risk reduction would have been achieved by the previously planned measures, which were almost 20 times more expensive.

The third approach to assess the event probabilities, the subjective or intuitive evaluation is often not considered as scientific and therefore not serious, or it is simply forgotten. In practice this approach means that event probabilities can be estimated, by experts who know about the conditions and circumstances of an activitiy, the sensitivity of materials, etc. This is called an educated guess (Ref. 8). If you have a group of experts for solving a problem, you can also use the more sophisticated Delphi method (Ref. 9). Quite often this approach is the only way to get a suitable result when there are no handy statistical data or no time for an analytical investigation.

These are the three principle possibilities to assess event probabilities (Figure 6). If we look at what we usually do when we estimate probabilities, we will see that in most cases we use a mixture of these three approaches. We start with some incomplete or limited statistical data, adjust them to our problem by a subjective or intuitive interpretation, combine this information by means of certain mathematical rules - and there we are!

Take an example: What is the probability of an explosion of 100 tons of dynamite stored in an igloo magazine? Let's try the intuitive guess first, before we are influenced by other approaches.

Nobody will know the exact answer. But actually we often know intuitively more than we are aware of. We know for sure that it is not once a year,

nor once in ten years and even once in 100 years would probably be the upper limit for most of us. Thus, if anything more frequent than once in several 100 years or, in other words, an event probability of 10^{-3}/year or higher results from our statistical or analytical investigation, we should be suspicious.

This kind of check of calculated result by common sense is something which I think should be done and trained, anyhow. And the last question of any analysis or investigation should always be: Does this make sense?

Let's now try the empirical, statistical or global approach. Maybe you think that's hopeless: we don't have any readily available statistics for explosions of dynamite storages. Let me now give you the following facts which are not too complicated to get (Figure 7):

In Western Europe and Canada we have a production of approximately 200'000 tons of dynamite per year. Every ton of dynamite is, on an average, lying about 1/10 of a year in a storage, waiting to be delivered to the customers. We found that in a period of about 20 years there were around 50 major accidents, all of them in production and none in storing. (Note that "no event" is also a statistical information.) From these facts we assumed that an accident in storing of dynamite has, as a conservative assumption, a return period of around 40 years which leads, on the average, to a probability about 100 times lower than in manufacturing (Figure 8).

From these figures we deduced:

Probability of a major accident in the lifetime of 1 t of dynamite

during production $50/20 \times 200'000 \cong 1 \cdot 10^{-5}$

during storing $1 \cdot 10^{-5}/100 \cong 1 \cdot 10^{-7}$

Probability of a major accident in a dynamite storage with a capacity of 100 tons (filled up 100 % of year)

$$P \text{ dynamite mag } 100\text{ t} \cong 1 \cdot 10^{-7} \times 10 \times 100$$

$$\cong \underline{1 \cdot 10^{-4} \text{ / year}}$$

The last approach, the analytical one, would attack the problem still from another side. Without going into details let me just indicate that here we would have to ask about the possible causes of an explosion in such a storage. From these different causes, their probabilities to occur and to cause an explosion, we can estimate the overall probability of an explosion in the storage.

This last approach is surely the most complicated one, but its advantage is on the other hand that we learn much more about our system than with a statistical or even intuitive approach.

Perhaps you have expected a precise mathematical formula, or a physical model to determine explosion event probabilities. Perhaps you find this procedure a bit homemade. But in fact it is the only sensible way to establish probabilities. We know that we are not very sophisticated and very precise in every case, but this is no reason for us to solve safety problems as if there were no event probabilities.

Let's leave this example now. I hope that you got a feeling that we really came from quite different sides and with quite different questions toward the probability we were looking for.

3. TOOLS

Let me now explain two tools which are of great help in dealing with event probabilities:

The first one which we call "Basic Frequency Rate System" is a table containing activities with dangerous goods listed against the so-called basic frequency rate. This is the probability of an event or, more precisely, the frequency rate F_e of its occurrence when one would uninterruptedly carry out a certain activity during a whole year (8766 hours) (Figure 9). The actual probability P_e per year of an event e can be established by simply multiplying it with the actual production hours t_e

$$P_e = \frac{F_e \times t_e}{8766}$$

In Figures 10 and 11 an actual and a simplified frequency rate table is presented. The fitting in of activities with dangerous goods into our basic frequency rate table has been established in the following way: some information has been taken from the accident statistics of the Swiss ammunition factories, other data has been found by global empirical considerations and others by means of analytical investigations. Many basic frequency rates, however, have been determined by a group of explosives experts in the subjective or intuitive approach I was talking about before. In this sense it represents a consensus among experts.

This Basic Frequency Rate System offers the advantage of making it possible to consistently classify dangerous activities. A consistent classification is often more important than absolute values when adequate safety measures have to be elaborated. Moreover, this system prevents gross misinterpretations and allows to incorporate new activities into the list so that they are easy to calibrate. There is a certain disadvantage inasmuch as a basic probability system cannot be applied universally, as it is often tailor-made for specific conditions such as manufacturing processes or general safety levels in a country or in a company. It goes without saying that it does not give any information on the cause of an event.

We have used - and continuously improved - this Basic Frequency Rate System for many years in risk analyses for entire factories and it was found to be very effective and practical.

The second vital tool for the assessment of event probabilities are statistics of explosion events. In fact, in many countries statistics about explosions are kept in one or the other way. But several years ago we realized that neither in Switzerland nor probably in other countries specially designed, easily accessible worldwide explosion event statistics exist for risk analysts who have to determine event probabilities and also explosion effects. For this reason we have started some years ago to collect reports of explosion and fire accidents in this field and to evaluate them in a way suitable for risk analysts.

The number of these reports (several thousands by now) has become so big that an evaluation by hand is no longer possible. We have started to develop a special computer program called EXPLOSTAT, wherein every accident is evaluated according to a given pattern, containing the following data (Figure 12):

- General information, i.e.
  . Date
  . Time
  . Country
  . Place
  . Company

- Event Data such as
  . Exact location of the event
  . Activity preceding the event
  . Involved substances
  . Type of reaction
  . Amount of involved substance
  . Cause of event

- Damage to Persons, such as
  . Number of deaths
  . Number of injured persons

- Damage to Material, i.e.
  . Total amount of loss
  . Range of window breakage
  . Range of debris throw
  . Crater dimensions
  . Propagation

A complete list of this data is given in Figure 13. The classification of the data is made by a code. Figures 14 and 15 give an example. This system makes it possible to answer almost any question with very little effort, such as "How many accidents are known in the USA during the melting and casting process of TNT between 1970 and 1980?" Several hundred

accidents have already been evaluated and implemented. Of course, we are fully aware that there is still a lot of work to do, but we are sure that this instrument will be of very big help, indeed.

4. CONCLUDING REMARKS

I hope that I have been able to show you what basic approaches exist for the determination of explosion event probabilities. Morover, I have described two tools which are handy when it comes to practical work.

Let me finish with two concluding remarks:

- We believe that we can no longer afford to guarantee the safety in the field of explosives and ammunition by limiting the consequences only, for instance by means of safety distances. Therefore, if we want to make use of the available financial means in the best possible way, we have to carry on with explicitly considering probabilities in our safety evaluations. As in other technical fields, where low probabilities are the most important safety guarantee.

- Today, there are means of establishing probabilities of rare accidents. One might refuse to believe this, and argue that an "exact" determination is not possible. Whatever is meant by "exact", it is my personal conviction that it is almost always possible to assess the probability accurately enough, which means that the result will be within the right order of magnitude. Nobody will expect that you assess the probability of an explosion up to three digits after the point. Here, as in other things, the phrase applies: "It's better to be roughly right than exactly wrong"!

REFERENCES:

1. Hans A. Merz: "Who ist Afraid of Risk Criteria?", presented at 22nd DDESB Seminar, Anaheim, 1986

2. Hans A. Merz, Andreas F. Bienz: "Methods of Quantitative Risk Assessment: The Case of the Propellant Supply System", presented at 21st DDESB Seminar, Houston, Texas, 1984

3. Hans A. Merz: "The Low Probability of Accidental Explosions; Isn't it Worth a Cent in Explosives Safety". presented at 20th DDESB Seminar, Norfolk, Virginia, 1982

4. Th. Schneider: "Practical Application of Quantitative Risk-Cost-Criteria to Explosives Safety", presented at 19th DDESB Seminar, Los Angeles, 1980

5. Th. Schneider: "How Much Should we be Willing to Pay for Explosives Safety?", presented at 18th DDESB-Seminar, San Antonio, Texas, 1978

6. Th. Schneider: "Some Principles for a Quantitative Approach to Safety Problems in Explosives Storage and Manufacturing in Switzerland", presented at 17th DDESB Seminar, Denver, Colorado, 1976

7. "EXPLORISK - Computer-Supported Risk Analysis for Explosives Storage Installations", Report by E. Basler & Partners Ltd., 8702 Zollikon, Switzerland, 1987

8. Samuel Kotz, Donna F. Stroup: "Educated Guessing - How to Cope in an Uncertain World", Marcel Dekker Inc., New York and Basel, 1983

9. Harold A. Linstone, Murray Turoff (eds.): "The Delphi Method - Techniques and Applications", Addison-Wesley Publishing Company, Reading, Mass., USA, 3rd printing, 1979

Safety Analysis

means

1. Thinking Quantitatively

2. Measuring the Danger in Terms of Actual Risks

3. Thinking in Terms of Cost/ Effectiveness

Figure 1

Definition of Risk

$R = f(P, C)$

$R = P \times C$ **(simplified)**

P = Probability of an Accident

C = Consequences of an Accident

Figure 2

Range of Probabilities for Explosion Events

Pressing of Primary Explosives

Storing of Insensitive Explosives

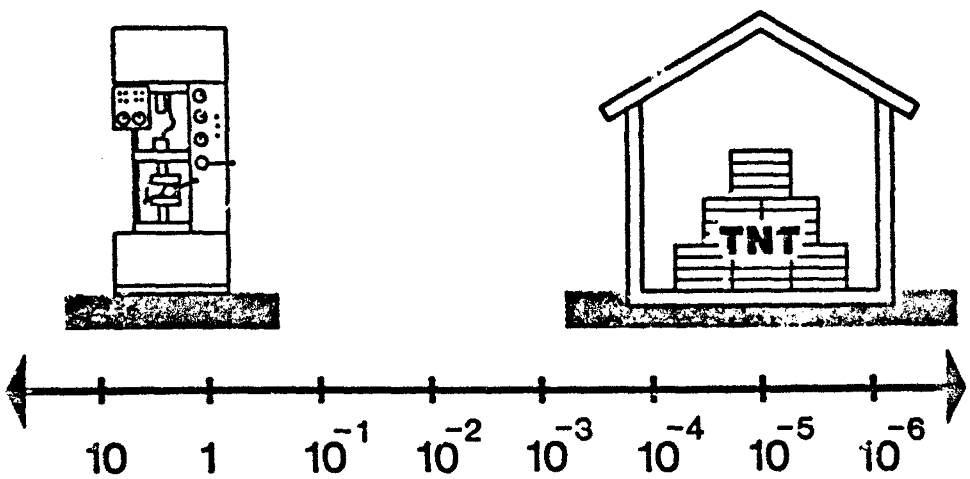

Frequency Rate of Event per Year

Figure 3

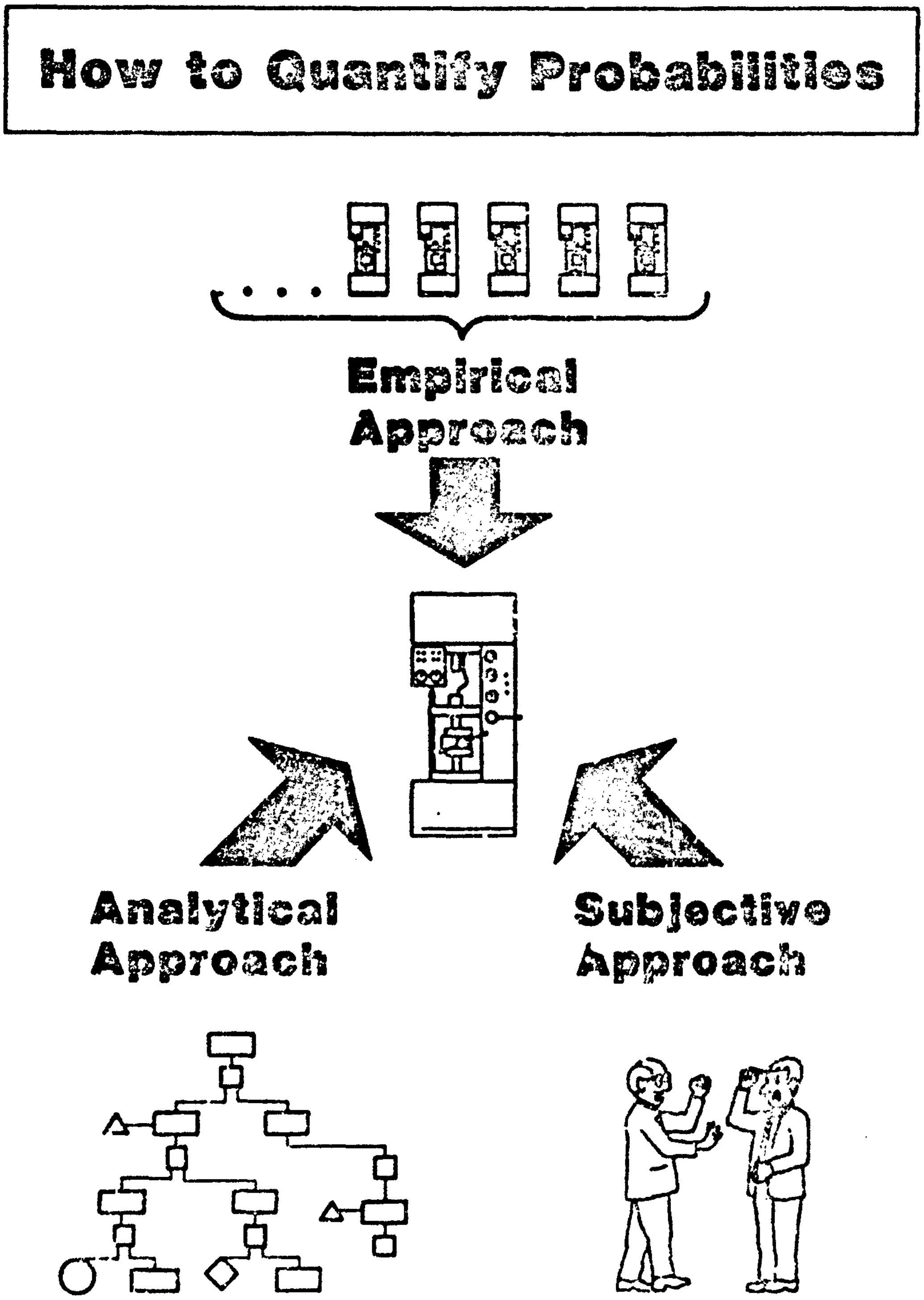
How to Quantify Probabilities
Empirical Approach
Analytical Approach
Subjective Approach

Figure 4

Example

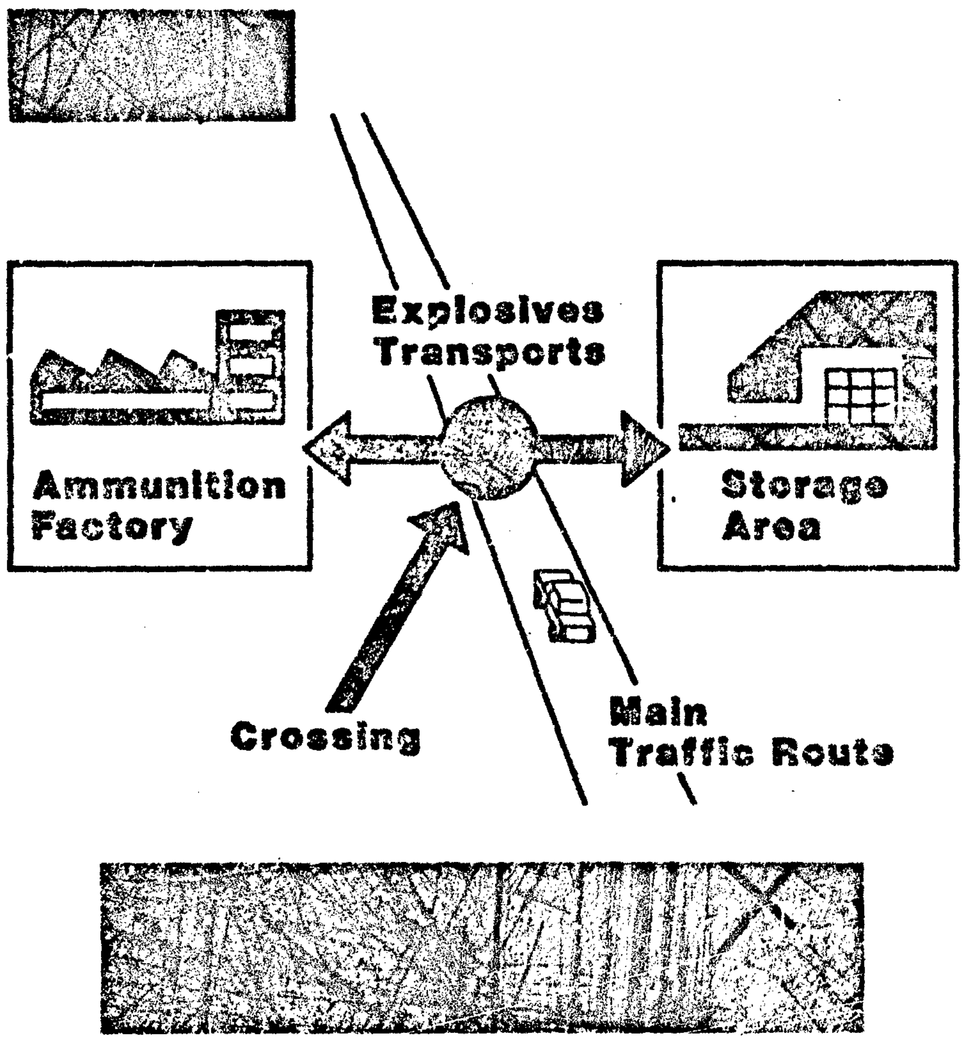

Underground Passage,
Costs 5 Million US $

Figure 5

Quantification of Probabilities

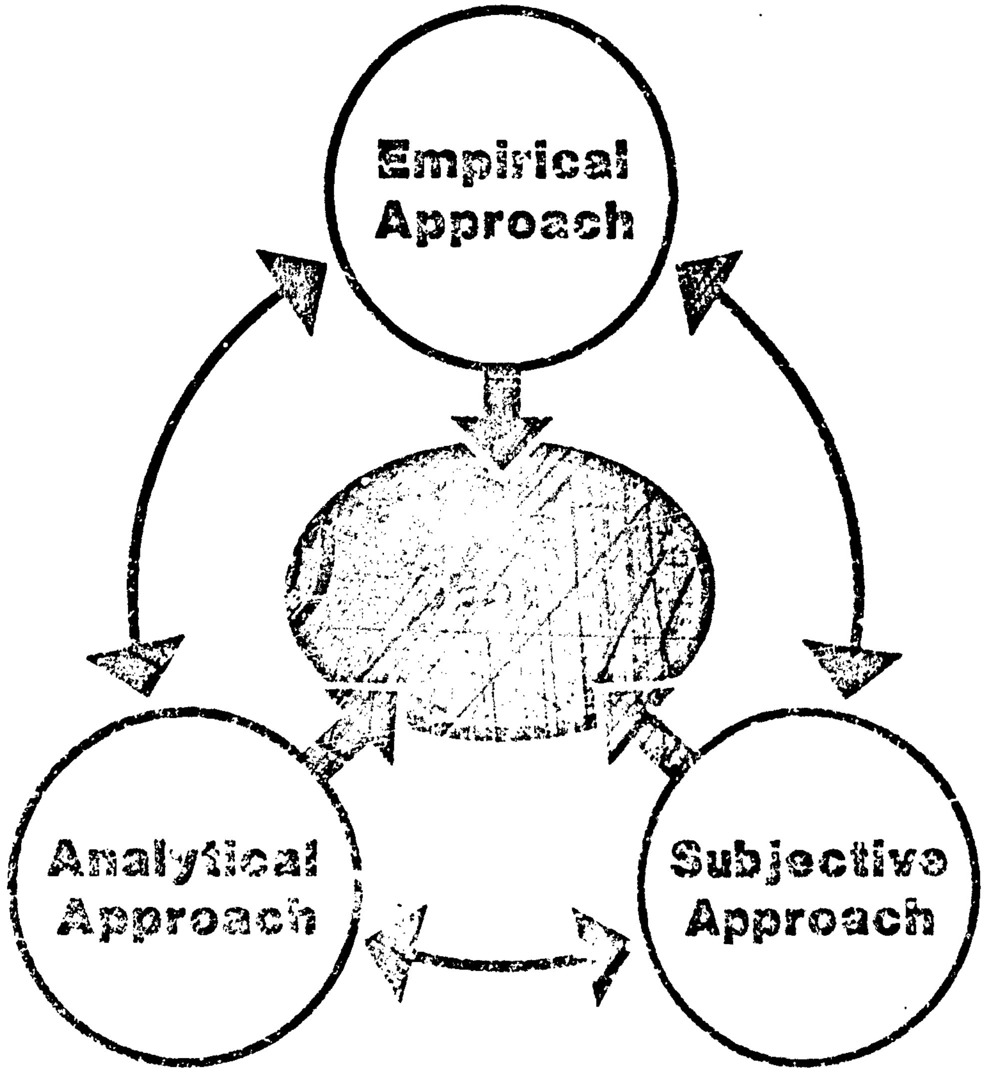

Figure 6

Example: Probability of Explosion Event in Dynamite Storage

- Production of 200'000 t of Dynamite per Year in Western Europe and Canada

- Every Ton of Dynamite is Stored 1/10 of Year on the Average

- Around 50 Major Accidents in Around 20 Years

- All Accidents in Manufacturing, <u>none</u> in Storing

Figure 7

Example:
Probability of Explosion Event in Dynamite Storage

Accident in Storing is About 100 Times Less Probable than in Manufacturing

$$\text{in Production} \quad \frac{50}{20 \times 200'000} \cong 1 \cdot 10^{-5}$$

$$\text{in Storing} \quad \frac{10^{-5}}{100} \cong 1 \cdot 10^{-7}$$

$$1 \cdot 10^{-7} \times 10 \times 100 \cong 1 \cdot 10^{-4}/\text{year}$$

Figure 8

Basic Frequency Rate System

Frequency of an Accident (Explosion, Fire) within 8766 Working Hours (1 Year)

$$P = \frac{F \times t}{8766}$$

F = Basic Frequency Rate

t = Actual Working Hours

Figure 9

Basic Frequency Rate System

Actual Example

Produkt	Verpackung, Zustand	Art der Einwirkung	Q_{TNT} %	100	1	10^{-2}	10^{-4}	10^{-5}
TNT	gegossen, geschuppt, gepresst	lagern						●
	geschuppt	sieben, maschinell					●	
	geschuppt	pressen				●		
	fest flüssig	schmelzen, giessen					●	
	fest	abbechern					●	
	Körper	laborieren, maschinell					●	
		laborieren, von Hand						●
Nitropenta (Penta)	20 % H_2O-feucht	lagern						●
	trocken	lagern						●
		volumetrisch dosieren					●	
		mech. bearbeiten				●		
		pressen			●			
Hextro, Oktol	Kessel	lagern						●
		pressen			●			
		giessen					●	
		abbechern					●	
Hexastit, Oktogen, Oktastit, Pentastit	Metalldose, Kartonfass	lagern						●
		pressen			●			
Trizin	Kanne 25 % H_2O-feucht	lagern						●
		einwägen						●
Div. neue Munition - ohne Sprengstoff (Menge < 1 t brutto)	fertig laboriert	lagern						■◐
		verpacken von Hand						■◐
	im Fabrikationsablauf	laborieren					■●	
- mit Sprengstoff ohne Zünder (Menge < 1 t brutto)	fertig laboriert	lagern						●
		verpacken von Hand						●
	im Fabrikationsablauf	laborieren (nicht am Sprengstoff)						●
		laborieren (am Sprengstoff)					●	
- mit Sprengstoff mit Zünder (Menge < 1 t brutto)	fertig laboriert	lagern						●
		verpacken von Hand						●
	im Fabrikationsablauf	laborieren (nicht am Sprengstoff od. Zünder)					●	
		laborieren (am Sprengstoff/Zünder)					●	

(Valid for Swiss Standards only)

Figure 10

Basic Frequency Rate System

Example

	Basic Frequency Rate ([illegible])
Pressing of Initial Explosives	10^{2}
Pressing of PETN	10^{1}
Pressing of RD	10^{0}
Pressing of TNT	10^{-1}
Drying of Initial Explosives	10^{-2}
Working with Wet Initial Explosives	10^{-3}
Melting and Casting of TNT	10^{-4}
Assembly of Ammunition without Fuse	10^{-5}
Storing of TNT (smaller amounts)	10^{-6}

(Valid for Swiss Standards only)

Figure 11

Data Base EXPLOSTAT

- **Date, Time, Country, City, Company**

- **Place of Event, Activity before Event, Type of Explosive, Amount of Explosive, Cause of Accident**

- **Damage to Persons**

- **Damage to Materials Cratering, Propagation**

Figure 12

Data Base EXPLOSTAT

Example of Output

```
DATA BASE EXPLOSION EVENTS (DETAILED INFORMATION)                                        No.   102

GENERAL        Date     :   11.  1.  1985                  Time            : 14.00
INFORMATION:   Country: d        West Germany              Place           : US-Base "Red Leg" near Heilbronn
               Company: -        US-Army                   Responsibility: N      US-Army
---------------------------------------------------------------------------------------------------
EVENT DATA:    Location      :  5040        3010     open place in a US-Army base
               Activity      :  3630.2               unpacking of a Pershing II rocket motor without war head out of a metall container with a
                                                     crane

               Substances    :  2040                 solid-fuel / propellant HTPB (Ammoniump.)

               Containment   :  2050                 rocket motor for Pershing II, 1. stage
               Reaction      :  2010                 intensive, fast burning fire (2 min)
               Quantity [kg]:       3500.0000        about 3500 to 4000 kg

               Cause         :  1311                 electro-static discharge because of extreme weather conditions could ignite the rocket
                                                     motor (confirmed by investigation)  --> 1),2)
---------------------------------------------------------------------------------------------------
PERSONAL INJURIES: Dead (total / not involved)     :  3 /  0      Lightly wounded (total / not involved)  :  7 /  0
                   Injured (total / not involved) : 16 /  0      Seriously wounded (total / not involved):  9 /  0
                   Further Details:  N       Remarks:  all dead and injured persons were Americans and suffered serious burns
---------------------------------------------------------------------------------------------------
DAMAGE TO      Range of Damage            :  K       Crater          : N           Propagation  :  N
MATERIAL:      . Building Destruction [m]:           . Depth [m]    :   0.00       . Distance [m]:
               . Window Breakage [m]     :           . Diameter [m] :   0.00       . Substance   :  rocket motor 2. stage
               . Debris Throw [m]        :   125.

               Amount of Loss [SFr]      :           Further Details  : N
               Barricades                :           Remarks          : the rocket motor disintegrated partially and "blew" fragments away up
                                                                        to 125 m
---------------------------------------------------------------------------------------------------
               Remarks:        1) the temperature was extremely cold (-20 C) and the humidity of the air very low
                               2) obviously the sensitivity of the rocket motor by a temperature of -20 C against electro-static discharge was never
                                  tested

               Source  : Z/U, d,e                   Classification:   -                   Size        :   40.00
               File    : EBP 12 / 59.3 / 3.2                                              Evaluation:        U
```

Figure 13

Data Base	EXPLOSTAT

1000	Explosives
2000	Powders (smokeless)
3000	Black Powders
4000	Initial Explosives
5000	Pyrotechnics
.	
.	
.	

Figure 14

Data Base EXPLOSTAT

[illegible]

[illegible]

1000 Explosives

1100 Nitric Acids

1101 PETN

1102 Nitroglycerine

1103 Nitroglycol

⋮

1200 Nitramine Explosives

1201 RDX

1202 HMX

⋮

Figure 15

TWENTY-THIRD EXPLOSIVE SAFETY SEMINAR
ATLANTA GEORGIA

TACTICAL MISSILES PRODUCTION FACILITIES APPLYING THE FRENCH EXPLOSIVE SAFETY CONCEPTS

By Maurice CHIZALLET
Explosive Safety Engineer

MATRA
37 avenue Louis Bréguet
78140 - VELIZY-VILLACOUBLAY
FRANCE

Presented with Gilbert CROZE

MATRA AEROSPACE
Crystal City Gateway IV - Suite 1102 -
1213 Jefferson Davis Highway
Arlington VIRGINIA 22 202

"Tactical Missiles" Production Facilities applying the French "Explosive Safety" concepts

•0•

ABSTRACT

The principles on which the Explosive Safety is based in France were presented during the 22nd E.S.S. in 1986. The aim of this Paper is to show the concrete application of the Explosive Safety regulations, within the context of the fabrication of tactical missiles, with the steps taken to perform the industrial operations, while guaranteeing a high safety level for the operators, as well as for the environment.

The method that enabled the general regulations to be applied to the particular activity of the missiles, to design and layout the missiles integration buildings, is described.

A detailed example is given of a modern workshop, permitting the mass production of a surface-to-air missile, with a maximum safety level for the personnel and the environment.

1. - INTRODUCTION

The principles on which the explosive safety are based in France were presented during the 22nd Explosive Safety Seminar by Engineer General AMIABLE who gave the viewpoint of the French official authorities, and by Mr RAT who expressed the opinions of explosives, powders and propellant manufacturers.

The same explosive safety regulation is applicable to the whole of French industry involved in the production of explosive products and items. But the evidence points to the fact that problems met with in the course of industrial activity in this area, whether at hazard or accident probability level, are rather different. Each manufacturer must therefore analyse his own specific case with regard to those major principles detailed in the safety regulations and then define the means he must implement to comply with them.

At MATRA, missile assembly in conditions assuring the safety of production personnel and the environment is undertaken in strict compliance with the regulation in force since 1980 when designing and implementing the required production facilities, and when setting the operating rules in order to justify its decisions with the official agencies.

The facilities described hereafter enable us to ensure a high safety level. Due to their innovative design, representatives of our various industrial partners, that is to say, our cooperants and customers, often ask to visit them.

2. - REMINDER ON THE PRINCIPLES OF THE FRENCH REGULATION FOR EXPLOSIVE SAFETY

The French regulation is based on the requirement for the establishment manager to conduct a safety analysis.

The goals of the analysis are :

- To detect all the possibilities of explosive accidents,

- To establish the type and importance of the risks incurred by the personnel in each case,

- To determine the steps to be taken to avoid accidents and to limit their effects.

During preparation of the safety analysis it will be necessary to determine :

- The classification of explosive materials or items in the appropriate risk class.

- The hazard zones (Zi) resulting from the presence of a quantity of explosive materials or items taking account :
  - Of the specific explosive properties in their implementation conditions,
  - Of existing conditions likely to change the hazard.

- The estimated accident probability (PJ).

The impact on personnel, facilities and the environment must be checked by means of these factors.

The above points are at the core of French thinking with respect to explosive safety. They are often cited under the form Zi/Pj/ak which represents the criteria : hazard zones (Zi), accident probability (Pj), and the layout rules for the facilities (ak) (see annex 1).

The safety analysis must be carried out prior to any new activity, construction of buildings or modification of workplaces likely to have an impact on personnel safety.

An extremely rigorous in-depth approach is necessary to meet these different goals.
The result allows the manufacturer to organize his plant so as :

- to expose personnel only to a strictly minimal risk after taking all necessary steps to avoid that risk, and

- to reduce, if not prevent, accident propagation.

One fundamental point of the spirit of the safety regulation consists also in not limiting safety matters to a restricted circle of informed persons but to heighten the awareness and involvement of all personnel concerned with safety to the level of a basic principle. So all persons involved are informed regarding any remaining risks deemed acceptable.

Lastly, safety analysis approval by the administration department responsible for the workplace and the environment facilitates a positive dialog, together with a further examination by an agency which is not directly linked with the working of the establishment.

3. - APPLICATION OF THE SAFETY REGULATION TO TACTICAL MISSILE ASSEMBLY OPERATIONS

In general, MATRA missiles essentially consist of the following explosive units :

- a warhead,
- a safety and arming unit,
- a rocket motor igniter,
- a solid rocket motor.

The principal phases encountered during missile manufacture are :

- The assembly and testing of non explosive equipment,
- the assembly of the complete operational missile,
- missile testing, and
- missile packaging and containerization.

Of course, some related operations, such as transportation, handling and storage also require logistic facilities.

All types of hazards inherent in the following units must be taken into account when defining missile production facilities :

- warhead : hazards due to the detonation and the projection of fragments,

- rocket motor : mainly hazards of thermal origin characterized by a brief jet of flame in one direction,

- warhead or rocket motor ignition devices : are often a small hazard, but have enhanced sensitivity and are therefore generally provided with effective safety barriers.

Lastly, account should be taken of rocket motor behavior in the event of accidental warhead detonation, notably to deduce the missile TNT equivalent mass.

Before the present regulation became applicable, missile assembly operations were conducted in buildings comprising 3 main rooms :

- 1 non explosive units assembly room,
- 1 missile assembly workshop where work was conducted on an assembly line basis,
- 1 test room.

The application in 1980 of the new regulation controlling explosive safety and the fundamental principle :

> "Buildings must be designed and built in a manner such that an explosive accident shall not generate a major risk for persons other than those who, due to their work, must remain exposed to the possible effects of a potential accident",

illustrated by the Zi/Pj/ak triptyque previously mentioned, has led us to review the general design and layout of our explosive production buildings.

3.1. - Determination of risk levels

The first criteria we had to fix were therefore the risk levels presented by the explosive assembly operations on our missiles.

All these operational phases take place with the warhead present, except where otherwise specified.

If the level of "risk" is considered to be the result of a "hazard" multiplied by the "occurrence probability", we can assume that the greatest hazard is always the possibility of a warhead exploding.

Three occurrence probability classes have been chosen, based on the administration's instructions. Thus, the risks incurred in the course of missile assembly may be grouped at three levels :

- Level 1 - Extremely rare :
  Risk related to missile storage and handling operations.

- Level 2 - Very rare :
  Risk related to missile assembly operations.

- Level 3 - Rare :
  Risk related to complete round missile test operations.

It must be stated that as regards our own industrial experience, no accident has ever occurred during missile production at MATRA's missile facilities. We would therefore imagine that these three risk probability levels are extremely severe.

3.2. - Transcribing these risk levels into general layout principles for assembly buildings

The goals assigned to the buildings are designed to ensure :

- personnel protection,
- environment protection,
- work tool preservation.

For this, 3 basic principles must be satisfied :

1°) Maximum risk separation,

2°) Directing the effects of an explosion in a specific direction,

3°) Matching every room to the risk level of operations performed in it :

- Level 1 - Extremely rare (P1)
  The buildings (or rooms) are constructed without any special constraints at roof or wall level, apart from avoiding detonation by propagation from one room to another.

- Level 2 - Very rare (P2)
  This risk level requires work stations to be partitioned off into separate work cells so as to limit the permanent staff in each work cell to two, three or occasionally four persons.

  These work cells are sized so that an explosion in one of them will not cause any serious bodily harm in adjacent cells. They have a concrete roof and walls reinforced with steel rods.

- Level 3 - Rare (P3)
  This risk level requires working without exposure to hazard.
  If the room is contained within the main building it has a concrete roof and walls like a single work cell.

3.3. - <u>Description of a missile assembly building according to these principles</u>
(see annex 2)

<u>ROOM 1</u> - <u>Inert section</u>
This is the non-explosive part of the building

- electronic equipment assembly,
- workshop foreman's office.

The roofing is in concrete or metal frame, depending on the over-pressure loading which may result from the potential seat of explosion (rooms 2 to 5).

A metal frame with a steel mesh under the roof generally suffices to prevent roof parts or other projections from falling into these rooms in case of accident.

ROOM 2 - Assembly and tests explosive section

There is only a single missile at a time in these cells :

- During assembly, 2 operators,
- During testing, no operator present. Testing is conducted from the inert zone or a neighbouring cell.

The cell structure consists of 3 blast walls and a strong concrete slab and ceiling. These 5 facings are very strongly interconnected by a steel lacing (angle plate to avoid stressing). A heavy door is provided to resist an accidental explosion inside the cell. The 4th wall is a blow out wall giving onto a barricade in order to protect against projections.

In case of an explosion, only the blow out wall is destroyed and fragments are ejected towards this wall by the external walls which extend as far as the middle of the barricade.

The back-pressure wave on the neighbouring cell does not demolish the adjoining blow out wall ; personnel working in it are therefore not likely to sustain injury by the accident. The blow out walls act like electrical diodes in that they are :

- destroyed on internal overpressure,
- but will resist if there is an external overpressure.

This design allows all work cells to be situated next to one another facing the same direction.

ROOM 3 - Daily magazine

This room is used to store several warheads and rocket motors on stand-by for assembly. Its design is of the igloo type and it is located far enough from the main building for an overpressure resulting from an accidental explosion, to be acceptable for the rest of that building.

ROOM 4 - Packaging and containerization room

It is built with strong walls and a light-weight roof. In case of explosion in this room, the walls and the roof are destroyed, but the explosion does not propagate beyond the room.

Should an explosion occur outside this room, the roof may be destroyed but not the metal frame supporting it. The sheet metal is held in place by the steel mesh under-frame to avoid injury to personnel below.

ROOMS 5 and 5' - Corridors

The walls of these corridors are strong. They have been calculated to withstand the accidental explosion of a missile. The concrete roofing is strong in the corridor area dividing it from the "inert" part (5).

The roofing can be in metal in those corridor segments which are further from the "inert" part (5').

These corridors act as an airlock by means of a servo system for opening the heavy cell doors, giving access to the inert section.

EXPLOSIVE YARD 6

The trailors linking up with the central stores are loaded and unloaded in this yard, for :

- bringing in crated warheads and rocket motors,
- dispatching complete containerized missiles.

This yard is an asphalted area surrounded by barricades or buildings. It is provided with a chicane entrance so that all grazing fragments would be stopped in the event of explosion.

3.4. - Determination of allowable explosive quantity in the rooms

The allowable explosive quantity in the rooms must be determined after freezing the design and layout principles of the buildings. Two parameters must be studied :

- The room explosion resistance rating, expressed in TNT equivalent mass. This value can be either specific to a program or an overall figure covering a missile family, and would allow a utilisation flexibility as the programs advance.

- The weight, speed and energy characteristics of the burst fragments which would be projected.

These parameters will allow to analyse and set up the various safety measures needed to ensure the personnel and plant safety in compliance with the regulation, notably :

- determination of the characteristics of the explosion-resistant walls,

- barricade sizing and location,

- calculation of the safety distances between different types of facility.

3.5. - PERSONNEL PROTECTION FACED WITH AN UNTIMELY FUNCTIONING OF A ROCKET MOTOR

The tools used for missile assembly in the assembly cell play an essential part in personnel safety as regards untimely rocket motor ignition.

Assembly is on a jig connected to the cell floor. The assembly jig is designed to retain the rocket motor securely in case of untimely ignition. This assumes that the rocket motors are fitted with mechanical devices with which they can be attached to the bench. This rocket motor securing is assured throughout P2- or P3-type operations.

In addition, the assembly jig is installed in the cell axis, closest to the blow out wall with the rocket motor nozzle pointing towards the latter.
A prefragilized diaphragm has been inserted in the blow out wall in line with the rocket motor so that if the rocket motor ignites, all the combustion gases are immediately expelled outside, without flame return toward the operators.

All these arrangements (the assembly jig and prefragilized diaphragm in the rocket motor axis) protect the operators most effectively. Solely operator hearing would be impaired in the event of untimely rocket motor ignition.

4 - ILLUSTRATION BY A REAL EXAMPLE OF A PRODUCTION FACILITY DESIGN AND DEVELOPMENT

4.1. - Definition of the requirement and design of the facility

We have designed some buildings for missile assembly and testing in the frame of a new ground-to-air tactical missile program.

In this case, each missile possesses :

- An explosive charge with its safety and arming unit consisting of a mechanical and electrical non-alignment of the ignition train.

- A propulsive section comprising a launch motor and a main rocket motor which is equipped with a safety ignition device based on the same principles as the warhead.

We have found the minimum explosive charge rating of each room from the unitary TNT equivalent according to the number of missiles liable to be inside the room and, in case of accident, of causing a mass detonation. However, we have chosen a rating higher than these calculated results to avoid tying down the use of these rooms to this one program.

The following rooms are required for production of this type of missile :

- Workshops for assembly and testing electronic subassemblies.

- A distribution corridor acting as an air-lock between the "inert" part of the building and its "potential seat of explosion".

- A daily magazine intended for supplying parts to the assembly machines rated at 600 kg TNT equivalent. Detonation transmission by propagation between neighboring explosive charges is prevented by partition walls to split the risk.

- Explosive assembly cells foreseen for achieving assembly in manual and automatic modes :

  1°) Manual and test assembly cells rated at 70 Kg TNT equivalent, complying with the principles stated in Ch. 3.3 above, i.e. comprising 5 strong walls, and a blow out wall bearing on two posts. A fragilized part in alignment with the rocket motor allows the combustion gases resulting from an untimely accidental ignition of the latter to be evacuated. An assembly jig secures the missile in this case.

  2°) Assembly and automatic test cells rated at 15 kg TNT equivalent, operated according to the following principles :

    - Automatic production chain procurement in explosive items from the daily magazine previously mentioned.

    - Missile section transfer to the assembly machines, then assembly and electrical connection.

    - Complete round ammunition transfer to the test cell.

    - This automatic facility is supervised by an operator who is protected from an accident at any potential seat of explosion.

  3°) An ammunition packaging room rated at 140 kg TNT.

4.2 - Installation safety analysis

The installation just described allows any hazards inside the buildings to be controlled by the 5 strong walls which are calculated in accordance with the data given in TM5-1300.
However, in the event of an explosion inside a cell the blow out wall would allow the escape of a leak pressure that has been calculated as a function of the TNT equivalent taken account of for the rating. Knowing the areas submitted to pressure it is then possible to determine the structure of other facilities which risk being damaged by an accidental explosion. This construction principle enables the reduction of overpressures, especially at the rear of the building, and thus to set up those activities related to the functioning of the facility which remains subject to risk. Such a hazard may be overcome at the cost of some simple precautions, such as installing steel mesh to avoid roofing falling on personnel.

As regards fragment projection, the blow out wall faces a barricade and the horizontal and vertical walls are extended to limit the projection angles.

Conformity to the fundamental principle of the safety regulation concerning personnel exposure to risk, i.e. rule Zi/Pj/aK, is then checked.
An explosion at a potential seat, or donor, designated ao, puts the other facilities at risk, called a1, in a hazard zone Z4 for a P3 risk probability. This procedure proves to be entirely in compliance with the French safety regulation (see table in annex 1).

In addition to these steps designed to control the effects of an accident, there are of course other precautions for preventing stresses, or accident escalation into the worst possible case. We specially note :

- Building air conditioning (both temperature and relative humidity),

- Equipotentiality of all conducting elements,

- Conducting floors,

- Antistatic garments, special conductive safety shoes and earthing bracelets,

- Firefighting by an automatic fast deluge system fed by two independent water supplies.

4.3. - Environment safety

The exposure to risk of the other facilities, workshops, offices, etc. of the plant shall form the subject of an analysis according to the Zi/Pj/ak rule.
Each risk donor will be considered a potential seat of explosion ; the other "active" or "inert" buildings may be installed if the safety of personnel and facilities is deemed acceptable.

For instance, missile production requires two quite distinct potential seats of explosion : the workshops, such as those previously presented, and storage bunkers which mainly consist of igloos. These two activities present a very different risk due to their hazards and accident probability levels.
The safety analysis for determining building installation therefore takes account of the exposure to reciprocal risks :

1°) The missile storage igloos, potential seats of explosion (risk donors) designated ao, have a P1 accident probability level.
The workshops (risk receivers) designated a2 installations (see annex 1) may be located in the Z2 zone, which is evaluated according to the igloo safety rating (function of "Q" kg and hazard class).

2°) Conversely, the igloos are risk receivers designated a2 of hazard coming from the workshops, which then become potential seats of explosion (risk donors) and have a higher accident probability level P3. Thus, the igloos cannot be located in a hazard zone less than Z3. The latter is calculated according to the workshop explosive safety rating (function of "Q" kg and hazard class).

This procedure is carried out for all the plant facilities.

Finally, depending on the explosive load rating of the plant's various potential seats of explosion, the hazard zones (Zi) of all the facilities are drawn to show the impact of an accidental explosion on the environment and, if need be, to enable adequate protection measures to be taken.

5. - CONCLUSION

The French regulation which defines the safety principles to be satisfied during the production of explosive materials or items can be a source of constraint for industrialists. This is specially true for financial investment, which is required both for conducting safety analyses as for the construction of production facilities.

The advantages however are clear. It is almost impossible to manufacture weapons systems without hazard. But as we have shown, acceptable risk criteria can be met, allowing to ensure that all possible risk avoidance steps have been carefully analysed. Therefore an explosion hazard and its impacts can be controlled.

ANNEX 1

RULE Zi/Pj/ak

DESIGNATION OF HAZARD ZONES

1)

Z_i	PERSONAL INJURY	PROPERTY DAMAGE
Z_1	LETHAL INJURY IN MORE THAN 50 % OF CASES	VERY SEVERE DAMAGE
Z_2	SERIOUS INJURIES WHICH MAY BE LETHAL	SEVERE DAMAGE
Z_3	INJURIES	MEDIUM AND SLIGHT DAMAGE
Z_4	POSSIBILITY OF INJURIES	SLIGHT DAMAGE
Z_5	VERY LOW POSSIBILITY OF SLIGHT INJURIES	VERY SLIGHT DAMAGE

DESIGNATION OF CLASSES OF PROBABILITY

2)

P_i	LEVEL	EXAMPLE
P_1	EXTREMELY RARE	STORAGE AND HANDLING
P_2	VERY RARE	ASSEMBLY OPERATIONS
P_3	RARE	COMPLETE ROUND MISSILE TEST OPERATIONS
P_4	*RATHER FREQUENT*	*OPERATIONS ON VERY SENSITIVE MATERIALS, PRODUCTION OF PRIMARY EXPLOSIVES*
P_5	*FREQUENT*	*MIXING, COMPRESSION OF PRIMARY EXPLOSIVES*

3) **DESIGNATION OF INSTALLATIONS TO PROTECT FROM DONOR "ao"**

1. FACILITIES INSIDE THE PLANT

- a_1 EXPLOSIVE FACILITIES HAVING TO BE LOCATED NEAR "ao"
- a_2 OTHER EXPLOSIVE FACILITIES AND INNER ROADS
- a_3 INERT BUILDINGS

2. ROADS OUTSIDE THE PLANT

- b_1 TRAFFIC < 200 VEHICULES/DAY
- b_2 TRAFFIC BETWEEN 200 AND 2000 VEHICULES/DAY
- b_3 IMPORTANT TRAFFIC > 2000 VEHICULES/DAY

3. BUILDINGS OR OTHER PLACES OUTSIDE THE PLANT

- C_1 UNINHABITED, SHORT PRESENCE
- C_2 INHABITED BY OR WITH PRESENCE OF PLANT PERSONNEL
- C_3 OTHER FACILITIES, HOUSES,
- C_4 GATHERING PLACES OF PEOPLE : MARKETS, SCHOOLS, HOSPITALS, DENSELY BUILT UP AREAS.

4) **RULES OF CONFORMITY "ak/ Zi/ Pi"**

probability / hazardous zone	P_1	P_2	P_3	P_4	P_5
Z_1	a_o	a_o	a_o(x)	a_o(xx)	a_o(xx)
Z_2	a_1 a_2	a_1 a_2(x)	a_1	a_1(x)	a_1(xx)
Z_3	a_1 b_1 c_1 a_2 a_3	a_1 b_1 c_1 a_2	a_1 a_2	a_1	a_1(x)
Z_4	a_1 b_1 c_1 a_2 b_2 c_2 a_3	a_1 b_1 c_1 a_2 b_2 c_2 a_3	a_1 b_1 c_1 a_2	a_1 a_2	a_1
Z_5	a_1 b_1 c_1 a_2 b_2 c_2 a_3 b_3 c_3	a_1 b_1 c_1 a_2 b_2 c_2 a_3 b_3 c_3	a_1 b_1 c_1 a_2 b_2 c_2 a_3 b_3 c_3	a_1 b_1 c_1 a_2 b_2 c_2 a_2 b_3 c_3	a_1 b_1 c_1 a_2 b_2 c_2 a_3 b_3

(x) presence limited to maximum 10 % of the working time.
(xx) no presence allowed except in particular circumstances.

TYPICAL MISSILE ASSEMBLY BUILDING

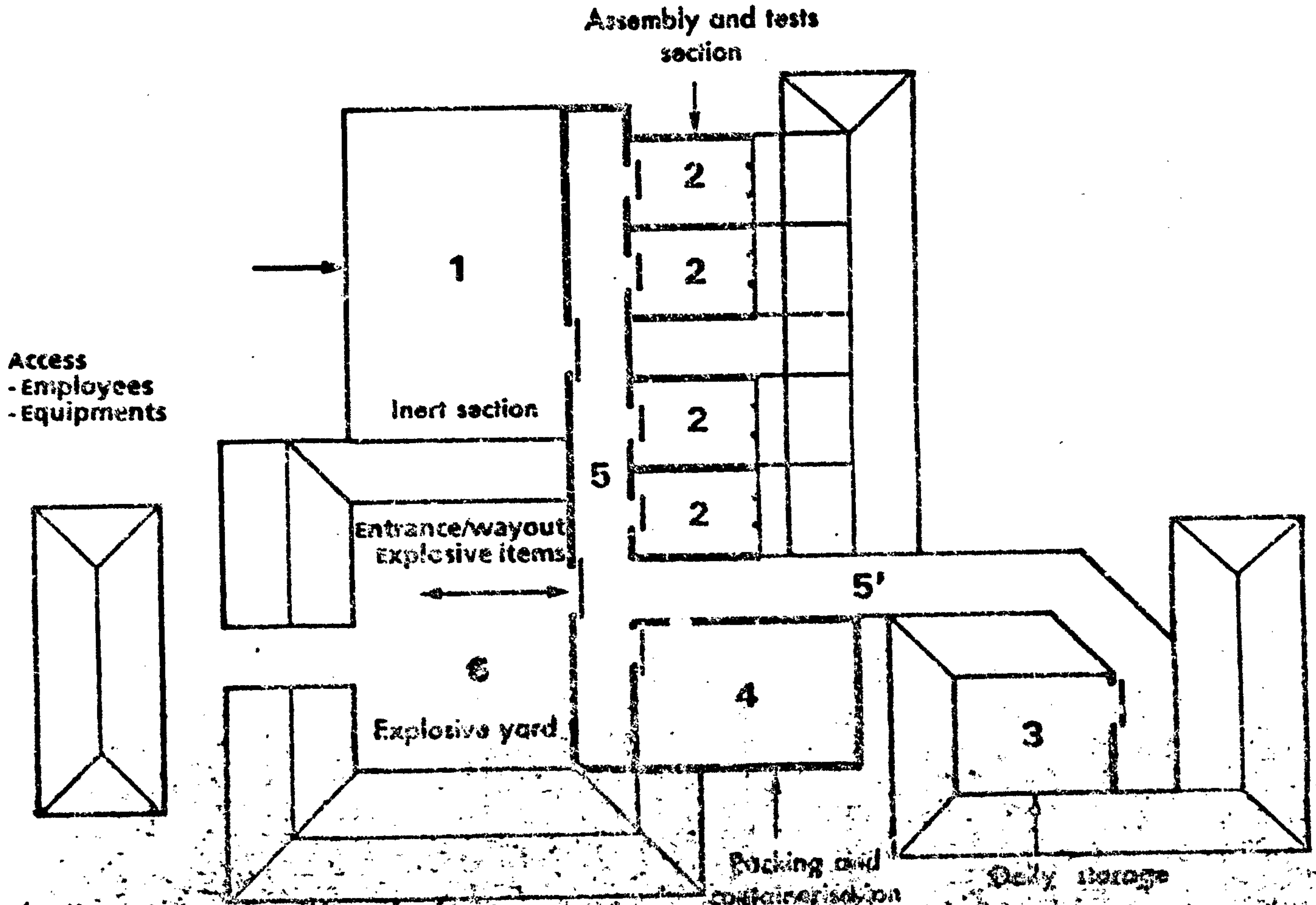

ANNEX 3

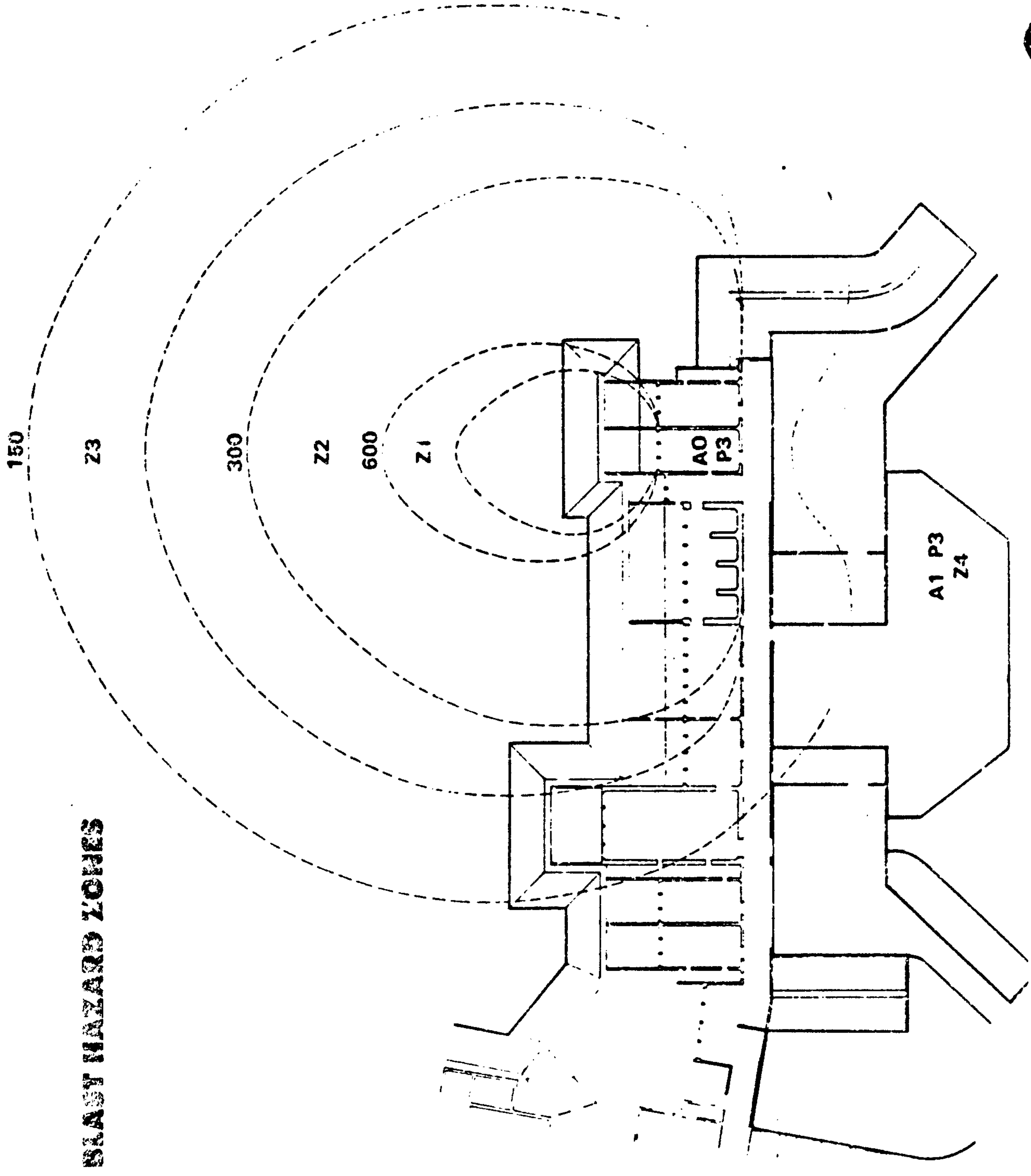

BLAST HAZARD ZONES

SAFETY DISTANCE UNDER BLAST LOADING

He Chengzhi and Li Zheng

Engineering Design and Research Institute

BEIJING, P. R. C.

ABSTRACT

In this paper, some results of experimental and theoretical studies and numerical calculation carried out in our country for determination of the intraline safety distance under detonation of explosives are presented.

SAFETY DISTANCE UNDER BLAST LOADING

INTRODUCTION

In the processing, transportation and storage of industrial explosives, and in the blasting applications of mineral, railway, highway and hydraulic engineering, we have to meet the problem of considering the building damage and human injury caused by airblast waves during explosion. Usually a building must be kept a certain distance away from the explosion source for safety measure. The safety distance to be considered, whether larger or smaller, is not only related to protection of the life and property of the people and the normal running of production, but also related to the saving of land and cost. Since the sixties some experiments and research work in this field had been started in our country, a brief and systematic description of our work are given in this paper.

I. AIRBLAST LOADING INDUCED FROM DETONATION OF EXPLOSIVES

According to the scaling law, the overpressure ΔP of shock wave front in standard air may be expressed as

$$\Delta P = K_1 \left(\frac{R}{C^{1/3}} \right)^{-n_1} \qquad \text{--- (1)}$$

and its positive time duration may be expressed as

$$t_+ = K_2 \left(\frac{R}{C^{1/3}} \right)^{n_2} C^{1/3} \qquad \text{--- (2)}$$

where ΔP — incident overpressure of shock wave front (kg/cm²)
t_+ — positive time duration of overpressure (ms)
R — distance from charge center to point to be measured (m)
C — blast energy, or weight of charge (kg)
K_1, n_1, K_2 and n_2 are experiential factors. Some values of these factors for different blast conditions from experimental or engineering data are shown in Table 1.

The P—R/C curves for different blast conditions are shown in Figure 1.

II. EQUATIONS OF SAFETY DISTANCE CONSIDERING POSITIVE OVERPRESSURE TIME DURATION AND DYNAMIC CHARACTERISTICS OF RECEIVER STRUCTURE

From equation (1), we get

$$R = KC^{1/3} \qquad \text{--- (3)}$$

where

$$K = \left(\frac{K_1}{\Delta P} \right)^{1/n_1} \qquad \text{--- (4)}$$

The expression of equation (3) is widely used among countries. The values of K given by some countries for some different conditions are shown in Table 2.

From test series of explosion ranging from 0.3 - 100t, carried out in our country, the relationships between overpressure and damage of structure are given in Table 3. There are two types of structure, brick wall with timber roof and brick wall with RC roof.

TABLE I

Item No.	Blast Condition	Direction	ΔP K_1	ΔP n_1	t_+ K_2	t_+ n_2	Range of Charge Wt.
1	Surface burst (without earth barricade)	0°-360° 0°-360°	14.49 17.20	2.00 1.82	1.50 1.50	0.50 0.50	Arbitrary Arbitrary
2	Surface burst (with earth barricade)	0°-360°	16.69	2.56	1.50	0.50	0.3-100t
3	Explosion of ammunition within earthcovered steel arch magazine [2] (charge concentrated)	0° 90° 180°	5.49 2.22 3.48	1.53 1.21 1.58	1.32 1.79 1.32	0.52 0.33 0.81	0.5-45t
4	Explosion of ammunition within earthcovered steel arch magazine [2] (charge scattered)	0° 90° 135° 180°	3.79 0.65 0.48 0.76	1.40 1.05 1.02 1.06	1.50 2.30 3.52 2.53	0.50 0.49 0.16 0.26	0.5-1.0t
5	Explosion of explosives within earthcovered steel arch magazine [3]	0° 90° 180°	13.93 2.76 2.20	1.91 1.25 1.33	0.72 0.76 0.73	0.71 0.67 0.69	< 45t
6	Explosion of explosives within earthcovered RC lat roof storehouse	0° 45° 90°	5.87 3.49 4.55	1.67 1.23 1.28	0.96 0.92 0.65	0.30 0.74 0.60	> 3t
7	Blast within tunnel	0° 45° 90°	2.21 0.96 0.69	1.68 1.36 1.10	1.36 0.63 0.48	0.95 1.07 0.50	> 4t
8	Blast for open excavation, deep hole ammonite, [5] differential blast simultaneous blast	0°-360°	 1.43 2.03	 1.55 1.55			0.8-30t

Remarks of Table 1:

$\rho = 1.50$ g/cm^2 TNT, unless otherwise specified.

Item 1: derived from Brode formula and Sadovskii formula.

Item 2: a 0.3 - 100t test series.

Item 3: depth of earthcover 0.60m, direction of opening along 0° - axis.

Item 4: same as item 3.

Item 5: same as item 3.

Item 6: depth of earth cover 0.50m, storehouse along hillside, 0°-axis perpendicular to charge length, door opening on 90°-axis.

Item 7: direction of opening along 0°-axis.

Item 8: $t_+ = 1.70\ (R/C^{1/3})^{0.82}$

TABLE 2

Item No.	Country	Blast Condition	Value of K (m/kg$^{1/3}$)
1	U. S. A.	1. Explosive storehouse with earth barricade:	
		to residence	14-16
		to passenger railway	6.5
		to highway	4-6
		to other explosive storehouse	1.4
		2. Intraline distance	3.55
2	F. R. G.	1. Explosive storehouse with earth barricade:	
		to factory building	2.5-8
		to building without blast risk	8-22
		to residence	22
		to zone without damage	> 22
		2. Intraline distance	4
3	Japan	1. To urban residence, school	16
		2. To village residence, garden	14
		3. To railway, gas tank, factory	3
		4. To highway, high-voltage wire	5

TABLE 3

Damage Level	Degree of Damage	Description of Damage	$\overline{R}=R/C^{1/3}$ ($m/kg^{1/3}$)	ΔP (kg/cm^2)
I	No damage	No damage at all.	23	0.02
II	Glass damage	Glass damage (partial or total)	10-23	0.09-0.02
III	Light damage	Glass debris, partial damage of door and/or window frame, small crack of brick wall (crack width < 5mm), or slightly inclined, roofing tile lifted and moved.	6-10	0.25-0.09
IV	Medium damage	Damage of door and window, large crack of brick wall (crack width 5-50mm), and inclined (sidesway =10-100mm), crack of RC roof, large extent damage of timber roof.	4-6	0.45-0.25
V	Severe damage	Failure of door and window, severe crack of brick wall (crack width > 150mm), inclined significantly, even partial collapse, severe crack of RC roof, fallen timber roof	3.5-4	0.70-0.45
VI	Collapse	Collapse of brick wall, fallen RC roof	3.5	0.70

Remark: Damage conditions for damage levels (II-VI) are shown in Photos (1-5).

From equation (4) we may see that if we take K_1, n_1 as constants, then the factor of safety distance, K, is only related to ΔP. This is not an overall consideration, since two important factors are missed out of equation (3).

1. The influence of positive time duration:

For the same building, according to the scaling law, when the scaled distance $\bar{R}=R/C^{1/3}$ is a constant value, the overpressures will be identical, but the positive time duration are not identical, t_+ will increase with the increasing charge. From test results we can see that when t_+ is longer the structural damage is more severe, when t_+ is shorter the structural damage is less severe.

2. The influence of dynamic characteristics of receiver structure:

For the same ΔP and the same positive time duration t_+, the degree of structural damage will be different for structures of different sizes, different materials or different structure types.

In order these two factors may be considered in equation(3), the dynamic characteristics of structure may be represented by its natural frequency (or period), and the structure may be simplified as a system with one degree of freedom. The vibration equation of motion without damping with mass m and stiffness k may be expressed as

$$m\ddot{y}(t) + ky(t) = P(t) \qquad \text{--- (5)}$$

where $P(t)=\Delta P\left[1-(t/\theta)\right]$, assuming the overpressure decays linearly with zero rise time, and θ is effective positive time duration. If we take displacement y_T at the end of the elastic stage to be the initial condition of the plastic stage, and consider that the structure usually reaches its maximum displacement at plastic stage, y_p, after the blast load vanishes, the established relationship between the dynamic load factor K_p at plastic range and the ductility ratio $\mu=y_p/y_T$ for a simply supported structure is given by

$$K_p^3 - 3K_p^2 + 3\left[3 + \frac{\mu}{0.79\,(\omega\theta)^2}\right]K_p - 1 = 0 \qquad \text{--- (6)}$$

Usually we use the method of numerical integration to solve equation (5). The external load and the resistance of structure system are assumed constant within a very short time interval, at any time t the equation (5) may be expressed as

$$\ddot{y}(t) = \frac{P(t)-ky(t)}{m}$$

or

$$\ddot{y}_n = \frac{P_n-R_n}{m} \qquad \text{--- (7)}$$

where $\omega=\sqrt{k/m}$, and $T=2\pi\sqrt{m/k}$, natural period of structure.

Response curves for idealized elastic-plastic system with one degree of freedom without damping under triangular impulse load with zero rise time are given in reference [4].

The equivalent static load imposed on a structure is

$$P_e = K_r K_p \Delta P \qquad \text{--- (8)}$$

The deflection of structure under equivalent static load is

$$y = \frac{1}{EJ} \varphi P_e L^4 = \frac{1}{EJ} \varphi L^4 K_r K_p \Delta P \qquad \text{--- (9)}$$

where φ— deflection factor for structure at elastic stage, its value depends on boundary conditions, e.g. for simple supported beam φ=5/384, L — span of structure, EJ — rigidity of structure.

Substituting equation (1) $\Delta P = K_1 (R/C^{1/3})^{-n_1}$ into equation (9), we get

$$R = \left(\frac{K_1}{y} \frac{\varphi L^4}{EJ} \right)^{1/n_1} K_r^{1/n} K_p^{1/n} C^{1/3}$$

$$= \alpha \beta \eta C^{1/3} \qquad \text{--- (10)}$$

where $\alpha = \left(\frac{K_1}{y} \frac{\varphi L^4}{EJ} \right)^{1/n_1}$ — factor of structural characteristics

$\beta = K_r^{1/n_1}$ — factor of reflection, $K_r = 2 + \frac{6 \Delta P}{7 + \Delta P}$

$\eta = K_p^{1/n_1}$ — factor of positive time duration

Equation (10) is the general equation for estimating safety distance, if the relative parameters of the structure, the blast load, and ductility ratio (or damage criterion) are given, then the safety distance may be computed.

The η—θ/T and K_p—θ/T curves that we need for investigation of safety distance are shown in Figure 2.

Let R_1 and R_2 be the safety distances under different conditions, then we have

$$R_1 = \alpha_1 \beta_1 \eta_1 C_1^{1/3} \qquad \text{--- (11)}$$

$$R_2 = \alpha_2 \beta_2 \eta_2 C_2^{1/3} \qquad \text{--- (12)}$$

by (12)/(11), we get

$$R_2 = \frac{R_1}{C_1^{1/3}} \frac{\alpha_2}{\alpha_1} \frac{\beta_2}{\beta_1} \frac{\eta_2}{\eta_1} C_2^{1/3} \qquad \text{--- (13)}$$

Equation (13) may be used for analyzing model tests and structure receiving blast loads of variable charge weight.

For example, an explosion with charge C = 1000kg, the identified safety distance for structure with brick wall and RC roof at certain damage level is 40m from test results, that is R =40m. If the increased charge weight is within the range of 1-100t, $\alpha_1 = \alpha_2$ for the same structure at same damage level, $\beta_1 \doteq \beta_2$ for varied range of ΔP with n_1 taken as 2.56, then equation (13) may be simplified as

$$R = R_2 = \frac{R_1}{C_1^{1/3}} \frac{\eta_2}{\eta_1} C_2^{1/3} = 4\bar{\eta} C^{1/3} \qquad \text{--- (14)}$$

where $\bar{\eta} = \eta_2/\eta_1$ varies with charge weight, equation (14) is a general equation for estimating intraline distance of certain structure type, and we call it an equation with variable coefficient.

III. EVALUATION OF INTRALINE DISTANCE

The natural period, T, of receiver structure used in the test series is controlled by that of the bearing brick wall, as it is more vulnerable and the natural period of brick wall is taken as T=100ms. When the charge of explosion is 1000kg TNT, the overpressure ΔP is 0.535 kg/cm^2 at a distance 40m from the charge center, the positive time duration t_+ is 30ms. The calculated maximum elastic displacement of structure is 3.05cm, and the measured displacement during test is 5.3cm, where rather large cracks occured on the brick wall, the structure entered into plastic deformation stage, thus we take the ductility ratio $\mu=2$ to obtain the dynamic factor of structure.

We need K_p for computing η, and we need θ/T for selecting K_p, as R and θ are interrelated and both are unknown, so we must take the calcution procedure of successive approximation. The procedure of calculation is first to assume a η_o, and then calculate seccessively $\eta_o \rightarrow R \rightarrow t_+ \rightarrow \theta \rightarrow \theta/T \rightarrow \eta_n$, repeat the process with η_n as the newly assumed η_o until $(\eta_o - \eta_n)/\eta_n < 4\%$.

For example, the computed results of intraline distance for receiver structure with natural period T=100-400ms and $\mu=2$ are shown in Table 4.

TABLE 4

T(ms)	C(kg) / R, η	300	1,000	3,000	5,000	10,000	40,000	100,000
100	η	0.62	0.72	0.82	0.86	0.92	1.00	1.10
	$\bar{\eta}$	0.82	1.00	1.14	1.19	1.28	1.39	1.53
	R	24.2	40.0	64.8	79.6	105	185	274
200	η	0.50	0.56	0.67	0.713	0.79	0.92	0.98
	$\bar{\eta}$	0.89	1.00	1.20	1.213	1.42	1.64	1.76
	R	23.0	40.0	67.0	84.5	120	217	323
300	η	0.42	0.50	0.60	0.64	0.72	0.84	0.91
	$\bar{\eta}$	0.84	1.00	1.20	1.28	1.43	1.69	1.83
	R	22.0	40.0	69.0	89.0	126	227	339
400	η	0.37	0.43	0.53	0.58	0.66	0.80	0.87
	$\bar{\eta}$	0.87	1.00	1.23	1.36	1.53	1.86	2.02
	R	21.0	40.0	72.2	94.0	132	254	372

IV. OTHER FORM OF EXPRESSION FOR INTRALINE DISTANCE DISTANCE EQUATIONS

1. Equation of Variable Exponent:

The exponent of charge weight C in the equation may not be considered as a constant value ⅓, and may be considered as a variable value which varies with the natural period of the structure.

If we plot the calculation results from Table 4 on a logarithmic coordinates paper, the $\bar{\eta}$ - C curves nearly a straight line, we obtain

$$\begin{aligned} &T=100ms, \quad \bar{\eta} = 0.53\ C^{0.072} \\ &T=200ms, \quad \bar{\eta} = 0.43\ C^{0.123} \\ &T=300ms, \quad \bar{\eta} = 0.406\ C^{0.131} \\ &T=400ms, \quad \bar{\eta} = 0.353\ C^{0.153} \end{aligned} \qquad \text{--- (15)}$$

Substitute (15) into (14), we get

$$\begin{aligned} &T=100ms, \quad R = 2.12\ C^{1/2.35} \\ &T=200ms, \quad R = 1.72\ C^{1/2.19} \\ &T=300ms, \quad R = 1.62\ C^{1/2.15} \\ &T=400ms, \quad R = 1.41\ C^{1/2.06} \end{aligned} \qquad \text{--- (16)}$$

In equation (16), the exponent of charge weight C is no longer a constant value ⅓, but a variable which varies with the natural period of the structure.

2. Estimating Safety Distance by Transfer Function

If we take the safety distance for a specified charge weight as a standard distance, then the safety distance for any arbitrary charge weight may be estimated by multiplying this standard distance by a function, this function is called a tranfer function.

If we take C=1000kg as the specified charge weight, the safety distonce for which is the standard distance, then from equation (14)

$$\frac{R_2}{C_2^{1/3}} = \frac{R_1}{C_1^{1/3}}\bar{\eta} \qquad \text{--- (17)}$$

Substituting (15) into (17), we get

$$\begin{aligned} &T=100ms, \quad R_2 = R_1[(1/18.9)C^{0.425}] \\ &T=200ms, \quad R_2 = R_1[(1/23.3)C^{0.456}] \\ &T=300ms, \quad R_2 = R_1[(1/24.6)C^{0.464}] \\ &T=400ms, \quad R_2 = R_1[(1/28.3)C^{0.486}] \end{aligned} \qquad \text{--- (18)}$$

From equation (18), we get the transfer function

$$K_T = \left(\frac{1}{18.9} \sim \frac{1}{28.3}\right) C^{0.425 \sim 0.486} \qquad \text{--- (19)}$$

V. INFLUENCE OF STRUCTURE TYPES ON SAFETY DISTANCES

The above mentioned intraline distance equation (14) is based on a structure with brick and flat RC roof. As compared with brick wall and timber roof, the degree of damage of timber roof is much severe than that of RC roof, but the degree of brick wall with timber roof is lighter than that of brick wall with RC roof. Therefore the timber roof governs the safety criterion.

The safety distance for brick wall structure with timber roof may be increased by 1.25 times that for RC roof, or

$$R_2 = 5\bar{\eta} C_2^{1/3} \qquad \text{--- (20)}$$

From test results and investigations of some accidental explosions, RC frame structures behave stronger resistance, the safety distance may be decreased by 0.75 times that for brick wall structure with RC roof, or

$$R_2 = 3\bar{\eta} C_2^{1/3} \qquad \text{--- (21)}$$

VI. INFLUENCE OF EARTH BARRICADE AROUND RECEIVER STRUCTURE ON SAFETY DISTANCE

The earth barricade around a receiver structure may decrease the effects of blast wave overpressure and flying fragments. Usually the earth barricade that we build is sloped 45° on both sides with a top width of 1m, the height of earth barricade is equal to the eaves height of the structure. Comparing the test results of incident overpressure in free field and that within an earth barricade (at the center point) at the same distance from the charge center, we get

$$\Delta P_b = K_b \Delta P \qquad \text{--- (22)}$$

where $$K_b = 0.7755 - \frac{0.0748}{\Delta P} \qquad \text{--- (23)}$$

ΔP_b —— overpressure within barricade
ΔP —— overpressure in free field at same distance
K_b —— reducing ceofficient

When ΔP=0.535-0.211 kg/cm², K_b = 0.64 - 0.42, that is to say the overpressure may decrease 36-58% under the protection of earth barricade, the safety distance may be multiplied by a reducing coefficient 0.71-0.84. Also considering that the positive time duration is decreased within a receiver earth barricade as compared to free field at same distance, the total reducing coefficient is about 0.55-0.75 at the center within a barricade. Here we shall notice that the influence of earth barricade decreases as the charge weight increases. For one ton TNT explosion, the safety distance may reduce 45%, but for a 100t TNT explosion, it only reduce 25%, if the size and configuration of the earth barricade are identical for both charges.

Many countries consider the influence of earth barricade around receiver structure with respect to safety distance a 50% reduction. Our opinion is that this conclusion holds true only when the charge weight is limited.

VII. INTRALINE DISTANCES COMPARED WITH OTHER COUNTRIES

For ground explosion with earth barricade around charge center, distance-charge curves are plotted on logarithmic paper as shown in Figure 3. These R-C curves represent the equation (14) in this paper, and the corresponding standards of U. S. A., U. S. S. R., Britain and F. R G.. We can see that

1. Since the damage criterions are somewhat different, the British distance is larger than that of U. S. A., and when $C \geqslant 7.0t$, the two curves become parallel to each other.
2. The U. S. S. R. standard seems to demand excessive distance requirement for large quantity of charge. The equation $R=1.2C^{1/2}$ fits relatively small quantity of charge where its effective positive time duration, θ, is relatively short, as compared to the natural period of structure, usually $\theta/T \leq 3/8$.

VIII. CONCLUSION

1. In this paper, equations are given for shock wave overpressure and its positive time duration which are need for evaluation of blast load.
2. A general equation for estimating safety distance is given, with the positive time duration and dynamic characteristics of receiver structure being considered in the equation for intraline distance. The application of law of comformity (or the scaling law) and tranfer function are discussed.
3. The influence of earth barricade around receiver structure upon decrease of overpressure and the safety distance from test results are discussed. the 50% decrease of safety distance seem valid only for limited charge weight.
4. The influence of structure type upon safety distance is discussed, and values of factor for structural characteristics are given for three structure types.

REFERENCES

1. J. Henrych, "The Dynamics of Explosion and Its Use", 1979.
2. A. R. Sound, AD 619241, 1965.
3. Charles N. Kingery, et. al., AD A031414, 1976.
4. R. E. Crawford, C. J. Higgins, E. H. Bultmann, "The Air Force Manuel for Design and Analysis of Hardened Structures" (AFWL-TR-74 102), 1980.
5. Кузнецов, Г. В., Ульйцн, В.П., Горныи Журнал, 5, 1973.

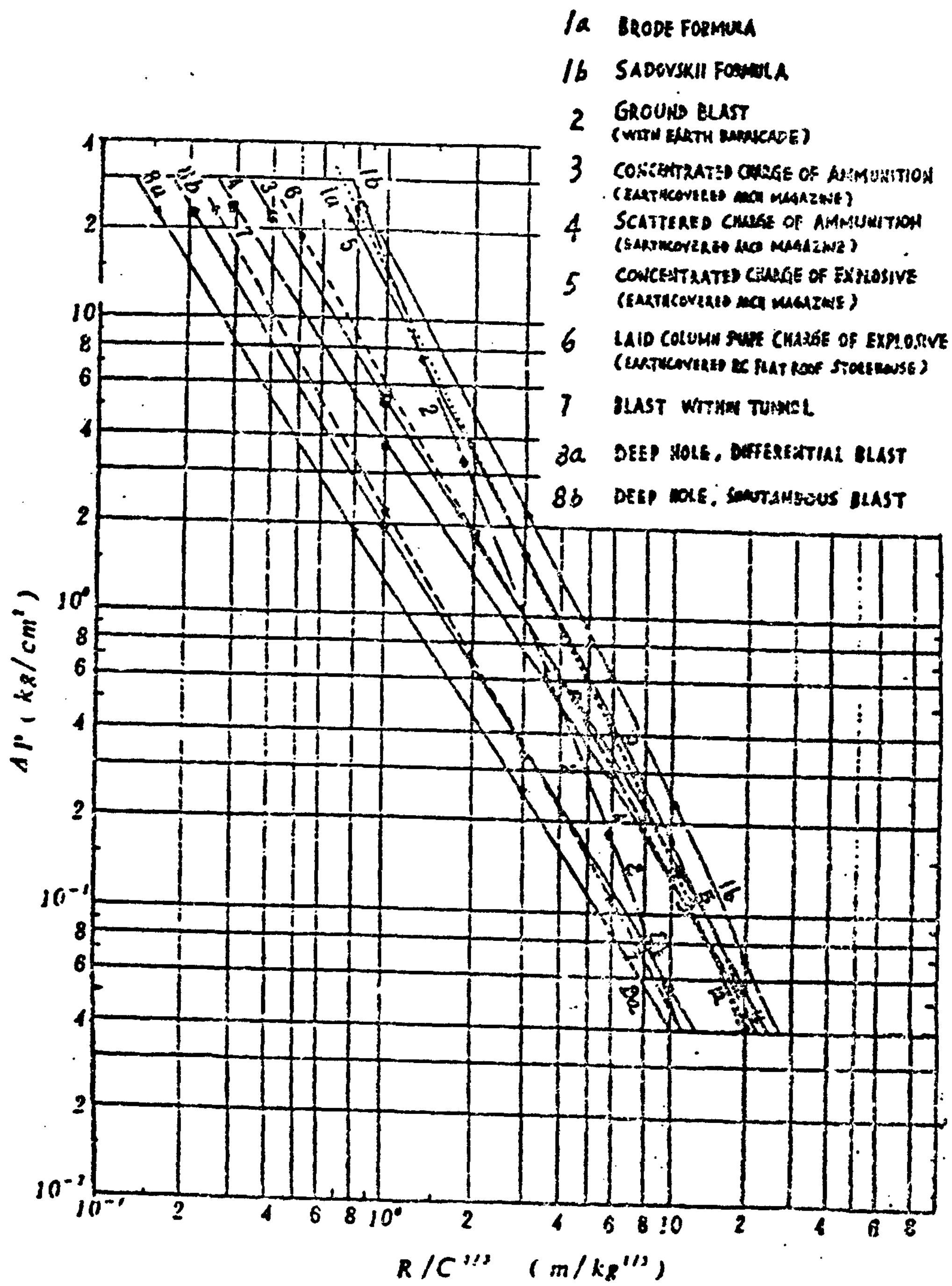

FIGURE 1 $\Delta P - R/C^{1/3}$ CURVES FOR DIFFERENT BLAST CONDITIONS

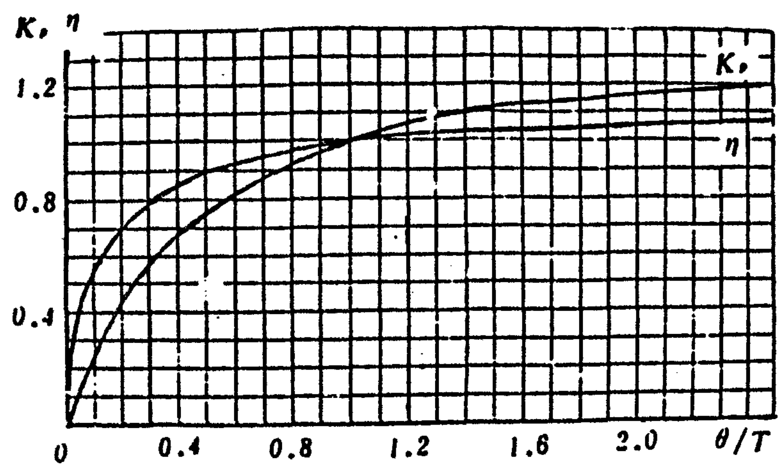

FIGURE 2 CURVES FOR $K_p - \theta/T$ (DUCTILITY RATIO $\mu=2$) AND $\eta - \theta/T$

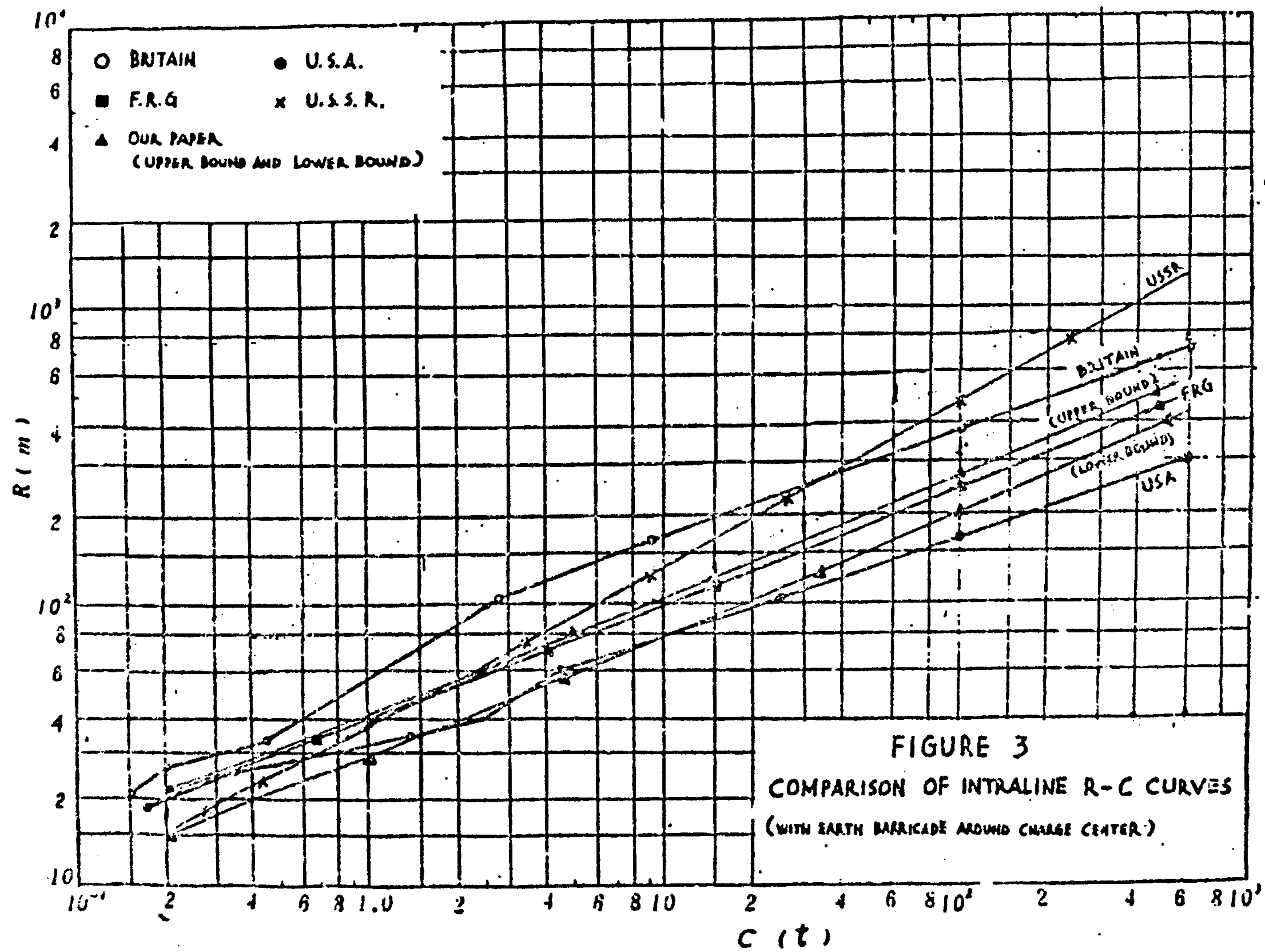

FIGURE 3
COMPARISON OF INTRALINE R-C CURVES
(WITH EARTH BARRICADE AROUND CHARGE CENTER)

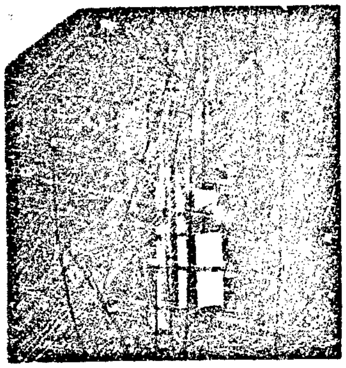

(1) Damage Level II
Glass Damage

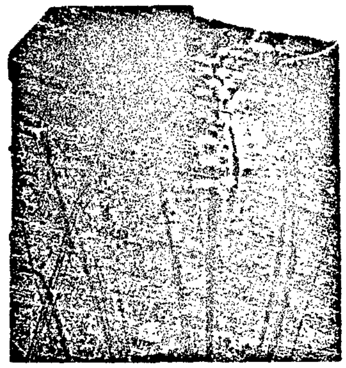

(2) Damage Level III
Light Damage

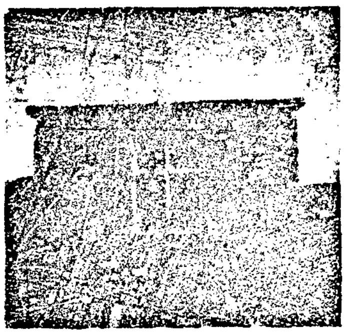

(3) Damage Level IV
Medium Damage

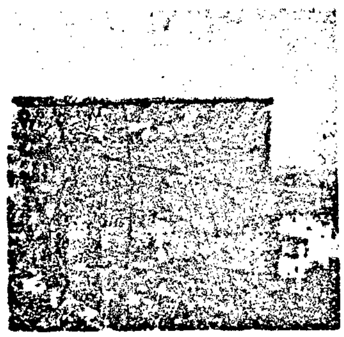

(4) Damage Level V
Severe Damage

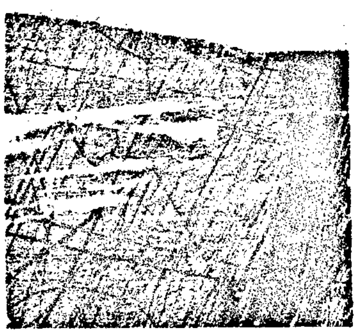

(5) Damage Level VI
Collapse

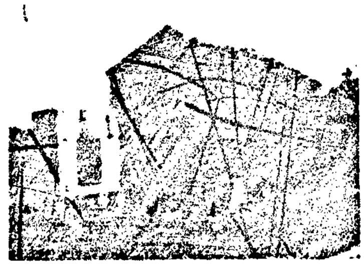

(6) Brick Structure
and Wood Model

PHOTOS

ULTRA HIGH SPEED DELUGE SYSTEMS

ROBERT A. LOYD

U.S. ARMY ARMAMENT, MUNITIONS AND CHEMICAL COMMAND
SAFETY OFFICE

23RD DEPARTMENT OF DEFENSE EXPLOSIVE SAFETY SEMINAR
9-11 AUGUST 1988

PORTABLE DELUGE PAPER OUTLINE

1. Army ammunition plants and ammunition depots perform many short-run maintenance, renovation, demil, surveillance, and rework jobs involving exposed thermally energetic material such as propellant and pyrotechnics. They frequently last less than a week. Each job requires a different equipment setup. Only a limited number of ammunition maintenance and surveillance facilities are equipped with installed ultra-high-speed deluge systems. Permanently installed deluge systems are: costly (up to $200,000 per building); must be programed into project funding cycle; require 4 to 6 months to install; require extensive modification for many of the jobs; and there are only a few permanently installed systems in ammunition maintenance facilities. This greatly reduces the commander's flexibility in planning, scheduling, and executing depot-type operations.

2. Several ammunition plants and depots, as well as the U.S. Army Depot System Command, requested the assistance of the U.S. Army Armament, Munitions and Chemical Command (AMCCOM) Safety Office to develop a deluge system capable of protecting these type of operations. The U.S. Army Central Ammunition Management Office-Pacific (CAMO-PAC) conducted a survey of the 8th Army's 19th Support Command's maintenance and surveillance operations in. Many of the operations involved exposed propellant and are performed in facilities without deluge systems or water supply. The CAMO-PAC requested the assistance of the AMCCOM Safety Office to develop a deluge system capable of protecting these type of operations. Other Army commands involved in maintenance and surveillance operations have the same problem.

3. The Department of Defense Explosives Safety Board surveys have repeatedly noted the need for ultra-high-speed deluge systems to protect operations involving exposed propellant and pyrotechnics material and has specially mentioned the need for a portable deluge system.

4. As a result of the interest in a self-contained deluge system, the AMCCOM Safety Office conducted a survey of potential users of a portable ultra-high-speed deluge system. Responses to the survey are summarized below. They indicated there was a definite need for a portable ultra-high-speed deluge system:

a. Typical types of operations requiring fire protection system?

- Surveillance, renovation, maintenance, and inspection operations.

b. Typical types of work being performed in these operations?

- Surveillance, renovation, maintenance, and inspection of bulk propellant, prop charges, and mortar increments.

c. Typical types of ammunition or explosives involved in these operations?

- Propellant for prop charges such as M1, M6, M10, and M30 plus propellant for mortar increments such as M8 and M9.

d. Typical quantities of ammunition or explosives present in the bay or area of these operations?

- 1-100 pounds.

e. Number of operators typically present during these operations?

- 2-5 operators.

f. Do buildings in which these operations are typically performed have running water or electric power?

- No running water or electricity from either a commercial source or portable generator.

g. Is there a need for portable deluge systems within your organization?

- Yes.

h. What is the typical size of the bay or area the operation is performed in?

- Operations usually take place in small bays such as 20 feet by 20 feet or 18 feet by 25 feet.

5. As a result of this interest, the AMCCOM Safety Office developed the concept of a portable ultra-high-speed deluge system. It would be a self-contained fire detection and suppression system capable of delivering water to the nozzles within 100 milliseconds from time of detection to water at the nozzle. The detectors would be ultraviolet (UV) and water would be supplied from a pressurized tank. It would protect an area approximately 10 feet by 10 feet. In a separate but parallel action, Automatic Sprinkler Corporation was looking at the possible development of a portable ultra-high-speed deluge system.

6. Before discussing the portable deluge system, we must understand exactly what an ultra-high-speed deluge system is. An ultra-high-speed deluge system is designed to start applying large volumes of water in an extremely short (milliseconds) period of time. Pre-primed, ultra-high-speed deluge systems are used to protect personnel, process equipment, and buildings from the fire and thermal hazard presented by exposed energetic material involved in munition operations such as weighing, pressing, pelletizing, propellant loading, melting, extrusion, mixing, blending, screening, sawing, granulating, drying, and pouring. A pre-primed, ultra-high-speed deluge system utilizes the following components:

a. Flame detector.

b. Controller.

c. Valve (squib- or solenoid-operated).

d. Piping.

e. Nozzles.

7. When a flame detector senses the radiant energy of a flame or fire within its field of coverage, it will respond within milliseconds sending a signal to the controller. The controller, in turn, sends a signal to the valve to open. Opening of the valve permits line water pressure to be applied to the priming water already in the pipe behind the nozzles, causing water to flow from the nozzles. At the same time, signals are sent to operate alarms and shut down process equipment.

8. The concept of the portable ultra-high-speed deluge system is valid. The Ammunition Equipment Directorate (AED), Tooele Army Depot, has developed a small self-contained system for two pieces of Ammunition Peculiar Equipment (APE). It utilizes UV detectors, a 15-gallon pressurized water tank, and explosive rupture disc valve. The MIGRAD mixer uses a similar setup to dump 30 gallons of water very quickly into the mixer bowl should an incident occur. In both cases, the water was being placed into an enclosed container or shield.

9. Automatic Sprinkler Corporation developed a prototype portable ultra-high-speed deluge system that could protect personnel and process equipment in an open area. It is a self-contained fire detection and suppression system capable of delivering water to the nozzles within 50 to 100 milliseconds from time of detection to water at the nozzle. It will protect an area approximately 10 feet by 10 feet.

a. It uses two UV detectors. The sensitivity range of the detectors is between 1,850 and 2,450 Angstroms; consequently, radiation from normal artificial lighting and sunlight do not readily trigger the system. Each detector is automatically verified for optical cleanliness and ability to detect UV energy several times per second. The detectors have an 80-degree cone of vision with middle 40 degrees being the most sensitive to UV energy. The UV detectors are gas-filled, cold-cathode sensor tubes mounted inside explosion-proof housings. When a photon of UV radiation is absorbed by the cathode of a UV tube, the energy of the photon is imparted to an electron in the metal of the cathode. Each sensor tube is filled with an ionizable gas, and a large voltage potential is present between the cathode and anode. When the electron is emitted from the cathode, it strikes the gas molecules with enough energy to cause ionization, resulting in an avalanche effect. The total number of electrons generated in this manner is typically several million times more than were emitted from the cathode. The net result is that a detectable signal pulse is transferred to the system controller.

b. The system includes a battery-operated (rechargable) controller housed in an explosion-proof enclosure. Pulses from the the detectors are counted by the microprocessor-based controller. When the count threshold (adjustable) per second is exceeded, the controller signals the pilot line solenoid valves to open. When the pilot line solenoid valves open, the pressure is bled off of the pilot lines allowing the deluge valves to open. When the deluge valves open, water travels from the water tank to the nozzles.

c. The water tank has a 120-gallon capacity, but the tank is normally filled with 100 gallons of water and is pressurized to 175 psi by a standard 200-cubit foot nitrogen bottle. Additional water could be provided via a connection to the building water supply, if available, or a second water tank. Electrical components would be suitable for use with exposed explosives (class II). Electricity for the system could be supplied by commercial power, generator, or battery. The detectors have a ball mount that permits the viewing angle to be adjusted. The nozzles can be adjusted up to 1 foot both vertically and horizontally to provide better coverage of hazard. The nozzles can be configured for different spray patterns including 40, 60, 90, and 120 degrees. The system would be mounted on a dolly or skid and be transportable.

10. Ultra-high-speed deluge systems have prevented serious or fatal injuries and serious damage to process equipment and facilities. Two typical examples are:

a. An operator was preparing a batch of ignition composition for screening when it initiated. The ultra-high-speed deluge system functioned. The operator received only minor burns to exposed skin. There was severe scorching to the front of her Nomex uniform. There was no propagation to another nearby batch of mix or damage to process equipment and the structure. The operator was wearing the protective clothing specified in the SOP.

b. Mortar increment bags containing M9 propellant were being sealed with an ultrasonic sealers when initiation of the propellant occurred. The ultra-high-speed deluge system functioned. Only two increment bags burned. The deluge system prevented propagation down the conveyor. There were no injuries or property damage.

11. The U.S. Department of Defense Ammunition and Explosives Safety Standards (DOD 6055.9-STD) states that where exposed thermally energetic materials are handled that have a high probability of ignition and a large thermal output, as indicated by a hazard analysis, they must be protected with an ultra-high-speed deluge system. The system must suppress potential fires in their incipient state. Other publications such as AMCR 385-100 (U.S. Army Materiel Command Safety Manual), Navy Sea System Command OP 5 (Ammunition and Explosives Ashore), DOD 4145.26M (Contractor's Safety Manual), Military Handbook 1008 (Fire Protection For Facility Engineering, Design, and Construction), and the National Fire Codes also provide guidance on ultra-high-speed deluge systems.

12. The concept of the portable deluge system needed to be evaluated. This could only be done through a systematic testing program. The AMCCOM Safety Office established the test criteria and developed the test plan outline. The U.S. Army Production Base Modernization Activity contracted with Day & Zimmermann to evaluate the portable deluge system, prepare a technical report, develop a purchase specification, and recommend changes to prototype. The AED, Tocele Army Depot, developed the detailed test plan, testing procedures, and instrumentation requirements. They also performed the actual tests. Only propellant was used due to: More propellant than pyrotechnics are involved in maintenance and renovation operations; time constraints; and funding constraints.

13. Test criteria established for an acceptable test of the portable deluge system were:

a. System would respond in 100 milliseconds or less from time of detector output to water at the nozzle.

b. System would prevent propagation of fire from the donor to the receptor.

14. Test setups were developed to simulate operations commonly performed in ammunition plants and depots. Three tests involved the removal and replacement propellant increments and one involved the collection of propellant in a hopper.

a. Propellant replacement operations. A table, approximately 4 feet by 4 feet was used to simulate the table typically found in ammunition maintenance facilities. A donor charge equalling one round plus 25-percent overcharge was placed near the center of the table to simulate an operator performing an operation on the round. Acceptor charges were placed 12 and 18 inches from donor charge to simulate the typical location of propellant items (complete rounds, scrap propellant, new propelling charge, etc.) required to support the operation. Three typical propellant charges used in maintenance, renovation, and demil operations were selected selected as donor charges. The weight includes the 25-percent overcharge. The donor charges were initiated by means of a electric squib buried in the propellant. The portable deluge system was placed to one side of the worktable so that the detectors were 5 feet from the donor and the nozzles were 4 feet from the donor. They were:

(1) M90, 81mm mortar increments, M9 propellant - .39 pounds.

(2) M36, 4.2-inch mortar increments, M8 propellant - .75 pounds.

(3) M67, 105mm howitzer increments, M1 propellant - 3.5 pounds.

b. Propellant collection operation: It simulated the typical propellant collection operation. The collection hopper for the APE 1023 Vacuum Collection System was used to hold the donor charge. Acceptor charges were placed on small trays at the same level as the top of the collection hopper.

They were located 12 and 18 inches from the collection hopper. The M26 propellant used with the many 106mm recoilless rifle rounds was selected for the donor because it represents one of the more energetic propellants commonly involved in maintenance, renovation, and demil operations. The donor charge consisted of 10 pounds of loose M26 propellant placed in the collection hopper. This represented a typical 106mm round with a 25-percent overcharge. The M26 propellant was also used for the acceptor charges. The portable deluge system as placed to one side of the hopper so that the detectors were 5 feet from the donor and the nozzles were 4 feet from the donor. The donor charges were initiated by means of a electric squib buried in the propellant.

c. To verify that propagation would take place between the donor and acceptors, a series of propagation tests was performed. Propagation occurred.

d. The tests were instrumentated to measure overpressure, heat flux, and temperature. They were recorded on normal speed video system, high-speed video system (200 frames per second), and high-speed camera system (500 frames per second). Still pictures were taken before and after each test. A manikin placed at the operator's position.

15. Test results are presented below. Each qualifying test was performed at least twice.

a. Propellant replacement operations with M90, M36, and M67 charges:

(1) No overpressures were noted. All readings were well below the 2.3 psi level established by MIL STD 398.

(2) No measured heat flux valves were in excess of standards established by DOD 6055.9-STD or MIL STD 398.

(3) No overpressures were noted. All readings were well below the 2.3 psi level established by MIL STD 398.

(4) There was no propagation from the donor to either acceptor charge.

(5) At least 70 percent of the propellant was recovered after each test.

b. M26 propellant (10 pounds).

(1) No overpressures were noted. All readings were well below the 2.3 psi level established by MIL STD 398.

(2) Response times were all less than 100 milliseconds. They ranged from 47 to 83 milliseconds (from time of detector output to water at the nozzle).

(3) The highest heat flux reading for the third qualifying propellant collection hopper test was 0.43 cal/cm^2 per second. It did not exceed the level established by MIL STD 398. However, it did exceed the 0.3 cal/cm^2 per second level established by the DOD 6055.9-STD. This qualifying test was not valid because one of the acceptor hoppers and the collection hopper were pushed over by the force of the water. The second qualifying test did not pass either heat flux standard because the water spray patterns did not adequately cover all of the energetic materials. The nozzles were changed for the third test. See paragraph 26 for additional details.

(a) There was no propagation from the donor to either acceptor charge during the third qualifying test.

(b) At least 83 percent of the propellant was recovered after the third qualifying test.

16. It was concluded that the prototype portable deluge system will adequately suppress the thermal hazards associated with typical renovation and maintenance operations on the types and quantities of propellant tested. This system will provide protection for an operator and personnel in the immediate vicinity from the heat flux generated in event of an incident. Additional testing needs to be performed for specific applications; e.g., type of energetic material, quantity of energetic material, equipment layout, and specific nozzle configurations. Testing also needs to be performed to establish methods for winterizing the portable deluge system.

17. As part of their evaluation of the portable deluge system, Day & Zimmermann developed a detailed purchase specification. See appendix A.

18. Ultra-high-speed portable deluge systems can be purchased from commercial vendors at this time. At least one installation has purchased several portable deluge systems. Several of major subordinate commands are considering a central purchase of the portable deluge systems.

19. Potential problems with portable deluge system include:

a. The proper setup of the portable deluge is critical to its successful operation. If the portable deluge system is incorrectly located, nozzles and/or detectors improperly aimed, or the wrong type of nozzle used, it will not protect the employee. This was borne out by the qualification tests performed at Tooele Army Depot.

(1) Detectors. The UV detectors for ultra-high-speed deluge systems should be located to provide two levels of protection. One or more detectors should be placed as close as physically possible to the most likely source(s) of ignition. They should be located so the detector's field of view is not blocked by shield, equipment, or personnel. One or more additional detectors should be located to provide general area coverage of the cubicle or bay, on the assumption that an ignition could occur at other points within the area.

The UV and infrared (IR) detectors are optical devices and, as such respond to the attenuation laws of optics, doubling the distance between the detector, and the flame will reduce the radiation perceived to one fourth; conversely, reducing the distance by one half results in four times more radiation to the detector. Tests done by Detector Electronics graphically demonstrated the effect of distance and obstructions have on the detection time (reaction time of the detector only) of UV detectors.

(a) In one test, 10 grams of black powder was ignited. The fire was viewed by identical detectors and controllers at 5, 10, and 15 feet. Note the almost 100 percent increase in time between 5 and 10 feet and the almost 200 percent increase between 5 and 15 feet. The detector response times were:

5 feet . . . 27 milliseconds
10 feet . . . 54 milliseconds
15 feet . . . 75 milliseconds

(b) In another test, 10 grams of black powder was ignited. The fire was viewed by three identical detectors and controllers located 10 feet from the fire. The detectors had a clear view, partially obstructed view, and completely obstructed view, respectively, of the target. Note the almost 100-percent increase in response time when the view is partially or completely blocked. The detector response times were:

Clear view . . . 20 milliseconds
Partial view . . . 38 milliseconds
Blocked view . . . 40 milliseconds

(c) The UV detectors are sensitive to weld arcs, lightning, X-rays (gamma radiation), cosmic and background radiation, and high electrostatic charges. They should be located away from the horizontal plane, and they should not be aimed toward doors or windows.

(d) The UV radiation will not transmit through smoke, water vapor, acetone, regular glass, plexiglass, or oil.

(2) The proper location of the nozzles is vital to the correct operation of the portable deluge system. They should be located as close as possible to the hazard but still provide adequate coverage. The nozzles must also be aimed at the hazard. If the nozzle is improperly aimed, the water spray may partially or completely miss the hazard. The water travel time from the nozzle to the hazard is the longest component of response time. See paragraph 32 for additional discussion of water travel time.

(3) The proper nozzle selection is also critical to the successful operation of the portable deluge system. A single type or combination of nozzles may be required. Nozzles with spray patterns of 40, 60, 90, and 120 degrees are available. All exposed energetic material must be protected by the water spray pattern for the portable deluge system to be effective. The operator's position should also be protected. The need to select the proper

nozzles was very graphically demonstrated in one series of the test runs at Tooele Army Depot. The test involved a propellant collection device as the donor and a tray of propellant located 18 inches from the hopper. In the first test, three 40-degree nozzles were used. The water spray pattern did not protect the acceptor charge and did not completely penetrate the flame of the donor charge, as 10 pounds of M26 propellant burned in the hopper. The fire propagated to the acceptor charge. When the test was repeated, one 40-degree nozzle was replaced with a 90-degree nozzle. The acceptor charges were protected with the water spray and the fire did not propagate from the donor.

(4) The portable deluge system must be located so that no personnel are working directly opposite it. When the system functions, it tends to push burning propellant across the table. This was noted during the Tooele tests. This is more a problem witn the narrow angle nozzles.

b. Maintenance of the portable deluge system is much more critical than for permanently installed systems because of the extra stress placed on the unit when it is moved from location to location and stored for long periods of time. A good preventive maintenance program is required. Experience has shown that increasing the time period beyond 4 to 6 weeks results in a significant increase of false activation and other system problems. A tri-service manual, Maintenance of Fire Protection Systems (TM 5-695/NAVFAC MO-117/Air Force AFM 91-37), provides guidance on the inspection and testing of fire protection systems. The following items should be considered when establishing maintenance procedures:

(1) System checks.

(a) Measure all voltages.

(b) Check for loose wires and or relays.

(c) Clean all dirt and debris from box housing the controller.

(d) Spot check conduit fittings for moisture and/or loose wire nuts.

(2) Detectors.

(a) Remove each lens and clean.

(b) Remove each barrel and check grounding springs, when used.

(c) Tighten each terminal screw in sensors.

(d) Clean and inspect all optical integrity rings.

(e) Check for moisture and or corrosion inside sensor housings.

(f) Check each sensor for proper alignment.

(g) Check housing for continuity.

(h) Reactivate system and check for problems.

(3) Flow tests should be conducted:

(a) After each job set or move.

(b) After major maintenance or modification.

(c) After reactivating an inactive system.

c. There is a need for backup water supply. The water supply of the portable deluge system is very limited (typically 100 gallons). Whenever possible, a backup water supply should be provided. This can be done by tying into the building water supply system. The first choice would be an existing fire protection system. The second choice would be the domestic water supply. The connection between the portable deluge and building water supply can be accomplished by means of a flexible hose, similar to the hose connection of a fire department standpipe system. When this is not feasible, the use of a second pressure tank should be considered. The primary purpose of the backup water supply is to prevent reignition of the energetic material due to the residual heat after the flames have been extinguished.

d. Whenever possible, the portable deluge system should also be tied into the building fire alarm system. If backup water is provided from the building water supply, a flow alarm could be provided on this system. An alternate method would be to wire a set of contacts in the controller enclosure into the building fire alarm system. However, this wiring must comply with the requirements for class I or II locations (explosion-proof).

e. The solenoid type of valve is better suited for the portable deluge system because, unlike squib valves, the entire system can be reset in less than 30 seconds. Also, the squib-operated valve uses an explosive squib that requires special handling, and is difficult to ship to military installations in foreign countries. It also provides redundancy. Water will flow from all nozzles even if one of the solenoids fails since the pressure in all the pilot lines will be reduced when the valves open, although the response of that one nozzle will be slower. See appendix B for additional information on deluge valves.

f. Training for operators and maintenance personnel is very important to ensure the proper operation of the portable deluge system. Detailed training procedures will be required. These should include a video tape on the setup, operation, preventive maintenance, and maintenance procedures.

g. Spare parts must be readily available for the portable systems. Most of the items are off-the-shelf. A recommended spare parts list should be developed and the critical items either stocked locally or be quickly available from vendors.

h. Procedures for storage of the portable deluge systems need to be developed to ensure proper storage. This should include winterization of the unit; e.g., draining of water lines and tanks and/or use of antifreeze solutions. Consideration should also be given to winterization procedures when the portable deluge system is used in facilities that have little or no heat during nonworking hours.

i. Because of the very real possibility for misapplication of the portable deluge system, control and accountability of any system in the field must be maintained. Concerns include: proper maintenance, distribution, standardization, usage, spare parts, winterization, etc. A good avenue to ensure the necessary control of the portable deluge system (for Government-operated facilities) is to make the item part of the APE inventory or some similar program.

20. Suggested modifications to prototype portable deluge system include:

a. Add an additional detector.

b. Make it easier to place the detectors and nozzles closer to the hazard by using extension hoses and clamping devices.

c. Increase the quantity of water.

21. When evaluating the thermal threat presented by exposed energetic material, all potential methods of protecting the employee must be considered. These include ultra-high-speed deluge systems, protective clothing/equipment, shielding, and remote operations. These can be used singly or in combination.

22. Advantages of portable deluge system:

a. Provides improved protection for ammunition maintenance, renovation, and surveillance operations by means of a system that can be arranged to protect the hazards presented by a variety of operations and can be moved from location to location.

b. Provides a substantial cost savings by reducing the need for permanently installed deluge systems in ammunition maintenance, renovation, and surveillance operations. Permanent systems can cost up to $200,000 per building while portable systems would cost about $30,000 or less. Only one or two systems per maintenance building would be required. Additional costs would also be saved when permanent systems do not have to be modified to meet job requirements.

c. Provides process fire protection for facilities without any permanent water supply.

d. Provides a system that can be quickly and easily moved to the location it is needed.

e. Provides improved management flexibility for the scheduling and execution of maintenance, renovation, demil, and surveillance operations requiring deluge protection.

23. There are many other potential users of the portable deluge system including: private munition manufactures, research and development labs, other military services, and foreign countries.

24. The portable ultra-high-speed deluge system is designed to be effective on limited quantities of exposed energetic materials. The testing already done proves the system can effectively contain some types of propellant fires and indicated that it would be effective on other types of propellants and pyrotechnics. The portable deluge system cannot replace or eliminate fixed/installed ultra-high-speed deluge systems where fixed systems are needed. The portable deluge system will allow more facilities to execute their mission for operations involving limited quantities of exposed energetic materials in operations such as rework, maintenance, renovation, surveillance, and demilitarization. The portable deluge system can fill the "gap" where a fixed deluge system is not feasible because of constraints such as water supply and changing processes and equipment layout.

25. The portable deluge system provides an excellent test bed for deluge system research, development, and testing. The nozzle and detectors can be easily relocated, different nozzles configurations used, different water pressures utilized, water flow rates tried, and different type valves utilized. The unit can be tailored to fit the test criteria.

26. The Tooele deluge tests of the portable deluge system pointed out problems related to heat flux measurement and defining response time.

a. The heat flux problems include:

(1) Two standards with different formula.

(2) Lack of correlation between heat heat flux standards and permitted exposure.

(3) No universally accepted method to measure heat flux.

b. No common agreement on how to define and measure response time.

27. There are currently two different heat flux standards. The DOD 6055.9-STD states that employees should not be exposed to a thermal threat of more 0.3 calories per square centimeter per second. The MIL STD 398 (Shields, Operational For Ammunition Operations, Criteria for Design of and Tests for Acceptance) states that employees should not be exposed to a thermal threat of more than the value established the following equation:

$$\text{Heat Flux} = 0.62t^{-0.7423} \text{ where}$$

Heat Flux = heat flux in cal/cm²-sec

t = total time in seconds that a person is exposed to the radiant

28. The value used in the DOD STD 6055.9-STD and AMCR 385-100 is an absolute value while the value used in MIL STD 398 is base on total exposure time. The formulas should be evaluated to determine which formula or combination is the best, then determine if the formula selected needs to be modified or changed.

29. Army ammunition plants and depots perform various ammunition-related operations involving production, maintenance, renovation, surveillance, and demil. The DOD 6055.9-STD requires that where thermally energetic materials are handled that have a high probability of ignition and a large thermal output, they must be protected with an ultra-high-speed deluge system capable of protecting personnel and limiting exposure to not more than 0.3 calories per square centimeter per second (first-degree burns). A similar requirement is contained in AMCR 385-100, AMC Safety Manual. The correlation between the degree of exposure permitted and the thermal protection provided by ultra-high-speed deluge systems has never been clearly defined or established.

30. The instrumentation used to measure heat flux, method of calibration, and instrumentation setup is not clearly defined or spelled out in DOD 6055.9-STD and MIL STD 398 or other publications.

31. There is a need to:

a. Establish the correlation between the degree of exposure permitted and the thermal protection provided by ultra-high-speed deluge systems.

b. Establish what formula should be used to measure heat flux.

c. Establish what type of instrumentation should be used to measure and record heat flux, method of calibration, and instrumentation setup.

32. There is no universally accepted agreement on the definition of deluge system response time, although the most commonly accepted definition is from time of detection to water at the nozzle. The U.S. Army Materiel Command Safety Manual (AMCR 385-100) defines the response time for ultra-high-speed deluge systems as: The sensing of a detectable event by the detector to the beginning of water flow from the critical nozzle(s) closest to the hazard or as determined by the hazard analysis. In lieu of testing, a small deluge system (design flow rate of 500 GPM or less) shall have a response time of 100 milliseconds and large deluge system (design flow rate of more than 500 GPM) shall have a response time of 200 milliseconds.

33. This definition does not consider the time required for the water to travel from the nozzles to the hazard being protected. The high-speed video tapes of the portable deluge tests at Tooele and and other tests conducted at Lone Star Army Ammunition Plant very graphically show the need to measure not only the time from detection to water at the nozzle but also from the nozzle to the target (hazard).

34. A proposed change to AMCR 385-100 states that:

a. While the water travel time from the nozzle to the target is not included in the definition of response time, it must be considered in the design of high-speed deluge systems.

b. Measurement of response time should start with detector input. When a digital timer is used, a saturating UV or IR source should be used to provide a source of UV or IR input energy for the detector.

This is a step in the right direction but still does not completely address the total time required for response of a deluge system or assign specific time.

35. In order to more precisely define response time requirements, it is necessary to understand the interrelation between development of an incident and deluge system functions. The following outlines a way of breaking down the fire dynamics and deluge system functions into understandable segments:

a. Ignition Time - T0: Ignition time is defined as the start of ignition. Ignition of an item is defined as self-sustained deflagration.

b. Ignition To Sensing Threshold Time - T1: Ignition to sensing threshold time is defined as the time from ignition until the buildup of energy reaches the sensing threshold of the sensor. This is dependent upon the configuration of the item being protected. For example, the ignition of propellant from the bottom of a hopper may require more than a second to reach the surface of the propellant where it can be sensed by a detector. If ignition occurred on the surface, the ignition to sensing threshold period would be much less - in the millisecond range.

c. Ignition To Sensor Response Time - T2: Ignition to sensor response time is defined as the time from ignition to transmission of the signal to the controller.

d. Ignition To Controller Response Time - T3: Ignition to controller response time is defined as the time from ignition to transmission of signal to deluge valve squib or solenoid.

e. Ignition To Valve Opening Time - T4: Ignition to valve opening time is defined as the time from ignition to the opening of the deluge valve permitting water to flow.

f. Ignition To First Water at the Nozzle Time - T5: Ignition to first water at the nozzle is defined as the time from ignition to the first flow of water from the critical nozzle(s). This is usually the nozzle(s) closest to the hazard or as determined by a hazard analysis.

g. Ignition To First Water on Target Time - T6: Ignition to first water on the target is defined as the time from ignition to the first drops of water to strike the target from the critical nozzle(s). There is usually an initial stream of water, followed by a break in the flow, followed by a full flow pattern.

h. Ignition To Full Flow Water On Target Time - T7: Ignition to full flow water on target is defined as the time from ignition to a fully developed spray of water strikes the target area.

i. Extinguishment Time - T8: Ignition to extinguishment is defined as the time from ignition to termination of the deflagration.

36. Deluge system response time should be redefined as total response time. This is the total time lapse from detector sensing threshold response to full flow of water on the target area (T1-T7). Total response time consists of two segments--detection time (T1-T4) and water delivery time (T4-T7). The total response time must be considered when designing deluge systems. The use of total response time provides a means to realistically evaluate the required response time of deluge systems. This will also provide a baseline for checking system response time during the annual flow tests and after a system has been inactive for an extended period of time, or a system has been modified.

a. Detection time is the time from detector sensing threshold of the fire to the time that the signal is amplified and fires the primer in the water control valve or opens the solenoid valve (T1-T4). The detection time is the fastest phase, and under ideal conditions, can be accomplished in as little as 10 milliseconds. Factors effecting detection time include:

(1) Distance between detector and target.

(2) Type of flame and amount of smoke.

(3) Signal processing sensitivity.

(4) Detector sensitivity.

b. Water delivery time is the time required from primer firing or solenoid valve opening to the time a fully developed spray of water strikes the target (T4-T7). It is the source of the most of the time consumption and is dependent on several factors:

(1) The completeness of water prime in the piping system from the valve to the nozzles. Tests show this is a vitally important factor, since an air pocket constituting only a small percent of the total volume of the system can cause drastic increase in operating time.

(2) Water pressure. Both analysis and tests show that all other factors being equal, the water pressure delivery time is inversely proportional to the square root of water pressure. This would mean, for example, that if the supply pressure on a specific system were increased from 50 psi to 100 psi, the water delivery time would be reduced by about 40 percent with all other factors being equal.

(3) The distance from the nozzle to the hazard.

37. The two methods frequently used to check response time of ultra-high-speed deluge systems are the digital timer and the high-speed video recording system. This seems to be acceptable by most authorizes for testing deluge systems in the field and also for periodic maintenance testing. This will also provide a baseline for checking system response time during flow testing on and after a system has been inactive for an extended period of time or a system has been modified or worked on.

a. The digital timing system consists of a timing circuit connected to a saturating UV or IR source at the detector and a water flow switch to measure first flow of water at the nozzle. Controller output could also be measured, if a second timing circuit is used. The timer is started the instant the UV or IR saturating source is activated and is stopped the instant first water leaves the critical nozzles (T1-T5). Several devices can be used to measure first water at the nozzle. One consists of a light metal disc approximately 2 inches in diameter held between electrically conductive contacts. The water from the nozzle pushes the disc out of the contacts opening the circuit and stopping the timer. Another is a water flow switch which replaces a nozzle. The measurement of full water on the target is more difficult (T1-T7). One method would be to place two electrically conductive screens on top of each other, but sufficiently separated so that a complete circuit is made only when water pass through the screens. The screens would need to be large enough to ensure the first water hit them, possibly 1 foot square. The digital timer is well suited for routine measurement of response time by maintenance technicians at ammunition plants and depots. It is inexpensive, easy to operate, and can be quickly set up and torn down.

b. The high-speed video system consists of a camera, recorder, and monitor. The system is capable of recording 60 to 300 frames per second or up to 3.3 frames per millisecond. The system provides a practical way to measure total system performance from initiation to suppression (T0-T8). The first visible indication of an incident can be identified long before the detector is saturated. The digital timer can only be activated when the detector is saturated. The high-speed video recording system costs less than $20,000. It can also be rented. It is the ideal tool for measuring total system performance (T0-T8), compliance with criteria specified in contract documents, evaluating new or modified systems, and determining total system response time.

38. There is a need to:

a. Redefine response time as "The time from detector input to full water at the hazard (target)".

b. Determine what are appropriate total response times.

c. Determine the method(s) used to measure response time.

39. The AMCCOM Safety Office has submitted four scopes of work to the U.S. Army Safety Center for research and development projects on ultra-high-speed deluge systems. One of the proposed projects deals with heat flux, while another deals with response time. The remaining projects deal with deluge system design and installation. See appendix C for copies of the scopes of work.

40. A list of technical reports is provided at appendix D, and a list of other references is provided at appendix E. These were utilized in the preparation of this paper. Additional technical material was provided by the following persons:

a. Mr. Paul Kennedy, Day & Zimmermann, Inc., Kansas AAP.

b. Mr. Jerry Miller, AED, Tooele Army Depot.

c. Mr. Gene Burns, Day & Zimmermann, Inc., Lone Star AAP.

d. Mr. Gary Fadorsen, Automatic Sprinkler Corporation.

e. Mr. Ken Klapmeier, Detector Electronic, Inc.

f. Mr. George O'Brien, U.S. Army Production Base Modernization Activity.

41. The point of contact for this paper is Mr. Robert Loyd, U.S. Army Armament, Munitions and Chemical Command, ATTN: AMSMC-SFP, Rock Island, IL 61299-6000. Telephone: commercial (309) 782-2975/2182 and AV 793-2975/2182.

ULTRA HIGH SPEED DELUGE SYSTEM COMPONENTS

— FLAME DETECTORS
  (ULTRAVIOLET OR INFRARED)

— CONTROLLER

— VALUE (SQUIB OR SOLENOID OPERATED)

— PIPING/NOZZLES

— WATER SUPPLY

FIGURE 1

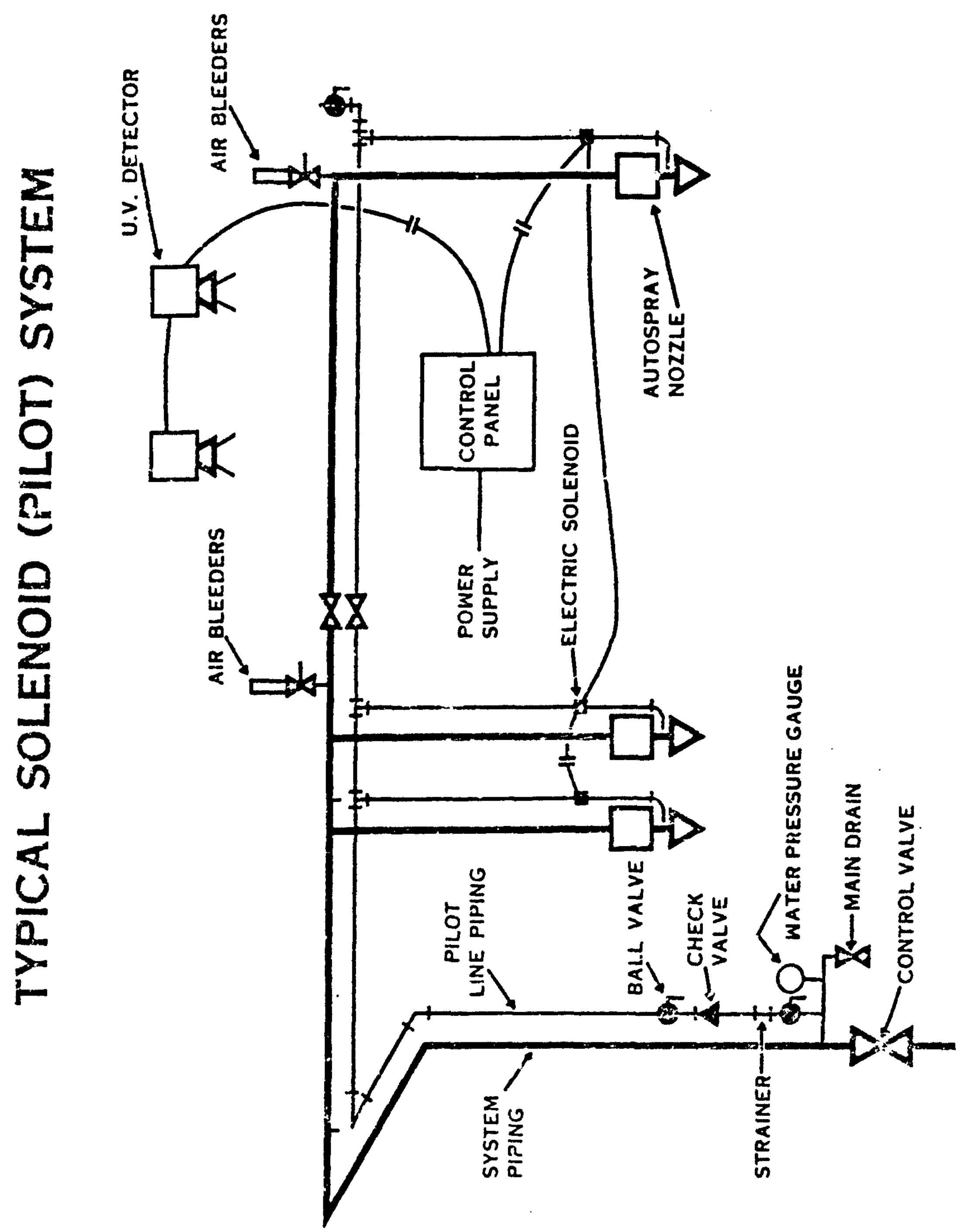
TYPICAL SOLENOID (PILOT) SYSTEM
U.V. DETECTOR
AIR BLEEDERS
AIR BLEEDERS
CONTROL PANEL
POWER SUPPLY
ELECTRIC SOLENOID
AUTOSPRAY NOZZLE
PILOT LINE PIPING
BALL VALVE
CHECK VALVE
WATER PRESSURE GAUGE
MAIN DRAIN
CONTROL VALVE
SYSTEM PIPING
STRAINER

FIGURE 1A

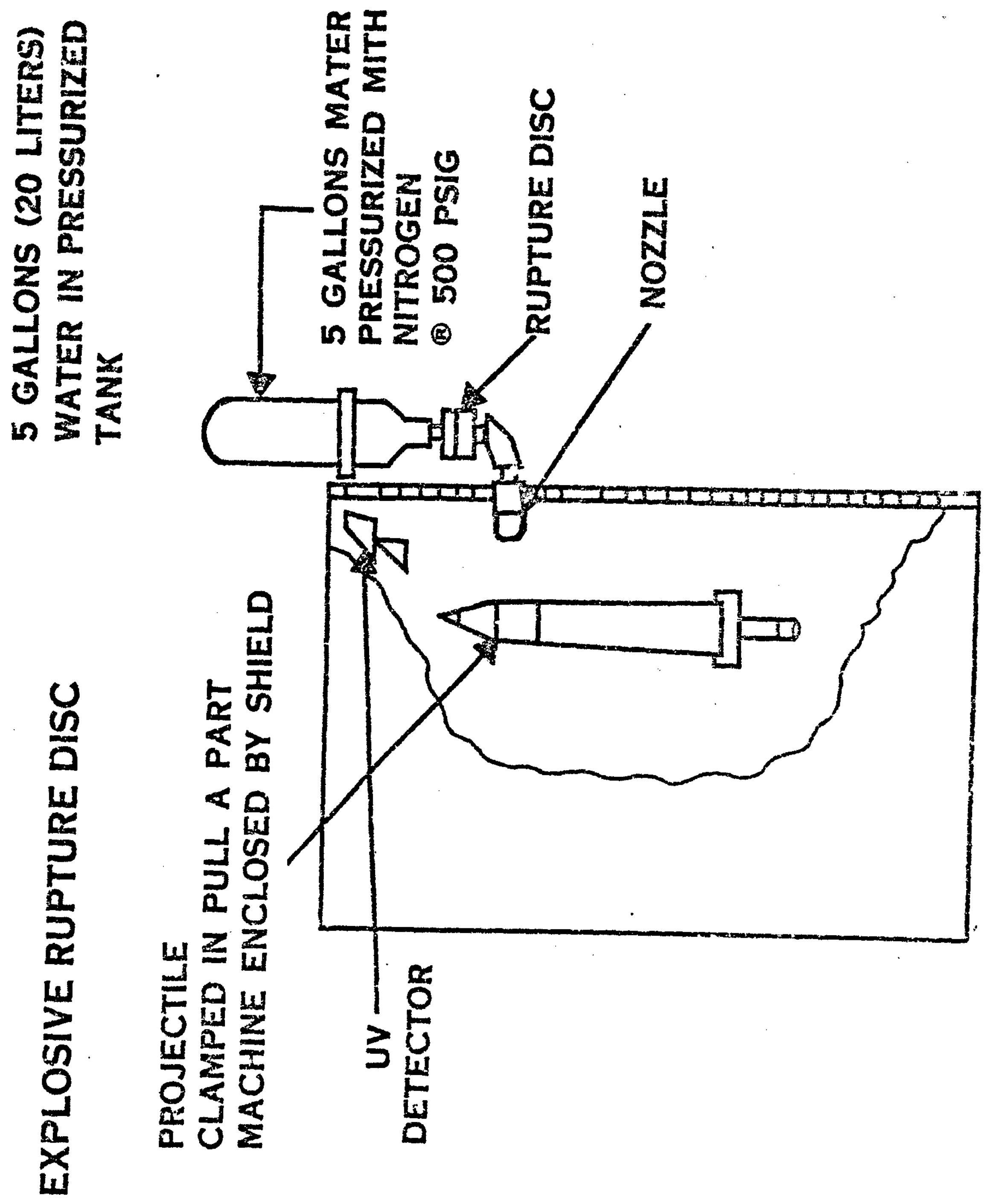
EXPLOSIVE RUPTURE DISC
5 GALLONS (20 LITERS) WATER IN PRESSURIZED TANK
5 GALLONS MATER PRESSURIZED MITH NITROGEN ® 500 PSIG
RUPTURE DISC
NOZZLE
PROJECTILE CLAMPED IN PULL A PART MACHINE ENCLOSED BY SHIELD
UV DETECTOR

FIGURE 2

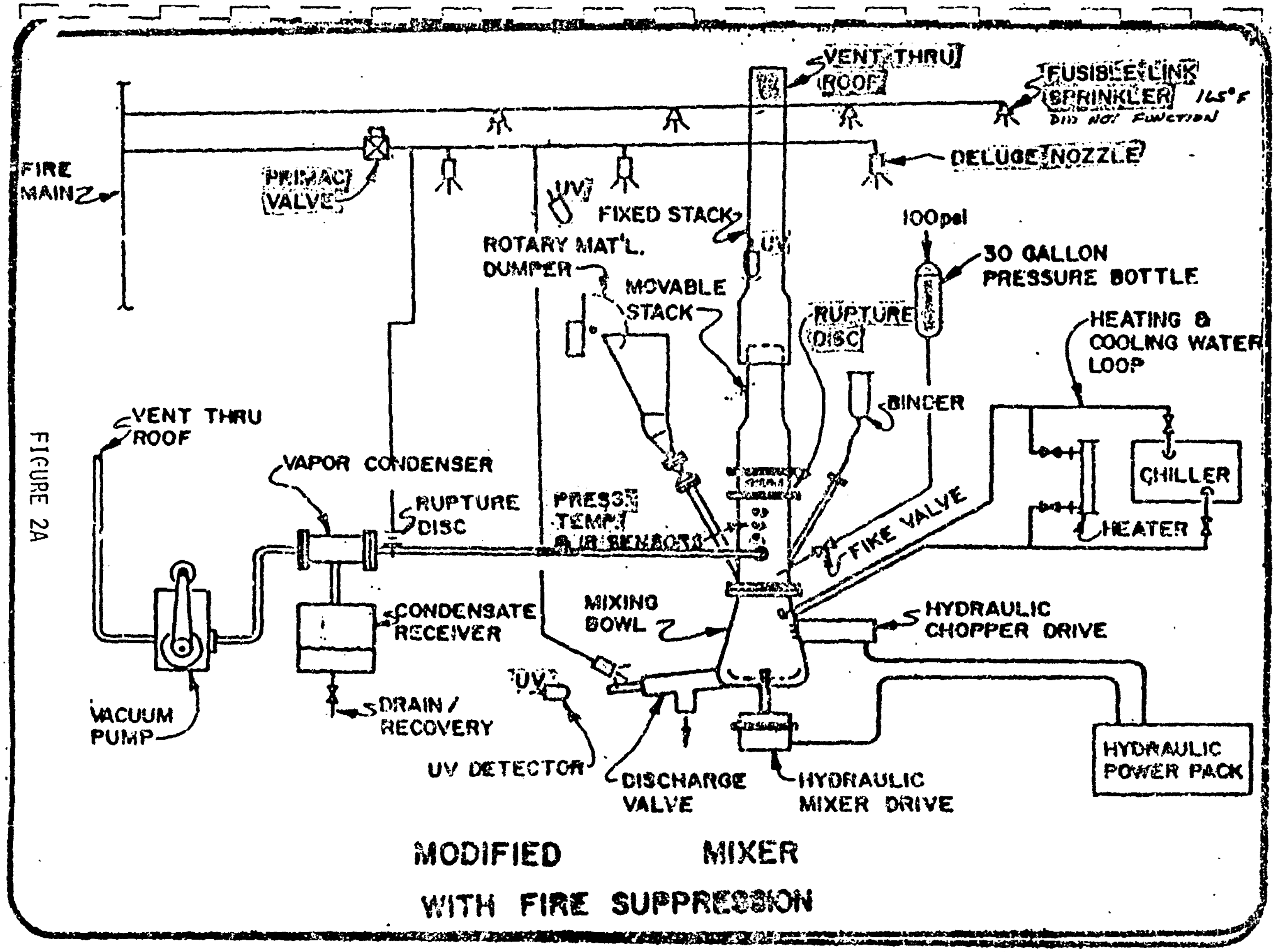
VENT THRU ROOF
FUSIBLE LINK SPRINKLER 165°F
DID NOT FUNCTION
DELUGE NOZZLE
FIRE MAIN
PRIMAC VALVE
UV
FIXED STACK
UV
100psi
30 GALLON PRESSURE BOTTLE
ROTARY MAT'L. DUMPER
MOVABLE STACK
RUPTURE DISC
HEATING & COOLING WATER LOOP
BINDER
CHILLER
HEATER
VENT THRU ROOF
VAPOR CONDENSER
RUPTURE DISC
PRESS TEMP IR SENSORS
FIRE VALVE
MIXING BOWL
HYDRAULIC CHOPPER DRIVE
CONDENSATE RECEIVER
UV
DRAIN / RECOVERY
VACUUM PUMP
UV DETECTOR
DISCHARGE VALVE
HYDRAULIC MIXER DRIVE
HYDRAULIC POWER PACK
MODIFIED MIXER
WITH FIRE SUPPRESSION

FIGURE 2A

FIGURE 3

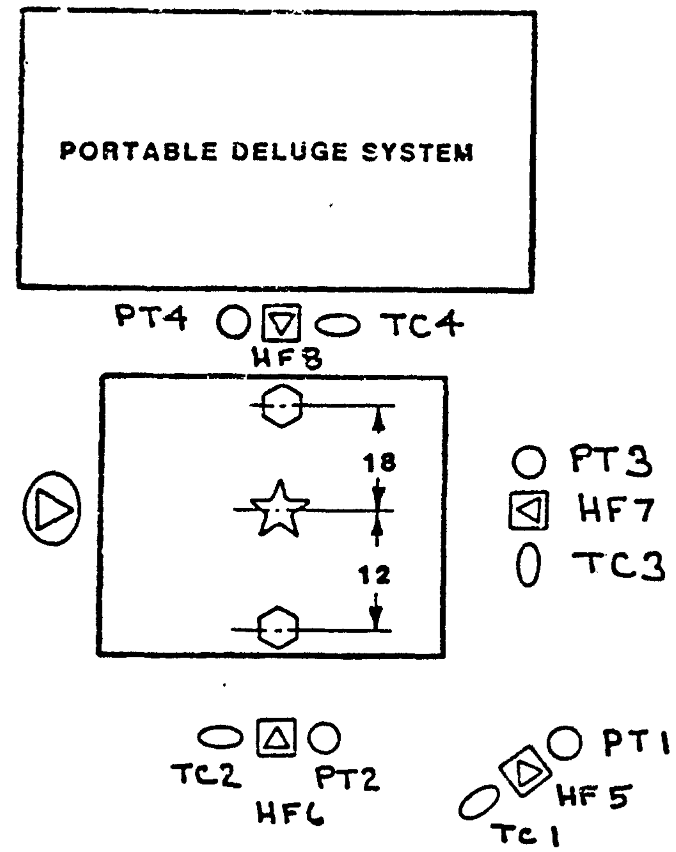

FIGURE 3

PRELIMINARY AED TEST

FACILITY BUILDING 1379 TEST LAYOUT

LEGEND

DONOR CHARGE	MANIKIN
ACCEPTOR CHARGE	PRESSURE
HEAT FLUX	THERMOCOUPLE

FIGURE 4

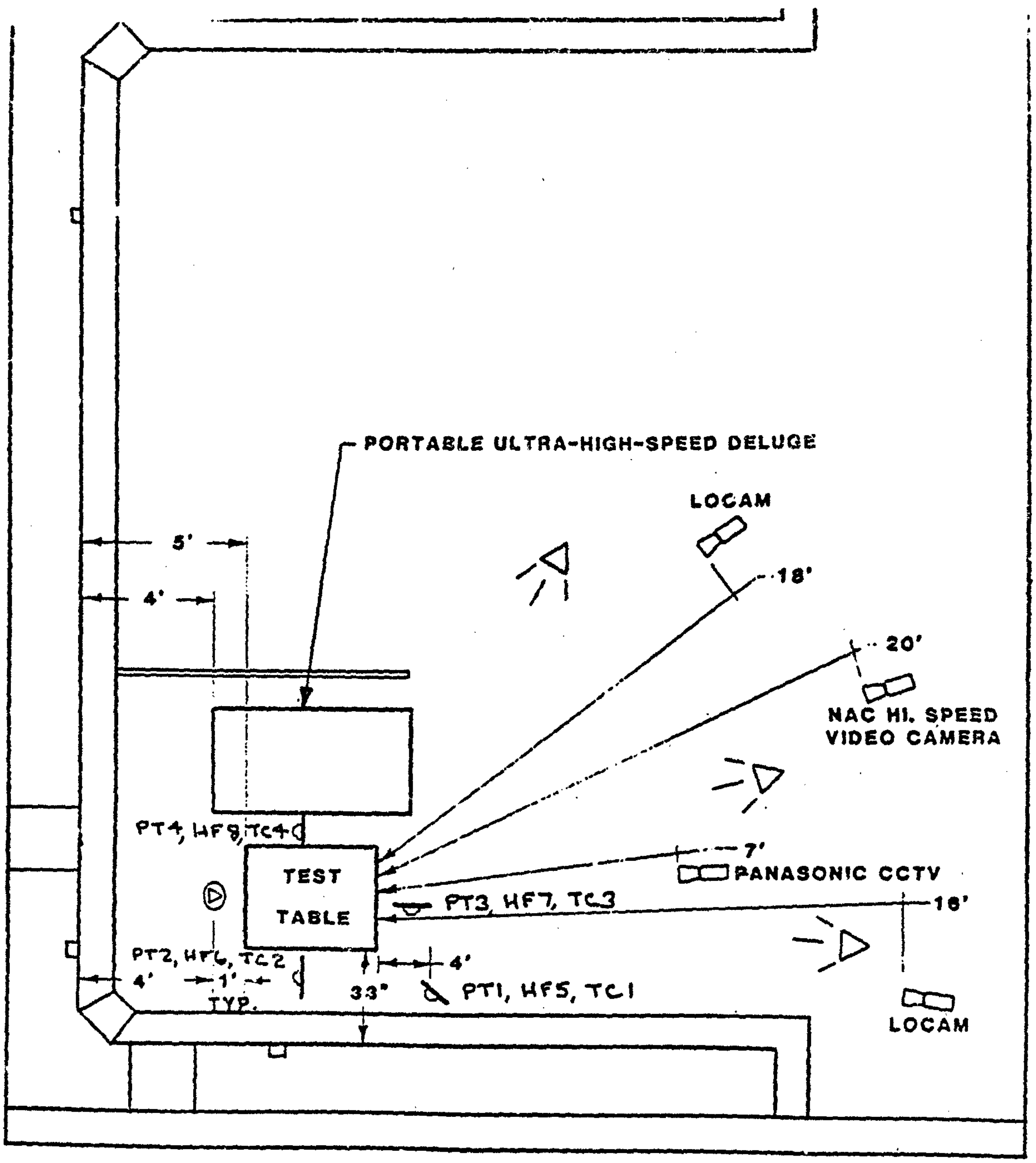

FIGURE 2
PRESSURE TRANSDUCER STANDS, CAMERAS, AND CCTV LOCATIONS BUILDING 1379

FIGURE 4A

APPENDIX A

DRAFT PURCHASE SPECIFICATION

The proposed purchase specifications for the portable ultra-high-speed deluge system were developed by Day & Zimmermann, Kansas Division, under contract with the U.S. Army Production Base Modernization Activity.

Proposed purchase specification is not approved for release. Release is expected in Sep or Oct 1988. Please contact Robert Loyd, U.S.Army Armament Munition and Chemical Command, ATTN: AMSMC-SFP, Rock Island, IL 61299-6000. Telephone is commerical: (309) 782-2975/2182 or Autovon 793-2975/2182.

APPENDIX B

DELUGE VALVES

There are three major types of deluge values. They are the solenoid-operated valve, squib-operated valve, and the explosive rupture disc. A brief description of each is provided below:

a. The solenoid valve uses a pilot-operated deluge valve located behind each nozzle. It operates on a pressure differential basis. When a signal is received from the controller, pressure in the pilot line is released. This permits the valve to open and water to flow from the nozzle.

b. The squib-operated valve uses an explosive squib to open a single deluge valve. This permits line water pressure to be applied to the priming water, located between the valve and the nozzles, causing the rupture discs or caps to blow off the nozzles.

c. The explosive rupture disc system does not use a valve. There is an explosive disc located behind eacn nozzle. When a signal is received from the controller, the explosive disc is fired, permitting water in the piping behind the disc to flow.

APPENDIX C

SCOPES OF WORK - ULTRA-HIGH-SPEED DELUGE SYSTEMS

The U.S. Army Armament, Munitions and Chemical Command has submitted four scopes of work dealing with ultra-high-speed deluge systems to the U.S. Army Safety Center for possible funding as research and development projects. The scopes of work are provided below:

Title: Correlation of the Thermal Flux Protection Requirement with the Protection Provided by Ultra-High-Speed Deluge Systems.

Problem Statement: Army ammunition plants and depots perform various ammunition-related operations involving production, maintenance, renovation, surveillance, and demil. The DOD Ammunition and Explosives Safety Standards (DOD 6055.9-STD) requires that where thermally energetic materials are handled that have a high probability of ignition and a large thermal output, they must be protected with an ultra-high-speed deluge system capable of protecting personnel and limiting exposure to not more than 0.3 calories per square centimeter per second (first-degree burns). A similar requirement is contained in AMCR 385-100, AMC Safety Manual.

The correlation between the degree of exposure permitted and the thermal protection provided by ultra-high-speed deluge systems has never been clearly defined or established.

Furthermore, a different thermal exposure standard is used in MIL STD 398 (Shields, Operational For Ammunition Operations, Criteria for Design of and Tests for Acceptance). The heat flux value is established using the following equation:

$$\text{Heat Flux} = 0.62t^{-.7423} \text{ where}$$

$$\text{Heat Flux} = \text{heat flux in cal/cm}^2\text{/sec}$$

t = total time in seconds that a person is exposed to the radiant

The value used in the DOD 6055.9-STD and AMCR 385-100 is an absolute value while the value used in MIL STD 398 is base on total exposure time. The formulas should be evaluated to determine which formula or combination is the best, then determine if the formula selected needs to be modified or change.

The instrumentation used to measure heat flux, method of calibration, and instrumentation setup is not clearly defined or spelled out in MIL STD 398 or other publications.

Research objective: To establish the correlation between the degree of exposure permitted and the thermal protection provided by ultra-high-speed deluge systems. To establish what formula should be used to measure heat flux. To establish what type of instrumentation should be used to measure and record heat flux, method of calibration, and instrumentation setup.

Title: Computer Model for Design of Ultra-high-speed Deluge System

Problem Statement: Army ammunition plants and depots perform various ammunition related operations involving production, maintenance, renovation, surveillance, and demil. The DOD Ammunition and Explosives Safety Standards (DOD 6055.9-STD) requires that "In those areas of facilities where exposed thermally energetic materials are handled that have a high probability of ignition and a large thermal output, . . . a fire detection and extinguishing system that is sufficiently quick acting and of adequate capacity to extinguish potential flash fires in their incipient state will protect both workers and property". A similar requirement is contained in AMCR 385-100, AMC Safety Manual.

The design, installation, maintenance, and testing of ultra-high-speed deluge systems for ammunition applications involves a technology which is substantially different from that associated with automatic sprinkler systems. Due to the speed of water delivery from all nozzles, ultra-high-speed deluge systems are highly dependent on the detection system, piping network, nozzles, and water supply characteristics; therefore, the design, installation, maintenance, and testing of ultra-high-speed deluge systems must be performed by experienced personnel who thoroughly understand the limitations and capabilities of these systems and the characteristics of the energetic material involved.

However, this is usually not the case. Deluge systems are frequently assembled rather than designed. Once it has been decided to install a deluge system, design is often accomplished by selecting the components based on personnel experience and installing them as best as possible to deal with a hazard that is not completely defined. Once a system is installed, there is usually little thought given to maintenance or testing requirements.

The improper design or installation of ultra-high-speed deluge systems has resulted in numerous false systems activations resulting in large loss of product, downtime, and water damage, and systems that provides little or no protection due to improper selection and/or placement of nozzles and detectors for a hazard that has not been adequately defined. The testing and evaluating the effectiveness of ultra-high-speed deluge systems with a variety of energetic materials with different equipment configurations is time consuming and expensive. The development of a computer model would make it possible to evaluate a large variety of energetic materials and equipment configurations used in the manufacturing, renovation, and ammunition. This should be an extension of the work already done in this area and reported in U.S. Army Armament Research and Development Command Report, AD-E400 315, dated May 1979, entitled "Dynamic Model of Water Deluge System for Propellant Fires".

The following factors should be considered in any model developed: quantity of exposed material; initiation sensitivity; heat output; rate of burning; potential ignition and initiation sources; munitions configuration; water flow rate; time to detection, time to extinguishment; water pressure; water density; water application rate; pipe size; pipe layout, nozzle spray pattern; number of nozzles; nozzle location; deluge valve location; pressure raise of

the energetic material; change in energetic material temperature; process equipment layout; packing density of the energetic material; volume of energetic material; heat of combustion; grain shape and size; water travel distance/time from nozzle to hazard.

Research Objective: To develop a computer model to aid in the design and testing of ultra-high-speed deluge systems.

Phase I: Perform literature search to identify work that has already been done in this and related areas.

Phase II: Develop and test a computer model to aid in the design and testing of ultra-high-speed deluge systems.

TITLE: Design, installation, maintenance, and testing of ultra-high-speed deluge systems for ammunition operations at ammunition plants and depots.

Problem Statement: Army ammunition plants and depots perform various ammunition-related operations involving production, maintenance, renovation, surveillance, and demil. The DOD Ammunition and Explosives Safety Standards (DOD 6055.9-STD) requires that "In those areas of facilities where exposed thermally energetic materials are handled that have a high probability of ignition and a large thermal output, . . . a fire detection and extinguishing system that is sufficiently quick acting and of adequate capacity to extinguish potential flash fires in their incipient state will protect both workers and property". A similar requirement is contained in AMCR 385-100, AMC Safety Manual.

The design, installation, maintenance, and testing of ultra-high-speed deluge systems for ammunition applications involves a technology which is substantially different from that associated with automatic sprinkler systems. Due to the speed of water delivery from all nozzles, ultra-high-speed deluge systems are highly dependent on the detection system, piping network, nozzles, and water supply characteristics; therefore, the design, installation, maintenance, and testing of ultra-high-speed deluge systems must be performed by experienced personnel who thoroughly understand the limitations and capabilities of these systems and the characteristics of the energetic material involved.

However, this is usually not the case. Deluge systems are frequently assembled rather than designed. Once it has been decided to install a deluge system, design is often accomplished by selecting the components based on personnel experience and installing them as best as possible to deal with a hazard that is not completely defined. Once a system is installed, there is usually little thought given to maintenance or testing requirements.

The improper design or installation of ultra-high-speed deluge systems has resulted in numerous false systems activations resulting in large loss of product, downtime, and water damage, and systems that provide little or no protection due to improper selection and/or placement of nozzles and detectors for a hazard that has not been adequately defined. The total fire protection requirements for the operation are frequently not considered. In more than one instance, an ultra-high-speed deluge system has been installed in a building already protected by an automatic sprinkler system or manual deluge system without regard to how the systems will interact should an incident occur. The definition of response time and how it is measured must also be considered.

Research objective: There is a need for a handbook on ultra-high-speed deluge systems. It would provide information on the design, installation, maintenance, and testing of ultra-high-speed deluge systems used in ammunition operations that are well defined. The handbook would be used by installations, headquarters, Corps of Engineers, and outside engineering design and consulting firms. To accomplish this, a three-phase effort is required. It would include a literature search, testing, and preparation of the handbook.

Phase I would consist of a literature search to identify and evaluate work that has already been done and that could be utilized in the development of a handbook for ultra-high-speed deluge systems. A test plan would be prepared to assemble additional information needed for the development of the handbook.

Phase II would be involve testing needed to develop the handbook. Specific topics should include: typical munition items and configurations; detector type, location, and sensitivity setting; nozzle type and location; water pressure; water application density; deluge valve location; locations of air bleeders; system response time; water travel distance from nozzle to hazard; definition of response time; and methods of measuring response time.

Phase III would involve the preparation of a handbook for the design, installation, maintenance, and testing of ultra-high-speed deluge systems utilized in ammunition operations.

Title: Improved Ultra-High-Speed Deluge System for M42/M46 Grenade Presses.

Problem Statement: During the consolidation of Composition A-5 into M42 and M46 grenade bodies, numerous press blows have occurred. Three of these have propagated to the hopper and resulted in the detonation of up to 15 pounds of Composition A-5. These incidents have resulted in major damage to M42/M46 grenade production facilities. The pressing operations are protected by ultra-high-speed deluge systems. They functioned as designed, but even with their 50 to 200 millisecond response time, failed to prevent propagation to the hopper. Propagation appears to be via Composition A-5 spilled on the dial (rotating table). It is estimated the time between initiation of the Composition A-5 on the dial and propagation to the hopper was approximately 24 milliseconds. The M42/M46 grenades are a submunition that is placed in the M483, 155mm, and M509, 8-inch projectiles.

Research Objective: To determine if a faster responding deluge system can prevent a detonation on the dial from propagating to the hopper. Many things affect the response time of ultra-high-speed deluge systems including: detector locations; detector type; deluge valve type; nozzle type; nozzle location; water flow rate; and water pressure. To achieve this objective the following areas must be looked at:

a. Determine the quantity and configuration of Composition A-5 that is spilled on the dial, and then determine the propagation rate of the Composition A-5 on the dial, and the total time from initiation to incident propagating to the hopper.

b. Determine the best type of detection system; e.g., UV, IR, pressure, or sound.

c. Determine the best location and number of detectors.

d. Determine the best type of deluge valve; e.g., squib, solenoid, or explosive rupture disc.

e. Determine the best type of nozzle; e.g., wide angle, medium angle, or narrow angle.

f. Determine the best location and number of nozzles.

g. Determine the best flow rate; pressure; and source; e.g., installation water system; pressure tank; or elevated tank.

APPENDIX D

TECHNICAL REPORTS ON DELUGE SYSTEMS

1. Design of a Deluge System to Extinguish Lead Azide Fires, No. AD-E400 204, Aug 78, approved for public release (APR).

2. Evaluation of Pyrotechnic Fire Suppression System for Six Pyrotechnic Compositions, No. AD-E401 306, Mar 85, APR.

3. Engineering Guide for Fire Protection and Detection Systems at Army Ammunition Plants, Vol I (Selection and Design), No. AD-E400 531, Dec 80, APR.

4. Engineering Guide for Fire Protection and Detection Systems at Army Ammunition Plants, Vol II (Testing & Inspection), No. AD-E400 874, Dec 82, distribution limited to U.S. Govt Agencies only - contains proprietary information.

5. On-site Survey and Analysis of Pyrotechnic Mixer Bays, No. AD-E401 141, Feb 84, APR.

6. Feasibility Study to Develop a Water Deluge System for Conveyor Lines Transporting High Explosives, Tech Rpt No. 4889, Aug 75, APR.

7. Development of a Water Deluge System to Extinguish M-1 Propellant Fires, No. E00 217, Sep 78, APR.

8. Design of a Water Deluge System to Extinguish M-1 Propellant Fires in Closed Conveyors, No. AD-E400 216, Sep 78, APR.

9. Fire Suppression System Safety Evaluation, No. AD-E401 083, Dec 83, APR.

10. Dynamic Model of Water Deluge System for Propellant Fires, No. AD-E400 315, May 79, APR.

11. Deluge Systems in Army Ammunition Plants, prepared by Science Applications, Inc., for the U.S. Army Munitions Production Base Modernization Agency, 30 Jun 81.

12. Minutes of the Rapid Action Fire Protection System Seminar, U.S. Army Armament, Munitions and Chemical Command, 23-24 Oct 84.

13. Fire Protection Systems Utilized in U.S. Army Munition Plants, Robert Loyd, U.S. Army Armament, Munitions and Chemical Command, No. A192447, 30 Nov 88.

14. Ultra High Speed Deluge Systems, Robert Loyd, U.S. Army Armament, Munitions and Chemical Command, 27 Jul 87.

15. Portable High Speed Deluge Cost Effective Explosion Suppression, Gary Fadorsen, Automatic Sprinkler Inc., 8 Mar 88.

16. Portable Ultra-High-Speed Deluge System, Day & Zimmermann Kansas Division, Paul Kennedy (Prepared for the U.S. Army Production Base Modernization Activity).

Most of these reports can be ordered from the Defense Technical Information Center, Cameron Station, Alexandria, VA 22314. Their telephone number is AV 284-7633.

APPENDIX E

REFERENCES

1. AMC Safety Manual, AMCR 385-100, 1 Aug 85.

2. DOD Ammunition and Explosives Safety Standards, DOD 6055.9-STD, Jul 84.

3. Maintenance of Fire Protection Systems, TM 5-695 (Army)/FAC MO-117 (Navy)/AFM 91-37 (Air Force), Oct 81 with Change No. 1.

4. Military Handbook - Fire Protection for Facilities Engineering, Design, and Construction, MIL-HDBK-1008, 30 Apr 85.

5. National Fire Codes, National Fire Protection Association.

ULTRA HIGH SPEED DELUGE FOR SUPPRESSION OF FIRE
AND EXPLOSION IN HIGH ENERGY CHEMICAL PROCESS FACILITIES

Gary A. Fedorsen

August, 1988

High Speed Deluge for the suppression of fire and explosion in explosive, pyrotechnic and propellant manufacturing process facilities has become widely accepted and has proven to be a viable life-safety system. Over the past fifteen years there have been many improvements in both the electrical and mechanical design of these high speed deluge systems. Because of the many different chemical compositions and processes involved in the high energy chemical field, it is impossible to write an effective generic coverall specification for high speed fire protection. Actual burn testing involving the product and the specific process would provide information for writing improved specifications, at this point burn testing with high speed deluge is still in its infancy. A great deal of work needs to be done in this particular field. The tests that were done at Toole Army Ammo Depot in March, 1988, using nitrocellulose type propellants are a good example of the type of testing that needs to be done. If nothing else, actual burn tests should emphasize and illustrate the different possibilities and scenarios that can crop up in a particular application. Actual burn testing provides an enormous amount of data such as the hazards that the personnel are exposed to, the effect of response time on the particular high energy compound. It is useful to determine the distance of nozzles and detectors, to establish a cone of view for the detectors and also to establish patterns for nozzles so that they can be used most effectively.

In the past, there have been large amounts of money spent on ineffective high speed deluge systems. Although this product burn testing is fairly expensive, I believe the long term savings in both lives, equipment and dollars would warrant more of this type of experimentation.

The following paper describes just a few of the many different high energy chemical compounds and processes that are encountered by the safety engineer. The paper is a reprint of one presented in July, 1988, at the INTERNATIONAL PYROTECHNICS SOCIETY'S THIRTEENTH SEMINAR IN GRAND JUNCTION, COLORADO.

Considering the small amount of exposure, I though it appropriate and permissable to reprint the paper for the DEPARTMENT OF DEFENSE EXPLOSIVE SAFETY BOARD, 23RD SEMINAR, AUGUST, 1988.

SYSTEM DESIGN

The topic of discussion is High Speed Deluge for explosion fire protection. However high speed deluge is probably not the easiest nor does it rank as the highest priority of all the safety methods and procedures utilized in the high energy chemical field. It is not a cure for all cases. Often explosive safety can be obtained by both obvious and relatively inexpensive means. For instance, cutting down on batch size, continuous mix operations (screw extruder mixers),training personnel and newer less sensitive compounds. Unfortunately, in the real world, this is not always possible, economical or applicable. There are cases where we will have personnel working with a hazardous mix and in quantities that could do some substantial damage. Hopefully, in the near future, all hazardous processes will be remote operations leaving the operators safe and out of the hazard area. Even if this were the case, the property costs involved if there was an incident, often would warrant some sort of protection or explosion prevention.

In very broad terms there are two (2) basic criteria that must be met in an explosion suppression system. (1) It has to be fast enough to perform the task before the incident gets beyond the

point where suppression is ineffective. (2) If the fire or explosion is meant to be suppressed or extinguished, the proper suppressant must be used. In the case of energetic chemical compounds, chemical extinguishments (CO_2, Halon, Dry Chemical) are not usually effective or feasible. The main reason being, that, in energetic chemical mixes (for example explosives, pyrotechnics, and propellants) there is an oxidizer that provides the oxygen required to sustain combustion. A few examples of oxidizers are ammonium perchlorate, potassium nitrate, sodium nitrate, etc.

The function of the water as a fire suppressant is to disperse and cool the mixture to halt the chemical reaction. Other extinguishments such as CO_2, dry chemical, Halon, would not be able to perform as well as water or at all in some cases, because their operation is based on smothering or cutting off oxygen to extinguish the fire.

The speed necessary to halt the explosion and deflagration is dependent on many variables including the type of mixture being processed, the type of process (whether it be an enclosed vessel, an extrusion, mixing, drying, pressing, etc.) and the proximity of the personnel and critical equipment. There are some cases where the only alternative or option is to allow it to burn. Conversely, there are instances in which high speed deluge, with reaction time in milliseconds, (usually less than 100 milliseconds) is necessary to protect the lives of personnel or costly equipment.

Some variables that may influence the speed of deflagration are, mass of the compound, density, temperature, moisture or solvent content, the physical geometric shape of particle size of the compound, and whether or not the substance is contained. The classic example of how different containments could affect the burning characteristics of explosives is in the example of black powder. Black powder, one of the oldest and most versatile

explosives, when burned in an open long train is relatively slow burning and is sometimes used as a fuse. Confined with one end open for exhaust, black powder can be used as a rocket propellant. When contained in a fairly rigid container, black powder could become explosive with deflagration speeds reaching detonation.

High speed deluge systems are sometimes installed with no thought or knowledge as to the hazards that they are to protect. Often, the system is designed or procured around specifications written for a completely different process. It is the responsibility of both the user and the vendor or contractor to be knowledgeable of both the processes and hazards involved and the variety and capabilities of different suppression systems available to meet the need. It is not uncommon to see deluge systems that are specified for fifty (50) milliseconds reaction time, installed sometimes fourteen (14) feet above the hazard, providing general overall coverage. Applications like this are a waste of effort and provide an ineffective, unsafe system. It is essential to get both detection and water spray nozzles as close as possible to the hazard. In most cases, this will also save on system cost.

There are many cases where various protection systems will provide adequate safety. Also, there are instances where only one (1) specific type system will handle the task. Alternately, one may encounter cases where a hybrid or combination of two (2) systems would provide the necessary safety margin. For example, high speed deluge combined with rupture disc or over pressure release mechanisms. Another example may be high speed deluge combined with product shut-off mechanisms to stop the flow of hazardous material.

The following are a few basic guidelines to consider when designing or specifying a high speed deluge system. For the sake of clarity, energetic chemicals are broken down into three (3) basic groups. The categories are High Explosives, Pyrotechnics/Low Explosives and Propellants.

HIGH EXPLOSIVES

Often, the first thoughts or reactions to high speed deluge protection for high explosives is that there is no fire protection system that could stop the detonation process when the explosive goes to a high order state and this of course is very true. But, in many cases prior to the explosion, there is a fire. Examples of high explosives process applications are extrusion dies for C-4 explosives or a TNT melt kettle. In these situations, there is a good chance that there will be a fire preceding the explosion. The fire could start and propagate until the pressure build-up was enough that we achieve high order detonation or, in other words, a cook-off type of reaction. In this situation high speed deluge would be quite feasible in stopping the initial fire which precedes possible explosion. Again, dealing with high explosives the processes must be considered. For example, a TNT melt kettle is a closed vessel with a steam heat jacket, in most cases, operating at approximately 180 degrees fahrenheit. Often the enclosure is operated at a slight vacuum. Presently, one of the best ways to attack the situation is to provide infra-red detection within the melt kettle. With this in mind, infra-red flame detection at the present state of the art is susceptible to ambient light. Design consideration should be made to disable the infra-red detection when the melt kettle is open either for cleaning or for adding material. Infra-red detection is less susceptible to the attenuation due to dirty lens caused by steam, smoke or particles than it's ultra violet counterpart. So, in this case, infra-red detection lends itself to a fairly good design option. Also, in the case of a TNT melt kettle, flooding of the kettle with water is necessary. There is no need for special spray nozzle patterns in this situation. The objective would be to get as much water as possible into the kettle for the flooding action to extinguish the fire. Deluge speed in this case is essential. Due to the fact that we have an enclosed vessel and a fire situation could build pressure rapidly in the vessel, possibly to a point high enough to cause detonation. One other option for melt kettles may be quick release venting, either mechanical gate or rupture disc method.

A common process in high explosive product manufacture is casting. Oftentimes TNT, RDX or HMX type materials are casted into a shell, bomb, or a mine housing. In this situation we have a molten explosive being physically poured into a chamber. There is a chance for spilling, overflow and there is exposed explosive often from the ejection point to the fill area. For casting and filling, ultra-violet detection with high speed deluge nozzles as close as possible to the hazard are recommended. Since ultra-violet detection is not susceptible to normal ambient light, it would be the least troublesome and beneficial type of detection. Again bring your nozzles as close as possible to the hazard.

Extrusion is a process encountered with explosives. For instance, extruding C-4 explosive blocks. One possible source of fire is at the extruder die. As the explosive leaves the extruder die, there is often friction and the explosive is under pressure making this a likely ignition point. Ultra-violet detection, with nozzles as close to the hazard as possible would be a viable method to help prevent an incident.

High explosive melt-out or steam-out is an application for high speed deluge. The design would have to vary with the particular process involved, which is actually more dependant on the munitions involved in the meltdown. A demil (demilitarization) process often encountered is the belt flaker or "candy maker". In the belt flaker the high explosive, often TNT or RDX is melted and extruded onto a stainless steel water cooled conveyor belt. As the conveyor moves along, the explosive solidifies and breaks off at the end and is either boxed or sent on to other processes. Detectors (ultra-violet) should be placed within the conveyor hood. Nozzles are installed within the hood as close as possible to the hazard. Because of the presence of steam and vapors, it is recommended that air shields are used to keep the detector lenses clean and maintain the system integrity.

PYROTECHNICS/LOW EXPLOSIVES

Design considerations for low explosives will be combined with pyrotechnics, since many of the methods for detection and suppression are the same. Items that fall into the low explosive and pyrotechnic category would be golden powder, black powder, illumination flare mixtures, mag-tef flare mix, smoke mixes, first fire, delay mixes, fireworks, salute mixes, etc. Some of the processes involved in the manufacture of low explosives include grinding, mixing, activation of binders, extruding, pressing, granulating, and drying, these being some of the most common processes encountered.

The initial grinding process is probably the least hazardous due to the fact that, in most cases, the ingredients are still separated. For example, the oxidizers are ground separately from the fuels. Processes such as roll milling or ball milling demand customized systems designed on a one-to-one basis. Each situation is unique and should be handled accordingly. Often encountered during pyrotechnic production is the use of solvents to activate binders. Solvents, are in most cases, flammable with flammable vapors. To compound that problem, certain vapors attenuate U.V. radiation emitted from the flame. The characteristics of the solvent must be determined along with its effect on the detection system. In past explosions the flammable solvent fumes where in some cases the initial source of fire that then propagated to the pyrotechnic mix. Even though as a rule, solvent dampened compounds are less sensitive than dry, the problem of the flammable solvent fumes must be considered.

Grinding and granulation is a hazard because we are exerting extreme physical forces on the completed pyrotechnic mix. Chances for impact, friction and even static initiation is much greater at this point. Compounding the hazard during this step of the processes is the fact that we are working, in most cases, with

large bulk amounts of the product. When protecting a container or hopper with large amounts of pyrotechnic product, it is recommended to not only apply water from the top but also to provide for flooding of the vessel from the bottom or the sides.

Composition pressing is a very common practice in pyrotechnics, especially in the case of smoke and flare compositions. During the pressing procedure, the pyrotechnic mixture is compacted at very high pressures exerting large physical force, up to thousands of PSI. Although it is almost impossible to stop any ignition or deflagration in the press or the object being pressed, it is often advantageous to suppress propogation of the flame or explosion to bulk hoppers containing mix yet to be pressed or finished pelletized product. Often the pressing machinery is designed and shielded to withstand initiation during the pressing procedure. In this situation, the objective would be to protect operators and counter propogation.

Application of first fire is a fairly dangerous task and often involves an operator in intimate contact with the hazard. The operator is working with a sensitive mixture, even though the mixture is wetted. If the first fire were to initiate, it could cause initiation of the parent product. One example would be the application of first fire to magnesium teflon flares. If done manually, the operator is directly exposed to the high temperature burning of the magnesium teflon flare. In this scenario, one option is to aim the fire suppression nozzles at the operator and also use nozzles configured to drive the burning flare into a hopper or chute so that it is driven away from the operator. The reason being that certain compositions, including magnesium teflon, mixes are very hard to suppress with the water spray, so it is best to separate the operator from the hazard.

Usually, the final stage in the production of a pyrotechnic mix is the drying phase. During this phase the solvents are removed from the final product or the product is allowed to cure. During the drying process the pyrotechnic mixture is often subjected to added heat to facilitate faster and more even drying, at this point, the pyrotechnic product is susceptible to ignition. Ignition may be due to spark, friction or impact but is sometime due to a chemical reaction during the drying process. In many cases this is an unpredictable reaction. High speed fire suppression is a very good safety measure unless the cost of product loss is low enough and equipment is built to withstand ignition, then it may not be economically feasible to use high speed fire protection unless of course operators are exposed to the hazard.

Frequently, fires occur during cleanup or equipment tear-down. This should always be considered when designing an explosive prevention system or high speed deluge so that the system will activate and do its job during the cleanup and tear-down process if it is deemed a possible hazard. In most all cleanup or repair situations, plant personnel are in the hazard area.

PROPELLANTS

Propellants offer some similarities in reference to hazards that the explosive and pyrotechnic categories present. However there are some processes that are unique to propellant. Propellants are extruded, which offers the same hazards as extruding high explosives, except for the fact that, in most cases, propellants will burn much more aggressively, although there is probably not as much of a chance of achieving detonation. A good rule of thumb, would be that anywhere there is action (movement, friction impact, static discharge) there is a chance for initiation. In other words, where the propellent leaves the

extruder die, or, if the extrusions are being cut into pellets, during the cutting action. For composite propellant mixing, high speed fire protection flooding the mixing bowl is advised. If using a closed mixer, infra-red detection is presently the state of the art method to use in the closed vessel. It offers faster reaction time and is less subject to blinding or obscuration.

Sometimes propellants are machined after casting or pressing. The propellant machining process should be monitored by ultra-violet type detection keying where the tooling comes in contact with the propellant and if operators are present protect the operator, stop propogation to hoppers or to propellant feeds. Often the propellant pellets, especially the nitrocellulose type propellants, are coated with graphite to help its flow through processing equipment and to prevent possibility of static discharge. The added graphite coating can cause two (2) potential problems. (1) Is that it can obscure the detector lens because it has the tendency to float in the air and (2) it can inhibit deluge water penetration into the propellant mix due to its ability to shed water. In the case of graphite coated propellants it may be advisable to use air shields on the detectors and provide penetrating and flood type spray configurations.

Propellants are often involved during demil (demilitarization) operations . During the demil process the item is separated or opened so the propellant may be poured into collection container. The equipment, and operator if present, should be protected during the step when the projectile is pulled from the shell or cartridge. Also, during the pouring of any propellant, there is a potential hazard because of friction and possible static initiation. There is also a chance, due to the age and storage condition, that the propellant may have become more sensitive than normal. Large quantities of propellants when contained in hoppers or similar containers should receive deluge water both from above and flooding from within the container as with some of the pyrotechnic mixes.

The nature of the progressive burning and increasing burn velocity of propellants emphasizes the need for a very fast fire protection system that will extinguish or suppress the flame before it can get to the point where it is out of control and the gas velocity is such that it will not allow for water penetration.

Thermal dehy during the propellant manufacturing process is another feasible and recommended application for high speed deluge. In this case, if hooded equipment is involved, infra-red detection is probably the best answer.

Triple base propellant (consisting of nitrocellulose, nitroglycerin and nitroguanidine), double based propellants (consisting of nitrocellulose and nitroglycerin), single base propellants (consisting mainly of nitrocellulose), do not exhibit different characteristics as far as the ability to be extinguished by water spray, although the burning rates and temperatures do vary. More testing would have to be done to verify the affects of the water spray (varying amounts and speed) on the different propellants. So far, water has proven to be very effective when delivered quick enough. Composite mixtures, i.e. ammonium perchlorate and aluminum can be protected during the pour and casting process and during the mix process. The system configuration would have to be determined specifically for the process.

Initiating explosives such as mercury fulminate, lead azide, lead styphinate, pose particular hazards due to their combustion characteristics. They are very sensitive to heat, static, friction and impact initiation and they seem to transcend the deflagration stage and almost evaporate into a detonation. With these compounds, probably the utmost safety measure would be small batches and isolating the material. High speed deluge for these initiators would probably only be effective as a deterrent to propogation. Avoid using brass fittings and nozzles in lead azide

areas as copper and brass, when combined with moisture, may cause lead azide to form extremely sensitive copper azide.

As previously stated, general overall coverage type systems located high in the ceiling, should be avoided, but as with all rules, there is an exception. The exception being, that, in an explosive area where there is chance of dust or explosive particles which had previously settled on equipment or parts of the building, a general coverage high speed deluge may help to eliminate the explosive hazard. Although, good housekeeping and a cleaner working environment would probably be a more cost effective way to handle this problem. If there is a chance of secondary explosion, i.e., an initial blast that is hopefully suppressed by the primary system, were to force out explosive dust or particles allowing for a secondary explosion. In this situation a secondary overall coverage system may help to eliminate this.

The preceding was a brief summary of high energy process applications where high speed deluge may be incorporated. There are many other substances and processes that warrant the use of high speed fire protection. This has been a review of some of the more common. It cannot be stressed enough that, both the substance and the process should be reviewed before designing and installing a high speed fire protection system. Specifications for the systems should be written per the application. More times than not, generic specifications do not provide for a system that would do the job adequately. Whenever possible, it is suggested that actual burn tests be performed using the same high energy substance and the same process situation for the test and design as will be used in the final application. As with other situations that we encounter; when in doubt, the best rule of thumb is to use common sense when designing your systems and to have intimate knowledge of the product and process involved.

PORTABLE HIGH SPEED DELUGE

Having quickly covered some fixed high speed deluge applications, it is appropriate now to introduce a new concept in high speed deluge for high energy chemicals, the Portable High Speed Deluge System. It is hoped that Portable High Speed Deluge could prove to be a viable life safety system, and at the same time provide cost savings, in certain unique applications. Portable High Speed Deluge is a totally self contained fire detection and suppression unit. Totally self contained meaning; battery power supply to provide power to detectors and to activate the system; self contained water supply and pressurizing capabilities to propel the water; and the ability to move not only the portable unit itself but also reconfigure and relocate the detectors and the nozzles. The Portable Deluge System should be able to achieve reaction times of at least fifty (50) milliseconds. Reaction time defined as: time from instant of flame detection to flow at nozzle. The batteries should provide power to the unit for at least eight (8) hours and be supervised to signal and annunciate the loss of power. The system should be completely supervised for detection, solenoid integrity, loss of pressure, low water, and any other function that might inhibit the system from operating correctly.

The Portable System is not intended to replace or eliminate Fixed High Speed Deluge but does suffice in filling the "gap" where Fixed High Speed Deluge is not feasible because of constraints such as water supply and changing processes or fixed deluge is not feasible for economic reasons.

Listed here are some examples and suggestions where the Portable High Speed Deluge would be advantageous. These are just a few of the many applications where Portable High Speed Deluge could prove useful and cost effective;

* Explosive or pyrotechnic spills. The portable could be rolled in and used to protect the area during the clean-up operation, in any area where fire protection may not normally be present.

* When there is not sufficient time or funding to install fixed fire protection quickly enough to satisfy the need.

* Depot re-work where maintenance or operations often change and machinery is moved or replaced with different equip- ment. In these applications, fixed systems are not practical from an operational, safety or economic standpoint. The area may have previously gone unprotected or improperly protected had portable deluge not been available.

* Anytime there is machining, milling, blending or drying, the portable system could be attached to the machinery. This may eliminate the need to move the machinery to a location with fixed high speed deluge; especially advantageous if only needed for a short time.

* When the existing system is shut down and production must go on. Loss of production can be costly, portable deluge may bridge the time involved in getting fixed system back on line.

* Clean up and decontamination operations when equipment is torn down or if there is fear of residual explosives. Clean up can be a most hazardous aspect of tasks at explosive facilities, often exposing operators to various and sometime unforseen risk.

* The portable system would be very cost effective to evaluate and test the design of fixed fire protection systems with actual burn test to prove the effectiveness of such systems. The system would allow for easy modification and variations providing more comprehensive test results.

* In research, evaluation and quality control laboratories hazards often vary as do the processes and material that the technicians are exposed to. Many times the energetic material has known properties such as sensitivity to spark, friction or impact. Sometimes in the case of experimental compounds the properties (possibly hazardous) are unknown. In either case it would be advantageous to be able to roll in a Portable High Speed Deluge System to protect personnel and equipment. Processes in the laboratory environment are also quite likely to change. For example; blending, mixing, granulating, extruding and drying. Changing operations (if hazardous) require an adaptable explosion or fire suppression system. Although personnel are more highly skilled and quantities often much smaller, the explosives laboratory can be a hazardous environment and in some cases warrant the use of such a system.

* Temporary depot and staging areas possibly off-shore or overseas applications. Portable High Speed Deluge can be applicable where fixed deluge could never have been considered possible because installation speed, lack of water supply or various processes.

* Used in areas where improper or insufficient water supplies are a problem. This would apply to the above mentioned areas (temporary depots and staging areas and domestic ammunition and pyrotechnic processing plants that have inadequate or no underground supply water supplies in some test areas or building locations.

* Temporary storage protection for in-process work. In the situation of production over runs where surplus must be stored and normal adequate fire protection is not available. Also in the case of rejected production runs where the product must be stored until it can be recycled or destroyed.

* Portable High Speed Deluge could be an additional back-up for existing High Speed Deluge, allowing for inadequately designed systems or unforseen changes in process.

* Additives can be included with the water supply; for instance, anti-freeze or wetting agents. Water coloring might be added to help evaluate different spray patterns utilizing high speed video (for added clarity). Possible advantages of water gels "sticky water" could be experimented with.

* Portable High Speed Deluge is easy to maintain; it can be moved to a shop or maintenance area for service, allowing it to leave the restircted (hazardous) area. Nozzles with different spray patterns can be adapted, moved and configured depending on operation. Very beneficial for design evaluation for fixed systems. Nozzles may be configured to propel the hazard away from the operator or to push the operator from the hazard with water spray.

The following are suggested guidelines for specifications of Portable High Speed Deluge systems.

Flow time -	Approximately one minute (1 min.)
Flow Rate -	Approximately twenty-five (25) gallons per nozzle per minute maximum, when all four (4) nozzles are fired simultaneously.
Detection -	Minimum two (2) ultra violet detectors (for redundancy) and compatible control unit to monitor detection, detect fire and provide fire output.

Actuation -	Four (4) Pilotox Deluge nozzles with two (2), 24 VDC solenoids and two (2) High Speed Module slave units.
Nozzle mobility -	Nozzles supply and pilot supply lines shall be flexible to allow a minimum of one (1) foot horizontal and vertical movement. Operator shall have the option to select the number of nozzles to protect the hazard by use of a ball valve or other suitable means. Nozzle configurations using flexible hose shall be available for placing nozzles up to fifteen (15) feet from portable unit. Nozzles shall be connected to process equipment by use of integral positioner clamp.
System reset -	System reset shall be accessible to the operator from <u>outside</u> the explosion proof electrical enclosure and accomplished in less than thirty (30) seconds from activation of reset switch.
Automatic Reset -	System shall be available with an (optional) automatic reset allowing up to one (1) minute of flow. Automatic reset shall not activate if fire is present.
Reaction time -	Shall be less than fifty (50) milli-seconds for the system described. Reaction time is defined as being instant of detection at the panel to waterflow at the nozzle. System reaction time may vary

according to hose length/nozzle distance from unit, reaction time shall always be less than one hundred (100) milli-seconds.

Fire test actuator -Panel shall have actuator to simulate "fire condition" for testing purposes.

Battery back-up -Minimum reserve power of eight (8) hours in stand-by; five (5) minutes in alarm. Shall plug into 120 VAC, 60Hz outlet (or other voltage as specified)

Power supply/battery charger - Shall provide sufficient power to charge battery system within eight (8) hours. Charge shall be integral part of control panel.

Annunciation - Visual fault indications for low water pressure, low water level, HCM/U.V. controller fault, low battery condition, "system ready" indication. Audible fault horn to annunciate any fault.

Auxiliary contacts - Shall provide minimum of two (2) form "C" contacts for fire condition and two (2) form "C" contacts for fault condition.

System mobility - Two (2) swivel casters
Two (2) fixed casters
Two (2) floor locks
Shall also be moveable by a fork lift.

Electrical explosion proof requirement:
Class II, Group G

Electrical enclosure:

Explosion rating : Class II, Group G
(with window for visual access)

Pressure tank - CAPACITY: - 100 gallons
* to be pressurized to 175 psi
WORKING PRESSURE: - 200 psi by nitrogen gas
Supply tank to have water inlet shut-off and air bleed ball valves.

Overall dimensions - SIZE: L-69" x W-48" x H-80"
(system fully extended)
WEIGHT: 1,200 lbs. (empty tank)

The Portable High Speed Deluge System shall be a completely self-contained deluge system which is portable by use of its casters or lift truck. The Portable High Speed Deluge System shall feature one (1) button reset, ultra-violet detection; four (4) Pilotex valves w/autospray nozzles; battery back-up and complete supervision. Because of the principals inherent in the design of the pilot nozzle, there shall be no need for replacement of squibs or rupture discs when resetting the system.

The Portable High Speed Deluge System shall be fired electronically through the use of a solenoid, thus it may be reset the same way.

By activating the reset button, the solenoid shall close. This restores pressure to the pilot line and restores the system to a "Ready" condition.

The four (4) pilot valves actually operate as four (4) small deluge valves. Each valve has two (2) water connections; one (1) for supply and one (1) for pilot.

The supply is held back by use of a poppet, which is held in the closed position through use of pilot pressure.

The system shall be fired by a solenoid which is attached to the pilot line. This solenoid opens, releases the pressure within

the pilot line and allows the poppet to "LIFT" inside the body of the pilot valve. When this poppet rises it allows the supply water to flow from the nozzle. This entire process shall be accomplished in less than fifty (50) milli-seconds.

Spray nozzles are designed to fit into the pilot valve in order to accomplish the flow pattern required.

The Portable High Speed Deluge System is supervised for AC loss, low system pressure, controlled faults and low water level.

When system in operational "Ready" mode, it is indicated with a green "System Ready" light.

All detectors and solenoids are supervised and any fault will be signaled with an audible fault horn.

As mentioned, the Portable High Speed Deluge is not intended to replace fixed explosion suppression systems but will fill the need for explosive safety in many situations. Portable Deluge is a cost effective alternative in many situations that otherwise would have called for loss of production and downtime.

CONCLUSION

Ultra High Speed Deluge is not a cure all panacea for all the hazards involved in the high speed chemical process field. It is a formidable solution for many safety problems encountered and has proven in the past to be a successful means of explosion suppression. If nothing else, one point should be understood and remembered. When designing or specifying high speed fire protection always consider both the compound being produced or processed and the type of process utilized. Above all, if an operator is present, how best to protect your personnel.

Any questions, comments or criticisms, please contact Gary A. Fedorsen, "Automatic" Sprinkler Corporation, (216) 526-9600, Ext. 378; Residence: (216) 467-2910.

RAPID RESPONSE DELUGE TESTS
USING A PORTABLE DELUGE SYSTEM

JERRY R. MILLER, P.E.
AMMUNITION EQUIPMENT DIRECTORATE
TOOELE ARMY DEPOT

Evaluation tests of a portable rapid response deluge system were conducted in March 1988, by the Ammunition Equipment Directorate (AED), Tooele Army Depot (TEAD) in conjunction with other government agencies and contractor representatives. Representatives of these agencies witnessed most of the performed tests. Among the representatives at the tests were Goerge Obrien, PBMA; Bob Loyd, AMCCOM Safety; Paul Kennedy, Project Coordinator, Day and Zimmermann, Inc, Kansas Div. Gene Burns, Day and Zimmermann, Inc., Lone Star AAP, Gary Fadorsen and Mike Lechko, Automatic Sprinkler Corp., of America. Dugway Proving Grounds personnel provided high speed video documentation of the tests.

A commercially manufactured portable ultra-high-speed deluge system was set up for the tests in Bldg. 1379 at the AED test facility, Tooele Army Depot, Tooele, Utah. These tests were to somewhat simulate propellant rework operations. Various types and quantities of propellants were initiated with electric matches and igniters.

Response times, overpressures, heat flux, temperatures and other measurements were taken during the tests and then compared to various certification criteria such as is found in MIL-STD 398. In general terms, under this standard:

1. The measured overpressures are not to exceed 2.3 psi peak positive incident pressure (P_{so}) measured at personnel locations.

2. The heat flux measured at personnel locations is not to exceed the value given by the equation:

$$\phi = 0.62t^{-0.7423}$$

Where ϕ = heat flux in cal/cm^2-sec

t = time interval of exposure to measured heat flux in seconds

3. Fragments must be contained within the shield, or directed away from personnel locations.

4. Shield movement or deflection shall not be such that personnel injury would result.

During this test series four (4) different types of propellant were tested:

1. M9 Propellant (81mm mortar)
2. M1 Propellant (105mm howitzer)
3. M8 Propellant (4.2 inch mortar)
4. M26 Propellant (106mm round)

Five propagation tests were performed utilizing the above propellants. The deluge system was not used during the propagation testing to demonstrate that fire would spread from the donor charge to the receptor charges and thus confirm the validity of the donor/receptor spacing for the qualifying tests which followed. On these tests, the instrumentation consisted of a real time video camera system, a high speed video camera system, four thermocouples with a datalogger system and a heat flux sensor with recording system. Figure 21 is a graph of the heat flux measured on four of the propagation tests and figure 36 is a graph of the measured temperatures on propagation test PT-4 (M26 propellant).

Following the propagation tests, ten qualification tests were performed on the same propellants. In addition to the same instrumentation which had been used on the previous tests, two high speed motion picture cameras operating at 500 frames per second, four pressure transducers, and three more heat flux sensors with associated instrumentation were used to record the results. A manikin with explosive handlers coveralls was also positioned in front of the munition test table to see what might happen to the surface of the coveralls/manikin. Figures 1 through 3B depict the instrumentation schematic, transducer and camera locations,and general test layouts. Figure 29 is a graph of the heat flux measured on qualification test no. QT-4B and figure 45 is a graph of the measured temperatures on the same test.

The pressure transducers were set up to measure peak side-on pressures. Since the tests basically involved unconfined burning or deflagration of the propellant, no detonations were measured. Consequently no pressure data was extracted.

With respect to these specific tests, the commercial rapid response deluge system performed well. Measured heat flux levels were significantly reduced with the deluge system functioning. All test results seemed to verify the effectiveness of this type of deluge system in providing operator protection for limited applications as can be seen from figures 24A, PT-2 vs QT-2 for M1 propellant, and figure 30A, PT-4 vs QT-4B for M26 propellant.

Sections of real time video vs high speed video and high speed film of these same two tests will now be shown.

Figure 29 Heat Flux QT-4A

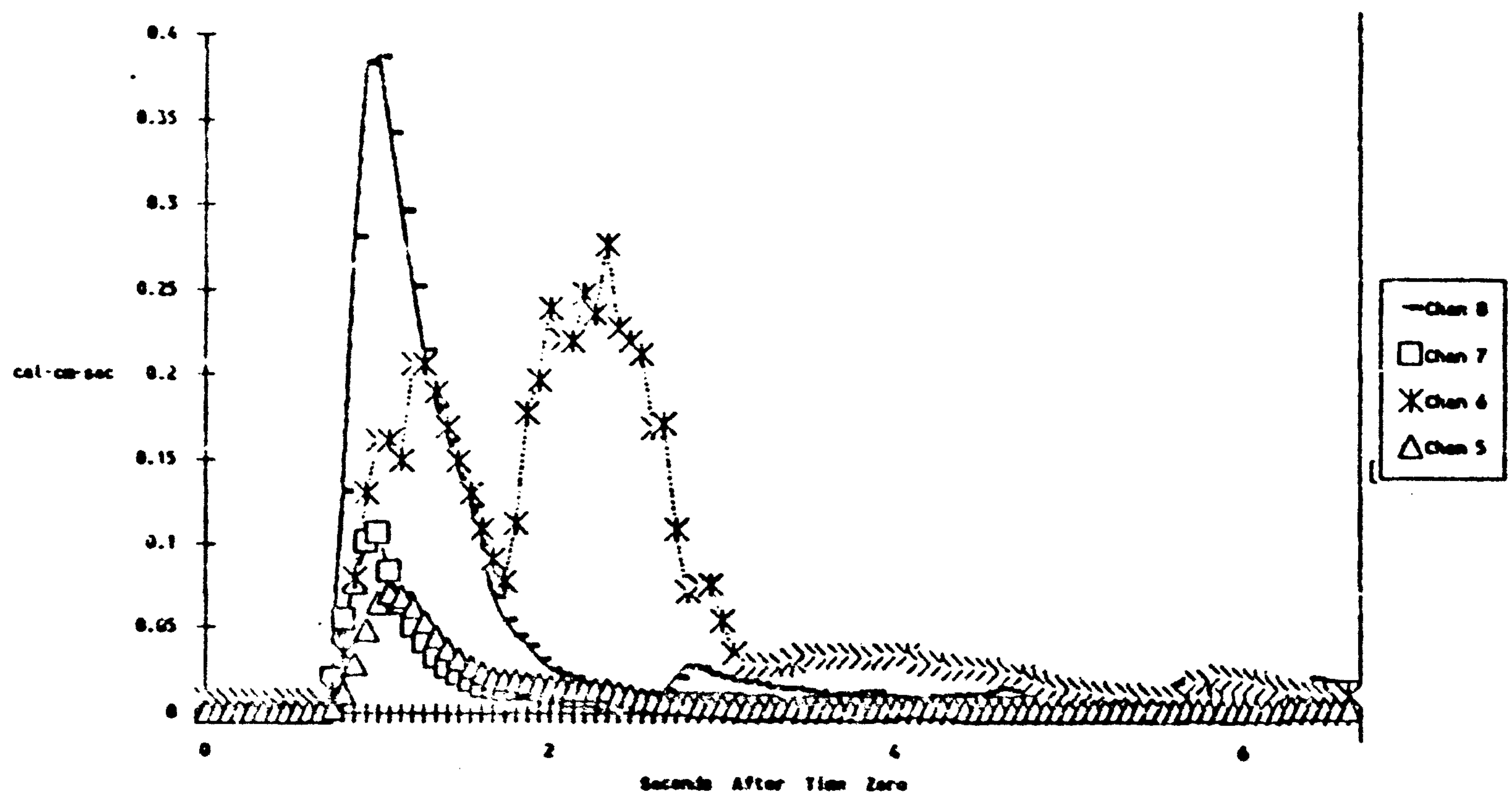

PROPAGATION TEST PT-4, 106mm (M26)

9 MARCH 1988

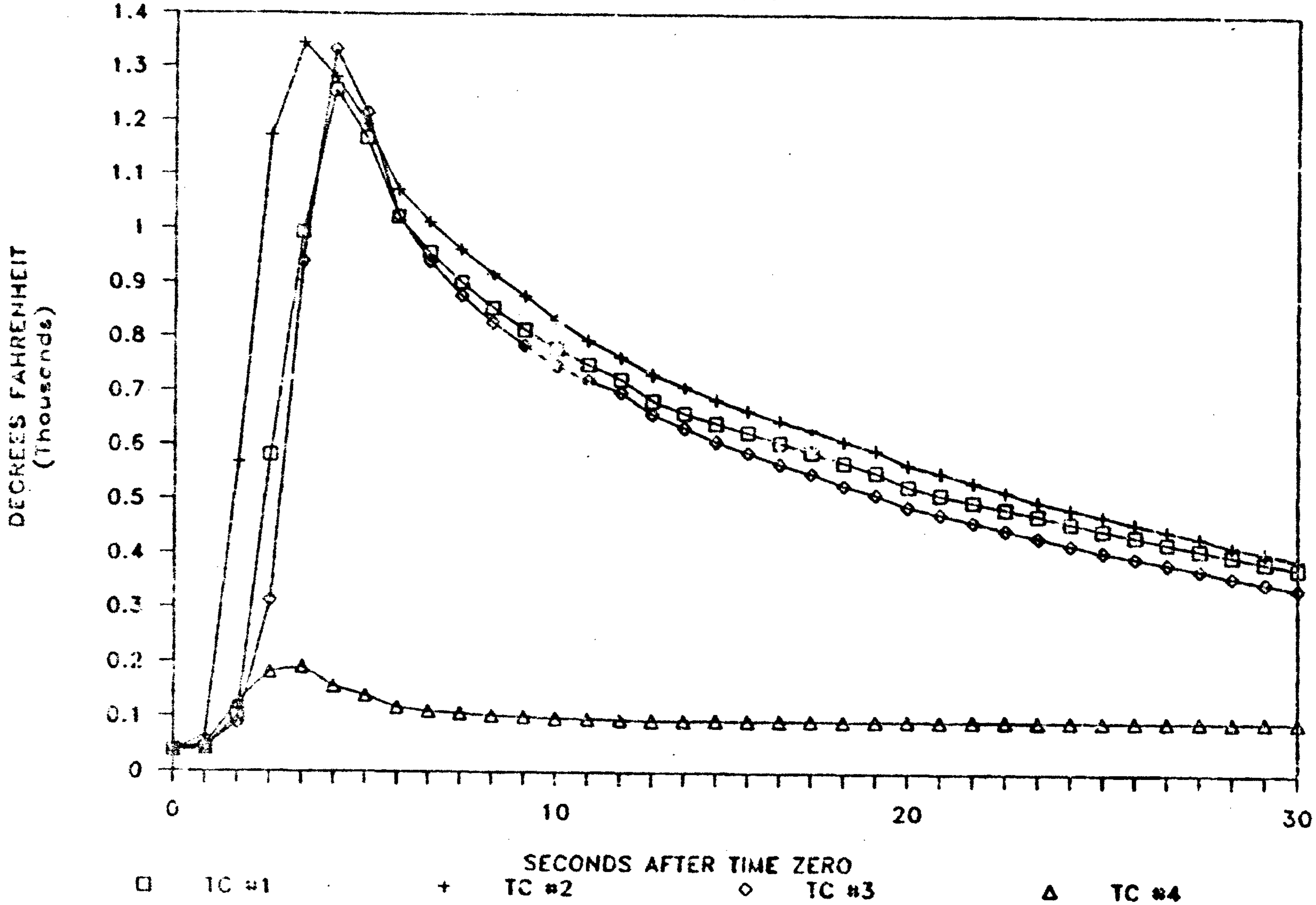

fig 36

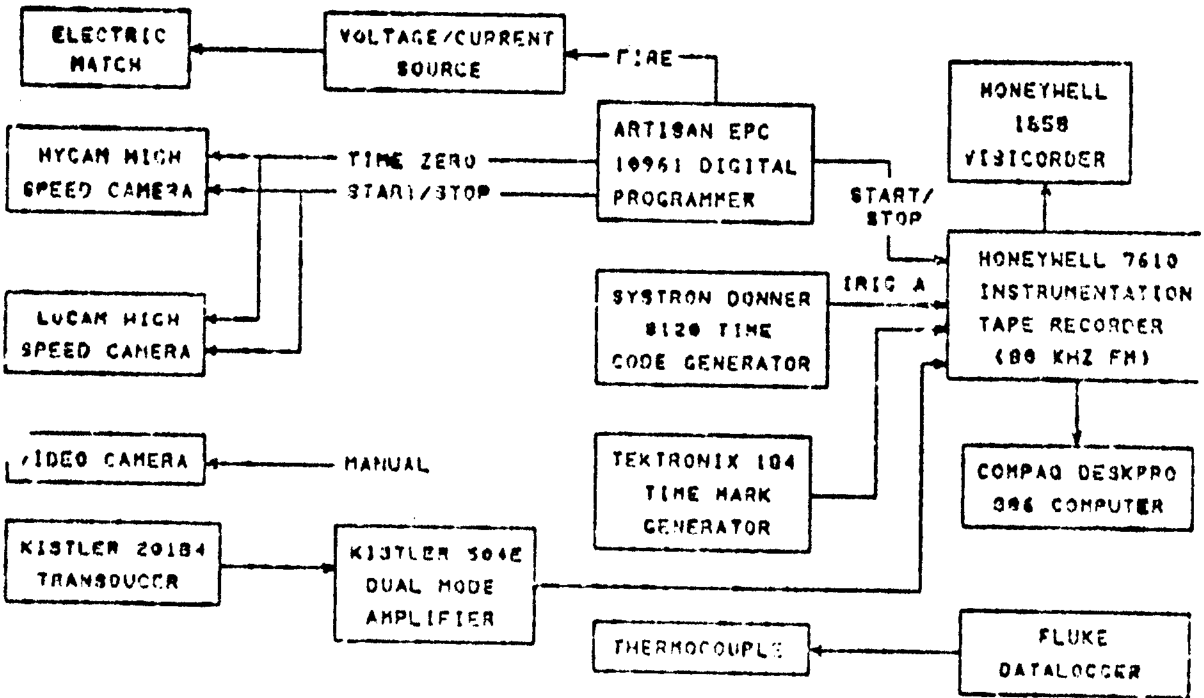

INSTRUMENTATION SCHEMATIC
FIGURE 1

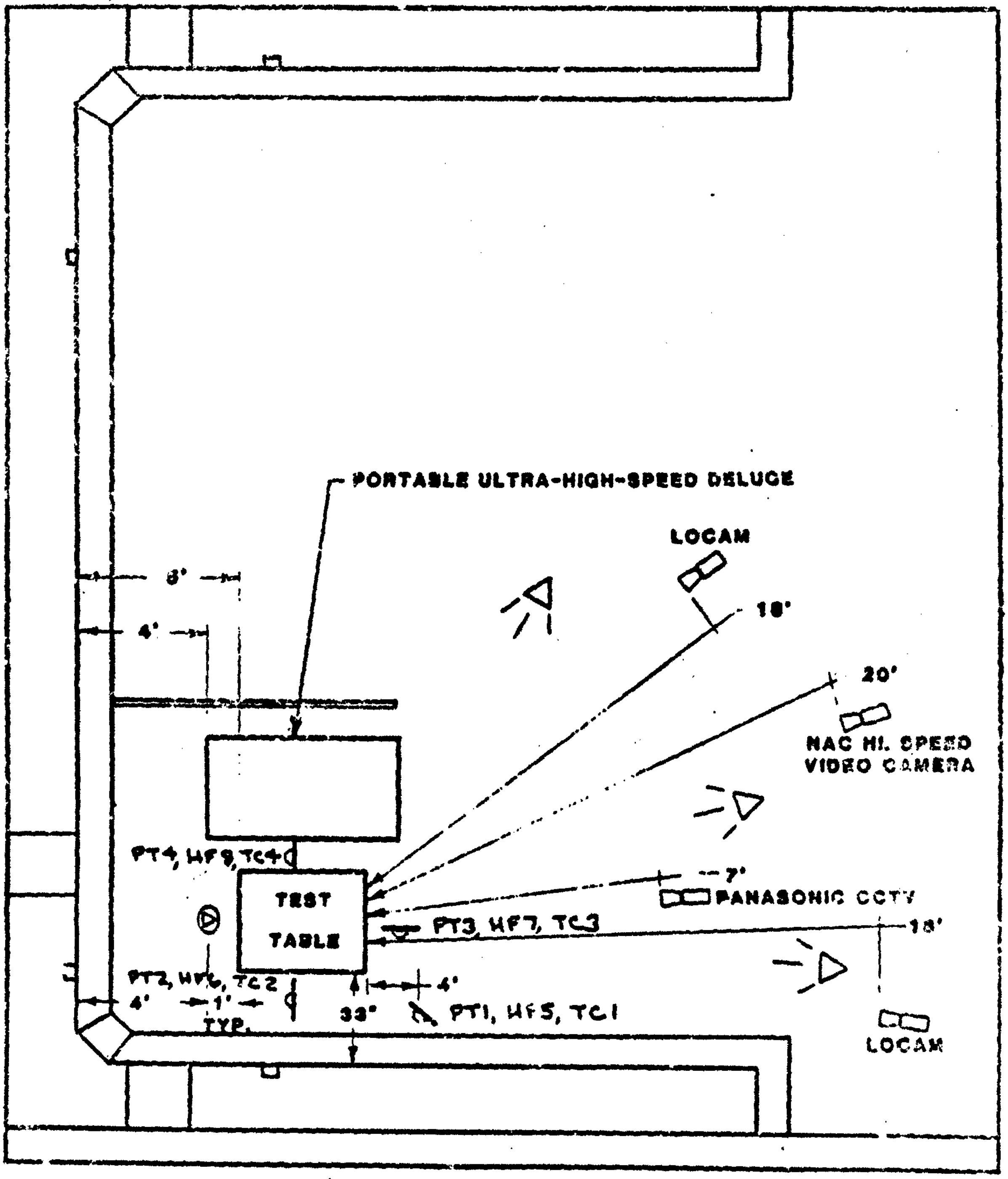

FIGURE 2
PRESSURE TRANSDUCER STANDS, CAMERAS, AND CCTV
LOCATIONS BUILDING 1379

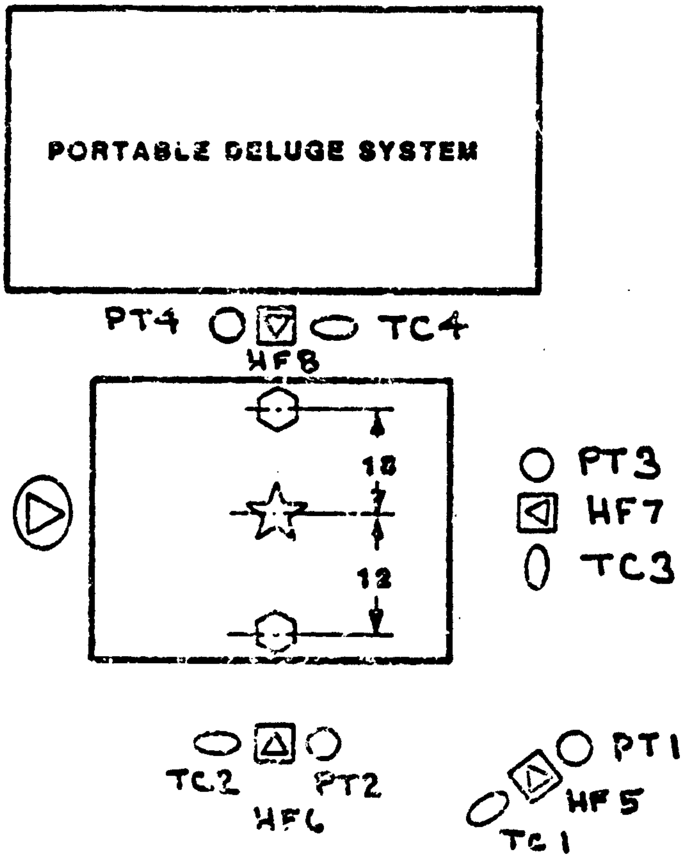

FIGURE 3

PRELIMINARY AED TEST

FACILITY BUILDING 1379 TEST LAYOUT

LEGEND

DONOR CHARGE	MANIKIN
ACCEPTOR CHARGE	PRESSURE
HEAT FLUX	THERMOCOUPLE

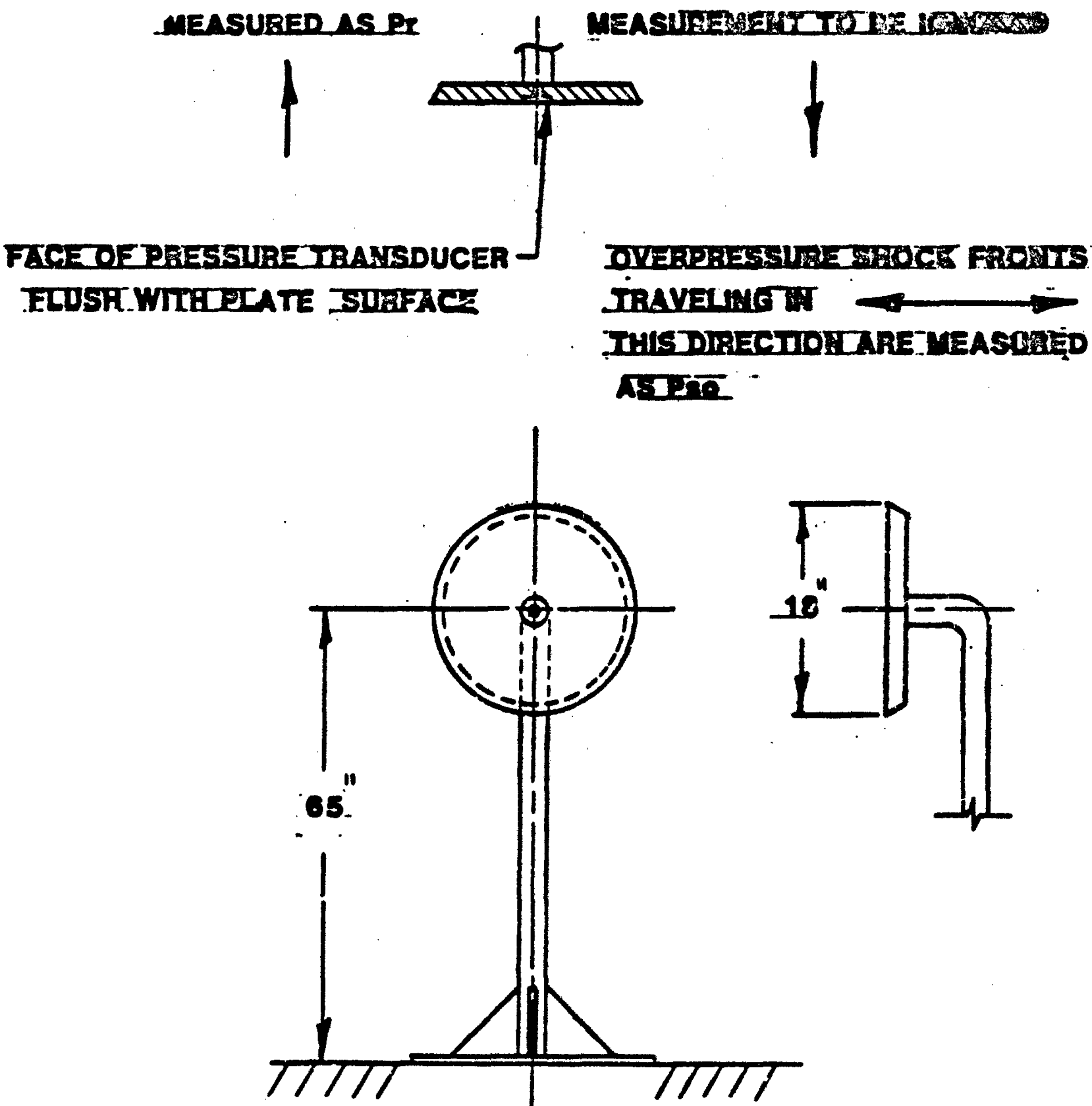

FIGURE 3A

BLAST PRESSURE TRANSDUCER STAND AND OVERPRESSURE SHOCK FRONT ORIENTATIONS

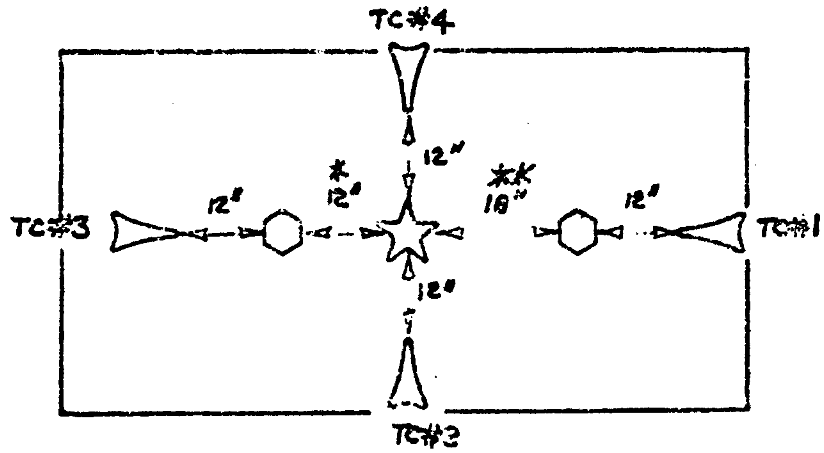

* 8" FOR PT-1
** 12" FOR PT-1

FIGURE 3B

PROPAGATION TEST

LAYOUT

LEGEND

☆ DONOR CHARGE

⬡ RECEPTOR CHARGE

▷ THERMOCOUPLE

Figure 29 Heat Flux QT-4A

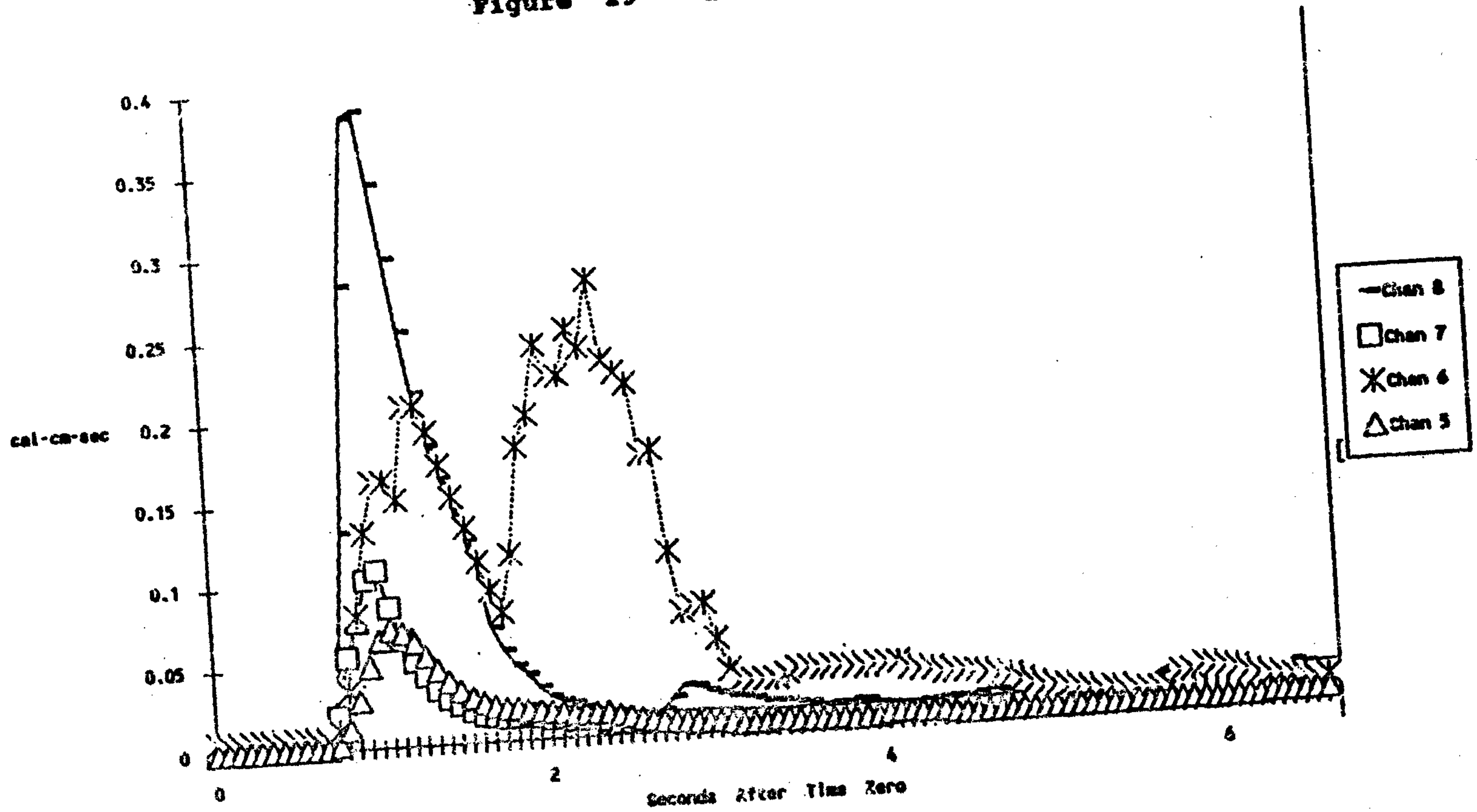

QUALIFICATION TEST QT-4B, 106mm (M26)

15 MARCH 1988

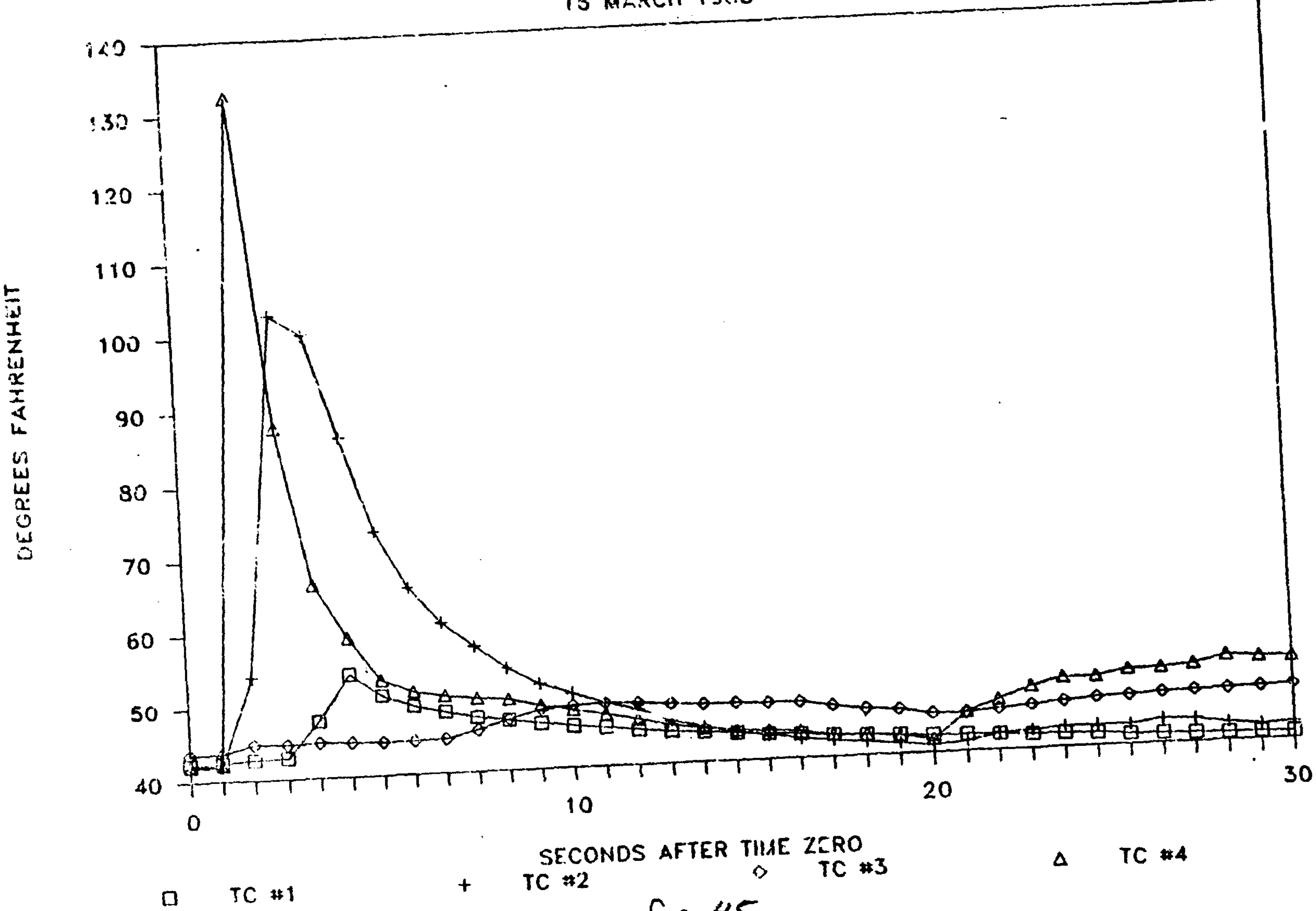

fig 45

Figure 24A Heat Flux PT-2 vs QT-2

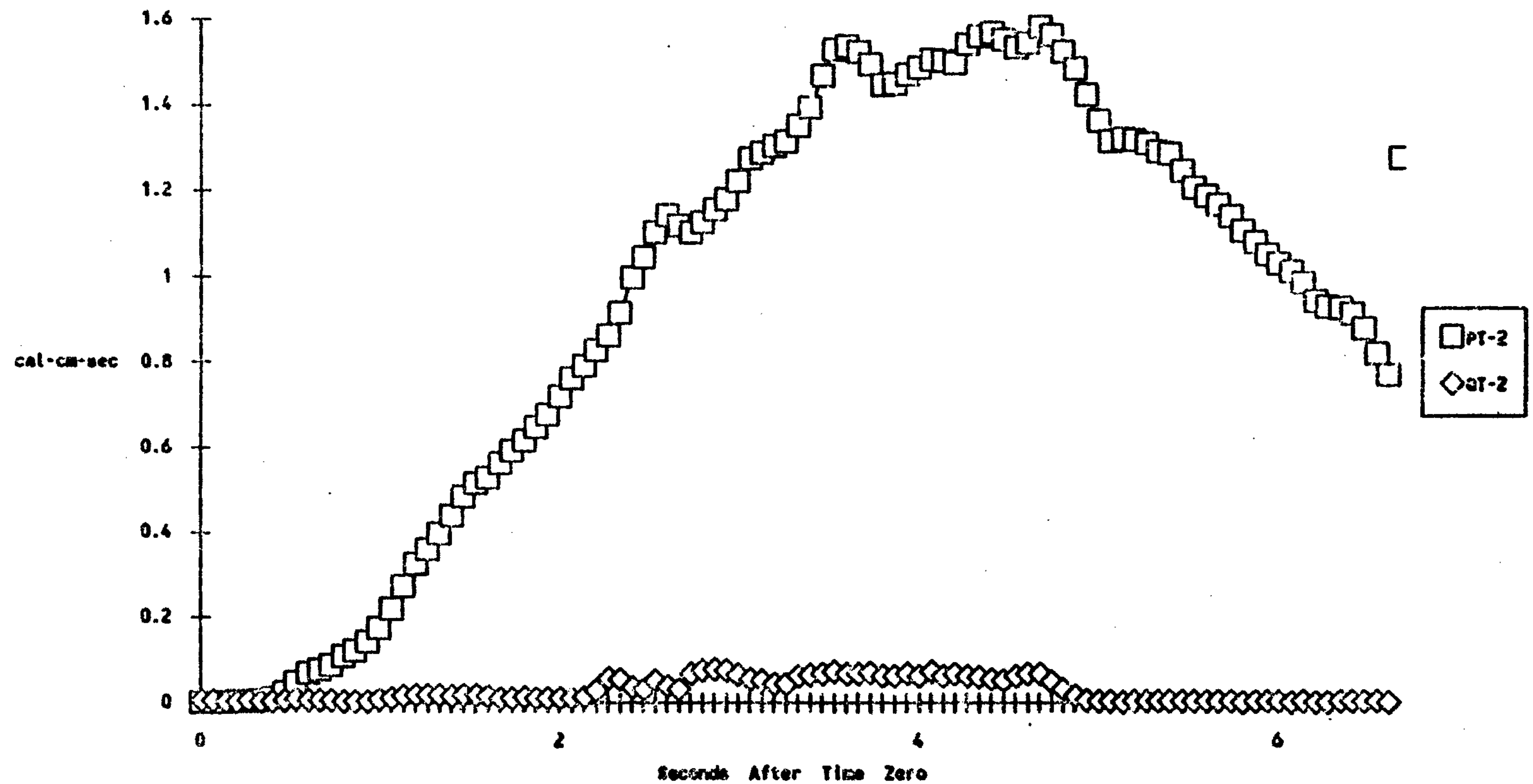

Figure 30A Heat Flux PT-4 vs QT-4B

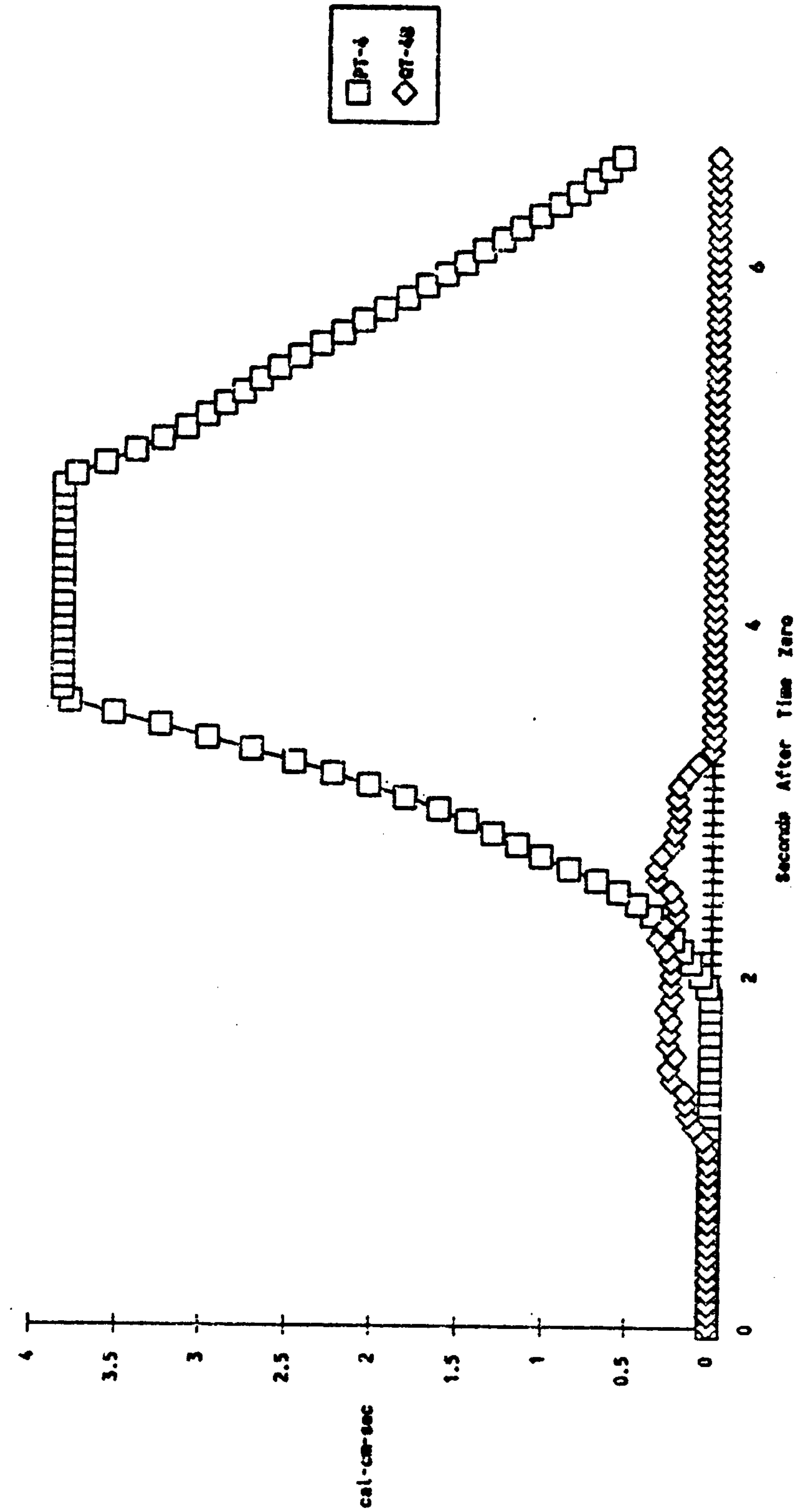

UK COLLABORATIVE EXPLOSIVES SAFETY TEST PROGRAMME

N J M Rees and J Henderson

Safety Services Organisation, Procurement Executive
Ministry of Defence, UK

Presented at the

US Department of Defence, Explosives Safety Board
Twenty-Third Explosives Safety Seminar

Atlanta GA, 9-11 August 1988

SUMMARY

In recent years there has been a recognition of the need to maximise the utilisation of the major investment in explosives facilities, particularly storage buildings. Unduly restrictive licensing limits based on over-conservative Q-Ds can no longer be tolerated and test programmes to define more precisely the basic explosion effects have been started by many countries.

Many problems are common and general collaboration to minimise national spending and maximise the acquisition of useful data is an obvious way forward. Even where a trial is specified and organised by a single nation, collaborative negotiations with other nations may permit more trials instrumentation leading to the acquisition of additional data with minimum disturbance to the conduct of the trial.

The UK MOD is presently collaborating in the following major test programmes:-

1. Australian/UK Stack Fragmentation Tests.
2. Norwegian/USA/UK Underground Storage Tests at NWC China Lake, California.
3. Klotz Club Underground Storage Tests at Alvdalen, Sweden.
4. USAF Bomb Communication Tests.
5. UK Home Office Structural Response to Blast Tests.

UK COLLABORATIVE EXPLOSIVES SAFETY TEST PROGRAMME

N J M Rees and J Henderson

Safety Services Organisation, Procurement Executive
Ministry of Defence, UK

Introduction

1. The need to carry out practical trials to determine the effects of accidental explosions is not new. Probably the most important trials in the last twenty years were the US ESKIMO series which investigated the safety of the igloo storage concept in response to an accidental explosion. This was the first time that a planned series of effects trials had been carried out to examine the safety in use of a specific type of building for explosives storage. In more recent times the US DISTANT RUNNER trials investigated, in a similar fashion to the ESKIMO series, the safety of the hardened aircraft shelter design for the protection and stabling of aircraft with their munitions loads, when an explosion occurred in an adjacent shelter.

2. The first question that comes to mind is "why does the UK perceive a need at this time for any major collaborative explosives safety test programme?" NATO, through the AC258 storage sub-group, has produced a comprehensive manual giving safety standards for dealing with all aspects of explosives storage and transport. One would have thought that extensive practical data was used in the development of the manual and hence the current Quantity-Distance (Q-D) criteria would be well established and understood.

3. Indeed, the AC258 manual (1) has been in existence for a decade and one of the primary source documents, the UK Explosives Storage and Transport Committee's (ESTC) Leaflet 5, (2) has been around for much longer. Thus one might expect that a large amount of data was available and consulted when these documents were written. Unfortunately this was not found to have been the case when these documents were reviewed recently. Over the last few years ESTC has conducted a study into Risk and Hazard Analysis, (3). Additionally, in an effort to establish the basic standards the editorial sub-group of AC258 has attempted to put together a historical summary of the development of their Q-Ds. Both the ESTC and AC258 studies have been severely hampered by an inability to identify when many of the Q-Ds originated, let alone produce the practical data on which they are based. This is no reflection on the efforts or abilities of the individuals involved in their original formulation. However it does reveal the lack of sufficient recorded information to constitute a respectable database for many of our Q-Ds. Disturbingly this leaves the whole Q-D philosophy shrouded in mystery and asks us to have confidence in the adequacy of both the quantity and quality of the information used by those who constructed the tables without verification now being possible. This makes life very difficult for those who have complex licensing problems and who need to assess the actual consequences of accidental explosions to obtain the most economic layout of an explosives facility. Equally when large sums of money are to be expended on new facilities or on the

refurbishment of existing ones, it is clearly important that the design and layout of the buildings are based on sound technical data.

4. Thus the current Q-D codes should be regarded as "rules of thumb", and there is a clear need to reassess these rules in detail to gain a better understanding of the degree of protection that they give. It must be remembered that structural design techniques and structural response analysis are improving all the time and those concerned with using and reviewing the Q-D rules should be aware of these new developments so that the consequence model they use for accidental explosions is as realistic as possible.

5. From the above discussion, I am sure you will agree there is a clear need to obtain relevant practical data. However the advantages of international collaboration over individual national trials programmes are less obvious.

6. Clearly the first major reason for conducting such a programme of trials collaboratively is to reduce costs. Construction of test buildings, even scaled down versions, is a relatively expensive and lengthy process and therefore worthwhile cost savings can be made when individual nations group together. Clearly the more participants, the lower the individual nation's cost. However this must always be balanced against the increasing difficulties in the planning and conducting of trials which inevitably arise as the number of organisations involved in the work increases. Every participating organisation wants the test to be conducted as near to their own specification as possible and consequently compromises will have to be agreed. This does not need to detract from the technical value of the trial although there is always the danger that the compromises can obscure the original individual test programmes to such an extent that the data produced is not then sufficiently relevant to the individual nation's original problem to be really useful.

7. However there are advantages in collaboration and the very fact that more than one organisation is involved in the work should lead to a broader and more realistic consideration of the test objectives. Too often a test is set up to consider one specific aspect, eg the required inter-magazine separation of igloos, whilst other aspects then perceived to be of lesser importance, eg the debris throw, are either inadequately treated or even ignored completely. The result is that when the question is raised on these other effects at some later date it is often realised, with hindsight, that the opportunity to obtain valuable additional data has been lost. If research funds were freely available then more tests could be carried out. However UK does not have a large testing budget and the money must be used efficiently. We believe it is essential that those responsible for this work ensure that the tests provide as much data, at as low a cost, as possible.

8. It is often forgotten that producing the data from a trial is usually only the half-way point of an investigation. Only by appropriate analysis and interpretation of the collected data can it be properly used for the intended purpose of improving the Q-D rules. Collaboration in this area is just as important as in the planning and conduct of the actual test. Nations, for historical reasons, have developed expertise in specific areas and it is therefore important to ensure that the data is analysed

appropriately by those experienced in such analysis. This can be done, often more effectively, by organisations separate from those more closely involved with the trial and the application of its results to explosives licensing situations.

9. It is also all too easy for individuals to become immersed in the data analysis to such an extent that possible alternative applications are missed. Too often one cannot see the wood for the trees. Discussion between the analysts and other interested parties can often be very helpful in ensuring that the data is correctly and fully exploited.

10. A further reason for such collaborative effort, certainly within NATO AC258, is that it aids member nations in interpreting and adopting the changes in the Q-D rules brought about by the new trials data. We have found on many occasions that the acceptance of data by an organisation is usually eased by its involvement in the collection and analysis of that data. Additionally during the joint analysis process it would be hoped that any perceived shortcomings in the data or its analysis would be recognised there and then rather than at some time in the future. This joint process also makes it difficult for any participating organisation to say in the future that they were not happy with the data and the conclusions reached, because they have been involved throughout. This has been found to be effective in concentrating participants minds on the data so that a thorough analysis is carried out leading to sound conclusions.

11. Enough of the reasoning behind the need perceived in UK for collaborative programmes of work in Explosives Safety. The remainder of the paper gives some examples of collaborative test work in which the UK is currently engaged and indicates some areas where UK believes future collaboration is necessary.

Australian/UK Stack Fragmentation Tests

12. In this series of tests, which began in the early '80s, the UK has collaborated extensively, in terms of both expertise and funding, with Australia to investigate the consequences of accidental explosions in the smaller above ground explosives storage buildings, typical of those used in both UK and Australia. Without co-operation from the Australian Department of Defence it would not have been possible for the UK to have carried out these tests on two main counts:

(1) UK has no national testing ground where it could have carried out full-scale testing of this kind,

(2) Because of the need to conduct these tests at a suitable location outside UK it is not possible for the UK MOD to economically provide the instrumentation and data collection effort required.

13. The current test programme at the Test Range, Woomera, South Australia, was completed earlier this year. It examined the consequences of explosions in larger brick and concrete storehouses, and in particular, the effects of debris throw from such structures. Very little information was currently available for such situations and the results are being presented at this conference by Mr Henderson. When fully analysed and

applied this data could produce significant cost savings in the utilisation of such brick and concrete storage buildings in both UK and Australia.

14. This is an example of the type of collaboration, which could be extended to the testing of other types of structures, eg igloos, so that good data can be obtained on the debris hazard from a wide range of structures. This is, of course, of major interest to all nations but particularly to those who are developing consequence models to aid probabilistic risk estimation for future explosives licensing procedures.

US/Norwegian/UK Underground Storage Tests

15. These tests have been planned collaboratively to investigate the debris, blast and ground shock effects from shallow buried magazines. While in the UK we do not have any true underground storage with overhead cover of several tens of metres or more of rock and earth, the Royal Navy does have many buried magazines with 15-30 metres of overhead cover. However, because the AC258 guidelines were not really intended for these shallow buried magazines, the guidance given by their Q-D rules is very conservative. Better, more appropriate data must be obtained which will almost certainly enable the magazines to be licensed for the storage of larger quantities of explosives than at present.

16. Preliminary work has been carried out by UK using 1:25 scale models but to validate the results it has always been accepted that some large-scale or even full scale trials would be necessary. However UK has never chosen to carry out such trials on their own, again primarily because of the high overall cost and also because we have no suitable test site where such a trial could be carried out.

17. UK has benefited considerably from the technical collaboration with both US and Norway whose experience in true underground storage is much greater than ours, particularly in designing associated test programmes and analysing the results. The present joint trial at the Naval Weapons Centre, China Lake will be in an approximately half-scale tunnel and storage chamber. About 20 tonnes HE will be detonated to represent an accidental explosion, the test taking place on the 24th August.

Klotz Club Underground Storage Tests

18. A greater degree of international collaboration has been achieved in these tests than in any other. The European nations who utilise underground explosives storage, together with the US, have been collaborating over a period of some five years to design, conduct and analyse a series of tests in an underground test facility at Alvdalen in Sweden. Despite the difficulties of co-ordinating the inputs from six nations a very useful test scheme has been developed and worthwhile results are now being produced. Charges of one and 5 tonnes HE have been detonated in the storage chamber which models a deep buried magazine. Dr Vretblad of the Swedish Fortifications Service will be reporting some of these trials at this meeting.

19. It was as a result of this collaboration that the aforementioned China Lake tests were generated. It is to be hoped that such collaboration will

continue and the UK believes that the AC258 element at the Klotz Club fully appreciate the benefits of such joint work.

USAF Bomb Communication Tests

20. The USAF have been conducting, since early 1985, an extensive series of tests to investigate whether stacks of general purpose HE bombs in useful quantities could be stored as a unitised risk in the current designs of igloo storage. Although USAF have funded these tests they have collaborated in the detailed planning and analysis of the test results with the Netherlands and UK. This collaboration was fundamental to the design and conduct of the trials since the results of the tests would be used to establish the safety of this method of storage of such bombs in both countries.

21. As a result of this collaborative effort the USAF progressed from testing bomb stacks in the open to testing in confined situations to represent igloo storage and subsequently in low-cost igloo mock-ups (the "Hayman" Igloo). The results of these tests have demonstrated the benefits of such collaborative work. Firstly, but regrettably negatively from the USAF point of view, the testing demonstrated graphically, by sympathetic detonation, the difficulties in extrapolating from open to confined storage without tests. Secondly, as a result of having to build low-cost igloo mock-ups, the USAF have developed the "Hayman" design as a low-cost alternative to conventional igloos which shows every indication of providing protection as good as conventional igloo construction with significant cost savings.

22. UK believes that such collaboration also amply demonstrates the major advantage of involving those nations who have to endorse the storage concept at all points in the testing procedure. It could have been extremely embarrassing for both US and UK, for instance, had the US only carried out the tests in the open, put forward a storage concept, and then had to answer the difficult question of the effect of the igloo confinement. A new series of tests would have been required by the host nations and the unfortunate effect of such confinement would have been demonstrated, resulting in much delay and difficulties in the programme, with possible political repercussions.

UK Home Office Studies of Structural Response to Blast

23. Collaboration is not only important between nations, as has been demonstrated in the above examples, but also between organisations within national boundaries. This is perhaps more important in the US where, to an independent observer, the three services appear to have developed independent expertise in a number of areas of explosives behaviour. However the authors of this paper are only qualified to discuss the situation pertaining to UK. The only UK government department, outside of the Ministry of Defence and Property Services Agency, which has expertise in structural blast response is the Home Office who, in this respect, are essentially concerned with structural response to nuclear blast. Although such response could be considered significantly different to the response from much smaller quantities of conventional explosives, we believe that a read across is possible at the Inhabited building Q-Ds (0.7 psi). Consequently collaboration is now underway in UK between all three

organisations to design a test series which will meet the objectives of all the participants. No trials dates have yet been set.

Future areas for collaborative work

24. As well as the continuation of the work outlined above more collaborative work is being proposed under the aegis of AC258 in the following areas:-

(1) Modelling of debris scatter from explosions in reinforced concrete structures, using small scale structures and computer programmes.

(2) Effects of explosions in storehouses containing HD 1.2 ammunition. Recent accidents in ammunition storage depots outside Europe and the US have indicated that the effect of lobbed ammunition from fires is perhaps a more important phenomenon than the large HD 1.1 explosion to which most attention has been paid in the past.

25. There is still however a need for further work to define and refine the current Q-D requirements. UK hopes to promote a greater awareness with AC258 of the need for such collaboration.

26. Finally international collaboration depends upon those involved in explosives safety communicating effectively with their counterparts in other countries to ensure that there is an up-to-date understanding of each other's areas of interest and planned and projected trials. Beyond this point it is up to each nation to respond quickly where the opportunity for collaboration presents itself if unnecessary duplication of trials work is to be avoided and the best value obtained for the overall international expenditure on this important work.

REFERENCES

1. Manual on NATO safety principles for the storage of Ammunition and Explosives : AC/258 - 0/259.

2. Quantity-Distances for Military Explosives. ESTC/220/Leaflet No 5 - Part 2.

3. The Application of Risk Assessment in the Field of Explosives and Ammunition Safety, F.R. Hartley et al - Minutes of 22nd Explosives Safety Seminar pp 1597-1603.

JOINT AUSTRALIAN/UK STACK FRAGMENTATION TRIALS

PRELIMINARY PHASE 3 REPORT

By

J Henderson

Dr N J M Rees

MOD (Procurement Executive)
Safety Services Organization
Orpington, Kent, UK

1 SUMMARY

This paper is a preliminary report of Phase 3 of the series of Joint Australian/UK Stack Fragmentation Trials. It is the last of the current series conducted to examine the explosion effects from limited quantities of explosives (< 6000 kg) in brick and concrete structures representing typical UK or Australian explosives storehouses. The paper describes the conditions for each trial and gives some preliminary results. No conclusions are drawn at this stage since the results from the overall series of trials are being consolidated into the UK's Quantity-Distance Leaflets. The full results and recommendations are considered in more detail in the final report which will be published in late 1988.

2 ACKNOWLEDGEMENTS

The UK authors wish to acknowledge the major contribution made by the Australian Department of Defence to the work reported here. The work was made possible by the use of the Woomera range and the support provided by and through the Directorate of Trials.

The trials were arranged through British Defence Research Scientific Staff Canberra (Dr R M Allen) with Director of Trials (Group Captain Coutts). The main contributors to the trials were the Australian Army (Project Officer, Major R M Baguley and Project Officer Field, Major C Brereton with EOD Staff and detachments from 21 Construction Squadron), RMB Salisbury (under Mr H Evans), WSRL Salisbury (under Mr K Scheballa) and DSCW Personnel at Woomera (under Mr D Fail). Staff were also supplied from Australian Ordnance Factories to carry out weighing and sorting of fragments.

The trials would not have been possible without the aid of the US Department of Defense Explosives Safety Board who supplied surplus 175mm shell for use in the trials.

The trials proposals were discussed in detail and approved by the UK Explosives Storage and Transport Committee (ESTC).

3 BACKGROUND TO PHASE 3

The Explosion Effects Sub-Committee (EESC) of ESTC recommended in 1980 the investigation of fragments and debris arising from an untraversed bomb stack, one having a standard 2 degree traverse and also one with a 10 degree traverse. In addition, the effect of having such a stack inside a typical brick built storehouse with a protective concrete roof, under comparable traversed conditions, was also to be determined. Consequently Phase 1 was planned and carried out at DSC Woomera during May 1982.

As a result of reservations expressed by RARDE concerning the symmetry of the bomb stacks used in Phase 1 it was decided to carry out a Phase 1B search over part of the sites used during Phase 1. A comprehensive sampling plan was devised, utilising visual search and metal detection techniques, and was carried out at DSC Woomera during May 1984. This sampling plan has formed the basis of all subsequent debris sampling.

Combination of the results from Phase 1 and 1B resulted in a recommendation to reduce minimum fragment throw distances and showed that the RARDE reservations were unfounded. The trials to date had shown that there appeared to be no reason to apply a minimum quantity-distance of 270/400m for fragment/debris throw to a building, of construction similar to those tested and traversed preferably to the eaves, or an open stack traversed with the standard UK 2 degree traverse. The recommendation was to use D13 distances for fragment/debris throw, with a minimum of 270m for quantities less than the 1800kg tested in Phase 1, as determined in ESTC Leaflet 5 Part 2. This would still give adequate protection from the effects of blast. The 270m minimum distance was an interim measure which was expected would be reduced when the results of Phase 2 were available.

A Phase 2 had been recommended because of some doubts as to the applicability of the trials to buildings which were considerably weaker than those tested, e.g. with 115mm brick walls and because it was not felt that the results allowed extrapolation down to small quantities of explosives (less than 1800 kg). Both of these doubts were based on the uncertainty over building break-up due to lighter construction or lighter loading.

Consequently Phase 2 was proposed using smaller quantities of explosives, typically of a few hundred kilograms, in a similar type brick built building to ascertain the effect of reduced loading. Similar trials were also proposed to ascertain the situation for a brick building of lighter construction and a concrete structure. Phase 2 was conducted at DSC Woomera in early 1985 and consisted of detonating a variety of charges in different structures (Ref 2). This confirmed the Phase 1 results but did not produce the expected reduction in the 270 m minimum distance.

However there remained some concern that the worst case situations had not been addressed and proposals were put forward to carry out a Phase 3 to examine the effects of larger quantities in buildings similar to those used in Phase 2.

4 AIM OF PHASE 3

The prime aim of Phase 3 was to obtain additional data on the distribution of hazardous fragments and debris from an explosion in a building to supplement those obtained from earlier trials. Phase 3 was to examine the situation with regard to typical UK style explosive storehouse structures loaded with fragmenting ammunition at Net Explosive Quantities (NEQ) of up to 5600 kg.

From this data it was hoped to consolidate the recommendations from the earlier trials to verify the existing and proposed Q-Ds based on fragment/debris throw considerations.

5 PROPOSALS FOR PHASE 3

Phase 3 was finalised at a total of 5 trials as detailed below. Since Phase 1 consisted of Trials 1 to 4 and Phase 2 consisted of Trials 5 to 8, the sequence was continued to Trials 9 to 12 for Phase 3. For Phase 3 the NEQs to be tested were primarily 1800 and 5600 kg which were considered to be more typical of limited storage situations.

Trial 9: A building was constructed of 395 mm cavity brick walls with a 150 mm reinforced concrete roof, internal dimensions of 6 m square by 2.5 m high, with a door of plywood and 16 gauge mild steel covering. The design also incorporated a concrete beam to support the roof panels. The explosive content of the building would be sufficient 175 mm fragmenting shell of Hazard Division 1.1 (Composition B filled) to give a total net explosives content for the building of 1800 kg.

Trial 10: A building was constructed of 395 mm cavity brick walls with a 150 mm reinforced concrete roof, internal dimensions of 9 m by 4.5 m by 2.5 m high, with a door of plywood and 16 gauge mild steel covering. The design also incorporated a concrete beam and pillar to support the roof panels. The explosive content of the building would be sufficient 175 mm fragmenting shell of Hazard Division 1.1 (Composition B filled) to give a total net explosives content for the building of 5600 kg.

Trial 11: A building was constructed of 200 mm reinforced concrete walls with a 150 mm reinforced concrete roof, internal dimensions of 6 m square by 2.5 m high, with a door of plywood and 16 gauge mild steel covering. The design also incorporated a concrete beam to support the roof structure. The explosive content of the building would be sufficient 175 mm fragmenting shell of Hazard Division 1.1 (Composition B filled) to give a total net explosives content for the building of 1800 kg.

Trial 12: A building was constructed of 200 mm reinforced concrete walls with a 150 mm reinforced concrete roof, internal dimensions of 6 m square by 2.5 m high, with a door of plywood and 16 gauge mild steel covering. The design also incorporated a concrete beam to support the roof structure. The explosive content of the building would be sufficient 175 mm fragmenting shell of Hazard Division 1.1 (Composition B filled) to give a total net explosives content for the building of 5600 kg.

Trials 9-12 were traversed to the level of the eaves of the building on three sides, the remaining side being left untraversed. In order to provide continuity and ease of comparison with Phases 1 and 2 the traverses erected in the SE and SW sectors for each building were the standard double slope type traverse and the door to the building was in the NE side. The remaining traverse on the NW side was a vertical faced traverse providing protection to the eaves of the building and backed with earth to the design given in ESTC Leaflet 6. As in Phases 1 and 2 local soil was used in the construction of the traverses.

Trial 13. Due to interest expressed in UK and the Australian Department of Housing and Construction and because of the ramifications of using Steelcrete cladding to improve security, UK added a further trial to ascertain the effects on debris throw of Steelcrete cladding on a conventional brick building. To allow read across from results already obtained during Phase 2, the building was constructed of 395mm cavity brick walls with a 150mm reinforced concrete roof, internal dimensions of 3.5 m square by 2.5 m high, with a door of plywood and 16 gauge mild steel covering. The explosive content of the building would be sufficient 175mm fragmenting shell of Hazard Division 1.1 (Composition B filled) to give a total net explosives content for the building of 500 kg. The building was traversed to the eaves using standard double slope traverses in the SE and SW sectors and the door to the building was again in the NE side.

Trial 12A. This trial was carried out to make good use of the additional shell which would otherwise simply have been demolished. It was instrumented using the gauges already laid out in the 45 degree direction on Trial 12 with the charge being placed at 50 metres from ground zero on the gauge axis. The intention was to measure the resultant blast pressures which should give two possible assessments:

a. A baseline for comparison of the various shots.

b. A figure for the TNT equivalence and casing factor for these particular shell.

The charge used was forty-five 175mm shell, primers and detcord giving a calculated NEQ of 650 kg.

All trial sites were on virgin ground, with minimum separation distances specified to ensure that there would be no fragment contamination between sites.

It was essential that all the munitions used in any one trial were initiated virtually instantaneously. UK would have preferred that the initiation followed a propagation mechanism as far as was possible, ie one shell being initiated normally and detonating cord used to ensure transmission of the detonation to the other shell present. This was in preference to each shell being initiated separately since this does not represent a practical accident situation. However in common with Phase 2 it was necessary to accept simultaneous detonation of all the munitions, to eliminate any subsequent possible EOD problems.

The main requirement for each trial was the collection of fragments and building debris generated by the explosion of the building and its contents. To this end it was necessary to mark out collection areas similar to those used for Phase 2. The initial collection areas would be 10 degree sectors running to the NE, SE, SW and NW of each site extending over the distances shown in Figure 1. This would then be supplemented with radial searches determined as a result of the analysis of the initial search sectors. The actual collection methods were two-fold, metal fragments being detected by visual search, backed up by the use of metal detectors where necessary, and building debris by a visual search. In common with Phase 2 it was only considered to be necessary to determine the search area in which the fragments or debris are collected and there was no requirement to plot the individual position of each piece collected, except where any large structural debris was found.

In addition to the basic search pattern shown a search was also undertaken of the crater and traverses on one site to determine the concentration of fragments which have been projected into the crater and traverses. This was intended as an attempt to establish a mass balance for the shell metal and should give some estimate for the efficiency of projection of the primary fragments.

Each trial was instrumented for blast to determine that a successful complete detonation was achieved and to allow an assessment of any attentuations afforded by the different structures and traverses under test. An arrangement of three lines, each of four blast gauges positioned as shown in Figure 2 running to the NW, NE and SE of each site was required.

Each trial was recorded on high speed cine film and video as a record of the trial. Still colour photographs were taken before and after each detonation and during the collection phases . A video record and still colour photographs of the construction phases were also obtained and provided a detailed coverage of the construction of each building.

Photographs taken overhead of the detonation in two of the Phase 2 trials had yielded some additional very relevant information, which would not otherwise have been obtained, and it was intended that this exercise should be repeated in Phase 3 for each of the four trials if possible but as a minimum for at least one of the brick building and one of the concrete building detonations. In practice only Trial 9 was actually photographed successfully because of various technical difficulties.

As a result of discussions with DRCS Salisbury during a planning visit in 1985 additional filming support was suggested which would provide a capability to analyse the trajectories and velocities of debris lobbed from each explosion site. These fragments were expected to be in the weight range of 50-1000g and 100-2000g with impact velocities of 50-70 m/sec and 30-40 m/sec for metal and building debris fragments respectively. Cine cameras were situated in pairs pointing across the major plane of fragment travel at distances of 270 metres and 400 metres, as these ranges are of particular concern and were expected

FIGURE 1
Fragment Search
Representative Layout

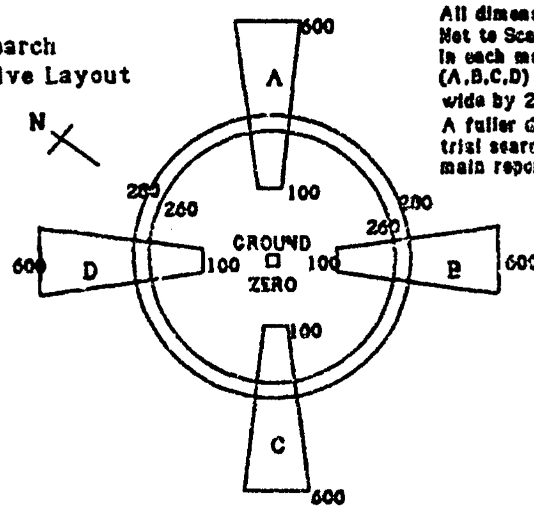

All dimensions in metres
Not to Scale
In each main vector search area (A,B,C,D) search grids are 10 degrees wide by 20 m deep
A fuller description of the individual trial search layouts are given in the main report

FIGURE 2
Air Blast Measurement
Representative Layout

Not to Scale
Each line has four measurement points

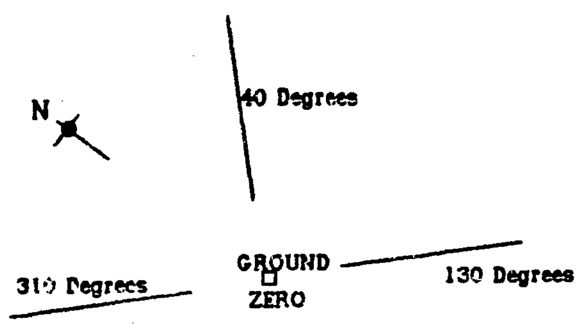

to yield the most productive results. A grid was laid out at these ranges to aid in the identification of the fragments and to give a reference for the subsequent velocity determinations.

As a result of discussions towards the end of the planning phase it was decided to employ a contractor to make laser photographic determinations of the volumes of the traverses before each trial and the volumes of traverses and crater afterwards. The intention was to make some estimate of the changes in the various volumes as an aid to estimating the effectiveness of the traversing and the energy loss through moving material from the crater and traverses.

The shell for the trials were the remainder of the American 175mm munitions which were transported to Woomera in April 1985 for use during Phase 2.

A detachment of 21 Construction Work, under the command of Major A G Schmidt, was tasked with carrying out the construction of all buildings and supportive earthworks. The detachment completed all tasks in less than the programmed time during September-November 1987. A further detachment provided manpower support for the fragment search and various technical tasks during the actual trial programme from February-March 1988. The performance of both detachments was very significant in the overall success of the trial.

6 FRAGMENT AND DEBRIS COLLECTION

The centre of explosion for each trial was established and a search pattern grid was laid out as shown in Figure 1. Each area was marked off with tape and searched by a visual sweep, backed up with a metal detector where appropriate.

In common with earlier trials it was quickly established that shell fragments had attained a distinctive blue colour due to tempering by the heat of the explosion which made them readily identifiable against the red coloured earth and stone.

All metal and masonry fragments were identified by collecting them into receptacles marked with the search area in which they were found. They were taken back to base camp where they were sorted by type and weighed.

All metal and masonry fragments over 50g and 100g weight respectively were weighed and recorded. To enable analysis and sorting by computer to be carried out all fragments were sorted into weight intervals by type and sector.

7 FRAGMENT AND DEBRIS CRITERIA AND ASSUMPTIONS

The fragment data was computer sorted using a LOTUS 123 program on COMPAQ and TOSHIBA portable microcomputers to calculate the numbers and densities of lethal fragments. The program will allow further analysis but for the present only totals of all lethal fragments have been fully anlysed. In common with earlier trials there is still some controversy over what the weight criteria for these lethal fragments should actually be. However the following three assumptions are still valid:

ASSUMPTION 1

Fragments, whether metal or masonry, are lethal, if their kinetic energy exceeds 80J (58ft lb).

ASSUMPTION 2

All fragments will be travelling at their free-fall velocities on impact which are in the range 50-60m/s for metal and 30-40m/s for masonry. It is anticipated that the actual values for these velocities will be determined from the photographic analysis of the final part of the trajectories of typical fragments filmed during the trials.

ASSUMPTION 3

The lethal fragment density is considered unacceptable if it rises above one lethal fragment per 56 square metres (600 square feet). This figure is also accepted internationally within AC 258 and is equivalent to approximately a 1% chance of being hit by a lethal fragment.

Having accepted the above assumptions it is then necessary to interpret the values given to allow analysis of the fragments and debris collected. Phase 2 (Ref 2) recommended the use of 75 and 150g for metal and masonry fragments respectively. The relative velocities of the two fragment types would suggest a ratio in the range between 1.6:1 to 4.1 for masonry fragment weight to metal fragment weight and

although the use of larger masonry fragment weights have been suggested they have not been considered further in this report. The choice of the metal fragment weight at 75g is still conservative in comparison to the criteria used by other countries.

8 PRELIMINARY RESULTS

8.1 TRIAL 13

Crater :

Approximately half the floor slab was still relatively intact, the crater (4 m long by 4 m wide by 0.8 m deep) being centred towards the rear of the slab where the charge had been placed at approximately 0.75m from the original position of the rear wall of the building.

Traverses :

The SE traverse appeared virtually intact whilst the SW traverse was eroded towards the open end.

Debris :

There was very dense debris up to 100m decreasing very rapidly beyond 100m. The significant debris appeared to be all of quarter brick size or equivalent (most is in fact either steelcrete or concrete debris). There were also large pieces or agglomerations of reinforcing bar.

There were several large pieces of concrete debris from the roof with attached reinforcing bars, some broken up on impact. One piece was approximately one metre square with a considerable amount of reinforcing bar attached and a similar piece had impacted just behind the firing unit. Some 15 of these large pieces of debris were identified, almost all within 200 m of ground zero.

The results of the main debris collections are shown graphically in the following two figures. The first figure shows the density variation with range for the four main sector searches at 45, 135, 225 and 315 degrees. The second figure shows the density variation with direction at a distance of 270 metres. Note that the density for all the figures published in this section are lethal fragment densities which are taken as the number of potentially lethal fragments, i.e. metal fragments greater than or equal to 75 grammes and masonry fragments greater than or equal to 150 grammes, per unit area of 56 square metres. The currently accepted AC 258 value for tolerable fragment density to the general public is one potentially lethal fragment per 56 square metres.

TRIAL 13 STEELCRETE

Directional Search

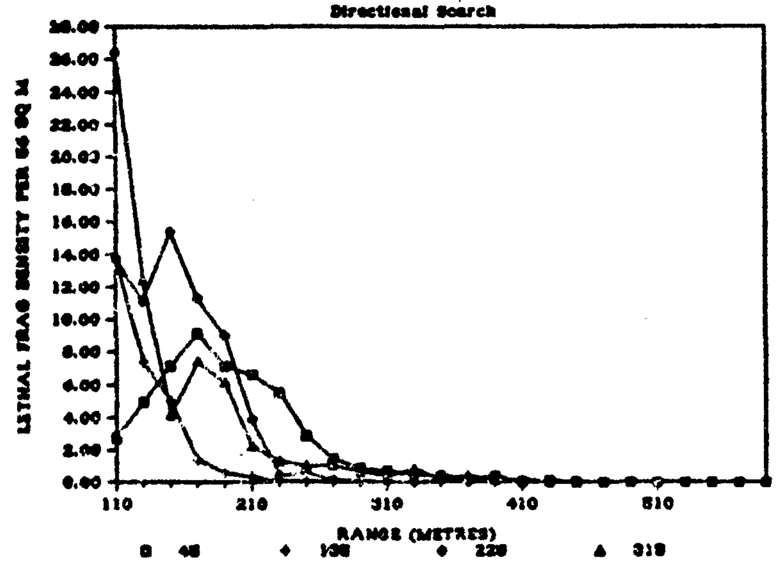

TRIAL 13 RANGE 270 METRES

Directional Search

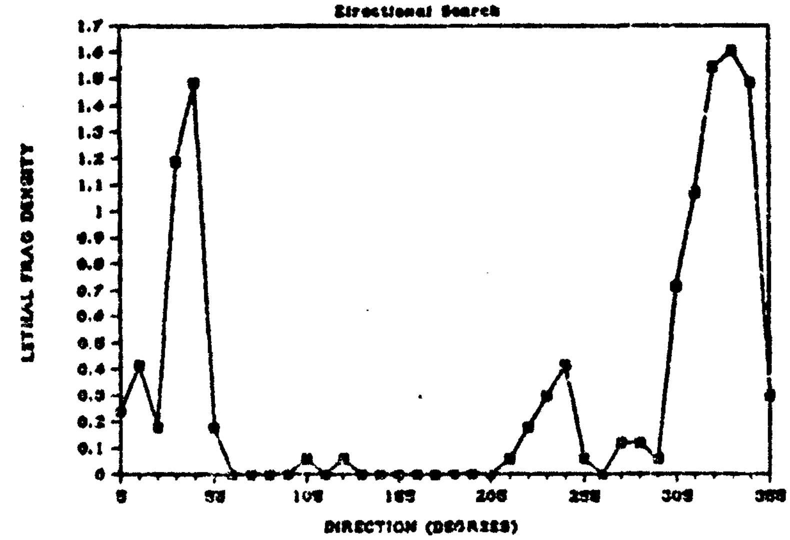

Blast Instrumentation:

A few problems had been encountered, primarily direct primary fragment attack on the gauges but also a great deal of noise prior to the arrival of the shock front. It was considered that the noise is due to either ground shock or the bow waves from the primary fragments. Ground shock noise had been noticeable on the records for Phase 1 and lead was used in the gauge mounts for Phase 2 to counteract the problem. Modifications were made to the gauge mounts for the later tests to see if the problem could be eliminated.

8.2 TRIAL 9

Crater :

The crater was approximately the size and shape of the floor slab, being 6.5 m wide by 7.5 m long by 1.8 m deep. The front part of floor slab was still in position but broken and heaved up.

Traverses :

The vertical faced traverse was blown over, the backfill being reduced to about 20% of original volume. Wood and earth from traverse was spread out behind traverse position to about 50 m. There was some, although not apparently significant, erosion of two double mound traverses.

Debris :

Several large pieces of concrete debris with attached reinforcing bar were found, the majority being inside 200 m.

Because of all the debris apparent on the ground at 200-300 metre range and the results shown by the main sector searches additional searches 10 degrees either side of the 135, 225 and 315 degree sectors from 200-400 m were conducted (except for NW sector where search was extended out to 480 m because of higher fragment densities).

The results of the main debris collections are shown graphically in the following two figures. The first figure shows the density variation with range for the four main sector searches at 45, 135, 225 and 315 degrees. The second figure shows the density variation with direction at a distance of 270 metres.

TRIAL 9 BRICK WALLS CONCRETE ROOF

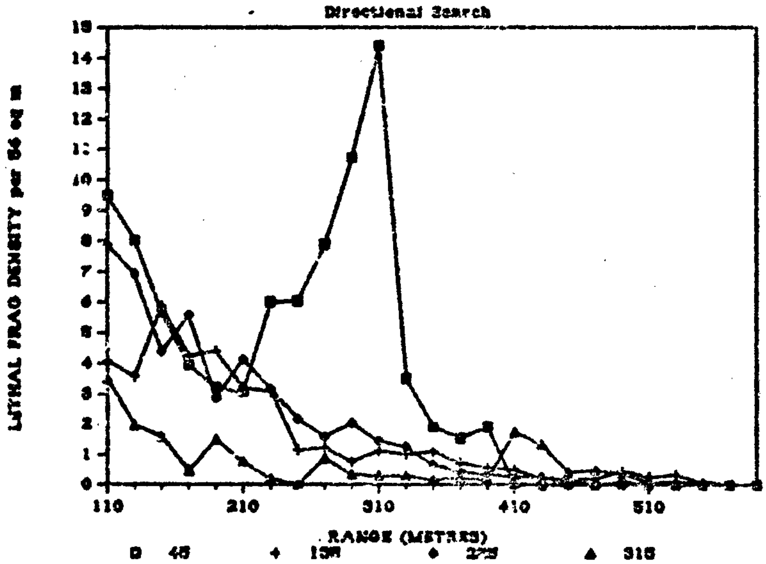

TRIAL 9 RANGE 270 METRES

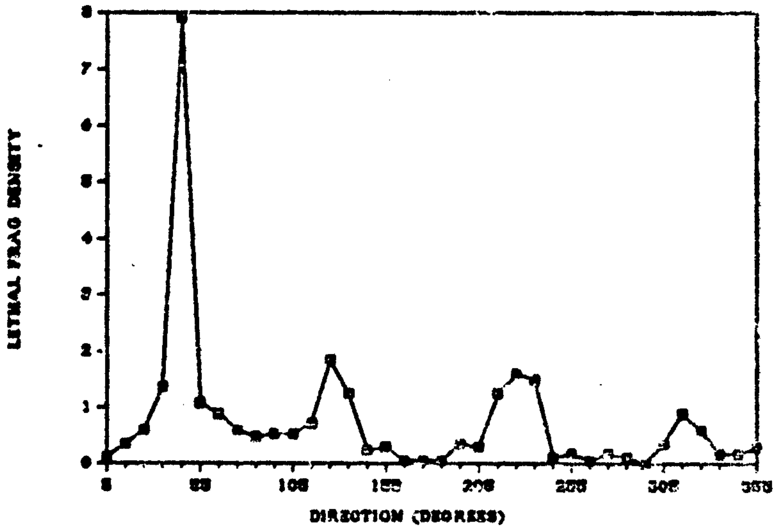

Blast Instrumentation:

Three gauges were mounted at 150 m in different mounts (including one gauge mounted as for Phase 2) to check the validity of measurements in 40 degree direction. The three gauges produced virtually identical records. Preliminary results indicate very good records from the 130 and 310 directions but with a lot of noise still apparent on the 40 degree direction.

8.3 TRIAL 10

Crater :

The crater was approximately the size and shape of the floor slab, being 10 m long by 9 m wide by 2 m deep, with large pieces of the footings on the lip of the crater.

Traverses :

The vertical faced traverse was almost totally destroyed. Only the supports in the corner junction with the rear traverse were still in place although displaced outwards. The bulk of the wood and earth fill from the traverse was strewn back behind the traverse position to about 50 m. The other traverses were eroded but remained still largely intact.

Debris :

The vast majority of the debris apparent inside a 100 m radius circle from ground zero were apparently less than the weights of interest. A sample of the typical brick debris confirmed this.

Some 40 large pieces of debris were identified, mostly concrete with associated reinforcing bar.

Additional search areas at 400-420 m from 135 to 315 degrees were also covered because of initial concern from Trial 9 results that there could be debris of interest at this range.

The results of the main debris collections are shown graphically in the following two figures. The first figure shows the density variation with range for the four main sector searches at 45, 135, 225 and 315 degrees. The second figure shows the density variation with direction at a distance of 400 metres.

TRIAL 10 BRICK WALLS CONCRETE ROOF

Directional Search

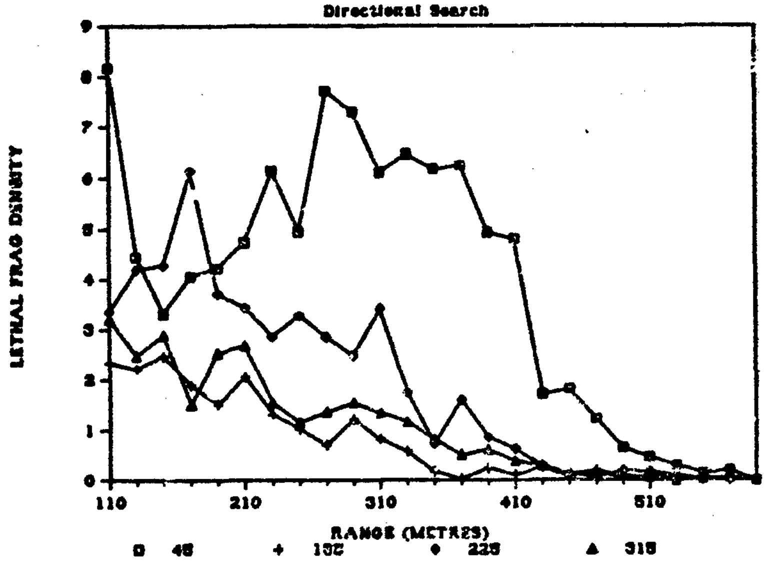

TRIAL 10 RANGE 400 METRES

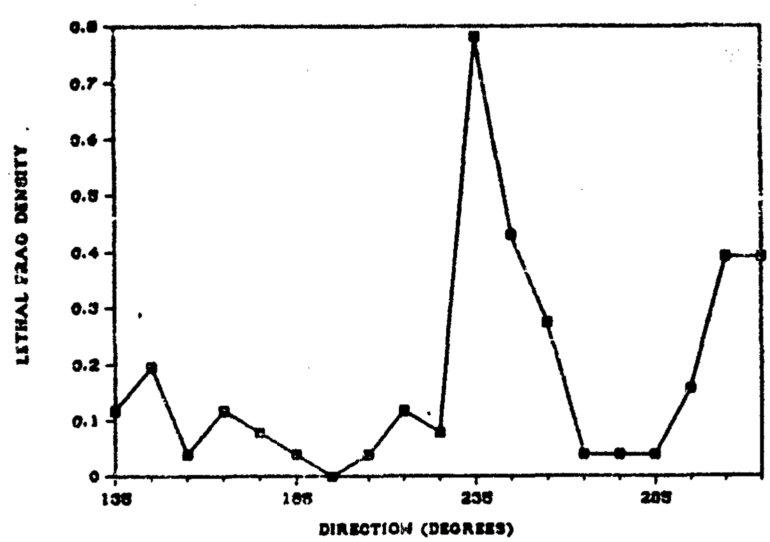

Blast Instrumentation:

There were no apparent problems with much less noise in the signals. Preliminary results indicated reductions from expected overpressures in all directions, with reductions being marginally greater in traversed directions.

8.4 TRIAL 11

Crater :

The crater was approximately the size and shape of the floor slab, being 7 m long by 5.5 m wide by 1.4 m deep, with the front part of the floor slab broken up but intact. The reinforcing tie bars for the walls were all very obvious, protruding to their full length (0.5m) from the displaced footings.

Traverses :

Damage to the traverses and the base of the building was virtually identical to that from Trial 9.

The vertical faced traverse was again blown out in the centre part with the uprights shorn off and thrown back over the traverse position. The outer parts were displaced but relatively intact. Traverse earth fill and wood were strewn back to approximately 150m behind the traverse position.

Debris :

An additional search area was covered out to 720m in the 45 degree direction to identify the density of fragments beyond 600 m.

Preliminary results from the prescribed search areas identified a potential problem in the SW direction with relatively high fragment densities being recorded from 210-260 degrees at 270m. This did not appear to be validated by qualitative searching either side of the 225 degree sector at 200-300m but to improve the data further search areas were covered from 210-260 degrees at 250 and 290 metres.

There was a great deal of reinforcing bar of various sizes scattered all round the site but in particular inside 100 metres. There appeared to be very few hazardous fragments of concrete inside 100 metres with most material being small and pulverised. A sample of this material was collected.

Some 30 large pieces of debris were identified, mostly concrete with associated reinforcing bar.

The results of the main debris collections are shown graphically in the following two figures. The first figure shows the density variation with range for the four main sector searches at 45, 135, 225 and 315 degrees. The second figure shows the density variation with direction at a distance of 270 metres.

TRIAL 11 CONCRETE WALLS AND ROOF

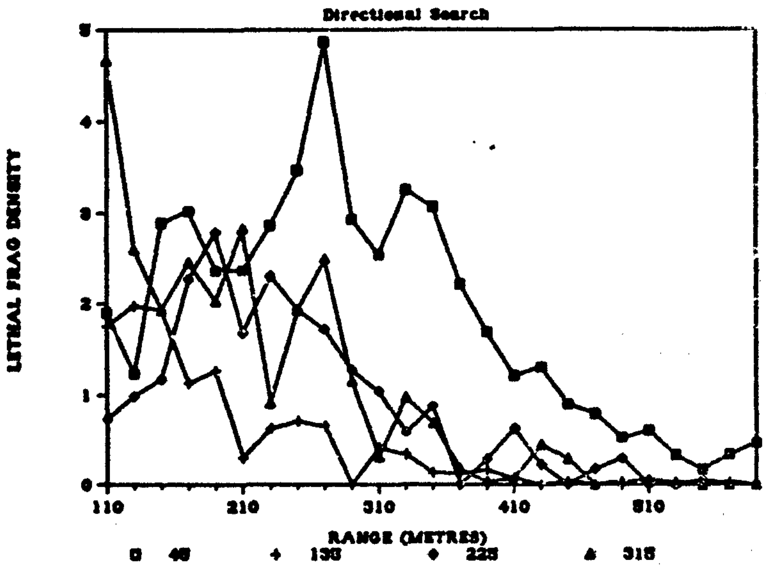

TRIAL 11 RANGE 270 METRES

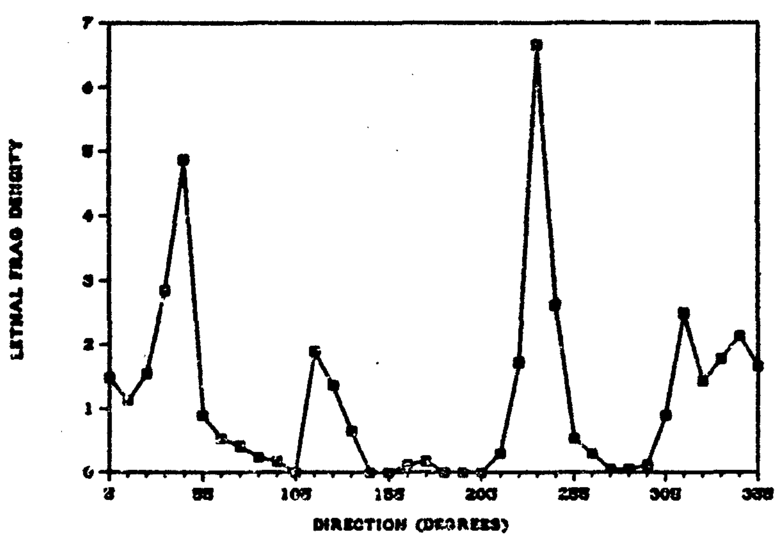

Blast Instrumentation:

Successful records were obtained from the shot.

8.5 TRIAL 12

Crater :

The crater was almost exactly the shape and size of the floor slab, being 6.6 m long by 6.2 m wide by 1.5 m deep. The footings had been thrown up on to the lip of the crater.

Traverses :

The vertical faced traverse was almost completely destroyed. Only the corner posts at the junction with the SW traverse were still close to their original positions. Timber and earth fill was scattered out to 100 metres from 315 to 45 degrees. There appeared to be very little erosion of the double mound traverses.

Debris :

A large amount of pulverised material was again observed up to 120 metres from ground zero.

Some 80 large pieces of debris were identified, mostly concrete with associated reinforcing bar.

There was a significant amount of debris in both the 45 and 135 degree direction comprising either pieces of concrete or reinforcing bar. The lethal fragment density out to 800m in both sectors was very low (considerably less than 1).

In the 45 degree direction there were still isolated pieces of concrete out to 1200m but there was no further debris found beyond 1200m. An impact area was noted at 1020m but no equivalent large fragment was found. The size of the impact area suggested that the concrete and reinforcing bar found out to 1100m from this point may be the remains of the impact.

In the 135 degree direction there was a further band of potentially lethal debris out to 900m approximately 25m either side of the 135 degree line. The apparent density was very low however. Some 15 fragments of concrete were found beyond 700 m in this direction but no further debris was found beyond 1000m.

Further searches were carried out from 400-600m either side of the 135 degree direction and in the 215 degree direction because of the amount of debris noted in these areas.

The results of the main debris collections are shown graphically in the following two figures. The first figure shows the density variation with range for the four main sector searches at 45, 135, 225 and 315 degrees. The second figure shows the density variation with direction at a distance of 400 metres.

TRIAL 12 CONCRETE WALLS AND ROOF

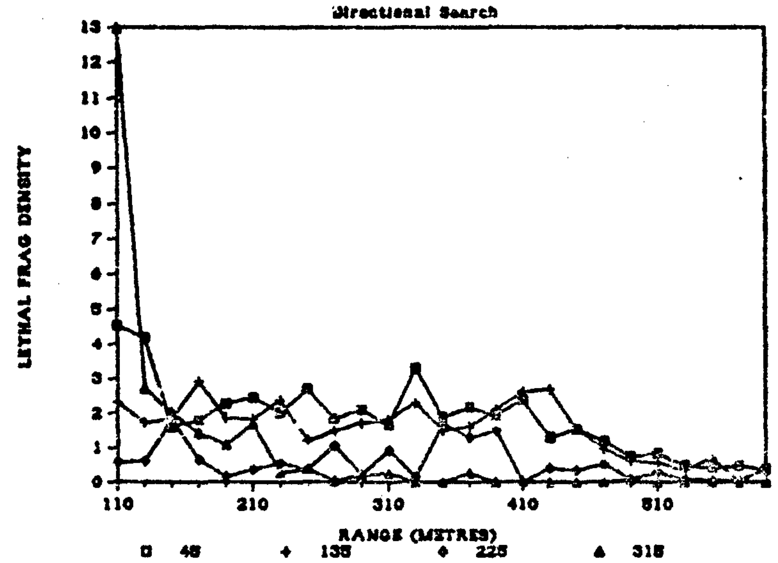

TRIAL 12 RANGE 400 METRES

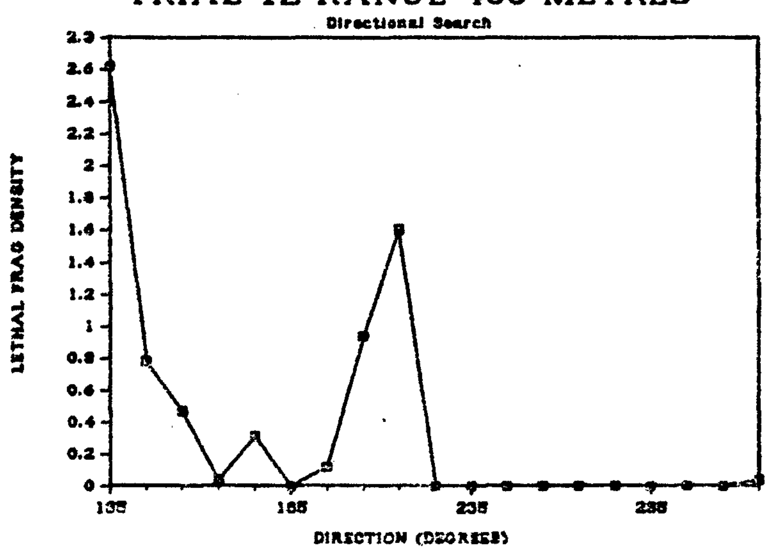

Blast Instrumentation:

Successful records were obtained.

8.6 Trial 12A

Crater:

Approximately 3 m diameter by 1.5 m deep.

8.7 Photographic Coverage:

Video coverage of the explosion for Site 13 and subsequent exlosions identified several fragments impacting on the grid areas. Later viewing of the cine film from the various trials showed that there were apparently a large number of fragments which should be amenable to velocity analysis.

Aerial coverage from a helicopter of the event in Trial 9 was very successful with good video and still camera coverage.

For Trial 10 there was no aerial coverage because of camera operational difficulties. Infra-red photographic coverage from the aircraft immediately after the explosion did not show up any fragments of interest as the resolution available was not high enough.

For Trial 11 the helicopter developed engine trouble and had to make an emergency landing. The firing was delayed in the hope that the problem could be resolved. However a new engine was required and the firing went ahead without aerial coverage. The helicopter team photographed the shot from the main observation point.

For Trial 12 because of problems with the firing circuit the cameras were started but no explosion took place. As the backup unit appeared to have the same problem the decision was made to proceed with the trial without photographic coverage since there were excellent photographs from which velocity measurements can be made from all the other trials and the high speed coverage of the actual events has shown no information to date. There was also no aerial coverage as the duration of the F-111 aircraft did not allow it to remain in the airspace during the long delay.

9 FUTURE WORK

The work carried out to date, including the current trials reported here, appear to consolidate the information required by UK to verify existing and proposed distances for fragment and debris throw from limited (< 6000 kg) quantities of explosives in a variety of explosive storehouse structures. Although no firm conclusions are offered at this stage from this phase of the work there is no apparent need to gather any more data for this part of the Quantity-Distance tables. However the series of trials have shown that it is not possible to take for granted the existing, often very subjective standards, for minimum fragment and debris standards for buildings.

Much work has been commissioned by the US DDESB to investigate the problems of open, untraversed stacks of fragmenting ammunition, in particular with respect to maximum and safe fragment distances. Similar work has been conducted for a variety of weapons by the UK Ordnance Board. However very little information exists for the situation when these same weapons and fragmenting ammuntion are stored inside a structure which does more than simply provide weather protection. This was the primary reason for the UK conducting the present series of Stack Fragmentation Trials.

However the question still remains whether the existing blast generated Quantity-Distances provide a sufficient degree of protection against fragment and debris effects for more typical storage quantities of several tens of tonnes NEQ of ammunition and explosives. Normally such quantities would be stored in igloos according to present day standards and the Explosion Effects Sub-committee of ESTC have considered that some work is needed to verify the existing Quantity-Distances for igloos in terms of debris hazard. This becomes especially important when it is realised that AC 258 reduced the outside Quantity-Distances from the rear and side of igloos with NEQs of less than 45,000 kg, and it is not apparent that any consideration was given to the debris hazard posed by these types of igloos. In addition, in the light of the UKs journey down the route of potential application of Risk Analysis techniques to the storage and handling of explosives it is even more essential to obtain some picture of the hazards posed by igloos , as well as other types of storage, at distances intermediate between ground zero and inhabited building distances (and beyond ?).

Consequently ESTC have opened negotiations with the Australian Department of Defence with a view to conducting a trial with a NATO Standard Igloo, loaded to some 50,000 kg NEQ, to investigate the explosion efffects from an accidental explosion of the contents of such a structure. At the present moment it is anticipated taht any such trials would take place in early 1990.

10 REFERENCES

1. Joint Australian/UK Stack Fragmentation Trials
   Phase 1 Report - F Bowman et al
   - 21st DDESB Seminar pp 1461-1484

2. Joint Australian/UK Stack Fragmentation Trials
   Phase 2 Report - J Henderson et al
   - 22nd DDESB Seminar pp 1867-1886

Q-D Requirements for New Norwegian Aircraft Shelter Design

by

Patricia Moseley Bowles
Mark G. Whitney
Michael A. Polcyn

ABSTRACT

Current quantity-distance (Q-D) safety criteria for siting NATO aircraft shelters are based on recommendations and conclusions from the DISTANT RUNNER test series. The DISTANT RUNNER program included full scale explosion tests of third generation, United States Air Force Shelters in normal munition storage configurations exposed to internal detonations. Data collected from these tests were utilized to establish hazardous debris range and hazardous blast contours to the front, side, and rear of a shelter. This information is the basis of current Q-D siting criteria for aircraft shelters which appear in DOD 6055.9 and AFR 127-100.

A new aircraft shelter design which has been termed the "combined Norwegian/US design" is being proposed for construction in Norway. Test data for debris or blast hazards do not exist for this specific shelter design. The Norwegian Defence Construction Service (NDCS) funded Southwest Research Institute (SwRI) to review the DISTANT RUNNER and new Norwegian shelter designs noting structural similarities and differences, and to recommend whether the differences preclude use of current Q-D criteria for siting the new Norwegian shelters. Conclusions of the study indicated insufficient confidence in using the current criteria for safe siting of structures to the front and side of the new shelter due to substantial variations in the arch and the front door designs. A plan of action for determining the proper Q-D environment for the new Norwegian shelter was developed as a result of the study. The plan includes testing recommendations and steps necessary to establish safety criteria which apply to the new shelter design.

1.0 INTRODUCTION

Current quantity distance (Q-D) safety criteria for siting NATO aircraft shelters are based on recommendations and conclusions from an explosion test series known as DISTANT RUNNER. The DISTANT RUNNER program included full scale tests of internal detonations of normal munitions storage configurations in third generation, United States Air Force shelters. The program is described in References 1, 2, and 3. Reference 3 presents results of two tests (Events 4 and 5) in which internal detonations resulted in the throw of hazardous debris and the venting of blast waves around the shelter site. The data collected from these tests were utilized to establish hazardous debris range and hazardous blast contours in various directions about the shelter. This information is the basis of current Q-D siting criteria for aircraft shelters which appear in Chapter 10 of DOD 6055.9 and Chapter 5 of AFR 127-100. The inhabited building distances are set at the 1.2 psi blast contours for the US and about 0.7 psi for NATO. After the DISTANT RUNNER test program was completed, the United States Naval Surface Weapons Center, Research and Technology Department completed the Aircraft Shelter Model Test (ASMT) series which repeated the DISTANT RUNNER explosion tests using small scale (1/10) replica models. The tests and results are documented and compared with the full scale tests in References 4 and 5.

The Norwegian Defence Construction Service (NDCS) has expended a large amount of research effort in developing aircraft shelter designs. NDCS completed a test program described in References 6 and 7 utilizing models of third generation Norwegian aircraft shelters to establish Q-D criteria for these structures. In addition, NDCS was very involved in the DISTANT RUNNER and the ASMT programs. NDCS has been asked to utilize a shelter design which has been termed the "Combined Norwegian/US Design". Test data for debris or blast hazards do not exist for this specific shelter configuration. However, structural similarities between the third generation US shelters tested in DISTANT RUNNER and the combined Norwegian/US design are apparent as indicated in

Figure 1. NDCS has three major questions for NATO and the explosives safety community:

- Are the differences in the two shelter designs significant, i.e. can DISTANT RUNNER results apply to the new combined design?

- If the differences are significant, are there any data available which might be utilized to establish Q-D criteria for the new design?

- If sufficient data are unavailable, what is the most cost effective method of collecting data (testing or engineering analysis)?

Southwest Research Institute (SwRI) was funded by NDCS to provide an answer to the first question and consider answers to the other questions. Thus, the objective was to review the DISTANT RUNNER and Norwegian/US shelter designs noting structural similarities and differences of importance which would affect shelter break-up under internal blast loads. In addition, SwRI was tasked to recommend whether the differences preclude utilization of current Q-D criteria.

2.0 SHELTER DESIGN REVIEW AND COMPARISON

SwRI reviewed as-built drawings of the DISTANT RUNNER shelters along with drawings of the combined Norwegian/US design in order to identify important structural differences which could affect debris formation and distribution due to an internal explosion. The buildings were evaluated by comparing three structural elements: the arch, the front door, and the rear wall. Of these three, the most dramatic difference is in the front door design. The Norwegian/US door is a hollow steel door which opens to the inside, and is supported by special thresholds at the top and bottom when closed. The door will be seated

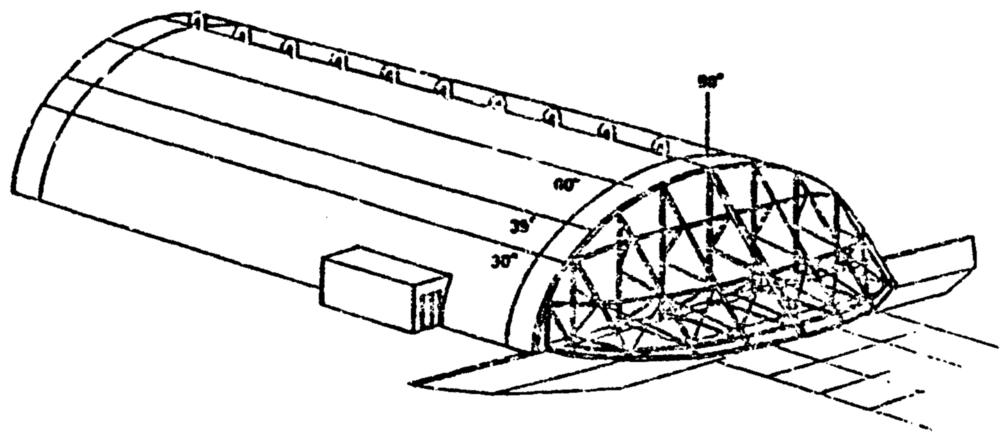

a) DISTANT RUNNER

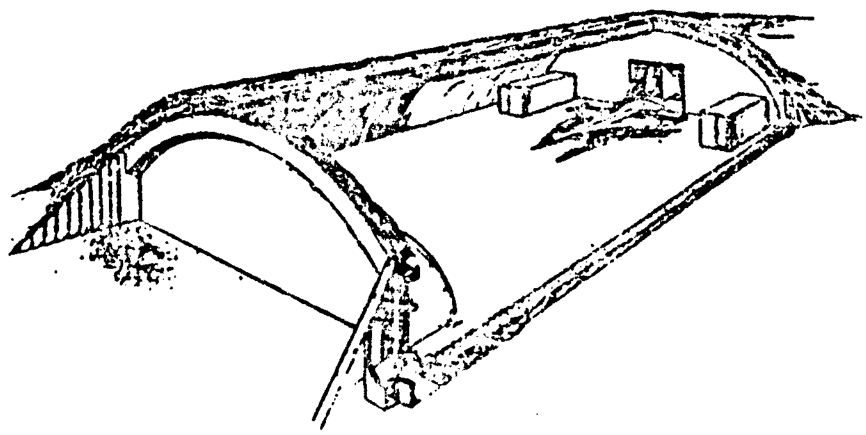

b) Norwegian/US

Figure 1. Aircraft Shelter Designs

in the thresholds when deflecting due to either external or internal loading. The DISTANT RUNNER door utilized a concrete/steel composite section with a large exterior support frame work. The door is designed to separate in the middle, and each piece moves sideways along a track when opening or closing. The door is supported by the arch structure when responding to external loads. The door is unsupported when responding to internal loads.

Other dramatic differences between the two structures include:

- The Norwegian/US shelter concept is earth covered (about 25 cm (10 in) soil cover at the top, with the arch base and rear wall supporting about a 5 m (16 ft) berm which contains rock rubble as well as soil in many cases), while the DISTANT RUNNER structures had no earth cover.

- The DISTANT RUNNER structures have a side entry door midway along the arch on one side. The Norwegian/US shelter has a personnel entry door by the front door.

- The exhaust chimney structure is different for the two buildings.

These are the more obvious differences in the two designs. A review of the plans identified a number of other variations which may affect shelter breakup. These are summarized in Table 1.

Although differences exist in the building dimensions and the size and weight/area of venting surfaces (doors), the predicted blast loads for the two structures are essentially the same. The quasi-static loads were predicted utilizing a method in the revised tri-service document, AFM 88-22, (NAVFAC P-397, TM5-1300), which accounts for the weight/area of vent covers. The explosive charge used in the calculations was 4158 kg (9162 lb) of Tritonal (same as in Event 5 of DISTANT RUNNER). The

TABLE 1. STRUCTURAL COMPARISON

Building Dimensions	Combined Norwegian/US	DISTANT RUNNER
inside plan width	23.5 m (77 ft)	21.6 m (70.8 ft)
inside plan length	37.2 m (122 ft)	36.6 m (120 ft)
inside height at crown	7.0 m (23.1 ft)	8.43 m (27.67 ft)
volume	5079 m^3 (179,400 ft^3) [third generation Norwegian was 3900 m^3 (137,747 ft^3)]	5221 m^3 (184,400 ft^3)
Arch		
corrugation depth	360 mm (14 in)	360 mm (14 in)
arch thickness at base (including corrugation)	1360 mm (53 in)	810 mm (32 in)
arch thickness at crown (including corrugation)	810 mm (32 in)	810 mm (32 in)
total circumferential reinforcement (area/unit spacing)	3.8 mm^2/mm (0.15 in^2/in)	1.31 mm^2/mm (0.0517 in^2/in)
total horizontal reinforcement (area/unit spacing)	2.5 mm^2/mm (0.10 in^2/in	1.31 mm^2/mm 0.0517 in^2/in)
typical circumferential reinforcement spacing	100 mm (3.9 in) o.c.	150 mm (6 in) o.c.
typical horizontal reinforcement spacing	100 mm (3.9 in) o.c.	150 mm (6 in) o.c
corrugation material (connections detailing the same for both)	3 mm (0.1 in) min. thickness	3 mm (0.1 in) min. thickness
arch base connection to footing	double legs at 100 mm (3.9 in) o.c., 2 m long	single #4 leg at 150 mm (6 in) o.c., 1.2 m long
floor slab connection at arch base	slab overlaps footing	no slab overlap
personnel door	near front door	at one side with protection wall
earth cover	present	not present

TABLE 1. STRUCTURAL COMPARISON

Front Door	Combined Norwegian/US	DISTANT RUNNER
panels	hollow-core steel plates with internal stiffeners: interior plate-20 mm (0.8 in) exterior plate-10 mm (0.4 in) stiffeners-10 mm (0.4 in) thickness-250 mm (9.8 in)	composite steel/concrete supported by exterior trusses: steel plate-3.2 mm (1/8 in) concrete-300 mm (12 in)
support against internal load	simple support top and bottom	track mechanism only
weight/area	280 kg/m^2 (58 lb/ft^2)	770 kg/m^2 (157 lb/ft^2)
Rear Wall		
thickness	1200 mm (47 in) no reinforcement details given	600 mm (24 in) 3.2 mm (1/8 in) plate on inside face, #6 bars @ 180 mm (7 in) o.c., e.f., e.w.
earth berm	present	not present

quasi-static impulse and duration predictions were based on the vent area of the front door only for both shelters.

The shock loading can be affected by the position of the munitions within the shelter. To make a comparison between the response of the two shelters, the same charge configuration should be used for each. However, the location of the bomb stacks near the front door for the DISTANT RUNNER layout (Figure 2) had to be altered when examining the load inside the combined shelter to allow space for the recessed area into which the front door opens. We evaluated the two munition distributions at various locations in the shelter and found relatively no difference in overall shock loading.

Based upon the predicted loads and the known structural details of the two buildings, some simple dynamic response comparisons were made. Arch response in extension was examined along with door debris throw.

We approximated the arch structures as single-degree-of-freedom systems to predict time response assuming restraint at the footing. (We realize that restraint is not provided; however, we want to compare the extensional behavior of the two arches to the predicted loads). As shown in Figure 3, the deflection histories of each are very similar out to very large predicted deflections, well beyond the point at which either structure will fail and begin to break apart. We expect that despite the differences in arch reinforcement, if the two were to break at the same point in time, the debris initial velocities should be similar. After failure, additional velocity will be imparted to the arch pieces as the internal pressure tries to "push" its way around and out past the pieces. This process will occur for both structures. However, the Norwegian/US arch is either bermed with rock rubble and soil which extend approximately 2.5 m (8 ft) up the side of the arch, or its foundation rests on solid rock and the arch is bermed with soil alone. The lower portions of the arch may be restrained enough to cause hinge formation and resultant higner velocities for debris from the upper arch of this shelter compared to the debris velocities for the DISTANT RUNNER arch.

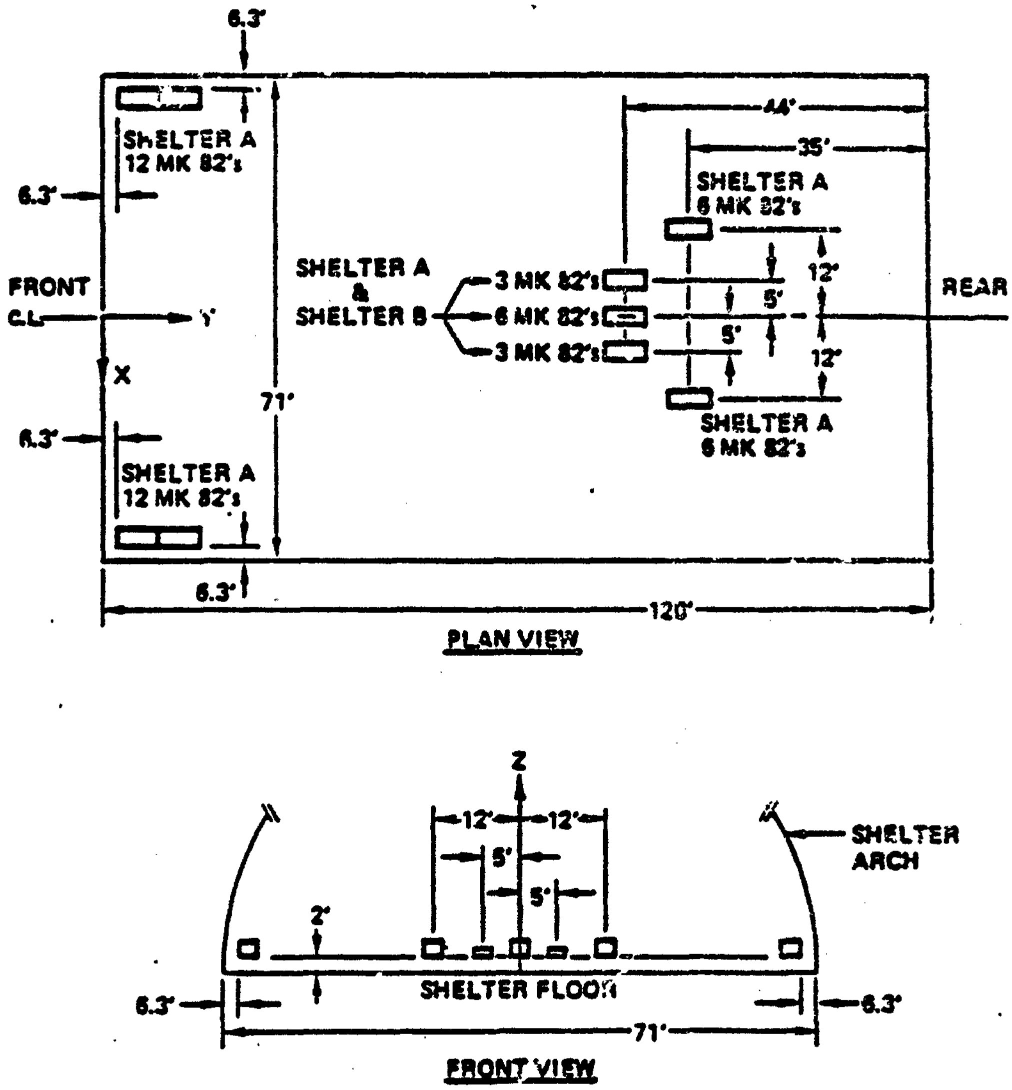

Figure 2. Plan View and Front View of Aircraft Shelter Bomb Placements

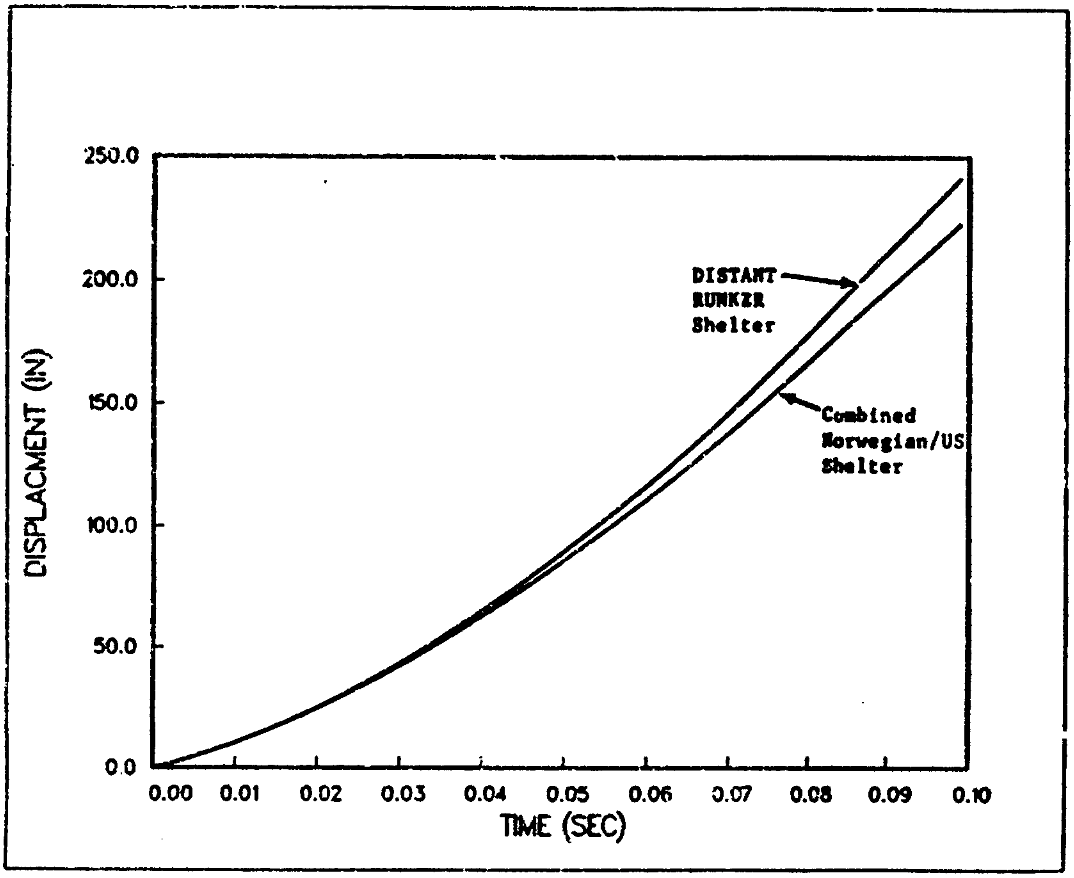

Figure 3. Displacement History for Both Shelters

The comparisons made in this report must be qualified by noting how differences such as those listed in Table 1 may affect shelter breakup from internal loads.

- Existing Q-D criteria were established based upon data collected in Events 4 and 5 of the DISTANT RUNNER program. Both shelters used in these tests had been exposed to substantial dynamic loads (external and internal) prior to the final events in the test series. This type of "pre-conditioning" of structures will not be present at potential accident sites in Norway except after action of war or nearby accidental explosions. It is not clear whether this pre-conditioning affected the breakup of either shelter and, hence, influenced the establishment of Q-D criteria.

- There are substantial differences in the arch connection at the foundation of the two buildings. The DISTANT RUNNER arch is attached to the footing by a single 1.2 m (4 ft) leg at 150 mm (6 in) o.c. The floor slab of the building does not overlap the footing, and the arch is the same dimension at its base as at its crown. The Norwegian/US design specifies that circumferential rebar legs continue through the construction joint to the bottom of the footing. The arch is thicker at the base than at the top. The floor slab overlaps the footing, and there is an earth berm at the side of the arch. In some geographical locations, there is rock rubble as well as soil in the berm. These factors result in the Norwegian/ US arch responding less in rigid body translation and more in extensional stretching than that expected in the DISTANT RUNNER shelters. We expect the DISTANT RUNNER arch to pull free from the footing earlier in its response than the Norwegian/US shelter. Note that in the DISTANT RUNNER tests, separation of the arch from the footing was observed early in the dynamic response after time of detonation. Also, the restraint caused by the rock rubble berm of the Norwegian/US shelter may prevent

horizontal movement and cause higher initial debris velocities for the arch above the rock rubble. The debris trajectory angles may depend on the hinge formation in the arch instead of being normal to the original arch shape.

- The Norwegian/US shelter utilizes a 100 mm (3.9 in) reinforcement spacing in the arch whereas the DISTANT RUNNER plans indicate a spacing of 150 mm (6 in) o.c. Debris formation can be related to rebar spacing when the structure is overwhelmed by an intense blast load, e.g. large quantities of explosives. This is evident in the DISTANT RUNNER test results (Reference 2).

- The DISTANT RUNNER shelters utilized 10 vent openings spaced evenly along the peak of the arch. Though a small percentage of the total length, the diameter of each [150 mm (10 in)] is large enough to interrupt circumferential reinforcement and possibly establish a preferred breakup location in the arch. This is not present in the Norwegian design. Note that in the DISTANT RUNNER tests, separation of the arch at the crown occurred early in the dynamic response after time of detonation.

- In Reference 4, the authors noted that DISTANT RUNNER shelter breakup was definitely influenced by the location of reinforcement splices and the amount of overlap. This is particularly true for lower charge amounts. The location and overlap of splices in the Norwegian/US design should have a similar influence in the breakup of this shelter. This is not to say that, for low charge amounts, the breakup will be the same as for DISTANT RUNNER, but that splice locations should have similar importance.

3.0 CONCLUSIONS

It should be obvious from the discussions in the previous sections that one definite conclusion can be made about the Norwegian/US and DISTANT RUNNER shelters; they are alike and they are different! There are many technical reasons we can cite that can be the basis of predicting differences in the breakup pattern and debris throw of the two shelters; however, it is our opinion that enough similarities are present between the rear walls to predict that the currently established Q-D criteria for the rear direction can be used for the Norwegian/US shelter for charge amounts equal to or greater than that used in Event 5 of the DISTANT RUNNER tests. This is not the case for the front direction, however, where enough differences exist between the front door systems of the two shelters to preclude drawing any conclusions on using existing Q-D criteria. There also is insufficient confidence in using current criteria for siting structures to the side of the new shelter due to substantial variations in the arch design. These comments apply to criteria established from the DISTANT RUNNER results, whether for protection of occupied areas, protection of assets, or prevention of explosion propagation. Again, this is an opinion, and not a statement of engineering fact. The comparisons made in this paper do not form an adequate basis of information to establish Q-D criteria. The level of confidence traditionally expected in making these decisions has not been reached through this comparison, as the two structures are not enough alike to make conclusive statements about the debris and blast hazards near the combined Norwegian/US shelters.

4.0 RECOMMENDATIONS

To develop a level of confidence necessary to establish Q-D criteria for the combined Norwegian/US shelter, a testing and analysis plan of action was recommended. The test program would utilize very small scale and small scale tests to develop important data. These data would be utilized to "fine-tune" analysis prediction methods which, once developed, could be applied to establish Q-D criteria for a general

group of structures which resemble the Norwegian/US shelter in size and construction and could be applied to a range of charge amounts.

A series of tests is recommended to provide an adequate data base to predict the hazards near aircraft shelters. Of most interest are hazards due to debris, since the greatest uncertainty exists here; however, data on exterior blast will also be collected. The recommended approach is to utilize very small scale (around 1/30 scale) and small scale (around 1/4 scale) models of the shelter in the test program. It is felt that the following steps are necessary:

1. Determine internal load history on the shelter utilizing very small scale structures.

2. Understand the arch response to dynamic loads. We wish to learn more of arch extensional, bending, and translational (uplift) behavior under internal loads. Debris formation and size are not of interest at this time, as we want to study the events leading up to failure utilizing very small scale models.

3. The formation of debris (size and shape) from the arch structure must be understood if hazards are to be defined. In addition, the door breakup must be studied. We suggest no less than small scale (around 1/4 scale) tests be performed to provide this information.

4. The test data collected in Items 1-3 above can be utilized to establish analysis predictions of shell response, breakup, and debris throw. From this, quantity-distance (Q-D) criteria can be established. If deemed necessary, full scale tests can be performed under the desired conditions.

REFERENCES

1. Flory, Robert A., "DISTANT RUNNER Results: A 5 Event High Explosive Test Series Involving U.S. Air Force 3rd Generation Aircraft Shelters," Minutes of the Twentieth Explosives Safety Seminar, Volume II, pp. 1817 - 1835.

2. Ward, Dr. Jerry M., "DISTANT RUNNER - Debris Recovery and Analysis Program for Events 4 and 5," Minutes of the Twentieth Explosives Safety Seminar, Volume II, pp. 1837-1881.

3. Ward, Dr. Jerry M., "DISTANT RUNNER - Debris Recovery and Analysis Program for Events 4 and 5," Naval Surface Weapons Center, White Oak Laboratory, Silver Spring, MD, April 1982.

4. Ward, Jerry M., et al., "Modeling of Debris and Airblast Effects from Explosions Inside Scaled Hardened Aircraft Shelters," NSWC TR85-470, May 1985.

5. Swisdak, Michael M., Jr., "Aircraft Shelter Model Test (ASMT) Follow-Up Analyses," NSWC TR 86-472, September 1986.

6. Riis, F., "Third Generation Aircraft Shelter Debris Throw and Air Blast Caused by Accidental Explosions in the Ammunition Cubicle, Report III, Model Tests, Scales 1:20 and 1:100," Fortifikatorisk Notat 149/80, November 1980.

7. Jenssen, A. and Riis, F., "Third Generation Aircraft Shelter, Debris Throw and Air Blast Caused by Accidental Explosion in Ammunition Cubicle, Report II, Pressure Measurements Within Steel Model, Scale 1:75," Fortifikatorisk Notat 150/80, November 1980.

HIGH EXPLOSIVE HOB AIR BLAST INTERACTION WITH A SIMULATED HEATED LAYER

R. E. Reisler, L. A. Dixon, J. H. Keefer

ABERDEEN RESEARCH CENTER
30 DIAMOND STREET, P. O. BOX 548
ABERDEEN, MARYLAND 21001

301 272-4200

HIGH EXPLOSIVE HOB AIR BLAST INTERACTION
WITH A SIMULATED HEATED LAYER

INTRODUCTION

Research studies of the interaction of reflected air blast with a non-ideal surface were carried out with a series of 1000-lb height-of-burst (HOB) experiments. Development of a technique to generate a heated layer as a non-ideal surface condition began in 1982 with the investigation and testing of pyro-chemicals as the source. Although work with these materials continued on a limited scale for several years, totally satisfactory results were not achieved and the emphasis shifted toward the use of helium gas as a simulator of a heated layer. A successful HOB test of a helium layer was conducted in 1984 while the authors were in the employ of the Ballistic Research Laboratory (BRL), and became the fore-runner of the experiments discussed in this paper.

The interaction of HOB blast with a helium layer along the surface generates a precursor wave as depicted in the schematic of the development of blast waves from a HOB explosion in Figure 1. A "snowplow" modification to regular Mach reflection is shown. A similar modification will be observed with irregular Mach reflection (IMR) when HOB conditions are such that IMR will occur.

Precursor waveforms from nuclear explosions have been evaluated in the past and grouped according to their shape as shown in Figure 2. Reproduction of these five types of waveforms was desired from the blast interaction with the helium layer.

EXPERIMENTAL PROGRAM

Four HOB experiments were conducted in 1986 using a 1000-lb TPH 3342 (85% HMX) spherical charge detonated at 19.8 feet with a 2-inch layer of helium over a rigid surface. Two HOB experiments were added in 1987 using the same type of charge but detonated at 36 feet, again with a 2-inch layer of helium over a rigid surface. The tests were conducted over a specially

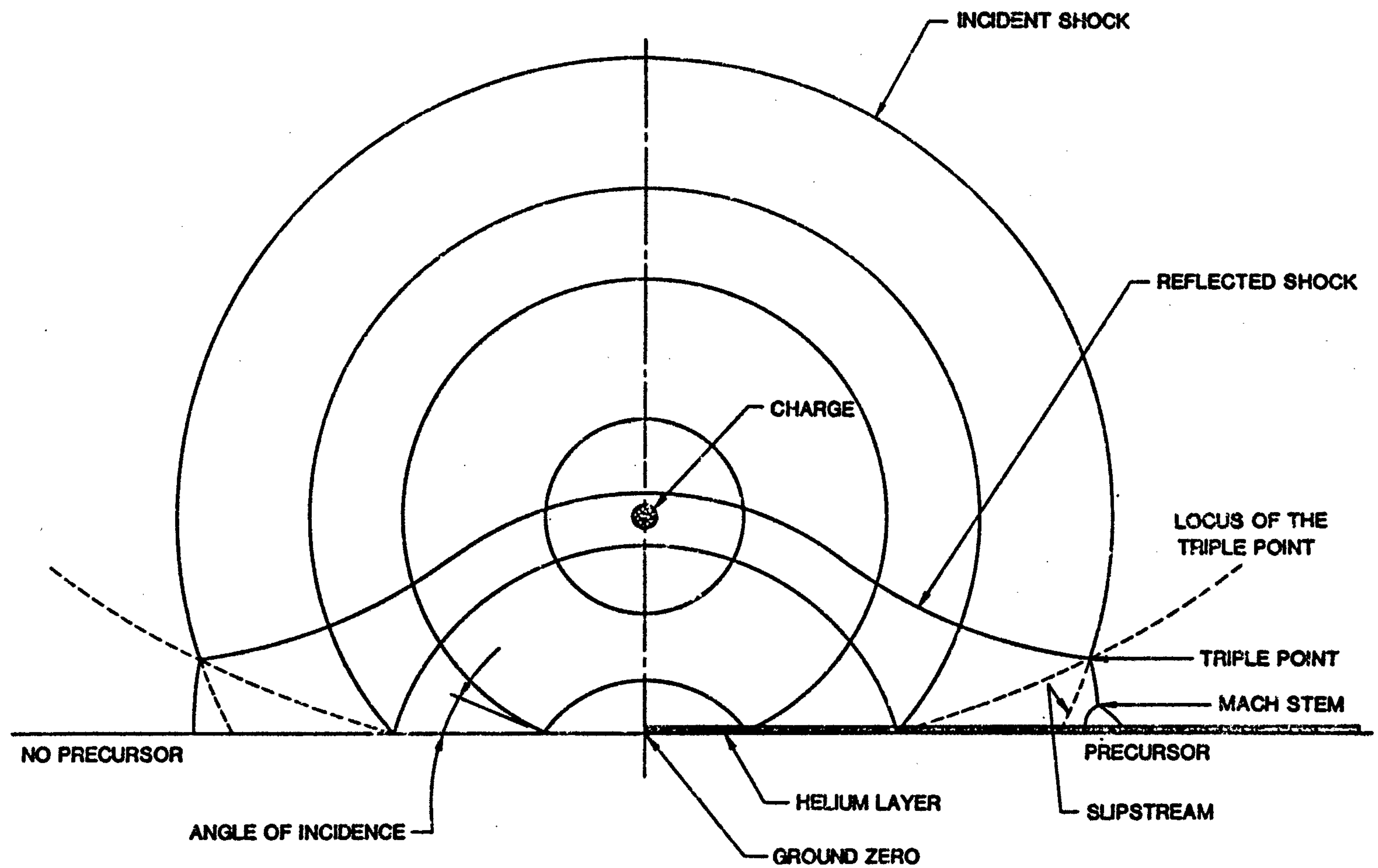

Figure 1. Schematic of the development of the blast waves from an airburst explosion for precursor and non-precursor conditions.

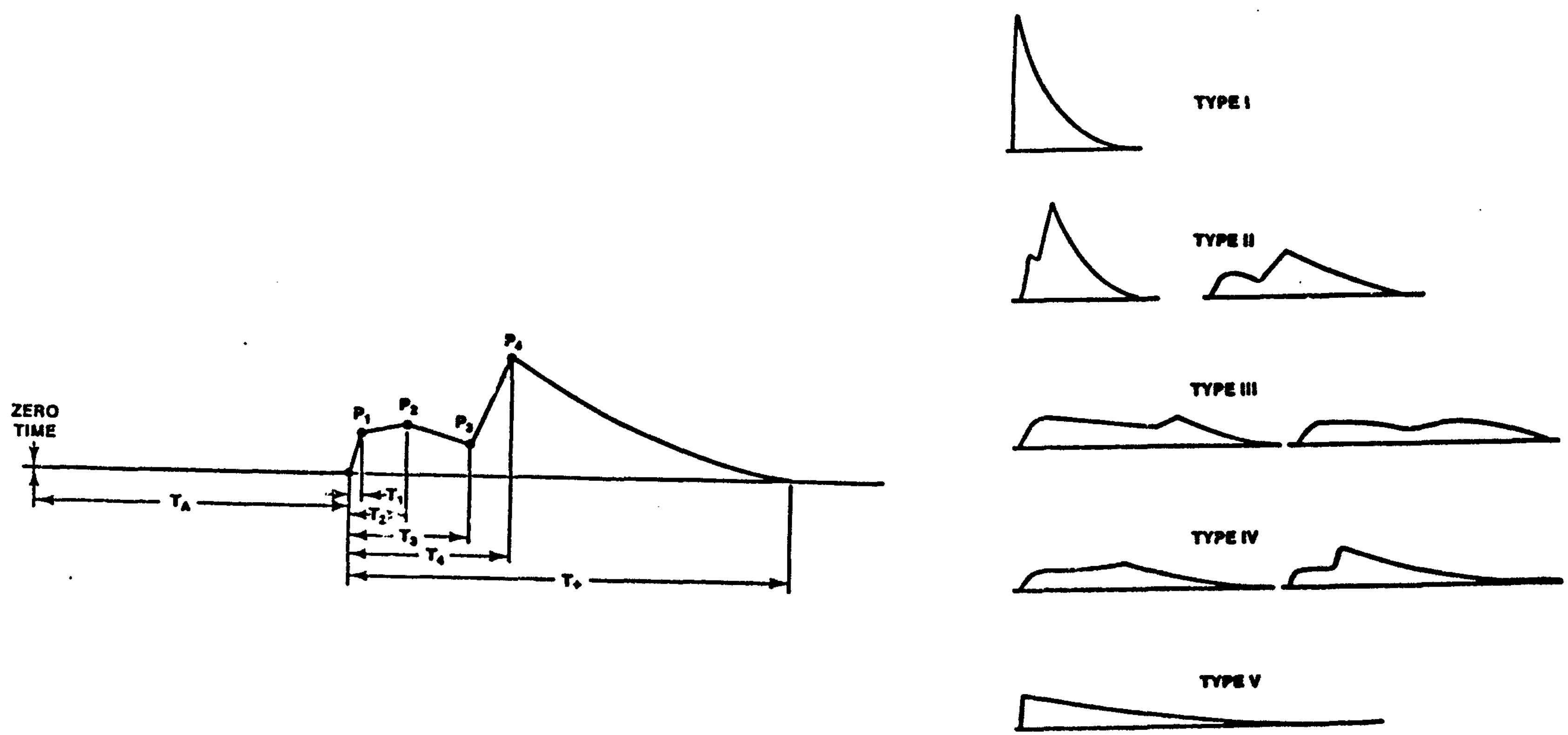

Figure 2. Left, time and pressure breakdown of precursor waveforms. Right, classifications of waveforms.

constructed concrete test pad at the Defence Research Establishment, Suffield, Alberta, Canada.

Table 1 presents a summary of the shots with the size of the layer and the concentration of the helium achieved. Of the experiments conducted in 1986, two had a single constant concentration and two had a decreasing concentration created by five segments in the containment system. Of the two experiments conducted in 1987, one had five segments for a decreasing concentration and one had four segments for a decreasing concentration.

A Mylar membrane, 1/2-mil thick and having a cord grid on one side, was used to contain the helium. Deployment of the membrane, as shown in Figure 3, was achieved by unrolling the pre-rolled membrane from an aluminum pipe supported on the ends by modified golf carts. The edges of the membrane were sealed to the concrete pad by the use of double-sided sticky tape and polyethylene tubing. Tension across the membrane was produced by attaching pre-anchored bungee cords to patches incorporated on the edges of the membrane at 2-foot intervals. Two-inch cord tie downs from patches on the membrane at 2-foot square intervals were hooked on to pre-installed anchors in the test pad to maintain a uniform 2-inch layer. Poly-tubing was used along several arcs in 1986 in order to segment the membrane for decreasing helium concentrations; in 1987 the poly-tubing was replaced by a skirt of the membrane material. Helium was released to fill the volume created by the membrane through a pipe network under the pad coupled to a reservoir of tanks near the facility. Helium concentration measurements in the form of the ratio of helium to air were obtained using sound probes. Filling operations took approximately 40-60 minutes. Shown in Figure 4 is a photograph of Shot 86-2 readied for charge arming and the final helium fill from the remote-control position. Figure 5 shows a photograph of the test pad with the membrane in place for Shot 87-1.

INSTRUMENTATION

The instrumentation for the tests was the analog FM data acquisition system as deployed on past experiments of this size. PCB piezoelectric quartz pressure transducers were connected with line drivers and coupled by

Table 1. Helium Layer Test Series

85% HMX Charge at 19.8 ft HOB

•	Shot 1	15 July 86	20 ft wide, single concentration (93%)
•	Shot 2	25 July 86	36 ft wide, single concentration (89.4%)
•	Shot 3	31 July 86	36 ft wide, segmented, decreasing concentration (93-33%)
•	Shot 6	26 Aug 86	36 ft wide, segmented, decreasing concentration (93% to less than 48%)

85% HMX Charge at 36.0 ft HOB

•	Shot 1	14 Oct 87	50 ft wide, segmented, decreasing concentration (84-27%)
•	Shot 2	28 Oct 87	50 ft wide, segmented, decreasing concentration (93-21%)

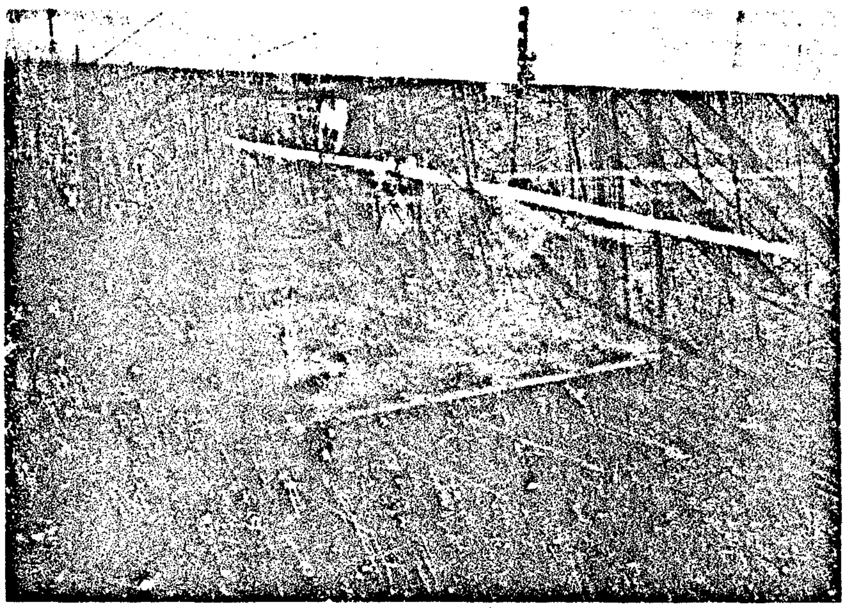

Figure 3. Membrane deployment, Shot 86-3.

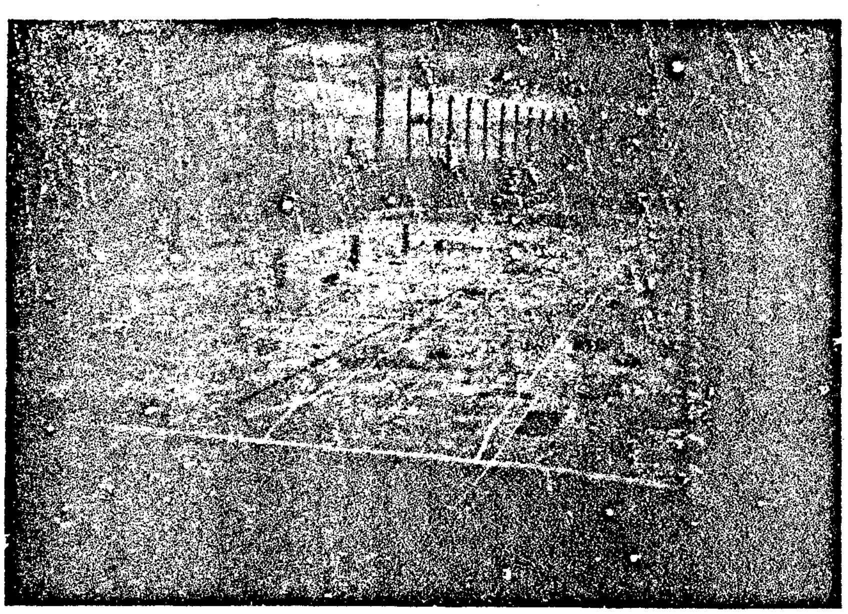

Figure 4. Membrane in position, Shot 86-2.

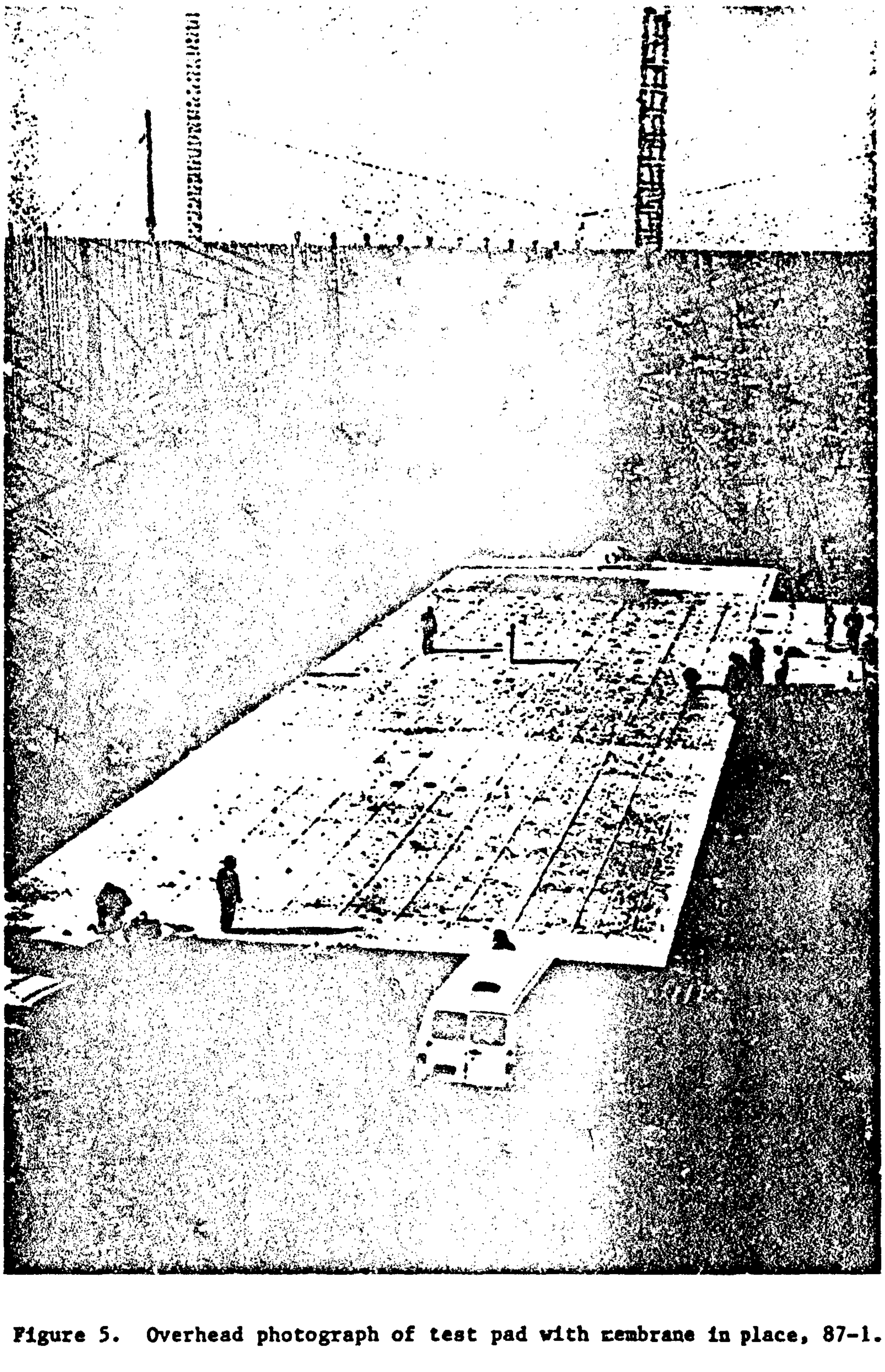

Figure 5. Overhead photograph of test pad with membrane in place, 87-1.

coax cabling to 500 kHz wide band II magnetic tape recorders to achieve response times of one to two microseconds. High-speed cameras were used at various locations on the layout to observe the detonation and shock development. The early time shock structure was observed by the laser photogrammetry technique deployed by the Denver Research Institute.[1]

RESULTS

Photographs of the shock structure obtained from laser photogrammetry in the region of highest helium concentration (93%) for Shot 86-6 are shown in Figure 6 together with a numerical simulation.[2] Correlation of the numerical simulation with the observed structure shows the laser photogrammetry recording the precursor front, the precursor triple point, the Mach stem, the triple point of the Mach stem, and the incident and reflected waves as labeled by the numerics. At the 19.8-foot HOB it is to be observed that irregular Mach reflection occurs. This is evident in the laser photographs. A hot thermal layer is indicated by the very short mach stem.

Photographs of the shock structure for Shot 87-1 are shown in Figure 7. This was a 36-foot height-of-burst where a regular Mach reflection occurs. Correlation of the numerical simulation with the observed structure is very similar to the 86-6 shot discussed above, however, a "cold" thermal layer is indicated by the lengthy Mach stem.

Pseudo comparisons were made between pressure-time signals generated at selected gage positions and laser-light images that were photographed over

---

[1] Wisotski, John, "Ultra High-Speed Ruby Laser Photographic Light System," Proceedings of the Sixth International Symposium on Military Applications of Blast simulation, Vol. I, Cahors, France, 25-29 June 1979.

[2] Kuhl, A.L., Glowacki, W.J., Glaz, H.M., and Colella, P., "Simulation of Air Blast Precursors in Large Shock Tubes," Proceedings of the Ninth International Symposium on Military Applications of Blast Simulation, Vol. II, Oxford, England, September 1985.

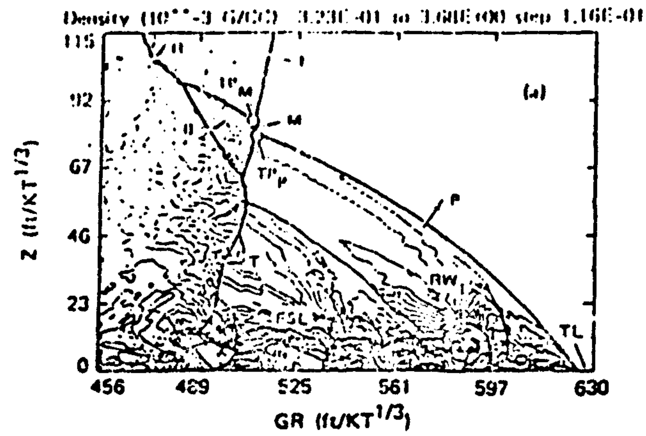

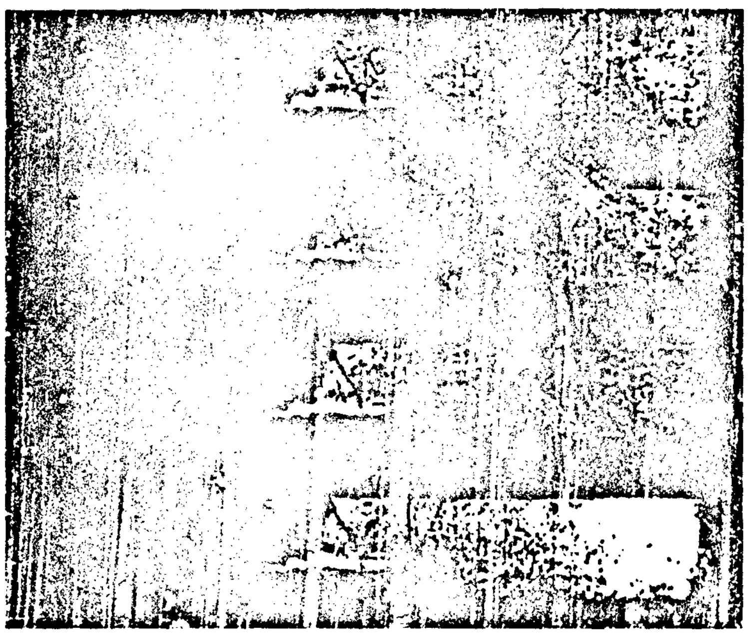

Figure 6. Top, inviscid numerical simulation of an airblast precursor for a "hot" thermal layer.
Bottom, laser lighted photograph of shock structure, Shot 6, time 6.006 msec.

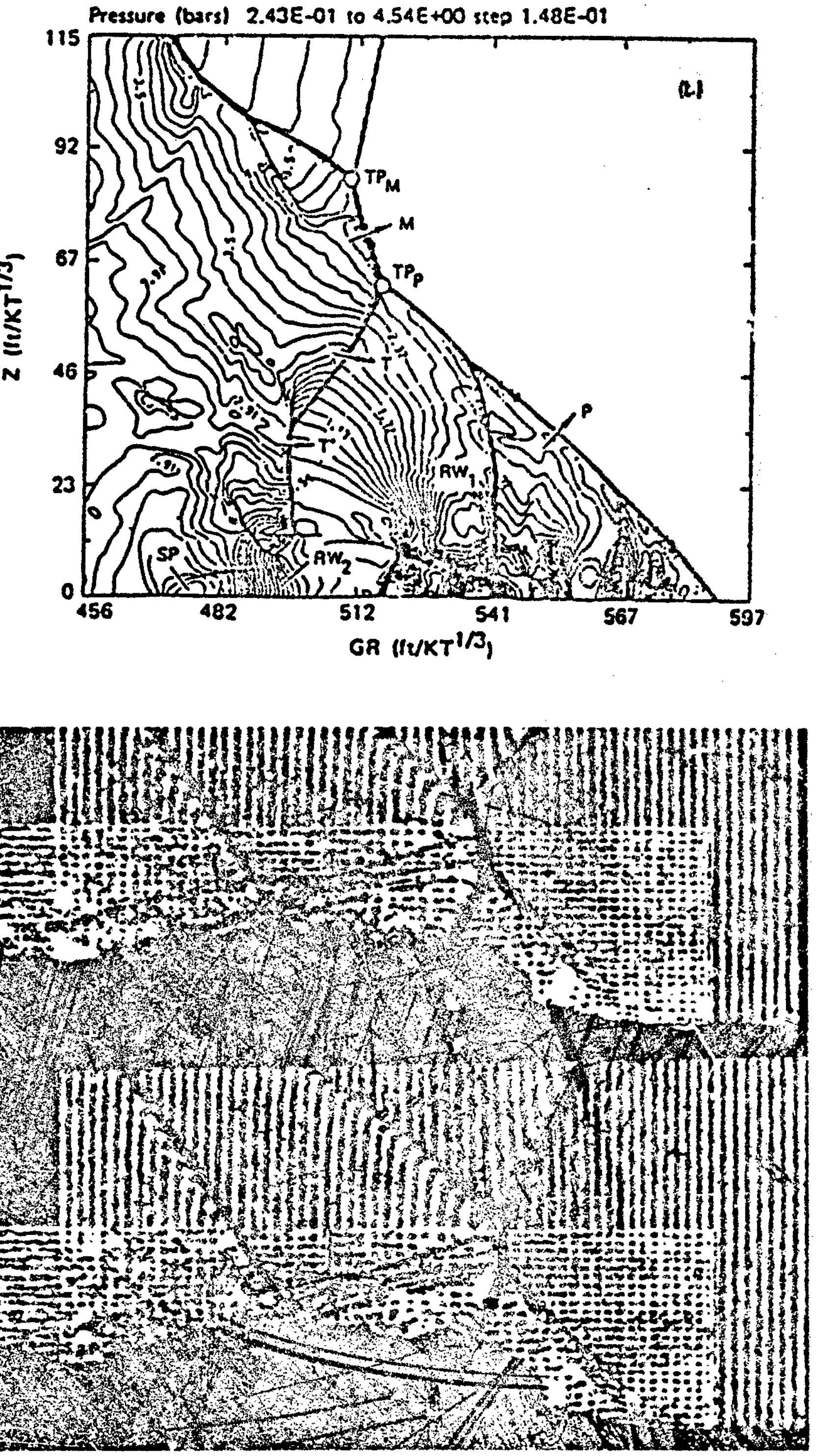

Figure 7. Top: Numerical simulation of a precursor for a "cold" thermal layer. Bottom: Laser-lighted photographs of shock structure at times 21.974 and 22.070 ms in the 45- to 60-foot precursed region.

the same time periods in which the gage signatures were being recorded.[3] These are shown for the gage record at 35 feet on Shot 86-3 in Figures 8.1 through 8.3. Comparisons were made at the start of the outrunning precursor peak (To), at the minimum prior to the maximum peak (Tm) and at the maximum peak (Tp) of the pressure record as obtained from the beginning of the record. Times were based on gage time-of-arrival measurements (To) and calculated differentials from Tm and Tp. Note that the minimum of the pressure record appears to occur slightly behind the triple point but probably ahead of the main vortex flow if one were to project and draw the vortex flow from the triple point down to the surface. The maximum at Tp appears to occur decidedly back within the main vortex flow if the same projection scheme were again used by the observer. These relative positions of Tm and Tp, with respect to the triple point, seem to be common to all gage positions.

Pressure waveforms from the surface gages were analyzed and where possible compared with available records from large-scale experiments. Pressure records from the experiments were analyzed following these procedures and where possible comparisons were made with records from large-scale experiments. In Figure 9.1 the waveforms from Shot 86-2, a constant helium concentration event, have been categorized by type and scaled to and compared with results from a large scale experiment at a comparable height of burst. Record types of II, III, and IV were recorded. Shot 86-2 may be classified as a "hot" layer, especially in the cleanup region where the last station is a Type IV record instead of the Type V recorded on the large scale event.

Figures 9.2 and 9.3 present records from the decreasing helium concentration event, Shot 86-6, which have been scaled to and compared with the same large scale event. Waveforms of Type II, III, IV, and V are evident. Some of the wave structure on the Type II and III records between the time of arrival and the time of minimum pressure, T3, Figure 2, was caused by the wall which separated the membrane into segments. The

[3] Wisotski, John and Plooster, Myron, "Photographic Analyses of HOB Shockwaves Generated With or Without Thermal Precursor Layers," Report No. 5-32916, Denver Research Institute, Denver, CO, December 1986.

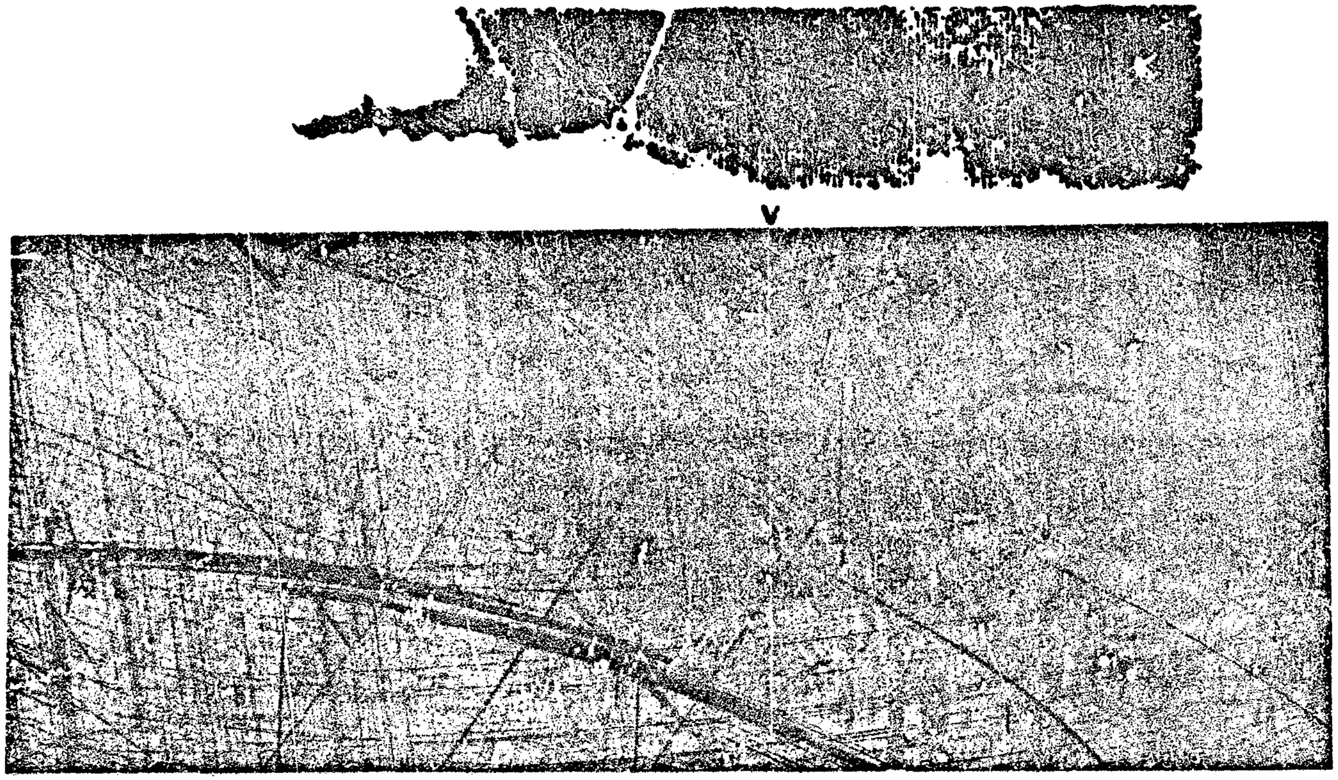

Figure 8.1. Pseudo comparison of Shot 86-3 pressure-time signature from the 35 ft gage and photographic image at instantaneous time, To.

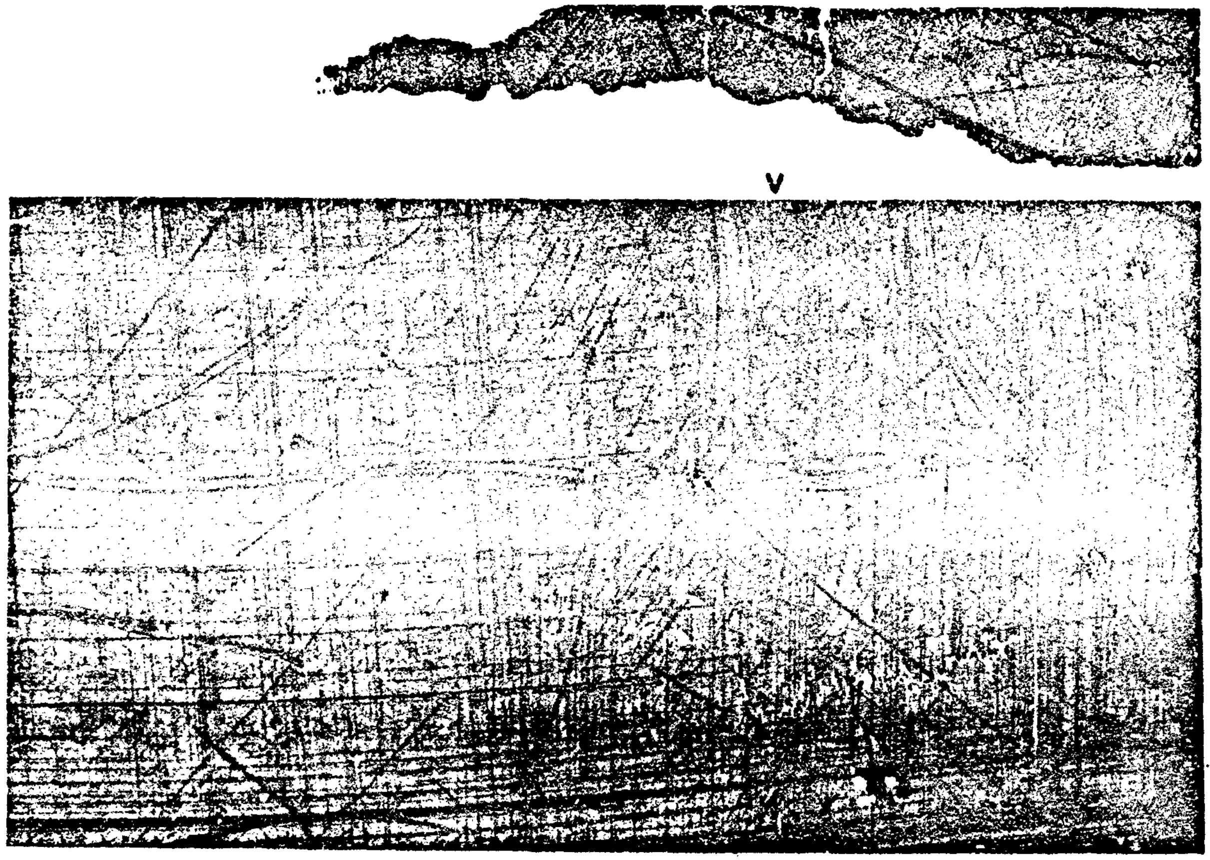

Figure 8.2. Pseudo comparison of Shot 86-3 pressure-time signature from the 35 ft gage and photographic image at instantaneous time, Tm.

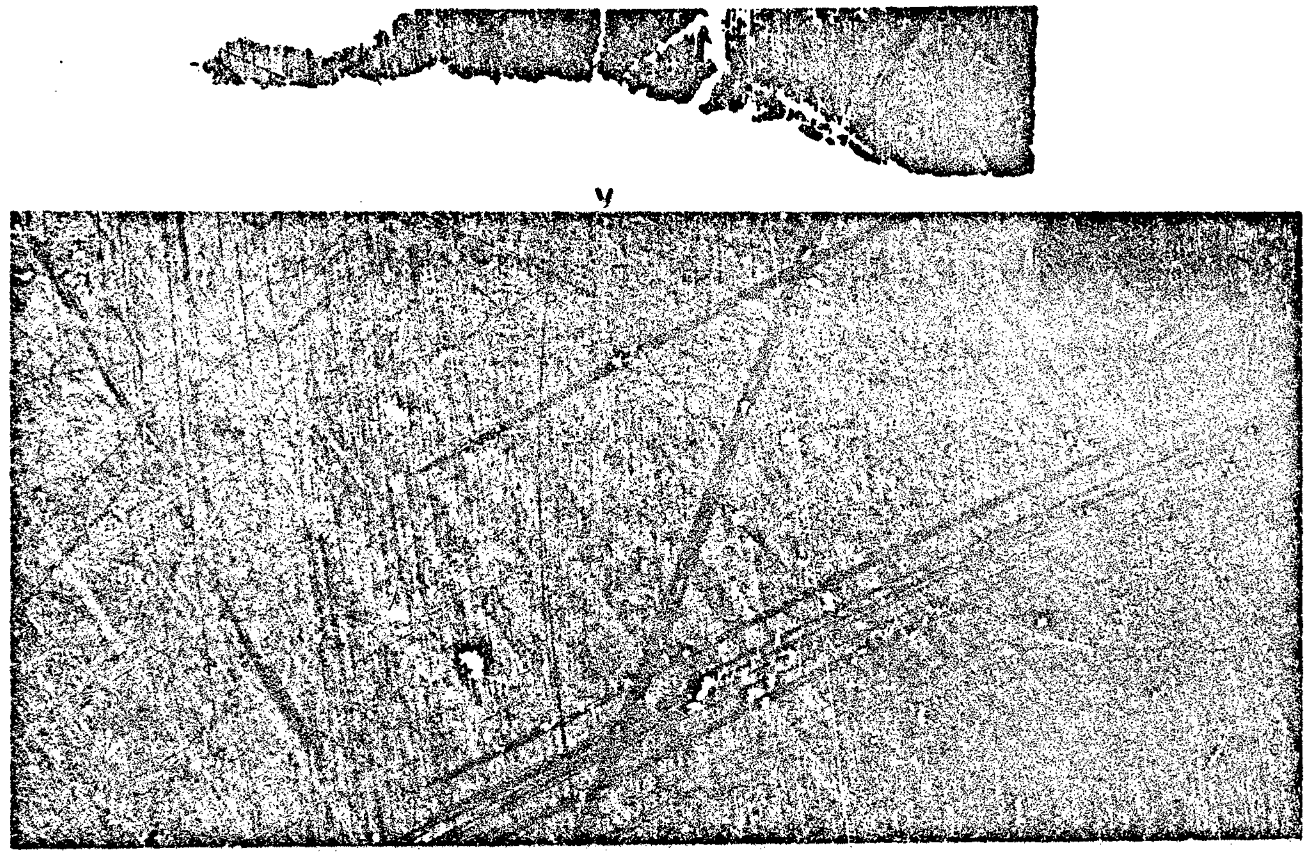

Figure 8.3. Pseudo comparison of Shot 86-3 pressure-time signature from the 35 ft gage and photographic image at instantaneous time, Tp.

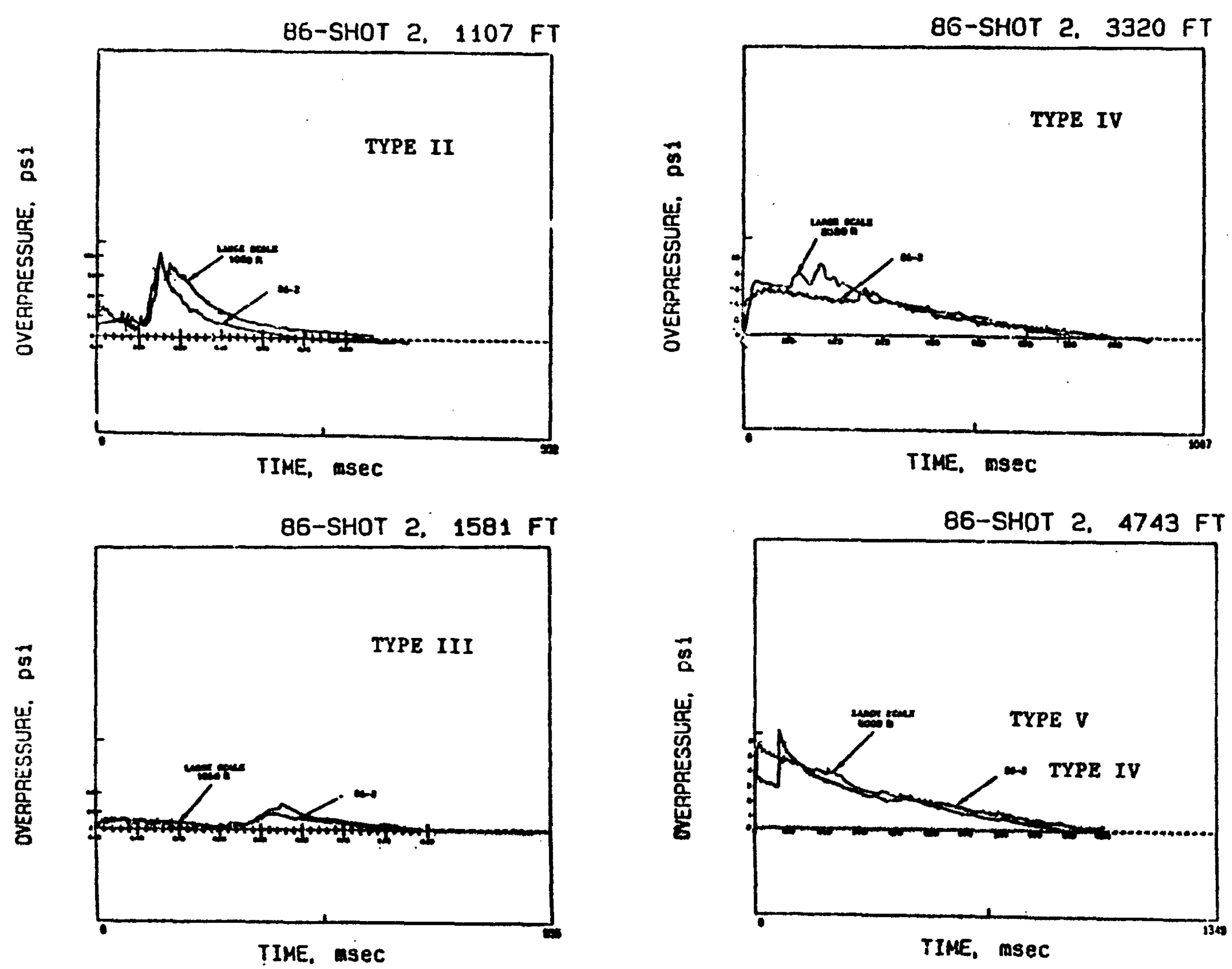

Figure 9.1. Static pressure time records on the surface from Shot 2, Stations 35.0, 50.0, 90.0, and 150.0, scaled to and compared with large scale experiment.

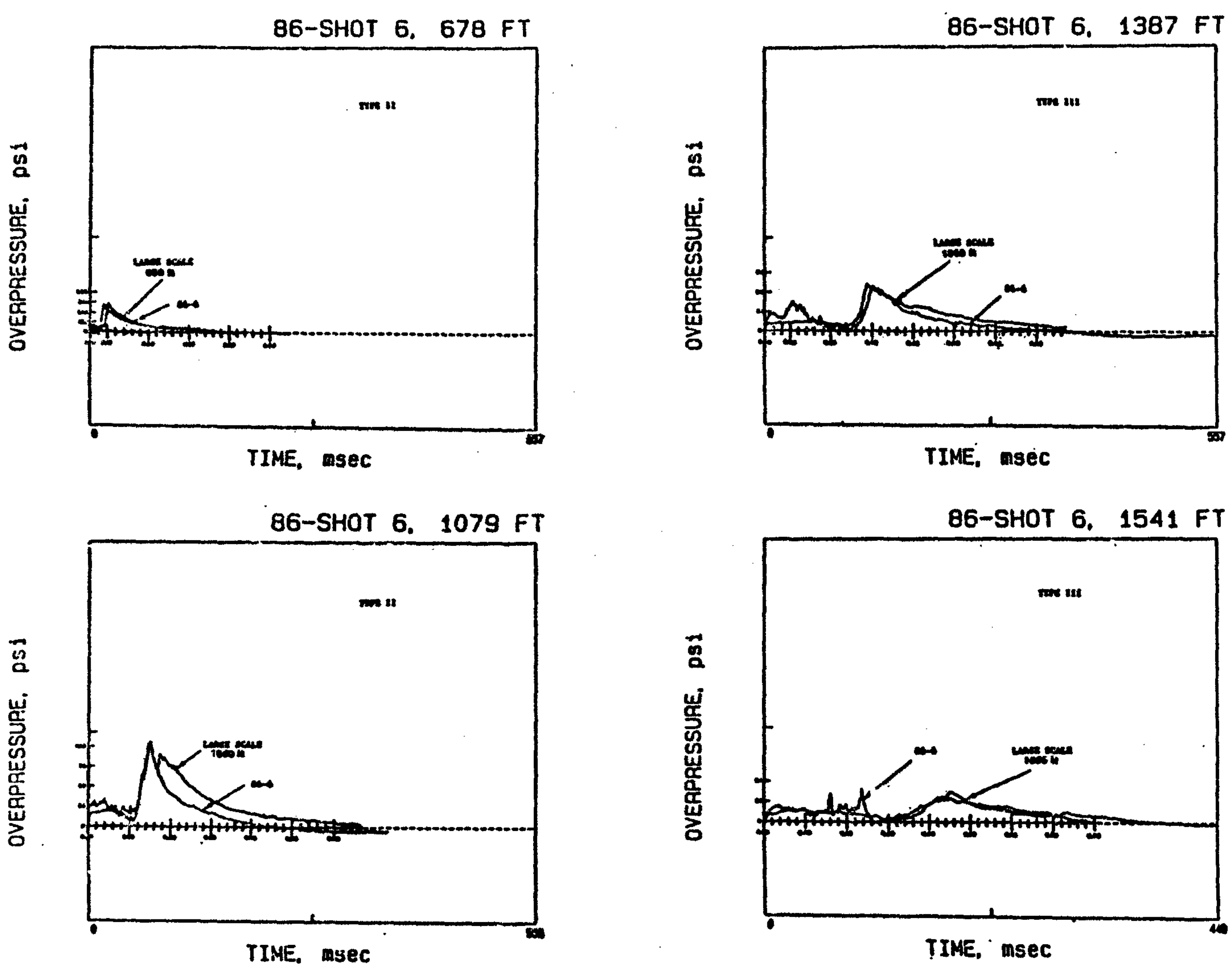

Figure 9.2. Static pressure time records on the surface from Shot 6, Stations 22.0, 35.0, 45.0, and 50.0, scaled to and compared with large scale experiment.

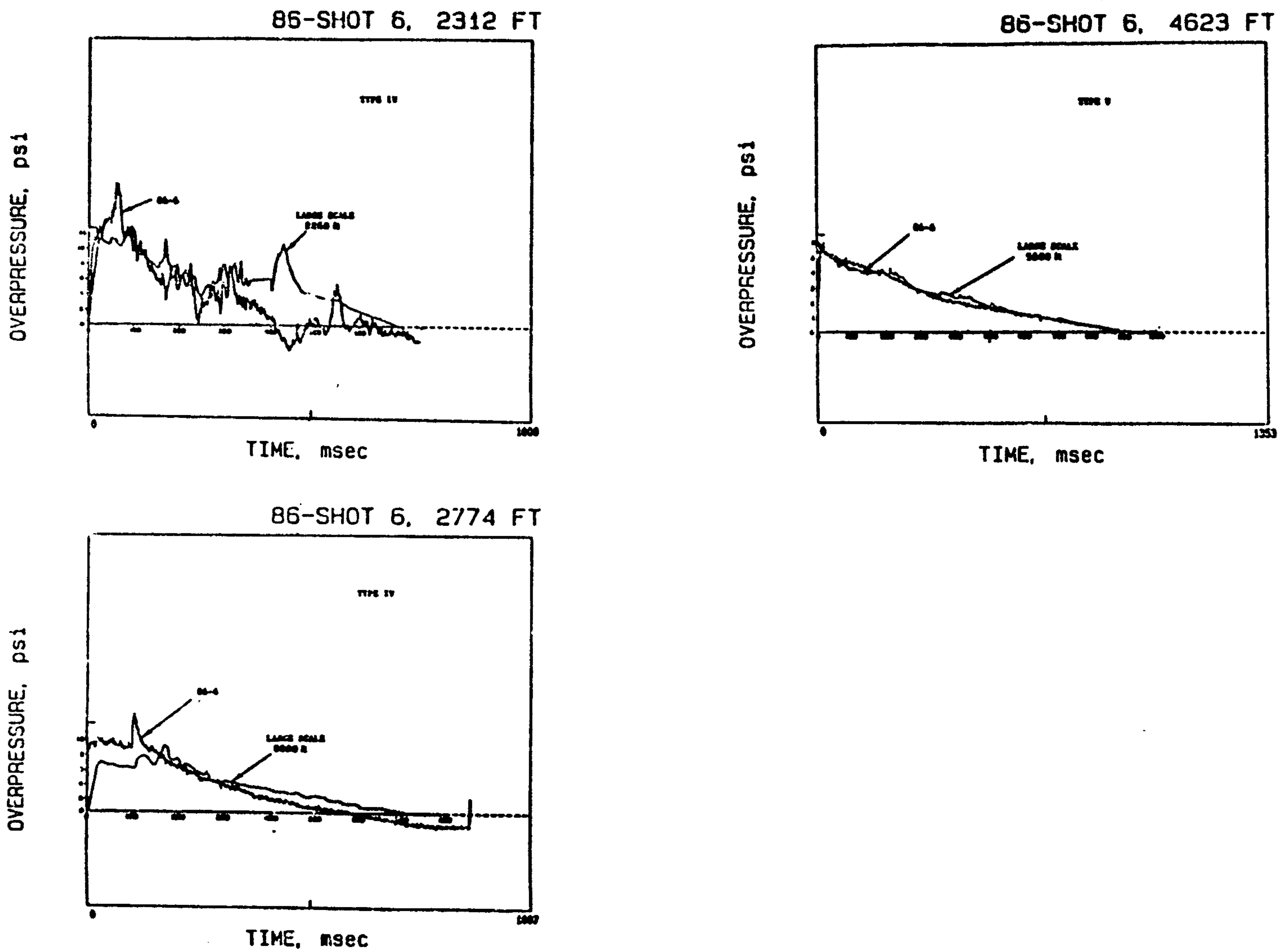

Figure 9.3. Static pressure time records on the surface from Shot 6, Stations 75.0, 90.0, and 150.0, scaled to and compared with large scale experiment.

precursor cleanup observed in the record at 2774 scaled feet occurred earlier in time than that of the large scale record. This would indicate a "cool" layer at this point, although the last comparable station shows a complete cleanup and excellent correlation with the large scale record.

Shot 2 of the two 1987 shots provided the best correlation with the large scale nuclear event of comparable scaled height of burst. The waveforms presented in Figure 10.1 show an excellent correlation with the large scale at the two 60-foot stations; the B station is 8 feet on the arc from the main station. A Type III wave form is observed. At the closer stations the record comparison shows the 87-2 layer to be "colder" than the large scale. This is seen by the higher initial pressure, P_1, and the shorter T_3 time of the precursor front. In Figure 10.2 the waveforms of the precursor cleanup are given. A slow rise and rounded peaks are characteristic of these records. At the 200-foot position of the 87-2 shot, the cleanup is complete - a sharp shock of the Type V record is evident. Waveforms, Types III - IV, have been presented although all types were recorded.

Overpressure versus ground range for Shot 86-2 and Shots 86-3 and 6 are scaled to and compared with the measured values of the same large scale test in Figure 11. Overpressures of Shots 86-3 and 6 correlate better than the data of 86-2; the helium layer of 86-2 was a single, constant concentration while those of 86-3 and 6 were of decreasing concentrations. The single concentration of 89.4% simulated a "hotter" layer than the large scale test while the decreasing concentrations indicate a cooler layer in the precursor cleanup region. Figure 12 presents the dynamic pressure versus ground range for 86-2 and 6 scaled to and compared with the same large scale experiment. Good agreement is observed.

Overpressure distance data from Shot 87-2 is given in Figure 13 compared with a large scale event. The 1987 shot replicates well in the mid- to far range especially in the cleanup region. In the close-in range the experiment generated a cooler precursor than was experienced on the large scale test.

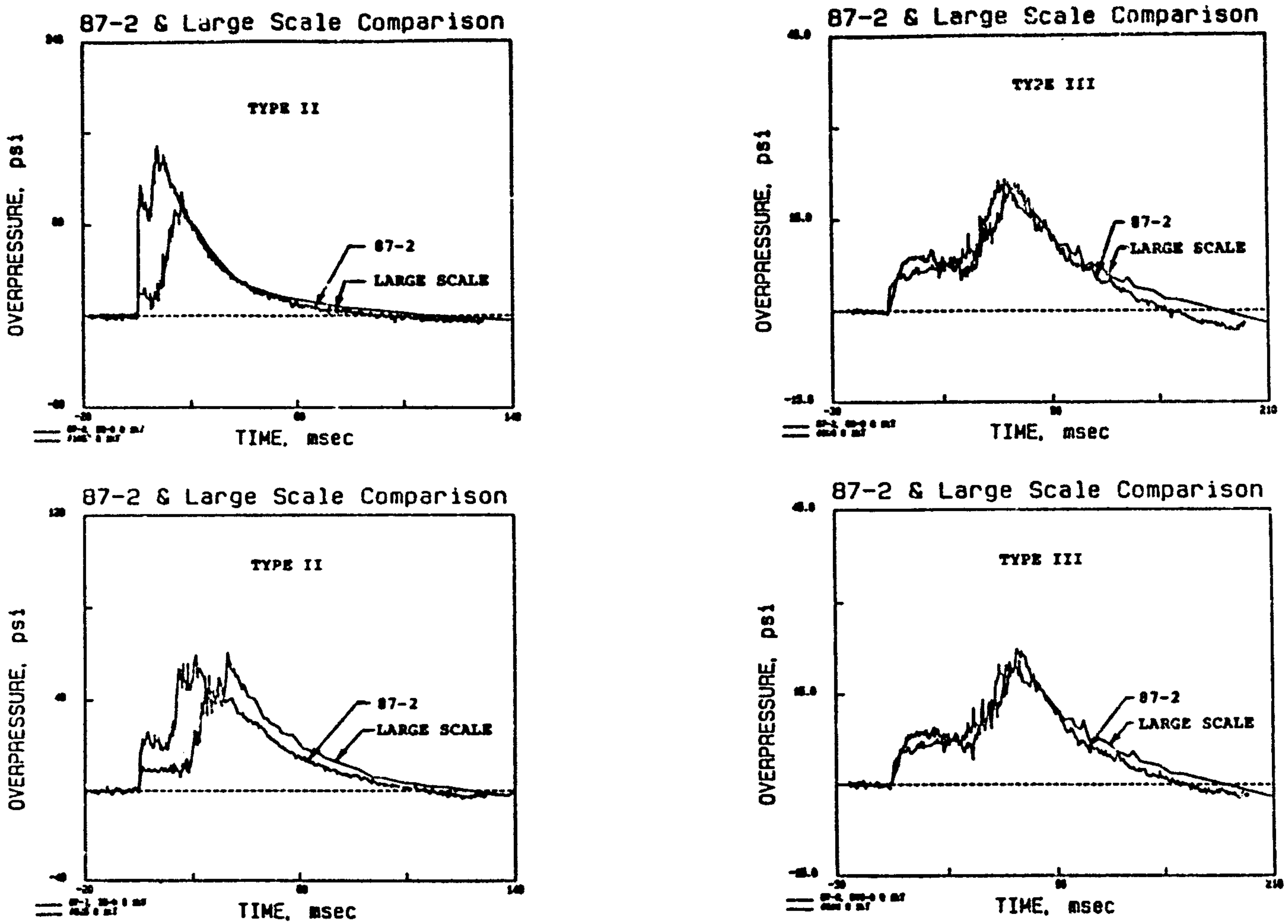

Figure 10.1. Shot 87-2 and large scale record comparisons, 87-2 stations 22.0, 35.0, 60.0, and B60.0.

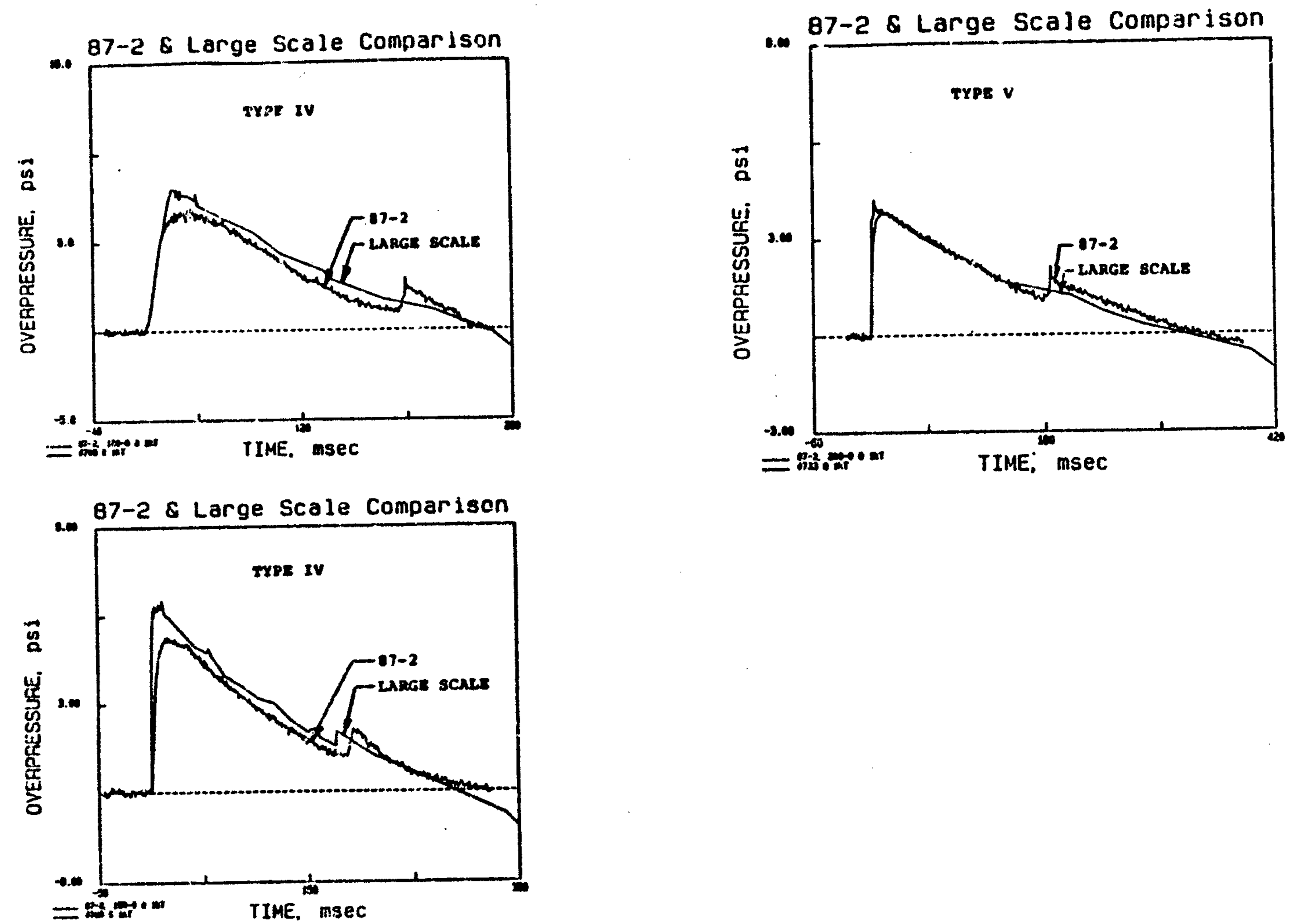

Figure 10.2. Shot 87-2 and large scale record comparisons, 87-2 stations 120.0, 150.0, and 200.0.

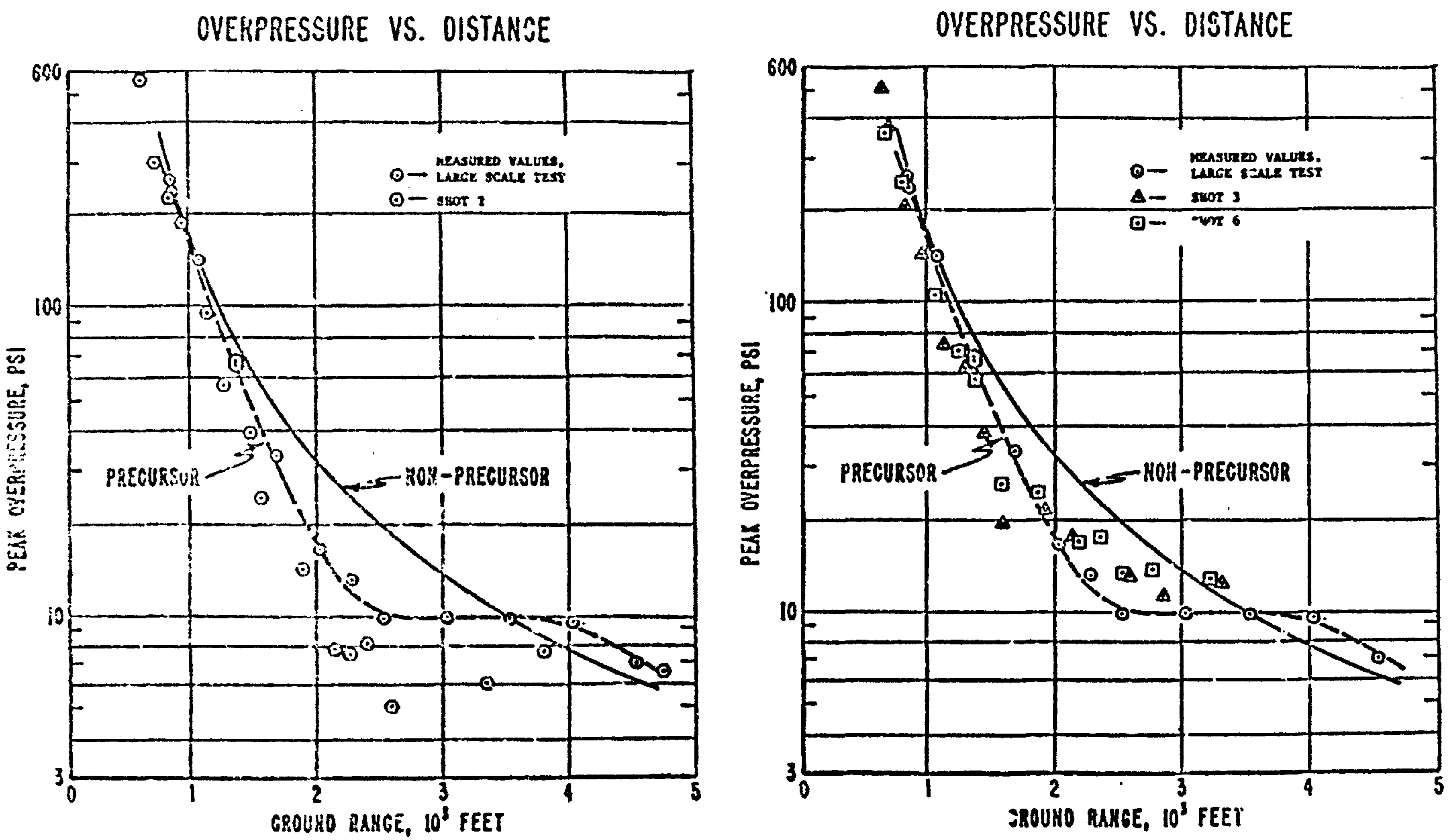

Figure 11. Overpressure versus ground range, Shot 2, and Shots 3 and 6, scaled to and compared with large scale test.

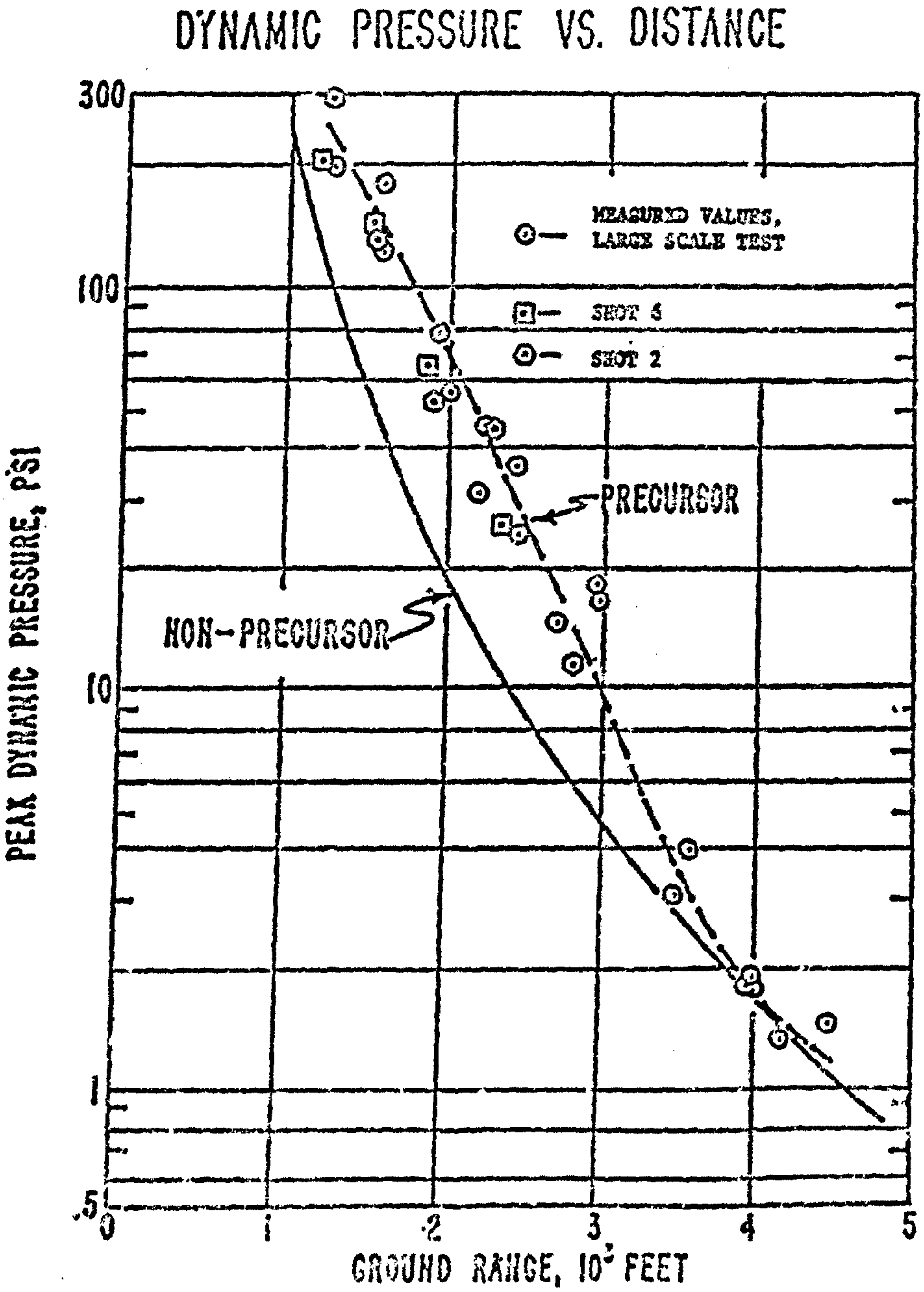

Figure 12. Dynamic pressure versus ground range, Shots 2 and 6, scaled to and compared with large scale test.

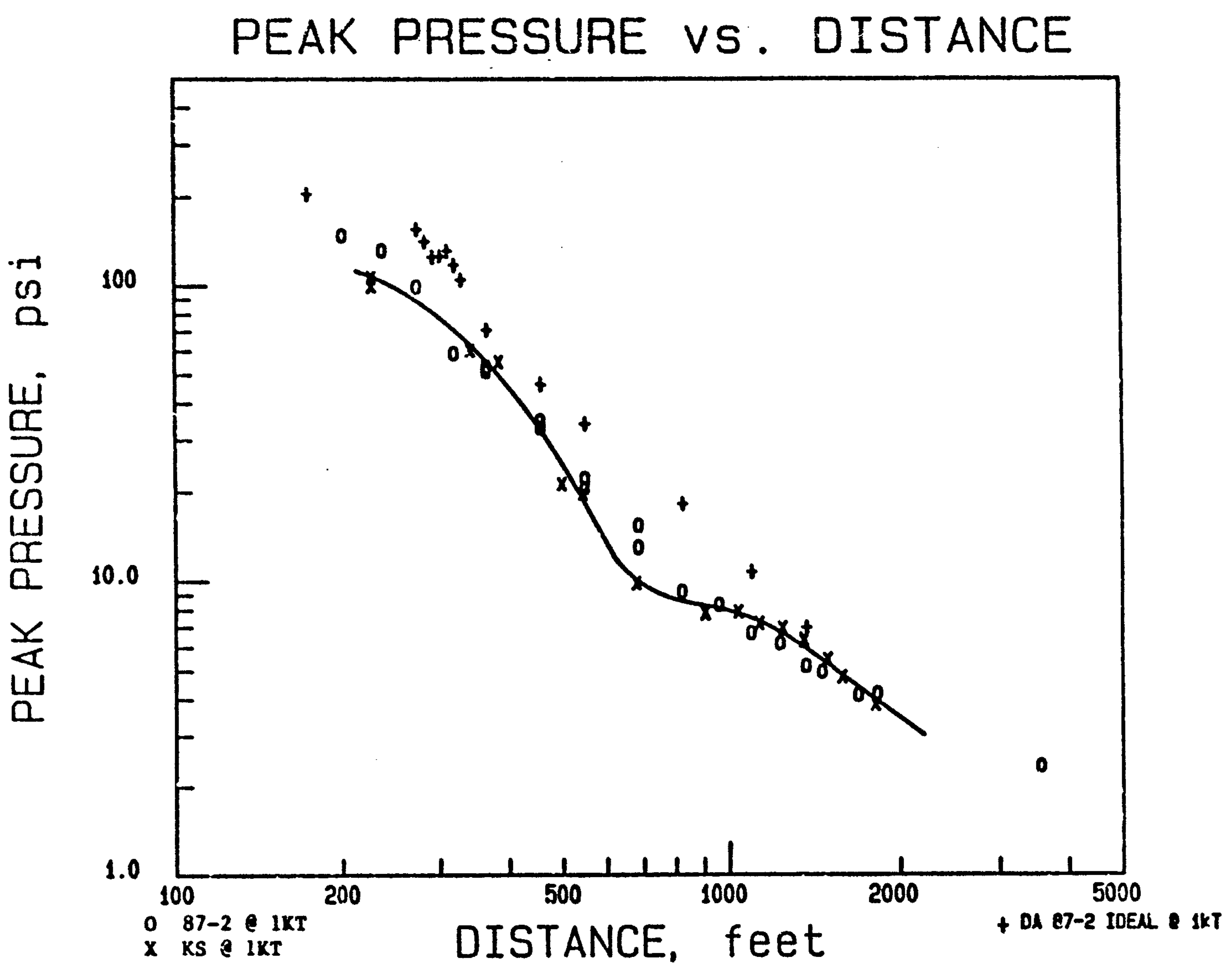

Figure 13. Shot 87-2 overpressure data compared with large scale.

The significance of surface temperature effects simulated by the percentage of helium is observed in Figure 14. The duration of the nuclear precursor for the hot layer is always longer and starts in the regular reflection region. Precursor development modifies the irregular or regular Mach region as the case may be. Past large scale data were used to predict the hot, warm, and cool precursor durations. Surface variations cause larger differences with increasing ground range as observed by the cool data of the 1986 experiments beyond 700 scaled feet. Shot 86-2, with a constant, uniform sound speed, resembles a very hot surface in the precursor cleanup phase.

CONCLUSIONS

A simulated heated layer was demonstrated in HOB experiments using a thin layer of helium. A high-fidelity simulation which generated the five types of waveforms of precursed blast was achieved. The 2-inch thick, 30-foot wide helium layer was found to be satisfactory for the production of precursed waves at this scale. A continuously hot precursor layer was observed on the single, constant concentration shots, whereas a hot layer was evident at the beginning of the decreasing helium concentration shots at the same HOB, but soon developed into a cool layer with increasing distance. This condition was very evident in the cleanup region for the 19.8-foot HOB.

The 2-inch thick, 50-foot wide helium layer was found to be satisfactory for the production of precursed waves in the cleanup region. The decreasing helium concentration produced a good precursor in the mid-range through the cleanup; the layer was "cold" in close and thus produced a weak precursor.

Tailoring of the experimental technique can provide for the study of precursors for specific requirements.

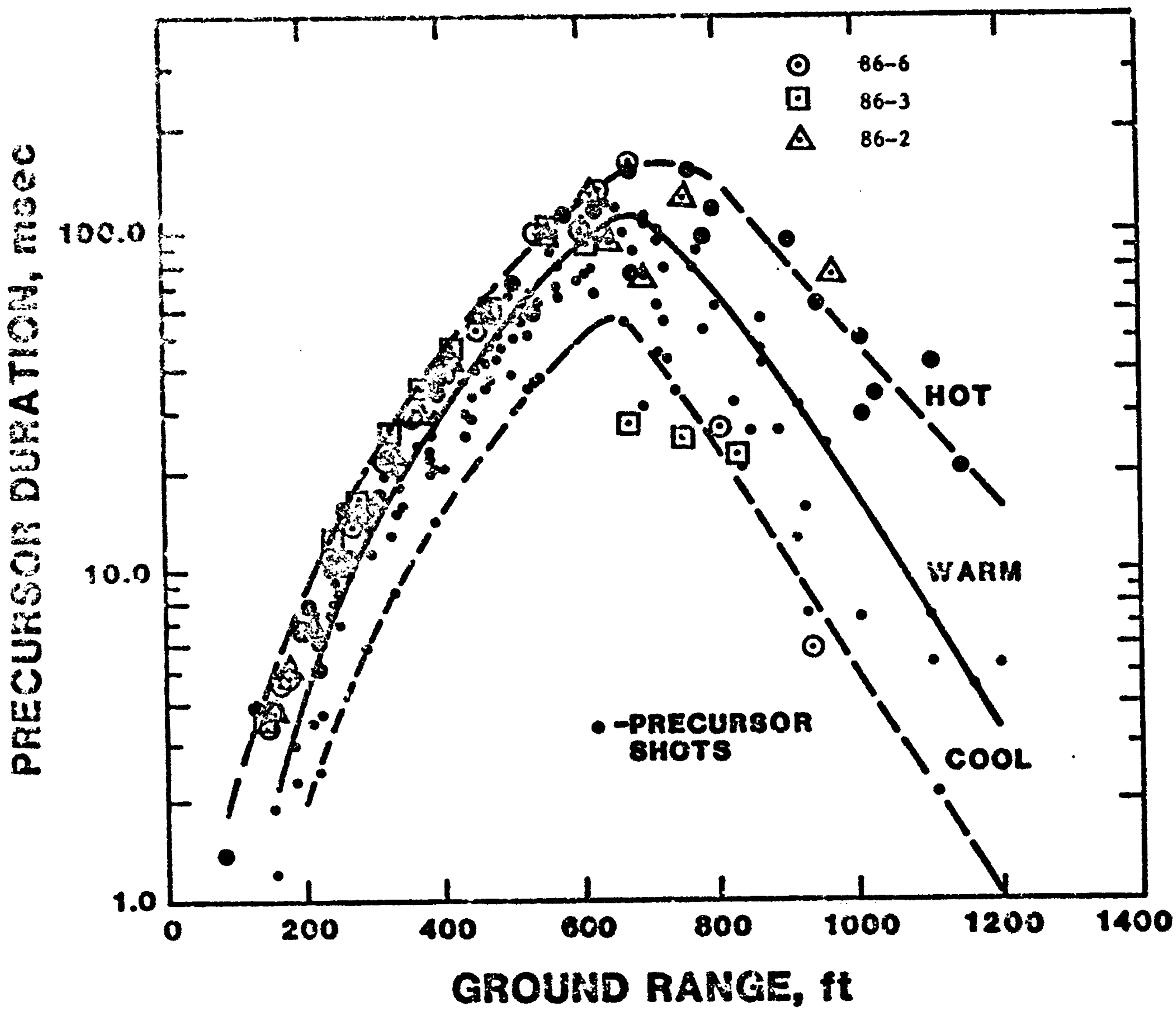

Figure 14. Correlation of precursor duration versus ground range, Shots 2, 3, and 6, scaled to 1-KT large scale test.

Mitigation of Far-field Airblast Associated with Explosive Detonations Near Populated Areas

James B. Cheek
James S. Shore
Frances M. Warren

ABSTRACT

The Structural Mechanics Division of the Structures Laboratory at the Waterways Experiment Station frequently subjects test structures to dynamic loads generated by explosive charges. Usually, the large shots are conducted in remote test ranges in the desert southwest. In the case of two recent tests, however, unique geologic requirements forced a test in an area that was close to large population centers in and around Ft.Knox, KY. Efforts were made to mitigate the effects of the airblast by monitoring weather conditions and predicting window damage probabilities right up to shot time. The two shots contained 25.5 tons and 42.9 tons of explosives, and were detonated on 5 December 1986 and 4 June 1987. The 25.5 ton shot resulted in two damage claims and the 42.9 ton shot had no claims.

This paper outlines the calculational and operational procedures used for these tests. Included are the weather watch, the ground shock and airblast/window damage calculations, the far-field airblast measurements, and the interaction with Ft. Knox officials to ensure no adverse public reaction would result.

MITIGATION OF FAR-FIELD AIRBLAST ASSOCIATED WITH EXPLOSIVE DETONATIONS NEAR POPULATED AREAS

James B. Cheek, James S. Shore, and Frances M. Warren
U.S. Army Engineer Waterways Experiment Station, Vicksburg, MS

INTRODUCTION

The Waterways Experiment Station (WES) conducted two large explosive tests at Fort Knox, Kentucky that required careful consideration of the effects of far-field airblast on surrounding populated areas. Since these tests could not be allowed to damage private property, a plan was outlined and executed to minimize the effects of far-field airblast on the surrounding areas. This paper presents the airblast mitigation procedures used for these tests.

BACKGROUND

The 1963 Limited Nuclear Test Ban Treaty ended above ground nuclear detonations and precipitated the development of high explosive simulators to generate nuclear-like airblast and groundshock loadings. These simulators have evolved to the point that virtually a complete time history of all blast effects can be generated. However, this requires large amounts of conventional explosives even when the articles being tested are small scale models. The two tests conducted at Ft. Knox contained total explosive weights of 25.5 and 42.9 tons.

Such large tests are generally conducted in sparsely populated areas. However, in this case the tests were conducted at Ft. Knox because no alternate site was found in the U.S. that met the special geological requirements. The tests were conducted to provide experimental validation of structural response calculations. One-eighth scale structures were instrumented and placed in an instrumented testbed. An explosive simulator was placed over each testbed and detonated. The structure and testbed responses were measured, recorded, and compared with the responses predicted by the calculations.

OBJECTIVE

The objective of the far-field airblast mitigation program was to prevent any damage to the populated areas around Ft. Knox.

SCOPE

The scope of the far-field airblast mitigation program incorporated the elements of collection, prediction, and documentation. The necessary demographic and atmospheric data was collected along with the proper

analytic tools. These were used to make predictions so that a safe shot time could be determined. The predictions were verified by measuring the far-field airblast at several locations.

SIMULATOR DESCRIPTIONS

The first test employed a Crater and Related Effects Simulator (CARES) to produce the airblast and groundshock from a 0.64 kt nuclear surface burst. The Near Source Simulator (NSS) portion of the simulator provided the direct-induced groundshock and consisted of a double walled fiberglass hemisphere with Nitromethane filling the space between the inner and outer walls. In addition, there were shallow fireball wing tanks also filled with Nitromethane around the lip of the hemisphere. The central subsurface tanks contained 14,200 pounds of Nitromethane and the wing tanks contained 7,100. A cross-sectional view of the NSS is shown in Figure 1.

Concrete tamping was placed over the area between the two walls of the central tank. The inner bowl was left open to the atmosphere with no tamping. There was no tamping over the fireball wing tanks.

The airblast simulator for the first test was a High Explosive Simulation Technique (HEST) charge. The HEST varied in areal explosive density from 4.28 psf at the close-in edge (r = 16 ft) to 0.187 psf at the outer edge (r = 120 ft). The explosives used were Iremite 60 (15,323 pounds) and PETN detonating cord (10,685 pounds). Strands of 1-inch diameter Iremite and 400 gr/ft det cord were placed in grooved polystyrene boards. The groove spacing and board thickness were varied to provide the proper explosive density. The HEST charge was tamped with 18 inches of finely crushed limestone with a density of 130 pcf.

A transition zone (r = 12 ft to r = 16 ft) provided simulator continuity between the NSS and the HEST. This portion contained 3,720 pounds of Iremite 60 strands placed side by side. No foam was used in the transition zone. The proper explosive loading over the zone was achieved by decreasing the number of Iremite layers as the radius from ground zero increased.

The simulator was detonated using a branching detonating cord initiation system. Tie-backs were used in the regions where a detonation velocity exceeding that of the detonating cord was required.

The simulator used in the second test was similar to that in the first (Figure 1.). The main differences were the larger explosive weight in the subsurface charge and the smaller explosive weight in the HEST. There was 74,200 lbs of Nitromethane in the central charge, 1,482 lbs of Iremite 60 in the transition zone, and 3,500 lbs of Iremite and 6,650 lbs of PETN detonation cord in the HEST. There were no wing tanks in the second simulator and the crushed limestone overburden depth was 22 inches instead of 18. The second test was designed to produce the airblast and groundshock loadings from a 0.39 kt nuclear shallow-depth-of-burst detonation.

COORDINATION WITH FT. KNOX AUTHORITIES

A feasibility study was done prior to asking the Ft. Knox Commander for permission to conduct these large explosive tests in the range area. Although this study showed that the tests could be conducted without damage to private property, it was necessary to prepare an Environmental Impact Assessment (EIA) before permission was granted for the second shot (Reference 1). The first test was granted a categorical exclusion based on a previous EIA. Since Ft. Knox must comply with various land use and noise mitigation programs, the EIA addressed the test's effects on the noise, groundshock, and air quality outside the post boundaries. The EIA also addressed the effects on the flora, fauna, groundwater, air quality, and archaeological sites.

The EIA led to a Finding of No Significant Impact (FONSI). A notice was published inviting inquiries from the public, but there were no inquiries made.

Ft. Knox regulations require that the public be notified anytime a larger than normal explosion is to occur. Notices for these two tests were published in the local paper and announced on local radio stations. The notices simply stated that the Corps of Engineers would conduct a demolition test. No specifics were given. These notices precipitated several comments from local citizens to the Ft. Know Public Affairs Office. but the comments were in the realm of curiosity and not complaints.

PEAK AIRBLAST PRESSURE CALCULATIONS

The explosion effect that was identified in the EIA as having the most potential to cause damage outside the boundaries of Ft. Knox was airblast. The parameter largely used to predict airblast induced damage to structures and animals is peak pressure. Therefore, a dependable way to predict peak pressure at various ranges from the blast site was needed. Actually, two types of calculations were required. One was needed to deal with the direct transmission of the pressure pulse in the air. The second would have to model the complex bending of the sound rays by the atmosphere.

As outlined in the ANSI standard (Reference 2), much progress has been made in mathematically modeling the variation of peak pressure with range for a one kiloton (kt) nuclear burst in free air. That work was initially done on very large, high-speed, digital computers. The early problems with numerical instability in the calculations at long ranges were finally resolved in the work completed at the Air Force Weapons Laboratory (AFWL). yielding results that agree with the known effects and experimental data. A product of that effort is a closed-form equation that models peak pressures from 62,199 to 0.000045 psi over ranges from 30 to 30 million feet.

By using Sach's scaling laws (Reference 3) the peak pressure produced by a specific nuclear explosion at a given range may be obtained from the pressure predicted by the above mentioned AFWL one kt model. This is accomplished by dividing the actual range (R) by the cube root of the

weapon yield (expressed in kt). That value (actually the scaled range, lambda) becomes the scaled range input to the peak pressure calculating equation. An example may be helpful.

What is the peak pressure at 7,000 ft from a 54,000,000 pound yield nuclear burst? In order to answer this question, we express the yield in kilotons, that is 27 kt. Taking the cube root of the yield (in kt) gives 3. This is the range scale factor. The actual range (7,000) divided by the range scale factor (3) gives a scaled range of 2,333 ft. The peak pressure predicted by the one kt model for that range (2,333 ft) is 2.04 psi. This, then, is also the peak pressure at the 7,000 ft range from a 54,000,000 pound yield nuclear burst.

As mentioned previously, the peak pressure predicted by the AFWL one kt model is for a free air burst. Under ideal conditions (point source and perfect horizontal reflector) the pressure produced by a surface burst will be the same as that produced by a free-air burst having twice the yield of the surface burst. In the above example, if the burst had been on the surface, the scale factor would have been the cube root of twice 27 kt which is 3.78. This yields a scaled range of 1852 ft (7,000 ft/3.78) and an associated peak pressure of 2.82 psi.

The fine analytical work represented by the AFWL model has applications well beyond the confines of nuclear weapons effects. Non-nuclear peak airblast pressures can also be predicted using this model. The yield of a nuclear weapon is described in terms of so many kilotons of TNT equivalent. One is inclined to think the same results would be obtained from the detonation of an equal amount of TNT. Such is not the case. For reasons outlined in References 2 and 4, the peak pressure from solid or liquid high-explosive (HE) sources (e.g.,TNT) is greater than that of an equal nuclear source. The yield scale factor varies with the scaled range, but for peak pressures below about 200 psi, the actual TNT charge weight must be doubled before calculating peak pressure with the procedure described above.

The AFWL model may be used in several ways for the many calculations that must be made during the planning and shot-day efforts. For low pressure levels, the model can be plotted on log-log graph paper for the planned charge weight. This is simple and quick. However, it is helpful to have the equation programmed (Reference 5) on both personal computers and hand-held calculators such as the Hewlett Packard 41 CX. The accuracy and convenience of the latter makes them clearly superior to the graphical approach. In the field, the ready availability and robust character of the hand-held units make them the calculating-engine of choice. They are particularly useful for answering the peak pressure questions that always seem to surface at the last minute.

The AFWL free-air model is used to determine the distances that residences, support equipment, and personnel should be located away from the explosive charge (Figure 2.). This model does not, however, account for far-field airblast as it is affected by atmospheric conditions. On a "perfect" day, the blast wave from the detonation would propagate outward and be directed upward in all compass directions (azimuths) around the site. Because of

this, the pressure at distant points on the ground would be much less than predicted for free-air because of the upward bending of the blast wave.

Such bending takes place when the speed of sound changes as the height above the ground (elevation) changes. Since the speed of sound in still air decreases with temperature and temperature decreases with elevation (on a "perfect" day), the lower (in elevation) portion of the blast wave will go slightly faster than the portion just above it. This is called a "gradient" condition, and the effect is to turn the wave upward and away; minimizing the airblast load on things at or near the ground surface.

On a not-perfect day, which is to say almost all of the time, in some azimuths the sound speed will not decrease with elevation. There are two reasons for this. First, there may be warm layers of air over the cooler layers beneath them. Second, the wind speed may increase as the elevation increases. In that situation the effective sound speed (with respect to the ground) is increasing with elevation because the sound is moving in the air at its sonic velocity, but the air is moving ,too. In both cases the sound rays will be turned back toward the ground.

It is, therefore, important to include the influence of atmospheric conditions when predicting far-field airblast and determining the advisability of detonating a given charge at a given time. In deciding if the weather conditions are acceptable for detonating the explosives, two questions must be answered. How much bending is taking place? Where will the bending rays return to the ground (both azimuth and range)? In the case of minor bending, the pressure at the ray return point will be just a bit higher than predicted. In the worst case of bending, many of the sound rays will be bent in such a was that they all return to the same point on the ground. In other words, they will be focused (called a caustic). Under those conditions, the peak pressure may be <u>seven to eight times</u> the predicted peak. This is why a ray tracing procedure must be employed.

If the temperature and wind velocity values for any point in the air were known in precise detail, then ray tracing would be a rather simple computer task (provided there were an automated way to get the data; how about "magic"). Even so, the problem would not be completely resolved because knowing where the rays focus is only part of the answer. The peak pressure must also be determined. However, knowing where the rays focus and knowing that the airblast is increased by a factor between one and eight is enough information in some cases to make go or no-go decisions. If the anticipated peak pressures are near the damage threshold at some locations, a coarse estimate of the azimuth and range of potential focus points is essential.

In practice, the best weather information that can be hoped for would be a velocity and temperature versus elevation profile taken shortly before shot time. Less satisfactory (but often all that is available) are the data taken by the weather people at nearby stations and /or short term forecasts based on computer processing of such data.

Suffice it to say that ray tracing based on such an out of date and sparse data base is as much art as it is high-science. In situations like this,

the skill of the weather-watch person is the key element in estimating the reliability of the input data and interpreting the significance of the predicted focus points. The current ray tracing programs used at WES (Reference 6) are operational on personal computers with supporting graphics. They are available, on the test site for use by the weather-watch personnel during the critical hours prior to the scheduled detonation time.

FAR-FIELD AIRBLAST MITIGATION PLAN

Since the explosive yield was set, the atmospheric conditions at shot time would determine the far-field airblast. A far-field airblast mitigation plan was developed to minimize the probability of damaged windows in and around Ft. Knox. The first step in this plan was to determine the window density at all distances and azimuths from the charge. The second step entailed obtaining a detailed report of the meteorological conditions that would exist at shot time. The AFWL model and the ray-tracing computer programs would then be used to obtain the magnitude and direction of any focused far-field airblast and the results combined with the window density map to predict the window damage probability. If there was a chance of damaging more than ten windows (roughly the window damage probability multiplied by the number of windows) in any area, the test would be postponed. When conditions permitted a test, observing personnel and instruments to measure the far-field environment would be dispatched to those locations most likely to experience damage.

The window density map was drawn with the test located at the center. Residence locations were plotted around the shot at increasing distances. The nearest large population concentrations were located in Shepherdsville (7 miles East-northeast) and Louisville (13 miles North). Other areas of concern were Bardstown (23 miles Southeast), Elizabethtown (18 miles South), and Radcliff (9 miles Southwest).

The most difficult phase of the mitigation plan would be the weather watch. Mr. Jack W. Reed from Sandia National Laboratories was enlisted to perform this phase of the plan. Mr. Reed has numerous years of experience in the field of weather effects on far-field airblast, and it was fortunate that he was available for these tests. Mr. Reed's reports concerning the weather for each of these tests can be found in References 7 and 8.

Test conditions necessitated a three day favorable weather window. Three days would allow one day for instrument hook-up and sensitizing the Nitromethane, one day for the shot, and one backup day. The backup day was very important because a long delay could produce an unsafe condition with the sensitized Nitromethane. Current state-of-the-art weather forecasting abilities yield good three-day forecasts which would allow time for labor crews to prepare for a possible shot day.

On shot day morning the weather conditions would be obtained from the National Weather Service. In addition, an artillery support group would make three special radio balloon ascensions; one at four hours before the

shot, one at two hours before the shot, and one at shot-time. This would provide local atmospheric conditions that are not available from the weather service.

TEST SCHEDULE

The tests were scheduled based on construction considerations. A finite amount of time was required to complete the various phases of each experiment. It took approximately eight months to fabricate the test structures and subsurface charge containers, buy the explosives, and accomplish the field construction. The first test's earliest possible shot day landed in early November. The construction activities for the first test were on schedule and the shot day was set for 4 November 1986.

The field work for the second test could not begin until after the first test was complete. The field work for the second test took about four and a half months. This meant that the second shot would occur about mid-March if the weather cooperated. It did not.

TEST 1 ACTIVITIES

As the scheduled shot day, 4 November, approached, the weather forecasts indicated that favorable conditions would not be present in the foreseeable future. Unfavorable conditions persisted for one month. Finally, on Sunday, 30 November, the 5-day long range forecast revealed a change in the weather patterns that might bring a potential shot day within the week. On Tuesday the shot day was set for Thursday, 4 December. The cold front slowed, however, and on Wednesday, the decision was made to delay the shot by one day. Shot day became 5 December 1986.

The first balloon ascension provided data that indicated that the winds were becoming more northerly and that focusing in the direction of Shepherdsville would not be a problem. It appeared that focusing could produce window damaging far-field airblast in Bardstown or Elizabethtown, however. Although there was a possibility of breaking windows, the small populations involved put only a few panes at risk.

The shot was scheduled for 1:45pm and far-field airblast units with microbaragraphs were dispatched to the house nearest the test site (Figure 3.) and to Bardstown. The simulator was detonated. The microbaragraph reading at the house nearest the test site did not record, but the reading at Bardstown was well below the window damage threshold. The data from the shot and the predictions are shown in Figure 4.

After the test there were several reports of an explosion being heard at the time of the test. One report from Elizabethtown indicated that the noise was loud enough to rattle some windows. There were two property damage claims. The first claimed that the shot caused a storefront window to crack in Radcliff (9 miles Southwest). The second claim was also from Radcliff and stated that the shot caused a living room ceiling to sag.

The post-test investigation of these claims determined that there was a remote possibility that the shot caused the broken window, but not the sagging ceiling. The investigation revealed that; there was only one window broken (not several in the area as might be expected), observers placed in the area could barely hear the detonation, and the far-field airblast prediction program using the actual shot-time weather conditions indicated that minor window damage was possible, but not structural damage to a house. At shot time the winds became more northerly causing some focusing in the vicinity of Radcliff (Figure 5.).

As a result of the investigation, the window damage claim was paid in its entirety. The sagging ceiling claim, however was not. Payment to cover superficial repairs was offered and initially refused. The homeowner threatened a lawsuit, but finally settled for the original offer. No other claims resulted from the first shot.

TEST 2 ACTIVITIES

The second test was scheduled for mid May 1987. The test did not occur, however, until 4 June 1987. The delay was needed so that the applicable environmental and land use procedures could be properly executed. There was a one day delay due to weather.

The weather patterns in May and June produced more numerous favorable shot days than did the November-December patterns. The shot was scheduled for Wednesday, 3 June. The three day forecast indicated that the passage of a front around Tuesday would make Wednesday an acceptable shot day. On Monday it appeared that the pre-frontal activity would make a Wednesday shot difficult, and by Tuesday morning it became obvious that the shot would have to be postponed until Thursday, 4 June.

On Thursday morning the 7:00 am balloon ascension indicated a shallow but strong temperature inversion that could cause strong airblast ducting and focusing in the direction of Shepherdsville (reference 6). Inversion ducting toward Elizabethtown would cause window damage threshold overpressures and in Radcliff the threshold would be exceeded. The inversion, however, was expected to dissipate as surface warming occurred during the day. Another balloon ascension was conducted at 10:00 am which indicated that the inversion had weakened. This cleared the way for the 1:00 pm shot. Technical difficulties delayed the test until 1:19 pm.

Far-field monitoring crews were dispatched to Shepherdsville, Radcliff, and the house nearest the test site. Micorbaragraphs were used at Shepherdsville and the house nearest the test site. Hand-held sound meters were used at Radcliff and also at Shepherdsville.

The shot time balloon ascension data indicated that only minor ducting would occur and that there should be no windows damaged from the shot (Figure 6). The far-field monitoring stations verified this with their measurements (Figure 7). The data and predictions are shown in Figure 8. The microbaragraph reading at the house nearest the test site did not

record, but the other three stations had good data. The noise from the airblast at Shepherdsville and Radcliff was will below the usual outside sounds (traffic, wind, etc.) and only sounded like distant thunder.

CONCLUSION

The procedures used to mitigate the far-field airblast from these large explosive detonations were effective. The objective of a successful mitigation plan is to ensure public safety and limit damage in surrounding areas. Current analytical techniques enable the test conductor to meet this objective. In most cases, a detonation should not be planned if damage due to far-field airblast is unavoidable. Once a detonation is planned, however, it is the responsibility of the test conductor to shoot only when damage will not occur. Since atmospheric conditions can increase or decrease the peak far-field airblast overpressures, the test conductor must evaluate the atmospheric effects before a shot is fired. This evaluation will require knowledge of the weather forecast for shot time and analytical tools that can predict far-field airblast and any focusing that will occur. The test conductor should also document the actual shot time conditions and far-field effects in the event damage claims are filed. This procedure was proven effective at Ft. Knox. With the help of Mr. Jack W. Reed of Sandia National Laboratories, the Waterways Experiment Station successfully conducted two large explosive tests near populated areas and kept the far-field airblast within acceptable limits.

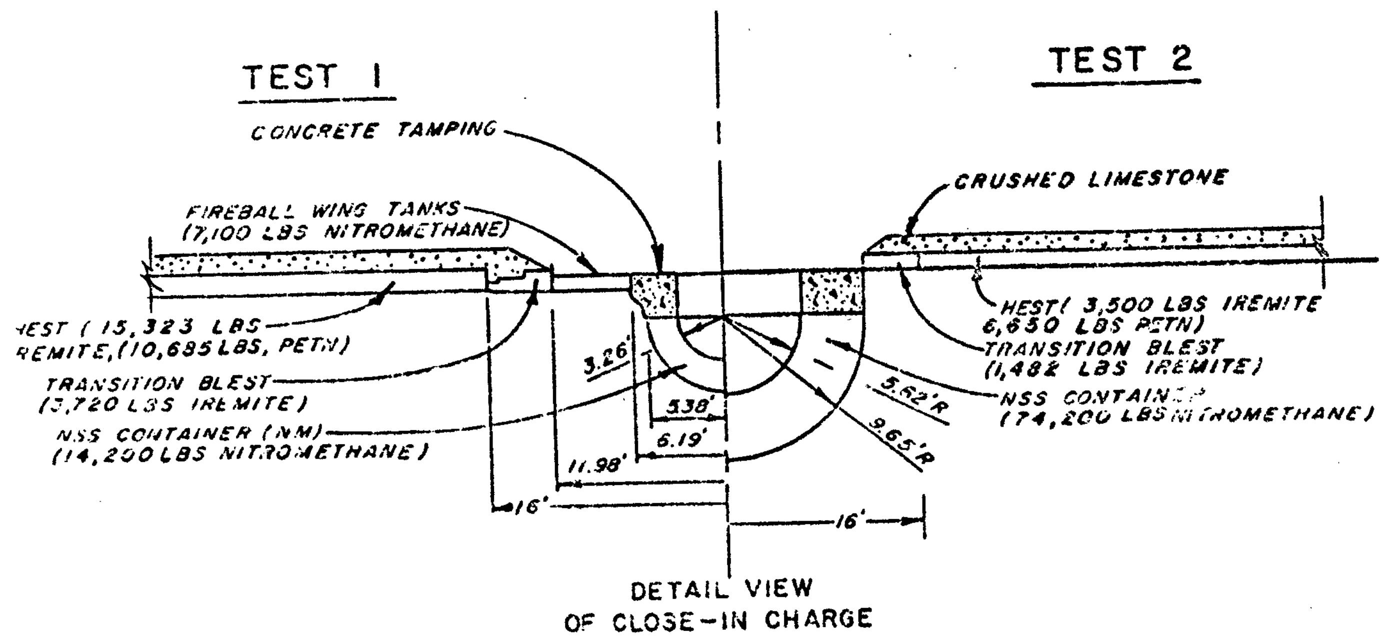

Figure 1. Crater and Related Effects Simulators (CARES) used in Test 1 and Test 2.

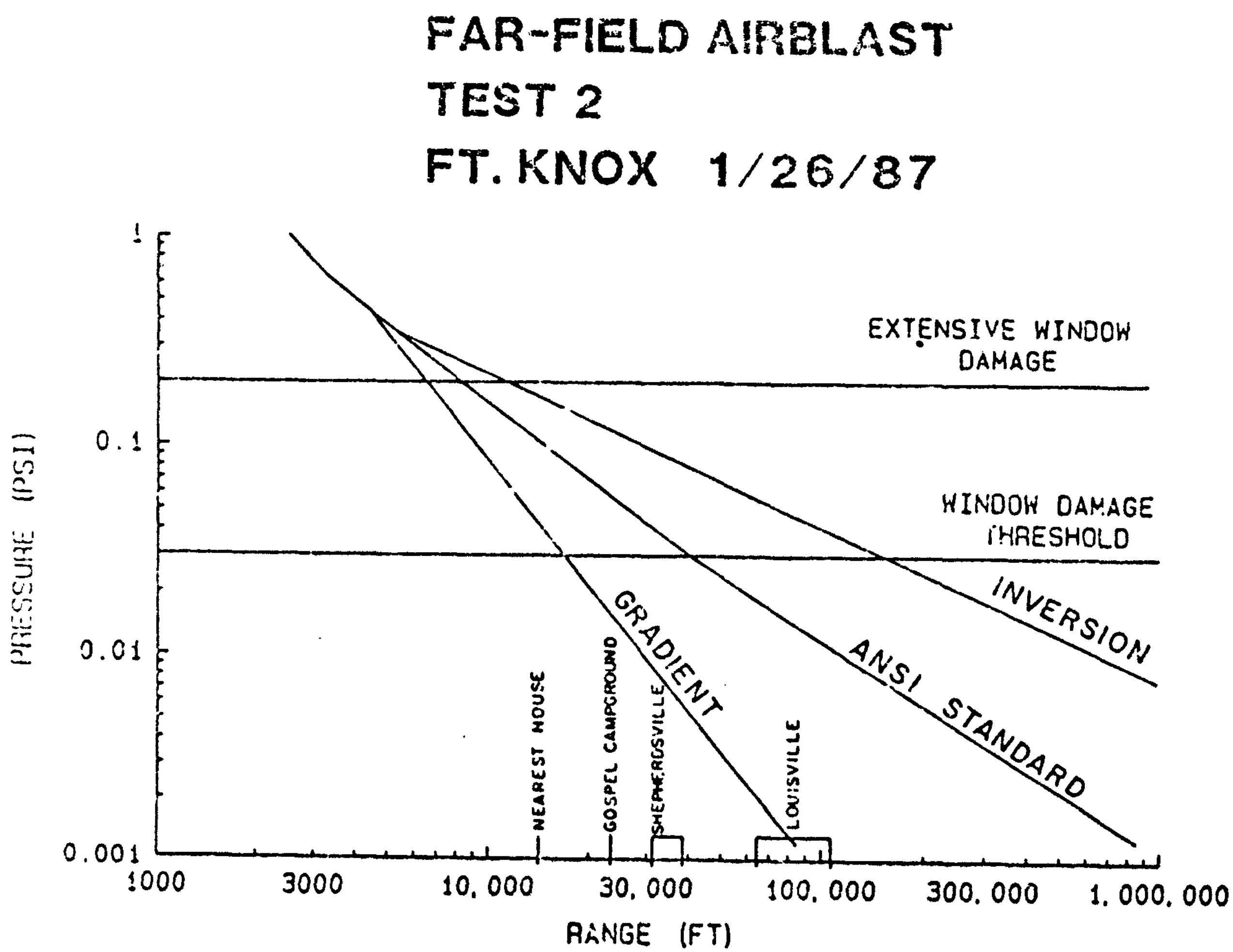

Figure 2. Airblast vs Range for Test 2.

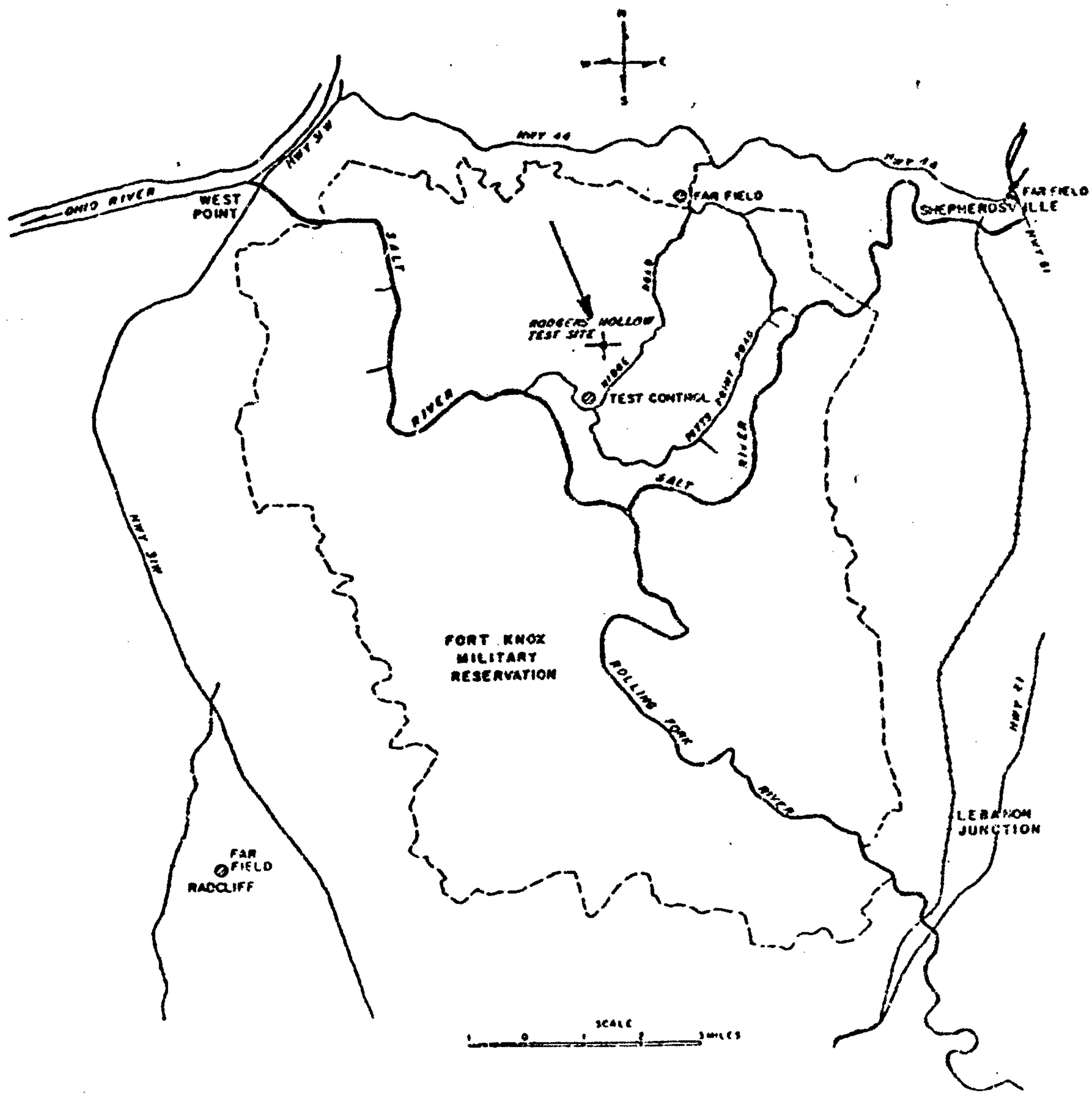

Figure 3. Area surrounding Rodgers Hollow Test Site.

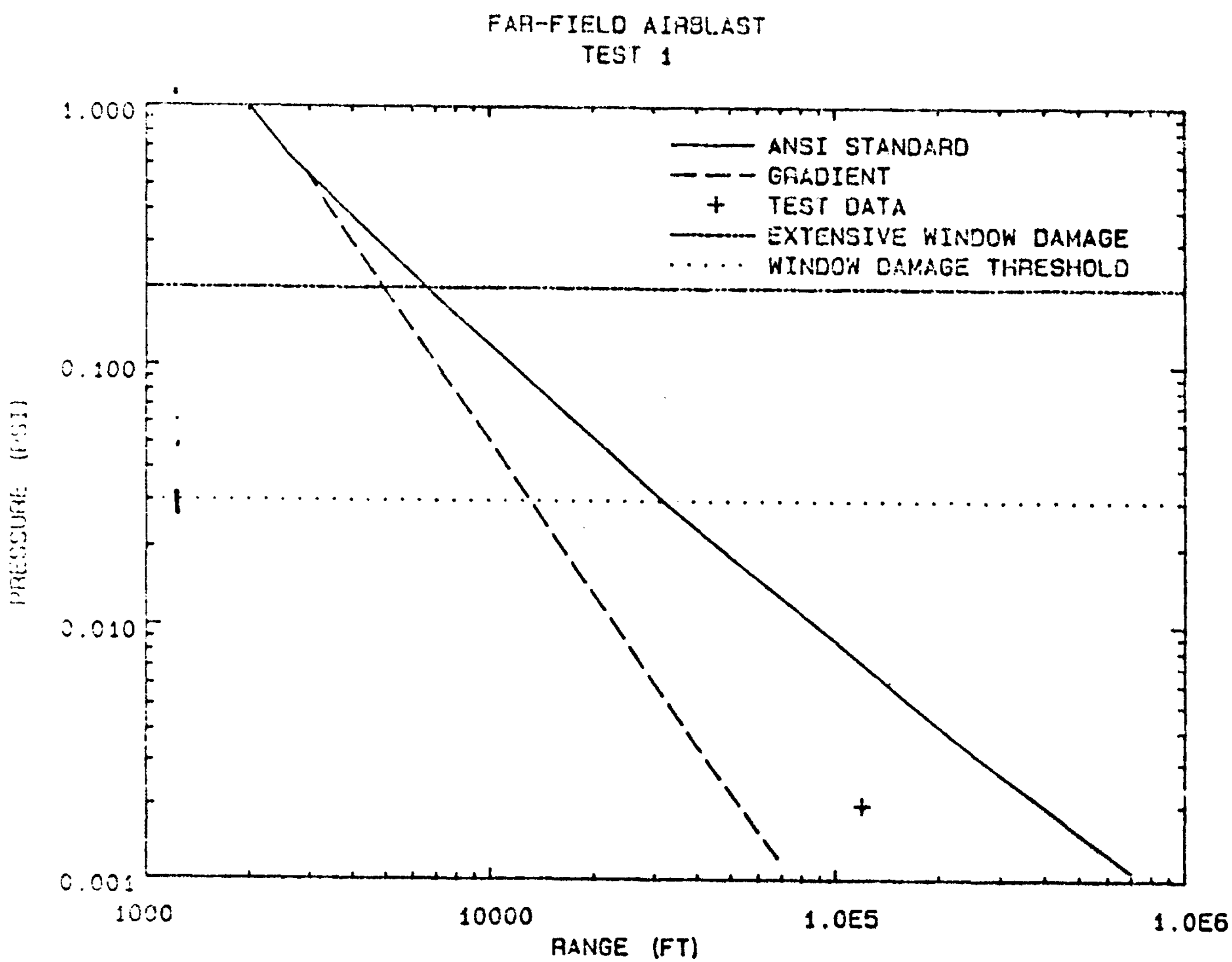

Figure 4. Far-field airblast predictions and data for Test 1.

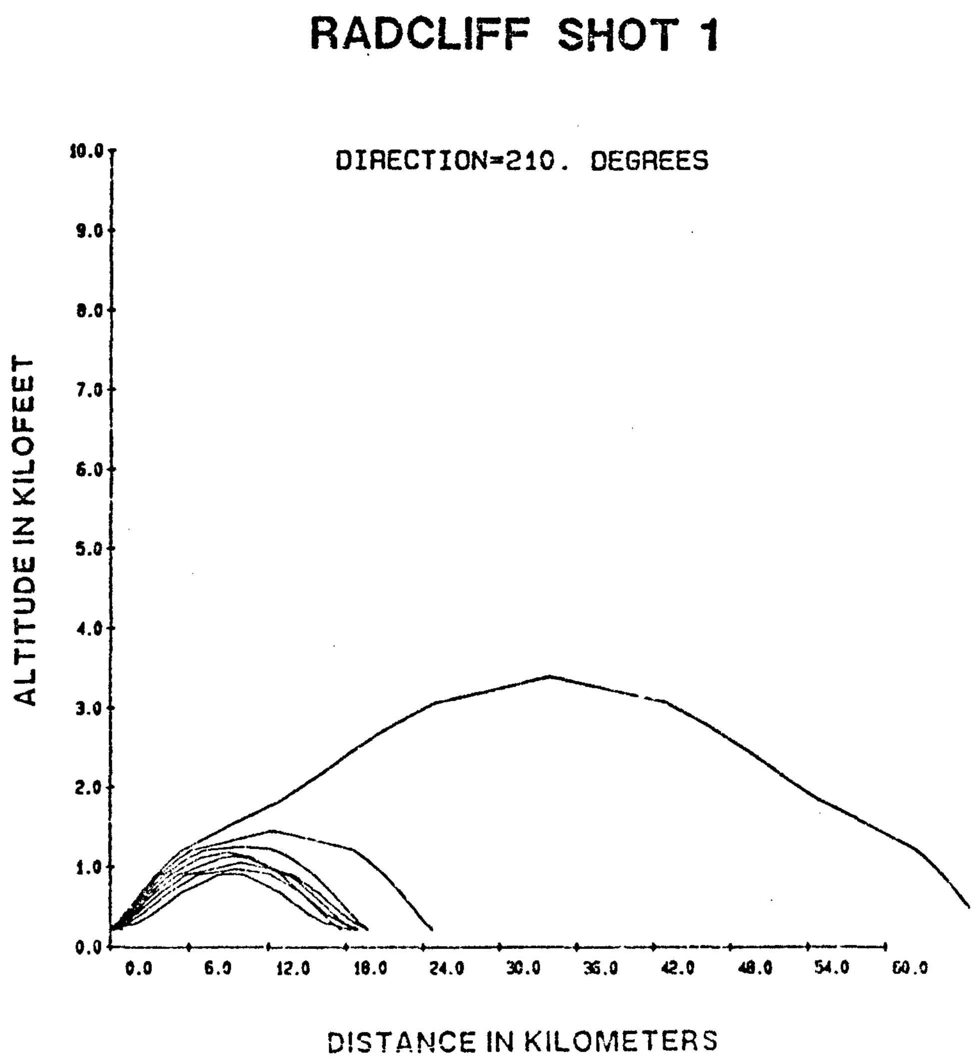

Figure 5. Shot time ray-trace for Test 1.

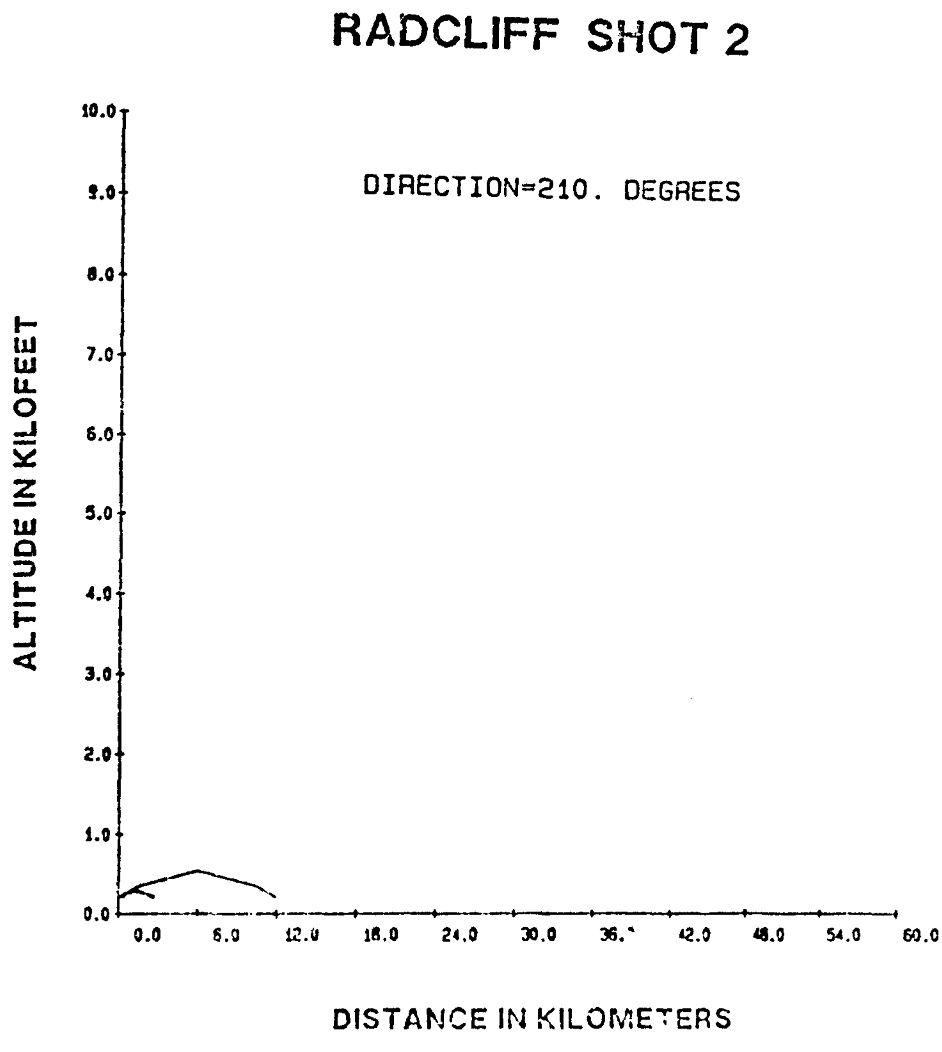

Figure 6. Shot time ray-trace for Test 2.

TEST 2
FAR-FIELD AIRBLAST
SHEPHERDSVILLE

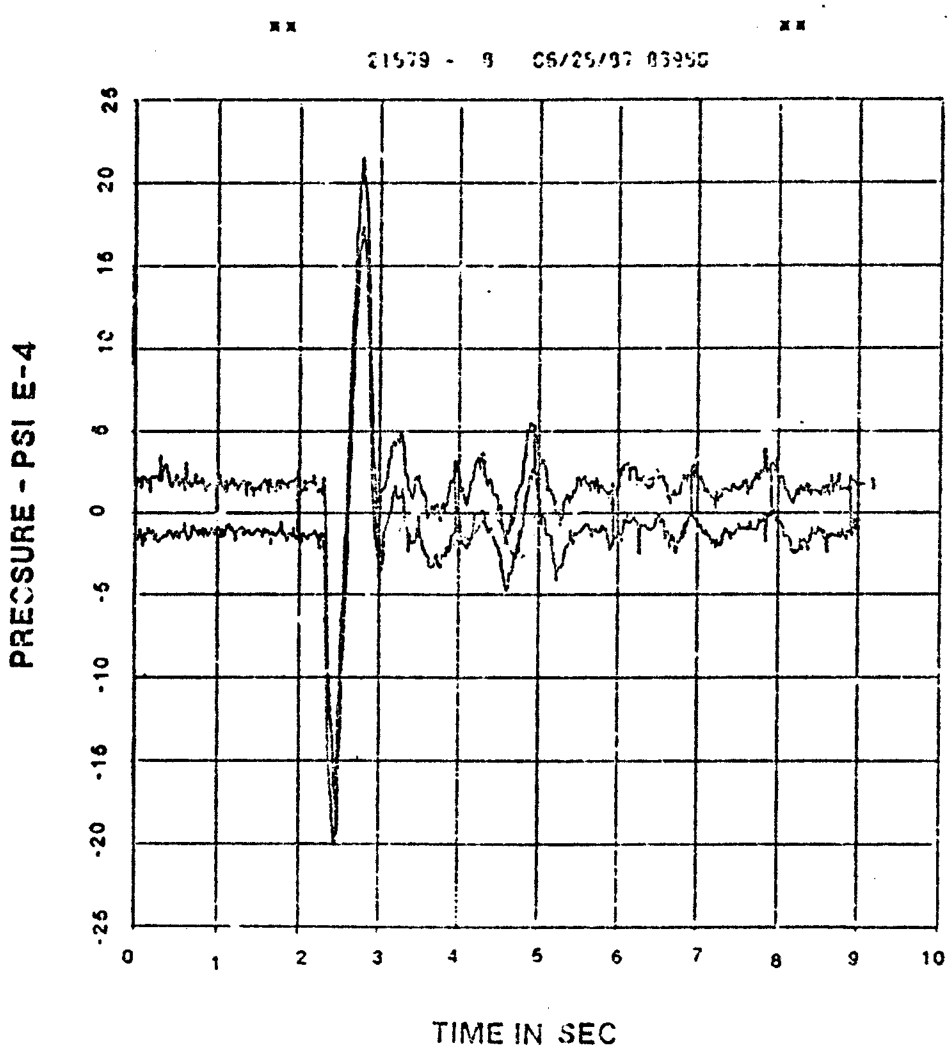

Figure 7. Test 2 far-field airblast measurement at Shepherdsville (zero time not shot zero).

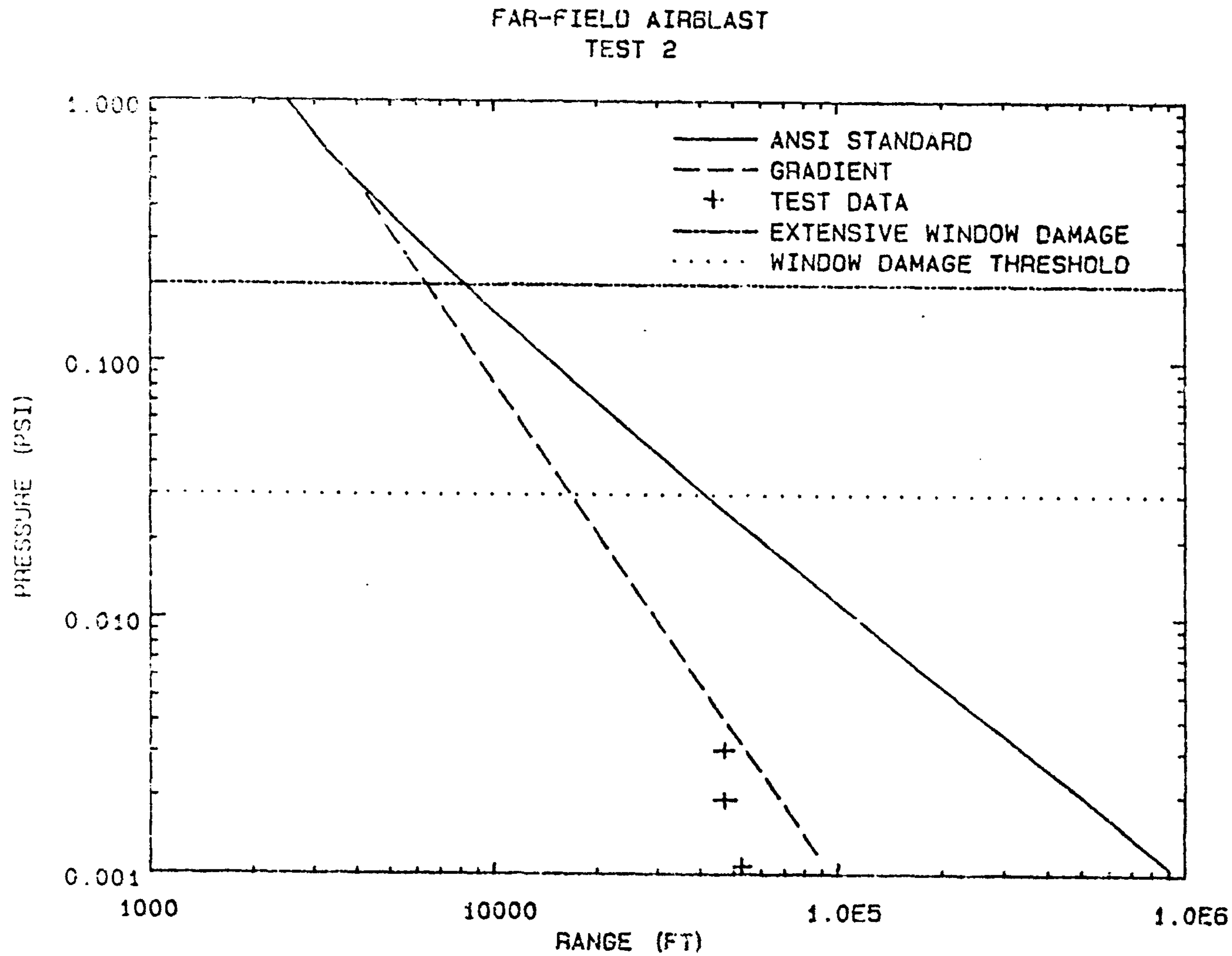

Figure 8. Far-field airblast predictions and data for Test 2.

REFERENCES

1. "Environmental Impact Assessment, Rodgers Hollow--Silo Test Program, Ft. Knox, Kentucky, 7 May 1987", USAE Waterways Experiment Station, Vicksburg, MS 39180, 1987.

2. "Estimating Airblast Characteristics for Single Point Explosions in Air, with a Guide to Evaluation of Atmospheric Propogation and Effects", S2.20-1983, American National Standards Institute, New York, NY, 1983.

3. Sachs, R. G., "The Dependence of Blast on Ambient Pressure and Temperature", BRL Report No. 472, Army Ballistic Research Laboratories, Aberdeen Proving Ground, MD, 1944.

4. Cheek, J. B. ,Far-Field Airblast Code "PFB" for HP 41CX, Waterways Experiment Station, Vicksburg, MS, 1987.

5. Warren, F. M., Ray-Tracing Code for Personal Computer, Waterways Experiment Station, Vicksburg, MS, 1987.

6. Reed, J. W., "Weather and Airblast Evaluations for Project STP-4a", Sandia National Laboratories, Albuquerque, NM 87185, 9 April 1987.

7. Reed, J. W., " Weather Watch and Blast Predictions for STP-4B", Sandia National Laboratories, Albuquerque, NM 87185, 22 June 1987.

DEPARTMENT OF DEFENSE
TWENTY-THIRD EXPLOSIVE SAFETY SEMINAR
ATLANTA, GEORGIA

IMPROVED GENERAL FIRING BARRICADE FACILITY
A CONCEPT STUDY

BY

FRANKLIN P. EPPERT, P.E.
BOOKER ASSOCIATES, INC.
1139 OLIVE STREET
ST. LOUIS, MISSOURI 63101
(314) 421-1476

ABSTRACT

The Aberdeen Proving Ground (APG) Firing Barricades were designed and built forty to sixty years ago. The army's weapons systems and the criteria for testing them have undergone significant changes since that time. Today, the weapons are more powerful and the safety and environmental testing criteria are more critical. Noise and blast generated at firing points on army installations are now being critically evaluated because of increasing concern about protecting personnel in the vicinity of the weapons. New government regulations on noise pollution are also increasing public awareness on this matter. With these safety and environmental constraints, the testing programs at Aberdeen Proving Ground have had to be compromised in many situations in order to maintain adequate safety and reduce noise. It is, therefore, necessary that the Aberdeen Proving Ground Firing Barricades be improved by modernization or replacement in order to regain the testing flexibility which they had in years past.

This paper will discuss the development of detailed conceptual schemes to be incorporated in the criteria proposed for the design of a new Improved Firing Barricde. Elements of the Study included:

a. Functional design criteria, configuration characteristics and a general arrangement of the improved barricades and support facilities at the Firing Line.

b. Establishment of separation distances between on-site and off-site structures, between individual on-site structures, and between on-site structures and off-site access roads. This was done in order to attentuate the blast overpressures resulting from an accidental explosion as well as the sound produced by normal firing operations.

c. Development of structural schemes, including concrete element thicknesses, types of reinforcement and associated blast-resistant items such as doors and fragment shields, which will provide improved protection for personnel and equipment, prevent propagation of an explosion, direct primary fragments in a safe direction, and attenuate noise generated by test firing.

1. INTRODUCTION

1.1 Objective

This concept study was prepared by Booker Associates, Inc. for the Baltimore District, U.S. Army Corps of Engineers, in cooperation with personnel at Aberdeen Proving Ground Maryland represnting both the Directorate of Engineering and Housing and the U.S. Army Combat Systems Test Facility. The purpose of the study was to develop functional design criteria and geometric configurations for a new General Firing Barricade with Temperature Conditioning Cells and a Control and Instrumentation Building. The Improved General Firing Barricade will replace existing firing barricades on the main range at Aberdeen Proving Ground, Maryland.

1.2 Background

The Aberdeen Proving Ground Firing Barricades were constructed forty to sixty years ago. Weapons systems and the criteria for testing them have undergone significant changes since that time. Today, the weapons are more powerful and the safety and environmental criteria are more demanding. Noise and blast effects generated at firing points on military installations are now being more critically evaluated because of increasing concerns for personnel protection in the vicinity of the weapons. New regulations on noise pollution are in effect, as well as increased public awareness. With these safety and environmental constraints, the testing programs at Aberdeen Proving Ground are being compromised in order to maintain safety and to abate noise. It was, therefore, necessary that an improved firing barricade be developed at Aberdeen Proving Ground to regain the testing flexibility which had existed for many years.

1.3 Basic Criteria

To initiate the study, basic criteria was established as follows:

a. Weapons to be test-fired at the improved barricade were tabulated and are listed in Figure 1 with dimensional data.

b. Line-of-fire for weapons was established requiring elevations ranging from 0 to 30 degrees above horizontal and lateral movement of 3-3/4 degrees left or right of the center line. Ability to quickly vary the elevation of the weapon being tested will be required.

c. The barricade must provide two firing positions: A permanent mount for weapon components and a mobile position for complete weapons on their carrier. The weapon components must be accessible for replacement in a short period of time.

d. The weapons being tested will be controlled and monitored from a safe remote position.

e. The barricade must provide weather protection, but allow for firing of the weapon at the stated maximum elevation.

f. The firing barricade must meet the criteria set forth in TM 5-1300, "Structures to Resist the Effects of Accidental Explosion".

1.4 Design Criteria

Blast design criteria was established as follows:

a. The maximum credible incident will be detonation of explosives totaling 200 pounds of TNT equivalency. The location of this charge for the worst case will be at a stand-off distance of 12 feet to the face of the closest wall, and three feet above the floor.

b. Fragmentation protection will be based on a weapon fragment weighting 500 pounds and traveling at 1000 feet per second. A breech failure will be a 700 pound fragment traveling 300 feet per second.

c. The firing barricade must withstand one maximum credible incident, however, it should be reusable after several accidental detonations of the magnitude of normal daily operations, firing one round at a time.

d. The control and instrumentation building must withstand an accidental explosion within the firing barricade.

Noise Criteria was established as follows:

a. Noise containment or attentuation during normal firing must be evaluated to provide the maximum results practical and economically obtainable.

b. Maximum noise criteria was established at 140 decibels during test firing at the face of the inhabited structures along Main Front Road, behind the barricade.

2. EXISTING FIRING BARRICADES

2.1 Facility Layout

The existing firing barricades are located along Main Front Road at Aberdeen Proving Ground as shown in Figure 2. This main road is fenced from the rest of the facility and only authorized personnel are permitted entry into the area.

2.2 Existing Facility Operation

The configuration of the existing barricade permits the test firing of large caliber military weapons systems. These weapons may be fired within the barricade from either a permanent gun mount or from the weapon's support vehicle or field carriage. Personnel required to load the weapon prior to firing leave the barricade and remain behind the back wall of the structure. Firing of the weapon is accomplished by pulling the lanyard which is brought over the back wall on a system of pulleys. Prior to firing, the crew chief visually inspects the area surrounding the barricades to ascertain that personnel are not exposed to the effects of firing. Ear protection must be worn by all personnel in the immediate area of the barricade.

Permanent instrumentation is not provided at the barricades, but is installed when required. These instruments are positioned in the vicinity of the barricade either in the open or behind make-shift shields.

Ammunition is brought from a remote storage location by truck which is parked in the vicinity of the barricade. The explosive items are carried into the barricade to be loaded in the weapon. The quantity of explosive contained in these vehicles is kept to a minimum, thereby requiring many deliveries of explosive items in order to complete the day's firings.

Delivery of the test weapons to the barricade is by truck. The truck may contain one or more weapons to be test-fired and is backed into the barricade alongside the gun position. At the same time, a long boom portable crane is positioned outside the barricade. The crane's boom reaches over the barricade wall and the weapon to be tested is then removed from the truck and placed in its proper position by the crane. The truck and the crane are removed from the barricade, but parked in the vicinity of the barricade during test firing.

2.3 Explosive Hazards

The major explosive hazard occurs in the firing barricade. A misfire or other malfunction before or during firing could cause an accidental explosion. The next lower level of hazard occurs in the preparation of the ammunition for firing. The least hazardous of all is the temporary storage of the ammunition.

The existing firing barricades are conventionally reinforced concrete structures as shown in Figure 3. The barricade is composed of two adjoining bays with open front walls facing down range, no roof and a labyrinth type common entrance through the back wall. The walls are not fixed at their bases to resist overturning by large blast forces but are merely embedded into the ground for several feet.

The blast capacity of the walls of the existing barricades is highly questionable due to the fact that they are conventionally reinforced and are not rigidly fixed at their bases. Conventionally reinforced members cannot sustain large deformations and are susceptible to local failures caused by the highly non-inform and high intensity blast loads associated with the blast effects of a close-in detonation. Since the walls are not rigidly fixed at their bases, resistance to the large overturning forces caused by close-in blast loads is due solely to inertial forces and the restraint afforded by their bases being embedded in the ground. Although the existing barricades will probably be able to resist an accidential explosion occurring in the smaller caliber weapons, the walls may fail due to an accidental explosion of larger caliber weapons.

The gun crew located behind the back wall of the barricade will be subjected to high blast pressures should an accidental explosion occur within the gun tube or should the warhead detonate soon after it leaves

the muzzle. Under current APG procedures, the crew is provided protection in strategically placed portable structures. This protection is from fragments resulting from a detonation of a projectile in the gun or soon after leaving the muzzle if the gun is fired in an elevated position. The crew will also be subjected to the blast and fragment effects associated with an accidental explosion of the ammunition which is and temporarily stored before firing. The explosion of this stored ammunition could be caused by an incident in the firing barricade since it is generally not shielded.

2.4 Noise Generation

An analysis was made of the firing noise to which personnel near the barricade, elsewhere on the Proving Ground, and in nearby communities are exposed. This noise exposure is based on the firing of the 120 MM M-1 Tank Gun. Results of field measurements are plotted on Figure 4. This data established a reference for further analysis based on the design proposed for the Improved Firm Barricade.

3. PROPOSED IMPROVED GENERAL FIRING BARRICADE FACILITY

3.1 Facility Layout

The Improved Firing Barricade Facility will include three structures. They are the barricade, control and instrumentation building, and temperature conditioning cells. These three structures are separated by intraline distances and have access roads from Main Front Road to the facility. Figure 5 shows the layout of the proposed facility.

The firing barricade will be a cubicle with the open face in firing direction. The barricade will be 74' wide and 70' deep with a 40' high ceiling. There will be two gun positions located within the firing barricade and an area between the two firing

positions for tractor-trailer access. This is shown on the floor plan on Figure 6. There will be ten ton bridge crane servicing both firing positions. Access to the firing barricade will be provided through personnel doors to the rear and to the side. Each door opening will be protected by a concrete wall capable of suppressing the door and any trailing primary or secondary fragment missiles in the event of an incident during firing.

The control and instrumentation building will be a harden structure constructed of reinforced concrete walls approximately 12" thick. The structure will be designed to resist missile fragments generated by an accidental explosion at the temperature conditioning cells and will also be capable of resisting the overpressure experienced from an accidental explosion either at the temperature conditioning cells or from the firing barricade.

The temperature conditioning cell will be a reinforced concrete box capable of withstanding the internal pressure developed by an accidental explosion of one 105mm round. However, the cell will not be designed to resist the maximum credible incident which would be a simultaneous detonation of the explosive limit for the temperature conditioning cell.

3.2 Explosive Hazards Due to Accidental Occurrences

The greatest probability for an incident is within the firing barricade. Such an incident could be a structural failure of the weapon or a pre-detonation of the projectile.

The maximum credible incident which could occur within the firing barricade would be during rapid firing of certain weapons, in which case, the total TNT equivalence of the accumulated rounds would be 200

pounds. The requirement for rapid firing of multiple rounds is not a frequent occurrence and recognizing that fact, the structure will be designed to resist this maximum credible incident on a one time basis. The structure would be substantially damaged and probably would have to be replaced following a maximum credible incident. On the other hand, an accident resulting from the more frequent requirement of single round testing will not significantly damage the firing barricade. The result of a single round detonation of 60 pounds of TNT would cause no more than 1 degree of support rotation as opposed to a 12 degree support rotation for the maximum credible incident.

The overpressure to the rear of the firing barricade due to a maximum credible incident within the firing barricade is less than 1.2 psi at the building along Main Front Road as shown on Figure 7. The temperature conditioning cells are located at intraline distance from the firing barricade and the control and instrumentation building. This intraline barricaded distance is 65 feet. The intermagazine distance between each of the temperature conditioning cells is 10 feet. The probability of an accident occurring at the temperature conditioning cells is much lower than within the firing barricade.

3.3 NOISE SUPPRESSION

To further enhance of sound attentuation, a modification of the barricade, partially closing the downrange side with movable doors, was investigated. Figure 8 shows estimated noise levels with the barricade open, indicating a level of 145 dB along Main Front Road. Figure 9 shows the results of partially closing the downrange side. Maximum noise level on Main Front Road is reduced to 125dB.

A cost estimate indicated that the doors and associated mechanisms would cost an additional $500,000. Although the attenuation results would be significant, the cost is high and the criteria requirements for 140 db at the buildings along Main Front Road will be satisfied with open barricade.

3.4 New Firing Barricade Construction

The design proposed for the Improved Firing Barricade is a laced reinforced concrete structure designed to resist, without significant damage, the blast effect of an accidental detonation during normal test firing operations. It will also resist the blast and fragment effects associated with accidental explosion equivalent to a maximum of 200 pounds of TNT located approximately 12 feet from the face of any wall.

The laced reinforced concrete wall system will include missile fragment protection immediately behind the firing point to suppress breech block failure. This protection will be provided by a 2 inch thick steel plate mounted on the face of the concrete wall. The reinforced concrete structure will be of sufficient thicknesses to suppress a steel fragment weighing 500 pounds and traveling 1000 feet per second.

The permanent gun mount will be attached to a massive concrete base. This foundation will be isolated from the rest of the firing barricade in order to prevent localized stress concentration in the structure due to firing at the permanent gun mount. The roof height was set such that a maximum elevation of 30 degrees can be obtained for both the mobile weapons and fixed mount weapons. The length of the side walls of the firing barricade was based on the longest barrel requirement of 24' plus 15' to the end of the walls.

The Control and Instrumentation Building shown on Figure 10 will be a conventionally reinforced concrete structure designed to protect personnel and instrumentation from the blast effects of normal firing operations as well as the blast and fragment effects associated with an accidental explosion which might occur in the Firing Barricade or at the Temperature Conditioning Cells. Personnel located within the building are also protected from the noise pressure caused by normal firing operations.

The Temperature Conditioning Cells will be reinforced concrete, earth covered structures as shown in Figure 11. In addition to the head wall doors, a pair of sliding steel grates are included to contain the contents of the room should a single round detonation occur. This is assuming, of course, a simultaneous detonation does not occur. To ensure that the cell can contain a single round detonation, a reinforced concrete structure was selected over a conventional metal arch type structure. A maximum credible incident of simultaneous detonation will destroy the cell, however, the adjacent Cells will withstand the external effect of such a detonation.

4. Conclusions

There are a number of conclusions from this study concerning the design and siting of the Improved Firing Barricade Facility. They are based on considerations of the mission of the facility, the present state-of-the-art in design and construction of blast resistant structures, and methods of noise attentuation. These conclusions are as follows:

a. It is both feasible and practical to construct an Improved General Firing Barricade Facility at Aberdeen Proving Ground, Maryland meeting the established criteria.

b. It is feasible to design and construct a Firing Barricade to sustain the blast and fragment effects of an accidental explosion which may occur during the testing of weapons systems.

c. Laced reinforced concrete construction is required for the Firing Barricade in order to resist the effects of close-in blast loadings.

d. Significant construction cost savings can be realized by establishing the support rotation limits for the blast walls at 12 degrees in lieu of 2 degrees for a maximum credible incident equivalent to 200 pounds of TNT.

e. The Improved General Firing Barricade with an openside downrange will attenuate noise to 140 db at the inhabited buildings.

REFERENCES

1. Structures to Resist the Effects of Accidental Explosion, TM 5-1300 June, 1969, U. S. Departments of the Army, Navy and Air Force.

2. Suppressive Shields, HNDM 1110-I-2, November, 1977, U. S. Army Corps of Engineers, Huntsville Division.

3. Blast Environment from Fully and Partially Vented Explosions in Cubicles, NCEL R-828, November, 1975, W. A. Kennan and J. E. Tancreto.

4. Safety Manual, DARCOM Regulation No. 385-100, Department of the Army Headquarters, United States Army Material Development and Readiness Command, August, 1985.

5. An Improved Computer Program to Calculate the Average Blast Impulse Loads Acting on a Wall of Cubicle, TR 4070, May, 1970, Stuart Levy, Picatinny Arsenal; Dover, New Jersey.

6. A Manual for the Prediction of Blast and Fragment Loadings on Structures, DOE/TIC 11268, U. S. DOE, Alburquerque Operations Office, Amarillo Area Office, Pantex Plant, Amarillo, Texas, November, 1980.

7. Noise Characteristics of Firing Barricades: Phase I Report, Report No. 4385, March 1981, Bolt Beranek and Newman, Inc.

FIGURE 1 – WEAPONS TO BE TESTED

Weapon Gun/Howitzer	Vehicle	Carriage	Weight (lb)	L	H	W	Lg	l	h	Remarks
Gun, 90mm M41	Tank M48	N/A	99,500(1)	24'-3.5"	10'-3"	11'-11.5"	-	-	-	-
Gun, 105mm M68	Tank M60	N/A	-	27'-1"	10'-8"	12'-0"	14'-10"	8'-2"	6'-10.5"	-
Gun, 105mm M68	Tank XM1	N/A	118,000(2)	25'-11.7"	7'-9.5"	11'-11.8"	13'-9"	6'-0.92"	6'-10.5"	-
Gun, 152mm M81	M551	N/A	29,960	-	9'-4"	9'-2.5"	-	-	-	Full track vehicle
Gun, 152mm XM162	Tank M60	N/A	109,500(2)	23'-10.85"(1)	10'-10.31"	11'-11"	-	-	-	-
Gun, 120mm M58	Tank M103A1	N/A	110,560(2)	29'-5"(3)	10'-10"	12'-2.3"	-	-	-	Tank M728 data given
Gun, 120mm XM1	XM1	N/A	-	-	-	-	-	-	-	-
Gun, 162mm M135	M728	N/A	-	-	-	-	-	-	-	-
Gun, 175mm M113	M107	N/A	62,100(2)	37'-.75"(4)	11'-4.75"	10'-4"	-	-	-	Full track with spade
Howitzer, 105mm (M137) (M102)	N/A	M31	3,140	21'-10.5"	-	6'-4"	-	-	-	Towed Howitzer
Howitzer, 155mm M185	M109	N/A	52,461	21'-3"	10'-8"	10'-4"	20'-7"(5)	9'-1.5"	6'-8.5"	Full track vehicle
Howitzer, 155mm M138	N/A	XM39	-	24'-6"(8)	-	9'-2"(7)	21'-5"(6)	11'-6"	3'-10"	Towed Howitzer with large trails
Howitzer, 8 in M201	M110	N/A	58,000(2)	22'-.5"	9'-7.76"	10'-4"	24'-7"	11'-7"	7'-1.3"	Full track with spade
Howitzer, 8 in M2A1E1	M110	N/A	58,506(2)	24'-6"(1)	9'-7.5"	10'-4"	-	-	-	Full track with spade

(1) May include gun.
(2) Combat-loaded.
(3) May include boom.
(4) Includes gun.
(5) 18'-5" without muzzle break.
(6) 20'-5" without muzzle break.
(7) 20'-0" trails open.
(8) Approximate carriage length with trails open.

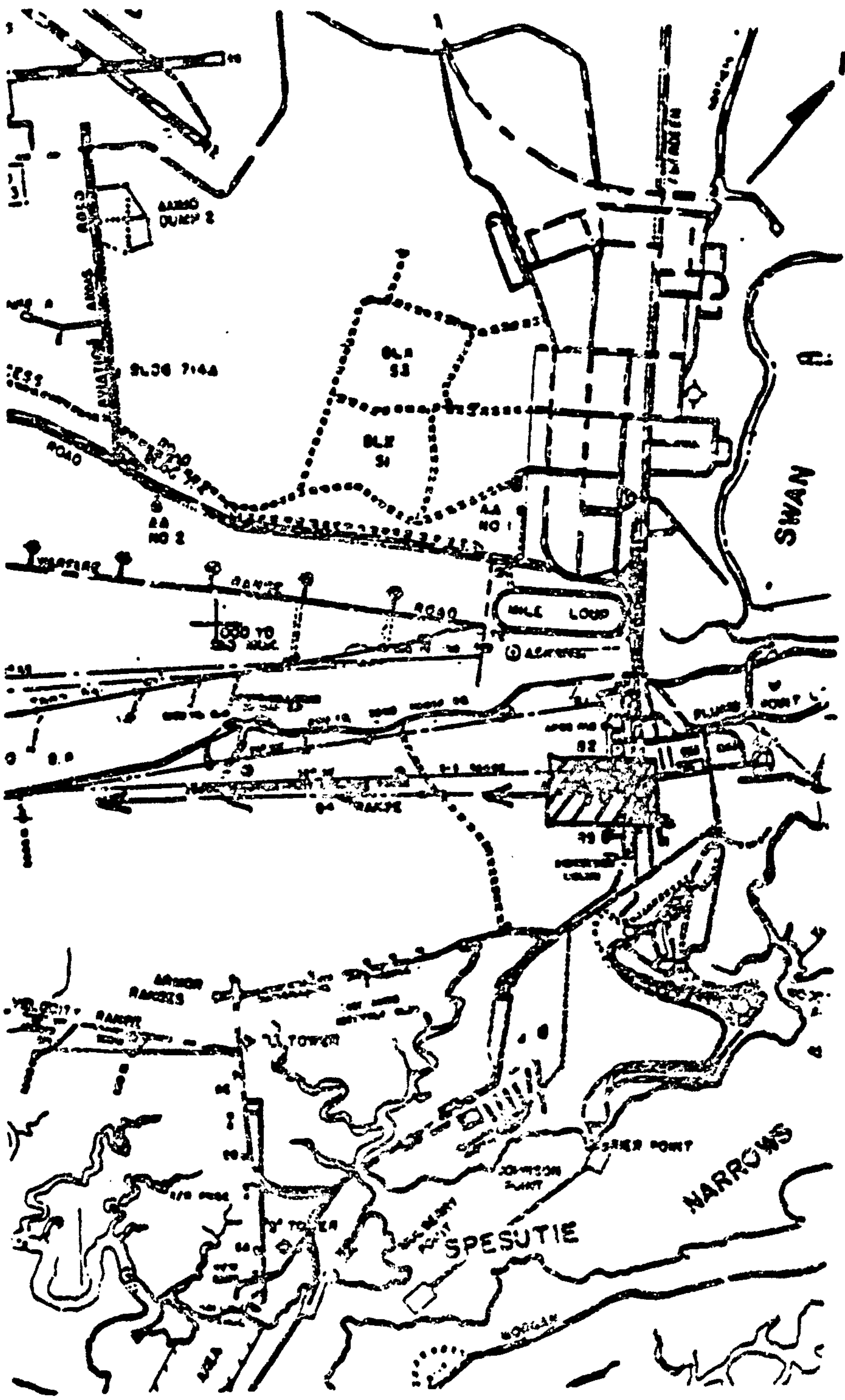

FIGURE 2 - MAIN RANGE - APG, MD

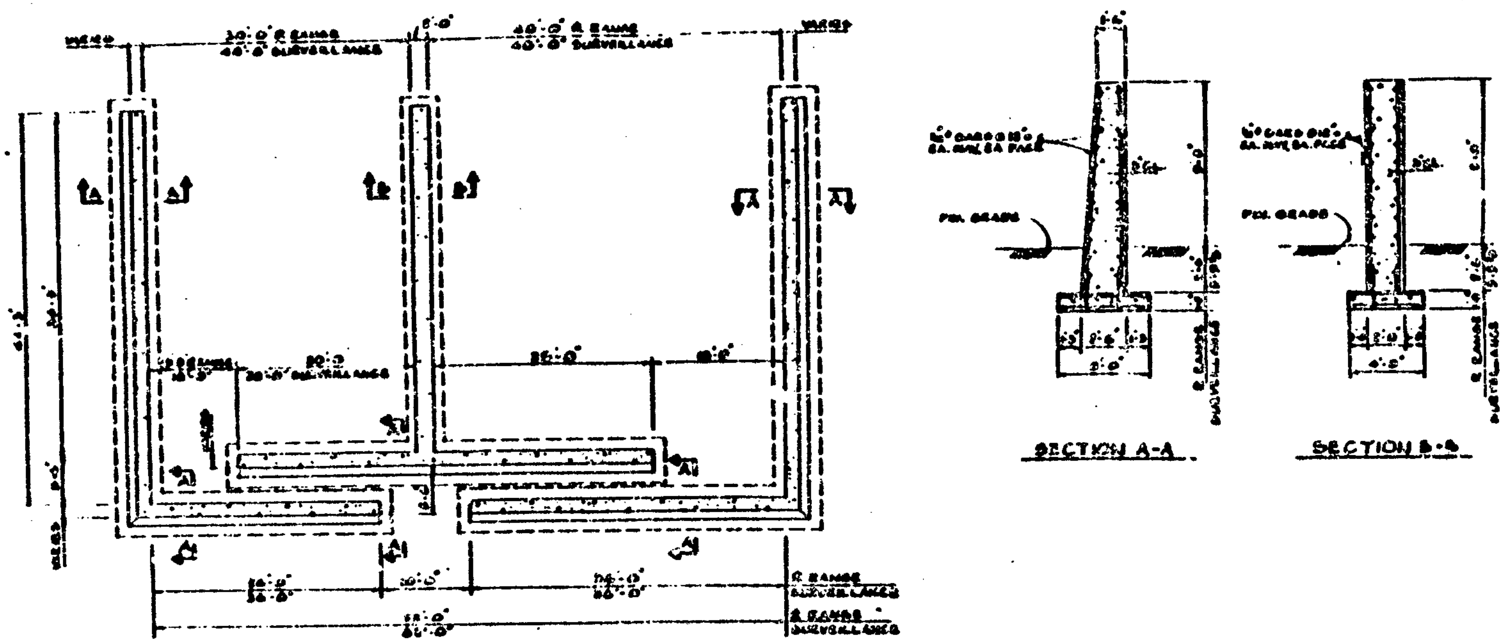

FIGURE 3

LAYOUT OF EXISTING FIRING BARRICADE

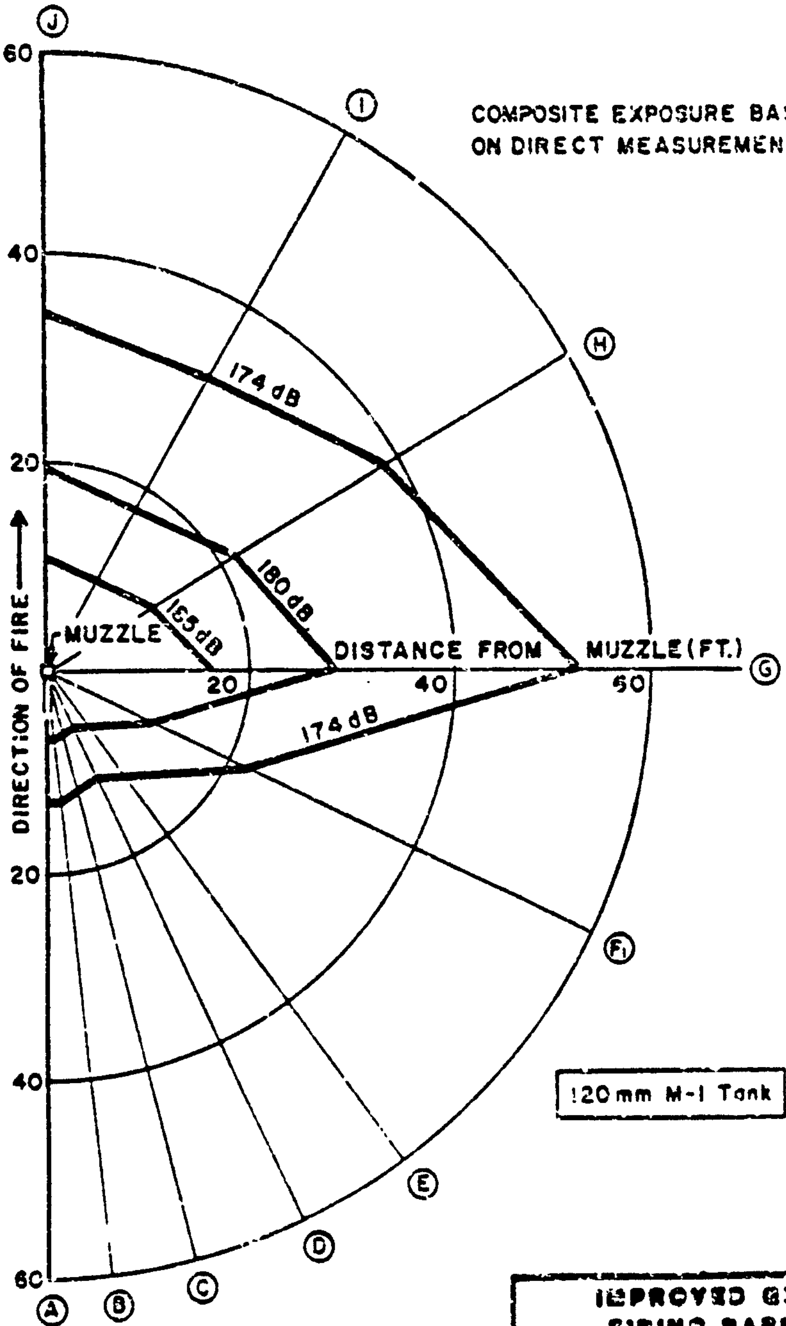

COMPOSITE, WORST-CASE PEAK
OVER-PRESSURE CONTOURS
NEAR 120mm M-1 TANK BASED
ON DATA FURNISHED BY ABERDEEN
PROVING GROUNDS.

IMPROVED GENERAL
FIRING BARRICADE

ABERDEEN PROVING GROUND

FIGURE 4

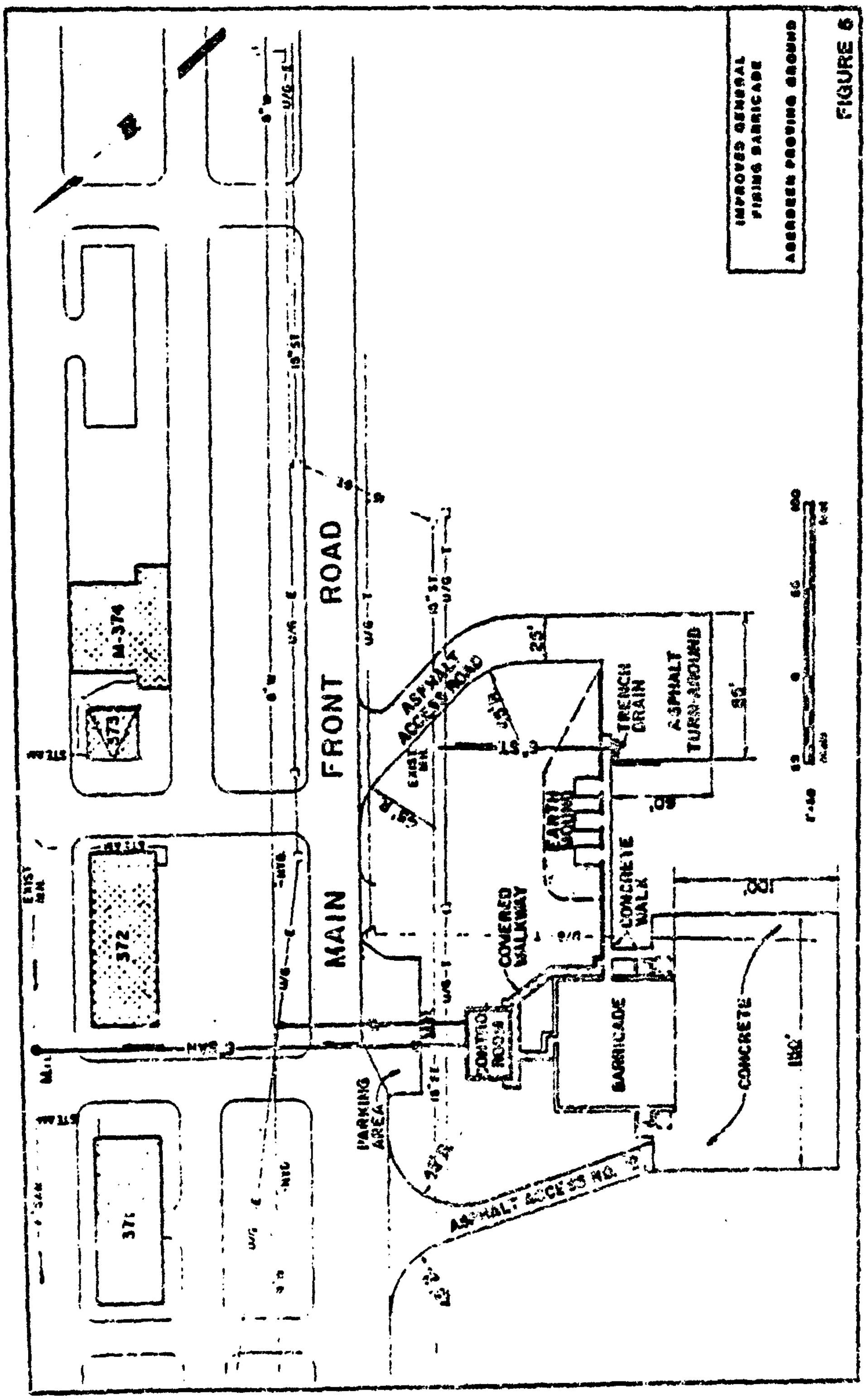
IMPROVED GENERAL
FIRING BARRICADE
ABERDEEN PROVING GROUND
FIGURE 6
MAIN
FRONT
ROAD
M-374
373
372
371
ASPHALT ACCESS ROAD
TRENCH DRAIN
ASPHALT TURN-AROUND
EARTH MOUND
CONCRETE WALK
COVERED WALKWAY
CONTROL ROOM
BARRICADE
CONCRETE
PARKING AREA
ASPHALT ACCESS NO. 19

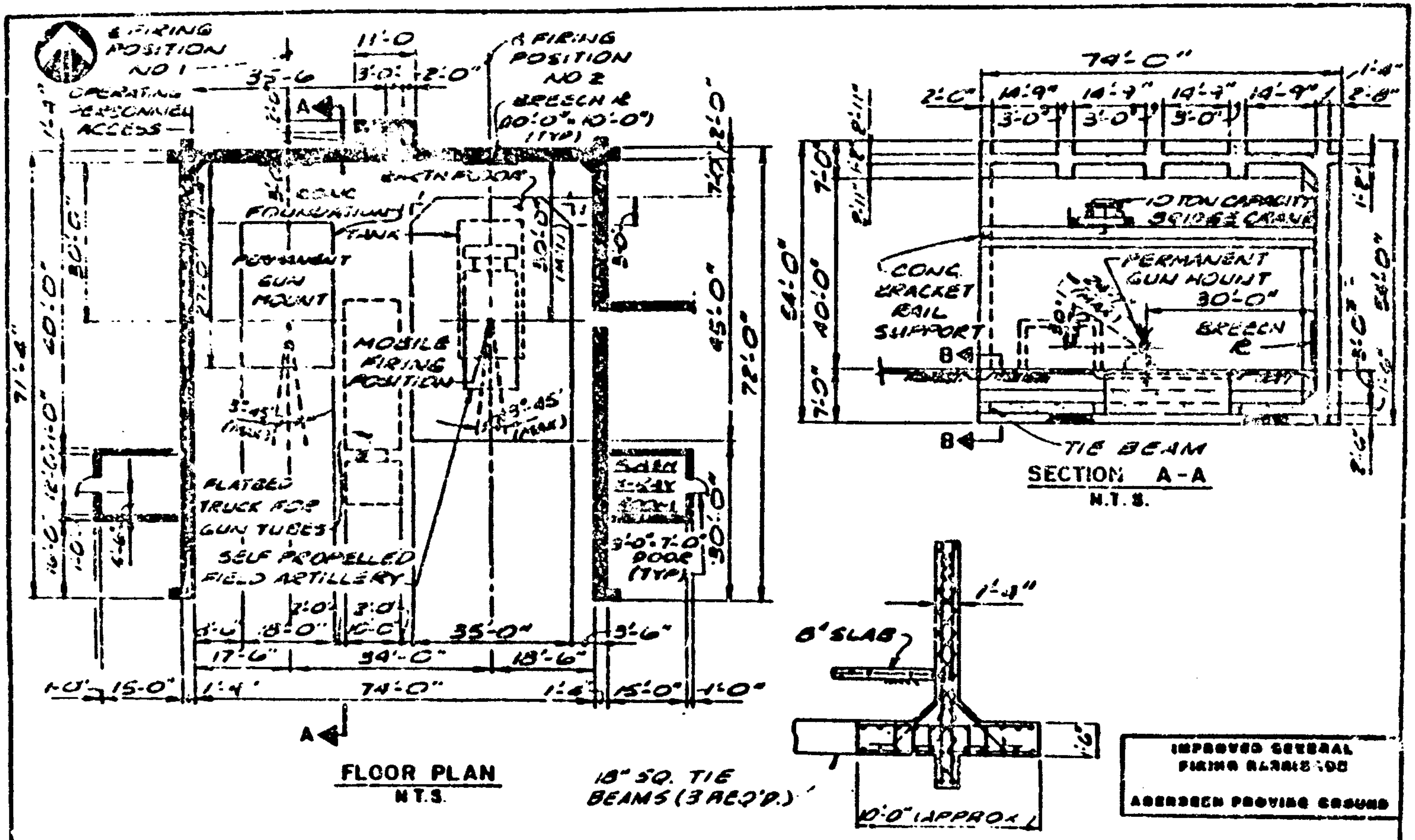
FIRING POSITION NO 1
OPERATING PERSONNEL ACCESS
FIRING POSITION NO 2
BREECH (10'-0" x 10'-0") (TYP)
EARTH FLOOR
CONC FOUNDATION
TANK
PERMANENT GUN MOUNT
MOBILE FIRING POSITION
FLATBED TRUCK FOR GUN TUBES
SELF PROPELLED FIELD ARTILLERY
3'-0" x 7'-0" DOOR (TYP)
74'-0"
72'-0"
45'-0"
35'-0"
FLOOR PLAN
N.T.S.
18" SQ. TIE BEAMS (3 REQ'D.)
10 TON CAPACITY BRIDGE CRANE
CONC BRACKET RAIL SUPPORT
PERMANENT GUN MOUNT
30'-0"
BREECH
TIE BEAM
SECTION A-A
N.T.S.
8" SLAB
1'-4"
10'-0" (APPROX)
SECTION B-B
IMPROVED GENERAL FIRING BARRICADE
ABERDEEN PROVING GROUND

FIGURE 6

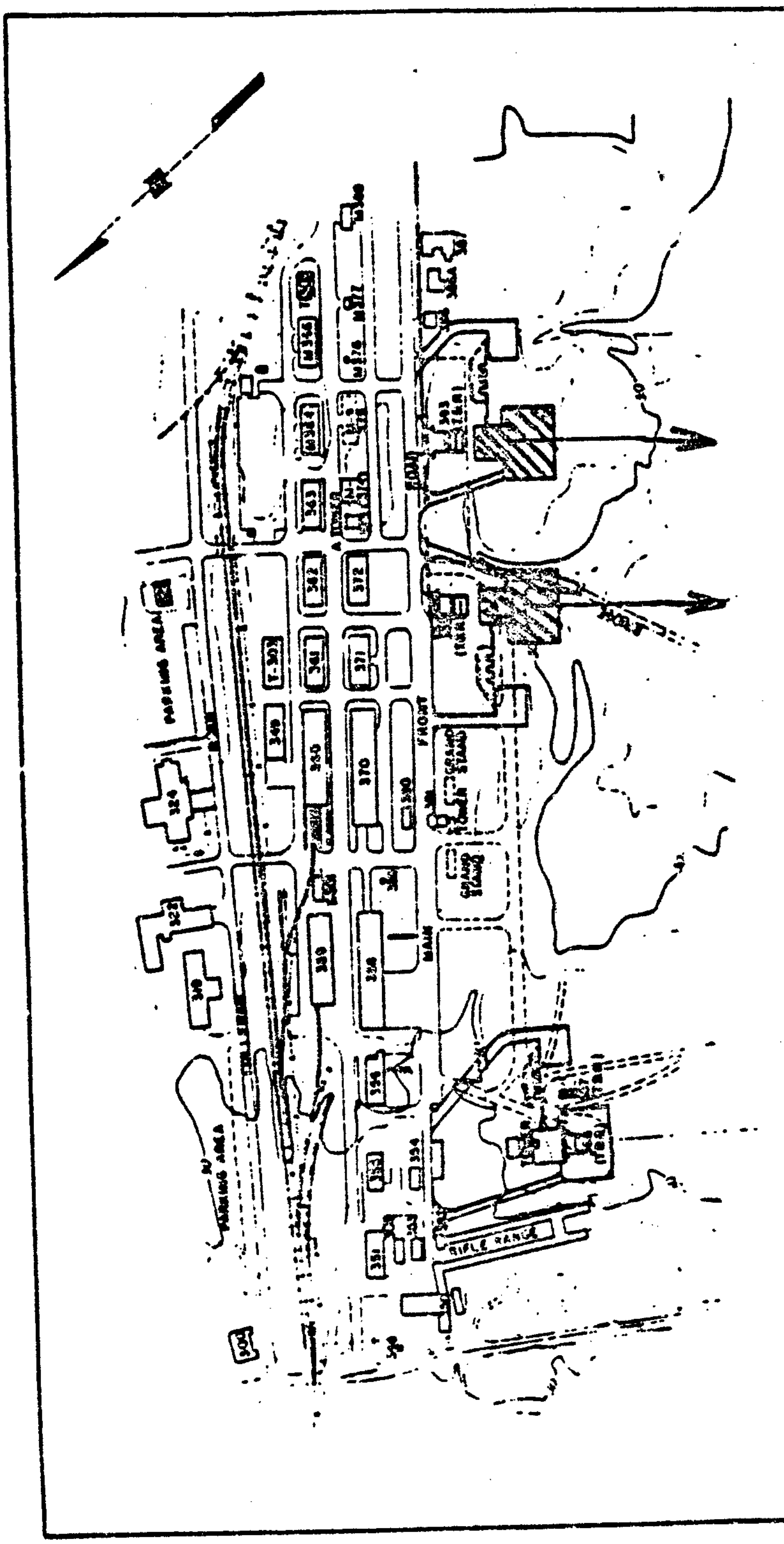

IMPROVED GENERAL FIRING BARRICADE

ABERDEEN PROVING GROUND

FIGURE 7

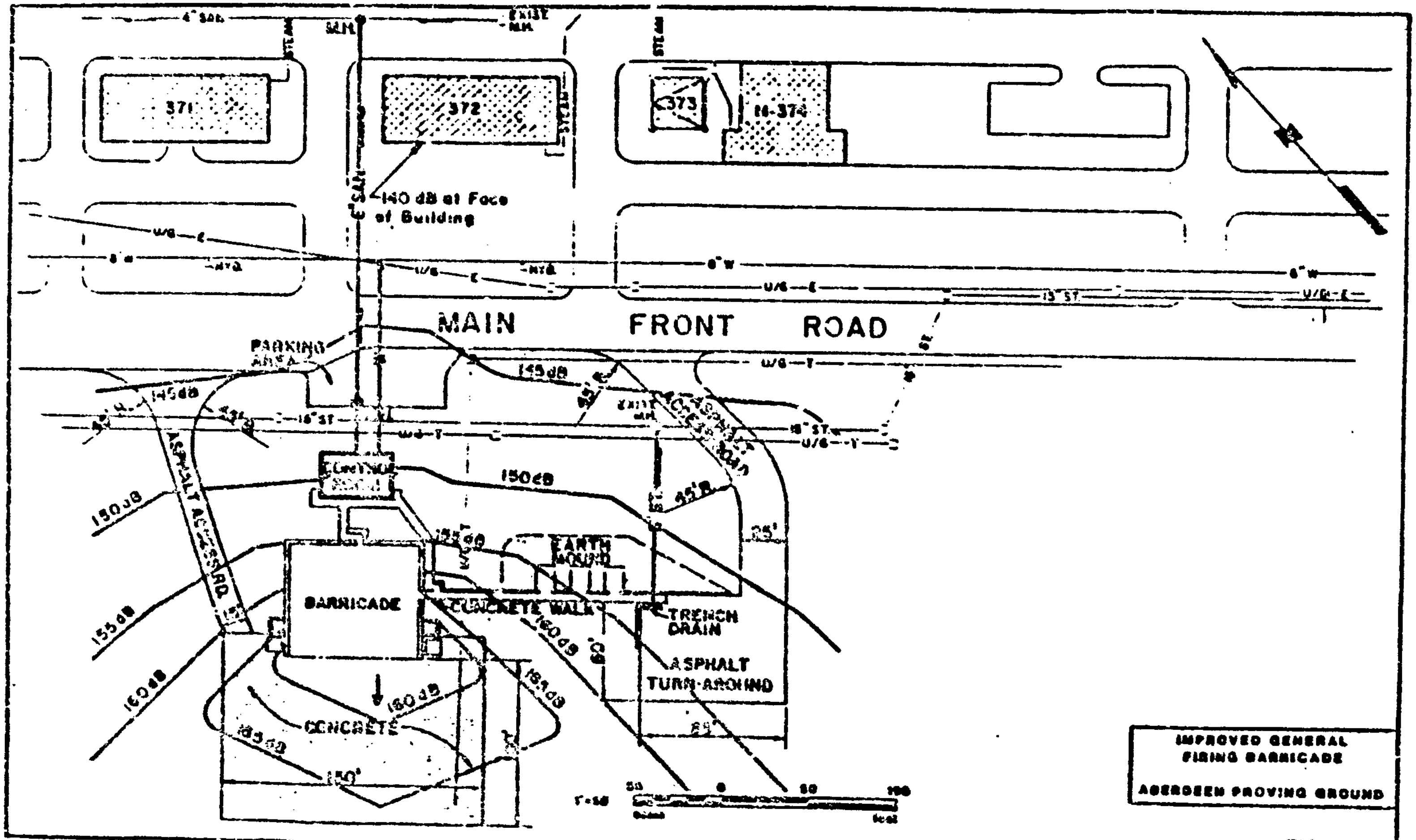

IMPROVED GENERAL FIRING BARRICADE

ABERDEEN PROVING GROUND

FIGURE 8

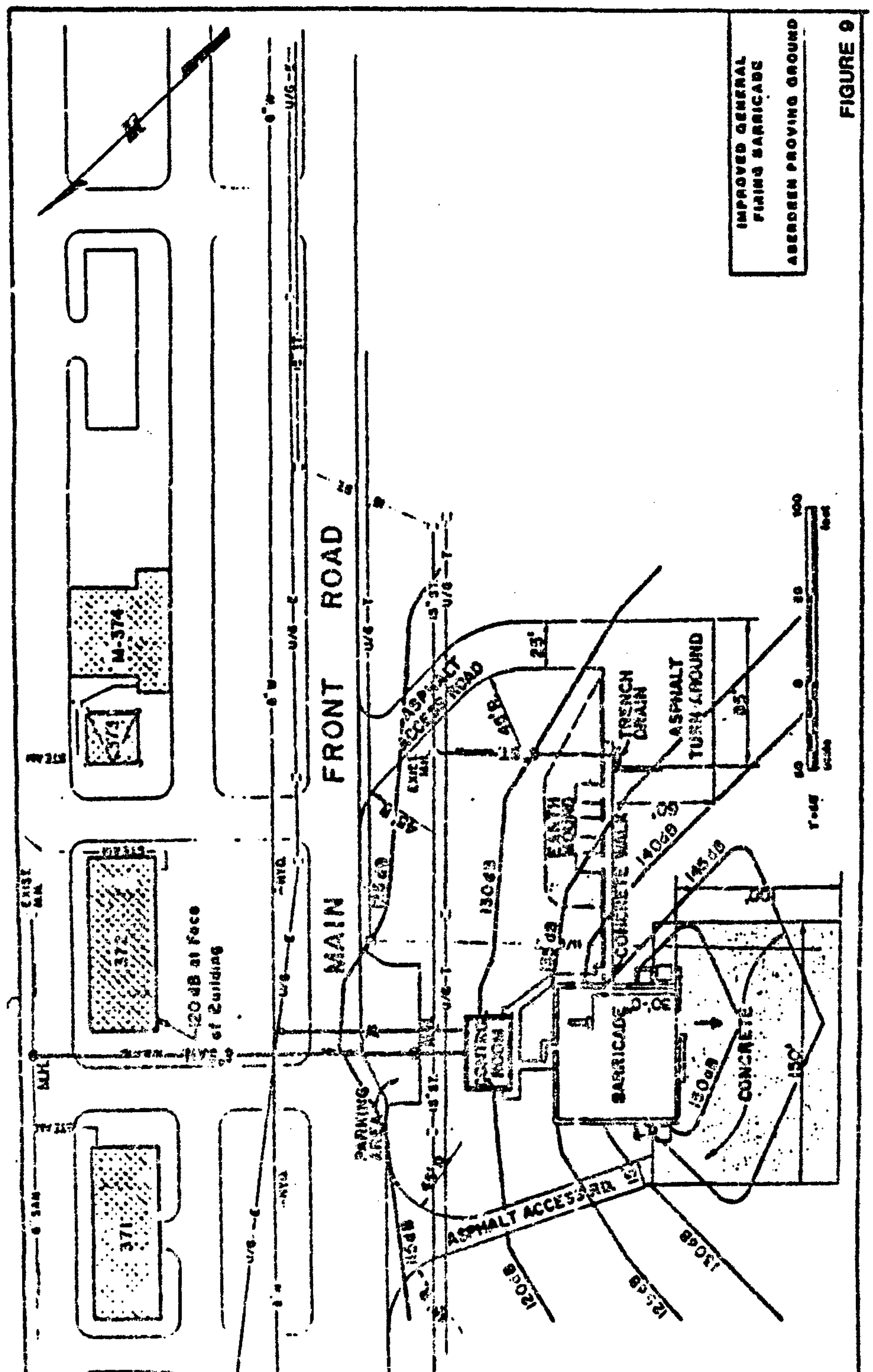
IMPROVED GENERAL FIRING BARRICADE
ABERDEEN PROVING GROUND
FIGURE 9
MAIN
FRONT
ROAD
BARRICADE
CONCRETE
ASPHALT ACCESS ROAD
EARTH MOUND
TRENCH DRAIN
ASPHALT TURN AROUND
CONCRETE WALK
PARKING AREA
FIRING ROOM
120 dB at Face of Building
M-374
374
372
371
130dB
140dB
145dB
120dB
125dB

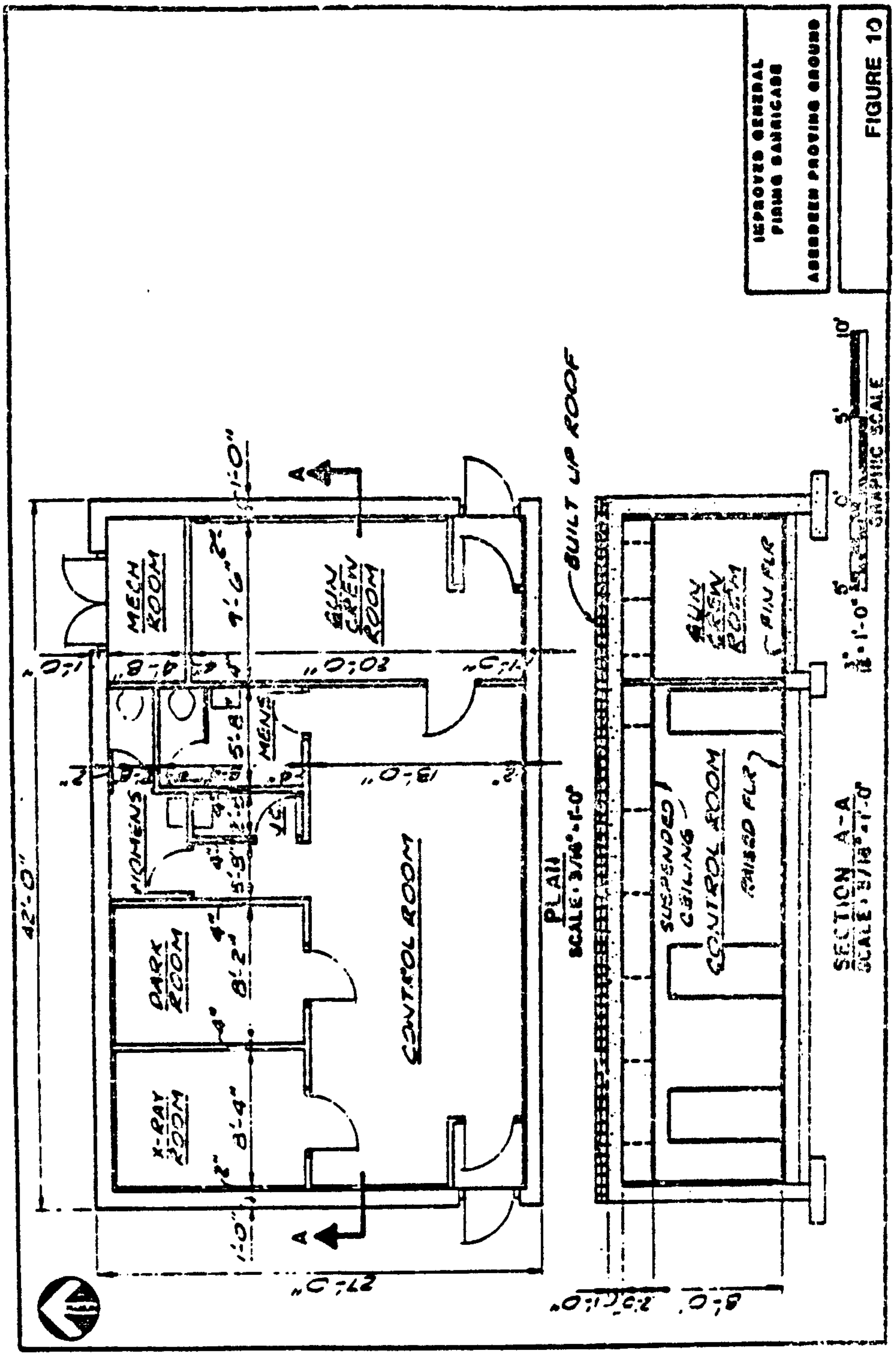

IMPROVED GENERAL FIRING BARRICADE
ABERDEEN PROVING GROUND

FIGURE 10

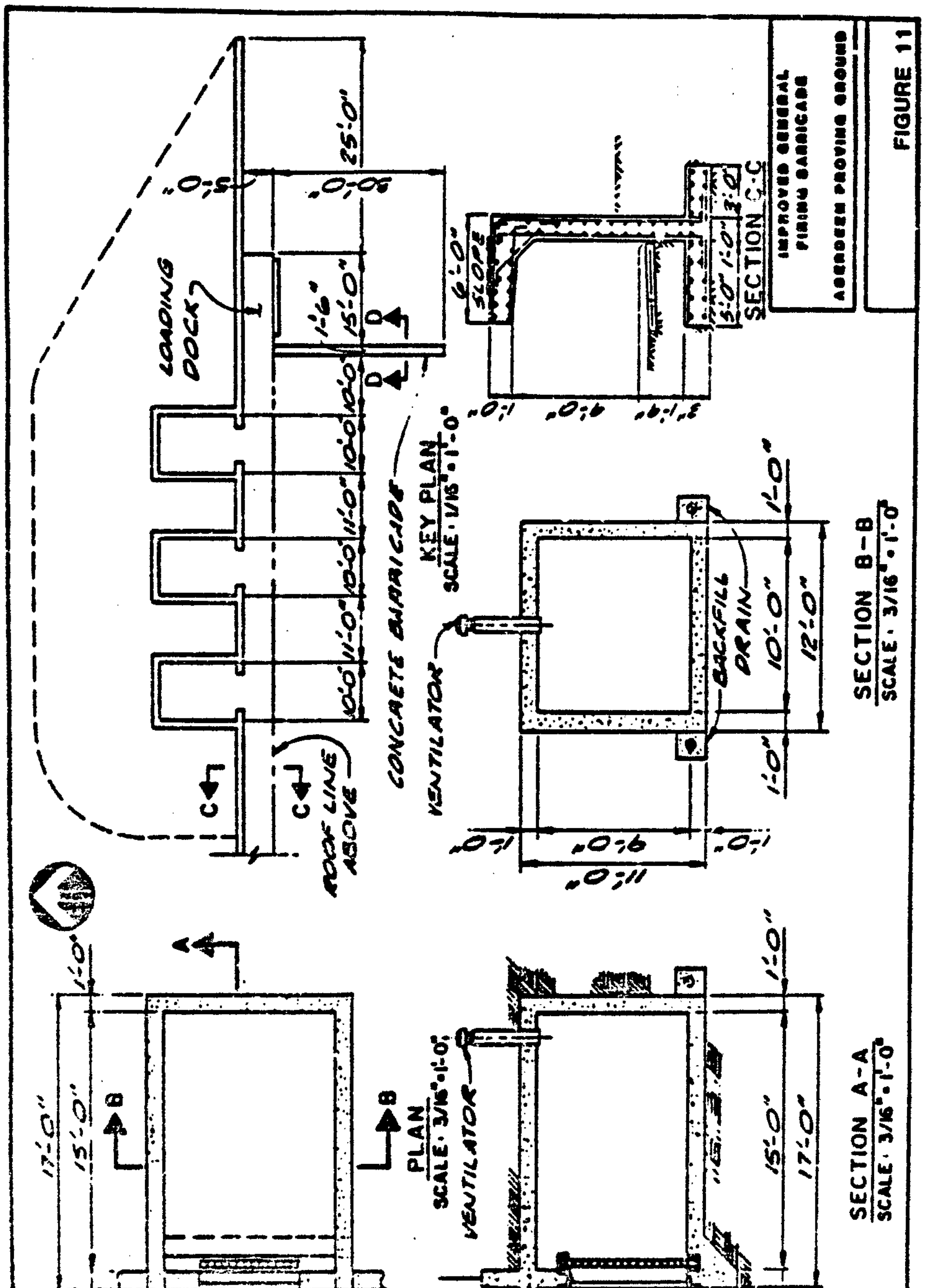
IMPROVED GENERAL FIRING BARRICADE
ABERDEEN PROVING GROUND
FIGURE 11
LOADING DOCK
CONCRETE BARRICADE
ROOF LINE ABOVE
KEY PLAN
SCALE: 1/16" = 1'-0"
PLAN
SCALE: 3/16" = 1'-0"
SECTION A-A
SCALE: 3/16" = 1'-0"
SECTION B-B
SCALE: 3/16" = 1'-0"
SECTION C-C
VENTILATOR
BACKFILL DRAIN
SLOPE

PACKAGING OF EXPLOSIVES -- IS ESD CONSIDERED?

E. E. Anspach, PE, CSP, CMS
Sverdrup Technology, Inc.
AEDC Group
Arnold Air Force Base, TN

M. D. Evans, CSP
Calspan Corporation
AEDC Division
Arnold Air Force Base, TN

ABSTRACT

Electrostatic Discharge (ESD) has been identified in the past as the probable cause of several propellant and electroexplosive device mishaps. ESD has become a subject of much interest in the solid-propellant rocket motor (SRM) community. Before static electricity can become active, it must be generated and have a location to accumulate. If the generation and accumulation phases can be controlled, then the risk of the ESD hazard can be significantly reduced. Means of such control are available, but materials now in use in shipping explosive devices often make those means either inapplicable or unnecessarily difficult to apply. This paper challenges the SRM and explosives communities to develop standard regulations to control the materials used in shipping and handling of explosives and explosive items.

INTRODUCTION

Arnold Engineering Development Center (AEDC) is an Air Force Systems Command (AFSC) facility involved in research, development and testing of new and existing weapons systems. The mission of the Center includes test firing of rocket motors at simulated altitude and handling of related and nonrelated electroexplosive devices (EED's). To accomplish this, many different manufacturers' explosive products must be received, inspected, stored, transported, prepared and fired. AEDC personnel involved in these operations have no control over selection of packaging and shipping container materials for the explosives transported to AEDC. Explosives items are often received in static-producing packing materials.

Electrostatic discharge (ESD) from packing materials and other sources is a well-documented hazard to explosive items. Electrostatic discharge occurs when a static charge moves from one material to another and can result in the inadvertent ignition of explosives. To understand the ESD hazard, knowledge of static electricity is necessary.

THE ESD PHENOMENON

Electrostatics has been looked upon as a potpourri of science, black art, and old wives' tales. In fact, it is a science that is not completely understood. Static electricity can be thought of as electric energy--that is, an electrical charge--at rest. Static electricity does not pose a problem until it is aroused from its resting place and made active. This activation is called electrostatic discharge. Static electricity can be represented by a triangle (Fig. 1).

Approved for public release; distribution is unlimited.

The sides of the triangle are 1) Generate, 2) Accumulate, and 3) Activate. For static electricity to pose a problem, all three sides of the triangle must exist. Therefore, elimination or effective control of any one of these triangle sides will provide control of risk associated with an ESD hazard.

Next, consider each side of the static triangle.

Generation

Static electricity can be generated by unbalancing the molecular construction of relatively non-conductive materials. The resulting phenomenon is called triboelectrification. Explained briefly, when two dissimilar materials make contact with each other, an exchange of electrons between the atoms in the surfaces of the materials takes place (Fig. 2). Electrons from one material move across the boundary between the two materials and associate with the other material. There will exist a difference in charge of the two materials, and when separated a significant potential difference (voltage) will result.

If both materials in contact are good conductors and they are separated, the charge imbalance at the interface will cease to exist because of the ease of electron flow between the two conductive materials. Both materials will then be at the same potential. If a dielectric material is in contact with a conductive material, then upon separation a charge will remain on both surfaces. However, the conductive material can be grounded to provide a path for the charge to bleed off. The dielectric does not have this capability and may maintain a charge accumulation for long periods of time. A composite listing of materials in the triboelectric series is shown in Fig.3. Cotton has been taken as the neutral material. The further apart paired materials are on the scale, the greater will be the charge transferred when they are separated.

Accumulation

The accumulation of electrostatic charge occurs when the charges generated on contact deposit themselves on the surfaces when the materials become separated. The ease by which the free electrons shared by the material surfaces during contact, return to equilibrium upon separation is a function of the material conductivity. The charge flows freely between the materials for good conduction. For nonconductors (dielectrics) the charge cannot flow freely and upon separation the materials retain their charges intact and accumulation occurs. The accumulation of charge for dielectrics is cummulative, depending on the number of times the materials make contact and are separated. That is, the more times the materials are separated, the greater will be the charge transferred, and consequently, the greater will be the static potential difference.

Charge generation/accumulation can occur simply by the wind blowing over a dielectric material. The charge that resides on a dielectric may remain for a significant period. The maximum charge density that can be accumulated on a dielectric surface is 2.65 x 10^{-5} coulombs/sq (Ref. 1). Above this value, corona discharge occurs.

Activation

The activation of static electricity (discharge) is a physical phenomenon dependent on both the generation and accumulation legs of the static triangle. The probability of activation is present if a charge can be generated and accumulated on the case of an electroexplosive device sufficient to initiate a case-to-ground discharge through the igniter explosive charge; or if the energy stored, resulting from separation of a nonconductive rocket motor case from mounting hardware, is sufficient to cause an electrical breakdown in the propellant and a high energy electrical discharge is possible. Therefore, if control of the static generation and/or accumulation legs of the triangle can be obtained, then the risk associated with activation can also be controlled.

Static Controls

How can static electricity be controlled? Based on the static triangle, eliminating any of the legs of the triangle will control static electricity. The control of activation is accomplished by the control of generation and/or accumulation. Without generation and accumulation activation cannot occur. There are five major methods available for controlling static generation and/or accumulation: 1) bonding and grounding, 2) relaxation time, 3) humidification, 4) ionization, and 5) increase electrical conductivity (Ref. 1). Bonding and grounding is the most effective technique for conductive materials.

At AEDC, a ground connection is made when a rocket motor is off-loaded, and a ground attachment remains until the motor leaves the Center. Grounding is providing a conducting path from the item in question to ground potential. Bonding is interconnecting items so they are all at the same potential.

Relaxation time is the time required for the generated/accumulated charge to dissipate to its surroundings. No material is totally nonconductive, the more conductive the dielectric, the more rapid the dissipation of charge.

Humidification enhances the conductivity of materials that have accumulated a static charge and can be accomplished simply by increasing the humidity of the work environment. However, humidification control is not possible for outdoor operation at extremely low temperatures or indoors when motors are being temperature-conditioned at low temperatures. Control of the humidity is not completely effective, it does not work for all materials because even in humid air, some plastics remain static-laden.

Ionization of the atmosphere surrounding and in contact with a charged material provides a conducting path for the charge to leak to ground. Ionization may be accomplished by placing a high voltage close to the material; however, the hazards associated with this technique make it impractical for use around explosives. Ionization can also be accomplished by the use of radioactive alpha particles. Another method of ionization is by induction. Induction may be accomplished by placing grounded combs, bristles and/or tinsel bars near the static-laden material.

The fifth major method of control is to increase the electrical conductivity of the connecting surfaces. This can be done with a topical antistat which is a chemical formulation possessing some degree of conductivity to bleed the static charge. Numerous sprays are available commercially; however, their period of activity is limited and they must be considered temporary.

Of the five methods presented for controlling static electricity associated with solid-propellant rocket motors, the increase of electrical conductivity is the best method; however, many times it is not a practical solution based on design constraints. The most practical and best technique is to adhere to the first two methods of control (bonding and grounding and relaxation time).

MISHAPS

To ignite bulk propellant by ESD, two conditons must exist (Ref. 2). First, the electric field in the propellant must be high enough to cause an electrical breakdown of the propellant. Second, there must be sufficient energy stored in the propellant to cause ignition once the electrical breakdown in the propellant occurs. Ignition may also be caused by an ESD from igniter case to the grounded leads through the igniter explosive charge. In summary, ESD ignites explosives by an electrical discharge through the propellant to ground resulting in the explosive material igniting during the energy dissipation.

Within The Department of Defense (DoD) and general industry, several explosives mishaps have occurred which were attributed to ESD. One of the earlier incidents involved the accidental ignition of the X-248 rocket motor used on the Delta launch vehicle (Ref. 3). In this instance, a plastic cover was removed from the motor during preparation procedures, resulting in an electrostatic discharge thru the igniter assembly and subsequent ignition of the rocket motor, killing three people and causing extensive damage. A more recent accident involving ESD occurred in West Germany in January 1985 when an operational rocket motor ignited during handling operations, killing three U.S. soldiers and injuring several others (Ref. 4). Investigation revealed that the propellant was ignited by an electrostatic discharge between the propellant grain and the rocket motor Kevlar[R] case.

AEDC EXPERIENCE

The recent receipt of several small retro-rockets at AEDC illustrates the need for regulations concerning electrostatic-producing packaging material. Twenty of the retro-rockets (fiberglass cases filled with solid propellant) arrived at AEDC in both wooden and metal containers. These motors had been in storage for 20 years at Vandenberg AFB, CA. The shipping containers for the motors complied with Department of Transportation (DOT) regulations and were properly marked for interstate shipment. When the motors arrived, eight of the 20 were chosen for testing. The remaining motors were returned to storage.

During the inspection, AEDC standard procedures were followed while removing the motors from the shipping containers. Electrostatic voltage was monitored using a static meter. The physical characteristics and the electrostatic measurements obtained for each motor are shown in Table 1.

Five of the 20 motors had been packed in wooden boxes with conductive bags and corrugated packing paper. During the unpacking and removal of these motors, the conductive bag was grounded and an electrostatic voltage was measurable (50 volts) on only one of the five motors . The remaining motors were packed in metal cans and contained in "form-fitting" foam-rubber protective cushions (Fig. 4).

The electrostatic voltages on these motors were significantly higher, ranging from 50 to 25,000 volts (Table 1). With the motors packed in this configuration, it was impossible to bleed the static charge to an acceptable level; therefore, the foam was separated from the motor over a period of hours to prevent a possible massive electrostatic discharge. This method took advantage of relaxation time to control charge generation.

Not only is static-producing packaging material found in the shipment of small explosives, but it is prevalent in large rocket motor shipping containers. A large solid-propellant rocket motor, tested at the AEDC originally consisted of a bare Kevlar case filled with solid propellant. Static potentials as high as 4500 volts were measured at AEDC when the bare Kevlar case was separated from the chocks on the mounting fixture during motor weighing operations (Table 2). The motor was separated from the mounting fixture six times (three to flex a load cell and three to obtain weight measurements).

The Ballistic Missile Office (BMO), through the "Propulsion Electro-Static Discharge Working Group" (PESDWG), sponsored an intensive effort and determined that the Kevlar cased SRM's were potentially susceptible to ESD ignition (Ref. 2). The PESDWG then recommended that Kevlar case rocket motors be coated with a conductive paint and relaxation time be incorporated in AEDC handling procedures. This corrective action resulted in no observable static potential during handling operations of the large SRM at AEDC and the effective control of an electrostatic hazard (Table 2). These are just a few examples of AEDC experience. Explosive initiators continue to be received in styrofoam and other static-producing packaging material.

STATIC MATERIAL TESTING

Research has been conducted on materials, and techniques have been developed to test material susceptibility to static buildup. A study conducted by NASA is representative of such research (Ref. 5). NASA, at the JFK Space Center, performed nine physical and chemical tests on 59 thin plastic films . One of the nine tests was "electrostatic testing". Two distinct electrostatic properties of a material were evaluated. The first test was the material's capability to develop a charge. This is shown by the peak triboelectric voltage generated. The second property evaluated was the material's ability to discharge the accumulated surface charge to ground. Data were obtained for both 30- and 45-percent relative humidity. The NASA electrostatic acceptance criteria (pass/fail) (Table 3) were determined by the decay of the generated voltage to a given level (350 volts) in a fixed period of time (five seconds). The peak value of the generated voltage was not evaluated. Only the achievement of the required final value of 350 volts in five seconds constituted acceptance.

The test method used in this study is a conservative approach; however, the study presents a listing of acceptable materials that are available for use with explosive items.

SUMMARY

Currently, there is no guidance or directive concerning the use of static-producing packaging materials with explosive items. Military Standard 1686 and Military Handbook 263 which discuss electrostatic discharge control for protection of electrical and electronic parts, assemblies and equipment (excluding electrically initiated explosive devices), specifically excludes EED's and explosive devices, leaving the manufacturer and distributors to determine proper packaging of these items. The technology and information to determine packaging material susceptibility to ESD are available. Materials used to package explosive items should minimize triboelectric and frictional charging and be slightly conductive to permit a safe slow distribution of generated charge. Use of these guidelines will virtually eliminate the possibility of ESD in explosive packaging material. Inquiries were made within the DoD community to determine if any specifications, regulations, policies, handbooks and/or standards exist for ESD packaging materials. No specific references other than the NASA study (Ref. 5) have been found. Information on suitable packaging material can be found in the literature; however, an extensive search and interpretation of results to determine use for explosive packaging is required.

The phenomenon of ESD is well known and the hazards are well documented. However, the explosives industry, the Department of Transportation, and other agencies regulating explosives shipments do not specify or regulate the materials which are used as packing materials for explosives shipments.

Industry and government agencies must develop standards or directives concerning the packaging material to be used with explosives devices to help prevent further damage and personal injury.

REFERENCES

1. Eichel, F. G., "Electrostatics," Chemical Engineering, March 13, 1967, McGraw Hill, Inc.

2. Peacekeeper Electrostatic Effects, Final Report of the Propulsion Electrostatic Discharge Working Group, January 1987, TRW Electronic and Defence Sector, BMO.

3. Electrostatic Ignition of X-248 Rocket Motors, Cornell Aeronautical Lab, Inc., Report DM-1934-E2-A, June 24, 1964 (Revised March 18, 1965).

4. Stephen, D., Technical Investigation of 11 January 1985 Pershing II Motor Fire, TR-RX-85-9, Vol. 1-11, June 1985.

5. Gompf, R. H., Physical and Chemical Test Results of Plastic Films, MTB-402-85, Materials Testing Lab, NASA, JFK Space Center, 3 March 1986.

ACTIVE STATIC ELECTRICITY
DEPENDS ON THREE (3) MECHANISMS

- CHARGE GENERATION
- CHARGE ACCUMULATION
- CHARGE ACTIVATION

WHICH CAN BE REPRESENTED BY THE
STATIC TRIANGLE

FOR ELECTROSTATIC ENERGIES TO BE ACTIVE (CAUSE IGNITION)
ALL THREE ELEMENTS OF TRIANGLE MUST OCCUR!

Fig. 1. Static Triangle

STATIC ELECTRICITY
IS
GENERATED
BY
UNBALANCING THE MOLECULAR CONSTRUCTION OF
RELATIVELY NON-CONDUCTIVE INSULATORS ---

-- WHICH HAPPENS --

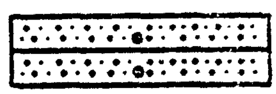

WHEN TWO (2) DISSIMILAR MATERIALS, THAT ARE IN CONTACT, ARE SEPARATED

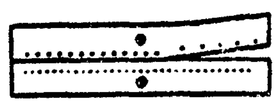

AN ELECTROSTATIC CHARGE REMAINS ON THE SURFACES OF
THE TWO MATERIALS AND A POTENTIAL DIFFERENCE (VOLTAGE)
BETWEEN THEM RESULTS.

THE AMOUNT OF CHARGE AT AN INTERFACE CAN BE GREATLY
ENHANCED BY MOVEMENT OR RUBBING THE MATERIALS TOGETHER.

Fig. 2. Triboelectric Charging Mechanism

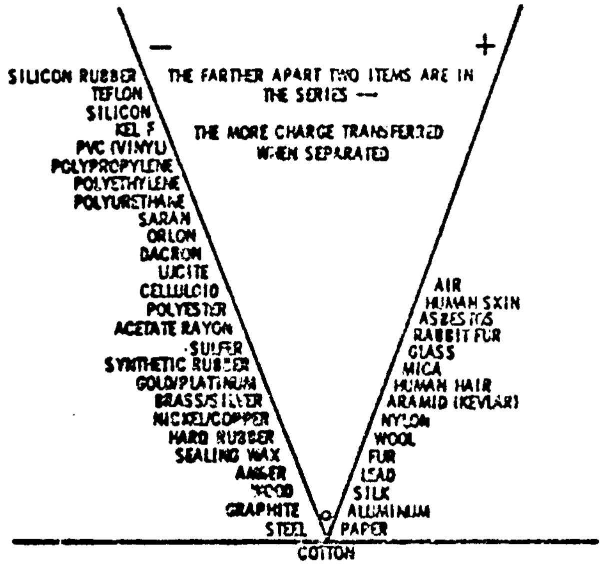

Fig. 3. Triboelectric Series

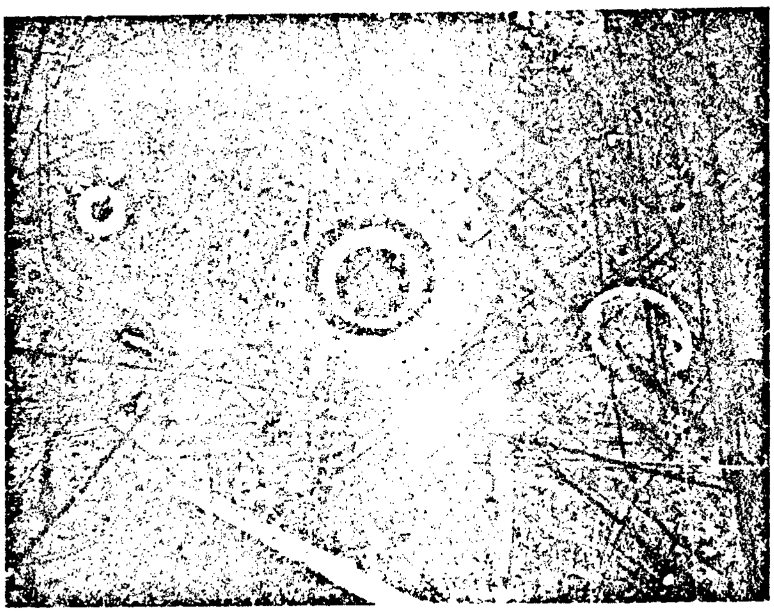

Fig. 4. Retro Rocket Protective Cushions

TABLE I. Summary of Retro Rocket Inspection Reports

Serial Number	External Packaging	Internal Packaging		Max. Volts	Comments
		Bag	Foam		
PN 2709	Wooden Box	Aluminized Velostat	---	50	
PN 2710	Wooden Box	"	---	0	
PN 2752	Wooden Box	"	---	0	
PN 2758	Wooden Box	"	---	0	
PN 2775	Wooden Box	"	---	0	
PN 2692	Metal Can	----	Soft White	600	Motor Removal - 100 v
PN 2699	Metal Can		Yellow	25000	Top Layer Foam - 25000 v Igniter Nylon Cover - 15,000 v Motor Case - 600 v
PN 2718	Metal Can	---	Pink	700	Decayed to 150 v in 12 min
PN 2741	Metal Can	Aluminized	Yellow	2000	
PN 2742	Metal Can	---	Pink/White	2000	Motor Removal - 300 v
PN 2745	Metal Can	---	Yellow	1500	Decayed to 200 v in 9 min
PN 2748	Metal Can	---	Mixed	3400	Fluctuated Between 2500 and 3400 v
PN 2761	Metal Can	---	Yellow	2700	Motor Case - 2000 v for 15 min Igniter Nylon Cover - 1500 v
PN 2762	Metal Can	---	White	500	
PN 2763	Metal Can	---	White/Yellow	23000	Waited 7 min to Remove Motor, Foam Removed from Can, 23,000 v Peak
PN 2767	Metal Can	---	Mixed	100	Fluctuated Between 50 and 100 v
PN 2768	Metal Can	---	Pink/White	700	Motor Removal - 150 v
PN 2769	Metal Can	Poly	Pink	3000	Fluctuated Between 2000 and 3000 v
PN 2771	Metal Can	---	Pink/White	2500	
PN 2774	Metal Can	---	White	2500	Remove Top Half Foam - 200 v Decayed to 300 v in 20 min Igniter Nylon Cover - 1600 v

TABLE II. Static Voltage Measurements.

Motor Designation	Date	Time	Temperature, °F	RH, percent	Operation	Max. Voltage	Location of Measurement
Q-6	09/04/85	0816	77	75	Motor Offloading from Martin Container	+200	Motor Mid-Barrel 40.5° Azimuth
Q-6	09/23/85	0905	72	63	Motor Weighing at Separation from Chock	+1500 (35 sec)	Fwd. Chock Contact Point
Q-6	09/26/85	1018	63	85	Motor Loading at Separation of Chock	+200	Motor Mid-Barrel
Q-6	10/14/85	0730	61	70	Test Preparation in J-4 Test Cell	0	All Points
Q-7	10/22/85	1031	65	95	Motor Offloading from Martin Container	+50	Mid-Barrel
Q-7	11/07/85	0930	56	43	Motor Weighing at Separation from Chock	+4500	Fwd. Chock Contact Point
Kevlar Motor Case Painted with Conductive Paint and Mounting Chocks Lined with Conductive Material.							
PQA-1	11/11/86	1000	65	38	Motor Offloading	0	All Points
PQA-1	12/18/86	1220	70	54	Motor Pre-Fire Weigh Separation from Chock	0	All Points

Note: All PQA-2 and PQA-3 Motor Handling Activities Yielded 0 Voltage - Static Measurement.

TABLE III. Electrostatic Test Results of Plastic Films

Brand Name	Generic Type	Electrostatics			
		30% Peak Voltage		45% Peak Voltage	
3M 2100	Polyester/Nickel	361	Pass	318	Pass
Aclar 22A	PCTFE	-6375	Fail	-15888	Fail
Aclar 33C	PCTFE	-16293	Fail	-21424	Fail
Altair 20	Polyester/Iridium	415	Pass	456	Pass
Ameri-Stat	Polyester/Metal/PE	486	Fail	297	Pass
AN-16	Nylon/PVF/Al	505	Fail	161	Pass
AN-18	Metallized PVF	286	Pass	342	Pass
AN-22	Nylon/PVF/Al	274	Pass	245	Pass
AN-CC	PVF/Metallized	331	Pass	177	Pass
Baltaron 2007	Polyvinyl Chloride	-1583	Fail	-5168	Fail
Black Polyethylene	Polyethylene (Black)	2555	Fail	2298	Fail
Capran 512	Nylon-6	24309	Fail	17726	Fail
Capran 512 - Stat	Nylon-6	8127	Fail	9806	Pass
Capran 980	Nylon	18328	Fail	17862	Fail
CF K-798	Kevlar/Teflon	-18900	Fail	-11349	Fail
Condulon Grid Bag	Nylon/C/Polyolefin	297	Pass	216	Pass
CRP Nylon	Nylon	18713	Fail	5574	Fail
CRP Pink Poly	Polypropylene	276	Pass	177	Pass
CRP Polyethylene	Polyethylene	13654	Fail	5558	Fail
CRP Polypropylene	Polypropylene	16935	Fail	5095	Fail
Faclon 1412	PVC/Nylon	18241	Pass	697	Pass
Glassclear A/S	PVC	18573	Pass	697	Pass
Griffolyn Nylon	Polyethylene/Nylon	22680	Fail	18643	Fail
Herculite 80	PVC/Dacron	1542	Pass	1012	Pass
Ipplon BW 900	Nylon	4075	Fail	421	Pass
Ipplon DP 1000	Nylon	16444	Fail	3729	Pass
Ipplon WN 1500	Nylon	20782	Fail	9558	Pass
Kapton LCL 1074	Polyimide	-14444	Fail	-14892	Fail
KN-80	Nylon/Kapton	5256	Fail	6049	Fail
Lectrolite	PVC/Polyester/C	467	Pass	233	Pass
Met Polyester 100	Polyester	497	Pass	184	Pass
Met Polyester 50	Polyester	492	Fail	202	Pass
MP 1880 (0.010 in.)	Polyurethane	15505	Fail	4111	Fail
MP 1880 (0.015 in.)	Polyurethane	14613	Fail	5063	Fail
MP 1880 (0.020 in.)	Polyurethane	5235	Fail	3819	Fail
PVC	Polyvinyl Chloride	-3463	Fail	6309	Fail
RCAS 1200	Polyethylene	737	Fail	242	Pass
RCAS 2400	Polyamide Nylon	6404	Fail	4787	Pass
RCAS 3600	Tyvek/Al/PE	981	Fail	683	Fail
RCAS 4200	Polyester/Al/PE	413	Pass	141	Pass
RCAS 4800	Polyester/SS/PE	392	Pass	213	Pass
Saran 18L	PVDC	14729	Fail	7797	Fail
Scharr Industries	Polyester/Al/PE	318	Pass	305	Pass
ST-500	Polyethylene (Pink)	266	Pass	232	Pass
ST-600	PE/PVA/Carbon	416	Pass	211	Pass
ST-700	PE w/Coating	326	Pass	—	Pass
ST-800	Polyethylene/Al	277	Pass	227	Pass
Tran-Polyethylene	Polyethylene	2566	Fail	1552	Fail
TX-300	Polypropylene	12263	Fail	12275	Fail
Velostat	Polyolefin (Black)	265	Pass	184	Pass
Wrightlon 4000A	PCTFE	-10623	Fail	-7745	Fail
Wrightlon 7000	Nylon (Green)	7009	Fail	10423	Pass
Wrightlon 7400	Nylon	18541	Fail	11334	Pass
Wrightlon 8400	Nylon	20233	Fail	9542	Pass
Wrightlon AS-3000	Nylon	16051	Fail	1470	Pass
Met Polyester 200	Polyester	No Data			
Proofilm	PVDC	No Data			
Teckfilm	Polyester/Gold	No Data			

HERO SAFE and Electrostatically Protected Electric Blasting Caps and Squibs

by

Robert L. Dov and Paul Proctor
NAVEODTECHCEN Indian Head, MD
10 August 1988

ABSTRACT

The Mk 11 Mod 0 Blasting Cap and the MK 20 Squib passed MIL STD 1385B testing and are HERO safe. The electromagnetic protection is provided by one MN-67 ferrite choke that is nonconductive, has a high curie temperature, and provides lover frequency attenuation than previous ferrites. The electrostatic protection is provided by a conductive mylar tape that dissipates both pin-to-pin and pin-to-case electrostatic changes. The combination protection fits inside the standard metal case and is lightweight, non-resonant, broad-banded, and low cost ($.15/unit).

This new protection approach is availalbe to be adapted to many currently unprotected EEDs. The only modifications required are to lengthen the case (to accommodate the choke) and to safely dissipate the heat generated when the RF energy is attenuated. All other EED characteristics remain unchanged.

The MK 11 Mod 0 provides an opportunity to buy military blasting caps at a lower unit cost than current unprotected caps. This can be accomplished by producing MK 11 Mod 0 on high speed blasting cap machines (instead of handline production) and combining buys for more efficient production runs.

The desingn concept is available to anyone working on DoD projects. US Patent 4,378,738 covers all applications. Assistance and consultation is available from the authors.

1. Introduction

The safety hazards associated with inadvertant firing of electroexplosive devices such as electric blasting caps, squibs and cartridges by stray electromagnetic or electrostatic are well known. The uncertainties associated with the levels of the energies in the field environments have lead to two types of solutions. The first was administrative procedures to limit the hazard levels, but this resulted in rather severe restrictions on use and greatly limited the user's flexibilty. The second was to formulate MIL STDs defining the worst expected environment and requiring all new designs to meet these requirements. The subject of this paper is a new technology combination that meet the requirements of MIL STD 1385B, provides electrostatic protection, and provides greatly improved safety protection. If fully implemented, it could provide the improved protection for many ordnance items at a lower unit cost.

2. HERO Safe and Electrostatically Protected Blasting Caps and Squibs

At last there are new electric blasting caps and squibs that have simultanious protection against both stray electromagnetic and electrostatic energy. The Mk 11 Mod 0 Blasting Cap and the Mk 20 Mod 0 Squib have successfully past MIL STD 1385B testing at NSWC Dahlgen and have been recorded as HERO Safe ordnance items. The Mk 11 Mod 0 Blasting Cap has the same explosive output and output diameter as the currently unprotected M6 Blasting Cap. The length was increased from 2.35 to 3.15 inches to allow inclusion of the choke assembly. The Mk 20 Mod 0 Squib was developed to ignite the Explosive Ordnance Disposal (EOD) Jet Perforater Tool. It also has the capability to ignite thermite grenades, diesel fuel (without using vicking material required by other squibs), atmospheric pressure ignition of scrap propellant, and can be used with adapters to ignite exsisting ordnance devices.

The electromagnetic protection is provided by a single MN 67 Ferrite Choke that fits inside the blasting cap's metal casing. The choke provides broadband protection from broadcast (below 1 megaHertz) through radar (35 giga- Hertz) frequencies without any resonances. The rf energy is attenuated by the choke and converted to heat. The heat is transferred to the metal case where it is safely dissipated. The choke design dissipates the same energy level as five ferrite beads, and the MN 67 ferrite attenuates at lower frequecies than previous formulations. These two factors combined to make a practical design where previous attempts had failed. The choke was fabricated with two orientation flats so automated equipment could be used to assemble the ordnance devices. NAVSEA Drawing 5206533 describes the design in detail.

The electrostatic protection is provided by a mylar tape with a special metal film that becomes conductive above 800 volts. This tape dissipates both pin-to-case and pin-to-pin stray electrostatic energy without significantly affecting the DC firing pulse energy. The Mk 11 Mod 0 Blasting Cap was successfully tested at Franklin Institute and Hercules Port Evan, New York up to 60,000 electrostatic volts without failure. The tape is also designed so it can be used on high speed automated production lines. NAVSEA Drawing 5206529 describes the design in detail.

The combination of the wire-wound ferrite choke and static resistant tape should cost between $0.10 and 0.15 per combination unit in high volume production.

3. Design Disclosure Package Information

The Mk 11 Mod 0 Blasting Cap and the Mk 20 Mod 0 Squib are Approved for Service Use and have coordinated design disclosure packages. The important characteristics of the designs are as follows:

Nomenclature: MK11 Mod 0 Cap, Blasting, Electric

HERO Safe Ordnance qualified to MIL STD 1385B

Electrostatically Protected to 60K electrostatic volts

Top Drawing Number: NAVSEA 5206524

Weapon Specification: WS 21886

NSN: 1385-01-145-1945

NALC Number: ML83

Nomenclature: Mk20 Mod 0 Squib, Electric

HERO Safe Ordnance qualified to MIL STD 1385B

Electrostatically Protected to 60K electrostatic volts

Top Drawing Number: NAVSEA 5761601

Weapon Specification: WS 21888

NSN: 1377-01-145-1947

NALC Number: MG 52

4. Standardization and Production Considerations

The Mk 11 Mod 0 Blasting Cap and the Mk 20 Mod 0 Squib share many of the same components to keep production and qualification costs low. The Mk 11 Mod 0 cap is being proposed as safer replacement for the currently unprotected M6 Blasting Cap. If the Mk 11 Mod 0 is produced in quantity on high speed automated production lines, it will be possible to produce a much safer cap at a lower unit cost. Costs as low as approximately $2.50 per cap may be possible if they are bought in lots over one million units and produced on commercial market high speed blasting cap lines.

The proposed standardization plan is as follows:

a. Standardize on the MK11 Mod 0 Blasting Cap because of its increased safety.

b. Remove the currently unprotected M6 from the inventory once current supplies are exhausted.

c. Combine requirements for current users and demonstrate increased safety to potential new users to get a lot size to approximately one million or larger.

d. Conduct competitive procurement with the following options to obtain lowest unit price:

(1) Multiyear or guaranteed total number buys.

(2) Standardize on the Mk20 Mod 0 Squib to get even larger lot sizes and lower costs.

(3) Automate choke winding.

(4) Investigate alternate packaging, bundle wrap, or other major cost savings design change.

(5) Offering design to the civilian market to get larger lot sizes and lower costs.

5. New Technology Applications

The new technology applications can be split into three categories. The first is the use the combination of the ferrite choke and tape in other currently unprotected devices. As an example, the combination will fit inside the Mk 1 Mod 0 Squib which currently without electromagnetic or electrostatic protection. The same approach could be attempted for the Mk 1 Mod 0 Squib as was done on the Mk 11 Mod 0 Cap:

a. Lengthen the case to accomodate existing choke, tape, and standoff.

b. Determine compatibility of the new design with existing commercial high speed blasting cap production line.

c. Qualify with a minimum of verification testing since nearly identical designs have already been qualified.

d. Perform a compatibility check to determine if incompatibilities exist and if adapters are required.

e. Produce pilot lot and qualify as required.

The retrofit program could continue as long as candidates are identified and funding made available for each new task.

The second category would be to use the existing technologies without the constraints of the existing design's dimensions. An example of this is the new EOD Firing Line Filter which was recently purchased. The design is detailed on NAVSEA Drawing 5206430 and the NSN is 1385 01-214-5397. The filter was recently tested to MIL STD 1385B and is part of the package required to make the MK 209 Mod 0 Electric Cartridge HERO Safe. Changing the dimensions of the ferrite choke did not adversely effect its performance.

The third category would be to make all new designs of electroexplosive devices use these technologies unless a lower cost alternative could be demonstrated. Standardization of the technologies required could be documented relatively easily now that the development is over. The current design has a significant safety factor so it should be a practical standardization candidate and applicable for the foreseeable future.

The design Concept is available to anyone working on DoD projects. US Patent 4,378,738 covers all applications contained in this paper. Assistance and consultation is available from the authors.

6. Summary

A new low cost design has been successfully demonstrated on the Mk 11 Mod 0 Blasting Cap and the Mk 20 Mod 0 Squib. Both designs have passed MIL STD 1385B and are classifed as HERO Safe Ordnance. With DoD wide standardization to get the lot size large enough, the Mk11 Mod 0 Blasting Cap will cost less and will provide greater protection than the currently unprotected M6 Blasting Cap. In high volume production, the wire-wound MN 67 Choke and Static Tape could cost between $0.10 and 0.15 per combination unit. The combined technologies have application to direct substitution in currently unprotected electroexplosive devices (EEDs), to incorporation in devices that will require changing the dimensions of the ferrite choke, and should become a standard and required in new design EEDs.

MDC H5025
AUGUST 1988

CONTROL OF TRIBOELECTRIC PHENOMENON ON PAM-DII

A. L. VAUGHER
C. M. WHITMEYER
E. A. WEBSTER

Presented to
XXIIIrd DOD Explosive Safety Seminar
Atlanta, GA
9-11 August 1988

MCDONNELL DOUGLAS ASTRONAUTICS COMPANY-HUNTINGTON BEACH

MCDONNELL DOUGLAS

CONTROL OF TRIBOELECTRIC
PHENOMENON ON PAM-DII

A.L. VAUSHER
C.M. WHITMEYER
E.A. WEBSTER

BACKGROUND

A catastrophic failure, inadvertent solid propellant ignition, occurred during erection operations of a Pershing II first stage in January 1985 at Heilborn, West Germany[1]. Because of the nature of the failure, it became apparent early on that the most likely cause was the presence of a nonconductive material (Kevlar motor case) that allowed the buildup of electrostatic charges. The exact failure mode, however, was questionable.

A massive effort by government agencies and industry attacked every aspect of the accident to determine the most likely failure mode, so that corrective actions could be implemented quickly. The investigation showed that the problem was most likely related to an electrostatic charge buildup, referred to as a triboelectric phenomenon, on the Kevlar motor case. Furthermore, details of the incident seemed to indicate that low temperature, low humidity, and motor handling contributed to the triboelectric charging.

At the time of the Pershing accident, the PAM-DII qualification program had been completed and the first vehicle was due to be shipped to Cape Canaveral within 6 months. Thus, very little time remained to solve what was felt to be an extremely critical risk management issue concerning the safety of solid rocket motors. PAM-DII would be the first upper stage with a Kevlar motor case to be launched by the Shuttle following the Pershing accident.

The aerospace industry has long been aware of the hazards associated with the electrostatic sensitivity of the motor ignition train. Accepted design practices for protecting the ignition system from electrostatic discharge (ESD) has centered around incorporating bonding, grounding, and shielding techniques, as well as procedure controls to prevent the buildup of electrostatic charges on the motor components. Based on the information at hand, it was believed that similar techniques should be expanded to mitigate

the problem of electrostatic charge buildup on a nonconductive motor case. This was tempered by the fact that the exact Pershing failure mode was not known at the time. Therefore, in developing a corrective action plan, all items, even those thought to be only remotely related, were thoroughly examined for completeness, safety, and practicality of the design.

DISCUSSION

Realizing the criticality and urgency of the problem, the PAM-DII design office formed an action group consisting of (1) a staff scientist to advise on the physics of triboelectric charging; (2) a manufacturing engineer to assure producibility; (3) a propulsion engineer to provide basic propellant formulation and motor construction advice as well as serving as an interface with the motor manufacturer; (4) an electronics engineer for bonding, grounding, and EMI/EMC concerns; (5) a safety engineer familiar with NASA/USAF ground operations and flight system safety requirements; (6) a structures designer; and (7) a project chief engineer.

The action group was responsible for adding all necessary protection to avoid a recurrence of the Pershing problem, as it was understood at the time, and re-examine existing features designed to abate related hazards. The latter was done to ensure the integrity of the design and the validity of a continuous conductive pathway to bleed off electrostatic charges. Practical steps that evolved from the action group recommendations were:

1. Ensure continuous electrical bonding, grounding, and shielding of the PAM-DII system flight hardware (Figure 1) consisting of the expendable vehicle (EV) and the airborne support equipment (ASE). MIL-B-5087, Class S electrical bonding requirements were emphasized and followed thoroughly. Redundant grounding provisions for the attachment of facility grounding cables directly to the motor case were implemented.

2. Provide positive electrostatic bleed-off for the motor case. After reviewing the physics of triboelectric charging, MDAC proceeded with engineering to protect the Kevlar motor case from the buildup of electric charges. It was decided that the best method would be to electrically bond the motor components together and cover the motor with a conductive material, creating a Faraday shield. Redundant grounding strips and aluminum foil tape were installed, as depicted in Figure 2.

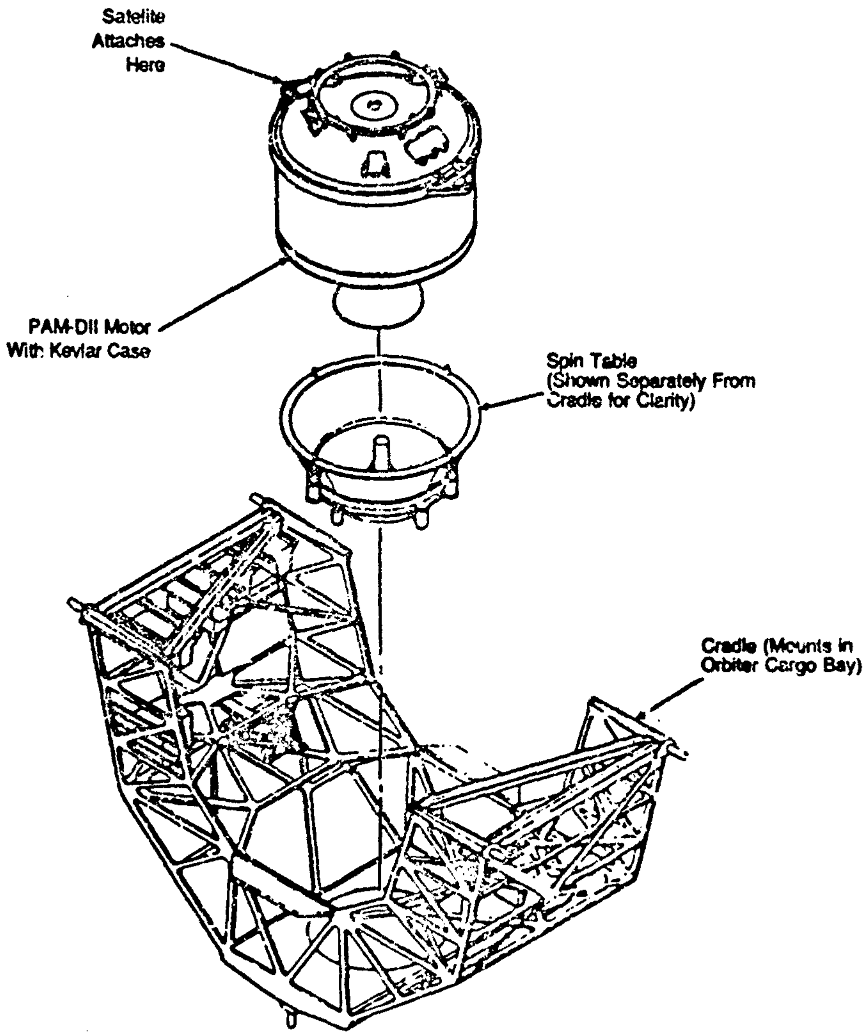

Figure 1. PAM-DII Flight System Hardware

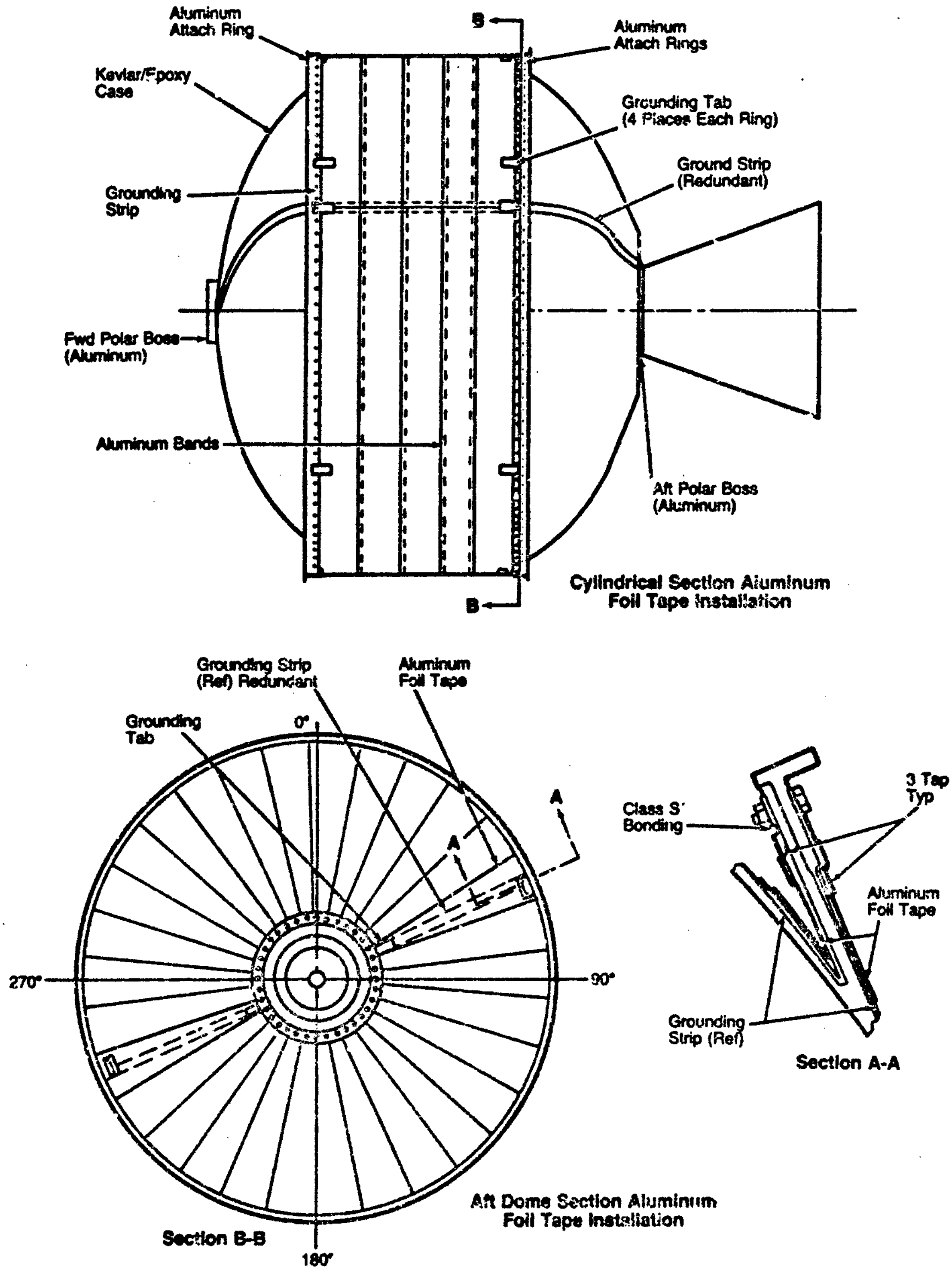

Figure 2. Aluminum Foil Installation and Grounding Provisions

3. Resolve possible ESD concerns related to other features of the motor design. The stress relief flap in the aft end of the motor (Figure 3) was also suspected of being susceptible to electrostatic charging. The face of the flap toward the motor case is Teflon and the matching surface is a rubber-like material. The concern was that if these surfaces made contact and then separated because of mechanical shock or vibration, a triboelectric charge could build up and produce an ESD. This was not thought to have a significant effect unless small propellant chips or particles were present in the gap between the flap and the motor case. The presence of these chips is possible after the propellant is machined to cut back unwanted propellant and contour the grain cavity for the desired burning surfaces. To prevent the propellant chips from entering the gap, the gap was blocked with conducting tape and filled with conductive plastic foam (Figure 3).

4. Review ground handling equipment designs (slings, lifting beams, hoists, handling fixtures, etc.) for proper and redundant bonding and grounding provisions.

5. Review motor shipping container grounding and Faraday cage provisions.

6. Review shipping and x-ray procedures for proper grounding.

7. Re-examine all motor assembly processing and handling procedures, especially prohibiting motor handling if the relative humidity drops below 30%.

8. Review facility designs (conductive floors, grounding straps, lightning protection, isolation, and personnel safety and training requirements).

Because of the Pershing incident, it was obvious that the methods used to secure against triboelectric charging would be subject to intense scrutiny. The choices for covering the Kevlar motor case included both metallic foils and conductive coatings. At the time, there were several concerns at McDonnell Douglas in connection with conductive coatings, including:

(a) Durability - possible deterioration over time.

(b) Verification - it could be difficult to determine if a change in the conductive coating resistance had occurred, and if so, what was the significance of the change. Both these factors could be important because if the shielding became isolated from ground, the motor might become a large capacitor, creating a more severe condition than a motor without shielding. Because of these uncertainties, and because a decision was needed immediately

VDP3748 T26K

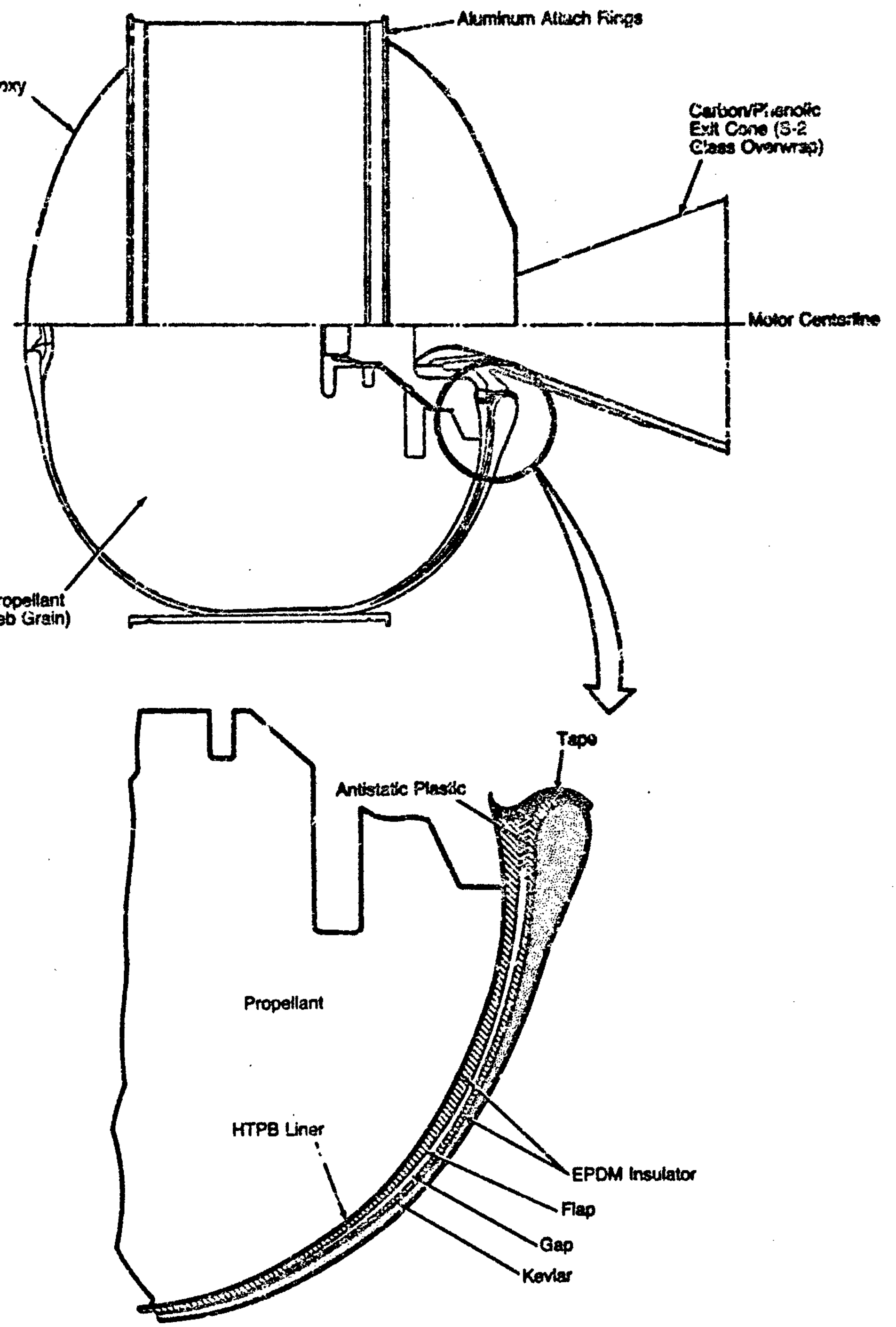

Figure 3. Blocking the Flap Gap With a Combination of Antistatic Plastic Foam and Tape

to support near-term PAM-DII launches, aluminum foil was chosen to form a complete Faraday cage around the motor. Such a system was not only predictably durable but easily verifiable with conventional ordnance-type ohmmeters.

SUMMARY

The approach to ESD control for the PAM-DII was to address all viable means by which inadvertent motor ignition could occur. Normal safety and grounding features were reviewed in great detail and enhanced. Ground handling, shipping, storage, launch processing procedures, and equipment were all included in the review and appropriate changes were implemented. The principal feature, an aluminum foil Faraday cage covering the Kevlar motor case, was chosen because of its effectiveness, durability, and simplicity, and because it could be easily verified with conventional instruments. Successive reviews by various agencies have confirmed the adequacy of the selected approach to ESD control.

REFERENCE

1. Knaur, James A. Technical Investigation of 11 January 1985 PERSHING II Motor Fire. Proceedings of the Twenty-Second Explosive Seminar, Anaheim, CA, 26-28 August 1986.

DETERMINATION OF ESD GROUNDING STRAP RESISTOR VALUES

BY

David R. Blinde, Honeywell DSG
and
C. Fred Mykkanen, Honeywell USD

INTRODUCTION

Electrostatic discharge (ESD) control grounding straps are a common precaution used in both the explosives industry and the electronics industry. These grounding straps are used to prevent the accumulation of static charge on an operator. In the explosives industry, accumulation of a static charge by an operator could inadvertantly cause initiation of a low energy initiator while in the electronics industry such static charges can degrade or destroy static sensitive electronic devices.

One feature common to grounding straps used in these two fields is a current limiting resistor. This resistor is used to assure that an operator would not be electrocuted if he /she were to come into contact with a high current source such as a standard electrical outlet. Commonly acepted safe electrical current levels (1 millamp to approximately 4 milliamp)[1] for people suggest that minimum resistor values in grounding straps should be in the range of 30K ohms to 440K ohms depending upon the selected safe current level and voltage source present (up to 440 volts is common in many manufacturing areas).

The latest revision of Safety Manual AMC R-385-100 states that the resistance value for an operator handling low energy initiators should be no greater than 250K ohms when measured from the opposite hand to ground. This value is clearly less than 440k ohms and almost certainly reflects a legitimate concern on the part of AMC that the standard must be conservative enough to assure that static voltages on operators could not achieve a level sufficient to cause initiation of an explosive component. The use of a simple maximum value in the standard however may lead some people to utilize extremely low resistance value resistors in their grounding straps and thus jeopordize employee health vis-a-vis common high current sources such as standard or high voltage electrical outlets. The Contractors Safety Manual, DOD 4145.26m takes a different approach stating that resistance should be between 250K ohms and 1 Megohm when measured from the opposite hand to ground.

Research reported in this paper was aimed at providing a sound technical basis for determing safe maximum resistor values that could be used without allowing dangerous static charges to develop on an operator. The research (see table 3), in fact, indicates that grounding resistance values substantially in excess of those allowed by AMC R-385-100 and DOD 4145.26m will satisfactorily limit operator static voltage levels for devices that are energy sensitive as low as 10 ergs (or even lower depending upon the desired safety factor).

THEORY

This paper develops a model (through the utilization of designed experiments) which describes the voltage generation process for a grounded operator. Utilization of the designed experiment results as well as work by the authors and other researchers[2] on the maximum voltage generation rates that can be produced by ungrounded operators, permitted development of an equation that computes the maximum voltage that an operator can develop for a given grounding resistance.

Designed Experiment methodology

Design of Experiments is a body of knowledge which relies heavily upon statistical analysis techniques and is used to improve the knowledge that can be gained from an experiment. This methodology has been used successfully for many years in many fields of work and has the significant advantage of minimizing the number of tests needed to perform an effective experiment. In simple terms, designed experiments differ from the more traditional "one variable at a time" experimental methodology because more than one independent parameter is varied at a time to determine the effect on the response of interest. The way in which these parameters are simultaneously varied is dependent upon the particular design that is used. All designs however possess the characteristic that it is mathematically possible to determine the effects of individual parameters on the response as well as to determine the interactions between parameters and the effects of those interactions upon the response. Interactions cannot be determined using the "one variable at a time" technique.

This study utilizes both a Box Behnken design and Central Composite design to analyze the response (voltage on an operator) as a function of the independent parameters of operator activity level, operator capacitance, environmental relative humidity, and grounding resistance value. Detailed information on the designed experiment methodology is available in a number of resource documents.[3,4,5,6]

Voltage generation by the capacitive shift process

The capacitive shift process is used in this paper as the most severe method currently recognized for rapidly generating voltages on an operator performing normal work activities. The voltage generation rates that have been found for the process are, in this paper, applied to the general findings of the designed experiments to develop an appropriate model for worst case voltage generation by a grounded operator. For that application to make sense, it is necessary to evaluate conditions associated with the capacitive shift process. That evaluation is hereafter performed using a simple capacitor analogy for an operator in order to simplify understanding of the process.

First, since the capacitive shift process involves a voltage increase (from V1 to V2) in concert with a lowering of operator capacitance from C1 to C2, it is clear that the energy stored on the operator by that process would not be as high as for someone whose capacitance remained fixed at the high initial level of C1 while being charged from V1 to V2 as a result of triboelectric charging. The ratio of energy deltas (final energy - initial energy) for the two processes would in fact vary from case to case depending upon the initial and final voltages of the operator. That situation can be expressed by the simple expressions listed below:

$$\text{EQ 1.} \quad \frac{E_2\text{-}E_1(\text{cap})}{E_2\text{-}E_1(\text{tribo})} = \frac{.5\,C_2V_2^2 - .5C_1V_1^2}{.5C_1V_2^2 - .5C_1V_1^2} = \frac{V_1}{V1 + V2}$$

Strictly speaking therefore, any general application of capacitive shift process voltage change rates to a model derived from triboelectric charging data (i.e. the designed experiments performed in this study) should consider the energy effects. Practically speaking however, it should be clear that the high voltage generation rates in the capacitive shift process when applied to the triboelectrically derived model produces conservative results with a safety factor which is the inverse of the ratio observed in equation 1. For large differences in V1 and V2 the safety factor would be very large while for small differences the safety factor would be small.

Second, since relative humidity is shown in the triboelectric Box Behnken experiment to be of little importance over the grounding resistance values used in this study, it is important to also understand how relative humidity might effect the capacitive shift process. If we again consider an operator to be represented as a simple parallel plate capacitor, it is possible to theoretically examine the factors which influence voltage. Equation 2 below indicates that voltage is a function of charge (Q), plate area (A), plate separation (D), and the permittivity of the dielectric (ε).

EQ 2. $V = DQ/A\varepsilon$

Differentiation of that equation with respect to time to represent what occurs when an operator moves yields equation 3 (which reasonably assumes that Q and A may be treated as constants):

EQ 3. $dV/dt = (Q/A\varepsilon)(dD/dt) - (D/\varepsilon^2)(d\varepsilon/dt)$

Both of the differential terms on the right side of the equation are clearly dependent upon the speed of movement and not dependent upon relative humidity. The one term which could have a dependence upon relative humidity is the permittivity of the dielectric (ε). In the situation we examine in this paper, that dielectric is in effect primarily composed of air, and shoe sole material. The combined effective permittivity of those materials is in fact essentially independent of relative humidity based upon test subject capacitance measurements performed during the experiments. This finding indicates that the lack of humidity dependence for the model derived through triboelectric generation data is consistent with the behavior of the capacitive shift process.

EXPERIMENT

Prior to the performance of this experiment, work performed by 3M corporation suggested that voltage generation by the capacitive shift process produced voltage levels on operators more rapidly than any other available mechanism. In order to confirm their conclusions with regard to voltage generation, an experiment was performed in which the voltage on three different test subjects with effective capacitances of 67, 155, and 294 pf was monitored while the subjects generated voltage through triboelectric charging. The accumulated voltage was monitored on a chart recorder with the subjects not grounded, grounded through 200 megohm, grounded through 20 megohm, and grounded through 1 megohm. These tests were performed at three different relative humidity levels (1%, 35%, and 61%).

Determination of voltage on the test subjects was performed by electrically connecting the subjects to a conductive plate which was monitored by a Monroe model 175 electrostatic voltmeter. The voltage monitoring plate was electrically connected by a wrist strap (no protective resistor employed) to the subjects' right wrist. The grounding wrist strap used in the experiment was connected to the subjects left wrist to assure that charge dissipation could occur only by current flow through the subject. Figure 1 (which provides a pictorial view of the test arrangement used for the two designed experiments that will be described later) is very similar to the test arrangment used in this portion of the study. For this portion of the study the Van De Graaff connection to the subject was broken.The subject held a rubbing plate in the left hand and a rubbing cloth in the right hand. This arrangement was found to produce greater voltages than observed by simply setting the rubbing plate on the table and rubbing with the right hand.

FIGURE 1
(TEST SYSTEM DIAGRAM)

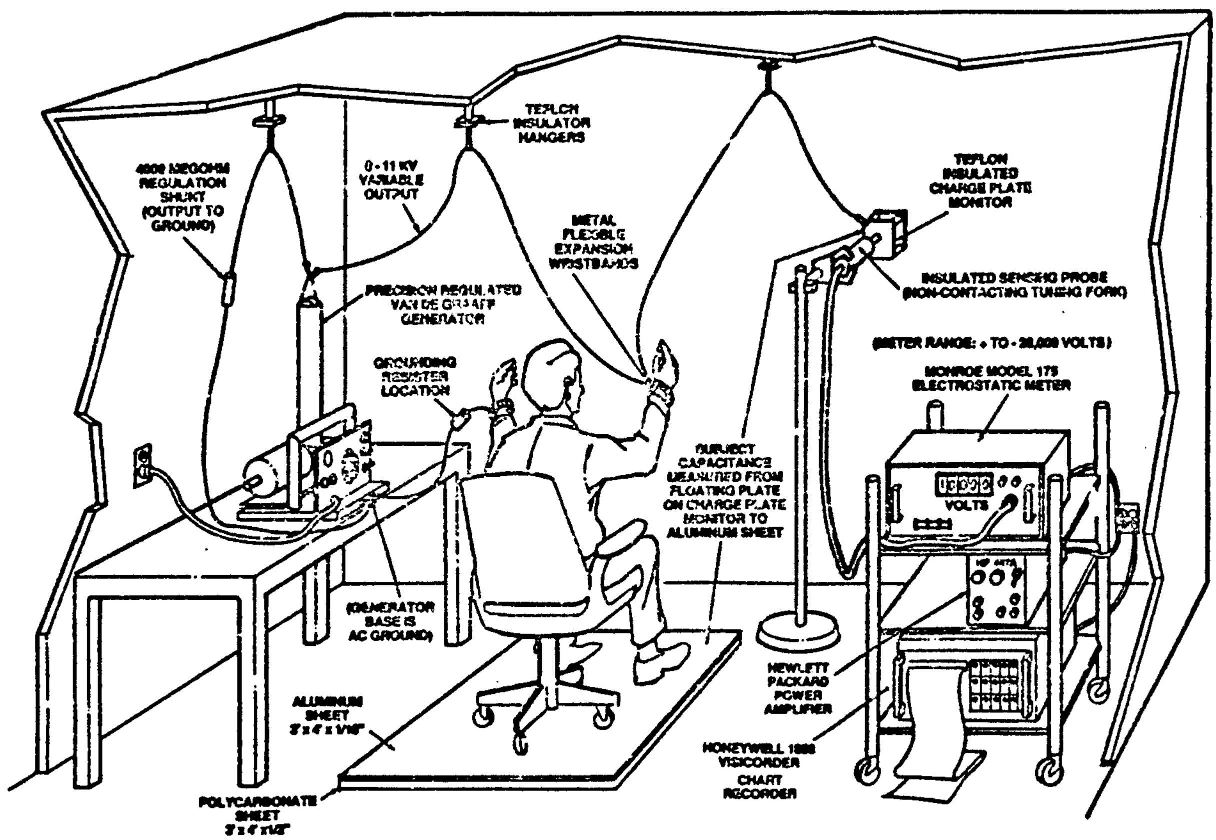

A number of different materials were used in this test. Rubbing plates of teflon, glass, aluminum, and polycarbonate were used. The rubbing cloth materials were cotton, polypropylene, conductive carpet, polyester, silk, nylon,and bare hand.These items were selected to provide a large number of combinations representing materials at opposite ends of the triboelectric series and were rubbed very vigorously to create the highest possible static potential.

The second portion of the study was a modeling effort utilizing designed experiments to analytically determine the effects of relative humidity, operator capacitance, operator activity level, and grounding resistance on operator voltage. These tests were performed using a modified commercial Van De Graaff generator to simulate operator activity level. Major modifications to the generator included replacement of the original belt motor with a 0 to 5000 rpm, 1/15 hp ac/dc motor; addition of a calibrated autotransformer; addition of a voltage regulation shunt of about 4000 megohms; and selection of a special belt, belt treatment and pulley materials. These modifications made it possible to control the voltage generation rate to within less than 2% of the desired value. Photographs of the Van De Graaff generator are shown in figure 2.

FIGURE 2
(VAN DE GRAAFF GENERATOR)

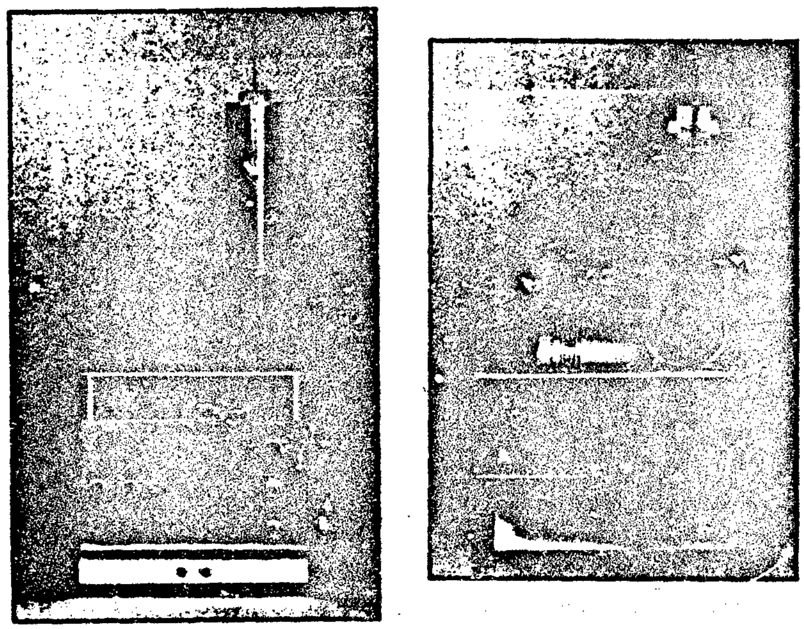

The two experimental designs used in this study were a modified three level, four variable Box Behnken design and a five level, two variable Central Composite design. As noted earlier, the experimental set-up for these tests is shown in figure 1. The Box Behnken design was utilized to determine which factors had significant influence on operator voltage while the Central Composite design was used to more precisely quantify the influence of the significant parameters.

Variable levels for the Box Behnken design were:

1. grounding resistance - 200 megohm, 10 megohm, 0.602 megohm
2. generator belt speed - 23.9, 21.7, and 18.4 inches/sec.
3. relative humidity - 44%, 15%, 2%
4. test subject capacitance - 294, 155, and 67 picofarad

Variable levels for the Central Composite design were:

1. grounding resistance - 200 megohms, 171 megohm, 100.5 megohm, 30 megohm, and 0.602 megohm
2. generator belt speed - 23.9, 23.3, 21.7, 19.5, and 18.4 inches/sec

TEST RESULTS AND DISCUSSION

Triboelectric charging tests

Some typical results from the triboelectric charging experiment are shown below in table 1. These results are typical of data when the charging plate was teflon (teflon produced the highest observed voltages).

TABLE 1
(TRIBOELECTRIC CHARGING DATA)

RUBBING MATERIAL	GROUNDING RESISTANCE	1% RH	|VOLTAGE| 35% RH	61% RH
COTTON	OPEN	410	580	60
	200 MEG	210	260	40
	20 MEG	30	120	30
	1 MEG	0	0	0
POLYESTER	OPEN	460	580	60
	200 MEG	210	340	30
	20 MEG	20	120	10
	1 MEG	0	0	0
WOOL	OPEN	440	520	90
	200 MEG	240	470	30
	20 MEG	40	90	10
	1 MEG	0	0	0

A simplified typical waveform for this data is shown in figure 3. Examination of the waveform clearly indicates that it consists of two components. The first and major component is a cyclic charging pattern which exhibited a frequency identical to the rubbing frequency associated with the charging materials. This bipolar pattern is believed to be the result of induction charging caused by movement of the operators hand over the highly charged (>> 10 k volts) teflon rubbing plate. The second and much smaller component was a unipolar voltage shift caused by the transfer of charge from the rubbing material to the body of the test subject. The triboelectric generation tests exhibited a maximum voltage generation rate of 3600 volts/sec.

FIGURE 3
(TRIBOELECTRIC CHARGING WAVEFORM)

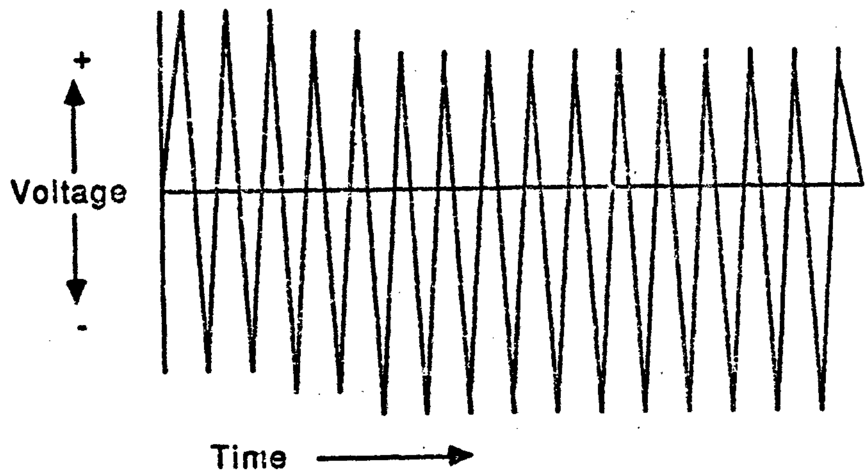

Examination of table 1 indicates that voltage on the operator decreases as expected as the grounding resistor value decreases. In addition, as suggested by this abbreviated table, no voltage was ever observed on a operator grounded through 1 megohm of resistance for any of the test plate /rubbing material combinations examined. Two characteristics of table 1 at first examination may appear in error if examined simplisticalty . These characteristics are the lack of a definite progression of voltage amplitude in concert with the triboelectric charging series and changing relative humidity. We believe these progressions do not exist due to 1) the dominance of the inductive component of the charging waveform, 2) the existance of uncontrollable variables associated with this process (i.e. rubing speed/pressure, etc.), 3) the fact that the reported voltages exist on the test subject and not the materials (i.e. charge transfer plays a dominant role), and 4) increasing relative humidity should increase human and insulator conductivity characteristics while decreasing triboelectric charging propensity.

These tests were primarily useful in determining general characteristics associated with the triboelectric charging process. They are of limited value for modeling purposes however due to uncontrollable parameters which have previously been described. Our major use of these findings in the study was, in fact, to simply compare the results to previously available data associated with the capacitive shift process. That comparison indicates that the maximun voltage shift rate of 5000 volts/sec which has been obvserved with the capacitive shift process represents the most severe charging senario currently known. Secondly, the triboelectric charging senario we examined represents an extreme situation which should never be seen in an ESD controlled environment unlike the capacitive shift situation which is very much a "real world" situation.

Designed Experiments

Modeling of operator voltage generation was accomplished through the use of two designed experiments. The first experiment which was a three level, four variable modified Box Behnken design demonstrated that, for the range of values examined, human activity level (i.e. Van De Graaff speed) and grounding resistance value are the primary controlling factors for human voltage level. Relative humidity also begins to become important at the upper end of the resistance range for significant activity levels, but the effect is still relatively small for the range of values we examined. Data from this experiment is listed in table 2.

TABLE 2
(VARIABLE EFFECTS - BOX BEHNKEN DESIGN)

A. Low speed (a) to high speed (b) voltage effects for listed test conditions

R.H.%	CAP. pf	RES. ohms	VOLTAGE (a)	VOLTAGE (b)	(b-a)/a	EFFECT
15	155	602k	0	1	undefined	n/a
15	155	200 meg	161	489	+2.04	yes
15	67	10.28 meg	8	24	+2	yes
2	155	10.28 meg	8	26	+2.25	yes
15	294	10.28 meg	8	23	+1.88	yes
44	155	10.28 meg	5	27	+4.4	yes

B. Low R.H. (a) to high R.H. (b) voltage effects for listed test conditions

SPEED dial value	CAP. pf	RES. ohms	VOLTAGE (a)	VOLTAGE (b)	(b-a)/a	EFFECT
37.5	67	10.28 meg	17	16	-.06	no
45	155	10.28 meg	26	27	+.04	no
37.5	294	10.28 meg	17	17	0.0	no
37.5	155	200 meg	367	330	-.10	small
30	155	10.28 meg	8	5	-.38	small
37.5	155	602k	0	2	undefined	n/a

C. Low capacitance (a) to high capacitance (b) voltage effects for listed test conditions

R.H.%	SPEED dial value	RES. ohms	VOLTAGE (a)	VOLTAGE (b)	(b-a)/a	EFFECT
2	37.5	10.28 meg	17	17	0.0	no
15	37.5	200 meg	297	298	0.0	no
15	37.5	602k	1	1	0.0	no
44	37.5	10.28 meg	16	17	+.06	no
15	45	10.28 meg	24	23	-.04	no
15	30	10.28 meg	5	5	0.0	no

D. low resistance (a) to high resistance (b) voltage effects for listed test conditions

R.H.%	CAP. pf	SPEED dial value	VOLTAGE (a)	VOLTAGE (b)	(b-a)/a	EFFECT
2	155	37.5	0	332	>+332	yes
15	67	37.5	1	297	+296	yes
15	294	37.5	0	296	>+296	yes
44	155	37.5	2	367	+183	yes
15	155	45	0	489	>+489	yes
15	155	30	1	161	+100	yes

Multiple regression analysis of the data listed in table 2 produced a predictive model for operator voltage as a function of the examined factors. That model had a confidence factor of 98.87%. In order to provide an even better model of the factors which were initially determined to be significant, a second designed experiment was performed. This experiment which was a five level, two variable Central Composite design produced a model with a 99.99% confidence factor. The predictive equation developed from that experiment (which relates activity level and grounding resistor value to operator voltage) is listed as equation 4. It should be noted that equation 4 is similar, but not identical to, the equation that can be developed from the modified Box Behnken experiment. The differences are primarily a result of the fact that different generator belts (with somewhat different triboelectric charging characteristics) were used in the two experiments. Nearly identical results are obtained from the two models for a given resistance value when generator speeds which produce the same charging characteristics are chosen.

EQ 4. volts = 234.7 + 85.924 (spd) + 165.089 (res) + 64.25 (spd)(res) - 1.551 (spd)(spd)

NOTE: spd = autotransformer dial set of Van De Graaff generator
res = resistance to ground for test subject
for equation 4 to yield the correct answer, both speed and resistance must be transformed linearly to the scales shown below:

dial speed transform		resistance transform	
32.1959	-1	29.7925 meg	-1
37.5	0	100.301 meg	0
42.8041	+1	170.809 meg	+1

In order for these findings to be useful in determining a reasonable upper limit for grounding resistors it is necessary to relate Van De Graaff output characteristics to dial speed. That relationship is provided in figure 4. Secondly it is necessary to determine the Van De Graaff level which simulates expected worst-case behavior for an operator. As noted earlier, the 3M study which found typical maximum voltage generation rates of 5000 volts/sec for different test subjects currently provides the best information available on worst-case voltage generation by an operator. Substituting into equation 4 the dial speed transform (+.2639) for a 5000 volt/sec voltage generation rate and the voltage value that can be permitted on an operator makes it possible to calculate a reasonable upper limit to the grounding resistor value. An exact solution for resistance can be determined by using the quadratic equation. Alternatively, since the coefficient of the R-squared term is very small, that term could be dropped and the equation solved as a simple linear function. Determination of the appropriate operator voltage level is based upon a simple calculation from a known energy sensitivity for the explosive device to be handled. That calculation is based upon equation 5 and assumes a human body capacitance (C) of 500 picofarad.

EQ 5. $E \text{ (joules)} = 0.5\, CV^2$

FIGURE 4
(DIAL SETTING VS. VOLTAGE RISE TIME)

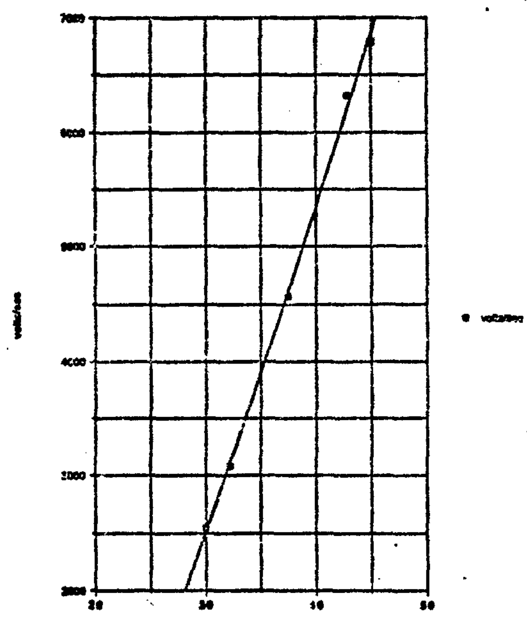

Operator voltages predicted on the basis of equation 4 are shown in figure 5 along with actual values seen for grounded test subjects in the 3M study. These curves show that the designed experiments provide more conservative resistance values. This difference is believed to be a direct consequence of the different time scales over which the Van De Graaff and capacitive shift process can produce voltage changes on the order of 5000 volts/sec. Equation 4 can be normalized to predict results equivalent to the capacitive shift data by multiplying the right side of the equation by .29 to yield equation 6 (notes which apply to equation 4 also apply to equation 6).

EQ 6. Volts = 68.063 + 24.918 (spd) + 47.876 (res) + 18.633 (spd)(res) - 0.45 (res)(res)

FIGURE 5
(PREDICTED VS. OBSERVED VOLTAGE)

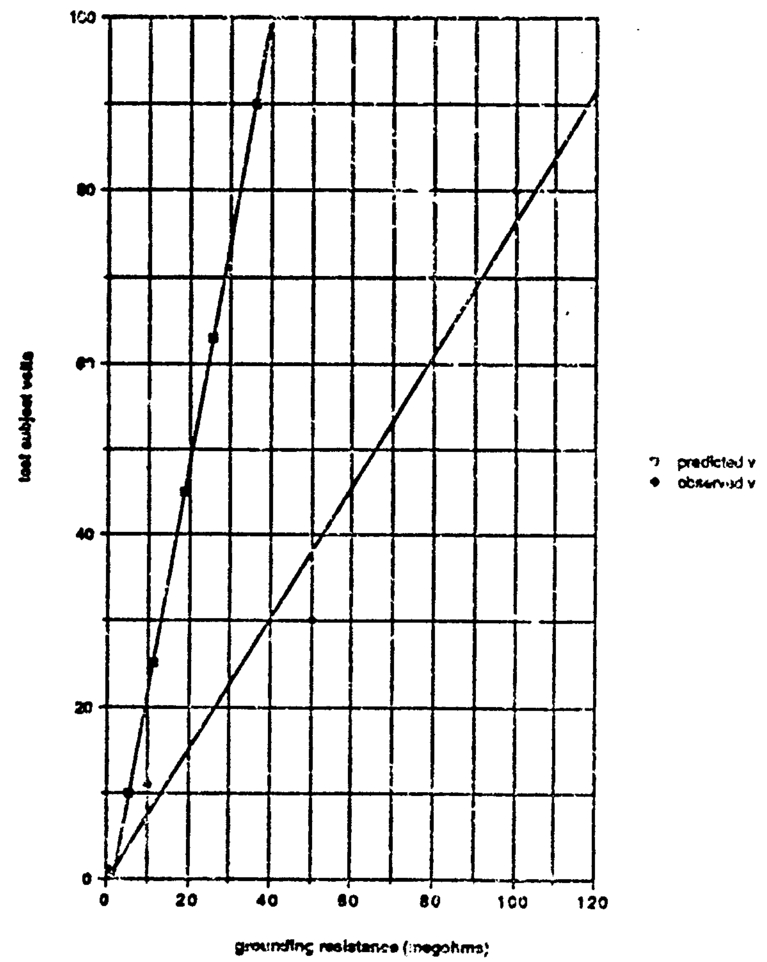

Table 3 provides an example of explosive detonation energy versus allowed grounding resistance value for an operator. The allowed resistance values are shown for four different safety factors. These safety factors are solely based upon the specified fractional reduction in the energy factor column and do not include previously described indeterminate factors which increase the safety margin or the potentially significant energy losses which can occur when energy is transferred from an operator to a device.

TABLE 3
(INITIATION ENERGY VS. ALLOWED RESISTANCE)

ENERGY FACTOR (ERGS)	RESISTANCE (MEGOHMS) FOR SPECIFIED SAFETY FACTOR			
	1 TO 1	1 TO 2	1 TO 5	1 TO 10
10	84.8	60.7	38.0	27.3
50	188.9	134.1	84.8	60.7
100	>200	188.9	119.5	84.8
200	>200	>200	188.9	134.1

Stated another way, an M100 point to case metal bridgewire detonator with a static energy sensitivity of 263 ergs is, from an energy point of view, protected at a level more than 450,000 times what is required when total grounding resistance is 1.25 megohm. This determination was made using normalized equation number 6 (resistance transform of -1.4048 and speed transform of +.2639) which predicts that at a 5000 volts/sec. charging rate and at 1.25 megohm total grounding resistance the voltage developed on an operator would be roughly .47 volts. Comparing the energy stored at that voltage on an 500 picofarad operator with the 263 erg sensitivity level of the detonator yields the heretofore listed safety factor.

CONCLUSIONS

1) A 5000 volts/sec. rise time, as observed for the capacitive shift process, currently represents the worst-case voltage generation senario for an operator.

2) Operator activity and grounding resistance value are the two major factors which effect operator voltage levels. Relative humidity and operator capacitance play no significant role at grounding resistance values below 200 megohms (for a 5000 volts/sec. charging rate).

3) Grounding resistance values considerably in excess of those permitted by AMC R-385-100 and DOD 4145.26m should safely limit electrostatic voltages on operating personnel (Ref. table 3).

ACKNOWLEDGEMENTS

The authors wish to acknowledge the contributions of the following people.

1) Mr. D. Clark for multiple regression analysis of the modified Box Behnken design data.
2) Mr. E. Edwards for his assistance with the experimental set-up.
3) Dr. A. Joglekar for general assistance with the designed experiment methodology.
4) Mr. J. Kremers for his assistance with the experimental set-up.
5) Mr. J. Lee of ICI Americas who provided initiator sensitivity information.
6) Mr. D. Swenson of 3M with whom we discussed the 3M capacitive shift experiment.

REFERENCES

1) MIL-STD-454 , Standard General Requirements for Electronic Equipment
2) James R. Huntsman and Donald J. Yenni, Jr., "Test Methods for Static Control Products", 1982 EOS/ESD symposium proceedings, p. 94.
3)G.E.P. Box, William G. Hunter, J. Stuart Hunter, Statistics for Experimenters, John Wiley and Sons, inc., 1978.
4)O. L. Davies (ed.), Design and Analysis of Industrial Experiments, Hafner (MacMillan), 1954.
5)Charles R. Hicks, Fundamental Concepts in the Design of Experiments, Holt, Rinehart and Winston, Inc., 1973
6) Bernard Ostle, Statistics in Research, The Iowa State University Press, 1963

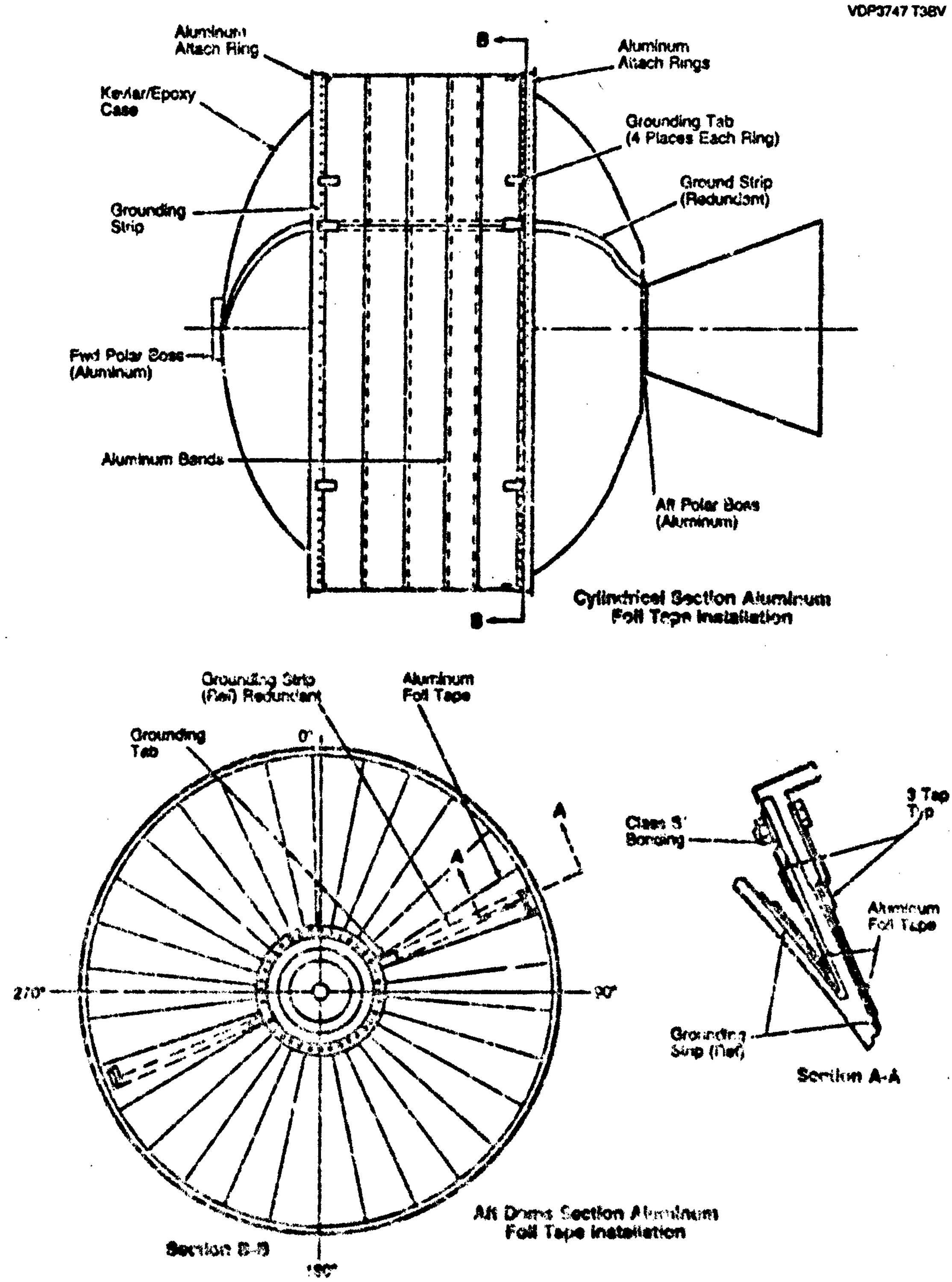

Figure 2. Aluminum Foil Installation and Grounding Provisions

3. Resolve possible ESD concerns related to other features of the motor design. The stress relief flap in the aft end of the motor (Figure 3) was also suspected of being susceptible to electrostatic charging. The face of the flap toward the motor case is Teflon and the matching surface is a rubber-like material. The concern was that if these surfaces made contact and then separated because of mechanical shock or vibration, a triboelectric charge could build up and produce an ESD. This was not thought to have a significant effect unless small propellant chips or particles were present in the gap between the flap and the motor case. The presence of these chips is possible after the propellant is machined to cut back unwanted propellant and contour the grain cavity for the desired burning surfaces. To prevent the propellant chips from entering the gap, the gap was blocked with conducting tape and filled with conductive plastic foam (Figure 3).

4. Review ground handling equipment designs (slings, lifting beams, hoists, handling fixtures, etc.) for proper and redundant bonding and grounding provisions.

5. Review motor shipping container grounding and Faraday cage provisions.

6. Review shipping and x-ray procedures for proper grounding.

7. Re-examine all motor assembly processing and handling procedures, especially prohibiting motor handling if the relative humidity drops below 30%.

8. Review facility designs (conductive floors, grounding straps, lightning protection, isolation, and personnel safety and training requirements).

Because of the Pershing incident, it was obvious that the methods used to secure against triboelectric charging would be subject to intense scrutiny. The choices for covering the Kevlar motor case included both metallic foils and conductive coatings. At the time, there were several concerns at McDonnell Douglas in connection with conductive coatings, including:

(a) Durability - possible deterioration over time.

(b) Verification - it could be difficult to determine if a change in the conductive coating resistance had occurred, and if so, what was the significance of the change. Both these factors could be important because if the shielding became isolated from ground, the motor might become a large capacitor, creating a more severe condition than a motor without shielding. Because of these uncertainties, and because a decision was needed immediately

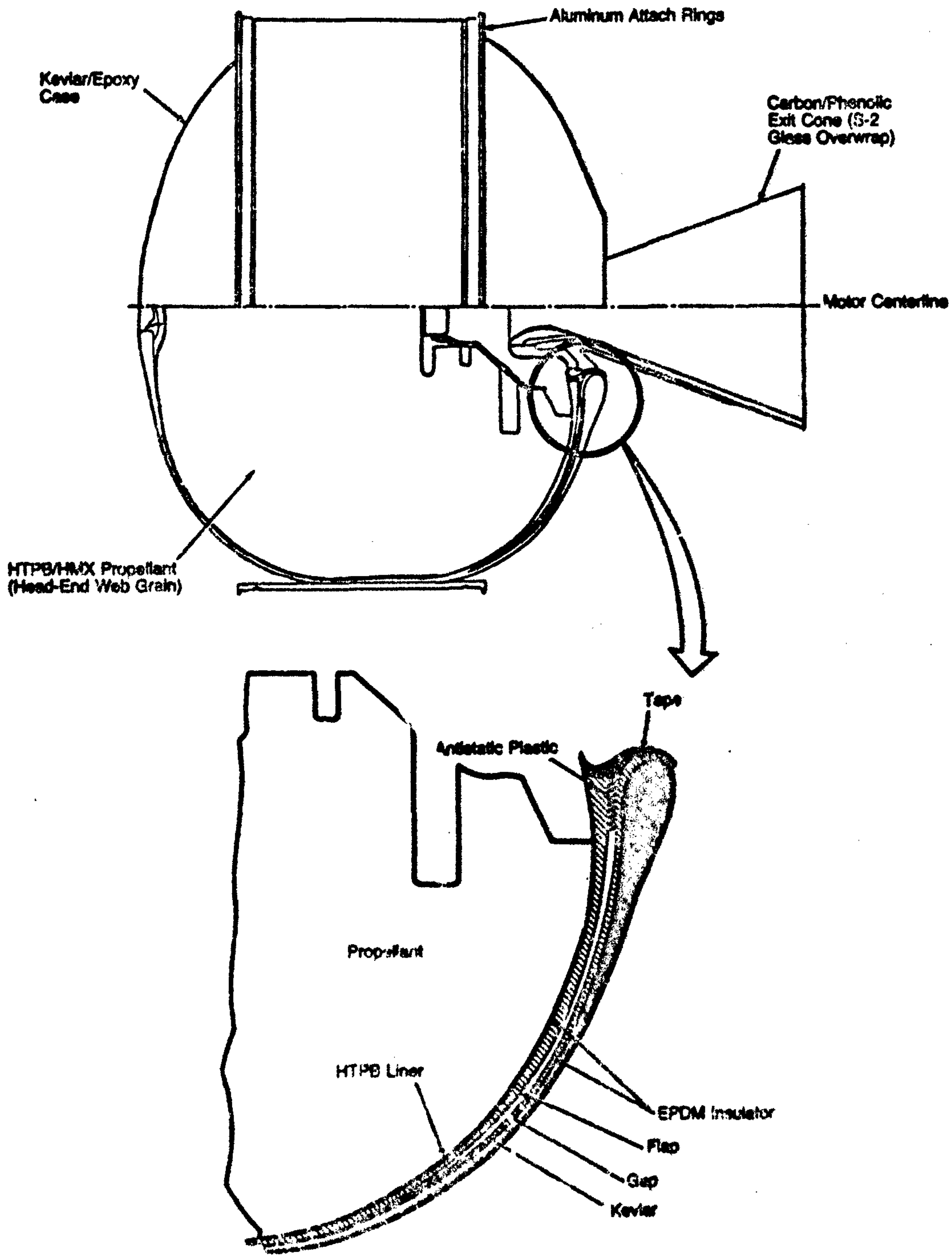

Figure 3. Blocking the Flap Gap With a Combination of Antistatic Plastic Foam and Tape

to support near-term PAM-DII launches, aluminum foil was chosen to form a complete Faraday cage around the motor. Such a system was not only predictably durable but easily verifiable with conventional ordnance-type ohmmeters.

SUMMARY

The approach to ESD control for the PAM-DII was to address all viable means by which inadvertent motor ignition could occur. Normal safety and grounding features were reviewed in great detail and enhanced. Ground handling, shipping, storage, launch processing procedures, and equipment were all included in the review and appropriate changes were implemented. The principal feature, an aluminum foil Faraday cage covering the Kevlar motor case, was chosen because of its effectiveness, durability, and simplicity, and because it could be easily verified with conventional instruments. Successive reviews by various agencies have confirmed the adequacy of the selected approach to ESD control.

REFERENCE

1. Knaur, James A. Technical Investigation of 11 January 1985 PERSHING II Motor Fire. Proceedings of the Twenty-Second Explosive Seminar, Anaheim, CA, 26-28 August 1986.

DETERMINATION OF ESD GROUNDING STRAP RESISTOR VALUES

BY

David R. Blinde, Honeywell DSG
and
C. Fred Mykkanen, Honeywell USD

INTRODUCTION

Electrostatic discharge (ESD) control grounding straps are a common precaution used in both the explosives industry and the electronics industry. These grounding straps are used to prevent the accumulation of static charge on an operator. In the explosives industry, accumulation of a static charge by an operator could inadvertantly cause initiation of a low energy initiator while in the electronics industry such static charges can degrade or destroy static sensitive electronic devices.

One feature common to grounding straps used in these two fields is a current limiting resistor. This resistor is used to assure that an operator would not be electrocuted if he /she were to come into contact with a high current source such as a standard electrical outlet. Commonly acepted safe electrical current levels (1 milliamp to approximately 4 milliamp)[1] for people suggest that minimum resistor values in grounding straps should be in the range of 30K ohms to 440K ohms depending upon the selected safe current level and voltage source present (up to 440 volts is common in many manufacturing areas).

The latest revision of Safety Manual AMC R-385-100 states that the resistance value for an operator handling low energy initiators should be no greater than 250K ohms when measured from the opposite hand to ground. This value is clearly less than 440k ohms and almost certainly reflects a legitimate concem on the part of AMC that the standard must be conservative enough to assure that static voltages on operators could not achieve a level sufficient to cause initiation of an explosive component. The use of a simple maximum value in the standard however may lead some people to utilize extremely low resistance value resistors in their grounding straps and thus jeopardize employee health vis-a-vis common high current sources such as standard or high voltage electrical outlets. The Contractors Safety Manual, DOD 4145.26m takes a different approach stating that resistance should be between 250K ohms and 1 Megohm when measured from the opposite hand to ground.

Research reported in this paper was aimed at providing a sound technical basis for determining safe maximum resistor values that could be used without allowing dangerous static charges to develop on an operator. The research (see table 3), in fact, indicates that grounding resistance values substantially in excess of those allowed by AMC R-385-100 and DOD 4145.26m will satisfactorily limit operator static voltage levels for devices that are energy sensitive as low as 10 ergs (or even lower depending upon the desired safety factor).

THEORY

This paper develops a model (through the utilization of designed experiments) which describes the voltage generation process for a grounded operator. Utilization of the designed experiment results as well as work by the authors and other researchers[2] on the maximum voltage generation rates that can be produced by ungrounded operators, permitted development of an equation that computes the maximum voltage that an operator can develop for a given grounding resistance.

Designed Experiment methodology

Design of Experiments is a body of knowledge which relies heavily upon statistical analysis techniques and is used to improve the knowledge that can be gained from an experiment. This methodology has been used successfully for many years in many fields of work and has the significant advantage of minimizing the number of tests needed to perform an effective experiment. In simple terms, designed experiments differ from the more traditional "one variable at a time" experimental methodology because more than one independent parameter is varied at a time to determine the effect on the response of interest. The way in which these parameters are simultaneously varied is dependent upon the particular design that is used. All designs however possess the characteristic that it is mathematically possible to determine the effects of individual parameters on the response as well as to determine the interactions between parameters and the effects of those interactions upon the response. Interactions cannot be determined using the "one variable at a time" technique.

This study utilizes both a Box Behnken design and Central Composite design to analyze the response (voltage on an operator) as a function of the independent parameters of operator activity level, operator capacitance, environmental relative humidity, and grounding resistance value. Detailed information on the designed experiment methodology is available in a number of resource documents.[3,4,5,6]

Voltage generation by the capacitive shift process

The capacitive shift process is used in this paper as the most severe method currently recognized for rapidly generating voltages on an operator performing normal work activities. The voltage generation rates that have been found for the process are, in this paper, applied to the general findings of the designed experiments to develop an appropriate model for worst case voltage generation by a grounded operator. For that application to make sense, it is necessary to evaluate conditions associated with the capacitive shift process. That evaluation is hereafter performed using a simple capacitor analogy for an operator in order to simplify understanding of the process.

First, since the capacitive shift process involves a voltage increase (from V1 to V2) in concert with a lowering of operator capacitance from C1 to C2, it is clear that the energy stored on the operator by that process would not be as high as for someone whose capacitance remained fixed at the high initial level of C1 while being charged from V1 to V2 as a result of triboelectric charging. The ratio of energy deltas (final energy - initial energy) for the two processes would in fact vary from case to case depending upon the initial and final voltages of the operator. That situation can be expressed by the simple expressions listed below:

$$\text{EQ 1.} \quad \frac{E_2\text{-}E_1(\text{cap})}{E_2\text{-}E_1(\text{tribo})} = \frac{.5\,C_2V_2^2 - .5C_1V_1^2}{.5C_1V_2^2 - .5C_1V_1^2} = \frac{V_1}{V1 + V2}$$

Strictly speaking therefore, any general application of capacitive shift process voltage change rates to a model derived from triboelectric charging data (i.e. the designed experiments performed in this study) should consider the energy effects. Practically speaking however, it should be clear that the high voltage generation rates in the capacitive shift process when applied to the triboelectrically derived model produces conservative results with a safety factor which is the inverse of the ratio observed in equation 1. For large differences in V1 and V2 the safety factor would be very large while for small differences the safety factor would be small.

Second, since relative humidity is shown in the triboelectric Box Behnken experiment to be of little importance over the grounding resistance values used in this study, it is important to also understand how relative humidity might effect the capacitive shift process. If we again consider an operator to be represented as a simple parallel plate capacitor, it is possible to theoretically examine the factors which influence voltage. Equation 2 below indicates that voltage is a function of charge (Q), plate area (A), plate separation (D), and the permittivity of the dielectric (ε).

EQ 2. $V=DQ/A\varepsilon$

Differentiation of that equation with respect to time to represent what occurs when an operator moves yields equation 3 (which reasonably assumes that Q and A may be treated as constants):

EQ 3. $dV/dt = (Q/A\varepsilon)(dD/dt) - (D/\varepsilon^2)(d\varepsilon/dt)$

Both of the differential terms on the right side of the equation are clearly dependent upon the speed of movement and not dependent upon relative humidity. The one term which could have a dependence upon relative humidity is the permittivity of the dielectric (ε). In the situation we examine in this paper, that dielectric is in effect primarily composed of air, and shoe sole material. The combined effective permittivity of those materials is in fact essentially independent of relative humidity based upon test subject capacitance measurements performed during the experiments. This finding indicates that the lack of humidity dependence for the model derived through triboelectric generation data is consistent with the behavior of the capacitive shift process.

EXPERIMENT

Prior to the performance of this experiment, work performed by 3M corporation suggested that voltage generation by the capacitive shift process produced voltage levels on operators more rapidly than any other available mechanism. In order to confirm their conclusions with regard to voltage generation, an experiment was performed in which the voltage on three different test subjects with effective capacitances of 67, 155, and 294 pF was monitored while the subjects generated voltage through triboelectric charging. The accumulated voltage was monitored on a chart recorder with the subjects not grounded, grounded through 200 megohm, grounded through 20 megohm, and grounded through 1 megohm. These tests were performed at three different relative humidity levels (1%, 35%, and 61%).

Determination of voltage on the test subjects was performed by electrically connecting the subjects to a conductive plate which was monitored by a Monroe model 175 electrostatic voltmeter. The voltage monitoring plate was electrically connected by a wrist strap (no protective resistor employed) to the subjects' right wrist. The grounding wrist strap used in the experiment was connected to the subjects left wrist to assure that charge dissipation could occur only by current flow through the subject. Figure 1 (which provides a pictorial view of the test arrangement used for the two designed experiments that will be described later) is very similar to the test arrangment used in this portion of the study. For this portion of the study the Van De Graaff connection to the subject was broken. The subject held a rubbing plate in the left hand and a rubbing cloth in the right hand. This arrangement was found to produce greater voltages than observed by simply setting the rubbing plate on the table and rubbing with the right hand.

FIGURE 1
(TEST SYSTEM DIAGRAM)

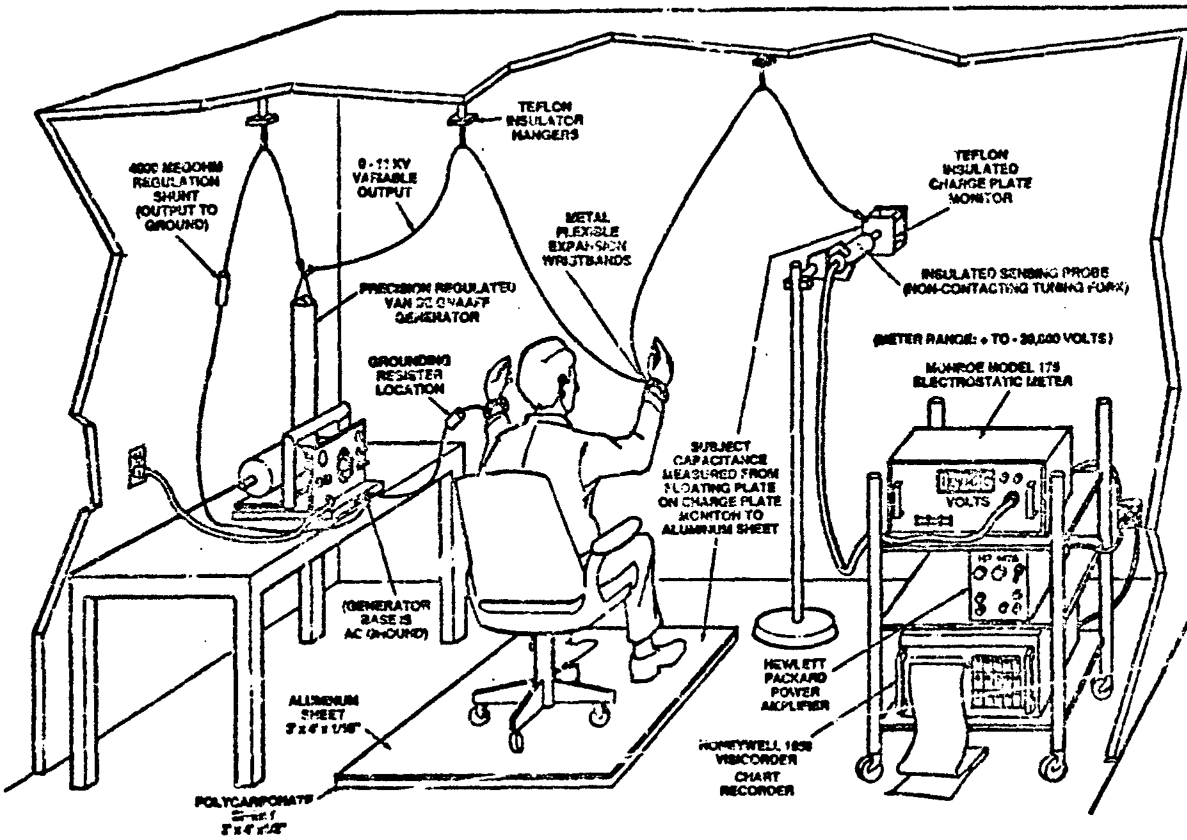

A number of different materials were used in this test. Rubbing plates of teflon, glass, aluminum, and polycarbonate were used. The rubbing cloth materials were cotton, polypropylene, conductive carpet, polyester, silk, nylon,and bare hand.These items were selected to provide a large number of combinations representing materials at opposite ends of the triboelectric series and were rubbed very vigorously to create the highest possible static potential.

The second portion of the study was a modeling effort utilizing designed experiments to analytically determine the effects of relative humidity, operator capacitance, operator activity level, and grounding resistance on operator voltage. These tests were performed using a modified commercial Van De Graaff generator to simulate operator activity level. Major modifications to the generator included replacement of the original belt motor with a 0 to 5000 rpm, 1/15 hp ac/dc motor; addition of a calibrated autotransformer; addition of a voltage regulation shunt of about 4000 megohms; and selection of a special belt, belt treatment and pulley materials. These modifications made it possible to control the voltage generation rate to within less than 2% of the desired value. Photographs of the Van De Graaff generator are shown in figure 2.

FIGURE 2
(VAN DE GRAAFF GENERATOR)

The two experimental designs used in this study were a modified three level, four variable Box Behnken design and a five level, two variable Central Composite design. As noted earlier, the experimental set-up for these tests is shown in figure 1. The Box Behnken design was utilized to determine which factors had significant influence on operator voltage while the Central Composite design was used to more precisely quantify the influence of the significant parameters.

Variable levels for the Box Behnken design were:

1. grounding resistance - 200 megohm, 10 megohm, 0.602 megohm
2. generator belt speed - 23.9, 21.7, and 18.4 inches/sec.
3. relative humidity - 44%, 15%, 2%
4. test subject capacitance - 294, 155, and 67 picofarad

Variable levels for the Central Composite design were:

1. grounding resistance - 200 megohms, 171 megohm, 100.5 megohm, 30 megohm, and 0.602 megohm
2. generator belt speed - 23.9, 23.3, 21.7, 19.5, and 18.4 inches/sec

TEST RESULTS AND DISCUSSION

Triboelectric charging tests

Some typical results from the triboelectric charging experiment are shown below in table 1. These results are typical of data when the charging plate was teflon (teflon produced the highest observed voltages).

TABLE 1
(TRIBOELECTRIC CHARGING DATA)

RUBBING MATERIAL	GROUNDING RESISTANCE	1% RH	|VOLTAGE| 35% RH	61% RH
COTTON	OPEN	410	580	60
	200 MEG	210	260	40
	20 MEG	30	120	30
	1 MEG	0	0	0
POLYESTER	OPEN	460	580	60
	200 MEG	210	340	30
	20 MEG	20	120	10
	1 MEG	0	0	0
WOOL	OPEN	440	520	90
	200 MEG	240	470	30
	20 MEG	40	90	10
	1 MEG	0	0	0

A simplified typical waveform for this data is shown in figure 3. Examination of the waveform clearly indicates that it consists of two components. The first and major component is a cyclic charging pattern which exhibited a frequency identical to the rubbing frequency associated with the charging materials. This bipolar pattern is believed to be the result of induction charging caused by movement of the operators hand over the highly charged (>> 10 k volts) teflon rubbing plate. The second and much smaller component was a unipolar voltage shift caused by the transfer of charge from the rubbing material to the body of the test subject. The triboelectric generation tests exhibited a maximum voltage generation rate of 3600 volts/sec.

FIGURE 3
(TRIBOELECTRIC CHARGING WAVEFORM)

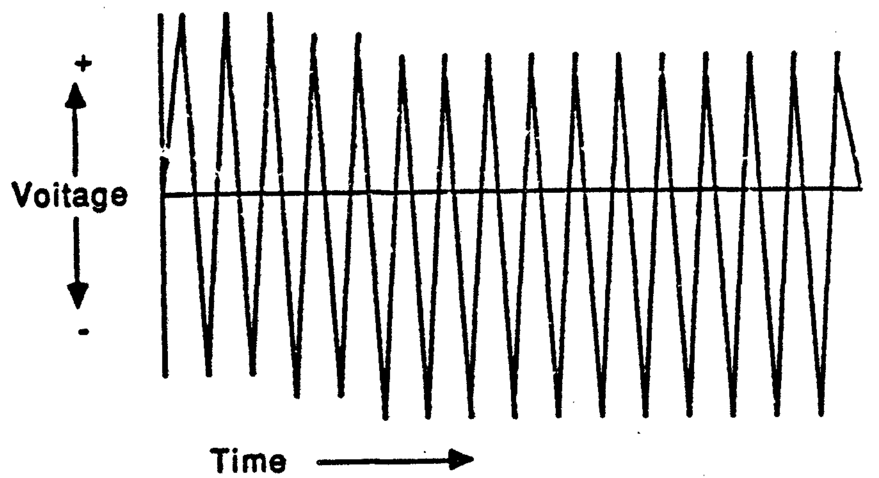

Examination of table 1 indicates that voltage on the operator decreases as expected as the grounding resistor value decreases. In addition, as suggested by this abbreviated table, no voltage was ever observed on a operator grounded through 1 megohm of resistance for any of the test plate /rubbing material combinations examined. Two characteristics of table 1 at first examination may appear in error if examined simplistically . These characteristics are the lack of a definite progression of voltage amplitude in concert with the triboelectric charging series and changing relative humidity. We believe these progressions do not exist due to 1) the dominance of the inductive component of the charging waveform, 2) the existance of uncontrollable variables associated with this process (i.e. rubing speed/pressure, etc.), 3) the fact that the reported voltages exist on the test subject and not the materials (i.e. charge transfer plays a dominant role), and 4) increasing relative humidity should increase human and insulator conductivity characteristics while decreasing triboelectric charging propensity.

These tests were primarily useful in determining general characteristics associated with the triboelectric charging process. They are of limited value for modeling purposes however due to uncontrollable parameters which have previously been described. Our major use of these findings in the study was, in fact, to simply compare the results to previously available data associated with the capacitive shift process. That comparison indicates that the maximun voltage shift rate of 5000 volts/sec which has been obvserved with the capacitive shift process represents the most severe charging senario currently known. Secondly, the triboelectric charging senario we examined represents an extreme situation which should never be seen in an ESD controlled environment unlike the capacitive shift situation which is very much a "real world" situation.

Designed Experiments

Modeling of operator voltage generation was accomplished through the use of two designed experiments. The first experiment which was a three level, four variable modified Box Behnken design demonstrated that, for the range of values examined, human activity level (i.e. Van De Graaff speed) and grounding resistance value are the primary controlling factors for human voltage level. Relative humidity also begins to become important at the upper end of the resistance range for significant activity levels, but the effect is still relatively small for the range of values we examined. Data from this experiment is listed in table 2.

TABLE 2
(VARIABLE EFFECTS - BOX BEHNKEN DESIGN)

A. Low speed (a) to high speed (b) voltage effects for listed test conditions

R.H. %	CAP. pf	RES. ohms	VOLTAGE (a)	VOLTAGE (b)	(b-a)/a	EFFECT
15	155	602k	0	1	undefined	n/a
15	156	200 meg	161	488	+2.04	yes
15	67	10.28 meg	8	24	+2	yes
2	155	10.28 meg	8	26	+2.25	yes
15	294	10.28 meg	8	23	+1.88	yes
44	156	10.28 meg	5	27	+4.4	yes

B. Low R.H. (a) to high R.H. (b) voltage effects for listed test conditions

SPEED dial value	CAP. pf	RES. ohms	VOLTAGE (a)	VOLTAGE (b)	(b-a)/a	EFFECT
37.5	67	10.28 meg	17	16	-.06	no
46	156	10.28 meg	28	27	-.04	no
37.5	294	10.28 meg	17	17	0.0	no
37.5	156	200 meg	367	332	-.10	small
30	156	10.28 meg	8	5	-.38	small
37.5	155	602k	0	2	undefined	n/a

C. Low capacitance (a) to high capacitance (b) voltage effects for listed test conditions

R.H. %	SPEED dial value	RES. ohms	VOLTAGE (a)	VOLTAGE (b)	(b-a)/a	EFFECT
2	37.5	10.28 meg	17	17	0.0	no
15	37.5	200 meg	297	296	0.0	no
15	37.5	602k	1	1	0.0	no
44	37.5	10.28 meg	16	17	+.06	no
15	46	10.28 meg	24	23	-.04	no
15	30	10.28 meg	8	8	0.0	no

D. low resistance (a) to high resistance (b) voltage effects for listed test conditions

R.H. %	CAP. pf	SPEED dial value	VOLTAGE (a)	VOLTAGE (b)	(b-a)/a	EFFECT
2	155	37.5	0	332	>+332	yes
15	67	37.5	1	297	+296	yes
15	294	37.5	0	296	>+296	yes
44	156	37.5	2	367	+183	yes
15	156	46	0	488	>+488	yes
15	155	30	1	161	+160	yes

Multiple regression analysis of the data listed in table 2 produced a predictive model for operator voltage as a function of the examined factors. That model had a confidence factor of 98.87%. In order to provide an even better model of the factors which were initially determined to be significant, a second designed experiment was performed. This experiment which was a five level, two variable Central Composite design produced a model with a 99.99% confidence factor. The predictive equation developed from that experiment (which relates activity level and grounding resistor value to operator voltage) is listed as equation 4. It should be noted that equation 4 is similar, but not identical to, the equation that can be developed from the modified Box Behnken experiment. The differences are primarily a result of the fact that different generator belts (with somewhat different triboelectric charging characteristics) were used in the two experiments. Nearly identical results are obtained from the two models for a given resistance value when generator speeds which produce the same charging characteristics are chosen.

EQ 4. volts = 234.7 + 85.924 (spd) + 165.089 (res) + 64.25 (spd)(res) - 1.551 (spd)(spd)

NOTE: spd = autotransformer dial set of Van De Graaff generator
res = resistance to ground for test subject
for equation 4 to yield the correct answer, both speed and resistance must be transformed linearly to the scales shown below:

dial speed transform		resistance transform	
32.1959	-1	29.7925 meg	-1
37.5	0	100.301 meg	0
42.8041	+1	170.809 meg	+1

In order for these findings to be useful in determining a reasonable upper limit for grounding resistors it is necessary to relate Van De Graaff output characteristics to dial speed. That relationship is provided in figure 4. Secondly it is necessary to determine the Van De Graaff level which simulates expected worst-case behavior for an operator. As noted earlier, the 3M study which found typical maximum voltage generation rates of 5000 volts/sec for different test subjects currently provides the best information available on worst-case voltage generation by an operator. Substituting into equation 4 the dial speed transform (+.2639) for a 5000 volt/sec voltage generation rate and the voltage value that can be permitted on an operator makes it possible to calculate a reasonable upper limit to the grounding resistor value. An exact solution for resistance can be determined by using the quadratic equation. Alternatively, since the coefficient of the R-squared term is very small, that term could be dropped and the equation solved as a simple linear function. Determination of the appropriate operator voltage level is based upon a simple calculation from a known energy sensitivity for the explosive device to be handled. That calculation is based upon equation 5 and assumes a human body capacitance (C) of 500 picofarad.

EQ 5. $E\ (\text{joules}) = 0.5\ CV^2$

FIGURE 4
(DIAL SETTING VS. VOLTAGE RISE TIME)

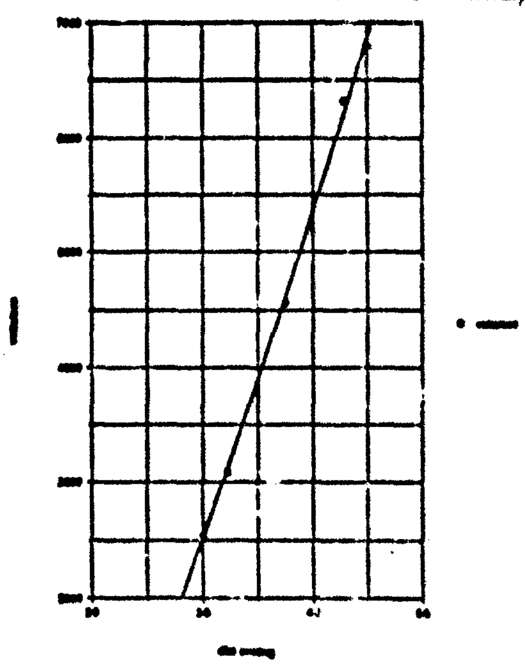

Operator voltages predicted on the basis of equation 4 are shown in figure 5 along with actual values seen for grounded test subjects in the 3M study. These curves show that the designed experiments provide more conservative resistance values. This difference is believed to be a direct consequence of the different time scales over which the Van De Graaff and capacitive shift process can produce voltage changes on the order of 5000 volts/sec. Equation 4 can be normalized to predict results equivalent to the capacitive shift data by multiplying the right side of the equation by .29 to yield equation 6 (notes which apply to equation 4 also apply to equation 6).

EQ 6. Volts = 68.063 + 24.918 (spd) + 47.876 (res) + 18.633 (spd)(res) - 0.45 (res)(res)

FIGURE 5
(PREDICTED VS. OBSERVED VOLTAGE)

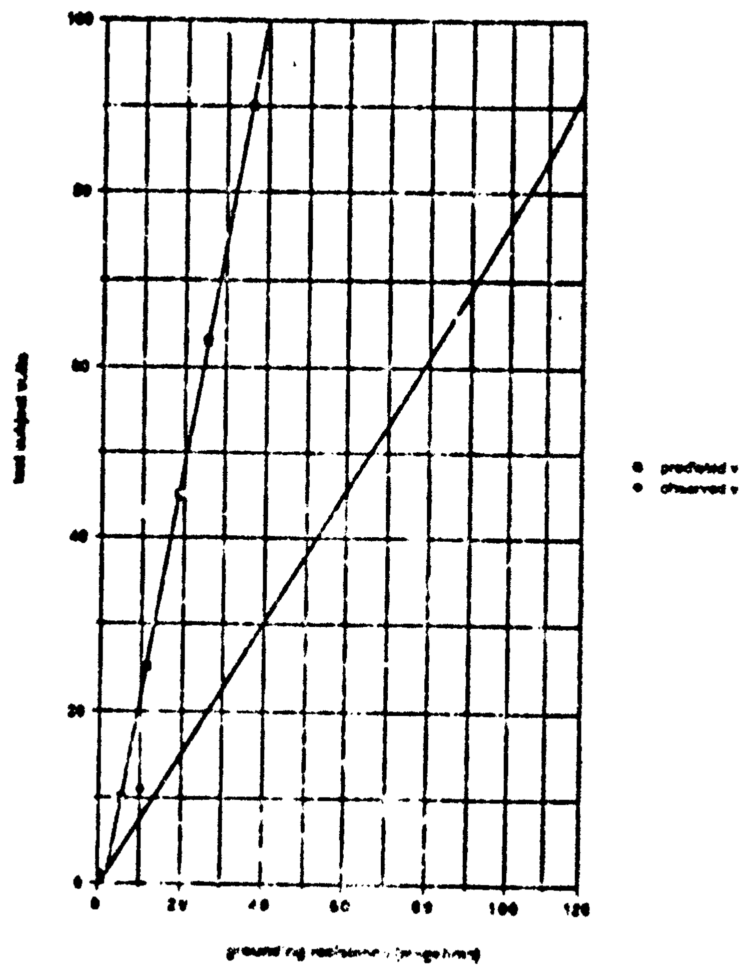

Table 3 provides an example of explosive detonation energy versus allowed grounding resistance value for an operator. The allowed resistance values are shown for four different safety factors. These safety factors are solely based upon the specified fractional reduction in the energy factor column and do not include previously described indeterminate factors which increase the safety margin or the potentially significant energy losses which can occur when energy is transferred from an operator to a device.

TABLE 3
(INITIATION ENERGY VS. ALLOWED RESISTANCE)

ENERGY FACTOR (ERGS)	RESISTANCE (MEGOHMS) FOR SPECIFIED SAFETY FACTOR			
	1 TO 1	1 TO 2	1 TO 5	1 TO 10
10	84.8	60.7	38.0	27.3
50	188.9	134.1	84.8	60.7
100	>200	188.9	119.5	84.8
200	>200	>200	188.9	134.1

Stated another way, an M100 point to case metal bridgewire detonator with a static energy sensitivity of 263 ergs is, from an energy point of view, protected at a level more than 450,000 times what is required when total grounding resistance is 1.25 megohm. This determination was made using normalized equation number 6 (resistance transform of -1.4048 and speed transform of +.2839) which predicts that at a 5000 volts/sec. charging rate and at 1.25 megohm total grounding resistance the voltage developed on an operator would be roughly .47 volts. Comparing the energy stored at that voltage on an 500 picofarad operator with the 263 erg sensitivity level of the detonator yields the heretofore listed safety factor.

CONCLUSIONS

1) A 5000 volts/sec. rise time, as observed for the capacitive shift process, currently represents the worst-case voltage generation senario for an operator.

2) Operator activity and grounding resistance value are the two major factors which effect operator voltage levels. Relative humidity and operator capacitance play no significant role at grounding resistance values below 200 megohms (for a 5000 volts/sec. charging rate).

3) Grounding resistance values considerably in excess of those permitted by AMC R-385-100 and DOD 4145.26m should safely limit electrostatic voltages on operating personnel (Ref. table 3).

ACKNOWLEDGEMENTS

The authors wish to acknowledge the contributions of the following people.

1) Mr. D. Clark for multiple regression analysis of the modified Box Behnken design data.
2) Mr. E. Edwards for his assistance with the experimental set-up.
3) Dr. A. Joglekar for general assistance with the designed experiment methodology.
4) Mr. J. Kremers for his assistance with the experimental set-up.
5) Mr. J. Lee of ICI Americas who provided initiator sensitivity information.
6) Mr. D. Swenson of 3M with whom we discussed the 3M capacitive shift experiment.

REFERENCES

1) MIL-STD-454 , Standard General Requirements for Electronic Equipment
2) James R. Huntsman and Donald J. Yanni, Jr., "Test Methods for Static Control Products", 1982 EOS/ESD symposium proceedings, p. 94.
3) G.E.P. Box, William G. Hunter, J. Stuart Hunter, Statistics for Experimenters, John Wiley and Sons, Inc., 1978.
4) O. L. Davies (ed.), Design and Analysis of Industrial Experiments, Hafner (MacMillen), 1954.
5) Charles R. Hicks, Fundamental Concepts in the Design of Experiments, Holt, Rinehart and Winston, Inc., 1973
6) Bernard Ostle, Statistics In Research, The Iowa State University Press, 1963

KLOTZ-CLUB TESTS IN SWEDEN

By

Bengt E Vretblad
FortF - Royal Swedish Fortifications Administration
Eskilstuna, Sweden

ABSTRACT

The Klotz-Club has been performing tests in Sweden to get more data in particular on debris and fragments thrown from detonations in rock storages. The test installation is described and the test program and some results are given in the paper.

INTRODUCTION

At the 22nd DDESB meeting, in Anaheim California, 1986, the Klotz-Club and parts of the work within it were described, /1/. The results from the tests given by then have been further analyzed and more tests have been performed.

TEST OBJECTIVES

The purpose of the test series made was to get additional data on

* debris and fragment dispersion
* blast propagation
* influence of geometry on debris flow and blast propagation
* groundshock effects
* TNT-equivalence for artillery rounds
* degrading effects of detonations on e.g. shotcrete.

THE INSTALLATION

The needs for the installation to meet with were:

* Chamber volume 200-300 m^3
* Smooth walls of access tunnels
* Debris-trap geometry
* Debris collecting area in a sector in front of the installation.

As the main objective with the installation was to make multiple tests with debris a site had to be selected where large amounts of explosives could be

detonated without impairing the community, where competent rock with adequate rock cover could be found and at the outside of which a surface suitable for collecting fragments and debris could be arranged.

This led to the shooting range at ArtSS, Älvdalen, Sweden.

The rock at the selected site consists of porphyritic granite, poor in quartz.

Outside the entrance cutting a sector -5° - +10° from the tunnel axis from which debris and fragments could be collected was made. The area was close to flat up to 150 m from the entrance and then steeper to form a target area in total more than 300 m from the tunnel.

Figure 1 depicts the geometry outside the installation.

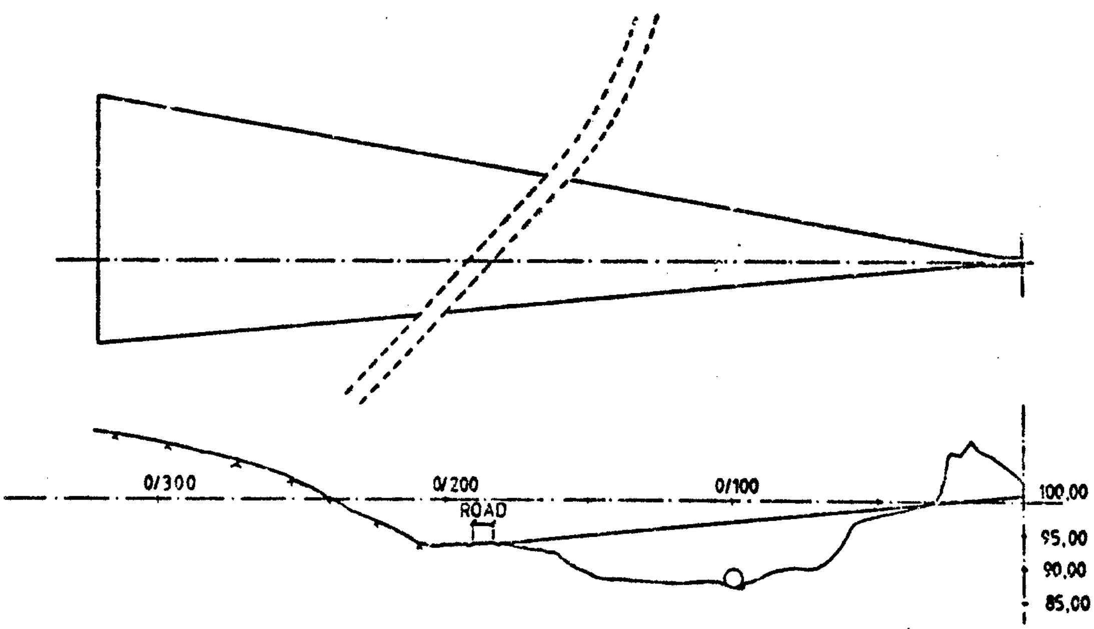

Figure 1. Geometry at the test site

For the tunnel a crossection of 6.3 m^2 was chosen. The walls were shotcreted. In the end of the tunnel was a chamber with a crossection of 12 m^2 and a volume of 300 m^3 e.g. a length of about 25 m designed. In 45° to the tunnel another tunnel with the same crossection was planned. At the end of one end of

that tunnel a chamber 17 m long with a volume of 200 m^3 was foreseen. At the other end of it a 10 m long tunnel with the purpose of collecting debris and fragments coming out of the 200 m^3 chamber was made.

The entrance part of the tunnel was made of reinforced concrete to ascertain that the geometry would not change during the test series. Also to facilitate a comparison with other test data a well defined geometry was needed.

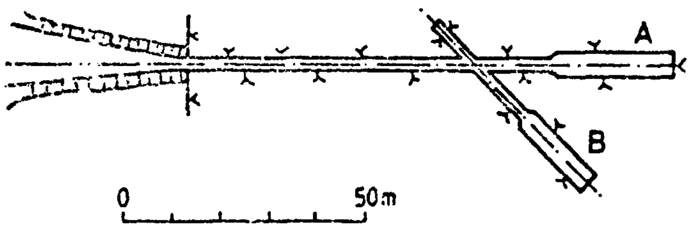

Figure 2. The installation

TEST PROGRAM

The program for the tests comprised

1. 10 kg TNT in chamber A
2. Ditto chamber B
3. 1 ton TNT in chamber A
4. Ditto chamber B
5. Artillery rounds with net explosive weight 1 ton in chamber A
6. Ditto chamber B
7. 1 ton of ANFO in chamber A
8. 5 tons of ANFO in chamber A
9. Ditto chamber B

The first two tests were mainly for calibration but also to give pressure vs charge-weight in and outside the chamber to compare with the tests 3 and 4.

The tests 1-6 were executed in 1986 and the tests 7-9 in 1987.

EXPLOSIVES

For the first four shots TNT was used. Then two tests with m/36 artillery shells followed. Shot number 7 was made with ANFO to permit a comparison with the earlier test, cf. also /2/. The last two tests were made with ANFO.

MEASUREMENTS

Measurements were made of blast, groundshock and fragments.

Blast measurements

The transducers for blast pressure measurements were placed according to figure 3.

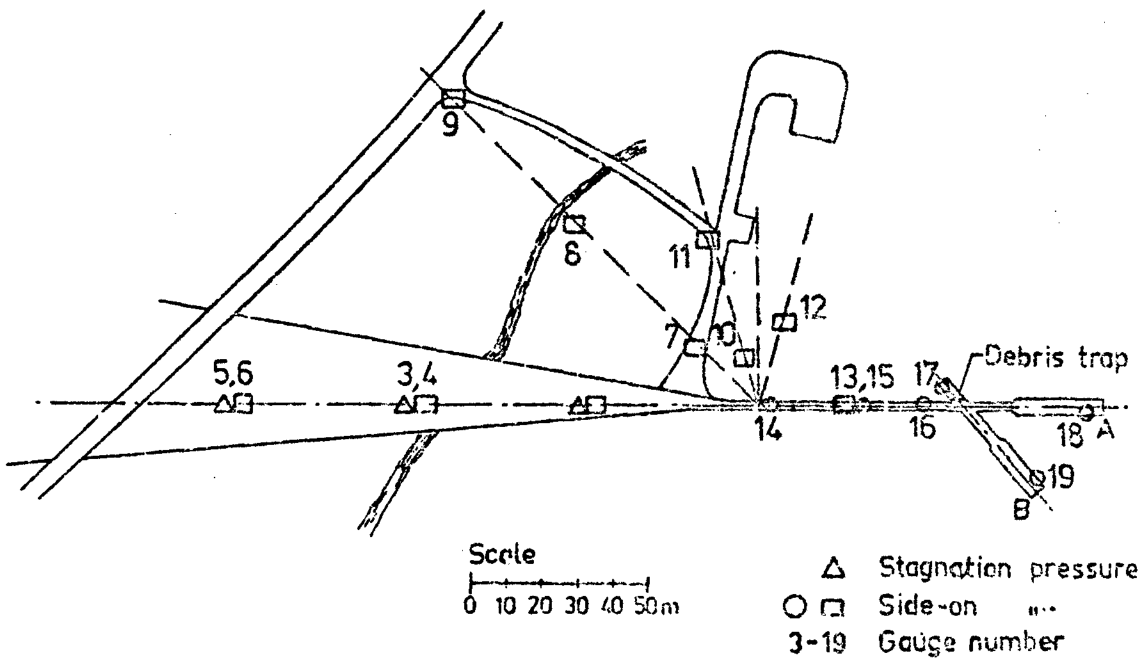

Figure 3. Positions for the airblast gauges.

The side-on pressure gauges outside the installation were PCB 113A51. For stagnation pressure Kistler 412 transducers were used. In the tunnel system PCB 113A24 gauges were placed.

The gauges outside the tunnel were placed about 0.5 m above the ground surface.

Ground shock

Groundshock measurements were made at different locations within the rock according to figure 4. The gauges 20 and 21 were triaxial (Bruel o Kjaer 2x4366+4368) and gauge 22 close to the upper surface of the rock was a vertical sensing geophone. The gauges were installed for the 1986 tests. They were grouted to the rock. Therefor they could not be recovered or inspected. One of the gauges had been destroyed during the winter 1986-87. It was not replaced.

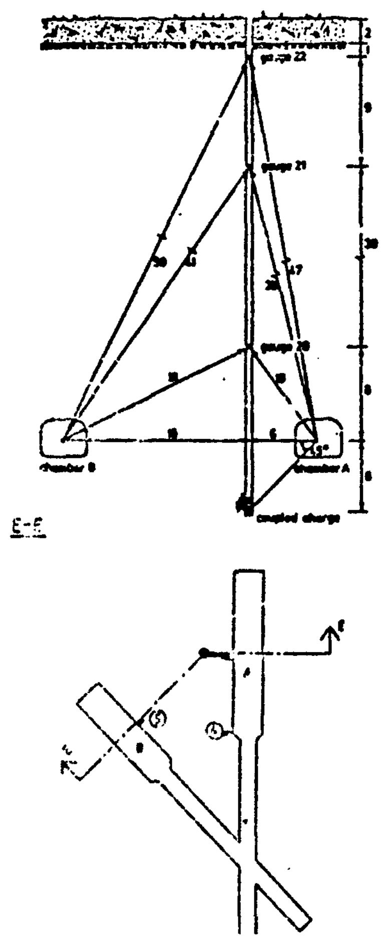

Figure 4. Ground shock gauge locations. Vertical (top) and horisontal (bottom) views.

Recording and data reduction systems

A Sangamo Sabre tape recording system with a 14 tracks 1" tape FM IRIG WB1 was used. Together with it was also used a digital recording system John & Reilhofer 8k13 with 8 channels.

The data reduction was made with a Data General Nova 4/x equipped with a Westward Pericom graph terminal and a Versatec V-80 high-resolution-printer-plotter.

Debris

Artificial debris in the shape and with the mass approximately like the artillery rounds for the major tests were used. These debris were 680 mm long 160 mm diameter steel pipes filled with concrete. The mass was 47 kg.

These tubes were placed in the chamber standing on the floor behind the charge (4 of them) and lying and standing in front of the charge on the same level (16 of each) at tests 3 and 4. In the tunnel pairs of cylinders were placed on the floor on four locations.

Figure 5 shows the location of the artificial debris.

To make a detailed study of the trajectories of the ejecta easier the area outside the tunnel was prepared with timber logs laid down perpendicular to the tunnel axis at 10 m interval. Highspeed cameras and videocameras were placed perpendicular to and along the tunnel axis as can be seen in figure 6.

In shot number 8 and 9 artificial fragments were sawn out of 10 mm thick steel plates and put into wooden boxes. The boxes were subsequently placed close to the charge.

The steel fragments were 25x25, 35x35 and 80x80 mm (50 g, 100 g and 500 g). Each box contained 250, 125 and 41 of each, respectively. the total weight of

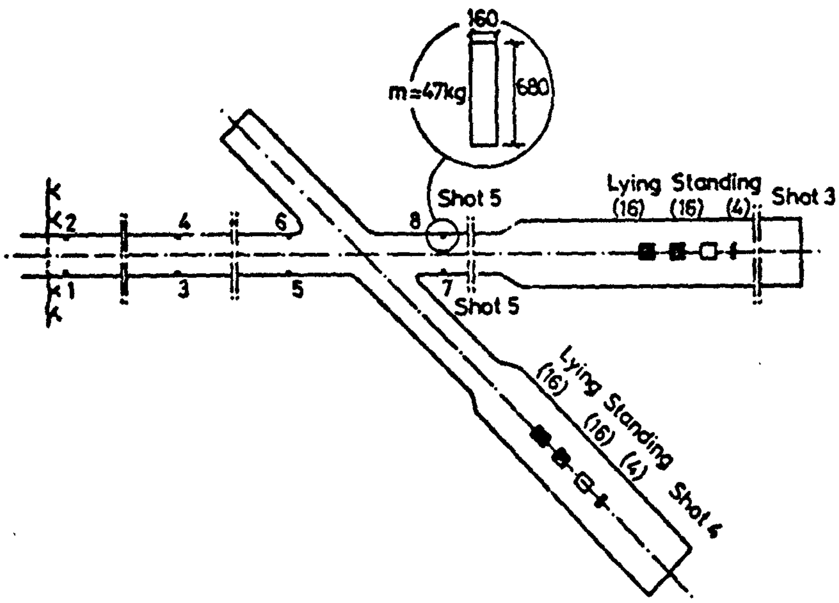

Figure 5. Location of artificial debris (shot 3-6)

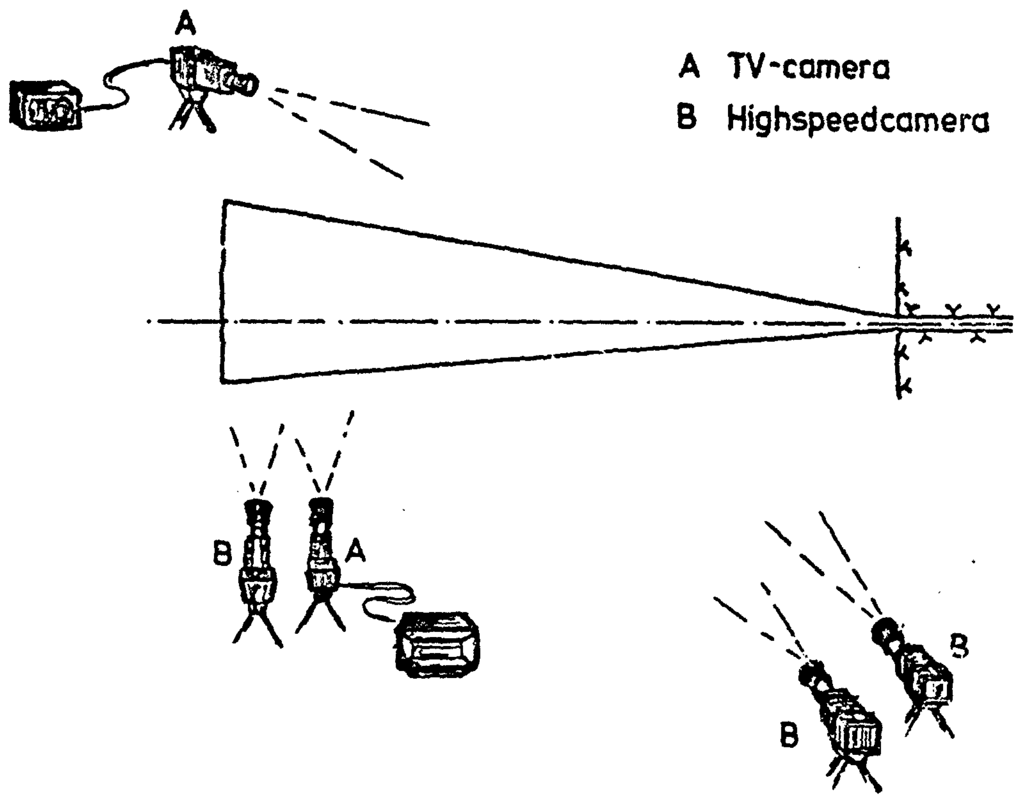

Figure 6. Highspeed- and video cameras during the tests.

the steel fragments in each box was therefor 446 kg. 12 boxes were used for each test giving a total of 5350 kg.

To check on the trajectories for the fragments and debris Peter Kummer at Basler & Partners, Zurich, suggested the use of debris traps of a multilayer configuration, /3/. Six such traps were included in the number 9 test. The design of the traps is shown in figure 7.

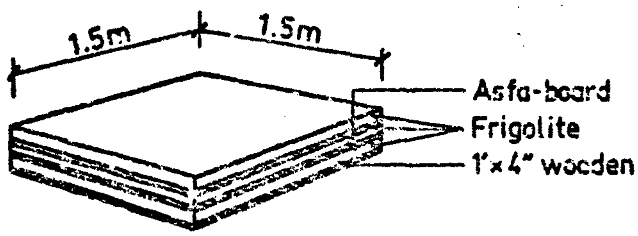

Figure 7. Multilayer debris trap.

The traps were placed at 45° from horisontal facing the tunnel entrance as can be seen in figure 8.

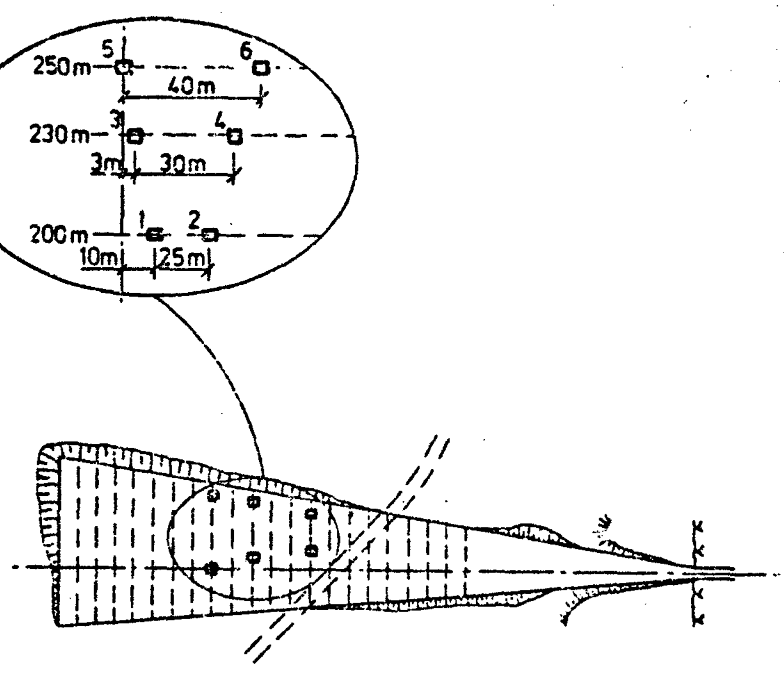

Figure 8. Location of the debris traps.

TEST EXECUTION

The explosives were put in the center of each chamber. The bare TNT charges were initiated in one point. The projectiles were initiated individually. (There were 180 at each of tests 5 and 6.) The 5 ton ANFO charges were initiated at six different locations in the explosive.

Just before the detonation of the charge the highspeed and the video cameras were started and the execution of the test was followed from an observation post. Figure 9 shows one test as an observer could see it.

Figure 9. The test area during the execution of a test.

After each shot the entrance to the tunnel had to be secured and the toxic gases must be ventilated. For this purpose a plastic hose was put into the tunnel and connected to a ventilating equipment. The day after the shot the air in the tunnel was good enough to permit people to go into the installation.

After the tests the debris was collected carefully in the tunnel system and outside the installation.

TEST RESULTS

Blast pressure

As the geometry outside the installation is very specific to the site selected a detailed comparison of blast measurements around the installation can only be made between the different shots and not with e.g. design code values based on more ideal geometries. A comparison of pressure data along the tunnel axis outside the installation where the surface is reasonably flat could however be of interest for comparisons also with design codes.

In figure 10 such a comparison is made for shots 3-6.

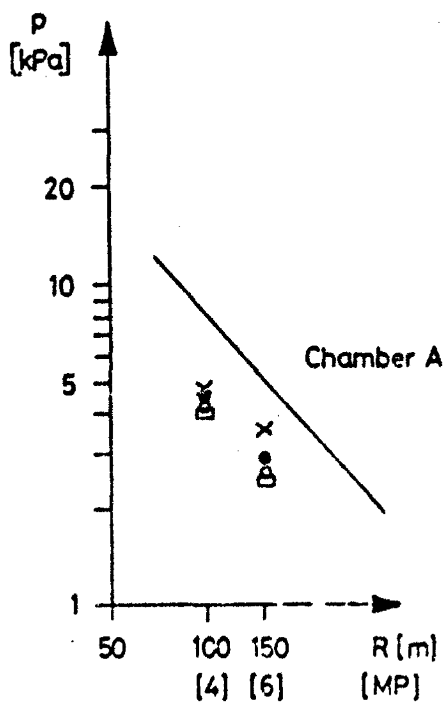

Figure 10. Pressure outside the tunnel along the tunnel axis

Typically, the pressure along the tunnel axis outside the installation shows a steep front, figure 11, while recordings in other directions show first a front then a gradual pressure increase, figure 12. The latter performance is due to geometrical and frictional effects. The effect of the debris trap on the pressure outside the installation is very minor as could be expected.

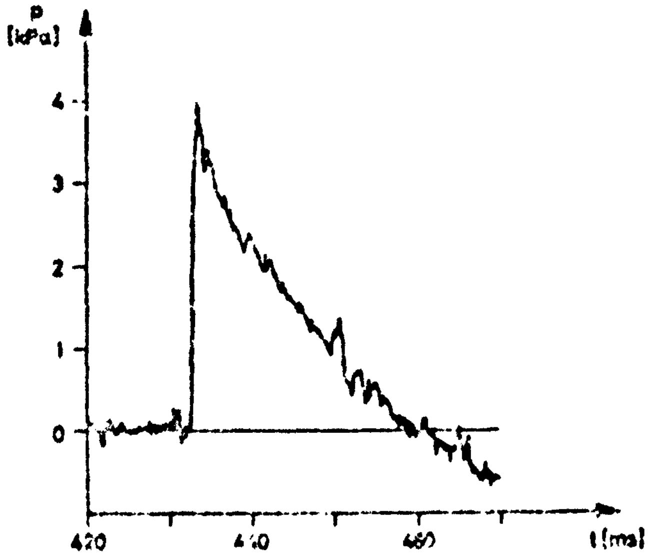

Figure 11. Blast pressure outside the installation along the tunnel axis (shot 5)

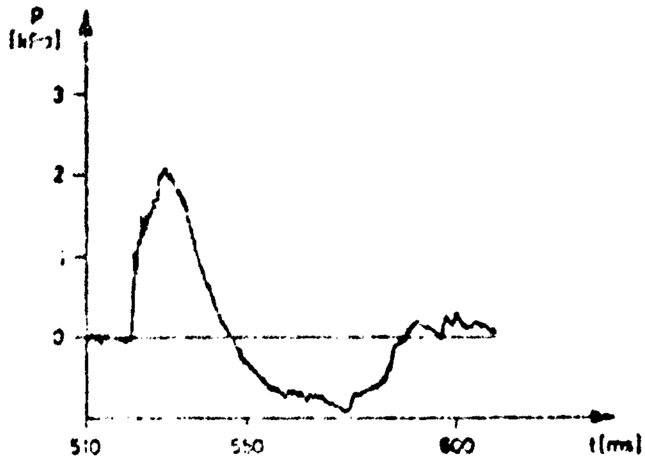

Figure 12. Blast pressure outside the installation at 45° (shot 5)

Groundshock

The groundshock measurements from the different shots in the Klotz-Club tests as well as from an additional coupled shot for comparison have been given in /4/. From the recordings in /4/ the following plot can be made:

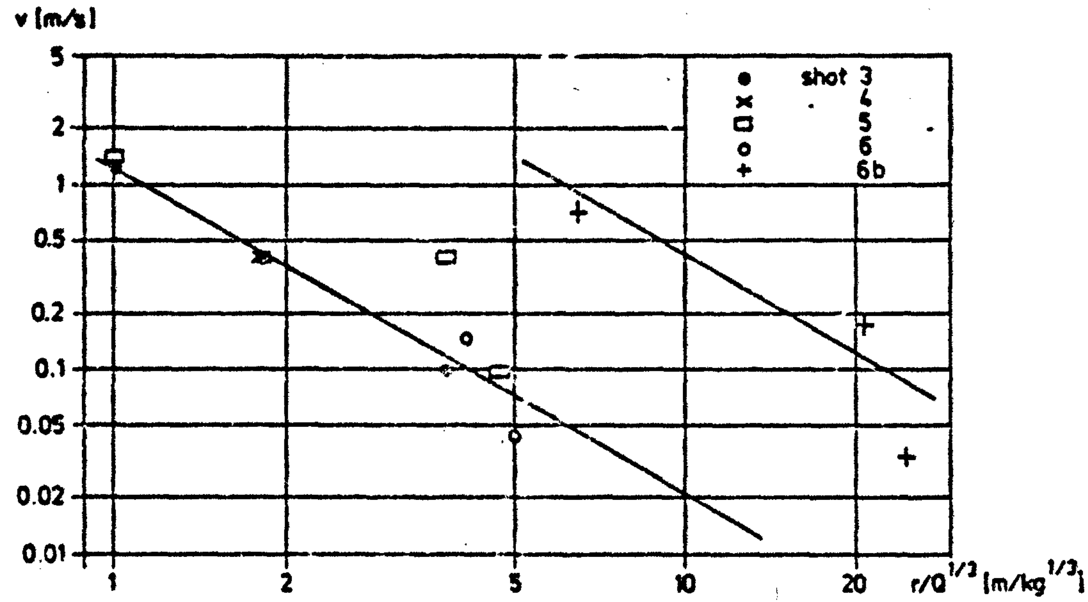

Figure 13. Maximum velocity vs scaled distance

From the recordings in the different tests a coupling factor can be calculated. From figure 13 can be concluded that a coupled charge gives appr. 20 times higher velocities for the same scaled distance. This means that the coupling factor with respect to groundvelocity is 1/20 ~ 5 % for the conditions in the tests. The tests do not indicate that a different coupling factor should be used for bare TNT charges and the ammunition used in the shots 5 and 6. It is to be expected, however, that the coupling factor varies with the loading density.

Debris

The artificial debris placed in the chambers at the shots 3 and 4 were heavily destroyed. The cylinders placed in the tunnel were also demolished in a way that they could not be identified to original position past test.

In figure 14 the positions of the cylinders after the different shots are shown. It can be seen that the cylinders all impacted within ± 10° from the tunnel axis.

It was clearly illustrated in each of the shots 3-6 that the debris initially at the inner part of the chambers remained there e.g. only debris from the outer part contributed to the hazards outside the installation.

In shot 5 and 6 large amounts of fragments were produced from the ammunition upon detonation. All fragments found in sample areas were collected and measured.

The debris density and its variation with the position of the collecting area is shown in figure 15 for shot number 5 and figure 16 for shot number 6.

The debris density vs distance from the tunnel entrance is shown in figure 17. From it can be concluded that the debris density is about an order of magnitude lower in shot number 6 than in shot number 5 e.g. the debris trap is highly efficient.

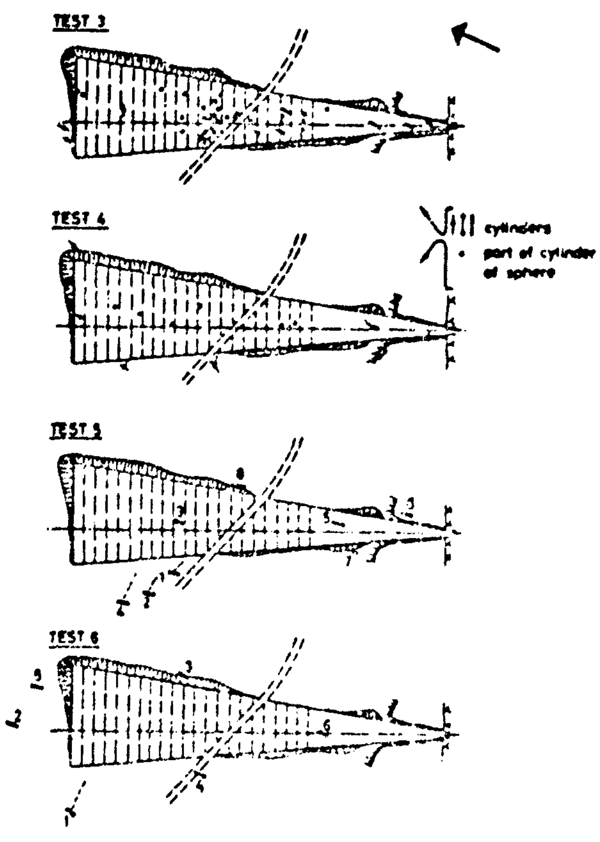

Figure 14. Artificial debris as recovered after test 3-6

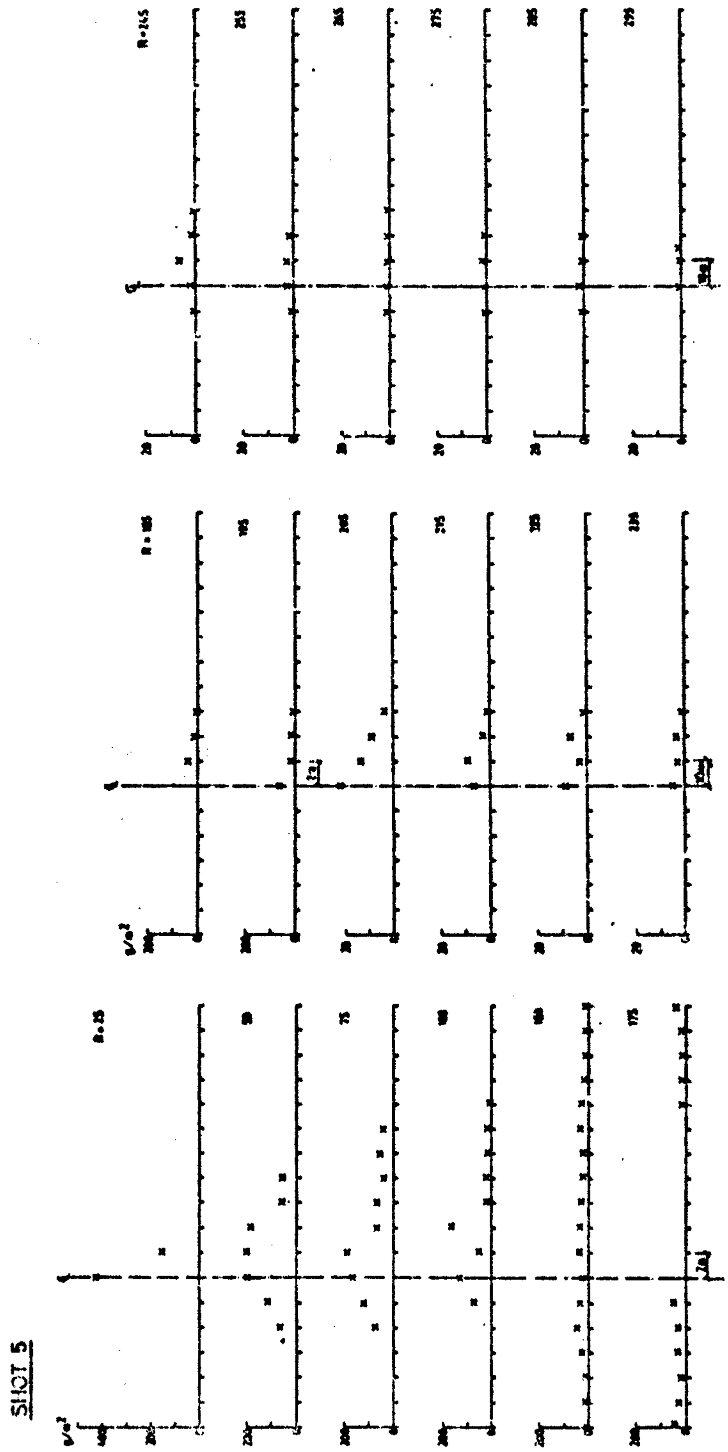

Figure 15. Debris densities at different distances from the entrance and from the tunnel axis. Shot 5.

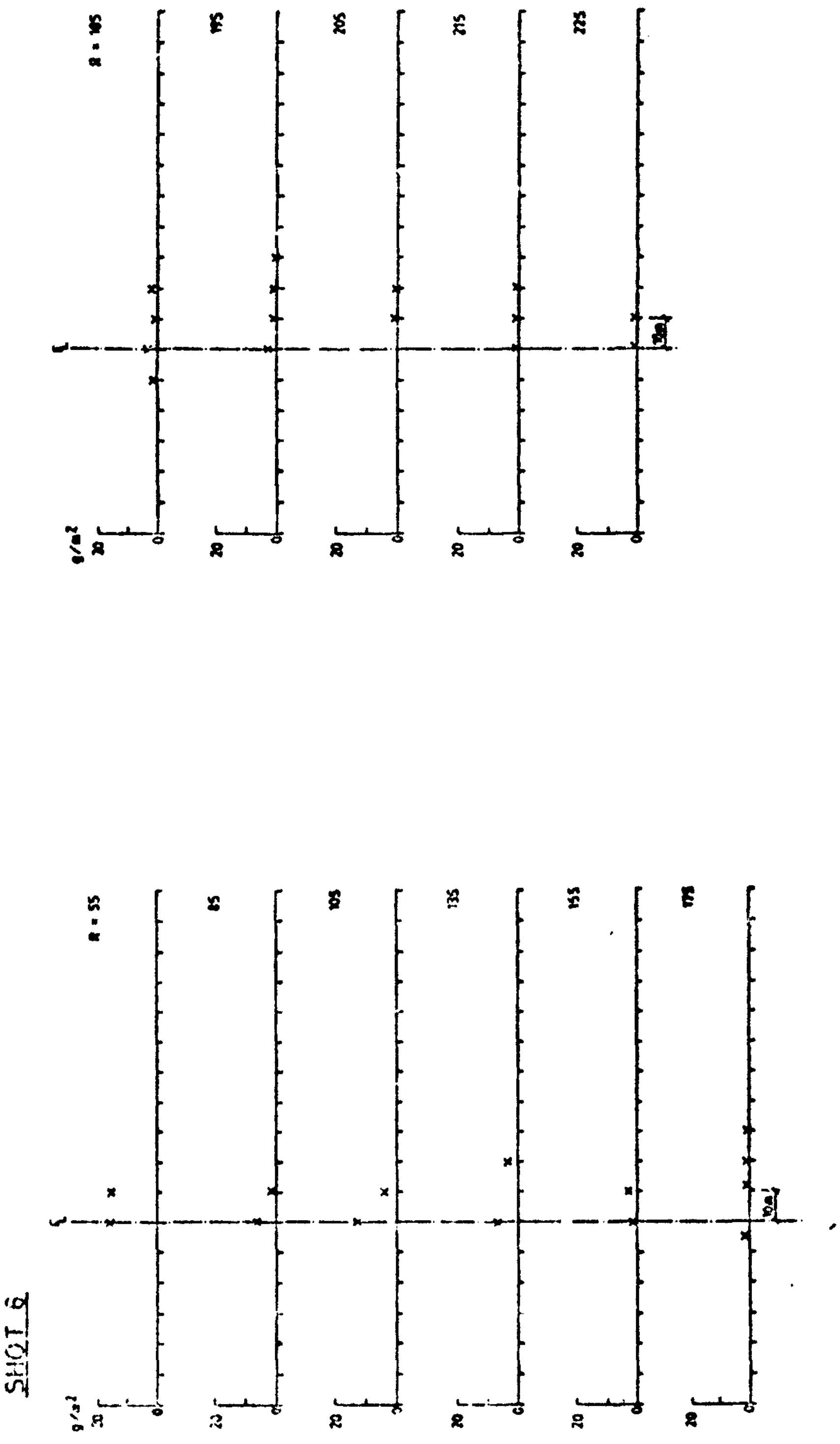

Figure 16. Debris densities at different distances from the entrance and from the tunnel axis. Shot 6.

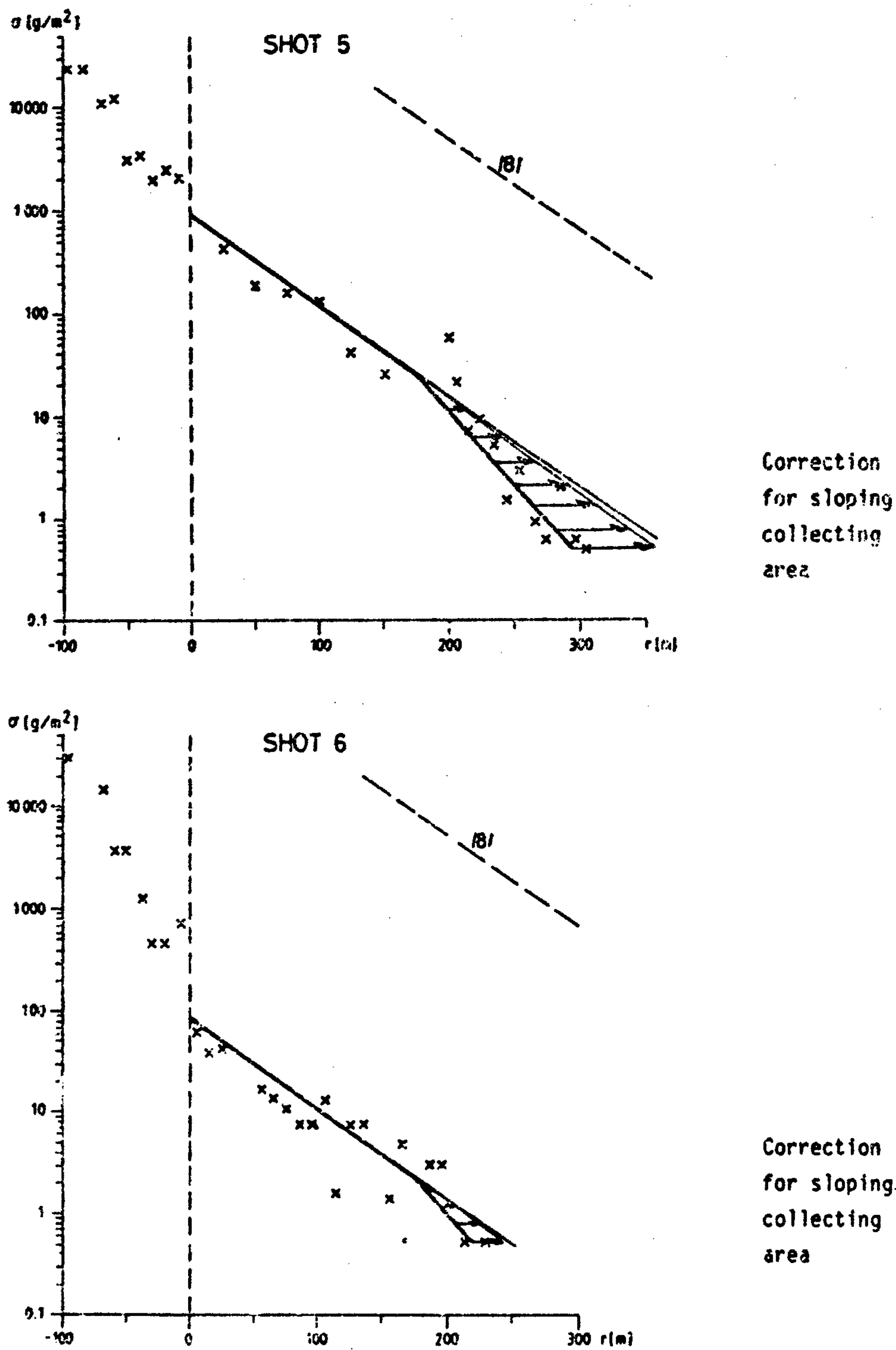

Figure 17. Debris density vs distance from tunnel entrance

CONCLUSIONS

The data have not yet been fully analyzed. The following conclusions can be made:

Debris and fragments

The blast/debris trap dead-end tunnel constructed as an extension of the branch passageway from chamber B, was able to reduce considerably the fragments outside (order of magnitude).

It has been demonstrated that the velocity of debris emerging from the main entranceway is a function of the loading density.

This hazardous sector from debris/fragments is considerably smaller than prescribed by most safety regulations.

Blast

These tests confirm the assumption that the air blast outside the main passageway blast pressure can be calculated based on the pressure in the main passageway close to the exit and the diameter of the passageway.

Ground shock

The tests have shown that for scaled ranged between 1 and 4 $m/kg^{1/3}$ and a loading density of about 15 kg/m^3 under conditions studied, the decoupling factor is 0.05.

A decoupling factor of 0.05 corresponds to a dangerous range of only a fraction of the range for a tamped charge. For higher loading densities the coupling factor can be expected to be higher.

ACKNOWLEDGEMENT

In the planning and during the execution of the tests many valuable suggestions have been made by members of the Klotz-Club and of the Steering Committee. Excellent efforts have also been made by a lot of individuals at ArtSS and FortF. The author is most grateful for all dedication and excellent achievements he has met during different stages of the project.

REFERENCES

/1/ Vretblad, B, Klotz-Club Tests in Sweden. Minutes 22nd Explosives Safety Seminar. Anaheim, California, 1986.

/2/ Eriksson, S, TNT vs ANFO in Klotz Club Tests. FortF/F Report A5:88. Eskilstuna, 1988.

/3/ Kummer, P, Private communication. 1987.

/4/ Hultgren, S, Ground Motion Measurements, KLOTZ II. FortF/F Report C4:87. Eskilstuna, 1987.

ANALYSIS OF THE DEBRIS PRODUCED BY EXPLOSIONS IN TUNNELS

by

Michael M. Swisdak, Jr.
and
Paul E. Montanaro

Naval Surface Warfare Center
10901 New Hampshire Avenue
Silver Spring, Maryland 20903-5000

ABSTRACT

Rock tunnels are sometimes used as storage facilities for significant quantities of Class 1 Division 1 (Mass Detonating) materials. In order to site these facilities properly, one of the questions which must be addressed is the definition of the hazard range associated with the event; i.e., what is the debris, is it hazardous, and at what range does the debris areal density reach the acceptable level of one hazardous fragment per 600 ft^2 ground surface area? Further, what are the effects of any significant terrain features on this hazard range? To answer these questions, a series of model tests were conducted. In addition, detailed debris analyses and trajectory calculations were performed. This paper presents the results of these tests and analyses for the debris hazard ranges.

BACKGROUND

In many parts of the world, rock tunnels are used as storage magazines for all Classes of explosive materials. Two phenomena drive the Explosive Safety Quantity Distance (ESQD) hazard range which must be associated with accidents in tunnels--airblast and fragmentation/debris. The operative criteria are: (1) less than 1.2 psi airblast and (2) less than one hazardous fragment per 600 ft^2 surface area, where a hazardous fragment is defined as having an impact energy greater than or equal to 58 foot-pounds.

The Department of Defense Explosives Safety Board (DDESB) has recommended that the unwaivered scaled distance be 76 $ft/lb^{1/3}$ to the front of each tunnel magazine (with other factors applying in other directions).[1] The phenomena driving the hazard range to this scaled distance was airblast. Often, tunnels are constructed with one or two baffles designed to eliminate the projection of primary fragments beyond the immediate vicinity of each tunnel. The effects of these baffles on airblast has not been fully understood. Further complicating the problem is the interaction of the surrounding terrain with both the airblast

and the debris. When tunnels are built into the sides of ravines or gullies or when the tunnel adit is surrounded by hills, the area encumbered by the ESQD arc is often on the top of the hill opposite the tunnel mouth. This is shown schematically in Figure 1. As the airblast range is reduced, it approaches the hazard range associated with the debris. Thus, both ranges must be considered when determining the actual ESQD range for tunnels.

In 1987, the Naval Civil Engineering Laboratory (NCEL) designed and conducted a series of model tests whose purpose was to study the phenomena of explosions within tunnels. As part of this program, the Naval Surface Warfare Center (NSWC) agreed to study the debris produced by these tests and to prepare debris hazard range prediction methodologies for tunnels. The test program will be described in detail in a paper being given by NCEL. This paper will concentrate on the debris effort. However, a brief description of both the tunnels and the tests are required for a general understanding of what will follow.

GENERAL TUNNEL DESCRIPTION

The tunnels considered in this study either faced flat terrain or hills. The tunnel overburden is rock and varies from about 20-50 feet at the entrance to between 150-350 feet at the rear of the tunnel. With these overburden thicknesses and the loading densities used in the tunnels, blowout of the overburden was not considered a problem. Although the topography looks severe from the tunnel entrances, the actual vertical angle from the tunnel entrance to the top of the opposite ridge (near the property line) is usually less than 15 degrees.

Each tunnel is essentially straight, with no side chambers. Each has a reinforced concrete headwall with a steel door on the outside. Each contains one or two fragment suppression baffles located a short distance inside the tunnel behind the entrance. The large majority of the tunnels have two baffles. These baffles are made from un-reinforced concrete and are not anchored in any significant way to the tunnel walls. Figure 2 is a drawing of a typical tunnel.

TEST DESCRIPTION

Model tests were conducted using models of two scale sizes: 1/15 and 1/6.43. The majority of the tests were conducted at 1/15 scale. One test was conducted at a scale of 1/6.43. The tunnels were modeled with circular cross sections, rather than the shape shown in Figure 2. However, the cross-sectional area of the tunnels was scaled properly in the models. In addition, the amount of blockage produced by the baffles was also scaled during the modelling program.

The 1/15 tests were conducted using a section of a steel gun barrel as the tunnel model. The 1/6.43-scale model was constructed from concrete pipe. For both models, dirt was piled over the test section for added confinement.

The models were fired with various combinations of charge weights and numbers of baffles/headwalls. The explosive charges were all bare charges of Composition C-4 for the 1/15-scale tests and a lightly aluminum clad TNT charge for the 1/6.43-scale test. Thus the only sources of debris were the materials contained in the headwall and the baffles (Note: This corresponds to the assumption that the baffles actually suppress all primary fragments produced by the detonation of the stored munitions.) The test program is shown in more detail in Table 1.

A nominal 5 ° recovery sector was established out the front of each tunnel. This sector was lined with plastic. After each test, the material remaining on the plastic was recovered, labeled as to its location, and analyzed for size, weight, and type. In addition, any large pieces found off the plastic were located, their range and bearing from the tunnel mouth determined, and their size and weight measured.

High speed photography and photo-grids were used to determine debris angles and velocities on each shot. The photographic portion of the program will be described in more detail in the following section.

PHOTOGRAPHIC ANALYSIS

A white backdrop with a black grid was placed at varying distances from the tunnel exit for each shot. The backdrop measured 12 feet wide by 18 feet high with 1-foot grid squares. Two to three cameras were used to photograph each shot. One camera had a narrow field of view and showed only the backdrop; the others viewed a much wider area which included the backdrop. Camera frame rates were generally 1000 to 2000 frames/sec.

The films showed many individual fragments coming from the tunnel exit. By tracking the positions of each fragment, frame by frame from the film, velocities and launch angles were determined. The backdrop grid was used as a distance and angle reference; the calibrated timing marks applied to each film were used as a timing reference. To insure accurate distance measurements, the fragments had to be approximately the same distance from the camera as the backdrop. Fragments which went behind the backdrop or which were in front of the backdrop but out of focus were ignored. Accuracy of the measurements was estimated by comparing the measured velocity and angle of a fragment as seen from two different cameras. From this, the accuracy of velocity measurements was estimated to be within 10%, and angle measurements to within 1°.

Waves of fragments could be seen coming from the tunnel at low angles. These waves contained many fragments which were all moving at the same velocity and angle. Velocities for low-angle fragments were generally high. Higher angle fragments were generally fewer in number, more scattered, and had lower velocities. To be sure that the fragments being measured were coming directly from the tunnel exit and not ricochetting, the fragment paths were traced backward to the distance at which the tunnel was located. Obvious ricochet fragments were noted in the tables and not used in further computations. Those fragments not originating in the tunnel were also not considered.

Three tests were done specifically for fragment analysis (NCEL test numbers 7a, 7b, and 7c). The first had only baffles, the second only headwall, and the third included baffles and headwall. A flash panel consisting of metal sheets was placed at a distance of 41 ft from the tunnel exit. Films from the baffle-only test showed that the baffle fragments were all ejected at low angles (below 5°). On this test, the flash panels were not hit by any fragments; however, the supporting frame was hit. Films from the headwall-only test showed that the headwall fragments were distributed over all angles. Several hits on the metal flash panels were recorded.

The fragment velocity and launch angle data for all shots were compiled and tabulated. Duplicates (where the same fragment was seen from two different cameras) were removed; i.e., the fragment was only counted once. Overall, over 200 debris tracks were analyzed.

For analysis purposes, all fragments with launch angles less than 5° were not considered. The remaining data were then curve fitted with an exponential fit. The results are shown in Figure 3. The fitted curve is a relationship between launch angle and launch velocity which can then be applied to the debris originating from these tunnels. This curve has the form:

$$V = 3225 * \theta^{-0.71} \quad (\theta > 5°)$$

where

V = Launch velocity (ft/s)

θ = Launch angle (°)

For launch angles <5°, use a constant velocity of 1100 ft/s.

Examination of the data does not show any distinguishable differences between the shots of various charge weights. Based on these data and for these test conditions, the launch velocities and angles appear to be independent of charge weight. One set of data that does stand out is the data from the headwall-only shot. This case, headwall without baffles, is not realistic and its differences from the remainder of the data can be explained. When baffles are present, energy must be expended both in breaking them up and in transporting the pieces. Without baffles, this energy can be dumped into the headwall, producing unrealistic results since all tunnels have baffles.

Based on both the photographic evidence and the post-test recovery of the fragments, the beam spray angle in the horizontal plane, the angle which contains most of the fragments, was approximately 10° on either side of center; a few fragments, however, were more than 10° off the center line of the tunnel.

DEBRIS ANALYSIS

The debris data taken during this program were used to define two things: (1) the characteristic shape of the fragments/debris (as defined by the debris shape factor, B), and (2) the characteristic size of the debris (as defined by the debris characteristic length, L_c). In addition, the location of the debris pieces helped to define the "debris beam angle", i.e., the angles between which the majority of the material were recovered.

SHAPE FACTOR

The concrete debris collected in the recovery areas were evaluated as to shape factor. The shape factor relates the debris weight with a length dimension according to the function:

$$M = B \rho_c L^3$$

where M = Debris mass or weight
B = Shape Factor
ρ_c = concrete mass or weight density = 2800 kg/m^3 = 175 lbs/ft^3
L = (debris length x width x thickness)$^{1/3}$

Figure 4 illustrates the linear dimensions measured for each fragment. The shape factor can be thought of as the ratio of the volume of a fragment to the volume of a rectangular box with the minimum dimensions required to hold the fragment (see Figure 4). The recovered debris pieces were analyzed and cataloged by the New Mexico Institute of Mining Technology.

Table 2 presents the shape factors determined for each of the tests. Even though the numbers of recovered fragments were small for the 1/15-scale tests, their results are presented here for completeness. Because the recovery numbers were so low for the 1/15-scale tests, the bulk of the analysis and interpretation was concentrated on the single 1/6.43-scale test. The average shape factor for the 1/6.43-scale test was 0.37; this is actually not statistically different from the shape factors determined for the 1/15-scale tests. The shape factor determined for the break-up of reinforced concrete in the Aircraft Shelter Model Test Program (ASMT) was 0.573, while that determined on the DISTANT RUNNER test series[2] was 0.42-0.443 . It should be remembered, however, that the debris from these tunnel tests was from a combination of reinforced and unreinforced concrete (headwall and baffles), while the ASMT and DISTANT RUNNER data were all reinforced concrete.

DEBRIS CHARACTERISTIC LENGTH

Using the above shape factor information, a number distribution of the form (taken from Reference 3):

$$N(>L) = N_0 \exp(-L/L_c)$$

where

$N(>L)$ = number of pieces of debris with length greater than L
L = $(M/(B\rho))^{1/3}$
M = debris weight
B = shape factor (determined above)
ρ = debris density
L_o = characteristic fragment dimension (determined by fit)
N_0 = total number of pieces of debris (determined by fit)

was fitted to the 1/6.43-scale test data. The results are shown in Figure 5. The fragment characteristic length is found to be 2.756 cm. When this result is scaled up to full scale, the characteristic fragment dimension becomes 7.0 inches (2.756*6.43/2.54).

DEBRIS HAZARD RANGE DETERMINED FROM 1/6.43-SCALE TEST

The technique for predicting full scale debris ranges based on model scale test results is described in detail in Reference 2. The following is a synopsis of the technique. Trajectory calculations are used to calculate initial launch conditions necessary to get the model debris to its final location (both high and low angle trajectories are considered). Once the initial conditions have been calculated, each piece of debris is scaled up to full scale by the scale factor, S (debris characteristic length is multiplied by S, drag area by S^2, and mass by S^3). The "scaled-up" debris are then flown out using the initial conditions just determined. At the debris final locations, evaluate each piece as to whether or not it is hazardous, and then compute an areal density.

For this technique to work, certain information is required--namely, (1) the type of debris, (2) the debris weight density, (3) the debris shape factor, (4) initial estimates for the high and low angle fragments (to start the iterations), and (5) velocity cut-offs for the high and low angle fragments.

For this test, the type of debris was concrete with a density of 2800 kg/m³. The shape factor (as determined above) was 0.37. The high and low angle trajectory estimates were 25° and 5° respectively. The associated velocity cut-offs were 490 feet per second for high angle trajectories and 800 feet per second for low angles. As described in Reference 2, the computational algorithm uses an iterative procedure to calculate a set of initial launch conditions (velocity and angle) for each piece of debris. Some of these calculated initial conditions are obviously unrealistic, with launch velocities which are not physically possible. In many cases, these unrealistic results are due to the debris which bounced or skipped

along the ground before it reached its final location (a phenomena which is known to have occurred on these tests). To handle these cases, upper limit velocity cutoffs are built into the procedures. All fragments whose initial velocities are calculated to be greater than this cutoff velocity are dropped from the calculations. The cutoff velocities used in these calculations were based on the observed relationship between launch angle and launch velocity described in a preceding section.

The output of the program is a table of the number of hazardous fragments as a function of the full scale range. The computational algorithm also uses the smoothing technique described in Reference 2 . This smoothed or normalized output as a function of range is shown in Figure 6 for the 1/6.43-scale test results.

A least squares regression was performed on the normalized data. The form of the function was:

$$N = A \exp (BR)$$

where A, B are determined by the fit and R is the normalized range in feet and N is defined as follows:

$$N = (N_c/N_A)_j = \sum_{i=j}^{k} (N_c)_i \Big/ \sum_{i=j}^{k} (N_A)_i$$

and

$$R = \sum_{i=j}^{k} R_i /(k-j+1)$$

N	=	Normalized Fragment Density
R	=	Normalized Range (feet)
$(N_c)_i$	=	Number of hazardous debris in zone i
$(N_A)_i$	=	The acceptable number of hazardous debris that corresponds to an areal density of 1 per 600 ft^2 for zone i
R_i	=	The distance from the tunnel mouth to the mid-point of zone i
i	=	Index for full-scale zone; varies from 1 to k (outermost zone)
j	=	Specific zone index between i=1 to i=k

Using the fitted curve in Figure 6, the range at which the hazardous fragment density reaches one (i.e. the number of hazardous fragments equals the allowed number of hazardous fragments) is 1145 feet. It must be remembered, however, that this result represents the case with no terrain effects; i.e., the test was conducted on flat ground. The effects of hills would be to reduce this range. These terrain effects will be discussed in a subsequent section.

ANALYTICALLY DETERMINED HAZARD RANGES

In order to compute fragment density as a function of range, two pieces of information are required: (1) the fraction of material falling into each range increment, and (2) the total number of debris pieces which must be apportioned among the various range increments.

The procedure for determining the fraction of material falling into each range increment begins with a series of trajectory calculations. In order to perform these calculations, three things are required: (1) the mass, shape factor, and type of debris involved, (2) the initial velocity and launch angles of the debris, and (3) the height and range (or profile) of the hill involved.

The following masses were arbitrarily chosen to characterize the full-scale debris produced by the tunnel explosion: 0.5, 1.0, 2.0, 5.0, 10.0, 20.0, 50.0, 100.0, and 200.0 pounds. The debris was assumed to be concrete, with a shape factor of 0.37 and a density of 175 lbs/ft^3, based on the model results.

The relationship between launch angle and initial velocity derived from the photographic data presented in an earlier section was used for the launch conditions. That relationship is:

$$V = 3225 * \theta^{-0.71} \quad (\theta > 5°)$$

$$V = 1100 \quad (\theta < 5°)$$

where

V = velocity (ft/s)
θ = launch angle (°)

The terrain (hill) was modeled with a polynomial expression (cubic), relating range and elevation. Figure 7 shows a sketch of one of the hills considered in these calculations. When debris items failed to clear the hill, their final location was taken as the X-coordinate of the impact point on the hill. The trajectory calculations were performed using the computer program TRAJ, described in Reference 3.

Once the trajectory calculations were completed, it was assumed that there was a uniform distribution of debris with respect to ejection angle (up to some maximum angle taken as 45°) and that spherical divergence applied. With these two assumptions, the fraction of material falling into arbitrary 100-foot increments out to the maximum range of each weight group was computed.

Using the distribution previously discussed, the numbers of fragments associated with each mass increment can be computed. The distribution has the form:

$$N(>L) = N_0 \exp(-L_L/L_c),$$

where

$N(>L)$	= number of debris with dimension greater than L_L
N_0	= total number of debris = W_T/m
m	= $6{*}B{*}\rho_c{*}L_c^3$ (Reference 3)
W_T	= total weight of fragmenting material
β	= fragment shape factor (use 0.37)
ρ	= debris density (use 175 lb/ft^3)
L_c	= fragment characteristic length (inches)
L_L	= fragment length associated with W_L (inches)
W_L	= assumed weight groups (0.5, 1.0, 2.0, 5.0, etc).

Associated with each mass is a length. These are related by:

$$L_L = (1728{*}W_L/(B{*}\rho_c))^{1/3}$$

where the symbols are defined above. The lengths associated with each weight group chosen were calculated using this equation and are shown in Table 3.

The only source of debris within the tunnels are taken to be the headwall and the baffles themselves. For low angles (ranges out to 600-700 feet) both (headwall plus baffles) contribute as sources of fragments. At the higher launch angles (ranges beyond 700 feet), only the headwall fragments contribute (see section on photographic results). Thus W_T, the total weight of fragmenting material is a combination of the assumed weights of the headwall and the baffles.

All material was assumed to be unreinforced concrete. The headwall was assumed to have nominal dimensions of 17 ft x 17 ft x 3.5 ft with an opening of 7 ft x 10 ft x 3.5 feet. This gives a weight of approximately 130,000 pounds. The baffles were assumed to have a front-face area of 75 ft^2 and a thickness of 4 feet, for a nominal weight of 51,000 pounds each. Therefore W_T is either 232,000 pounds (headwall plus two baffles) or 130,000 pounds (headwall, only).

The characteristic length (L_c) determined from the 1/6.43-scale test and scaled up to full scale was 7.0 inches (see section on Debris Analysis).

Everything that is needed for computing N(>L) is now either known or can be calculated from the information presented above. The results (debris lengths and numbers) are also shown in Table 3.

Thus, for any range increment, the fragment density can be computed using the following relationship:

$$D_i = \sum_{j=1}^{9} (FRAC_j * N_j)$$

where

D_i	= fragment density in i-th range increment
$FRAC_j$	= fraction of material of j-th weight group landing in i-th range increment
N_j	= number of debris pieces in j-th weight group
i	= identifier for each range increment
j	= identifier for each weight group; when j=1, W_L=0.5 pounds, j=2, WL=1.0 pounds, j=3, WL=2.0 pounds, etc.

This computational technique was first applied to the flat terrain case. The computed fragment densities were then "smoothed" using the technique described earlier in the analysis of the model results. Again, the hazard range is defined as the range at which the hazardous fragment density reaches one (i.e., the number of hazardous fragments equals the allowed number of hazardous fragments; in these calculations with the weight groups assumed, all fragments are hazardous). The calculation indicates that this density of hazardous fragments would be obtained at a range of 1300 feet. This differs from the model-derived result by 13.5%.

Not all the baffle material will become involved as analytically assumed. On several of the model tests, at least one of the baffles remained nearly intact and did not fracture into a large number of pieces. Moreover, the analytic procedure assumed that all of the headwall material would become debris. In actuality, not all of this material will become involved; rather, an amount of material slightly larger than the tunnel diameter would be broken up and projected as debris. Because of these differences between the model results and the analytic procedures, the analytically-derived ranges should he considered as overly-conservative estimates.

If we assume that the flat-terrain, 1/6.43-scale model results give a realistic hazard range, then a "normalization factor" of (1145/1300) can be derived and applied to the analytic results to bring them into agreement with the test results.

The prediction technique described at the start of this chapter was then applied to terrain containing 8.1° and 14° hills, and the normalization factor derived above was applied to the calculated hazard ranges.

Thus, for flat terrain the fragment hazard range is 1145 feet, for an 8.1° hill, the range decreases to 950 feet, and for a 14° hill the range becomes 850 feet. These results are shown in Figure 8 and in Table 4.

REFERENCES

1. Ammunition and Explosives Ashore: Safety Regulations for Handling, Storing, Production, Renovation, and Shipping, NAVSEA OP5, Volume 1, Fourth Revision, Change 15, 15 February 1988.

2. "DISTANT RUNNER--Debris Recovery and Analysis Program for Events 4 and 5," Ward, J. M., Minutes of the Twentieth Explosives Safety Seminar, Aug 1982.

3. "Technology Base of the Navy Explosives Safety Improvement Program," Porzel, F. B., Minutes of the Nineteenth Explosives Safety Seminar, Los Angeles, CA, 9-11 September, 1980.

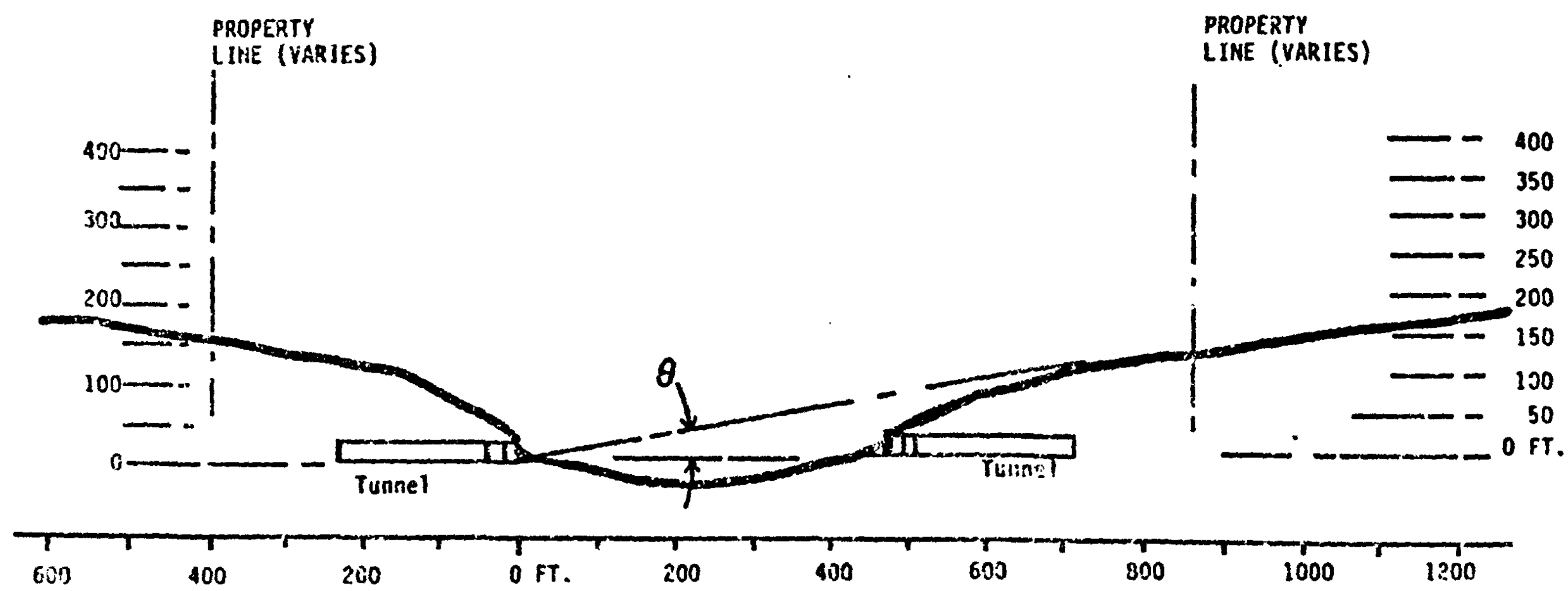

FIGURE 1 REPRESENTATIVE TUNNEL TOPOGRAPHY

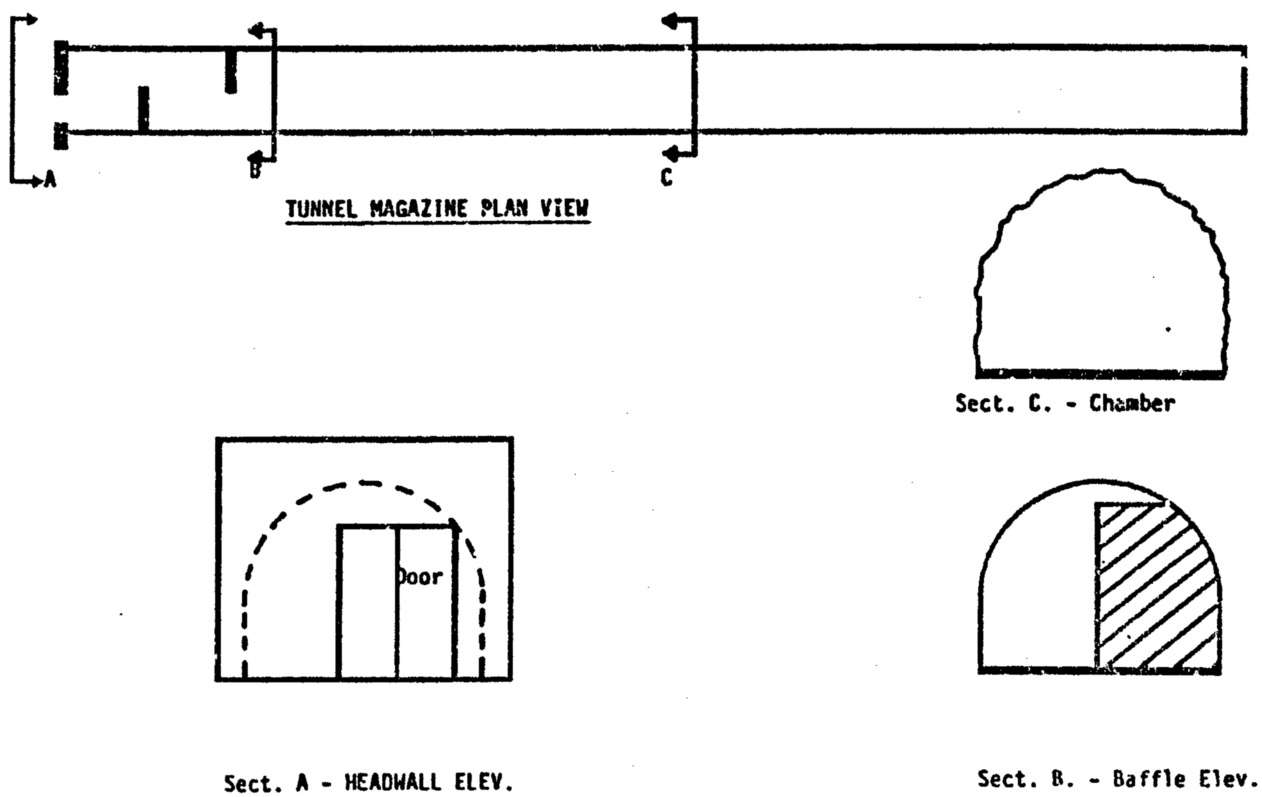

FIGURE 2 SCHEMATIC OF TUNNEL MAGAZINE

FIGURE 3 COMPOSITE TUNNEL DEBRIS DATA

(DATA <5° OMITTED)

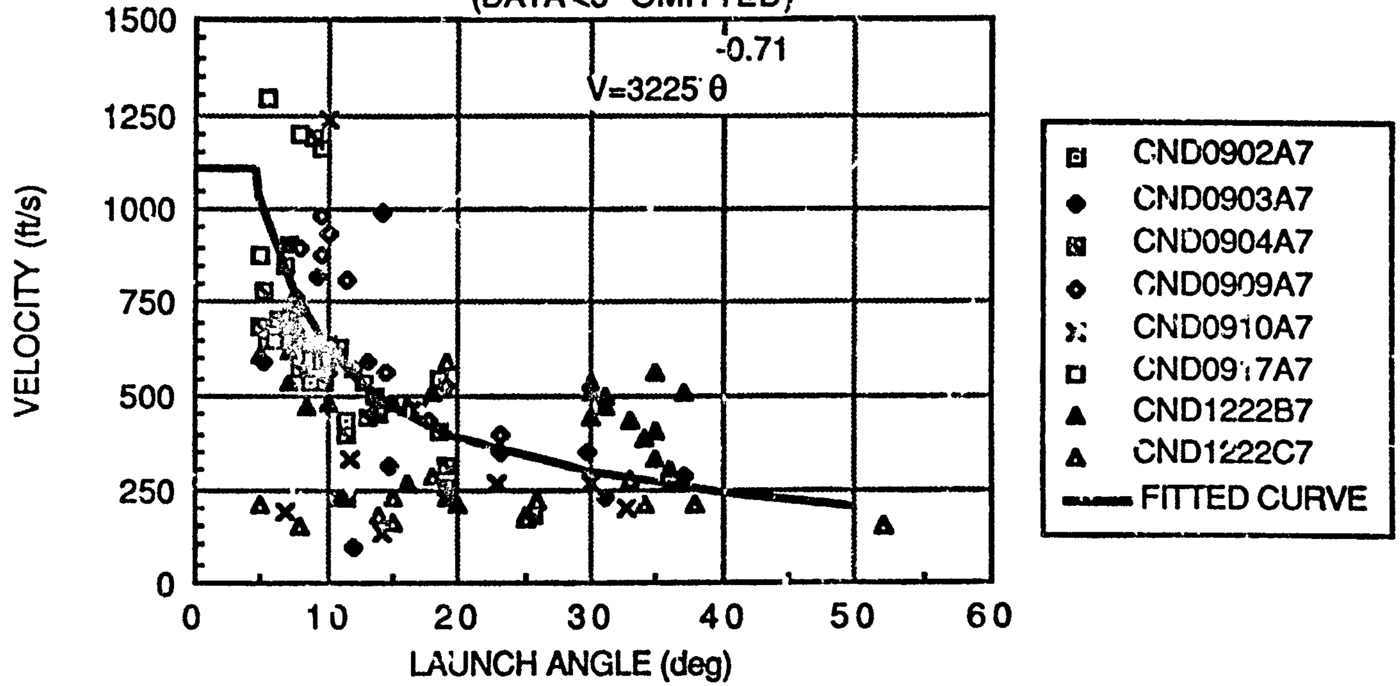

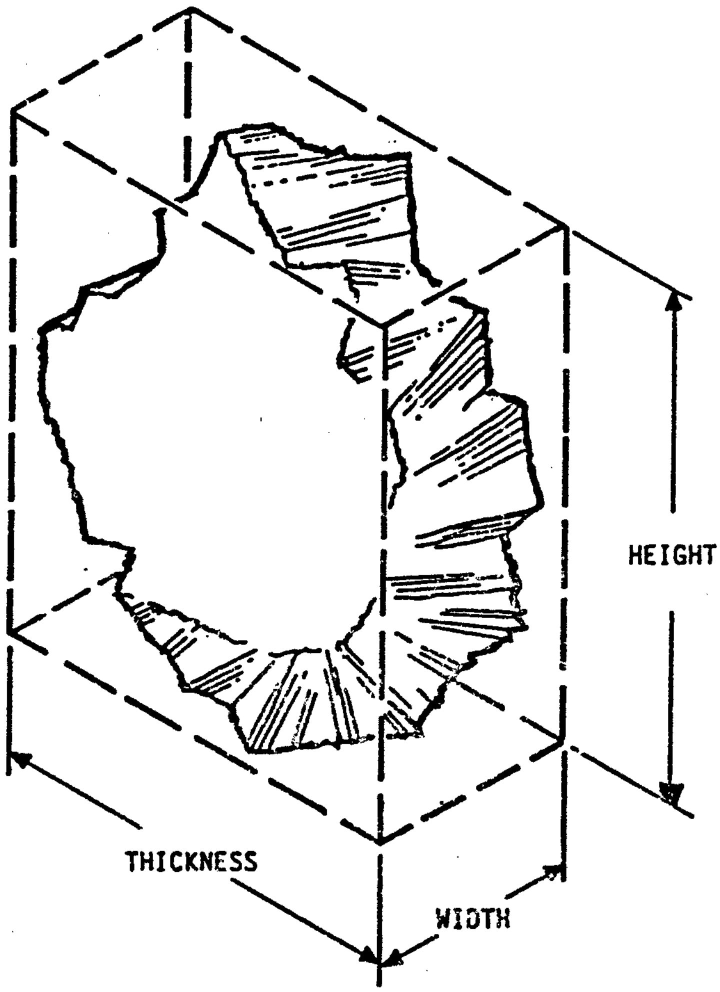

FIGURE 4 SHAPE FACTOR MEASUREMENTS

FIGURE 5 1/6.43-SCALE DEBRIS NUMBER DISTRIBUTION

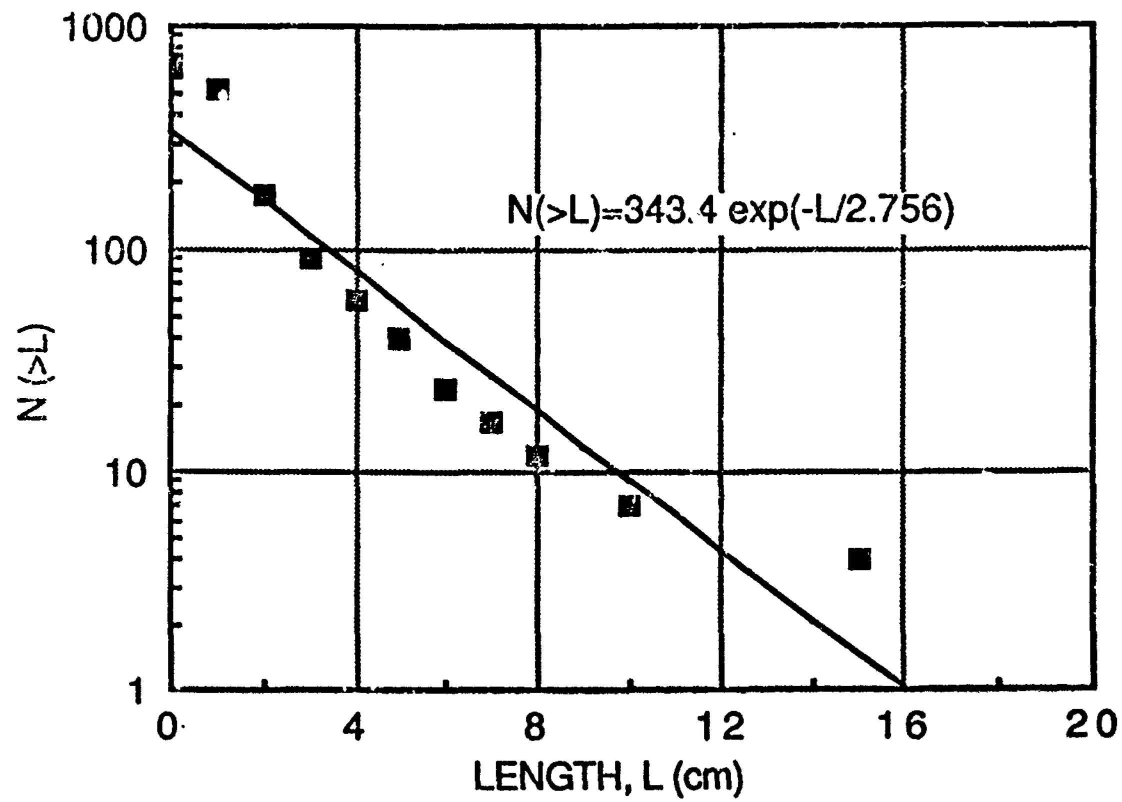

FIGURE 6 FULL SCALE DEBRIS DENSITY VERSUS RANGE
(BASED ON 1/6.43-SCALE TEST)

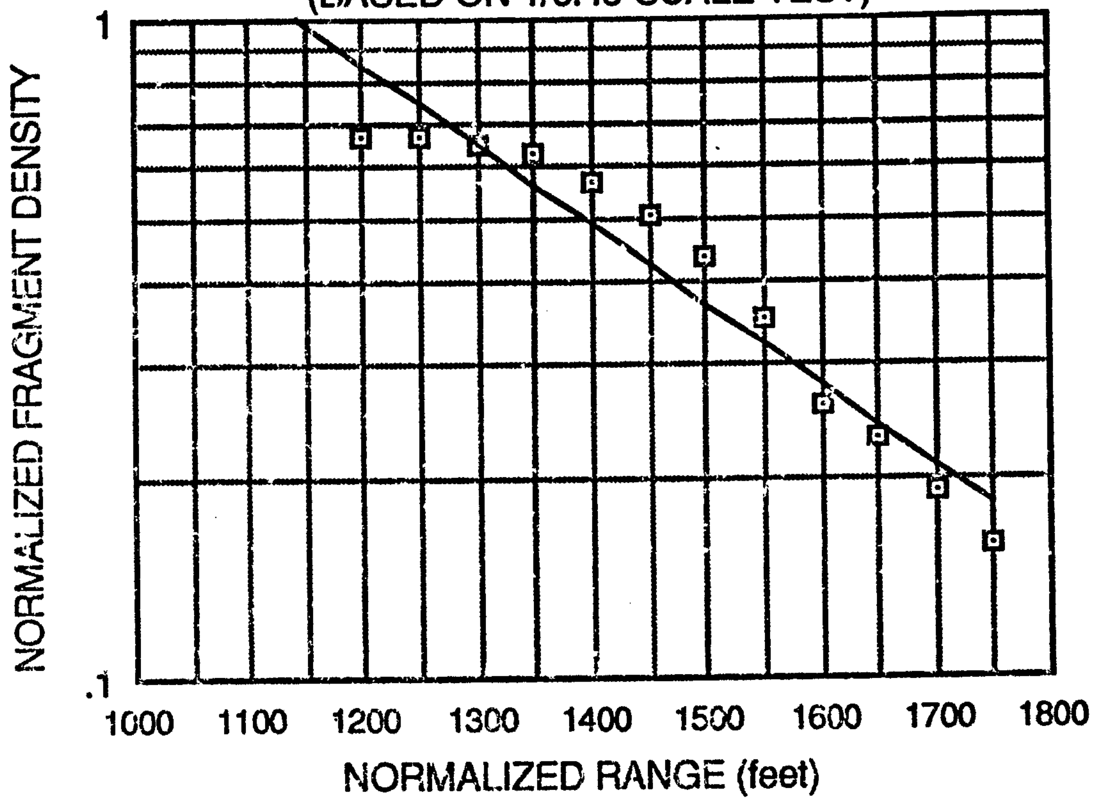

FIGURE 7 HILL PROFILE

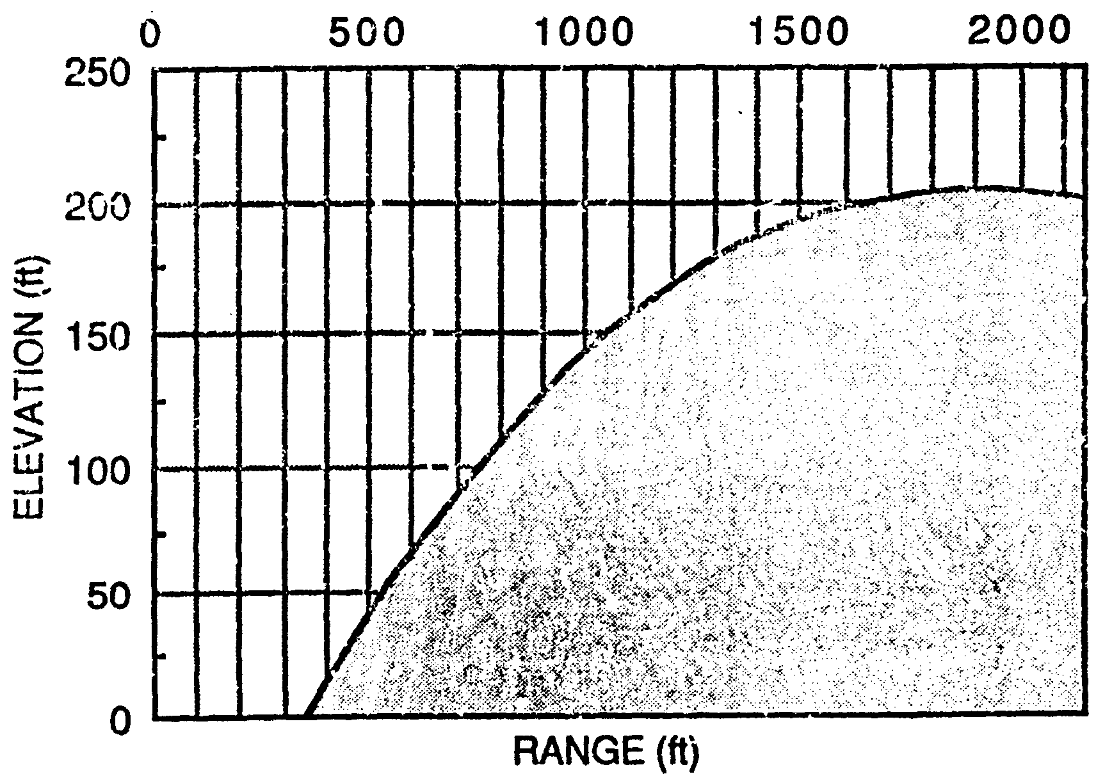

FIGURE 8 DEBRIS HAZARD RANGE

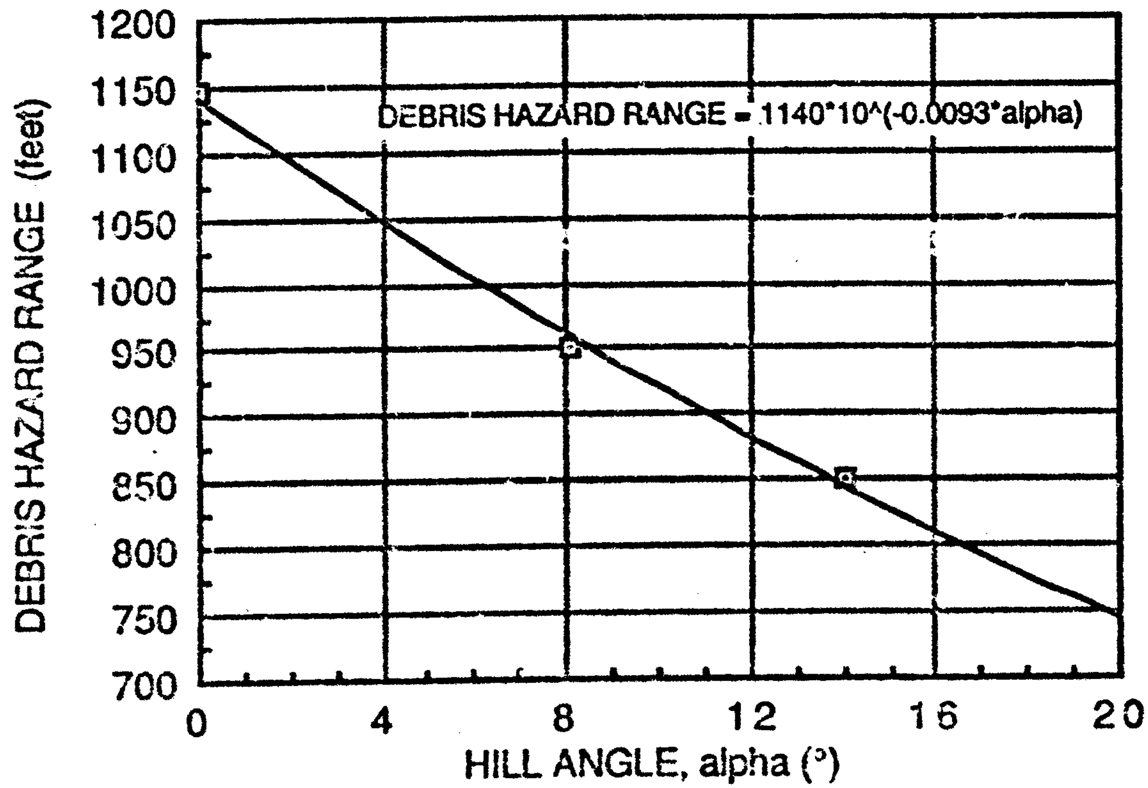

TABLE 1 DEBRIS TEST PROGRAM

NCEL TEST NUMBER	TERA SHOT NUMBER	SCALE FACTOR	EXPLOSIVE WEIGHT (pounds)	CONFIGURATION
2	CND0821A7	15	12	Headwall & 1 Baffle
4	CND0902A7	15	12	Headwall & 2 Baffles
5a	CND0903A7	15	6	Headwall & 2 Baffles
6a	CND0904A7	15	3	Headwall & 2 Baffles
6b	CND0909A7	15	3	Headwall & 2 Baffles
5b	CND0910A7	15	6	Headwall & 2 Baffles
8	CND0917A7	6.43	96	Headwall & 2 Baffles
7a	CND1222A7	15	6	2 Baffles
7b	CND1222B7	15	6	Headwall
7c	CND1222C7	15	3	Headwall & 2 Baffles

TABLE 2 TUNNEL DEBRIS SHAPE FACTORS

	CND0821A7	CND0902A7	CND0903A7	CND0904A7	CND0917A7
MODEL SCALE	15	15	15	15	6.43
SAMPLE SIZE	35	35	92	62	421
SAMPLE MEAN	0.47	0.36	0.36	0.33	0.37
SAMPLE STANDARD DEVIATION	0.11	0.11	0.10	0.10	0.11
SAMPLE MEDIAN	0.44	0.36	0.36	0.36	0.36
SAMPLE MODE	0.44	0.28	0.36	0.36	0.28

TABLE 3 DEBRIS LENGTHS AND NUMBERS

WEIGHT (lbs)	LENGTH, L (in)	HEADWALL+2 BAFFLES	HEADWALL
		(N>L)	(N>L)
0.5	2.36	185	94
1	2.97	189	107
2	3.74	283	160
5	5.08	231	131
10	6.40	234	133
20	8.06	295	167
50	10.94	195	110
100	13.79	154	88
200	17.37	232	131

TABLE 4 FRAGMENT RANGE VERSUS HILL ANGLE

HILL ANGLE (°)	FRAGMENT HAZARD RANGE (feet)
0	1140
1	1120
2	1090
3	1070
4	1050
5	1030
6	1000
7	980
8	960
9	940
10	920
11	900
12	880
13	860
14	850
15	830
16	810
17	790
18	780
19	760
20	740

TUNNEL EXPLOSION TEST

A Progress Report

by

William F. Durbin
Ordnance Evaluation Branch (Code 3269)
Ordnance Systems Department
Naval Weapons Center, China Lake, California

Presented to the Twenty-Third DoD Explosives Safety Seminar
Hyatt Regency Hotel
Atlanta, Georgia
9-11 August 1988

ABSTRACT

The Department of Defense Explosives Safety Board (DDESB) and KLOTZ Club member nations Norway and the United Kingdom proposed to fund construction and testing of an underground explosives storage facility to verify the data obtained from modeling and scale studies. The Ordnance Evaluation Branch of the Naval Weapons Center (NWC), China Lake, California, agreed to perform the construction and testing work at NWC.

This report summarizes, to date, work performed at the Naval Weapons Center in preparation for the Tunnel Explosion Test.

I. Background and Introduction

The necessity of providing a safe environment for persons and property located in the vicinity of explosives storage facilities has long been recognized by the world-wide explosives safety community. Numerous test programs have been carried out over the years to develop and expand the quantity/distance (QD) database which is used to provide minimum safe siting distances for personnel, roadways, and structures subject to airblast, debris scatter, and ground motion effects resulting from detonations occurring in explosives storage facilities. The requirements for increasing the database in QD measurements extend not only to above ground facilities but to underground storage centers, as well. Until recently, the majority of QD data for underground facilities has been generated through computer modelling and small-scale testing programs.

The Ordnance Evaluation Branch of the Ordnance Systems Department, Naval Weapons Center, accepted the task proposed by the DDESB and KLOTZ Club member nations Norway and the United Kingdom, to construct and perform tests on a one-half scale model of an underground explosives storage magazine (tunnel/chamber) with shallow overhead cover in an effort to verify data from modeling studies and small-scale test programs.

The work performed by the Naval Weapons Center has been conducted during Fiscal Years 1987 and 1988 and includes the following:

* Site Selection

* Site Environmental Clearance

* Preparation and Award of Contract for Tunnel/Chamber Construction

* Completion of the Tunnel/Chamber

* Geologic and Geophysical Analysis of Rock

* Test Planning and Coordination with NWC Range Department

NOTE: As of this date — 10 August, 1988, the instrumentation groups and experimenters who are supporting the Tunnel Explosion Test are on-Center installing their equipment and making final preparations for the test.

For the reader's convenience, all figures are located at the back of the report text.

II. Site Selection

The Tunnel Explosion Test site is situated on the north side of a northeast-southwest trending hillside of weathered granitic rock near the western boundary of the Naval Weapons Center (Figure 1). The site was selected following a series of Center-wide reconnaissance trips via road and helicopter. The site was most promising for the following reasons: The rock outcrop was weathered but generally competent; the Sponsors' requirements for depth of tunnel/chamber overhead cover could be met at this site; there was a large gently-sloping open area to the north quite suitable for unobstructed fragment collection and gauge placement locations; the site was easily accessible by good roads, and the site was relatively isolated from the main NWC ranges, thus eliminating numerous logistics and scheduling conflicts with other test groups. A view of the proposed test site is shown in Figure 2. The view is oriented looking southeasterly along the centerline bearing.

III. Site Environmental Clearance

Prior to construction or land disturbance for a test program at NWC, an environmental impact study must be conducted. This study involves field examination, analysis of data and preparation of documentation for potential program impact upon cultural and biological resources and endangered species.

The Tunnel Explosion Test site required an environmental impact study for a circular area of radius approximately 900 meters from "ground zero" (the center of the chamber). Work was performed by the NWC Environmental Office of the Public Works Department and their environmental contractor during the period September 1987 through January 1988. The completed environmental report was reviewed by the State Historical Preservation Office and Federal environmental agencies.

A finding of "Negative Environmental Impact" was determined for the Tunnel Explosion Test site and approval to proceed with the program was granted on 1 February 1988.

IV. Funding and Contract Requirements

Funding for the Tunnel Explosion Test was provided in increments from the Sponsors which were received by NWC in April, November and December of 1987, and in January of 1988.

Because of the size and nature of the effort required for the tunnel/chamber construction, concrete work, and associated services, it was necessary for NWC to prepare and award a contract to have this work performed. Contract preparation and execution was conducted by the NWC Supply Contracts Branch.

NWC contract policy requires that full funding is available for a contract before that contract can be awarded. The funding increment that provided the full amount to cover the contract arrived on-Center on 25 January 1988; therefore, the major elements of the contracting process, and the final contract award occurred after 25 January.

V. Contracting Process

In preparing the specifications and requirements for the contract, the Ordnance Evaluation Branch included construction work, engineering and geologic evaluations of rock and concrete, and a portion of the pre-and post-test data collection. The elements of work incorporated into the contract are listed below:

* Site Preparation
* Construction of the Tunnel/Chamber Configuration (Figure 3 A and B)
* Form and Pour Concrete Tunnel Floor, Portal Apron, Tunnel Liner, and Portal Arch
* Drilling of Holes in Chamber for Instrumentation Cabling
* Shotcreting of Tunnel and Chamber
* Geologic Mapping of Surface and Underground
* Conduct Engineering Property and Thin Section Analysis of Rock Samples
* Conduct Concrete Compressive Strength Testing
* Survey and Map the Completed Tunnel/Chamber -- Prepare Plan Map, Longitudinal Section and Cross-Sections
* Survey Debris Collection Pads
* Survey Artificial Debris Items Following Test
* Compile Post-Test Debris Scatter Data

Table 1 shows the highlights and dates for each of the steps in the contracting process.

On 14 April 1988, the Tunnel Explosion Test contract was awarded to the joint venture group of Mine Engineering and Development Corporation and Valley Engineers (MDEC/VE) of Bakersfield and Fresno, California.

VI. Construction and Service Milestones Completed by the Contractor (MDEC/VE)

The contractor mobilized to the test site on 25 April 1988 with a crew of 6 persons and the full complement of equipment to perform the contract work. The small crew demonstrated capability in all phases of mining work, heavy equipment operation, engineering design, surveying, concrete forming/finishing, welding, electrical, and maintenance.

STATEMENT OF WORK (SOW) PREPARED DEFINING SERVICES AND SPECIFICATIONS REQUIRED OF CONTRACTOR	4 DEC 87
REQUISITION FOR MATERIALS/SERVICES PREPARED	4 JAN 88
REQUEST FOR PROPOSAL ADVERTISED IN COMMERCE BUSINESS DAILY	13-27 JAN 88
BID PACKAGES SENT OUT (25 REQUESTS RECEIVED)	28 JAN 88
SITE VISIT FOR PROSPECTIVE BIDDERS	5 FEB 88
BID PROPOSALS RECEIVED (2)	7 MAR 88
TECHNICAL EVALUATIONS COMPLETED	14 MAR 88
CONTRACT AWARDED	8 APR 88
POST AWARD CONFERENCE WITH SELECTED BIDDER	14 APR 88

TABLE 1. MILESTONES IN THE CONTRACTING PROCESS.

Table 2 shows the progression of construction and service tasks performed by the contractor from 25 April 1988 through the present time.

Following the Tunnel Explosion Test, the contractor will survey the direction and distance of throw of artificial debris items which were located on the overhead cover along the tunnel/chamber centerline prior to the test. The contractor will also weigh, measure, and catalog debris found on debris collection pads following the test.

VII. Geology and Geophysics

The test site is built in a gently-sloping hillside composed primarily of the intrusive igneous rock called granodiorite. The granodiorite is coarse-grained (1-4mm grain size) and deeply weathered and fractured. Numerous fine-grained black to dark gray dikes have been injected along the fractures and these stand as resistant topographic "highs" in contrast to the granodiorite (Figure 2).

Weathering of the granodiorite is attributed to the combined effects of infrequent rain and snowmelt waters and the intense range of temperatures from below freezing to well above 100 degrees F. Mineral grains are often destroyed through repeated freeze/thaw conditions while others are chemically attacked by reaction with rain and snow melt waters which seeps into fractures and produces clays or other soft weathering products (Figure 14). The dike rocks present are younger, generally much finer grained and more silica rich than the granodiorite host rock, and are therefore less susceptible to weathering. These tend to break up into angular blocks rather than decompose grain by grain (Figure 15).

The contractor was tasked with mapping the surface and underground geology of the site and providing thin section analysis, compressive strength, and specific gravity data for a representative suite of rocks. As of this writing, the mapping and thin section data are unavailable but will be included in the final report produced following the Tunnel Explosion Test. Personal communications with the contract geologist (July 1988) indicate that the underground geology is highly complex, particularly in the chamber where there are at least 4 different types of dikes within faulted and fractured granodiorite. The dikes join at fracture intersections and in some cases, cross-cut one another. A fault occurs at the entrance to the tunnel which was not visible on the surface before the portal site cut was made. This fault is primarily responsible for the extremely fractured ground encountered during the start-up of the tunnel (Figure 6).

Rock property data provided by the contractor is listed below:

Compressive strength measurements for the granodiorite range from 3,475 to 3,664 pounds per square inch (psi) and specific gravity measurements ranged from 2.58 to 2.61 grams per cubic centimeter (g/cc).

Compressive strength measurements for the dike rocks ranged from 14,318 to 44,153 psi and specific gravity measurements ranged from 2.63 to 2.85 g/cc.

The Sponsors requested that a seismic geophysical survey be made of the rock cover over the tunnel/chamber in order to determine the rock mass seismic velocity — information considered important in predicting the severity of overhead rupture and fragment throw from the explosion. The Geosciences Branch

25	Apr	Contractor began mobilization at NWC
26	Apr	Contractor began drilling on site
2	May	First shot on surface cut (Figs. 4 and 5)
2-6	May	Surface geology mapping completed
6	May	First tunnel round shot (Fig. 6)
7	June	8- by 8-foot (2.4 by 2.4m) tunnel driven to 141 feet (43m) (Fig. 7)
1	July	Chamber enlargement completed
2-3	July	Underground geologic mapping completed
13	July	Tunnel floor/Portal apron poured (Figs. 8 and 9)
22	July	Rock compressive strength/specific gravity data completed
16/23	July	Debris collection pads surveyed
23/26	July	Tunnel liner/Portal arch poured (Figs. 10, 11, and 12)
30	July	Shotcreting of Tunnel/Chamber completed (Fig. 13)
2	Aug	Drilling of Chamber Instrumentation Holes completed
4	Aug *	Surveying/Measuring of finished Tunnel/Chamber

* In progress that date.

Table 2. MDDC/VE CONTRACT WORK MILESTONES. APRIL THROUGH AUGUST 1988.

of the NWC Research Department conducted a series seismic surveys in July 1988 employing detonations from the contractor's underground blasting work to obtain compressional and shear wave velocities. These tests were followed up by hammer seismic measurements which were employed to narrow the wide range of velocities encountered in the blast-generated measurements. The wide velocity range was apparent through both seismic methods and is attributable to jointing, dike emplacement, localized weathering, and irregularities in overburden thickness.

The overburden rock mass seismic velocities are as follows:

Compressional Waves (Vp):	3096-5332 f/s	(944-1626 m/s)
	Average (Vp): 4292 f/s	(1309 m/s)
Shear Waves (Vs):	1985-3514 f/s	(605-1071 m/s)
	Average (Vs): 3071 f/s	(936 m/s)

VIII. Work Currently in Progress and Up-Coming

1. Studies of tunnel/chamber Rock Quality Data (RQD), i.e., fracture spacing, fracture roughness, and fracture/fault orientation, and additional Schmidt Hammer rock compressive strength testing were performed by The Earth Technology Corporation, Long Beach, California. This data is to be employed in calculations and predictions for tunnel/chamber rupture and debris throw. A summary report is expected at NWC on 3 August.

2. Chamber volume measurements and as-completed wall smoothness measurements were conducted during 2-3 August by S-Cubed of Albuquerque, New Mexico. The data will be employed in modeling pressure build-up, gas volume, and air blast effects. A report is expected prior to the Tunnel Explosion Test.

3. Personnel from the Army Corps of Engineers Waterways Experiment Station (WES) are on-Center installing air blast and ground motion gauges and performing equipment check-outs.

4. The NWC Range Department has completed Safe Operating Procedures for the mass detonation test and the Ordnance Evaluation Branch has prepared Re-Entry Procedures. Both are approved for use through required NWC channels.

5. The NWC Range Department photography and video groups are preparing equipment and camera sites for the test.

6. Experiment groups who are providing the tethered balloon camera platform, air densitometers, smoke puffs, wire drag gauges, and blast cubes will be arriving during the weeks of 8-12, and 15-19 August to install and prepare their various items.

IX. Tunnel Explosion Test Schedule

At the time of this writing, the dry run for the Tunnel Explosion Test is scheduled for Friday, 19 August, 1988. The Tunnel Explosion Test is scheduled for 24 August, 1988 at 1030 hours.

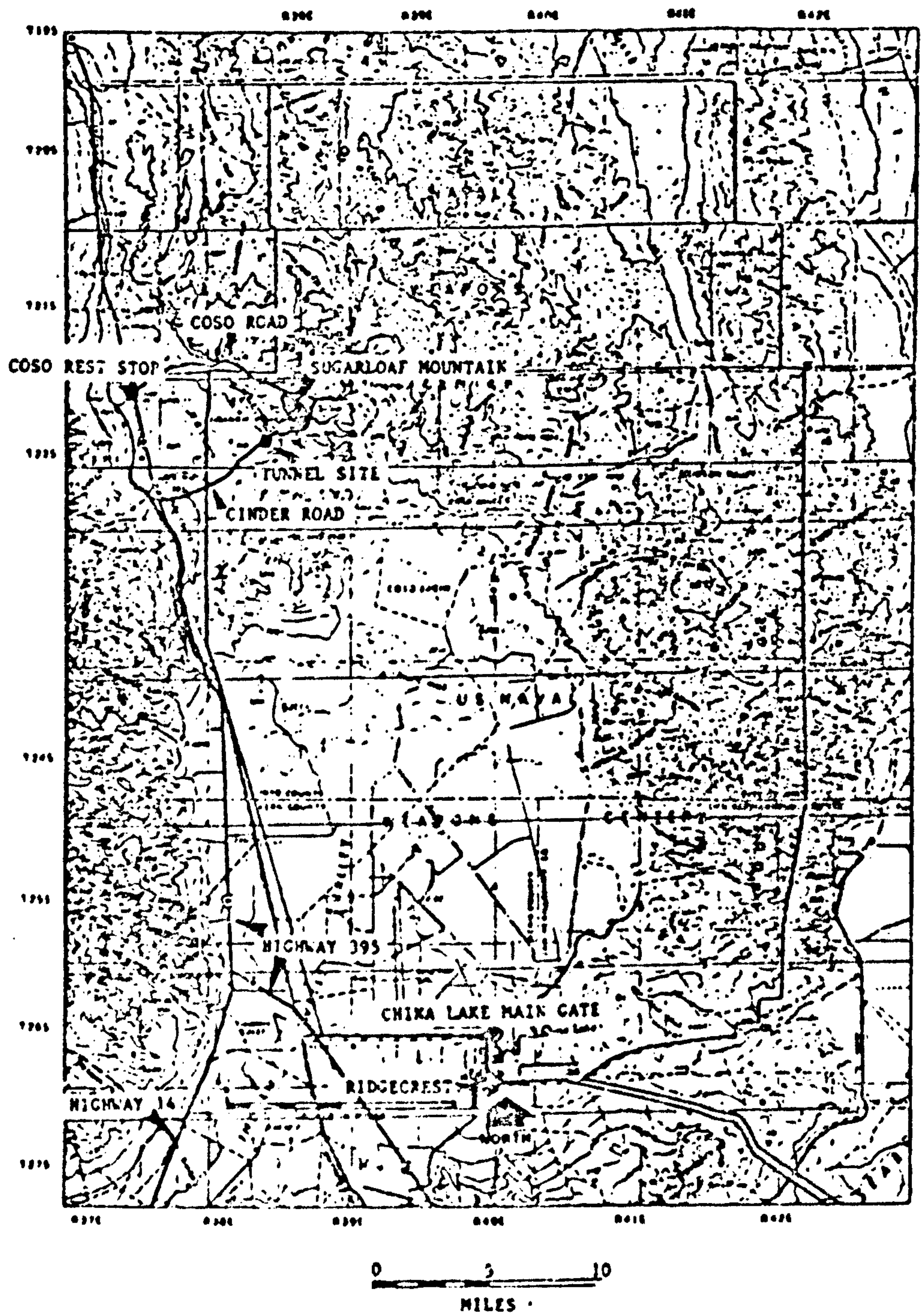

FIGURE 1. Tunnel Site Location Map

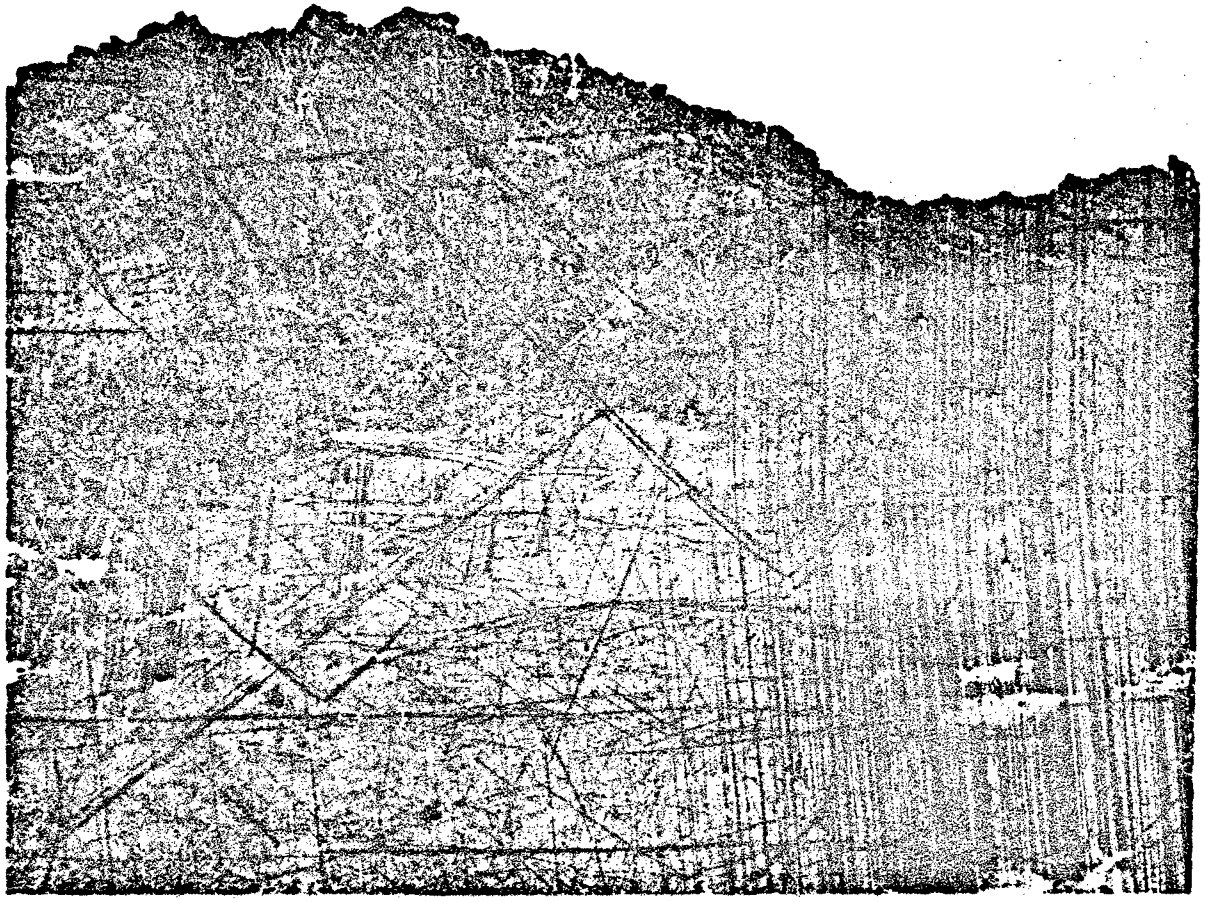

FIGURE 2. View of the proposed Test Site looking to the sou heast. Stakes mark the centerline bearing

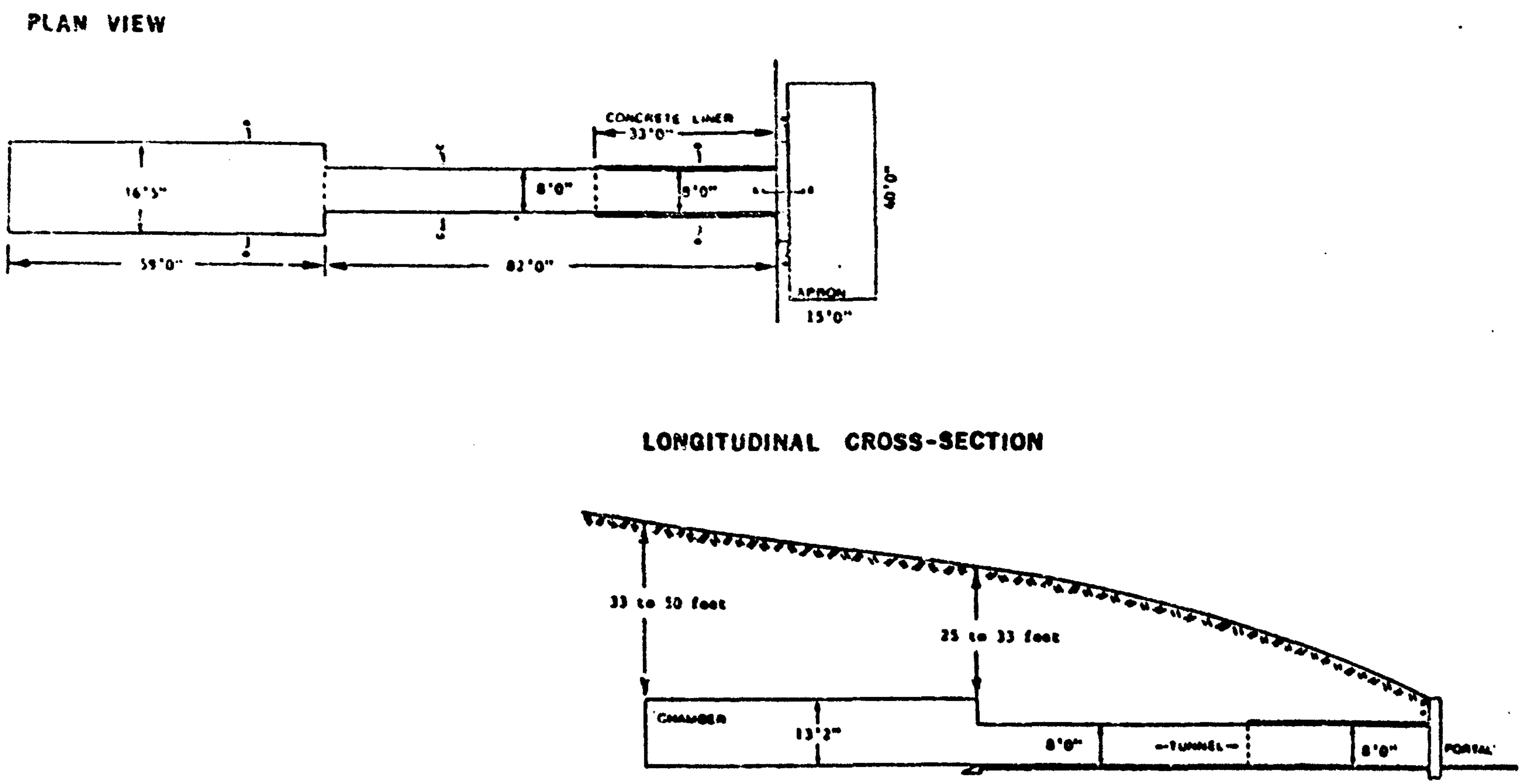

FIGURE 3A. Plan View and longitudinal Cross-Section of Tunnel/Chamber configuration as presented in specification package for prospective bidder.

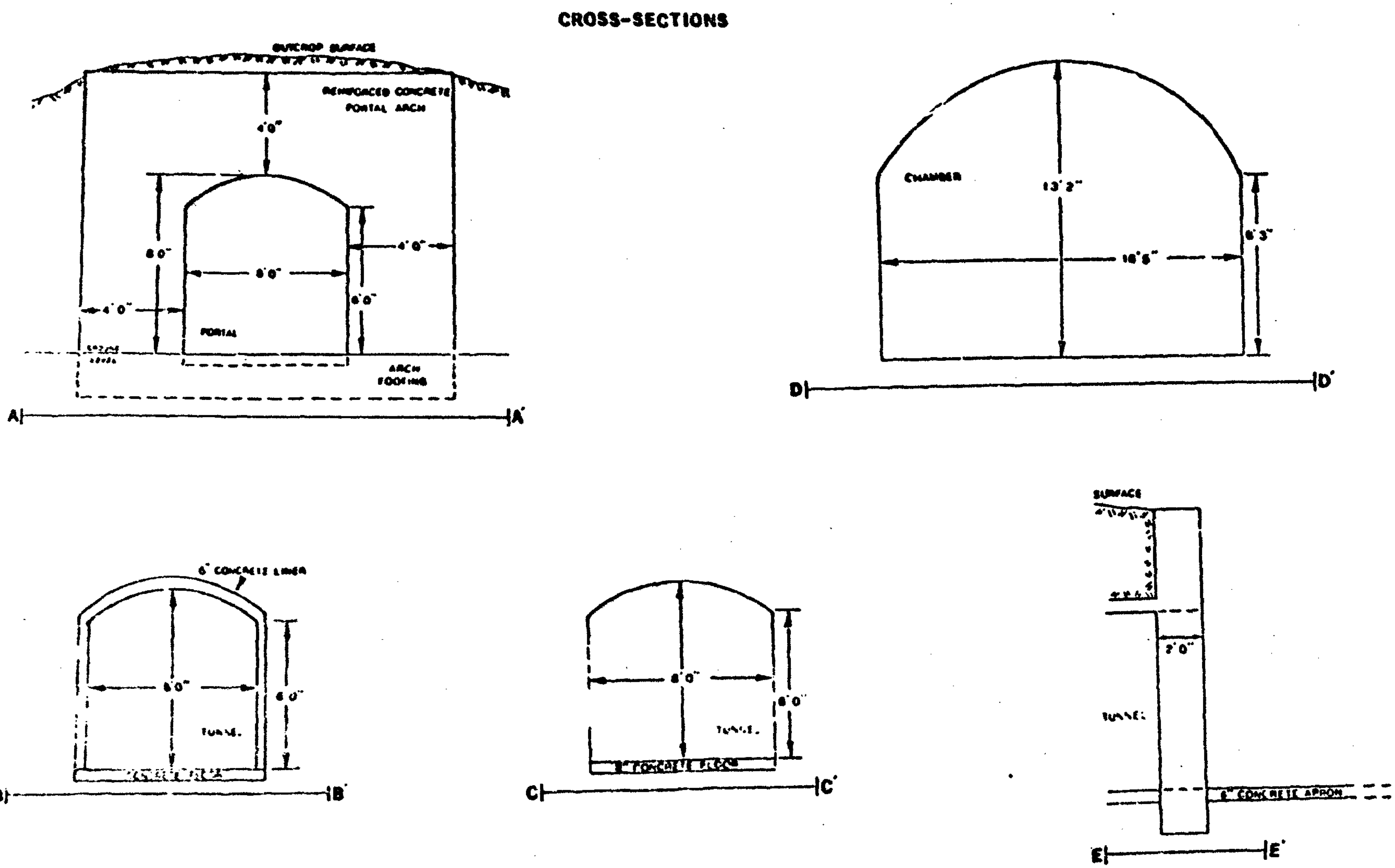

FIGURE 3B. Tunnel/Chamber Cross-Sections as presented in specification pack for prospective bidder.

FIGURE 4. Excavation of rock at portal site, following surface blasting operations.

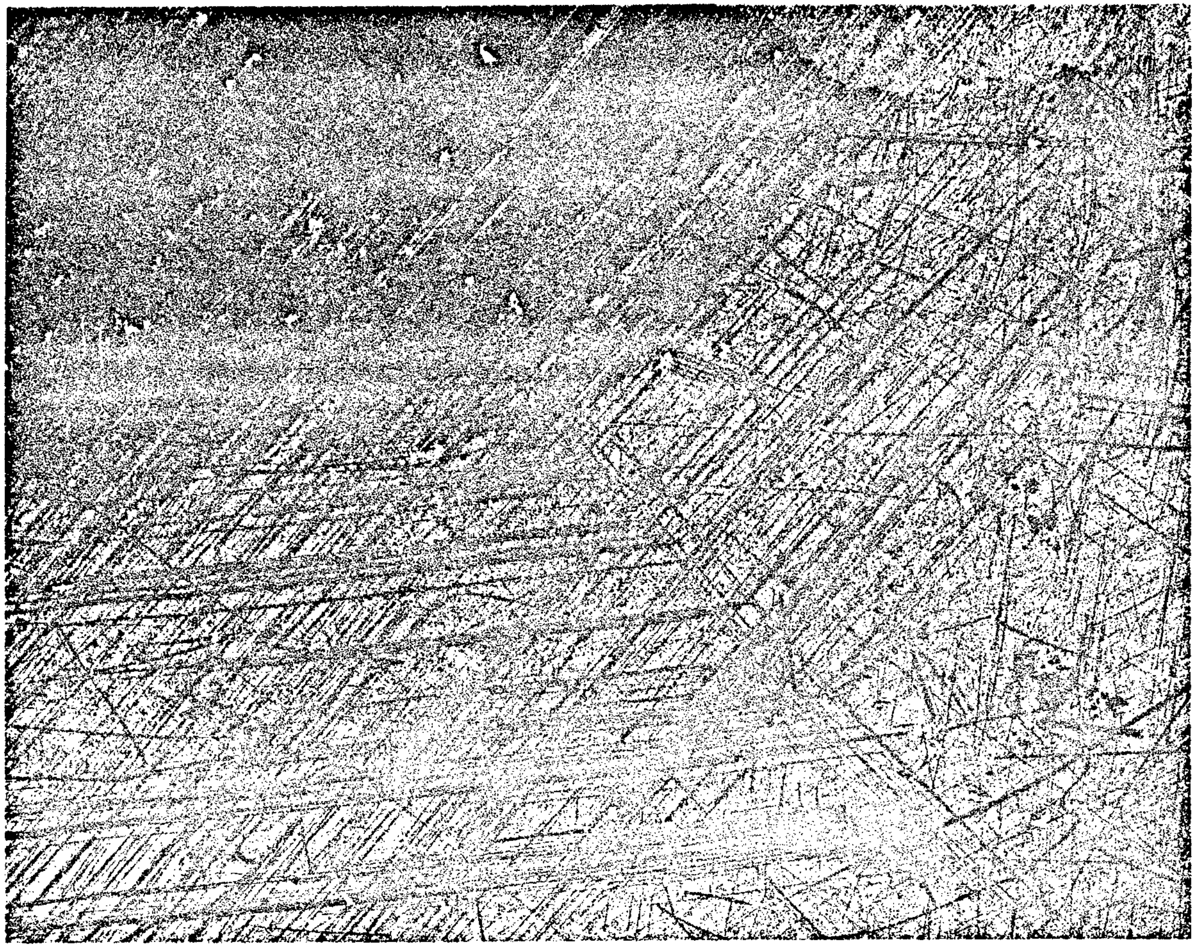

FIGURE 5. View of vertical surface cut following surface blast and clean-up. Photo taken looking southeasterly along centerline beering.

FIGURE 6. Drilling to establish tunnel opening. Note: First shot on the tunnel resulted in caving of highly fractured rock from the top and sides of the blast area.

FIGURE 7. View inside tunnel looking southeasterly along centerline bearing.

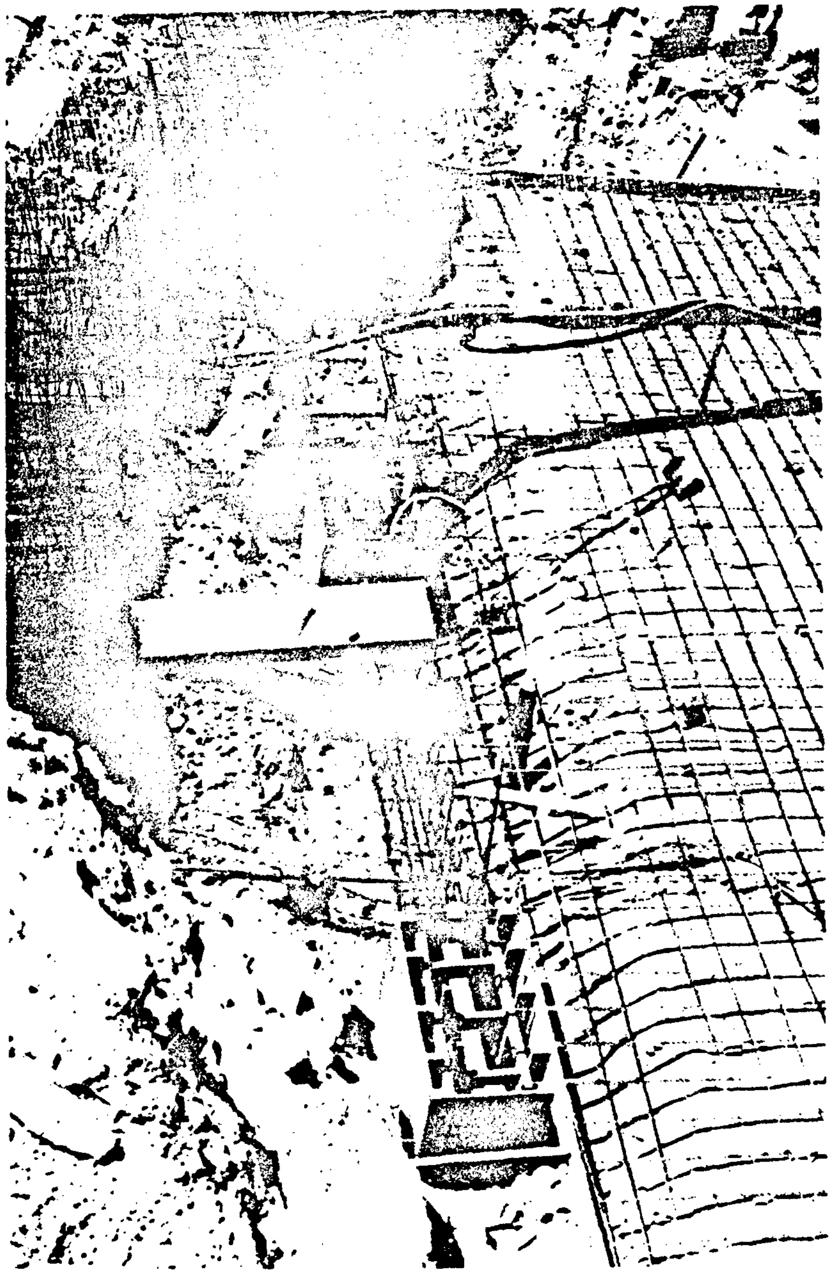

FIGURE 8. View from above looking down on portal apron forms, portal arch footing, and tunnel entrance.

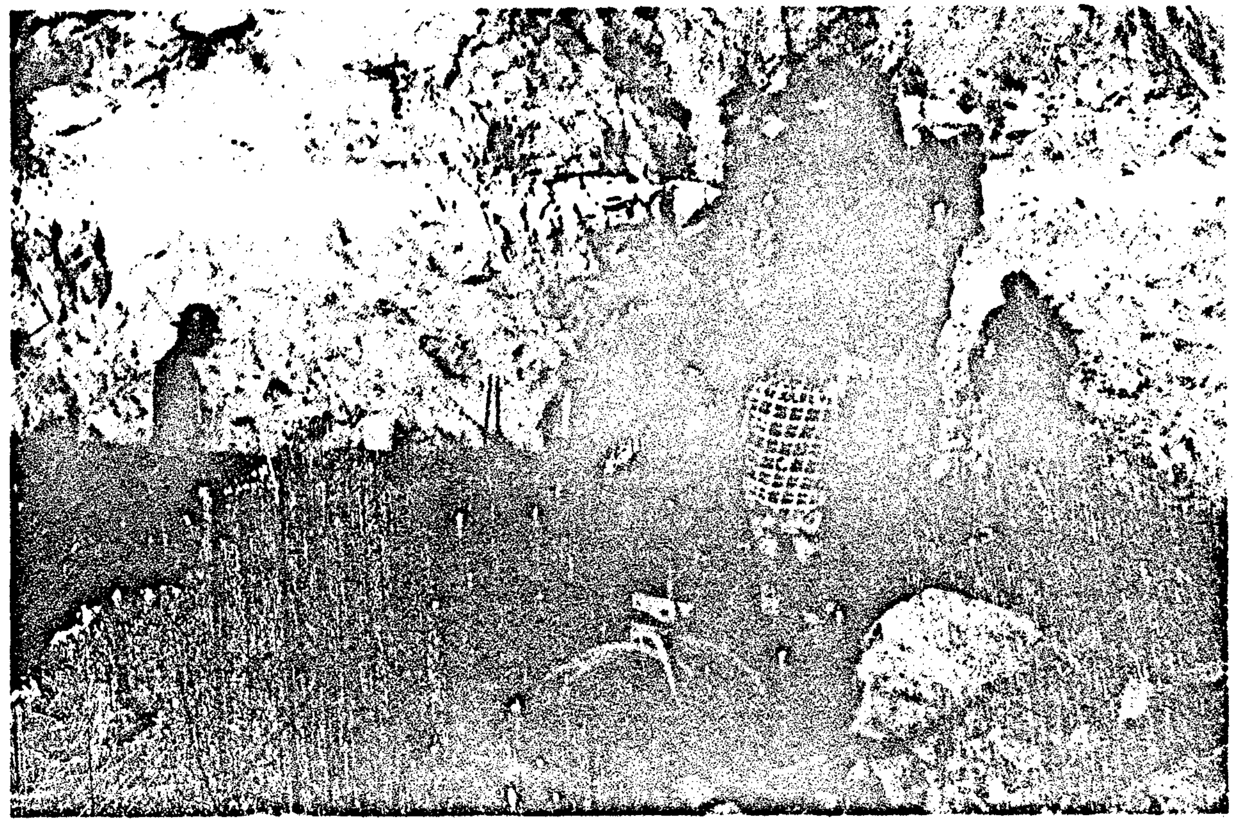

FIGURE 9. Concrete pour of tunnel floor, and portal apron.

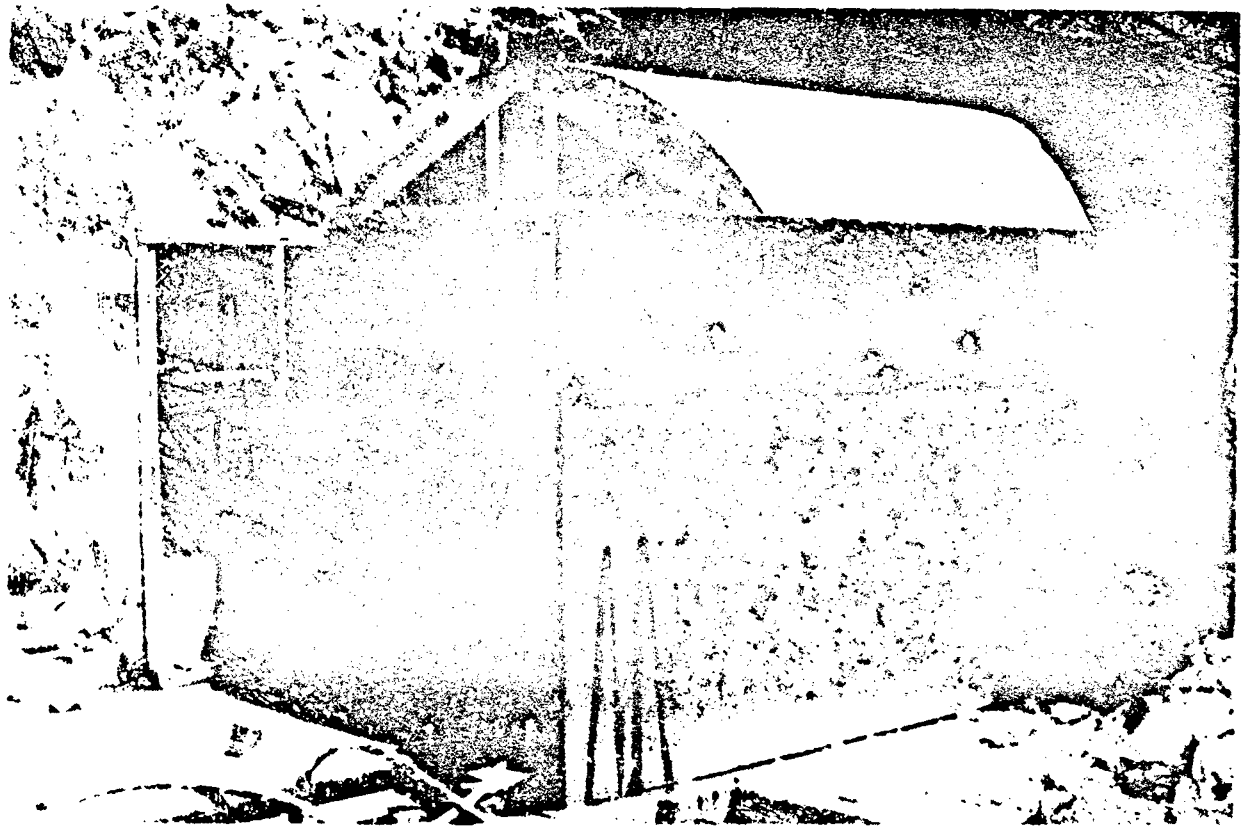

FIGURE 10. Side view of tunnel liner forms.

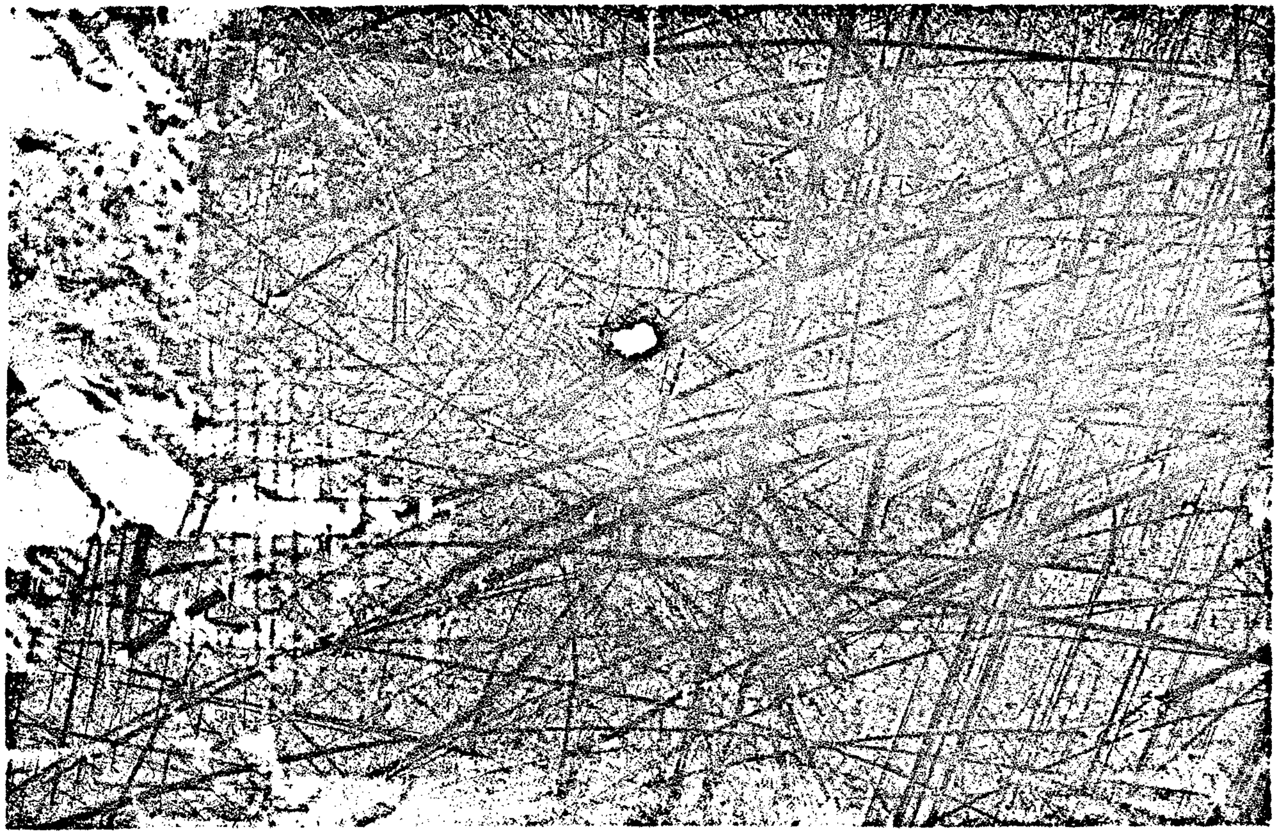

FIGURE 11. Front view of tunnel liner forms and reinforcing mats constructed for concrete pour of portal arch.

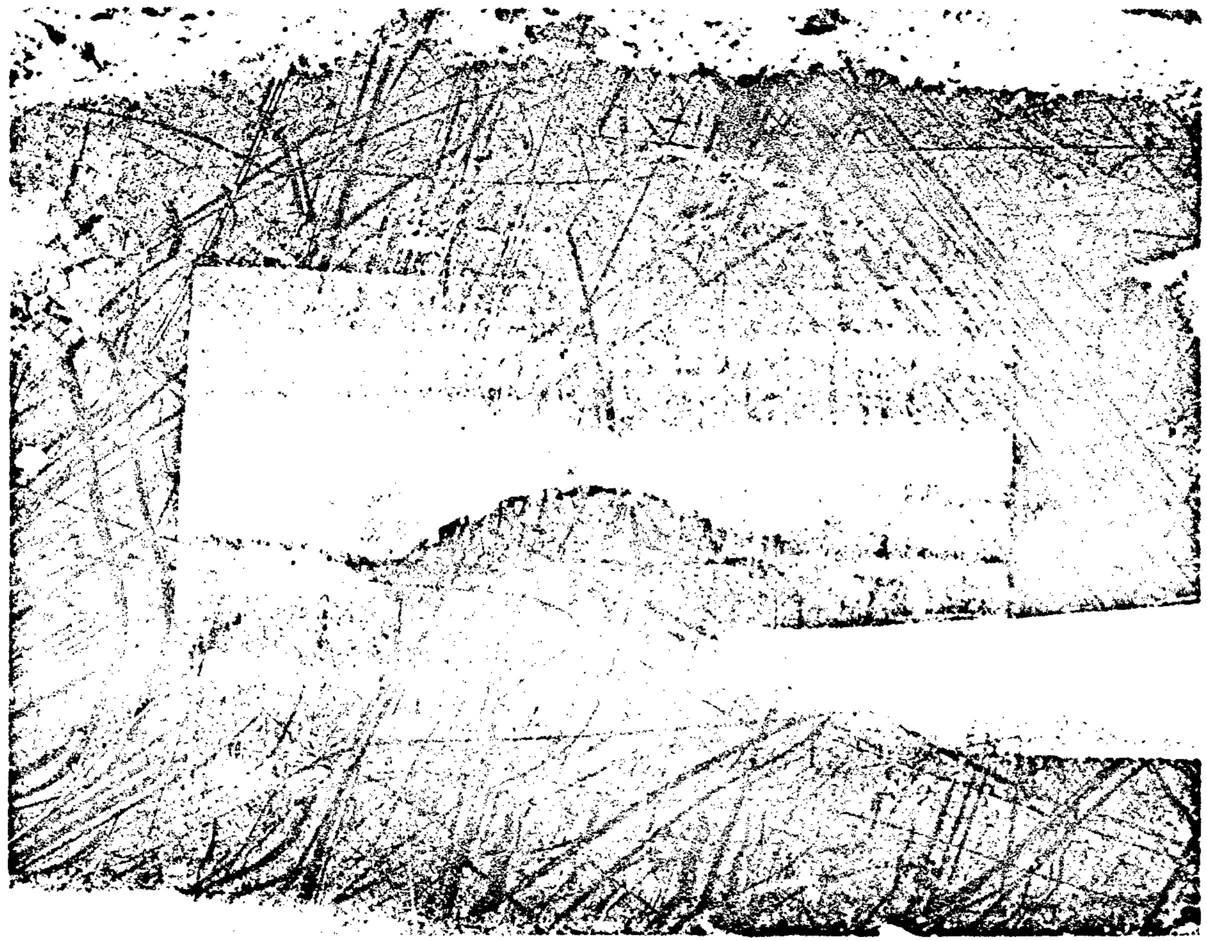

FIGURE 12. Completed portal arch.
Portal viewed along centerline bearing.

FIGURE 13. View of chamber during shotcrete application. Photo taken along centerline bearing.

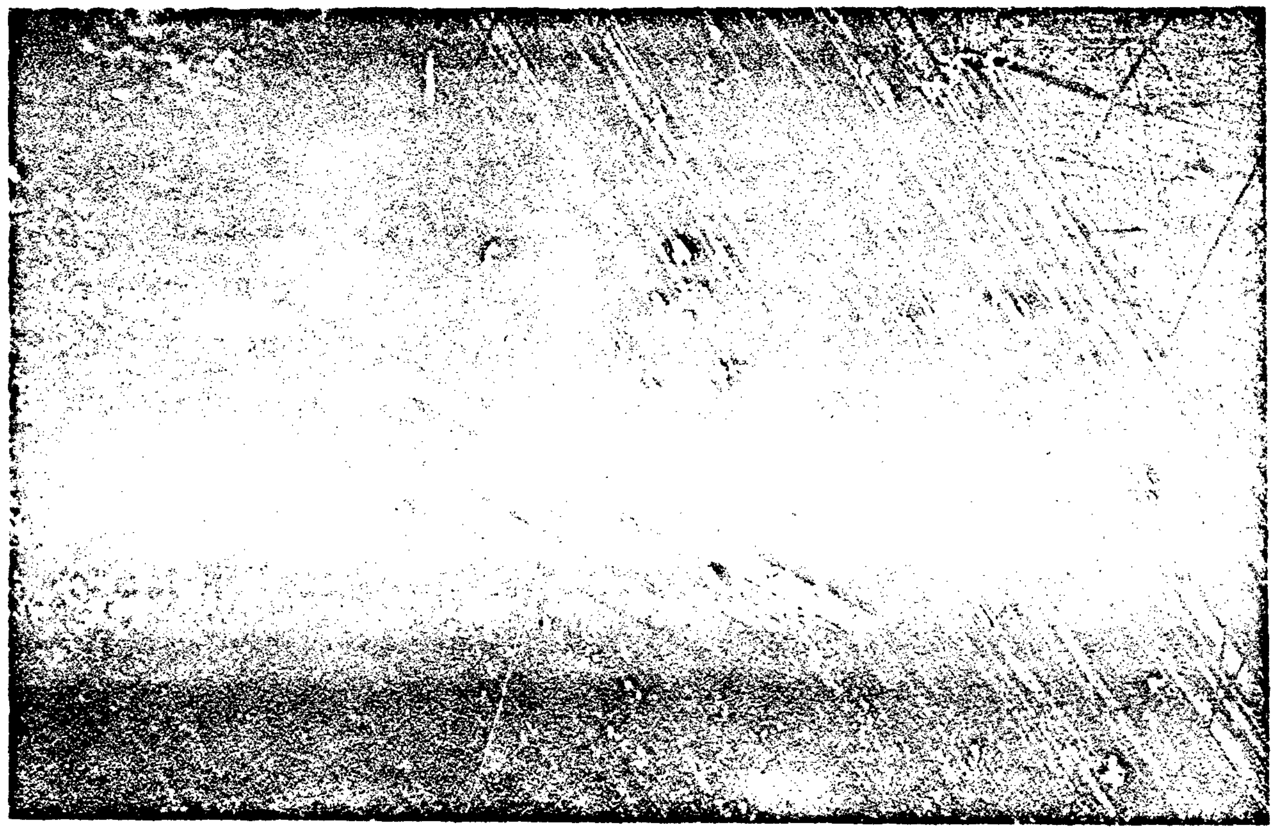

FIGURE 14. Granodiorite host rock.
Note: Many clay filled fractures.

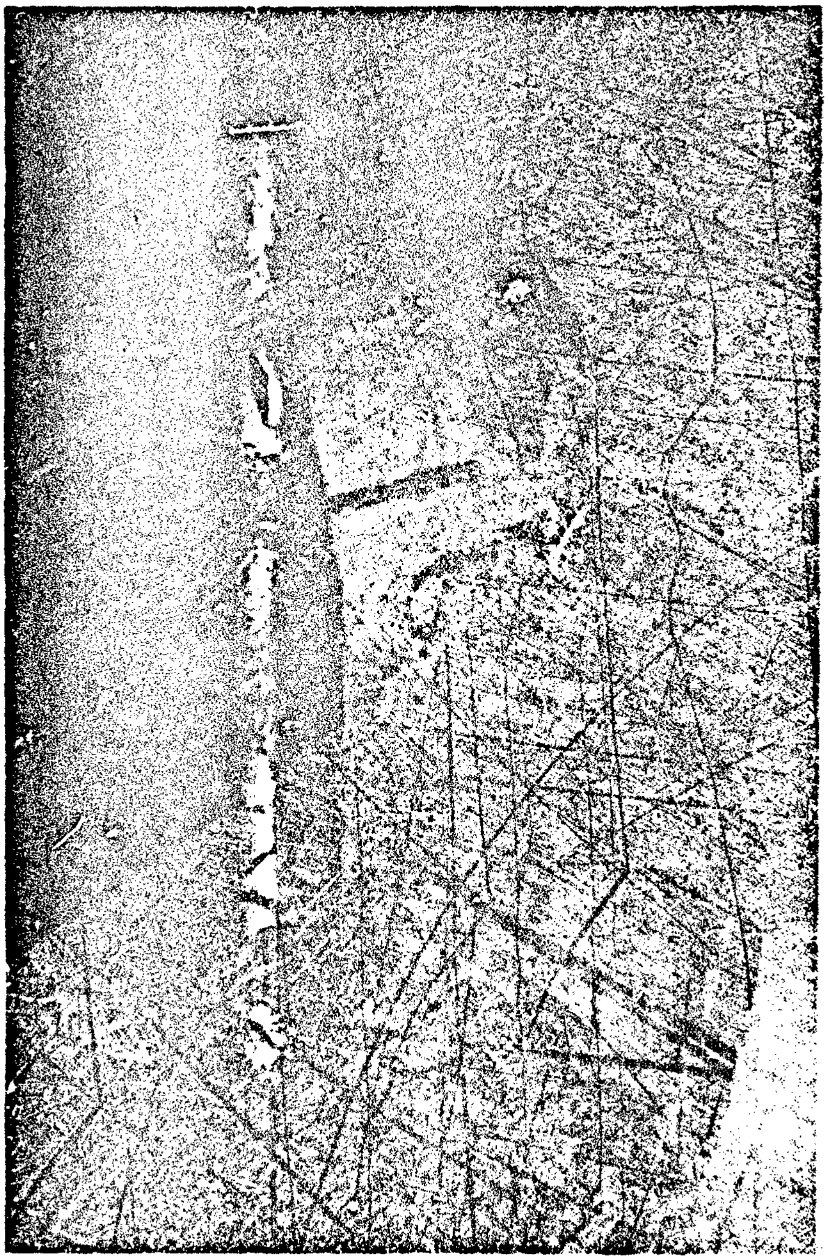

FIGURE 15. Fine-grained dike rock.
Note: Blocky appearance.

SHALLOW UNDERGROUND AMMUNITION MAGAZINE TRIALS
AT
NAVAL WEAPONS CENTER, CHINA LAKE

Arnfinn Jenssen
Ottar Krest
Norwegian Defence Construction Service
Oslo, Norway

Presented to the Twenty-Third DoD Explosive Safety Seminar
The Hyatt Regency Hotel, Atlanta Georgia
9 - 11 August 1988

Abstract

The paper describes 1:24.8 scale tests of the shallow underground ammunition magazine test (1/2 scale) planned to be carried out at the Naval Weapons Center (NWS), China Lake, CA, late in 1988. The objective of these Ad Hoc Model Tests was to acquire information which could serve as a guide when preparing the data acquisition plan for the large test at NWC. Two tests were carried out. One test with sand around a thin steel structure, to simulate an extremely poor rock, and one test using concrete, to simulate a high quality rock. Blast gauges were installed in the tunnel and on radials at different distances outside. Oak and aluminium cubes were located outside to observe the throw distance and thereby indirectly measure the dynamic pressure impulse. Aluminium rods were imbedded in the sand/concrete above the tunnel and storage chamber in order to determine the throw distance of the scattered overburden. Overpressure-distance, impulse-distance, and throw-distance tables and curves are presented. The blast waves emerging through the overburden can be distinguished from the blast wave emerging from the tunnel. More energy is dissipated into sand than into concrete.

TABLE OF CONTENTS

TABLES AND FIGURES

TABLE OF CONTENTS (Continued)

ABSTRACT

The paper describes 1:24.8 scale tests of the shallow underground ammunition magazine test (1/2 scale) planned to be carried out at the Naval Weapons Center (NWS), China Lake, CA, late in 1988. The objective of these Ad Hoc Model Tests was to acquire information which could serve as a guide when preparing the data acquisition plan for the large test at NWC. Two tests were carried out. One test with sand around a thin steel structure, to simulate an extremely poor rock, and one test using concrete, to simulate a high quality rock. Blast gauges were installed in the tunnel and on radials at different distances outside. Oak and aluminium cubes were located outside to observe the throw distance and thereby indirectly measure the dynamic pressure impulse. Aluminum rods were imbeded in the sand/concrete above the tunnel and storage chamber in order to determine the throw distance of the scattered overburden. Overpressure-distance, impulse-distance, and throw-distance tables and curves are presented. The blast waves emerging through the overburden can be distinguished from the blast wave emerging from the tunnel. More energy is dissipated into sand than into concrete.

1. INTRODUCTION

A large scale Shallow Underground Amunition Magazine Test is planned to be carried out at Naval Weapons Center (NWC), China Lake, California. The test is jointly sponsored by UK, USA and Norway and financially supported also by France, Switzerland and Sweden. The main objective of the test is to determine the effect of rupturing the overhead cover of an underground chamber by observing:

a. The break-up and initial velocity of the overhead cover and the scatter of crater ejecta.

b. Scatter of fragments and debris thrown out through the tunnel by the dynamic forces of the blast wave.

c. Blast propagation from the storage chamber, through the exit tunnel and through the crater.

d. Ground shock

The objective of the Ad Hoc Model Tests was to acquire information which could serve as a guide when preparing the data acquisition plan for the large scale test:

a. Position and setting of blast gauges

b. Initial position and recovery area of artificial debris

- rods embedded in the surface above the tunnel and chamber
- cubes placed inside the tunnel and arranged on radials outside

c. Collecting area for crater ejecta

d. Film rates and area to look at

2. TEST set up

Two tests at a linear scale of 1:24.8 were carried out:

- One with sand arround a thin steel structure to simulate an extremely poor rock (Density 1800 kg/m^3)
- One with concrete arround a thin steel structure to simulate a high quality rock. (Density 2400 kg/m^3)

A drawing of the steel and concrete/sand structure is shown in Figure 1 and a sketch of the layout at the test site is shown in Figure 2.

Blast gauge lines were arranged as shown in Table 1

Table 1. Blast gauge lines.

Direction	Distance (m)	Measuring Point No. (MP)
0° Extended centerline	17 30 53	3 4 5
30°	15 27 37 (Test 2, concrete) 48 (Test 1, sand)	6 7 8
60°	12 20	9 10

Measuring point 1 and 2 (MP1 and MP2) were located in the floor on the centerline of the tunnel - flush mounted - and separated 100 mm. Gauges and instrumentation used are shown in Figure 3.

Aluminium and oak cubes - 40 mm × 40 mm × 40 mm - were placed outside the tunnel exit as shown in Table 2:

Table 2. Location of cubes.

Direction	Distance, m	
	Test 1, Sand	Test 2, Concrete
0°	1 6 12	1 2 3
30°	1 6 12	1 2 3
60°	1 6 12	1 2 3

The average weight of the cubes were:

Aluninium: 170 grams

Oak : 44,2 grams

The aluminium rods - diameter 20 mm, length 20 mm - with a bolt screwed into one end onto which a strip of cloth was fastened were sligntly embedded into the surface of the sand/concrete overburden directly above the tunnel/chamber. The exact locations are shown in Figure 4.

The weight of the rods were:

- Rod only 15.3 grams
- Rod and bolt 30.2 grams

Location and type of technical cameras are shown in Figures 2 and 4.

Explosive used was 1.40 kg C4 formed as a sausage approximately 600 mm long. This "sausage" was located in the center of the chamber and initiated from the end facing the tunnel exit. The loading density is 64.59 kg/m^3 (Chamber alone). If the tunnel is included in the volume, the loading density will be 43.51 kg/m^3.

3. WEATHER CONDITIONS

Both tests were carried out Thursday 15 Oct 1987 at the Raufoss test site. Speed of sound (Accustic speed - a) was 333 meters per second and the barometric pressure 931 mbar (ambient pressure, Pa). It was overcast with heavy continuous rain.

4. RESULTS

4.1 Air Blast

Pressure-time histories are shown in Appendix A. Because of the complexity of the pressure-time history in the tunnel, peak pressure (PO) in the tunnel close to the exit were calculated using the ideal gas equation:

$$\frac{Po}{Pa} = \frac{2\gamma}{\gamma + 1}\left(M^2 - 1\right)$$

γ = ratio of heat capacity = cp/cu = 1.4

m = Mach number = $\frac{a_s}{a}$

a = sound velocity

a_s = shock wave velocity based on travel time from MP1 to MP2

The Po found this way were:

Test 1, Sand: 5.361 MPa (Test site or
5.758 Mpa when corrected to sea level (1000 mbar)

Test 2 concrete: 5.575 MPa (Test site) or
5.988 MPa when corrected to sea level (1000 mbar)

The peak pressures measured outside the tunnel are shown in Table 3, the impulses in Table 4 and the scaled distances and scaled pressures are shown in Table 5. These tables are also presented as diagrams in Figures 5, 6 and 7.

Time of arrival is shown in Table 6 and in Figure 8. Pressure waves exiting through cracks in the overburden have been observed for test 2. The measured peak pressures are shown in Table 3. These pressures are not presented in any diagram.

The distance (d) - pressure (Po) relations derived from Figure 7 are:

Sand:(30°)

$$\frac{d}{D} = 0.42 \frac{(Po)^{0,75}}{p}$$

Concrete (0°)

$$\frac{d}{D} = 0.60 \frac{(Po)^{0,75}}{p}$$

d = distance from the tunnel exit
D = Equivalent hydraulic diameter of the tunnel
Po = Peak overpressure in the tunnel close to the exit
P = Peak overpressure at distance d

4.2 Break up of overhead cover and scatter of ejecta

Both tests resulted in the break up of the overhead cover (Scaled overhead cover ranged from about 0.3 to 0.5 m/kg $^{1/3}$). The crater diameter was about 3 m. The visual crater bottom was close to the tunnel/chamber floor. The distance (vertical)-time history of the overburden as seen by the camera behind the installation is shown in Figure 9. Based on these figures the velocities of the overburden were found to be:

Sand : 33.3 m/sec
Concrete: 25 m/sec

The max throw distances assuming no drag (vacuum) and 45° elevation of ejection would be 110 m and 62 m. The observed maximum throw distances of concrete debris were as follows:

0°	70 m (landed on asphalt pad and rolled?)
30°	37 m
60°	22 m
90°	6.5 m
180°	3 m

All these distances are measured from the tunnel exit.

Table 3. Distance - overpressure.

Direction	Distance* (m)	Test 1 Sand Overpressure (Pa)	Test 2 Concrete Tunnel Overpressure (Pa)	Test 2 Concrete Crater Overpressure (Pa)
0°	17	1430.0	2914.4	2450
	30	898.77	1508.7	700
	53	----	782.88	430
30°	15	----	4534.2	2300
	27	946.13	2238.3	1480
	37	----	1607.6	1100
	48	498.68	----	----
60°	12	2571.3	5575.0	2200
	20	1753.6	2500.2	2800

*Distances are referenced to the tunnel exit.

Table 4. Distance - impulse.

Direction	Distance (m)	Test 1 Sand Impulse (Pa ms)	Test 2 Concrete Impulse (Pa ms)
0°	17	2490	5022.5
	30	1468.4	4606.3
	53	----	2332.8
30°	15	----	11105.0
	27	1500.5	6346.9
	37	----	4632.2
	48	954.71	----
60°	12	3375.8	11256.0
	20	2696.2	10291.0

*Distances are referenced to the tunnel exist.

Table 5. Scaled distance and scaled overpressure.

Direction	Distance (m)	Scaled Distance $\frac{d}{D}$ $D = 0.112867$ m	Scaled Overpressure $\frac{Po}{P}$ Concrete $Po = 5575000$ Pa	$\frac{Po}{P}$ Sand $Po = 5361000$ Pa
0°	17	150.62	1913.93	3748.94
	30	265.80	3697.21	5964.81
	53	469.58	7129.96	----
30°	15	132.90	1230.20	
	27	239.22	2492.06	5666.23
	37	327.82	3469.75	----
	48	425.28	----	10750.37
60°	12	106.32	1000.42	2084.93
	20	177.20	2231.02	3057.13

Table 6. Time of arrival (Reference MP1).

Direction Distance	MP	Test 1, Sand (ms)	Test 2, Concrete (ms)
100 mm	MP 2	0, 0438	0, 043
0° 17 m	MP 3	44, 5	42, 5
0° 30 m	MP 4	83, -	80, -
0° 53 m	MP 5		149, 5
30° 15 m	MP 6		36, 5
30° 27 m	MP 7	74, -	71, 5
30° 37 m	MP 8		101, 5
30° 48 m	MP 8	137, -	
60° 12 m	MP 9	31, -	29, 5
60° 20 m	MP 10	54, 5	52

The throw distances of the aluminium rods are shown in Table 7:

Table 7. Throw distance aluminium (rods).

Rod Number (See Figure 2)	Throw Distance,* m	
	Test 1	Test 2
1	+ 2.8	+ 9.84
2	+10.9	+15.64
3	+63	+44.14
4	+21	+27.94
5	+ 6.1	+ 2.64
6	-12 (Rolled downhill?)	+ 1.04
7	- 2.8	- 0.68
8	- 0.7	- 0.56
9	- 0.3	- 0.25
10	0	0

*Distances are referenced to the original locations of the rods.

The film proved to be to dark to be able to distinguish the rods from smoke, dust and sand/concrete. The ejection angle and the trajectory could therefore not be determined.

4.3 **Throw of cubes**

The throw distances for cubes are shown in Table 8 and 9:

Table 8. Test 1, sand.

Position		Throw Distance, m	
Direction	Distance, m	Aluminium	Oak
0°	1 6 12	0.63 and 1.0 ---- ----	7.6 and 6.43 ---- ----
30°	1 6 12	0.7 and 0.2 ---- ----	2.95 and 0.7 ---- ----
60°	1 6 12	0.15 and 0 ---- ----	0.8 and 0.37 ---- ----

Table 9. Test 1, concrete.

Position		Throw Distance, m	
Direction	Distance, m	Aluminium	Oak
0°	1 2 3	2.1 and 1.8 1.15 and 0.9 0.25 and 0.2	20.25 and 10.05 17.9 and 13.4 3.5 and 2.05
30°	1 2 3	0.80 and 0.55 0.60 and 0.25 0.10 and 0.5	9.15 and 4.85 3.75 and 3.55 0.2 and 0.05
60°	1 2 3	0.80 and 0.75 0 0 0 0	8.25 and 1.0 0.05 and 0 0 0

These results are plotted in Figure 10.

5. DISCUSSION AND RECOMMENDATION

5.1 The difference between MP1/MP2 for Test 1 (sand) and Test 2 (concrete) is noticeable. The pressure-time history for Test 1 has only one peak and blast waves recorded outside have also one peak only. For Test 2 the pressure-time history is similar to Test 1 for the first few milliseconds but then the pressure rises to about twice the pressure at the front.

This second peak can also be observed outside. It is also clearly demonstrated that this second peak gradually catches up with the first peak. At MP 05 (0°, 53 m, Page A-8) the second peak is higher than the first peak.

In Figure 7, the first peak is used as Po. When the second peak is used, the curves for sand and concrete fall close together. This may be a coincidence since the duration (and impulse) for MP1/MP2 for Test 2 is longer than for Test 1, but how to take duration into account is as of now not validated.

For Test 2, concrete, a distinct separate blast wave is observed in the 0° and 30° direction (Pages A-6 to A-11) arriving about 10 ms after the first one. In the 60° direction a pressure pulse is observed at 12 m (Page A-12). This is also the nearest measuring point and similar pressure pulses may have been seen also in the 0° and 30° direction if gauges had been installed closer in. This pressure wave has developed into a strong blast wave at 20 m (Page A-13). It is assumed that this separate blast wave stems from pressure waves exiting through large cracks in the overburden. For Test 1, sand, this separate blast wave is not seen although a weak pressure pulse can be imagined.

Both peak pressures (first peak) and impulses are larger in all directions for the concrete test than for the sand test (Figures 5 and 6). Time of arrival (Figure 8) shows also a slightly higher front velocity for the concrete than for the sand test. It seems quite obvious that more energy is dissipated into the sand media than than into the concrete media. Before this can be said with certainty, several more elaborate tests have to be carried out.

5.2 The peak pressure (Po) measured in the tunnel is not very well defined (Page A-1 - A-5). Blast gauges should therefore be located along the tunnel (floor, wall or roof) such that the velocity of the shock front can be determined and the peak pressure calculated assuming that ideal gas equations can be used. The pressure-time history shown in Appendix A is felt to be fairly accurate also for the large shallow underground test when the charge is initiated at the front end.

5.3 The environment in the tunnel is such that direct measurement of the dynamic pressure impulse (or particle velocity and density) is difficult. Since the dynamic pressure impulse in the tunnel is very important for the judgement of debris hazard, it is recommended to use calibrated cubes located in the tunnel and observe the throw distances outside. In this way the dynamic pressure impulse in the tunnel may be determined indirectly.

5.4 The dynamic impulse outside the tunnel may cause considerable damage. Very little is know quantitatively about the magnitude and directivity. It is therefore recommended to use cubes on several radials at different distances to observe the throw distances and thereby be able to determine the dynamic pressure impulse indirectly. At a few (3) stations it is recommended to colocate cubes and blast diagnostic stations (side on pressure, head on pressure and density) in order to be able to "calibrate" the cubes. The debris hazard for the blast diagnostic stations and the minimum acceptable throw distances for the cubes have to be balanced. Based on the result from these model tests it is recommended to locate the blast diagnostic stations on the 15°, 30° and 45° radial at a distance of 50 m to 75 m.

5.5 Table 3 and Figure 5 can be used for location and setting of side on blast gauges in the 0° to 60° direction. For overpressures in other directions the following directivity factors could be used:

0° - 1 Reference
30° - 1 (May be larger than 1)
60° - 0, 7
90° - 0, 3
180° - 0, 1

The data base for equations presented in paragraph 4.1 on page 5 are very limited and the overpressure range investigated is also narrow--0.5 kPa to 5.5 kPa. The exponent 0.75 should be used with caution. Previous investigations have shown that the exponent may be as high as 0.90 for low overpressures and as low as 0.6 for overpressures in the 50 kPa range. Reference is made to Figure 11 where the variation of the exponent with overpressure is given for a range of overpressures. This figure was provided by Mr. Charles Needham, S-Cubed in Albuquerque.

5.6 It is highly recommended to embed large aluminium rods or steel tubes filled with reinforced concrete (SIFCON) on the surface above the tunnel and chamber. The velocity of these will, based on the result from these model tests, be between 25 m/sec and 40 m/sec; therefore, the camera frame rates do not need to be very high. It will be difficult to see these rods or tubes. They should therefore be as large as possible and also marked with a piece of cloth or have a light or smoke tracer incorporated.

5.7 Smoke trails have previously been used with success to observe direction and velocity of air molecules. These trails give air blast time of arrival as well and thereby indirectly the peak pressure.

The blast propagation close to the tunnel exist is complex and it is difficult to properly install a large number of blast gauges which also will survive (debris, etc.). It is recommended to use several (20) smoke trails in front of the exit (0°) and above the tunnel (180°).

5.8 The directivity of the blast wave emerging from the tunnel is very much dependent on the exact geometry at the exit and the topography close to the exit. A wire drag gauge has been used (Suffield Technical Note No. 80) to observe the symmetry of the blast wave around large charges, the direction of ground zero and to give the approximate yield of the charge. It is recommended to use wire drag gauges on several radials at 5 kPa and 20 kPa overpressures.

5.9 Many of the problems encountered in understanding the blast and flow field could be alleviated by performing a high-quality hydrodynamic computer code calculation of the test configuration, and it is recommended that this be undertaken. It is easy to place a large number of measurement points in a calculation, and hence the development of features of the blast wave can be monitored where experimental data is lacking. Fidelity of the calculations can be verified by comparison with experimental data records acquired at a few key points, if measurements as proposed in paragraphs 5.2, 5.3, 5.4, 5.7 and 5.8 are carried out. In addition, parameters not easily measured directly, such as air flow velocity, dynamic pressure and dynamic pressure impulse in all directions, are directly available from calculated results.

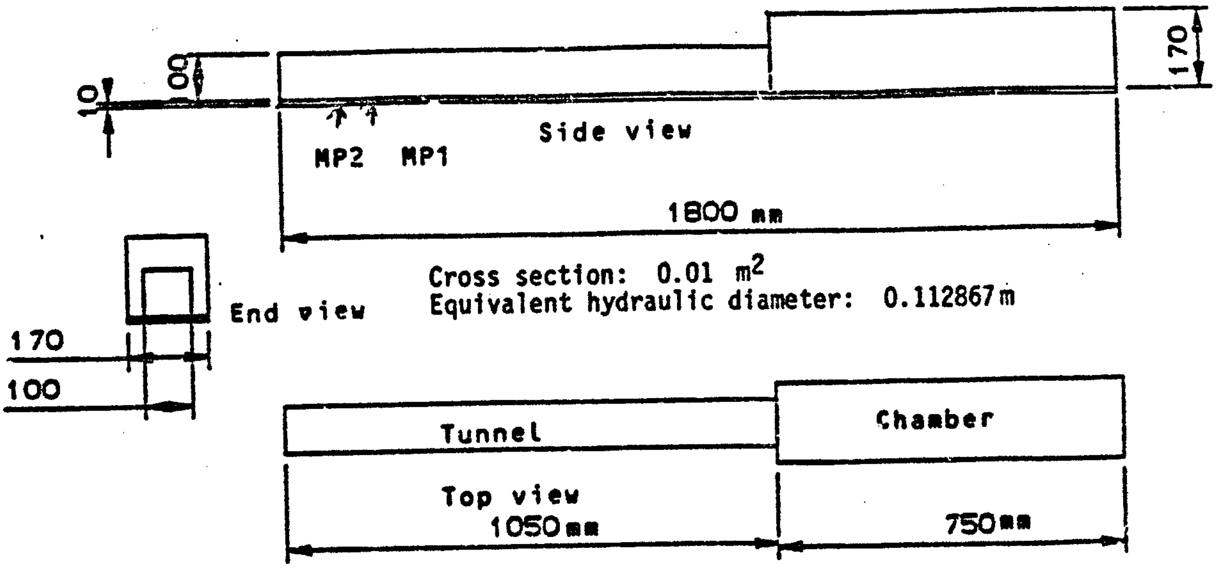

Figure 1 a Steel structure

Volume:

Chamber: 0.021675 m3

Chamber + tunnel: 0.032175 m3

Loading density: (1.4 kg C4)

Chamber : 64.59 kg /m3

Chamber + tunnel: 43.51 kg /m3

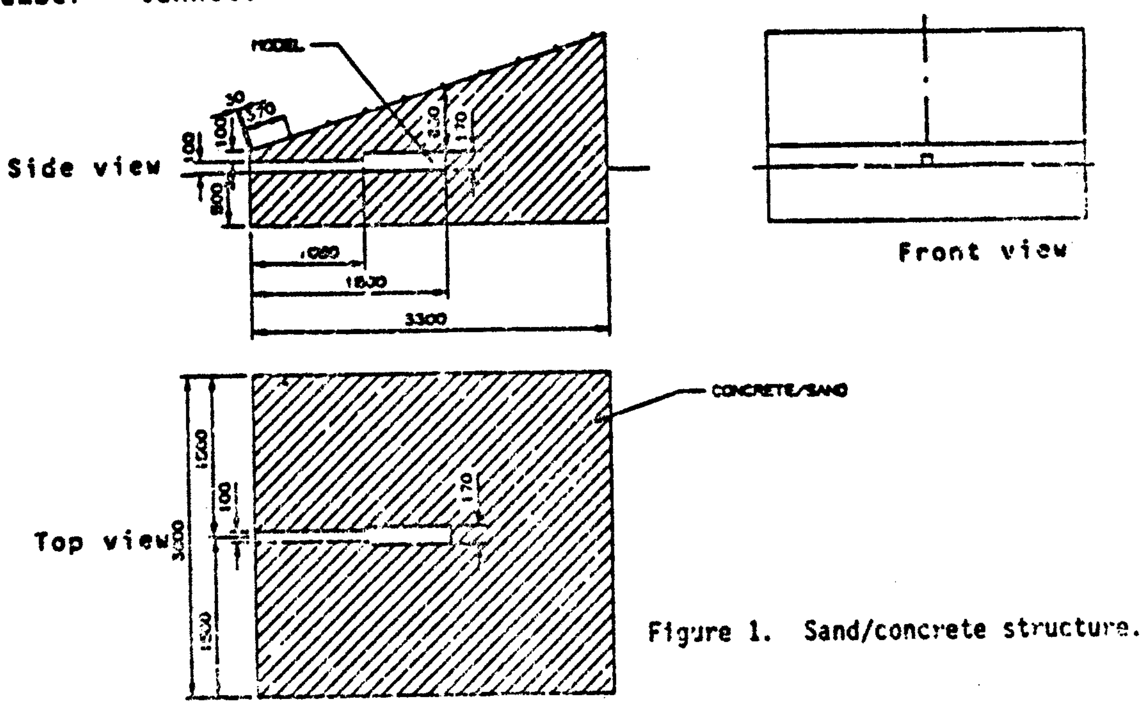

Figure 1. Sand/concrete structure.

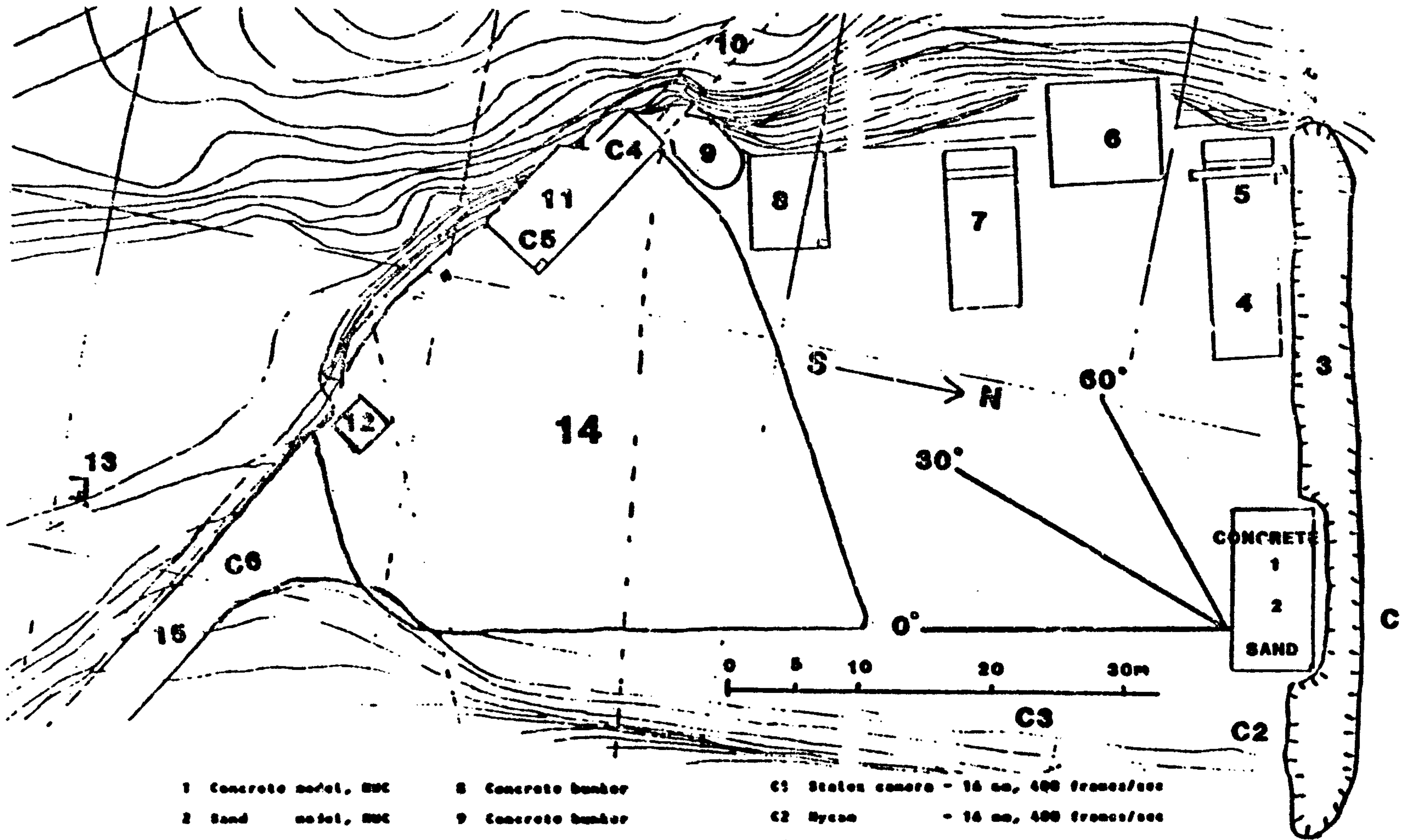

1 Concrete model, NWC	8 Concrete bunker	C1 Stalex camera - 16 mm, 400 frames/sec
2 Sand model, NWC	9 Concrete bunker	C2 Hycam - 16 mm, 400 frames/sec
3 Soil berm	10 Underground tunnel	C3 Hycam - 16 mm, 400 frames/sec
4 Concrete platform	11 Concrete bunker	C4 Beaulieu - 16 mm, 80 frames/sec
5 Concrete wall	12 Concrete platform, gun mount	C5 TV camera
6 Ammunition magazine	13 Observation bunker, concrete	C6 Beaulieu - 16 mm, 64 frames/sec
7 Concrete platform	14 Asphalt pad	
	15 Access road	

Figure 2 Test site

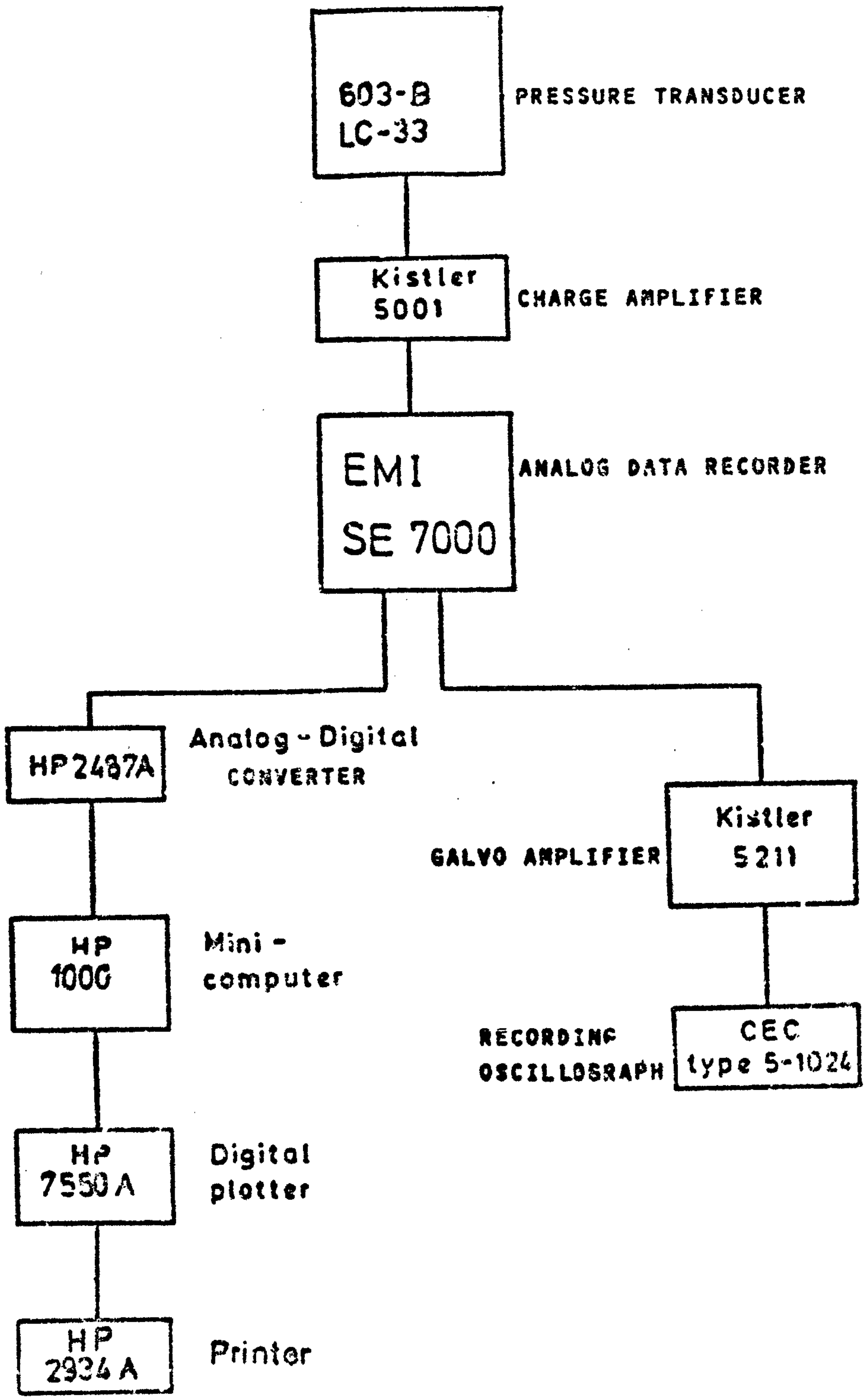

Figure 3

Gauges and instrumentation

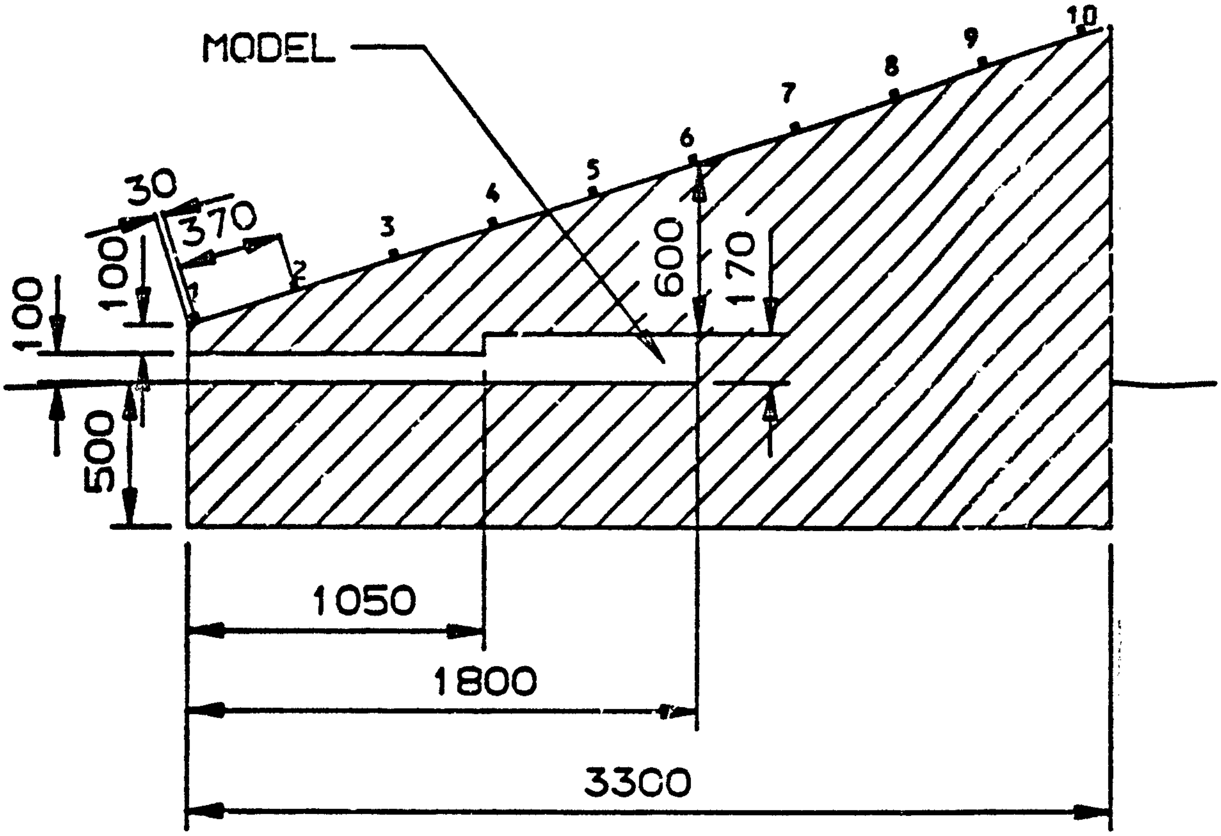

1 — 10 Rod number. Ref table 7

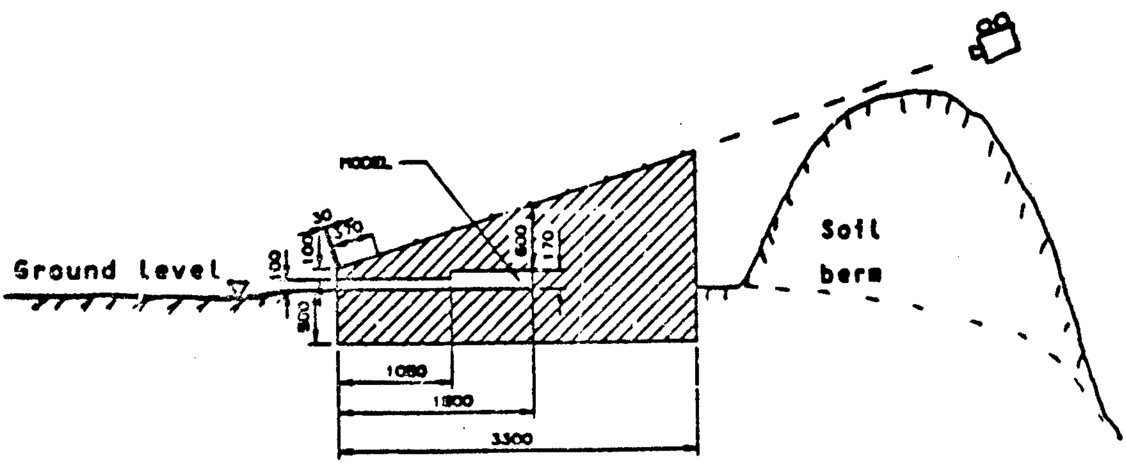

Figure 4

Location of aluminium rods and technical cameras

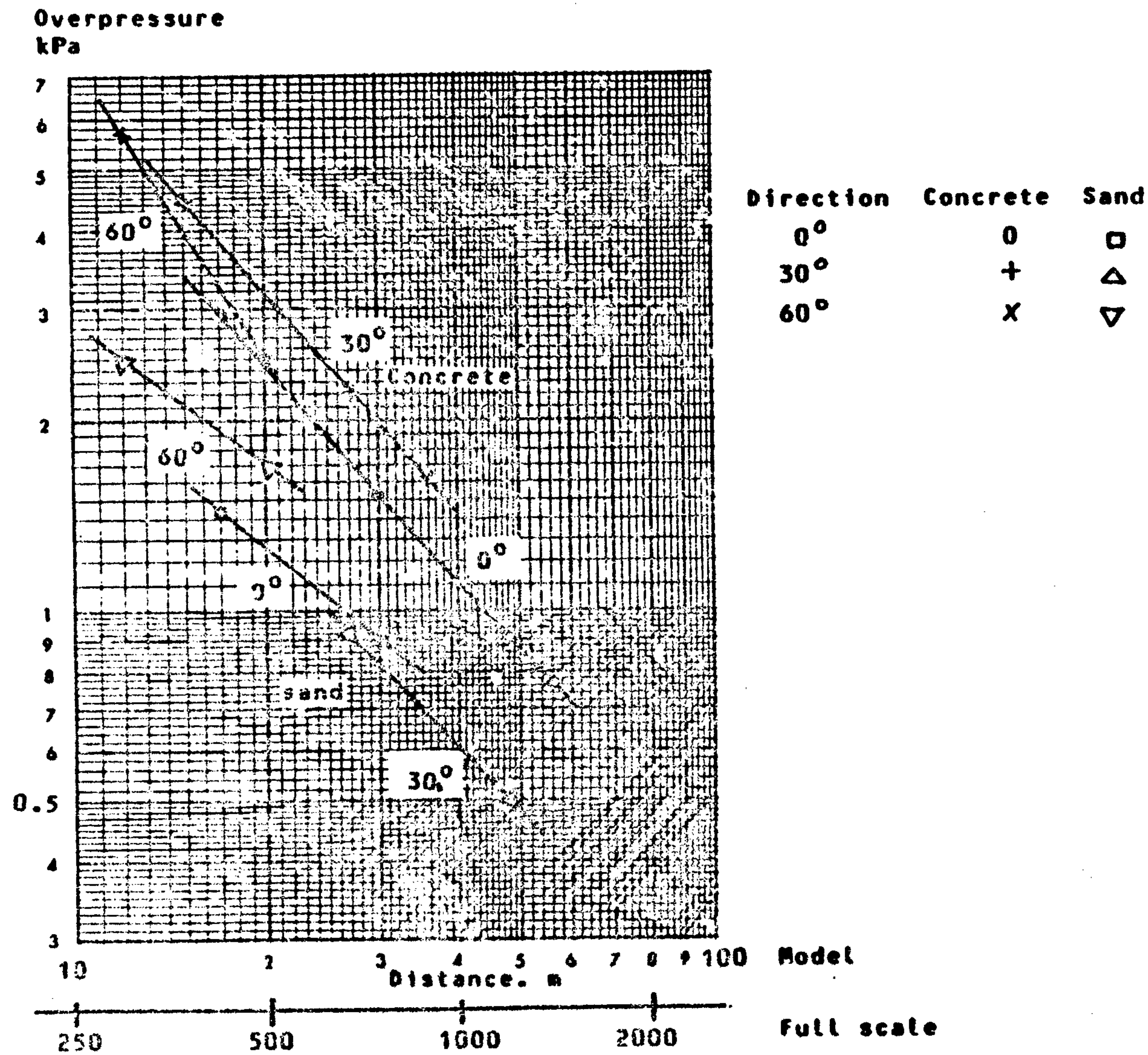

Figure 5
Overpressure versus distance

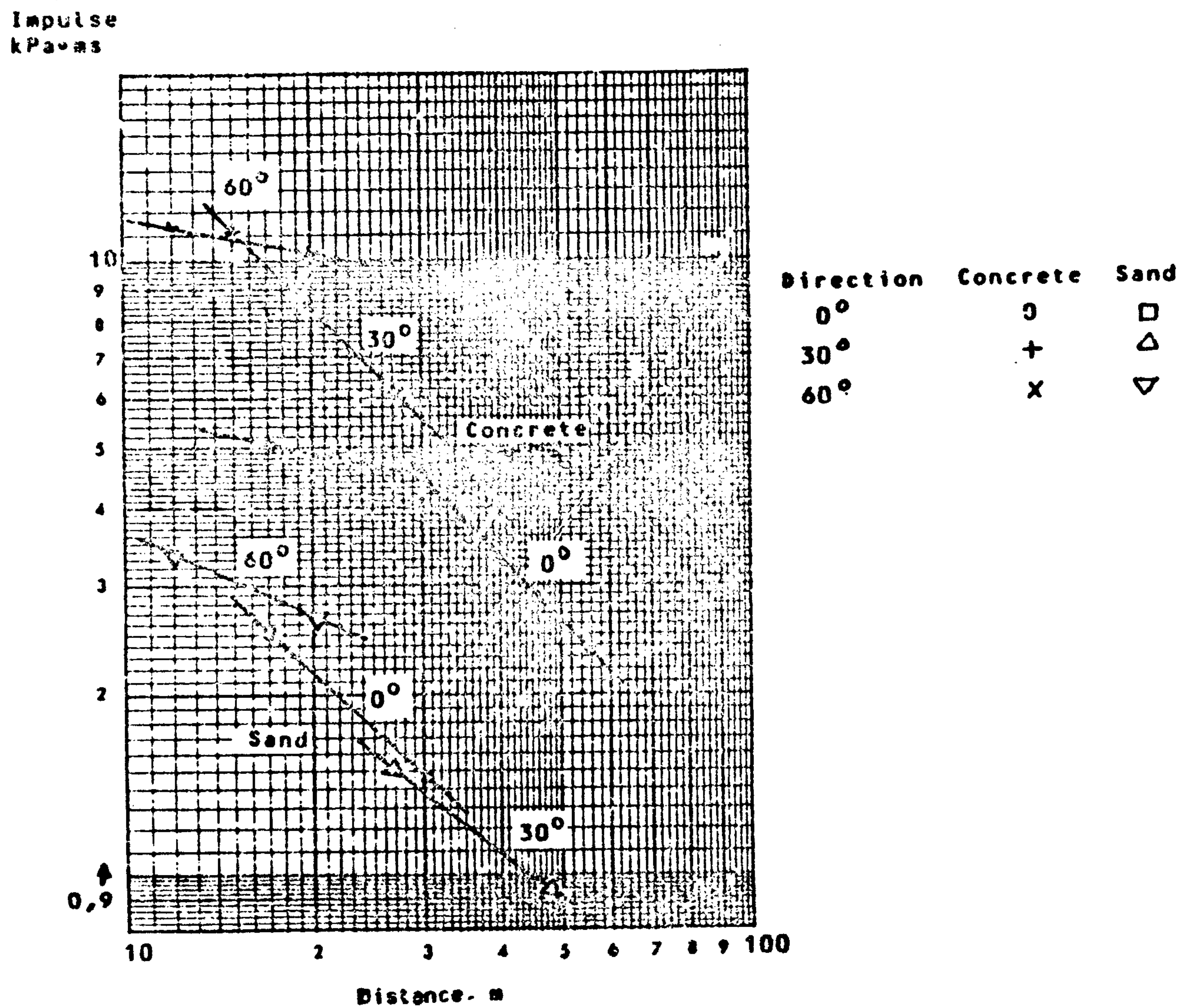

Figure 6

Impulse versus distance

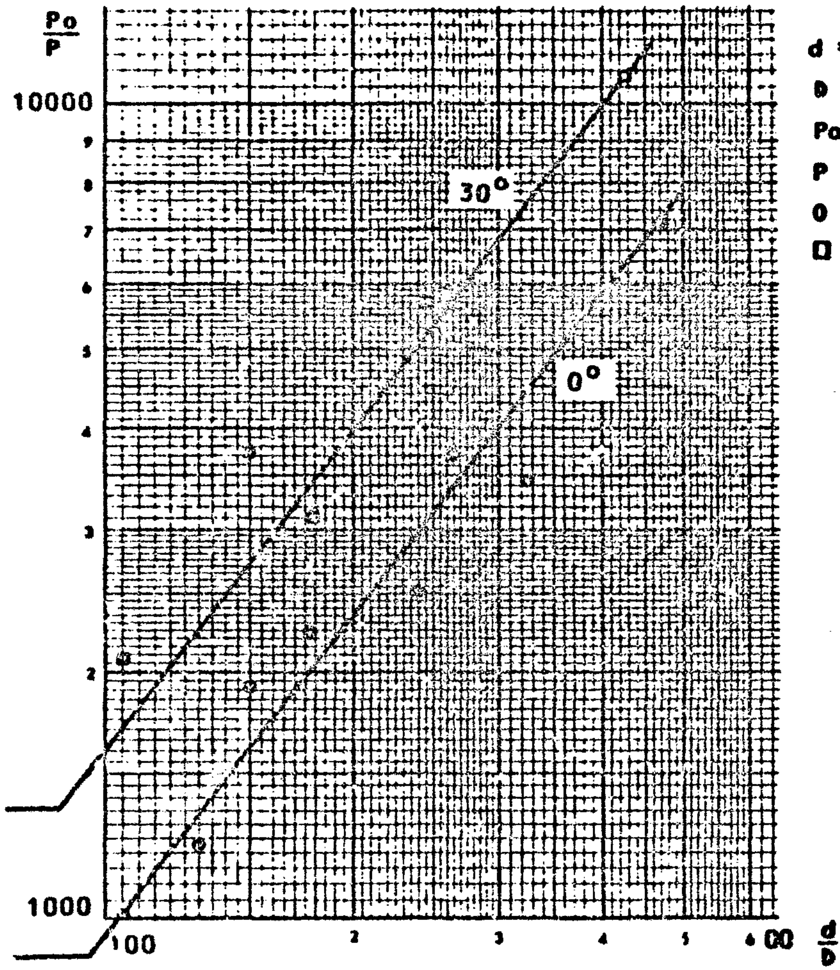

d = distance
D = diameter of tunnel
Po = overpressure in the tunnel
P = overpressure outside
O = concrete
□ = sand

<u>Sand</u> (30°)

$\frac{d}{D} \sim 0.42 \cdot (\frac{Po}{P})^{0.75}$

<u>Concrete</u> (0°)

$\frac{d}{D} \sim 0.60 \cdot (\frac{Po}{P})^{0.75}$

Figure 7
Scaled overpressure versus scaled distance

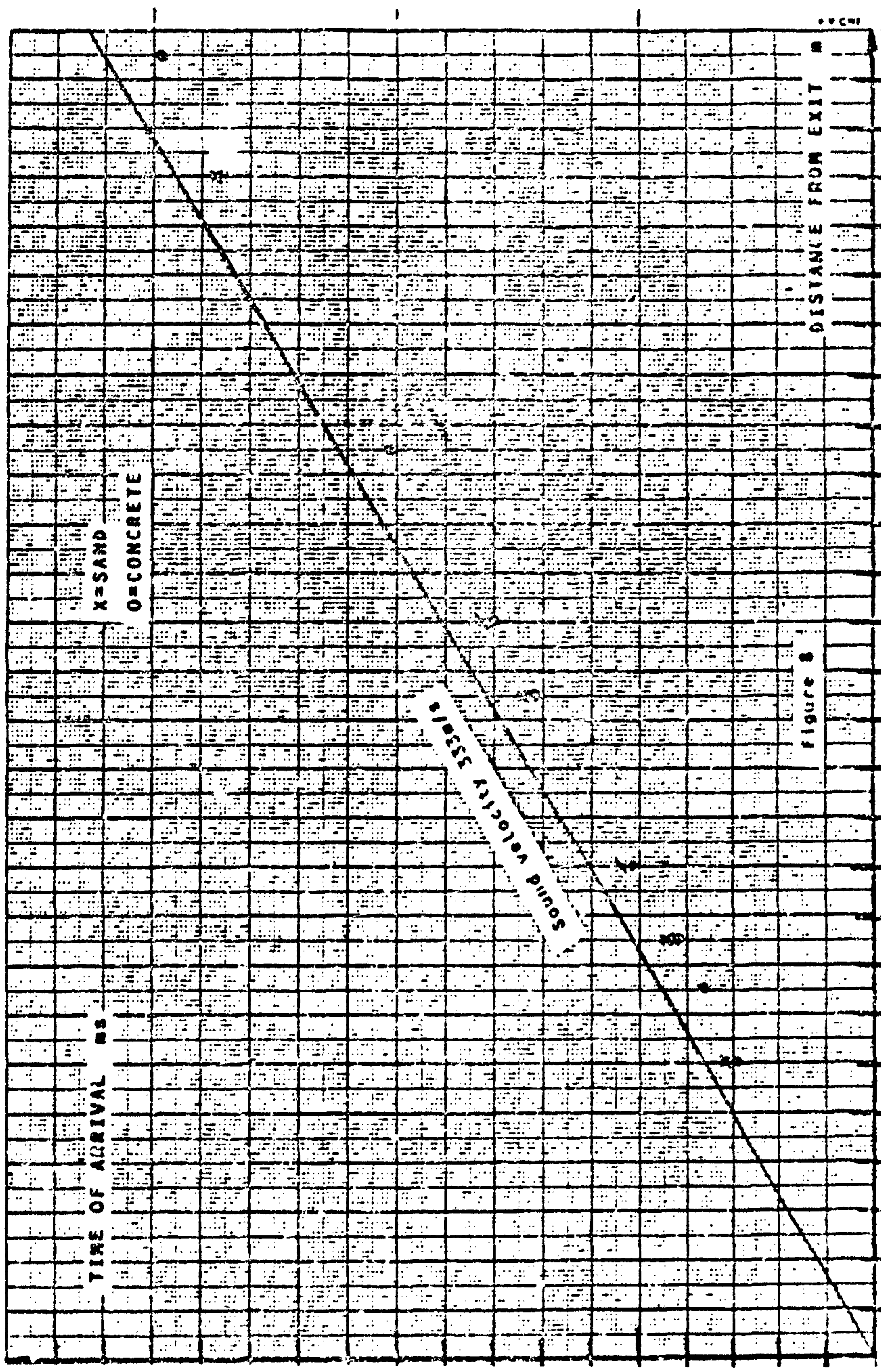
TIME OF ARRIVAL ms
X=SAND
O=CONCRETE
Sound velocity 333m/s
DISTANCE FROM EXIT m
10
20
30
40
50
Figure 8

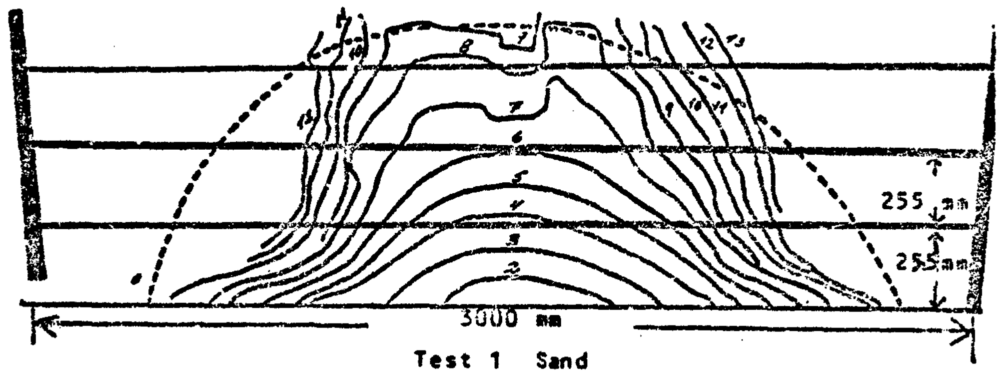

Test 1 Sand

0 = Fireball outside the tunnel = 0 time reference
2 = 5 ms
3 = 7,5 ms
— — —
10 = 250 ms

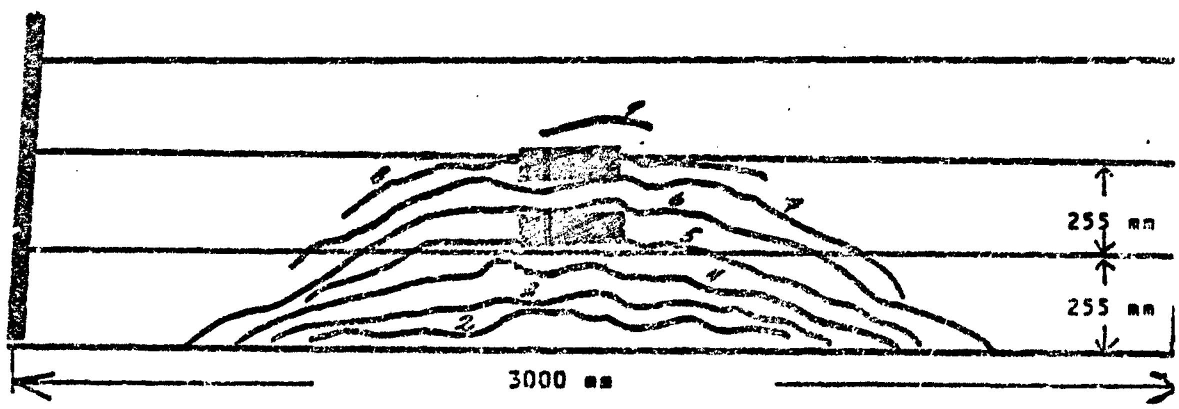

Test 2 Concrete

2 = 5 ms
3 = 7.5 ms
— — —
9 = 22.5 ms

Figure 9 Uplift of overburden

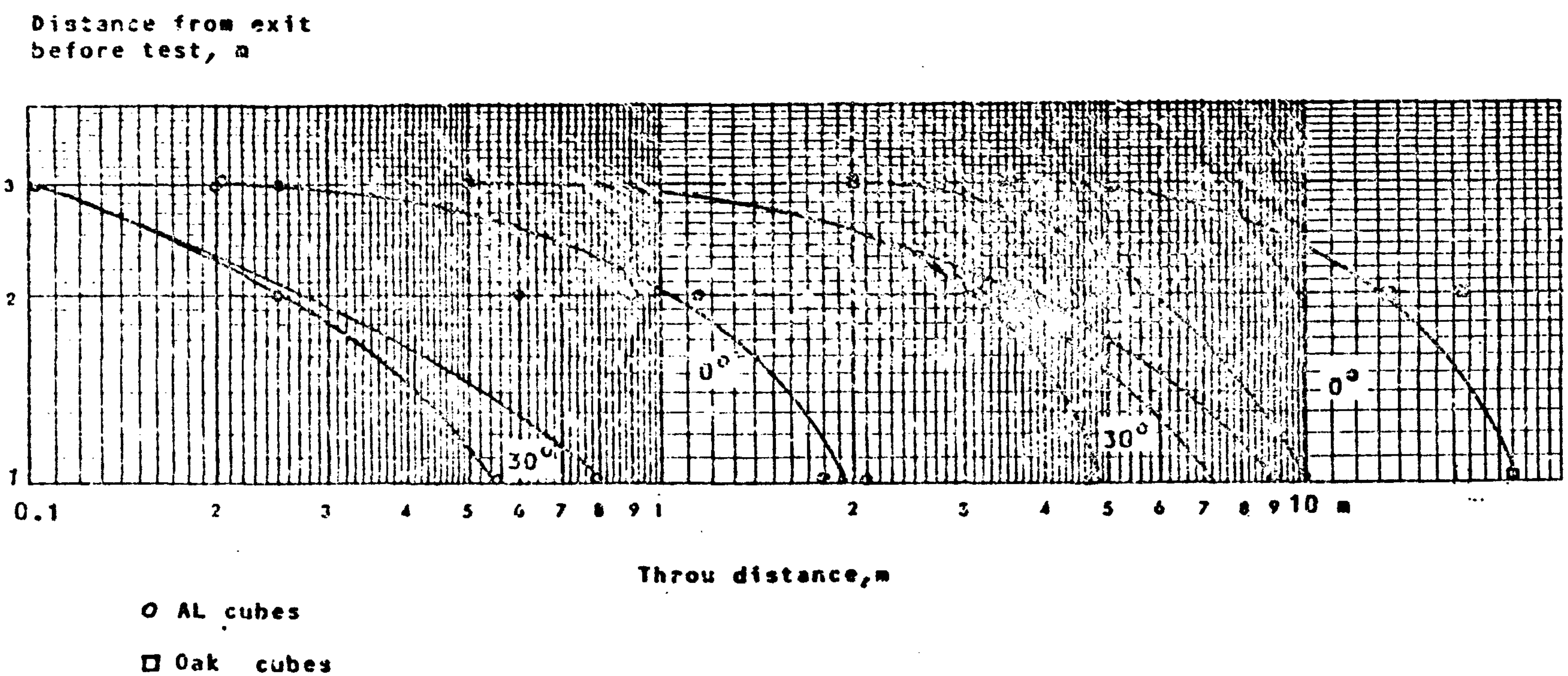

Figure 10 Throw distances for cubes, Test 2 Concrete

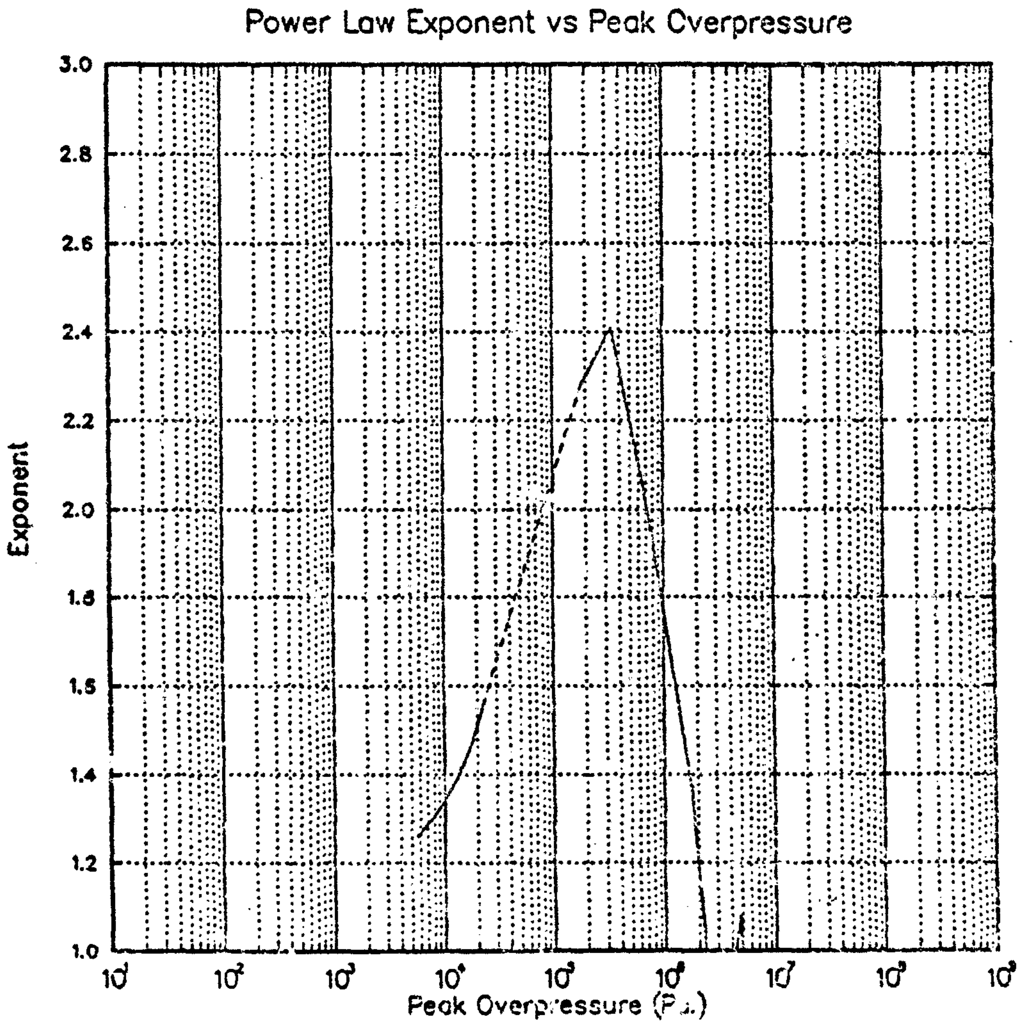

Exponent =−Log(p1/p2)/Log(r1/r2) at 0 Deg.

Figure 11

Power law exponent versus
peak overpressure

APPENDIX A

Pressure-Time Histories

Identification

SHOT: ID01 Test 1 Sand

ID02 Test 2 Concrete

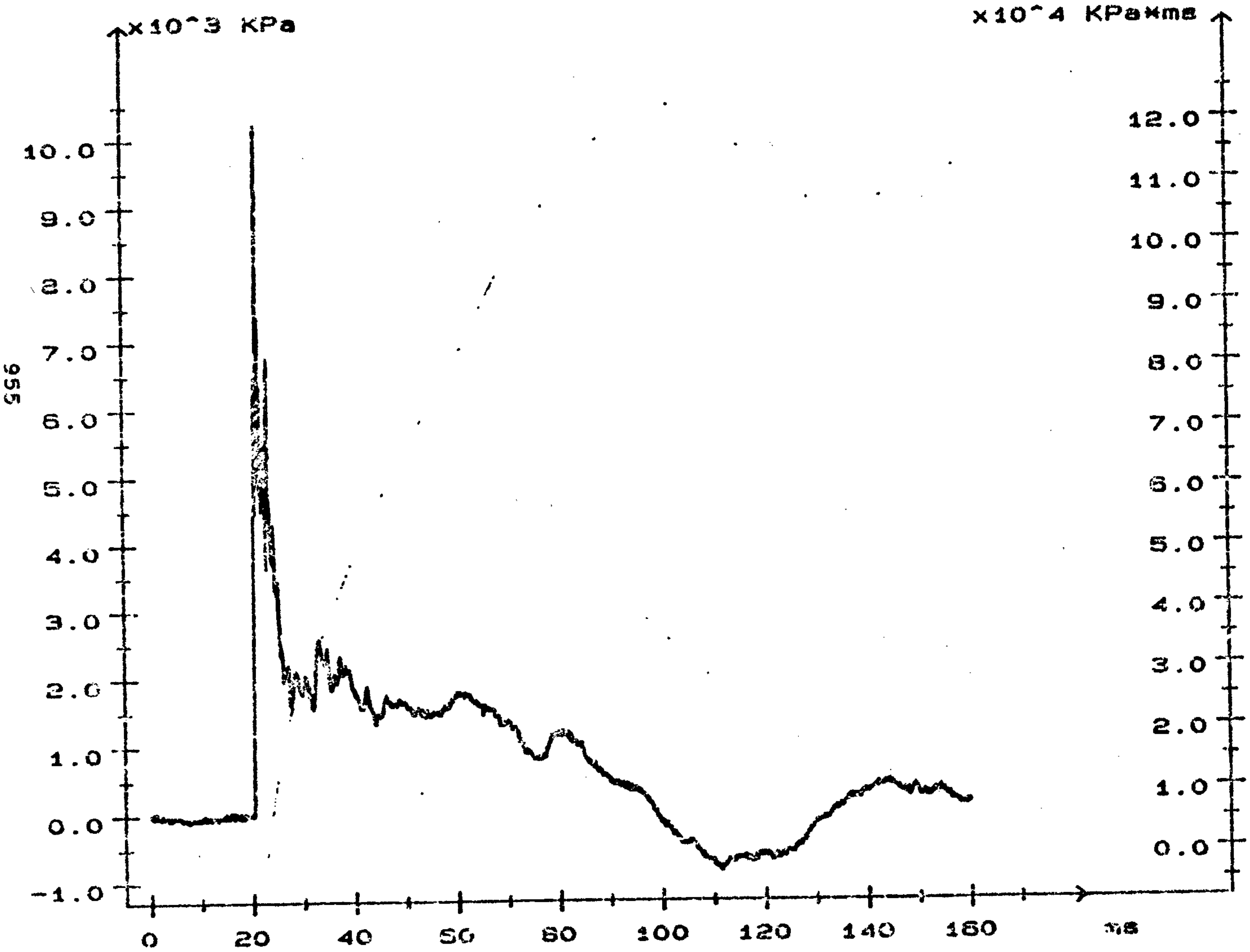

SHOT : ID02
MPKT : MP02
PMAX : 10231. KPa
PMIN : -866.85 KPa
IMAX :
IMIN : -676.43 KPa*ms

DATO 15 10 87

UAMT
NWC
CONCRETE
SCALE 1:24.8

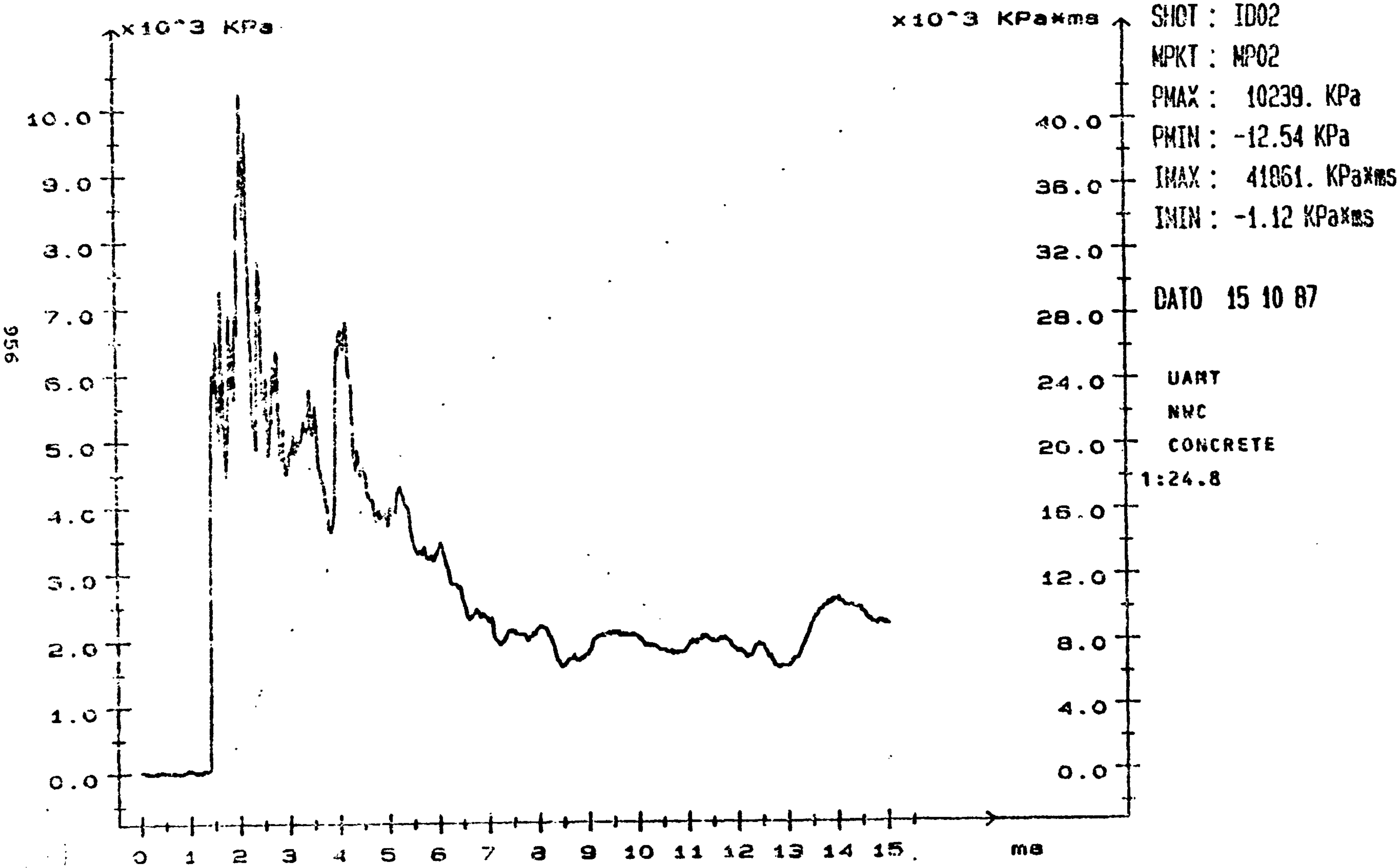
x10^3 KPa
x10^3 KPa*ms
SHOT : ID02
NPKT : NP02
PMAX : 10239. KPa
PMIN : -12.54 KPa
IMAX : 41861. KPa*ms
IMIN : -1.12 KPa*ms
DATO 15 10 87
UART
NWC
CONCRETE
1:24.8
10.0
9.0
3.0
7.0
6.0
5.0
4.0
3.0
2.0
1.0
0.0
40.0
36.0
32.0
28.0
24.0
20.0
16.0
12.0
8.0
4.0
0.0
0 1 2 3 4 5 6 7 8 9 10 11 12 13 14 15
ms

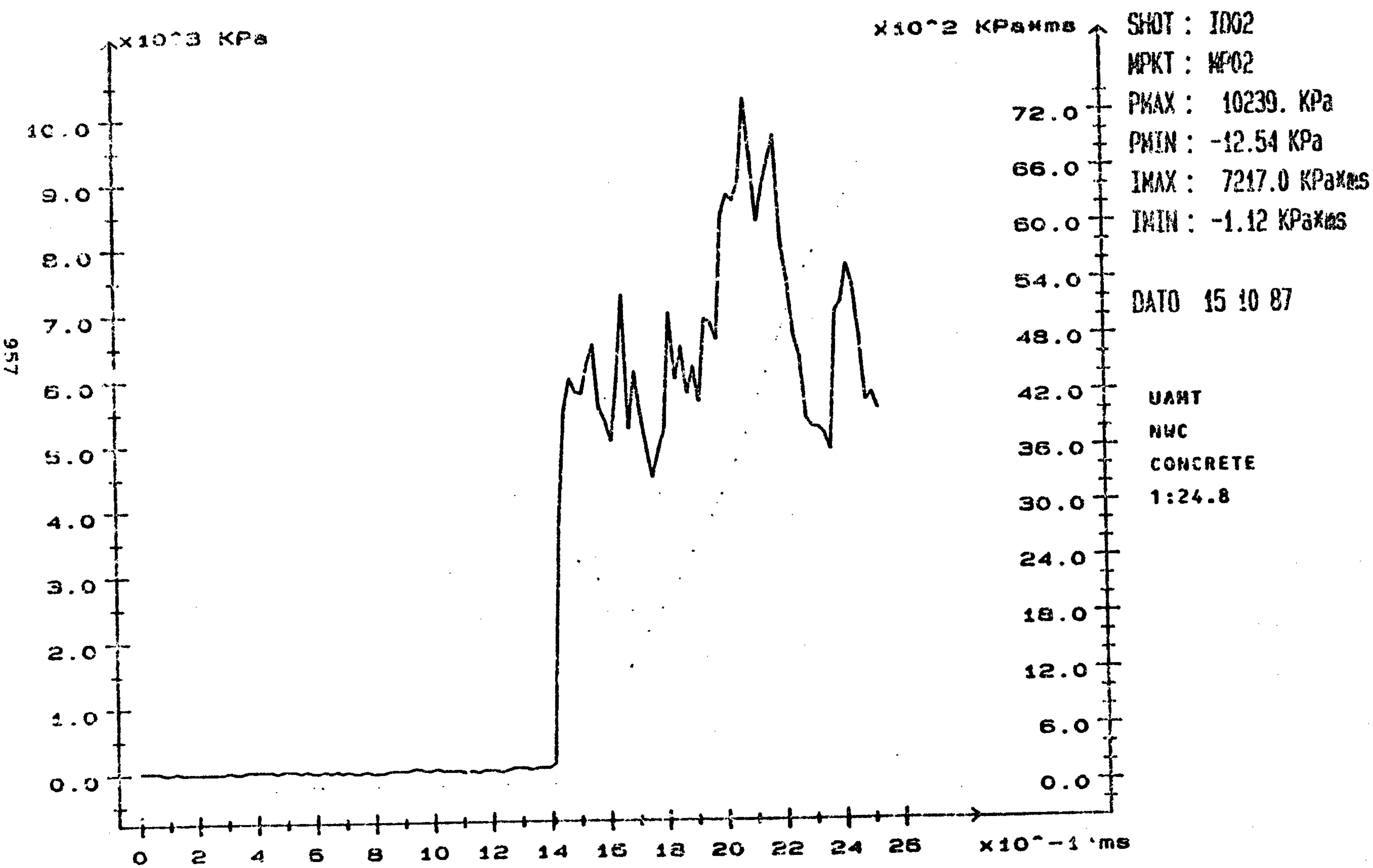
x10^3 KPa
10.0
9.0
8.0
7.0
6.0
5.0
4.0
3.0
2.0
1.0
0.0
x10^2 KPa*ms
72.0
66.0
60.0
54.0
48.0
42.0
36.0
30.0
24.0
18.0
12.0
6.0
0.0
0 2 4 6 8 10 12 14 16 18 20 22 24 26
x10^-1 ms
SHOT : I002
MPKT : MP02
PMAX : 10239. KPa
PMIN : -12.54 KPa
IMAX : 7217.0 KPa*ms
IMIN : -1.12 KPa*ms
DATO 15 10 87
UANT
NWC
CONCRETE
1:24.8

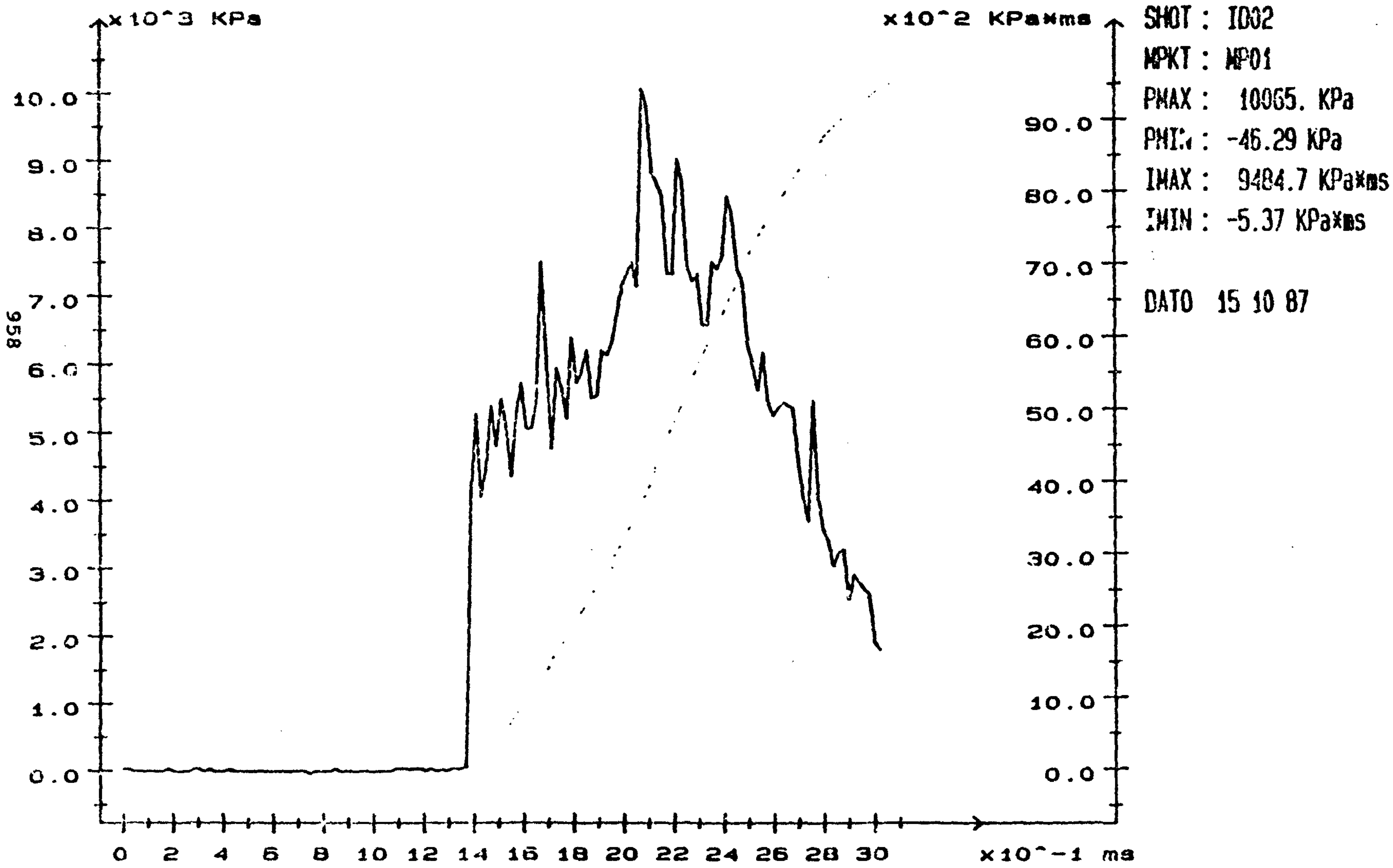
x10^3 KPa
10.0
9.0
8.0
7.0
6.0
5.0
4.0
3.0
2.0
1.0
0.0
x10^2 KPa*ms
90.0
80.0
70.0
60.0
50.0
40.0
30.0
20.0
10.0
0.0
0 2 4 6 8 10 12 14 16 18 20 22 24 26 28 30
x10^-1 ms
SHOT : I002
MPKT : MP01
PMAX : 10065. KPa
PMIN : -46.29 KPa
IMAX : 9484.7 KPa*ms
IMIN : -5.37 KPa*ms
DATO 15 10 87

958

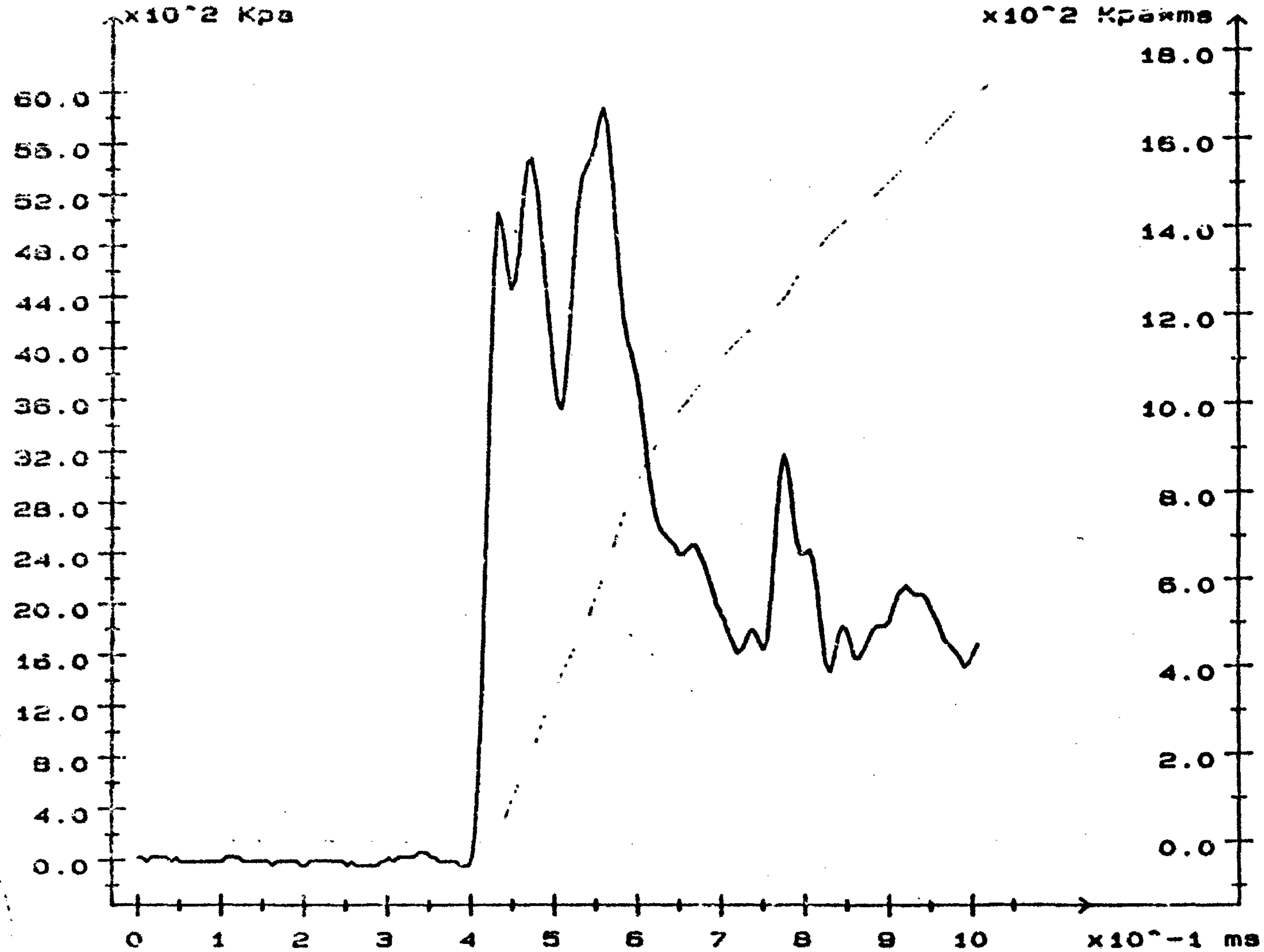

SHOT : ID01
MPKT : MP01
PMAX : 5881.0 Kpa
PMIN : -47.92 Kpa
IMAX : 1718.5 Kpa*ms
IMIN : -3.48 Kpa*ms

DATO 14 10 87

UAMT
NYC
SAND
SCALE 1:24.8

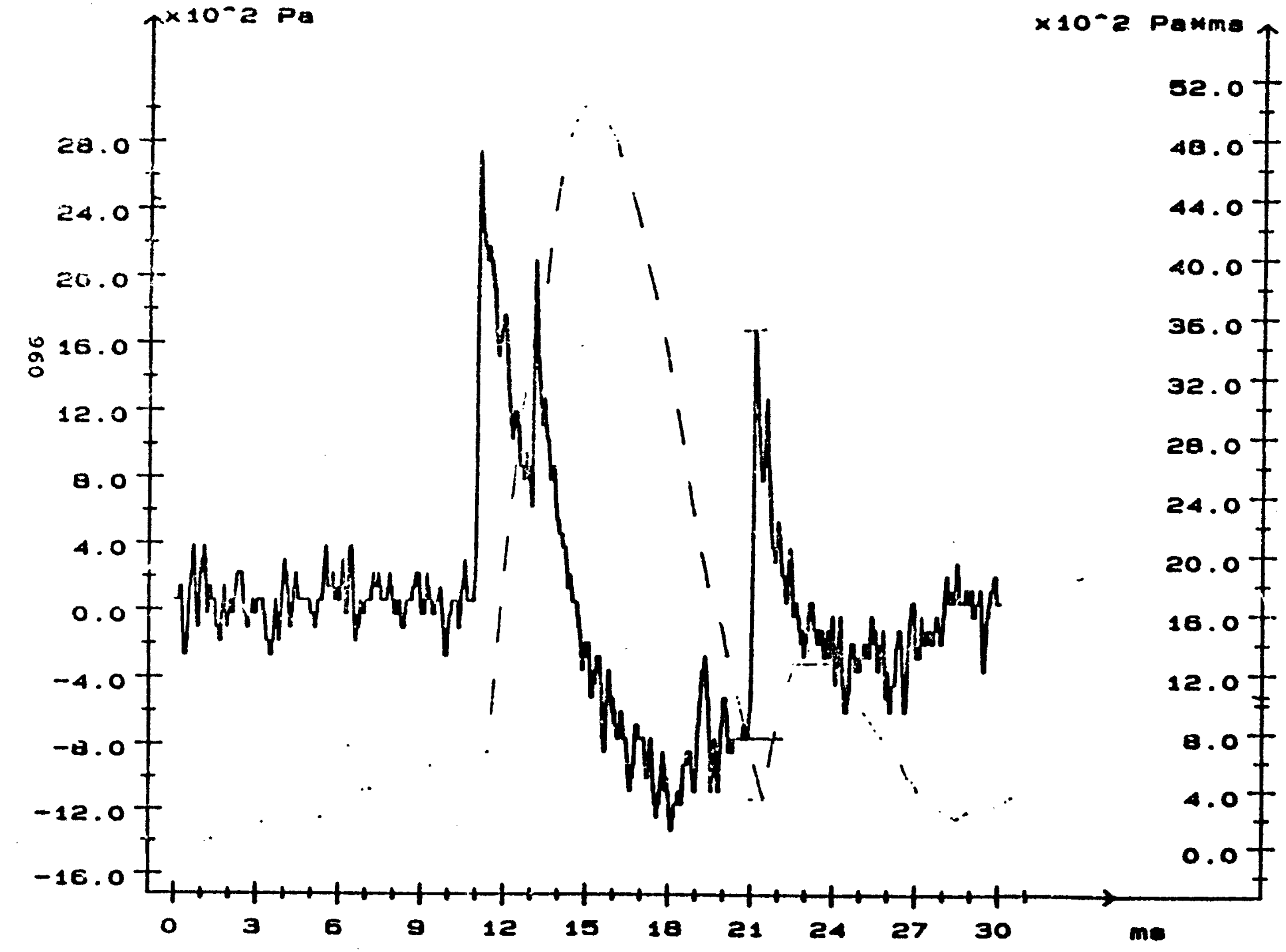

SHOT : ID02
MPKT : MP03
PMAX : 2914.4 Pa
PMIN : -1569.3 Pa
IMAX : 5022.5 Pa*ms
IMIN : -20.78 Pa*ms

DATO 14 10 87

UART 17M 0"
NWC
CONCRETE
SCALE 1:24.8

960

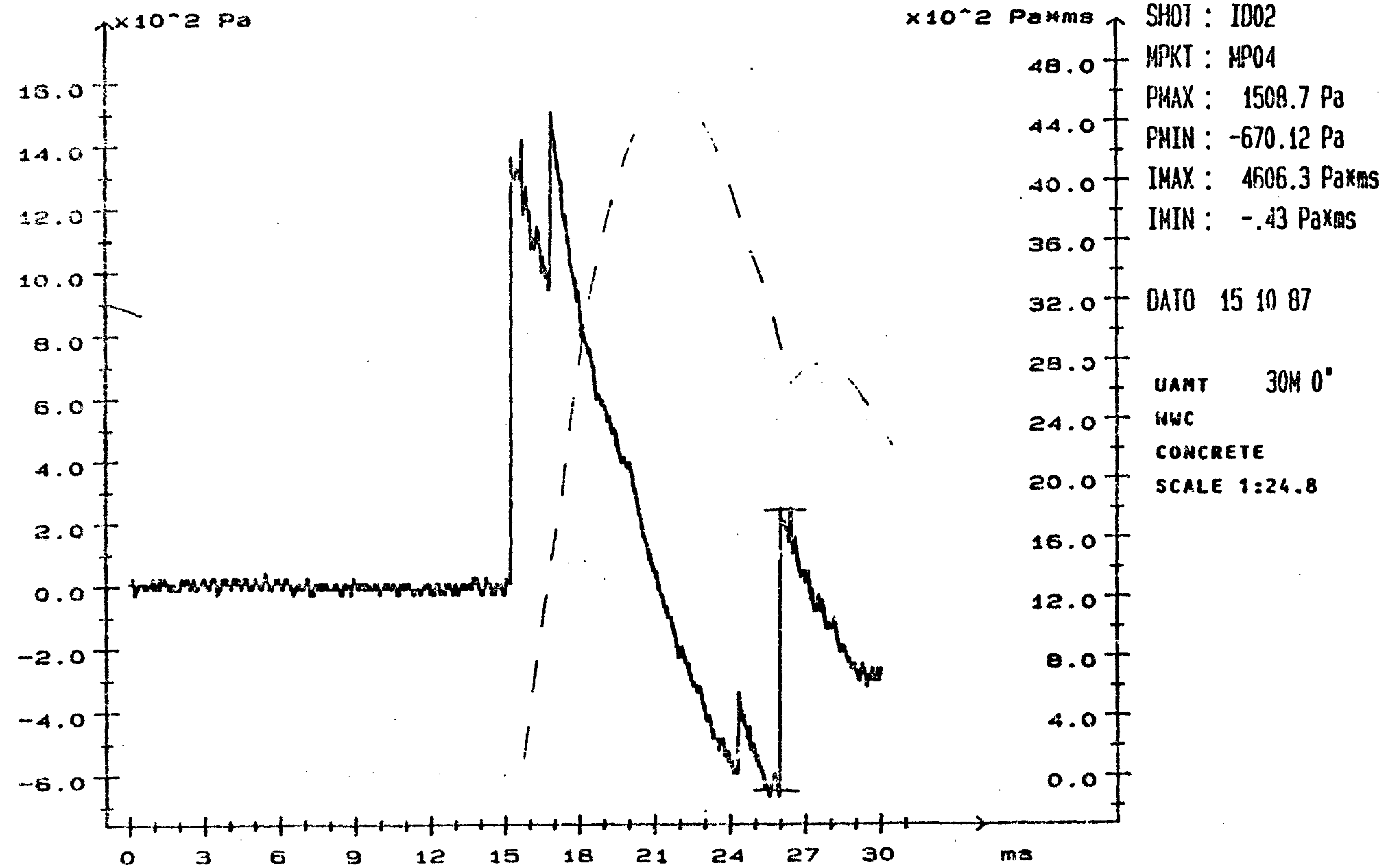
x10^2 Pa
x10^2 Pa*ms
16.0
14.0
12.0
10.0
8.0
6.0
4.0
2.0
0.0
-2.0
-4.0
-6.0
48.0
44.0
40.0
36.0
32.0
28.0
24.0
20.0
16.0
12.0
8.0
4.0
0.0
0 3 6 9 12 15 18 21 24 27 30 ms
SHOT : ID02
MPKT : MP04
PMAX : 1508.7 Pa
PMIN : -670.12 Pa
IMAX : 4606.3 Pa*ms
IMIN : -.43 Pa*ms
DATO 15 10 87
UANT 30M 0"
NWC
CONCRETE
SCALE 1:24.8

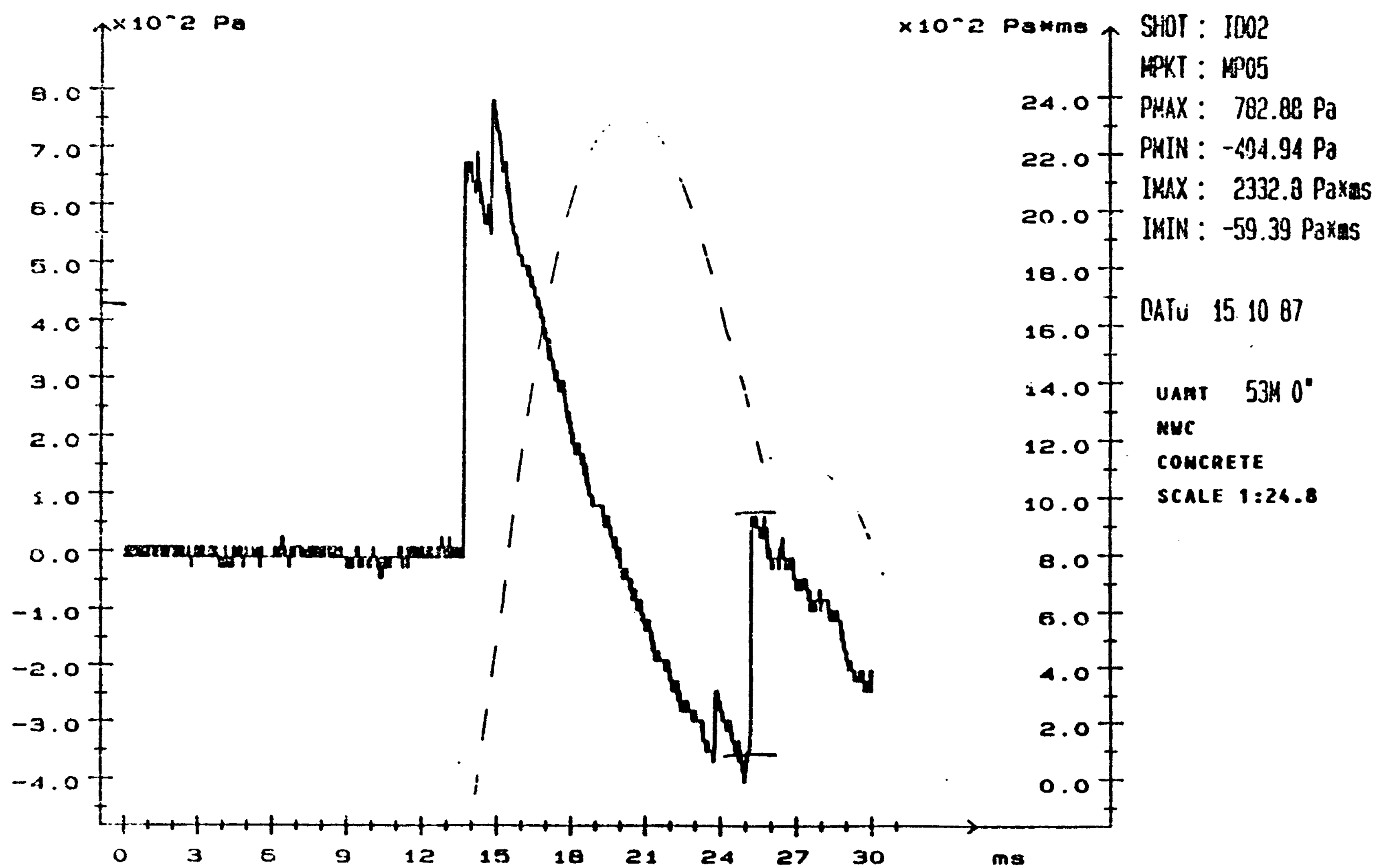

x10^-2 Pa
8.0
7.0
6.0
5.0
4.0
3.0
2.0
1.0
0.0
-1.0
-2.0
-3.0
-4.0
x10^-2 Pa*ms
24.0
22.0
20.0
18.0
16.0
14.0
12.0
10.0
8.0
6.0
4.0
2.0
0.0
0
3
6
9
12
15
18
21
24
27
30
ms
SHOT : I002
MPKT : MP05
PMAX : 782.88 Pa
PMIN : -404.94 Pa
IMAX : 2332.8 Pa*ms
IMIN : -59.39 Pa*ms
DATu 15 10 87
UANT 53M 0°
NWC
CONCRETE
SCALE 1:24.8

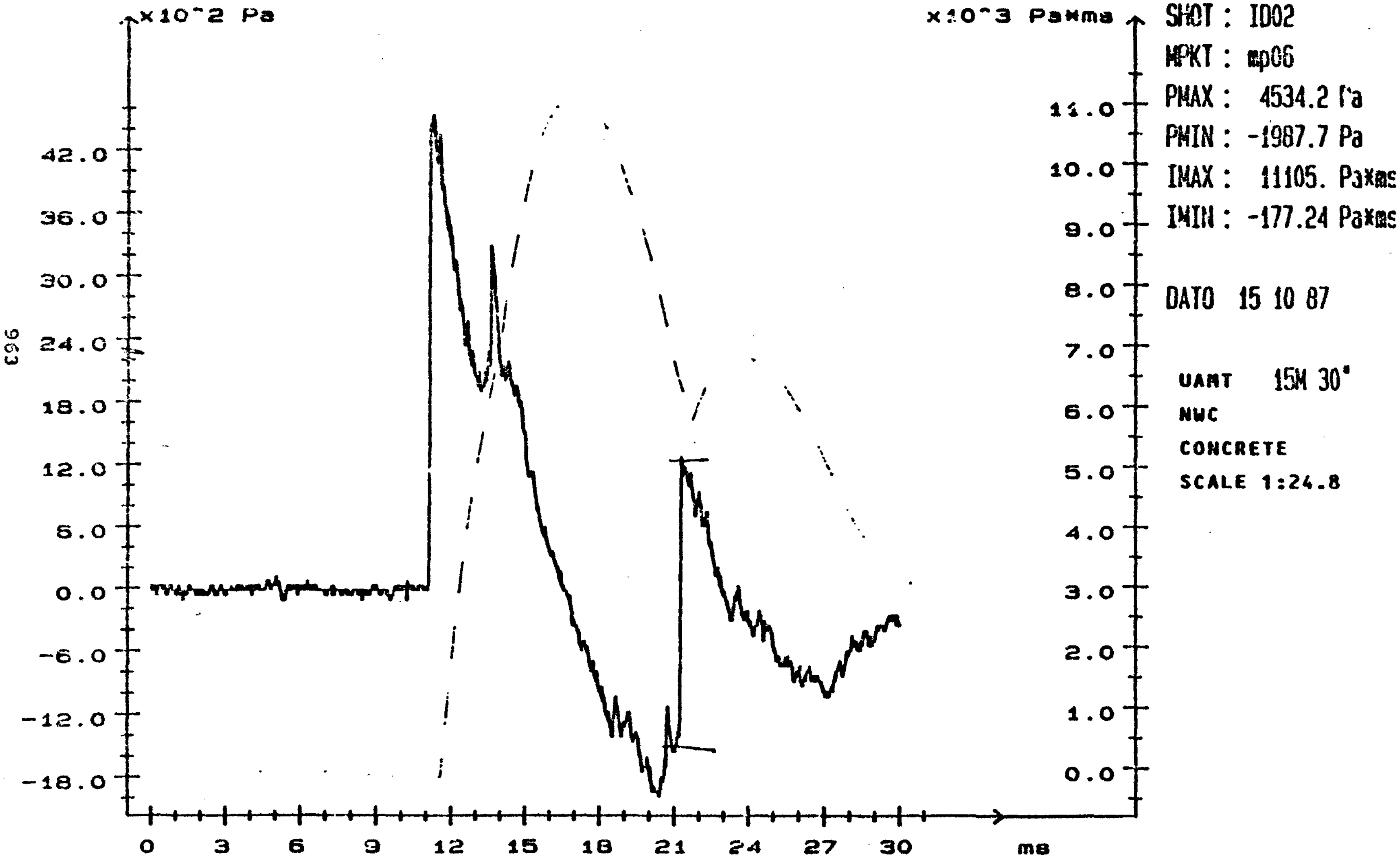
x10^2 Pa
x10^3 Pa*ms
42.0
36.0
30.0
24.0
18.0
12.0
6.0
0.0
-6.0
-12.0
-18.0
11.0
10.0
9.0
8.0
7.0
6.0
5.0
4.0
3.0
2.0
1.0
0.0
0
3
6
9
12
15
18
21
24
27
30
ms
SHOT : ID02
MPKT : mp06
PMAX : 4534.2 Pa
PMIN : -1987.7 Pa
IMAX : 11105. Pa*ms
IMIN : -177.24 Pa*ms
DATO 15 10 87
UANT 15M 30°
NWC
CONCRETE
SCALE 1:24.8

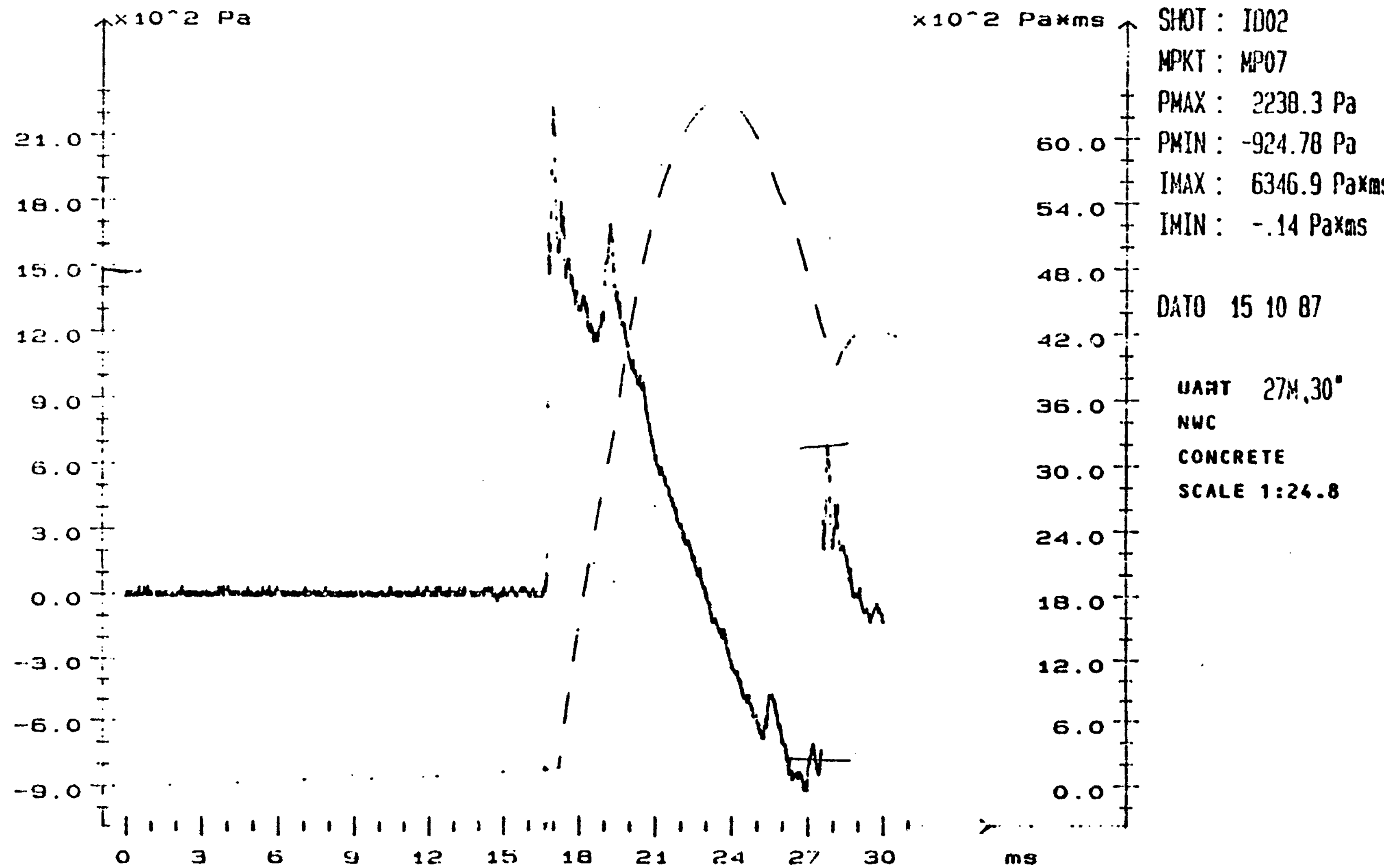
x10^2 Pa
21.0
18.0
15.0
12.0
9.0
6.0
3.0
0.0
-3.0
-6.0
-9.0
0
3
6
9
12
15
18
21
24
27
30
ms
x10^2 Pa*ms
60.0
54.0
48.0
42.0
36.0
30.0
24.0
18.0
12.0
6.0
0.0
SHOT : ID02
MPKT : MP07
PMAX : 2238.3 Pa
PMIN : -924.78 Pa
IMAX : 6346.9 Pa*ms
IMIN : -.14 Pa*ms
DATO 15 10 87
UART 27M,30"
NWC
CONCRETE
SCALE 1:24.8

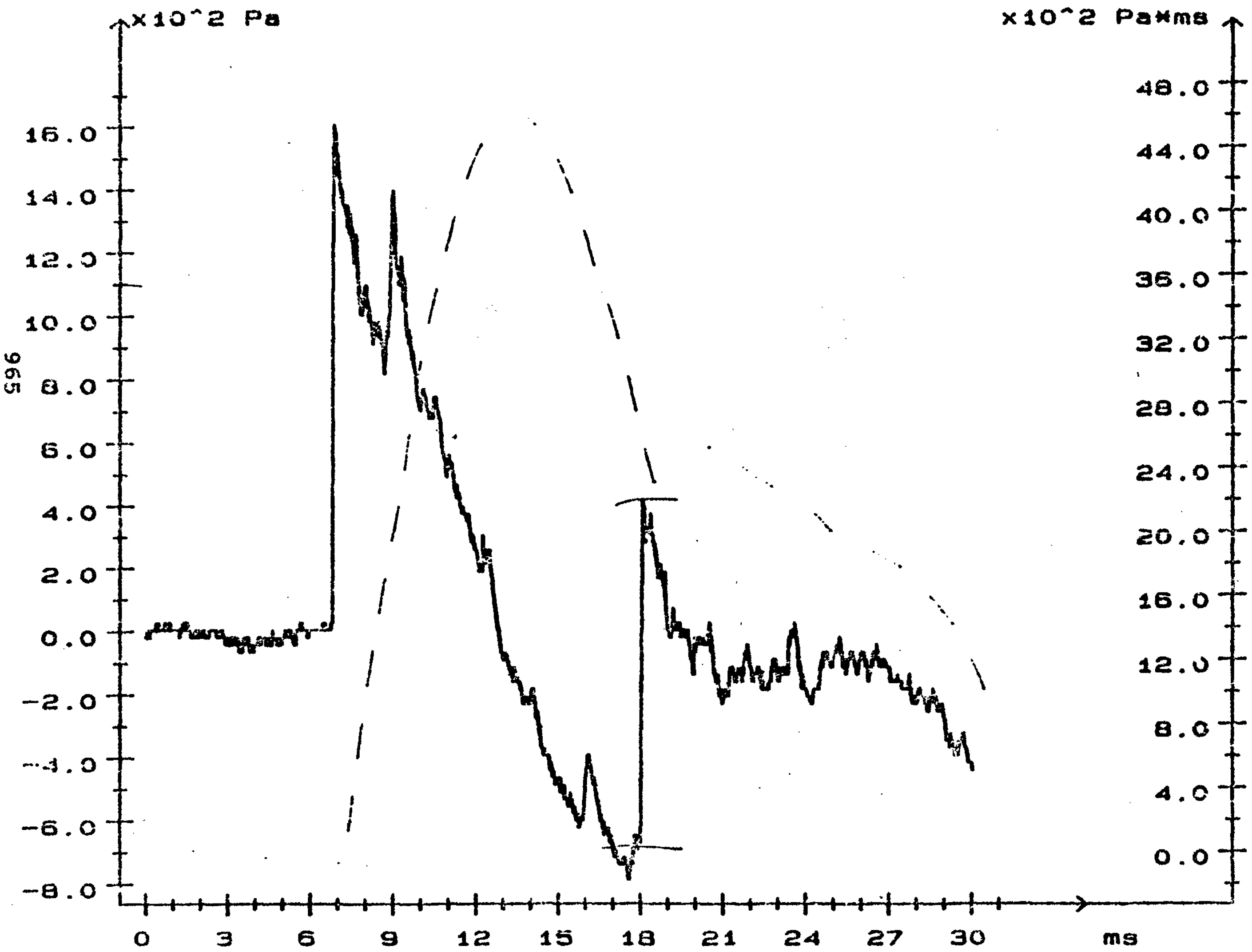

SHOT : ID02
MPKT : MP08
PMAX : 1607.6 Pa
PMIN : -705.25 Pa
IMAX : 4632.2 Pa*ms
IMIN : -74.43 Pa*ms

DATO 15 10 87

UANT 37M 30"
NWC
CONCRETE
SCALE 1:24.8

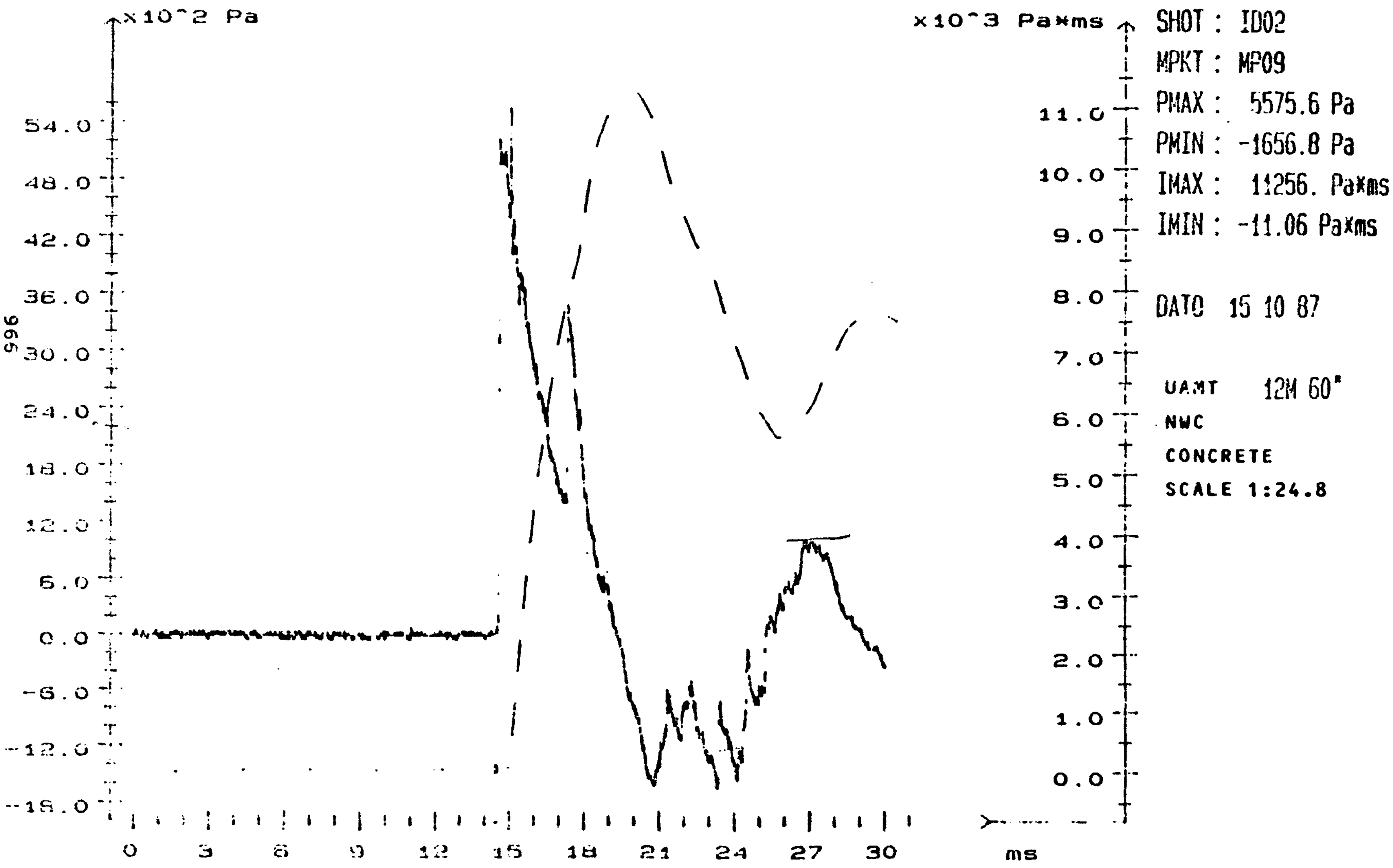
x10^2 Pa
x10^3 Pa*ms
54.0
48.0
42.0
36.0
30.0
24.0
18.0
12.0
6.0
0.0
-6.0
-12.0
-18.0
11.0
10.0
9.0
8.0
7.0
6.0
5.0
4.0
3.0
2.0
1.0
0.0
0
3
6
9
12
15
18
21
24
27
30
ms
SHOT : ID02
MPKT : MP09
PMAX : 5575.6 Pa
PMIN : -1656.8 Pa
IMAX : 11256. Pa*ms
IMIN : -11.06 Pa*ms
DATO 15 10 87
UAMT 12M 60"
NWC
CONCRETE
SCALE 1:24.8

996

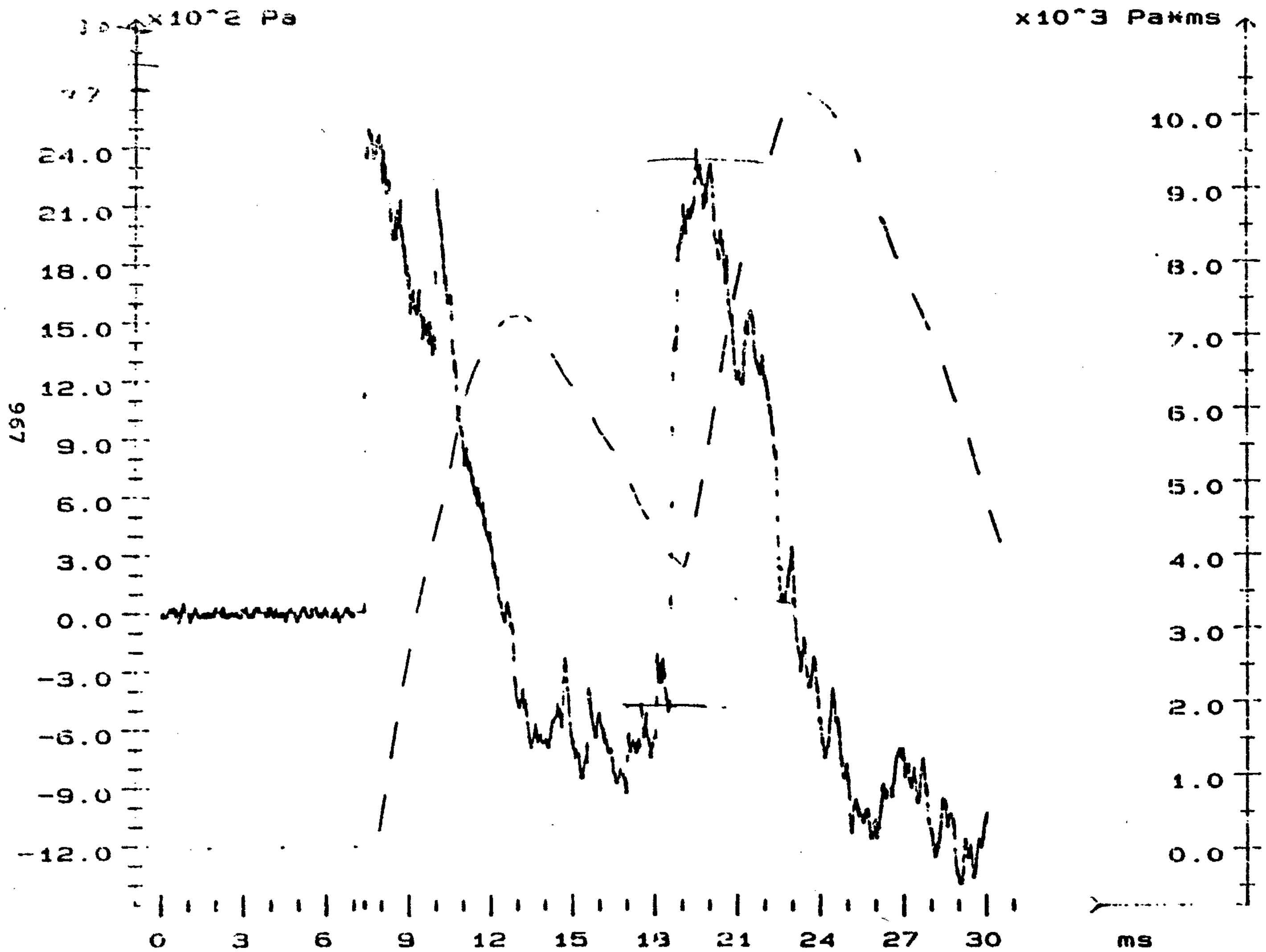

SHOT : ID02
MPKT : MP10
PMAX : 2500.2 Pa
PMIN : -1394.2 Pa
IMAX : 10291. Pa*ms
IMIN : -2.75 Pa*ms

DATO 15 10 87

UANT 20M 60"
NWC
CONCRETE
SCALE 1:24.8

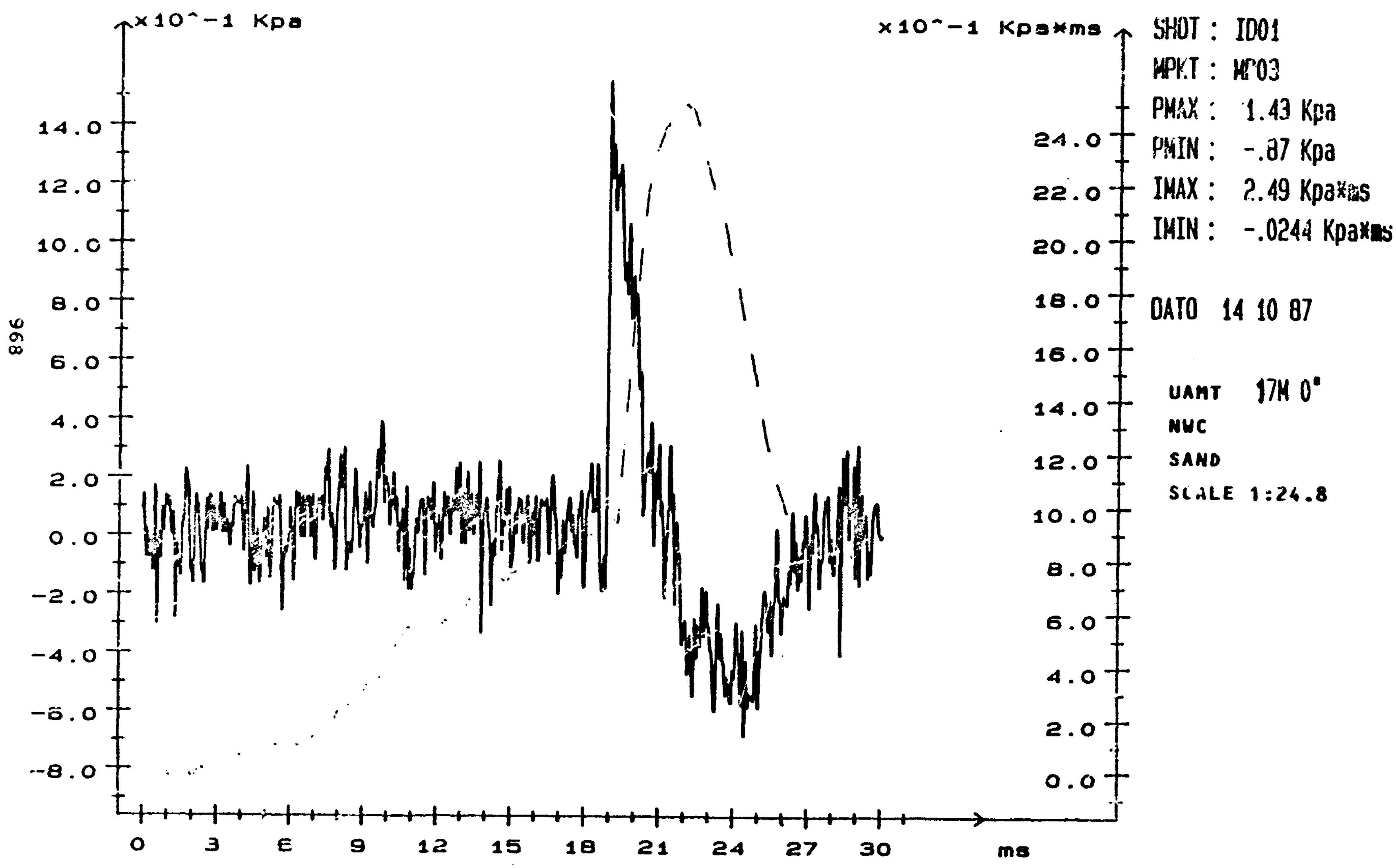
x10^-1 Kpa
x10^-1 Kpa*ms
14.0
12.0
10.0
8.0
6.0
4.0
2.0
0.0
-2.0
-4.0
-6.0
-8.0
24.0
22.0
20.0
18.0
16.0
14.0
12.0
10.0
8.0
6.0
4.0
2.0
0.0
0 3 6 9 12 15 18 21 24 27 30
ms
SHOT : ID01
MPKT : MP03
PMAX : 1.43 Kpa
PMIN : -.87 Kpa
IMAX : 2.49 Kpa*ms
IMIN : -.0244 Kpa*ms
DATO 14 10 87
UAMT 17M 0°
NWC
SAND
SCALE 1:24.8

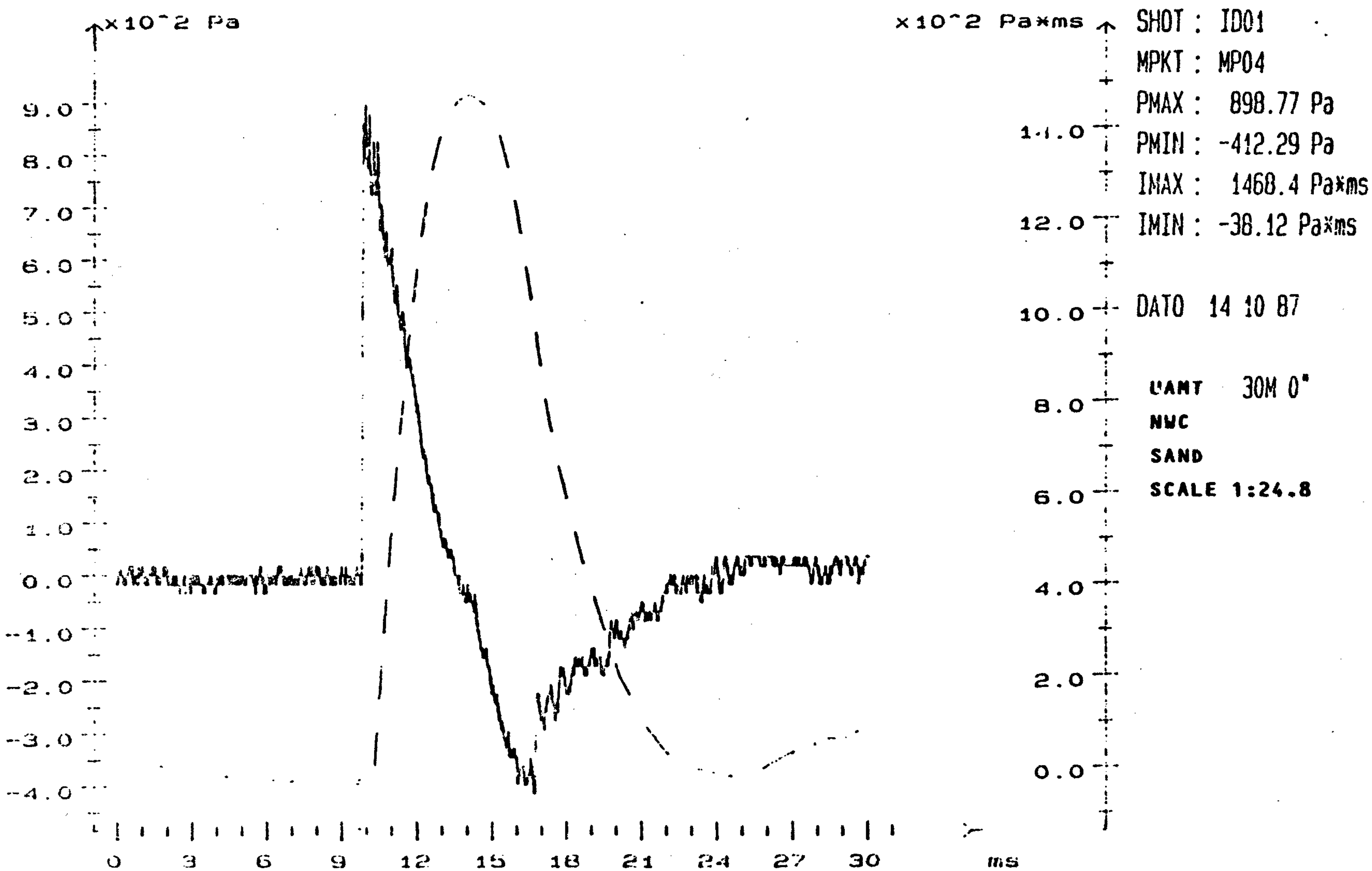
x10^2 Pa
9.0
8.0
7.0
6.0
5.0
4.0
3.0
2.0
1.0
0.0
-1.0
-2.0
-3.0
-4.0
0
3
6
9
12
15
18
21
24
27
30
ms
x10^2 Pa*ms
14.0
12.0
10.0
8.0
6.0
4.0
2.0
0.0
SHOT : ID01
MPKT : MP04
PMAX : 898.77 Pa
PMIN : -412.29 Pa
IMAX : 1468.4 Pa*ms
IMIN : -38.12 Pa*ms
DATO 14 10 87
UANT 30M 0"
NWC
SAND
SCALE 1:24.8

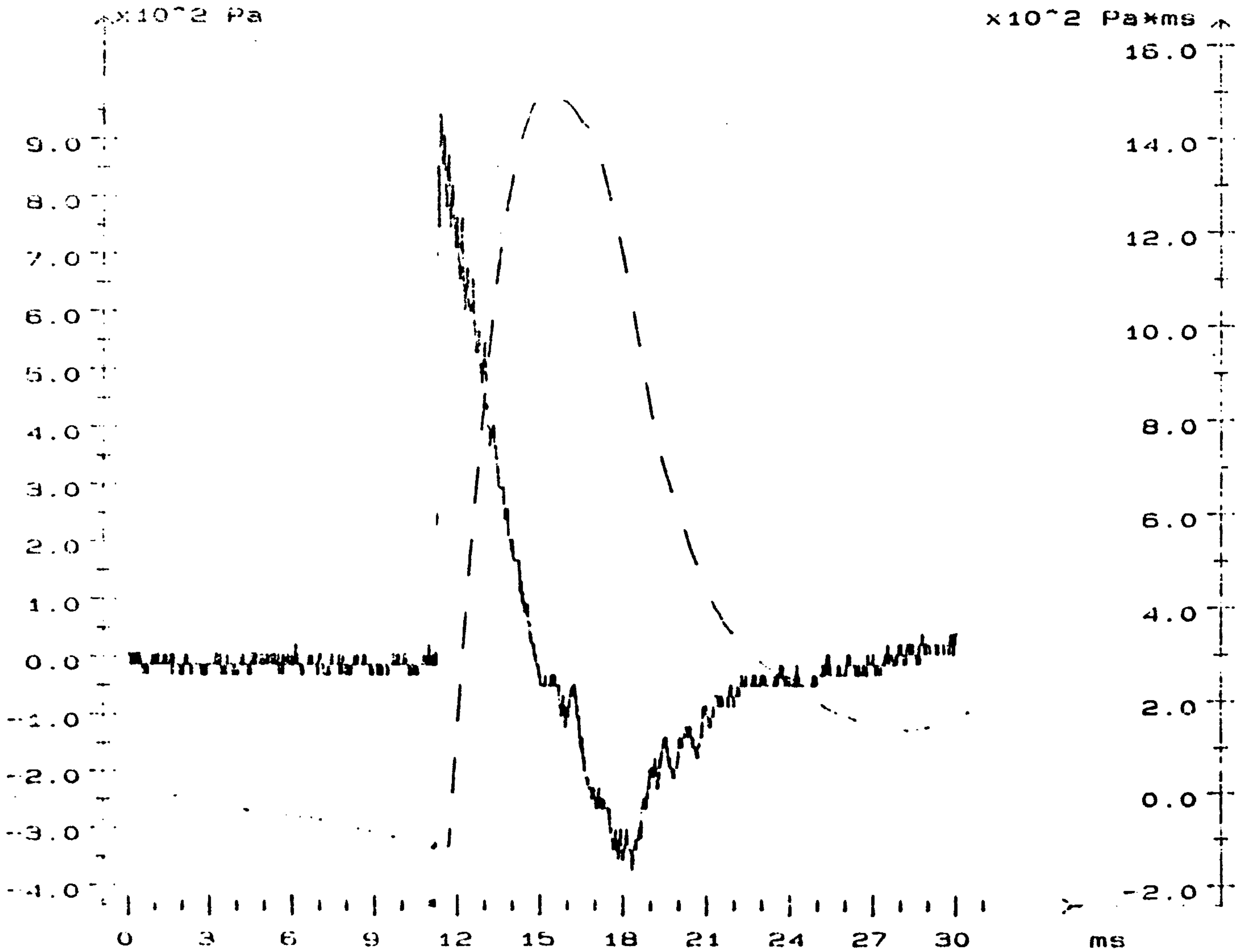

SHOT : ID01
MPKT : MP07
PMAX : 946.13 Pa
PMIN : -373.21 Pa
IMAX : 1500.5 Pa*ms
IMIN : -116.98 Pa*ms

DATO 14 10 87

UANT 27M 30°
NWC
SAND
SCALE 1:24.8

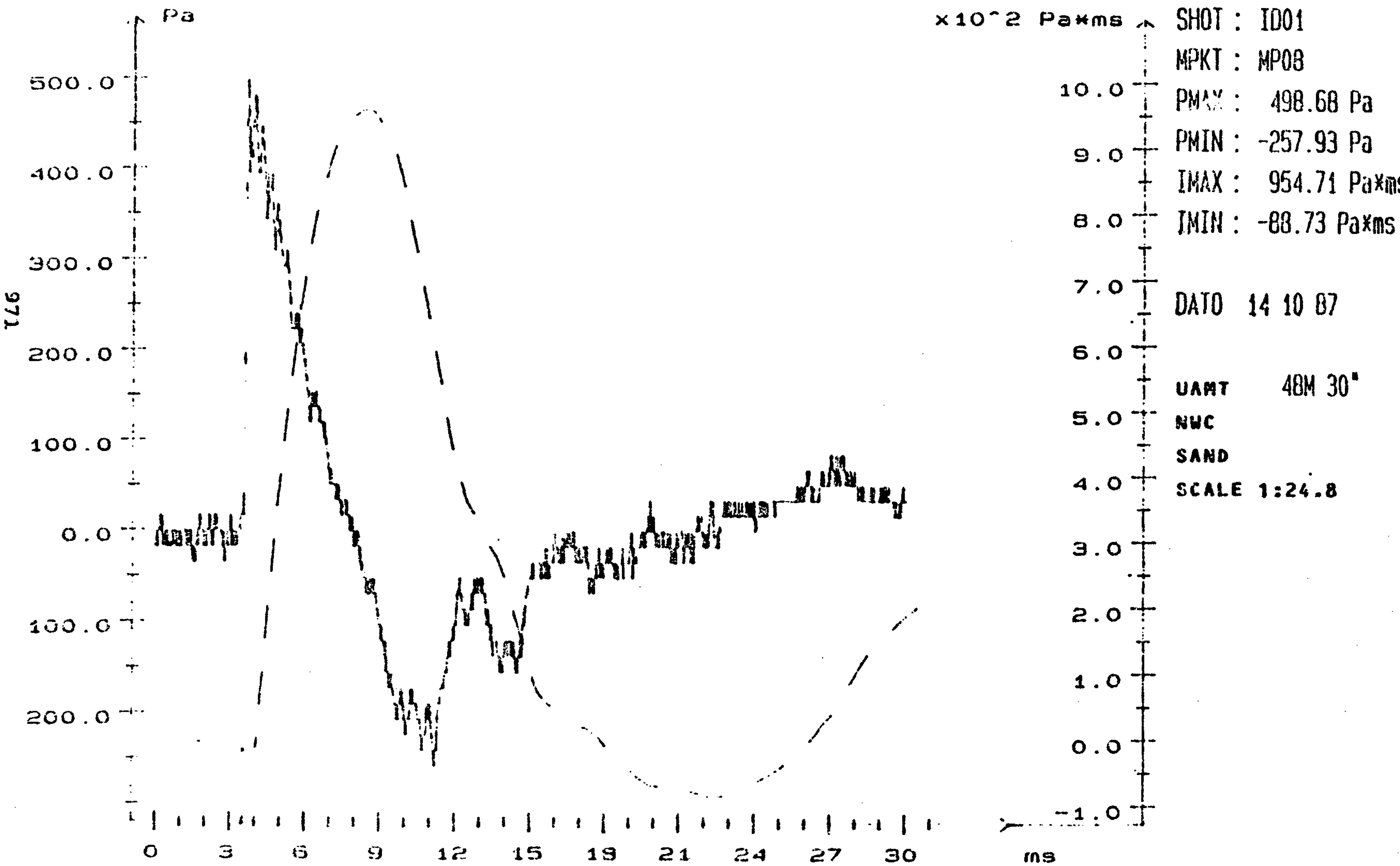

Pa
500.0
400.0
300.0
200.0
100.0
0.0
100.0
200.0
0
3
6
9
12
15
18
21
24
27
30
ms
x10^2 Pa*ms
10.0
9.0
8.0
7.0
6.0
5.0
4.0
3.0
2.0
1.0
0.0
-1.0
SHOT : ID01
MPKT : MP08
PMAX : 498.68 Pa
PMIN : -257.93 Pa
IMAX : 954.71 Pa*ms
IMIN : -88.73 Pa*ms
DATO 14 10 87
UAMT 48M 30"
NWC
SAND
SCALE 1:24.8

971

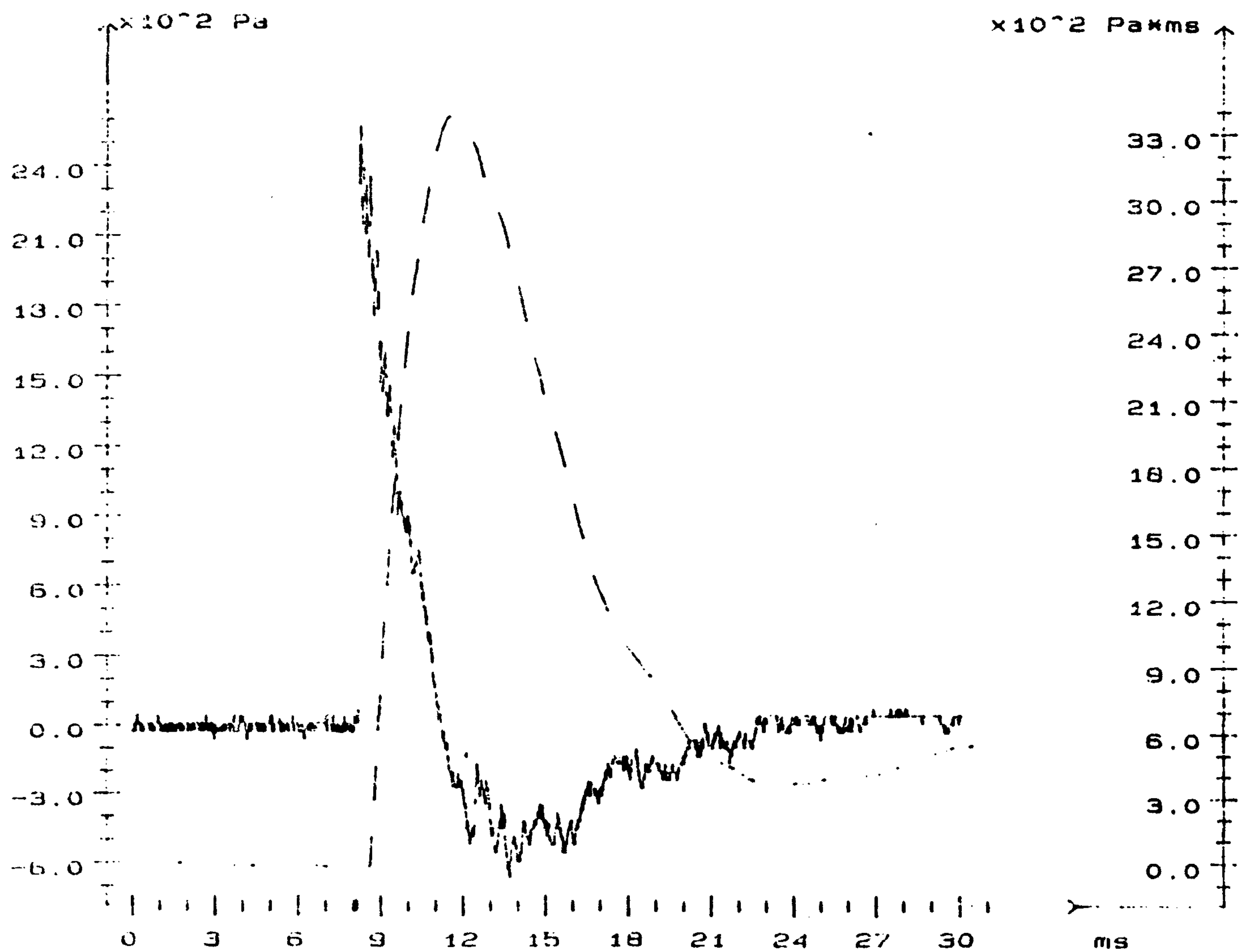

SHOT : ID01
MPKT : MP09
PMAX : 2571.3 Pa
PMIN : -667.30 Pa
IMAX : 3375.8 Pa*ms
IMIN ; -15.83 Pa*ms

DATO 14 10 87

UANT 12M 60°
NWC
SAND
SCALE 1:24.8

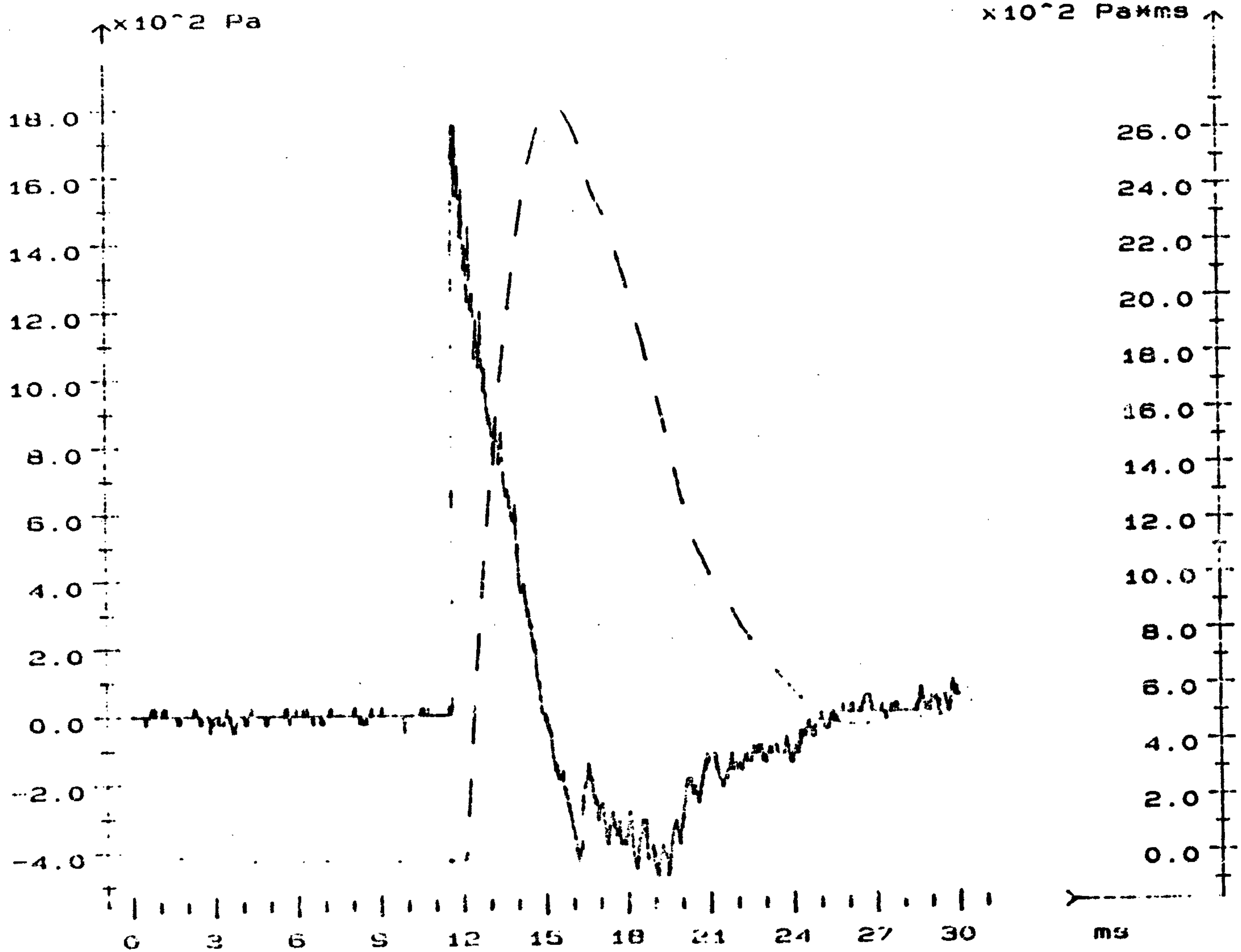

SHOT : ID01
MPKT : MP10
PMAX : 1753.6 Pa
PMIN : -480.44 Pa
IMAX : 2696.2 Pa×ms
IMIN : -14.89 Pa×ms

DATO 14 10 87

UAKT 20M 60"
NWC
SAND
SCALE 1:24.8

APPENDIX B

Documentary Photographs

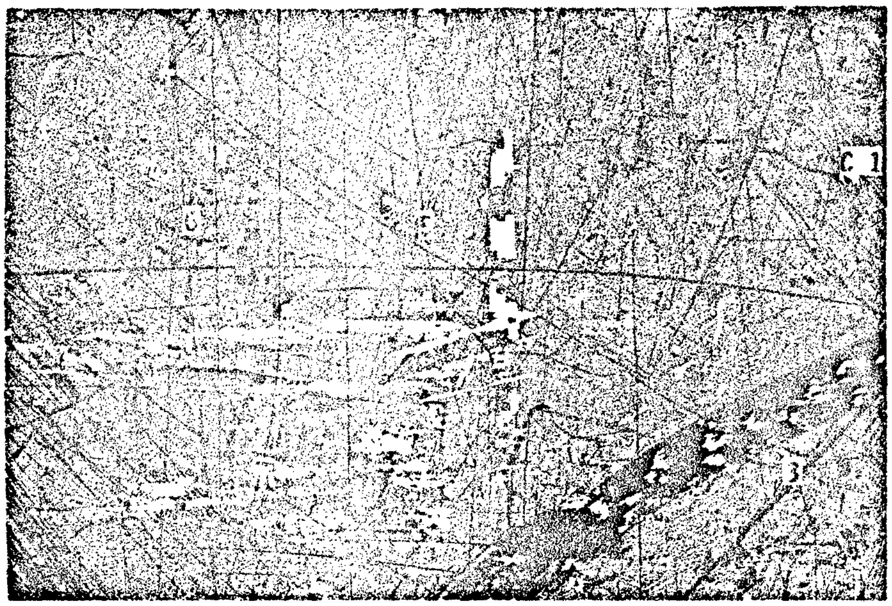

Sand and concrete models seen from EAST.
Ref Figure 4

Sand and concrete models seen from WEST.
Gauge lines marked with tape.

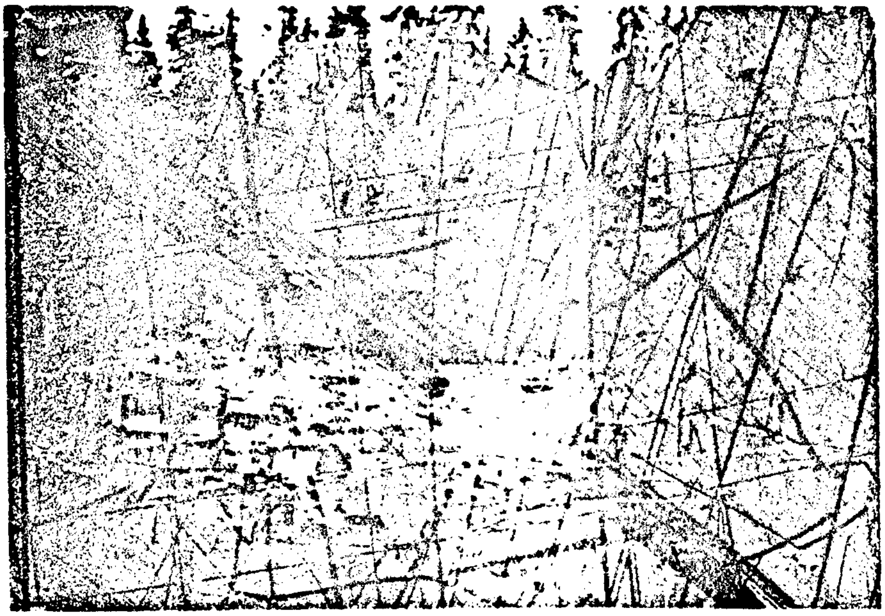

Models seen from SOUTH.
Asphalt pad in front.

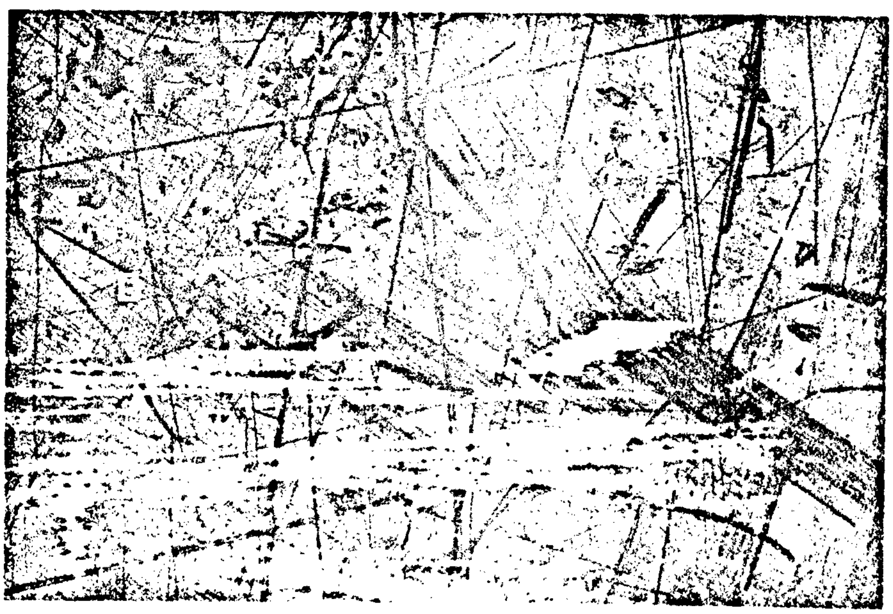

Models seen from SOUTH-EAST

Aluminium rod with bolt and cloth strip.
Oak and aluminium cubes.

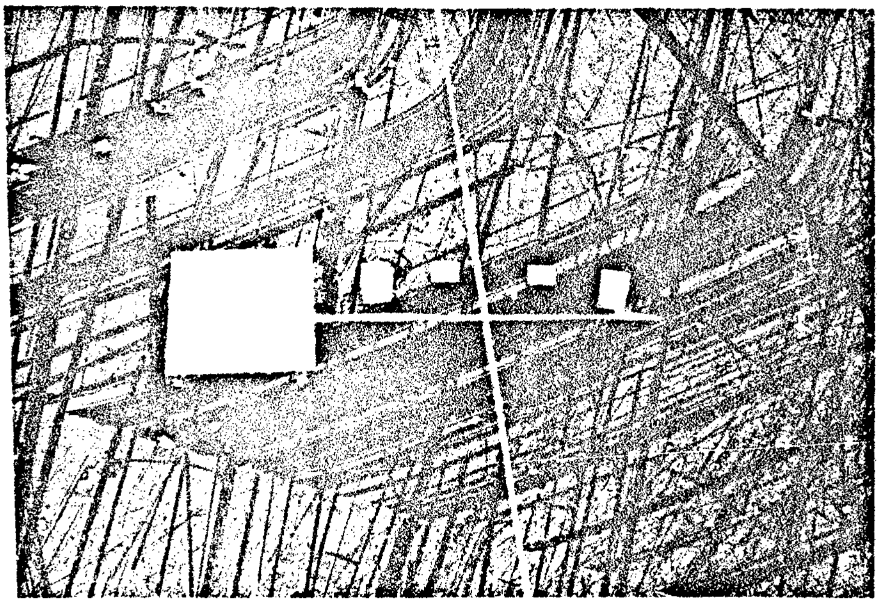

Oak and aluminium cubes located at the 0° radial

Sand model seen from the top of the soil berm in the 0^{o} direction.

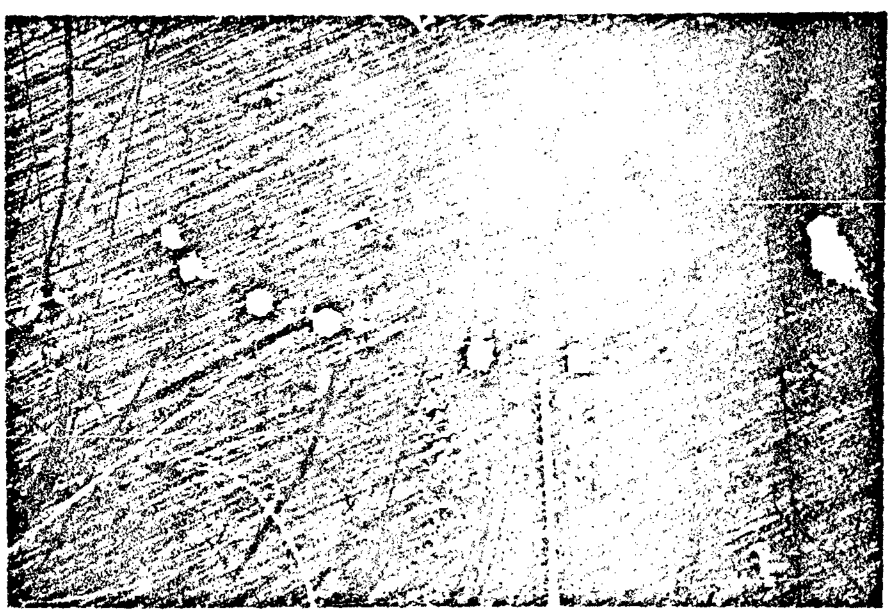

Cubes in front of the sand model

Sand model after test seen from SOUTH
Camera 1 on top of berm.

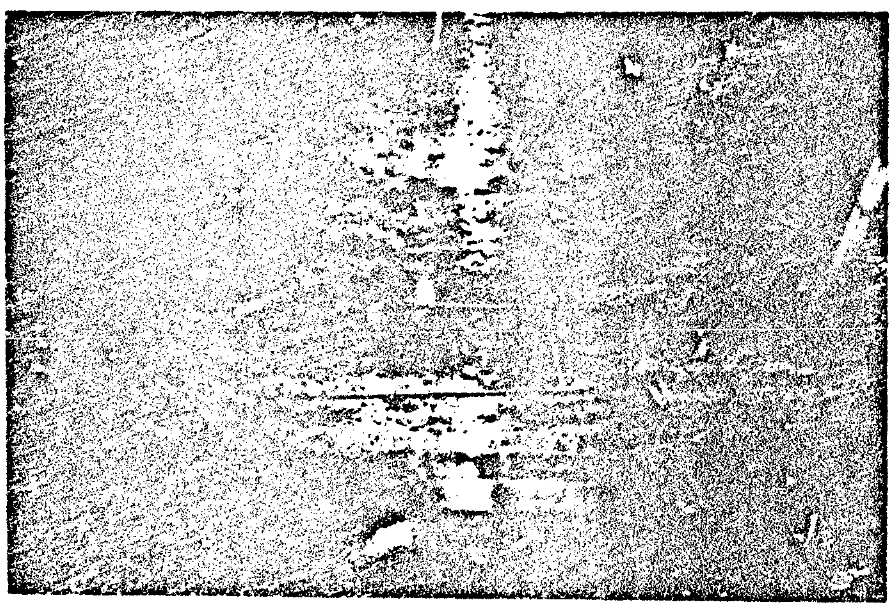

Sand model after test seen from top of the berm

Concrete model after test seen from SOUTH

Close up of tunnel exit.
Concrete model.

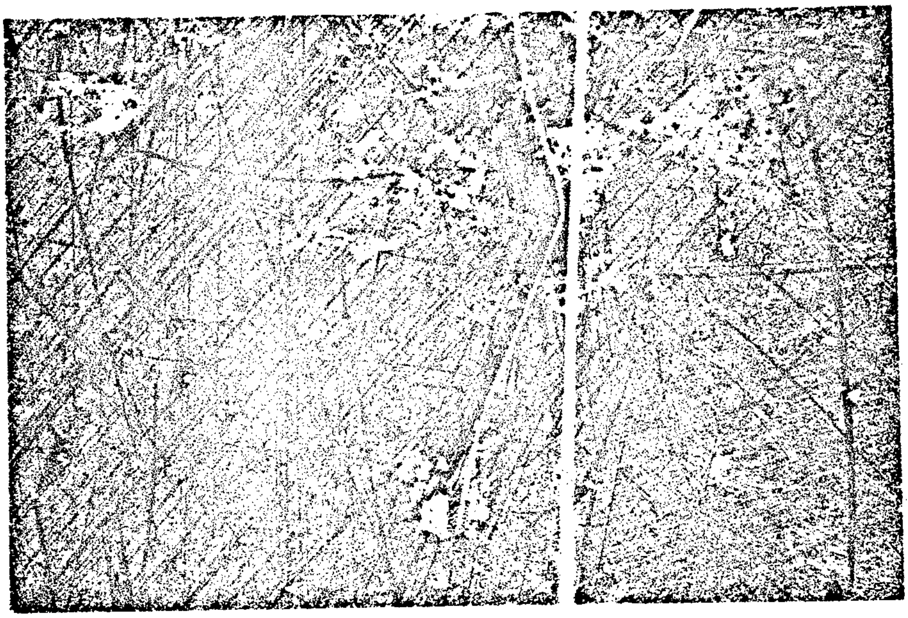

Concrete model. Chamber after test seen from SOUTH.

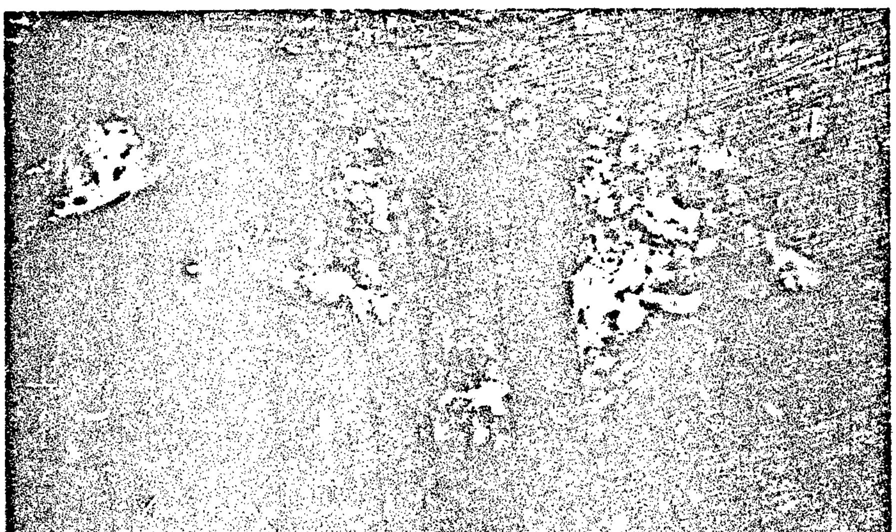

Concrete model. Chamber seen from SOUTH after debris have been removed.

Concrete model after test seen from the top of the soil berm.

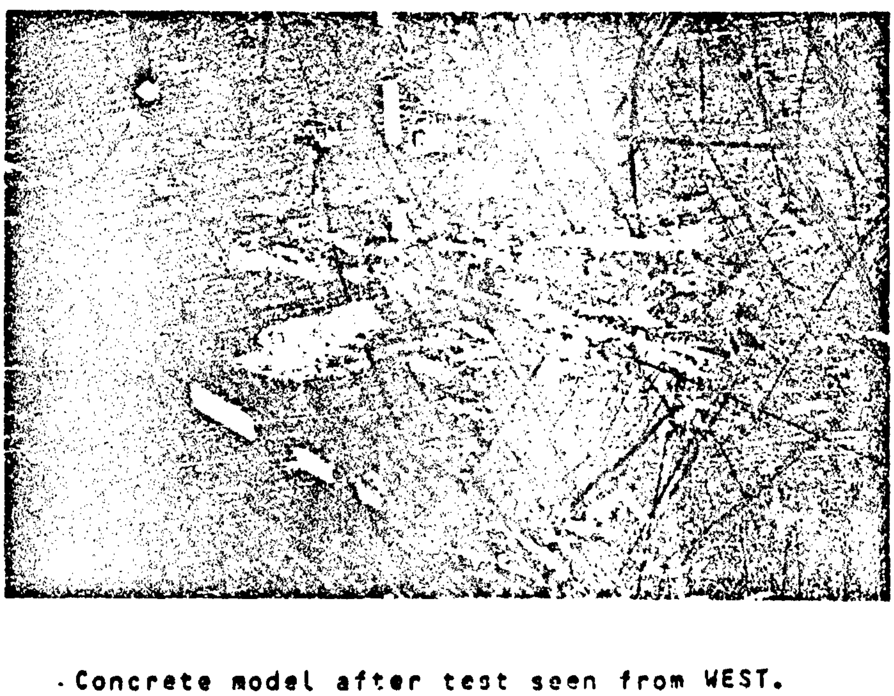

Concrete model after test seen from WEST.

Concrete model after test seen from the top of the soil berm.

Concrete model after test seen from the top of the soil berm after that some debris have

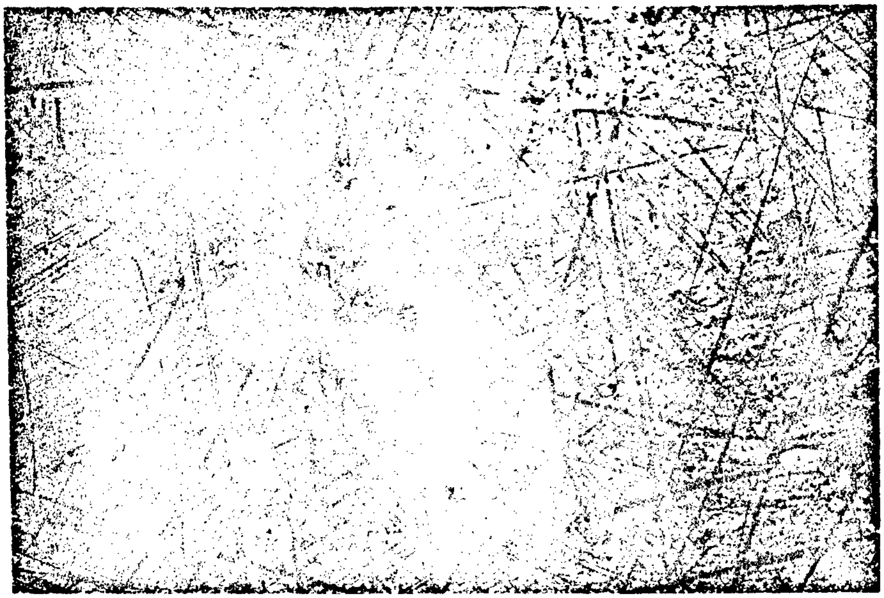

Debris after test 2 - concrete - seen in the 0° direction.

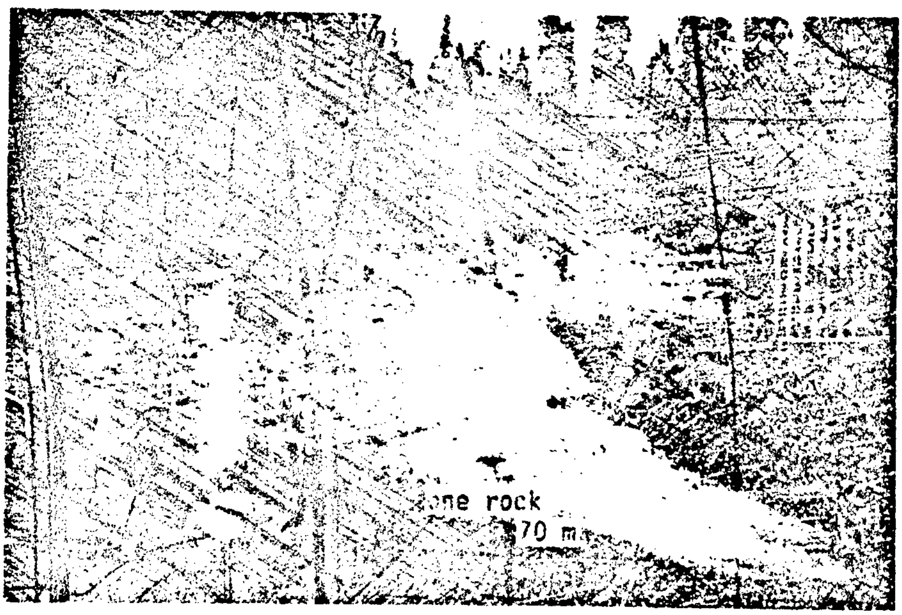

Test 2 - concrete - seen from SOUTH after the test.

SHEAR REINFORCEMENT IN BLAST-RESISTANT DESIGN

S.A. Kiger
S.C. Woodson and F.D. Dallriva
U.S. Army Engineer Waterways Experiment Station
Vicksburg, Mississippi

SHEAR REINFORCEMENT IN BLAST-RESISTANT DESIGN

S.A. Kiger, S.C. Woodson, and F.D. Dallriva

U.S. Army Engineer Waterways Experiment Station
Vicksburg, Mississippi

INTRODUCTION

The use of shear reinforcement and, if used, the type and amount of shear reinforcing selected can have a significant effect on the cost of construction. Shear reinforcement, i.e., reinforcement tying the mats of principal reinforcement together, used in blast-resistant design usually consists of either lacing or single-leg stirrups (see Figure 1).

Lacing bars are reinforcing bars that extend in the direction parallel to the principal reinforcement and are bent into a diagonal pattern between mats of principal reinforcement. The lacing bars enclose the transverse reinforcing bars which are placed outside the principal reinforcement. The cost of using lacing reinforcement is considerably greater than that of using single-leg stirrups due to the more complicated fabrication and installation procedures. Most blast resistant design guides and manuals stipulate the use of shear reinforcement irrespective of shear stress levels. In blast resistant designs, the primary purpose of this type of reinforcement, normally considered to be shear reinforcement, is not to resist shear forces but rather to improve performance in the large deflection region by tying the two principal reinforcement mats together.

Requirements for shear reinforcement are based primarily on data from static beam tests, and its primary purpose is to prevent the formation and propagation of diagonal tension cracks. Very little study has been devoted to examining the role of this type of reinforcement in slabs under distributed dynamic loads, especially in the large deflection regime. In blast resistant design, structures are typically designed to survive only one loading and relatively large deflections are acceptable as long as catastropic failure is prevented. There exist a considerable amount of data that indicate the extensive shear reinforcement typically required in blast resistant design may be excessive. A better understanding of the role of shear reinforcement should allow the design of lower cost structures without loss of blast resistant capacity.

CURRENT PRACTICE

In civilian practice the primary source of design guidance for placement of reinforcing steel in reinforced concrete structures, including shear reinforcement, is the American Concrete Institute's ACI 318-83 (Reference 1). No such single, widely accepted criteria document exists for blast resistant design guidance; however, the most widely used reference ...

the area of designing for explosive safety is the Tri-Service Manual, "Structures to Resist the Effects of Accidental Explosions," (References 2 and 3). Other references for guidance include the Army manual on Protective Construction, TM 5-855-1 (Reference 4) and the NATO Semihardened Design Criteria document published by the U.S. Air Force (Reference 5). A summary of the guidance for shear reinforcement from each of these references follows.

The Tri-Service Manual, "Structures to Resist the Effects of Accidental Explosions":

The Tri-Service Manual is the most widely used manual for structural design to resist blast effects. Its Army designation is TM 5-1300, for the Navy it is NAVFAC P397, and for the Air Force it is AFM 88-22. For convenience it will be referred to as TM 5-1300 (Reference 2) in this paper. A recently completed revision of TM 5-1300 is available in draft form and criteria from volume IV of the draft (Reference 3) will also be discussed here.

In Section 3-11 of TM 5-1300 (Reference 2), the use of lacing (see Figure 1) is required for "close-in" detonations, i.e. whenever pressures much larger than 200 psi are expected. The use of unlaced concrete elements is allowed at lower pressures if support rotations of less than 2 degrees are predicted.

In volume IV of the new draft version of TM 5-1300 (Reference 3) these restrictions are relaxed slightly. Considering the resistance-deflection relationship for flexural response of a reinforced concrete element, Section 4-9.1 of the manual states that, within the range following yielding of the flexural reinforcement, the compression concrete crushes at a deflection corresponding to 2 degrees support rotation. This crushing of the compression concrete is considered to be "failure" for elements without shear reinforcement. For elements with shear reinforcement (single-leg stirrups or lacing reinforcement) which properly tie the flexural reinforcement, the crushing of the concrete results in a slight loss of capacity since the compressive force is transferred to the compression reinforcement. As the reinforcement enters into its strain-hardening region, the resistance increases with increasing deflection. Section 4-9.1 of the manual states that single-leg stirrups will restrain the compression reinforcement for a short time into its strain hardening region until failure of the element occurs at a support rotation of 4 degrees. It further states that lacing reinforcement will restrain the flexural reinforcement through its entire strain-hardening region until tension failure of the principal reinforcement occurs at a support rotation of 12 degrees. Draft TM 5-1300 distinguishes between a "close-in" design range and a "far" design range for purposes of predicting the mode of response. In the far design range, the distribution of the applied loads is considered to be fairly uniform and deflections required to absorb the loading are comparatively small. Section 4-9.2 states that non-laced elements are considered to be adequate to resist the far-design loads with ductile

behavior within the constraints of the allowable support rotations previously discussed. The design of the element to undergo deflections corresponding to support rotations between 4 and 12 degrees requires the use of laced reinforcement. An exception is when the element has sufficient lateral restraint to develop in-plane forces in the tensile-membrane region of response. In this case, Section 4-9.2 states that the capacity of the element increases with increasing deflection until the reinforcement fails in tension. A value of support rotation is not given here, but one might deduce that a support rotation of 12 degrees is intended since it is the value given in Section 4-9.1 for tension failure of the reinforcement in a laced slab. However, a value of 8 degrees is given elsewhere in the draft manual as a limit of support rotation for elements containing stirrups and experiencing tensile membrane behavior.

Section 4-9.3 of the Draft TM 5-1300 discusses ductile behavior in the close-in design range. Again, the maximum deflection of a laced element experiencing flexural response is given as that corresponding to 12 degrees support rotation. This section states the following:

> "Single leg stirrups contribute to the integrity of a protective element in much the same way as lacing, however, the stirrups are less effective at the closer explosive separation distances. The explosive charge must be located further away from an element containing stirrups than a laced element. In addition, the maximum deflection of an element with single leg stirrups is limited to 4 degrees support rotation under flexural action or 8 degrees under tension membrane action. If the charge location permits, and reduced support rotations are required, elements with single leg stirrups may prove more economical than laced elements."

Section 4-25.3 of the Draft TM 5-1300 explains that for simplicity, the energy absorbed under the actual resistance-deflection curve with a maximum support rotation of 12 degrees, is approximated with an elastic-plastic model having a maximum support rotation of 8 degrees as shown in Figure 4-18 of the manual and Figure 2 of this paper. Due to the use of this model, one might presume that the criteria for maximum support rotation is identical for non-laced elements with lateral support and laced elements. However, no such elastic-plastic analogy is given for laced slabs. All other discussion in the draft manual indicates that the 12 degrees support rotation for laced elements is not equivalent to the 12 degrees support rotation for non-laced elements modeled with 8 degrees using the elastic-plastic curve. For example, Section 4-32 states:

> "... Also, the blast capacity of laced elements are greater than corresponding (same concrete thickness and quantity of reinforcement) elements with single leg stirrups. Laced elements may attain deflections corresponding to 12 degrees support rotation whereas elements with single leg stirrups are designed for a maximum rotation of 8 degrees. These non-laced elements must develop tension membrane action in order to

develop this large support rotation. If support conditions do not permit tension membrane action, lacing reinforcement must be used to achieve large deflections."

It is implied throughout Draft TM 5-1300 that laced elements may attain support rotations of 12 degrees whether they are restrained against lateral movement or not. The manual also implies that a non-laced element may only achieve its maximum support rotation of 8 degrees when it is restrained against lateral movement.

In addition to being required for large-deflection behavior, lacing reinforcement is required in slabs subjected to blast at scaled distances less than 1.0 ft/(lbs^1/3). Section 4-9.4 of the Draft TM 5-1300 indicates that lacing reinforcement is required due to the need to limit the effects of post-failure fragments resulting from flexural failure. It is implied that the size of failed sections of laced elements is fixed by the location of the yield lines, whereas the failure of an unlaced element results in a loss of structural integrity and fragments in the form of concrete rubble. Section 4-22 discusses the use of single-leg stirrups in slabs at scaled distances between 1.0 and 3.0. Support rotations in slabs with stirrups are limited to 4 degrees in the close-in design range unless support conditions exist to induce tensile membrane behavior. In addition, a non-laced element designed for small deflections in the close-in design range is not reusable and, therefore, cannot sustain multiple incidents.

Army Technical Manual 5-855-1

TM 5-855-1 (Reference 4) is intended for use by engineers involved in designing hardened facilities to resist the effects of conventional weapons. The manual includes design criteria for protection against the effects of a penetrating weapon, a contact detonation, or the blast and fragmentation from a standoff detonation.

Chapter 9 of TM 5-855-1 discusses the design of shear reinforcement. The criteria presented is primarily based on the guidance of ACI 318-83 (Reference 1) with consideration of available test data. The maximum allowable shear stress to be contributed by the concrete and the shear reinforcement is given as $11.5(\sqrt{f'_c})$ for design purposes as compared to $8(\sqrt{f'_c})$ given by ACI 318-83. An upper bound to the shear capacity of members with web reinforcing is given as that corresponding to a 100 percent increase in the total shear capacity outlined by ACI 318-83 and consisting of contributions from the concrete and shear reinforcing. An important statement concerning shear reinforcement in one-way slabs and beams is given in Section 9-7 and reads as follows:

"Some vertical web reinforcing should be provided for all flexural members subjected to blast loads. A minimum of 50-psi shear stress capacity should be provided by shear steel in the form of stirrups. In those cases where analysis indicates a requirement of vertical shear reinforcing, it should be provided in the form of stirrups."

TM 5-855-1 states that shear failures are unlikely in normally constructed two-way slabs, but that the possibility of shear failure increases in some protective constrution applications due to high-intensity loads. Shear is given as the governing mode of failure for deep, square, two-way slabs. In the event shear capacity is required above that provided by the concrete alone, additional strength can be provided in the form of vertical and/or horizontal web reinforcing. For beams, one-way slabs, and two-way slabs, the manual recommends a design ductility ratio of 5.0 to 10.0 for flexural design.

Air Force NATO Semihard Design Criteria

The purpose of the document (Reference 6) is to give guidance for semihardened and protected facilities with conventional, nuclear, biological, and chemical weapon protection. It states that these structures shall be designed to provide a ductile response to blast loading. Ductility of structural members is considered imperative to provide structural economy, energy absorption capability and to preclude catastrophic (brittle) failures. All reinforced concrete sections are required to be doubly reinforced (both faces) in both longitudinal and transverse directions. Where flexural response is significant, the structural element is to be reinforced symmetrically, i.e. the compression and tension reinforcement is the same. The use of stirrups is discussed as follows:

> "Ties and/or stirrups shall be provided in all members to provide concrete confinement, shear reinforcement, and to enable the element to reach its ultimate section capacity. Without stirrups, cracking and dislodgement of the concrete from between the reinforcement layers and buckling of the compression steel usually produce failure long before the ultimate strain of the reinforcement and the maximum energy absorption are attained. Stirrups contribute to the integrity of the element in the following ways:
>
> a. The ductility of the primary flexural steel is developed.
>
> b. Integrity of the concrete between the two layers of flexural reinforcement is maintained.
>
> c. Compression reinforcement is restrained from buckling.
>
> d. High shear stresses at the supports are resisted.
>
> e. The resistance to local shear failure produced by the high intensity of the peak blast pressures is increased.
>
> f. Quantity and velocity of post-failure fragments are reduced. Stirrups shall be bent a minimum of 135 degrees around the interior face steel and 90 degrees around the exterior face steel. Shear, splice, and anchorage details shall receive added design attention. Designers shall refer to protective design

manuals and/or seismic design manuals for appropriate details."

The document does not address the use of laced reinforcement. The above list of ways that stirrups enhance the integrity of structural elements is similar to the wording given in TM 5-1300 for the ways that lacing enhances the integrity of structural elements, except for the stirrup details given in Item f above.

Summary of Design Criteria

The above review indicates that guidance documents differ considerably on the type of shear reinforcement required; however, the use of some type of shear reinforcement is uniformly required for blast design. The current TM 5-1300 (Reference 2) limits the use of stirrups to those elements designed to undergo support rotations of less than 2 degrees. The Draft TM 5-1300 (Reference 3) allows the use of stirrups in elements designed to undergo support rotations of up to 8 degrees for scaled ranges greater than one and when restraint against lateral support movement exists. Lacing bars are required by References 2 and 3 for most cases and in every case for "close-in" detonations. Although TM 5-855-1 and the NATO Semihardened Criteria do not require lacing, they do require some form of shear reinforcement in all elements designed to resist blast loads.

RELATED RESEARCH

Data from several research programs investigating structural response to static and blast loads over the past 10 years indicate that reinforced concrete structures can sustain large deflections (rotations in excess of 12 degrees) without failure. None of these structures had laced reinforcement. Most had stirrup reinforcement, but some sustained large deflections without failure with no shear reinforcement at all. A selected sample of this data is summarized below. Although no specific recommendations for revising current design guidance can be made based on this data, it does indicate that a well designed research program could result in design guidance that allows much more flexibility in the use of shear reinforcement for blast resistant design without degrading the structural capacity to sustain large deflections safely. Such guidance would allow the designer to select shear reinforcement (or design around its use) to arrive at the least costly design for a specific application.

Woodson (Reference 6) statically tested ten one-way reinforced concrete slabs, primarily to investigate the effects of stirrups and stirrup details on the load response behavior of the slabs. The slabs were rigidly restrained at the supports and were loaded with uniformly distributed pressure. The slabs had span-to-effective-depth ratios of about 12, and principal reinforcement ratios of about 0.008 in each face. Support rotations between 13 and 21 degrees were observed (see Figure 3). Due to the increase in resistance with increasing deflections of a slab with a large number of single-leg stirrups, the loading of the slab was not terminated until support rotations were approximately 21 degrees (see Figure 4). A slab having no shear reinforcement achieved support rotations greater

than 16 degrees without failure. These slabs had sufficient lateral restraint to develop in-plane forces in the tensile membrane region of response. In this case, TM 5-1300 (Reference 2) would require lacing for support rotations greater than 2 degrees and the Draft TM 5-1300 (Reference 3) would allow a slab with single-leg stirrups to undergo maximum support rotations up to only 8 degrees. The slab with 21 degrees of support rotation contained single-leg stirrups (135-degree bend on one end and a 90-degree bend on the other end) spaced at about 0.4 d (d = effective depth of slab). The maximum spacing allowed in the Draft TM 5-1300 is 0.5 d and 180-degree bends are required on each end of the stirrup (an expensive requirement).

Guice (Reference 7) statically tested 16 one-way reinforced concrete slabs with uniformly distributed load, primarily to investigate the effects of edge restraint on slab behavior. Each slab contained single-leg stirrups spaced at approximately 1.5 d (compared to a minimum of about 0.5 d required by Reference 3). Again, the stirrups had 135 degree bends on one end and 90 degree bends on the other end. Support rotations of about 20 degrees were sustained. Regardless of support rotational freedom, the tests showed that the percentage of load carried by tensile membrane action is dependent upon the slab's span-to-thickness ratio. Guice concluded that elements which have a span-to-thickness ratio of about 15, have 1.0 to 1.5 percent of steel in each face, and are supported with a relatively large lateral stiffness and a moderate rotational stiffness will probably result in a structure which best combines the characteristics of strength, ductility, and economy.

Keenan (Reference 8) tested four laced reinforced concrete one-way slabs. All slabs were supported at clamped ends and longitudinally restrained. One slab was tested with an increasing static load applied by water pressure, and the other three slabs were subjected to two or more short-duration dynamic loads. Keenan reported that the rotation capacity at the critical sections of the slab was greater than 9.2 degrees, but could not be measured due to safety limitations on the loading device. Slab behavior was similar under static and dynamic load. The type of loading did not change the extent of cracked or crushed concrete, the collapse mechanism, the mode of failure, or the rotation capacity at supports. Keenan reported that the stress in the lacing bars at the hinges was induced by rotation of the cross-section in addition to shear. Lacing bars yielded at midspan, where the shear is theoretically zero. No lacing bars yielded under static load, but some yielded under dynamic load. The tests showed that the effects of rotation, in addition to shear, should be considered in designing lacing reinforcement for sections near a support.

Keenan (Reference 9) tested nine reinforced concrete two-way slabs. Six slabs were tested under uniform static pressure, and three slabs were tested under dynamic loads of long duration. The slabs were square and restrained against rotation and longitudinal movement at the edges. Keenan discussed the observation of tensile-membrane fragments that were the size of the reinforcing mesh in a slab that contained no lacing at midspan. This slab only had lacing near the supports and contained no stirrups. It was observed that lacing prevented this type of fragmentation in a slab with

lacing at midspan. However, lacing did not prevent severe spalling. It was concluded that slabs should contain lacing or closely spaced principal reinforcement to prevent fragmentation caused by dynamic deflections in the tensile membrane region of behavior. None of the slabs contained stirrups.

Although the new Draft TM 5-1300 does not address the use of closely spaced principal reinforcement, test data indicate that using smaller principal reinforcing bars with a reduced spacing will enhance the ductile response of slabs. This is reported by Keenan (References 9 and 10) and Woodson (Reference 6).

Slawson (Reference 11) dynamically tested eleven shallow-buried reinforced concrete box elements, primarily to evaluate dynamic shear failure criteria. The structures were subjected to high-pressure (greater than 2000 psi peak pressure) short-duration loads. Shear reinforcement consisted of single-leg stirrups with a 90-degree bend and a 135-degree bend. When dynamic shear failure occurred, severing the roof slab from the walls, the concrete was severely crushed and fell from the roof slab reinforcement mats when lifted from the floor for post-test examination.

The one-way roof slabs of four of Slawson's structures did not experience total collapse. One of these roof slabs, having a span-to-effective-depth ratio of 10, experienced a deflection at midspan of about 10 inches for the 48-inch clear span (about 23 degrees support rotation). Some spalling occurred at the walls, but the rest of the slab was cracked without spalling action (see Figure 5). This slab contained single-leg stirrups spaced at about 0.8 d with two stirrups at each location. The remaining three slabs contained one single-leg stirrup at each location, and the spacing varied from about 0.25 d near the supports to 0.5 d at midspan. These slabs had span-to-effective-depth ratios of 7. One slab responded predominantly in shear with a permanent midspan deflection of about 4.5 inches. The unloaded face of the slab experienced cracking with disintegration of the concrete occurring only at the supports. Another roof slab experienced a midspan deflection of about 12 inches (about 26 degrees support rotation). The concrete cover spalled, and the concrete between the principal reinforcement mats was broken up over the entire span but did not fall from the reinforcement cage (see Figure 6). These data indicate that slabs with single-leg stirrups can resist high-pressure short-duration loads without total collapse.

Several experiments have been conducted on buried box-type structures with stirrups (90- and 135- degree bends) as shear reinforcement. In Reference 12 a close-in high explosive produced a wall deflection of about 10.5 inches on a 4- by 16-foot, 5.6-inch thick wall (support rotations were about 24 degrees). A posttest photograph of the inside of the wall is shown in Figure 7. This same box structure was subjected to simulated nuclear overpressures (about 2000 psi peak pressures) in Reference 13. Damage to the structure buried 2 feet deep in a clay backfill is shown in Figure 8. Permanent deflection was about 6 inches (about 14 degrees support rotation), with some concrete cover broken free. In another simulated nuclear overpressure test on this box (Reference 14), it was buried 10 inches deep

in sand and loaded at about 2000 psi peak pressure. Posttest photographs of the structure show a partial failure of the roof (Figure 9) and again some loss of concrete cover from the reinforcement (Figure 10). Permanent roof deflections were about 12.5 inches (about 28 degrees support rotation). Although the roof was clearly on the verge of collapse, it did sustain this level of damage at a very high pressure without catastropic failure.

As a final example, a full-scale 100-man capacity blast shelter was tested in a simulated nuclear overpressure environment (see Reference 15). The 3-bay structure had a roof span of about 11 feet for each bay, a roof thickness of about 10.25 inches, and average tension and compression steel ratios of 0.011 and 0.0036, respectively. Some principal steel (25 percent) was "draped" so that it served as tensile reinforcement at both the supports (top) and center (bottom) of the roof. No shear reinforcement was used in the roof, and the bottom face of the roof was corrugated sheet metal that served as form work and effectively prevented spallation of the concrete from the roof. A posttest view of the interior of Bay 1 is shown in Figure 11. Maximum roof deflection was 17 inches (about 14 degrees support rotation). Due to the protection of the thin metal covering the roof, no concrete spall can be seen.

SUMMARY

Some type of shear reinforcemment in the form of lacing or stirrups is required by applicable design manuals for almost all blast resistant structures. The data reviewed in this paper indicate that these requirements for shear reinforcement may be much more restrictive (and expensive) than necessary.

For reinforced concrete beams, the use of transverse shear reinforcement can provide additional confinement for the concrete core. However, this type of reinforcement provides very little, if any, additional confinement for slabs. Also, shear reinforcement will not help in preventing spallation of the concrete cover over the reinforcement. Shear reinforcement might mitigate the break-up of the concrete core of a slab into rubble; however, some of the data reviewed indicate that the use of smaller, more numerous principal reinforcing bars may be a more effective way to prevent this type of failure.

Several examples of dynamic and static tests on structures using stirrups demonstrated that rotations in excess of 20 degrees without failure are possible. In one case for both static and dynamic tests, rotations of over 14 degrees were incurred with no shear reinforcement at all. In light of this data, the requirement in Draft TM 5-1300 (Reference 3) that lacing be used for all designs with rotations in excess of 8 degrees seems overly restrictive.

In virtually all of the data cited where stirrups were used, they were stirrups with 135 degree bends on one end and 90 degree bends on the other end. These stirrups performed satisfactorally under both static and high intensity blast loads and were much easier (cheaper) to install than

stirrups with 180 degree bends on each end (as required in Draft TM 5-1300 (Reference 3)).

The series of experiments performed by Guice (Reference 7) indicate that if stirrups are required for other than shear reinforcement, a larger spacing may be acceptable (he used 1.5 d). In many cases the 0.5 d spacing of stirrups required in TM 5-1300 could be relaxed.

The data reviewed in this paper may be too fragmented and undirected to base firm recommendations on. However, it clearly indicates that research to determine, quantitatively, the relative advantages of using stirrups verses lacing or possibly no shear reinforcement should be conducted. The results could allow a designer to make decisions on the type and quantity of shear reinforcement based on economics of the particular situation of this design problem.

REFERENCES

1. American Concrete Institute, "ACI 318-83, Building Code Requirements for Reinforced Concrete," Detroit, Michigan, 1983.

2. Department of the Army TM 5-1300, "Structures to Resist the Effects of Accidental Explosions," June 1969.

3. M. Dede and N. Dobbs, "Structures to Resist the Effects of Accidental Explosions, Volume IV, Reinforced Concrete Design," Special Publication ARLCD-SP-84001, U.S. Army Armament Research, Development, and Engineering Center, Picatinny Arsenal, New Jersey, April 1987.

4. Department of the Army TM 5-855-1, "Fundamentals of Protective Design for Conventional Weapons," November 1986.

5. HQ USAFE EUROPS/DEX, Design Criteria for Semihard & Protected Facilities with Nuclear, Biological, and Chemical (NBC) Protection, 15 June 1986.

6. S. C. Woodson, "Effects of Shear Stirrup Details on Ultimate Capacity and Tensile Membrane Behavior of Reinforced Concrete Slabs," Technical Report SL-85-4, U.S. Army Engineer Waterways Experiment Station, Vicksburg, Mississippi, August 1985.

7. L. K. Guice, "Effects of Edge Restraint on Slab Behavior," Technical Report SL-86-2, U.S. Army Engineer Waterways Experiment Station, Vicksburg, Mississippi, February 1986.

8. W. A. Keenan, "Strength and Behavior of Lace Reinforced Concrete Slabs Under Static and Dynamic Load," R620, U.S. Naval Civil Engineering Laboratory, Port Hueneme, California, April 1969.

9. W. A. Keenan, "Strength and Behavior of Restrained Reinforced Concrete Slabs Under Static and Dynamic Loads," R621, U.S. Naval Civil Engineering Laboratory, Port Hueneme, California, April 1969.

10. W. A. Keenan and others," NCEL Products Supporting DOD Revision of NAVFAC P-397," Technical Memorandum 2591, U.S. Naval Civil Engineering Laboratory, Port Hueneme, California, March 1983.

11. T. R. Slawson, "Dynamic Shear Failure of Shallow-Buried Flat-Roofed Reinforced Concrete Structures Subjected to Blast Loading," Technical Report SL-84-7, U.S. Army Engineer Waterways Experiment Station, Vicksburg, Mississippi, April 1984.

12. S. A. Kiger and G. E. Albritton, "Response of Buried Hardened Box Structures to the Effects of Localized Explosions," Technical Report SL-80-1 U.S. Army Engineer Waterways Experiment Station, Vicksburg, Mississippi, March 1980.

13. J. V. Getchell and S. A. Kiger, "Vulnerability of Shallow-Buried Flat-Roof Structures," Technical Report SL-80-7, Report 4, U.S. Army Engineer Waterways Experiment Station, Vicksburg, Mississippi, December 1981.

14. J. V. Getchell and S. A. Kiger, "Vulnerability of Shallow-Buried Flat-Roof Structures," Technical Report SL-80-7, Report 2, U.S. Army Engineer Waterways Experiment Station, Vicksburg, Mississippi, October 1980.

15. T. R. Slawson, "Vulnerability Evaluation of the Keyworker Blast Shelter," Technical Report SL-87-10, U.S. Army Engineer Waterways Experiment Station, Vicksburg, Mississippi, April 1987.

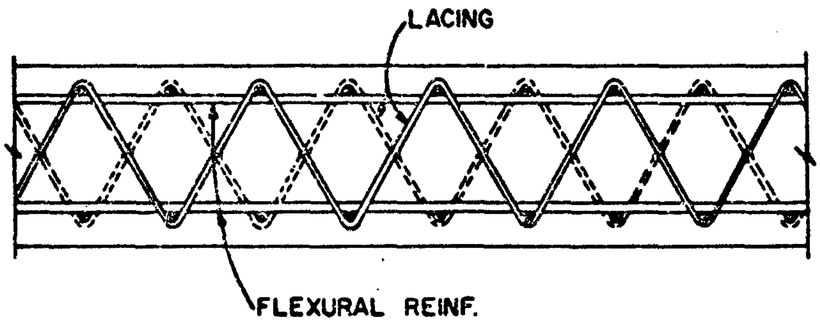

a. Lacing reinforcement

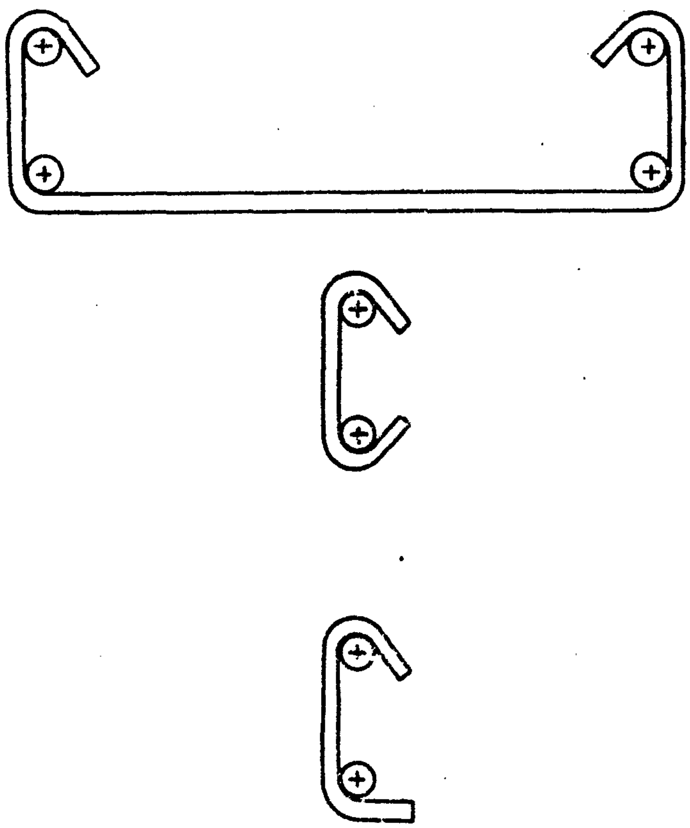

b. Stirrup configurations

Figure 1. Shear reinforcement

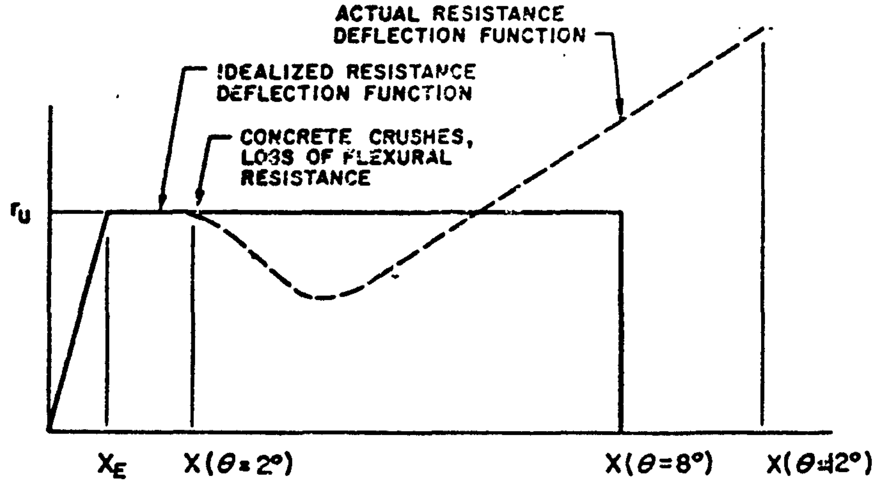

Figure 2. Idealized resistance deflection curve for large deflections

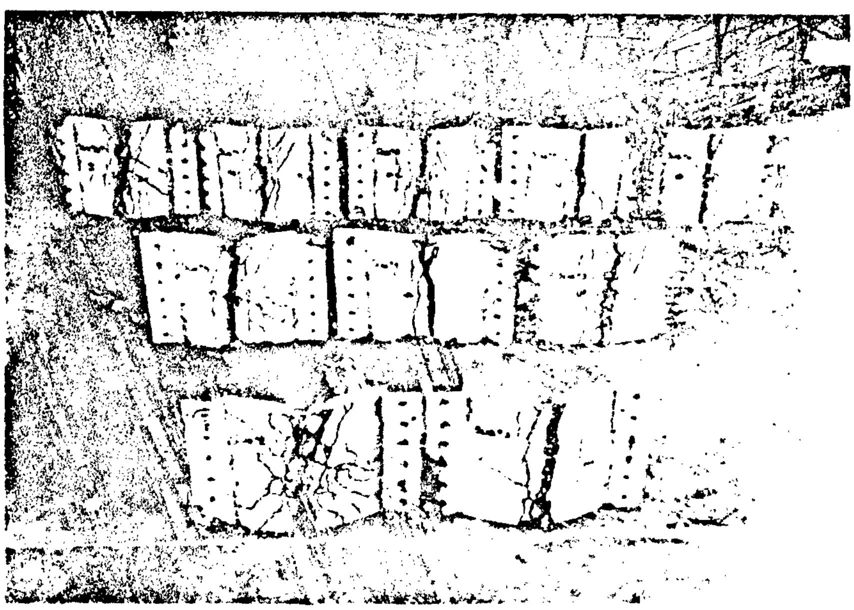

Figure 3. Posttest view of slabs with stirrups

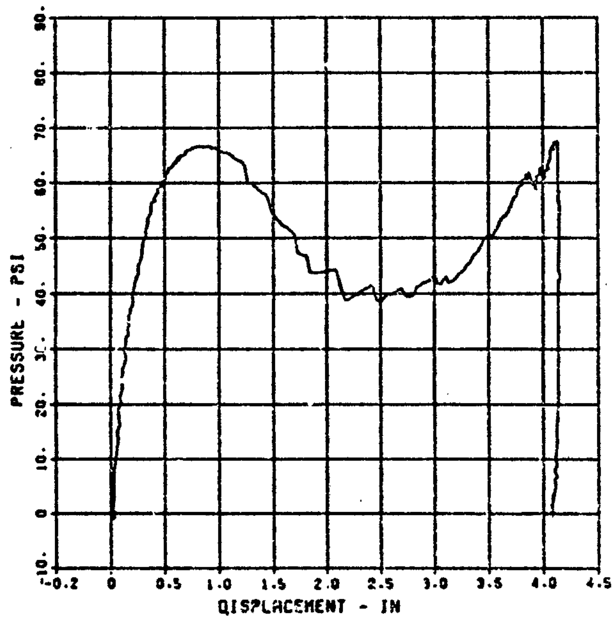

Figure 4. Load deflection curve for close stirrup spacing

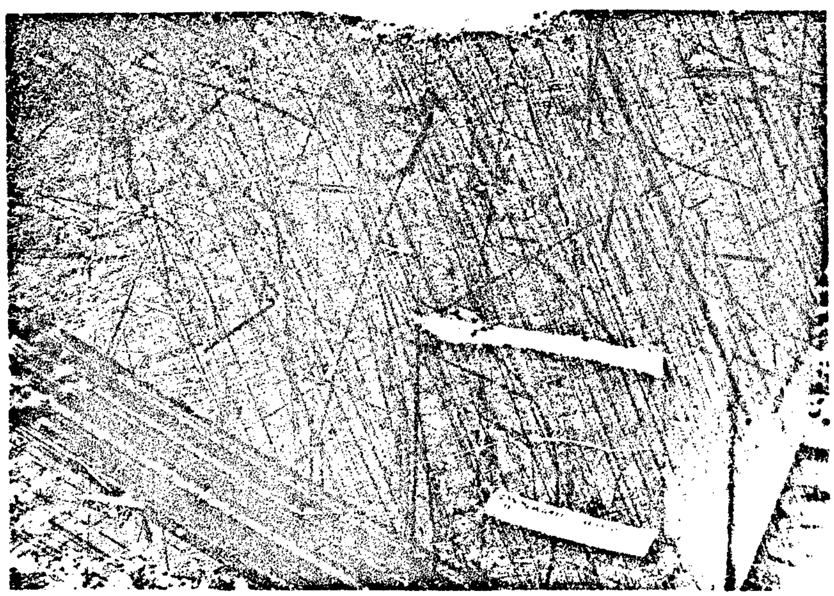

Figure 5. Shallow-buried box with 10-inch roof deflection

Figure 6. Shallow buried box with 12-inch roof deflection

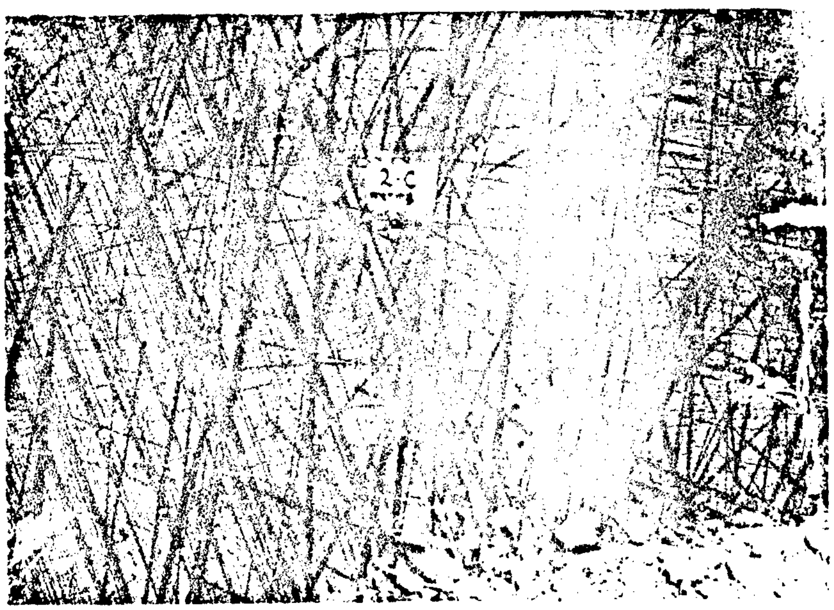

Figure 7. Posttest view of wall with stirrups

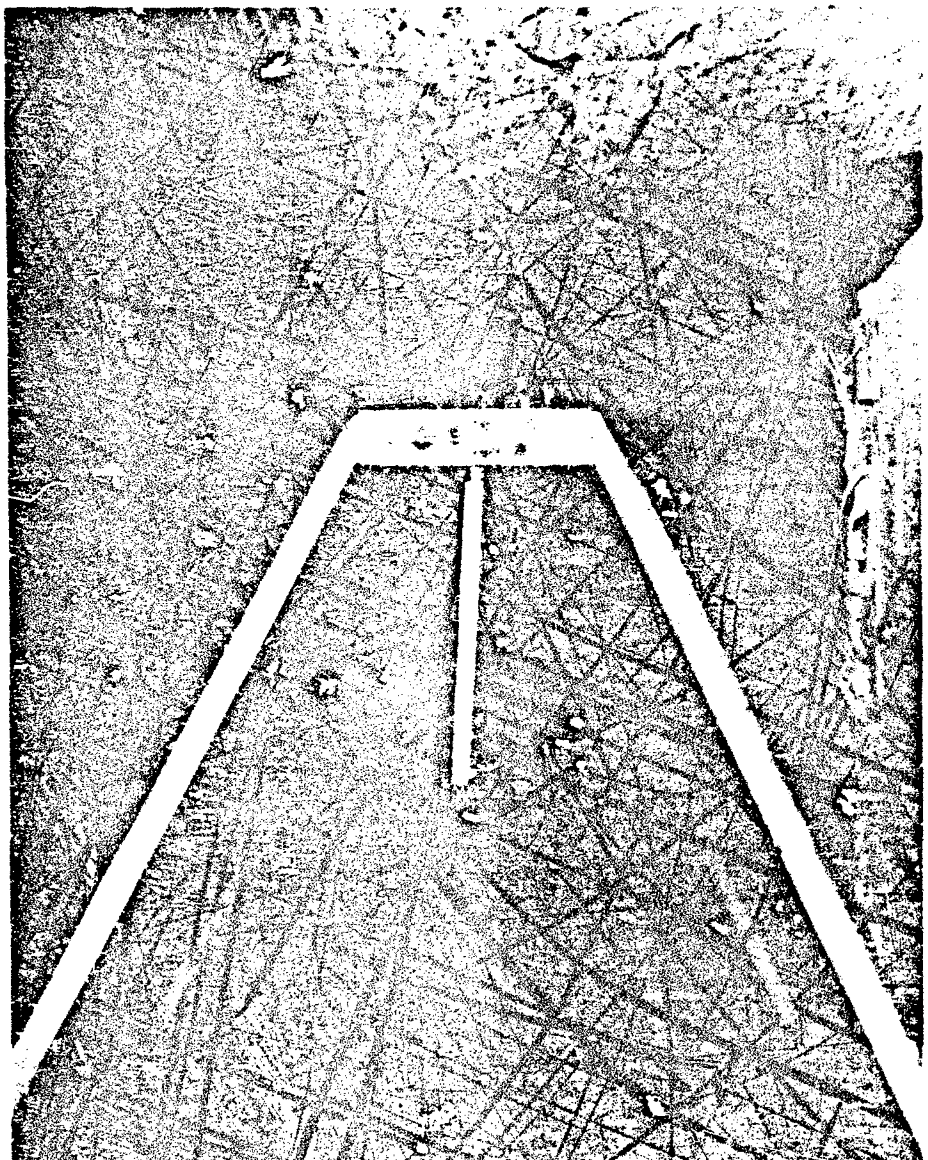

Figure 8. Damage to structure tested in clay backfill

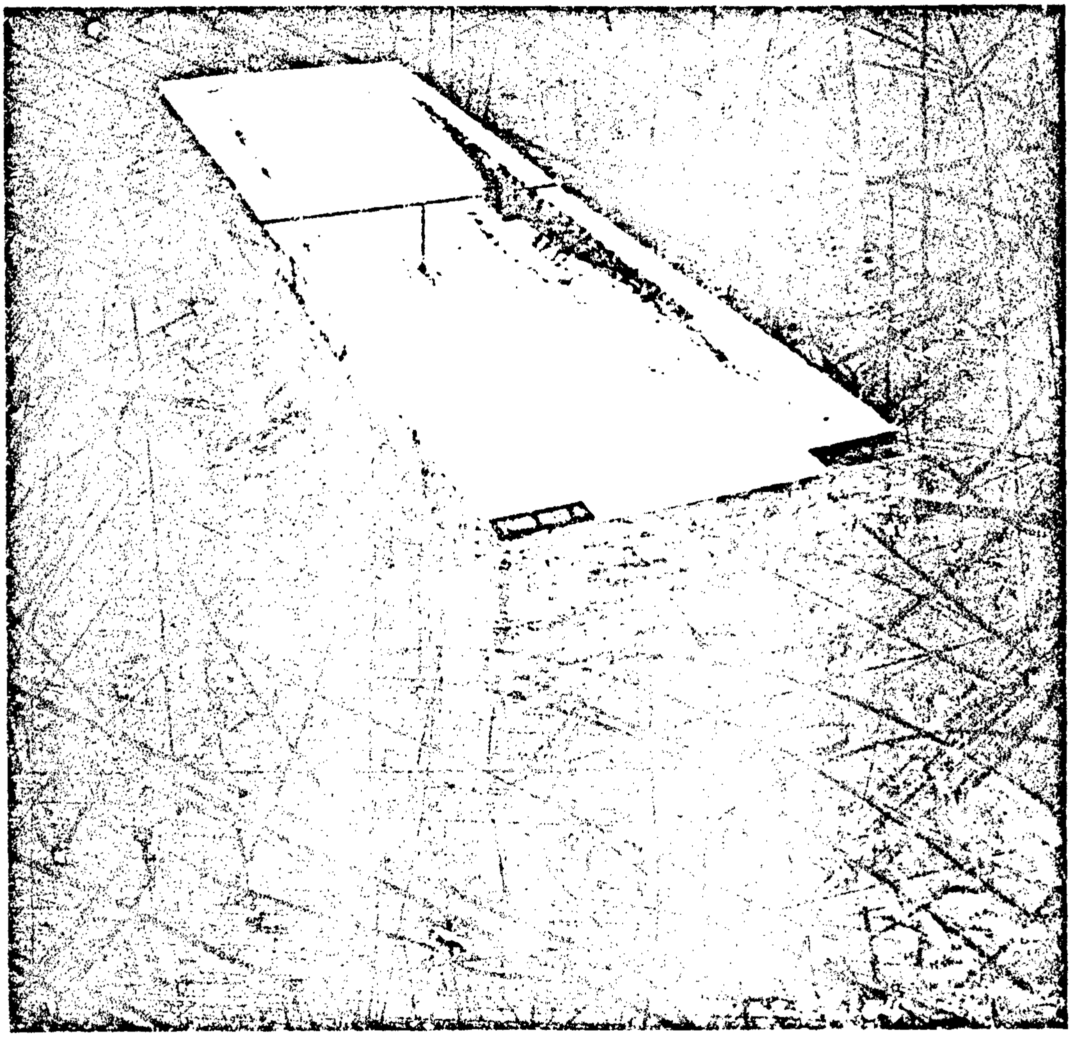

Figure 9. Damage to structure tested in sand backfill

Figure 10. Interior view of structure tested in sand

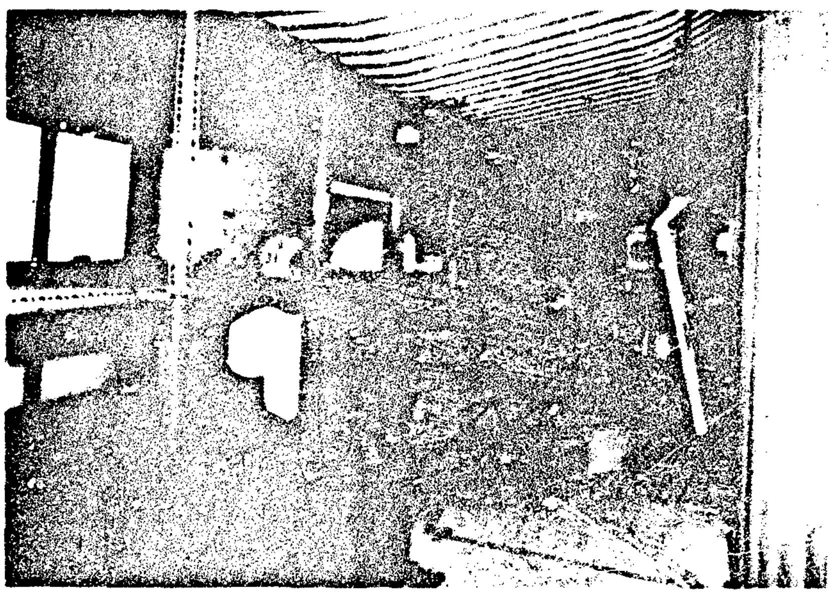

Figure 11. Interior view of 100-man blast shelter

THE APPLICABILITY OF THE FE-TECHNIQUE TO DYNAMIC FAILURE

ANALYSIS OF CONCRETE STRUCTURES.

by

J. WEERHEIJM, P.J.H. VAN ZANTVOORT and G. OPSCHOOR.

Prins Maurits Laboratory TNO

P.O. Box 45, 2280 AA Rijswijk

The Netherlands.

presented at the

23rd DoD Explosives Safety Seminar

Atlanta, Georgia, 9-11 August 1988

THE APPLICABILITY OF THE FE-TECHNIQUE TO DYNAMIC FAILURE ANALYSIS OF CONCRETE STRUCTURES.

by

J. WEERHEIJM, P.J.H. van ZANTVOORT (*) and G. OPSCHOOR

Prins Maurits Laboratory TNO
P.O. Box 45, 2280 AA Rijswijk
The Netherlands.

1. INTRODUCTION.

Concrete is commonly applied in protective structures in which the protection level is determined by the local or structural failure mode and the absorbed energy during the failure process. For this reason it is important to understand the failure mechanisms under transient loading and to have the opportunity to predict and calculate the response of a structure due to these loadings.
Studies at the Prins Maurits Laboratory, in which the normal mode technique was applied [1], have shown that differences exist between the internal force distribution due to transient loading and geometrically corresponding static loading. In the structure high peaks of shear forces and bending moments occur and the chance of a different failure mode, in respect of the static loading conditions, seems to be inevitable. On the other hand, however, the strength of concrete increases with increasing loading rate [2,3]. Due to these opposing effects more information is needed to predict the failure process and the ultimate dynamic load level.

* Graduate student of the Faculty of Civil Engineering of Delft University, Department of Structural Engineering, Section Applied Mechanics. Graduated in 1988.

For this reason at the PML a comparison has been made between the final failure mode of reinforced concrete slabs due to a uniformly distributed static load and an impulse load [4]. From the test results it emerged that, in spite of the initially completely different force distribution, in several cases the static failure mode of bending occurred. Apparently the material can withstand the high peaks of shear forces and bending moments that run through the structure immediately after loading. However the slabs with relatively rigid supports collapsed due to shear failure.

At this state of knowledge the question was raised whether the response and failure of reinforced concrete structures under transient loading could be calculated and predicted with an actual advanced finite element program. To investigate the applicability of the finite element technique for the situations described and to gain an impression of the difficulties and the unsolved problems, one category of the experiments mentioned has been simulated with the FE-code DIANA (IBBC-TNO).

The experiments, the simulation and the results are described and discussed in this paper.

2. THE EXPERIMENTS.

At the PML the failure mode due to impulsive loading of slabs which are simply supported at two or four edges has been investigated experimentally. The slabs were loaded by a shock wave of very short duration originating from an exploding charge at a short distance [4]. The results were compared with data from static tests.

For the sake of simplicity tests with slabs supported at two edges have been selected for numerical simulation and the slabs have been regarded as beams. These tests were performed with small slabs ($50x50x6\ cm^3$) in a cubical set-up. The sides were formed by the slabs to be tested, while the top was open and the bottom consisted of a steel plate [5]. The rigidness of the supports was varied by the application of thin wooden laths.

In the series of tests selected for simulation wooden laths were applied. The static failure mode of bending occurred by detonating 160

gram of TNT at a distance of 0.25 m. The slabs were made of high quality concrete and were reinforced in two directions on both sides of the slab. Pictures of the experimental set-up and a slab with the bending failure mode are given in Figures 1 and 2.

Figure 1. Experimental set-up.

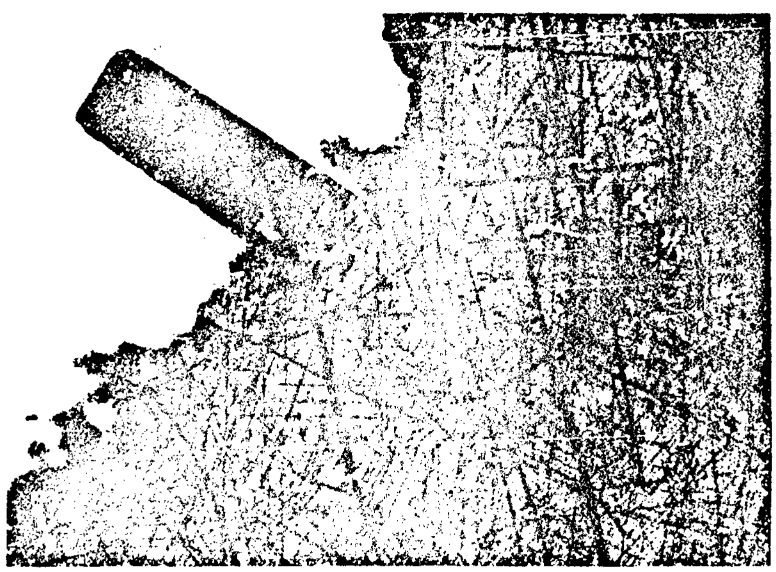

Figure 2. Slab showing bending failure.

In the experimental set-up the load configuration is very complex due to the reflections of the shock wave inside the cube. As the correct loading geometry is unknown and the objective of the numerical simulation was to investigate the applicability of the FE-technique to dynamic failure analysis, the loading condition had to be simplified for the calculation. It was assumed that the slabs were part of an infinite plane, so that no reflections and difractions at the edges had to be taken into account. The amplitude, distribution and duration of the loading were determined using graphs taken from literature.

3. FINITE ELEMENT MODELLING

When applying the FE-technique to linear and nonlinear dynamic response analysis the choices for a distinct discretization of the geometry into elements and the time into time steps and the choice for a specific type of material model are of major importance. These aspects and the way they have been assimilated into the computations are the subjects of the current chapter. For detailed information on the calculations see [6].

3.1 The discretizations

The choice for a distinct discretization is determined by the answers to several questions concerning the modelling of the problem. The first question that has to be answered is which type of elements will be appropriate. Since the aim of the study was among other things to predict the final failure modes with extensive bending and shear cracking the most suitable type of elements to describe these cracks are the plain stress or plain strain elements.

The next question that arises is which element mesh refinement in conjunction with which time step will yield representative results. From linear-elastic normal mode analysis it was concluded that the duration and the shape of the load influence the distribution of the normal mode contributions. For instance, when the duration of the load is shorter the number of normal modes that contribute in the response will be larger. Thus in dealing with blast loads the choice for the

discretizations is based on the wish to describe the response by means of the modelling of a sufficient number of these normal modes. In most cases this results in the application of a refined mesh and small time steps.

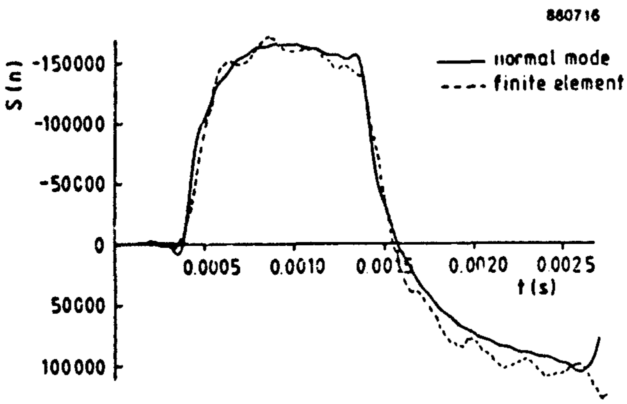

Figure 3. Comparison of the normal mode and the finite element technique for a linear-elastic shear force calculation.

Figure 3 represents an example of the comparison of the normal mode technique and the FE-technique for a linear-elastic high frequency response calculation. The shear force at one eighth of the length of a simply supported concrete beam has been calculated for a uniformly distributed impulse load with relative load duration $t_r = t_d/T_1$ of 0.0085 in which t_d is the duration of the load and T_1 the first natural period. The normal mode calculation has been performed with the lowest 64 normal modes. For this example a refined mesh was applied consisting of a division of the length into 32 quadratic isoparametric plain stress elements and a division of the height into 2 elements of the same type. This mesh should be capable of describing 64 transversal normal modes. In that case the time step should be estimated , at the most, at a fraction of the period of the 64^{th} normal mode. Previous normal mode analyses showed 15 normal modes to be sufficient so the capability of the mesh was limited to an accurate representation of only the first 15 normal modes by the choice of the

time step at 3.10^{-5} s. Still higher normal modes will be represented in the response but with decreasing accuracy. The differences between peak values predicted by normal mode and by FE calculations did not exceed the value of 4 percent. Hence these results show that accurate computations can be performed by using small enough elements and small time steps.

3.2 The material model

The non-linear dynamic FE analysis with a refined mesh and small time steps offers the possibility of representing a high frequency response but at the same time another problem arises. Due to the high frequency contributions the loading rate of the material will be correspondingly high and as a result the material strength f_{ct} will increase significantly. When the material model is not capable of modelling the increase in strength, the possibility exists that the numerical model predicts collapsing of the structure even before the maximum blast loading is attained. Right now it is possible to describe the relationship between the loading rate and the increase in strength for the uniaxial stress state [3]. Since this relationship is not a simple one, difficulties exist in implementing it in an FE-code. The relationship for the multiaxial stress state along with the energy absorbing and deformation capacity as a function of the loading rate are still subjects of intensive study.

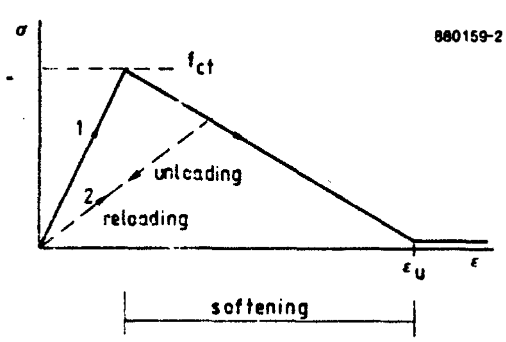

Figure 4. Static tension-softening representation of concrete.

To be able to perform non-linear dynamic FE analyses, for this type of problem anyway, a common approach is to apply a static material model in which the strength of the concrete is raised by some 10 to 20 percent. Therefore in the calculations a static material model has been used. The tension-softening behaviour of concrete under tension is represented in this model. In Figure 4 this model is depicted for the uniaxial stress state. The Figure also shows the possibility for the material to unload, which is indicated by path (2). In most cases subsequent reloading will go along this same path. Only when the direction of the principal stress deviates more than 60 degrees from the original principal stress direction, the reloading of the material will follow path (1) instead.

4. SIMULATION OF THE FAILURE OF THE REINFORCED CONCRETE SLABS

The presentation of the simulation will here be divided into two separate sections. Before performing the successful final run a specific difficulty which is illustrative for the FE applicability had to be overcome. The first section will deal with the first simulation attempt showing this difficulty, while the second section will present the final run.

4.1 The first simulation

To perform the first simulation the blast load was modelled for groups of elements by means of prescribing the maximum load that occurred during the experiment. For 7 distinct sections of the slab 4 different uniformly distributed loads were applied on the top surface of the slab. In this first estimate the blast load was taken to decrease linearly to the unloaded situation in 150.10^{-6} s. Because the relative load duration (0.063) for this case was larger than for the linear-elastic case fewer normal modes were expected to contribute in the response. As a result the mesh with a division of the length and the height into 12 and 3 elements respectively was less refined. For an accurate representation of the first 10 normal modes the time step was estimated at 5.10^{-6} s.

Between the 5^{th} and the 10^{th} time step the FE-model collapsed completely. Due to the reflection of the downwards propagating pressure wave against the lower surface of the slab, the resulting tension wave which propagated upwards caused the concrete to crack completely in the horizontal direction. This type of cracking, which

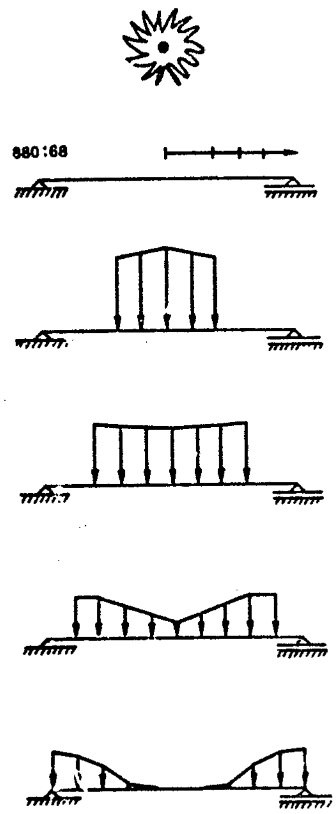

Figure 5. Blast load discretization for 4 subsequent points of time.

is related to spalling, did not occur in the test specimen. To perform a successful simulation with the static material model, a way to avoid these cracks is to raise the material strength by about 900 percent. In doing so all further cracking will be prevented since the increase in strength is raised with a constant and not expressed as a function

of the gradually decreasing loading rate. In the final run the difficulty of preliminary horizontal cracking was, if not elegantly, bypassed by means of distributing the blast load over the height of the slab with the result that the wave propagation in the vertical direction is neglected.

4.2 The final run

The final run was carried out using the complex loading condition presented in Figure 5. In this case the value of t_r equalled 0.0168. For this reason the mesh from the first simulation was changed to 20 and 3 elements. The calculation was performed with a time step of 2.10^{-6} s which garanteed the first 23 normal modes to be represented accurately. With respect to the final failure mode of bending that

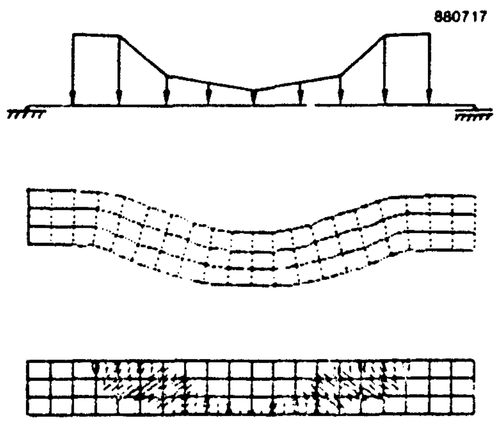

Figure 6. Load, deformation and initiatory dense crack pattern at time 36.10^{-6} s.

occurred at a late stage of time, the time step was probably too small. However, for the investigation of the period in which the loading and the deformation expand over the slab, the time step was appropriate. During the performance of 346 time steps three distinguishable crack patterns occurred in sequence of time:

1. A dense pattern of arising and arresting cracks due to the expanding of blast load and initiatory deformations (see Figure 6).
2. A pronounced pattern of concentrated shear cracks near the supports. The crack deformation exceeded the ultimate deformation e_u (see Figure 7).
3. A pronounced pattern of completely developed bending cracks near the mid-section of the slab. Again the ultimate deformation e_u was exceeded (see Figure 8).

Figure 7. Open shear cracks near the supports at time 240.10^{-6} s.

Figure 8. Open bending cracks near the mid-section at time 630.10 s.

Although the shear cracks exposed excessive crack deformation the final failure mode proved to be the bending mode. This is well illustrated by the fact that the shear cracks closed partially and by the fact that the largest amount of deformation took place around the mid-section. The resulting total deformation of the mid-section was close to the experimental data.

5. EVALUATION.

The numerical simulations have proven the applicability of the FE-technique to response calculations for structures under transient loading. The limitations of the FE-code arose in the non-linear, dynamic response calculations because a proper material model was not available. The final run shows that, even with the static material model, the same final failure mode is predicted as observed in the experiments. The question must be raised whether this has been a lucky coincidence or that the rate effects on the material properties are of minor importance for the structural response. This question is discussed in the current chapter on the basis of the crack patterns mentioned in section 4.2 and the shape of the stress-strain curve (Figure 4).

The first mentioned calculated crack pattern arises in the very first of the response directly after loading. The loading rates of the travelling stress waves are high and the strength increase should oppose or prevent this cracking like the horizontal cracking in the first simulation.
The second crack pattern is generated at the beginning of the structural response when the loading rates have decreased considerably. This pronounced pattern of macro cracks could have led to shear failure under slightly different loading conditions or material properties. This cracking illustrates the possibility of a change in failure mode due to dynamic loading. The macro shear cracks are closed in a later stage of the response and the completely developed bending cracks cause the final structural failure. At this stage of the study the influence of the static material model on the second crack pattern is not demonstrable and may be negligible. In any, case the applied deformation capacity, e_u, proves to be of great influence on the eventual appearance of the ultimate failure mode.

The influence of neglecting the rate dependency on the stress-strain relation, as given in effect on the strength is most evident and will be discussed first. Although the effect on the deformation capacity has hardly been investigated several comments can be made.

The horizontal cracking in the first simulation illustrates clearly the possible consequence of the underestimation of the dynamic strength. Although the stress rates are not calculated, it is obvious that also in the final run most of the early stage cracking is not realistic. This is shown by the rate of crack extension which was determined to be about 2500 m/s. This rate is unrealistic because it is limited by the velocity of the Rayleigh wave (approx. 2000 m/s). If the crack extension rate reaches this ultimate value the strength has already increased significantly and has become very rate sensitive, which makes the calculated cracks unrealistic. In spite of this early stage cracking, the final run led to the bending failure mode as has been observed in the experiments, and apparently the initial dense shear crack pattern near the mid-section did not influence the failure mode. This can be explained as follows. Figure 9 shows that most of the calculated cracks are closed afterwards. In contradiction to static conditions the direction of the principal stresses changes

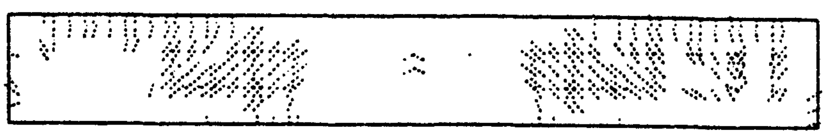

Figure 9. Closed initiatory cracks at time 90.10^{-6} s.

continuously, especially during the early stage response, due to the travelling stress waves. As illustrated in Figure 4, the applied material model has two opportunities of dealing with reloading (see section 3.2). If the direction of the subsequent principal stresses during reloading differs more than 60 degrees from the previous direction the earlier cracking is neglected. This condition probably appeared during the final run with the consequence that the calculated initial cracking, which ought to be prevented by the increased

strength, has been ignored afterwards, and the bending failure mode developed. This thesis still has to be checked by changing the 60 degree threshold up to 90 degrees.

Finally some comments are given on the rate dependency of the energy dissipation during the fracture process which is reflected in the stress-crack width relation or less directly in the stress-strain curve of a chosen volume (Figure 4). The first comment concerns the determination of the stress-crack width relation.
The relation can be determined statically in so-called "deformation-controlled" tests. Up to now the tests with high loading rates are "load-controlled" in which especially the descending branch cannot be compared with the branch under "deformation-controlled" conditions. So the question how the shape of the stress-strain curve is influenced by the loading rate cannot be answered. Possibly this question is not even relevant because in real structures the redistribution of stresses is limited under transient loading and the created loading conditions of the material are rather "load-controlled" than "deformation-controlled". Whether it is justifiable to apply the shape of the static curve in (FE-)response calculations to transient loading conditions has to be examined by comparing the static and impact relations observed.
In the comparison attention must be paid to the conversion of crack width into strain. This necessity arises most clearly from impact tests where multiple cracking occurs at high loading rates. The multiple cracking leads to an apparently increased deformation capacity [2,7,8] but the amount of cracking depends also on the size of the specimen. Consequently the value of e_u in Figure 4 will increase with increasing loading rate but only for sufficiently large specimen and large elements in which multiple cracking can occur.
Test results at high loading rates can be gathered for instance from the extensive impact tests at the Delft University of Technology (DUT) and the current PML/DUT program.

In this chapter questions and problems are summarized which were encountered during interpretation of the FE results and the PML research program on the material response of concrete under

(multiaxial) transient loading. From these studies it emerges that still much attention has to be paid to the material itself and to the model before the FE-codes can be applied for response predictions of concrete structures under arbitrary transient loading.

6. CONCLUSIONS.

1. Linear-elastic FE-analysis of structures under transient loading can be performed successfully without the need for excessively refined meshes and time steps.
2. Non-linear dynamic FE-analysis will in most cases give rise to problems because a proper loading rate dependent material model is still not available. Representative results may be obtained by means of the use of a static model in which preliminary cracking can be avoided or ignored.
3. Further extensive study of the dynamic material model and the implementation in FE-codes has to be performed. Special attention must be paid to the rate dependency on the:
   - Material properties (strength, Young's modulus, bond, etc.).
   - Deformation capacity.
   - Energy dissipation in the fracture process.

REFERENCES

[1] Mercx, W.P.M. and Harmanny, A.
The Normal Mode Technique: A useful tool to investigate the behaviour of structures subjected to local impulsive loading.
Symposium: Interaction of Conventional Munition with protective structures.
Mannheim, March 9-13, 1987.

[2] Kormeling, H.A., Zielinski, A.J. and Reinhardt, H.W.
Experiments on concrete under single and repeated uniaxial impact loading.
Stevin report 5-80-3, Delft University of Technology 1980.

[3] Weerheijm, J.
The strength of concrete under dynamic loading.

Journal de Physique, Colloque C5, supplement au no. 8, Tome 46, aout 1985.

[4] Harmanny, A.
Reinforced concrete plates under static and dynamic loading.
Symposium: Military Applications of Blast Simulation.
Oxford, England, September 23-27, 1985.

[5] Harmsma, R.E. and Nijhout, J.M.
The response of concrete slabs under explosive loading (Dutch).
Royal Military Academy, April 1982.

[6] Zantvoort, Van, P.J.H.
The failure process of reinforced concrete slabs under blast loading (Dutch).
PML-TNO, Rijswijk, 1988.

[7] Zielinski, A.J.
Fracture of concrete and mortar under uniaxial impact loading.
Delft University Press, Delft, 1982.

[8] Kormeling, H.A.
Strain rate and temperature behaviour of steel fibre concrete in tension.
Delft University Press, 1986.

BLAST RESISTANT POLYCARBONATE WINDOWS

by

Gerald E. Meyers, P.E.

United States Department
of
State

This paper presents background, theory, design curves and design procedures for blast resistant polycarbonate glazing. Use of these design curves will peermit the employment of polycarbonate in for many safety threats affecting DOD munition storage and industry. They are general enought to be used to enhance the combat survirability or physical security of a strucuture. Mandatory frame design and frame bite criteria and data are also included. Finally, equations to ascertain the fragment resistance of common glazing materials are reported.

POLYCARBONATE GLAZING

Glazing is often the weakest element in the protective capability of a structure against blast or fragments. Over the last few years, the U.S. Navy has developed and validated design charts and tables for thermally tempered glass (Ref 1 and 2) for use where blast overpressure is the predominate threat. However, glass does not provide a comparable level of protection against fragments, ballistics, or forced entry. Also, even if a laminated thermally tempered glass remains intact after fragment or ballistic impact, it will lose both its transparency and operational effectiveness.

Polycarbonate and glass-clad polycarbonate can overcome these deficiencies. As a glazing material, it has established a long track record against fragments, ballistics, forced entry and assault. This paper, in an attempt to fill this immediate and pressing need, presents design charts and procedures to guide the reliable design of blast resistant glazing containing one or more polycarbonate layers against blast. The U.S. Department of State has successfully conducted nine blast tests and six static load tests to validate the design curves. Required design of the frame and edge engagement or bite of the glazing are also included as they are requisite for a successful blast-resistant design.

Polycarbonate is available monolithically in thicknesses up to 1/2 inch. Greater required thickness must be obtained by lamination or fusion. As both aircraft and architectural grade PVB will chemically attack polycarbonate, they are precluded as interlaminar materials. At present, most glass-clad polycarbonate fabricators manufacture proprietary polycarbonate-compatible interlaminar materials. Research is now underway at the U.S. Department of State to determine what percentage of the monolithic strength can be developed with these materials

Polycarbonate is thermoplastic and is often marketed under trade names such as Lexan or Tuffak. It should not be confused with acrylic which is flammable and can exhibit a brittle failure mode.

Polycarbonate will burn when a flame is held to it. However, it will tend to extinguish itself when the flame is removed. Rated as a class CC-1 material, it is much less combustible than acrylic plastic (Plexiglas or Lucite). It is often used in visors of firefighting helmets. Preliminary investigation indicates that while polycarbonate will not generate the cyanide or chloride gases often associated with burning plastics, some carbon monoxide and carbon dioxide will be generated. Polycarbonate will often test with a smoke density rating over 500 according to the ASTM E84 Smoke Density Rating. However, many experts question whether the horizontal method of mounting the test specimen should be applied to a thermoplastic material.

Polycarbonate is resistant to most chemicals. However, it is particularly susceptible to contact with aromatic hydrocarbons, gasoline, kerosene, carbon tetrachloride, esters, ketones, and acetone phenols, which cause embrittlement and hazing. Most, if not all, commercial window cleaning preparations are compatible with polycarbonate. Glass cladding of polycarbonate will provide a barrier against chemical degradation.

Polycarbonate's main disadvantage is that it experiences greater environmental degradation than glass, especially due to the effects of ultraviolet radiation, abrasion, and aging. However, chemical coatings, such as Lexan's MARGARD or Tuffak's CM3, are available to provide some protection from abrasion. Ultraviolet inhibitors are also available for most commercial polycarbonate. Greater protection against both abrasion and ultraviolet attack is afforded by encapsulating the polycarbonate in glass. Incidentally, this will enhance both the ballistic and chemical resistance of the glass. Unfortunately, testing of older glass-clad polycarbonate indicates that even glass-encapsulated polycarbonate with ultraviolet inhibitors will suffer degradation of load carrying and penetration resistance over time. Research on the effects of aging is currently being conducted. In recognition of this fact, and to be conservative, a reduced maximum stress for polycarbonate that does not employ the potential benefits of ductile or post-elastic yield is assumed.

Pane Design Theory

A maximum design flexural stress of 9,500 psi is assumed for polycarbonate. This conservative stress value should account for degradation in ultraviolet stabilized polycarbonate exposed to long term solar exposure. While more research is required in this area, it is reasonable to expect at least a 10-year useful life for ultraviolet stabilized polycarbonate. A Young's modulus of 345,000 psi and a Poisson's ratio of 0.38, as reported by industry, are also assumed for polycarbonate. The potential of significant increases in blast capacity through the development of post ductile response is presently ignored. This is because long term environmental degradation may erode this potential. Research is underway to develop reliable ways to mobilize this response mode.

The polycarbonate glazing is modeled as a simply supported plate subjected to nonlinear center deflections up to 15 times the pane thickness. Using the finite element solution of Moore (Ref 3), the resistance function is generated for each pane under consideration. Typically, the resistance function is shaped concave up. This occurs because membrane stresses induced by the stretching of the neutral axis of the pane become more pronounced as the ratio of the center pane deflection to the pane thickness increases. In a few cases (usually with 1/4-inch-thick polycarbonate), where the center deflection associated with a maximum stress of 9,500 psi exceeds 15 pane thickness, a lower design stress associated with a center deflection of 15 times pane thickness is chosen to govern design. This limitation both restricts the solution to the valid range of the Von Karman equations used by the finite element program to develop the resistance function and the practical edge engagement available in commercially available frames.

The blast load is modeled as a triangular-shaped overpressure time curve. The blast overpressure rises instantaneously to peak overpressure, B, then decays linearly with a blast pressure duration, T. The pressure is uniformly distributed over the surface of the pane.

Monolithic action is assumed between adjoining polycarbonate layers for the following reasons. First, recent static load testing sponsored by the State Department indicated this to be a good assumption. Second, the large deflections experienced by the relatively flexible polycarbonate means that a relatively high proportion of the load is being carried in membrane action rather than bending. Interlaminar shear capacity between plates does not affect this very efficient mode of structural capacity. It is also anticipated that the high strain rates associated with blast loading will further increase the shear capacity of most, if not all, interlaminar plastics in current commercial use. Finally, blast testing of nine test samples indicates that our design methodology is conservative in predicting center deflections and maximum stress levels.

To prevent failure due to disengagement of the pane out of the frame or edge, engagement depths are required. They are based upon the conservative assumption that the plate will distort as a spheroid surface. To be conservative, a 1/2-inch safety margin is added to all calculations and all bites are required to be at least 1 inch.

It is worth noting the blast capacity of a polycarbonate pane is sensitive to the duration of the blast load. Because polycarbonate is extremely flexible and responds with a relatively long natural period of vibration compared to glass, polycarbonate will perceive blast loads as more impulsive. This effect can significantly increase the blast protection capability of polycarbonate when blast overpressure durations are relatively short.

Blast Pressure Design Charts

Figures 2 through 21 are design charts for ultraviolet protected and stabilized polycarbonate under blast load. Charts are provided for pane thickness of 1/4, 3/8, 1/2, 3/4, 1, 1-1/4, 1-3/4 and 2 inches for pane areas up to 25 square feet at pane aspect ratios (pane length to width ratios) of 1.00, 1.50, 2.00 and 4.00. The charts relate the peak experienced blast overpressure capacity, B, for convenient pane dimensions across the spectrum of encountered blast durations. Depending on the orientation of the window to the charge, the blast overpressure experienced may either be incident or reflected. The pane dimensions (measured across the span from the gasket centerline.); peak blast capacity at 1,000 msec, B; static frame design pressure, r_u; and the minimum required bite are printed to the right of each design curve. Whenever possible, a minimum bite of 1 inch is recommended, even if the posted value is less. To reflect manufacturing tolerances and to be conservative, design thicknesses used to calculate blast capacities were limited to 95% of the nominal thickness. Figure 1 presents an example of how the charts are used.

Engineering judgment is also required in assessing the blast capacity of glass-clad polycarbonate. Because in some cases the annealed, semi-tempered, or sodium-based chemically tempered glass does not contribute substantially to the blast load capacity of the cross section, it is conservative to base blast upon the polycarbonate layers alone. Research and development is now underway at the U.S. Department of State to develop design procedures and user friendly computer programs to analyze and design composite glass-polycarbonate blast resistant glazing.

In many cases, the dynamic amplification factor or the ratio of static load to dynamic load capacity will exceed two. This is because of the concave up shape of the load-resistance function and the mobilization of membrane resistance at large deflection to thickness ratios. Because of this phenomenon, it is unconservative to assume the peak blast capacity of polycarbonate glazing to be no less than one half of its static pressure load capacity.

At very short blast durations, some small area panes exhibit slightly less blast capacity than panes with larger areas. This occurs because the small panes are acting as linear plates with small deflections under blast loads while the larger panes can mobilize membrane resistance without exceeding the maximum design stress of 9,500 psi.

Because these design charts cover a wide spectrum of loading parameters, they can also be used for protection from many high-explosive industrial, fuel-air, or nuclear threats.

Hand Calculation Method

General Design Theory. Polycarbonate and glass-clad polycarbonate can be designed to resist as a simply supported plate according to large deflection and nonlinear elastic plate theory. Although new polycarbonate exhibits considerable ductility and a flexural modulus (yield stress in flexure) of 13,000 psi, design should be based upon no ductility and a flexural modulus of 9,500 psi. These design values are consistent with values obtained from testing of used and environmentally degraded polycarbonate with a history of long solar exposure. Currently, neither glass cladding nor ultraviolet (UV) stabilizers will completely prevent UV attack on the polycarbonate.

When analyzing a glass-clad polycarbonate, the structural contribution of the glass is presently ignored. However, the inertial effects of the mass of the glass can be included.

Detailed Design. The following theory can be used to calculate the blast resistance of a polycarbonate plate to blast loading. First, calculate the static design resistance, r_u, of the pane. Then calculate an equivalent linear resistance, r_e, based upon absorbable strain energy. For this equivalent linear system, calculate the dynamic amplification factor, D_{LF}, induced by the blast. The static design resistance, r_u, is then divided by the dynamic amplification factor to determine the blast capacity.

Use the following procedure to calculate the design peak blast pressure capacity, B, of the pane:

Step 1. Calculate the nondimensional stress, S_{ND}, as:

$$S_{ND} = \frac{sb^2T}{D} \qquad (1)$$

where:

s = Design stress for polycarbonate (9,500 psi)

b = Short span of polycarbonate pane measured between center lines of gaskets, in

t = Actual thickness of polycarbonate

$D = Et^3/12\ (1-u^2)$ = Modulus of rigidity, lb-in

E = Modulus of elasticity (345,000 psi)

u = Possion's ratio (0.38)

Step 2. Enter Figure 22 with S_{ND} and the aspect ratio, a/b and read the nondimensional load, L_{ND}.

Step 3. Calculate the ultimate resistance, r_u, of the lite as follows:

$$r_u = \frac{L_{ND}\ D\ t}{b^4}, \text{ psi} \quad (2)$$

Step 4. Read the nondimensional center deflection, X/t by entering Figure 23 with the value of L_{ND} and a/b. Calculate the design center deflection, X_u, as:

$$X_u = (X/t)t, \text{ in.}$$

Step 5. Calculate the design resistance of a linear elastic structural system. The highly nonlinear resistance function is converted to a linear resistance that contains the equivalent amount of absorbable strain energy in the pane. The equivalent linear resistance, r_e, is calculated as:

$$r_e = 0.4(r_1 + r_2 + r_3 + r_4 + 0.5\ r_u), \text{ psi} \quad (4)$$

where: r_1 = Resistance at 0.2 X_u

r_2 = Resistance at 0.4 X_u

r_3 = Resistance at 0.6 X_u

r_4 = Resistance at 0.8 X_u

r_u = Resistance at X_u (calculated by Equation 2)

Step 6. Calculate the equivalent linear stiffness, K_e, as:

$$K_e = r_e/X_u, \text{ psi/in.} \quad (5)$$

Step 7. Calculate the natural period of vibration, T_N, as:

$$T_N = 2\ (3.14)\ (K_{LM}.m/K_E)^{1/2} \quad (6)$$

where: $K_{LM} = 0.63 + 0.16\ (a/b - 1),\ 1 \leq a/b \leq 2$

$K_{LM} = 0.79, \qquad a/b \geq 2$

$m = 104t + 243t_g$ (lb-msec^2/in^3)

t = Actual thickness of the polycarbonate, in.

t_g = Actual thickness of the glass in a glass-clad polycarbonate pane, in.

Step 8. Calculate the blast capacity of the polycarbonate. Enter Figure 24 with the ratio of the effective positive pressure blast duration. T (msec) to the fundamental period of vibration of the polycarbonate, T_N. Read the dynamic amplification factor, D_{LF}, which is the ratio of the center deflection caused by the peak blast over pressure to the same pressure applied statically. The peak blast overpressure, B of the glazing can be defined as:

$$B = r_e/D_{LF}, \text{ psi} \tag{7}$$

For T/T_N ratios greater than 10, set D_{LF} to 2. For ratios less than 0.05, set D_{LF} to 0.03. If effective blast duration is unknown, it is conservative to set D_{LF} to 2.

If the blast overpressure capacity of the polycarbonate, B is equal to or greater than the design blast overpressure, P, the design is acceptable.

Step 9. Design adequate bite into the polycarbonate. If a spherical deflection shape of the polycarbonate is conservatively assumed, the required bite, b_{req}, can be calculated as:

$$b_{req} = (S_{arc} - b)/2 + 1/2, \text{ in.} \tag{8}$$

where S_{arc} is the deformed arc length of the polycarbonate. S_{arc} is calculated as:

$$S_{arc} = R_{cur} \cdot O_r \tag{9}$$

Where R_{cur}, the radius of curvature, is calculated as:

$$R_{cur} = (X_u{}^2 + b^2/4)/2X_u \tag{10}$$

The radian angle of curvature, O_r, is calculated as:

$$O_r = 2 \text{ arcsine } (h/2R_{cur}) \tag{11}$$

It is recommended that the minimum bite of 1 inch be used even if the calculated value is less. The frame should be designed in accordance with the following section.

Frame Requirements

To be effective, the blast load carried by the polycarbonate glazings must be transferred to the frame and ultimately through the structure. If not properly designed, the pane or pane and frame will disengage and become a large and dangerous fragment. Also, care must be taken to properly design the supporting structure for the frame loads. Failure to do this can increase the probability of structural collapse. This is especially true in retrofit construction.

While the design loads for the frame are based upon large deflection plate theory, the design loads for the frame are based on an approximate solution of small deflection theory for normally loaded plates. Analysis indicates this approach to be considerably simpler and more conservative than that of large deflection plate behavior. The effect of the static design load, r_u, applied directly to the exposed frame members of width, w, is also considered by superposition. The design load, r_u, produces a line shear, V_x, applied by the long side, a, of the pane equal to:

$$V_x = C_x r_u b \sin(3.14x/a) + r_u w, \text{ lb/in.} \tag{12}$$

The design load, r_u, produces a line shear, V_y, applied by the short side, b, of the pane equal to:

$$V_y = C_y r_u b \sin(3.14y/b) + r_u w, \text{ lb/in.} \tag{13}$$

The design load, r_u, also produces a corner concentrated load, R, tending to uplift the corners of the window pane equal to:

$$R = C_R r_u b^2, \text{ lb} \tag{14}$$

Distribution of these forces as loads acting on the window frame and symbol identification are shown in Figure 25. Static frame design loads, r_u, are provided for each pane in the third column of the design data to the right of each design chart or in the middle of the design threat tables. Table 1 presents the design coefficients, C_x, C_y, and C_R for practical aspect ratios of the pane. Linear interpolation can be used for aspect ratios not presented. Frame deflections should be limited to no more than 1/100 the length of the supporting span. This is a significant benefit compared to the more rigid restrictions associated with tempered glass. The allowable design stresses for the frame and connections are as follows:

- Design stress of any frame member is $f_y/1.65$, where f_y is the static yield stress of the frame material obtained from its catalogued specification.
- Design stress of any fastener is $f_y/2.00$, where f_y is the static yield stress of the fastener material obtained from its catalogued specification.

Although frames with mullions are covered in the design criteria, it is recommended that single pane frames be used. Experience indicates that mullions complicate the design and reduce reliable fabrication of blast-resistant frames.

Frame Bite, Edge Clearance. Minimum frame bites or frame edge engagements are required for polycarbonate to provide enough support to carry the blast load and prevent pane disengagement. The fourth column to the right of each design chart, the bottom threat design table or Equation (8), presents the required bite for each pane. At least 1/4 inch should be allowed for edge clearance to account for pane expansion during hot weather.

Rebound

Response to the dynamic blast load will cause the window to rebound with a negative (outward) deflection. The outward pane displacement and the stress produced by the negative deflection must be safely resisted by both the pane and frame. If operational requirements dictate an operational window after the blast, the frame connections, and wall should be designed to also resist the static frame design load, r_u, in the outward direction. If the window can be permitted to fail after the positive blast pressure has decayed, more economical frames can be used, as the negative static design load can be reduced to 0.67 % of r_u. For blast durations greater than 250 msec, significant rebound does not occur during the positive pressure phase.

GLAZING DURABILITY

All glazings fabricated from polycarbonate will degrade over time from the ultraviolet (UV) radiation contained in sunlight. Indoor glazing can also suffer this degradation due to fluorescent light exposure.

Degradation has been demonstrated to result in loss of ductility and the reduction of yield strength in even ultraviolet stabilized polycarbonate sheet. The blast design values in the design tables and design charts take this loss of strength into account. When blast resistance governs design, a 10-year useful life can be expected.

Some practical steps are currently available to mitigate and limit the rate of this phenomenon.

- All polycarbonate should be ultraviolet (UV) stabilized. Adherence with Military Specification MIL-P-46144C Type II, Class II or Type III, Class 1A will assure UV stabilization.
- Polycarbonate, that is not glass cladded, should be treated with a UV resistant coating such as Margard.

- Polycarbonate with an external exposure should be glass cladded. This will reduce UV exposure by over 50% as well as providing greater abrasion and chemical attack resistance. If spalling is deemed to be a hazard on an exposed surface, apply a 4-mil (0.004-inch) thick polyester plastic security film to the inhabited face of the glazing. Tests have proven this to be an effective countermeasure to spall.

Some sealants and gaskets can poison polycarbonate. The polycarbonate manufacturer should be consulted for the latest list of compatible products. Currently, EPDM rubber gaskets and SEALPRUF are known to be compatible with polycarbonate.

Preliminary research indicated that the following modification of polycarbonate and glass-clad polycarbonate cross sections may dramatically extend useful glazing service life:

- Use laminated safety glass (semi-tempered) with polyvinyl butyral (PVB) between the glass layers on all UV exposed surfaces. The laminated glass will be bonded to the polycarbonate with urethane to account for differences in the temperature expansion rate of polycarbonate as it can chemically poison the polycarbonate. Product literature indicates that both architectural (S.R.) and aircraft grade (A.G.) PVB will block 99% of the intensity of the ultraviolet spectrum.

- Use a sacrificial layer of 1/4-inch UV stabilized polycarbonate on all UV exposed surfaces. The engineering literature indicates that polycarbonate is opaque to UV radiation and may protect the inner layers of polycarbonate from degradation.

FRAGMENT-RESISTANT GLAZING

The Thor equation (Ref 4) is convenient to predict the fragment resistance of glass, polycarbonate, and glass-clad polycarbonate. The equations are empirically developed from statistically significant testing by the Ballistic Research Laboratories and have been used extensively in aircraft survivability design. The equations can be used for compact fragments (a convex polyhedron) or adjust for fragments that present a large impact area. Ballistic threats can be conservatively approximated by a compact fragment.

To use the equations, calculate the exit or residual velocity, V_r, of the fragment through successive layers of glass or polycarbonate until it is less than zero. An extra inboard layer of polycarbonate or plastic security film should be considered to contain spalling. Since acrylics (Lucite or Plexiglas) are also included in security glazing and they have exhibited resistance against fragments, they are included in this chapter. These equations have been computerized and are available in Diplomatic Security.

Compact Fragments

The exit or residual velocity of a compact fragment, V_r, exiting a thickness of glass or polycarbonate can be calculated as:

$$V_r = V_s - 10^{c}\, t^{f}\, m_s^{g}\, (\sec \theta)^{h}\, V_s^{q}, \text{ ft/sec} \qquad (15)$$

where: V_s = Fragment striking velocity in fps

V_r = Fragment residual velocity in fps

t = Glazing thickness in inches

m_s = Weight of the original fragment in grains (437.5 grains = 1 oz)

θ = Angle between the striking trajectory of the fragment and the normal to the glazing surface and c, f, g, h, q are constants determined separately for each material (listed in table below).

The observed values of the constants for resistance against compact fragments are:

Material	c	f	g	h	q
Polycarbonate	1.387	0.720	-0.177	0.773	0.603
Glass	2.254	0.705	-0.253	0.690	0.465
Stretch acrylic	1.255	1.112	-0.161	0.715	0.686
Cast acrylic	3.035	1.044	-0.338	1.073	0.242

The remaining weight, m_r, of each fragment as its mass is degraded through each layer can be computed as:

$$m_r = m_s - 10^{c}(t\theta)^{f}\, m_s^{g}\, (\sec \theta)^{h}\, V_s^{q}, \text{ grains} \qquad (16)$$

The exponent constants are defined as:

Material	c	f	g	h	q
Polycarbonate	-7.288	0.480	0.785	1.171	1.765
Glass	-6.571	0.305	0.632	0.747	1.819
Stretch acrylic	-6.267	0.437	0.460	0.620	1.583
Cast acrylic	-5.305	1.402	0.797	0.674	1.324

In many calculations, this adjustment to weight is not significant. It is also conservative to ignore.

Non-Compact Fragment

This exit or residual velocity, V_r, of a fragment with a large striking area (greater than 2 square inches) can be calculated as:

$$V_r = V_s - 10^{c}(eA)^{f}\, m_s^{\,g}\, (\sec O)^{h}\, V_s^{\,q}, \text{ fps} \qquad (17)$$

where: V_s = Fragment striking velocity in fps

V_r = Fragment striking velocity in fps

t = Glazing thickness in inches

A = Average impact area of the fragment in square inches

m_s = Weight of the original fragment in grains (437.5 grains = 1 oz)

O = Angle between the striking trajectory of the fragment and the normal to the glazing surface

The exponential constants are defined as:

Material	c	f	g	h	q
Polycarbonate	2.908	0.720	-0.567	0.773	0.603
Glass	3.743	0.705	-0.723	0.690	0.465
Stretch acrylic	3.605	1.112	-0.903	0.715	0.686
Cast acrylic	5.243	1.044	-1.035	1.073	0.242

The residual weight, m_r, exiting from each glazing layer is defined as:

$$m_r = m_s - 10^{c}(tA)^{f}\, m_s^{\,g}\, (\sec O)^{h}\, V_s^{\,q}, \text{ grains} \qquad (18)$$

Material	c	f	g	h	q
Polycarbonate	-6.275	0.480	0.465	1.171	1.765
Glass	-5.926	0.305	0.429	0.747	1.819
Stretch acrylic	-5.344	0.437	0.169	0.620	1.683
Cast acrylic	-2.342	1.402	0.137	0.674	1.324

REFERENCES

1. G.E. Meyers. "Design Criteria and Acceptance Test Specification for Blast Resistant Thermally Tempered Glass Glazing," Department of Defense Explosive Safety Seminar, Anaheim, CA, Aug 1987.

The exponential constants are defined as:

2. Naval Facilities Engineering Command. MIL-HDBK-1013/1: Design guidelines for physical security of fixed land-based facilities. Alexandria, VA Jun 1987.

3. Jet Propulsion Laboratory. FSA Task Report No. 5101-291: Thickness sizing of glass plates subjected to pressure loads, by J.M. Moore. Pasadena, CA, Aug 1982.

4. Ballistic Research Laboratories. Project Thor Technical Report No. 51: The resistance of various non-metallic materials to perforation by steel fragments: Empirical relationships for fragment residual velocity and residual weight. Aberdeen Proving Ground, MD, Apr 1963, AD# 336461.

TABLE 1. Coefficients for Frame Loading

a/b	C_r	C_x	C_y
1.00	0.065	0.495	0.495
1.20	0.074	0.535	0.533
1.40	0.083	0.570	0.562
1.60	0.086	0.590	0.583
1.80	0.090	0.609	0.600
2.00	0.092	0.623	0.614
3.00	0.093	0.664	0.655
4.00	0.094	0.687	0.685

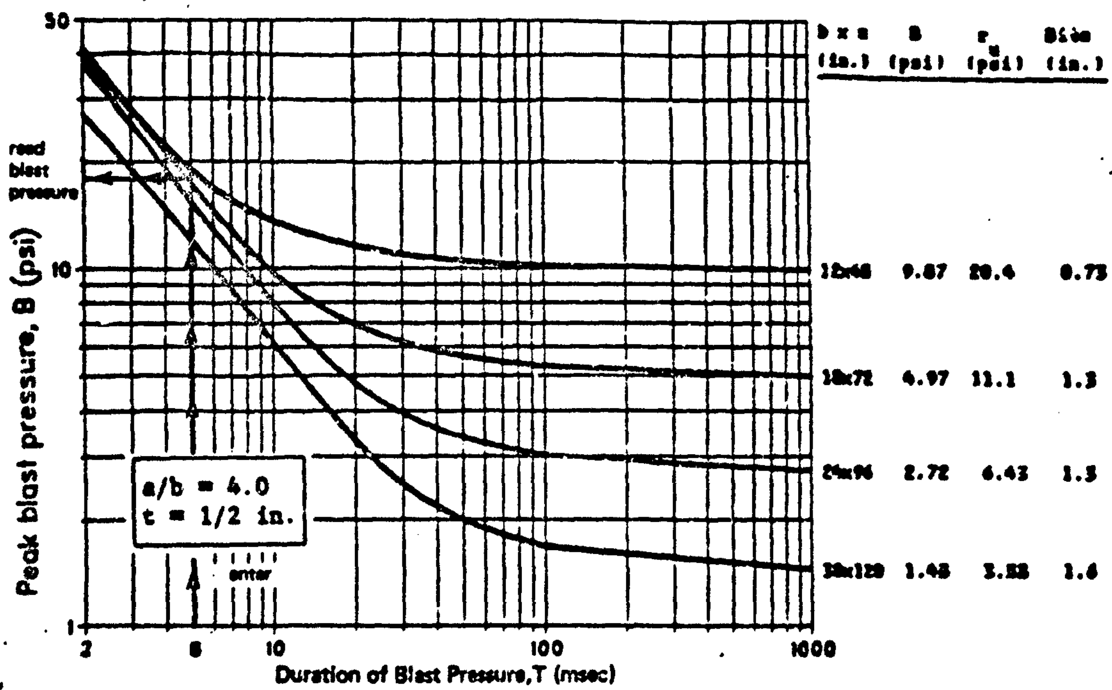

Problem: Evaluate the blast resistance of a 1/2 inch thick polycarbonate window with dimensions of 72 x 18 inches.

Solution: Step 1
Compute the aspect ratio, a/b (length to width ratio):
a/b = 72/18 = 4

Step 2
With a/b = 4 and a nominal thickness, t, of 1/2 inch locate the appropriate design chart, which in this case is the top chart on Figure 18 (pictured above).

Step 3
Locate the curve corresponding to the 18 x 72 inch polycarbonate. The blast capacity corresponds to the positive pressure for the 18 x 72 x 1/2 inch subjected to a positive blast duration of 5 msec is 17.4 psi.

Figure 1. Design chart example for blast resistant polycarbonate window.

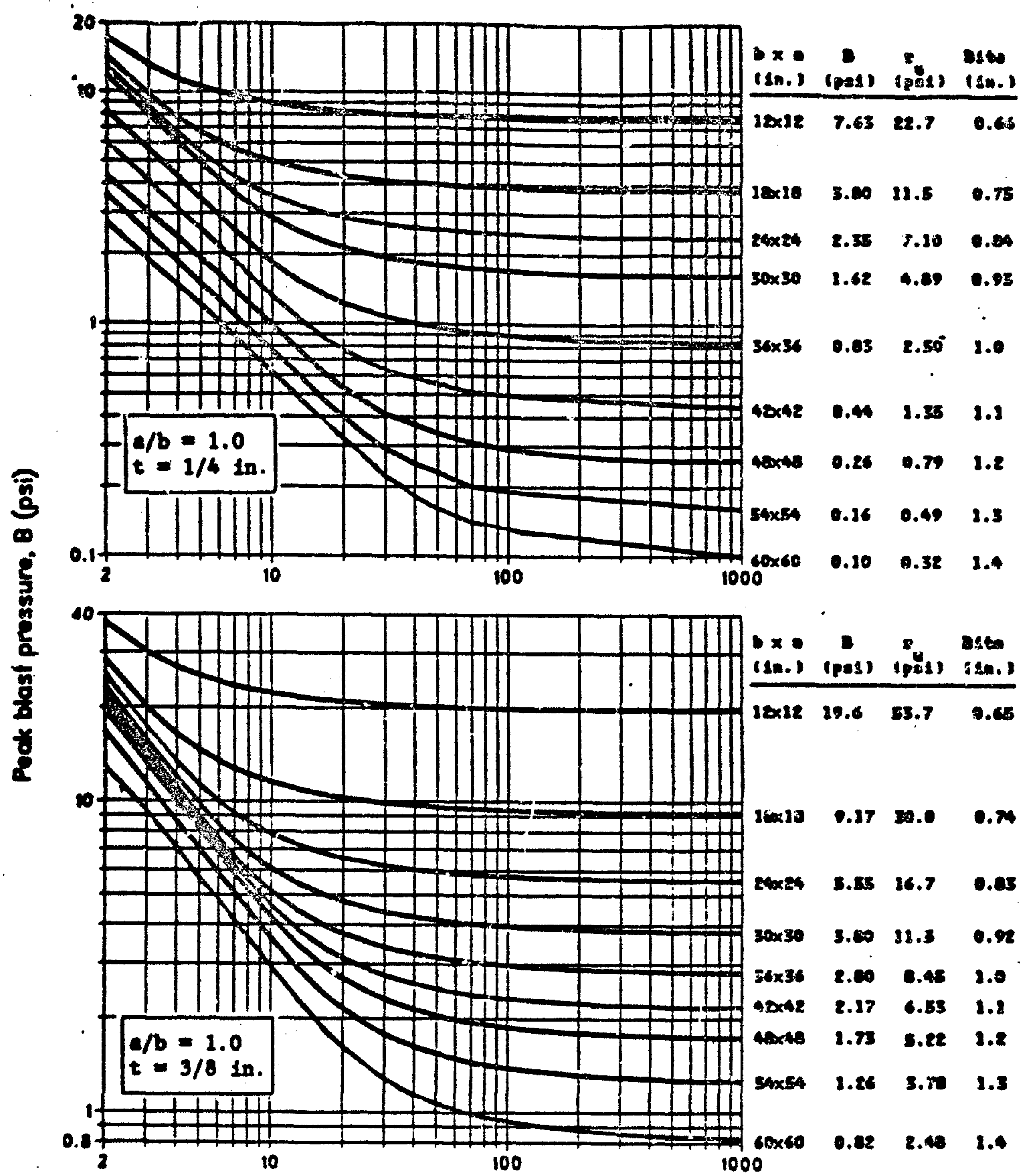

Figure 2. Peak blast pressure capacity for polycarbonate: a/b = 1.0; t = 1/4 and 3/8 in.

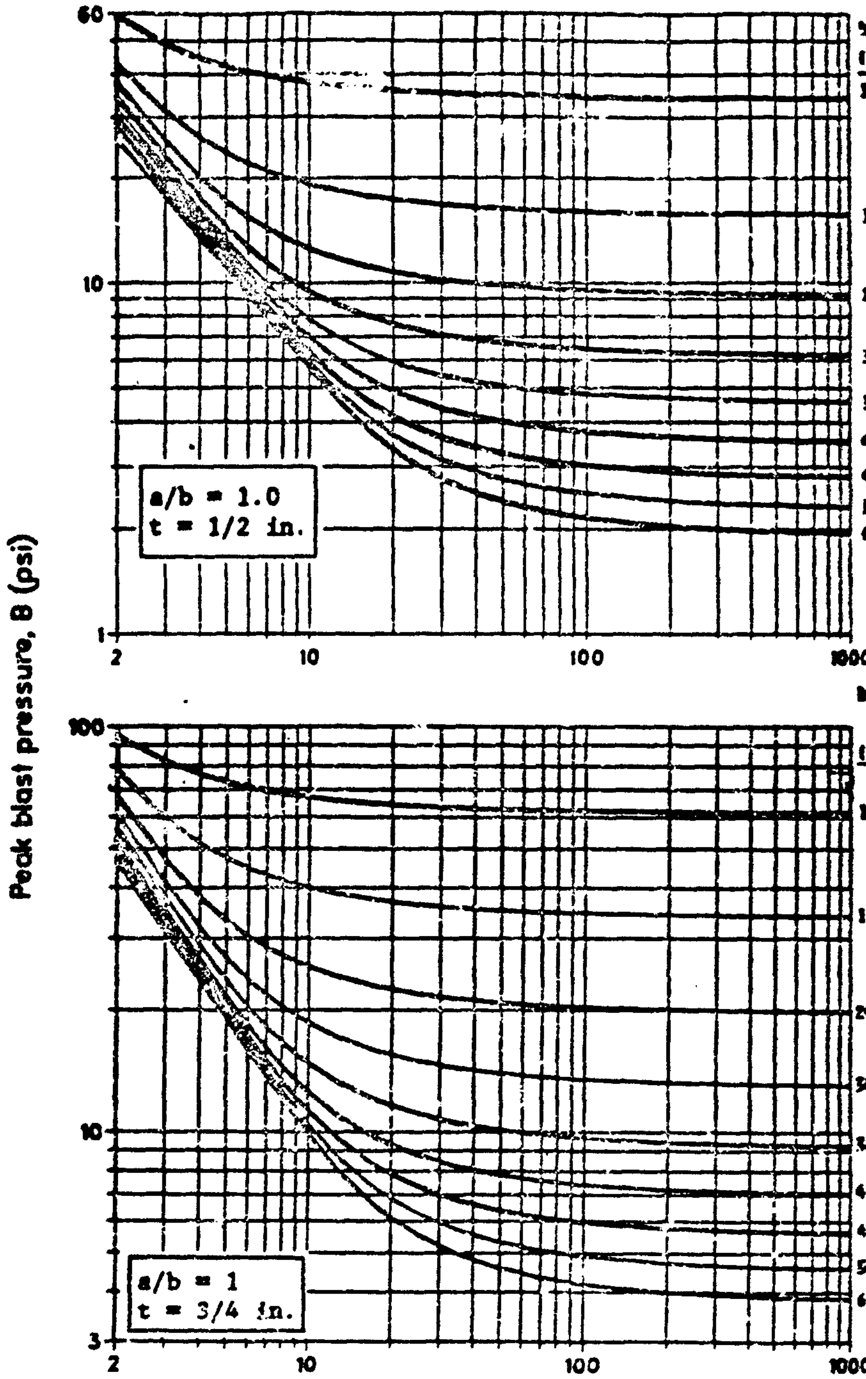

b x a (in.)	B (psi)	r_u (psi)	[illegible] (in.)
12x12	33.9	86.1	0.65
18x18	15.8	43.9	0.73
24x24	9.19	27.0	0.82
30x30	6.21	18.6	0.91
36x36	4.55	13.7	1.0
42x42	3.51	10.6	1.1
48x48	2.81	8.46	1.2
54x54	2.31	6.94	1.3
60x60	1.94	5.82	1.4

b x a (in.)	B (psi)	r_u (psi)	[illegible] (in.)
12x12	61.4	134	0.57
18x18	33.4	86.2	0.70
24x24	19.7	53.8	0.80
30x30	13.0	36.7	0.89
36x36	9.21	27.9	1.0
42x42	7.02	20.9	1.1
48x48	5.59	16.7	1.2
54x54	4.57	13.7	1.2
60x60	3.82	11.5	1.3

Figure 3. Peak blast pressure capacity for polycarbonate: a/b = 1.0; t = 1/2 and 3/4 in.

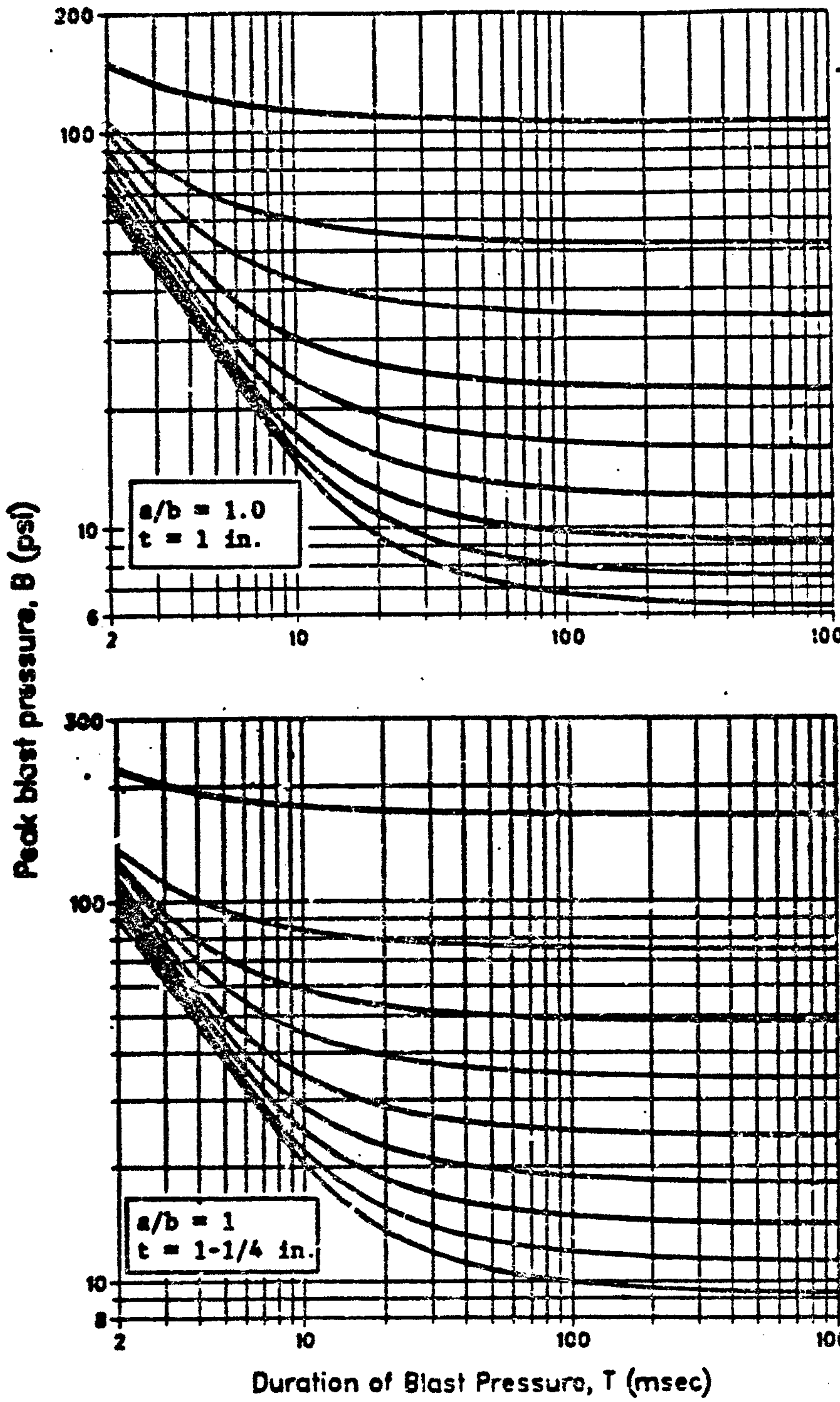

b x a (in.)	B (psi)	r_u (psi)	Bite (in.)
12x12	105	219	0.55
18x18	51.8	121	0.63
24x24	34.0	86.1	0.76
30x30	22.3	60.1	0.86
36x36	15.7	43.9	0.96
42x42	11.3	33.8	1.0
48x48	9.22	27.0	1.1
54x54	7.49	22.2	1.2
60x60	6.24	18.6	1.3

b x a (in.)	B (psi)	r_u (psi)	Bite (in.)
12x12	167	535	0.53
18x18	74.6	161	0.60
24x24	48.0	115	0.70
30x30	34.1	86.4	0.83
36x36	23.9	64.1	0.93
42x42	18.8	49.6	1.0
48x48	14.1	39.4	1.1
54x54	11.3	32.3	1.2
60x60	9.27	27.1	1.3

Figure 4. Peak blast pressure capacity for polycarbonate: a/b = 1.0; t = 1 and 1-1/4 in.

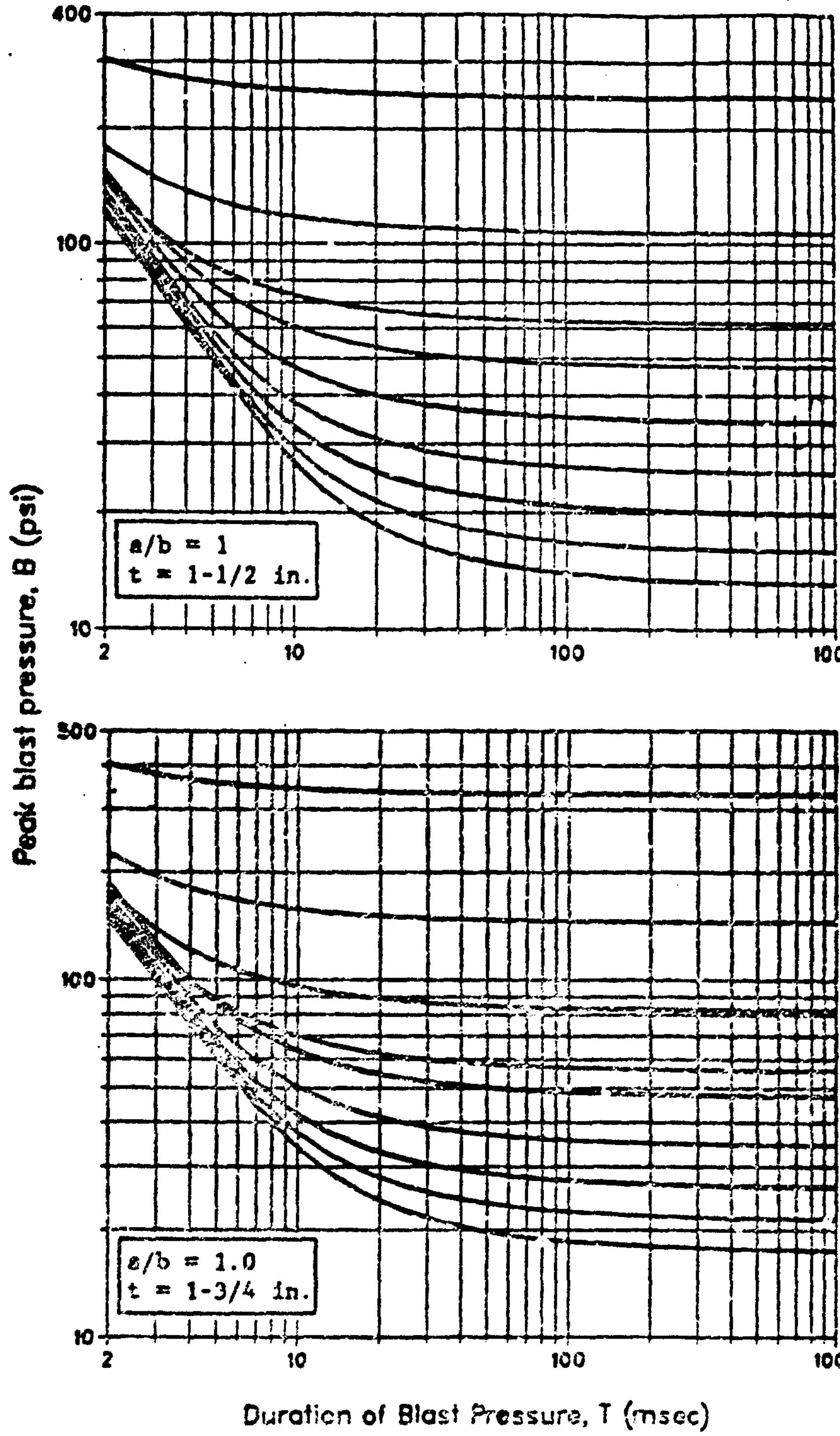

b x a (in.)	B (psi)	r_u (psi)	[illegible] (in.)
12x12	242	404	0.52
18x18	106	221	0.56
24x24	61.6	134	0.64
30x30	47.4	115	0.78
36x36	34.3	86.6	0.90
42x42	25.3	67.0	1.0
48x48	19.9	54.1	1.1
54x54	15.9	44.1	1.2
60x60	13.1	36.9	1.3

b x a (in.)	B (psi)	r_u (psi)	[illegible] (in.)
12x12	331	660	0.52
18x18	148	293	0.54
24x24	82.3	176	0.61
30x30	56.7	127	0.70
36x36	47.0	116	0.86
42x42	34.3	86.7	0.96
48x48	26.3	69.2	1.0
54x54	21.3	57.7	1.2
60x60	17.5	48.1	1.3

Figure 5. Peak blast pressure capacity for polycarbonate: a/b = 1.0; t = 1-1/2 and 1-3/4 in.

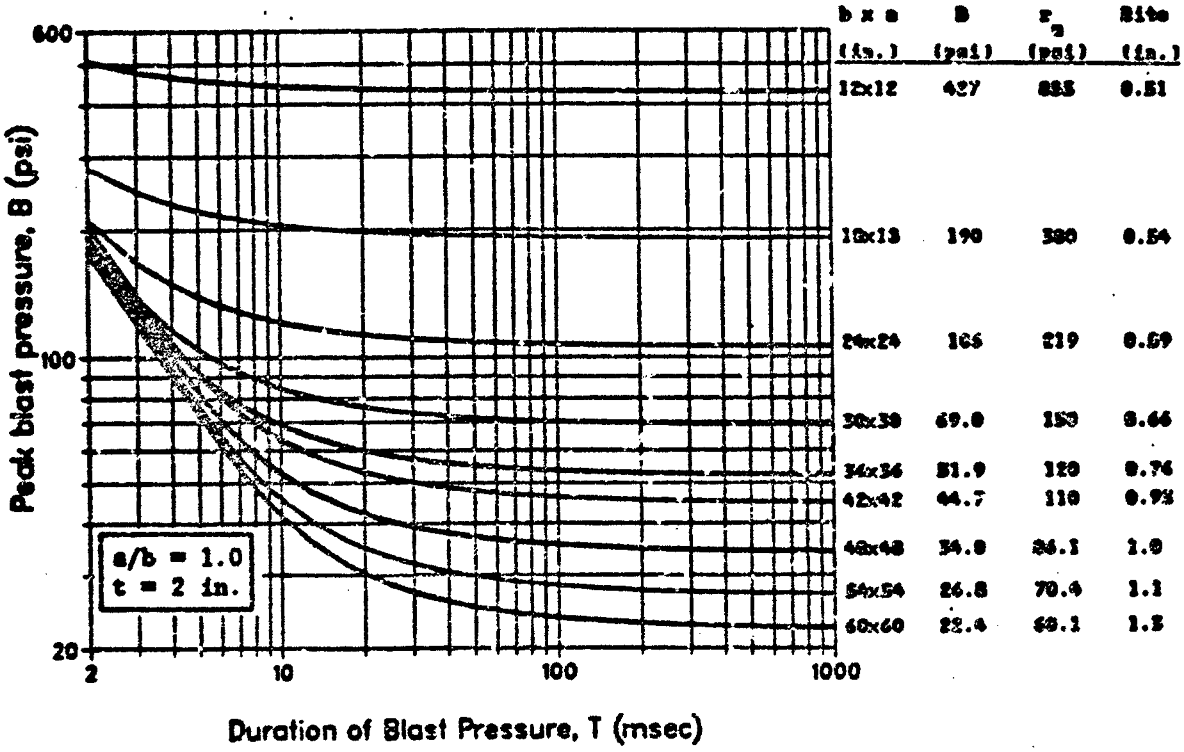

Figure 6. Peak blast pressure capacity for polycarbonate: a/b = 1.0; t = 2 in.

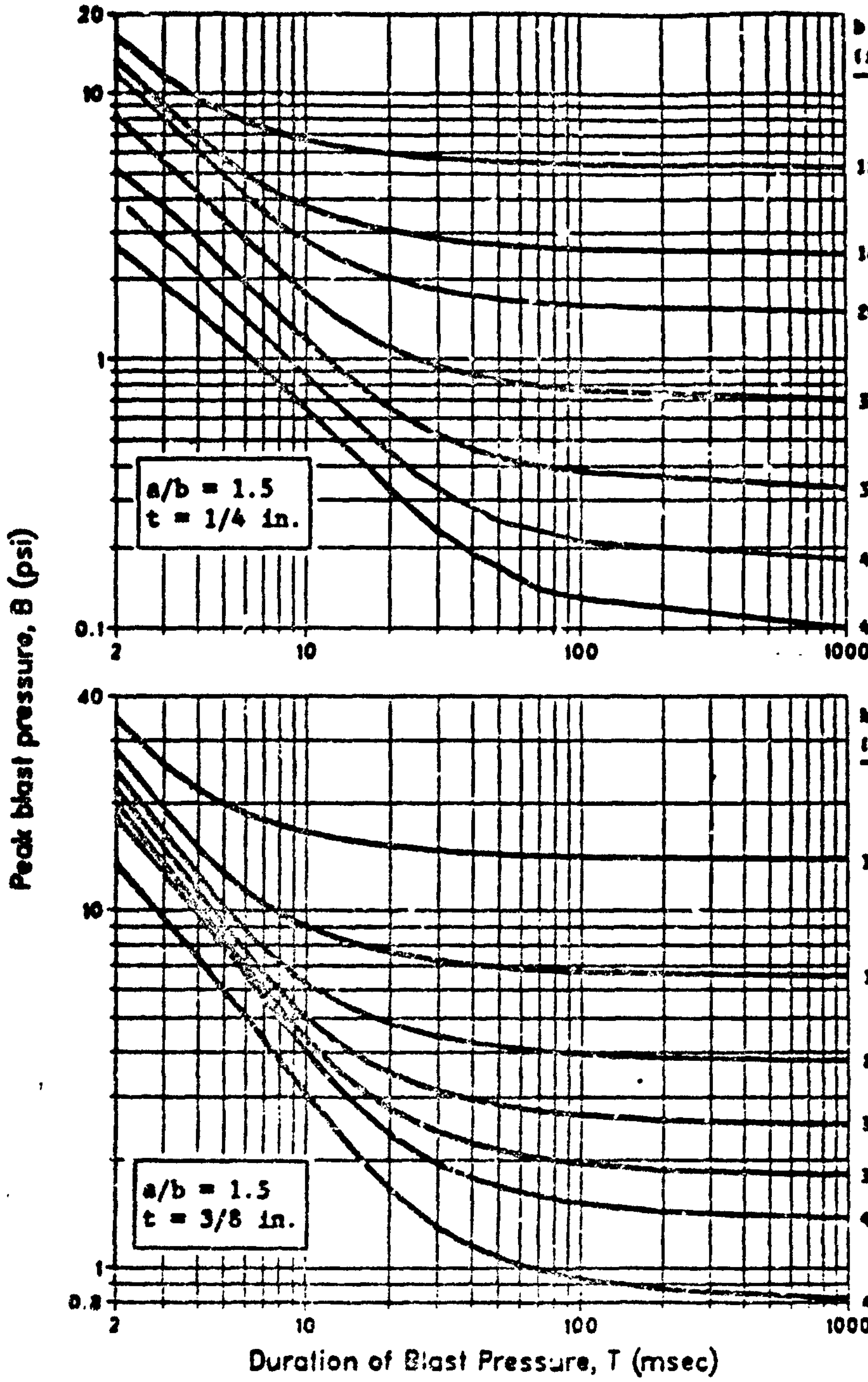

b x a (in.)	B (psi)	r_u (psi)	B/t (in.)
12x18	5.53	15.7	0.76
18x27	2.51	7.57	0.88
24x36	1.50	4.52	1.0
30x45	0.70	2.11	1.1
36x54	0.33	1.02	1.3
42x63	0.18	0.56	1.4
48x72	0.10	0.32	1.5

b x a (in.)	B (psi)	r_u (psi)	B/t (in.)
12x18	13.9	37.9	0.74
18x27	6.52	18.9	0.89
24x36	3.78	11.3	1.0
30x45	2.51	7.55	1.1
36x54	1.81	5.44	1.3
42x63	1.37	4.13	1.4
48x72	0.82	2.46	1.5

Figure 7. Peak blast pressure capacity for polycarbonate: a/b = 1.5; t = 1/4 and 3/8 in.

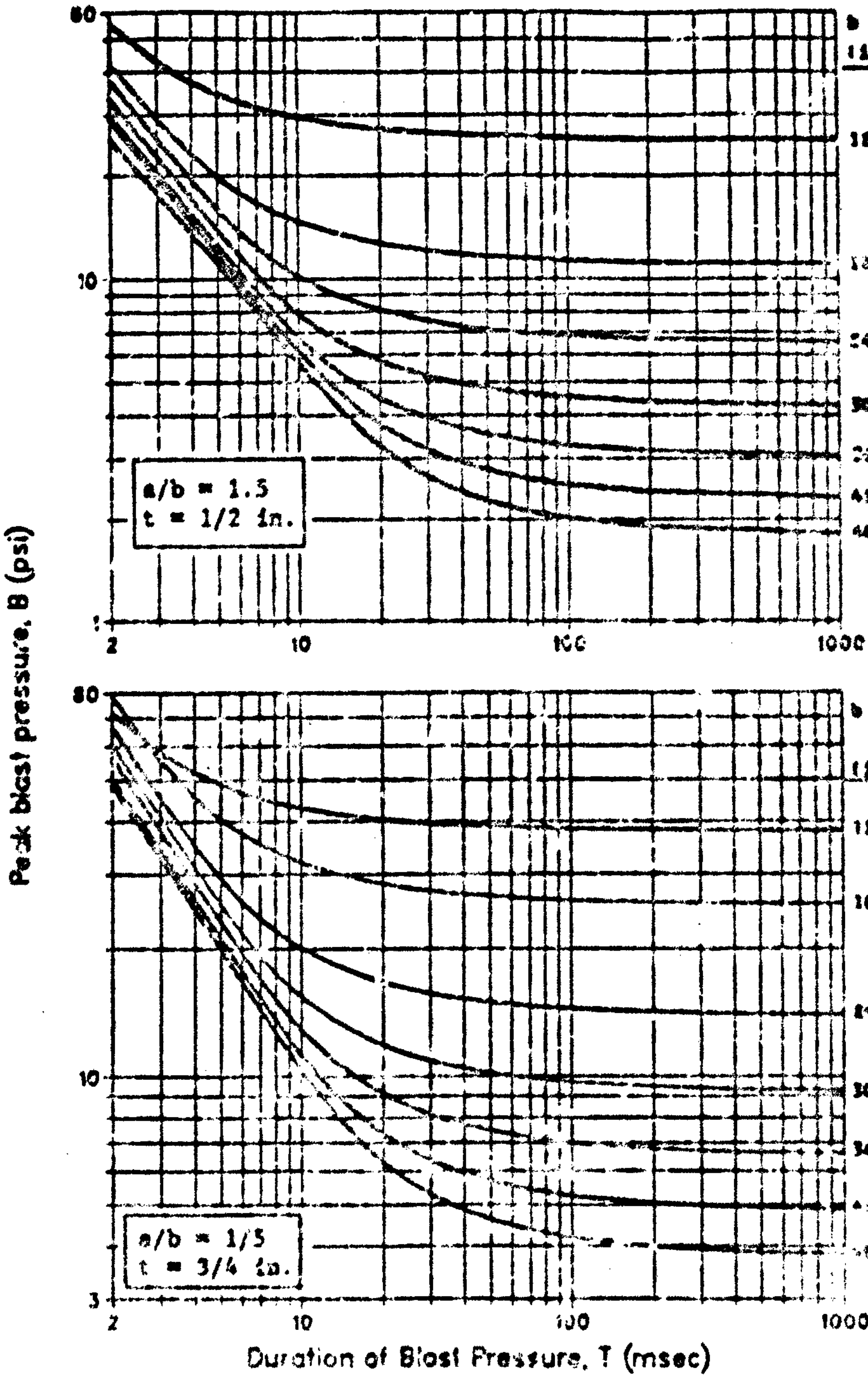

b x a (in.)	B (psi)	r_u (psi)	Dito (in.)
12x18	25.3	65.9	0.73
18x27	11.1	30.6	0.86
24x36	6.54	18.9	1.0
30x45	4.27	12.7	1.2
36x54	3.08	9.13	1.3
42x63	2.31	6.92	1.4
48x72	1.81	5.45	1.5

b x a (in.)	B (psi)	r_u (psi)	Dito (in.)
12x18	37.8	84.0	0.59
18x27	25.4	44.5	0.84
24x36	13.9	28.0	0.97
30x45	9.25	26.1	1.1
36x54	6.84	18.9	1.3
42x63	4.87	14.4	1.4
48x72	3.80	11.3	1.5

Figure 8. Peak blast pressure capacity for polycarbonate: a/b = 1.5; t = 1/2 and 3/4 in.

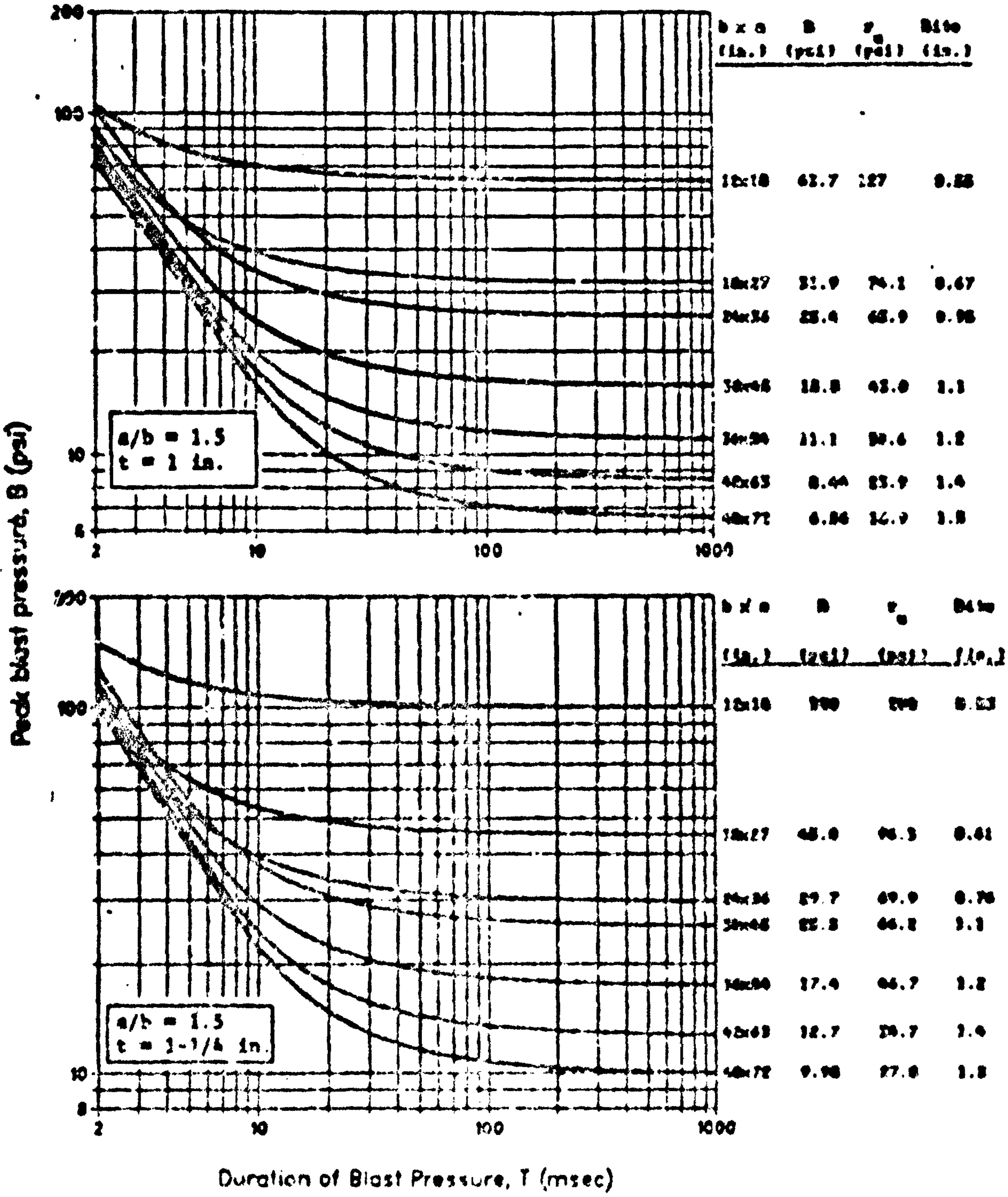

Figure 9. Peak blast pressure capacity for polycarbonate: a/b = 1.5; t = 1 and 1-1/4 in.

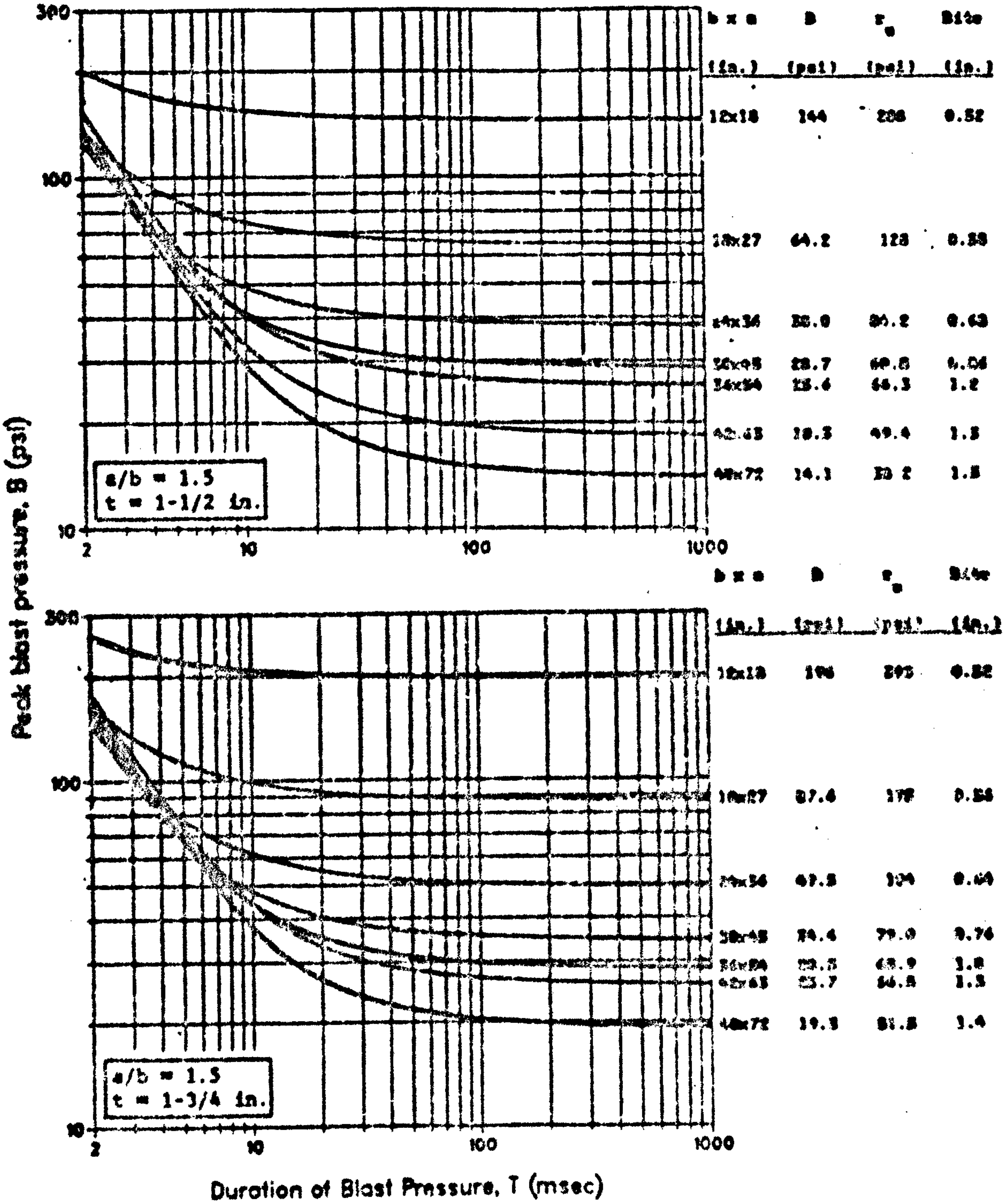

Figure 10. Peak blast pressure capacity for polycarbonate: a/b = 1.5; t = 1-1/2 and 1-3/4 in.

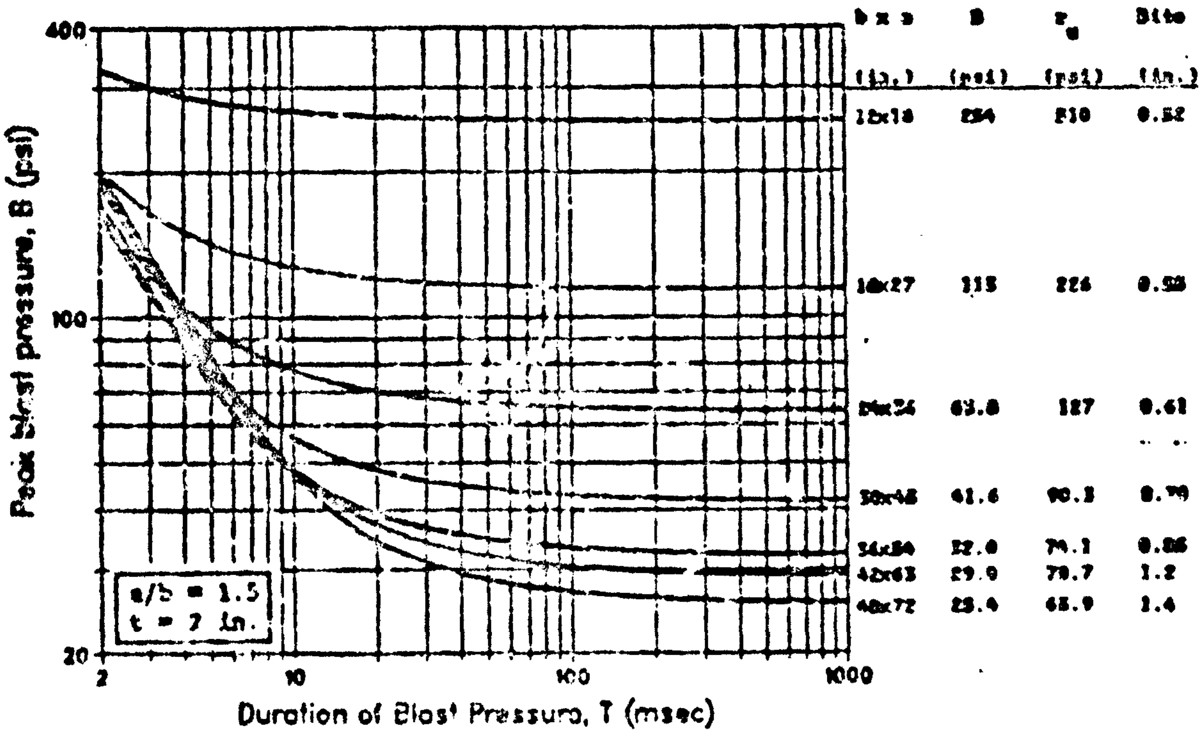

Figure 11. Peak blast pressure capacity for polycarbonate: a/b = 1.5; t = 2 in.

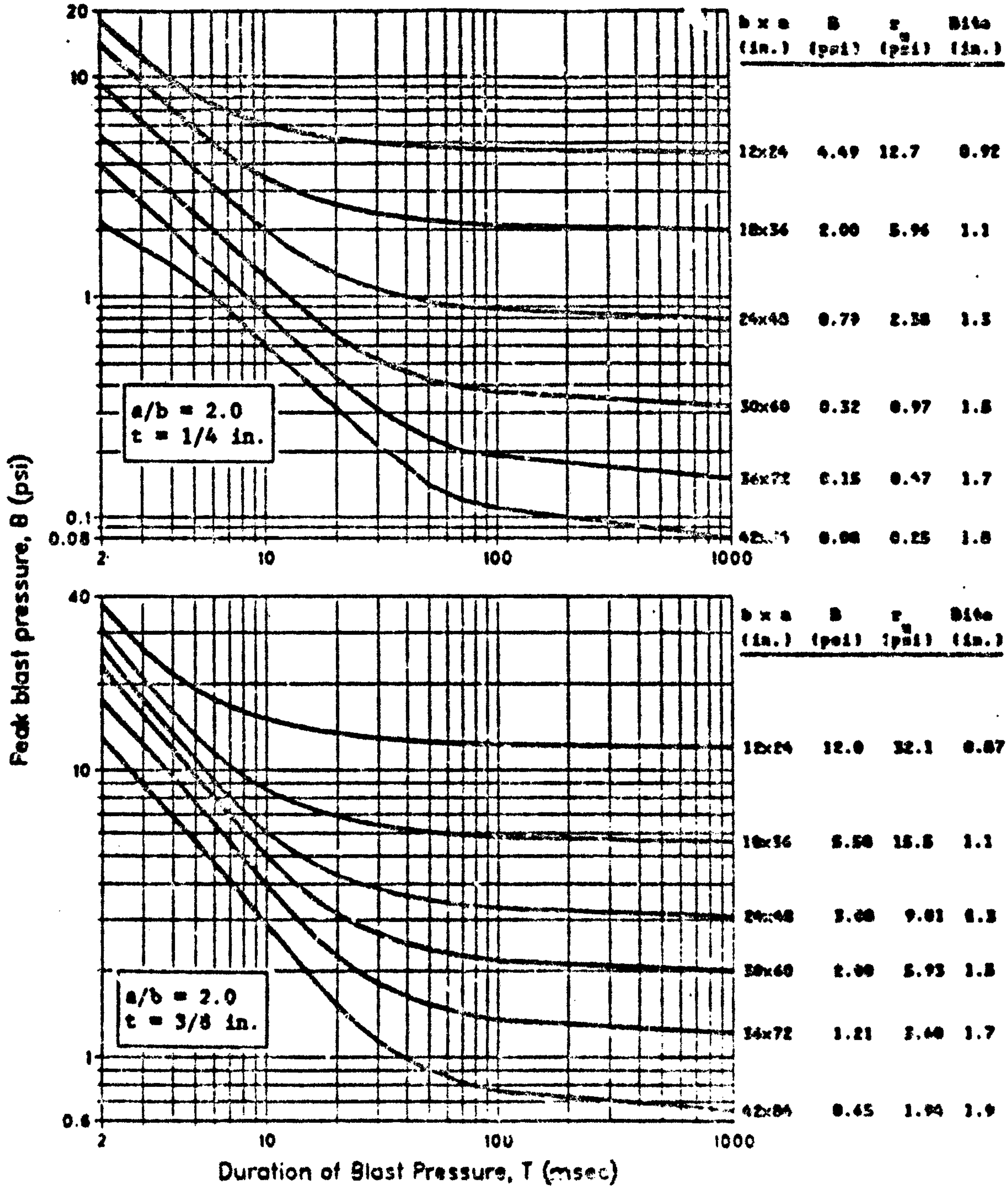

Figure 12. Peak blast pressure capacity for polycarbonate: a/b = 2.0; t = 1/4 and 3/8 in.

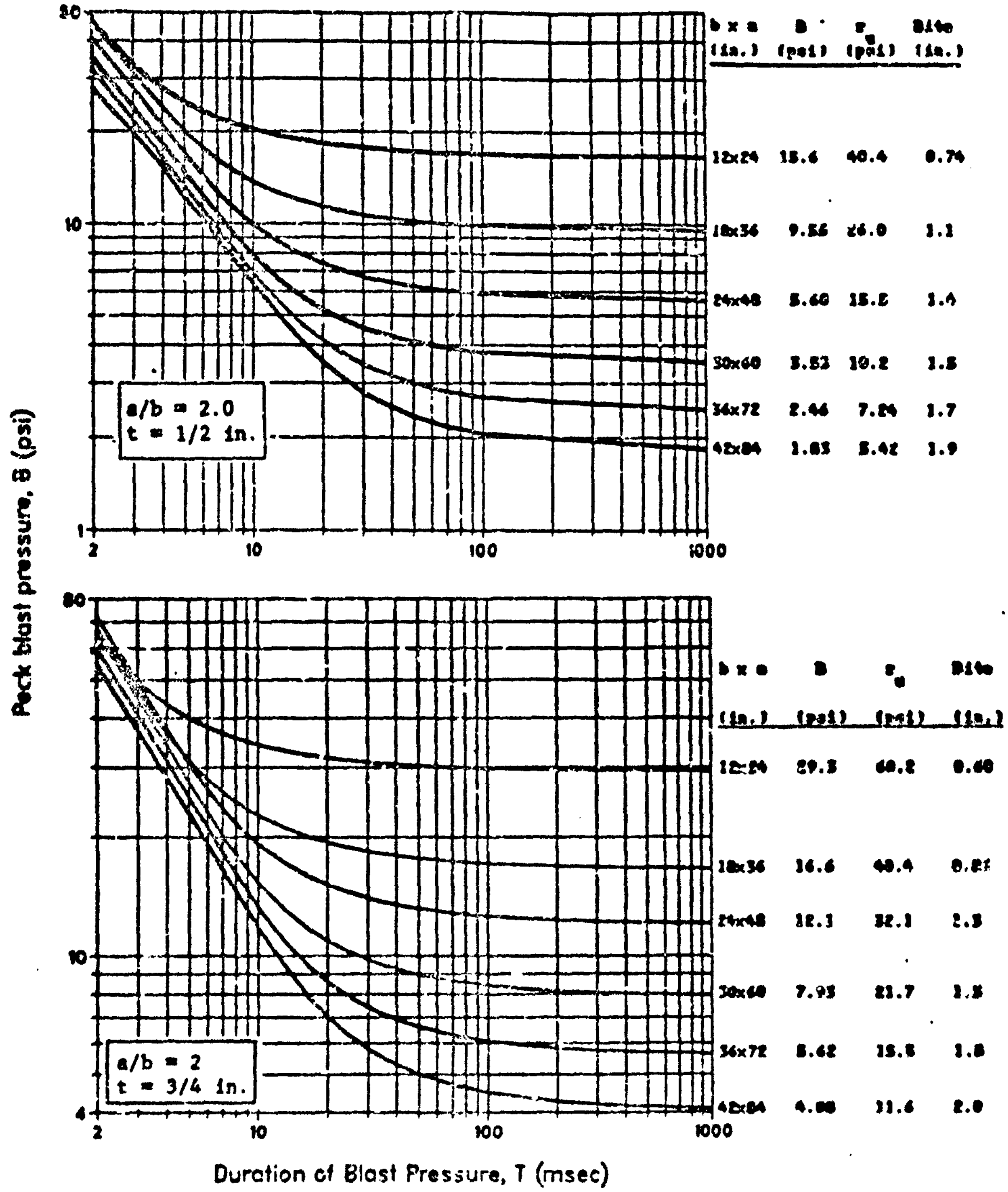

Figure 13. Peak blast pressure capacity for polycarbonate: a/b = 2.0; t = 1/2 and 3/4 in.

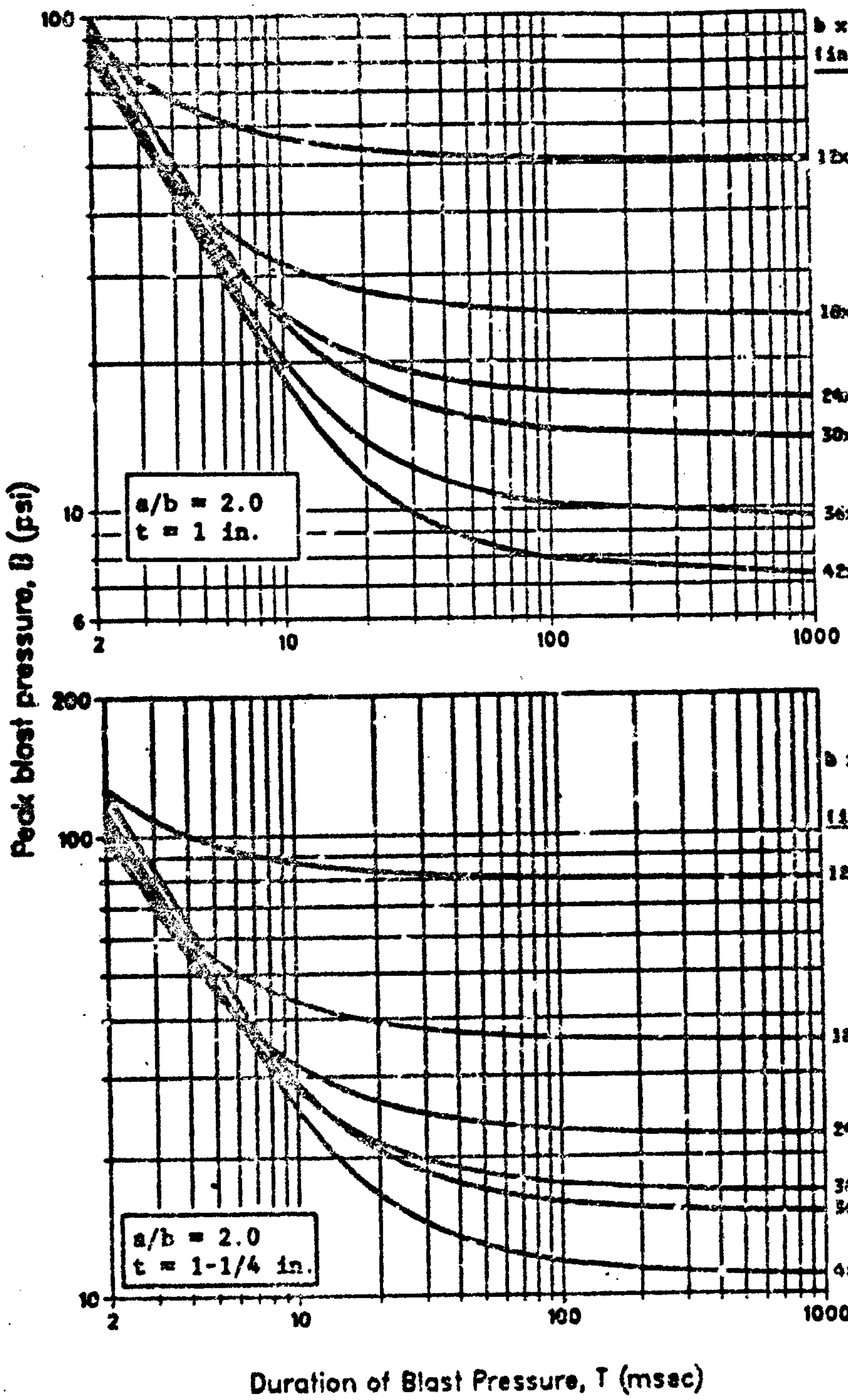

b x a (in.)	B (psi)	r_u (psi)	Bite (in.)
12x24	50.6	101	0.53
18x36	24.5	52.1	0.70
24x48	16.6	40.4	0.92
30x60	13.8	36.3	1.4
36x72	9.39	26.8	1.7
42x84	7.27	19.9	1.9

b x a (in.)	B (psi)	r_u (psi)	Bite (in.)
12x24	79.5	160	0.53
18x36	35.4	71.4	0.62
24x48	27.1	48.3	0.80
30x60	16.7	40.4	1.1
36x72	14.3	39.0	1.6
42x84	11.8	29.4	1.8

Figure 14. Peak blast pressure capacity for polycarbonate: a/b = 2.0; t = 1 and 1-1/4 in.

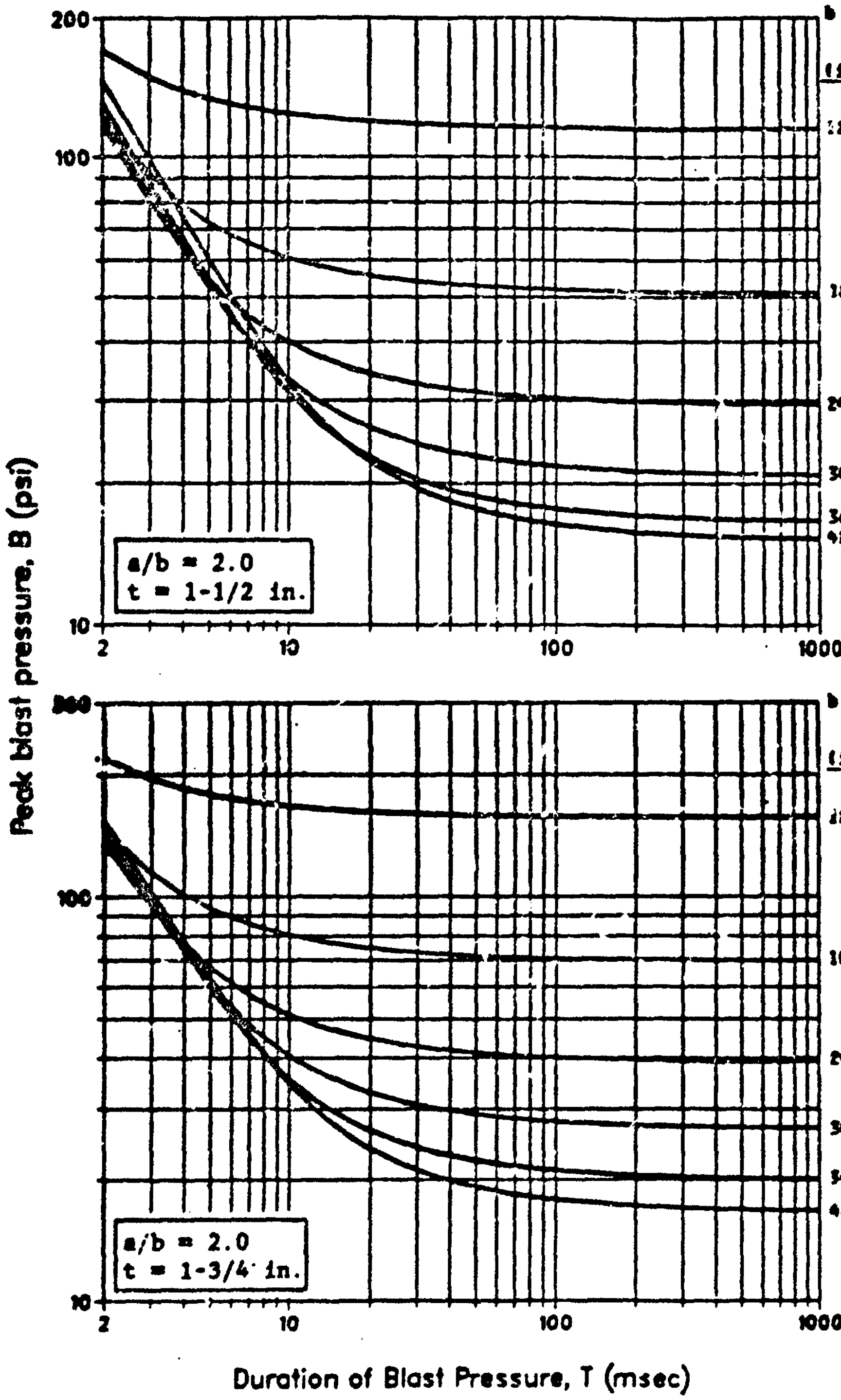

b x a (in.)	B (psi)	r_u (psi)	B/t (in.)
12x24	115	229	0.52
18x36	51.0	102	0.58
24x48	29.4	60.4	0.69
30x60	20.8	46.8	0.90
36x72	16.7	40.5	1.3
42x84	15.3	35.5	1.7

b x a (in.)	B (psi)	r_u (psi)	B/t (in.)
12x24	156	312	0.52
18x36	69.6	139	0.56
24x48	39.2	78.1	0.64
30x60	26.8	55.6	0.79
36x72	20.0	44.5	1.1
42x84	16.7	40.5	1.4

Figure 15. Peak blast pressure capacity for polycarbonate: a/b = 2.0; t = 1-1/2 and 1-3/4 in.

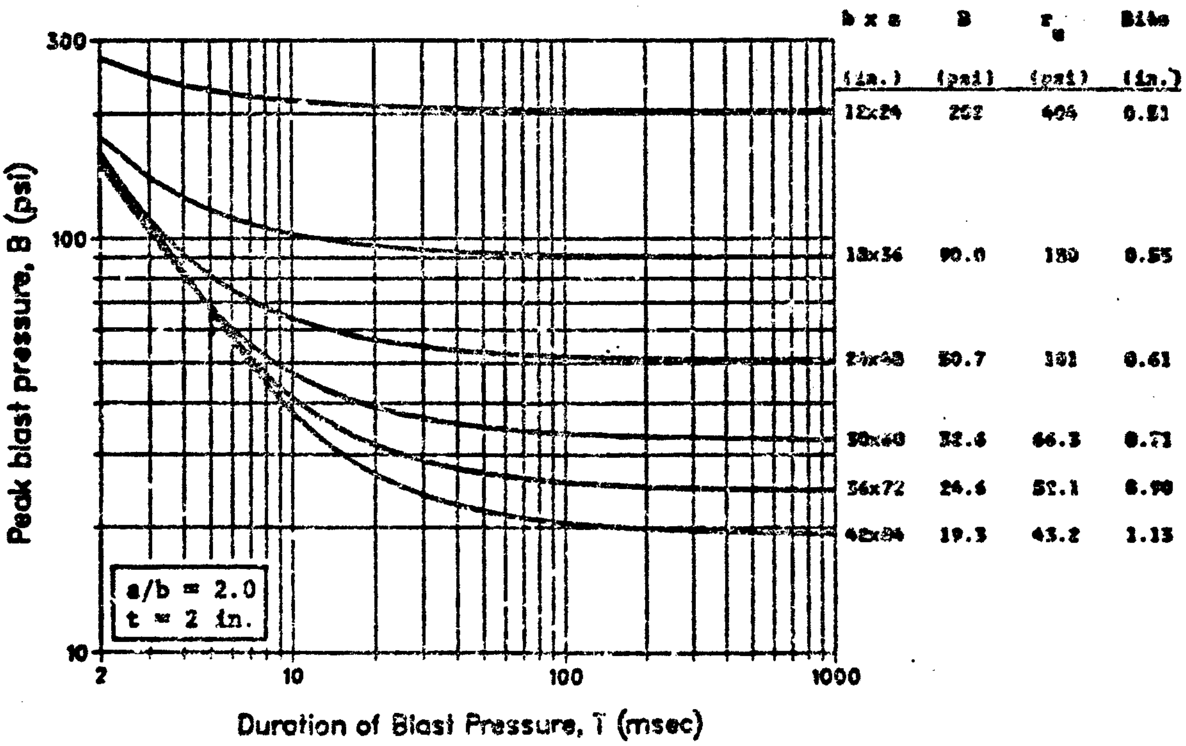

Figure 16. Peak blast pressure capacity for polycarbonate: a/b = 2.0; t = 2 in.

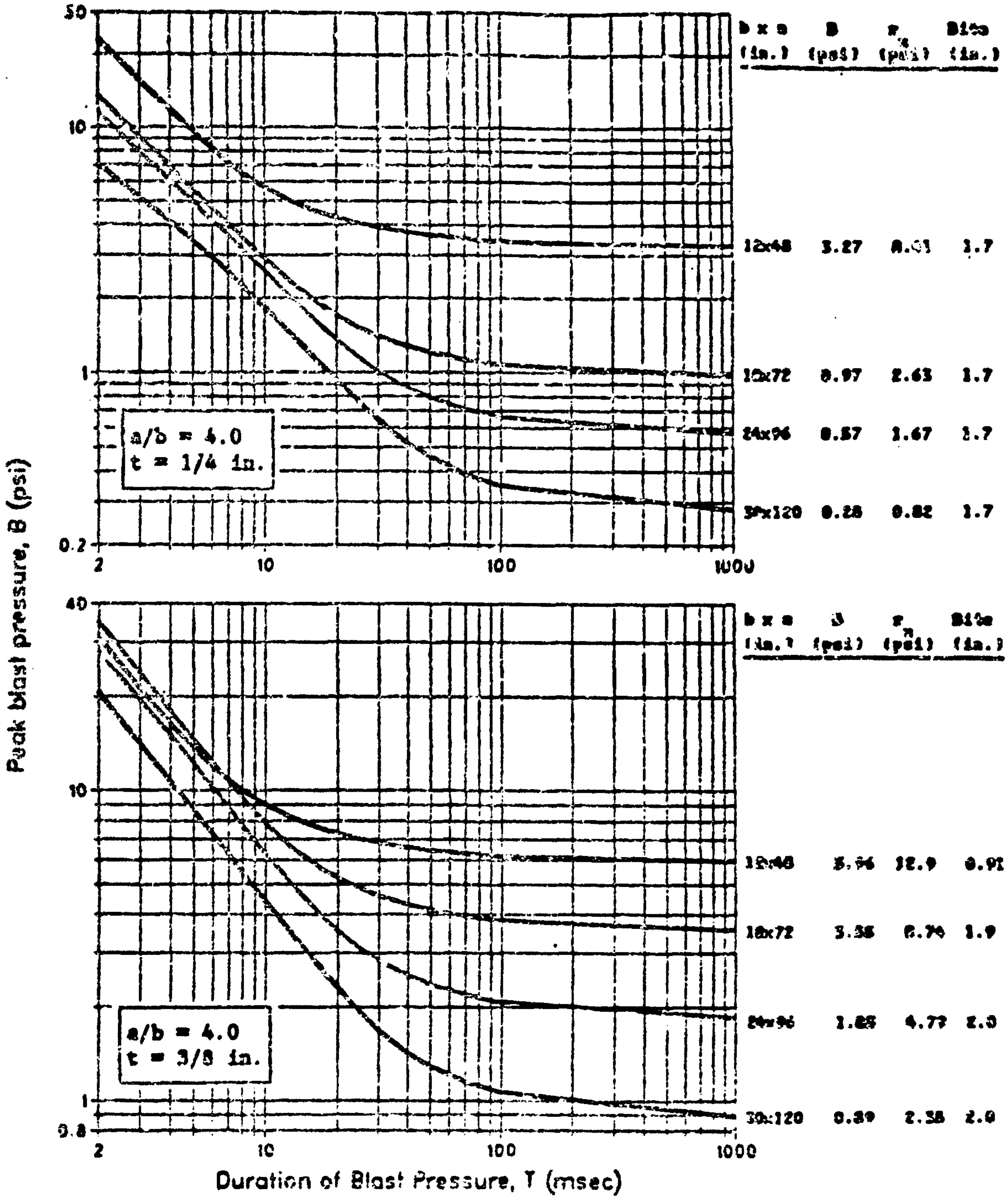

Figure 17. Peak blast pressure capacity for polycarbonate: a/b = 4.0; t = 1/4 and 3/8 in.

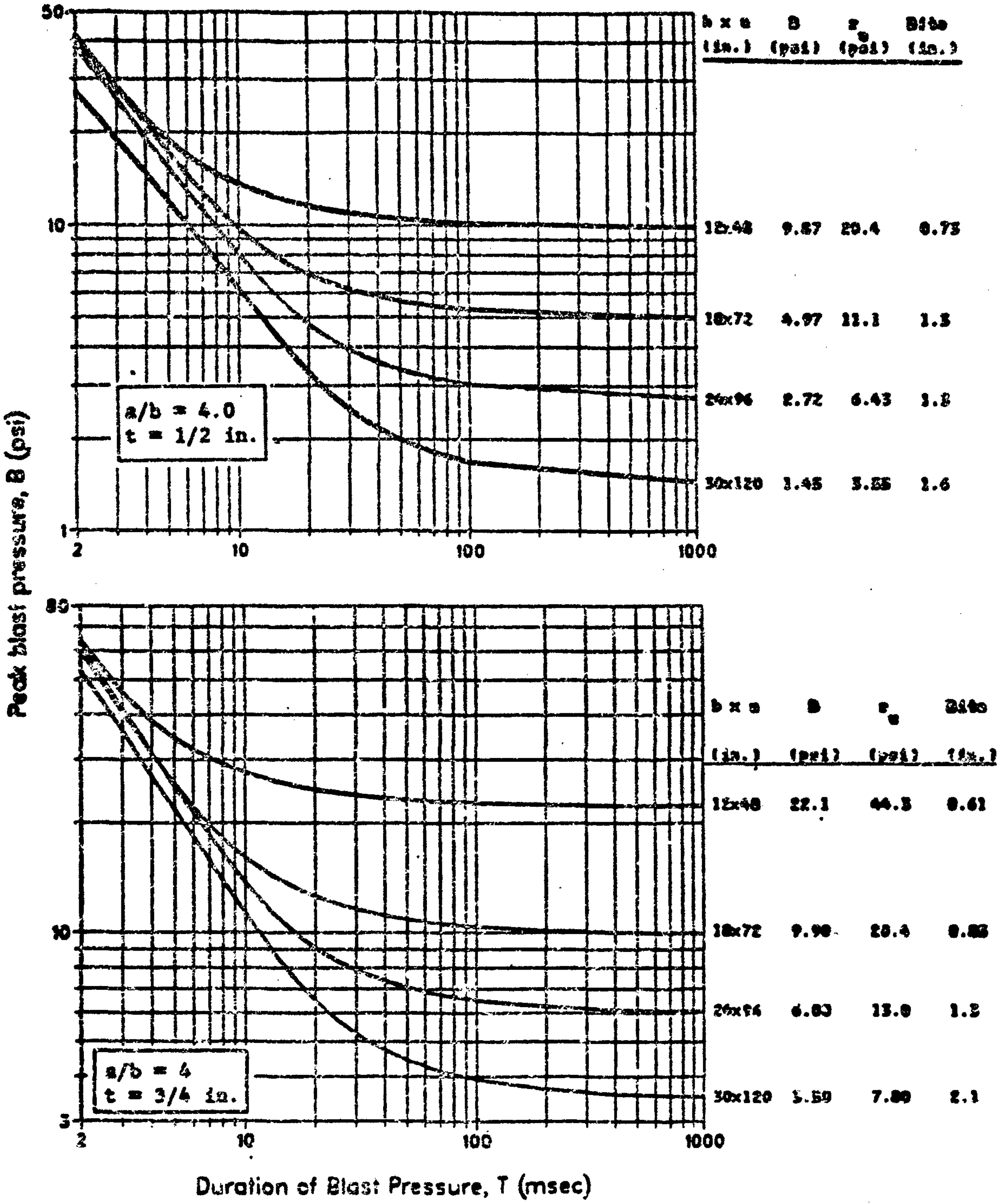

Figure 18. Peak blast pressure capacity for polycarbonate: a/b = 4.0; t = 1/2 and 3/4 in.

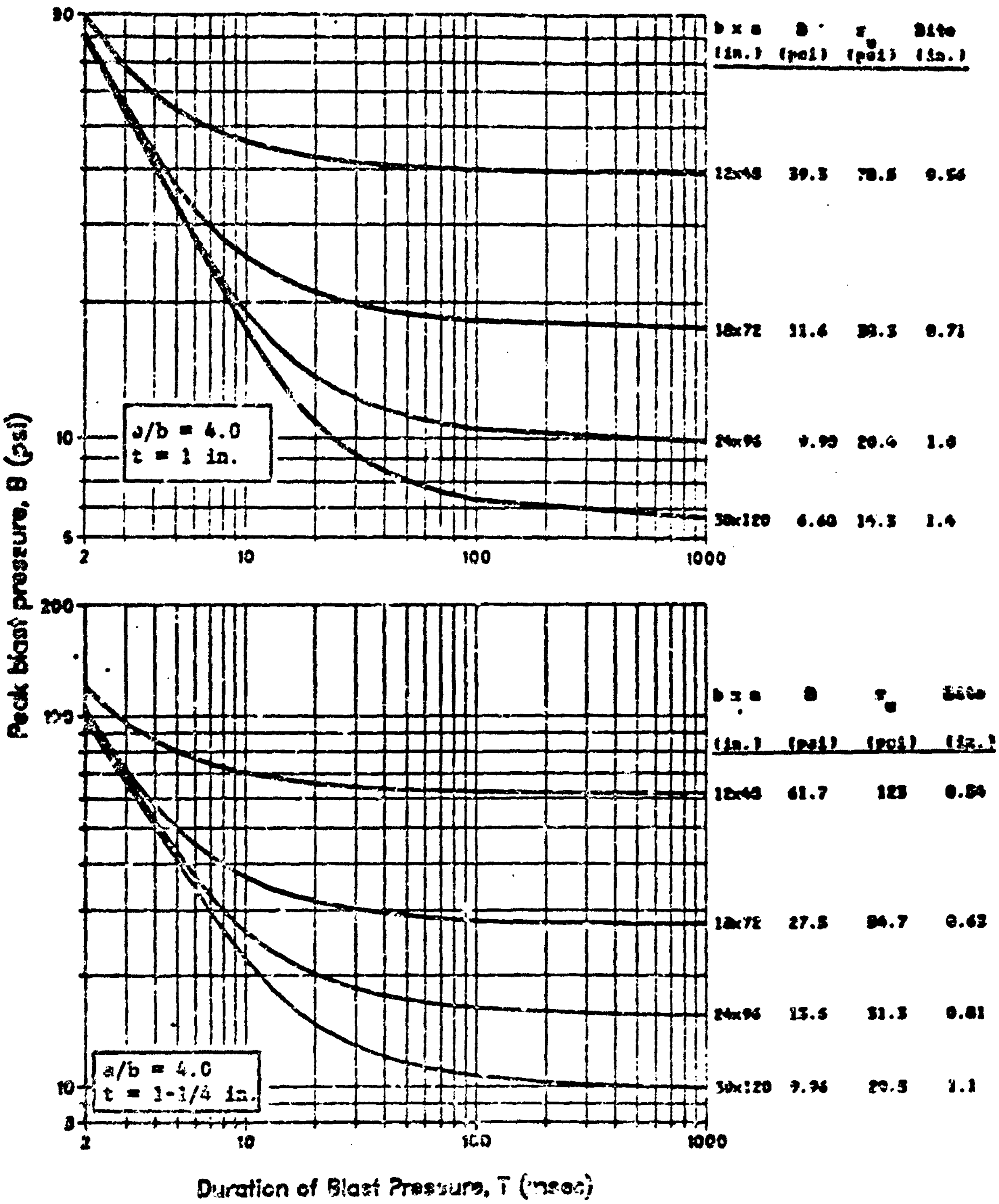

Figure 19. Peak blast pressure capacity for polycarbonate: a/b = 4.0; t = 1 and 1-1/4 in.

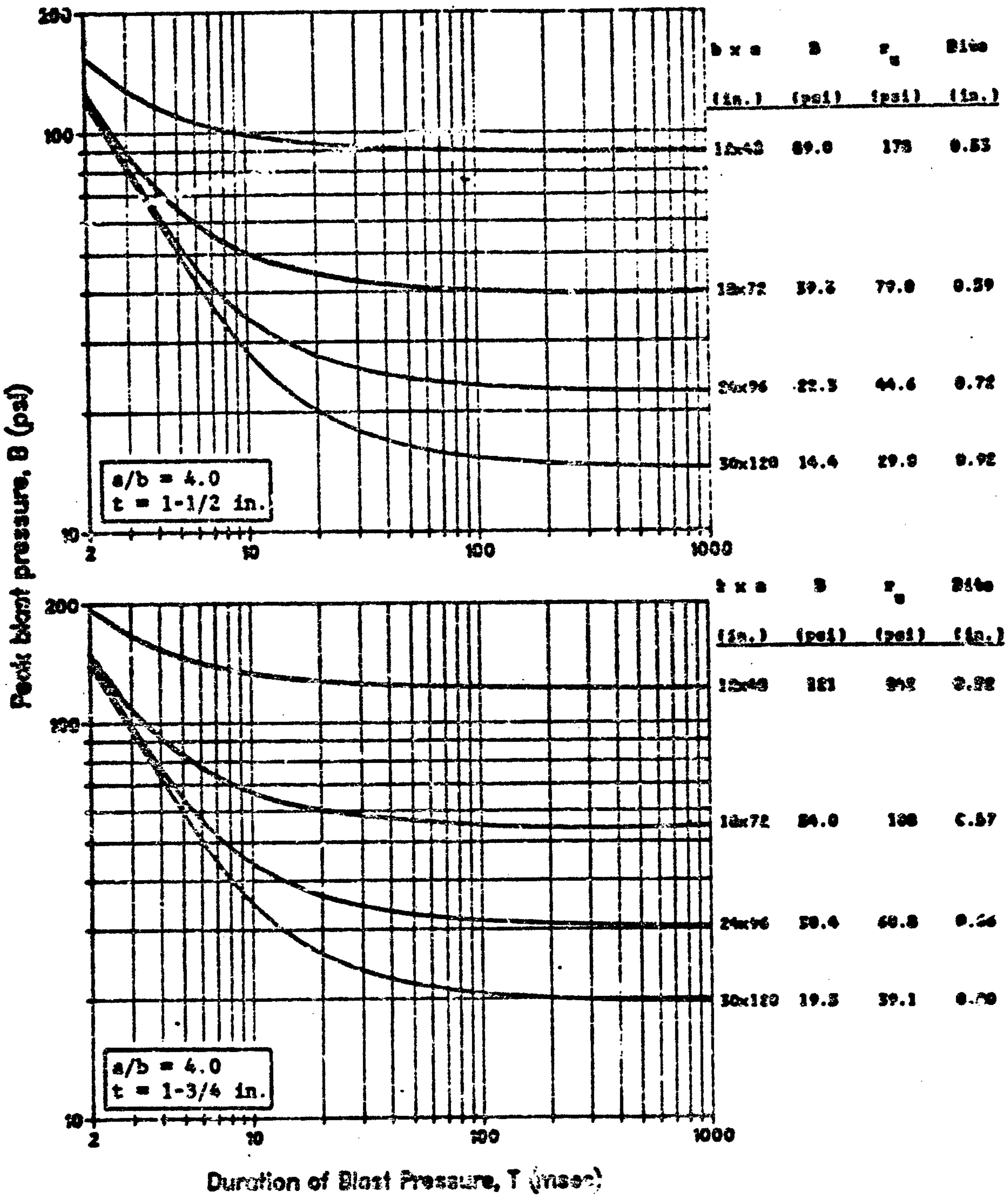

Figure 20. Peak blast pressure capacity for polycarbonate: a/b = 4.0; t = 1-1/2 and 1-3/4 in.

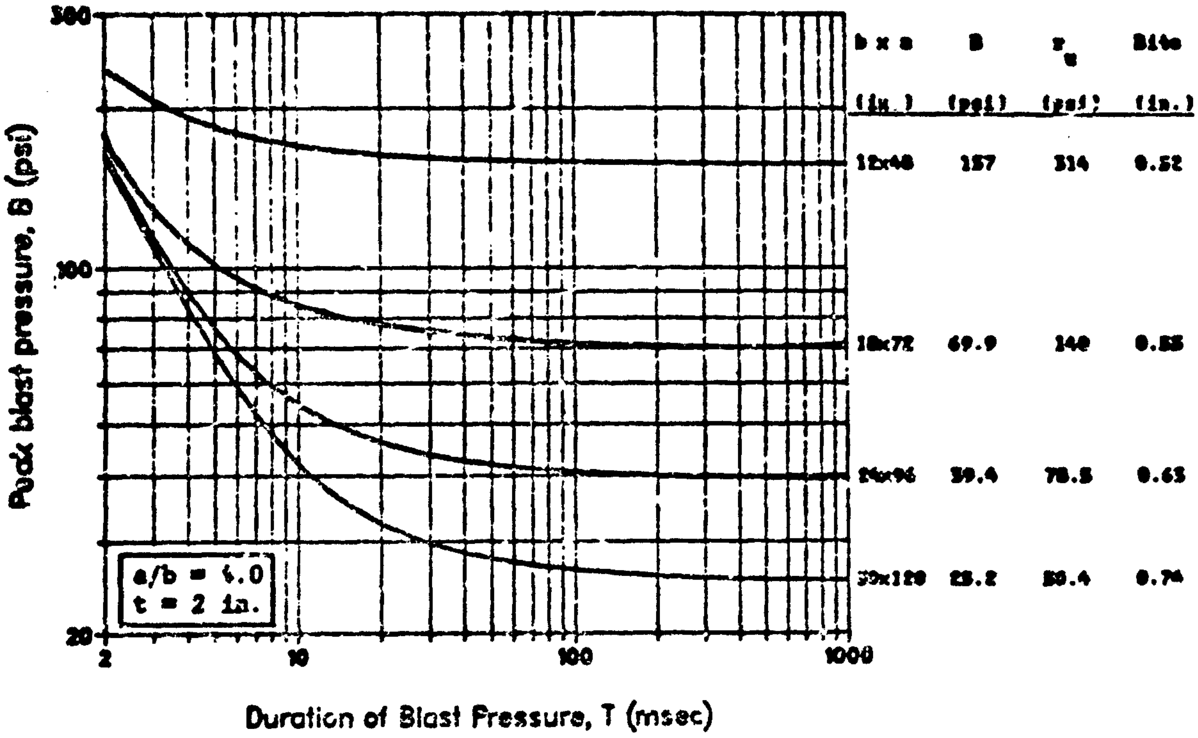

Figure 21. Peak blast pressure capacity for polycarbonate: a/b = 4.0; t = 2 in.

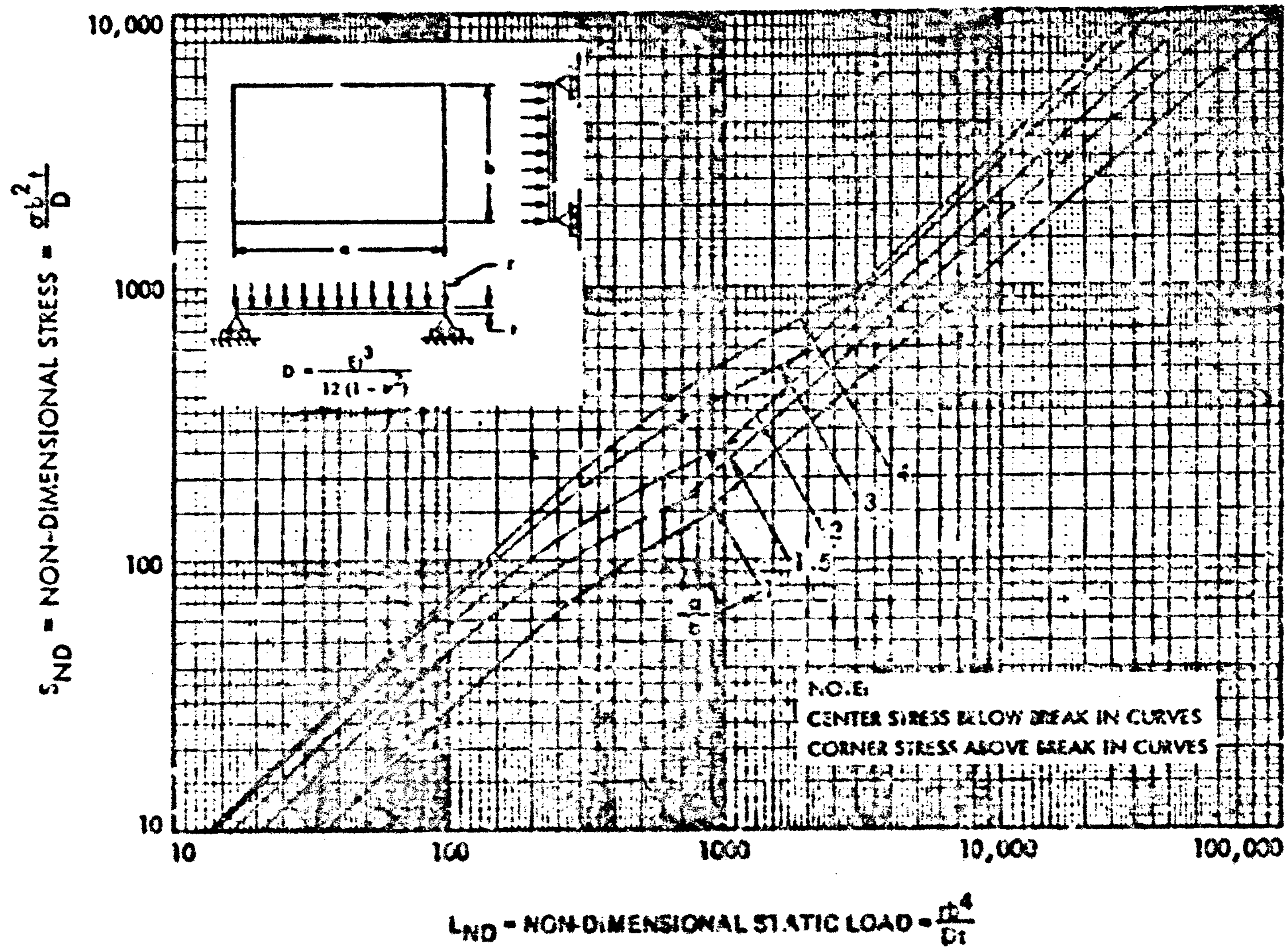

Figure 22. Non-dimensional static load-stress relationships for simply supported plates (from Ref 5).

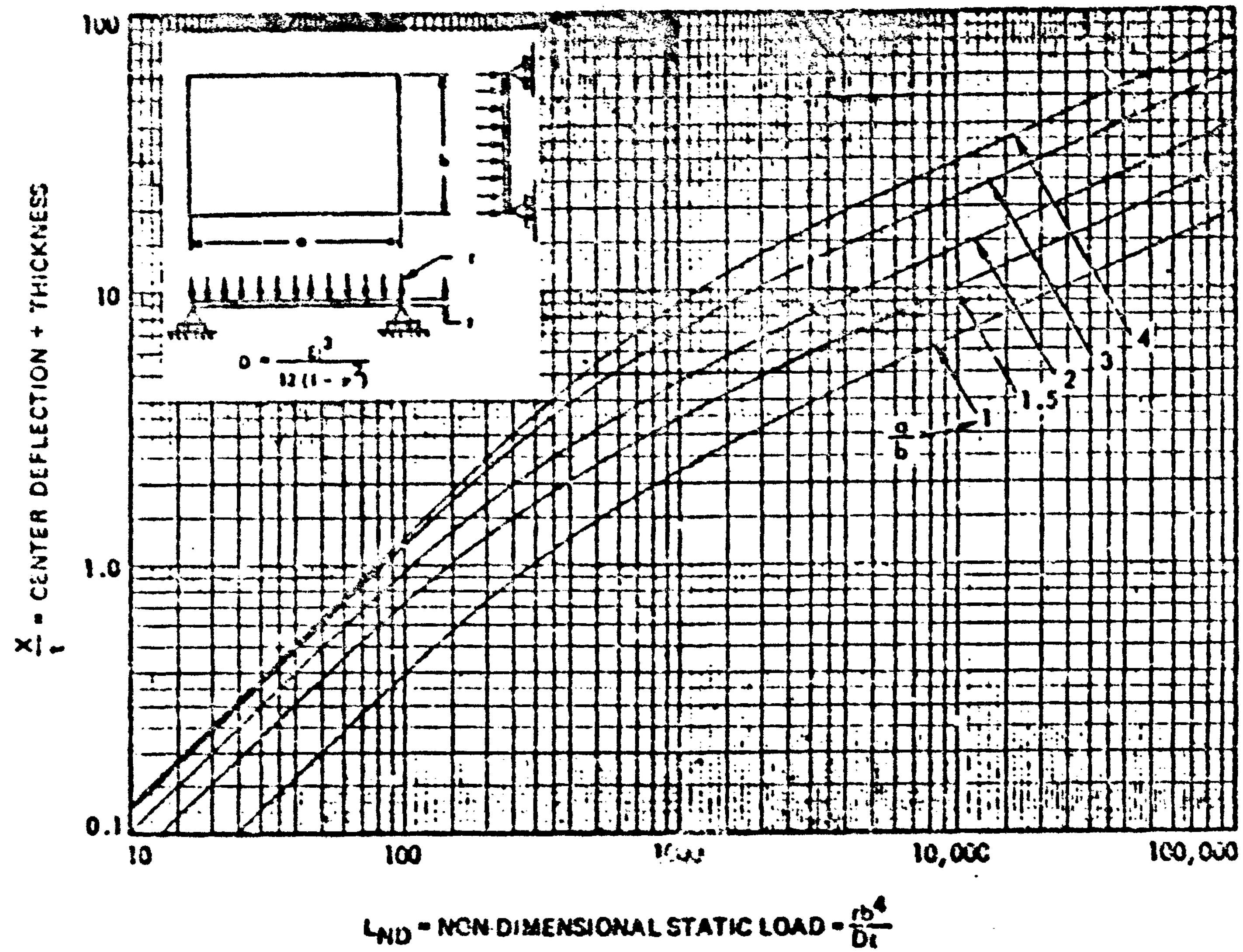

Figure 23. Non-dimensional static load-crater deflection relationships for simply supported plates.

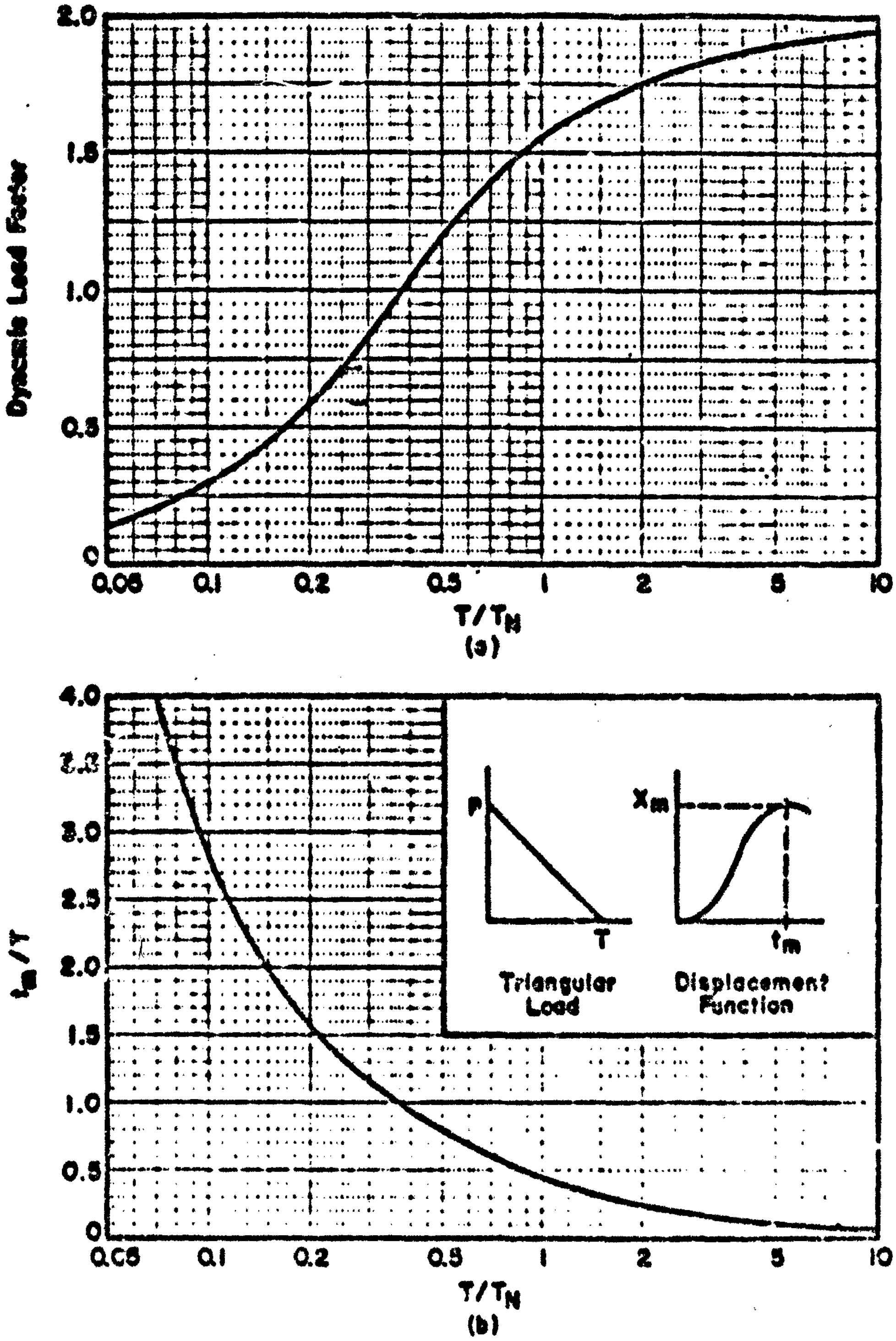

Figure 24. Maximum response of elastic one-degree-of-freedom system for triangular load (Figure 3-49 NAVFAC P-397 draft).

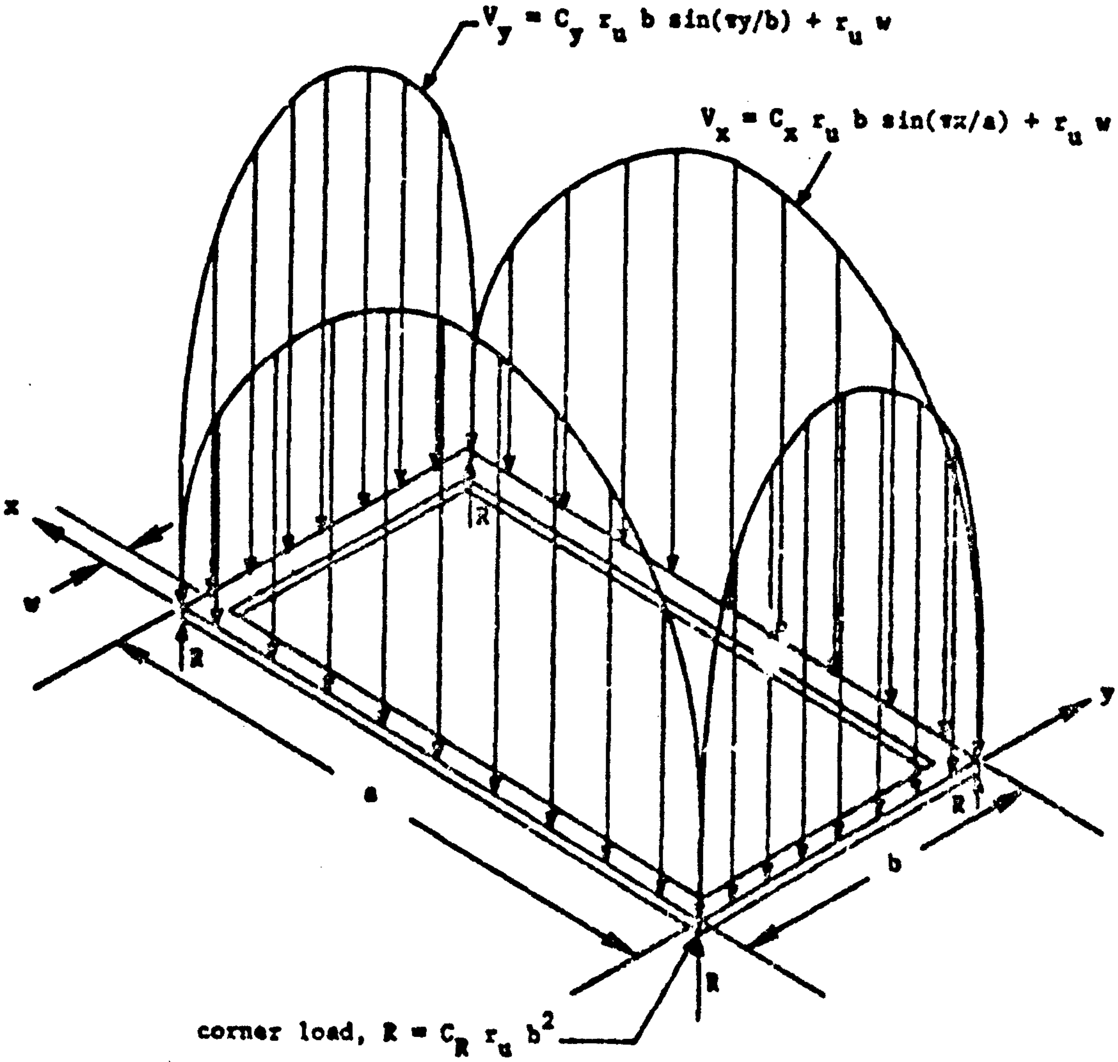

Figure 25. Frame design loading to be applied by the pane to the frame.

BLAST RESISTANCE OF LAMINATED WINDOWS

David L. Tilson and James M. Watt, Jr.
US Army Engineer Waterways Experiment Station
Vicksburg, Mississippi 39180

ABSTRACT: Windows that have some degree of resistance to forced entry are used in US Embassy buildings throughout the world. Because of the increase of worldwide terrorism and the concern for US personnel in foreign service, the US Department of State has funded research to determine the blast resistance of these window systems. This research will be used to develop a standard method for analyzing laminated glazings and their framing systems.

Static tests were conducted, subjecting each window/frame system to a hydrostatic pressure, to determine the nonlinear resistance function. Using these resistance functions, single-degree-of-freedom analyses were performed to predict dynamic response, and a dynamic test was conducted to verify the analysis. The analysis was accomplished by using a computer code (SDOF) developed at the US Army Engineer Waterways Experiment Station. On 17 December 1987, a dynamic test was conducted to verify this analysis.

For three of the four windows, the results from the dynamic test were in good agreement with the predictions from the SDOF code. For these three windows the maximum difference between predicted and actual deflection was 16 percent. From these results, it was concluded that a single-degree-of-freedom analysis, employing a resistance function developed from static test, predicts reasonably well the dynamic response of window systems.

BLAST RESISTANCE OF LAMINATED WINDOWS

David L. Tilson
James M. Watt, Jr.
US Army Engineer Waterways Experiment Station
Vicksburg, Mississippi

INTRODUCTION

Windows that have some degree of resistance to forced entry and high-powered rifle are used in US Embassy buildings throughout the world. Because of the increase of worldwide terrorism and the concern for the safety of US personnel in foreign service, there is a need to determine the blast resistance of these window systems. This information would identify the level of blast protection of current window systems and would provide a means for accessing future window needs.

A study was conducted to determine the blast resistance of four window systems and to develop a method for predicting their dynamic response. The method is to conduct static test, subjecting each window/frame system to a hydrostatic pressure, to determine the nonlinear resistance function. Using this resistance function, a single-degree-of-freedom analysis is performed to predict dynamic response, and a dynamic test is conducted to verify the analysis. This paper presents the results of the study and a comparison of analysis data to test data.

STATIC TESTING

Static Test Device

The static test device was designed to subject a test article to a maximum hydrostatic pressure of 200 psi. The three parts of the device are a U-framed base, a wall slab, representing the building; and a hold-down slab. An isometric view of the static test device is shown in Figure 1.

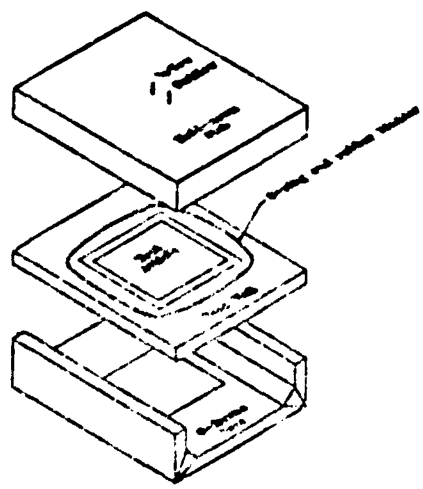

Figure 1. Isometric View of Static Test Device

The idea is to test a window system as if it were installed in a building. Once the window is installed in a slab, ensuring conformance with exact manufactures installation procedures, the hold-down slab is placed on top and the two slabs are bolted together. A chamber is formed between the test article and the bottom of the hold-down slab. The hold-down slab is equipped with two vertical vent pipes, one provided for pumping water into the chamber and the other to allow the evacuation of air from the chamber. When the chamber is completely filled with water, the outflow pipe is closed and a uniform hydrostatic pressure is provided over the entire window system. Two pressure gages are mounted in the bottom of the hold-down slab and are used to measure the hydrostatic water pressure of the chamber.

To insure a water tight seal in the chamber, a rubber bladder is assembled over the test article and sealed with a silicon caulk. An O-ring is then placed around the edge of the bladder to seal any irregularities in the concrete of the two slabs. A maximum pressure of 300 psi has been sustained with this sealing procedure.

The U-framed base was designed to allow for locating instrumentation beneath the test window. A 1/4-inch thick steel plate was embedded in the concrete, allowing for the welding of gage supports in the required locations. This design also allows clearance for videotape equipment to be used in recording the response of the test article.

The test wall, housing the windows, represents the Department of State's current embassy wall design. The wall was constructed with reinforced concrete and has a thickness of 8 inches. The reinforcement used is #5 reinforcing bars (5/8-inch diameter) that maintains a horizontal and vertical spacing of 5 inches. (See Reference 1.)

A design requirement for the hold-down slab was that the centerline deflection could not exceed 1/10-inch at 200 psi. Using plate theory for a simply-supported slab, it was calculated that the hold-down slab would be required to be 18-inches thick. The reinforcement used in the fabrication was #5 bars, consisting of 3 mats. The horizontal and vertical spacing was maintained at 5 inches (center to center). The concrete specified was a 5000 psi mix at 28 days.

Test Articles

The four test articles were commercially available windows that were designed to resist ballistics and forced-entry. All the windows were 42-inches in width and 48-inches in length. The clear span varied depending on the frame and amount of frame bite placed on the glazings. The laminated glazings contain sheets of polycarbonate and various types of glass. These glazings varied in nominal thickness from 1-1/8-inches to 1-15/16-inches, depending on the number and thickness of each layer. Figure 2 shows a cross-sectional view of each glazing type.

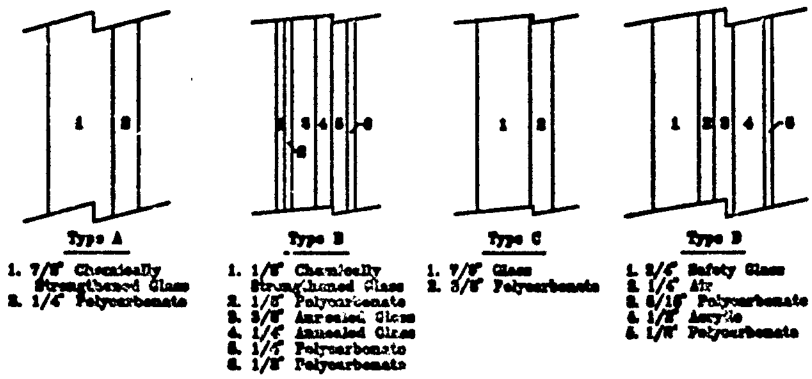

Figure 2. Cross-Sectional View of Glazing Types

Static Testing

Each window system was subjected to a hydrostatic pressure that produced failure. Failure was taken to be the point at which the window would not resist any additional load. In three tests, the failure mechanism for the window system was shear in the frame anchorage. The other failure mechanism was bending of the inner frame of a two frame system. This use of the inner frame was to maintain the bite on the glazing, but allowed for reglazing when required. See Table 1 for a summary of the static test results.

Table 1. Static tests summary.

Type Glazing	Avg. Chamber Pressure (psi)	Maximum Centerline Deflection (in)	Maximum Centerline Strain (microin/in)
A	13.50	2.15	4500
A Retest	15.25	4.00	7800
B	19.55	1.34	960
C	27.00	2.07	5625
D	22.30	2.47	6100

Single-Degree-of-Freedom Analysis

SDOF Analysis

The determination of the dynamic response of a simple structural system using numerical procedures is presented in detail in References 2, 3, and 4. More complex systems, such as the window systems reported herein, can also be analyzed with a single-degree-of freedom, provided an accurate representation of the load function $P(t)$, resistance function (load-deflection curve), and mass (M), can be obtained.

The selection of the idealized spring-mass system in Figure 3a is such that the deflection of the mass, y, is the same as the centerline deflection of the window glazing. From this freebody diagram (Figure 3b), the equation of motion is derived and then solved numerically.

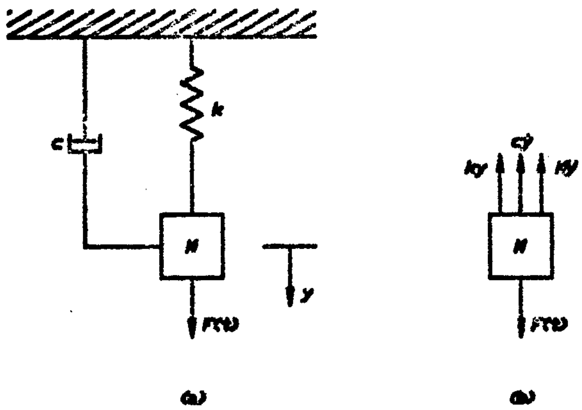

Figure 3. Single-Degree-of-Freedom Freebody Diagram

Resistance Functions

To develop a resistance function from the static tests, the centerline deflection was plotted against the chamber pressure loading the window. This resistance function is simplifyed by selecting specific points to be used in the SDOF code. Figure 4a through 4d show the actual load-deflection curves and the simplified resistance functions used in the SDOF analysis.

The specific points used in the resistance functions were points where layers of glass broke which caused an instant reduction in chamber pressure and where the pressure is sustained and begins to increase (Figure 4a - 4d). The maximum deflection of the resistance function was that point where the window could not sustain any additional loading. The unload slope used in the SDOF analysis was selected as the initial slope of the load-deflection curve before any glazing broke.

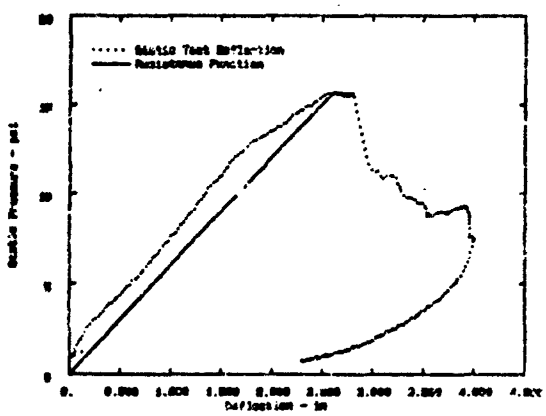

(a) Type A Glazing

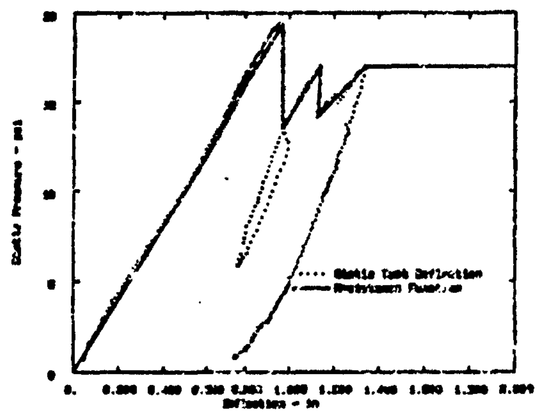

(b) Type B Glazing

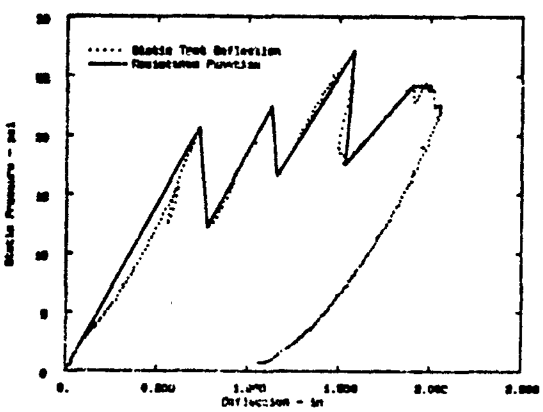

(c) Type C Glazing

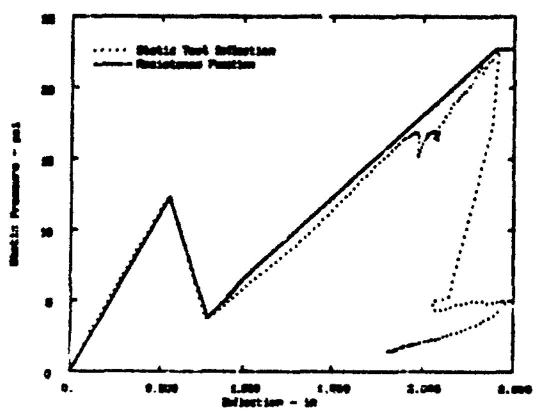

(d) Type D Glazing

Figure 4. Resistance Function for Each Glazing Type

Single-Degree-of-Freedom Code

The SDOF code was developed at the Waterways Experiment Station and uses the procedure described in Reference 2. The procedure is referred to as the constant-velocity, or lumped-impulse, procedure. The code requires the following information to preform the calculation: mass (M), area (A), load-mass factor (K_{LM}), percent of damping (c), time step (d_t), resistance function $f(R)$, and forcing function $P(t)$.

In the pretest analysis of the window systems, the calculations are done with the entire mass of the window glazing and frame. The total mass was used because there was some measured deflection in the frame before the anchorage sheared.

The area was calculated by using the length and width of the frame (48 in. by 42 in.). The values for the load-mass factor and percent of damping were chosen to be 0.67 and 0.03, respectively. The K_{LM} selected is for a uniformly loaded, two-way slab where the strain in the polycarbonate is in the elastic range (Reference 2). The percent of damping was chosen arbitrarily from discussions with personnel familiar in the response of glazings. A numerical iterative time step of 0.0001 seconds was used for the calculation.

The forcing function $P(t)$ was derived from equations developed from Reference 3. The analysis was performed by using a reflected pressure-time history, with and without clearing time[1], for a hemispherical high explosive (HE) charge of TNT weighting 1300 lbs. The distance from the HE charge to the test structures was selected as 100 ft. This HE charge and range produced a positive reflected peak pressure of 29.4 psi and a negative phase peak pressure of -3.1 psi. Figure 5 shows the calculated pressure-time history.

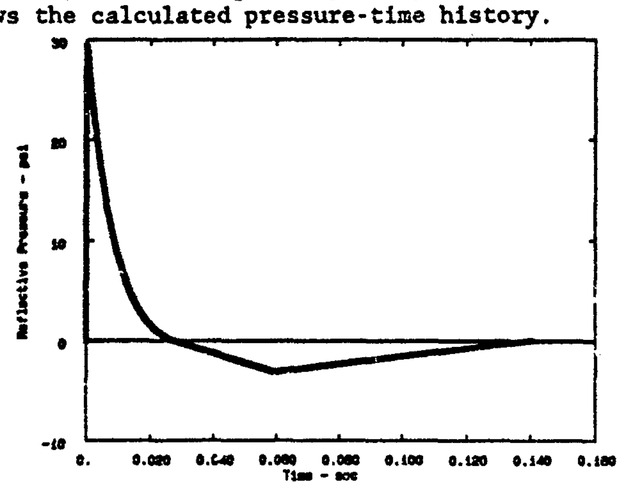

Figure 5. Calculated Pressure-Time History for 1300 lbs of TNT at a Range of 100 ft.

1 "The reflection effect may be assumed to diminish linearly and to disappear at the clearing time t_c, which is approximately $t_c = 3S_c/U$ where U is the shock front velocity and S_c is either the height of the reflecting surface aboveground or one-half the width, whichever is smaller." Reference 3

Charge Design

In determining the size of the charge, several assumptions were applied in the analysis. The first assumption was that an average resistance function represent the four windows. To arrive at an average resistance function, the individual static resistance functions were plotted and a hand fitted average resistance function was determined (Figure 6). It is seen from this plot that three of the four curves are very similar to the hand developed resistance function, however the fourth is well below the average curve. In the second assumption, a limit of 2 inches was selected for the allowable peak window deflection.

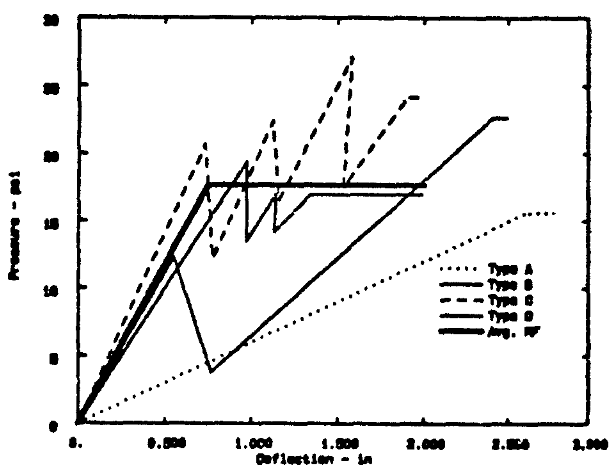

Figure 6. Development of Average Resistance Function

In determining the amount of high explosive required to produce 2 inches of deflection, a series of pressure-time histories were calculated (Reference 3) by using different weights of TNT at a range of 100 ft. Once these *P(t)'s* were calculated, an SDOF analysis was conducted. The input to the SDOF code consisted of the average resistance function, individual properties for each window, and the different loading functions. From these calculations, the peak dynamic deflections were determined and compared. This procedure indicated that a charge weight of 1300 lbs of TNT at a standoff of 100 ft would be required to produce the desired dynamic window response.

Window Analysis

Once the high explosive charge for the test was determined, a single-degree-of-freedom analysis was performed on each of the window/frame systems using the respective properties of that window. The results of the analysis are shown in Table 2 and represent the expected response of each window.

Table 2. SDOF analysis results.

Type Glazing	Predicted Peak Dynamic Deflection (in)	
A	4.10*	3.01#
B	2.25*	1.30#
C	1.64*	1.59#
D	2.70*	2.15#

* Pressure-Time History without clearing time
\# Pressure-Time History with clearing time

Dynamic Testing

A dynamic test was conducted on Range 37 at the Fort Polk Military Reservation, LA. The high explosive charge used in the test was 1092.5 lbs of Composition - 4 (C-4). The charge weight was derived by using an equivalent factor for TNT of 1.19 (Reference 3). This factor is for matching the impulse between TNT and C-4 explosives. The dynamic test setup, Figure 7, shows the two reaction structures and windows as viewed from a point behind the high explosive charge.

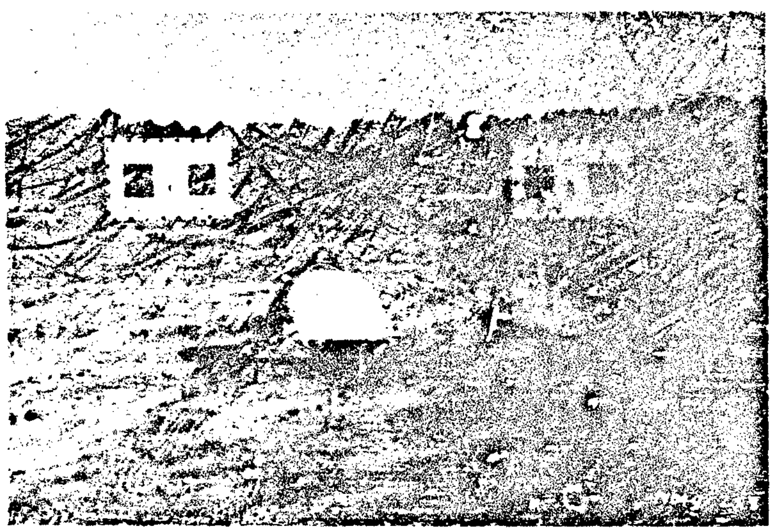

Figure 7. View of the Dynamic Test Setup

A total of 14 pressure gages were used (7 per structure) to measure the pressure-time history across the face of the structures and windows. The data records were processed and an average pressure across the face of the windows was determined. To establish the average pressure-time history for each structure, the time of arrival for each record was adjusted to coincide and the records were averaged. Figures 8a through 8d show a comparison of the calculated reflected pressure and impulse (with and without clearing time) and the averaged test data.

Two deflection gages were used to obtain the centerline deflection for each glazing type. The gages used were Trans-Tek Linear Variable Differential Transformers (LVDT) with an total travel of 6 inches.

DISCUSSION OF RESULTS

Table 3 contains the window response results from the SDOF pre- and posttest analyses and the test data. A review of this data reveals several interesting points.

Table 3. Comparison of Actual and Calculated Deflection

Type Glazing	Dynamic Test Deflection (in)		Pretest Predictions (fm Table 2)		Posttest Analysis (in)	
	Gage 1	Gage 2				
A	4.30	3.90	4.10*	3.01#	3.24	3.59@
B	1.90	1.98	2.25*	1.59#	1.60	1.75@
C	1.25	1.26	1.64*	1.30#	1.38	1.47@
D	0.89	0.90	2.70*	2.15#	2.17	2.31@

* Pressure-Time History without clearing time
\# Pressure-Time History with clearing time
@ Average Pressure-Time History and reduced mass (glazing only)

It was concluded from these comparisons that the window/frame systems were subjected to a reduced pressure (Figures 8a - 8d). One possible reason was that the clearing time effects at the top and sides of the reaction structures were neglected. Another reason was that the equivalence factor in matching the impulse produced with TNT and C-4 is not an exact number.

Two deflection gages were used to record centerline displacement for each of the window glazings. The successful survival of both deflection gages and their close agreement gives confidence in the accuracy of the data.

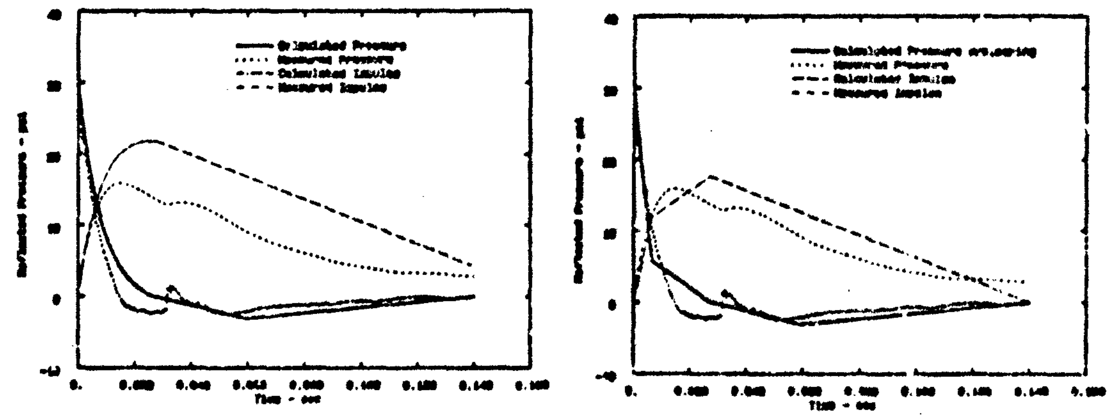

(a) (b)

Reaction Structure 1

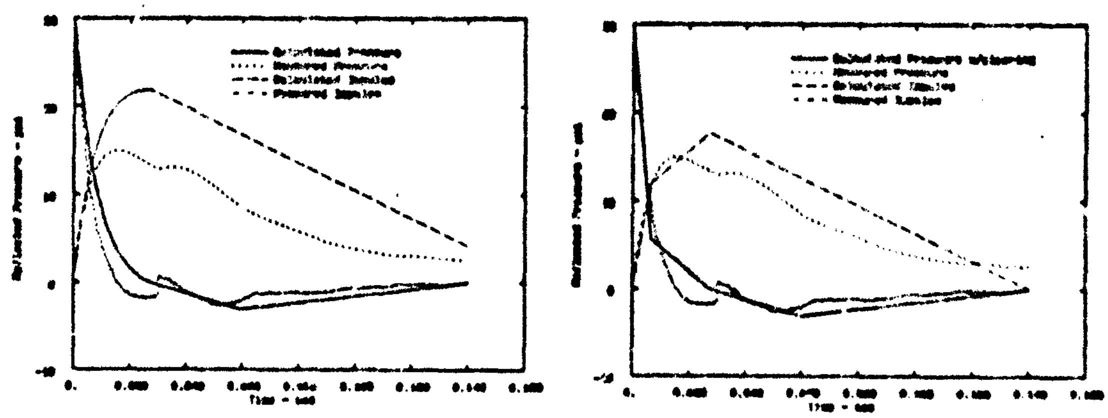

(c) (d)

Reaction Structure 2

Figure 8. Comparison of P-T Histories

Window glazing types A, B, and C behaved in a very consistent manner, whereas, the type D glazing appeared to depart significantly from the predicted behavior. Type D glazing is comprised of two glazing panels separated by an air gap. It appears that this glazing geometry will require some modification to the SDOF before better agreement can be achieved.

For glazing types A, B, and C the following observations can be made. First, one pretest SDOF analysis was calculated using a pressure-time function $P(t)$ (Reference 3) without considering clearing time of the shock wave. The $P(t)$ had a greater impulse and resulted in greater response of the windows. However, when the $P(t)$ was corrected for clearing time, the impulse was reduced and the response was calculated to be smaller. With clearing time accounted for, the SDOF calculation is in closer agreement with the measured test data.

A posttest SDOF calculation was conducted using the average of the measured pressure-time histories for the respected reaction structure. This calculation identified the difference in the window response as a function of the calculated $P(t)$, with clearing time, and the measured $P(t)$. The response calculated using these two pressure-time histories was in very close agreement.

As previously stated, the mass selected for the pretest SDOF calculation was taken as the total mass for the glazing and frame. A posttest SDOF calculation was done using only the mass of the glazing. This reduction in mass better represents the major responding element of the window system and resulted in a closer agreement between calculated and measured data.

Conclusions

The response of type A, B, and C glazings and frames were predicted very well by the SDOF code. Better agreement between the calculated and measured response can be achieved by using the calculated $P(t)$, with clearing time, and the mass of the glazing only.

The good agreement between calculated and measured window response data suggest that the resistance function developed from static testing correctly described the spring (k) of the SDOF system.

Although this verification of the static test/SDOF procedure is based on a limited number of tests, it appears to be a valid method for accessing the blast capacity of window systems.

ACKNOWLEDGMENTS

This research was sponsored by the Department of State, Physical Security Branch, Washington D.C. under the project entitled "Blast Standards Verification Program." The technical monitors were Messrs. Larry Binner, Jerry Felt and Gerald Meyers. This work was accomplished by the US Army Engineer Waterways Experiment Station (WES), Structures Laboratory, Structural Mechanics Division. Project Manager was Mr. James M. Watt, Jr. (WES). Project Engineers were Messrs. David L. Tilson and Lebron Simmons.

REFERENCES

1. US Department of State, Bureau of Diplomatic Security. 1986, "Physical Security Standards Handbook (Limited Official Use)," Washington, D.C.
2. Biggs, John M., "Introduction to Structural Dynamics," McGraw-Hill Book Company, New York, 1964.
3. "Fundamentals of Protective Design for Conventional Weapons," Technical Manual (TM) 5-855-1, Department of the Army, Washington, D.C.
4. "Structures to Resist the Effects of Accidental Explosives" Technical Manual (TM) 5-1300, Department of the Army, Washington, D.C., 1969.

OPTIMAL DESIGN OF AMMUNITION FACILITIES FOR CONFLICTING REQUIREMENTS OF SURVIVABILITY AND SAFETY

REUBEN EYTAN

EYTAN BUILDING DESIGN LTD

TEL AVIV, ISRAEL

ABSTRACT

The paper deals with the optimal design of ammunition storage and facilities for conflicting requirements of safety and survivability. The structures discussed are storage magazines and assembly/maintenance facilities and represent actual projects already constructed worldwide.

Three case histories involving aboveground and underground facilities designed to withstand different survivability requirements are presented and discussed.

The conflicting safety and survivability requirements are described and our solutions for optimal design are presented.

INTRODUCTION

In the design of ammunition magazines and ammunition related production/assembly/maintenance facilities we have encountered lately conflicting requirements of safety and survivability.

The safety requirements aim to reduce the risks to surrounding installations, for both life and property, in case of an accidental internal explosion.

The survivability requirements aim to reduce the risks to the ammunition facility and its personnel from different external types of attacks.

In many cases, the safety and survivability requirements are conflicting and the designer is faced with the task of finding such features that will be optimally adequate for both safety and survivability.

In this paper we are presenting three cases histories from our practical experience, pointing out the conflicting safety and survivability requirements and the solutions we have found in each case.

We are presenting only cases of survivability for conventional warfare and terrorist attacks and do not address cases of survivability for chemical, biological and nuclear warfare.

FIRST CASE HISTORY - STANDARD ABOVEGROUND AMMUNITION MAGAZINE

Our first case history is the design of standard aboveground ammunition magazines with the "normal" safety requirements covered by the safety distances codes and with the survivability requirement of withstanding direct hits of artillery shells.

In order to satisfy the safety requirements the magazines were designed with a roof soil cover of 60 cm. (see figure no. 1).

This however was not sufficient for the survivability requirements; the above soil cover could not withstand the direct hit effects of an artillery shell.

Therefore a design consisting of protective layers was considered : a top burster layer which would stop the artillery shell penetration and a soil absorbtion which would absorb the explosion energy and reduce the blast pressures reaching the magazine roof to acceptable levels. (see figure no. 1).

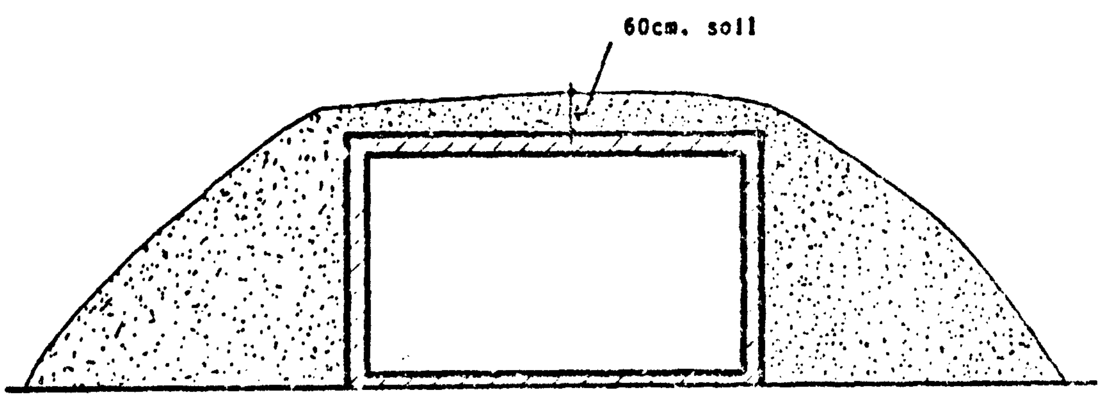

a. Normal roof soil cover

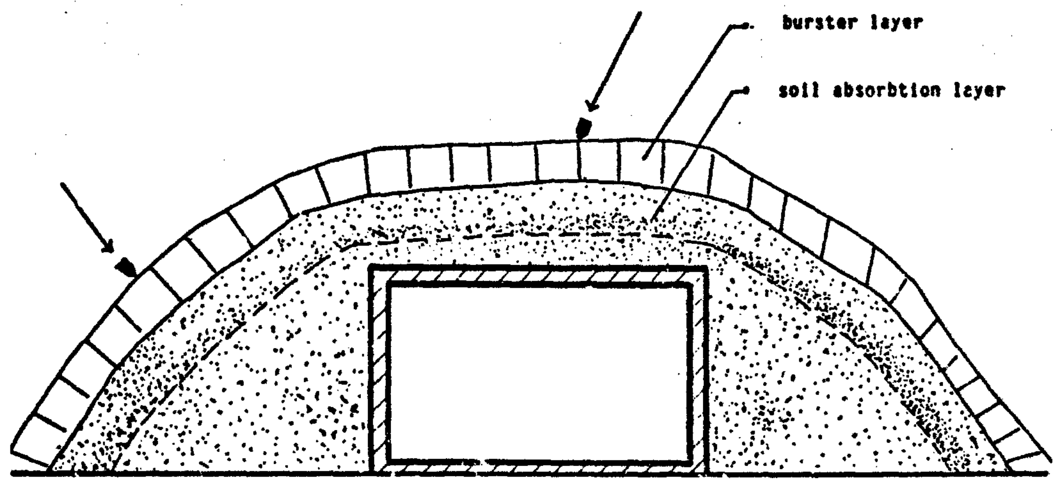

b. Protective layers roof cover

Figure no. 1 - Aboveground standard ammunition magazine

Obviously, the survivability requirement expressed in the design of additional protective layers led to a much stronger magazine structure required to carry the dead loads of the protective layers and the blast pressures induced by the artillery projectile explosion.

The most cost-effective solution for the burster layer is known to us to be the use of rock rubble with appropriate rock sizes and arrangement. However, the use of rocks presents a conflict with the safety requirements due to the fact that following an internal accidental explosion the rocks in the burster layer would be thrown at large distances and would provide an increased risk to the surroundings (see figure no. 2).

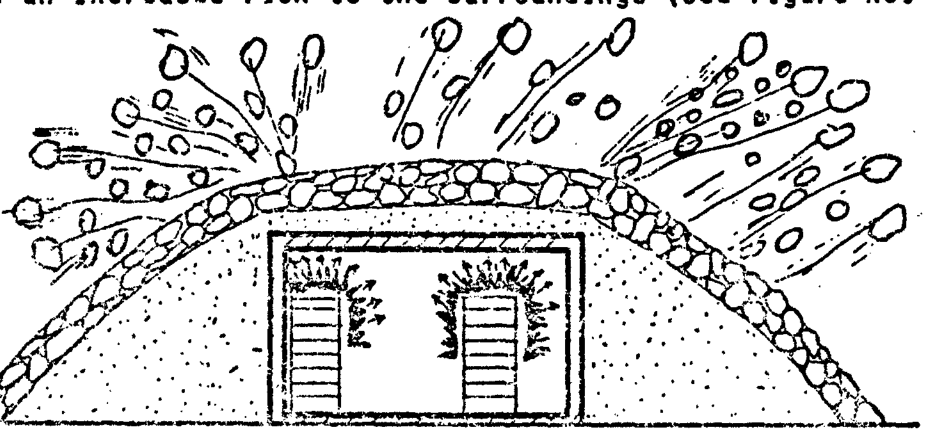

Figure no.2 - Increased risks from the protective layers rock

The solution required to respond to the conflicting requirements for safety and survivability was a roof configuration that would provide the required resistance to the artillery shell direct hit effects on one hand and will not increase the risks to the surrounding installations on the other hand.

From the different solutions considered in this case, two were found to be feasible and cost-effective :

a. A "layered" structure consisting of a concrete-air-concrete construction (see figure no. 3).

b. A protective layers configuration with a burster layer consisting of reinforced concrete or rocks in gabions or rocks bonded by mortar (see figure no. 4).

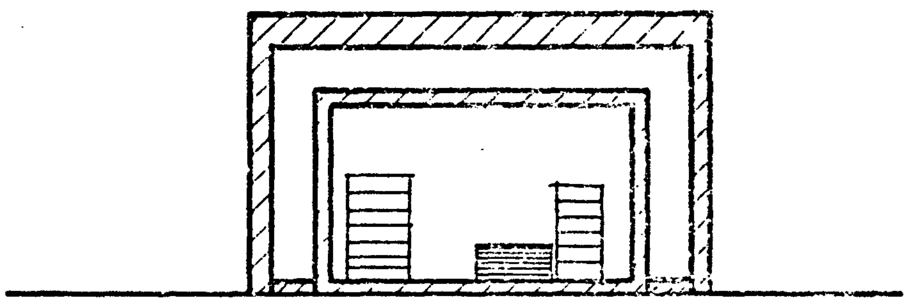

Figure no. 3 - Layered structure

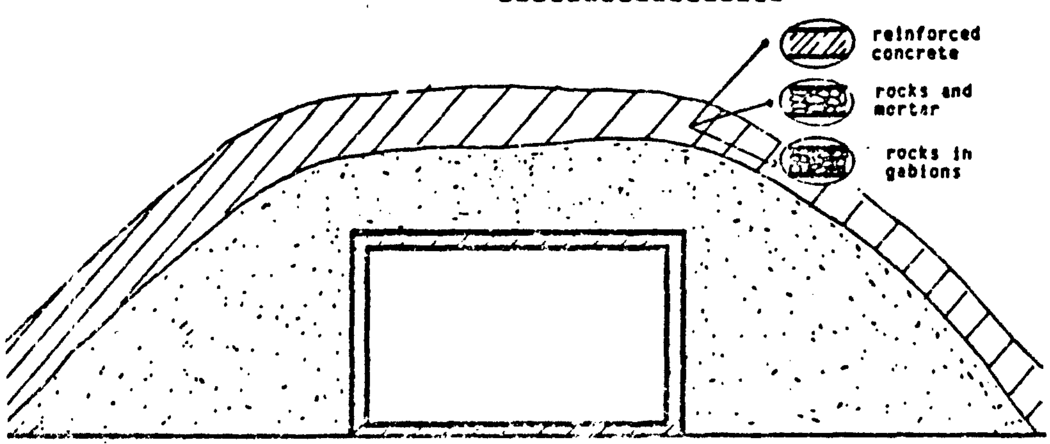

Figure no. 4 - "Safe" protective layers

The above described "safe and hardered" ammunition facilities were designed in all the described alternatives and large numbers of structures were built in numerous locations.

SECOND CASE HISTORY - ABOVEGROUND AMMUNITION FACILITY

Our second case history is the design of an aboveground ammunition related facility with the "normal" safety requirements covered by the safety distances codes and with the survivability requirement of withstanding forced entry terrorist attacks.

The safety requirements included the controled release of blast pressures from an accidental internal explosion which was achieved by designing "normal" venting elements in the structure's walls. These weaker elements normally designed as brick/masonry construction, light panel walls, etc. would be thrown outwards by the internal explosion in a pre-designed direction and will reduce the explosion effects toward surrounding installations (see figure no. 5).

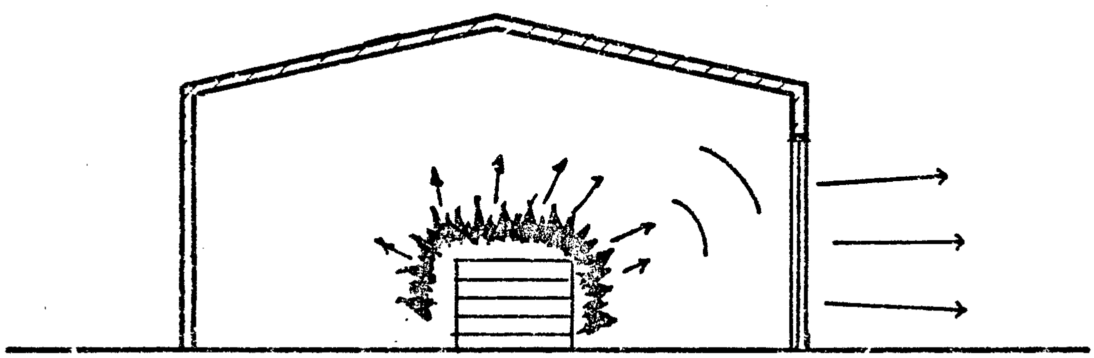

Figure no. 5 - Weak venting wall elements

However, these weak wall elements presented no obstacle for the case of terrorist forced entry and could not respond to the survivability requirement.

The conflict between the safety and survivability requirements was solved in the described case by the following two features :

a. The design of roof venting elements for most of the installation's internal areas.

b. The design of wall venting elements made of strong resistant materials withstanding the defined threats but with specially designed connections which would allow the elements blow-out but would not be easily defeated by the attackers. (see figure no. 6).

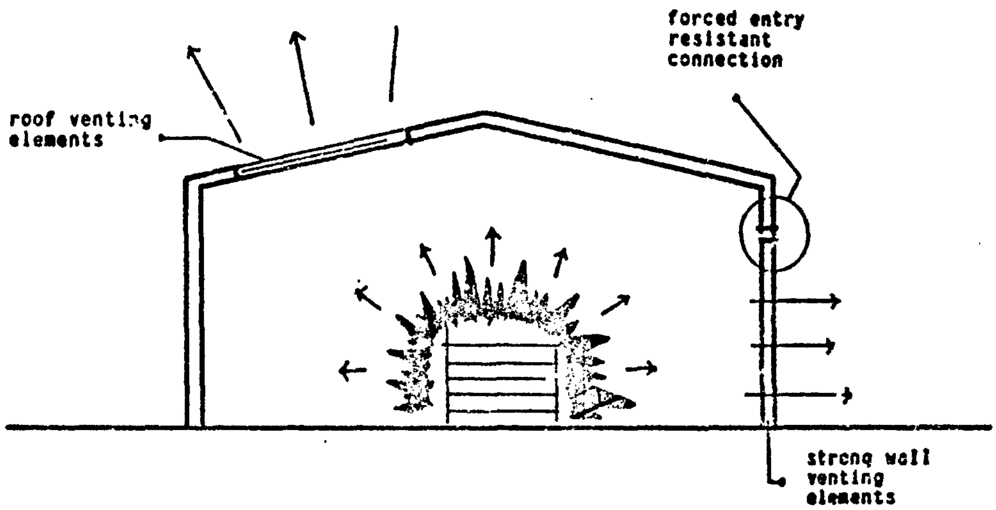

Figure no. 6 - Forced entry resistant design

The possibility of terrorist forced entry through the weak roof venting elements was minimized by the provision of anti-climbing measures and intrusion detection and alarm systems, as well as by appropriate camouflage and deceiving measures.

The above described "terrorist forced entry resistant" ammunition related facilities were designed and built in significant numbers and locations.

THIRD CASE HISTORY - UNDERGROUND AMMUNITION FACILITY

Our third case history is the design of an underground ammunition related facility with the "normal" safety requirements covered by the safety distances codes and with the survivability requirements of withstanding direct hits of air bombs.

The safety requirements were fully satisfied by designing the facility deep underground with controled blast and debris propagation at the entrances.

The survivability requirements were fully satisfied by designing the facility deep underground in rock caverns with sufficient rock cover and blast resistant entrances. (see figure no. 7).

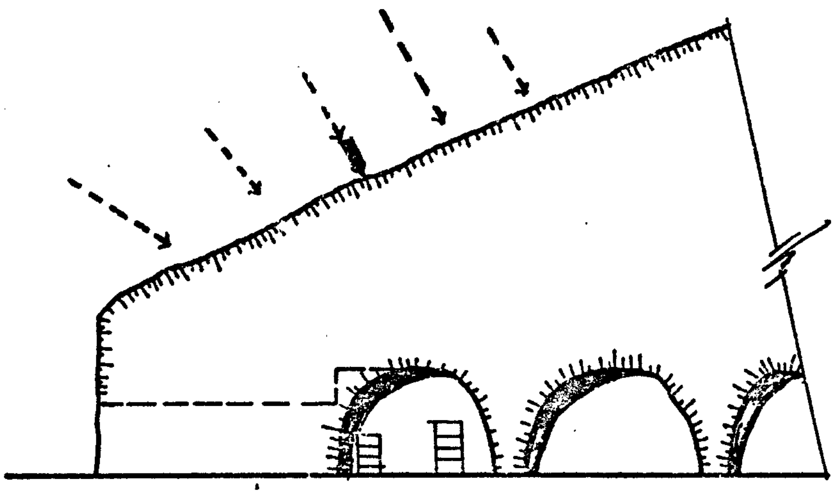

a. Survivability by rock cover

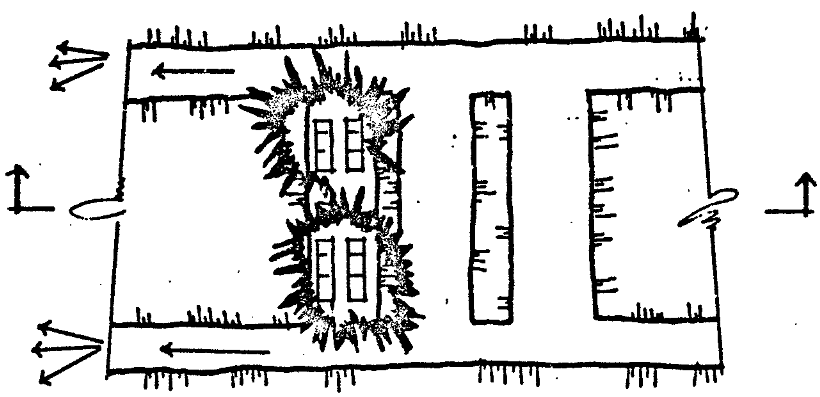

b. Safety by controled entrances design

Figure no. 7 - Underground rock caverns facility

Although it seemed that both the safety and survivability requirements were fully satisfied, at the stage of master planing it was realized that a new survivability/safety problem was created : in the case of an internal explosion induced by accident or sabotage, the damages to the internal equipment and installations as well as the possible number of injured personnel would be extensive with "normal" internal designs.

The solutions for minimizing these risks was to change the facility layout in such a way that the effects of an internal explosion will influence only a controled area and to provide strong explosion-resistant elements between the internal controled areas (see figure no. 8).

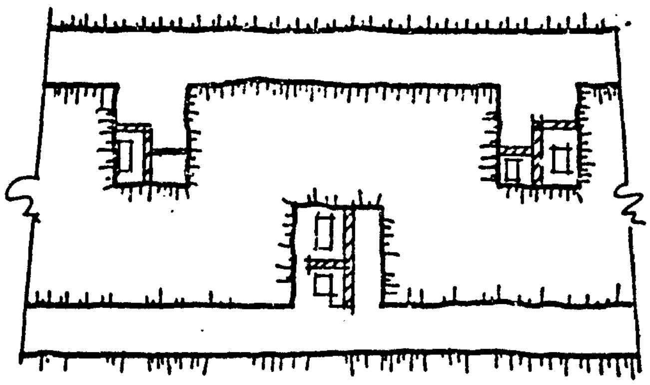

Figure no. 8 - Optimal cavern layout and strong internal division elements

CONCLUSIONS

We have shown some of the problems occuring in the design of ammunition storage and facilities due to the conflicting requirements of safety and survivability.

We have described three of our case histories with the solutions reached to provide the optimal response to both the safety and survivability requirements.

These solutions, based on practical experience and engineering judgement, proved to be cost-effective in many projects, worldwide.

ACKNOWLEDGEMENT

I would like to thank my wife and partner, Mrs. Micaela Eytan, Chief Architect and Director of Eytan Building Design Ltd, for her help in preparing this paper.

Paper Distributed at the:

Twenty-Third DoD Explosives Safety Seminar
Atlanta, Georgia

LITHIUM BATTERY TEST FACILITY PRELIMINARY HAZARDS ANALYSIS

by

C. James Dahn
Safety Consulting Engineers, Inc.
Rosemont, Illinois 60018

ABSTRACT

A Preliminary Hazards Analysis, Energy Trace and Barrier Analysis of the Lithium Battery Test and Analysis Facility at the Naval Weapons Support Center in Crane, Indiana yielded an optimum building design concept which provides ease of operation without compromising safety. A one building, one-story facility was selected which will satisfy the safety criteria provided good controls are followed for capturing noxious gases and scrubbing them without leakage. Three safety zones, divided by two protective vapor barriers, were established to protect office personnel from potential noxious vapor leaks in test areas. Also, blast protection in the hazardous test cells and the wall adjoining the nonhazardous laboratory areas was incorporated. Vapor containment and scrubbing, in the hazardous test cells, will be required. Vapor alarms will be installed in all personnel occupied areas, including entrances to the office area and its associated HVAC system.

Over 253 hazard conditions have been identified, with appropriate corrective actions, in the upgraded preliminary hazards analysis.

1.0 INTRODUCTION

Safety Consulting Engineers, Inc. conducted a Preliminary Hazards Analysis (PHA) on the Battery Test and Analysis Facility to be built at the Naval Weapons Support Center in Crane, Indiana.

The purpose of the Preliminary Hazards Analysis was to evaluate potential safety hazards and recommend controls to the upgraded facility design so that safety corrections can be made during the design phase. By incorporating safety features in the design of the facility, the potential of personnel injury and the cost of installing safety equipment are significantly reduced.

This Preliminary Hazards Analysis is prepared in accordance with Task 202 of MIL-STD-882B.

An Energy Trace and Barrier Analysis (ETBA), which systematically identifies the energy sources in the facility that could lead to potential hazards, was conducted. Based on the ETBA results, undesired events were identified and evaluated. Also, recommended controls to prevent the following were developed:

1. Death and/or serious injury to personnel.
2. Serious damage to facilities and/or equipment resulting in large dollar loss.

1.1 Project Description

Military Construction Project P-217, Lithium Battery Test Facility, will provide a new facility to support the life-cycle engineering and testing of lithium batteries. Testing and evaluation of lithium batteries must be performed for all

phases of the weapon system life-cycle. Lithium batteries are discharged by simulating weapon system load profiles to verify performance specifications. Lithium batteries are also dropped, punctured, short-circuited, charged and heated to determine safety characteristics under abusive conditions. Failure analysis and dissection are performed to assess and evaluate internal configuration and quality.

Hazardous lithium battery abusive testing had been conducted in an outdoor facility located in a remote portion of the Crane Complex. This outdoor facility is inadequate because it was not designed for repeated deflagrations or to contain the dangerous gases and fragmentation. Because the engineering analysis and computer support function are located twelve miles away, excessive equipment and personnel transport time was consumed between these facilities severely hampering battery test productivity. Thus a centralized test and analysis facility was persued.

2.0 HAZARDOUS CONSIDERATIONS

2.1 Evaluation

Various hazardous conditions associated with lithium batteries can arise during battery testing.

A runaway reaction of the lithium and the electrolyte can occur under easily predictable conditions (e.g., externally applied heat, shorting, charging, and similar abusive environments), or under unpredictable conditions such as internal failure of a defective or peculiarly damaged cell. Nearly all runaway reactions result only when the lithium anode becomes

heated to, or near, its melting point of about 180°C. The possible consequences of such a reaction can be one, or a combination of the following:

a. Slow release of minimal, moderate, or large quantities of highly corrosive and noxious smoke and gases.

b. Rapid venting of the smoke and gases, with potential of pressure build-up if in restricted enclosures.

c. An explosive pressure spike or shock wave, and possible flying projectiles of battery cell parts, and/or associated fixtures.

When batteries are abusively tested, the likelihood of a destructive reaction increases significantly. Thus the new test facility design must completely contain the maximum potential explosion to that no corrosive vapor release will occur.

Unfortunately, the safety provisions normally selected to control these types of hazards (blowout panels) tend to become compatible with maintaining vapor containment. Test cells and work rooms, where noxious gases can be generated, must be completely sealed to prevent the gases from entering areas occupied by personnel. Suitable vapor cleaning devices must be utilized to protect the air environment where personnel are working. Normally, such environmental protection devices are not blast resistant.

An initial survey of the lithium battery industry revealed that some facilities were built to handle moderate sized cell runaway reactions by incorporating both blast resistant and vapor scrubbing provisions.

2.1.1 Blast Output

Planned activities dictate that the maximum size battery to be tested in the proper facility would yield blast output less than eight pounds TNT equivalent.

Thus from a blast standpoint, two of the hazardous test cells (15' x 20' x 10' high) are to be designed to withstand the equivalent detonation of ten pounds of TNT.

The rest of the hazardous test cells (15' x 20') are to be designed to withstand the equivalent detonation of five pounds of TNT. One test cell will be 24 feet high to accommodate impact testing; while the others will be 10 feet high.

The control of released noxious vapors is a more challenging problem.

2.1.2 Toxic Gases

Lithium-Sulfur Dioxide (LI/SO_2) batteries can vent Sulfur Dioxide gas. Lithium-Thionyl Chloride ($LI/SOC1_2$) batteries can vent Thionyl Chloride, which breaks down into SO_2, and HCL with LI_2O particles in the smoke.

Based on Navy upgrade data, one battery design containing eight liters of Thionyl Chloride ($SOC1_2$), is the largest battery to be tested in the facility. Noxious gases released from this battery would be $SOC1_2$ along with its decomposition products SO_2 and HCl. Because the amount of each gas would vary depending on conditions, safe distance was estimated using the maximum volume of each gas that could be formed.

Assuming all the $SOC1_2$ becomes gas and none of it decomposes, 87.22 cu. ft of $SOC1_2$ gas will be released

at Standard Temperature and Pressure (STP). No SO_2 and HC1 will be present. The maximum amount of SO_2 and HC1 will be formed if all the $SOC1_2$ is decomposed in the presence of water. The volume of SO_2 and HC1 released would be 87.22 and 174.44 cu. ft respectively.

The estimated safe distances as shown in Table 1 varies greatly from 680 feet to 75 feet depending on which gases are present and how they are dispersed into the air.

3.0 BUILDING CONCEPTUAL DESIGN SAFETY STUDY

Three different building designs were analyzed to determine which concept would be safest for operation in case of noxious vapor release or an explosion. The Energy Trace and Barrier Analysis technique was used for each concept to determine which was safest for production without compromising operational effectiveness.

The following building designs (see Figure 1) were under consideration:

(1) One building with two stories

(2) One building with one story

(3) Two buildings (administration building separate from testing and lab areas)

The following considerations were used to determine safe separation distances from personnel:

- Radius of noxious gas release from battery undergoing tests in test cells.

- Explosion blast from battery undergoing tests in test cells.

TABLE 1

ESTIMATED SAFE DISTANCES FROM A

MAXIMUM BATTERY SIZE DURING

NOXIOUS GAS LEAKAGE

NOXIOUS GAS	SAFE DISTANCE USING HEMISPHERE MODEL	SAFE DISTANCE USING CYLINDER MODEL (CYLINDER HEIGHT) (6 ft)	SAFE DISTANCE USING CYLINDER MODEL (CYLINDER HEIGHT) (12 ft)
HCl @100 ppm	94 ft	309 ft	215 ft
SO_2 @100 ppm	75 ft	215 ft	152 ft
$SOCl_2$ @10 ppm	161 ft	680 ft	481 ft

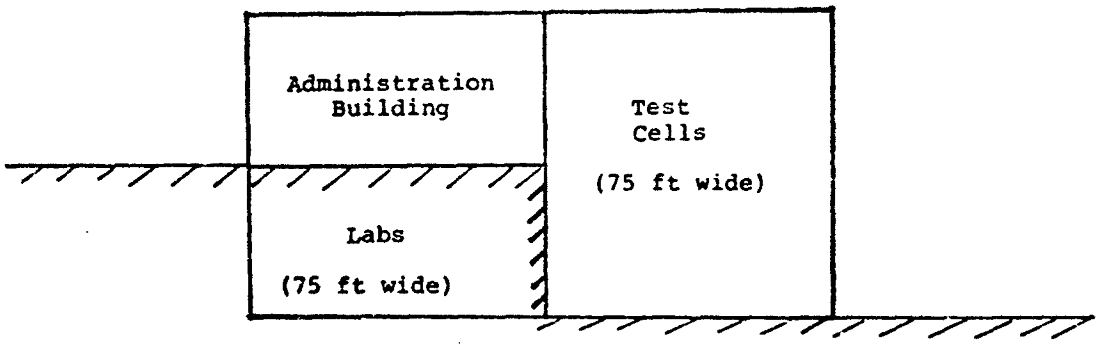

Configuration 1. One building with two stories

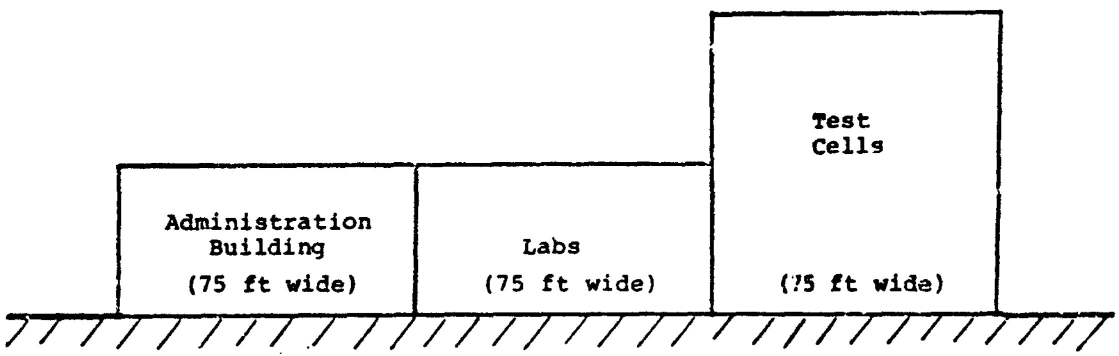

Configuration 2. One building with one story

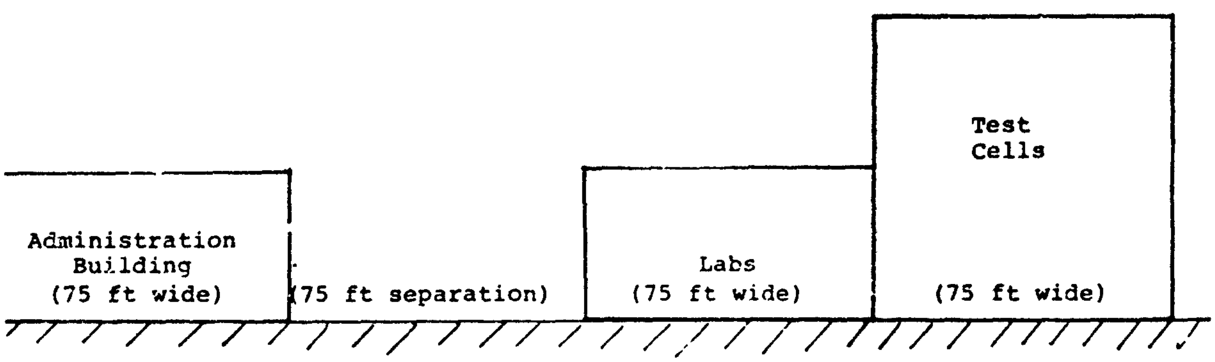

Configuration 3. Two separate buildings

Figure 1. Lithium battery test facility building configurations.

3.1 Explosion Considerations

Building wall and roof blast pressures from a 10 lb TNT equivalent in a test cell (doors open) were also calculated to determine if the single building concept could withstand such an explosion. Based on the calculations, the wall blast pressure calculated at a distance from the north side of the interim storage room to the middle of the closest test cell (which separates the office complex from the nonhazardous test area) is 0.39 psi. This is below the 0.5 psi maximum safe blast pressure.

The wall blast pressure was calculated from the middle of the closest test cell to the wall adjoining the test support equipment lab (28 ft) to be 2.83 psi. Therefore, the protective walls surrounding the hazardous test cell areas should be designed to withstand a blast pressure of at least 2.83 psi.

Blast pressure along the roof of building in configuration 2 were calculated for 5/10 lb TNT equivalent blasts (see Table 2). The roof blast pressure versus distance from blast on the roof is shown in Figure 2. At the point where the roof of the administration building begins (105 ft), the blast pressure on the roof is 0.39 psi, which falls in the safe limit.

3.2 Noxious Gas Considerations

Analysis was conducted to determine safe open air separation distances if a gas release should occur in the test cells. A summary of calculated values is shown in Table 3.

3.3 Process Description

When the batteries arrive at the Crane, Indiana

TABLE 2

ROOF BLAST PRESSURE AND DISTANCE OF

5 AND 10 LB TNT EQUIVALENT BLASTS

DISTANCE FROM BLAST (ft)	PRESSURE (10 lb)	PRESSURE (5 lb)
28	2.83	2.00
30	2.55	1.80
50	1.19	0.84
75	0.65	0.46
105	0.39	0.28
130	0.28	0.20
150	0.23	0.16
175	0.18	0.13

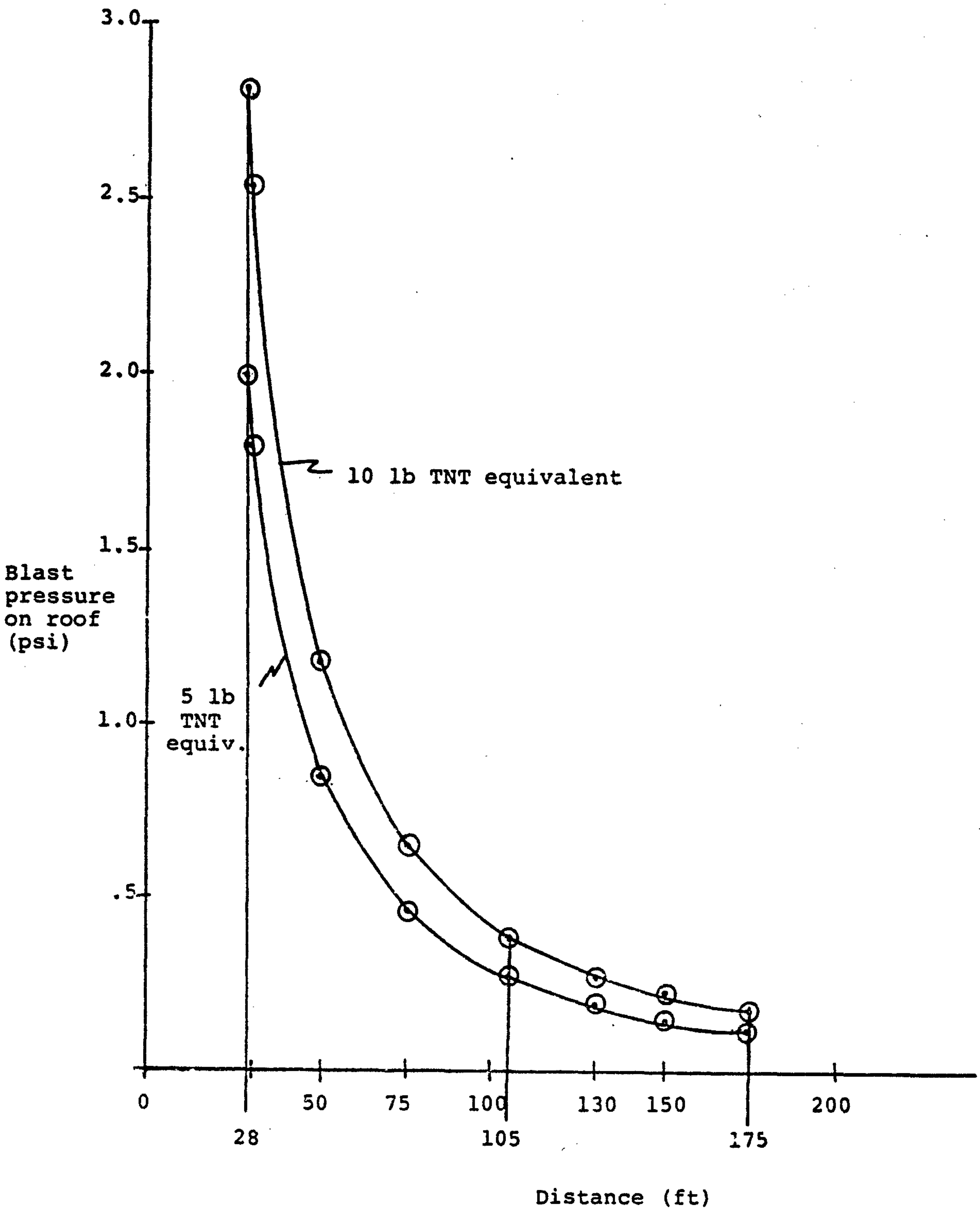

Figure 2. Roof blast pressure versus distance.

TABLE 3

BUILDING CONFIGURATION VERSUS

SAFE DISTANCE

BUILDING CONFIGURATION	DISTANCE FROM ADMINISTRATION BUILDING TO TEST CELL (ft)	EXAMPLE - SAFE DISTANCE FOR $SOCl_2$ HEMISPHERE VAPOR (ft)
1	30	160
2	105	160
3	225	160

facility, they will be checked in at a Receiving dock and placed into interim storage until time of inspection. See Figure 3 Process Flow.

In the physical inspection, the batteries are unpacked, physically inspected for damage, electrically inspected for internal resistance and open circuit voltage. Reserve batteries are checked to see if they have been activated.

In the sample setup room, the batteries are prepared for testing by drilling holes in them, intentionally making an internal short, bypassing the battery's internal protection, and installing thermocouples. Thet are immediately taken to an appropriate test cell for testing. If, for some reason, the batteries cannot be tested, they would be stored in a Hazard Storage Test Cell.

All tests which usually cause the battery to vent noxious gases, burn or explode are conducted in the two abusive test cells. Tests, such as constant current discharge to voltage reversal, will cause the battery to heat up and probably lead to venting of noxious gases, burning or explosion. The batteries would then be inspected for failure under control conditions at a failure analysis lab.

The batteries are moved then to various low yield cells to perform temperature conditioning, drop shock, vibration, climatic conditioning testing. After testing, the batteries may be inspected for failure (failure analysis lab) or moved to a hazardous storage test cell.

The Recycling/Staging dock is then used to log out

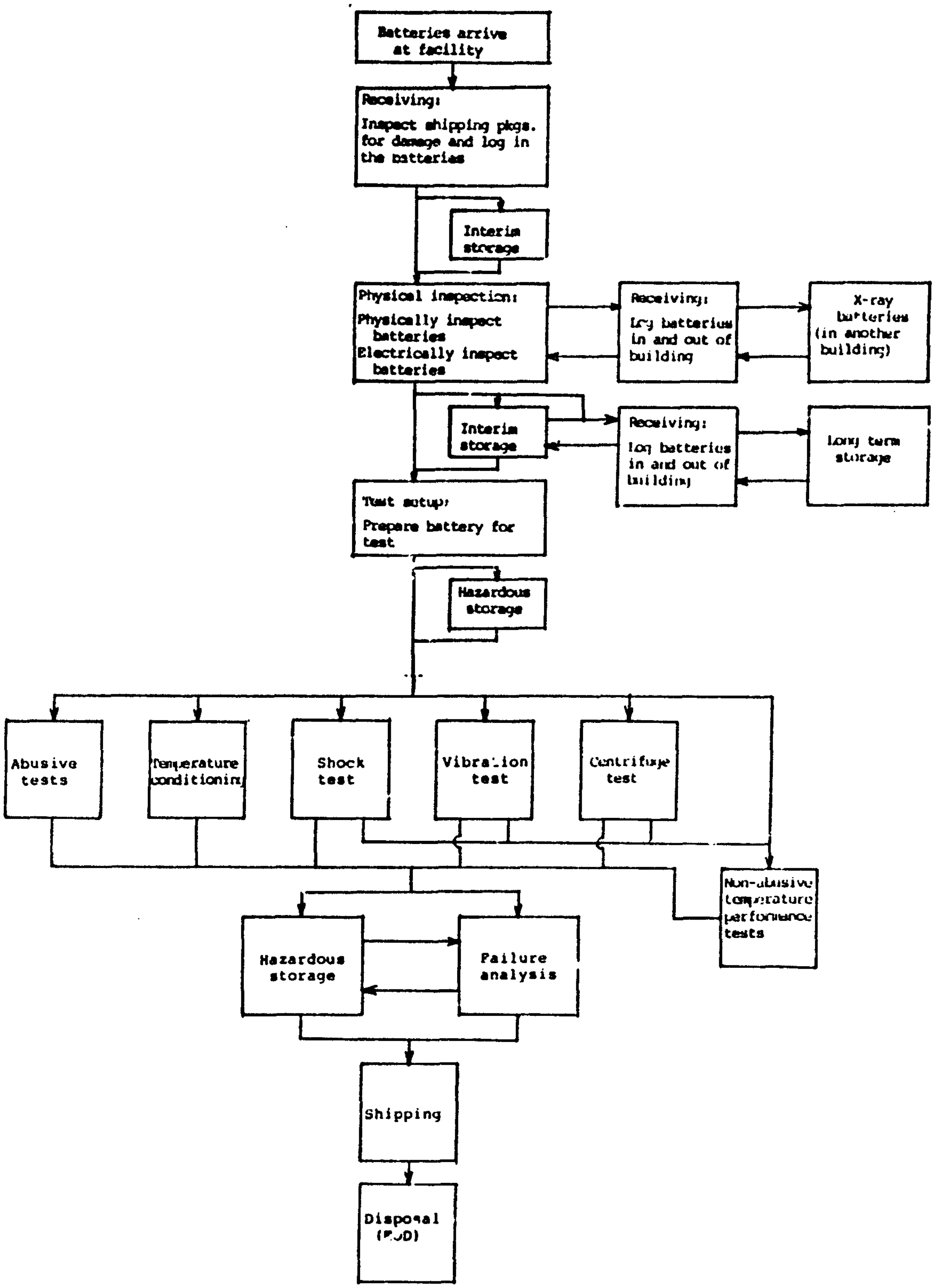

Figure 3. Diagram of lithium battery flow through testing facility.

tested batteries for disposal by EOD (Explosive Ordnance Disposal) personnel.

3.4 Preliminary Hazards Analysis Description

Energy Trace and Barrier Analysis (ETBA) was the method used for the Preliminary Hazards Analysis upgrade per MIL-STD-882B, Task 202.

3.4.1 Energy Trace and Barrier Analysis Method (ETBA)

The basic concept used for the ETBA method of hazards analysis is that anywhere an energy source exists, there is a chance of inadvertent release that could result in injury and/or equipment damage. Therefore, by identifying energy sources and how they can be transferred to a target in the absence of a barrier, potential hazards can be determined.

3.4.1.1 Input Required

To conduct the ETBA, a thorough understanding of the facility, personnel interactions, and its interaction with other facilities was necessary. Basic information about the following was determined in the analysis:

- Facility operations/functions equipment
- Location and siting
- Environments
- Personnel
- Process, material and people flow
- Nature of hazards and exposure

3.4.1.2 Process Steps

a. Identifying Hazards

The first step conducted was to identify the potential energy sources and their targets if no barriers were present. The targets identified (e.g., personnel) were placed into the "Object" column (column No. 1 on Table 4) for each room or cell. The potential energy sources then were identified and placed into column 2 (Energy Source). Typical energy sources could be: corrosive, electrical, electromagnetic, explosive, flammable materials, kinetic-linear, kinetic-rotational, mass-gravity-height, nuclear, pressure-volume, thermal, and toxic/noxious (see Table 5).

Potential causes and effects of the identified hazards were placed into columns 3 and 4 respectively.

b. Risk Assessment

After all potential hazards are identified, a risk assessment is performed by evaluating the hazard severity and likeliness of occurrence per MIL-STD-882B, Task 202. The hazard severity is estimated based on criteria shown in Table 7. The failure mode likelihood is estimated based on Table 8 criteria. Column 5 of the ETBA worksheet (Table 4) contains the Risk Assessment Code (RAC). The RAC consists of the hazard severity category (Table 6) followed by the failure mode likelihood (Table 7). For example, a RAC of I-B represents a hazard severity category of I (Catastrophic) and a failure mode likelihood of B (Reasonably Probable).

TABLE 4

PRELIMINARY HAZARDS ANALYSIS
ENERGY TRACE AND BARRIER ANALYSIS
Work Sheet

Project LITHIUM BATTERY TEST FACITLITY

System/Subsystem ____________

NO.	(1) OBJECT	(2) ENERGY SOURCE	(3) POTENTIAL CAUSES	(4) POTENTIAL EFFECTS	(5) RISK ASSESSMENT SEVERITY EXPOSURE PROBABILITY	(6) RECOMMENDED CONTROLS	(7) HAZARD CONTROL	(8) STATUS

TABLE 5

TYPICAL EXAMPLES OF ENERGY SOURCES

A. Corrosive

Caustics
Decon Solutions

B. Electrical

Battery Banks
Transformers
Wiring
Switchgear
Underground Wiring
Cable Runs
Service Outlets
Pumps
Motors
Heaters
Small Equipment

C. Explosive Pyrophoric

Hydrogen (incl. Battery Banks
and Water Decomp.)
Gases-Other

D. Flammable Materials

Packing Materials
Rags
Hydrogen (incl. Battery Banks)
Gases-Other

E. Kinetic-Linear

Forklifts
Carts
Obstructions
Presses
Crane Loads in Motion

F. Kinetic-Rotational

Centrifuge
Motors
Pumps
Shop Equipment

G. Mass, Gravity, Height

Human Effort
Lifts
Cranes
Hoists

H. Pressure-Volume

Test Loops and
Facilities
Gas Bottles
Pressure Vessels
Gas Receivers

I. Thermal (Except
Radiant

Convection
Exposed Steam Pipes
Electrical Wiring &
and Equipment

J. Toxic Pathogenic/
Noxious

Chlorine and
Compounds
Sulfur Dioxide
Hydrogen Chloride
Thionyl Chloride

TABLE 6

HAZARD SEVERITY CATEGORIES

FROM MIL-STD 882B PARAGRAPH 4.5.1

SYSTEM SAFETY REQUIREMENTS

"Hazard severity. Hazard severity categories are defined to provide a qualitative measure of the worst credible mishap resulting from personnel error; environmental conditions; design inadequacies; procedural deficiencies; or system, sub-system or component failure or malfunction as follows:

DESCRIPTION	CATEGORY	MISHAP DEFINITION
Catastrophic	I	Death or system loss.
Critical	II	Severe injury, severe occupational illness, or major system damage.
Marginal	III	Minor injury, minor occupational illness, minor system damage.
Negligible	IV	Less than minor injury, occupational illness, or system damage.

These hazard severity categories provide guidance to a wide variety of programs. However, adaptation to a particular program is generally required to provide a mutual understanding between the MA and the contractors as to the meaning of the terms used in the category definitions. The adaptation must define what constitutes system loss, major or minor system damage, and severe and minor injury and occupational illness."

TABLE 7

FAILURE MODE LIKELIHOOD

ESTIMATED PROBABILITY	DESCRIPTIVE WORD	DEFINITIONS
A	FREQUENT	Likely to occur repeatedly during Life-Cycle of system (test/activity operation)
B	REASONABLY PROBABLE	Likely to occur several times in Life-Cycle of system
C	OCCASSIONAL	Likely to occur sometime in Life-Cycle of system
D	REMOTE	Not likely to occur in Life-Cycle of system but possible

c. Hazard Control

Methods of reducing and controlling the level of energy are analyzed next. Then, methods of controlling the energy flow and of absorbing free energy (to comprise damage if loss of control happens) are also analyzed. Finally, strategies for energy control are established. Examples of energy control strategies are as follows:

1. Suppress or prevent the amount and release of energy.
2. Separate the energy source and the target with a barrier.
3. Strengthen the target source and the target with a barrier.
4. Provide rapid response to hazard to minimize damage.

The recommended controls to remove or mitigate hazards (removal of energy or protection from energy) were identified and recorded in column. Hazard control techniques (e.g., standards, procedures or references) or follow-up analysis were identified as shown in column 7.

The status of each hazard and its control is documented in column 8 and upgraded as the hazards analysis and the facility develops.

3.5 Results

It is recommended that the administrative office area be located at the opposite end of the building from the test cells and preferably upwind from potential vapor leaks with its own separate, specially designed HVAC system which includes sensors on its air inlets. If >2ppm $SOCl_2$ is detected, the system

will shut down, and an auxiliary air supply will be activated. Also, the doors joining the administration and test areas should be sealed. At a distance of 105 feet from the hazardous test cells, the administrative offices are considered far enough away so that under an alarm condition, personnel could evacuate the site to a safe distance of 160 feet from the building in sufficient time, without contacting a cloud spread. With double protection (blast walls vapor sealed and a second vapor seal), the likelihood of cloud spread is very minimal especially with good air scrubbing in the hazardous areas.

The one building, one-story design (configuration 2) is recommended provided that certain safety features are incorporated into the building design. Based on the calculations for safe distance for explosion blast and noxious vapor clouds (see Table 3), building configuration 2 is acceptable provided a special HVAC system is installed in the administration building and protective vapor and blast barriers are placed between the test cell area and nearby labs. See Figure 4 for final building configuration.

From the ETBA analysis, building configuration 3 is most desirable but presents additional personnel interface problems. From an operational and safety standpoint, the configuration 2 layout is most desirable.

4.0 PROCESS SAFETY EVALUATIONS

4.1 Hazard Areas Hierarchy

An analysis was conducted to determine locational safety of the rooms and cells relative to nonhazardous

operations. Arrangements of hazardous operational rooms were modified until common hazard (i.e., explosion, noxious, or both) groupings were achieved. As shown in Figure 4, the areas have been divided into three major categories as follows:

Category	Situation
3	Explosion, fire and/or noxious possibilities
2	High potential noxious vapor release areas with remote possibility of explosion.
1	Slight possibility of noxious vapor release with no explosion possibility.

Note that the Failure Analysis Lab falls between categories 2 and 1 because it will be limited to very small quantities of potentially hazardous material after a failure has occurred.

A listing of each room/cell, its possible explosion or noxious vapor potential and its hazard area is shown in Table 8.

5.0 HAZARDS ANALYSIS RESULTS

The energy Trace and Barrier Analysis on the final building concept yielded a total of 253 hazard events. Typical ETBA result is shown in Table 9. Corrective actions were cited for all of the hazard events identified. The following is a list of the hazards identified based on areas in the facility:

Area	Hazards
Abusive Test Cells (2)	40
Vibration Test Cell	38

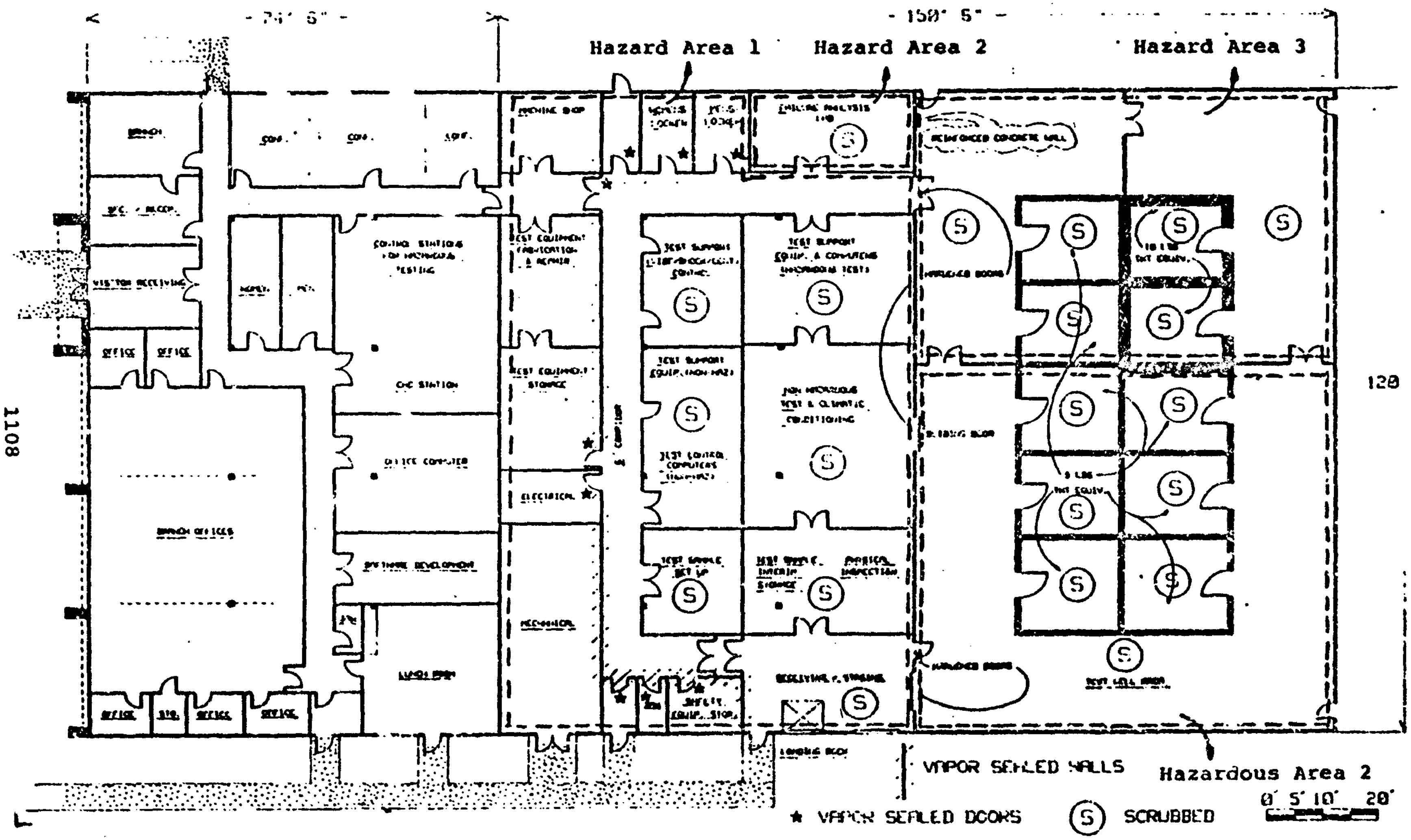

Figure 4. Final configuration and hazard zoning of test facility.

TABLE 8

HAZARD HIERARCHY

		EXPLOSION	HAZARD AREA	NOXIOUS
1.	Abusive Test Cells (2 each)	x	3	x
2.	Temperature Conditioning (2 each) Test Cells	x	3	x
3.	Shock Test Cell	x	2	x
	Vibration Test Cell	x	2	x
	Centrifuge Test Cell	x	2	x
4.	Non-Abusive Test Cell	x	2	x
	Hazardous Storage Cell	x	2	x
5.	Failure Analysis Lab	-	2	x
6.	Runway	-	2	x
7.	Test Sample Setup	-	1	x
	Interim Storage/Physical Inspection	-	1	x
	Receiving/Staging	-	1	x
	Non-Hazardous Test and Climatic Conditioning	-	1	x
8.	Test Support Equipment and Computers	-	1	-
	Test Equipment Fabrication and Repair	-	1	-
	Test Support Control	-	1	-
	Test Equipment Storage	-	1	-
	Machine Shop	-	1	-
	Mechanical Shop	-	1	-
	Electrical Shop	-	1	-
9.	Computers	-	-	-
	Offices	-	-	-

TABLE 9

PRELIMINARY HAZARDS ANALYSIS
ENERGY TRACE AND BARRIER ANALYSIS

Project Lithium Battery Test Facility

System/Subsystem Abusive Test Cell

NO.	OBJECT	ENERGY SOURCE	POTENTIAL CAUSES	POTENTIAL EFFECTS	RISK ASSESSMENT SEVERITY EXPOSURE PROBABILITY	RECOMMENDED CONTROLS	HAZARD CONTROL	STATUS
3	Personnel in Failure Analysis, Test Support Equipment & Computers, Non-hazardous & Climatic Conditioning, Test Sample Interim Storage/Physical Inspection or Receiving/Staging	Chemical toxic/noxious	Battery explodes and doors are open, no protective barrier present.	Personal injury/death	I-B	Install vapor barrier between test cell and room entrance to minimize personnel exposure.		
4	Personnel in Failure Analysis, Test Support Equipment & Computers, Non-hazardous & Climatic Conditioning, Test Sample Interim Storage/Physical Inspection or Receiving/Staging	Chemical toxic/noxious	Ruptured battery, scrubber fails, toxic/noxious vapors enter building through air inlet.	Personal injury/death	I-C	Install monitor on air inlet and special HVAC design.		

Drop/Shock Test Cell	33
Temperature Condition Cells (2)	33
Centrifuge Cell	31
Non-Abusive Cell	24
Non-Hazardous Test Areas	55

Corrective actions for all test cells relate to providing blast protective walls, gas sensors and alarms, gas scrubbing, and vapor sealed rooms. Walls between the test cells and the nonhazardous rooms also must be blast resistant and vapor sealed. A secondary vapor seal between the nonhazardous rooms and the office complex is also cited.

6.0 CONCLUSIONS AND RECOMMENDATIONS

Based on the building concept design study, the Lithium Battery Test and Analysis Facility will be a one building, one-story design which will allow safe separation of office personnel areas and the hazards potential in the test cell area.

6.1 Hazardous Test Rooms Recommendations

The ten test cells will be enclosed inside a large outer room which includes the runway. The ceiling of this room will be higher than any of the test rooms for total enclosure in case of failure of a cell to contain the noxious gases. The four most hazardous test cells (two Abusive Test Cells and two Temperature Conditioning Test Cells) should be isolated from the rest of the test cells. The exterior area surrounding these cells should be constantly ventilated and sensor installed to detect a buildup of noxious gases.

Each cell should have a blast rated exhaust vent

port, which would have a remotely-opened failsafe blast protective cover. The control system should allow only one cover to be open at a time, and not allow testing in a room if the cover is open. All the test rooms should contain noxious gas sensors which will be connected to a central control for monitoring.

Two scrubbers should be used to clean up the noxious gases in hazardous areas 2 and 3. One would be continually operated and be used for the venting of the test cells and one would be operated as needed. This second scrubber should be connected to the first scrubber system in case an accident temporarily overloads the first.

The vapor removal system should have a particle separator to remove the particles associated with these gases (SO_2, $SOCl_2$, and HCl), and then pass the gases through packed type scrubbers using alkaline buffered water for removal of the gases. A separate scrubbing system should be utilized for the nonhazardous area.

The internal surfaces of the test cells and exposed surfaces of equipment, installed in rooms where batteries are present, should be suitably coated with corrosive resistant material, such as resin coated fiberglass. These surfaces should also be water resistant to facilitate cleanup after a battery explosion. Water from remote washdown should be treated and disposed of properly. The drain in each room should be sealed with a blast protecting cover to prevent gases from leaking out to other cells or rooms.

The access door into each cell must be blast

resistant to the rating of the cell and be designed to allow both personnel and forklift access while forming a reliable seal to prevent noxious gas leakage in a blast condition.

6.2 Facility Layout Recommendations

To minimize exposure to the hazardous reaction of a malfunctioning battery during handling or testing, a safe separation distance has been incorporated between the test cells and the office area (area where most personnel are located). Also, if a release should occur, two vapor barriers are present between the test cells and the office area. Although the hazardous reactions are occurring in specially designed test cells, there is an inescapable possibility that a hazardous reaction will occur outside such a cell (e.g., during transport, setup, post test handling). If this unplanned event should occur, a primary vapor seal will protect personnel from noxious hazards.

The recommended facility layout consists of a one-story building, divided into thirds. One-third of the building will be upwind of the test cells for offices, the middle third will be used as lab areas. The hazardous labs requiring wet scrubbing will be located farthest from the office area. Vapor barriers must be installed between the scrubbed and the non-scrubbed labs to prevent vapor leak from entering the non-scrubbed areas. The final third of the building will contain the blast resistant and vapor tight test cells.

In all areas (other than the test cells) where batteries will be handled while electrically connected, overhead hoods, chemical hoods, verted glove boxes, etc. should be incorporated to handle any accidental gas release.

DESIGN OF A MAGNESIUM POWDER PRODUCTION FACILITY

by

W. E. Baker and K. H. Spivey
Wilfred Baker Engineering
San Antonio, Texas

and

S. K. Brauer
Southwest Research Institute
San Antonio, Texas

ABSTRACT

In its Arkansas Operations, Tracor Aerospace has been developing methods and equipment for production of magnesium powder for use in manufacturing magnesium flares. This work has been done in a facility converted from part of a Navy ammunition plant which was originally designed and built in 1945. The development has progressed to the production stage, requiring the design and construction of either a new production facility or a redesign and modification of the existing facility.

This paper describes the redesign of the existing facility as a magnesium powder production facility. The authors discuss the required facility equipment and arrangement. Then, various aspects of the design are covered. These include features dictated by explosives safety, efficient operation, and by limitations of the existing facility size, configuration, and strength. Details of the completed facility revision are illustrated.

ACKNOWLEDGEMENTS

The authors gratefully acknowledge support in preparing this paper by Messrs. David Wallace and Danny Dunagan of Tracor Aerospace, Arkansas Operations, and permission by Tracor management to publish the work.

I. INTRODUCTION

The facility which we discuss was originally part of a U.S. Navy ammunition plant, designed and built in 1945. The structure consisted of a single-story, reinforced concrete building which included a number of bays used for ammunition production operations. Construction was typical of blast-resistant design for that era, incorporating either foot-thick single walls or pairs of foot-thick walls with sand fill as dividing walls between bays. Exterior walls were all one foot thick, and the roof was somewhat lighter, but was supported at intervals with substantial reinforced concrete beams. Expansion joints were spaced every two bays.

Several years ago, two adjacent bays of this structure were modified, and a light metal superstructure was added, to adapt the facility for pilot plant operations for magnesium powder production. A safety analysis was conducted to determine if explosion venting was adequate in the atomizer rooms which had been the original explosive bays (see Ref. 1). Vent areas were increased, based on the analyses in Ref. 1.

Pilot plant results dictated development of a full-scale magnesium powder production facility. Options then included construction of a completely new production facility, or the redesign and modification of the existing facility.

This paper reports the analysis, design and re-work of the existing facility which was selected as the preferred option.

II. DESIGN REQUIREMENTS

A. General

Magnesium powder production is a batch process. Magnesium ingots are melted in a large tilt furnace. The furnace is pivoted to allow gravity pour into smaller crucibles, which are in turn poured into the top of a cylindri-conical vessel for atomization. The atomization vessel is sealed and pressurized with argon for atomizing. Resulting magnesium powder is transferred by pressure difference through piping to another building where it is discharged into containers.

The powder production facility includes a furnace room, a control room and an atomization room. The furnace room must be located over the atomization room to allow gravity feed of molten magnesium to the atomizer. Control of the process is best achieved if the control room is on the same level as the furnace room. Direct observation of the tilt furnace operation from the control room is very desirable.

Accidental explosions are possible in both the furnace room and the atomizer room. In the furnace room, low-energy physical explosions can occur if molten magnesium contacts water. In the atomizer room, discharge of a cloud of magnesium powder and a subsequent magnesium powder explosion is possible.

Design requirements for various parts of the facility based on this description follow.

B. Furnace Room

This room contains the heavy tilt holding furnace, a storage area for magnesium ingots, a preheat oven and some other lighter pieces of equipment. These items and their desired arrangement apply significant dead loads to their supporting structure. The room must be protected from the weather, and must have a door large enough to allow pallets of ingots to be brought in. A personnel door to the control room is also required.

Although great care is taken to prevent water from contacting molten magnesium, it is still remotely possible that molten magnesium spills could occur, trapping a small quantity of water. A stream explosion could then occur, causing blast loading of the walls and roof of the furnace room. For design, the amount of water assumed to cause a stream explosions was one pint.

The general layout of equipment in the furnace room is shown in a plan view in Figure 1.

C. Control Room

This room is adjacent to the furnace room. It contains a number of fairly heavy pieces of control equipment, and typically houses up to eight people. It is separated from the furnace room by a blast-resistant wall. A single, blast-resistant observation window in the blast wall allows an operator to observe tilt furnace operation. An emergency exit door and stairs to ground level are for safety.

The required size and location for the control room dictate that it must be either cantilevered from the existing structure, or supported from ground level.

D. Atomizer Room

This room must be located beneath the furnace room. It is adapted from a bay of the original structure, with modifications to allow adequate magnesium powder explosion venting.

E. Other Requirements

The postulated steam explosion in the furnace room applies blast loads to the blast wall between the furnace room and control room, the observation window, the personnel door in this wall, all walls and roof of the furnace room structure, and transmitted loads to the (steel) superstructure. All structures must be designed to withstand these dynamic loads, or checked for adequate resistance to these loads.

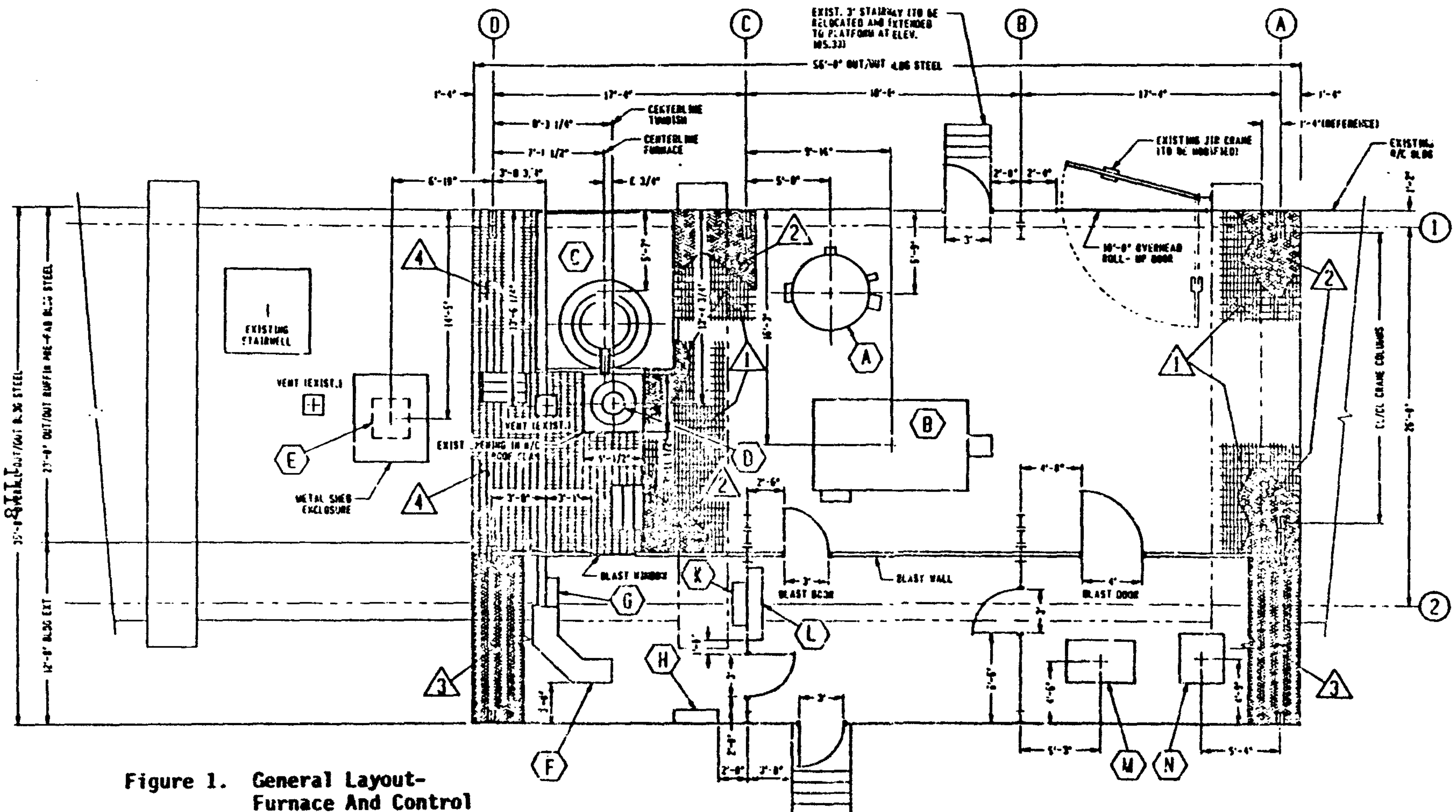

Figure 1. General Layout-
Furnace And Control
Rooms (Above Atomization Room)

EQUIPMENT LIST							
LETTER	DESCRIPTION	WEIGHT (LBS)	OS DIM. (X,Y)*	LETTER	DESCRIPTION	WEIGHT (LBS)	OS DIM. (X,Y)*
A	MPM HALOGIC FURNACE	12,000	5'-3" DIA	H	MPM HOLDING FURNACE CONTROL		(3'-0", 1'-0")
B	PREHEAT OVEN	9,400**	(10'-0", 6'-3")	J	AIR CONDITIONING UNIT		
C	MPM TILT FURNACE	21,500	(9'-3", 10'-10")	K	MPM TILT FURNACE CONTROL		(1'-0", 3'-0")
D	TUNDISH		1'-6" (I.D.)	L	ARGON CABINET		(1'-0", 5'-0")
E	INDUCTION WORK STATION	900	(2'-6", 2'-9")	M	INDUCTION POWER SUPPLY	11,275	(4'-6", 3'-0")
F	ATOMIZATION CONTROL PANEL	500		N	INDUCTION H_2O SUPPLY	900	(3'-0", 3'-6")
G	INDUCTION PANEL SUPPLY CONTROL						

The amount of magnesium powder which could explode in the atomizer room is greater for production operation than for the pilot plant operation discussed in Ref. 1. So, vented blast loads within this room must be recalculated, and the structural strength reassessed.

III. ANALYSIS AND DESIGN

A. General

The weight of the large tilt furnace, holding furnaces and peripheral equipment were great enough that the reinforced concrete roof deck of the existing structure was inadequate to carry these loads safely. A superstructure floor system was designed to transfer the furnace room loads to the reinforced concrete walls of the existing structure below which then carry the load directly into the foundation. Additionally, a pre-engineered manufactured metallic building was purchased to provide an environment protected from the elements for furnace room operations.

Space requirements for furnace room operations dictated that the adjacent control room extend beyond the existing facility wall below. By cantilevering the support structure for the furnace room beyond the existing support wall, the control room was constructed without the additional expense of providing new support columns.

A metallic building 'lean-to' type structure was designed to provide the adjacent control room area. By attaching to the furnace room structure, the lean-to design takes advantage of lateral bracing provided by the furnace room rigid frame design. A typical cross-section of the furnace and control room structure located above the atomization bay is shown in Figure 2.

Additional features of the design included a stainless steel sheet cover attached to the existing concrete roof deck to prevent contact of any molten magnesium from an accidental spill. A sheet pan was provided of a size large enough to capture th largest probable accidental spill. Floor grating around the tilt-furnace area provided a work platform as well as a means for any split magnesium to be collected by the sheet pan. A bridge crane was also incorporated into the furnace room design to handle the movement of the manganese ingots from the storage pallets to the pre-heat furnace and finally to the tilt furnace. A jib crane lifts the pallets from ground level into the roof-top furnace bay.

Additional details of the analysis and design for each area are provided in the following sections.

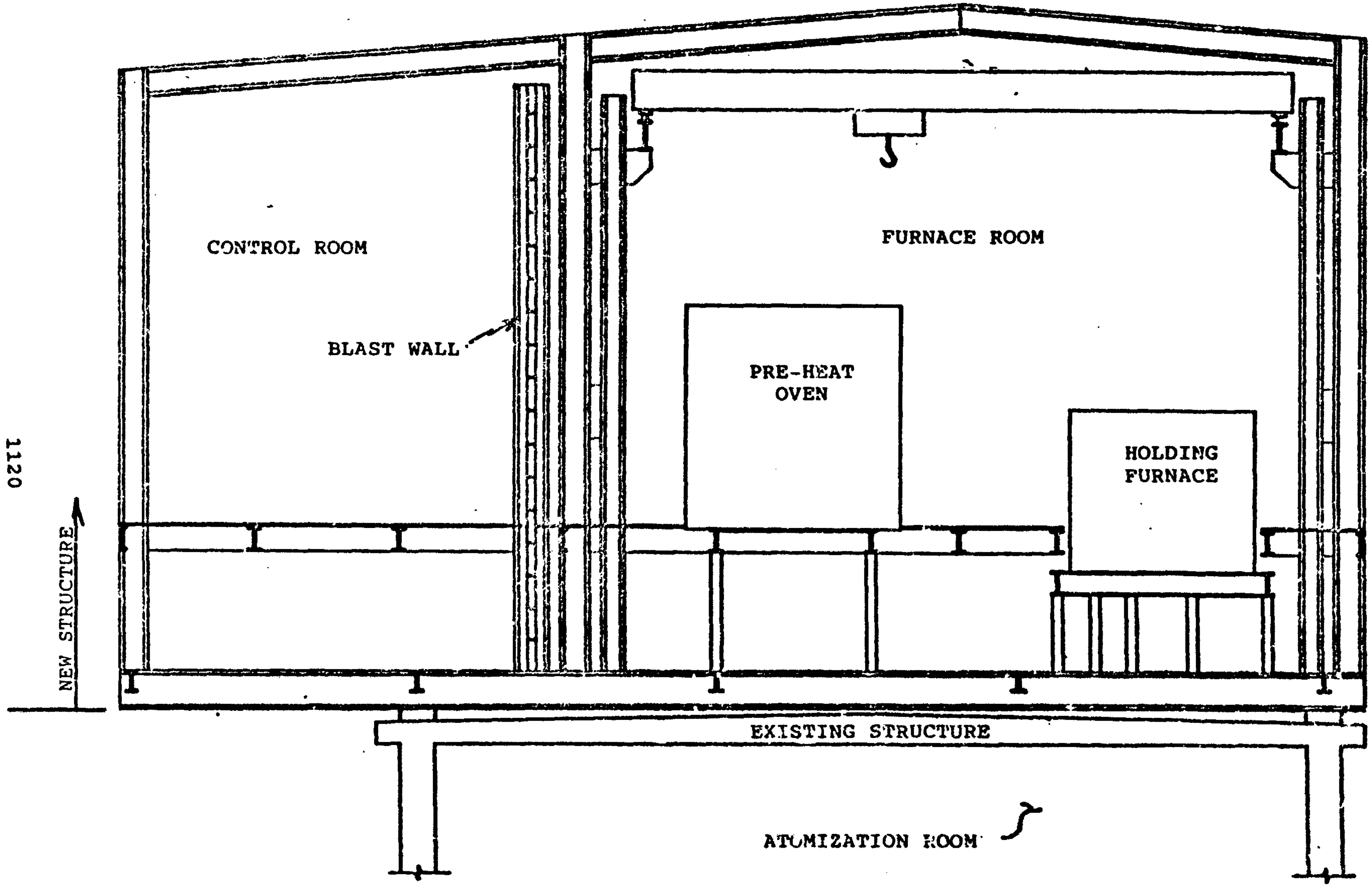

Figure 2. Typical Facility Cross Section

B. Furnace Room and Control Room

These operational areas are grouped together for discussion since both share the same principal support structure. A gridwork of W16 steel girders were placed spanning the roof deck and cantilevered on one end. These girders are braced at regular intervals with W8 steel beams. The W16 framing plan is shown in Figure 3. The elevation of the top of the W16 girders was set such that the tilt furnace would sit directly on top of two of these girders, thus most effectively transferring its 21,500 lb. weight to the reinforced concrete support walls.

Other significant furnace area equipment loads are applied to different floor level beams which eventually transfer all loads to the main W16 girders through stub-type pipe columns. These weights include a 12,000 lb holding furnace and a 9,000 lb loaded pre-heat oven.

Safety lug pattern floor plate is used in the work area away from the potential spill area near the tilt furnace. This plate has a coating applied to reduce the corrosive effects of the magnesium chloride vapors. Additionally, all structural steel in the furnace room was coated with a coal-tar epoxy.

The purchased pre-engineered metallic building was sized initially only to house the furnace room. The metallic building columns were attached directly to the W16 support girders. A structural steel frame 'lean-to' was subsequently designed to provide an adjacent control room. Standard metallic building components matching those of the furnace room were then used to enclose the control room.

Investigations were made to determine if by attaching the blast wall (located between the furnace and control rooms) directly to the columns of the metallic building, advantage could be taken of the stiffness of the entire structure thereby reducing costs associated with any type of vertical cantilevered blast wall support structure. The two conditions analyzed are shown in Figure 4. The results of these analyses however, indicated that the loads induced in the control room structure would impact the structural design requirements significantly and it was best to develop a full moment resistant connection at the W16 girder and provide cantilevered support for the blast wall independent of the control room or furnace room framing. Details of the blast wall design are given in the next section.

A brief summary of the structural design approach for the entire superstructure is provided in Table 1.

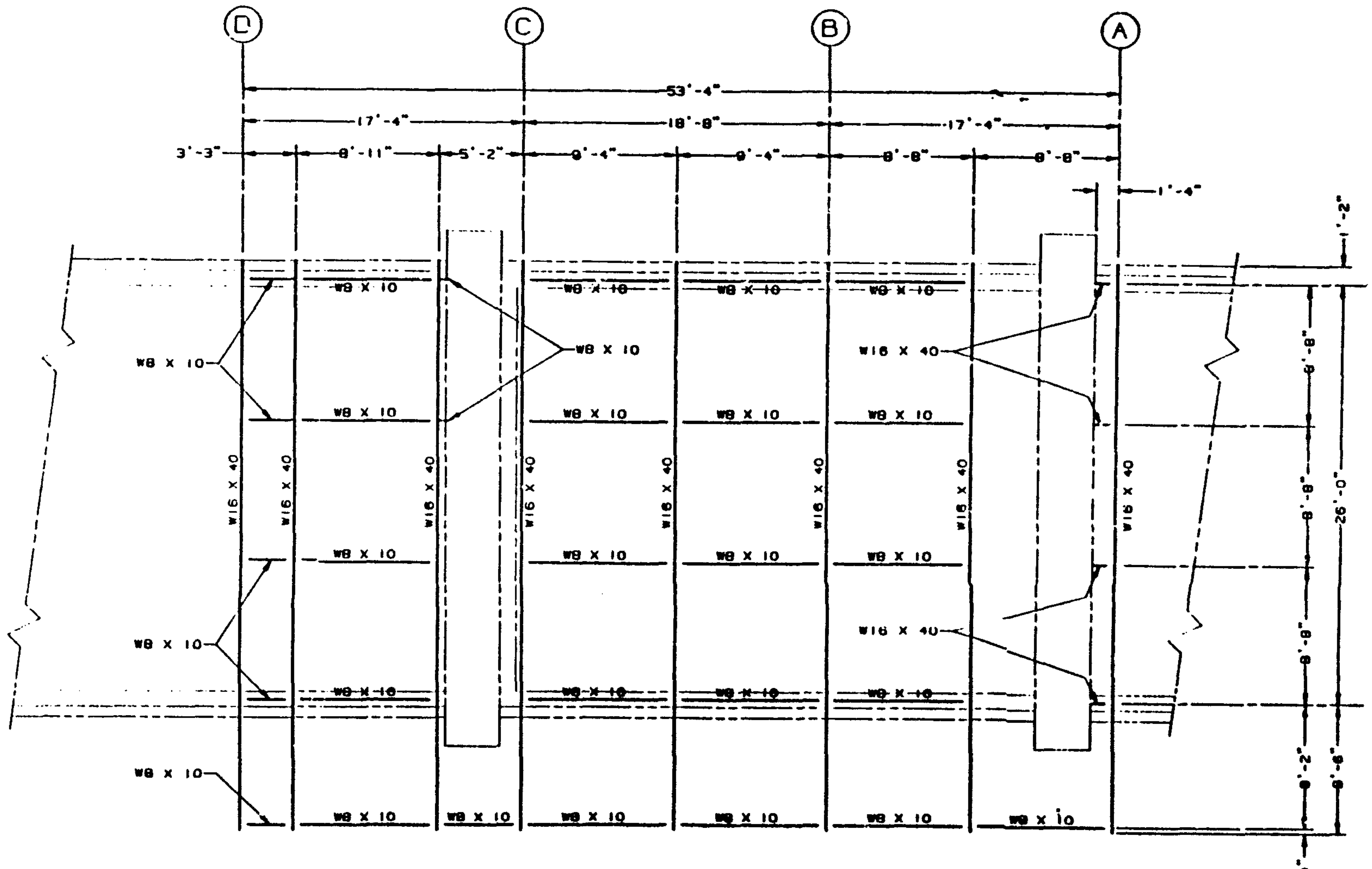

Figure 3. Primary Structural Support Grid For New Furnace And Control Room Superstructure

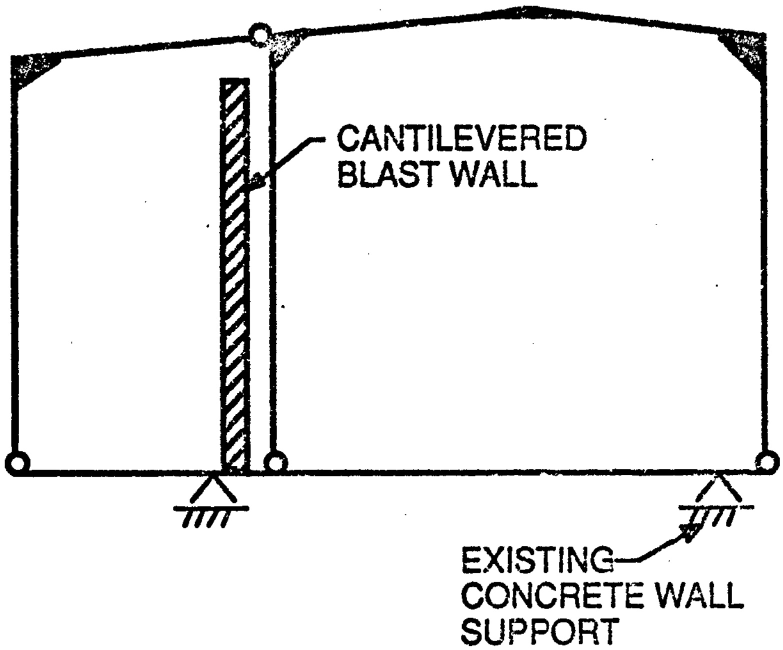

CASE 1

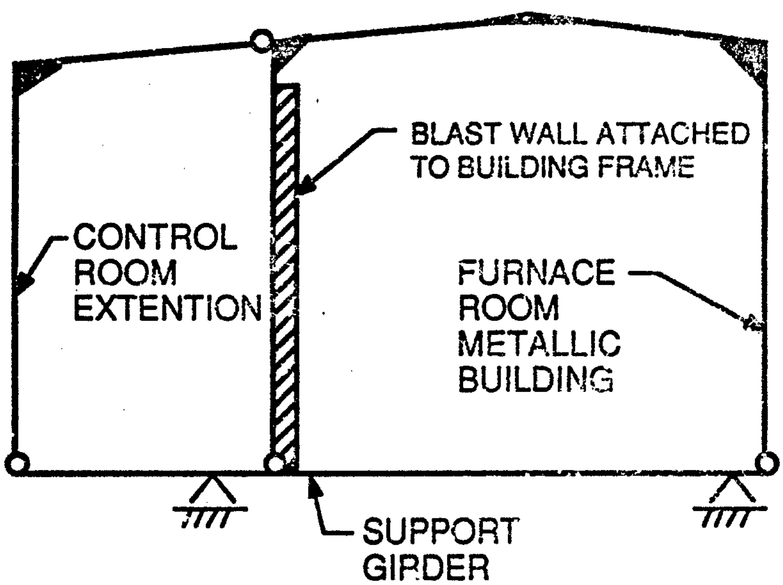

CASE 2

Figure 4. Schematic Of Structural Systems Investigated

Table 1.

Structural Design Methodology for Facility Upgrade

1. Identify all dead load and live load requirements for the new superstructure to be built above and supported by the existing reinforced concrete bay structure housing the proposed atomization room.

2. Initially size the main structural support girders based on the equipment dead loads and assumed live loads distributed on girder tributary areas.

3. Perform a detailed frame analysis investigating wind and snow loads acting on the complete system incorporating a steel lean-to frame attached to the metallic building purchased for the furnace area. The control room frame is assumed to be pinned at the connection to the metallic building with a rigid knee design at the outside wall. The rigid knee provides additional stiffness to the complete structural system. A schematic of the analyzed frame is provided in Figure 4.

4. Design a full moment-resistant connection between the blast wall column and the W16 support girder.

5. Design the remaining floor structure required to transfer furnace room operation loads to the W16 support girders.

6. Check the capacity of the existing reinforced concrete support walls for adequacy to carry the superstructure loads.

7. Design the bridge crane runway girder and support frame structure.

C. Blast Walls

An upper limit for the explosive energy release of a steam explosion due to molten magnesium being dropped into a small amount of water was calculated using the properties of steam and an estimate of the maximum amount of water which could be accidentally left or trapped in a furnace when molten magnesium is poured into it. Because of the emphasis and awareness by operating staff of problems which could occur in this situation, it was assumed that, at most, one pound of water could be accidentally trapped and contribute to a steam explosion. The energy release from this explosion was calculated to be 1556 BTU. Accident investigations of foundry steam explosions show effects very similar to TNT explosions, with strong air shock waves being developed. Converting the energy from the steam explosion into an equivalent TNT energy and accounting for enhancement due to reflection from the bottom of furnace or ladle, an equivalent weight of TNT was calculated to be 1.602 lb.

The blast wall separating the control room from the furnace room had a height of 18 ft 4 in and a length of 56 ft. Separated into three large panels and two narrow strips by I-beams with the blast source positioned 10 ft from the wall as illustrated in Figure 5, Panels 1 and 2 will be the most heavily loaded sections. Panel 3 will receive only minor blast loads in comparison. For Panels 1 and 2, a BASICA program was incorporated to aid blast load calculations. The program calculated the geometry and scaled distances for blast loads on a wall at certain standoff distances, which were then applied to standard TNT curves to retrieve reflected pressure and specific impulse. Because the program assumes the blast source is centered on the span, this method yielded a good approximation for average blast loads over Panel 1 and half of Panel 2. For Panel 3, the blast load was calculated using the average of the independent loads at each of the four corners. Besides the three panels on the blast wall, there are two 1 ft 4 in wide strips of wall on either side of the panels. Both are subjected to a blast load, with the one closest to the blast source being the worst case. To calculate the blast loads on the worst-case strip, it was divided into two sections and the average of the two independent loads was used in further calculations.

Results of the loading on the blast wall are given in Table 2. The duration of the load is given by:

$$td = \frac{2\, ir}{Pr}$$

where td is duration of the load
ir is reflected specific impulse
Pr is reflected overpressure.

Table 2.

Average Loads on Blast Wall Panels

	Pr (psi)	ir (psi-sec)	td (sec)
Panel 1	10.22	1.28×10^{-2}	2.50×10^{-3}
Panel 2	10.22	1.28×10^{-2}	2.50×10^{-3}
Panel 3	3.34	4.04×10^{-3}	2.42×10^{-3}
Strip	10.25	7.84×10^{-3}	1.53×10^{-3}

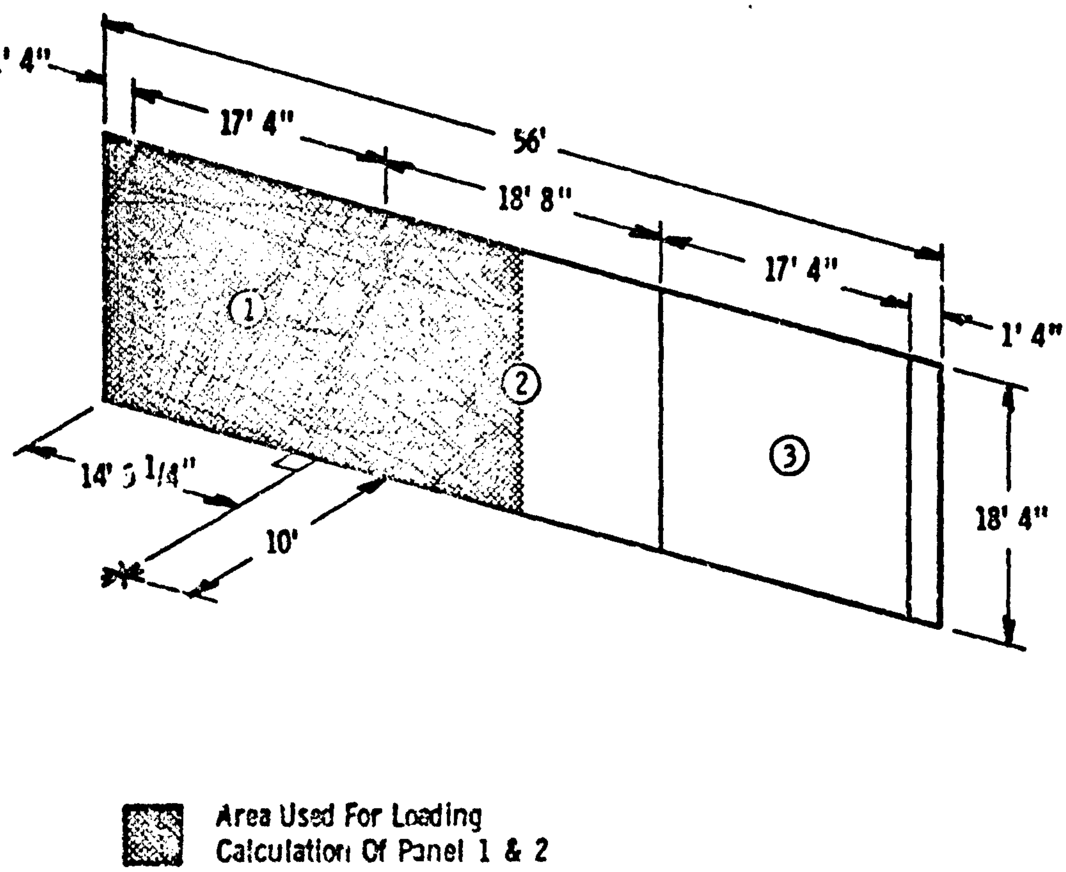

Figure 5 . Control Room Blast Wall Sections

The dynamic analysis methods used are described in Refs. 2-4. In these methods, the real structural elements are first converted to equivalent single-degree-of-freedom (sdof) systems. The methodology for calculating the elastic-plastic response of these sdof systems is found in both references and was aided by a computer program written in BASICA. The program gives both numerical solutions and graphs of the displacement-time histories of the responses. To use Biggs' sdof response methods, a few preliminary calculations to convert properties for the real elements to the equivalent sdof value were made. Dynamic strength properties must be used rather than static properties. Thus, we see that

$$\sigma dy = 1.25\ \sigma y$$

$$\sigma dy = 1.25\ (36000) = 45000\ \text{psi}$$

For a rectangular element, the plastic section modulus is

$$Z = bh^2/4$$

and the moment of inertia is

$$I = bh^3/12$$

The modulus of elasticity is

$$Es = 30 \times 10^6\ \text{psi}$$

From References 2 and 3, conversion factors are established for the panels and strips.

The blast wall panel design was a built-up structure with C3x4.1 channels and 1/8" thick steel cover plates, all of which were made of A36 steel. The panels were then placed within the flanges of the I-beams which separated the panels (see Figure 6). For the dynamic structural response analysis, Panel 2 was considered worst-case due to its longer span and assumed to be simply-supported at the sides. Due to the fact that the spacings of the chosen number of channels are not equal, the panel as a whole was considered in the analysis. Bending of the face plate between channels was also analyzed assuming clamped-clamped boundary conditions. The 1/8" thick A36 steel wall strip was considered as a cantilevered beam. The S12 x 40 I-beam supporting the blast-loaded panels was assumed to be fixed on one-side and cantilevered on the other with one-half of a blast loaded panel on either side. All the structural elements were designed not to exceed a maximum dynamic deflection of $\mu = 15$.

The results of the elastic-plastic sdof system analyses for the blast wall panels, strips, and beams are shown in Table 3. The dynamic response calculations show that all elements were within the design requirements. Since the elements analyzed were the most heavily loaded, the worst-case elements were adequate to support the structure at other locations.

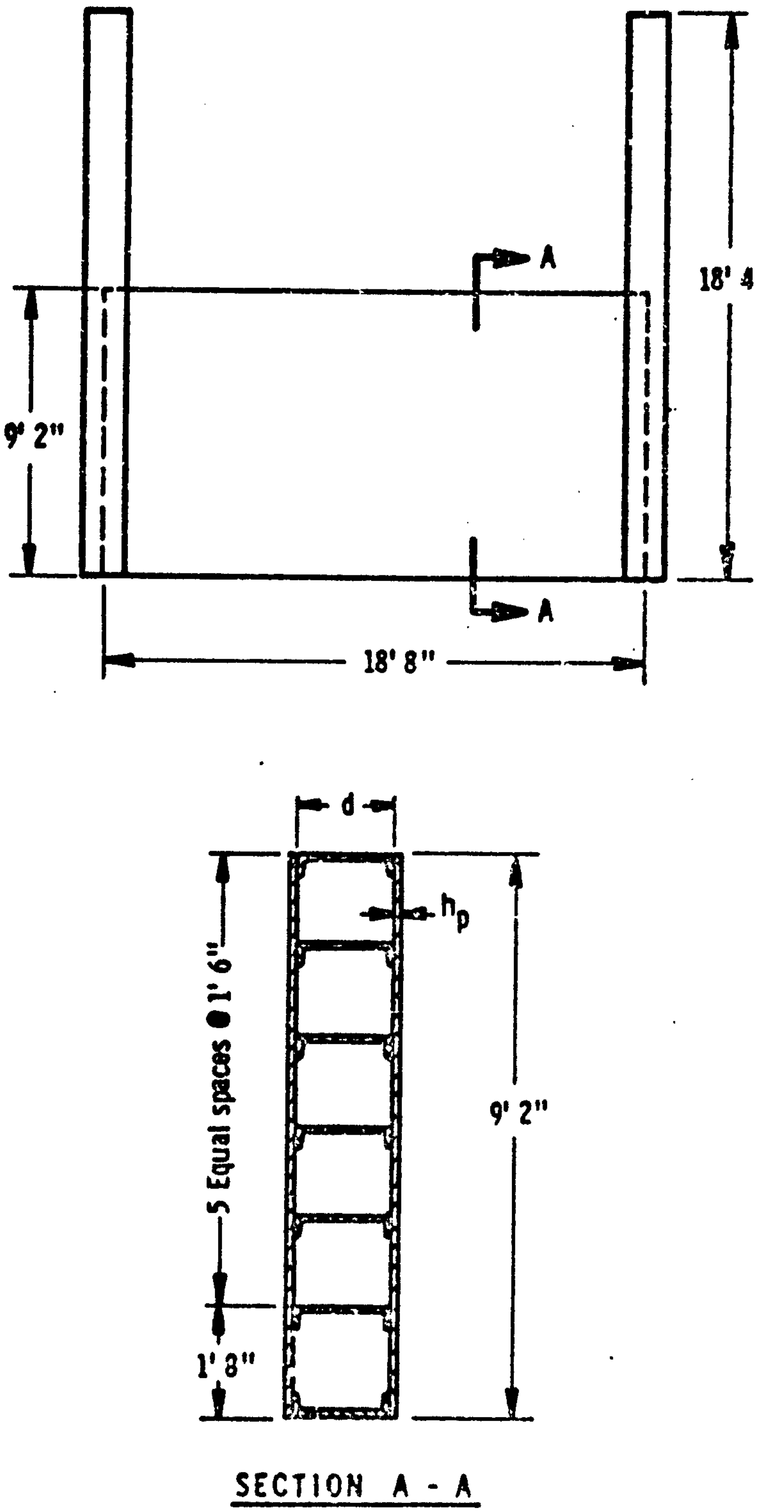

Figure 6 . Blast Wall Panel Construction

Table 3.
Maximum Responses of Blast Wall Structural Elements

Element	ym(in)	yel(in)	μ*
Panel 1 Panel 2	2.21	4.28	0.52
Bending Face of Panel	0.384	0.460	0.84
Strip	2.48	2.29	1.08
Beam	13.77	3.37	4.09

* $\mu \leq 15$ is acceptable (μ is the ductility ratio and is defined as μ = ym/yel)

The steel blast wall contains two doors, one 3 ft x 7 ft personnel door and one 4 ft x 7 ft 3 in equipment door, and one 3 ft x 1 ft viewing window. The doors and windows must be blast proof in the event of an accidental steam explosion. All three items were designed for a maximum dynamic deflection not to exceed μ = 15. The blast window was made of polycarbonate 1/4 in thick with the following properties:

$\gamma = 74.9\ \mathrm{lb/ft^3}$

$\sigma y = 9.8 \times 10^3$ psi

$E = 3.2 \times 10^5$ psi

where γ is specific weight

σy is the static yield stress

E is the modulus of elasticity.

The window had at least one inch of clamping distance on each edge and was positioned in a steel clamping plate which in turn was bolted in place in the blast wall (see Figure 7). Both the personnel door and the equipment door were made of 1/4 in thick A36 steel with a one inch wall overlap on the blastward side of the blast wall and a channel frame around the wall opening (see Figure 7). The doors were assumed to be simply-supported on two sides. Blast load calculations were made to the center of each element, taking into consideration the angle of incidence (Reference 4).

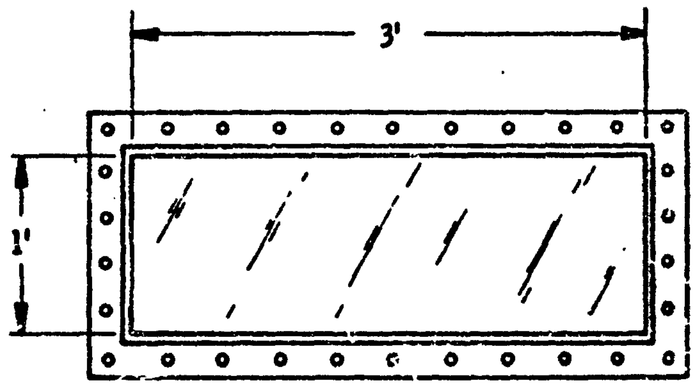

Figure 7 a. Blast Wall Viewing Window

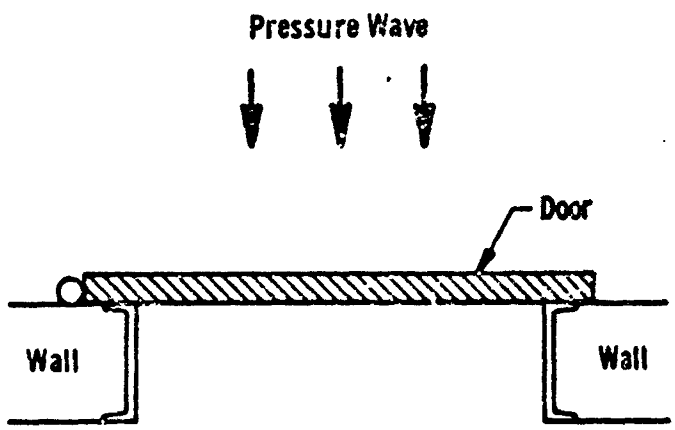

Figure 7 b. Blast Wall Door Connection

The results of the pressure loading calculations and the elastic-plastic sdof system analyses for the blast wall window and doors are given in Table 4 and 5, respectively. All elements stayed well within the maximum dynamic deflection allowed, and did not deform plastically.

Table 4.

Pressure Loads on Window and Doors in Blast Wall

Element	$P_{r\alpha}$ (psi)	$i_{r\alpha}$ (psi-sec)	td (sec)
Window	16	1.7×10^{-2}	2.125×10^{-3}
Personnel Door	1.3	2.23×10^{-3}	3.42×10^{-3}
Equipment Door	0.7	1.29×10^{-3}	3.68×10^{-3}

Table 5.
Maximum Responses of Elements in Blast Wall

Element	Ym (in)	Yel (in)	μ
Window	1.566	10.9	0.143
Personnel Door	0.144	2.43	0.059
Equipment Door	0.185	4.32	0.043

D. Atomization Room

In Reference 1, a safety analysis was made to determine the required vent area in the atomizer room to prevent a catastrophic failure of the structure in the event of an accidental dust explosion of magnesium powder in air. With the new production plant, it was decided to increase the vent area significantly with an increase in the mass of magnesium present in the room at any time. The vent area was increased from two vent areas of 9′ 6" x 8′ and 76" x 7′ to three areas of 9′ 10" x 10′ 6", 9′ 10" x 7′ 1", and 9′ 10" x 8′ 1". The amount of magnesium was increased from 100 lb to 1500 lb. The procedure for determining the elastic-plastic response of the structure to an accidental dust explosion was given in Reference 1 and those methods were used in this analysis on the wall, roof and door of the atomization room, except that in this analysis we allowed the nitrogen and unburned magnesium to absorb the heat of the reaction.

The bay structure is reinforced concrete and of World War II vintage. We assumed the rebar was Grade 40, the most common grade then in use. The front and rear walls are 12 inches thick and have reinforcing consisting of #4 rebars, 12 inches on centers, each way, each face. The rebar grids are placed on both sides of the wall about 1.5" from the wall face. The pressure-time history of such an explosion is given in Figure 8 and the results of elastic-plastic sdof system analyses on the structural elements are given in Table 6. The table shows that the steel door has only small elastic deformations; the rear wall has permanent deformation with $\mu = 1.47$, but well below the acceptable limit of $\mu = 15$; while the roof experiences the greatest deformation with $\mu = 3.13$, but is still quite safe. The conclusion was that the venting was adequate to limit the effects of worst-case magnesium dust explosions to safe levels, for structural integrity. But, a large dust fireball would be ejected out the vents, and burn outside the building.

Table 6.
Maximum Structural Response of Atomization Room Elements

Element	Ym (in)	Yel (in)	μ
Wall	0.45	0.361	1.47
Roof	1.13	0.361	3.13
Door	0.52	42.8	0.012

The roof of the bay varies somewhat in thickness, being thickest along a transverse centerline and tapering uniformly to an edge which overhangs the fore and aft walls by several feet. The average thickness is about 8 inches and reinforcing consists of #3 rebars, 12 inches on centers, both ways, both sides. The rebar grids are displaced on opposite sides of the roof such that the center of the outermost rebars are nominally 1.0 inch from the wall face. The entrance door is a 3' x 7' steel plate located in the rear wall of the atomizer room.

IV. DISCUSSION

The magnesium powder production facility now in operation at Tracor Arkansas operations is a good example of careful rebuilding and modification of an old explosives facility for new and very different uses. Lessons learned in pilot plant operations in the same facility guided the modifications for production use. The design modifications include explosion-resistant components, but they are dominated by design for dead loads for heavy equipment needed in the production operation.

Modification of an existing facility proved to be considerably less costly and required less time than the design and construction of a new facility.

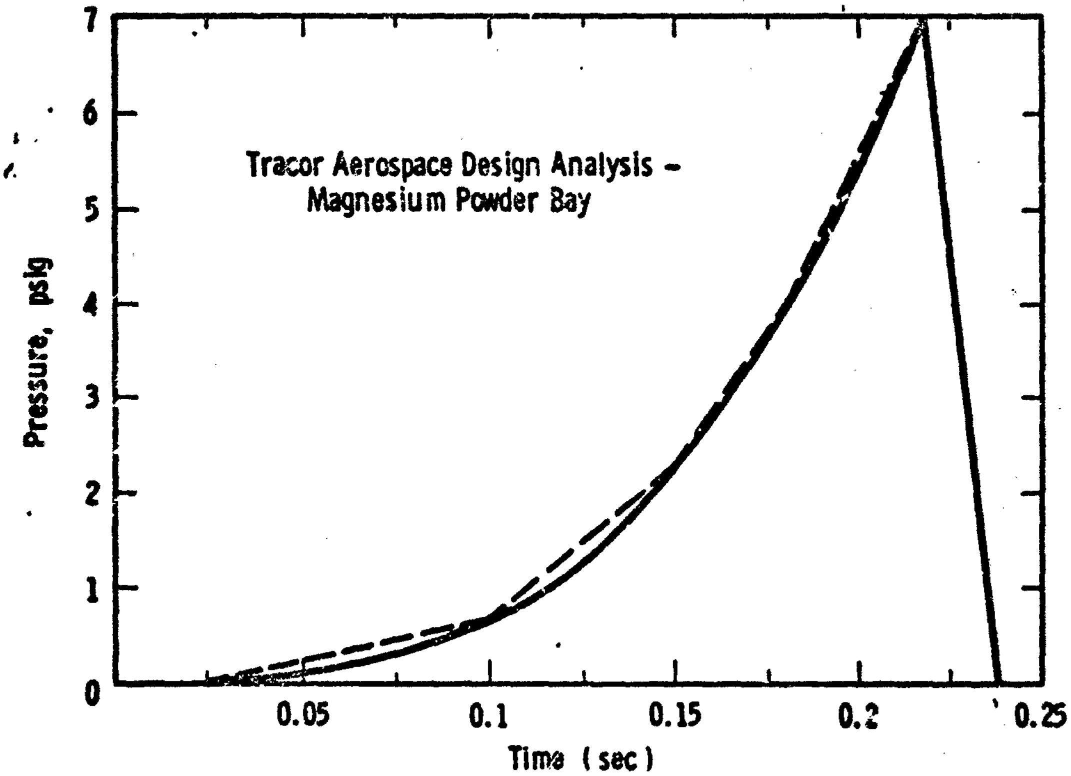

Figure 8 . Pressure - Time History in Atomization Room

References

1. J. J. Kulesz and W. E. Baker, "Safety Analysis for Vented Dust Explosions," Minutes of the 22nd Explosives Safety Seminar, August 1986, pp. 2073-2084.

2. Introduction to Structural Dynamics, John M. Biggs, McGraw-Hill Book Co., New York, NY, 1964.

3. "Structures to Resist the Effects of Accidental Explosions, Vol. III - Principles of Dynamic Analysis," U.S. Army Armament Research and Development Center, Large Caliber Weapon Systems Laboratory, Dover, NJ, June 1984.

4. "Structures to Resist the Effects of Accidental Explosions, Vol. II - Blast, Fragment, and Shock Loads," U.S. Army Armament, Research, Development and Engineering Center, Dover, NJ, December 1986.

COMPUTERIZED BANK OF EXPERIENCES FROM ACCIDENTS IN THE EXPLOSIVES INDUSTRY

Alf Rosberg
Safety Manager
Nobel Industries, Karlskoga, Sweden

An accident occurred some years ago while "rings" of propellant for mortars were being pressed out of flat propellant foil. A pressing tool which is illustrated below was being used.

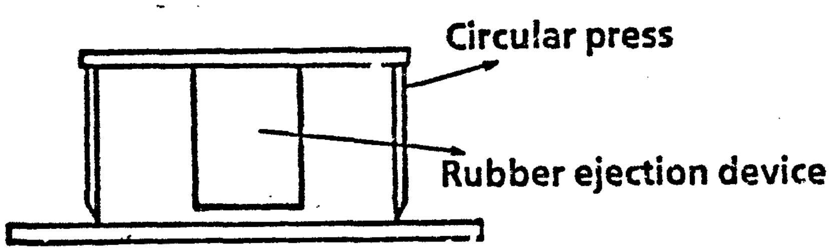

In order to test a new tool, rings were cut out of single propellant foils.

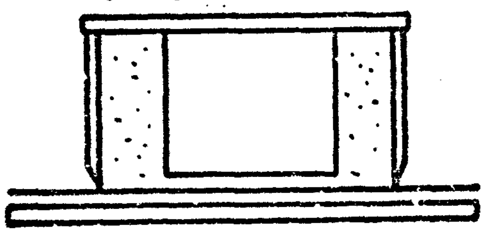

This worked very well. In order to increase capacity, several propellant foils were placed on top of each other so that several rings could be pressed out together.

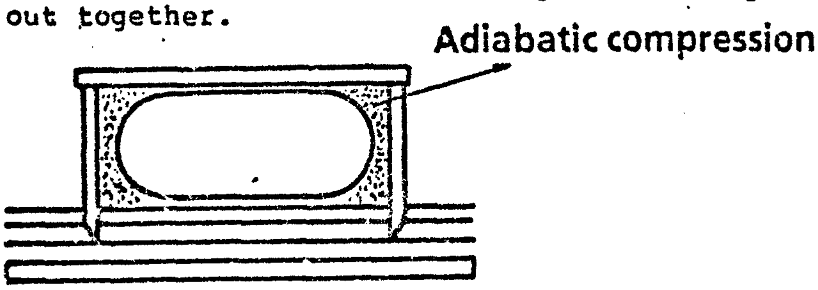

At this point en explosion occurred in which three people were injured (eye injuries and burns).

In the subsequent investigation, the following comment was pronounced by an experienced designer:

"- There must be a ventilation hole in the press otherwise air is compressed adiabatically inside the press. The air becomes so hot that it can ignite the propellant. This is a well-known fact".

There are old and good traditions within the explosives industry concerning the careful investigation of accidents and near-accidents. The intention is to gather all the information and experience we can so that safer handling methods can be implemented in the future. This information relating to actual accidents is especially significant when it comes to justifying a method of working for example.

We have, however, seen obvious difficulties within the Swedish explosives industry in keeping this information up-to-date and in transferring this information to the new generation of designers and operations managers. Unfortunately, when an accident occurs, we often see that a similar accident has occurred previously.

In an attempt to solve this information problem, we here in Sweden, have started a project to build up a computer-based system for storing and retrieving information in previous reports of accidents and near-accidents. The aim is that it shall be possible to find adequate information for every individual situation. If I am to take out a tool for propellant pressing, I should be able to investigate if these sorts of experiences exist from "pressing of propellant".

The project has been divided into the following stages:

* Selection of computer system.
* Designing of format for report summaries.
* Gathering of accident and near-accident reports.
* Producing report summaries for all reports (translating foreign reports).
* Filing these in the computer system.
* Producing a manual for users.

Computer system

We have had access to an information retrieval system called STAIRS which is an IBM product. This allows free text searching in all the material filed in the computer bank.

Format for report summaries

The reports which are available differ widely as regards design and contents etc. In order to make the reporting of information more systematic we have produced a model format for report summaries (Appendix 1).

Collecting accident and near-accident reports

We collected all the reports we could get hold of from the Swedish and Scandinavian explosives industry. We have also made use of all the reports distributed by SAFEX and a smaller number of reports from FEEM and IME.

Report summaries

After the basic material has been produced in the form of original reports, the contents have been treated systematically in accordance with the report summary format described earlier.

Filing in computer bank

The text in these report summaries has been filed manually in the computer bank using a conventional terminal.

Manual for users

Finally, a summarized manual for users has been produced in order to facilitate the use of the computer bank.

Using the computer bank

As stated earlier, the computer bank is built up so that it is possible to search freely within all filed text. This is an important function in order to obtain a user-friendly system.

As an introduction, we can take the accident described as an example:

* A designer has the task of producing a tool for pressing propellant. He then wants to investigate if there are any experiences from accidents or near-accidents to which he should take consideration. The designer can then make a search in the computer bank as an individual or through us in the Safety Service.

  In this case, the important words to be searched for are propellant (the substance in question) and pressing (the work operation).

  We also ask if there are any reports in which the words propellant and pressing appear in the text at the same time. When this extraction has been made, we take all or part of the report summary in order to see if it can provide any usable information. If we wish to know more, we can easily go back from here to the original report or contact the company where the event occurred.

  Already, we can see that if there had been a hole for evacuation of air, the accident could have been avoided.

  In this way we can make the information in accident reports available at the starting point for each separate need.

Situation today - Experiences

The computer bank today includes c. 1000 accident reports.

The computer bank has begun to be used as a source of information in connection with risk analyses, design of new equipment and for training. The response so far has been good, but there still remains a great deal of work before the system is complete. One of the most important requirements is to find further sources of information to feed into the computer bank.

The system is now based on the Swedish language but if the interest exists, it should be relatively easy to translate into English. A company or an organization would then be required, however, to take responsibility for running a computer bank of this type.

Format -- Report summary

DATE 030680

HEADING

COUNTRY/COMPANY

EQUIPMENT

WORK OPERATION

PRODUCT

SUBSTANCE

QUANTITY

SEQUENCE OF EVENTS

PERSONAL INJURIES

MATERIAL DAMAGE

CAUSE

MEASURES TO BE TAKEN

REFERENCE
R0601 * END OF DOCUMENT IN THE RECORD - PRESS
OR GIVE COMMAND

PICTURE OF REPORT SUMMARY

SEARCH - QUERY
00001 'PROPELLANT' AND 'PRESSING'
BOO11 Document = 1 of 1
DATE 030680
CLASS 001
CLASS 1 000
CLASS 2 001
CLASS 3 000

HEADING
EXPLOSION AND FIRE IN PROPELLANT PRESS BZ6

COUNTRY/COMPANY
Sweden/Nobel Chemicals, Dept. NVK 1

EQUIPMENT
Excenter press

WORK OPERATION
Pressing

PRODUCT
Propellant

SUBSTANCE
Test propellant NZK 5098 'Horse-shoe shaped propellant'

QUANTITY
7 kg

SEQUENCE OF EVENTS
Propellant foil was laid out in packs on the pressing pad, sizes - 0.1 mm foil in 3-4 mm thick packs, and 0.12 mm foil in 5-10 mm thick packs. The pressing of the 0.1 mm foil was completed and when the first pressing of the 0.12 mm foil was carried out, the foil in the pressing tool exploded and the foil next to it burned up.

PERSONAL INJURIES
1 with eye injuries and grade 2 burns
2 with grade 1 and 2 burns

MATERIAL DAMAGE
Inconsequential

CAUSE
Probably adiabatic compression in the inner ring of the pressing tool.

MEASURES TO BE TAKEN
Pressing tool shall be ventilated. Foil pressing shall take place in shelter. Sprinklers shall not be turned off during work with explosives. Positioning of sprinkler detectors must be carried out very carefully.

REFERENCE
OPH10 - report.

RESULTS OF AN EXPLOSION IN A SWEDISH MUNITION STORAGE

By

Bengt E Vretblad & Siwert E Eriksson
FortF - Royal Swedish Fortifications Administration
Eskilstuna, Sweden

ABSTRACT

On November 26, 1986, a military ammunition depot in Järna 50 km southwest of Stockholm blew up due to criminal actions.

After the blew up the area had to be cleaned up and secured from unexploded munitions. Also studies were made of the breakup of the building, cratering effects, demolition in the close in range, throw of fragments and debris and effects on buildings at larger distances.

Comparisons were made with regulations.

The main results from the studies and comparisons are given in the paper.

BACKGROUND

In Sweden there are many ammunition storages, both for the forces in the defense and for the civilian community. There are both aboveground magazines and magazines in rock. For the two kinds of magazines a large variety of technical solutions exists depending e g on the location, the amount of and the kind of explosives to be stored and the materials available for building.

In Järna 50 km southwest of Stockholm a munition storage of concrete had been built. On November 26, 1986, it was blown up.

In Sweden FortF has the responsibility to make the buildings for the national defense. Conclusively, the magazine in Järna was of FortF design.

The geometry of an aboveground magazine is regulated in /1/ together with maximum equivalent amount of TNT to be stored in it as well as the QED under these conditions. The drawings for construction as well as technical details are available from standard drawings from FortF.

The magazine in Järna is shown in figure 1.

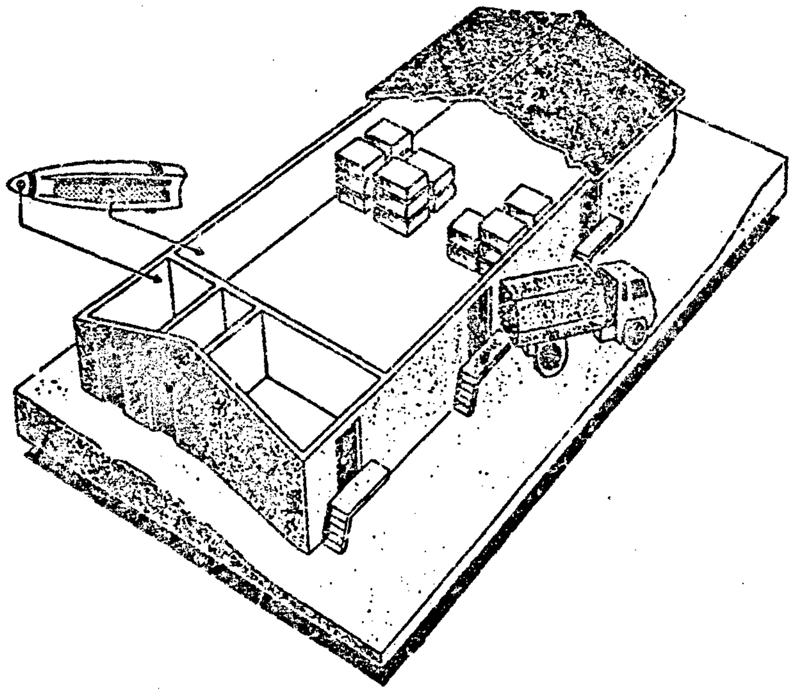

Figure 1. The aboveground munition storage in Järna.

In this design different rooms in the building are separated from each other and are only to be reached from the outside. The walls consist of reinforced concrete.

The QED for this type of magazine can be calculated according to the formula:

$$QED = K \sqrt[3]{Q} \ (m),$$

where

Q = amount of explosives (kg)
K = 30 for groups of houses
    9 for roads

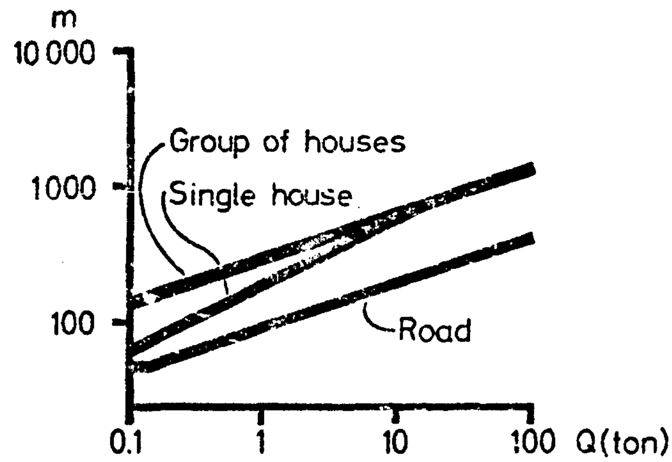

Figure 2. QED according to /1/.

Before the event on November 26, 1986, the munition storage at Järna contained an amount of explosives equivalent to a little more than 15 tons of TNT.

In the smaller rooms along one of the short sides of the building blast caps and munition with very low Q-values were placed. The major portion of the content in the main room was mines, plastic explosives and different kinds of artillery shells.

EFFECTS OF INTERNAL EXPLOSIONS IN ABOVEGROUND AMMUNITION STORAGES

When a detonation takes place in an ammunition storage a blast wave and a gas overpressure are generated. Depending on the kind of explosive products fragments may be generated as well.

Only if the amounts of explosives are very small the building can sustain the effects without serious damages.

The most elaborate systematic study of the effects of internal explosions in munition storages has been made for Amt für Bauten in Switzerland. The tests were made by FortF on contract and the subsequent analysis by Basler and Hoffman (now Basler and Partners) in Zurich. The tests and the analysis have been documented and reported, /2/.

In these tests simple concrete models were used. In the models only a structure with heavy reinforcement could withstand an internal explosion equivalent to a loading density of 0.15 kg/m^3 without being torn into parts. At higher loading densities and/or small amounts of reinforcement the walls and roof were broken up. Higher loading densities caused more complete disintegration of the structure.

The tests also showed how the debris from the walls was distributed primarily perpendicular to the original wall panes. The debris distribution in principle from the tests is indicated in figure 3.

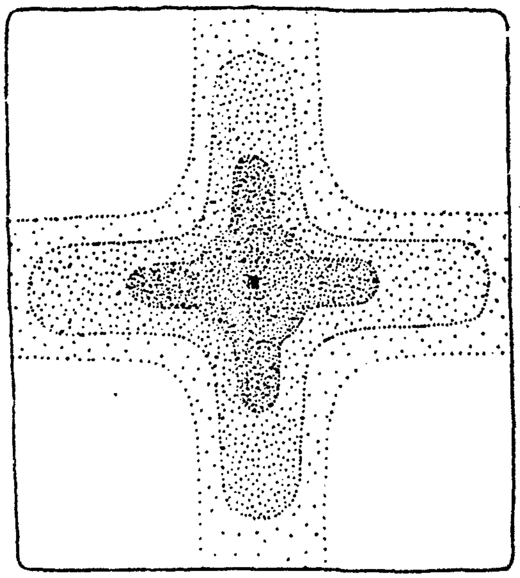

Figure 3. Debris distribution from model tests, /3/.

THE EVENT

Just before 10.30 am on Wednesday November 26th, 1986, the depot was blown up. Nobody was injured but the explosion was heard more than 20 km away.

The technical investigation started the same day with representatives not only from the Police and the Army but also from SÄI (National Inspectorate of Explosives), FMV (The Defence Material Administration) and FortF. In an early phase it was obvious that the storage had been the object of burglary and at a

trial in the springtime 1987 a couple of people were found guilty of grand larcency and dangerous devastation. The involved persons have not been entirely co-operative and there are contradictions in the individual statements. Therefor the cause of events can only be guessed.

It seems as the motorized thieves, after having appropriated some goods - e.g. hand-grenades, plastic explosives, detonating devices - decided on trying to clear away clues and make it impossible at least to find out the extent of the larcency by detonating munition in the storage.

According to one statement three persons prepared ignition at three different locations in the large room with use of some HE-plastics, a cap and an ignition cord. Neither the locations nor the environments of the booster charges are known. Furthermore, some muddle seems to have arisen when they tried to simultaneously light the cords, but at least one of the ignitions succeeded. The burning time of the cords has been estimated to five minutes.

At the interesting time the temperature in the area was 10-11°C, it was partly clouded with 84-86 % humidity and the wind - 10-12 m/s - was coming from southwest. From more detailed meterological data it has been concluded that there was no inversion in the air above the area.

WITNESSES

A number of witnesses has been questioned about the explosive effects. There is a difficulty, however, to get reliable data from such interviews depending on that the people interviewed were unprepared, some of them were shocked and most of them were very unfamiliar to detonations.

The questioning of the witnesses indicated that there was more than one explosion. It can not tell, though, how many there were and which of them was the bigger.

Among the witnesses can be mentioned an amateur seismologist, who had made registrations during the event. His registrations indicated four discrete

detonations,three minor preceding a bigger one. The time delays between the registrations were 54, 10 and 8 seconds. The equipment was not calibrated to permit an analysis of the size of the detonations, unfortunately.

OBSERVATIONS POST EVENT

At the very first approach - the main purpose was to look for injured persons - it was noticed that

* Nothing seemed to remain of the building.
* There was only one crater.
* There had been - and still were - some minor fires in the vicinity (up to 100 m away) ignited - as it seemed - by star shells.
* The terrain was difficult to access in particular because of broken trees.
* There were lots of unexploded ammunitions in the area.

Figure 4 and figure 5 show the site after the event.

The ammunition gave problems. Not so much the HE-fragments and the more or less intact mines and grenades in- and outside the crater but the fuzes. Some of these time-fuzes had to be destroyed on site. It was, however, decided to take advantage of the "accident" and collect as many primary data as possible from this "full scale test".

It was also agreed that every object taken away from the site had to be registrated - door fragments for the police investigation by size and coordinates and unexploded ammunition by type, condition and place in a 15 x 15 m square-net. In practice, however, it was not possible to come up to that standard regarding the ammunition. Surprisingly, many antitank mines - mainly cast HE in a plastic casing - which were a substantial part of the explosives, had not detonated but were found intact, smashed or partly burnt.

However, the number of burnt casings - indicating deflagration - and the amount of HE-fragments could not be accurately estimated during the investigation. Furthermore, on destroying items on the spot many of the explosions revealed ammunition or a resulting crater bigger than expected indicating that

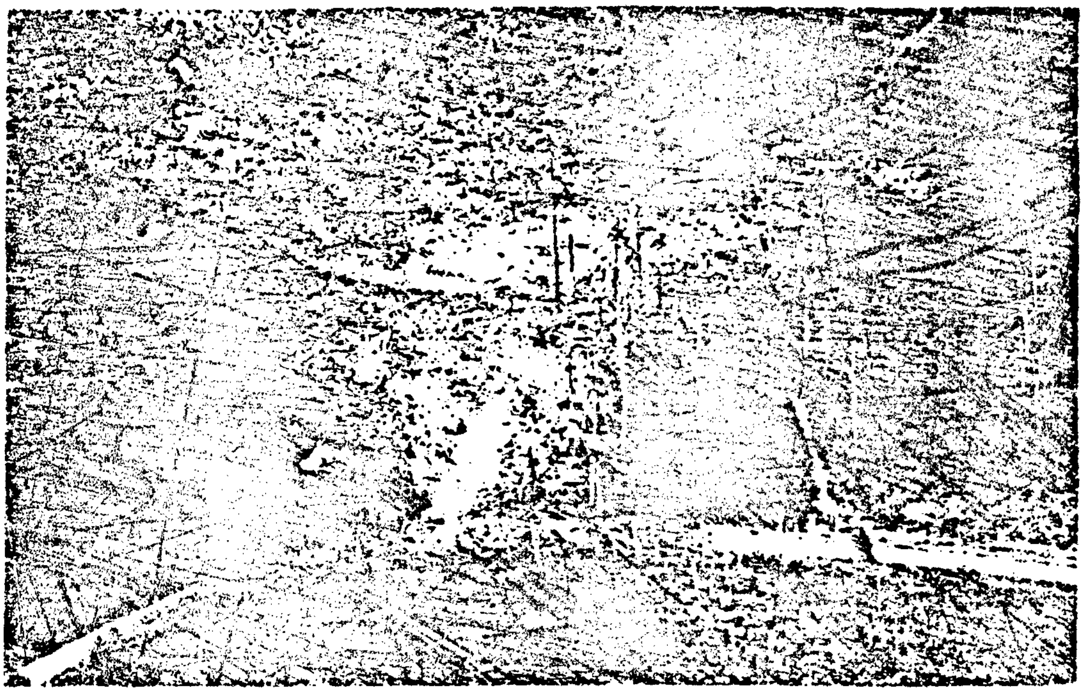

Figure 4. The sita post event seen from west

Figure 5. The site post event seen from the south

more had detonated than the fuzes visible in the first place. Thus, no archaeological digging was performed and, especially in the crater, many items could not be identified.

The season reduced the time available for collection since adequate daylight was limited to between 9 am and 2 pm. Five days after the event a temporary tiny covering of snow prevented the investigation for one day. December 12th, finally, the site had to be left. The clearing and restoring was completed in May 1987.

The Building

As could be expected the building was totally disintegrated. The distribution of debris around the storage could not be examined in detail due to the large amounts of it in the close in region, the hazards involved and the terrain conditions with forests and moors. In certain open areas where the fragments could be found and identified the debris density was estimated, see figure 6. With very few fragments the debris density is difficult to define.

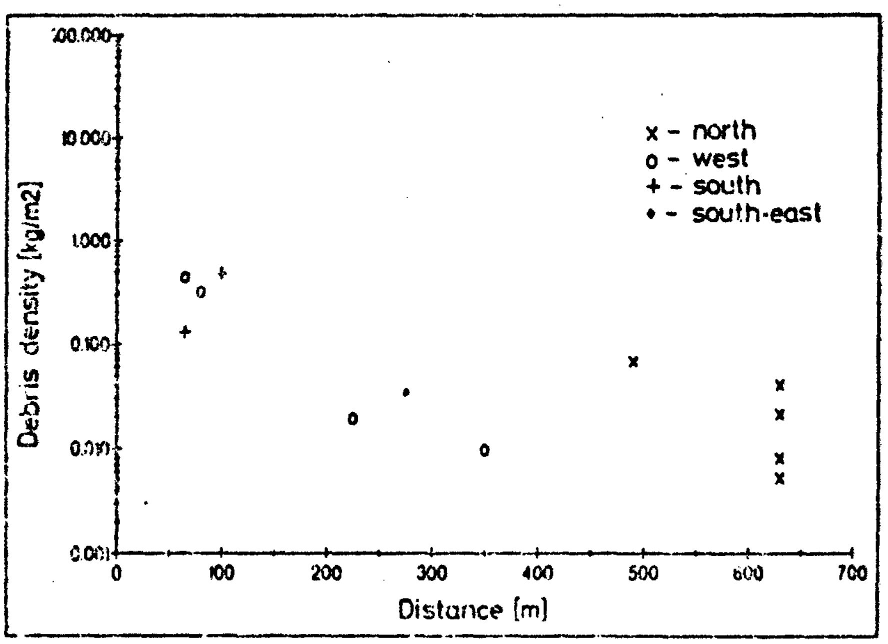

Figure 6. Debris density vs. distance.

The sizes of the fragments varied and differed between the examined areas. In the northern fields - at approximately 600 m distance - the debris were the size of a head while they were much smaller in the southeast direction.

Much effort was put into finding the most remotely travelling debris. A 5 kg piece at 720 m distance was the one found.

Door Fragments

Fragments of the doors and doorframes are shown in figure 7. Since there were two single doors in the western gable and the other doors - one single and two double - in the south wall fragments are of course mostly found in the western and southern directions. In most cases it is possible to do a puzzle with the fragments. This is illustrated in figure 8 for the single door in the southern wall.

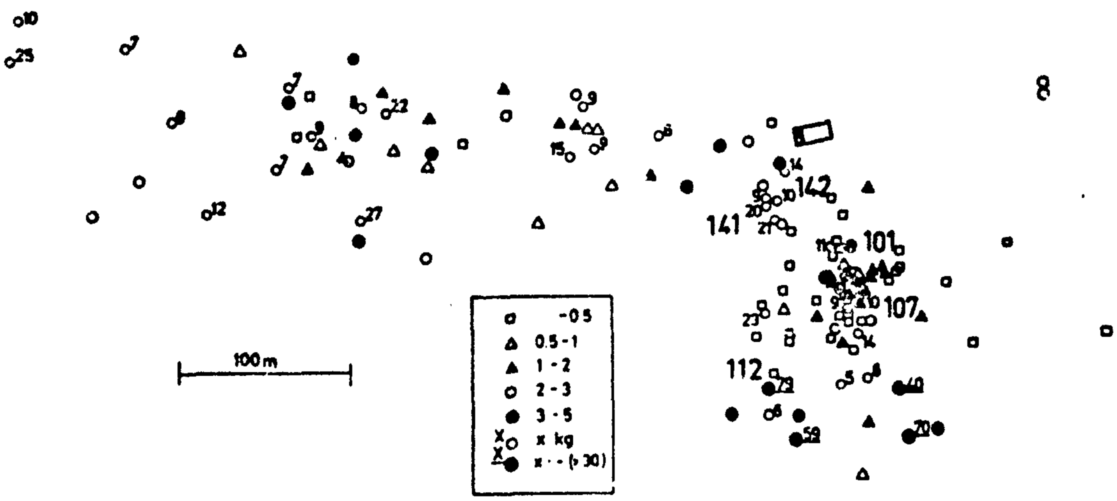

Figure 7. Locations where fragments from doors and frames were found. The numbers refer to items identified in figure 8.

Figure 8. Some parts of the smaller door in the southern wall. The locations where the parts were found are identified in figure 7. The outside 5 mm steelsheet was found double-folded. Photo from /4/.

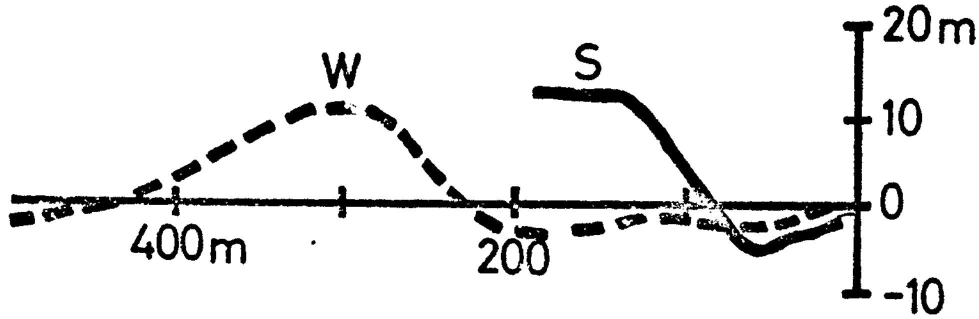

Figure 9. Contour of the ground in the south and west directions where most of the door fragments were found

The Crater

As the terrain below the storage before the event was far from flat, cf. figure 9, it was somewhat difficult to identify and measure the true crater. Also, the measures of it waried from one direction to another. There was no typical embankment surrounding the crater. The original location of the storage could be identified from aerial photos taken before the event. In some spots the level of the approaching drive way could be found.

The crater dimensions (m) observed are given in the table:

Depth	2.1
Width	
Maximum	20
Minimum	14
Average	17

The shape and some crater profiles can be identified from figures 10 and 11.

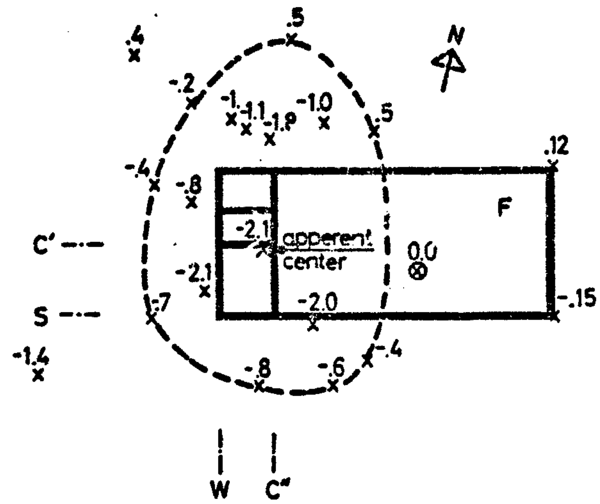

Figure 10. The apparent crater with some ground level values relative to an arbitrarily chosen origin (0.0). F indicates some parts of the remaining concrete floor and the directions c', c'', s and w are referred to in figure 11.

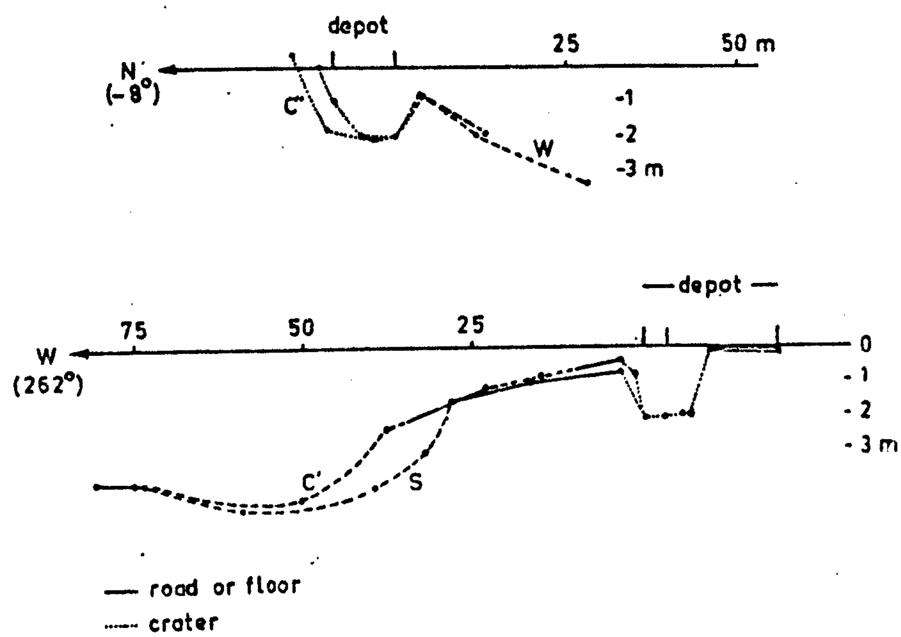

Figure 11. Crater sections. c', c'', s and w refer to figure 10.

Damages to the Forest

The forest in the neighborhood was irregular both with respect to density and age with bare areas at the east, buckwood to the northwest and grown-up pine-trees in the southwest. Close to the depot the existing wood was destroyed with all trees cut down and/or overthrown. The borders of this area were easily defined except of course in the east direction were there were no trees, see figure 12. Naturally, many lone trees were damaged far outside these borders. Figure 13 shows one of the more spectacular hits.

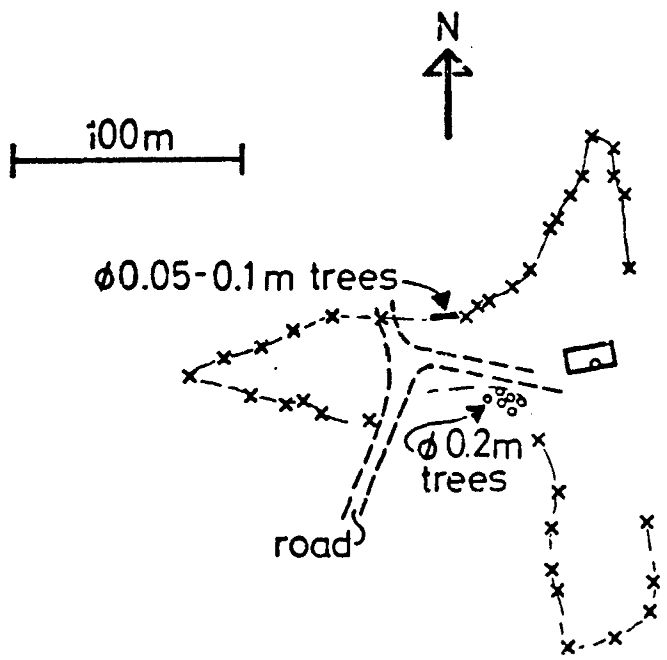

Figure 12. The borders between damaged and undamaged forest.

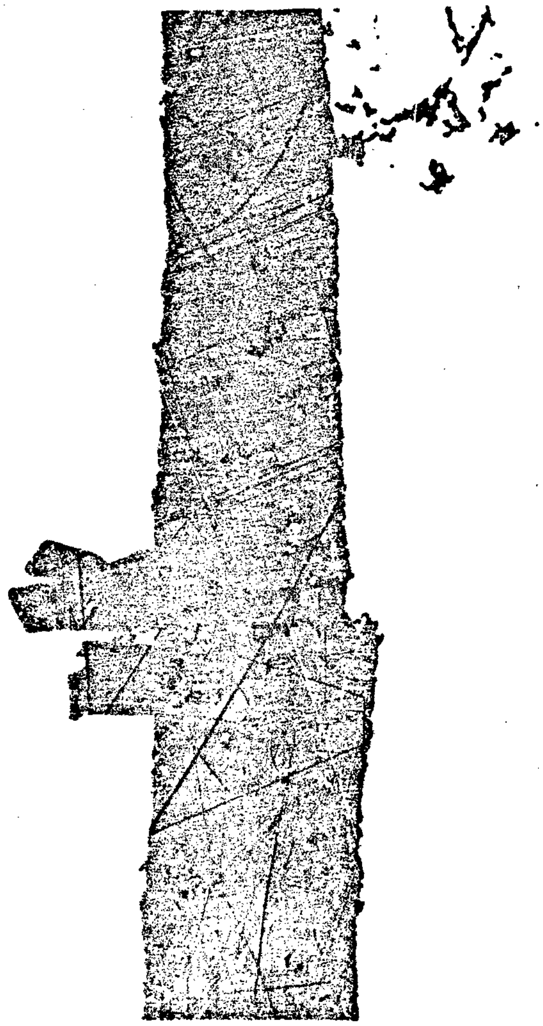

Figure 13. A 0.2 m diameter pine tree hit 4.5 m above the ground 290 m west of the depot by one of the steel fragments (weight 7.4kg) from a door frame.

Damages to the vicinity

More than 100 claims for damages have been registered, most of them from people in houses to the south and east of the storage. This, basically, reflects the fact that most buildings were in these directions.

In some cases the connection between the explosions and the reported damages is obvious in other cases not.

COMPARISONS WITH EXPECTATIONS

It is of particular interest to compare the observations made with calculations using different models. One problem with such a comparison is that the net amount of explosives participating is not known in detail. First of all the original amount of explosives in the storage was reduced as the burglars took some ammunition away before the event. Secondly, all of the munition did not participate due to the fact of improper initiation - a factor, though, which should be given adequate consideration for risk and damage calculations at this kind of events.

The Building

Obviously, the loading density was higher than what was needed to disintegrate the building. Only a part of the floor was with less than major damages.

In Switzerland Basler & Partners has developed a computer code to calculate the fragmentation of a building with an internal explosion and the distribution of these fragments. The physical model is based among other on results in /2/. The program, WATOMA, is described in /5/. The program has been modified by Carl Elfving, /6/, to give additional data.

As examples the calculated number of debris from one of the walls and the distance travelled from the depot are shown in figure 14. Obviously, the major parts of the debris remain in the vicinity of the magazine. The calculation has been repeated with different amounts of explosives in the storage. Also calculations have been made considering the terrain, the elevation of the magazine as well as the forest and combinations. A comparison, cf. figure 15 for 5 and 8 tons of explosives at 200 m distance clearly shows the terrain and other obstacles around the magazine to be effective in catching debris.'

At further distances very few debris can be expected according to these calculations. After the event also very few remote pieces were found. The fragments localized are not numerous enough to permit a more detailed comparison e.g. to make an estimation of the yield of the explosion.

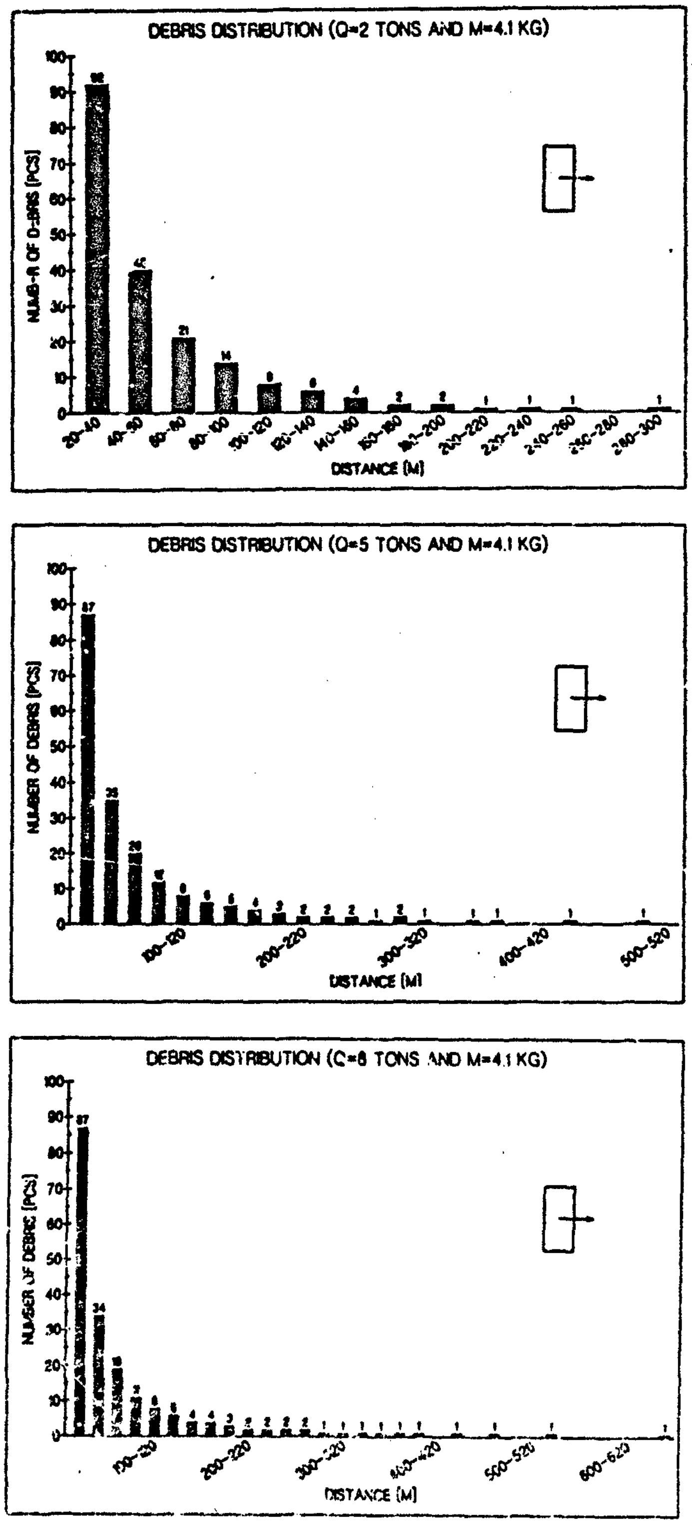

Figure 14. Debris distribution vs range. From /6/.

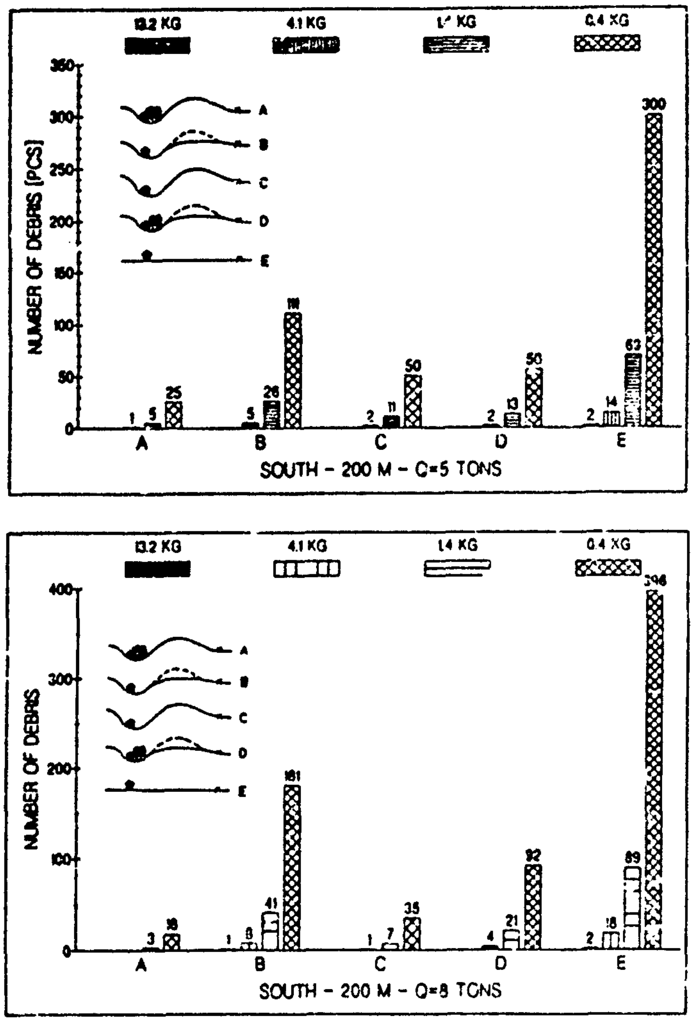

Figure 15. Number of debris of different sizes and with different obstacles. From /6/.

The Crater

From the location of the crater, cf. figure 10, with its maximum depth near one of the short walls, it is obvious that all of the explosives did not detonate simultaneously. Probably, the sloping terrain has facilitated the creation of the crater in the south and west directions. the shape of the crater can be explained to one part by the sloping terrain but also to the distribution of the ammunition in the storage and/or by multiple detonations.

The size of a crater can be calculated according to /7/. The diameter and depth versus charge weight is shown in figure 16 and 17 respectively. The upper lines give upper bounds (95 % fractile) and the lower lines the average values to be expected. (Of course the crater size varies with soil conditions, the shape and the position of the charge at detonation etc).

The crater dimensions given above can be used for calculating Q-values according to the table:

Measures (m)	Q (t)
H=2.1	2.5
D=20	15.6
D=14	5.4
D=17	9.6

As can be concluded from this table a difference exists in the charge weight as calculated from H and D. If separate charges had detonated it would give this result - an increase in diameter but less so for the maximum depth. This indicates that the biggest of the detonations was at least 2.5 tons and less than 5 tons. This conclusion is supported by the amount of remains found post event. The explosives participating in the other detonations noted would total a smaller amount.

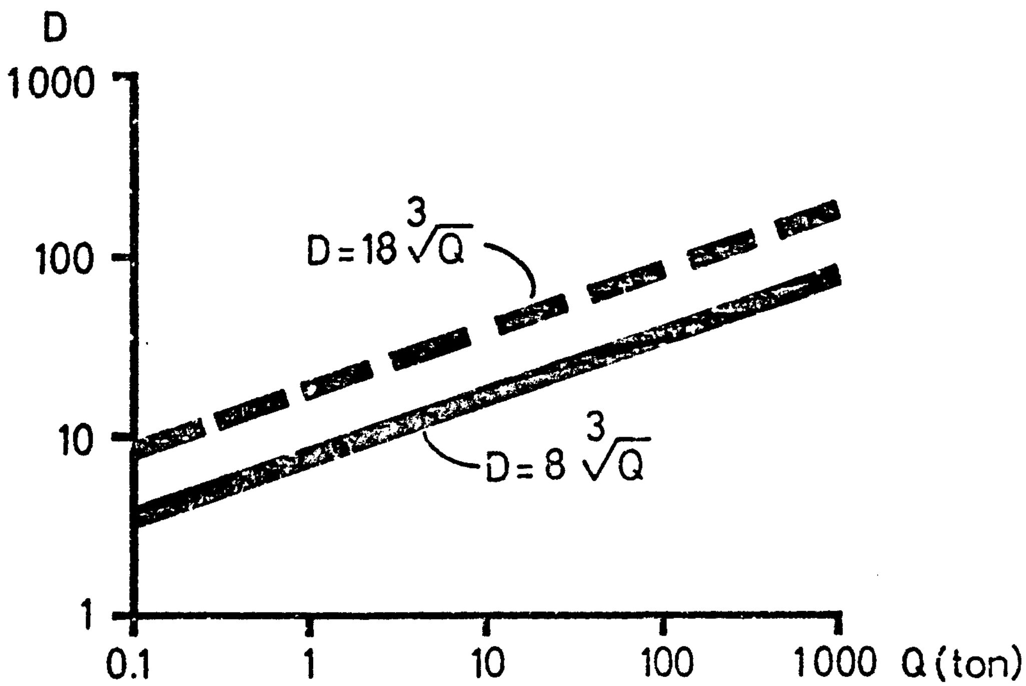

Figure 16. Crater diameter vs yield. From /7/.

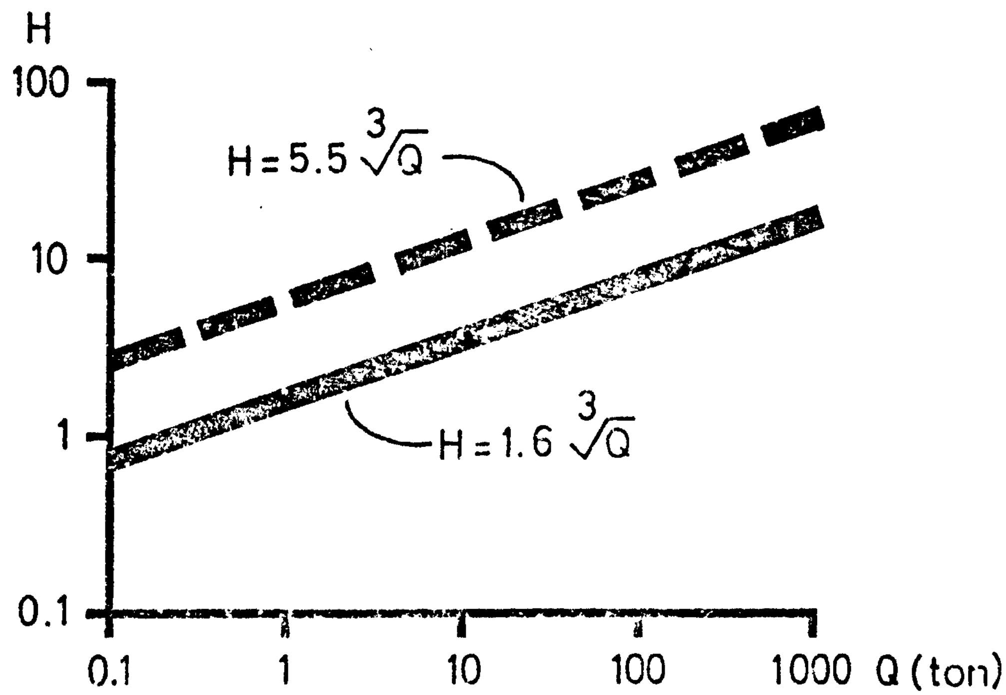

Figure 17. Crater depth vs yield. From /7/.

Damages to the vicinity

A commonly used expression to calculate the pressure (Pa) from yield (kg) and distance (m) is

$$p = k \cdot 70000 \sqrt[3]{Q}/R,$$

where k is depending on focusing effects. With k = 2.5 in the direction of the wind at the site and with k = 1.0 where no wind existed the distance corresponding to p = 250 Pa and p = 1000 Pa can be calculated:

k	Q (t)	p (Pa)	R (km)
2.5	2.5	250	9.5
		1000	2.4
	5.4	250	12.3
		1000	3.1
1.0	2.5	1000	0.9
	5.4	1000	1.2

The range 250-1000 Pa is where windows might begin to break. The calculations show that some damages to windows can be expected about 1 km from the site with no wind and about three times further away in the windward direction. Most of the claims for where from owners to houses within or about this distance. However claims were made also from the owner of a building 24 km away!

CONCLUSIONS

Though many efforts have been put into the collection of data the conditions at the site do not permit extremely sophisticated conclusions. The uncertainty about how the detonation took place also adds uncertainty to the calculations.

legarding this, however, the observations post event showed reasonable agree-
ment with expectations based on calculations.

The outcome of the event supports the risk assessments on which the Swedish regulations are based.

ACKNOWLEDGEMENT

The data in this reported were available only because of the combined efforts and good will from the representatives from the Swedish Army, the Police and other authorities involved in the aftermath of the event. Many individuals at FortF have done an outstanding job in collecting data. Peter Kummer at Basler and Partners has contributed in valuable discussions and is the author of /8/. The same company has also made the WATOMA computer program available to FortF. Carl Elfving has devoted much effort to make calculations. The authors want to extend their thanks to all.

REFERENSES

1/ IFTEX. Instruktion för förvaring och transport av försvarets explosiva varor.(Instruction for Storage and Transportation of Explosive Goods for the Defense.) FMV, 1985. (In Swedish.)

2/ Basler & Hofmann, Modellversuche fuer Oberirdische Explosiv-stoff-magazine.amt Fuer Bundesbauten, Abteilung Bauwesen. Bern 1980.

3/ Merz, Hans, Debris Hazards from Explosions in Above-Ground Magazines. Minutes of the 19th Explosives Seminar. Los Angeles, California. September 9-11, 1980.

4/ Stockholms Polisdistrikt Kriminalavdelningen Tekniska Roteln, Undersökningsprotokoll angående Sprängningen av förrådet i Järna m m. (Police Investigation.) Stockholm 1987. (In Swedish.)

/5/ Basler & Partner, Truemmerwurf bei Explosionen in Oberirdischen Munitionsmagazinen. TM 3113-34. Zurich 1984.

/6/ Elfving, Carl, Private communication. 1988.

/7/ FortH 1.(Fortification handbook).Stockholm 1987. (In Swedish.)

/8/ Basler & Partner, Die Explosionim Munitionsmagazin von Södertälje (S) am 26.11.1986. Reisebericht und erste Schlussfolgerungen. Zurich 1987.

ANALYSIS OF THE DEBRIS PRODUCED BY A PROCESSING BUILDING ACCIDENT

by

Michael M. Swisdak, Jr.
Naval Surface Warfare Center
10901 New Hampshire Avenue
Silver Spring, Maryland 20903-5000

ABSTRACT

In 1986, there was an explosives mishap (accident) at an explosives processing building owned by the United States Air Force. As part of the investigation, as much of the fragments/debris which could be located were found and cataloged. This catalog included item descriptions and locations within an arbitrarily imposed grid system. Also provided as part of the investigation were maps showing the location of each fragment or piece of debris. This information was used to calculate the range at which the hazardous fragment density reached a value of 1 per 600 ft^2 for various azimuth angles around the building location. The data presented can be used to help evaluate the effects of terrain and barricades on the ranges areal densities produced by fragments/debris from explosive incidents.

BACKGROUND

In 1986, there was an explosives mishap (accident) at an explosive processing facility owned by the United States Air Force. As part of the investigation, approximately 4926 fragments or pieces of debris were located and cataloged. This information was included as part of the package provided to the Department of Defense Explosives Safety Board (DDESB).

The facility was of reinforced concrete construction. The north wall was 36" thick while the south wall was 12" thick. ~~The east wall was 24"~~ thick and was backed by earth; the west wall was 12" thick and was constructed of cinder block. The terrain at the facility rose sharply to the East and Southeast. The facility was cut back into the hillside with a barricade located directly to the North. The main section of the building (where the accident occurred) was approximately 40 feet long, 14 feet high, and 36 feet wide. The remainder of the building, including the truck well loading area, was constructed from metal beams with corrugated metal siding. A sketch of the important part of the building is shown in Figure 1. Post-accident investigations estimated the explosive yield of the event to be equivalent to the detonation of 4200 pounds of TNT.

DATA DESCRIPTION

A copy of both the debris catalog and the debris location maps were provided to the Naval Surface Warfare Center (NSWC). These included an item number, item description, the approximate weight of the item, and the map grid location of each item's final resting place. The area around the accident site was divided into a series of blocks. Each block was divided into a series of 100 ft x 100 ft grids (each 100 x 100 grid will, hereafter, be referred to as a cell) and the location of each piece mapped into these cells.

GENERAL ANALYSIS

An analysis of the debris/fragment information described above was begun by Dr. Jerry Ward of the DDESB. At his request, NSWC has completed this analysis.

Trajectory calculations were performed on representative samples of the items contained in the debris catalog. The results of these calculations indicated that all items in the catalog (each piece of recovered debris) must be considered hazardous (i.e., their impact energies were > 58 foot-pounds).

DOD Standard 6055.9[1] requires an Explosives Safety Quantity-Distance (ESQD) arc of 1250 feet (as a default minimum distance) around buildings such as this facility with sited net explosives weights less than 30,000 pounds. There were 368 fragments which went beyond 1250 feet. Table 1 (prepared by Dr. Ward at the DDESB) summarizes the weights and final impact ranges for these fragments. Because the hazard range is stated as 1250 feet does not mean that there are no hazardous fragments beyond this range; rather, it means that the density of hazardous fragments will be below a value of 1 per 600 ft^2 at that range.

As indicated above, detailed maps showing the location of each fragment within each cell were provided. As part of the analysis procedure, the total number of fragments within each cell was determined; if a fragment were shown as being exactly on the dividing line between two cells, the fragment was divided and half assigned to each cell. These total fragment numbers are shown in Table 2 for each cell.

Questions that should be addressed by this data include:

(1) Where (at what range) does the hazardous fragment density fall below 1 per 600 ft^2?
(2) How does this range vary with azimuth around the building?
(3) How is this range influenced by terrain, barricades, building construction details, or other possible mitigating factors?

ANALYSIS PROCEDURE

It was decided that the range at which the fragment density fell below 1 per 600 ft^2 would be computed at 15° intervals around the building (0°, 15°, 30°, 45°, etc). The coordinate system was chosen such that 0° was at the top of the grid system described above. This corresponds to a direction of due East. It was further decided to consider 100 ft x 100 ft sections along each azimuth. These sections would be 100 feet long and have a width of 50 feet on either side of the azimuth center line. The fragment density calculations were started in the cells located 200 feet from the explosion source. The explosion source was defined as a four cell area and is shown as a darkened area near the center of Table 2.

The procedure basically involved mapping the rectangular recovery grid into polar coordinates. Once the data were mapped into polar coordinates, the number of hazardous fragments in each cell was computed. In addition, the number of hazardous fragments that would be allowed in each cell and still not exceed the fragment density of 1 per 600 ft^2 was also computed. Finally, the ratio of these two quantities was determined for each cell. To meet DOD Standards, this ratio must be ≤ 1.00.

A smoothing procedure developed during the analysis of the debris produced by explosions inside hardened aircraft shelters (Operation DISTANT RUNNER)[2] was then applied to these data. This procedure utilizes two new variables which are defined below:

$$N = (N_c/N_A)_j = \sum_{i=j}^{k} (N_c)_i \Big/ \sum_{i=j}^{k} (N_A)_i$$

and

$$R = \sum_{i=j}^{k} R_i/(k-j+1)$$

where

N	=	Normalized (smoothed) Fragment Density Ratio
R	=	Normalized Range (feet)
$(N_c)_i$	=	Number of hazardous debris in zone i
$(N_A)_i$	=	The acceptable number of hazardous debris that corresponds to an areal density of 1 per 600 ft^2 for zone i
R_i	=	The distance from the explosion center to the mid-point of zone i

i = Index for full-scale zone; varies from 1 to k (outermost zone)
j = Specific zone index between i=1 to i=k

These smoothed data are presented in Table 3 for each azimuth angle in the form of N vs R for each normalized range increment.

As indicated above, what is needed is the range at which the fragment density ratio becomes $\leq$ 1.00. Again, the same procedure that was developed during the analysis of the Operation DISTANT RUNNER data was applied to the material in Table 3. This procedure involves fitting an equation of the form:

$$N=A\,e^{BR}$$

where N is the fragment density ratio, R is the normalized range, and A and B are fitting constants. The values of the fitting constants are given in Table 4 for each azimuth direction. Also included on this table is a measure of the goodness of fit for each angle (a perfect correlation would have an r^2 value of 1.000). The fitted curves were then used to calculate the range at which the fragment density ratio becomes 1.00. Further statistical analyses of this information provide a 95% confidence interval for this range. Thus, for each azimuth angle, there is a calculated hazard range. Associated with that range is an upper and lower bound (corresponding to the 95% confidence interval). These values are presented in Table 5.

RESULTS AND INTERPRETATION

Figure 2 presents a plot of the N=1 fragment density ratio as a function of range around the facility. Figure 3 presents the 95% confidence interval for the hazard range. Superimposed on both of these plots are circles whose radii are 1250 feet--the ESQD arc required by the current DOD standards.

Figures 2 and 3 and the equations for the fragment density as a function of range and azimuth (Table 4) provide the information needed to answer the questions raised above. The average hazardous fragment range (averaging over all azimuth angles) was 1123 $\pm$105 feet. The actual variation with azimuth angle is readily seen in both Figures 2 and 3.

There was an area of essentially flat terrain at the site. It extended between the azimuth angles of 135° and 195°. In this area, the hazard range was 1289 feet. The greatest hazard range was determined to be 1349 feet (8% greater than the 1250 foot standard). The terrain rose sharply in a direction generally toward the East. Specifically,

the upsloping area was assumed to lie between the azimuths of 345° and 45° (remember, East is defined as 0°). In this general direction, the average hazard range was 1100 feet. The barricade covered an azimuth extending from 225° to 285°. In this region, the average hazard range was 1073 feet. These effects are compared in Figure 4.

The effect of the barricade was to reduce the average hazard range by 16.6% when compared to the "flat terrain" range. The upsloping terrain had the effect of reducing the average hazard range by 14.5%.

In general, the 1250-foot hazard range, as prescribed in DOD-Standard 6055.9, was found to be a good (if slightly conservative) estimate of the true hazard range.

REFERENCES

1. DOD 6055.9-STD, Department of Defense Ammunition and Explosives Safety Standards, July 1984.

2. Ward, Dr. Jerry M., "Distant Runner--Debris Recovery and Analysis Program for Events 4 and 5," Minutes of the Twenthieth Explosives Safety Seminar, 24-26 August 1982.

TABLE 1. FRAGMENT SUMMARY

RANGE (feet)	NUMBER OF FRAGMENTS	WEIGHT <1 POUND	WEIGHT =1 POUND	WEIGHT >1 POUND	WEIGHT >10 POUNDS
1250-1500	161	49	38	74	26
1500-2000	153	31	57	65	14
2000-2500	40	8	8	24	6
2500-3000	12	1	3	8	1
>3000	2	0	1	1	1
TOTAL	368	89	107	172	48
Percentage		24.2	29.1	46.7	13.0

TABLE 2. NUMBER OF FRAGMENTS RECOVERED PER CELL

									1		1	0.5	0.5																		
										2	2	1				1	1				1										
							2	2	1	1	1		1		2		1	1	2	1	1										
		2				1	1	2	1	4	1	3	4	4	3	4	6.5	5	3	4	7	5									
		1	1	1			2	2	1	3	5	5	3	3	2	9	0.5	5	8	3	7	6									
			2			4	2	1	2	3		4	1	2	5	4	6	10	3	4	4	2									
				2	2	1			2	5	7	1	10.5	6.5	7	16	7	3	4	10	5	4	1								
				4				3	1	2	5	4	3	4	3	9	6	5	5	5	4	2		1							
		1		12	1.5	4.5	5	6	12	4	15	6	3	5	7	6	2	3	3	3	8	4									
	4	2	4	14	9	10	3	4	8	7	14	11	20.5	4.5	5	7	4	1	5	6	9		0.5	0.5							
	1	2	1	1	7	5	10	13	1	3	10	5	21	9	11	11	8	4	2	3	2	1	1								
			2	4	5	24	21	3	11.5	7.5	7	6	12	14	8	9	3	3.5	1		2			1							
2	1			6	4	13	21	32	16	32	3	6	5	15	14	20		0.5	2	1											
			1	5	5	13	18	46	26	28	19			17	11	19	6														
			6	2	4	5	21	18	49	13	22			55	15	15.5	17														
				1	1	2	40	6	7	10	31	17	61	60	14	12.5	12	5													
	1	1		2	2	1	10	9	31	4	5	28.5	92	45.5	26	12	3	6													
			2	5	8		1	3	12	3	3	17	41.5	60	23.5	11		2		1		4									
		1		4	2		0.5	4	24	26	44	19	20	45	25	8	11			2											
		2		1	4	5	8.5	10	18	59	86.5	78.5	81.5	18.5	15.6	9	7	1				1	2				1	1			
		1		1	2	3	2	14	18	258.5	95.5	105	32.5	38	20	20	22	1	8	2								1			
				1	2	2	2	3	6	8	61	68	84	75	23	10	9	6	3	2	3						1	1			
1					3	1	1	2	1	1	14	36	45	38	21	19	12	6	2	2	4						1				
				2	1				2	1	15	38	39	35	20	7	6	2			3	2	1	6	7						
				1					1	2	3	6	22	14.5	9.5	7	8	5		1	4	6	1.5	0.5		5	6	2			
		0.5				1			1		8	13	22	12	13	7	7	5	2	2	3		2	5	2		4				
		0.5			3	1			2	3	5	9	9	6	12	4	5	4		3	2	1	6	6	3	2	2	2			
		1					1		2		1		7	8	5	1	1	2	4	1.5	4	4			2	1	6	1			
											0.5	2.5		2	2.5				1	0.5	1		3	8			1	3			
										1				2	6.5				1			6	6	1		1	4				
								1				1	2	1	1	2	2										2				
							1	1				1					2		1	1	1	2		1				1			
												1								1	0.6	2.5			2	1					
							2													2					1			1			
																		0.5	0.5	1		1						3		2	
																1			3	1			1		1						
										1										1										1	
												1																			2
																												1			
																	0.5	1	0.5												

BUILDING

E

N S

W

NOTE: EACH CELL REPRESENTS AN AREA OF 100 FT X 100 FT

TABLE 3 FRAGMENT AZIMUTH-DENSITY-RANGE DATA

NORMALIZED RANGE (feet)	BEARING 0°	15°	30°	45°	60°	75°	90°	105°	120°	135°	150°	165°
900	2.76	2.72	3.88	4.25	4.55	4.36	2.67	4.70	5.86	10.85	16.81	24.13
950	2.40	1.91	3.01	3.38	3.73	3.73	1.83	2.34	2.24	6.61	12.26	19.80
1000	2.10	0.93	2.25	2.83	3.16	2.51	0.93	1.48	1.24	4.44	8.93	17.01
1050	1.44	0.35	1.79	2.17	2.77	1.56	0.18	0.68	0.54	2.93	6.10	15.47
1100	1.08	0.32	1.49	1.76	2.40	1.32	0.00	0.16	0.38	2.30	4.61	12.24
1150	0.84	0.23	1.25	1.58	1.99	1.07	0.00	0.00	0.25	1.75	3.64	9.43
1200	0.78	0.17	1.05	1.37	1.26	0.63	0.00		0.23	1.43	2.40	5.29
1250	0.54	0.12	0.70	1.08	0.79	0.37	0.00		0.15	1.34	1.82	3.37
1300	0.24	0.05	0.27	0.66	0.52	0.24	0.00		0.12	1.05	1.07	1.88
1350	0.05	0.03	0.04	0.32	0.25	0.06	0.00		0.04	0.92	0.76	1.29
1400	0.06	0.00	0.00	0.00	0.07	0.00	0.00		0.00	0.76	0.46	0.58
1450	0.00				0.00		0.00			0.56	0.27	0.11
1500										0.38	0.20	0.00
1550										0.15	0.07	
										0.00	0.00	

NORMALIZED RANGE (feet)	BEARING 180°	195°	210°	225°	240°	255°	270°	285°	300°	315°	330°	345°
900	25.17	20.11	5.03	3.79	2.93	5.93	9.06	7.41	6.20	3.30	2.48	3.25
950	23.46	19.10	4.36	2.98	2.31	4.28	7.44	5.80	4.47	2.06	2.07	2.87
1000	22.44	18.85	4.14	2.14	1.71	2.59	3.90	4.13	3.59	1.78	1.73	2.30
1050	21.35	18.54	3.35	1.22	1.21	1.62	1.98	2.29	3.08	1.51	1.47	1.56
1100	16.65	12.16	1.97	0.99	0.70	0.29	1.05	1.23	2.07	0.99	0.94	0.94
1150	10.35	0.78	1.00	0.86	0.66	0.20	0.51	0.61	1.52	0.78	0.39	0.75
1200	6.27	0.30	0.23	0.41	0.43	0.11	0.21	0.33	1.08	0.49	0.22	0.48
1250	4.11	0.22	0.07	0.21	0.22	0.06	0.03	0.13	0.49	0.40	0.22	0.30
1300	1.83	0.14	0.01	0.09	0.09	0.03	0.00	0.07	0.07	0.37	0.13	0.18
1350	1.47	0.06	0.00	0.00	0.09	0.00		0.02	0.02	0.25	0.03	0.09
1400	0.69	0.00			0.00			0.00	0.00	0.20	0.00	0.03
1450	0.15									0.11		0.02
1500	0.15									0.04		0.00
1550	0.00									0.00		

TABLE 4. LEAST SQUARES FITTING COEFFICIENTS

AZIMUTH ANGLE (°)	A Coefficient	B Coefficient	r^2
0	4771.7	-0.0078	0.894
15	13327.3	-0.0096	0.974
30	7465.3	-0.0080	0.794
45	414.4	-0.0050	0.930
60	5417.2	-0.0073	0.875
75	12585.8	-0.0085	0.930
90	25302346.0	-0.0175	0.901
105	9884776.0	-0.0160	0.952
120	19378.7	-0.0096	0.954
135	991.9	-0.0053	0.956
150	25507.7	-0.0079	0.981
165	115460.8	-0.0087	0.891
180	231269.8	-0.0092	0.914
195	40694388.0	-0.0150	0.895
210	8799436.0	-0.0148	0.848
225	14209.9	-0.0089	0.954
240	6659.0	-0.0083	0.967
255	2639652.0	-0.0141	0.976
270	16055596.0	-0.0154	0.941
285	1658913.5	-0.0131	0.974
300	362131.5	-0.0114	0.838
315	1085.1	-0.0064	0.961
330	15545.6	-0.0092	0.929
345	26304.3	-0.0094	0.959

NOTES: (1) Fit is of the form $Y=Ae^{Bx}$

(2) r^2 is a measure of the goodness of fit

(r^2 = 1.000 is perfect correlation)

TABLE 5. FRAGMENT HAZARD RANGE VERSUS AZIMUTH ANGLE

AZIMUTH ANGLE (°)	RANGE (feet)	RANGE-Upper (95% confidence) (feet)	RANGE-Lower (95% confidence) (feet)
0	1091	1127	1049
15	994	1014	971
30	1120	1178	1061
45	1212	1245	1187
60	1173	1216	1135
75	1112	1139	1084
90	972	1125	725
105	1007	1038	980
120	1032	1056	1003
135	1294	1314	1274
150	1289	1302	1276
165	1343	1409	1296
180	1349	1400	1310
195	1168	1212	1131
210	1082	1129	1029
225	1079	1100	1058
240	1060	1077	1041
255	1047	1062	1029
270	1080	1107	1053
285	1094	1110	1078
300	1122	1172	1071
315	1098	1119	1075
330	1043	1078	1013
345	1083	1106	1057
AVERAGE	1123	1160	1083
STD. DEV.	105	107	125

(note: 0° corresponds to East)

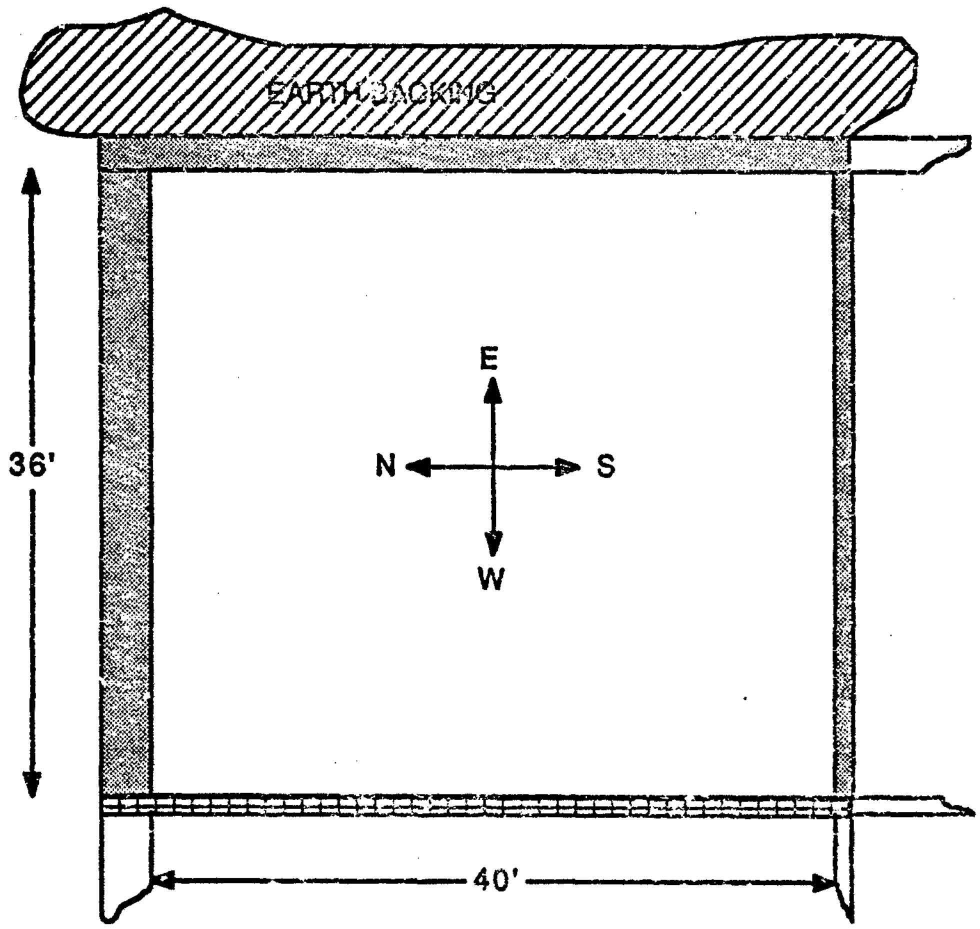

FIGURE 1 EXPLOSION SITE SCHEMATIC

FIGURE 2 FRAGMENT HAZARD RANGE CONTOUR

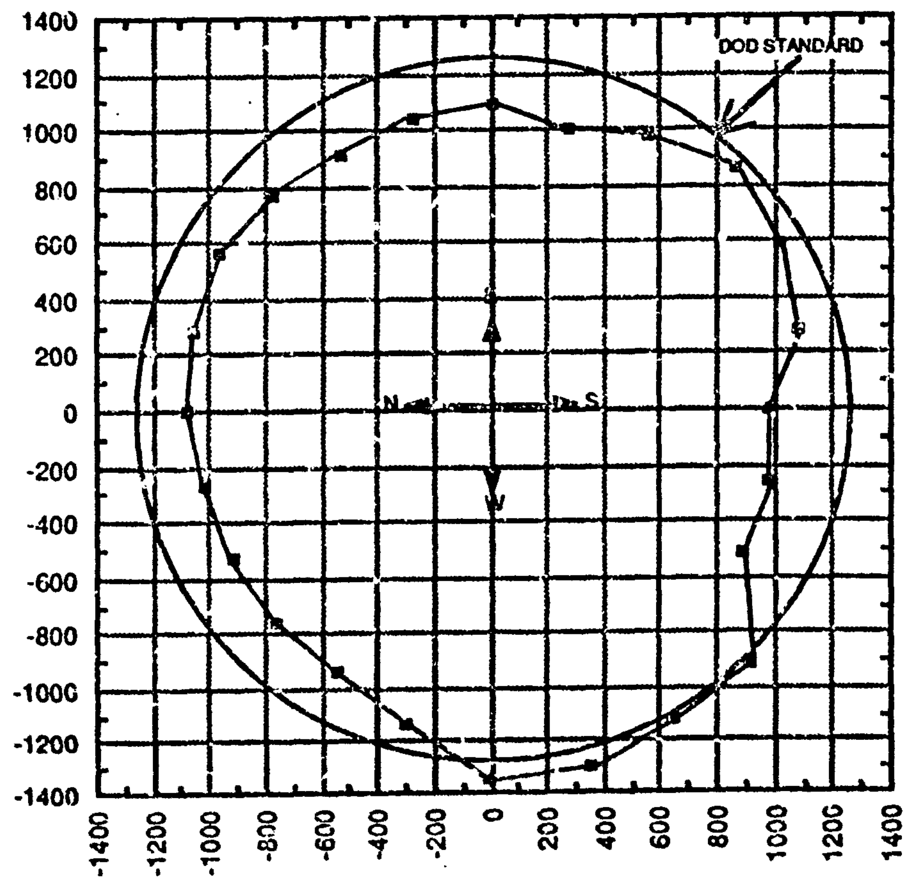

FIGURE 3 95% CONFIDENCE INTERVAL FOR FRAGMENT HAZARD RANGE

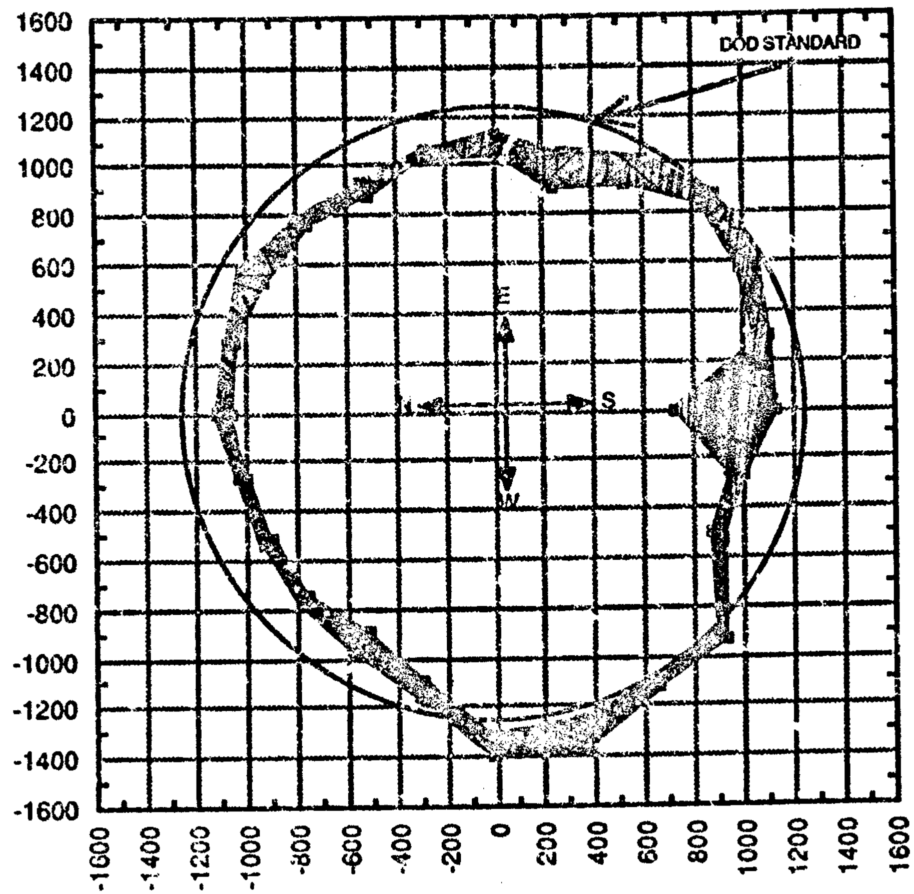

FIGURE 4 THE EFFECTS OF BARRICADES AND TERRAIN ON DEBRIS HAZARD RANGE

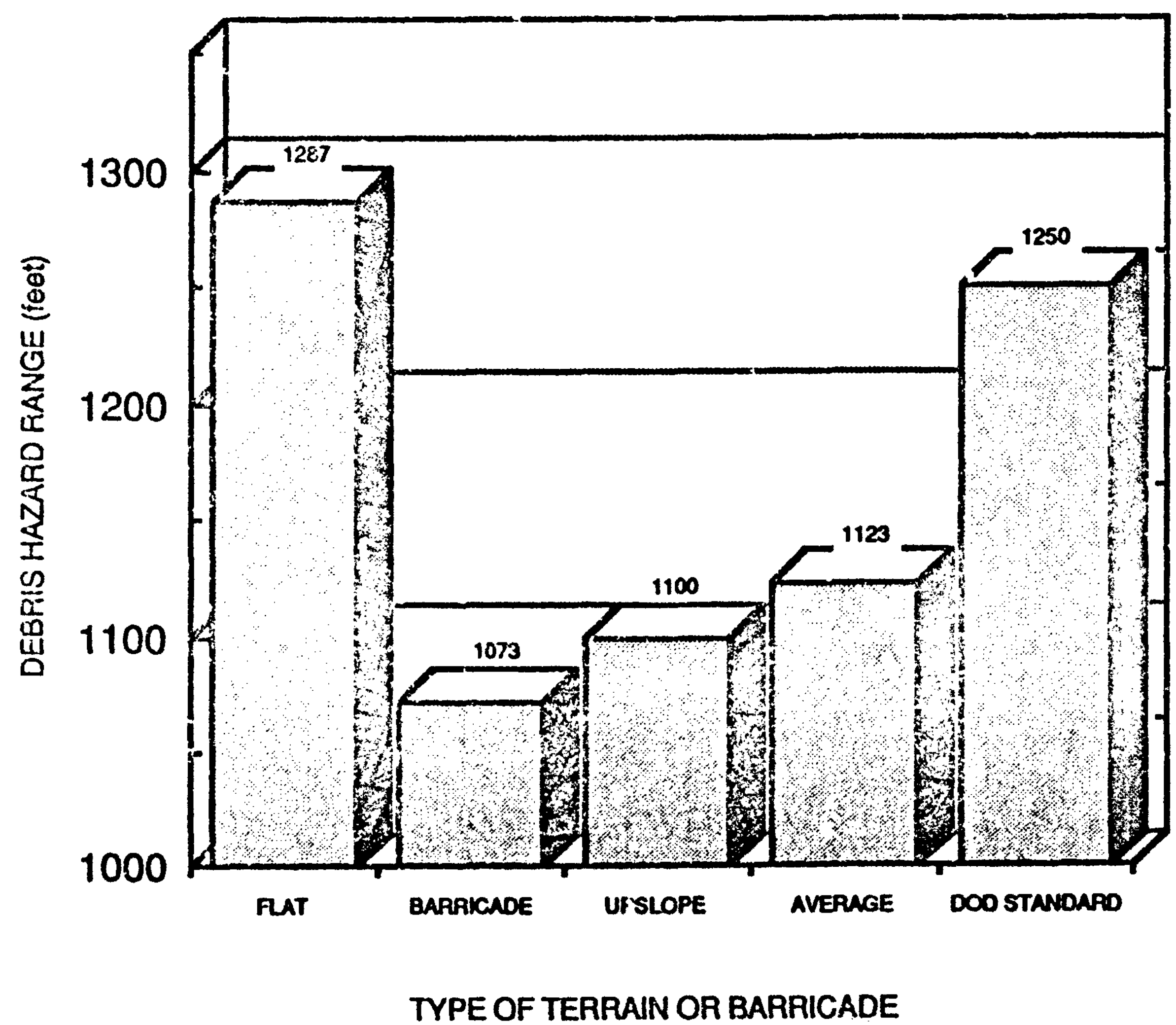

Photo Reconnaisance Acquisition Program (PRAP)

Richard W. Ash

Despite all of our efforts and successes at preventing explosive accidents, we still find the perfect explosive safety program illusive. Tragically, sophisticated and well established procedures fail to prohibit all explosive mishaps. Given that the unforeseen will continue to occur, we must strive to hone our response procedures.

With these thoughts in mind, I have endeavored to establish a program that utilizes existing DOD resources to provide investigation teams with timely aerial photography of explosive accident sites.

The U.S. Air Force provides the resources with its tactical reconnaissance squadron (TRS) aircraft of the active and national guard forces. Three active duty and five national guard squadrons of RF-4C aircraft provide conus coverage of potential explosive sites. The active duty squadrons are the 91st and 12th TRSs at Bergstrom AFB, TX and the 16th TRS at Shaw AFB, SC. The national guard sites are the 192nd TRS in Reno, Nevada, 173rd TRS in Lincoln, NE, 190th TRS in Boise, ID, the 106th TRS in Birmingham, AL, and the 153rd TRS in Meridian, MS.

A Memorandum of Understanding (MOU) between the Tactical Reconnaissance Operations and Programs Division and the USAMC Field Safety Activity (FSA) formalizes PRAP operations (See Appendix A). The MOU of March 1987 documents individual service responsibilities for the FSA PRAP under the authority of DOD 4000.19-R Defense Regional Interservice Support (DRIS) Regulation, March 1984, and Air Force Regulation 95-8, Requesting and Reporting Aerial Imagery, dated 16 April 1982.

FSA desires to manage a system to obtain aerial photography of major accidents/incidents through a single source. This program is simple to initiate and has a short response time. Timely aerial photographs are beneficial to accident investigation boards. They can be used to:

a. Preserve evidence.

b. Aid in the estimated quantity of explosive material involved.

c. Enhance the verification of AMC quantity-distance tables.

d. Identify fragment dispersion pattern.

e. Locate fragments.

f. Verify storage compatibility charts.

g. Give investigators an overview of the accident/incident site.

The following are established as guidelines for the conduct of PRAP operations and may be amended informally as particular circumstances dictate.

a. Office of responsibility for AMC is: USAMC Field Safety Activity, AMXOS-SE, Charlestown, IN 47111-9669.

b. Office of responsibility for the Air Force is: HQTAC, Reconnaissance Operations and Programs Division, DOP-DOPR, Langley AFB, VA 23665.

c. Requests made as a result of an accident/incident will not normally require funding by the requestor.

d. Photography will be black and white.

e. FSA will receive five copies of 9 inch x 9 inch prints, and all negatives within 96 hours of their request.

In May 1987, FSA and the Naval Sea Systems Command (NAVSEASYSCOM) completed an MOU for PRAP services (See Appendix B). The FSA is NAVSEASYSCOM's point of contact for PRAP services in the event of an explosive accident on a Navy installation.

Since its inception, FSA utilized the PRAP program on four occasions. Our first initiation followed initial program placement and tested our procedures to ensure its successful accomplishment (See Appendix C). The second occasion supported an Department of Army exercise conducted by the Surety Field Activity at Savannah, IL on 11 August 1987. Accidents at the Lone Star Army Ammunition Plant (10 October 1987) and Radford Army Ammunition Plant (19 March 1988) were the first real tests of the PRAP.

Our experiences with the PRAP have demonstrated its capabilities as a valuable tool. It serves as an excellent example of interservice cooperation that maximizes scarce resources by utilizing existing assets.

For more information on this program, please contact the U.S. Army Materiel Command, Field Safety Activity, Charlestown, IN 47111-9669.

APPENDIX A

DEPARTMENT OF THE ARMY
U.S. ARMY MATERIEL COMMAND
FIELD SAFETY ACTIVITY
CHARLESTOWN, INDIANA 47111-9669

REPLY TO
ATTENTION OF:

MEMORANDUM OF UNDERSTANDING
BETWEEN
TAC, RECONNAISSANCE OPERATIONS AND PROGRAMS DIVISION, AND
ARMY MATERIEL COMMAND (AMC) FIELD SAFETY ACTIVITY (FSA)

SUBJECT: AMC Photo Reconnaissance Program (PRP)

1. Purpose. This Memorandum of Understanding (MOU) formalizes the responsibilities and procedures for execution of the AMC PRP.

2. Reference. This MOU documents individual service responsibilities for the AMC PRP under the authority of DOD 4000.19-R Defense Regional Interservice Support (DRIS) Regulation, Mar 84, and AFR 95-8, Requesting and Reporting Aerial Imagery, dated 16 Apr 82.

3. Problem. AMC desires to establish a single source for aerial photography of major accidents/incidents. This program must be simple to initiate and have a short response time. Timely aerial photographs are beneficial to accident investigation boards, they can be used to:

a. Preserve evidence.

b. Aid in the estimate of explosive material quantity involved.

c. Enhance the verification of AMC quantity - distance tables.

d. Identify fragment dispersion pattern.

e. Locate fragments.

f. Verify storage compatibility charts.

g. Give investigators an overview of the accident/incident site.

4. Scope of responsibilities, procedures, and limitations. The following are established as guidelines for the conduct of PRP operations. They may be amended informally as particular circumstances dictate.

a. Office of responsibility for AMC is: USAMC Field Safety Activity, AMXOS-SE, Charlestown, IN 47111-9669, AUTOVON 366-7825.

b. Office of responsibility for TAC is: HQ TAC, Reconnaissance Operations and Programs Division, DOF-DOFR, Langley AFB, VA 23665, AUTOVON 574-3527.

SUBJECT: AMC Photo Reconnaissance Program (PRP)

c. Requests made as a result of an accident/incident will not normally require funding by the requestor.

d. Requests will be made by AMC FSA via telephone, and followed up by a message from FSA within 48 hours.

(1) Telephone: HQ-TAC, DOF-DOFR
During duty hours - AUTOVON 574-3527
During non-duty hours - AUTOVON 574-7771 (ask for DOF duty officer)

(2) Message: TO: HQ TAC, LANGLEY AFB, VA //DOF/DOFR//
INFO: 9 AF, SHAW AFB, SC //DO//
12 AF, BERGSTROM AFB, TX //DO//
Installation Safety Office

e. Photography will be normally black and white. High cost and limited availability preclude color film in most cases.

f. When requesting photographic support AMC FSA will provide:

1. Location of site to include, a. Name and location of installation and b. Longitude and latitude of point(s) to be photographed or points defining area to be photographed.

2. Desired scale of vertical pinpoint photograph if known. Specify "best possible" if unknown.

3. Name and autovon phone number of installation POC to answer specific questions.

g. Type of photographic coverage available.

(1) Vertical pinpoint.

(2) Forward oblique.

(3) Side oblique.

(4) Infrared imagery.

h. HQ TAC will issue a priority tasking within 24 hours of FONECON to accomplish paragraph 4d request.

i. Five copies of 9" X 9" prints will be delivered to AMC Field Safety Activity within 96 hours of phone request. All negatives will also be forwarded.

SUBJECT: AMC Photo Reconnaissance Program (PRP)

Billington

GORDON F. BILLINGTON, Col, USAF
HQ TAC/DOF
Langley AFB, VA 23665-5001

3/30/87

James D. Lloyd

JAMES D. LLOYD
Director
USAMC Field Safety Activity
Charlestown, IN 47111-9669

MARCH 25, 1987

APPENDIX B

DEPARTMENT OF THE NAVY
NAVAL SEA SYSTEMS COMMAND
WASHINGTON, DC 20362-5101

IN REPLY REFER TO
OPR: 6522
Ser 06/375
13 May 87

Memorandum of Understanding between

Naval Sea Systems Command (COMNAVSEASYSCOM) and

Army Material Command (AMC) Field Safety Activity (FSA)

Subject: PHOTO RECONNAISSANCE ACQUISITION PROGRAM (PRAP)

1. Purpose. This Memorandum of Understanding (MOU) formalizes the responsibilities and procedures for execution of the COMNAVSEASYSCOM/AMC PRAP.

2. Reference. This MOU documents individual service responsibilities for the COMNAVSEASYSCOM/AMC PRAP under the authority of DOD 4000.19-R Defense Regional Interservice Support (DRIS) Regulation, Mar 84.

3. Problem. AMC agrees to act as a source for aerial photography of major accidents/incidents within the Navy. This program is simple to initiate and has a short response time. Timely aerial photographs are beneficial to accident investigation boards; they can be used to:

a. Preserve evidence.

b. Aid in the estimate of explosive material quantity involved.

c. Enhance the verification of quantity-distance tables.

d. Identify fragment dispersion pattern.

e. Locate fragments.

f. Verify storage compatibility charts.

g. Give investigators an overview of the accident/incident site.

SUBJECT: PHOTO RECONNAISSANCE ACQUISITION PROGRAM (PRAP)

4. Scope of Responsibilities, Procedures, and Limitations. The following are established as guidelines for the conduct of PRAP operations. They may be amended informally as particular circumstances dictate.

a. Office of responsibility for AMC is: AMC Field Safety Activity, AMXOS-SE, Charlestown, IN 47111-9669, Autovon 366-7825.

b. Office of responsibility for Navy is: Naval Sea Systems Command, SEA 652, Washington DC 20362, Autovon 222-2080.

c. Requests made as a result of an accident/incident will not require funding by the requestor.

d. COMNAVSEASYSCOM should make initial request to FSA via telephone.

e. FSA will coordinate the accomplishment of requests in accordance with Air Force (TAC)/Army (AMC) agreements presently in effect.

f. Photography will be black and white. High cost and limited availability preclude color film in most cases.

g. When requesting photographic support, COMNAVSEASYSCOM will provide:

(1) Location of site to include: Name and location of installation; longitude and latitude of photographic point(s), or points defining photographic area.

(2) Desired scale of vertical pinpoint photograph if known. Specify "best possible" if unknown.

h. Type of photographic coverage available:

(1) Vertical pinpoint.

(2) Forward oblique.

(3) Side oblique.

(4) Infrared imagery.

i. COMNAVSEASYSCOM will issue a follow-up priority message tasking the request (paragraph 4g) within 24 hours of PHONCON to DIRAMC FSA CHARLESTOWN IN //AMXOS-SE//.

Subj: PHOTO RECONNAISSANCE ACQUISITION PROGRAM (PRAP)

j. Five copies of 9" x 9" prints will be delivered to COMNAVSEASYSCOM within 7 working days of message request. All negatives will also be forwarded.

C. J. CAMPBELL
Acting Director
AMC Field Safety Activity
Charlestown, IN 47111-9669

M. E. CHANG
Deputy Commander for
Weapons and Combat Systems
Washington, DC 20362-5015

APPENDIX C

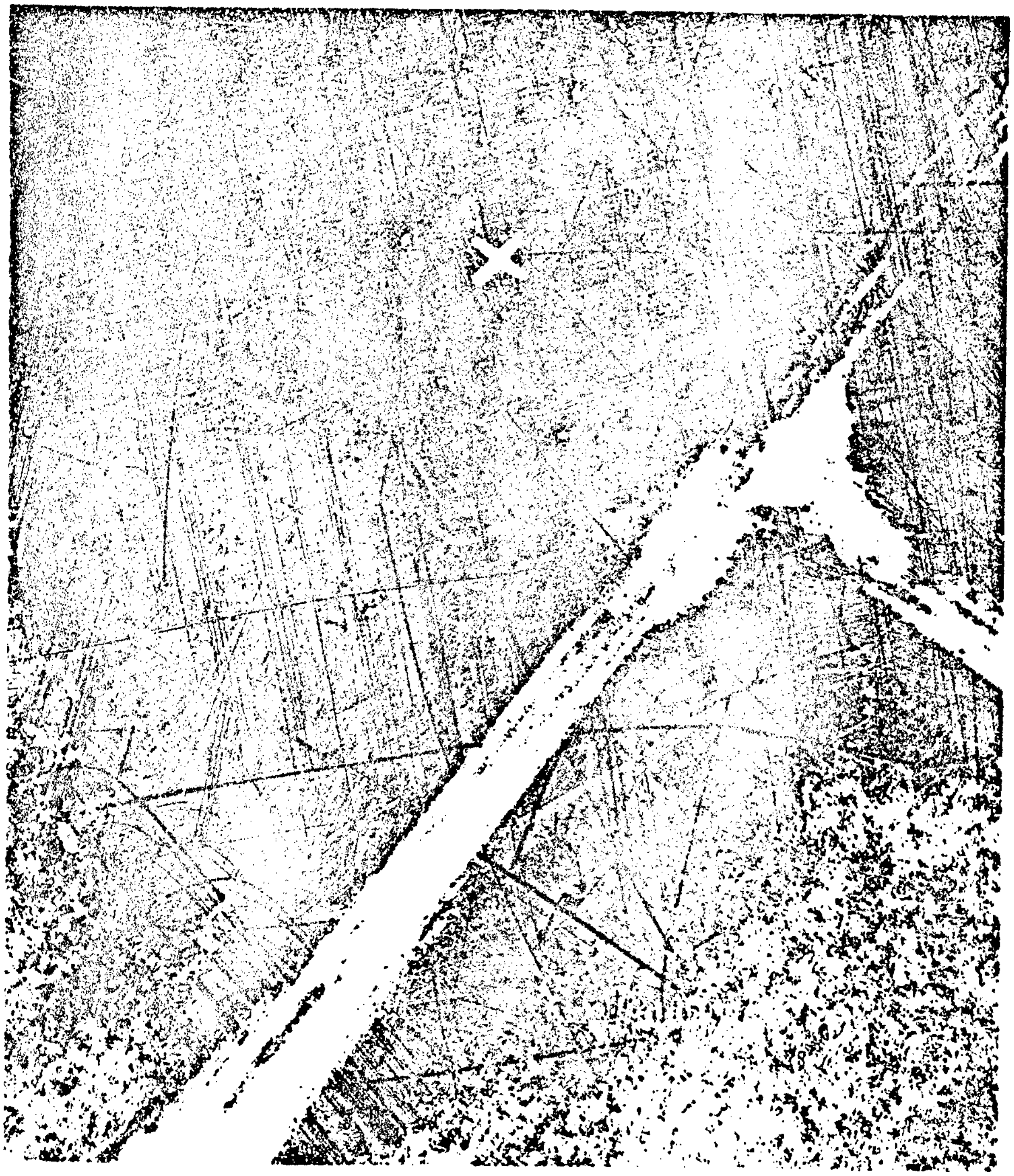

SHOCK SENSITIVITY TESTS, INSENSITIVE MUNITIONS, AND UNDERWATER EXPLOSIVES

Richard R. Bernecker
Naval Surface Warfare Center
10901 New Hampshire Ave.
Silver Spring, Md. 20903-5000

ABSTRACT

The shock loading characteristics of gap tests used in DoD funded research are reviewed and discussed in terms of corresponding data from recent numerical simulations of the detonation of various donor configurations in a water environment. These numerical computations of shock attenuation in water surrounds have been compared to recent pressure-distance experimental data for several donors and found to be in good agreement. The importance of donor diameter and height on the peak pressure-distance relationships, shock duration, and the pressure gradient behind the shock wave has also been discussed. These parameters are used to recommend a configuration of an IM "small scale" gap test for insensitive energetic materials as well as all underwater explosives.

INTRODUCTION

In recent years the Department of Defense has placed great emphasis on the deployment and utilization of insensitive munitions. While the main areas of concern are fast cookoff, bullet impact, and sympathetic detonation, the shock sensitivity of the energetic material(s) in the munition is of fundamental importance. For example, in order to conduct a numerical simulation of the munition in a hazard scenario where an explosion or detonation may be the ultimate event, it is necessary to have some quantitative measure of the shock reactivity of the material. In our recent studies, we have been attempting to conduct experiments of the shock-to-detonation transition (of explosives and propellants) from which a quantitative description of shock reactivity can be ascertained.[1,2] However, as we work with more insensitive explosives (which normally have large critical diameters), it is necessary to consider the applicability of the experimental arrangement to the desired outcome. The same is also true for the insensitive munitions community and it is evident that that community is addressing the importance of critical diameter in consideration of shock reactivity and sensitivity. However, it is not evident that all researchers/program managers are considering another important factor in shock sensitivity experiments - namely, shock duration. Thus, we would like to discuss the interplay of shock pressure, shock duration, and critical diameter in shock initiation studies, particularly as they pertain to the various current experimental shock sensitivity tests, used in DoD funded research, and the interpretation of data from these tests.

SHOCK SENSITIVITY EXPERIMENTAL ARRANGEMENTS

Until the end of the 1970s, the principal experiments used to measure shock reactivity and shock sensitivity of booster and warhead explosives, as well as propellants, were the NOL large scale gap test[3] (LSGT) and the LANL wedge test[4]. The former defines only the shock sensitivity of a material while the latter defines not only shock reactivity (since it measures distance to detonation as a function of pressure) but defines shock sensitivity if one fixes the distance to detonation and selects the corresponding pressure.

LANL WEDGE TEST

The wedge test[5], as implemented by Los Alamos National Laboratory[4,6], is a very versatile and highly useful experimental arrangement. The run distance to detonation is determined from the digitization of a streak camera trace (record) of the top surface of the wedge. In addition to measuring the run distance to detonation (x*), it also yields "inert" Hugoniot data. The driver (donor) system is basically composed of a plane wave lens and explosive pad, followed by various layers of attenuating materials (metals and plastics). These driver systems (there are a variety[4]) provide different pressure-time loading conditions, all of which have been experimentally calibrated. For these systems, the pressure-time (p - t) gradient behind the initial shock front was considered to be sufficiently close to zero that one-dimensional computer models, used for its description and simulation, would be quite applicable for the typical distance to detonation (< 25 mm). However, recent studies have been directed toward more exact descriptions of the p-t loading history.[7] For the Comp B driver system, it is currently estimated that the gradient behind the shock, for a high density cast energetic material (EM), is 1.8 GPa/μs and is 0.55 GPa/μs for the Baratol system with the same acceptor. Thus, in five microsec (close to the maximum shock duration for x* of 20 mm) the pressure drops very significantly during the buildup process. The effect of these gradients on numerical modeling of shock reactivity in wedge tests is uncertain at present.[7]

NOL LARGE SCALE GAP TEST

The LSGT has been used extensively in research and industrial applications of shock sensitivity of energetic materials[8]. There are a variety of other gap tests (e.g., the LANL large scale gap test[8]) but the LSGT is the only one which has been experimentally calibrated to yield a pressure-gap length relationship. This feature, its extensive experimental data base[3] and its required usage in some explosive hazard classification procedures[9] undoubtedly are responsible for its wide usage. Like all gap tests, the LSGT consists of a donor (in this case a pressed pentolite cylinder, density of 1.56 Mg/m^3, composed of two 2.54 cm high by 5.08 cm diam. pellets), a gap (attenuator) and acceptor (energetic material). Instead of using air, water, wax, or a metal as attenuator, the LSGT uses a cylinder of cast polymethylmethacrylate (PMMA) as the gap material; its diameter is also 5.08 cm. To extend the utility of the test to materials with "large" critical diameters, the acceptor is encased in a steel tube[3]; its inner and outer tube diameters are 3.65 and 4.76 cm, respectively. The criterion used to determine the detonation of the encased acceptor is a hole punched in 9.5 mm (0.375 in.) thick steel plate. The critical gap or 50% gap is the experimental measure of the shock sensitivity of the energetic material. (As opposed to the LANL

wedge test, normally instrumented gap tests provide no information about the run distance to detonation associated with the 50% gap.) The pressure-distance gradient behind the attenuating shock front (in the gap) and shock duration change with gap length; knowledge of these is necessary for complete characterization of the shock sensitivity data.

NSWC EXPANDED LARGE SCALE GAP TEST

In order to extend the applicability of the LSGT to insensitive munitions, Liddiard and Price developed[10,11] the expanded large scale gap test (ELSGT) by basically scaling the pentolite donor and PMMA attenuator (gap) of the LSGT by a factor 1.875. The inner and outer tube diameters, however, are 7.32 and 9.53 cm, respectively - a factor of 2.00 in scaling. Again, the criterion used to determine the detonation of the encased acceptor is a hole punched in a steel plate - 19.1 mm (0.75 in.) thick in this case. No experimental calibration of the ELSGT has thus far been made although a correlation has been made between 50 % gap data from the LSGT and the ELSGT[11]. A numerical simulation of this test has recently been made by Bowman[12].

AFATL SUPER GAP TEST

A much larger gap test has been described by Foster et al.[13]. The super gap test (SGT) uses an encased donor and an encased acceptor (both have 8.9 mm steel walls and 12.7 mm steel plates at both ends) while retaining the PMMA attenuator of the above gap arrangements. The donor is a 18.2 cm (7.15 in.) diameter by 20.3 cm (8.0 in.) long cast Comp B cylinder (unknown density). On occasions, the Comp B cylinder is unconfined on both ends and, as expected, the results with this laterally confined donor arrangement are different from those of the confined donor system. The energetic acceptor has the same diameter as the Comp B but is 40.6 cm (16.0 in.) long. The diagnostic analysis of detonation is much more extensive than either the LSGT or the ELSGT; ionization pins and an axial steel witness plate help to define the run distance to detonation (estimated uncertainty appears to be about 12 mm). In lieu of an experimental calibration of their donor and attenuator systems, Foster et al. made a numerical study of the pressure and impulse loading of their system (as discussed later). The steel end plates of the donor complicate significantly the interpretation of the pressure-time loading of the acceptor.

NWC AQUARIUM GAP TEST

NWC has recently developed an aquarium gap experiment in conjunction with studies of the shock sensitivity of high energy propellants.[14] Because of the readily available supply of pentolite pellets for the NOL LSGT, it was recommended[15] that the donor system of the LSGT also be used as the donor for this aquarium arrangement. Thus the NWC aquarium gap arrangement currently utilizes a pressed pentolite cylindrical donor (5.08 cm x 5.08 cm); the donor and acceptor are both surrounded by water. The acceptor shape can vary, sometimes being a cylinder but at others a rectangular solid. There are two arrangements for the NWC aquarium gap experiment; one arrangement utilizes a bucket to contain the apparatus (donor, water and the acceptor). In this case, the determination of a detonation is a hole punched in a 6.3 mm thick steel plate. For calibration purposes and in instances in which the run distance to detonation is to be determined, the apparatus is confined in an

aquarium and a streak camera (occasionally a framing camera) is used. An experimental pressure-distance calibration curve has been obtained for this latter arrangement.

NSWC LARGE SCALE AQUARIUM GAP EXPERIMENT

In order to explore the usage of an aquarium arrangement to obtain shock reactivity and sensitivity data where the pressure gradient behind the shock front approaches that of the LANL wedge test, we have used computer modeling[16] of various donor systems to select the appropriate donor system. We have also reproduced the NWC aquarium arrangement in order to conduct some experimental calibrations of the system[1] and to evaluate the various donor arrangements in an aquarium environment. Based upon our initial computational studies, the donor systems of the LSGT and the ELSGT, as well as a single pellet of the ELSGT, have been evaluated as donors. Table I lists the donor systems which are of interest experimentally and whose pressure-distance relationships were to be outlined in the numerical simulations. Because of explosive weight limitations in our firing chamber, our current donor system consists of the donor of the LSGT (5.08 cm long) followed by one pellet (9.53 cm diam. x 4.765 cm long) of the ELSGT. It appears that the characteristics of this donor arrangement, Donor D, are basically the same as those provided by Donor B (ELSGT). (In the earlier experimental work,[1] the donor was the same as in the NWC arangement - a 5.08 x 5.08 cm cylinder of pressed pentolite). Both the donor and the acceptor (usually unconfined cylindrical charges of various diameters and lengths) are surrounded by water. A streak camera is used to measure run distance to detonation and experimental peak pressure-distance relationships; front lighting and back lighting are used to outline the propagation of the various shock fronts and also the detonation wave.[2]

Table I

Donor	Configuration
A	5.08 cm high x 5.08 cm diam. (LSGT)
B	9.53 cm high x 9.53 cm diam. (ELSGT)
C	4.765 cm high x 9.53 cm diam.
D	5.08 cm high x 5.08 cm diam. followed by a pellet 4.765 cm high x 9.53 cm diam. (Composite of Donor A and Donor C)

PRESSURE-DISTANCE SHOCK LOADING CHARACTERISTICS

Experimentally, knowledge of the variation of shock amplitude with distance from the donor is most important in order to define shock sensitivity on an absolute basis. The relationship can be obtained from special calibration experiments; however, it is highly desirable to conduct a numerical simulation of the experimental arrangement for comparative and predictive purposes. Numerical simulations have been carried out for most of the tests described above but the results may not always be of comparable quality. For example, zoning considerations and choices of constitutive equations vary from study to study.

Our main considerations in this paper are the variation of both pressure and the p-t gradient, behind the shock, with distance from the donor. In

later reports, the variation of pressure with radial direction will also be addressed.

SIMULATION AND EXPERIMENTAL CALIBRATION OF THE LSGT

The experimental calibration of the NOL LSGT (peak pressure on axis vs. distance) has been reported by Erkman et al.[17] while a numerical simulation of it has been made by Bowman using the 2DE hydrodynamic code.[18] Bowman's original pressure-distance relationship has been improved significantly in recent work by using a Forest Fire routine for the detonation of the pentolite donor instead of a volume burn routine.[13] Tarver and James[19] have also simulated the LSGT using the DYNA2D hydrodynamic code but have not reported a pressure-distance relationship. The current accuracy of these numerical models of the LSGT are undocumented in the open literature.

SIMULATION AND CALIBRATION OF THE NWC and NSWC AQUARIUM TESTS

Hudson and Sternberg have simulated, using the DYNA2D hydrodynamic code, the detonation of various pentolite donors in a water environment.[16] One of the objectives of the calculations was to understand how the shape and size of the donor influenced the peak pressure-distance relationship and the pressure gradient of the water shock wave. Since the donors included those in Table I, it was planned that the water gap would eventually be replaced with a finite diameter PMMA gap such that the LSGT and the ELSGT arrangements could also be simulated with the same code parameters and constitutive equations.

The LSGT donor, Donor A, and the ELSGT donor, Donor B in Table I, are composed of two pentolite pellets. Each pellet has a diameter to height (d/h) ratio of 2 while the diameter to height ratio of the donor is 1. In the numerical simulations, a 1 cm diam. x 1 cm high donor was used to represent both the LSGT and ELSGT donors while a 2 cm diam. x 1 cm high donor was used to simulate one pellet of each donor. The results were scaled accordingly. Using scaling, the simulation of Donor C, d/h of 2, would allow the comparison of output with the experimental data for one pellet of the ELSGT and the simulation of Donor A, d/h of 1, would permit comparison with the calibration datal of the NWC (NSWC version) aquarium gap experiment. In addition, scaling would allow a comparison on computations for hypothetical donors of any constant height but of different d/h ratios.

The pressure-distance relationship calculated for the 5.03 x 5.08 cm donor (Donor A) in a water environment is shown in Figure 1 along with the corresponding experimental pressure-distance relationship[1]; in addition, the calibration curve of the LSGT[17] is displayed. It is evident that there is good agreement between the computed and experimental p-x data for Donor A and that there is a great similarity between the experimental calibration curves for the two gap materials. The extra confinement of the donor and the "infinite" diameter of the gap for the aquarium arrangement does not appear to affect significantly the p-x relationship relative to LSGT data. The difference between the two experimental p-x curves appears to correlate in large part with the difference in density between the two gap materials.

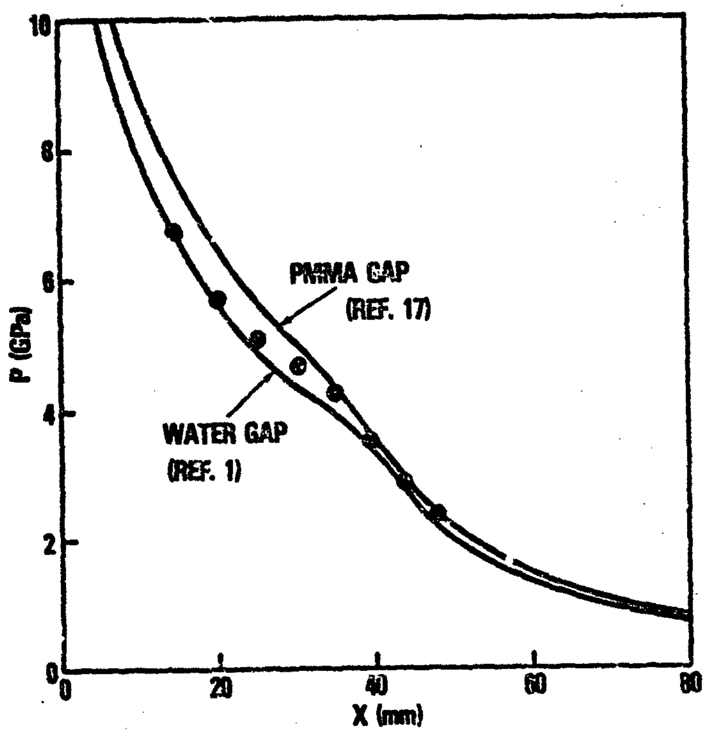

FIGURE 1. VARIATION OF PRESSURE WITH DISTANCE IN GAP EXPERIMENT FOR DONOR A, 5.08 CM HIGH X 5.08 CM DIAMETER. (● HUDSON–STERNBERG CALCULATIONS)

During the calibration of the LSGT[17], significant effort was taken to document the presence of the "knee" seen in the p - x data at about 35 mm. Its presence was attributed to rarefactions from the lateral surface (of the gap (?)). Since the water gap is essentially of infinite diameter in terms of the calibration considerations, it is evident that the knee, as seen in the data in Figure 1, can not be associated with rarefactions from the gap boundary. The p - t data for the two donor shapes (d/h of 1 and 2) provide the answer to the occurrence of the knee. In Figure 2 are shown the pressure-time data for a 5.00 x 5.00 cm donor (slightly smaller than Donor A) at several locations in the water (gap). The pressures are standardized to the maximum pressure seen at a location, left side of the figure, while the maximum value of that pressure is referenced on the right side of the figure. In Figure 3 are the corresponding data for a 5.0 cm high x 10.0 cm diam. donor (a slightly larger version of Donor C). By comparing Figures 2 and 3, the influence of charge diameter (for a constant height) are immediately evident. For locations near 0 and 10 mm, the p - t data of Figures 2 and 3 essentially overlay each other; for locations of approximately 20, 30, and 40 mm the contours in Figure 2 are significantly shortened in time, relative to Figure 3. Thus, the knee in the p - x plane marks the location where the rarefactions from the edge of the explosive donor (farthest from the detonator) overtake, on axis, the initial water shock wave (whose amplitude decreases in an

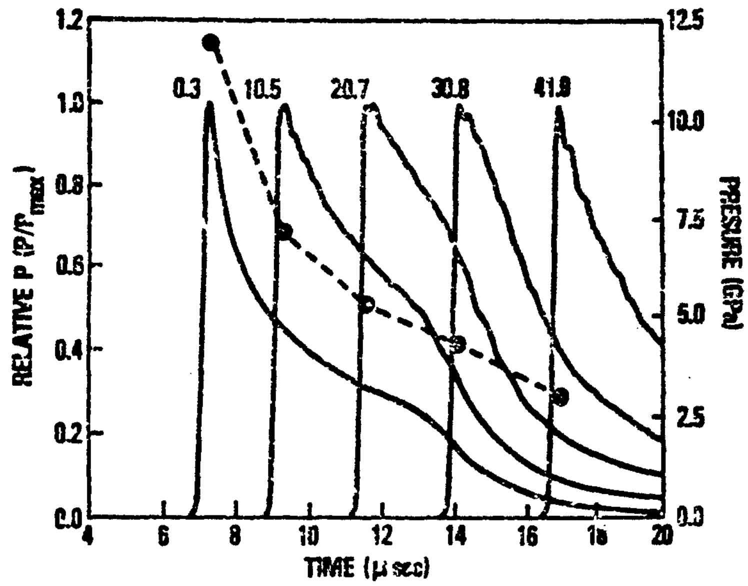

FIGURE 2. PRESSURE–TIME DATA FOR VARIOUS LOCATIONS ON AXIS FOR 5.0 CM HIGH X 5.0 CM DIAMETER DONOR (D/H = 1). (NUMBERS ARE LOCATIONS IN MM FROM DONOR; ● P_{max})

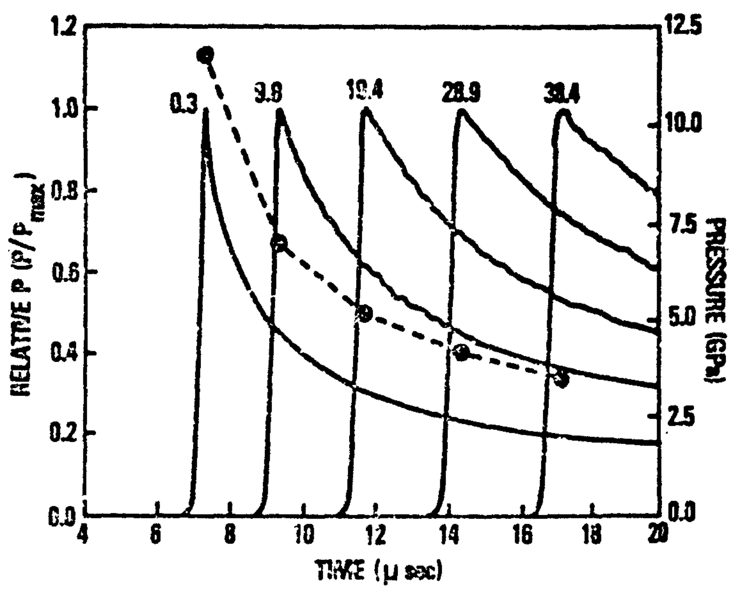

FIGURE 3. PRESSURE–TIME DATA FOR VARIOUS LOCATIONS ON AXIS FOR 5.0 CM HIGH X 10.0 CM DIAMETER DONOR (D/H = 2). (NUMBERS ARE LOCATIONS IN MM FROM DONOR; ⊕ P_{max})

exponential manner with distance to about 35 mm) to produce a shock wave which also attenuates in an exponential manner with distance but at an even faster rate than seen in the region next to the donor. The arrival of the rarefaction at the 0.3 mm location can be seen in Figure 2 at about 13 microseconds; in Figure 3 its arrival would be after 20 microseconds.

The interpretation of the knee in the pressure-distance plane is confirmed by the data of Tasker.[20] Tetryl cylindrical donors (1.50 Mg/m^3) were used in PMMA gap experiments to study the thresholds for reaction and detonation. Two sizes of donor were used: they were 5.08 cm high but one had a diameter of 5.08 cm while the other had a diameter of 7.62 cm. Thus, their d/h ratios were 1 and 1.5, respectively. Calibrations of these systems showed identical p - x relationships down to approximately 35 mm where the 5.08 cm diameter system had a knee. For the 7.62 cm diameter system, the knee appeared in the p - x plane at about 54 mm. That is, the knee occurred at a longer distance for the larger diameter system.

This correlation is confirmed by our experimental calibration of Donor C[21] as shown in Figure 4. Also shown in the figure are computed data for Donor C by Hudson and Sternberg. It is seen that the latter data agree well

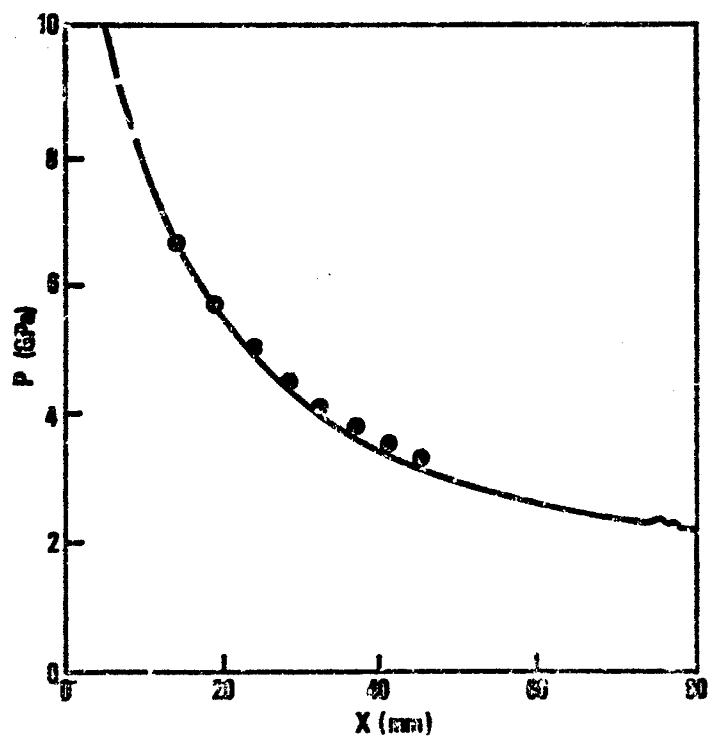

FIGURE 4. VARIATION OF PRESSURE WITH DISTANCE FOR DONOR C, 4.795 CM HIGH X 9.53 CM DIAMETER, IN WATER. (● HUDSON–STERNBERG CALCULATIONS)

with the experimental data and that there is no evidence of a knee in the experimental data, at least to 70 mm. Thus, we see that the location of the knee in the data of Tasker for a donor with d/h of 1.5 is intermediate between the locations of the knees for Donors A (d/h of 1) and C (d/h of 2), confirming the interpretation of the p - x relationships and also demonstrating that the simulations of Hudson and Sternberg agree very nicely with experimental observations.

SIMULATION OF THE AFATL SGT

As mentioned earlier, Foster et al. did not experimentally calibrate their super gap test but did conduct a numerical simulation with the Hull hydrodynamic code.[13] They performed simulations for both the confined and the laterally confined Comp B donor (no end plates). The laterally confined donor is similar to a configuration whose d/h is between 1 and 2; thus, it should also have a knee in the p - x plane. In Figure 13 of Ref. 13, the knee appears to lie between 105 and 125 mm for the laterally confined donor. It is interesting to note that (because of the steel end plates) a knee was not observed in the Hull p - x data for the confined SGT donor. These end plates make it difficult to compare pressure-time loadings from the SGT with other gap experiments where the donors are unconfined at the ends. The pressure time contours, as seen in Figures 2 and 3, are modified significantly by reflections due to the end plates. Hence, in the following discussions we can only address the laterally confined donor situation since there are no published p - t data available for the confined donor; the laterally confined donor and the attenuator system of the super gap test can be semi-quantitatively understood in terms of the p - t contours shown in Figures 2 and 3 and the p - x data in Figures 1 and 4.

PRESSURE-TIME SHOCK LOADING CHARACTERISTICS

The shock durations from the various gap arrangements have not been determined experimentally. Hence, the numerical simulations of the gap experiments provide the insight concerning the important variable - shock duration (or the total available shock reaction time). The data shown in Figures 2 and 3 were used to estimate both the pressure gradient behind the shock front and the duration of the shock wave. As is evident from the figures, both are subjective parameters. Hence, the pressure gradient was associated with the time for a 20% decrease in the maximum pressure; this is the value shown in the second column of the following tables. The shock duration was determined at two locations; at 80% of the maximum pressure (and thus associated with the pressure gradient in the second column) and at 50% of the maximum pressure. The two durations help to outline changes due to rarefactions. Tables II, III, and IV contain the corresponding data for Donors A, B, and C, respectively. (These data were determined directly from figures such as Figures 2 and 3; hence, there is an estimated 10 to 15% uncertainty in the quoted values.) It is quite evident from these data, as well as the contours shown in Figures 2 and 3, that the shock durations will reach a maximum value, determined by the location where the rarefactions from the donor overtake the initial shock wave. At pressures below 3 GPa, calculations show that the shock durations again increase with decreasing pressure.

Table II

PRESSURE GRADIENTS AND SHOCK DURATIONS FOR DONOR A*

P GPa	-dP/dt (0.8Pmax) GPa/microsec	t @ 0.8Pmax microsec	t @ 0.5Pmax microsec
12.0	6.7	.36	1.7
7.07	1.23	1.15	4.0
5.28	.63	1.7	3.2
4.79	.64	1.5	2.9
4.30	.75	1.15	2.4
3.00	.87	.69	2.4

* on axis

Table III

PRESSURE GRADIENTS AND SHOCK DURATIONS FOR DONOR B*

P GPa	-dP/dt (0.8Pmax) GPa/microsec	t @ 0.8Pmax microsec	t @ 0.5Pmax microsec
12.0	3.6	.67	3.25
7.07	.65	2.15	7.6
5.28	.34	3.15	6.1
4.79	.34	2.8	5.4
4.30	.40	2.15	4.55
3.00	.46	1.3	4.55

* on axis

Table IV

PRESSURE GRADIENTS AND SHOCK DURATIONS FOR DONOR C*

P GPa	-dP/dt (0.8Pmax) GPa/microsec	t @ 0.8Pmax microsec	t @ 0.5Pmax microsec
11.8	7.1	.33	1.62
7.00	1.36	1.0	4.0
5.20	.66	1.6	6.5
4.69	.51	1.85	7.35
4.19	.41	2.05	(9.5)**
3.54	.24	2.9	-

* on axis
** estimated

DISCUSSION

The shock sensitivity of an energetic material is defined in terms of the pressure-time loading provided by the donor of the test. That is why, of course, the shock initiation pressure from the LSGT is different from that of the ELSGT, for example, and rankings of the shock sensitivity from gap tests are usually relative rather than absolute. From a theoretical modeling viewpoint, knowledge of the pressure-time gradient behind the entering shock front is most important since the reaction time available to the ingredients will influence the shock initiation threshold. That is why it is important for researchers and program managers to understand completely any limitations of a particular gap test in defining shock sensitivity.

The importance of the shock duration (and the gradient behind the shock wave) on the shock reactivity and sensitivity of an EM is typically seen in comparisons of gap test data and wedge test data.[1,18] Because of the shorter durations and larger gradients found in the donor/attenuator of the LSGT, the run distance to detonation is longer in the LSGT. The data in Table II give us a measure of the variation of these important parameters for the LSGT but what are the corresponding data for the wedge test? Kury is conducting numerical simulations of some of the drivers used in the wedge test in order to understand more completely the influence of the shock gradient on the reaction kinetics occurring behind the shock front.[7] His data for a typical high density EM shows that the Comp B driver system has about a 1.8 GPa/μs gradient behind the 7.4 GPa front with a shock duration time at 3.7 GPa of about 4 microseconds. The Baratol driver system has about a 0.55 GPa/μs gradient behind the 4.2 GPa front with a shock duration approaching 5 microseconds at 2.1 GPa. The comparison of the shock durations in Tables III and IV with wedge test data indicate that shock loadings from the ELSGT and AFATL SGT (unconfined and laterally confined donors) are very well suited for usage in the evaluation of insensitive explosives and propellants. The same can not be said for the use of the LSGT donor attenuator system where the shock duration times may be close to a critical range for insensitive and underwater explosives; an example of potential problems with the a LSGT donor/attenuator system is outlined in Ref. 1. Thus, we consider the use of the LSGT "too risky" for the evaluation of shock sensitivity for insensitive energetic materials (IEMs) as well as underwater explosives which contain ammonium perchlorate, ammonium nitrate, aluminum, nitroquanidine, etc.

IM "SMALL SCALE" GAP TEST FOR IEMs

Earlier papers at this meeting were concerned with the proper small scale tests to use in the development of IEMs. We would like to address this concern for shock sensitivity testing. We propose that there may not be one ideal small scale shock sensitivity test for IEMs. Let us first evaluate separately the requirements for the donor, the attenuator and the acceptor. For the donor, the data in Tables II - IV and previous discussions indicate Donor B, along with the laterally confined SGT donor, has the more desirable shock loading characteristics of the gap tests that we have examined. Because it is smaller, Donor B (or its near equivalent, Donor D) is our selection for the donor of a small scale test for IEMs.

The next consideration is the type of material to use for the gap. At present with our incomplete knowledge of shock durations in the PMMA gap tests (LSGT, ELSGT, SGT), there is no definitive answer. To this writer, it presently appears that no significant gain arises from the use of Donor B in an aquarium arrangement as opposed to using Donor B in air with a PMMA gap; this is contrary to our expectations before the computations were made by Hudson and Sternberg and the calibration data shown in Figure 1 were obtained. Since the PMMA in air arrangement appears easier to use on a routine basis, we select the Donor B/PMMA system (i.e., the donor/attenuator of the ELSGT) as the donor/attenuator system for a "small scale" test of shock sensitivity of IEMs and all underwater explosives.

The choice of the configuration of the acceptor is the more difficult selection in the absence of a large data base of ELSGT results. Based upon the consideration that a small scale test should use the smallest amount of acceptor EM in the formulation stage, we believe that the selection of the acceptor size should not be fixed; the known (or estimated) critical diameter characteristics of the IEM should determine the selection of the acceptor size. The minimum size of the acceptor would be the LSGT acceptor size. If this minimum size is unacceptable, then the diameter and confinement of the ELSGT should be used but the length should be kept the same as the LSGT, 14 cm. What we are advocating for standard, routine testing situations is the use of a modified version of the ELSGT as the "small scale" shock sensitivity test for IEMs.

This modification can be improved still further with additional instrumentation. For example, if a facility has a streak camera, then the methodology discussed in Ref. 1 provides a procedure where the minimum amount of EM can be used. On the other hand, a researcher could select another criterion for the occurrence of detonation in the test (a dent in a steel plate[22] instead of a hole punched in a plate, etc.) or use a shorter acceptor[22]. These approaches may involve development of a modified procedure and are not as straightforward as the use of the proposed modified version of the ELSGT. However, they may be more useful as a "small scale" gap test for IEMs.

If one wants to keep approximately the shock duration of the LSGT, then the use of only one pentolite pellet in the proposed modified version of the ELSGT would allow the usage of larger diameter acceptors with the shock loading characteristics of the LSGT.

SHOCK DURATION OF THE LSGT DONOR/ATTENUATOR SYSTEM

Gap tests such as the LSGT and ELSGT have a major feature which must be considered in routine and non-routine usage. Namely, the shock duration goes through a maximum as peak pressure decreases. Ideally, in shock initiation studies one would like to keep the shock duration fixed at some large value and vary the input pressure to evaluate shock reactivity. If the shock duration has to vary, then it is better to have it increase as peak pressure decreases. Unfortunately, this is only partly true for gap tests. As seen in Tables II and III for donors with d/h ratios of 1, the shock duration decreases in the 5 to 3 GPa range of the p - x plane. As an example of the non-routine application, if one is comparing shock sensitivities over a

pressure range, such as in Refs. 1 and 2, then it must be kept in mind that pressure is not the only variable changing. In that situation, the shock duration should be long enough such that it plays no role in the evaluation of shock reactivity. Thus, Donor B is preferable to Donors A or C. As mentioned earlier, our current donor system (Donor D) consists of the donor of the LSGT (5.08 cm high) followed by one pellet (9.53 cm diam. x 4.765 cm high) of the ELSGT. (It appears that the characteristics of this donor arrangement are basically the same as those provided by Donor B but with less explosive weight.) Donors B and D can approximate the driver systems of the wedge test and any measurement of the axial distance to detonation should be equivalent to x^*.

Another example of where the decrease of the shock duration in the LSGT is important is in the evaluation of delayed detonation using the LSGT. Keefe[23] and others have studied the probability of detonations as a function of gap length (or gap pressure) using the LSGT. Keefe found for some propellants that the probability curve had two maxima, one associated (at high pressures) with SDT and a second (at lower pressures) associated with delayed detonation. (Delayed detonation has the characteristics that the distance to detonation and time to detonation at the 50% gap are much greater than in the SDT process.) Interestingly, the delayed detonation process occurred in the pressure region (gaps > 40 mm) where the shock duration is decreasing rapidly. It would be of great interest to know how the probability of detonation and distances to detonation vary in that pressure region for donors with longer shock durations (e.g., the ELSGT donor/attenuator system). This knowledge could be of significant mechanistic importance.

SUMMARY

The shock loading characteristics of gap tests can be more fully understood using the simulations carried out by Hudson and Sternberg. The importance of shock duration - a poorly characterized parameter in gap tests - is discussed. For insensitive explosives and propellants and for all underwater explosives, a modified version of the ELSGT is the IM "small scale" shock sensitivity test while the laterally confined donor AFATL SGT is the desired IM "large scale" shock sensitivity test; our understanding of the shock loading from the confined AFATL SGT is insufficient to make any suggestions or recommendations. The use of the LSGT can be "too risky" for the evaluation of shock sensitivity of insensitive energetic materials. However, if one wants to continue to use the shock duration and shock gradient of the LSGT but with larger diameter acceptors, then only one ELSGT pentolite pellet should be used as the donor; the gap diameter must be increased while the acceptor diameter and length can vary. The ELSGT and the laterally confined donor AFATL SGT have donor systems which approach the p - t characteristics of the wedge test driving systems and thus are useful in general studies of shock sensitivity.

ACKNOWLEDGEMENTS

This work was sponsored by the NSWC Explosive and Undersea Warheads Technology Block Program. Dr. Sigmund J. Jacobs provided many helpful and valuable discussions, throughout the course of our studies, which have contributed to this paper. Dr. Donna Price contributed valuable comments during the review of this paper.

REFERENCES

1. Bernecker, R. R., Clairmont, A. R. Jr., Sandusky, H. W., and Smith, M. S., "Participation of Aluminum in Two-dimensional Shock Initiation Experiments," Proc. of 1987 APS Topical Conference on Shock Waves in Condensed Matter, to be published.

2. Bernecker, R. R., "Chemical Aspects of Shock Reactivity," this meeting.

3. Price, D., Clairmont, A. R., Jr., and Erkman, J. O., "The NOL Large Scale Gap Test. III. Compilation of Unclassified Data and Supplementary Information for Interpretation of Results," NOL TR 74-40, Silver Spring, Maryland, March 1974.

4. Gibbs, T. R. and Popolato, A., Eds.,"LASL Explosive Property Data," University of California Press, Berkeley, California, 1980.

5. Majowicz, J. M. and Jacobs, S. J., "Initiation to Detonation of High Explosives by Shocks," NAVORD 5710, NOL, Silver Spring, Maryland, 1958.

6. Dick, J. J. and Engelke, R., "Reproducibility of Planewave Transit Times in Three Explosives during Initiation: Comparison to Wedge Experiments," Propellants and Explosives, Vol 5, 1980, p. 139.

7. Kury, J., LLNL, private communication.

8. Urizar, M. J., Peterson, S. W., and Smith, L. C., "Detonation Sensitivity Tests," LA-7193-MS, LASL, Los Alamos, New Mexico, April 1978.

9. TB 700-2/ NAVORDINST 8020.3/TO 11A-1-47, 19 May 1967.

10. Liddiard, T. P. and Price, D., "The Expanded Large Scale Gap Test," 1986 Propulsion Systems Hazards Subcommittee Meeting, CPIA Publication 446, Vol. I, March 1986, p. 443.

11. Liddiard, T. P. and Price, D., "The Expanded Large Scale Gap Test," NSWC TR 86-32, NSWC, Silver Spring, Maryland, March 1987.

12. Bowman, A., LANL, private communication.

13. Foster, J. C., Jr., Forbes, K. R., Gunger, M. E., and Craig, B. C., "An Eight-Inch Diameter, Heavily Confined Card Gap Test," Proc. Eighth Symposium (International) on Detonation, NSWC MP 86-194, July 1985, p. 228.

14. Graham, K.J., Richter, H. D., Lind, C. D., and Lepie, A. H. "Shock Sensitivity of Damaged Explosives and Propellants," 1987 Propulsion Systems Hazards Subcommittee Meeting, CPIA. Publication 464, Vol. I, March 1987, p. 145.

15. Jacobs, S. J., AT&R, private communication.

16. Hudson, L. and Sternberg, H. M., AT&R, Progress Report for Contract 4106-111, 9 July 1987.

17. Erkman, J. O., Edwards, D. J., Clairmont, A. R., Jr., and Price, D., "Calibration of the NOL Large Scale Gap Test; Hugoniot Data for Polymethyl Methacrylate," NOL TR 73-15, April 1973.

18. Bowman, A. L., "A Numerical Study of the NOL Large Scale Gap Tests," 1980 Propulsion Systems Hazards Subcommittee Meeting, CPIA. Publication 330, Vol. I, December 1980, p. 267.

19. Tarver, C. M. and James, E., "Two-dimensional Reactive Flow Modeling of the Minimum Priming Charge, LANL Large Scale Gap and NOL Large Scale Gap Tests," 1986 Propulsion Systems Hazards Subcommittee Meeting, CPIA. Publication 446, Vol. I, March 1986, p. 497.

20. Tasker, D. G., "Shock Initiation and Subsequent Growth of Reaction in Explosives and Propellants: The Low Amplitude Shock Initiation Test, LASI," Proc. Seventh Symposium (International) on Detonation, NSWC MP 82-334, June 1981, p. 285.

21. Unpublished data of Bernecker, R. R., Sandusky, H. W., and Clairmont, A. R., Jr.

22. Forbes, J. W., Watt, J. W., and Adolph, H. G., "The Insensitive High Explosive (IHE) Gap Test," NSWC TR 86-58, NSWC, Silver Spring, Maryland, July 1986.

23. Keefe, R. L., "Delayed Detonation in Card Gap Tests," Proc. Seventh Symposium (International) on Detonation, NSWC MP 82-334, NSWC, Silver Spring, Maryland, June 1981, p. 265.

LOW AMPLITUDE SHOCK INITIATION

OF COMMERCIAL EXPLOSIVES

K.K. FENG

CANADIAN EXPLOSIVES RESEARCH LABORATORY

P. KATSABANIS

MINING RESOURCE ENGINEERING LIMITED

LOW AMPLITUDE SHOCK INITIATION OF COMMERCIAL EXPLOSIVES

K.K. FENG

Canadian Explosives Research Laborotory, CANMET, EMR
555 Booth Street, Ottawa, Ontario, Canada K1A 0G1
P. Katsabanis*
Mining Research Engineering Limited
Kingston, Ontario, Canada

ABSTRACT

This paper describes a study into the low amplitude shock initiation of three explosives using experimental and theoretical techniques. Experimentally these explosives were tested using a modified gap test to determine the pressure threshold to initiation for each. This gap test is similar to the method used by Tasker and Kroh. The free surface velocity of the acceptor plate is recorded as a function of the thickness of the plexiglas attenuator. The results of these tests are used to determine the pressure threshold for the onset of shock to deflagration and deflagration to detonation transition.

In order to compare these test values, the pressure profile and particle velocity profile under the shock wave for the threshold of these explosives were calculated by Lagrangian Code. From the pressure profiles, the critical energies for the explosives were obtained by evaluating the integral of pressure profile of the shock wave in the acceptor and particle velocity profile [p(t)Up(t)dt]. To determine the performance of these explosives, Tiger Code calculations have been carried out for detonation pressure, detonation velocity and Gurney velocity.

The explosives used in this study consisted of pressed RDX/WAX (90/10) which was used as a standard, a slurry explosive and an emulsion explosive. These commercial products are typical small diameter mining explosives with both containing less than 5% aluminum.

* present address: Dept. of Mining Engineering, Queen's University, Kingston, Ontario, Canada, K7L - JN6

INTRODUCTION

The Canadian Explosives Research Laboratory regularly evaluates commercial explosives for authorization under the Canada Explosives Act. As part of the evaluation process safety characteristics such as impact sensitivity and shock sensitivity are evaluated. Low velocity impacts or low amplitude shock waves can be a cause of a violent event which can lead to a major catastrophy, for example, in a transportaation accident. For this purpose the sensitivity of commercial products to low amplitude shock waves was examined experimentally and theoretically. The effort was concentrated in establishing the low amplitude impact sensitivity of commercial explosives by using calibrated gap tests. In addition, knowledge of both the sensitivity and performance enables us to find commercial explosives with high performance and low sensitivity. Such explosives include slurry and emulsion explosives.

This paper describes theoretical and experimental investigations which were conducted on two types of commercial explosives to obtain shock sensitivity and performance data.

BACKGROUND

The process of shock impact can lead to a deflagration or detonation. The shock wave, if it is strong

enough will shock initiate the explosive and deflagration to detonation transition can occur. In order to determine shock to detonation transition, projectile tests on slurry and emulsion explosives were conducted previously (1). A series of tests were conducted by varying projectile velocity and diameter. Aluminum projectiles were fired from a cannon towards targets of explosive. The projectile diameters used were 2.5 cm, 5.1 cm, 10.2 cm and 15.4 cm. The explosives were tested unconfined and confined in steel tubes. The projectile velocity was calculated by reading the time interval for passage of the projectile between two light sensors placed a known distance apart in front of the explosive target. The impact was observed by a high speed camera having a writing speed of 3000 frame per second. Thus the detonation or failure of the target was determined. The experimental set up is shown in Figure 1. The results of the tests are shown in Table 1. The result conclude that the slurry and emulsion explosives tested did not detonate from low velocity impact under unconfined conditions and that it was a case of shock to detonation transition.

PROPERTIES OF EXPLOSIVES

Three explosives were tested by the above technique to obtain the threshold to initiation. These explosives were pressed RDX (90% RDX, 10% WAX) and, a slurry at density of 1.15 g/cc and an emulsion at density of 1.15 g/cc. The waxed RDX was used as a standard because of the reproductibility of the acceptor charges. The slurry and the emulsion products were typical cap sensitive commercial explosives. Both of

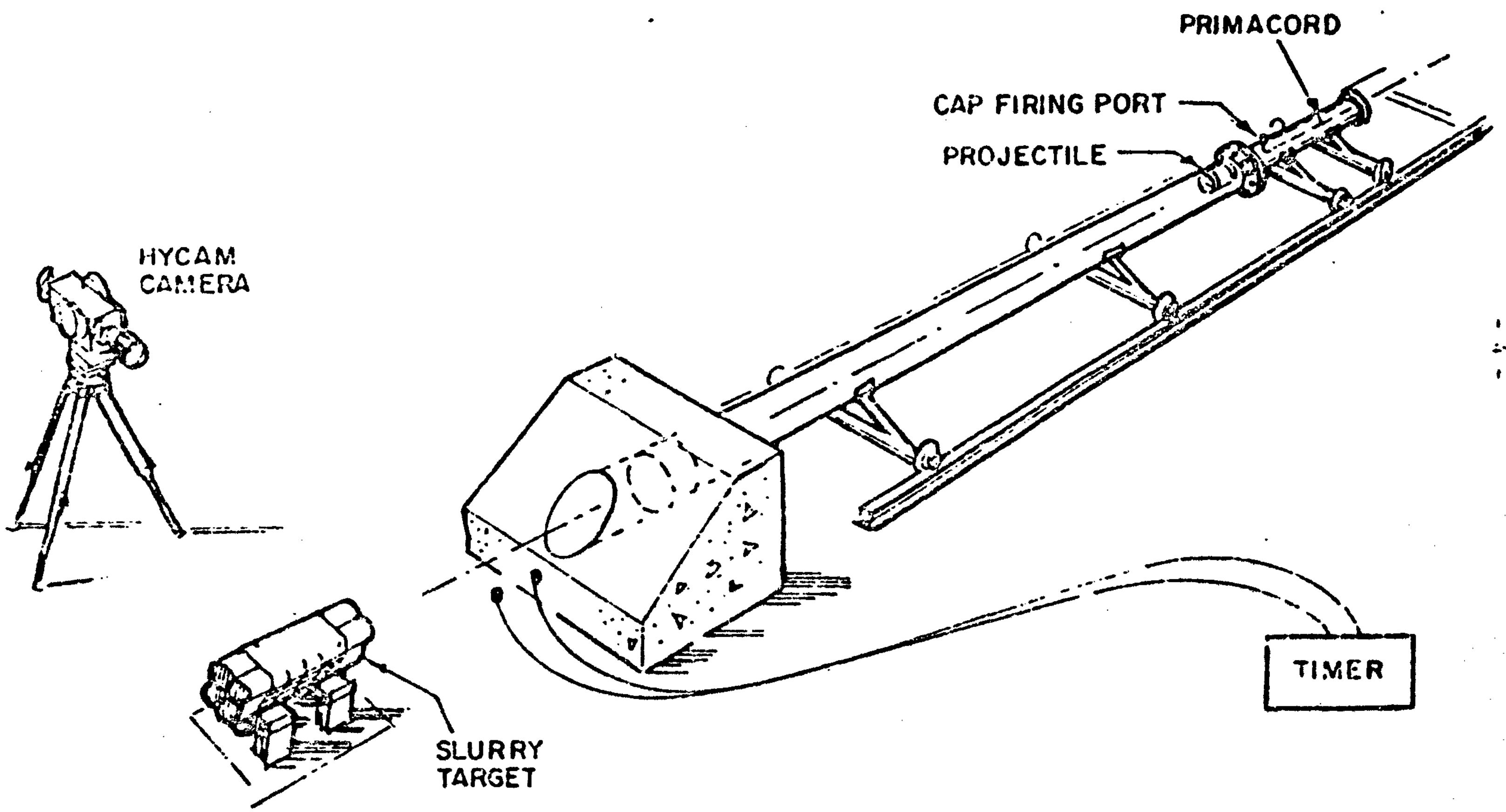

FIGURE 1 : EXPERIMENTAL ARRANGEMENT FOR THE PROJECTILE TESTS.

TABLE 1 : PROJECTILE IMPACT TEST RESULTS FOR SLURRY AND EMULSION EXPLOSIVES

Explosives	Slurry A					Slurry B			Emulsion
Projectile Dia. (mm)	25	25*	50	100	152	25	50	152	25
Projectile Length (mm)	50	50	100	150	152	50	100	152	50
Projectile Velocity (m/s)									
33			F						
132					F				
219			F						
296	F								
315								F	
330		F		F					
337		F		F			F		F
342					F				F
344			F	F	D				
347	F		D/F						
350			D	D			F		
356		D							
358							D	F	
363		D			D				
369								D	
380									F
396									
410		D							
417									F
421	F	D							
444	D					F			
460						D			F
537	D								F

* CONFINED IN 50 mm STEEL PIPE

them are used in small diameter applications and they contain a small amount of aluminum (less than 5%). The major components of the slurry explosive used are ammonium nitrate, calcium nitrate, ethylene glycol, aluminum and water. the major components of the emulsion explosive used are ammonium nitrate, sodium nitrate, calicum nitrate, aluminum, water and oil.

The slurry uses air bubbles in order to achieve the desirable sensitivity. The air bubbles vary in size from a few microns to a few millimeters. The emulsion uses glass microballoons with an average size of 70 microns. The pressure of the gas inside the microballoons is normally below the atmospheric pressure.

Further differences in the two products are found in their physical characteristics. In the slurry, the discontinuous phase consists of fuels and oxidizer salt crystals and the continuous phase is the oxidizer solution.

In the emulsion, the continuous phase is the oils while the discontinuous phase consists of the oxidizer salt solution. There are no crystals in the emulsion and the mix is much more intimate than in the case of the slurry.

CALIBRATED GAP TESTS

From the projectile impact data, it is apparent that the results apply to a transition to detonation and not

initiation to deflagration which may not result in detonation. For this reason a modified gap test was used to provide data for low amplitude shock initiation. The test is similar to the one implemented by Tasker [2], Liddiard [3] and Kroh [4].

The experimental set up is shown in Figure 2. The test consisted of a donor charge, an attenuator plate, an acceptor charge and an Argon filled light bomb. The free surface velocity of the acceptor plate is recorded as a function of the thickness of the plexiglas attenuator. The donor is made of three disks of pressed RDX (90% RDX, 10% Wax). Each disk has a diameter of 7.64 cm and a height of 2.54 cm. The density of the charge is 1.55 g/cc. The attenuator is made of square plates of plexiglas with dimensions of 17.8 cm X 17.8 cm. The block of plexiglas is normally polished so that it is transparent. The acceptor has the same diameter as the donor and a height of 2.54 cm and it is place in such a way that they have a common axis of symmetry. Donor, attenuator and acceptor are glued without air bubbles. The charge is placed exactly perpendicular to the slit of the streak camera.

The donor is initiated by a 10 g PETN primer and the event is recorded by using a streak camera. The slit of the camera is placed at the centre of the charge, parallel to the axis of symmentry of the charge. At a specific time the light bomb is detonated to produce the back light necessary for the shadow graphic streak camera techniques. From the cutoff of this light, as the shock wave passes through the plexiglas,

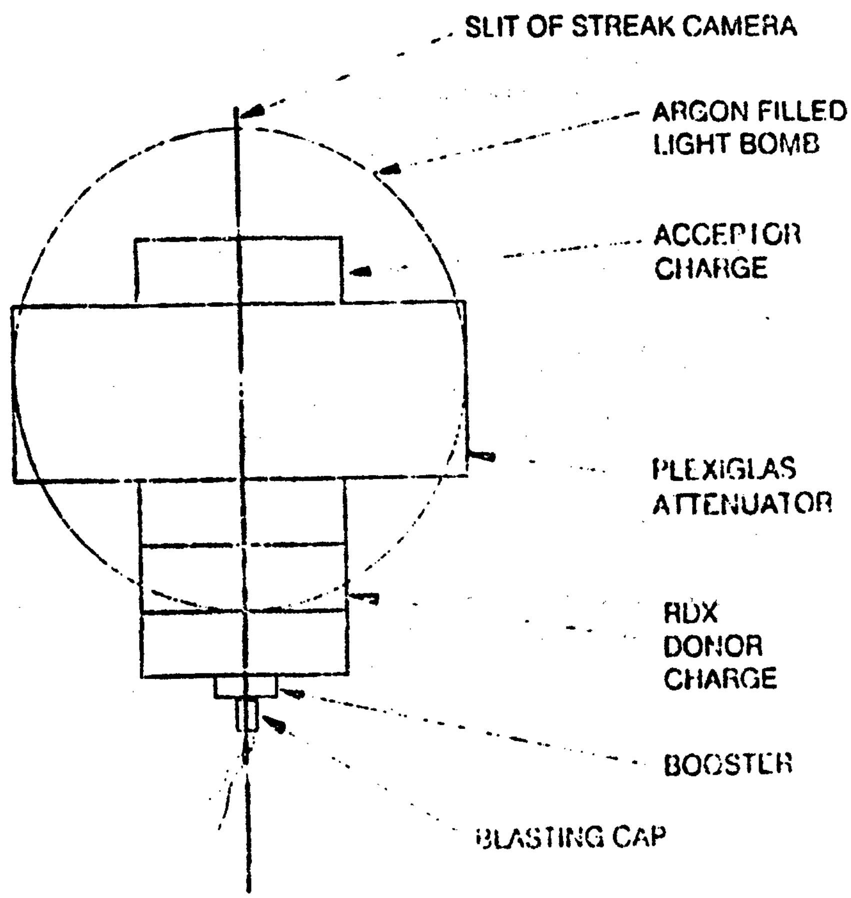

FIGURE 2 : EXPERIMENTAL ARRANGEMENT OF THE CALIBRATED GAP TESTS.

it is possible to obtain the shock velocity in the plexiglas attenuator as a function of thickness of the plate. Furthermore when the shock wave reaches the free surface of the acceptor, it moves it, producing a cutoff of light. From the slope of this line, the free surface velocity can be measured. If the acceptor detonates, a bright flash is normally seen in the streak camera record. Streak camera records of a calibrated gap test for RDX/WAX. Slurry A and Emulsion A are shown in Figures 3, 4 and 5 respectively.

INTERPRETATION OF EXPERIMENTAL RESULTS

The results of the calibrated gap test are reported as free surface velocity vs impact pressure curves which indicate the thresholds to deflagration and detonation. In order to obtain these curves it is necessary to calculate the pressure in the plexiglas attenuator as a function of the thickness of the attenuator for the case of the shock provided by the standard donor. The calculation steps are as follows:

a) From the streak camera records, the shock velocity in the plexiglas can be obtained at various points of the attenuator. The relationship between shock velocity and thickness is shown in Figure 6.

b) From the shock velocity and the Hugoniot of the plexiglas ($Us=2430+1.5785xUp$), the particle velocity can be calculated.

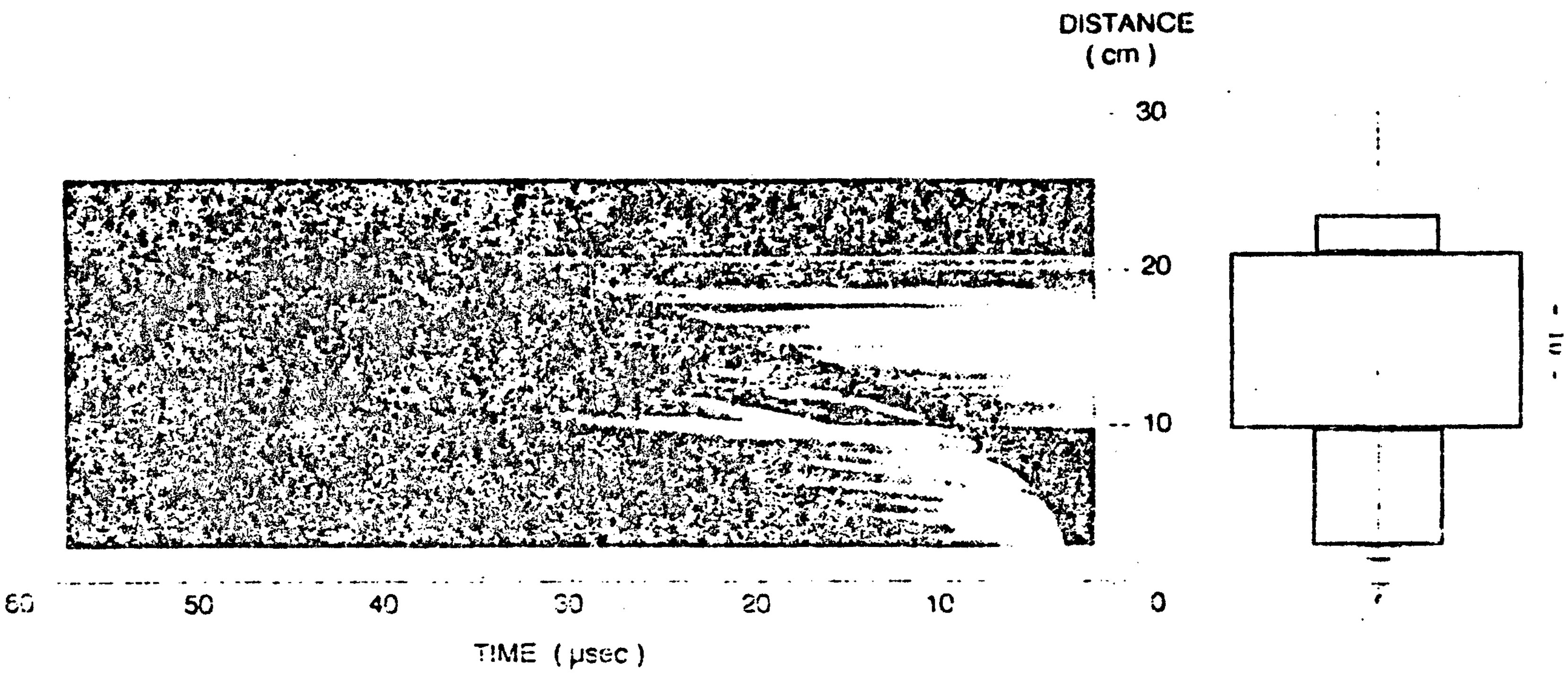

FIGURE 5 : STREAK CAMERA RECORD OF A CALIBRATED GAP TEST FOR WAXED RDX.

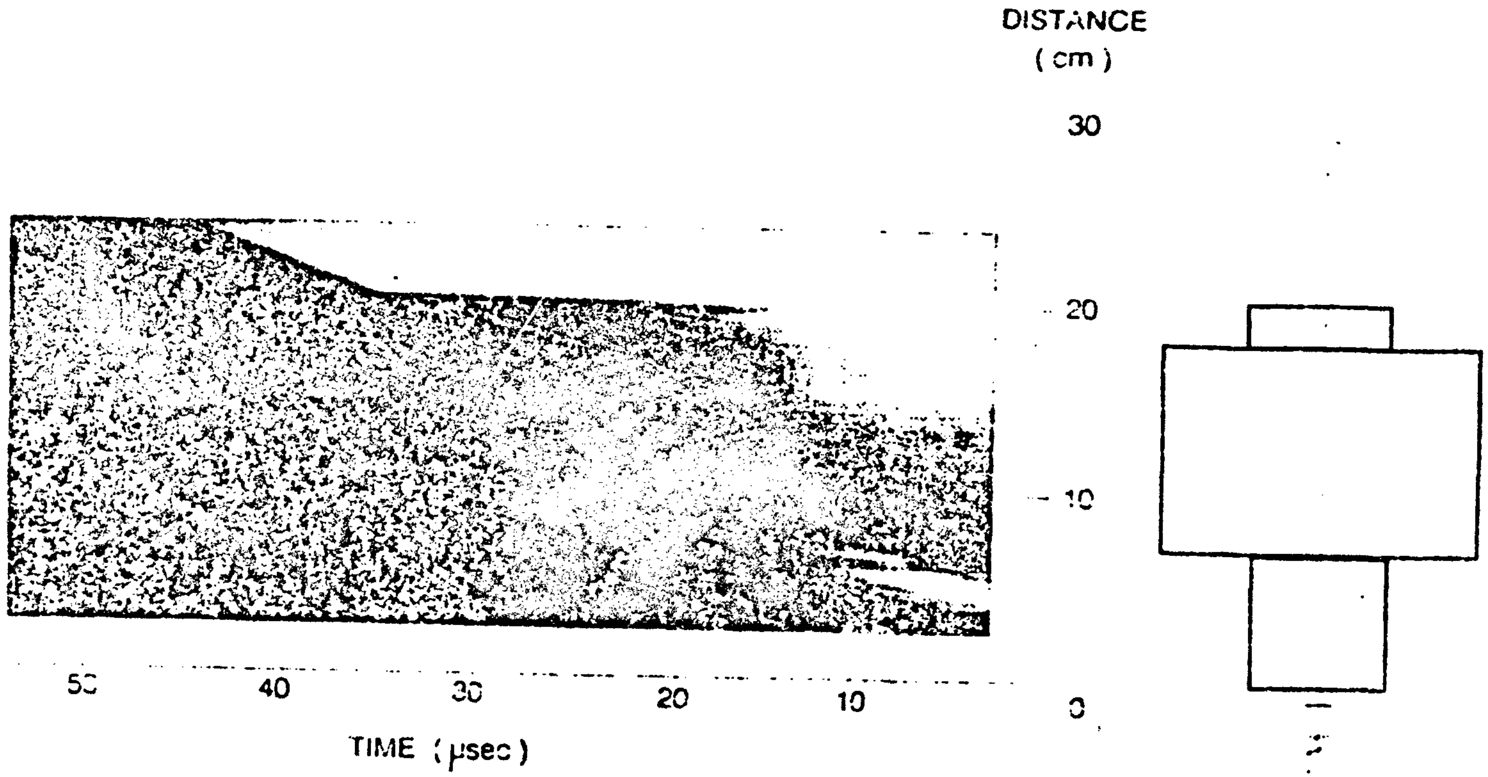

FIGURE 4 : STREAK CAMERA RECORD OF A CALIBRATED GAP TEST FOR SLURRY A.

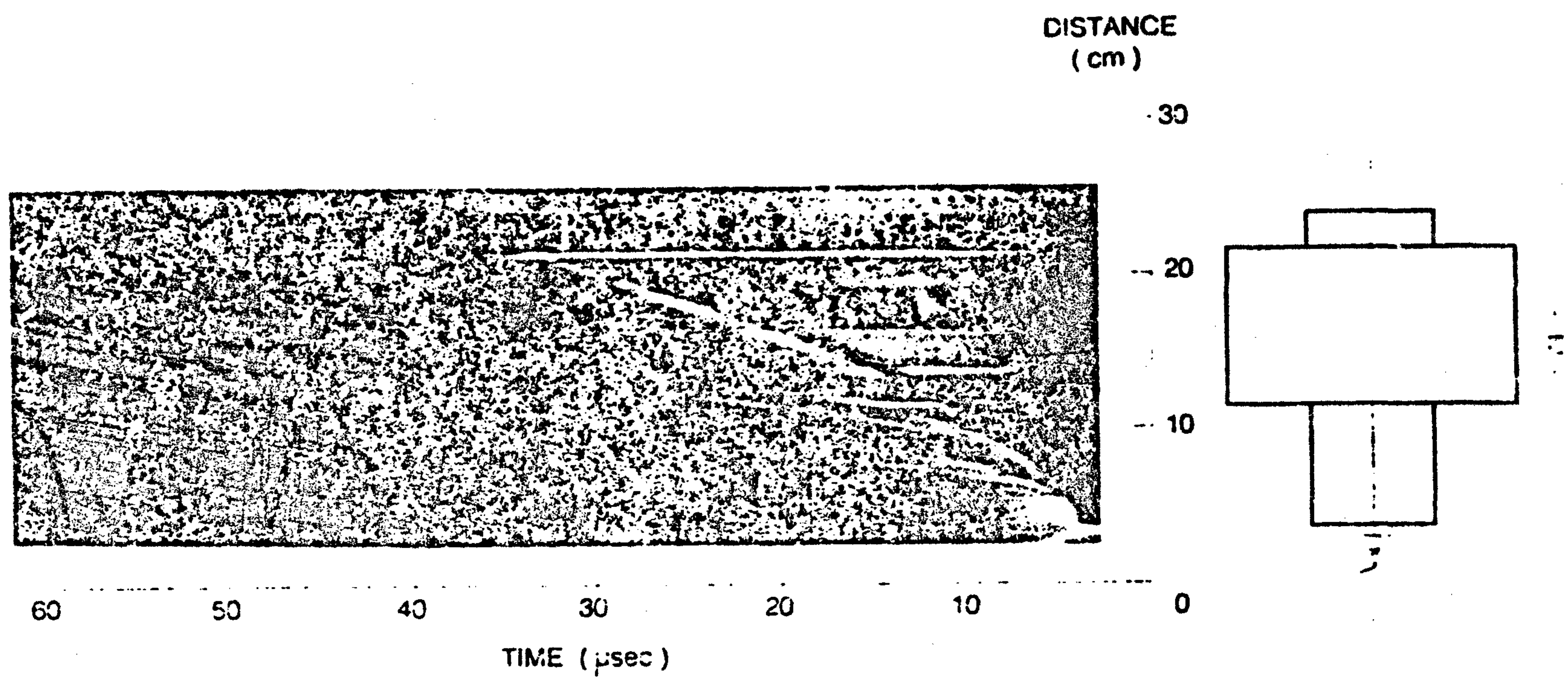

FIGURE 5 : STREAK CAMERA RECORD OF A CALIBRATED GAP TEST FOR EMULSION A.

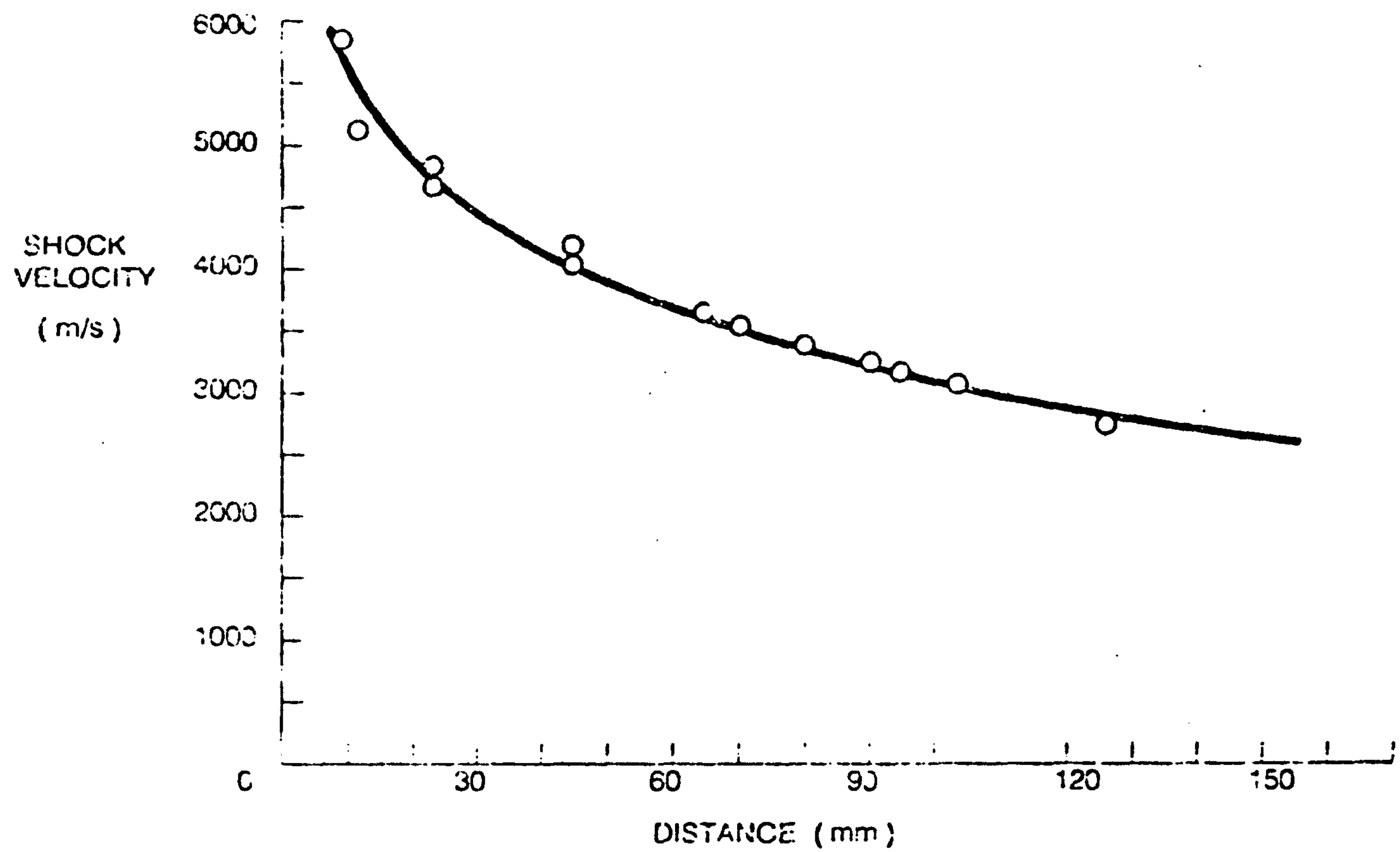

FIGURE 6 : SHOCK VELOCITY VERSUS PLEXIGLAS THICKNESS FOR THE CALIBRATED GAP TEST.

c) The pressure in the plexiglas can be calculated from the density, shock velocity and particle velocity, ($P = \rho UpUs$).

The relationship between pressure in the plexiglas and the plexiglas thickness is shown in Figure 7.

The initial pressure in the explosive can be caluculated if the Hugoniot of the unreacted explosive is known. It is assumed that the pressure and particle velocity are the same on both sides of the attenuator - explosive interface. Since the shock pressure and the particle velocity in the attenuator are known, the pressure P and the particle velocity Up in the explosive are found by reflecting the attenuator Hugoniot along the line Up = constant, and finding the intersection of this curve and the line provided by the Hugoniot of the explosive . The process is illustrated in Figure 8.

Hugoniots of explosives were estimated based on values from previous work (5), (6). The particle velocity of the unreacted explosive is half of the free surface velocity of the acceptor. The pressure of the unreacted explosive can be estimated from the Hugoniot for the explosive and the momentum conservation equation. $P_1 = \rho\ (CUp + SU^2p.)$

RESULTS

The experimental results for waxed RDX are shown in Figure 9. Figure 10 shows the relationship between the

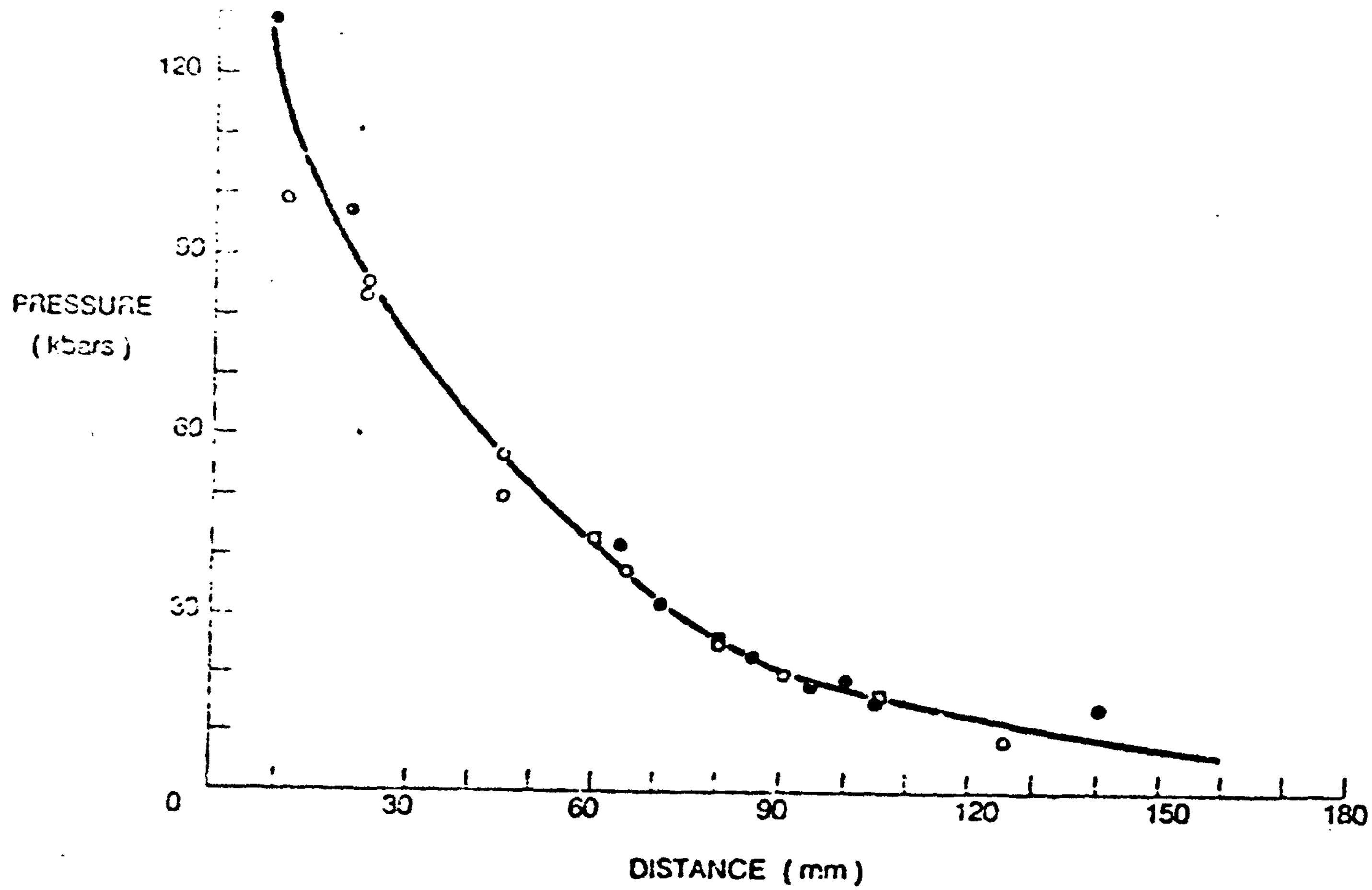

FIGURE 7 : ATTENUATION OF THE SHOCK WAVE PRODUCED BY THE DONOR IN THE CALIBRATED GAP TEST.

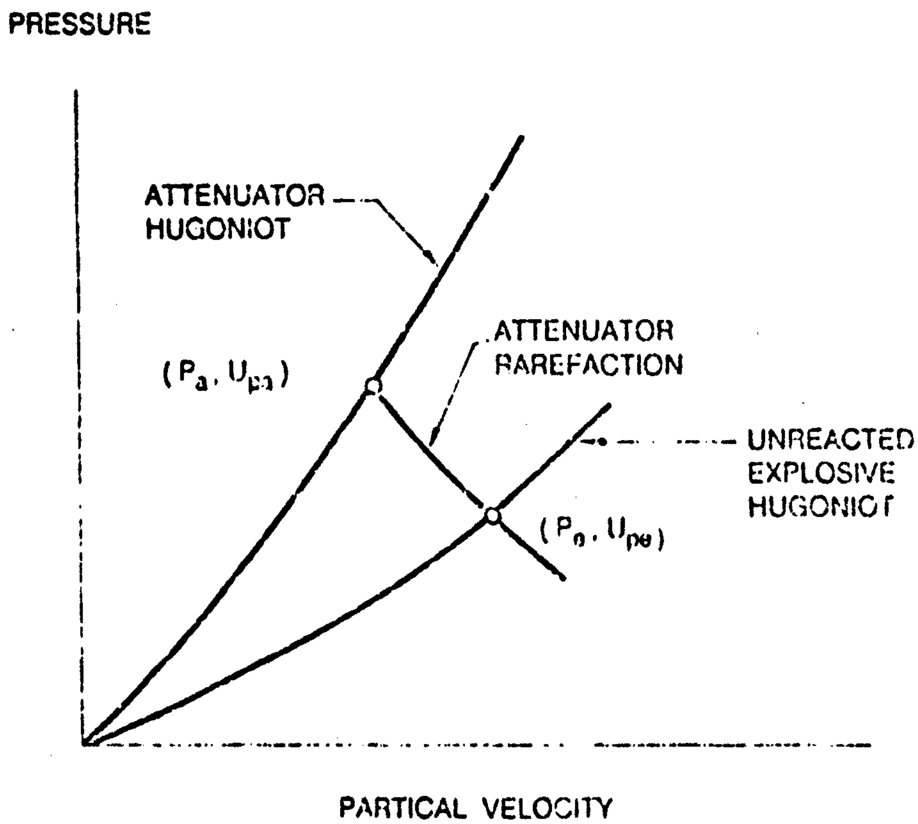

FIGURE 8 : GRAPHICAL METHOD OF OBTAINING SHOCK PRESSURE AND PARTICAL VELOCITY IN UNDER INITIATED EXPLOSIVE.

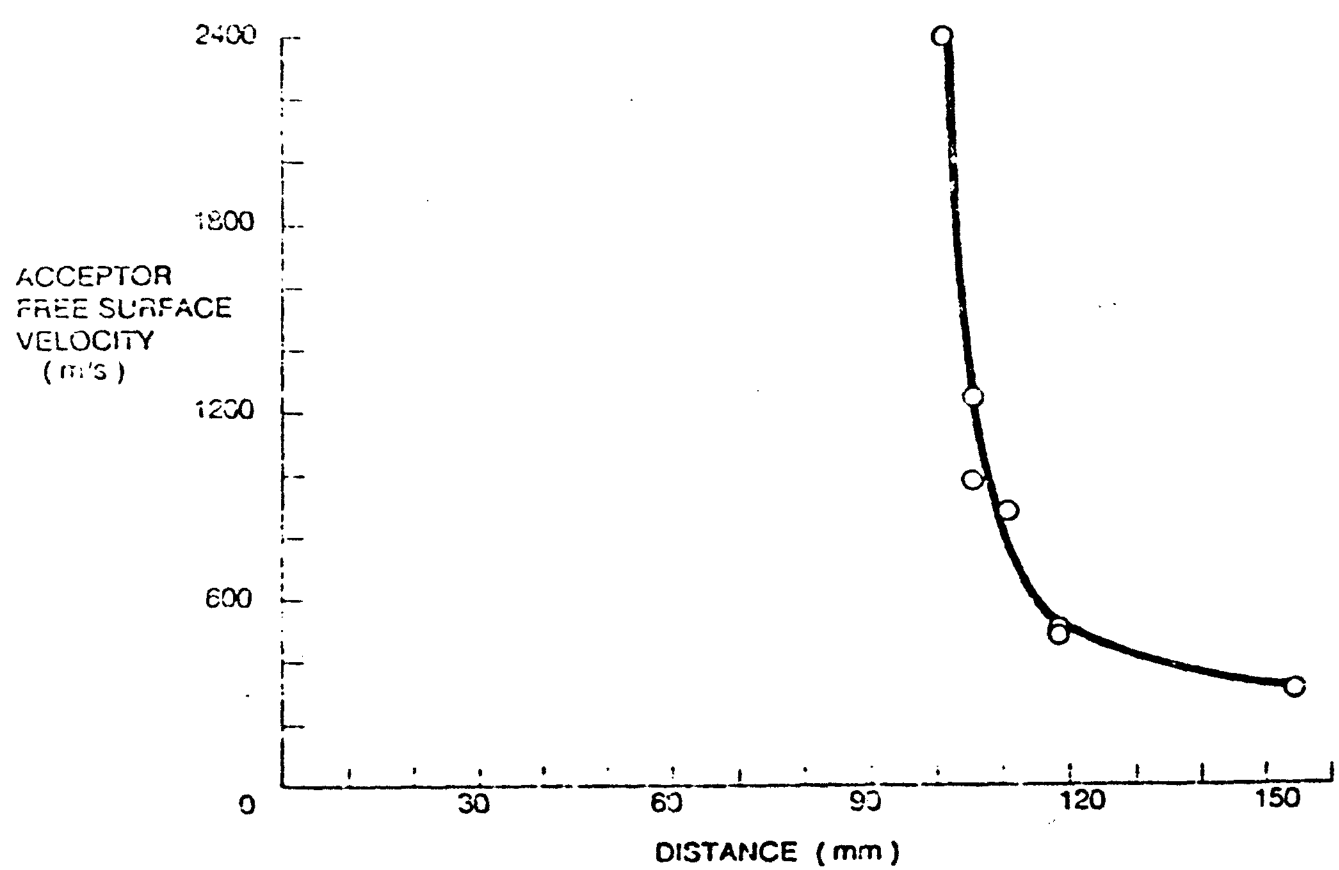

FIGURE 9 : ACCEPTOR FREE SURFACE VELOCITY VERSUS PLEXIGLAS THICKNESS FOR WAXED AND PRESSED RDX.

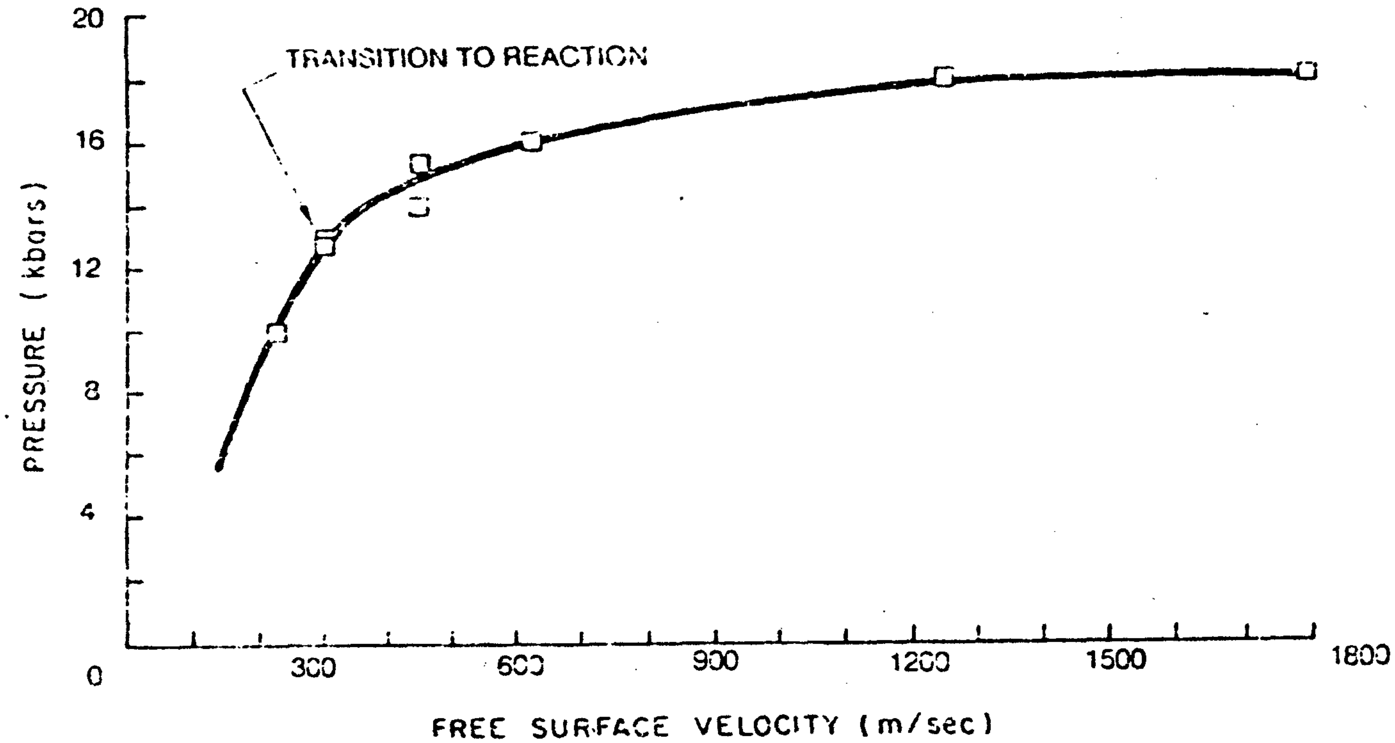

FIGURE 10 : PRESSURE VERSUS FREE SURFACE VELOCITY FOR WAXED RDX

plexiglas shock pressure and acceptor free surface velocity for waxed RDX. It follows that the trigger initiation threshold is at a plexiglas thicknesss of 115 - 125 mm or at a shock pressure in the plexiglas of between 11 and 13 kbars.

The experimental results for Slurry A are shown in Figure 11. Figure 12 illustrates the relationship between plexiglas shock pressure and acceptor free surface velocity. The trigger initiation threshold is at a thickness of 135 - 145 mm or a shock pressure in the plexiglass of between 10 and 15 kbars.

The experimental results for the emulsion explosive are plotted as plexiglas thickness - acceptor free surface velocity and plexiglas shock pressure - acceptor free surface velocity curves in Figures 13 and 14 respectively. The trigger initiation threshold is at a thickness of 105-115 mm or at shock pressure in the plexiglas of 13-15 kbars. The experimental work shows that a threshold to initiation could be found in all three explosives tested. These results are summarized in Table 2.

TABLE 2 : RESULTS OF MODIFIED GAP TESTS

Explosive	Density (g/cm^3)	Trigger Initiation Threshold (kbar)	Detonation Threshold (kbar)
Slurry A	1.15	10.2	30.33
Emulsion A	1.15	13.15	23.25
Waxed RDX	1.55	11.13	18.20

CRITICAL ENERGY CALCULATION

The gap test values of the critical pressure for initiation are dependent not only on the chemical composition and the physical properties of the acceptor charge, but also on the dimensions of the tests. A donor of different dimensions will produce different impulses and an acceptor of a different diameter will also change the pressure-time profile inside the acceptor charge. Obviously, the threshold values given represent only the test described previously. As such the test is good only for comparative purposes. In order to obtain values which are not dependent on the geometry, the pressure profile has to be considered. This can be performed by calculating the critical energy for initiation and detonation (7), (8), (9), (10).

In order to evaluate the computer code calculations, the calcuates results were compared to available experimental data. Hence, the relationship between plexiglas pressure and plexiglas thickness for the standard donor was used. Figure 15 illustrates both the experimental and the calculated curves. The agreement is good. Figure 16 shows pressure histories for various points along the axis of symmetry of the experiment. The critical energy in calculated as $Ecr = \int PU_p dt$ where p is the pressure, Up is particle velocity, t is the time duration. This is the time until the particle velocity vector has a direction opposite to the direction of the propagation of the initial shock wave created by the impact.

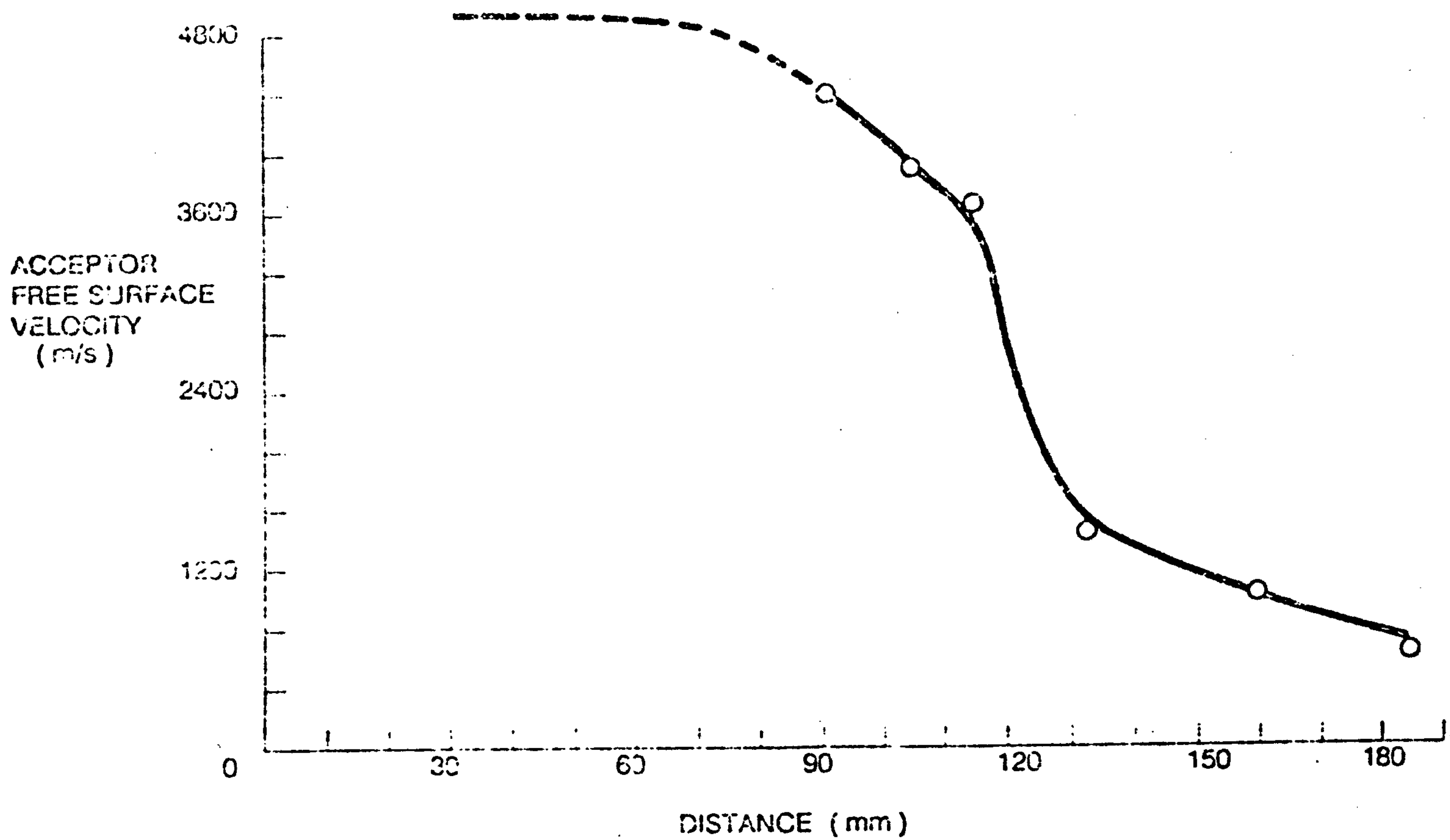

FIGURE 11 : ACCEPTOR FREE SURFACE VELOCITY VERSUS PLEXIGLAS THICKNESS FOR SLURRY A.

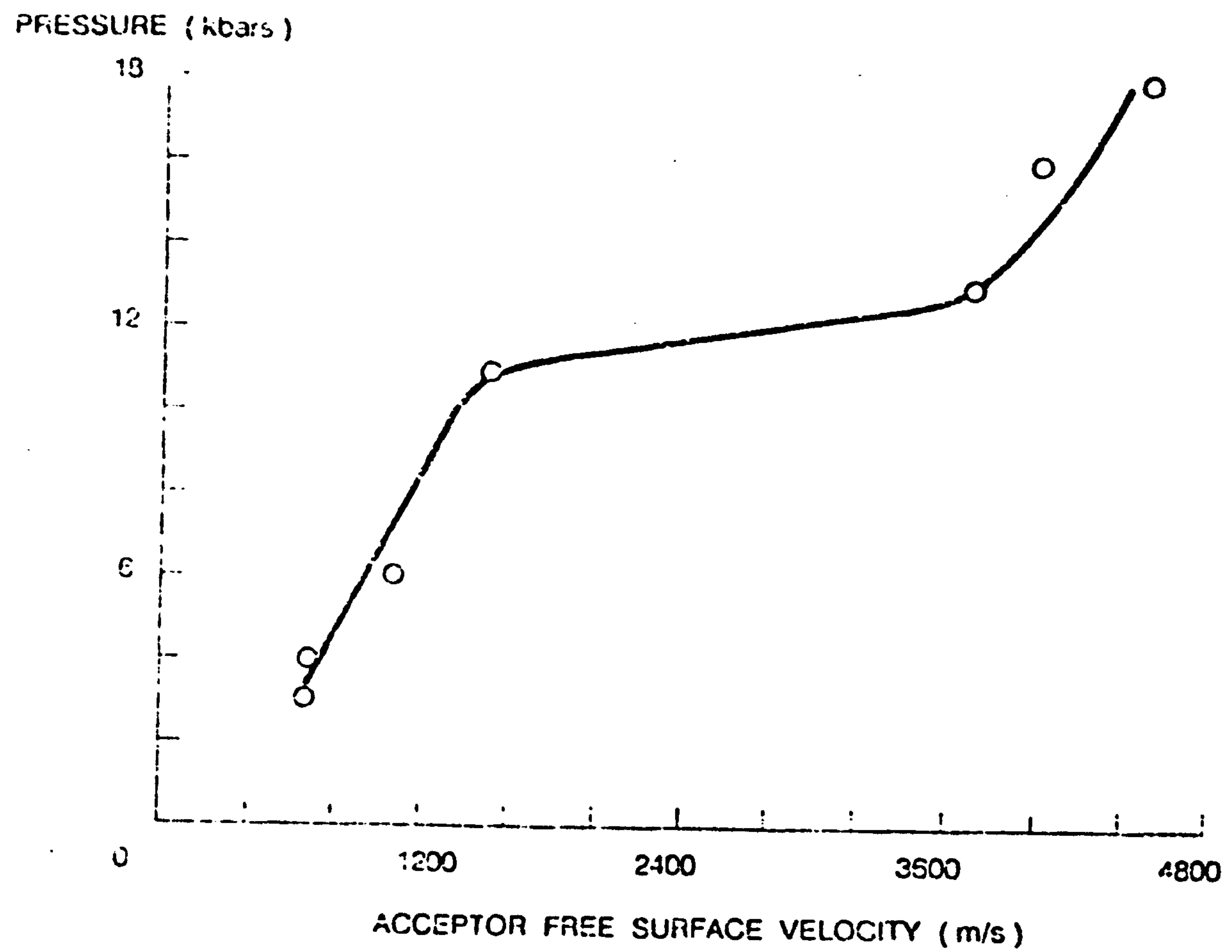

FIGURE 12 : PRESSURE VERSUS FREE SURFACE VELOCITY FOR SLURRY A.

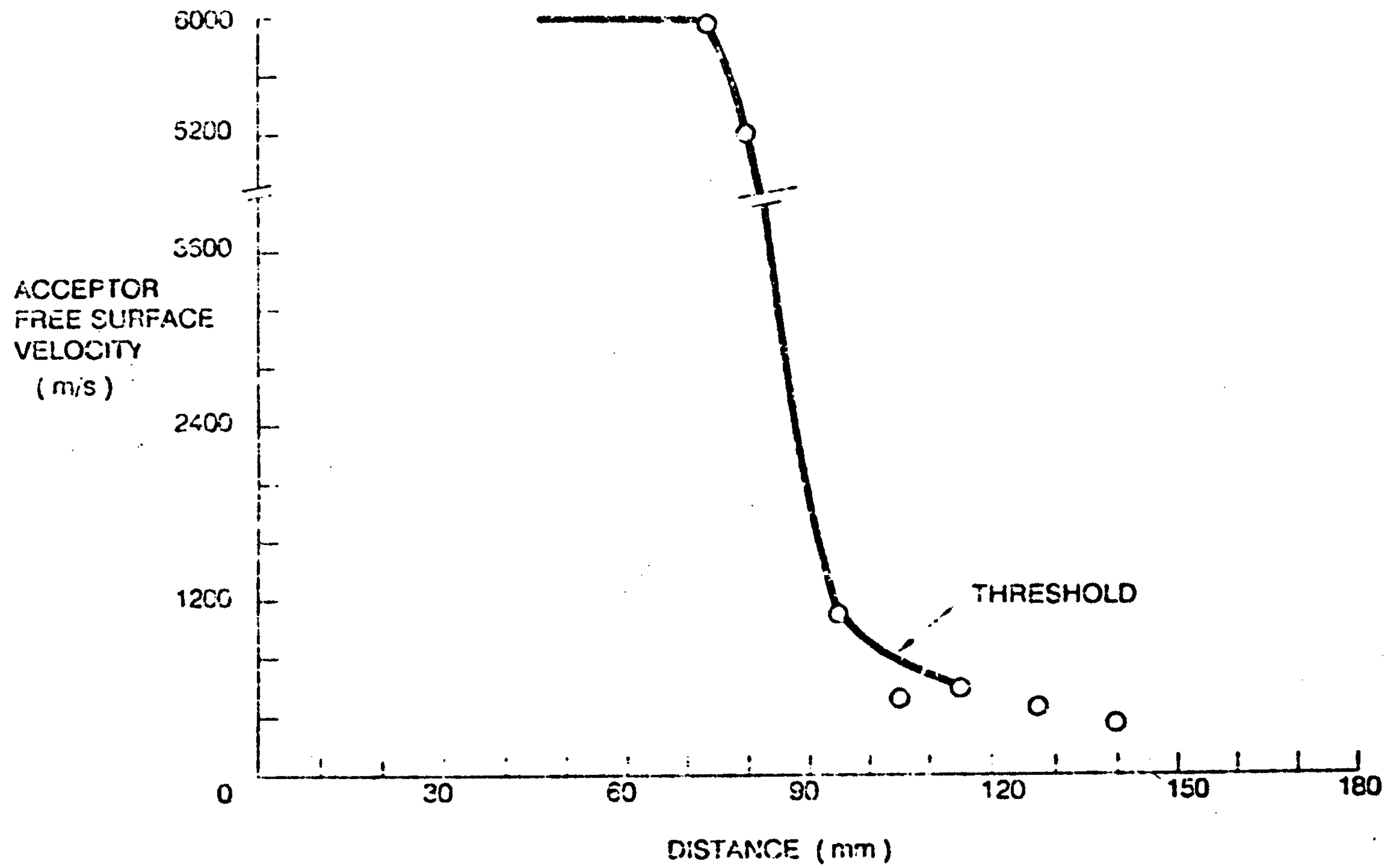

FIGURE 13 : ACCEPTOR FREE SURFACE VELOCITY VERSUS PLEXIGLAS THICKNESS FOR EMULSION A

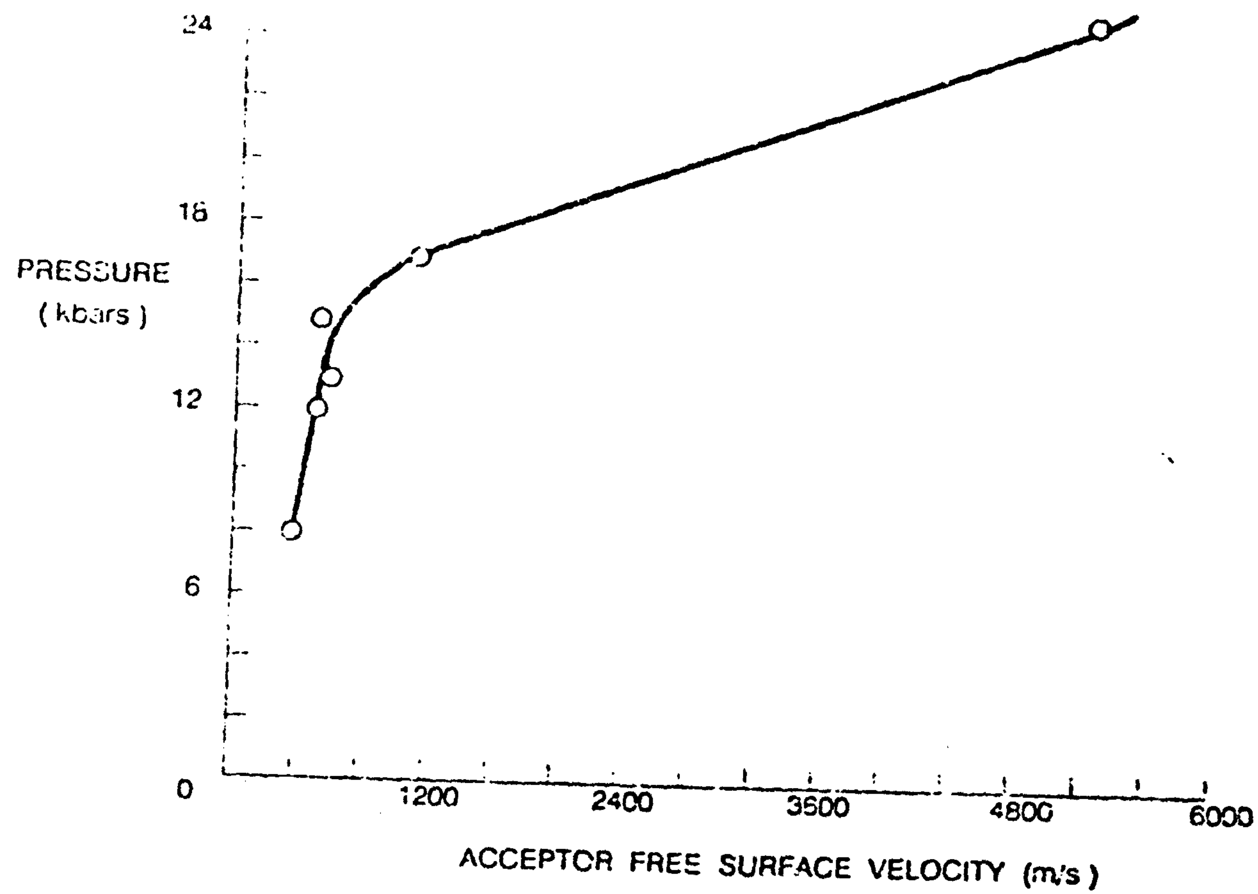

FIGURE 14 : PRESSURE VERSUS FREE SURFACE VELOCITY FOR EMULSION A.

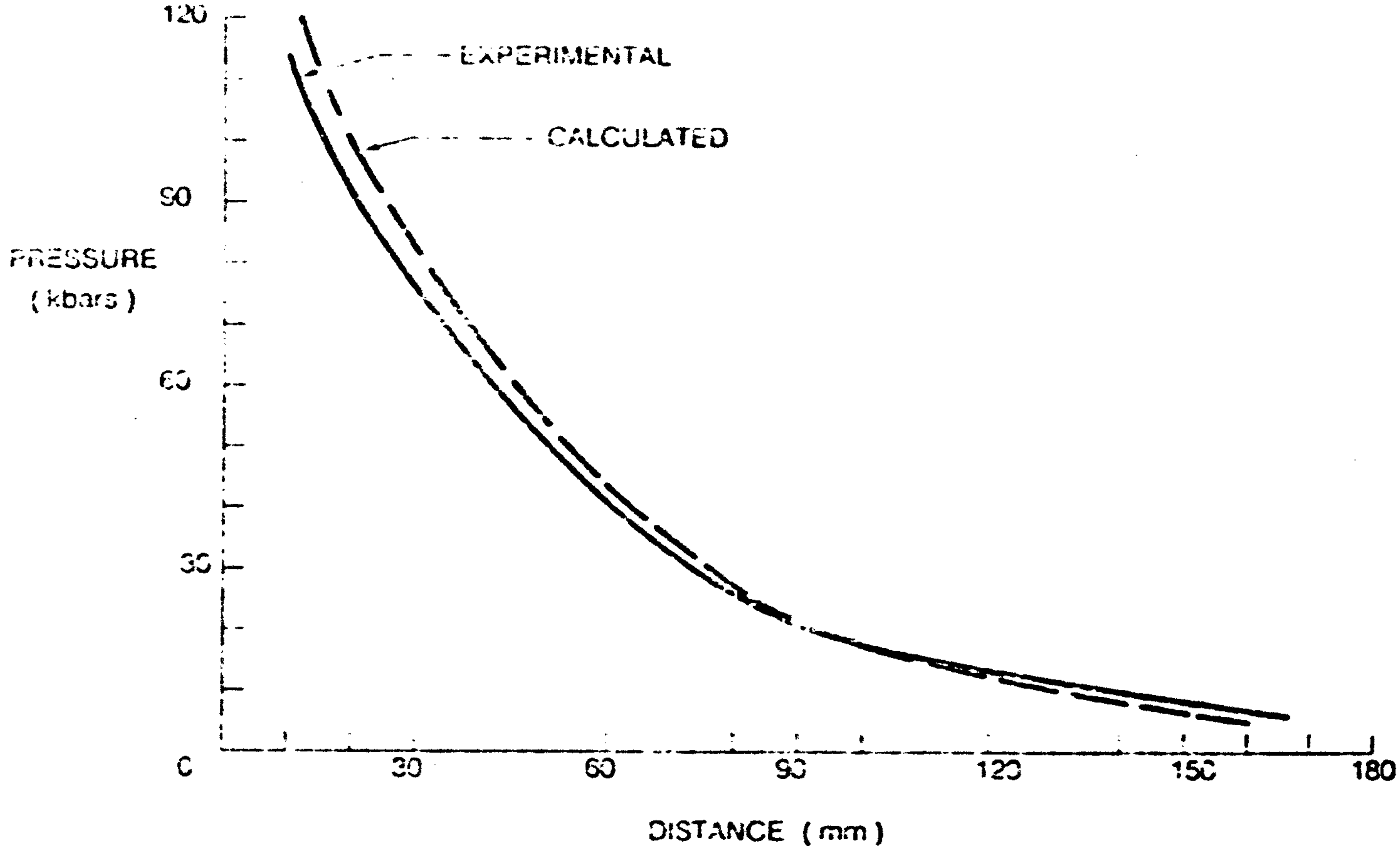

FIGURE 15 · EXPERIMENTAL AND CALCULATED CURVES SHOWING PLEXIGLAS PRESSURE AS A FUNCTION OF DISTANCE IN THE CALIBRATED GAP TEST.

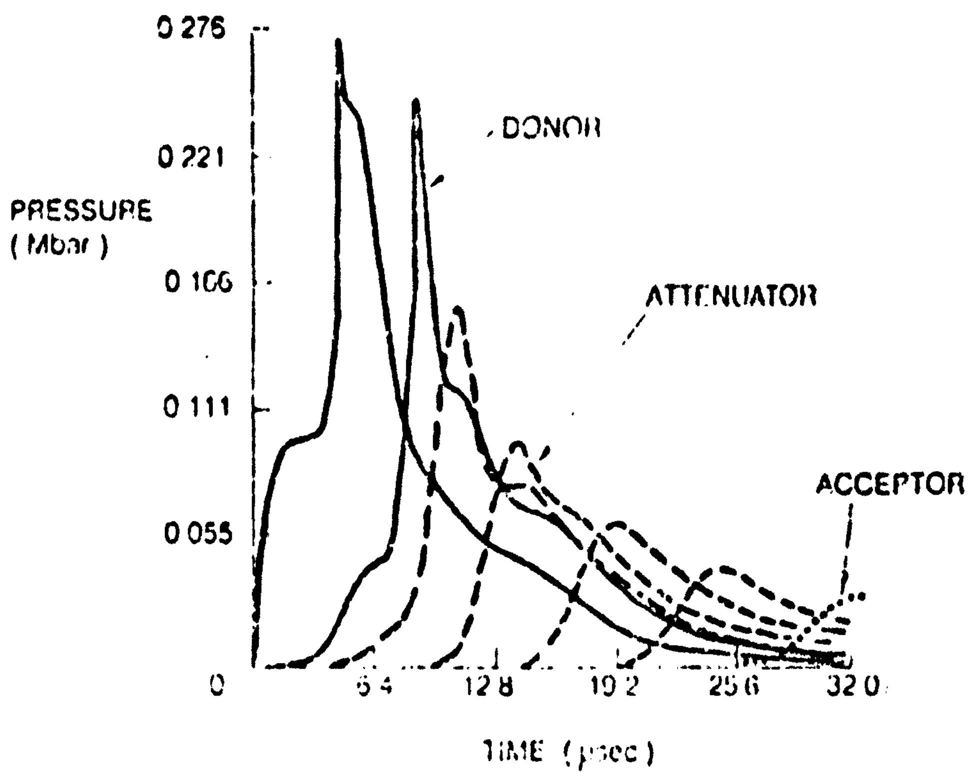

FIGURE 16 : TYPICAL PRESSURE HISTORIES FOR VARIOUS POINTS ALONG THE AXIS OF THE GAP TEST ARRANGEMENT.

According to the experiments and the pressure histories the critical energies for the studied explosives were obtained by evaluating the integal P(t)Up(t)dt. The results are listed in Table 3.

TABLE 3 : RESULTS OF CRITICAL ENERGY CALCULATIONS

Explosive	Density (g/cm^3)	Modified Gap (kJ/m^2)	Projectile Impact (kJ/m^2)
Slurry A	1.15	672	1202
Emulsion A	1.15	2430	4142
Waxed RDX	1.55	1382	1476

PERFORMANCE CALCULATIONS

The detonation pressure and velocity were calculated by Tiger Code (11) using the JCZ3 Equation of State. The Gurney velocity was estimated by Kamlet's formula (10). The calculation of detonation velocity is in a reason agreement with the experimental values. The results from the calculation are summarized in Table 4.

TABLE 4 : THE RESULTS OF PERFORMANCE CALCULATIONS

Explosive	Density (g/cc)	Tiger Code		Experimental Value (km/s)	Gurney Velocity (km/s)
		Detonation Velocity (km/s)	Detonation Pressure (kbar)		
Slurry A	1.13	4.6	72	4.1	1.712
Emulsion A	1.12	5.4	68	5.2	2.084
Waxed RDX	1.55	8.0	250	-	2.786

From Table 4, the emulsion explosive has higher performance than the slurry explosive, the value for the emulsion explosive is about 20% higher than for the slurry explosive. The calculated of detonation velocities are in reasonable agreement with the experimental values measured using nichome resistance wire velocity probes.

DISCUSSION

The experimental results using the modified gap test show that a first threshold to deflagration before detonation occurred in all three type of explosives. On the contrary, projectile impact tests are a case of shock to detonations transition without indication of the first transition. The results of the projectile impact tests are reported as detonations or failures. Therefore, any initiation which did not propagate to a detonation is reported as a failure. There appears to be no general agreement on the exact role that the first transition plays in the sheok initiation process determined from the modified gap tests. We call this transition point the trigger initiation transition. The energy required for this transition, we call trigger initiation energy.

The slurry explosive was shown to be more sensitive than the emulsion explosive or waxed RDX. It exhibited a large zone where buildup of reaction occurred. In addition to this, Figure 5 shows that a significant amount of burning takes place before detonation occurs as evidenced by the relatively long and flat transition area (Figure 12). In the case of the emulsion explosive and waxed RDX, a rapid build up to detonation is observed in Figures 3 and 4 when the shock pressure increased above the threshold for the initiation transition.

In a few cases, detonation was observed several microseconds after the arrival of the shock wave at the interface between plexiglas and acceptor. These events occurred in both the slurry and emulsion explosives. Figure 17 shows a streak camera record illustrating this. However, it was more common in the experiments conducted for the slurry explosive. This might be an indication of the role of air bubbles in slurry explosives or microballoon in emulsion explosives.

The emulsion explosive was somewhat more sensitive than the waxed RDX. This is due to the high density of the waxed RDX. One would expect waxed RDX to be more sensitive than the emulsion explosives at the same density.

The behaviour of an explosive subjected to impact is dependent on the test method and such variables duration of impact, deformation of sample and confinement. For example, Table 1 indicates the critical impact velocity for the slurry explosive is 447 m/s in non-confined test conditions and 337 m/s confined in 50 mm ID steel pipe.[4] This is due to the arrival of rarefaction waves from the wall of the pipe and other effects.

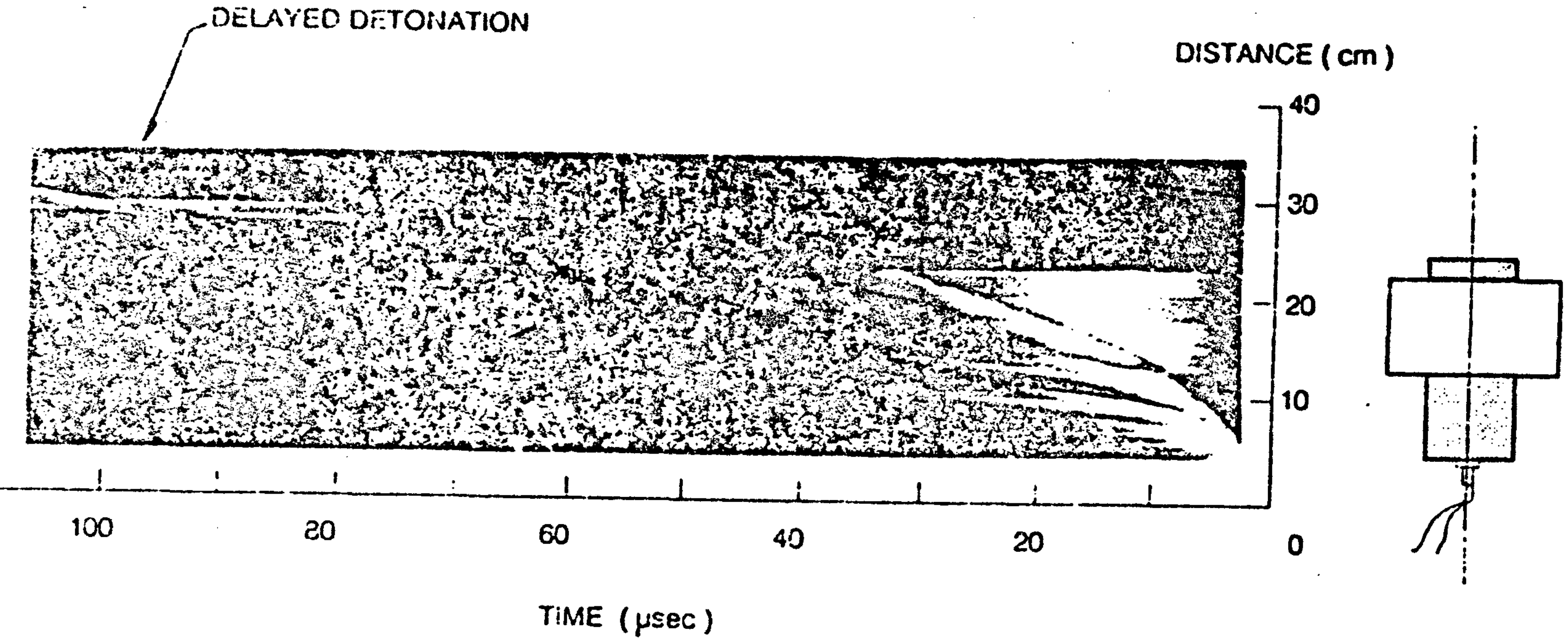

FIGURE 17 : STREAK CAMERA RECORD FOR EMULSION A

CONCLUSIONS

The experimental work shows that an initiation threshold to detonation could be formed in all three explosives tested. The slurry explosives was shown to be the most sensitive of the three. This agrees with the projectile test results for a detonation threshold.

From critical energy calculations, the slurry explosive exhibited considerably lower critical energy for initiation due to low amplitude shocks and for detonation due to high velocity projectile impact. Therefore, it is expected that the slurry explosive will be more susceptiable to accidental initiation than the emulsion explosive tested.

Two thresholds, one for initiation and one for detonation, SDDT curve could be identified by modified gap tests, instead of one detonation threshold by projectile impact tests. The initiation and detonation thresholds from modified gap tests could be identified by interpreting the experimental shock pressure and particle velocity curves for the explosives.

ACKNOWLEDGEMENTS

The authors would like to thank Mr. R.R. Vandebeek, Manager of the Canadian Explosives Research Laboratory for fruitful discussion and reading the manuscript .

REFERENCES

1) A. Bauer, K.K. Feng, P. Katsabanis and J. Moroz, R.R. Vandebeek, "High Velocity Impact Sensitivity of Commercial Slurry and Emulsion Explosives" presented at the First International Symposium on Intense Dynamic Loading and Its Effects, Beijing, China, 1986.

2) D.G. Tasker, "Shock Initiation and Subsequent Growth of Reaction in Explosives and Propellants", Seven Symposium (International) on Detonation, 1981, pp. 285-298.

3) T.P. Liddiard and J. Forbes," Initiation of Burning and Detonation in Cast H-6 and Cast PGXW-109" Seven Symposium (International) on Detonation, 1981, pp. 308-315

4) M. Kroh, K. Thomas, W. Arnold and V. Wallenweber, "Shock Sensitivity and Performance of Several High Explosives", 8th Symposium (International) on Detonation, 1985, pp. 502-508.

5) A. Bauer, K. Feng, P. Kaisabanis, J. Moroz and R. Vandebeek, "High Velocity Impact Sensitivity of Commercial Slurry and Emulsion Explosives" Minutes of the 22nd Explosives Safety Seminar of Department of Defence Explosives Safety Board.

6) S.P. Marsh, "LAST Shock Hygoniot Data" University of California Press, 1980.

7) L. Seamen, "TROTT Computer Program", Stanford Research Institute, 1976.

8) M.S. Shaw and G.K. Straub, "HYDROX CODE - A One Dimensional Lagrangion Hydrodynamics Code" Los Alamos Scientific Laboratory, LA - 8642-M, March 1981.

9) J. Zukas, T. Nicholas, H. Swift, L. Greszczuk and D. Curran, "Impact Dynamics", John Wiley & Sons, 1982.

10) B.M. Dobratz, "Properties of Chemical Explosives and Explosives Simulants" LLNL Explosives Handbook, March 16, 1981.

11) M. Cowperthwaite and W.H. Zwisler, "Theoretical and Mathematical Formulations for the Tiger Computer Programs" Stanford Research Institute, California, 1973.

Factors Affecting the Response of Munitions to Shaped Charge Jets

M.C. Chick

Materials Research Laboratory

Australia

R. B. Frey

Ballistic Research Laboratory

USA

1. INTRODUCTION

Shaped charge jets represent a formidable threat/hazard to target munitions. An understanding of the response of munitions to jets is of fundamental importance in assessing the threat/hazard situation in several areas of munition deployment. Specific areas of concern include: the mass detonation hazard from the premature firing of a warhead jet during transport or storage into neighbouring rounds; development of safe and predictable Explosive Ordnance Disposal [EOD] techniques for the removal of unwanted munitions; and the vulnerability assessment of munitions from shaped charge jet attack in wartime and from urban guerillas in peacetime. The review has treated the subject in terms of a generic jet and target munition system. Jets were produced from conventional shaped charge warheads and the generic munition is defined as an unfuzed cylindrical case filled with energetic material (see Figure 1). From the point of view of shaped charges it is convenient to consider the generic munition as either having a thin or thick case. This classification arises since thin cased fillings are generally initiated by the jet impact shock whereas thick cased fillings are initiated by the bow wave ahead of the penetrating jet and these two processes have different characteristics. The demarcation thickness between the two systems is normally taken as equivalent to about a few jet diameters. This treatment is a guide only since in some situations other factors (eg presence of air cavities, see Section 3.6; the influence of critical detonation diameter, see Section 3.2) can predominate in determing the initiation mechanism and level of the filling's senstivity to jets.

Most surveyed work has been concerned with studying factors and processes that influence the initiation of detonation or the detonation/lower order reaction threshold of the filling. However USA (Ballistic Research Laboratory, BRL)[1] and Australian (Material Research Laboratories, MRL)[2] studies suggest that jet stimulation or lower order reactions in confined solid fillings can lead to quite violent deflagrations. The fragment/blast from these deflagrations may be a potential cause of

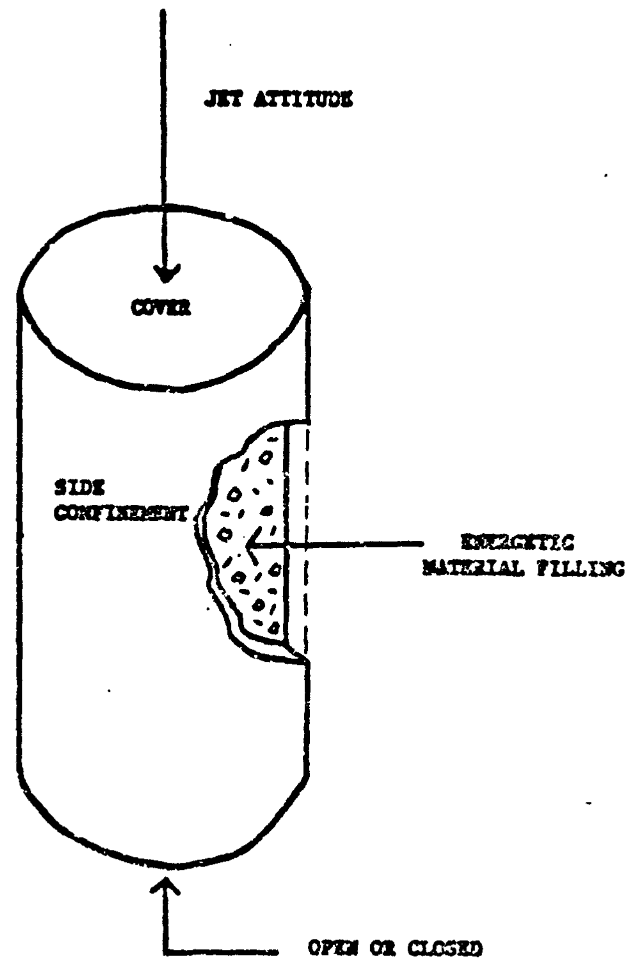

FIGURE 1. ILLUSTRATION OF A FILLED GENERIC MUNITION SHOWING DIRECTION OF JET STIMULUS

sympathetic detonation and represents a technological gap in our knowledge. In this paper the threat/hazard level is mostly considered from the effect of the jet on the detonation/lower order reaction threshold of the generic munition.

2. BASIC JET INITIATION PROCESSES

2.1 MECHANISMS OF INITIATION

2.1.1 COVERED EXPLOSIVES

The following summary is mostly based on Australian work and from results of a joint Australian (MRL)/USA (BRL) program sponsored by TTCP Subgroup W. The results have been progressively reported within TTCP and the open literature over recent years.[3-8]

When the jet hits the surface of the cover a large impact shock is produced. The impact shock propagates through the cover ahead of the jet but decays very rapidly. For thin covers of less than a few jet diameters impact is most likely to cause detonation. Pressures up to a few thousand kilobars are produced at the cover surface and about 1000 kbar can be transmitted to the explosive - this compares to an initiation pressure in Composition B in the large scale gap test of 20-25 kbar The penetrating jet sets up a bow wave that overtakes the impact shock within a few jet diameters of the cover surface. The characteristics of the bow wave are dependent on the properties of the jet and the host material. The jet and bow wave continue steady penetration towards the cover/explosive interface. If the penetration rate in the cover is supersonic a shock is formed with a velocity equal to the penetration rate. It is expected that this shock would detonate the filling in some situations. When the penetration rate is subsonic or the bow wave shock is weak initiation is unlikely and the wave is transmitted to the explosive. The precursor wave (decaying jet impact or cover bow wave) ahead of the jet can desensitise the explosive filling (see Section 2.2). When the jet penetrates the explosive a new bow wave is set up. The initial pressure at the jet tip in the explosive is several orders of magnitude greater than the bow wave pressure. It can also be several orders of magnitude greater than the critical initiation pressure without detonation occurring. Reaction occurs within the thickness of the bow wave which can either build up to detonation or cause the round to fail. The process by which the bow wave desensitises the explosive is discussed in the next Section. Jet penetration of the explosive is supersonic and considerable evidence[3-8] suggests that the bow wave shock formed is the usual method of initiating energetic fillings with thick covers.

Depending on the velocity of the jet and the cover characteristics several types of event are possible;

(a) for very thin covers and high jet velocities the impact shock can cause detonation. This occurs within a few milimetres of the explosive surface and before the arrival of the jet,

(b) for thin covers strong bow waves can cause prompt detonation within a few millimetres of the explosive surface,

(c) as the jet velocity decreases with increasing cover thickness bow wave strength in the explosive decreases and the run distance and time to detonation increases. Thus near the critical condition, detonation in Composition B can take 11 μs and 40 mm for initiation by the 38 mm diameter shaped charge jet,

(d) for bow waves below the critical condition the explosive fails; the jet penetrates through the explosive with the bow wave causing disruption and/or reaction,

(e) jet bow waves reflected back into the explosive from a steel surface at the far end of test samples can cause detonation. This has been observed near the critical jet initiation condition with explosive samples of up to 50 mm long for jets from a 38 mm shaped charge and with samples up to 100 mm long for jets from a 81 mm charge. This must be considered as a potential mechanism for initiation in munition systems, at least in smaller geometries with heavy confinement near the jet initiation threshold.

For covered explosives Australian work has never observed initiation occurring directly at the jet, it has always occurred in the shock ahead of the jet or not at all.

2.1.2 BARE EXPLOSIVES

For bare explosives the jet impact either causes detonation at (or very near) the surface or not at all. Mader and Pimbley in the USA (Los Alamos National Laboratory)[9-11] have undertaken an extensive numerical modelling study of the process and attributed the surface nature of the process to the rapid quenching action of the rarefactions on any shock that does not establish a prompt, curved detonation front. The results of the computer modelling study are in accord with measurements using multiple, orthogonal, flash radiography of the detonation build-up in explosives carried out by the joint Australian (MRL)/USA (BRL) program.[3,5,12] Held[33] produced the original proposal for the influence of jet velocity and diameter on the detonation threshold of bare explosives (see Section 4)

However, recent Australian work [12,13] has shown that if the ratio of an explosive's critical detonation diameter to the jet diameter is large then there is a transition in the mode of initiation from that produced at the surface by the impact shock to that produced in the bulk of the explosive by the bow wave of the penetrating jet - this transition is accompanied by a marked drop in jet sensitivity. These observations are discussed in Section 3.2.

2.2 BOW WAVE INITIATION AND DESENSITISATION

The jet bow wave initiation and desensitisation of explosive has different characteristics than those associated with conventional shock initiation. The long detonation build-up distances and times at the critical condition were indicated in Section 2.1.1. The summary of the process described below is taken from the Australian (MRL)/USA (BRL) work.[3-5]

The initial waves transmitted to the explosive from the cover by the penetrating jet may precondition the initial layer of explosive and cause desensitisation of the type initially postulated by Campbell et al[14,15] (this considers that the initial low pressure precursor wave deactivates the hot spots to the higher pressure in the jet tip region). However, direct evidence from flash radiographs and results using different cover materials have shown that during jet penetration of the explosive a bow wave developes with associated reaction (termed bow wave burn). As the jet penetrates further in the explosive bow wave burn produces increasing reaction with the front becoming more defined on flash radiographs. Consequently bow wave burn alters the state of the explosive and the shock profile by decreasing the pressure in the zone adjacent to the jet tip. Thus the jet penetrates mostly products rather than unreacted explosive and the bow wave desensitises the explosive by causing it to undergo a fast reaction rather than a detonation. If the bow wave shock is strong enough the front runs up to detonation. For weaker bow waves, however the burn process helps stop detonation altogether. This is demonstrated by the introduction of an air gap in an explosive charge which would otherwise fail. The air gap dissipates the bow wave and the jet produces prompt detonation at the explosive surface on the far side of the void (see Section 3.6 for further discussion on the sensitising effect of voids). The similar critical jet velocities for the threshold initiation of Composition B with steel, aluminium and plexiglas cover materials (and which transmit very different shaped precursor waves into the initial layer of explosive) demonstrates that the characteristics of the bow wave of the jet penetrating the explosive (including the bow wave burn desensitisation) are responsible for determining the initiation and failure processes. Measurements from radiographs suggest the bow wave region in Composition B to be up to about 10 mm thick with a duration of up to 3 μs for the jet from a 38 mm diameter shaped charge.

In two recent papers Held[23,24] (MBB, West Germany) has repeated several of the Australian (MRL)/USA(BRL)[3-8] experiments with similar results. However, these two papers do not attempt to interpret the results in terms of jet bow wave initiation and desensitisation.

Mader[25] has numerically modelled the form of the precursor wave desensitisation (hot spot deactivation) that occurs in the initial layer of explosive at the barrier boundary. The basis of Mader's code calculations were the arrangements and results from the Australian and joint Australian (MRL)/USA(BRL) studies.

An experimental and numerical modelling study carried out by Pirotais[26] et al in France examined two thinly covered explosives. The numerical method was similar to that reported by Mader et al.[9-11] The HMX composition exhibited impact initiation similar to that reported in 2.1.2[3-11] Although reaction in the TATB composition faded from the impact shock as per the Mader et al study[10-11] it subsequently detonated several millimetres below the explosive surface following support from a compression wave produced in the explosive by the jet at the interface with the cover.

Although experimental work[3-8,12-13] over recent years has lead to the discovery and characterisation of jet bow wave initiation and desensitisation there is a requirement for further work. More information is needed on the characteristics of bow wave mechanisms in a range of

energetic materials (the joint Australian (MRL)/USA (BRL) study is proposing further work in this area), reactive numerical models need to be expanded to take account of the processes and the lack of theoretical work requires addressing.

3. EFFECTS OF GENERIC MUNITION CHARACTERISTICS

3.1 CHARACTERISTICS OF THE ENERGETIC FILLINGS

From the point of view of the shaped charge jet threat/hazard, fillings of energetic materials may be considered in 3 classes; explosives, solid propellants and loose propellants (propellant beds). The survey on which this paper is based found that most work has been carried out on explosives; studies on propellant beds have been confined to BRL and a recent investigation on solid propellants has commenced in Australia. Information to date suggests that the similar physical state of explosives and solid propellants may confer similar general characteristics in their response to jets. It is expected, however that some controlling parameters will produce large differences in the degree of the response from the two types of energetic material e.g. the large critical diameter of many propellants would be expected to have an overriding influence on their sensitivity to jets. Clearly there is a requirement to remedy the lack of information on the response of solid propellants to jets.

Although this survey is primarily concerned with the response of explosives and solid propellants information on propellant beds is summarised in Section 3.1.1.

3.1.1 PROPELLANT BEDS

The general physical structure of the grain packing of a propellant bed would be expected to play an important role in its response to shaped charge jets. Thus the network of voids and the low density may discourage the growth of a regular bow wave but promote the development of burning.

Work by Majerus et al[16,17] at BRL in the 1970's studied the effect of shaped charge jets on propellant beds and found that localised violent reaction (detonation) was produced by jet impact and along the jet's path through the propellant. They found that violent reaction went out but the majority of the remaining propellant was consumed by burning, for example, the low velocity portion of the jet consumed about 90% of the propellant. The study concluded that the amount of both violent reaction and burning reaction increased with the kinetic energy of the jet (i.e. increased with jet velocity and diameter). Anderson[18] subsequently produced a model to approximate the work of Majerus et al. Further work at BRL by Brown et al[19] found that the severity of the rupture of the cartridge case increased with residual jet velocity and jet path length in the propellant bed. Recent work by Watson[15] also of BRL developed a method for assessing the amount of violent reaction induced in the propellant bed by a shaped charge jet. This method measured the shock decay curve in the propellant from the localised violent reaction. The results showed that the rate of decay of the curve was related to the degree of violent reaction and that the method was capable of distinguishing between the reactivity of different types of propellants. Thus, Watson's method offers the possibility of using a small

scale test to assess the response of the interaction of various types of propellant beds and jets. This would appear to open a way to study the physical and chemical characteristics of propellant beds with a view to minimising their violent response to shaped charge jets.

3.1.2 EXPLOSIVES AND SOLID PROPELLANTS

Jet impact is a conventional shock initiation process and has been extensively modelled by Mader et al at LANL[9-11]. It is also expected that the small diameter rod initiation of Composition B modelled by Starkenberg[21] et al at BRL would have application to jet impact. Generally these modelling studies are supported by LANL[9-11] and Australian (MRL)[7,22] experimental work on bare explosives which shows a correlation between the shock sensitivity (as measured on the gap test) and the critical jet velocity. An important limitation to the interpretation of both the modelling and experimental results is the effect of the explosives critical detonation diameter. However, as discussed in Section 3.2, this failure may be only temporary if the bow wave set-up in the explosive by the penetrating jet is strong enough and exceeds the critical detonation diameter.

Jet bow wave initiation is assumed to be a shock type process. This is supported by the joint Australian (MRL)/USA(BRL)[5-8,22] work in which the measured critical jet penetration velocities for several explosives have been shown to be greater than the sonic velocity, hence the initiating bow wave will be in the form of a shock. Furthermore these studies also found a good correlation between the critical jet penetration velocity and the shock sensitivity (as measured on the gap test) for 7 different types of explosive composition.

Since both the jet impact shock and bow wave initiation mechanisms are shock processes then it may be assumed that properties related to the physical state of the explosive are important in jet sensitivity; e.g. density, particle size and surface area, porosity, method of fabrication. This is demonstrated by results using TNT.[7,8] Pressed TNT was found to be significantly more jet sensitive than cast TNT although both had a similar density - this is typical shock sensitivity behaviour.

3.2 INFLUENCE OF CRITICAL DETONATION DIAMETER

Australian[12,13] and joint Australian (MRL)/USA (BRL)[5-8] studies have investigated the effect of the ratio of the jet diameter (d) to critical detonation diameter (D) on the level of sensitivity and mechanism of initiation of bare explosives.

Jets from 15, 38 and 81 mm diameter shaped charges were fired into bare fillings. The explosives represented a range of critical detonation diameters and included the common munition fillings Composition B, H-6, Octol and TNT. Multiple flash radiography was used to observe and measure events occurring inside the explosive.

Table 1 shows that depending on the jet/target explosive combination, initiation was produced either by the jet impact at the explosive surface or from the bow wave of the jet penetrating the

TABLE I. Effect of minimum detonation diameter and jet diameter on the type of jet initiation of bare explosives.

Explosive		Type of initiation in the region of the detonation/failure threshold	Minimum diameter of explosive for detonation D mm	Jet diameter d mm	D/d
Type	Density Mg/m^3				
Pressed TNT	1.52	Impact	2.6	1.5	1.7
Composition B	1.65	"	4.3	1.5	2.9
PBX 9502	1.90	"	9	3.0	3
Octol	1.78	"	< 6.4	1.5	< 4.3
H-6	1.74	"	= 6.4	1.5	= 4.3
Composition B	1.65	Bow Wave	4.3	0.75	5.7
H-6	1.74	"	= 6.4	0.75	= 8.5
Cast TNT	1.57	"	14.6	1.5	9.7

explosive. The observed impact initiation conforms to that normally associated with the action of jets on bare explosives.[3-11] Jet bow wave initiation occurred within the bulk of the explosive which is the common jet initiation mechanism for medium and thickly covered explosives. It is important to note that Composition B and H-6 exhibited either jet impact or jet bow wave initiation at the threshold conditions depending on the jet diameter. The explanation for this observation is that the impact shock reaction failed to expand to the minimum detonation diameter before being quenched by rarefactions whereas the subsequent jet penetration bow wave built-up and expanded to greater than the minimum diameter required for detonation. Further evidence is given by Australian flash radiographic results which show similar critical jet velocities for cast TNT in both the bare and covered configuration.[7,8,12,13] Mader et al[10,11] have numerically modelled the limiting effect of critical detonation diameter on the jet impact mechanism and in the failure cases detonation was quickly quenched by side and rear rarefactions. However, the treatment did not consider the subsequent effect of the bow wave from jet penetration

In Table 1 it is proposed that the empirical ratio, D/d, may be used to estimate the transition in the mode of initiation. The data indicates that there is no contradiction to the predictive criterion,

$$D/d = 5 \qquad (1)$$

Thus for bare explosive where $D/d < 5$, jets would be expected to produce impact initiation and where $D/d > 5$ jet penetration bow wave initiation is predicted.

Results for several explosives have shown that jet bow wave initiation requires velocities between 40-70% higher than for jet impact initiation.[3-8] Therefore a consequence of the results is that the transition is accompanied by a sharp jump in the critical jet velocity and hence a significant drop in the explosive's measured sensitivity to jets.

Hence it is most important to select the correct form of the predictive equation for the detonation threshold depending on the mechanism of initiation - See Section 4.

The application of the D/d criterium is particularly relevant to;

(a) insensitive explosive fillings which generally have large critical detonation diameters,

(b) solid rocket propellants with large proportions of secondary explosives which have small critical detonation diameters, and

(c) Explosive Ordnance Disposal and the producton of predictable events.

Further work is required to confirm the influence of critical detonation diameter of explosives and solid propellants on the mechanism of jet initiation and level of jet sensitivity. These results will also allow further testing/modification of the D/d predictive criterium. Energetic

materials of particular interest are insensitive explosive fillings and solid propellants containing large proportions of secondary explosives. The Australian (MRL)/USA (BRL) program is proposing further work in this area.

3.3 EFFECT OF FILLING DIAMETER

The effect of unconfined sample size on the jet initiation of covered Composition B has been assessed in Australian work (MRL).[13] The study used 38 mm and 76 mm diameter steel covered charges with no side confinement and copper jets 1.5 mm diameter fired from 38 mm diameter shaped charges.

Several fi ings for both charge diameters in a Bruceton go/no-go sequence gave the same mean critical jet velocity for the detonation threshold of 5.2 m/µs which is thus assumed represents the limiting value. These results may suggest that for a charge/jet diameter ratio greater than at least 25 (38/1.5) there is no charge diameter effect where side confinement is not an issue - see Section 3.5 for an assessment of side confinement. This result is useful in the design of small scale testing for the determination of jet sensitivity values of energetic fillings and were (instrumented) tests are undertaken to assess controlling parameters for jet bow wave initiation.

3.4 ROLE OF THE COVER

The thickness of the cover in the region of jet impact is of prime importance in determining the mechanism of initiation and level of jet sensitivity. For thin covers of less than a few jet diameters the impact is most likely to cause detonation. This shock is very strong but attenuates rapidly. Starkenberg et al[21] have numerically modelled impact initiation of thin covered Composition B by small diameter projectiles and the trend in results is useful for assessing the characteristics of jet impact. Thus, for example, the study showed that for the smallest diameter projectile (5 mm) the Jacobs-Roslund formula[34] failed to correct for case thickness and detonation either occurred very close to the cover/explosive interface or not at all.

Detonation close to the thin cover surface at the critical jet velocity is supported by the experimental and numerical code study by Pirotais et al[26] in France on an aluminium covered HMX composition. For covers greater than a few jet diameters the impact shock is attenuated and overtaken by the jet penetration bow wave in the cover. The mechanisms of initiation of energetic fillings through thicker covers are summarised in Section 2, this includes reference to the role of the bow wave in the cover.

When penetrating the cover the fastest elements of the jet are progressively erroded and this process is governed by the density relationship of the jet and cover materials as per the penetration equations.[27] Consequently the jet penetration velocity in the explosive decreases with increasing cover thickness and the associated bow wave shock becomes a less efficient initiator. Australian (MRL)/USA (BRL) work has demonstrated that the critical jet velocity for bow wave initiation is independent of the cover material (steel, aluminium, plexiglas and steel/plexiglas were used) except that the critical thickness increases as

a function of decreasing density. However, a direct correlation with density is complicated by the degree of stretching of the jet. These observations suggest that the cover forms a protective role by attenuating the impact shock, erroding the jet and forming desensitising precursor waves.

3.5 FULL CONFINEMENT EFFECTS

The effect of confinement on the response of explosive fillings to shaped charge jets can be partly assessed from USA(BRL)/Australian (MRL) work.[1-8] There are two aspects of the results that should be noted; the effect of confinement on the critical jet velocity for the detonation threshold and the degree of voilence of the non-detonative reactions.

Preliminary work by Zernow et al[28] of BRL in 1955 demonstrated that the type and degree of confinement affected the probability of the jet initiation of covered explosives. However, the study was of a limited nature and the explosive filling geometry and jet quality appears to have complicated the interpretation of the data.

Jets fired at covered explosive with no side confinement close to the detonation threshold of both cast and pressed explosives produced bulk burning. Flash x-ray showed that creamed TNT underwent bulk deflagration within the bow wave. No explosive was recovered. Flash x-ray indicated that Composition B, H-6 and pressed TNT exhibited localised bow wave burn in the jet tip region. For H-6 this reaction probably spread to the bulk of the filling since no explosive was recovered but for Composition B some powder was recovered from the firing cell walls. However, lower velocity jets produced limited amounts of burning. Unconsumed explosive was recovered as powder and various size pieces with signs of surface melting.

38 mm diameter Composition B in steel cylinders with a 12 mm thick wall and Composition B and H-6 filled 105 mm shell consistently produced violent deflagrations even when stand-off plates were used to allow only the lower velocity portion of the jet to enter the filling. These experiments suggest that the puncturing of the case by the jet does not produce effective release of the confinement and that there is no quenching of the reaction started by the jet. Thin cases, however, may rupture from early reaction thus avoiding the build-up of violent non-detonative events - this may particularly apply to solid propellants and types of non-TNT based explosives. Some form of bow wave burn would still be expected. Further work is required to investigate this aspect of confinement.

There is also a need to assess whether larger, confined fillings will undergo the deflagration to detonation transition in these situations and whether the fragmentation and blast from violent deflagrations is a sympathetic detonation hazard.

Depending upon its proximity to the jet entry into the explosive filling, side confinement can have a significant effect on the critical jet velocity for bow wave initiation at the detonation threshold. Thus for the jet from the 38 mm diameter shaped charge the critical velocity of 5.2 mm/μs for an effectively infinitely large diameter, unconfined filling was reduced to 4.7 mm/μs for symmetrical steel confinement at 19 mm radius from the jet axis. However, side confinement at about 40 mm radius from the jet axis showed no decrease in the critical jet velocity. These

results indicate that beyond a certain limit (for these trials a filling diameter to jet diameter ratio of 30/1.5 = 53), side confinement has no effect. It is interesting to note that the critical jet velocity of 5.2 mm/μs produces an initiation bow wave pressure in Composition B of about 25 kbar (similar to the large scale gap test value) which is significantly reduced to about 12 kbar (similar to the Eglin super gap test value) for the bow wave initiation pressure from the 4.7 mm/μs velocity jet. The effect of the side confinement is attributed to a change in the shape of the initiation bow wave pulse to be flatter, with a steeper front. Work is currently underway in the Australian (MRL)/USA(BRL) program to further asses confinement effects and determine whether a predictive equation can be developed for estimating the effect of symmetrical side confinement. The development of numerical modelling routines would assist in predictive work.

3.6 EFFECT OF CAVITIES IN THE ENERGETIC FILLING

Cavities can be classified as two types; those between the case and the energetic filling and those within the bulk of the filling. Australian (MRL)/USA (BRL) work[3,5-8,29] has shown that both types can have a strong sensitising effect.

The major sensitising effect of a cavity between the cover and filling has been demonstrated by flash radiography and can be assessed from Table 2 where the critical jet velocity for the detonation threshold has been determined with and without an air gap between the filling and cover. The effect arises since any precursor wave is dissipated in the air gap and

TABLE 2

Jet Detonation/Failure Threshold Velocities for Explosive Fillings with and without an Air Gap Between the Cover and Filling

Explosive	Shaped Charge Diameter	Critical Jet Velocity (mm/μs)	
		Covered With No Air Gap	Covered With Air Gap (Bare Explosive)
Cast TNT	38 mm	6.6	6.8
Composition B	38 mm	5.2	3.2
H-6	38 mm	4.9	3.3
Octol	38 mm	4.9	2.8
Pressed TNT	38 mm	4.1	2.9
PBX 9502	81 mm	6.5	3.8

an impact shock can again form when the jet strikes the bare explosive surface. Thus the results in Table 2 also represent the difference in the jet sensitivity of bare (impact initiation) and covered explosives (bow wave initiation). Energetic fillings with a large critical detonation diameter with respect to the jet diameter would not be expected to show this effect. This is demonstrated by the cast TNT result which is initiated by the bow wave in both configurations - see Section 3.2.

Cavities within a filling can perform a similar sensitising role to that described above since they can also dissipate the bow wave and allow the jet to form an impact shock on the far, exposed surface of the void. This has been demonstrated experimentally using multiple flash radiography for both spherical and laminer cavities. Aspects of the effect have been discussed in detail in Reference 29 where it has been calculated that the maximum depth for a void to retain a sensitising effect in Composition B and pressed TNT is about 320 mm and 290 mm respectively for the 38 mm diameter shaped charge jet. Again, however, fillings with large critical detonation diameters with respect to the jet diameter (see Section 3.2) would not be expected to show this effect. German work[24] has recently repeated some of the void experiments with similar results.

These results may have application to solid rocket propellants with small critical detonation diameters where cavities are produced by internal shaping.

R.B. Frey[30] has proposed that an energetic material may be initiated by the penetration process of a particulated jet. In this proposal sufficient time may elapse between well separated individual impacts for dissipation of the desensitising bow wave and for the following particle to produce impact initiation on the exposed surface.

4. JET CHARACTERISTICS AND PREDICTIVE EQUATIONS FOR THE DETONATION THRESHOLD

An early British study[31] at RARDE (then ARD) demonstrated that the jet and not the slug initiated bare explosive. Later James[32] also of RARDE postulated that jet initiation occurred when the jet penetration velocity was equal to or exceeded the maximum particle velocity in the explosive detonation - this proposal is not supported by the measured critical jet velocities for a number of explosives.[4-8]

Jet velocity and diameter[1-11,33] are important in determing the detonation of an explosive filling by either the impact or bow wave shock. Jet velocity determines the peak pressure while the jet diameter controls the shape of the shock and contributes to the pressure profile; large jet diameters produce flatter topped waves which are less affected by rarefactions and will therefore be more effective at initiation. Jet density is important for impact initiation in that it contributes to energy transfer at the jet/explosive boundary. Higher density jets are also more effective at penetrating the cover.

Using a range of copper jets Held[33] demonstrated that the initiation of bare explosive was controlled by jet velocity and diameter in the form of the predictive equation,

$$V_j^2 d = \text{constant} \qquad (2)$$

where V_j the critical jet velocity for initiating bare explosive and d jet diameter.[11] This conclusion was supported by later experimental work by Campbell.[11] The numerical modelling study by Mader et al[10,11] also confirmed equation (2) and went on to propose a predictive relationship independent of jet material by including a jet density term,

$$V_j^2 d\rho = \text{constant} \qquad (3)$$

where ρ jet density.

Expressions (2) and (3) will have application to impact shock initiation through thin covers. This shock will attenuate very quickly and hence the jet velocity will need to be increased in order to maintain detonation with increasing cover thickness. Thus for the thin covered situation the explosive sensitivity value would show an apparent increase from the limiting value of equation (2) set with bare explosive. The Starkenberg et al[21] modelling study on thin cased Composition B indicated that the Jacobs-Roslund formula[34] for correcting for case thickness on the critical impact velocity of a projectile was not obeyed for 5 mm diameter rods and persumably therefore not by jets.

After travelling a few jet diameter thicknesses the decaying impact shock is overtaken by the bow wave and expressions (2) and (3) are replaced by predictive equations based on bow wave initiation.

Australian (MRL)/USA (BRL)[7,8] work has proposed the form of the predictive equations for the jet bow wave in the explosive at the detonation threshold. The equations were obtained from the measurements of the detonation/lower order reaction threshold in Composition B for an aluminium and 2 types of copper jets. The equations take the form,

$$Up^2 d = \text{constant} \qquad (4)$$

or

$$V_{jb}^2 d\rho^{\frac{1}{2}} = \text{constant for any jet material} \qquad (5)$$

or

$$V_{jb}^2 d = \text{constant for a given jet material} \qquad (6)$$

where Up critical jet penetrating velocity in the explosive, and

V_{jb} critical jet velocity in air prior to striking the explosive for bow wave initiation.

Equation (4) directly relates to bow wave initiation and indicates that critical jet penetration velocity is independant of jet density.[27] Although Up and V_{jb} were measured independently they are related by,

15.

$$Up = \frac{V_{jb}}{1 + \gamma}$$ where γ the square root of the ratio of target to jet density.

It is stressed that although expressions (2) and (6) are similar in form they do not use the same critical jet velocity values and hence produce significantly different jet sensitivity constants. For example, Australian work has measured the jet impact shock sensitivity value for bare Composition B using equation (2) at 15 $mm^3/\mu s^2$ which is markedly different to the measured jet bow wave sensitivity value for covered Composition B using equation (6) at 40 $mm^3/\mu s^2$.

Section 3.2 has suggested that a qualification on the use of equation (2) for bare explosives is when D/d > 5 when equations (4) to (6) are appropriate.

Equations (2) to (6) are used to measured the jet sensitivity constants of an explosive which can then be used to predict the velocity, and diameter values (and density if other materials are used) for another jet at the detonation threshold. Work at Sandia National Laboratories[35] using jet diameters from 0.041 to 1.10 mm applied equation (2) thus assuming jet impact initiation. Further, equations (4) to (6) have only been tested over a limited diameter range and no experimental work has been reported to support equation (3). Further verification is required for the predictive equations over a larger range of jet diameters and densities and for energetic materials with a greater range of properties. The Australian (MRL)/USA(BRL) program is undertaking further work to asses the validity of the jet bow wave predictive equations (4) to (6).

5. RELEVANCE OF STUDIES ON BARE ENERGETIC MATERIALS

Generic munitions with cases up to a few jet diameters thick will be initiated by the impact shock. Thus studies on bare energetic fillings will have application to this type of munition when account is taken of the changing profile of the decaying shock through the case. However, for thicker covers the jet penetration bow wave in the energetic filling becomes the controlling mechanism which has different initiation characteristics and results in a much lower level in jet sensitivity. This is shown in Table 2 where the critical jet velocity for the detonation threshold of a covered material is in the region of 30% greater than for the same material in the bare configuration. These considerations suggest that studies on bare energetic fillings have limited value when applied to generic munitions with thick cases. If not treated with caution they will lead to using incorrect jet parameters for the detonation threshold and to erroneous predictions on whether a detonation or lower order reaction will occur. An exception will be when there is a cavity between the case and filling or within the bulk of the filling when measurements on bare materials will allow an estimate of the sensitising effect of the cavity.

A further qualification on the use of data from studies on bare materials arises if the critical detonation diameter is large with respect to the jet diameter when there is a change in the mechanism of initiation and level of sensitivity - this effect is discussed in Section 3.2.

CONCLUSION

The survey has shown that in recent years considerable progress has been made in understanding the processes that underlie the shaped charge jet threat/hazard situation. Thus there has been a growth in understanding the mechanisms of jet initiation, identifying the parameters that control the detonation threshold and the determination of the characteristics that influence a generic munitions response to a shaped charge jet strike. The information suggests that generic munitions can be classified as thin or thick cased from the point of view of the jet threat/hazard and that it is important that the correct form of the predictive equation is used for the detonation threshold. Most work has been undertaken using explosive fillings although the results suggest that solid propellants may exhibit similar general characteristics.

There are no tests that assess the response of a generic munition to the shaped charge jet threat/hazard. Basic information and test measurements (e.g., gap test) of the shock initiation process are of general relevance to jet initiation and critical detonation diameter is an important property. Australia has developed a small scale, calibrated test to measure the jet sensitivity of energetic material and the results are applicable to both thin and thick cased generic munitions. An instrumented form of the test has been used to assess the role of various parameters that are relevant to generic munition response.

Recent information has allowed a start at constructing detonation threshold maps and a proposal has been developed for a hazard assessment flow chart. It is proposed that current data provides a good base for an extension of technical knowledge to cover a greater range of jets and energetic fillings. This should include experimental theoretical and numerical modelling studies. Shaped charge jets, like other threat/hazard stimuli require an understanding of the consequences of a deflagration occurring within a generic munition.

REFERENCES

1. R.B. Frey, G. Melani and S.M. Carter BRL Report ARBRL-MR-2753 (May 1977).

2. M.C. Chick and T.J. Bussell. Report in course of publication.

3. M.C. Chick and D.J. Hatt Proceedings Seventh Symposium (International) on Detonation, p 352 (1981).

4. M.C. Chick and D.J. Hatt, Propellants, Explosives, Pyrotechnics, 8 121, (1983).

5. M.C. Chick, I.B. Macintyre and R.B. Frey, Proceedings of Eighth Symposium (International) on Detonation (1985).

6. M.C. Chick and R.B. Frey, Proceedings First Australian Explosives Seminar, p 237 (1985).

7. M.C. Chick, T.J. Bussell, R.B. Frey and G. Boyce, Proceedings of Ninth International Ballistics Sympoisum p 2-241 (1986).

8. M.C. Chick, T.J. Bussell, R.B. Frey and G. Boyce, MRL report 1026 (1986).

9. C.L. Mader and G.H. Pimbley, LANL Report 8647 (1981).

10. C.L. Mader, G.H. Pimbley and A.L. Bowman, LANL Report LA-9527-MS 1982.

11. C.L. Mader and G.H. Pimbley, J. Energetic Materials 1, p 3 (1983).

12. M.C. Chick and T.J. Bussell, Preprints Second Australian Explosives Safety Seminar (1987).

13. M.C. Chick and T.J. Bussell, Paper in course of publication.

14. A.W. Campbell, W.C. Davis, J.B. Ramsay and J.R. Travis, Phys. Fluids, 4, p 511 (1961).

15. A.W. Campbell and J.R. Travis, Proceedings of Eighth Symposium (International) on Detonation (1985).

16. J.N. Majerus and A.B. Merendino, BRL Report ARBRL-TR-02103 (1978).

17. J.N. Majerus, T. Martin and W. Jones, BRL Report BRL-MR-2665 (1976).

18. W.H. Anderson, J. of Ballistics, p 1479.

19. F.T. Brown, W.S. Jackson, R.G. Hippensteel, R. Abrahams, G. Coulter, C. Kingery BRL Report ARBRL-MRL-02977 (1979).

20. J. Watson, Proceedings of Ninth International Ballistics Symposium, p 2-391 (1986).

21. J.J. Starkenberg, Y.K. Huang and A.L. Arbuckle, BRL Technical Report ARBRL-TR-02548 (1984).

22. M.C. Chick, M.G. Wolfson and L.A. Learmonth, Proceedings of 18th International ICT Conference, p 56-1 (1987).

23. M. Held, Propellants, Explosives, Pyrotechnics, 12, p 35 (1987).

24. M. Held, Propellants, Explosives, Pyrotechnics, 12, p 97 (1987).

25. C.L. Mader LANL Report LA-UR-85-2429 (1986).

26. D. Pirotais, J.P. Plotand and J.C. Braconnier, Proceedings of the Eighth Symposium on Detonation (1985).

27. G. Birkoff, D.P. MacDougall, E.M. Pugh and G. Taylor, J. App. Phys, 19, p 563 (1948).

28. L. Zernow, I. Lieberman and S. Kronman, BRL Memo Report 944 (1955).

29. M.C. Chick, J. Energetic Materials 3, 5, p 221 (1985).

30. R.B. Frey Private Communication.

31. Anon., ARD Mot. Report 45/45 (1945).

32. Referenced in F.C. Ledsham, Ordnance Board Report (1959).

33. M. Held, Explosivstoffe, 5, p 98 (1968).

34. L.A. Roslund, J.W. Watt, and N.L. Coleburn, NOL Technical Report NOLTR-73-124 (1974).

35. M.G. Vigil, Proceedings of the Eighth Symposium (International) on Detonation (1985).

36. M.C. Chick, M.G. Wolfson and L.A. Learmonth, MRL Report MRL-R-1016 (1986).

NUMERICAL SIMULATIONS OF

SHOCK INITIATION OF EXPLOSIVES BY FRAGMENT IMPACTS

by

Larry Libersky

As a part of a study to determine the vulnerability of high explosive warheads to fragment impact, three-dimensional numerical simulations of detonation in Comp-B explosive initiated by steel cubes have been performed. These calculations address the phenomena of shock initiation as a function of fragment size, impact speed, and orientation. A simultaneous fragment impact was calculated as a start on the problem of multiple fragment impacts.

The MESA (Multi-Material Eulerian Shock Algorithm) hydrodynamics code was used to simulate the impact and detonation. MESA was written at the New Mexico Institute of Mining and Technology TERA (Terminal Effects Research and Analysis) Group and is a combination of the "best" procedures used in many well known and established hydrocodes. The code is second order accurate throughout and uses the SLIC (Simple Line Interface Calculation) algorithm for multi-material fluxing, and BKW equation of state for detonation products. MESA code predictions are in good agreement with the experiments of Roslund (NOL Report 73-124) which was used as a test case for the shock initiation calculation.

The basic mechanism of shock initiation of high explosives is the interaction of the shock with density discontinuities which produce local hot spots that initiate decomposition and thus propagate the detonation. Since it is not possible to model in detail all the density discontinuities of a heterogeneous explosive, Forest Fire, a simplified model, was used.

Results for a few cases in which a 60 grain steel cube impacted a 1/8-inch thick steel plate covering Comp-B explosive are shown in the accompanying figure. The critical speeds for detonation in mm/μs are displayed on the cube face. Notice that the critical speed is strongly dependent on the orientation of the cube. The critical speed for a "flat" impact was 1.7 mm/μs while the critical speed for the "edge-on" impact was 2.8 mm/μs. For flat impacts at obliquity angles of 22.5° and 45°, the critical speeds were 1.9 mm/μs and 2.3 mm/μs, a significant difference. For the case of simultaneous flat impacts at one cube separation, the critical speed was computed to be 1.6 mm/μs, as opposed to 1.7 mm/μs for the single fragment impact. These critical speeds were computed to the nearest one-tenth of a mm/μs, so that for the single fragment and flat impact case, detonation was observed at 1.7 mm/μs but not at 1.6 mm/μs.

In summary, the MESA code has been used to simulate impacts of steel cubes against a steel plate covering Comp-B explosive. These three-dimensional calculations were done on a relatively modest HP-9000 computer at TERA. Results show that the critical velocity for detonation is strongly sensitive to the fragment orientation and impact angle, and therefore an important safety consideration.

RESULTS

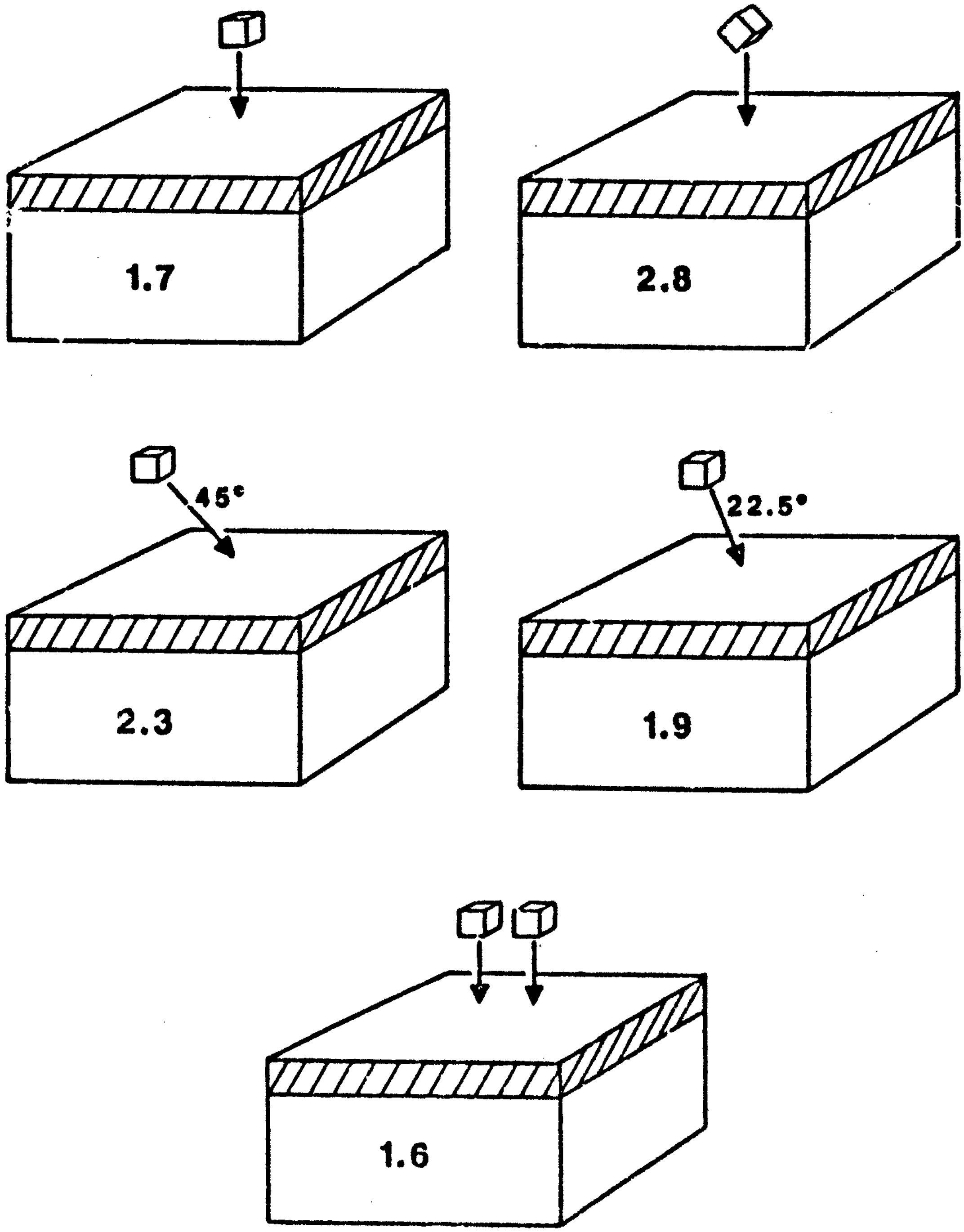

Critical speeds in mm/µs for 60 grain steel cube impacting covered Comp-B as computed by MESA3D. The steel plate is 1/8 inch thick. The critical speeds are computed to 0.1 mm/µs.